



Snow, Water, Ice and Permafrost in the Arctic (SWIPA) 2017

AMAP

Arctic Monitoring and Assessment Programme (AMAP)

Educational use: This report (in part or in its entirety) and other AMAP products available from www.apmap.no can be used freely as teaching materials and for other educational purposes.

The only condition of such use is acknowledgement of AMAP as the source of the material according to the recommended citation.

In case of questions regarding educational use, please contact the AMAP Secretariat (amap@apmap.no).

Note: This report may contain material (e.g. photographs) for which permission for use will need to be obtained from original copyright holders.

Disclaimer: The views expressed in this peer-reviewed report are the responsibility of the authors of the report and do not necessarily reflect the views of the Arctic Council, its members or its observers.

Snow, Water, Ice and Permafrost in the Arctic (SWIPA) 2017

**Arctic Monitoring and Assessment Programme
(AMAP), Oslo, 2017**

Snow, Water, Ice and Permafrost in the Arctic (SWIPA) 2017

Citing whole report

AMAP, 2017. Snow, Water, Ice and Permafrost in the Arctic (SWIPA) 2017. Arctic Monitoring and Assessment Programme (AMAP), Oslo, Norway. xiv + 269 pp

Citing individual chapters

[Lead author list], 2017. [Chapter title]. In: Snow, Water, Ice and Permafrost in the Arctic (SWIPA) 2017. pp. [??-??]. Arctic Monitoring and Assessment Programme (AMAP), Oslo, Norway.

ISBN 978-82-7971-101-8

© Arctic Monitoring and Assessment Programme, 2017

Published by

Arctic Monitoring and Assessment Programme (AMAP), Oslo, Norway. (www.apmap.no)

Ordering

This report can be ordered from the AMAP Secretariat, Gaustadalléen 21, N-0349 Oslo, Norway

This report is also published as electronic documents, available from the AMAP website at www.apmap.no

Production

Production management

Janet F. Pawlak (AMAP Secretariat)

Editing

Carolyn Symon (carolyn.symon@btinternet.com)

Technical production

Burnthebook, United Kingdom (www.burnthebook.co.uk)

Jane White and Simon Duckworth (Burnthebook)

Cover photograph

Sea ice edge. Photo: ©Richard Waters/Shutterstock

Printing

Narayana Press, Gylling, DK-8300 Odder, Denmark (www.narayananpress.dk).



AMAP Working Group (during period of preparation of this assessment)

Martin Forsius (Chair, Finland), Morten Olsen (Vice-Chair, Denmark), Sarah Kahlk (Canada), Mikala Klint (Denmark), Outi Mähönen (Finland), Helgi Jensson (Iceland), Marianne Kroglund (Vice-Chair, Norway), Tove Lundeberg (Sweden), Yuri Tsaturov (Vice-Chair, Russia), J. Michael Kuperberg (United States), Eva Krummel (Inuit Circumpolar Council), Jannie Staffansson (Saami Council), Bob van Dijken (Arctic Athabaskan Council)

AMAP Secretariat

Lars-Otto Reiersen, Janet Pawlak, Simon Wilson, Jon L. Fuglestad, Jan-Rene Larsen, Tom Armstrong, Inger Utne

Arctic Council Member States and Permanent Participants of the Council

Canada, Kingdom of Denmark, Denmark/Greenland/Faroe Islands, Finland, Iceland, Norway, Russia, Sweden, United States, Aleut International Association (AIA), Arctic Athabaskan Council (AAC), Gwitch'in Council International (GCI), Inuit Circumpolar Council (ICC), Russian Association of Indigenous Peoples of the North (RAIPON), Saami Council

Contents

Chapter 1. Introduction

Lead authors: Morten S. Olsen, Janet Pawlak, Lars-Otto Reiersen, Jason E. Box, James Overland, John Walsh

Chapter 2. Trends and feedbacks

Lead authors: James Overland, John Walsh, Vladimir Kattsov

Chapter 3. Arctic terrestrial snow cover

Lead authors: Ross Brown, Dagrun Vikhamar Schuler, Olga Bulygina, Chris Derksen, Kari Luojus, Lawrence Mudryk, Libo Wang, Daqing Yang

Chapter 4. Changing permafrost and its impacts

Lead authors: Vladimir Romanovsky, Ketil Isaksen, Dmitry Drozdov, Oleg Anisimov, Arne Instanes, Marina Leibman, A. David McGuire, Nikolay Shiklomanov, Sharon Smith, Donald Walker

Chapter 5. Arctic sea ice

Lead authors: David G. Barber, Walter N. Meier, Sebastian Gerland, C.J. Mundy, Marika Holland, Stefan Kern, Zhijun Li, Christine Michel, Donald K. Perovich, Takeshi Tamura

Chapter 6. Changes to Arctic land ice

Lead authors: Jason E. Box, Martin Sharp

Chapter 7. Freshwater

Lead authors: Terry D. Prowse, Arvid Bring, Eddy C. Carmack, Marika M. Holland, Arne Instanes, Johanna Mård, Timo Vihma, Frederick J. Wrona

Chapter 8. Arctic carbon cycling

Lead authors: Torben R. Christensen, Søren Rysgaard, Jørgen Bendtsen, Brent Else, Ronnie N. Glud, Ko van Huissteden, Frans-Jan W. Parmentier, Torsten Sachs, Jorien E. Vonk

Chapter 9. Sea level rise contribution from Arctic land ice: 1850-2100

Lead authors: Jason E. Box, William T. Colgan

Chapter 10. Cross-cutting scientific issues

Lead authors: Johanna Mård, Jason E. Box, Ross Brown, Michelle Mack, Sebastian H. Mernild, Donald Walker, John Walsh

Chapter 11. SWIPA 2017 Synthesis: summary and implications of findings

Lead authors: James Overland, John Walsh, Vladimir Kattsov, David Barber, Jason E. Box, Ross Brown, Johanna Mård, Morten S. Olsen, Vladimir Romanovsky

Acronyms and abbreviations

Coordinating lead authors shown in bold

Acknowledgments

Guðfinna Aðalgeirsdóttir, Maria Ananicheva*, Morten L. Andersen, **Oleg Anisimov**, Roberto Azzolini, **David G. Barber***, **Jørgen Bendtsen**, Jørgen Berge, Uma S. Bhatt, Bodil Bluhm, Jeff Bowman, **Jason E. Box***, **Arvid Bring**, **Ross Brown***, **Olga Bulygina**, Terry Callaghan, Anders Carlson, Eddy C. Carmack, Rachel Carr, **Torben R. Christensen***, Jørgen S. Christiansen, Caroline Clason, **William T. Colgan**, Luke Copland, **Chris Derksen**, Ralf Döscher, **Dmitry Drozdov**, Jens K. Ehn, **Brent Else**, Howard E. Epstein, Steve Ferguson, Greg Flato, Sandro Fuzzi, **Sebastian Gerland***, Andrey Glazovsky, **Ronnie N. Glud**, Mats A. Granskog, Pavel Groisman, Guido Grosse, Mauro Gugliemin, Carling Hay, Gina Henderson, Lawrence Hislop, **Marika M. Holland**, Haakon Hop, Øystein Hov, Alun Hubbard, **Ko van Huissteden**, Christine Hvidberg, **Arne Instanes**, **Ketil Isaksen***, Hans-Werner Jacobi, Margareta Johannsen, Benjamin M. Jones, M. Torre Jorgensen, Mikhail Kanevskiy, **Vladimir Kattsov***, **Stefan Kern**, Takashi Kikuchi, Alexander Kizyakov, Kristian K. Kjeldsen, Harri Kuosa, **Marina Leibman**, Antoni Lewkowicz, **Zhijun Li**, Bonnie Light, Magnus Lund, Nina

Lundholm, **Kari Luojus**, **Michelle Mack**, Galina Malkova, Sergey Marchenko, **Johanna Mård***, **A. David McGuire**, Walter N. Meier, Igor A. Melnikov, **Sebastian H. Mernild**, Christine Michel*, Geir Moholdt, Twila Moon, **Lawrence Mudryk**, **C.J. Mundy***, Isla H. Myers-Smith, Dmitry J. Nicolsky, **Morten S. Olsen***, **James Overland***, **Frans-Jan W. Parmentier***, Janet Pawlak*, **Donald K. Perovich**, Alek Petty, Tad Pfeffer, Chris Polashenski, **Terry D. Prowse***, Martha K. Raynolds, **Lars-Otto Reiersen***, **Vladimir Romanovsky***, **Søren Rysgaard***, **Torsten Sachs**, Christina Schädel, Martin Schneebeli, E.A.G. Schuur, Mark Sereze, **Dagrun Vikhamar Schuler**, **Martin Sharp**, **Nikolay Shiklomanov**, Lars H. Smedsrød, **Sharon Smith**, Gunnar Spreen, Martin Stendel, Dmitry Sterletskiy, Mikkel Tamstorf, **Takeshi Tamura**, Thorsteinn Thorsteinsson, Mark Tschudi, Martin Vancoppenolle, **Timo Vihma**, **Jorien E. Vonk**, Thomas Wagner, **Donald Walker**, **John Walsh***, **Libo Wang**, Melinda Webster, Sebastian Westermann, Steven Wofsy, Bert Wouters, **Frederick J. Wrona**, Wesley Van Wychen, **Daqing Yang**, Lujun Zhang

* Participant in the SWIPA lead author team

Bold text denotes lead authors

Preface

This report presents the findings of the *Snow, Water, Ice and Permafrost in the Arctic (SWIPA) 2017* assessment performed by the Arctic Monitoring and Assessment Programme (AMAP). The SWIPA 2017 assessment is the fourth AMAP assessment addressing Arctic climate issues and is a direct follow-up to the first *Snow, Water, Ice and Permafrost in the Arctic (SWIPA): Climate Change and the Cryosphere* assessment report published in 2011. The SWIPA 2011 report reviewed the state of knowledge regarding ongoing change in the Arctic climate, and particularly the status and impacts of global warming on the cryosphere – the frozen components of the Arctic; it represents the benchmark against which this updated assessment of change in the Arctic cryosphere has been developed.

The findings and recommendations from SWIPA 2011 were considered by the Arctic Council at its 2011 Ministerial Meeting in Nuuk after which it launched two major initiatives to follow up on the findings of the report: the Arctic Resilience Assessment work and the AMAP-led Adaptation Actions for a Changing Arctic (AAC) process (see Chapter 1 for further details). Both activities were conducted in parallel to the present assessment and provide parallel, complementary information to SWIPA 2017. In particular the AAC assessments cover the impacts of climate change and other stressors on the ecosystem services, human societies and socio-economic conditions in three regions of the Arctic.

The SWIPA 2017 assessment was conducted between 2010 and 2016 by an international group of over 90 scientists, experts and knowledgeable members of the Arctic indigenous communities. Lead authors were selected by an open nomination process coordinated by AMAP and several national and international organizations. A similar process was used to select international experts who independently reviewed this report. A SWIPA team of coordinating lead authors for the eleven chapters was responsible for scientific oversight and coordination of all work related to the preparation of the assessment report. Documentation available on the website www.apmap.no includes listings of the comments received from the peer reviewers and how they were addressed.

Information contained in this report is fully referenced and based mainly on research and monitoring efforts published since 2010 (i.e., information gathered since the SWIPA 2011 report was undertaken). It includes peer-reviewed material accepted for publication up until September 2016, and in some cases later. Unpublished monitoring information, including both *in situ* and satellite observations, with well-established national and international standards and QA/QC (quality assurance / quality control) protocol are also part of the assessment.

Acknowledging national differences in scientific quality assurance, the SWIPA assessment therefore draws mainly on peer-reviewed publications and work accepted for publication in respected scientific journals, including works reviewed by Russian scientific committees. Other sources of information, such as government reports, design standards, official records, statistics and other publicly available material have also been included in the work. All such references have been collected and are available upon request (at cost of reproduction) from

the AMAP Secretariat. Care has been taken to ensure that no critical probability statements are based on these materials.

Access to reliable and up-to-date information is essential for the development of science-based decision-making regarding ongoing changes in the Arctic and their global implications. To allow readers of this report to see how AMAP interprets and develops its scientifically-based assessment product in terms of more action-orientated conclusions and recommendations, an extract from the *Snow, Water, Ice and Permafrost in the Arctic: Summary for Policy-makers* report is reproduced in this report on pages vii to xiv. The SWIPA Lead authors have confirmed that this Summary for Policy-makers accurately and fully reflects their scientific assessment. The present report constitutes the fully-referenced scientific basis for all statements made in the SWIPA Summary for Policy-makers. The SWIPA reports are available from the AMAP Secretariat and on the AMAP website www.apmap.no.

AMAP would like to express its appreciation to all experts who have contributed their time, effort, and data to this assessment, with particular gratitude to the chapter lead authors and members of the SWIPA lead authors team who coordinated the production of this report. Thanks are also due to the many referees and reviewers who contributed to the SWIPA peer-review process and provided valuable comments that helped to ensure the quality of the report. A list of the main contributors is included at the start of each chapter. The list is not comprehensive. Specifically, it does not include the many national institutes, laboratories and organizations, and their staff, which have been involved in the various countries. Apologies, and no lesser thanks are given to any individuals unintentionally omitted from the list.

The support of the Arctic countries and non-Arctic countries implementing research and monitoring in the Arctic is vital to the success of AMAP. The AMAP work is essentially based on ongoing activities within these countries, and the countries also provide the necessary support for most of the experts involved in the preparation of the AMAP assessments. In particular, AMAP would like to thank Canada, the Kingdom of Denmark, the Norwegian Ministry of Foreign Affairs and the Nordic Council of Ministers for their financial support to the SWIPA work, and to sponsors of programs and projects that have delivered data for use in this assessment. The AMAP Working Group is pleased to present its assessment to the Arctic Council and the international science community.

Morten S. Olsen (SWIPA Chair)

Martin Forsius (AMAP Chair, April 2017)

Lars-Otto Reiersen (AMAP Executive Secretary)

Oslo, August 2017

Disclaimer: The views expressed in this peer-reviewed report are the responsibility of the authors of the report and do not necessarily reflect the views of the Arctic Council, its members or its observers.

Extract from the *Snow, Water, Ice and Permafrost in the Arctic: Summary for Policy-makers*

The *Snow, Water, Ice and Permafrost in the Arctic (SWIPA) 2017* assessment performed by the Arctic Monitoring and Assessment Programme (AMAP) presents key findings and implications of the second SWIPA assessment, conducted from 2010 to 2016 and published in 2017. Access to reliable and up-to-date information is essential for the development of science-based decision-making regarding ongoing changes in the Arctic and their global implications.

Key Findings of the SWIPA 2017 assessment

The Arctic's climate is shifting to a new state

Rising concentrations of greenhouse gases are driving widespread changes in the Arctic's sensitive climate, hydrological, and ecological systems. Since 2011, downward trends have continued in sea ice thickness and extent, land ice volume, and spring snow cover extent and duration, while near-surface permafrost has continued to warm.

With each additional year of data, it becomes increasingly clear that the Arctic as we know it is being replaced by a warmer, wetter, and more variable environment. This transformation has profound implications for people, resources, and ecosystems worldwide.

While SWIPA 2017 includes many important new findings, summarized below, three points in particular deserve special emphasis:

- The Arctic Ocean could be largely free of sea ice in summer as early as the late 2030s, only two decades from now.
- The recent recognition of additional melt processes affecting Arctic and Antarctic glaciers, ice caps, and ice sheets suggests that low-end projections of global sea-level rise made by the Intergovernmental Panel on Climate Change (IPCC) are underestimated.
- Changes in the Arctic may be affecting weather in mid-latitudes, even influencing the Southeast Asian monsoon.

Climate change in the Arctic has continued at a rapid pace

• **Arctic temperatures are rising faster than the global average.** The Arctic was warmer from 2011 to 2015 than at any time since instrumental records began in around 1900, and has been warming more than twice as rapidly as the world as a whole for the past 50 years. January 2016 in the Arctic was 5°C warmer than the 1981–2010 average for the region, a full 2°C higher than the previous record set in 2008, and monthly mean temperatures in October through December 2016 were 6°C higher than average for these months. Sea temperatures are also increasing, both near the surface and in deeper water.

• **The frequency of some extreme events is changing.** Recent observations include a widespread decline in periods of extreme cold during both winter and summer, and increases in extreme warm periods in some areas, such as northern Alaska and northeastern Russia in autumn and spring.

The role of Arctic glaciers and ice caps in global sea-level rise

Scientific advances since 2011 show that while Arctic glaciers and ice caps represent only a quarter of the world's land ice area, meltwater from these sources accounts for 35% of current global sea-level rise.

Traditional and Local Knowledge

The SWIPA scientific assessment is based primarily on peer-reviewed observations, methods, and studies, which in many cases include contributions from traditional and local knowledge. However it is recognized that this approach does not necessarily capture all relevant knowledge held by Indigenous and local communities.

- **The decline in sea ice continues, with variation from year to year.** Sea ice thickness in the central Arctic Ocean declined by 65% over the period 1975–2012. Sea ice extent has varied widely in recent years, but continues a long-term downward trend. A record low minimum sea ice extent occurred in 2012 and a record low maximum sea ice extent occurred in 2016.

Older ice that has survived multiple summers is rapidly disappearing; most sea ice in the Arctic is now 'first year' ice that grows in the autumn and winter but melts during the spring and summer.

Except for the coldest northern regions of the Arctic Ocean, the average number of days with sea ice cover in the Arctic declined at a rate of 10–20 days per decade over the period 1979–2013, with some areas seeing much larger declines. Warm winds during the autumn of 2016 substantially delayed the formation of sea ice.

Sea ice is becoming more mobile as its extent and thickness decrease, increasing ice-related hazards.

More open water occurs in all months of the year compared with observations reported in 2011.

- **The area and duration of snow cover are decreasing.** Snow cover has continued to decline in the Arctic, with its annual duration decreasing by 2–4 days per decade. In recent years, June snow area in the North American and Eurasian Arctic has typically been about 50% below values observed before 2000.

• **Permafrost warming continues.** Near-surface permafrost in the High Arctic and other very cold areas has warmed by more than 0.5°C since 2007–2009, and the layer of the ground that thaws in summer has deepened in most areas where permafrost is monitored.

- **The loss of land-based ice has accelerated in recent decades.** Since at least 1972 the Arctic has been the dominant source of global sea-level rise. Seventy percent of the Arctic's contribution to sea-level rise comes from Greenland, which on average lost 375 gigatons of ice per year—equivalent to a block of ice measuring 7.5 kilometers or 4.6 miles on all sides—from 2011 to 2014. This is close to twice the rate over the period 2003–2008.
- **Freshwater storage in the Arctic Ocean has increased.** Compared with the 1980–2000 average, the volume of freshwater in the upper layer of the Arctic Ocean has increased by 8,000 cubic kilometers, or more than 11%. This volume equals the combined annual discharge of the Amazon and Ganges rivers, and could—if it escapes the confines of the Arctic Ocean—affect circulation in the Nordic Seas and the North Atlantic.
- **Ecosystems are changing.** The decline in sea ice thickness and extent, along with changes in the timing of ice melt, are affecting marine ecosystems and biodiversity; changing the ranges of Arctic species; increasing the occurrence of algal blooms; leading to changes in diet among marine mammals; and altering predator-prey relationships, habitat uses, and migration patterns. Terrestrial ecosystems are feeling the effects of changes in precipitation, snow cover, and the frequency or severity of wildfires. The occurrence of rain-on-snow and winter thaw/refreezing events affects grazing animals such as caribou, reindeer, and muskox by creating an ice barrier over lichens and mosses. While many tundra regions have become greener over the past 30 years, reflecting an increase in plant growth and productivity, recent satellite data show shifts toward browning (indicating a decrease in plant cover and productivity) over large areas of the Arctic, particularly in Eurasia.
- **Arctic climate trends affect carbon storage and emissions.** New estimates indicate that Arctic soils hold about 50% of the world's soil carbon. While thawing permafrost is expected to contribute significantly to future greenhouse gas emissions, the amount released over the past 60 years has been relatively small.
- **The impacts of Arctic changes reach beyond the Arctic.** In addition to the Arctic's role in global sea-level rise and greenhouse gas emissions, the changes underway appear to be affecting weather patterns in lower latitudes, even influencing Southeast Asian monsoons.

Changes will continue through at least mid-century, due to warming already locked into the climate system

- **Warming trends will continue.** Models project that autumn and winter temperatures in the Arctic will increase to 4–5°C above late 20th century values before mid-century, under either a medium or high greenhouse gas concentration scenario. This is twice the increase projected for the Northern Hemisphere. These increases are locked into the climate system by past emissions and ocean heat storage, and would still occur even if the world were to make drastic near-term cuts in emissions.

- **The Arctic Ocean may be ice-free sooner than expected.** Extrapolations of recent observed data suggest a largely ice-free summer ocean by the late 2030s, which is earlier than projected by most climate models. Natural variability and model limitations make precise predictions impossible.
- **Declines in snow and permafrost will continue.** The duration of snow cover is projected to decrease by an additional 10–20% from current levels over most of the Arctic by mid-century under a high emissions scenario, and the area of near-surface permafrost is projected to decrease by around 35% under the same scenario.
- **The melting of land-based ice will contribute significantly to sea-level rise.** If increases in greenhouse gas concentrations continue at current rates, the melting of Arctic land-based ice would contribute an estimated 25 centimeters to sea-level rise between 2006 and 2100. Many of the smallest glaciers across the Arctic would disappear entirely by mid-century.
- **The Arctic water cycle will intensify.** Climate models project increases in cold-season precipitation of 30–50% over the Arctic Ocean toward the end of this century, with an increasing portion of that precipitation falling as rain instead of snow.
- **Arctic ecosystems will face significant stresses and disruptions.** Changes in sea ice are expected to affect populations of polar bears, ice-dependent species of seals and, in some areas, walrus, which rely on sea ice for survival and reproduction. There will also be losses of ice-associated algae. Physical disturbance arising from an increasing frequency of wildfire and abrupt thawing of permafrost could accelerate ecological shifts, such as the expansion of tall shrubs and trees into tundra. Boreal forests will be affected by thawing permafrost, increases in wildfires, insect pest outbreaks, and climate zone shifts.
- **Arctic changes will affect sources and sinks of important greenhouse gases.** The amount of atmospheric carbon dioxide absorbed by the Arctic Ocean may be significantly affected by changes in sea-ice cover, the structure and functioning of marine ecosystems, and the hydrological cycle. Thawing permafrost is expected to increase emissions of methane.

Substantial cuts in global greenhouse gas emissions now can stabilize impacts after mid-century

- **Reducing concentrations of greenhouse gases in the atmosphere will make a difference.** While the changes underway in the Arctic are expected to continue through at least mid-century, substantial global reductions in net greenhouse gas emissions can begin to stabilize some trends (albeit at higher levels than today) after that. Reversing trends would require reductions in atmospheric greenhouse gas concentrations.
- **Compliance with the Paris Agreement will stabilize snow and permafrost losses, but there will still be much less snow and permafrost than today.** Climate models show

that reducing greenhouse gas emissions and stabilizing concentrations, under a scenario roughly consistent with the Paris Agreement, could stabilize the further loss of snow cover and permafrost after mid-century. In contrast, higher emissions would result in continued losses.

- **Efforts to control greenhouse gas emissions can have a major impact on sea-level rise after mid-century.** For example, a scenario roughly consistent with the Paris Agreement would reduce end-of-century sea-level rise by 43% compared with that projected to occur under a business-as-usual emissions scenario.
- **However, the Arctic will not return to previous conditions this century under the scenarios considered in the SWIPA 2017 assessment.** The near-future Arctic will be a substantially different environment from that of today, and by the end of this century Arctic warming may exceed thresholds for the stability of sea ice, the Greenland ice sheet, and possibly boreal forests.

Adaptation policies can reduce vulnerabilities

- **Adaptation at the community and regional levels, both in the Arctic and globally, is essential.** The near inevitability of accelerating impacts in the Arctic and globally between now and mid-century reinforces the urgent need for local and regional adaptation strategies that can reduce vulnerabilities and take advantage of opportunities to build resilience.

Effective mitigation and adaptation policies require a solid understanding of Arctic climate change

- **Reducing knowledge gaps will improve our ability to respond to current and future changes in the Arctic.** Efforts are needed to increase the geographic coverage of observations, improve local-level projections, and reduce uncertainties.
- **Coordination across monitoring efforts, modeling studies, and international assessments can facilitate information-sharing and avoid duplication of effort.** As international attention becomes increasingly focused on Arctic climate change and its impacts, the need to coordinate among assessment processes and studies becomes greater.

Water in the Arctic

While liquid water and water vapor might seem irrelevant in a region where so much water is frozen, water in all its forms plays key roles in Arctic processes and ocean systems. For example, the increase in freshwater flow to the ocean from rivers and melting glaciers has implications for ocean circulation and climate that extend far beyond the Arctic.

The Arctic Transformed

The Arctic is still a cold place, but it is warming faster than any other region on Earth. Over the past 50 years, the Arctic's temperature has risen by more than twice the global average. Increasing concentrations of greenhouse gases in the atmosphere are the primary underlying cause: the heat trapped by greenhouse gases triggers a cascade of feedbacks that collectively amplify Arctic warming.

As a result, the Arctic of today is different in many respects from the Arctic of the past century, or even the Arctic of 20 years ago. Many of the changes underway are due to a simple fact: ice, snow, and frozen ground—the components of the Arctic cryosphere—are sensitive to heat. As the cryosphere changes, so do the Arctic's physical, chemical, and biological systems, with complex consequences within and beyond the region.

Since 2011, evidence for the Arctic's evolution toward a new state has grown stronger. Additional years of data show continued or accelerating trends in record warm temperatures, changes in sea ice and snow, melting of glaciers and ice sheets, freshening and warming of the Arctic Ocean, thawing of permafrost, and widespread ecological changes.

Beyond the trends, new data also show stronger evidence for fundamental shifts in some elements of the cryosphere, the ocean, and ecosystems. Sea ice in the Arctic is entering a new regime in which vast areas of ocean that used to be covered by ice throughout the year are now seasonally ice-free and dominated by younger, thinner ice. The composition of many boreal forests is changing: coniferous trees are increasingly being replaced by deciduous species normally found farther south.

Together, these findings portray a system whose component parts are changing at different speeds, affecting the Arctic's role as a regulator of global temperature and its influence on Northern Hemisphere weather, its contribution to sea-level rise, the livelihoods of those who live and work in the Arctic, and the habitats of Arctic species. Today's Arctic is a new environment, evolving rapidly and in unexpected ways.

Despite the many changes already underway or projected, some of which appear irreversible (such as thawing permafrost and melting of the Greenland ice sheet), climate models show that a scenario roughly equivalent to that under the 2015 Paris Agreement of the United Nations Framework Convention on Climate Change would slow or stop some trends, especially after the middle of this century, with the Arctic's average temperature stabilizing at a new, higher level. These findings offer encouragement for the long term, although the Arctic environment will continue to undergo significant changes far into the future, requiring northern countries, communities, and operators in the Arctic to focus on adaptation.

The Importance of Feedbacks

A number of feedback mechanisms, some of them unique to the Arctic, are responsible for the more rapid warming observed over the Arctic compared with the rest of the world. These feedbacks amplify warming well beyond the effects caused by increasing greenhouse gas concentrations alone. By

analyzing climate models, scientists have identified the relative contribution of the different feedbacks to warming in the Arctic.

The largest feedbacks, according to climate models, are related to the Arctic's inefficiency at radiating heat. Cold regions radiate heat slowly, so the warmth trapped by greenhouse gases tends to build up. Furthermore, warming in the Arctic is concentrated close to the Earth's surface, slowing the rate at which heat is lost to space from the top of the atmosphere.

The next-largest warming feedback comes from changes in surface reflectivity due to the melting of snow and ice. As reflective surfaces are replaced by darker surfaces such as open water or land, less energy is radiated back to space and the region warms further, leading to still more melting. Water vapor (a powerful greenhouse gas) also provides a warming feedback. Warmer temperatures increase evaporation, and a warmer atmosphere can hold more water vapor.

Follow the Water: The Changing Interactions between the Cryosphere and the Hydrosphere

The amplifiers of warming described above have contributed to an intensified water cycle in the Arctic, in which flows of freshwater between the land, the atmosphere, and the ocean are increasing. This pattern has important implications for human populations and ecosystems in the Arctic, as well as weather at lower latitudes.

For example, when precipitation increases in a warmer climate, much of that water ends up in rivers. As does the meltwater from snow, glaciers, and ice caps. The Arctic's rivers account for roughly 10% of the world's total river discharge, pouring enormous quantities of freshwater, sediment, nutrients, and organic carbon into the Arctic Ocean every year. Non-Arctic rivers, such as the St. Lawrence River in Canada, also contribute freshwater that ends up in the Arctic. Increases in freshwater flow into the ocean affect ocean circulation, ocean acidification (see AMAP's 2013 report on Arctic Ocean acidification), and biological productivity, and affect weather patterns far to the south. Melting sea ice also contributes to freshening of the ocean's surface. As the sea ice thins and shrinks it also becomes more mobile, creating hazards to shipping and other activities, while increasing the risk that currents will push it to warmer waters where it will melt.

Following the path of water through the hydrological cycle reveals many complex interactions between water and the cryosphere.

The Decades Ahead

With the warming already committed in the climate system plus the additional warming expected from rising concentrations of greenhouse gases in the atmosphere, the Arctic will experience significant changes during this century even if greenhouse gas emissions are stabilized globally at a level lower than today's. If emissions continue to increase, future changes in the Arctic would be even more substantial and long-lasting.

Climate models, using scenarios that depict plausible changes in future greenhouse gas emissions and concentrations over time, offer the following updated projections for the Arctic in SWIPA 2017:

The Paris Agreement and Arctic Change

Efforts to reduce emissions can have an impact in the later years of this century. Projections suggest that reducing greenhouse gas emissions under a scenario roughly similar to that under the Paris Agreement would have the following effects by the end of this century:

- Stabilize temperature at 5–9°C above the 1986–2005 average over the Arctic Ocean in winter.
- Reduce global sea-level rise from 2006–2100 by more than 20 centimeters.
- Stabilize the duration of snow cover at about 10% below current values.
- Stabilize near-surface permafrost extent at roughly 45% below current values.

While the Paris Agreement, if implemented, would limit the extent to which the Arctic climate changes, the Arctic environment in 2100 would still be substantially different from that of today.

Scenarios and Projections

Climate models project future conditions, based on scenarios. What does that mean?

Scenarios depict a range of plausible alternative futures, based on assumptions about future economic, social, technological, and environmental conditions that drive greenhouse gas emissions and their concentrations in the atmosphere.

Climate modelers use these scenarios to project, rather than predict, future climate under each scenario. Projections answer the question: if emissions and concentrations were to proceed along this pathway, what changes in climate would result?

SWIPA 2017 compared the outcomes of two different greenhouse gas concentration scenarios, RCP4.5 and RCP8.5. In the RCP4.5 scenario, reductions in emissions lead to stabilization of greenhouse gas concentrations in the atmosphere by 2100 and a stabilized end-of-century global average temperature rise of 1.7–3.1°C above pre-industrial levels. RCP8.5 is a high-emission business-as-usual scenario, leading to a global non-stabilized temperature rise of 3.8–6°C by 2100.

Temperature

Autumn and winter temperatures will increase by a regional average of 4°C over the next 30 years—twice the warming projected for the Northern Hemisphere as a whole—with new record temperatures observed in some regions and years. The strongest warming is projected to occur during the cold season, including spring and autumn for northern Eurasia. Even several years of cold weather due to natural variations are unlikely to affect the long-term trend, and efforts to reduce greenhouse gas emissions will not affect projected temperatures until the

latter half of this century. The warming climate will increase the amount of freshwater in the Arctic, with important implications for people, industries, ecosystems, and infrastructure.

Sea Ice

The Arctic is expected to be largely free of sea ice in late summer within the next few decades, possibly as early as the 2030s, although natural variability and other factors make it impossible to make precise predictions. The ice that appears in winter will be thinner, more salty, less rigid, and more mobile than today's sea ice. More open water is expected in winter, affecting temperature and the exchange of moisture between the atmosphere and ocean, leading to more extreme weather locally and at lower latitudes. Sea ice is currently thinning and shrinking more rapidly than projected by most models.

Snow and Permafrost

Projected changes in snow cover and maximum accumulation vary widely over the Arctic. Warmer coastal areas such as those in Alaska and Scandinavia will see the fastest and largest declines. The cold high latitudes of the Arctic will experience an increase in the annual accumulation of snow. The largest reductions in snow cover are projected in the spring in most regions of the Arctic.

The area of near-surface permafrost in the Northern Hemisphere is projected to decline by 20% relative to today's area by 2040, and could be reduced by as much as two-thirds by 2080 under a scenario of high greenhouse gas emissions. Impacts will vary widely at regional and local scales, but local effects are difficult to project given the lack of fine-scale detail in models.

Land-based Ice and Sea Level

The loss of land ice is expected to accelerate after the middle of this century. New projections of glacier changes since 2011 provide more regional detail, showing for example that some glaciers in northeastern Russia, Siberia, and the Kamchatka Peninsula could completely disappear by mid-century.

Global sea-level rise is expected to accelerate, although uncertainties about the Greenland ice sheet's response to ongoing warming hamper scientists' ability to project the rate and magnitude of the increase. A recent analysis developed for SWIPA estimates that the Arctic will contribute 19–25 centimeters to global sea-level rise by the year 2100.

The SWIPA analysis estimates that when all sources of sea-level rise are considered (not just those from the Arctic), the rise in global sea level by 2100 would be at least 52 cm for a greenhouse gas reduction scenario and 74 cm for a business-as-usual scenario. These estimates are almost double the minimum estimates made by the IPCC in 2013.

After the Greenland ice sheet, the largest Arctic contributions to sea-level rise will come from glaciers in the Canadian Arctic, Alaska, and the Russian Arctic, along with glaciers surrounding the Greenland ice sheet.

Freshwater

The Arctic water cycle is expected to continue to intensify during this century. Mean precipitation and daily precipitation extremes will increase over mid- and high latitudes, with implications for the management of water resources, flow of freshwater into the Arctic Ocean, changes in sea ice temperature, and amplification of regional warming (through reduced surface reflectivity caused by a shift from snow to more rain in the warmer seasons).

Ecosystems

The rate and magnitude of changes projected for the Arctic will push some species out of their ranges, while other species may colonize new areas. For example, many species depend on sea ice for survival and reproduction and their populations may decline with changes in sea ice thickness and extent (as well as changes in the timing of ice formation and melt), while phytoplankton and populations of non-native species may increase due to the warmer waters and reductions in sea ice. More frequent wildfires and abrupt thawing of permafrost could accelerate ecological shifts, such as the spread of tall shrubs and trees into tundra.

Carbon Cycling

Reductions in sea ice and other changes may affect the amount of carbon dioxide absorbed by the Arctic Ocean, while thawing permafrost is expected to increase emissions of methane. However, projections of future impacts on Arctic sources and sinks of greenhouse gases are still hampered by data and knowledge gaps.

What Are the Implications?

Changes underway in the Arctic have wide-ranging consequences for Arctic ecosystems and people living and working in the Arctic. The Arctic also plays an important role in global climate and weather, sea-level rise, and world commerce, which means that impacts in the Arctic resonate far south of the Arctic Circle. A recent economic analysis of the global costs of Arctic change estimated the cumulative cost at USD \$7–90 trillion over the period 2010–2100.

Adapting to Multiple Drivers of Change

Climate change is only one of many factors contributing to change in the Arctic. Oil and gas activities, mining, tourism, shipping, fisheries, economic development, and pollutants are just some of the other stressors faced by the Arctic today. Many of these factors interact with each other.

To better understand the interrelationships among multiple drivers of change in the Arctic, and to help decision-makers plan integrated adaptation strategies, AMAP is preparing an assessment on Adaptation Actions for a Changing Arctic, published in 2017.

The Arctic's Role in the Global Climate System

Compared with mid-latitudes and the tropics, the Arctic receives relatively little energy from the Sun. Because most of the Arctic's surface is covered in snow and ice, much of the energy that it does receive is reflected back to space. These factors account for the Arctic's cold climate.

The Arctic acts as a global refrigerator by drawing warm ocean water from the south, cooling it, and ultimately sinking it toward the ocean bottom. Surface water moves in to replace the sinking water, creating ocean currents. This movement of warmer ocean waters to the north has a major influence on climate; it accounts for northern Europe's relatively mild climate compared with that of Canadian provinces at the same latitude, for example, and it keeps the tropics cooler than they would be otherwise.

Meltwater from Arctic glaciers, ice caps, and the Greenland ice sheet also influences climate by flooding the ocean with freshwater, affecting ocean circulation and weather patterns.

The Arctic is both a source and sink for greenhouse gases. Changes in the quantities of greenhouse gases such as carbon dioxide and methane stored or released in the Arctic can have a long-term impact on global climate.

The implications of most findings in SWIPA 2017 are not fundamentally different from those reported in 2011, but are supported by more evidence and in some cases warrant greater concern due to more significant impacts or new knowledge. A major new finding is that Arctic changes may influence weather far to the south (see box on page xvi).

Challenges and Opportunities in the Arctic

The rapid changes underway in the Arctic affect lives, livelihoods, and ecosystems throughout the region, with both positive and negative consequences.

Access and Transportation

- The Arctic Ocean's open water season has already increased by 1–3 months over much of the ocean since the late 1970s, creating more opportunities for marine shipping, commercial fisheries, tourism, and access to resources.
- In contrast, losses and decreases in the thickness of lake and river ice and changes in permafrost conditions affect or threaten ice roads, restricting access to remote communities.
- Some northern communities have found it harder to obtain wild sources of food due to the shorter snow cover season (which affects travel to hunting grounds as well as animal habitat). The thinning of sea ice and the lengthening melt season also affect access to resources.

Risks and Hazards to Arctic Communities

- Reductions in coastal (landfast) sea ice, combined with loss of land-based ice and permafrost, are leading to coastal erosion and flooding, affecting safety and in some cases the very existence of coastal communities.
- The increased mobility of sea ice, as well as the increased export of land ice into the ocean, lead to an increase in marine ice hazards.
- Future climate change may bring higher risks of avalanches and floods from rapid melting in some regions of the Arctic. In 2015, above-average precipitation and record spring warmth in north-central Alaska led to extensive flooding that closed the Dalton Highway—the only road to Alaska's North Slope oil fields—for 3 weeks, leading to an estimated USD \$15 million in damages.
- Warmer and drier conditions have contributed to an increase in severe wildfires in the Arctic areas of North America and Eurasia. For example, the severity and frequency of fires in the taiga forests of interior Alaska are higher now than at any point in the last 10,000 years, based on paleoecological reconstructions of fire history in the region.
- Communities and infrastructure built on frozen soils are significantly affected by thawing permafrost, one of the most economically costly impacts of climate change in the Arctic. The bearing capacity of building foundations has declined by 40–50% in some Siberian settlements since the 1960s, and the vast Bovanenkovo gas field in western Siberia has seen a recent increase in landslides related to thawing permafrost. Thawing permafrost may also contaminate freshwater resources when previously frozen industrial and municipal waste is released.
- Climate change presents risks to food and water security through changes in access to hunting areas and the distribution range of traditional food sources, contamination of drinking water supplies (including by harmful algal species), changes in traditional food preservation techniques, and potential increases in food contaminants.

Impacts on Wildlife and Ecosystems

- Reductions in snow cover change the availability of habitat for microorganisms, plants, animals, and birds.
- Winter thaws and rain-on-snow events can damage vegetation, while refreezing creates a layer of ice over the vegetation that may be difficult for animals to penetrate with their hooves, adversely affecting conditions for grazing animals such as caribou, reindeer, and musk ox.
- The thinning and loss of sea ice has many impacts on Arctic life, from promoting the growth of marine phytoplankton and creating more habitat for open-water species to loss of ice-associated algal species and disrupting the feeding platforms and life cycles of seals, polar bears and, in some areas, walrus.
- Food webs are affected by changes in the structure of ecological communities and shifts in the geographic ranges of species.

Arctic Changes Affect Mid-Latitude Weather

One of the major new areas of research since 2011 is on connections between Arctic changes and mid-latitude weather. Some studies have linked the loss of land and sea ice, along with changes in snow cover, to changes in Northern Hemisphere storm tracks, floods, and winter weather patterns, and have even found evidence that Arctic changes influence the onset and rainfall of Southeast Asian monsoons.

While it is clear that Arctic changes can influence weather outside of the region, scientists are still working to characterize the nature, magnitude, and extent of the effects.

Implications for Key Industries

- Increases in precipitation could make the Arctic a potential future source of freshwater and hydropower for southern areas.
- Climate change may facilitate access to oil, minerals, and other resources, although market forces may play a larger role than climate change in those industries' activities in the Arctic. Extraction of oil and gas will lead to more greenhouse gas emissions, exacerbating the impacts described here.
- Commercial fisheries may also be affected by climate change, in both positive and negative ways, due to changes in phytoplankton growth, changes in ocean temperature, northward shifts in the ranges of some fish species (e.g., the recent migration of mackerel into waters around Svalbard and Greenland), and acidification of the ocean by carbon dioxide.

Global Implications

Changes in the Arctic affect the rest of the world, not only in obvious ways (such as the Arctic's contribution to sea-level rise), but through the Arctic's role in the global climate system, its influence on ocean circulation, and its impacts on mid-latitude weather.

- Coastal communities, low-lying islands, and ecosystems throughout the world will be affected by the melting of land ice (glaciers and ice sheets) in the Arctic, which is projected to increase the rate of global sea-level rise. Impacts include coastal flooding, erosion, damage to buildings and infrastructure, changes in ecosystems, and contamination of drinking water sources.
- The implications mentioned above for shipping; access to oil, gas, and minerals; and impacts to fisheries have economic consequences outside the Arctic.
- Changes in Arctic sea ice cover, marine ecosystems, and the water cycle affect the amount of carbon dioxide that the Arctic Ocean absorbs from the atmosphere. The ocean becomes more acidic as it absorbs more carbon dioxide, with potential implications for marine life. Changes in snow cover and permafrost also affect carbon and nitrogen cycling, as well as methane emissions.

Improving Our Understanding

The authors of SWIPA 2017 identified a number of areas where addressing data gaps and improving understanding of key processes would aid efforts to characterize the changes underway and to project changes in the future. Two overarching needs identified in the SWIPA 2017 report include 1) improving predictions for the timing of future Arctic changes (which requires a better understanding of feedbacks in the Arctic cryosphere); and 2) improving confidence in predictions of interactions between the Arctic and global systems.

The report also identifies many more specific data gaps and research needs. For example, detailed data on permafrost are lacking from important areas, such as the High Arctic regions of Canada and Russia. Gaps in our understanding of other factors, such as the storage and drainage of glacial meltwater, storage and export of continental freshwater and resulting effects on marine processes, the role of snow in the evolution of sea ice, interactions between snow and vegetation, and connections between Arctic changes and weather at lower latitudes, hamper efforts to model future impacts of warming in the Arctic. Data gaps also impede predictions of how Arctic ecosystems will respond to climate change, making it difficult to identify specific regions of the Arctic that may be most vulnerable to ecosystem shifts in the future.

Increasing the coverage of observations, in space and time, will help fill some of these gaps. Remotely sensed data from satellites, balloons, ships, aircraft, and underwater instruments have greatly improved our capability to monitor change in the Arctic, although the data have limitations in terms of resolution and applicability, and still need to be verified with on-site observations.

Some important needs relate to the difficulty of providing useful climate model projections at the local scale. The lack of local-level projections can impede efforts to develop adaptation strategies—especially in the case of permafrost, where impacts are influenced strongly by local topography and hydrology.

The reliability of future projections will be improved by reducing uncertainties related to factors such as the sensitivity of the Greenland ice sheet to climate change and the impacts of freshwater inflows on ocean processes. Other modeling-related challenges include capturing the effects of natural climate variability, which can obscure trends, and resolving differences across models' projected changes past mid-century. Despite these concerns, it is important to note that projections for the next several decades differ little across models or scenarios, and models do a generally good job of recreating past and current trends.

Recommended Action Steps

The key findings of SWIPA 2017 have implications for policy and planning in four broad areas:

Limit Future Change

Stabilizing Arctic warming and its associated impacts will require substantial near-term cuts in net global greenhouse gas emissions. Full implementation of the Paris Agreement under the United Nations Framework Convention on Climate Change

(UNFCCC) will cause Arctic temperatures to stabilize—at a higher level than today—in the latter half of this century. This will require much larger cuts in global greenhouse gas emissions than those planned under current nationally determined contributions to the fulfillment of the UNFCCC.

The Arctic states, permanent participants, and observers to the Arctic Council should individually and collectively lead global efforts for an early, ambitious, and full implementation of the Paris COP21 Agreement, including efforts to reduce emissions of short-lived climate forcers.

Raise Public Awareness of the Implications of Changes in the Arctic Cryosphere

Outreach and public sharing of information about Arctic climate change, its consequences, uncertainties, risks, adaptation options, and effects of emission reductions are key to informed governance and policy development.

The Arctic Council, permanent participants, and observers to the Council should prioritize informing and educating the public about observations, projections, and implications of Arctic climate change.

Adapt to Near-Term Impacts

The transformative changes underway in the Arctic will continue and in some cases accelerate until at least mid-century regardless of efforts to reduce emissions. Impacts from climate change are thus expected to intensify for at least the next three to four decades, creating a clear and urgent need for knowledge and strategies to help Arctic communities and global society adapt to new conditions and reduce vulnerabilities to expected impacts. Addressing major knowledge gaps will help ensure adaptation strategies are grounded in a solid understanding of potential impacts and interactions.

The Arctic Council and other international organizations should prioritize research and knowledge-building efforts leading to enhanced certainty in predictions of changes and their consequences at local to global scales, facilitating the development of effective adaptation responses to changes in the Arctic cryosphere.

Support the Advancement of Understanding

SWIPA 2017 demonstrates great advances in our understanding of changes in the Arctic cryosphere, but also reveals major knowledge gaps. It also identifies several unmet scientific goals and specific areas where more observations and research are needed. As awareness of Arctic climate change and its consequences has grown, a number of international organizations, such as the Intergovernmental Panel on Climate Change (IPCC), the World Meteorological Organization (WMO), and the International Council for Science (ICSU) through the International Arctic Science Committee (IASC), have become increasingly engaged in understanding the implications of Arctic change. Making advances in these areas will require international coordination; long-term commitments to funding; the application of traditional and local knowledge; engagement with stakeholders; and coordinated and enhanced observation networks.

The Arctic Council should continue its efforts to monitor, assess, and understand Arctic climate change and its implications. It should also support and interact with efforts of international organizations and conventions such as IPCC, WMO, the UNFCCC, and the Convention on Long-Range Transboundary Air Pollution (CLRTAP) to promote the inclusion of Arctic perspectives in their work.

1. Introduction

LEAD AUTHORS: **MORTEN S. OLSEN, JANET PAWLAK, LARS-OTTO REIERSEN, JASON E. BOX, JAMES OVERLAND, JOHN WALSH**

Coordinating lead authors shown in bold

Contents

1.1 Assessing climate-related changes in the Arctic cryosphere	2
1.2 Previous AMAP climate assessments and follow-up	2
1.2.1 Follow-up to SWIPA 2011	2
1.2.2 Aims of SWIPA 2017	2
1.3 An Arctic cryosphere assessment	4
1.3.1 Geographical delineation	4
1.3.2 What is the cryosphere?	4
1.3.3 Roles and relevance of the cryosphere	4
1.4 The SWIPA 2017 assessment process	5
1.5 What is in each chapter?	6
1.6 The situation in autumn–winter 2016	6
1.7 SWIPA 2017 and the Paris Agreement	6
1.8 Final comments	8
References	8

1.1 Assessing climate-related changes in the Arctic cryosphere

This report by the Arctic Monitoring and Assessment Programme (AMAP) presents the findings from its fourth scientific assessment of Arctic climate change and its regional and global consequences. Building on previous assessments, this updates trends in observations for Arctic climate change and concurrent changes to the Arctic cryosphere during the 2010–2016 period. The report synthesizes and assesses observations and scientific developments since 2010, and evaluates possible near- to mid-term (next few decades) trajectories and impacts for future snow, water, ice and permafrost conditions in the Arctic, and their potential impacts outside the Arctic within this century.

The SWIPA 2017 assessment had two overall aims.

- Update, synthesize and assess current knowledge on Arctic climate development and changes in the cryosphere since 2010.
- Establish pan-Arctic projections of future changes in the Arctic cryosphere as a baseline for, among others, the regional Arctic change assessments performed under the Arctic Council initiative *Adaptation Actions for a Changing Arctic* (AACa).

SWIPA 2017 focuses mainly on physical changes in the Arctic and its cryosphere, while contemporary and possible future effects of climate change and other drivers of change in Arctic ecosystems, ecosystem services and human wellbeing have been assessed in the AACa work (see Section 1.2.1).

1.2 Previous AMAP climate assessments and follow-up

Mandated by the Arctic Council to monitor and assess the state of the Arctic environment and climate, AMAP produced its first assessment of Arctic climate change and its impacts as part of the State of the Arctic Environment Report (AMAP, 1997, 1998). In this first assessment, AMAP pointed to studies suggesting that the Arctic would warm more than the global average and that warming would cause substantial changes in the Arctic cryosphere, which could in turn have major consequences for the Arctic as a whole and for its role in global climate.

The findings of the 1998 assessment led the Arctic Council to initiate an independent and comprehensive assessment of Arctic climate change and its impacts – the Arctic Climate Impact Assessment (ACIA). This was undertaken by AMAP in cooperation with the Arctic Council Working Group on the Conservation of Arctic Flora and Fauna (CAFF) and the International Arctic Science Committee (IASC). The resulting *Arctic Climate Impact Assessment* and its derivative *Impacts of a Warming Arctic* (ACIA, 2004, 2005) documented Arctic-wide warming and ongoing changes in Arctic snow, water and ice conditions that were impacting Arctic ecosystems and human living conditions. It also highlighted the potential global impacts of Arctic climate change. These reports showed that the Arctic climate was now warming rapidly, that much larger changes were projected, and that Arctic warming and its consequences have worldwide implications (ACIA, 2004, 2005).

With its findings of fundamental and ongoing Arctic climate change and the regional and global implications of this, the ACIA was an eye-opener for Arctic and global societies, drawing attention to the regional and global challenges and opportunities arising from climate change and the associated shifts in Arctic snow, water and ice conditions.

Focusing on climate-related changes in the Arctic cryosphere, AMAP published its third Arctic climate assessment in 2011: *Snow, Water, Ice and Permafrost in the Arctic (SWIPA): Climate Change and the Cryosphere*. Building on and up-dating the findings of ACIA, the observations reported in the SWIPA 2011 assessment (AMAP, 2011) confirmed that accelerated change and rapid Arctic warming are occurring in the Arctic cryosphere, corroborating the findings of ACIA. These changes in the cryosphere were found to cause fundamental changes in the Arctic ecosystems, which will have important implications for Arctic livelihoods and living conditions. The SWIPA 2011 assessment highlighted regional and global-scale climatic feedbacks caused by changes in the Arctic cryosphere and the cascading climate change impacts, while recognizing that climate change is not the only the only driver of change in the Arctic (see Box 1.1).

1.2.1 Follow-up to SWIPA 2011

The findings and recommendations from SWIPA 2011 were reflected in the Arctic Council Nuuk Declaration (Arctic Council, 2011), in which Ministers representing the eight Arctic States “note with concern the accelerated change in major components of the cryosphere and the profound local, regional and global effects of observed and expected changes, emphasize the need for forward looking Arctic cooperation with a view to increase Arctic resilience and to enhance Arctic Council leadership to minimize the human and environmental impacts of climate change...”

Two major initiatives were launched to follow up on the concerns expressed in the Nuuk Declaration. One was the Arctic Resilience Assessment work carried out by the Stockholm Environment Institute and the Stockholm Resilience Center (Arctic Council, 2016), and the other was the Adaptation Actions for a Changing Arctic (AACa) process led by AMAP (see Box 1.2). The AACa assessments provide parallel, complementary information to SWIPA 2017 and cover the impacts of climate change and other stressors on the ecosystem services, human societies and socio-economic conditions of several regions in the Arctic. Both initiatives are science-based assessments that aim to better understand the integrated impacts of change in the Arctic, but have different end-goals and so use different methodologies to reach them.

Rising atmospheric concentrations of carbon dioxide (CO₂) are also the cause of ocean acidification in the Arctic and elsewhere, and AMAP has initiated an update of its 2013 report on Arctic Ocean Acidification (AMAP, 2013). This update is planned for release in 2018.

1.2.2 Aims of SWIPA 2017

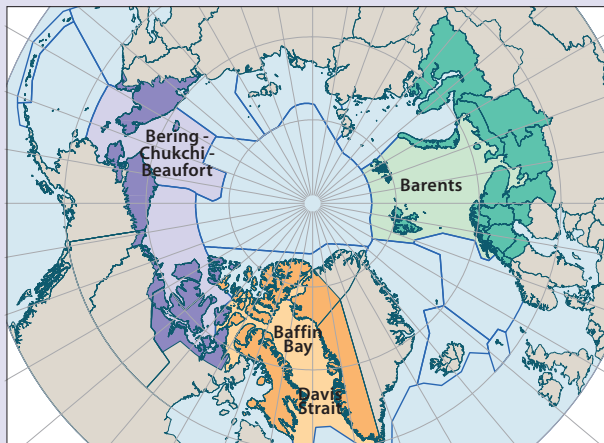
The objectives of the SWIPA 2017 assessment are to provide the Arctic Council with timely, up-to-date, and synthesized scientific knowledge about the present status, processes, trends,

Box 1.1 Key findings from SWIPA 2011

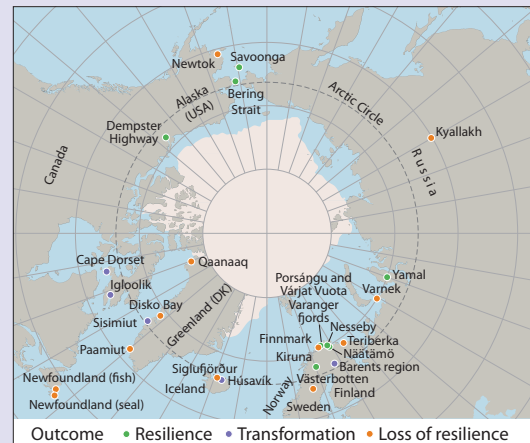
1. The past six years (2005–2010) have been the warmest period ever recorded in the Arctic. Higher surface air temperatures are driving changes in the cryosphere.
2. There is evidence that two components of the Arctic cryosphere – snow and sea ice – are interacting with the climate system to accelerate warming.
3. The extent and duration of snow cover and sea ice have decreased across the Arctic. Temperatures in the permafrost have risen by up to 2°C. The southern limit of permafrost has moved northward in Russia and Canada.
4. The largest and most permanent bodies of ice in the Arctic – multi-year sea ice, mountain glaciers, ice caps and the Greenland ice sheet – have all been declining faster since 2000 than they did in the previous decade.
5. Model projections reported by the Intergovernmental Panel on Climate Change (IPCC) in 2007 underestimated the rates of change now observed in sea ice.
6. Maximum snow depth is expected to increase over many areas by 2050, with greatest increases over Siberia. Despite this, average snow cover duration is projected to decline by up to 20% by 2050.
7. The Arctic Ocean is projected to become nearly ice-free in summer within this century, likely within the next thirty to forty years.
8. Changes in the cryosphere cause fundamental changes to the characteristics of Arctic ecosystems and in some cases loss of entire habitats. This has consequences for people who receive benefits from Arctic ecosystems.
9. The observed and expected future changes to the Arctic cryosphere impact Arctic society on many levels. There are challenges, particularly for local communities and traditional ways of life. There are also new opportunities.
10. Transport options and access to resources are radically changed by differences in the distribution and seasonal occurrence of snow, water, ice and permafrost in the Arctic. This affects both daily living and commercial activities.
11. Arctic infrastructure faces increased risks of damage due to changes in the cryosphere, particularly the loss of permafrost and land-fast sea ice.
12. Loss of ice and snow in the Arctic enhances climate warming by increasing absorption of the sun's energy at the surface of the planet. It could also dramatically increase emissions of carbon dioxide and methane and change large-scale ocean currents. The combined outcome of these effects is not yet known.
13. Arctic glaciers, ice caps and the Greenland ice sheet contributed over 40% of the global sea level rise of around 3 mm per year observed between 2003 and 2008. In the future, global sea level is projected to rise by 0.9–1.6 m by 2100 and Arctic ice loss will make a substantial contribution to this.
14. Everyone who lives, works or does business in the Arctic will need to adapt to changes in the cryosphere. Adaptation also requires leadership from governments and international bodies, and increased investment in infrastructure.
15. There remains a great deal of uncertainty about how fast the Arctic cryosphere will change in the future and what the ultimate impacts of the changes will be. Interactions ('feedbacks') between elements of the cryosphere and climate system are particularly uncertain. Concerted monitoring and research is needed to reduce this uncertainty.

Box 1.2 Adaptation Actions for a Changing Arctic and the Arctic Resilience Assessment

Adaptation Actions for a Changing Arctic: Seeks to inform adaptation actions based on assessments of drivers of change and resultant impacts in the Barents area (AMAP, 2017a), the Baffin Bay / Davis Strait region (AMAP, 2017b), and the Beaufort-Chukchi-Bering region (AMAP, 2017c).



Arctic Resilience Assessment: Seeks to evaluate pan-Arctic strategies for communities and governments to adapt based on case studies of socio-ecological systems, and identification of potential shocks and large shifts in ecosystem services affecting human well-being (Arctic Council, 2016).



and future consequences of Arctic climate change and its effects on Arctic snow, water, ice and permafrost conditions. Cryospheric change and variability are fundamentally linked to climate change and climate variability.

Global climate models use mathematical formulations of atmospheric behavior to simulate climate. These models reproduce historical climate variations with considerable success, and so are used to simulate future climate under various scenarios of greenhouse gas emissions. These simulations of possible future conditions are driven by different atmospheric greenhouse gas concentration trajectories (known as Representative Concentration Pathways or RCPs), which provide a means to examine how future climate could be affected by differences in climate policy scenarios and greenhouse gas emissions. These scenarios of future atmospheric greenhouse gas concentrations used to drive global climate models have been employed to estimate future trajectories in Arctic temperature and their impacts on major components of the Arctic cryosphere (snow, permafrost, sea ice, land-based ice), establishing pan-Arctic projections. SWIPA 2017 has relied on the global scenarios and climate projections of the Fifth IPCC Assessment Report (IPCC, 2013, 2014a,b) as the 'climate framework' for developing the SWIPA 2017 assessment. The IPCC projections have been used in comparisons of effects on parts of the Arctic cryosphere for different greenhouse gas concentration trajectories (see Section 1.7) in this assessment, as well as in the concurrent Arctic Council AAC project.

The SWIPA 2011 assessment constitutes the benchmark for the present assessment. Due to the concurrent assessment activities, the SWIPA 2017 assessment focuses on large-scale changes and their potential consequences. Recent updated analyses of the impacts of climate change and other changes in the Arctic on ecosystems, ecosystem services, socio-economics and human well-being can be found in the Arctic Resilience report (Arctic Council, 2016) and the reports from the AAC project (AMAP, 2017a,b,c).

1.3 An Arctic cryosphere assessment

1.3.1 Geographical delineation

The geographical delineation of the Arctic as used in the SWIPA assessment is based on that adopted by AMAP (Figure 1.1). The 'AMAP area' essentially includes the terrestrial and marine areas north of the Arctic Circle ($66^{\circ}32'N$), and north of $62^{\circ}N$ in Asia and $60^{\circ}N$ in North America, modified to include the marine areas north of the Aleutian chain, Hudson Bay, and parts of the North Atlantic Ocean including the Labrador Sea. However, for certain chapters there may have been some deviation from this delineation depending on the cryosphere component covered.

1.3.2 What is the cryosphere?

Water in its frozen state is a defining aspect of polar and high altitude regions of the globe, and depending on its form, origin, location and longevity, it constitutes the different components of the cryosphere dealt with in this assessment. In the Arctic, the various components of the cryosphere include the following: snow, including solid precipitation; permafrost (i.e. soil that remains at or below $0^{\circ}C$ for two or more consecutive years), present in terrestrial and sub-sea marine environments; river

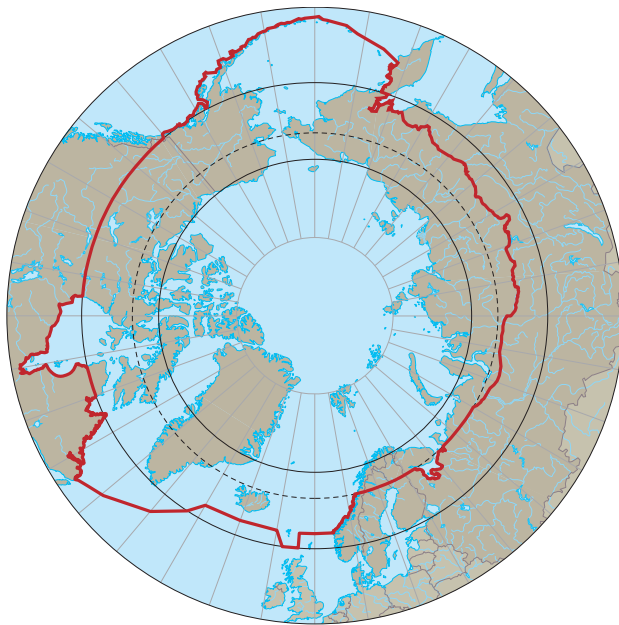


Figure 1.1 The Arctic, as defined by AMAP and as used in this assessment.

and lake ice; mountain glaciers and ice caps; the Greenland ice sheet; and sea ice in all its forms (i.e. multi-year ice, first-year ice, and land-fast ice) (Figure 1.2). These cryospheric components represent a globally unique system, parts of which are inextricably linked with each other, with the landscapes, seascapes, ecosystems and humans in the Arctic, and with the global climate and ecological systems themselves. As the Arctic warms, the temporal and spatial distribution of those cryospheric components that represent the solid (frozen) state of water change, and so does the distribution of water in its liquid and gaseous forms. Consequently, shifts in the Arctic cryosphere are also closely tied to shifts in the Arctic hydrosphere, and changes in the Arctic cryosphere (and the temporal and spatial distribution of water in its different states) have great significance, not just for the Arctic, but for the planet as a whole.

1.3.3 Roles and relevance of the cryosphere

Whereas division of the cryosphere into major categories such as snow, ice and permafrost may be useful for oversight and for practical linguistic purposes, it must be acknowledged that such an approach also entails a simplification. A simplification that is not able to capture the different properties of the specific components and interactions between the different parts of the cryosphere, or the different roles that the components play in the Arctic ecosystems and thus the services provided to humans by the systems. Something that is reflected in Arctic indigenous languages, where specific words precisely describe different forms of snow and ice based on their properties and relationship to ecosystem services.

For the millions of inhabitants in the Arctic region, snow, snow-drifts, lakes and rivers with solidly frozen ice layers, ice caps and mountain glaciers, sea ice, icebergs, permafrost, etc., constitute important parts of the physical environment that impede some human activities, while making others possible.

The cryosphere is a fundamental regulator or controller of local and regional climate, and global climate. Heat from the warmer lower latitudes is transported by ocean currents and the

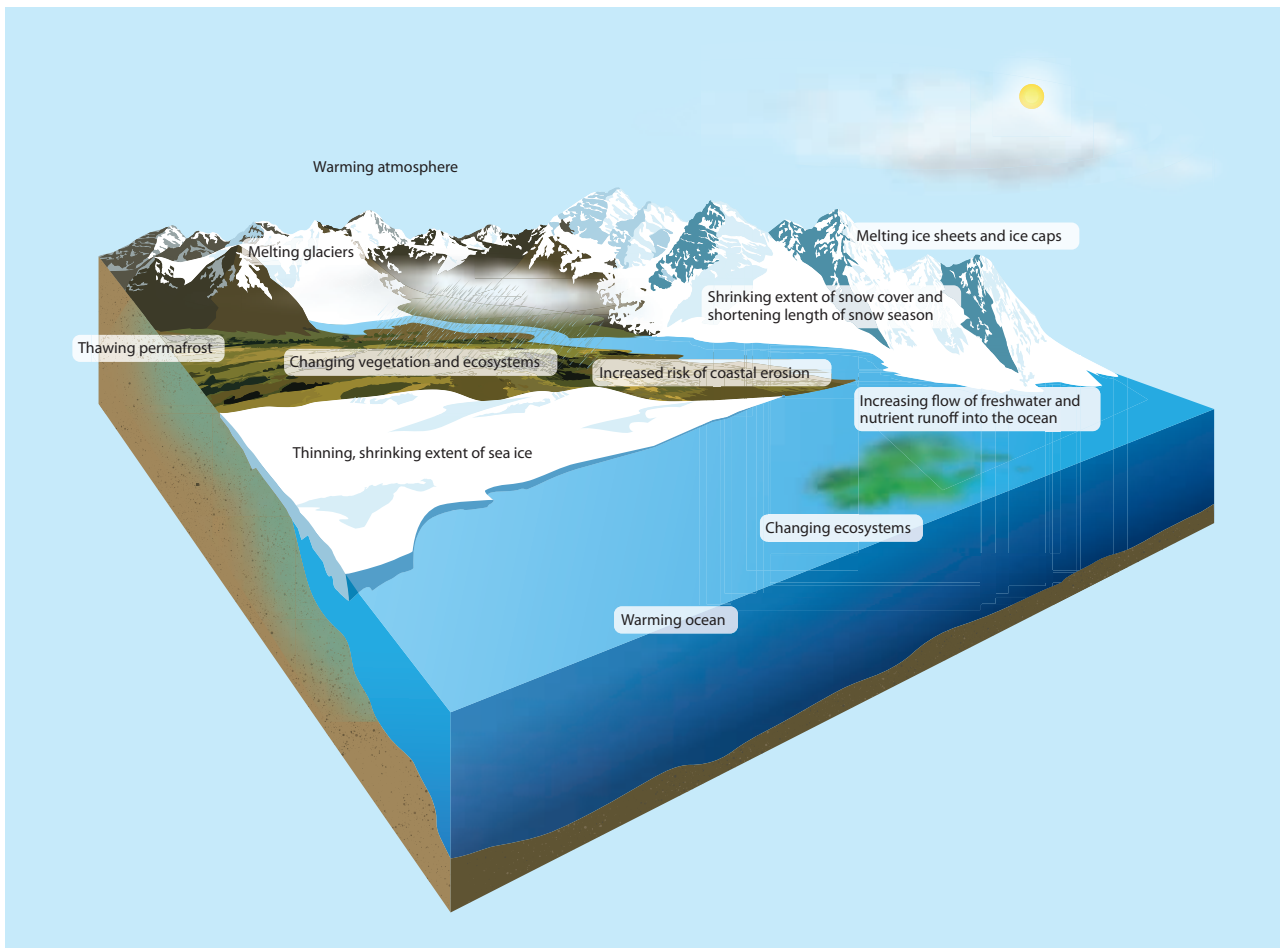


Figure 1.2 Schematic representation of major observed changes in the Arctic caused by global warming (graphic adapted from an image created by the U.S. National Center for Atmospheric Research).

atmosphere to the Arctic, where air and water masses are cooled and then returned to southern latitudes as cold air outbreaks and cold ocean currents. The properties of the cold sink enable heat transfer northward (thus cooling more southerly source regions) and with that, the physical transport of atmospheric and water constituents (i.e. gases, freshwater, seawater). The Arctic also cools the Earth by its snow- and ice-covered surfaces reflecting radiation back into space (termed the albedo effect).

Over time, cycles of summer vegetation growth and subsequent slow winter decomposition have resulted in a capture of atmospheric CO₂ in organic matter in soil, accumulating in large carbon sinks in Arctic permafrost soils, some of which are sub-sea.

Since the 1980s, a diminishing of the Arctic cryosphere has been observed. Put simply, there has been a downward trend in the proportion of Arctic water frozen at any given time, and the timing of the melt-freeze cycle has changed. This has driven corresponding changes in the spatial and temporal distribution of liquid water and water vapor, implying major changes in the physical and chemical environment of the Arctic, a shift in conditions for living species, and potentially altering the role of the Arctic in the global system.

1.4 The SWIPA 2017 assessment process

The SWIPA 2017 assessment involved over 90 scientists and experts from Arctic and non-Arctic countries. All were

nominated by countries and relevant international bodies and selected on the basis of scientific qualifications by appointed convening lead authors. These experts were charged with compiling and evaluating information from Arctic monitoring networks and recent national and international research activities.

Each chapter was drafted by experts covering relevant expertise from different scientific disciplines and geographical areas. A SWIPA assessment lead authors group, comprising the coordinating lead authors for each chapter was responsible for the organization and accuracy of the assessment.

This assessment report is fully-referenced and peer reviewed. The assessment is based on the peer-reviewed scientific literature or on new results obtained using well-documented observational methods and models. The peer-reviewed observations, methods, and studies used in the assessment in many cases include contributions from indigenous, traditional and local knowledge; it is recognized that this approach does not necessarily capture all relevant knowledge held by indigenous and local communities.

Chapter authors have followed recommendations to promote the use of common terminology as far as possible. This included use of terminology associated with probability statements where discussion of future events and conditions need to take into account the likelihood that these conditions or events will occur. To ensure consistency of the summarized material, the procedures used by ACIA and SWIPA 2011 (as

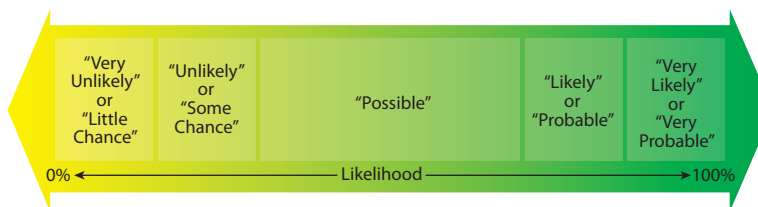


Figure 1.3 Five-tier lexicon describing the likelihood of expected change.

refined from those of the IPCC) were used throughout this report (see Figure 1.3).

Statements regarding the likelihood that particular events or conditions will occur reflect expert evaluation of peer-reviewed results, typically from multiple lines of evidence.

The statements and assessments presented in this report were subject to a comprehensive review process, which also involved national experts that contributed data and information to the assessment. These national experts verified that the interpretation of their data was correct and acceptable to the primary sources. A rule-based, independent international peer review process was established by AMAP to secure and document the integrity of the process (see the Preface for further details of the review process). Documentation of the results of the peer review process applied to the SWIPA assessment is available on the AMAP website: www.apmap.no.

1.5 What is in each chapter?

The report comprises four parts. The first (this chapter and Chapter 2) introduces and defines the scope of the assessment; it presents background climate information and summarizes recent Arctic changes to establish a framework for further assessment of Arctic cryospheric change. The second (Chapters 3 to 6) describes the physical and other aspects of individual components of the Arctic cryosphere, including discussion of the impacts. The third (Chapters 7 to 10) focuses on cross-cutting issues of importance at the global and regional levels. The last (Chapter 11) contains a synthesis of the preceding chapters, providing a summary of the observations and projections as well as the implications of these findings. This chapter presents a review and assessment of some of the major consequences of changes in the physical components and states of the Arctic cryosphere based on progress in understanding the complex interactions in the overall Arctic system.

Recent observations of Arctic climate development are assessed in Chapter 2, which also summarizes and analyzes results of climate model outcomes for northern latitudes and discusses the treatment of 'Arctic amplification' in global circulation models. Thus, Chapter 2 presents an overview of past, present and projected future climate.

The current status and climate impacts on the components of the Arctic cryosphere are described in the next four chapters. Chapter 3 describes the terrestrial snow component, focusing on climate-related spatial, interannual and seasonal variations, and changes in snow-cover extent and depth and snow properties. Changes in permafrost conditions in different regions of the Arctic are described in Chapter 4, together with the consequences of these changes and disturbances for the terrestrial environment. In Chapter 5, recent changes in Arctic sea-ice extent, thickness and duration are described together with some of the implications of the extended period of open

water for Arctic biota, biological productivity, and biodiversity. Changes in Arctic land-based ice bodies, including mountain glaciers, ice caps and particularly the Greenland ice sheet, are reported in Chapter 6.

Based on the findings of the joint IASC/CliC/AMAP Arctic Freshwater Synthesis (Prowse et al., 2015), Chapter 7 is devoted to an assessment of changes in the temporal and spatial distribution of the liquid and gaseous states of water in the Arctic. This chapter assesses the various Arctic freshwater sources, fluxes, storage and effects, most of which are directly or indirectly controlled by cryospheric components and processes.

Chapter 8 synthesizes observations and recent scientific progress in understanding the effects of climate change (and resultant changes in the Arctic cryosphere) on Arctic carbon cycling in marine and terrestrial environments, and assesses possible consequences of cryospheric change. Chapter 9 presents an assessment of future global sea-level rise under different greenhouse gas scenarios based on estimated future Arctic land ice contributions. Chapter 10 presents integrated assessments of cross-cutting scientific issues that affect or are affected by components of the cryosphere. Subsections include: an assessment of thresholds and the potential irreversibility of changes in the Arctic; an examination of Arctic tundra vegetation greening and browning in relation to snow, water, ice, and permafrost; an assessment of physical disturbance in Arctic terrestrial ecosystems and a synthesis of effects of changes in precipitation. The topics presented in Chapter 10 were selected by the lead authors of the assessment report as important supplements to the cross-cutting issues dealt with in Chapters 7, 8 and 9.

Finally, Chapter 11 presents an integrated synthesis of the findings presented in the preceding chapters, together with the conclusions and recommendations arising from the assessment as a whole.

1.6 The situation in autumn–winter 2016

Owing to the timing and scientific nature of the SWIPA 2017 assessment, the effective cut-off date for material to be included in the assessment was mid-2016; hence, a full assessment of conditions during late 2016 was not possible. However, owing to the magnitude and importance of some 2016 observations, important new data are summarized in Box 1.3.

1.7 SWIPA 2017 and the Paris Agreement

The SWIPA 2017 assessment primarily used two atmospheric greenhouse gas concentration pathways to evaluate future developments of Arctic climate, snow, permafrost, sea- and land-based ice conditions and sea level. These pathways represent two of the so-called Representative Concentration Pathways (RCPs) which are foundational for modelling efforts performed under the IPCC: namely, RCP4.5 and RCP8.5.

Box 1.3 Arctic extremes continued into autumn–early winter 2016

As was the case in January through March 2016 (see Section 2.1.1), near-surface air temperature extremes recurred during autumn–early winter 2016 (October through December, Figure 1.4). Such extremes show clear examples of amplifying feedbacks between warm winds and the formation of sea ice. The Arctic air temperature extremes were nearly double ($+6^{\circ}\text{C}$) those of the previous monthly maximums. Throughout autumn–early winter, warm air traveling north originated in eastern Siberia and the North Atlantic. This transport of warm air delayed sea-ice freeze-up in the Chukchi and Kara Seas (see Figure 1.5) that in turn allowed the warm air to advance further toward the North Pole.

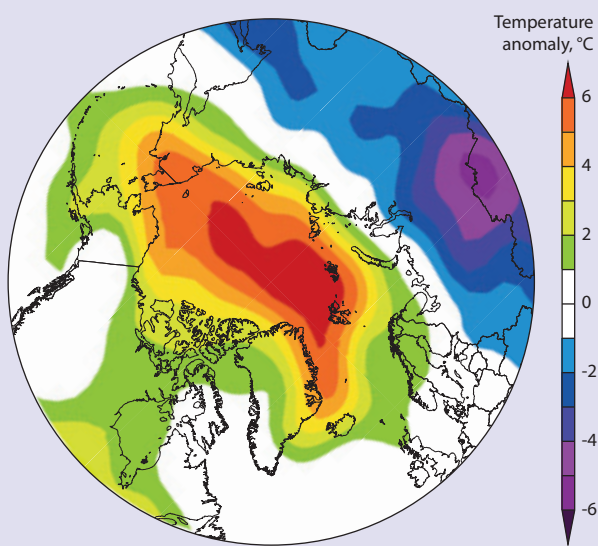


Figure 1.4 Air temperature anomalies October through December 2016 relative to the 1981–2010 baseline.

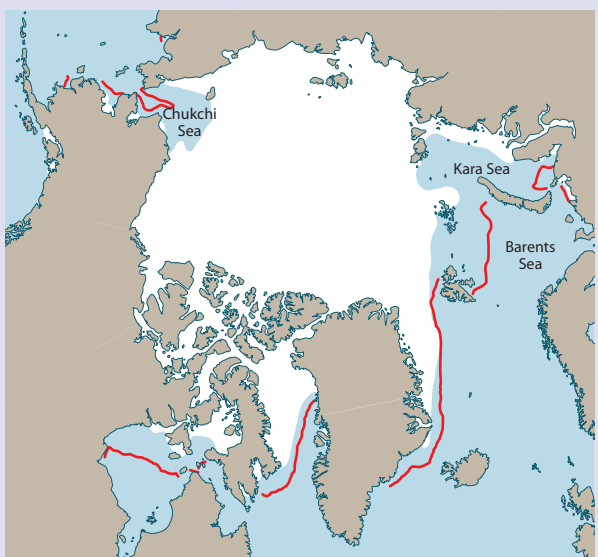


Figure 1.5 Sea-ice extent in November 2016. Red lines show the median climatological ice edge position for the period 1981–2010. Note, in particular the November 2016 sea ice-free regions in the Chukchi Sea to the northwest of Alaska and in the Barents and Kara Seas to the north of western Russia.

Box 1.4 The Paris Agreement

At the 21st Conference of the Parties (COP21) to the United Nations Framework Convention on Climate Change (UNFCCC) in December 2015, the Parties reached consensus on an agreement for how to enhance the implementation of the Convention. What has come to be known as the ‘Paris Agreement’ entered into effect in November 2016 when its ratification criteria were met.

The aim of the Paris Agreement is to strengthen the global response to the threats of climate change, with a central aim to hold the increase in global average temperature to well below 2°C above pre-industrial levels as well as to pursue efforts to limit the temperature increase to 1.5°C above pre-industrial levels. Furthermore, the agreement aims to strengthen adaptation efforts by providing continued and enhanced international support to developing countries for climate-related adaptation measures.

The Paris Agreement requires all Parties to the Convention to report their best efforts through ‘nationally determined contributions’ (NDCs) and to strengthen these efforts in the years ahead; this includes requirements that all Parties report regularly on their emissions and on their efforts to reduce emissions.

The IPCC is currently preparing two special reports related to SWIPA 2017, one due in 2018 on the impacts of global warming of 1.5°C above pre-industrial levels and related global greenhouse gas emission pathways, and the other planned for 2019 on climate change and oceans and the cryosphere. AMAP intends to facilitate Arctic contributions and perspectives to both of these efforts.

In the RCP4.5 scenario, carbon emissions peak around mid-century and atmospheric CO_2 concentrations stabilize around 2100 at about 25% above present levels. Under the RCP4.5 scenario, global temperatures relative to pre-industrial levels are projected to rise by a likely range of $1.5\text{--}2.6^{\circ}\text{C}$ by mid-century and approach $2.4\pm0.7^{\circ}\text{C}$ at the end of the century. The RCP8.5 scenario, which present-day emissions follow most closely, assumes little additional mitigation actions through 2100; it is essentially a business-as-usual scenario. Carbon dioxide concentrations are projected to be more than double their present values by 2100, and the corresponding projected increase in temperature is a non-stabilized global mean temperature (relative to pre-industrial levels) of $4.3\pm1.1^{\circ}\text{C}$ by 2090. Although temperature increases for both scenarios tend to follow the same general path in the near-term (decades), by mid-century projected temperatures begin to be higher for RCP8.5 ($2.0\text{--}3.2^{\circ}\text{C}$) than for the RCP4.5 ($1.5\text{--}2.6^{\circ}\text{C}$).

While the global mean temperature rise projected under RCP4.5 is almost compliant with the aims of the Paris Agreement at the maximum rather than target level (see Box 1.4), a comparison of results from models forced by the RCP4.5 and RCP8.5 greenhouse gas concentrations provide clear indications of how and when the Arctic cryosphere would respond to a mitigation scenario (i.e. RCP4.5), as opposed to a business-as-usual scenario (i.e. RCP8.5).

Even if global temperature were to stabilize near 2.0°C , Arctic temperatures would increase to nearly double that value, with large local and distant ecological and societal impacts.

1.8 Final comments

The SWIPA 2017 lead authors group considers that the aims of SWIPA 2017 have been met. New data and insights from the 2010–2015 period, preliminary data from 2016, and qualitative interpretations of model projections show that the Arctic cryosphere continues to move into uncharted territory, and this is expected to continue.

Based on this assessment report, a SWIPA 2017 Summary for Policymakers was prepared by AMAP and presented to the Arctic Council Ministers at their meeting in Fairbanks, Alaska in May 2017 (included at the start of the present report). This summary report contains an overview of the main findings of SWIPA 2017 presented in non-technical language, as well as scientifically based policy-relevant recommendations. The present report provides the scientific basis for statements made in the summary for policymakers, as confirmed by the lead authors.

References

ACIA, 2004. Impacts of a Warming Arctic: Arctic Climate Impact Assessment. Cambridge University Press.

ACIA, 2005. Arctic Climate Impact Assessment: Scientific Report. Cambridge University Press.

AMAP, 1997. Arctic Pollution Issues: a State of the Arctic Environment Report. Arctic Monitoring and Assessment Programme (AMAP), Oslo, Norway.

AMAP, 1998. The AMAP Assessment Report: Arctic Pollution Issues. Arctic Monitoring and Assessment Programme, (AMAP), Oslo, Norway.

AMAP, 2011. Snow, Water, Ice and Permafrost in the Arctic (SWIPA): Climate Change and the Cryosphere. Arctic Monitoring and Assessment Programme (AMAP), Oslo, Norway.

AMAP, 2013. AMAP Assessment 2013: Arctic Ocean Acidification. Arctic Monitoring and Assessment Programme (AMAP), Oslo, Norway.

AMAP, 2017a. Adaptation Actions for a Changing Arctic: Perspectives from the Barents Area. Arctic Monitoring and Assessment Programme, (AMAP), Oslo, Norway.

AMAP, 2017b. Adaptation Actions for a Changing Arctic: Perspectives from the Baffin Bay / Davis Strait Region. Arctic Monitoring and Assessment Programme, (AMAP), Oslo, Norway.

AMAP, 2017c. Adaptation Actions for a Changing Arctic: Perspectives from the Bering, Chukchi, Beaufort Region. Arctic Monitoring and Assessment Programme, (AMAP), Oslo, Norway.

Arctic Council, 2011. Nuuk Declaration. The Seventh Meeting of the Arctic Council, May 12, 2011. Nuuk, Greenland. <https://oarchive.arctic-council.org/handle/11374/92>

Arctic Council, 2016. Arctic Resilience Report. Carson, M. and G. Peterson (eds.). Stockholm Environment Institute and Stockholm Resilience Centre, Stockholm.

IPCC, 2013. Climate Change 2013: The Physical Science Basis. Contribution of Working Group I to the Fifth Assessment Report of the Intergovernmental Panel on Climate Change. Stocker, T.F., D. Qin, G.-K. Plattner, M. Tignor, S.K. Allen, J. Boschung, A. Nauels, Y. Xia, V. Bex and P.M. Midgley (eds.). Cambridge University Press.

IPCC, 2014a. Climate Change 2014: Impacts, Adaptation, and Vulnerability. Part A: Global and Sectoral Aspects. Contribution of Working Group II to the Fifth Assessment Report of the Intergovernmental Panel on Climate Change. Field, C.B., V.R. Barros, D.J. Dokken, K.J. Mach, M.D. Mastrandrea, T.E. Bilir, M. Chatterjee, K.L. Ebi, Y.O. Estrada, R.C. Genova, B. Girma, E.S. Kissel, A.N. Levy, S. MacCracken, P.R. Mastrandrea and L.L. White (eds.). Cambridge University Press.

IPCC, 2014b. Climate Change 2014: Mitigation of Climate Change. Contribution of Working Group III to the Fifth Assessment Report of the Intergovernmental Panel on Climate Change. Edenhofer, O., R. Pichs-Madruga, Y. Sokona, E. Farahani, S. Kadner, K. Seyboth, A. Adler, I. Baum, S. Brunner, P. Eickemeier, B. Kriemann, J. Savolainen, S. Schlömer, C. von Stechow, T. Zwickel and J.C. Minx (eds.). Cambridge University Press.

Prowse, T., A. Bring, J. Mård and E. Carmack, 2015. Arctic freshwater synthesis: Introduction [Special issue]. *Journal of Geophysical Research: Biogeosciences*, 120, 2121–2131.

2. Trends and feedbacks

LEAD AUTHORS: JAMES OVERLAND, JOHN WALSH, VLADIMIR KATTSOV

Contents

Key Findings	10
2.1 Recent Arctic changes	10
2.1.1 System components	10
2.1.2 Changes in extremes	15
2.2 Attribution and feedback processes	16
2.3 Potential Arctic and mid-latitude weather linkages	16
2.4 Projections of future changes	17
2.4.1 Projected changes in temperature	19
2.4.2 Projections for other variables	20
2.5 Summary	20
References	21

Key Findings

- Multiple lines of evidence show a continuing shift in the climate state of the Arctic, forced by increases in atmospheric levels of carbon dioxide (CO_2) and other greenhouse gases (GHGs). Changes include a shift from mostly multi-year to first-year sea ice, loss of late spring snow, thawing permafrost, biome changes, and record warm winter temperatures. Even several random cold years are unlikely to change the long-term trends, yet there is no evidence for an internally caused tipping point of rapid change.
- Given the projected increase in GHG concentrations over the next two decades, it is likely that average autumn and winter Arctic temperatures will increase by 4°C by 2040, and an essentially sea-ice-free late summer Arctic is a distinct possibility within the coming decades. This expected temperature increase is more than double that projected for the northern hemisphere. Whether temperatures stabilize in the latter half of the 21st century depends on new climate mitigation efforts.
- The past five years (2011–2015) have been the warmest of the instrumental record. January/April 2016 showed extreme Arctic-wide temperatures; January was 5°C above 1981–2010 average values, 2°C greater than the previous record. Regional and temporal variability in temperature will remain large, and when combined with the long-term trend, will increase the frequency of regional warm events that are unprecedented in the instrumental record.
- A major change is the loss of sea-ice volume in the past decade. Sea-ice thickness in the central Arctic Ocean declined from an average of 3.6 m to 1.3 m between 1975 and 2012. The nine lowest sea-ice extents have occurred in the past nine years (2007–2015).
- Greenland has been prone to rapid melting events in individual years based on the location of supporting weather patterns.
- There is emerging evidence that Arctic warming impacts mid-latitude weather, especially during winter in eastern Asia. However, such impacts are masked by internal variability and remain an active subject of research.

2.1 Recent Arctic changes

Confirmation of ongoing and future projections of Arctic change continues, and the changes are pervasive. The Arctic has continued to warm and the various components of the cryosphere are diminishing. This chapter summarizes multiple lines of evidence of interacting processes that serve as an indicator for the overall change. Subsequent chapters discuss cryospheric elements in detail. Since the previous SWIPA assessment (AMAP, 2011), new information has reinforced self-consistent, interlocking evidence of continuing rapid changes across lengthening, diverse Arctic data sets. There is evidence that global drivers of increased levels of atmospheric anthropogenic carbon dioxide (CO_2) and other greenhouse gases (GHGs) play a role in forcing large changes in the Arctic system through a set of Arctic-unique amplification processes and feedbacks (Notz and Stroeve, 2016). Understanding of feedbacks is advancing with research based on observational data and models.

There is emerging evidence that the Arctic influences the globe through changes in the northern hemisphere heat sink, Greenland ice loss and sea-level rise, and connections to mid-latitude weather. These have become active areas of research since the previous SWIPA assessment (AMAP, 2011).

This assessment shows increased confirmation that the Arctic is now considerably different from the Arctic of the late 20th century. Chapter 2 considers the Arctic system as a whole and addresses consilience: when multiple sources of evidence are in agreement, conclusions can lead to scientific consensus even when individual sources of evidence are less conclusive on their own. New thresholds since the previous SWIPA assessment (conducted 2008–2011) are established when a time series representing Arctic processes obtains new record values. These thresholds can be from trends (e.g. continuous change like increasing temperatures or declining spring snow cover) or as a regime shift when there is a qualitative change in the structure of the basic system, such as transitions from multi-year to first-year sea ice and coniferous to deciduous boreal forests. There are clear irreversible changes such as permafrost thaw and coastal melting of the Greenland Ice Sheet. Current evidence for a tipping point (a run-away condition based on internal climate physics) is not seen. Section 10.2 does discuss potential tipping points at other times such as abrupt warming and cooling during the previous glacial period (13,000 years BP) and for the late 21st century.

Based on new Arctic data and analyses, SWIPA 2017 confirms the Intergovernmental Panel on Climate Change (IPCC) in its latest assessment, “*Warming of the climate system is unequivocal, and since the 1950s, many of the observed changes are unprecedented over decades to millennia... It is extremely likely (95–100% probability) that human influence has been the dominant cause of the observed warming since the mid-20th century.*” (IPCC, 2013), and provides a basis for further global assessment.

2.1.1 System components

The Arctic has warmed at more than twice the global rate over the past 50 years. Arctic amplification of temperature is apparent in Figure 2.1, which shows the spatial pattern of temperature increase in the cold and warm seasons. The greatest increase of more than 2°C since 1960 occurred

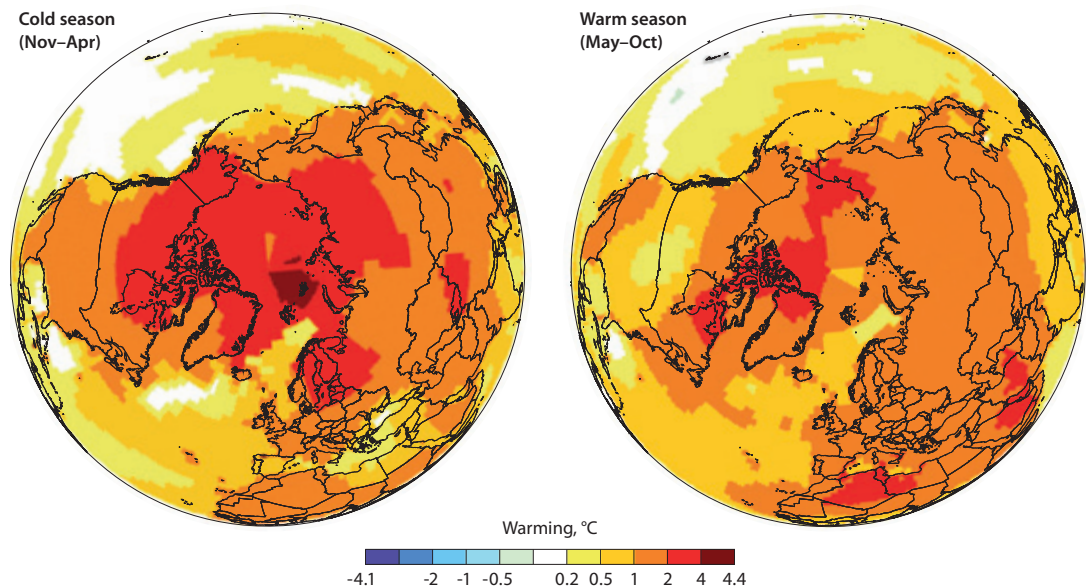


Figure 2.1 Spatial pattern of Arctic warming for the period 1961–2014 in the cold season (Nov–Apr) and warm season (May–Oct) (NASA GISTEMP <http://data.giss.nasa.gov/gistemp/maps/>).

during the cold season. The differential warming of the Arctic has become even more apparent over the past two decades, when the rate of global temperature rise underwent a decadal-scale slowdown (Figure 2.2), related to generally cool conditions in the North Pacific (Trenberth and Fasullo, 2013; Kosaka and Xie, 2014). This Pacific influence has reversed since 2014, as global temperatures have increased with the return of warm ocean temperatures in the tropical and northeastern Pacific Ocean.

While the Arctic has warmed more than the rest of the globe in recent decades, variability in space and time is also large. Observed spatial features of temperature change are largely governed by changes in atmospheric circulation patterns, which may either enhance or compensate the effect of the anthropogenic radiative forcing. For example, central and eastern Siberia show cooling for winter (DJF) from 1990 through 2013 (Cohen et al., 2014; Kug et al., 2015). In January and February 2016, the central Arctic exhibited extreme warm

months (Overland and Wang, 2016). January anomalies were 5°C north of 66°N, 2°C greater than the previous maximum January anomaly, based on the average of four reanalysis products (anomaly baseline 1981–2010). Several regions had anomalies over 7°C (Figure 2.3). Such extremes were due to ongoing Arctic amplification and warm air advection from mid-latitudes; note the southerly winds (orange) extending towards the very high latitudes (Figure 2.3). In terms of the ability of regions to adapt, differences between rates of change in different Arctic regions can be as important as the magnitude of change.

The Arctic warmed at a greater rate than the global mean in the early 20th century and cooled at a greater rate in the mid-20th century. Figure 2.4 shows the contribution of natural variability and GHG contributions to Arctic temperature trends during three periods of the 20th century. Natural variability made a positive contribution before 1939, but opposed the emerging GHG contribution during the mid-20th century (Fyfe et al., 2013). In the last third of the century, GHG is the dominant contributor to warming. The Atlantic Multidecadal Oscillation can also influence Arctic temperature variability (Kravtsov et al., 2014; Miles et al., 2014).

Updating the findings of the previous SWIPA assessment (AMAP, 2011), it is now clear that (1) the Arctic has been warmer over the past five years (2011–2015) than at any time since 1900, (2) the recent (post-1998) ‘hiatus’ in global warming (red curve in Figure 2.2) is less evident in the Arctic, and (3) an anthropogenic warming signal has emerged in the Arctic (Figure 2.4; also see Hawkins and Sutton, 2012).

While changes in sea ice and snow cover can be considered as impacts of climate change, the role of these changes in the albedo-temperature feedback also makes them agents of change (Chapters 3 and 5). The recent decline in Arctic sea-ice extent is well documented and has been highlighted as a key indicator of global change. The nine lowest September minima of the satellite record are the nine most recent years. Winter 2015/2016 had the lowest amount of sea-ice area at maximum extent for the period back to 1979.

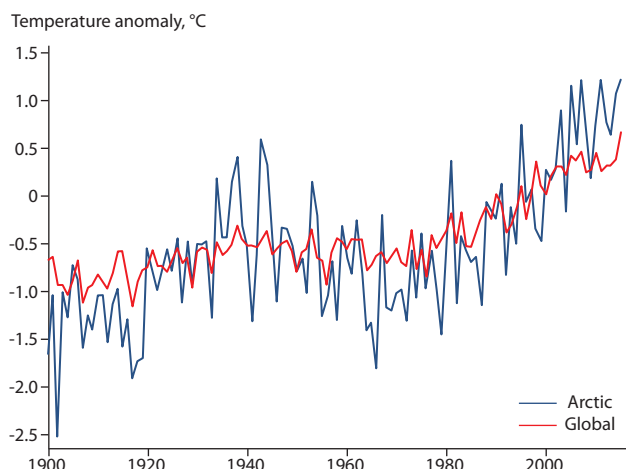


Figure 2.2 Arctic (60–90°N) and global annual surface air temperature anomalies relative to the 1981–2010 mean value (revised from NOAA, 2015).

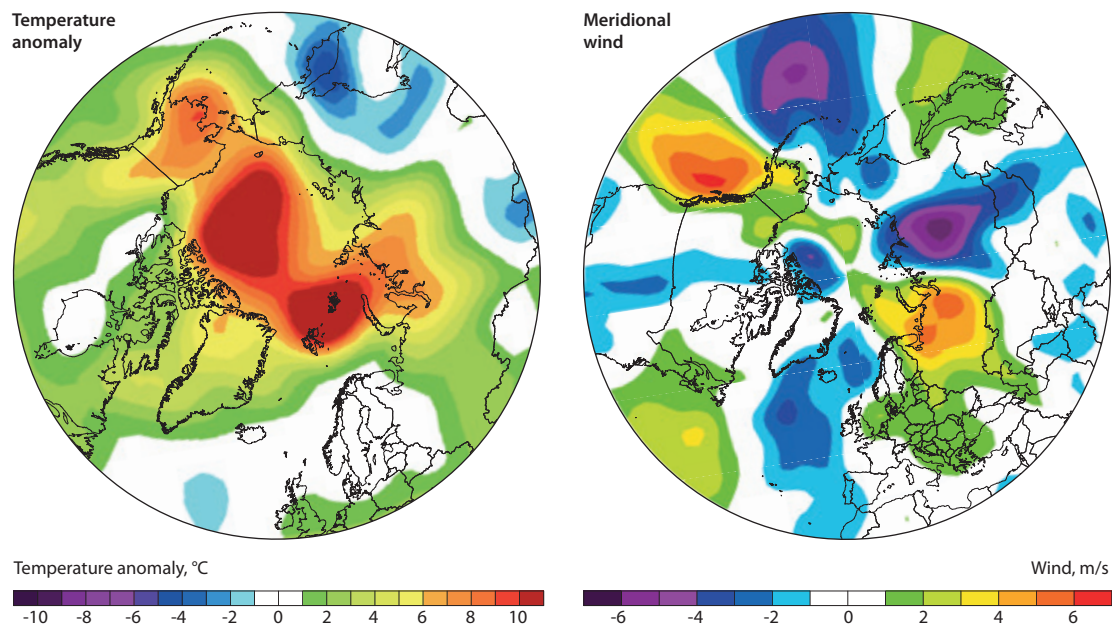


Figure 2.3 Temperature anomalies for January–February 2016 relative to the 1981–2010 mean value (left) and meridional wind components (positive northward) for the same months (right) (NOAA/ESRL).

The most striking new information is the loss of sea-ice volume and the transition of most of the Arctic from multi-year sea ice to first-year sea ice. Lindsay and Schweiger (2015) provide a long-term view of ice thickness, compiling a variety of subsurface, aircraft, and satellite observations. They found that ice thickness over the central Arctic Ocean has declined from an average of 3.6 m to 1.3 m, a reduction of 65% over the period 1975 to 2012. From a combination of observational data and model results it is estimated that sea-ice volume reduced by two-thirds between 1980 and 2013 (Overland and Wang, 2013). Satellites can distinguish between multi-year and first-year sea ice; Figure 2.5 shows the transition from multi-year sea ice (red) to first-year sea ice (blue) is strongest after 2005. As it would take multiple years of low temperatures to reverse this shift to first-year sea ice, Figure 2.5 provides evidence, combined with steady

global increases in GHG, for the irreversibility of Arctic change. The loss of sea-ice volume and summer retreats in all years since the previous SWIPA assessment (AMAP, 2011) increases the level of confidence that the Arctic has transitioned beyond conditions of the late 20th century (Chapter 5). Nevertheless, data since the previous SWIPA assessment (AMAP, 2011) also show considerable interannual variability (Kwok and Cunningham, 2015; Tilling et al., 2015).

The duration of newly sea-ice free areas is particularly relevant to shipping, resource exploration, and ecosystems. Parkinson (2014) showed the number of days with ice cover declined by about 20 days per decade between 1979 and 2013, with the greatest decrease (~30 days per decade) occurring in the Barents and Chukchi/East Siberian Seas. As there is always sea ice in the central Arctic in winter, the future duration of

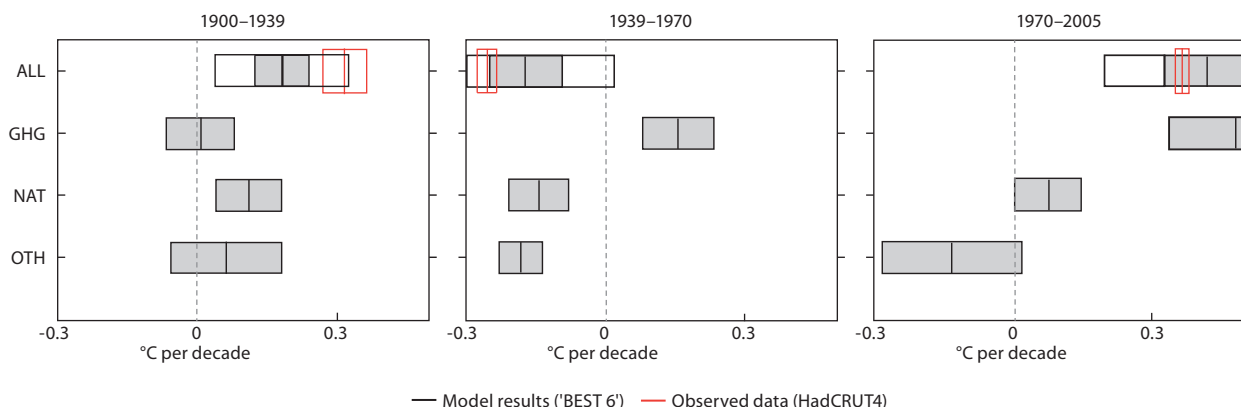


Figure 2.4 Attribution graphic showing impacts of greenhouse gases (GHG), natural variability (NAT) and other drivers (OTH) on total Arctic temperature change (ALL) during three consecutive periods of the 20th century. NAT is taken in this study to include El Niño/Southern Oscillation effects, volcanic effects and dynamically-induced atmospheric variability such as the cold ocean-warm land. Results in black are from a subset of CMIP5 models found to be the 'Best 6'; gray bars denote across-model ranges. Red boxes are based on observational data (HadCRUT4 = HadCRUT4 temperatures), with uncertainty ranges indicated by box width (Fyfe et al., 2013).

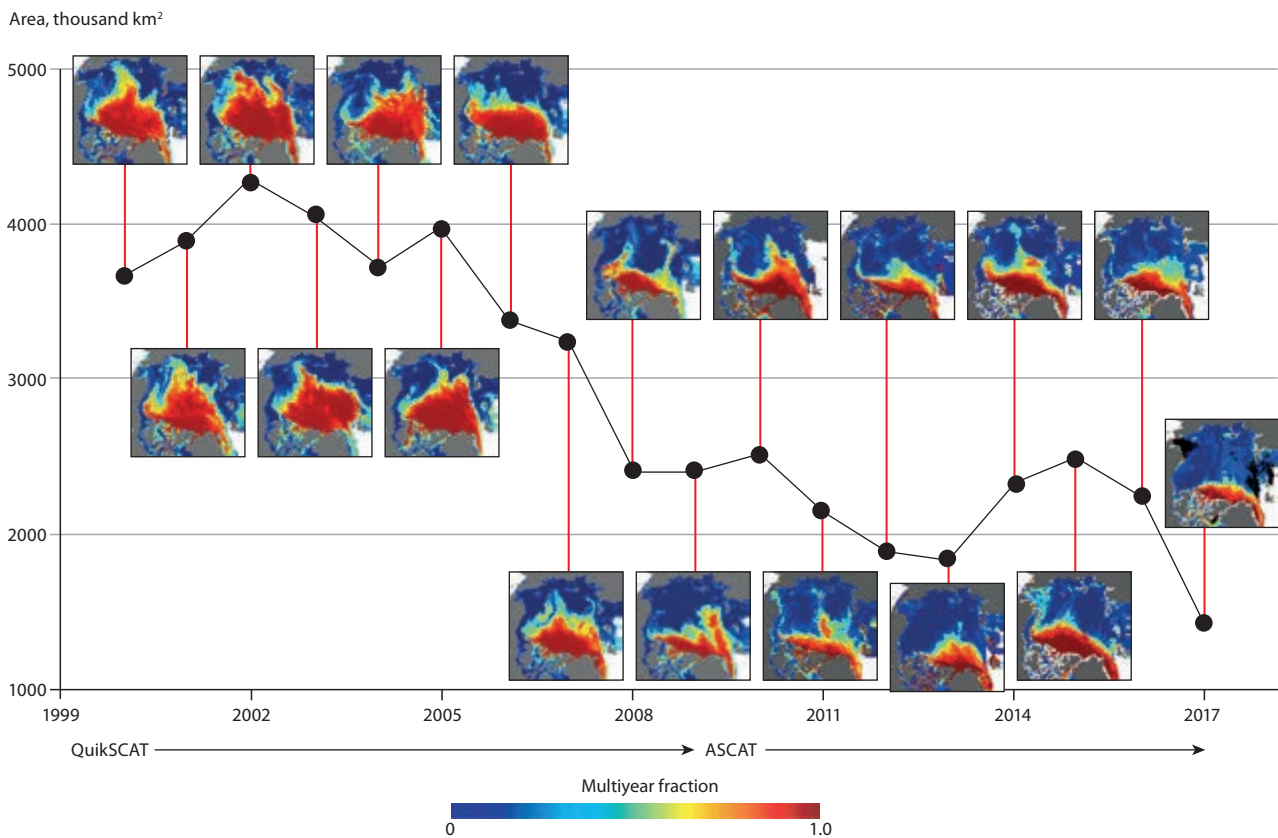


Figure 2.5 Decline in multi-year sea ice since the start of the 21st century, images relate to 1 January for each year shown (R. Kwok, NASA/JPL).

open waters in the central Arctic is unlikely to exceed three months (Wang and Overland, 2015).

Sea surface temperatures have increased in most of the Arctic's marginal seas. For the period 1982–2014, the following August decadal trends have been reported: Chukchi Sea, 0.5°C; Kara Sea: 0.2°C; East Siberian and Laptev Seas: 0.1°C; Barents Sea: -0.1°C (Timmermans and Proshutinsky, 2014). Below the surface, warmer ocean water has entered the Arctic Ocean in the past decade from the North Atlantic and the North Pacific. Pulses of increasingly warmer Atlantic water, entering the Arctic Ocean through Fram Strait and from the Barents Sea, have been documented by Alexeev et al. (2013), Dmitrenko et al. (2014) and Carmack et al. (2015), among others. A major exception is the cooler temperatures of the southern Bering Sea until 2014, as it is associated more to climate shifts in the Pacific than in the Arctic. The Bering Sea and Barents Sea, both marginal seas, were particularly warm in 2015 and 2016 related to anomalous southerly winds.

The reduced ice cover and increased upper-ocean temperatures of the Arctic have led to changes in primary production in the high-latitude seas (Ardyna et al., 2014). As shown in Figure 2.6, areas without a phytoplankton bloom (i.e. a 'flat' seasonal cycle) decreased between 1998–2001 and 2007–2012, whereas areas with autumn/secondary blooms increased. The increase in areas with double blooms was largest in the shelf seas north of Russia and the Bering Strait (Figure 2.6), consistent with the greatest loss in sea ice in this region.

Late spring and early summer snow cover in the Arctic has undergone a marked decrease in recent decades (Chapter 3) with values of June snow cover extent since 2008 typically averaging

about half the values observed in the period prior to 2000. June snow-cover extent decreased 17% per decade over the period 1979–2016 which is greater than the loss in September sea-ice extent over this period (a reduction of 13.4% per decade).

Various studies point to increased long-term photosynthetic activity in Arctic terrestrial regions (e.g. Bhatt et al., 2013; Urban et al., 2014). This is most apparent in tundra biomes, where the combination of higher temperatures and sufficient moisture availability result in increased greenness. While the tundra regions of the Arctic have greened over the past decades, since AMAP (2011) there has been a decrease in the greenness of some parts of the boreal forest. Figure 2.7 shows long term positive trends in vegetation greenness over most of the Arctic and subarctic during the period 1982–2011. More recently positive changes dominate Eurasia, but 'browning' (less photosynthetic activity) is indicated over areas of Alaska and northern Canada's boreal forest (Chapter 10). Possible contributory factors to browning include drier conditions during the growing season, fires, animal and insect activity, and industrial pollution (Xu et al., 2013).

An additional cryosphere indicator of recent change is permafrost (Chapter 4). Permafrost temperatures have risen in many areas of the Arctic (Romanovsky et al., 2013). Active layer thickness increased by 20–30 cm between 1990 and 2013 over most sub-regions of northern North America, northern Europe and northern Asia, although decreases were detected in western Canada and western Siberia. Deeper active layers are consistent with the warming documented earlier, although permafrost temperatures and active layer thicknesses are both affected by snow cover (Park et al., 2013).

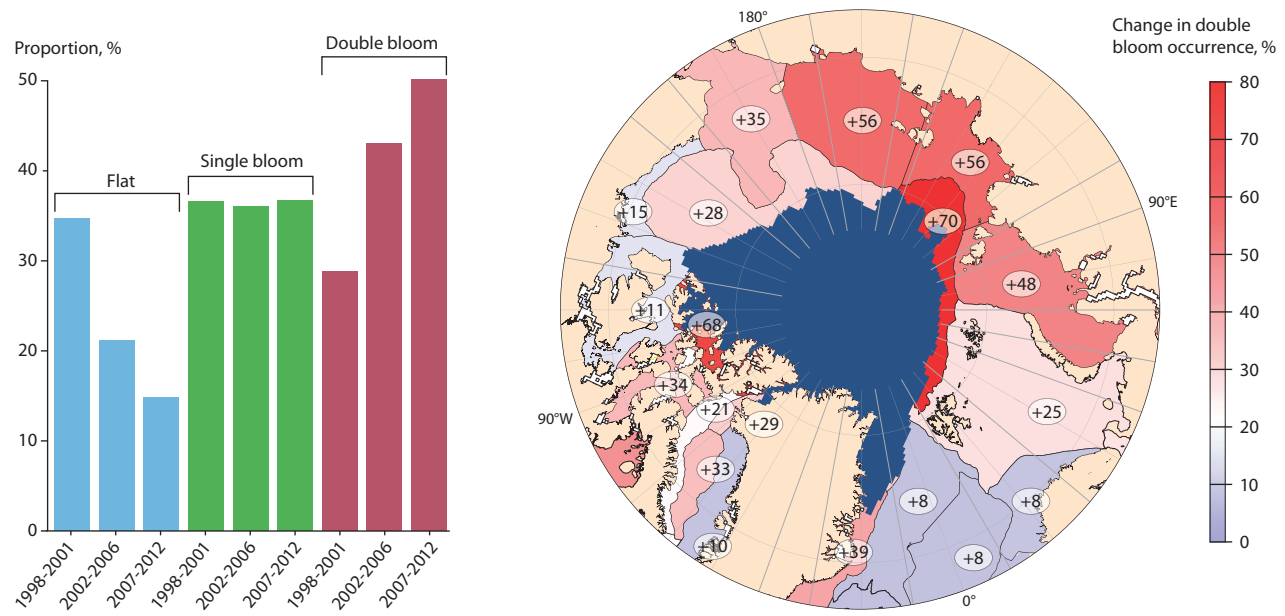


Figure 2.6 Shifts in Arctic phytoplankton phenology within the Arctic Circle ($>66.58^{\circ}\text{N}$). The histogram shows three types of annual phytoplankton bloom cycle (flat, single bloom, double bloom) for three consecutive periods since the late 1990s. The circumpolar map shows percentage change in autumn/secondary bloom occurrence between the earlier and later periods for 19 Arctic areas. The minimum September sea-ice extent in 2012 is shown in dark blue (Ardyna et al., 2014).

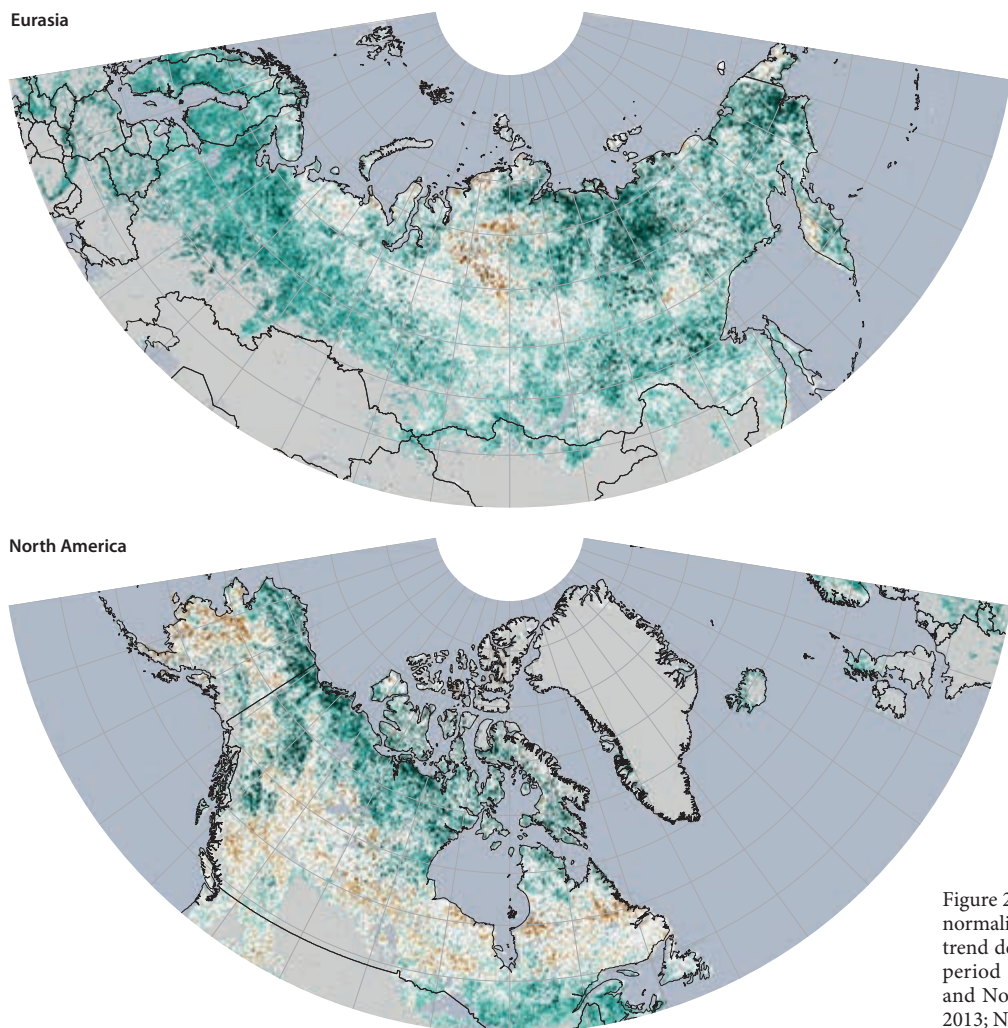


Figure 2.7 Vegetation greenness (NDVI; normalized difference vegetation index) trend derived from satellite data for the period 1982–2011 for Eurasia (upper) and North America (lower) (Xu et al., 2013; NASA Earth Observatory).

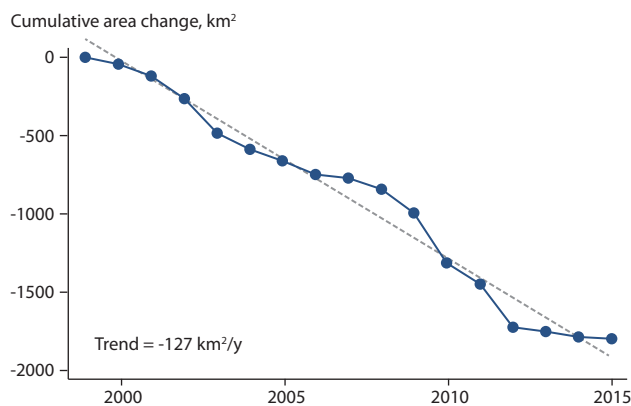


Figure 2.8 Cumulative net area change at the 45 widest and fastest-flowing marine-terminating glaciers of the Greenland Ice Sheet (after Box and Decker, 2011).

Changes in Greenland are also indicators of Arctic change (Chapter 6). The ongoing loss of coastal glacier extent in western Greenland can increase in years when southerly winds predominate, such as between 2009 and 2012 (Figure 2.8). Such increases are not seen in climate model projections (Tedesco et al., 2016). There was a major large-scale snow melt event in 2012.

An indicator of global change from an Arctic contribution is sea-level rise, which is increasing in response to discharge from glaciers and ice sheets (Chapter 9). While Greenland ice loss is an important climate change indicator, part of the contribution to global sea-level rise is from non-Arctic regions: thermal expansion of the oceans and, potentially, mass loss from the Antarctic Ice Sheet. The global average sea level has risen by more than 20 cm since 1900. However, sea-level changes are not spatially uniform. Notably for the Arctic, there is a tendency for falling sea level near regions where large decreases of glacier and ice cap mass are occurring or have recently occurred, such as much of eastern Canada, southeast Alaska, and northwestern Europe. Sea-level impacts from Greenland melt are expected to increase in the latter half of the century.

2.1.2 Changes in extremes

Changes in extremes often have greater impacts on ecosystems, infrastructure, and humans than changes in climatic means (CCSP, 2008; IPCC, 2012). While an absence of studies of extreme events in the Arctic was noted in the previous SWIPA assessment (AMAP, 2011), this situation has improved. Historical data from Alaska show recent trends for less frequent cold extremes and more frequent warm extremes in northern high latitudes (Figure 2.9).

On the Arctic scale, Matthes et al. (2015) showed widespread decreases in extreme cold spells, although there are small areas of statistically significant increases in cold spells in Siberia. Changes in extreme warm spells were found to be generally small throughout the Arctic except in Scandinavia, where increases of up to 2.5 days per decade have occurred. Long cold spells (cold events lasting more than 15 days) have almost completely disappeared since 2000.

The contribution of heavy daily precipitation amounts to the total precipitation has increased over Fennoscandia since 1950 (Hartmann et al., 2013). A type of extreme event with major impact in the Arctic is freezing rain, or rain-on-snow events. Hansen et al. (2014) examined the recent occurrence of such events in Svalbard and concluded that the frequency of rain-on-snow events is likely to increase in the Arctic, with implications for wildlife, infrastructure, transportation and other human activities.

Individual cyclones in the Arctic and their impacts on sea ice have been studied in recent years (Simmonds and Rudeva, 2012; Parkinson and Comiso, 2013). Comprehensive data-based studies of storms in the central Arctic are lacking, and evaluations of historical trends in subarctic storminess have not provided compelling evidence of trends (USGCRP, 2014). There are some indications from models of a northward shift in the storm tracks over the North Atlantic Ocean, but the northern hemisphere observational data show a less spatially coherent poleward shift in storm tracks (Collins et al., 2013).

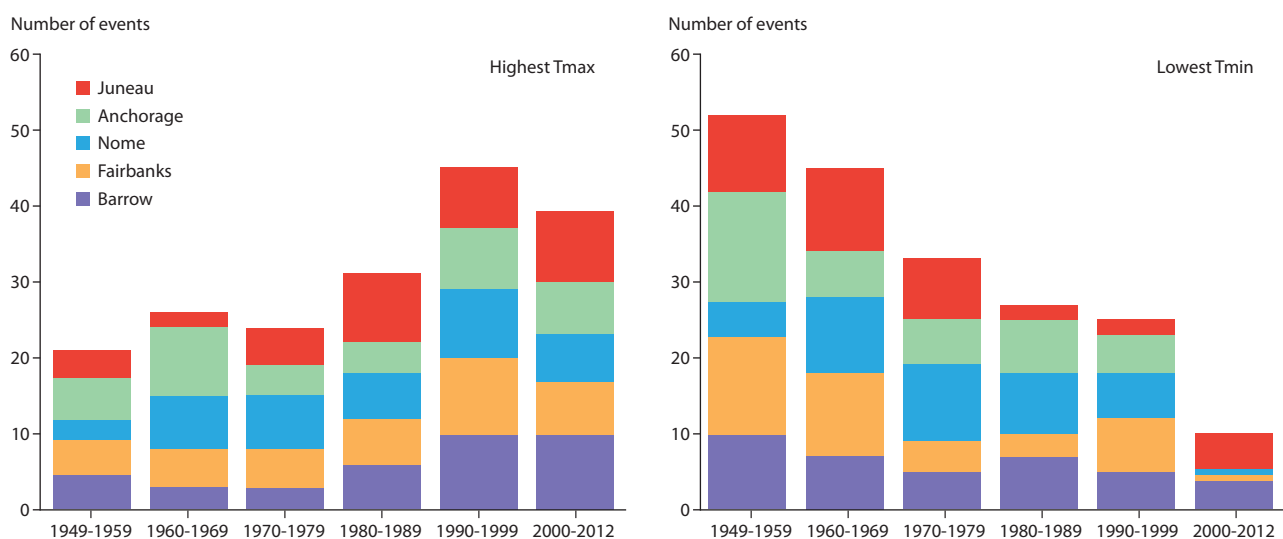


Figure 2.9 Decadal distributions of record-high daily maximum temperatures (left) and record-low daily minimum temperatures (right) for the period 1949–2012 at five first-order weather stations in Alaska. The bars for 2000–2012 have been adjusted to represent the number of events over 10 years (Bieniek and Walsh, 2017).

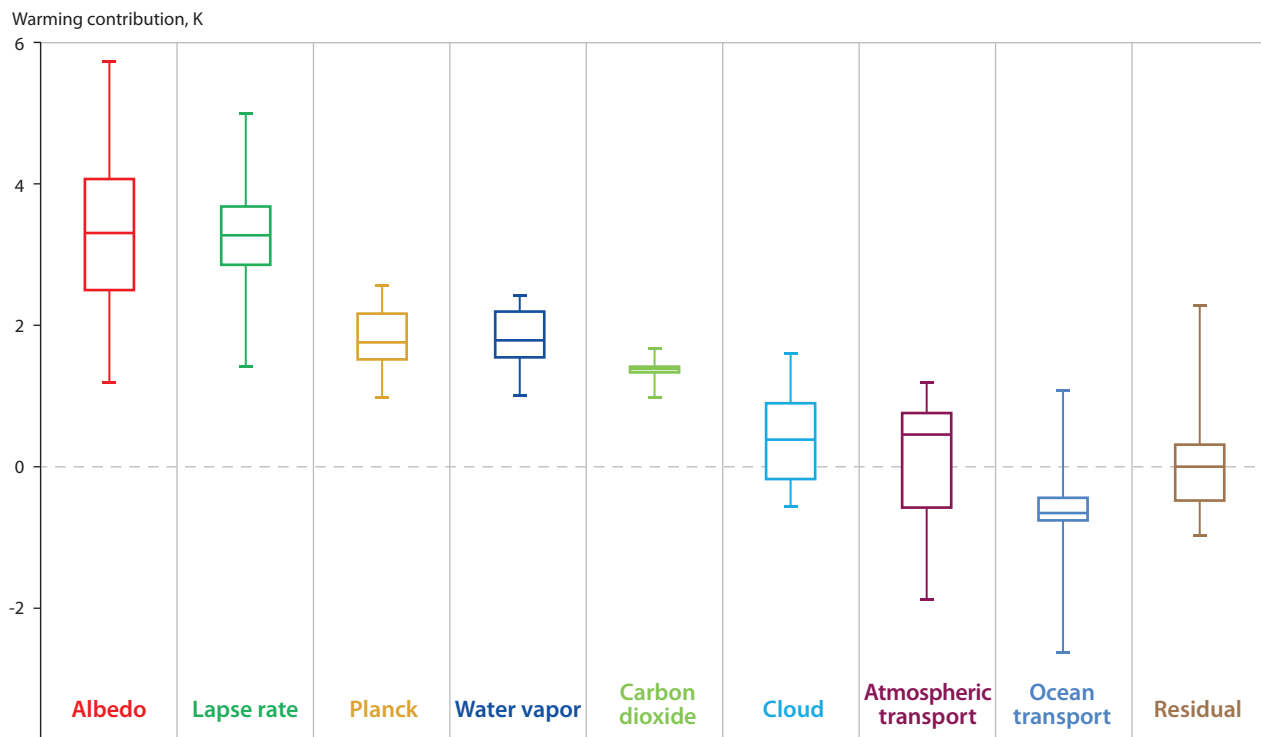


Figure 2.10 Contributions of various feedbacks to total Arctic warming in CMIP5 global climate models (Pithan and Mauritsen, 2014).

2.2 Attribution and feedback processes

Attribution of pan-Arctic temperature changes was discussed in regards to Figure 2.4. Global climate changes ultimately affecting the Arctic are driven by radiative forcing, as summarized by the IPCC (Myhre et al., 2013). The largest contributions to the increase in radiative forcing since 1750 have arisen from increasing atmospheric concentrations of CO₂ (~1.7 W/m²) and methane (~1.0 W/m²). Black carbon has contributed an increase of ~0.6 W/m². Other aerosols have had a cooling effect, decreasing radiative forcing by ~0.8 W/m². Clouds and land use (albedo) changes have also had small cooling effects, while the impact of changes in solar irradiance is negligible.

The contributions of various feedbacks to Arctic amplification in global climate model simulations was recently evaluated by Taylor et al. (2013) and Pithan and Mauritsen (2014) (Figure 2.10). The largest contributions arise from (1) the surface albedo (snow and ice) with related warming of newly sea-ice-free ocean areas and (2) the different vertical structure of the warming at high and low latitudes (lapse rate and Planck effect). The Planck effect arises because the Arctic is colder at the top of the atmosphere than in the subtropics and radiates less energy to space. The water vapor feedback is the next largest contributor to polar amplification. These contributions are followed by the direct radiative effect of increased CO₂ concentrations. The net role of clouds is small, but can be large in a particular season of a particular year. The only substantial negative feedback is ocean heat transport, which decreases as the Arctic warms, thereby reducing the rate of Arctic warming. The vertical range of values in Figure 2.10 shows how these different contributions vary among the global climate models. The feedbacks associated with clouds and atmospheric and ocean transport have wide ranges.

Four-year lagged correlations between Chukchi and Beaufort Seas, September northern hemisphere temperature increases, and sea-ice extent over the past two decades support the rise in temperature as preceding the dramatic regional sea-ice reductions in the Alaskan Arctic. Thinning of the ice cover and preconditioning of the upper ocean are mechanisms by which higher temperatures contribute to the substantial end-of-summer loss of sea ice (Ballinger and Rogers, 2014).

2.3 Potential Arctic and mid-latitude weather linkages

Linkages between Arctic and mid-latitude weather and climate have emerged as a research focus in the years since the previous SWIPA assessment (AMAP, 2011). The potential of recent Arctic changes to influence hemispheric weather is a complex and controversial topic with considerable uncertainty, as time series of potential linkages under the new sea-ice regime are short (~10 years) and understanding involves the relative contribution of direct forcing by Arctic changes on a complex mid-latitude climatic system (Barnes and Screen, 2015; Francis and Skific, 2015; Overland et al., 2015). However, potential mechanisms are emerging that are regional, episodic and based on amplifying existing long-wave weather patterns in central Asia and northeastern North America.

Figure 2.11 shows a set of 'links' to parse the potential connections from the Arctic to mid-latitudes (Overland et al., 2015). The top link is well established, because Arctic temperatures are increasing more than twice as fast as those at mid-latitudes. The second link connects increased Arctic temperatures to weaker zonal winds through changes in the geopotential height (GPH) field. As high-latitude temperatures increase disproportionately, the air becomes less dense, which

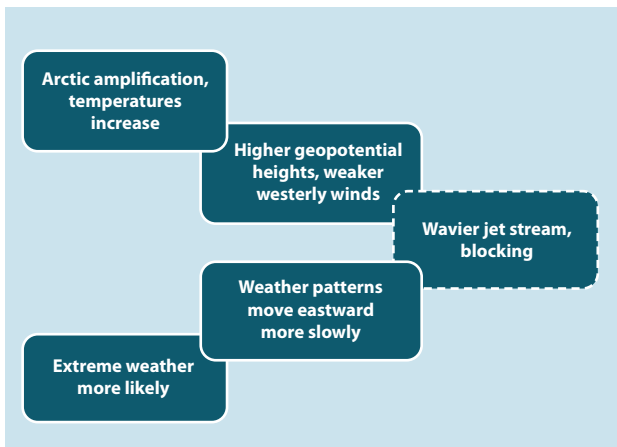


Figure 2.11 Schematic representation of the linkage between Arctic warming and extreme weather in mid-latitudes. The dashed link represents the most uncertain part of the chain (Overland et al., 2015).

increases the high-latitude geopotential thickness, reduces the poleward GPH gradient, and thus weakens upper-level westerly winds through the thermal wind relation (Overland and Wang, 2010; Cvijanovic and Caldeira, 2015; Francis and Vavrus, 2015). The last two links are that large-amplitude planetary waves in the jet stream tend to progress more slowly, which creates more persistent weather conditions that may cause extreme weather events (Screen and Simmonds, 2014). The dashed link in the middle of the chain relates to regional dynamics and represents the large uncertainty in the Arctic/mid-latitude causal linkage.

During several exceptionally warm Arctic winters since 2007, the loss of sea ice and warmer temperatures north of central Asia led to an increase in the intensity of the Siberian high pressure system. The temperature differences associated with this weather feature in turn fuel cold storms that can reach Japan, South Korea, and parts of China (Dethloff et al., 2006; Petoukhov and Semenov, 2010; Kim et al., 2014; Kug et al., 2015; Semenov and Latif, 2015).

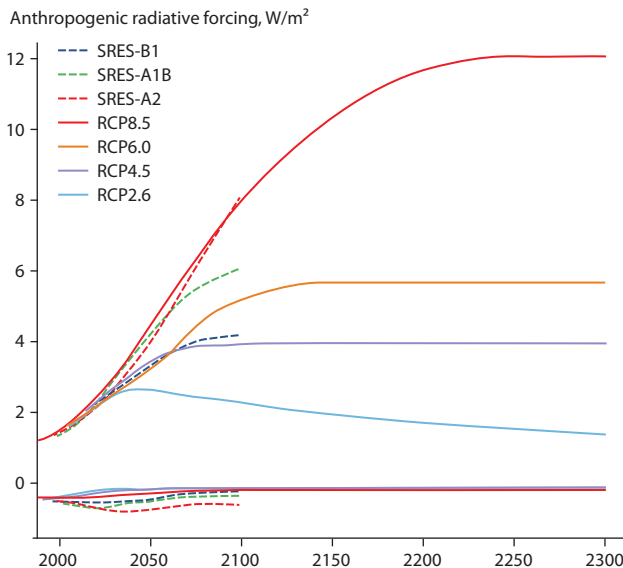


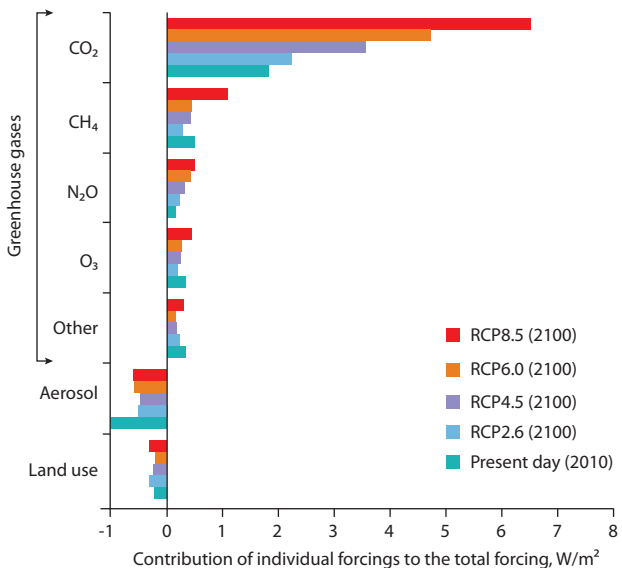
Figure 2.12 Total radiative forcing as a function of time under the RCP scenarios through 2300 (negative lines represent anthropogenic aerosol forcing) and the SRES scenarios through 2100 (left), and the contributions of individual forcings to the total forcing at present and under the RCP scenarios (right) (Collins et al., 2013).

The quantitative impact of Arctic change on mid-latitude weather may not be resolved within the foreseeable future. Yet continuing studies of the changing Arctic and subarctic low-frequency atmospheric dynamics can contribute to improved skill in extended-range mid-latitude forecasts (Jung et al., 2014).

2.4 Projections of future changes

There are presently over 30 global climate models (GCMs) being run by major modeling centers and modeling groups, in some cases with variants of the same model used by different groups. There are several arguments for suggesting that these models can provide credible projections for large-scale temperature changes. First, the models are built on well-known physical principles, and many large-scale aspects of the observed and past climate are simulated quite well by these models (Knutti, 2008). Second, biases in the simulated climates from different models tend to be unsystematic (e.g. Raisanen, 2007).

Projections of future climate change are dependent on scenarios of external forcing, which includes anthropogenic increases in GHG emissions. Because these scenarios of forcing are not assigned a probability, it is customary to utilize a range of scenarios to illustrate impacts of alternative scenarios of emissions. For its most recent assessment (AR5), the IPCC utilized Representative Concentration Pathways (RCPs) that provide a time-varying range of anthropogenic radiative forcing (Figure 2.12; Collins et al., 2013). The previous IPCC assessment (AR4; IPCC, 2007) utilized an earlier generation of global climate models and SRES (Special Report on Emission Scenarios; Nakicenovic and Swart, 2000) scenarios of external forcing (Figure 2.12 left). Under the RCP scenarios, the radiative forcing in 2100 ranges from 2.6 W/m² (an extreme scenario of emission reductions) to 8.5 W/m² (a scenario close to the current trajectory of emissions). SWIPA 2017 uses RCP4.5 and RCP8.5 as plausible low-end and high-end emission scenarios. It is noteworthy that, in spite of the different emission scenarios



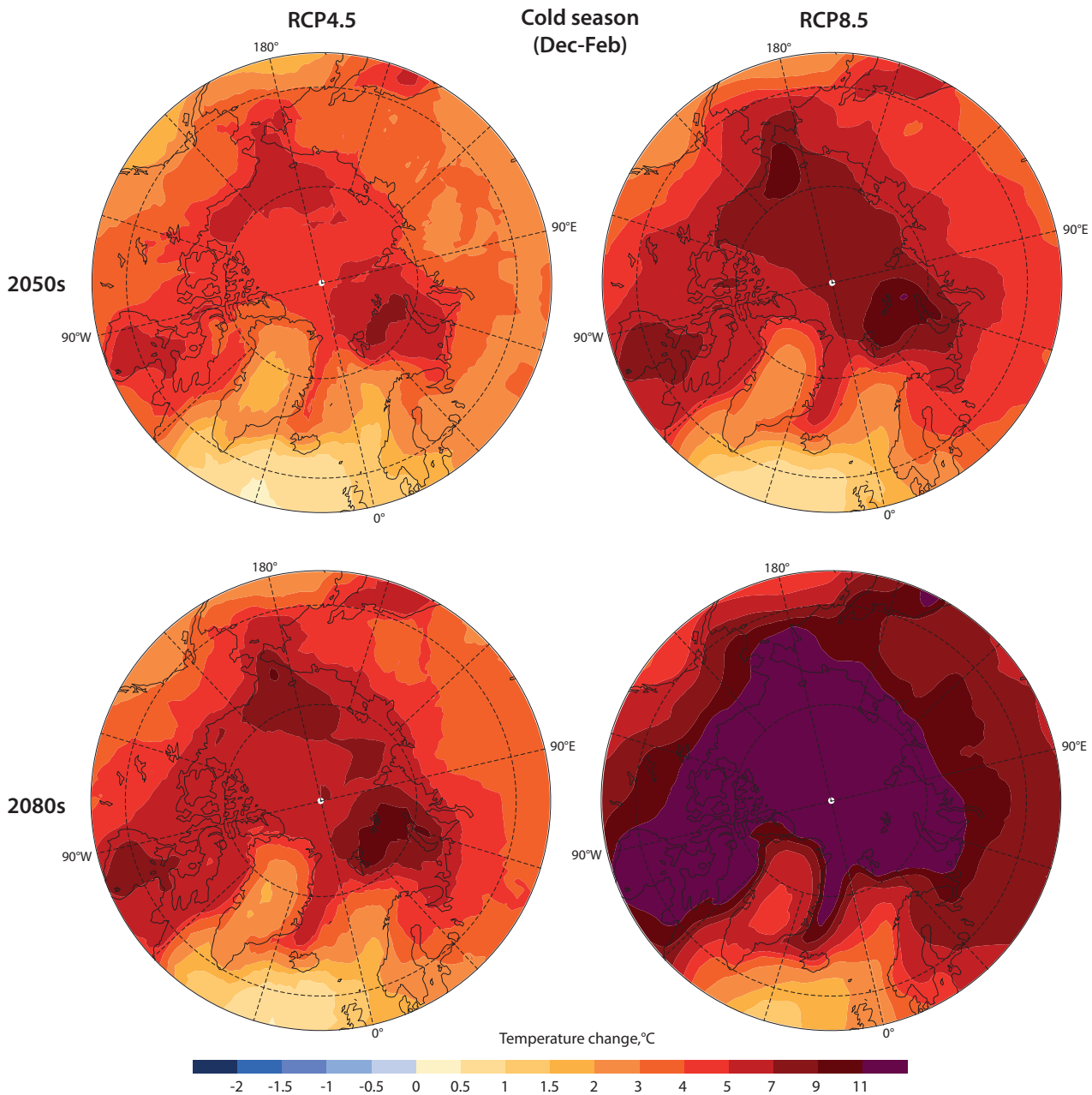


Figure 2.13 Projected changes in near-surface temperature (50th percentile), relative to 1986–2005, for December–February under the RCP4.5 scenario (left panels) and the RCP8.5 scenario (right panels). Upper panels are for the decade of the 2050s, lower panels are for the 2080s (graphic courtesy of G. Flato, Environment and Climate Change Canada).

(SRES vs. RCP) and the different generations of climate models, there is qualitative agreement between the groups of climate models (CMIP3 and CMIP5) that formed the basis of AR4 and AR5 assessments of Arctic climate change estimates, at least for temperature and precipitation. The ratio of Arctic to global SAT (surface air temperature) change by the end of the 21st century is robust for the two generations of models (Kattsov and Pavlova, 2015; Pavlova and Kattsov, 2015).

Uncertainty in the future scenarios of external forcing (emissions) is one of three major sources of uncertainty in climate projections obtained from global models. The other two sources of uncertainty are (1) internal variability, which can have major impacts on decadal or even multi-decadal timescales, and (2) differences in model formulation and the associated differences in systematic errors. Internal variability

and model uncertainty dominate over the first few decades, while the emission scenario uncertainty becomes the largest source of uncertainty late in the century. By 2050, the inter-scenario global temperature spread is 0.8°C whereas the model spread for each scenario is 0.6°C (Collins et al., 2013). Given the spread between model results, even though the models are ostensibly solving the same climate problem, there is no current consensus on the question of synthesizing results by cross model averaging versus model selection. In its AR5 the IPCC chose not to use model selection (Flato et al., 2013) due to the lack of unique selection criteria. However, model selection may be advisable for regional studies (Overland et al., 2011; Wang and Overland, 2012; Anisimov and Kokorev, 2016).

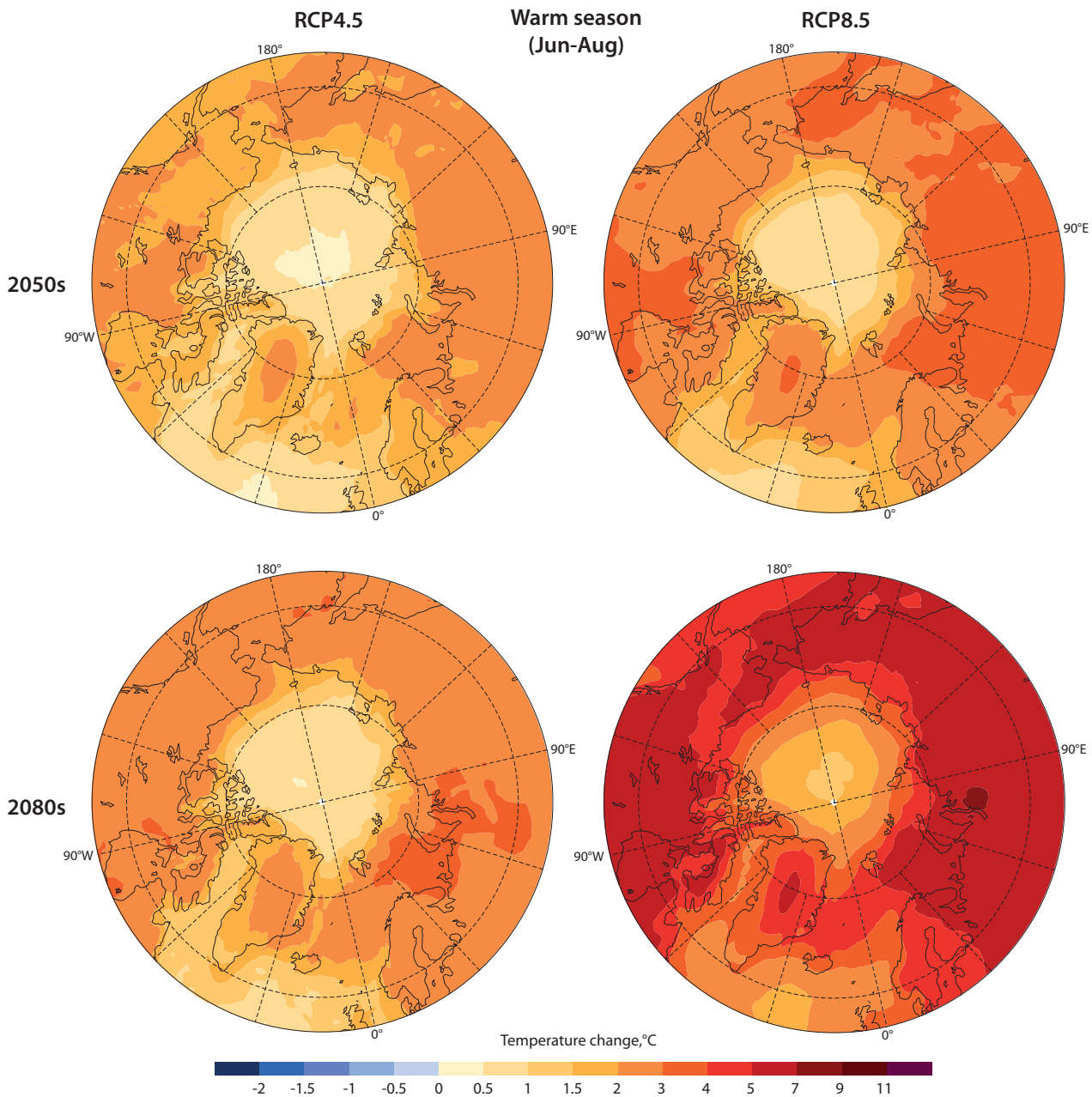


Figure 2.14 Projected changes in near-surface temperature (50th percentile), relative to 1986–2005, for June–August under the RCP4.5 scenario (left panels) and the RCP8.5 scenario (right panels). Upper panels are for the decade of the 2050s, lower panels are for the 2080s (graphic courtesy of G. Flato, Environment and Climate Change Canada).

2.4.1 Projected changes in temperature

Future changes projected by global climate models are larger in the Arctic than in the mid-latitudes. Figure 2.13 shows mid-21st century (2050s) and late-21st-century changes (relative to 1986–2005) of the cold-season (December–February) surface air temperature projected by the CMIP5 models under the RCP4.5 and RCP8.5 forcing scenarios. For each location, the plotted value is the median of results from 30 CMIP5 models run under the particular RCP forcing scenario. Over the Arctic Ocean, which is ice-free in early winter in some models and covered by thin sea ice during late winter, the warming is 3–5°C by mid-century and 5–9°C by late century under RCP4.5. The warming over the subarctic seas is slightly greater than over the central Arctic Ocean because the duration of open water (and hence absorption of solar radiation) increases southward

even when the ice cover is seasonal in the Arctic Ocean. Under the RCP8.5 scenario, the warming in each time-slice is typically 50–75% greater than under RCP4.5. Under both scenarios, there is a relative minimum of the warming in the subpolar North Atlantic.

Figure 2.14 shows the corresponding projections for the warm season (June–August). The spatial pattern is different to that of winter, as there is a minimum of warming over the Arctic Ocean in both time-slices under both scenarios. The minimum arises because of the large heat capacity of the ocean, relative to the surrounding landmasses. The spatial patterns for the transition seasons of spring and autumn more closely resemble the winter pattern with considerable polar amplification, especially during autumn when the Arctic Ocean is essentially ice-free in most models.

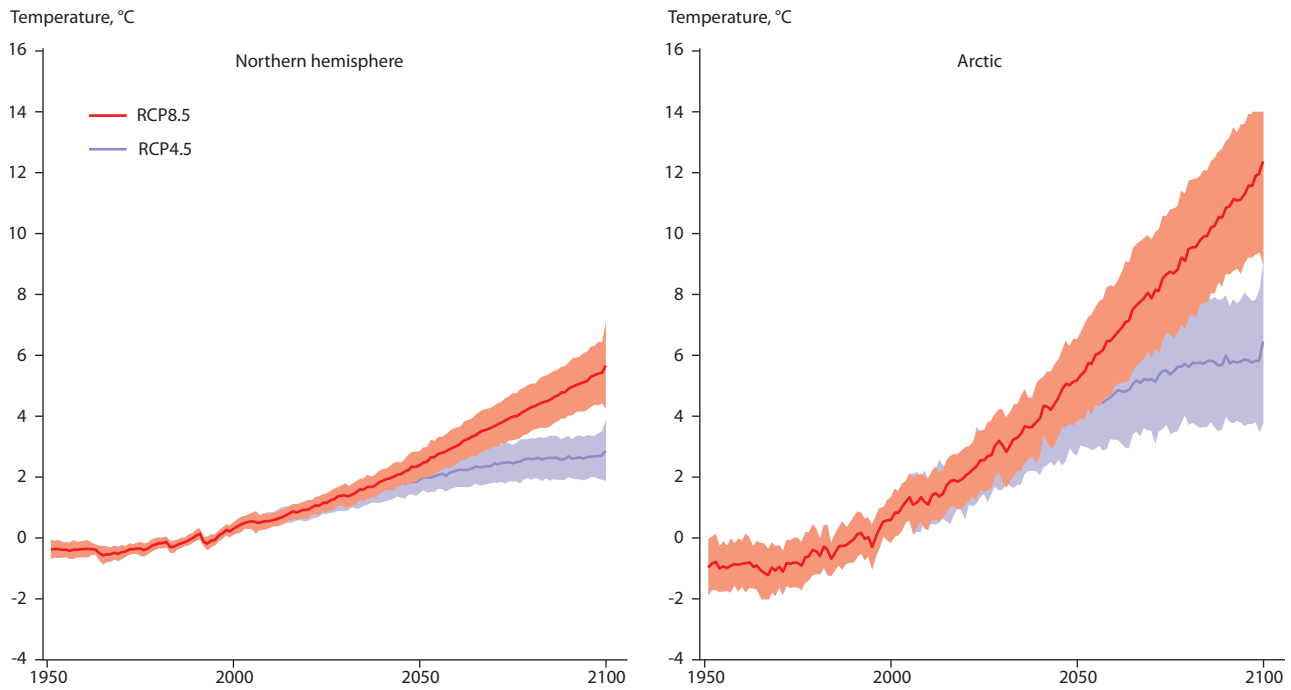


Figure 2.15 Winter season future temperatures for the northern hemisphere ($0\text{--}90^\circ\text{N}$) and Arctic ($60\text{--}90^\circ\text{N}$) averaged over 36 CMIP5 global climate models and expressed as departures from the means for the 1981–2005 period. The red line is the ensemble mean for RCP8.5, the blue line is for RCP4.5. Shaded areas denote \pm one standard deviation from the ensemble mean (Overland et al., 2014).

Figure 2.15 highlights the difference between the near-term ‘adaptation timescale’ and the long-term ‘mitigation timescale’ for the Arctic-wide warming, averaged over $60\text{--}90^\circ\text{N}$ relative to northern hemisphere changes for the winter half of the year (NDJFM). Only in the latter half of the century do the projections from the RCP4.5 and RCP8.5 emission scenarios noticeably separate. By the end of the century the warming is approximately twice as large under the higher-emission RCP8.5 scenario, pointing to the impact of emission reductions with RCP4.5. Over the adaptation timescale (to about 2040), the one-standard-deviation range of projected warming (shaded areas in Figure 2.15) is dominated by across-model differences and internal variability.

2.4.2 Projections for other variables

Four variables of particular importance are sea ice, permafrost, precipitation, and sea level. All are projected to undergo changes over the next half century, with strong dependencies from 2050 onward on which emission scenario is followed.

While the model ensemble-mean is essentially sea-ice-free around 2060 under the RCP8.5 forcing, extrapolation of the recent observed trend advances the ice-melt out date by two to three decades (Chapter 5). Some publications suggest that a seasonally ice-free Arctic Ocean within the next few decades is a distinct possibility (Massonnet et al., 2012; Stroeve et al., 2012; Overland and Wang, 2013; Rogers et al., 2015). Models consistently show winter refreezing of a substantial portion of the Arctic Ocean, even in the late 21st century under the RCP8.5 scenario (Collins et al., 2013). This seasonal sea ice can be expected to be thinner, more mobile and more deformable than sea ice has historically been during the cold season.

As is the case with sea ice, permafrost extent is projected to decrease substantially during the remainder of the 21st century. Projections are discussed in Chapter 4.

Future increases in precipitation in the Arctic are larger in a percentage sense than elsewhere in the northern hemisphere. However, this is because the Arctic precipitation totals are relatively small. Discussion of future precipitation is presented in Chapter 10.

Model projections of global mean sea-level rise in IPCC, driven by the atmospheric forcing of the various RCP scenarios, are shown in Figure 2.16. While the uncertainty range for each scenario is large, because of the weakly constrained contributions from the Greenland and Antarctic ice sheets, there is still a considerable dependence on the forcing scenario: the mean of the RCP2.6 projections for 2100 is 0.45 m compared to 0.75 m for the RCP8.5 scenarios. The overall range of the individual simulations is about 0.3 to 1.0 m. More recent assessments (USGCRP, 2014; Jevrejeva et al., 2016) show a higher upper limit and thus a wider range: 0.3 to 1.2 m. A new analysis of sea level rise in SWIPA 2017 (Chapter 9) supports higher upper limits.

The next generation of climate models, CMIP6, is expected towards the end of this decade. It is encouraging to note that multiple groups are now evaluating how individual feedbacks, including important Arctic processes, are currently handled in the models and are making recommendations for their improvement.

2.5 Summary

Additional data and peer-reviewed analyses have become available in the period since the release of the previous SWIPA assessment (AMAP, 2011). The Arctic is continuing to undergo rapid warming and change since the end of the 20th century,

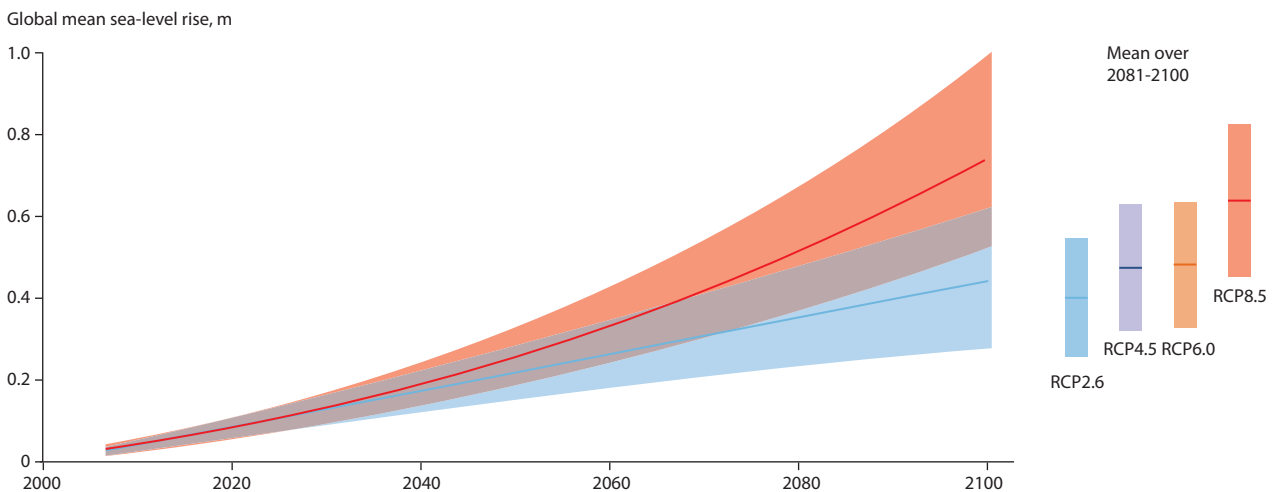


Figure 2.16 Projections of global mean sea level rise relative to the 1986–2005 mean sea level, based on forcing from the CMIP5 models. Medians (solid lines) and ranges (shading) are shown for RCP2.6 and RCP8.5. End-of-century median values and ranges for all RCP scenarios are shown to the right (IPCC, 2013).

as seen in mean annual temperature increases of 2.5°C , losses of two-thirds of the sea-ice volume and half of the June snow-cover extent, extreme winter/spring positive temperature anomalies in 2016, and secondary effects such as changes in the tundra, shifts in marine ecosystems, and sea-level rise. These multiple lines of evidence of interacting processes provide strong confirmation of the overall Arctic shift. Such interactions add further confidence to a self-consistent story of continuing Arctic change since the previous SWIPA assessment (AMAP, 2011).

These changes are driven by increases in GHG concentrations and multiple feedbacks that result in Arctic amplification. The combination of albedo plus a lower radiative cooling rate in the Arctic (lapse rate and Planck mechanism) and local and transported increases in water vapor, are large relative to the direct radiative effect of CO_2 . A modest global increase in temperature resulting from increased atmospheric GHG levels, activates a set of mostly one-way Arctic-specific feedbacks, and the changes are maintained in the state memory of the Arctic heat storage system. Feedbacks can be thermodynamic, involving radiative processes, or dynamic, involving advection of warm temperature anomalies by variation in wind patterns (Figure 2.17). Arctic change continues as GHG emissions continue.

The Arctic climate is very likely to continue to change, with autumn/winter temperatures rising by 4°C over the next three decades, augmented by natural variability and providing new record temperatures in some regions and years. Stronger mitigation efforts can have an impact in the latter half of the century. Increased duration of the summer sea-ice free season will continue, as well as permafrost loss and vegetation shifts. Such changes will affect local ecosystems, shipping, resource exploration, and other human activities. There is emerging evidence that as Arctic temperatures increase, they may influence mid-latitude weather; but such conclusions remain controversial. The rate of sea-level rise is very likely to increase, but uncertainties related to the potential accelerated loss rate of the Greenland Ice Sheet remain.

References

Alexeev, V.A., V.V. Ivanov, R. Kwok and L.H. Smedsrød, 2013. North Atlantic warming and declining volume of arctic sea ice. *The Cryosphere Discussions*, 7:245–265.

AMAP, 2011. *Snow, Water, Ice and Permafrost in the Arctic (SWIPA): Climate Change and the Cryosphere*. Arctic Monitoring and Assessment Programme (AMAP), Oslo, Norway.

Anisimov, O.A. and V.A. Kokorev, 2016. Climate in the arctic zone of Russia: Analysis of current changes and modeling trends for the 21st century. *Vestnik of the Moscow State University, Geographical Series*, 5:61–70.

Ardyna, M., M. Babin, M. Gosselin, E. Devred, L. Rainville and J.-É. Tremblay, 2014. Recent Arctic Ocean sea ice loss triggers novel fall phytoplankton blooms. *Geophysical Research Letters*, 41: doi:10.1002/2014GL061047.

Ballinger, T. and J.C. Rogers, 2014. Climatic and atmospheric teleconnection indices and western Arctic sea ice variability. *Physical Geography*, 35:459–477.

Barnes, E.A. and J.A. Screen, 2015. The impact of Arctic warming on the midlatitude jet-stream: Can it? Has it? Will it? *WIREs Climate Change*, 6:277–286.

Bhatt, U.S., D.A. Walker, M.K. Reynolds, P.A. Bieniek, H.E. Epstein, J.C. Comiso, J.E. Pinzon, C.J. Tucker and I.V. Polyakov, 2013. Recent declines in warming and arctic vegetation greening trends over pan-Arctic tundra. *Remote Sensing (Special NDVI3g Issue)*, 5:4229–4254.

Bieniek, P.A. and J.E. Walsh, 2017. Atmospheric circulation patterns associated with monthly and daily temperature and precipitation extremes in Alaska. *Int. J. Climatol.* doi:10.1002/joc.4994.

Box, J.E. and D.T. Decker, 2011. Greenland marine-terminating glacier area changes: 2000–2010. *Annals of Glaciology*, 52:91–98.

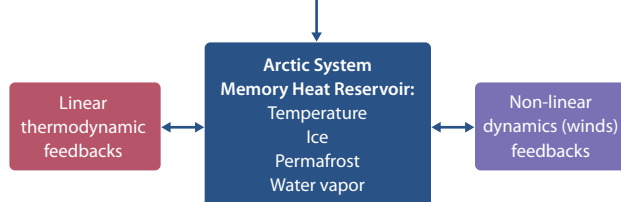


Figure 2.17 Key processes within the Arctic climate system.

Carmack, E., I. Polyakov, L. Padman, I. Fer, E. Hunke, J. Hutchings, J. Jackson, D. Kelley, R. Kwok, C. Layton, H. Melling, D. Perovich, O. Persson, B. Ruddick, M.-L. Timmermans, J. Toole, T. Ross, S. Vavrus, and P. Winsor, 2015. Toward quantifying the increasing role of oceanic heat in sea ice loss in the new Arctic. *Bulletin of the American Meteorological Society*, 96:2079-2105.

CCSP, 2008. Weather and Climate Extremes in a Changing Climate. Synthesis and Assessment Product 3.3. U.S. Climate Change Science Program (CCSP). Karl, T.R., G.A. Meehl, C.D. Miller, S.J. Hassol, A.M. Waple and W.L. Murray (eds.).

Cohen, J., J.A. Screen, J.C. Furtado, M. Barlow, D. Whittleston, D. Coumou, J. Francis, K. Dethloff, D. Entekhabi, J. Overland and J. Jones, 2014. Recent Arctic amplification and extreme mid-latitude weather. *Nature Geoscience*, 7:627-637.

Collins, M., R. Knutti, J. Arblaster, J.-L. Dufresne, T. Fichefet, P. Friedlingstein, X. Gao, W.J. Gutowski, T. Johns, G. Krinner, M. Shongwe, C. Tebaldi, A.J. Weaver and M. Wehner, 2013. Long-term climate change: projections, commitments and irreversibility. In: Stocker, T.F., D. Qin, G.-K. Plattner, M. Tignor, S.K. Allen, J. Boschung, A. Nauels, Y. Xia, V. Bex and P.M. Midgley (eds.), *Climate Change 2013: The Physical Science Basis. Contribution of Working Group I to the Fifth Assessment Report of the Intergovernmental Panel on Climate Change*. Cambridge University Press.

Cvijanovic, I. and K. Caldeira, 2015. Atmospheric impacts of sea ice decline in CO₂ induced global warming. *Climate Dynamics*, 44:1173-1186.

Dethloff, K., A. Rinke, A. Benkel, M. Koltzow, E. Sokolova, S. Kumar Saha, D. Handorf, W. Dorn, B. Rockel, H. von Storch, J.E. Haugen, L.P. Røed, E. Roeckner, J.H. Christensen and M. Stendel, 2006. A dynamical link between the Arctic and the global climate system. *Geophysical Research Letters*, 33:L03703, doi:10.1029/2005GL025245.

Dmitrenko, I.A., S.A. Kirillov, N. Serra, N.V. Koldunov, V.V. Ivanov, U. Schauer, I.V. Polyakov, D. Barber, M. Janout, V.S. Lien, M. Makhotin and Y. Aksenov, 2014. Heat loss from the Atlantic water layer in the northern Kara Sea: causes and consequences. *Ocean Science*, 10:719-730.

Flato, G., J. Marotzke, B. Abiodun, P. Braconnot, S.C. Chou, W. Collins, P. Cox, F. Driouech, S. Emori, V. Eyring, C. Forest, P. Gleckler, E. Guilyardi, C. Jakob, V. Kattsov, C. Reason and M. Rummukainen, 2013. Evaluation of climate models. In: Stocker, T.F., D. Qin, G.-K. Plattner, M. Tignor, S.K. Allen, J. Boschung, A. Nauels, Y. Xia, V. Bex and P.M. Midgley (eds.), *Climate Change 2013: The Physical Science Basis. Contribution of Working Group I to the Fifth Assessment Report of the Intergovernmental Panel on Climate Change*. pp. 741-866. Cambridge University Press.

Francis, J. and N. Skific, 2015. Evidence linking rapid Arctic warming to mid-latitude weather patterns. *Philosophical Transactions of the Royal Society A*, 373:20140170, doi:10.1098/rsta.2014.0170.

Francis, J.A. and S.J. Vavrus, 2015. Evidence for a wavier jet stream in response to rapid Arctic warming. *Environmental Research Letters*, 10:014005, doi:10.1088/1748-9326/10/1/014005.

Fyfe, J.C., K. von Salzen, N.P. Gillett, V.K. Arora, G. Flato and J.R. McConnell, 2013. One hundred years of Arctic surface temperature variation due to anthropogenic influence. *Nature Scientific Reports*, 3:2645, doi:10.1038/srep02645.

Hansen, B.B., K. Isaksen, R.E. Benestad, J. Kohler, A.O. Pedersen, L.E. Loe, S.J. Coulson, J.O. Larsen and O. Varpe, 2014. Warmer and wetter winters: Characteristics and implications of an extreme weather event in the High Arctic. *Environmental Research Letters*, 9:114021.

Hartmann, D.L., A.M.G. Klein Tank, M. Rusticucci, L.V. Alexander, S. Brönnimann, Y. Charabi, F.J. Dentener, E.J. Dlugokencky, D.R. Easterling, A. Kaplan, B.J. Soden, P.W. Thorne, M. Wild and P.M. Zhai, 2013. Observations: atmosphere and surface. In: Stocker, T.F., D. Qin, G.-K. Plattner, M. Tignor, S.K. Allen, J. Boschung, A. Nauels, Y. Xia, V. Bex and P.M. Midgley (eds.), *Climate Change 2013: The Physical Science Basis. Contribution of Working Group I to the Fifth Assessment Report of the Intergovernmental Panel on Climate Change*. Cambridge University Press.

Hawkins, E. and R. Sutton, 2012. Time of emergence of climate signals. *Geophysical Research Letters*, 39:L01702, doi:10.1029/2011GL050087.

IPCC, 2007. Contribution of Working Group I to the Fourth Assessment Report of the Intergovernmental Panel on Climate Change. Solomon, S., D. Qin, M. Manning, Z. Chen, M. Marquis, K.B. Averyt, M. Tignor and H.L. Miller (eds.). Cambridge University Press.

IPCC, 2012. Managing the Risks of Extreme Events and Disasters to Advance Climate Change Adaptation. A Special Report of Working Groups I and II of the Intergovernmental Panel on Climate Change. Field, C.B., V. Barros, T.F. Stocker, D. Qin, D.J. Dokken, K.L. Ebi, M.D. Mastrandrea, K.J. Mach, G.-K. Plattner, S.K. Allen, M. Tignor and P.M. Midgley (eds.). Cambridge University Press.

IPCC, 2013. Summary for Policymakers. In: Stocker, T.F., D. Qin, G.-K. Plattner, M. Tignor, S.K. Allen, J. Boschung, A. Nauels, Y. Xia, V. Bex and P.M. Midgley (eds.), *Climate Change 2013: The Physical Science Basis. Contribution of Working Group I to the Fifth Assessment Report of the Intergovernmental Panel on Climate Change*. Cambridge University Press.

Jevrejeva, S., L.P. Jackson, R.E.M. Riva, A. Grinsted and J.C. Moore, 2016. Coastal sea level rise with warming above 2°C. *Proceedings of the National Academy of Sciences*, 113:13342-13347.

Jung, T., M.A. Kasper, T. Semmler and S. Serrar, 2014. Arctic influence on subseasonal midlatitude prediction. *Geophysical Research Letters*, 41:3676-3680.

Kattsov, V.M. and T.V. Pavlova, 2015. Expected Arctic surface air temperature changes through the 21st century: projections with ensembles of global climate models (CMIP5 and CMIP3). *MGO Proceedings*, 579:7-21.

Kim, B.-M., S.-W. Son, S.-K. Min, J.-H. Jeong, S.-J. Kim, X. Zhang, T. Shim and J.-H., 2014. Weakening of the stratospheric polar vortex by Arctic sea-ice loss. *Nature Communications*, 5:4646 doi:10.1038/ncomms5646.

Knutti, R., 2008. Why are climate models reproducing the observed global surface warming so well? *Geophysical Research Letters*, 35:L18704, doi:10.1029/2008GL034932.

Kosaka, Y. and S.-P. Xie, 2014. Recent global-warming hiatus tied to equatorial Pacific surface cooling. *Nature*, 501:403-407.

Kravtsov, S., M.G. Wyant, J.A. Curry and A.A. Tsonis, 2014. Two contrasting views of multidecadal climate variability in the twentieth century. *Geophysical Research Letters*, 41:6881-6888.

Kug, J.-S., J.-H. Jeong, Y.-S. Jang, B.-M. Kim, C. K Folland, S.-K. Min and S.-W. Son, 2015. Two distinct influences of Arctic warming on cold winters over North America and East Asia. *Nature Geoscience*, 8:759-762.

Kwok, R. and G.F. Cunningham, 2015. Variability of Arctic sea ice thickness and volume from CryoSat-2. *Philosophical Transactions of the Royal Society A*, 373:20140157; doi:10.1098/rsta.2014.0157.

Lindsay, R. and A. Schweiger, 2015. Arctic sea ice thickness loss determined using subsurface, aircraft, and satellite observations. *The Cryosphere*, 9:269-283.

Massonnet, F., T. Fichefet, H. Goosse, C.M. Bitz, G. Philippon-Berthier, M.M. Holland and P.-Y. Barriat, 2012. Constraining projections of summer Arctic sea ice. *The Cryosphere*, 6:1383-1394.

Matthes, H., A. Rinke and K. Dethloff, 2015. Recent changes in Arctic summer temperature extremes: warm and cold spells during winter and summer. *Environmental Research Letters*, 20:114020, doi:10.1088/1748-9326/10/11/114020.

Miles, M.W., D.V. Divine, T. Furevik, E. Jansen, M. Moros and A.E.J. Ogilvie, 2014. A signal of persistent Atlantic multidecadal variability in Arctic sea ice. *Geophysical Research Letters*, 41:463-469.

Myhre, G., D. Shindell, F.-M. Bréon, W. Collins, J. Fuglestvedt, J. Huang, D. Koch, J.-F. Lamarque, D. Lee, B. Mendoza, T. Nakajima, A. Robock, G. Stephens, T. Takemura and H. Zhang, 2013. Anthropogenic and natural radiative Forcing. In: Stocker, T.F., D. Qin, G.-K. Plattner, M. Tignor, S.K. Allen, J. Boschung, A. Nauels, Y. Xia, V. Bex and P.M. Midgley (eds.), *Climate Change 2013: The Physical Science Basis. Contribution of Working Group I to the Fifth Assessment Report of the Intergovernmental Panel on Climate Change*. Cambridge University Press.

Nakicenovic, N. and R. Swart (eds.), 2000. Special Report on Emissions Scenarios: A Special Report of Working Group III of the Intergovernmental Panel on Climate Change. Cambridge University Press.

NOAA, 2015. What's new in 2015? Arctic Report Card: Update for 2015. National Oceanic and Atmospheric Administration (NOAA).

Notz, D. and J. Stroeve, 2016. Observed Arctic sea-ice loss directly follows anthropogenic CO₂ emission. *Science*, doi: 10.1126/science.aag2345

Overland, J.E. and M. Wang, 2010. Large-scale atmospheric circulation changes are associated with the recent loss of Arctic sea ice. *Tellus A*, 62:1-9.

Overland, J.E. and M. Wang, 2013. When will the summer Arctic be nearly sea ice free? *Geophysical Research Letters*, 40:2097-2101.

Overland, J.E. and M. Wang, 2016. Increased variability in early winter subarctic North American atmospheric circulation. *Journal of Climate*, 28:7297-7305.

Overland, J.E., M. Wang, N.A. Bond, J.E. Walsh, V.M. Kattsov and W.L. Chapman, 2011. Considerations in the selection of global climate

models for regional climate projections: the Arctic as a case study. *Journal of Climate*, 24:1583-1597.

Overland, J.E., M. Wang, J.E. Walsh and J.C. Stroeve, 2014. Future Arctic climate changes: adaptation and mitigation timescales. *Earth's Future*, 2:68-74.

Overland, J.E., J.A. Francis, R. Hall, E. Hanna, S.-J. Kim and T. Vihma, 2015. The melting Arctic and mid-latitude weather patterns: Are they connected? *Journal of Climate*, 28:7917-7932.

Park, H., J. Walsh, A.N. Federov, A.B. Sherstukov, Y. Ijima and T. Ohata, 2013. The influence of climate and hydrological variables on opposite anomaly in active-layer thickness between Eurasian and North American watersheds. *The Cryosphere*, 7:631-645.

Parkinson, C.L., 2014. Spatially mapped reductions in the length of the Arctic sea ice season. *Geophysical Research Letters*, 41:4316-4322.

Parkinson, C.L. and J.C. Comiso, 2013. On the 2012 record low sea ice cover: Combined impact of preconditioning and an August storm. *Geophysical Research Letters*, 40:1356-1361.

Pavlova, T.V. and V.M. Kattsov, 2015. Expected Arctic precipitation and evaporation changes through the 21st century: projections with an ensemble of global climate models (CMIP5). *MGO Proceedings*, 579:22-36.

Petoukhov, V. and V.A. Semenov, 2010. A link between reduced Barents-Kara sea ice and cold winter extremes over northern continents. *Journal of Geophysical Research*, 115:D21111, doi:10.1029/2009JD013568.

Pithan, F. and T. Mauritsen, 2014. Arctic amplification dominated by temperature feedbacks in contemporary climate models. *Nature Geoscience*, 7:181-184.

Raisanen, J., 2007. How reliable are climate models? *Tellus*, 59A:2-29.

Rogers, T.S., J.E. Walsh, M. Leonawicz and M. Lindgren, 2015. Arctic sea ice: Use of observational data and model hindcasts to refine future projections of ice extent. *Polar Geography*, 38:22-41.

Romanovsky, V.E., S.L. Smith, H.H. Christiansen, N.I. Shiklomanov, D.A. Streletskiy, D.S. Drozdov, N.G. Oberman, A.L. Kholodov and S.S. Marchenko, 2013. Permafrost. *Arctic Report Card: Update for 2013*. National Oceanic and Atmospheric Administration (NOAA).

Screen, J.A. and I. Simmonds, 2014. Amplified mid-latitude planetary waves favour particular regional weather extremes. *Nature Climate Change*, 4:704-709.

Semenov V.A. and M. Latif, 2015. Nonlinear winter atmospheric circulation response to Arctic sea ice concentration anomalies for different periods during 1966–2012. *Environmental Research Letters*, 10:054020, doi:10.1088/1748-9326/10/5/054020.

Simmonds, I. and I. Rudeva, 2012. The great Arctic cyclone of August 2012. *Geophysical Research Letters*, 39:L23709, doi:10.1029/2012GL052676.

Taylor, P.C., M. Cai, A. Hu, J. Meehl, W. Washington and G.J. Zhang, 2013. A decomposition of feedback contributions to polar warming amplification. *Journal of Climate*, 26:7023-7043.

Tedesco, M., T. Mote, X. Fettweis, E. Hanna, J. Jeyaratnam, J.F. Booth, R. Datta and K. Briggs, 2016. Arctic cut-off high drives the poleward shift of a new Greenland melting record. *Nature Communications*, 7:11723, doi:10.1038/ncomms11723.

Tilling, R.L., A. Ridout, A. Shepherd and D.J. Wingham, 2015. Increased Arctic sea ice volume after anomalously low melting in 2013. *Nature Geoscience*, 8:643-646.

Timmermans, M.-L. and A. Proshutinsky, 2014. Arctic Ocean Sea Surface Temperature. *Arctic Report Card: Update for 2014*. National Oceanic and Atmospheric Administration (NOAA).

Trenberth, K.E. and J.T. Fasullo, 2013. An apparent hiatus in global warming? *Earth's Future*, 1:19-32.

Urban, M., M. Forkel, J. Eberle, C. Huettich, C. Schmullius and M. Herold, 2014. Pan-Arctic climate and land cover trends from multi-variate and multi-scale analyses (1981-2012). *Remote Sensing*, 6:2296-2316.

USGCRP, 2014. Highlights of Climate Change Impacts in the United States. Melillo, J.M., T.C. Richmond and G. Yohe (eds.). U.S. Global Change Research Program (GCRP).

Wang, M. and J.E. Overland, 2012. A sea ice free summer Arctic within 30 years—an update from CMIP5 models. *Geophysical Research Letters*, 39:L18501, doi: 10.1029/2012GL052868.

Wang, M. and J.E. Overland, 2015. Projected future duration of the sea-ice-free season in the Alaskan Arctic. *Progress in Oceanography*, 136:50-59.

Xu, L., R.B. Myneni, F.S. Chapin III, T.V. Callaghan, J.E. Pinzon, C.J. Tucker, Z. Zhu, J. Bi, P. Ciais, H. Tommervik, E.S. Euskirchen, B.C. Forbes, S.L. Piao, B.T. Anderson, S. Ganguly, R.R. Nemani, S. Goetz, P.S.A. Beck, A.G. Bunn, C. Cao and J.C. Stroeve, 2013. Temperature and vegetation seasonality diminishment over northern lands. *Nature Climate Change*, 3:581-586.

3. Arctic terrestrial snow cover

LEAD AUTHORS: **ROSS BROWN, DAGRUN VIKHAMAR SCHULER, OLGA BULYGINA, CHRIS DERKSEN, KARI LUOJUS, LAWRENCE MUDRYK, LIBO WANG, DAQING YANG**

Coordinating lead authors shown in bold

Contents

Key Findings	26
Summary	26
3.1 Introduction	27
3.2 Drivers of change in Arctic snow cover	27
3.2.1 Arctic warming	28
3.2.2 Arctic atmospheric moistening	29
3.2.3 Changing vegetation	29
3.2.4 Increased atmospheric downward longwave radiation	29
3.2.5 Light absorbing particles	29
3.2.6 Changing atmospheric circulation	30
3.3 Observed changes in Arctic snow cover	30
3.3.1 Current monitoring status	30
3.3.2 Observed trends in snowfall and snow cover	34
3.4 Projected changes in snow cover	44
3.4.1 Snow-cover change scenarios	44
3.4.2 Snow cover and snow water equivalent	45
3.4.3 Snow properties	51
3.5 Impacts of a changing Arctic snow cover	51
3.5.1 Coupled soil-climate-vegetation system	52
3.5.2 Biological systems and geochemical cycling	52
3.5.3 Hydrological systems	53
3.5.4 Human systems	53
3.5.5 Feedbacks to northern hemisphere atmospheric circulation	54
3.6 Conclusions and recommendations	54
Acknowledgements	55
References	55

Key Findings

- There is increasing awareness that Arctic snow cover is responding to multiple environmental drivers and feedbacks (such as warming, increased moisture availability, changing atmospheric circulation, changing vegetation, increased frequency of winter thaws, rain-on-snow events). These drivers and feedbacks interact to produce spatially, temporally, and seasonally varying responses in Arctic snow-cover extent, accumulation and snow properties.
- There is widespread multi-dataset evidence of continued reductions in Arctic snow cover. The annual duration of snow on the ground is shortening by 2 to 4 days per decade with the largest negative trends occurring at high latitudes and elevations, which is consistent with polar amplification of warming and enhanced albedo feedbacks. Trends in annual maximum snow accumulation are more uncertain and vary regionally, by elevation and between different data sources, but with a consensus for declining maximum snow accumulation when averaged over the pan-Arctic region. The European sector shows consistent negative trends in annual maximum snow accumulation across all data sources.
- Projected changes in Arctic snow cover with the CMIP5 model ensemble are very similar to those presented in SWIPA 2011 based on the CMIP3 model ensemble. Annual snow-cover duration is projected to decrease by 10–20% over most of the Arctic by 2055 under RCP8.5 but with much larger relative decreases (>30%) over the European sector and western Alaska. Projected changes in annual maximum accumulation show a region of increasing accumulation over the cold high latitudes of the Arctic (of 15–30%), surrounded by a region of decreasing snow accumulation with the largest reductions (>30%) over the European sector and western Alaska. Snow accumulation in the shoulder seasons is projected to decline in all regions in response to a shortening of the snow season. Climate model projections for RCP4.5 show that efforts to limit carbon dioxide emissions result in Arctic annual snow-cover duration stabilizing at a new equilibrium level about 10% lower than current values by 2100, while RCP8.5 results show accelerating losses in snow cover throughout the 21st century.
- Current and projected changes in snow cover generate a cascade of interactions and feedbacks that affect Arctic climate, ground thermal regime, lake and river ice, hydrology, vegetation, biogeochemical activity, exchanges of carbon dioxide and trace gases, and ecosystem services. For some northern communities, a shorter snow-cover season has been linked to declining access to country foods, with important implications for health and disposable income. Increased risk of avalanches and spring flooding are projected in some regions of the Arctic.

Summary

Drivers: Arctic snow cover responds to multiple environmental drivers and feedbacks (e.g. warming, increased moisture availability, changing atmospheric circulation, changing vegetation, increased frequency of winter thaws and rain-on-snow events). These drivers and feedbacks interact to produce spatially, temporally, and seasonally varying responses in Arctic snow-cover extent, snow accumulation and snow properties. Current climate and Earth System Models (ESMs) incorporate many of the drivers (e.g. temperature, precipitation) and feedbacks (e.g. changing circulation, snow-albedo feedback), while others, such as changing vegetation, are not yet fully represented.

Observing systems: The past decade has seen a major increase in the availability of satellite and reanalysis snow products over the Arctic as well as rapid development of a number of new technologies for measuring snow at point-to-local scales. However, there has been relatively little progress in mapping snow depth and snow water equivalent over the Arctic with passive microwave satellite data since the GlobSnow product was developed. New work is exploring the potential of satellite-based radar for Arctic snow cover mapping. There have been some improvements in the real-time reporting and transmission of *in situ* snow depth observations but the development of a coordinated historical archive of *in situ* snow observations for the pan-Arctic region has yet to be realized. A coordinated international effort is underway to develop standard correction methods for automated snowfall and snow depth measuring systems that are being increasingly used in Arctic surface climate networks. Validation of snow products remains a challenge because of the limited surface observing network for snow over the Arctic.

Observed change: There is widespread multi-dataset evidence of continued reductions in annual snow-cover duration over Arctic regions (at rates ranging from -2 to -4 days per decade) over the past 30 to 40 years with the largest decreases observed in the warmer sectors of the Arctic. The influence of greenhouse gas induced warming has been detected in observed decreases of spring snow cover and snow water equivalent. Most of the change is occurring from earlier melt, but delayed snow onset is more important in some regions such as the eastern Canadian Arctic. Trends in annual maximum snow water equivalent (SWE_{max}) are less coherent and vary with dataset, region, elevation and time period. Available evidence suggests that SWE_{max} has decreased over pan-Arctic land areas over the past ~20 years, but with large uncertainties in trend magnitude and regional pattern. There is evidence of increased ice layer development in snowpacks from several regions of the Arctic in response to winter thaw and rain-on-snow events.

Arctic snow modelling: The current generation of detailed physical multi-layer snowpack models is capable of providing realistic simulations of Arctic snow cover including the formation of ice layers. Climate and ESMs employ simpler schemes and while some progress has been made since SWIPA 2011, climate models still exhibit a large spread in the strength of snow albedo feedbacks during the snowmelt period that contribute to an underestimate of observed decreases in Arctic spring snow-cover extent over the past 30 to 40 years. The treatment of snow in forests and the representation of

vegetation distribution and parameters in models have been identified as contributing to the observed model spread in snow albedo feedback. Blowing snow processes need to be included in ESM dynamic vegetation models to capture snow-vegetation interactions (e.g. trapping of snow) from changing Arctic vegetation.

Projected changes: Projected rates of snow cover decrease vary considerably over the Arctic with the largest and fastest changes in the relatively warmer coastal regions (e.g. Alaska, Scandinavia). Larger changes are projected in the spring period in response to positive feedbacks but in some regions of the Arctic (e.g. eastern Canada) the onset date of snow cover is projected to shift more rapidly than the snow-off date. Only northern Siberia and the Canadian Arctic Archipelago are projected to have increased maximum snow accumulation in a warmer climate. Climate model projections with the RCP4.5 stabilization scenario show that efforts to reduce carbon dioxide emissions can contribute to a stabilization of Arctic snow cover loss by the end of the 21st century. The ability to model the potential impact of warming on contaminant cycling is limited by major gaps in the current understanding of snow chemistry processes.

Impacts of changing snow cover: Snow cover is part of a tightly coupled soil-climate-vegetation system with multiple interactions and feedbacks which makes it challenging to isolate the impacts of snow cover changes in Arctic ecosystems. Snow cover sensitivities are complex and may include timing dependencies that create transient phenological and trophic mismatches from rapidly changing snow cover. The sensitivity of vegetation to snow cover change is observed to vary strongly across local scales which makes it difficult to generalize results across regions. Arctic hydrologic systems are changing in response to shifting seasonal distribution of solid and liquid precipitation and the loss of the perennial snow banks that buffer low flow periods in dry Arctic environments. Traditional activities of northern residents such as hunting are sensitive to snow conditions and the Arctic-wide trend towards a shorter snow season is adversely impacting access to country foods with important implications for health and disposable income.

Gaps: The period since SWIPA 2011 has seen important advances in snow science and greater understanding of the role and interactions of snow in Arctic soil-climate-vegetation systems. However, there are still fundamental knowledge gaps and scaling issues that need to be addressed to narrow uncertainties in observing, understanding, and predicting Arctic snow cover and snow-cover processes. Critical areas include: documenting and narrowing the uncertainties in snow observing systems over the Arctic (snow water equivalent in particular); more realistic treatment of sub grid-scale processes and snow-vegetation interactions in ESMs; and fully coupled snow chemistry and physics models. New initiatives such as Global Cryosphere Watch and ESM-SnowMIP will make important contributions to addressing some of these issues.

3.1 Introduction

Seasonal snow covers the Arctic for 7 to 10 months of the year (Figure 3.1) and through its unique physical properties (high reflectivity and low thermal conductivity) and water storage, plays critical roles in energy and water exchanges, ice

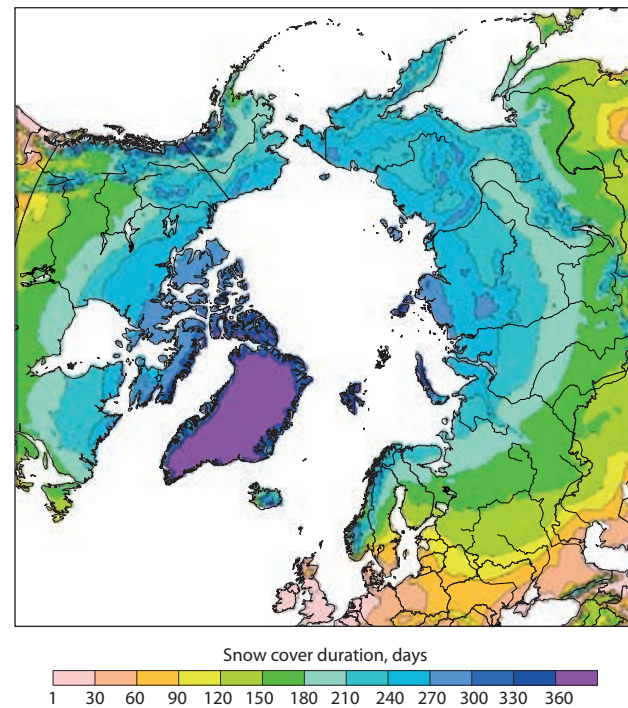


Figure 3.1 Mean annual snow cover duration over Arctic land areas from the NOAA IMS-24 daily snow cover analysis for the snow seasons 1998/99 to 2013/14.

growth, hydrology, ground thermal regime, carbon cycling, and many ecosystem services. The 2011 SWIPA assessment report presented a detailed baseline of Arctic snow cover changes and their impacts (AMAP, 2011; Callaghan et al., 2011a,b). The key message coming out of that assessment was that Arctic snow cover was changing in non-uniform ways via a warmer and moister climate, with demonstrable and widespread impacts. The 2011 assessment also concluded that the rates of observed and projected change in snow cover were likely to challenge adaptive capacity in several ways. The main objective of the present update is to revisit these key messages in the light of five additional years of observations, the newer CMIP5 climate model projections, and recent advances in Arctic snow science (e.g. measurements, modelling, snow processes, feedbacks). Advances in understanding of snow modelling and snow cover change impacts on human systems are addressed in more detail in a parallel IASC (International Arctic Science Committee) cross-cutting report *Arctic winter snow changes: Recent developments and roadmap for observing, modeling and determining impacts* (Bokhorst et al., 2016). While the present update mainly focusses on terrestrial snow cover, it is also recognized that snow cover plays critical roles in the thermodynamics and ecology of sea ice and freshwater ice. This topic is covered extensively in Chapter 5.

3.2 Drivers of change in Arctic snow cover

The amount of snow that falls in the Arctic and is stored on the land surface is a net result of a complex series of processes and interactions. Proximity to moisture, latitude, and elevation are key factors determining the duration of the snowfall season and the total amount of snowfall. Once on the ground, terrain

and vegetation take over as the most important factors in determining the spatial variability in snow cover during winter (Assini and Young, 2012; Clark et al., 2013; Rees et al., 2014; Homan and Kane, 2015) due to frequent wind redistribution of snow (Déry and Yau, 2002; Essery and Pomeroy, 2004; Sturm and Stuefer, 2013). Atmospheric and oceanic circulation as well as variable local moisture sources contribute to year-to-year variations in snow cover.

Arctic snow cover responds to multiple environmental drivers and feedbacks (such as warming, increased moisture availability, changing vegetation, increased frequency of winter thaws and rain-on-snow events (ROS) – see Figure 3.2). These drivers and feedbacks interact to produce spatially, temporally, and seasonally varying responses in Arctic snow cover. The feedbacks are too numerous to include in Figure 3.2 but are usually positive. For example, increasing shrubiness of Arctic tundra allows more snow to be trapped, providing more insulation and warming of the ground (Stieglitz et al., 2003). A warmer soil and deeper active layer provide positive feedbacks to the climate system through enhanced shrub growth (lower albedo) and additional carbon release (Chapin et al., 2005). Increased snow accumulation is playing an important role in observed trends toward permafrost warming and deepening of the active layer in several regions of the Arctic (Park et al., 2014, 2015; Sannel et al., 2016; and Chapter 4). The following sections outline current understanding of some of the main drivers involved in Arctic snow-cover change.

3.2.1 Arctic warming

The Arctic has warmed at twice the global average over the past 50 years due to a number of processes and feedbacks that amplify warming over high latitudes (Pithan and Mauritsen, 2014). A detailed discussion of Arctic Amplification is provided in Chapter 2. Warming of the Arctic has continued

largely unabated since the previous SWIPA assessment in 2011, with the past decade the warmest of the instrumental record (Chapter 2). There is less evidence in the Arctic of the ‘hiatus’ in global warming attributed to a variety of physical mechanisms (e.g. Schmidt et al., 2014; Fyfe et al., 2016) and inadequate sampling of high latitudes (e.g. Cowtan and Way, 2014; Saffioti et al., 2015). Paleoclimate evidence from Canada indicates that current summer temperatures are likely to be the warmest in more than 44,000 years (Miller et al., 2013).

The recent warming of surface air temperatures over Arctic land areas is characterized by a pronounced peak in the October–December period and a secondary peak in April–May (Figure 3.3) that reflect feedbacks from decreasing sea ice and snow cover. The autumn warming is more pronounced over land areas and is more pan-Arctic in nature than spring warming. Much of the observed reduction in snow-cover duration (SCD) at coastal communities in the eastern Canadian Arctic since 1950 is related to a later snow-onset (Brown et al., 2017), which is consistent with the enhanced warming during autumn.

Arctic warming has direct impacts on the timing and duration of snow cover, and on the fraction of precipitation falling as snow which together play a major role in determining the annual maximum snow accumulation. Warming affects snow properties and thermodynamics through temperature dependencies in turbulent energy exchanges, incoming longwave radiation, snow metamorphism, and snow albedo. It also affects the frequency of winter thaw and rain-on-snow events that contribute to ice layer development and changes in snow cover properties. Anthropogenic warming contributions have been identified in northern hemisphere spring snow-cover extent (SCE) reductions (Najafi et al., 2016) and in reductions in snow water equivalent (SWE) over the European sector of the Arctic (Bichet et al., 2016).

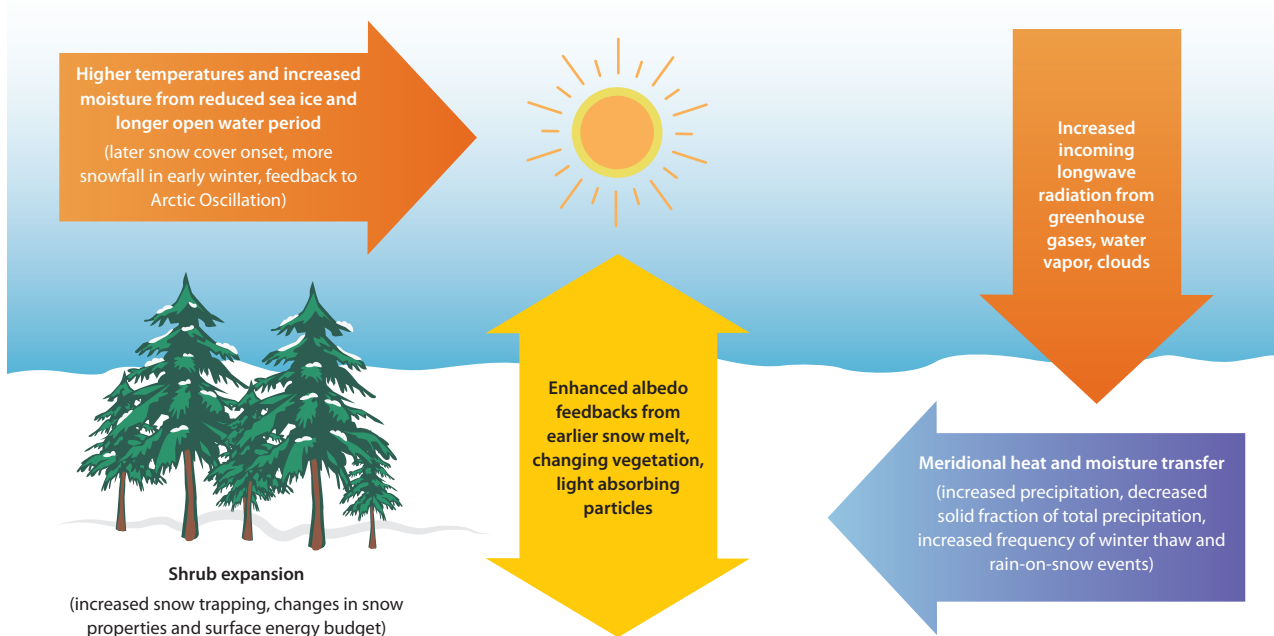


Figure 3.2 Schematic illustration of some of the important drivers influencing Arctic snow cover.

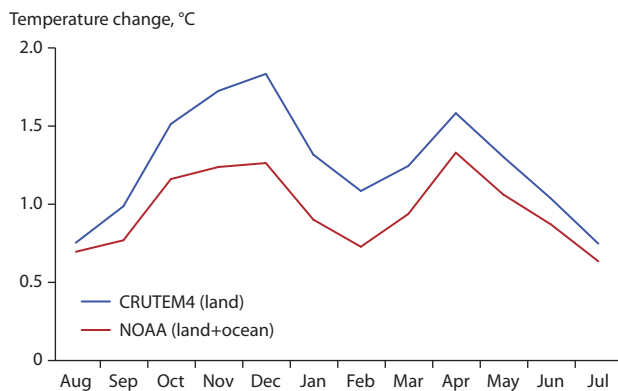


Figure 3.3 Seasonal nature of recent warming of Arctic surface air temperatures (difference between 2006–2015 average and 1951–2010 average) from two datasets, CRUTEM4 (Jones et al., 2012) and NOAA (Karl et al., 2015).

3.2.2 Arctic atmospheric moistening

Human-induced warming, loss of ice cover and enhanced poleward atmospheric moisture transport are contributing to increased atmospheric moisture and increasing precipitation over Arctic land areas (Min et al., 2008; Callaghan et al., 2011c; Zhang et al., 2013). There is also evidence of increasing precipitation extremes accompanying warming in many regions of the globe (Min et al., 2011; Donat et al., 2013) but there is insufficient data coverage over the Arctic to reach conclusions about trends in extremes. Increased evaporation rates also provide positive feedbacks to melting snow and ice through latent heat flux energy, water vapor and cloud cover (Boisvert and Stroeve, 2015). Bintanja and Selten (2014) estimated a precipitation sensitivity of 4.5% per K for the Arctic from a modelling study that suggests precipitation increases of around 2% per decade based on the observed warming, which is comparable to the observed 1.5% per decade increase in cold season precipitation over the 1936–2009 period reported in the previous SWIPA assessment (Callaghan et al., 2011c). Ye et al. (2015a) found evidence of increasing daily precipitation intensity over the 1966–2000 period from stations in northern Eurasia in response to warming and increasing humidity which is consistent with positive trends in precipitation extremes. Changes in precipitation intensity and the solid/liquid fraction of precipitation have important consequences and feedbacks to climate and the hydrological system (see Chapter 10).

3.2.3 Changing vegetation

Snow is a key component of the coupled climate-vegetation system in the Arctic that is thought to provide positive feedbacks to global warming (Jeong et al., 2012; Pearson et al., 2013; Urban et al., 2014). There is extensive evidence since the previous SWIPA assessment of shrub expansion over the Arctic (e.g. Rundqvist et al., 2011; Urban et al., 2014), although available evidence suggests the changes are neither uniform nor simple (Xu et al., 2013; Epstein et al., 2014; Myers-Smith et al., 2015; Ogden 2015). Increased plant mass provides greater potential to trap snow (Whittington et al., 2012), reduces blowing snow sublimation losses, reduces albedo (Loranty et al., 2014), affects snow thermal properties (Domine et al., 2015) and melt season energy budget (Marsh et al., 2010), and provides mostly positive feedbacks to soil warming and plant growth (Gouttevin et al., 2012; Johansson et al., 2013).

There is recent evidence that the rate of tundra greening inferred from satellite NDVI (Normalized Difference Vegetation Index) time series has declined since 1999 (termed ‘browning’) suggesting a decrease in growing season length (Epstein et al., 2014). The reasons for this browning are unclear as there are many factors influencing NDVI, including regional atmospheric circulation and snow depth anomalies (Bieniek et al., 2015), as well as reductions in plant moisture availability from changing hydrology linked to permafrost degradation (Frost and Epstein, 2014; Kim et al., 2014). However, there are also concerns about the robustness of satellite-derived NDVI trends, particularly those from AVHRR (Fensholt and Proud, 2012; Pattison et al., 2015). Landsat-derived greenness trends over Canada and Alaska for the 1984–2012 period (Ju and Maskek, 2016) show that the greening trend dominates the browning trend for all land cover types. Arctic greening/browning is addressed in more detail in Chapter 10.

3.2.4 Increased atmospheric downward longwave radiation

Atmospheric downward longwave radiation (DLR) varies in response to several factors including atmospheric moisture and temperature, the optical depth or thickness of the atmosphere above the surface, the concentration of atmospheric aerosols and greenhouse gases, and cloud cover. DLR is important for snow and ice over high latitudes because it is the main energy source for much of the year during the polar night (Sicart et al., 2006) and has a direct impact on cryospheric processes such as snow sublimation, ice growth (Burt et al., 2013) and snowmelt (Hock, 2005; Wang et al., 2015b).

Obtaining reliable estimates of trends in DLR is a challenge because the global surface observing network is biased to land areas, while DLR estimates from reanalyses and satellite data contain large uncertainties (Wang and Dickinson, 2013). Wang and Liang (2009) evaluated trends in DLR from surface observations made at 3200 stations over 1973 to 2008 and found an average increase of 2.2 W/m² per decade related to increasing air temperature, atmospheric water vapor and carbon dioxide (CO₂) concentrations. The Arctic region was dominated by significant increases where there were stations with sufficient data for analysis. Ma et al. (2014) estimated a significant global DLR increase of 1.54 W/m² per decade over the 1979–2005 period from CMIP5 climate models which was consistent with values obtained from atmospheric reanalyses.

3.2.5 Light absorbing particles

The term ‘light absorbing particles’ (LAP) is applied to various impurities in the snowpack that can affect melt rates through a reduction in surface reflectance (Bokhorst et al., 2016). These include black carbon (BC), brown carbon and dust as well as micro-organisms such as algae. BC is one part of a larger group of short-lived radiative climate forcers that also includes ozone and atmospheric aerosols (AMAP, 2015). The major source of LAP in Arctic snow and ice (~60%) is biomass burning (including burning of agricultural waste) with industrial sources dominating in Svalbard and the central Arctic (Bond et al., 2013; Qian et al., 2015). Dust is an important LAP in areas with patchy snow cover and mountains (Bond et al., 2013). LAP in snow and

ice has been identified as one of the forcings contributing to global warming (Hadley and Kirchstetter, 2012) but with high uncertainty (Qian et al., 2015). LAP are concentrated on the snow surface during the melt season (Doherty et al., 2013) and enhance melt during spring through the reduction in the reflectivity of the snow. In areas with perennial snow cover, such as glaciers, LAP accumulate over successive melt seasons during periods of extended mass loss such as the Arctic is currently experiencing (see Chapter 6). This enrichment in LAP essentially decouples the melt enhancement effect of LAP in these environments from current atmospheric deposition. Tedesco et al. (2016) showed that LAP accumulation on the Greenland Ice Sheet from the recent period of strong summer ablation is one of the factors contributing to the darkening of the ice sheet.

Spring albedo reductions through the presence of BC exhibit significant space-time variability with the highest reductions over the Russian Arctic (1.25%) compared to the Arctic average (0.4–0.6%) (Dou et al., 2012). Bond et al. (2013) estimated the current climate forcing from LAP in snow and sea ice to be $+0.13 \text{ W/m}^2$ with 90% uncertainty bounds of $+0.04$ to $+0.33 \text{ W/m}^2$. Yasunari et al. (2015) estimated that the snow darkening effect of LAP significantly enhances spring surface warming over northern hemisphere mid-latitudes, and raises surface temperatures by approximately 3–6°C near the snowline. Ménégouz et al. (2013) estimated that current BC deposition is responsible for up to ten days less snow cover over the northern hemisphere compared to pre-industrial levels. There is evidence that BC from anthropogenic emissions is declining in the Arctic in response to switches to cleaner burning fuels (Bond et al., 2013), and Skeie et al. (2011) estimated that the maximum BC burden in the Arctic was reached in the 1960s. However, there are exceptions to this trend such as on Svalbard where Ruppel et al. (2014) presented evidence of positive trends in BC over the period 1970–2004 from studies on a Svalbard glacier. A detailed review of BC as a climate forcer in the Arctic is provided by AMAP (2015).

Future trends in LAP from dust, forest fires and burning of agricultural waste are uncertain but decreasing snow cover favors increased potential for dust generation and forest fire frequency (Dumont et al., 2014). Some local increases in BC emissions are anticipated from increased shipping (Ménégouz et al., 2013). There are widely varying treatments of BC in climate and Earth System Models but only a few global models are able to simulate the effects of BC and other LAP in snow (Qian et al., 2015). A recent model assessment of the effect of BC radiative forcing on climate (Namazi et al., 2015) concluded that the impacts of BC emission changes on snow albedo since 1950 were small compared to the net warming of surface air temperatures over the latter half of the 20th century.

3.2.6 Changing atmospheric circulation

Atmospheric variability exerts important controls on snow cover variability at interannual to multi-decadal time scales (Callaghan et al., 2011c; Peings et al., 2013; Wang et al., 2013; Ye et al., 2015b) and snow cover can also influence atmospheric variability through various feedback mechanisms (see Chapter 2 and Section 3.5.5). There is some evidence that Arctic atmospheric circulation may be changing in response to warming and sea ice loss (Overland et al., 2012; Screen et al., 2013;

Petrie et al., 2015) and to Arctic greening (Jeong et al., 2012). As discussed in Chapter 2, these changes contribute to a weakening of westerly winds and more persistent weather patterns such as the prolonged blocking patterns observed over the eastern Canadian Arctic and Greenland from 2007 (Overland et al., 2012) that contributed to enhanced summer melt of snow and ice over the region (Bezeau et al., 2015). However, attributing this change to global warming is still uncertain as Belleflamme et al. (2015) found that similar periods of anomalous circulation have occurred in the past. Another effect of declining sea ice is increased moisture availability and heat in early winter (Screen et al., 2013). This provides enhanced warming and moistening of the lower troposphere, and can also influence circulation. For example, Wegmann et al. (2015) showed that declining sea ice in the Barents and Kara Seas created anomalies in the planetary wave pattern that generated enhanced moisture transport and greater snow depth over western Siberia. This is consistent with the modelling results of Park et al. (2013) who found that anomalously greater snow depths over northeastern Siberia during autumn and winter were significantly correlated to declining September sea-ice extent. The future response of atmospheric circulation over the Arctic to warming and declining sea ice (and the associated impacts and feedbacks with snow cover) is highly uncertain because it involves the nonlinear interactions of many factors (Barnes and Screen, 2015).

3.3 Observed changes in Arctic snow cover

3.3.1 Current monitoring status

The ability to monitor snow cover in the Arctic is constrained by the availability and limitations of the observing networks and satellite data streams, as well as by the availability and limitations in driving data (especially precipitation) for the physical snowpack models used in the growing number of atmospheric reanalyses and snow-cover reconstructions. A detailed review of Arctic snow observing systems was provided in Appendix 4.1 of the SWIPA 2011 report along with a list of online snow data products (Callaghan et al., 2011c). The following sections update this material to reflect current status and new developments. An updated inventory of snow data products and information is available online¹.

3.3.1.1 In situ observations

Regular daily snow depth observations continue to be made at climate and synoptic stations by Arctic countries as part of World Meteorological Organization (WMO) observing requirements. The overall network is largely unchanged since 2011 although there is a growing tendency for automated snow depth and SWE measuring systems in countries outside the Russian Federation where manual observations of snow depth and SWE are still carried out over an extensive network (Bulygina et al., 2011). While there are several issues with automation (Rasmussen et al., 2012), it does enable the expansion of the network into more remote locations and provides new opportunities such as the estimation of sub-daily precipitation amount and phase (Mair et al., 2015). Efforts

¹ http://globalcryospherewatch.org/reference/snow_inventory.php

are currently underway within the WMO Solid Precipitation InterComparison Experiment (SPICE) to characterize measurement uncertainties and errors in automated snowfall and snow depth measurement systems (Nitu, 2013). Activities being carried out under SPICE are contributing to the development of wind undercatch corrections over a wider range of wind speeds and gauge types than in previous assessments (Wolff et al., 2015), which will help reduce or eliminate cross-border inconsistencies in solid precipitation (Scaff et al., 2015) and provide more realistic estimates of winter precipitation across the Arctic.

The representativeness of point snow depth measurements made in open areas at climate and synoptic stations is an important issue for Arctic snow cover monitoring due to the strong spatial variability of snow and because observations may not reflect snow conditions across the surrounding terrain. For example, snow depth observations made at open locations will not detect changes in snow cover related to changing vegetation, while snow surveys made in forested terrain can be influenced by changes in canopy interception and sublimation over time from forest growth (Varhola et al., 2010). Daily snow depth observations at synoptic stations are reported on the WMO circuit in real-time and are used by meteorological centers to generate snow analysis fields for initializing weather prediction models (e.g. de Rosnay et al., 2014). Three key issues with this data stream are that (1) not all synoptic station snow depth observations are reported in real-time; (2) there are major gaps in the reporting network over the Arctic, particularly over northern Canada; and (3) zero depths are not reported consistently (zero depths provide important information for establishing snow-cover boundaries). The WMO Global Cryosphere Watch project has undertaken several initiatives to increase real-time reporting and consistent reporting of zero depths. There is currently no official mechanism for real-time reporting of *in situ* SWE observations to WMO.

Another related issue is the lack of a coordinated historical archive of *in situ* snow observations for the pan-Arctic region. Real-time reports of snow depth data are archived in the Global Historical Climatology Network (Menne et al., 2012) at the U.S. National Centers for Environmental Information and form an important resource for snow-cover monitoring. However, this archive does not include the large body of snow depth and SWE observations that are not reported in real time. These data are widely dispersed in various agencies and institutes and there is currently no coordinated funded activity to merge these data into a consolidated, quality controlled Arctic snow data archive. A workshop was held in 2014 under the Copernicus CORE-CLIMAX project to identify historical snow data sources and mechanisms to develop global archives for snow depth and SWE (WMO, 2015). This resulted in the Finnish Meteorological Institute developing a prototype global archive for historical and near-real-time snow survey data (see Table 3.4 in Section 3.6).

A number of new technologies for *in situ* snow-cover monitoring have recently emerged. These include ground-based LiDAR (Kaasalainen et al., 2011; Deems et al., 2013) and photogrammetry (Bühler et al., 2015); exploiting signal attenuation around GPS antennae to estimate snow depth (Koch et al., 2014; McCreight et al., 2014; Jin et al., 2016); applying optical and near-IR methods to estimate snow grain size and snow surface specific area (Arnaud et al., 2011; Montpetit et al.,

2012; Gallet et al., 2014); visualization of snow crystal structure from micro-tomography (Ebner et al., 2015) and high vertical resolution penetrometer measurements for estimating density and microstructure characteristics (Havens et al., 2013; Proksch et al., 2015). Surface-based ground penetrating radar has also been applied to measure end-of-winter snow depth variability on glaciers in Alaska and the Italian Alps (Forte et al., 2015; McGrath et al., 2015), and over a mountain transect in Alaska (Holbrook et al., 2016). Revuelto et al. (2016) combined terrestrial laser scanner with the physical snowpack model CROCUS to provide high resolution mapping of snow cover at a 5-m resolution over a small catchment in the central Spanish Pyrenees. With these new technologies coming on stream, intercomparison of different measurement methods under controlled conditions (like SPICE) is essential for documenting measurement uncertainties. For example, Proksch et al. (2016) compared snow density estimated from micro-tomography and a variety of gravimetric methods and found the different methods agreed to within 9%.

A number of recent coordinated Arctic snow measurement transects have made important contributions to understanding the characteristics and spatial variability in Arctic snow cover (Derkzen et al., 2009). For example, analysis of data collected over transects made in 2007 and 2011 showed that compared to sites across the subarctic, high-Arctic snow was more spatially variable, thinner, colder, comprised fewer layers, and had a proportionally higher fraction of wind slabs, with these slabs comparatively denser (often exceeding 450 g/cm³) than in the subarctic (350 g/cm³) (Derkzen et al., 2014).

3.3.1.2 Remotely sensed observations

Remote sensing is a powerful tool for monitoring the presence and physical properties of snow cover especially over the Arctic where *in situ* networks are sparse. A vast array of remotely sensed products and information currently exist, with varying temporal and spatial resolution for addressing a wide range of operational and scientific needs from initialization of numerical weather prediction models to climate monitoring. Increasing use and sophistication of land surface models in weather, climate and hydrology has also increased demands for higher resolution and more accurate information on snow-cover variables such as fractional coverage, snow water equivalent, albedo, and melt state. For example, Luus et al. (2013) showed that uncertainty in estimates of Arctic net ecosystem exchange could be reduced by including remotely sensed observations of snow cover in net ecosystem exchange models, providing better understanding of the climate response of the northern carbon cycle. The challenges and research questions related to satellite retrieval of snow cover information have changed little since the previous SWIPA assessment: cloud and forest cover are still key limiting factors for optical satellite systems (Nolin, 2010; Metsämäki et al., 2015) and scaling issues remain an ongoing challenge for evaluating gridded snow products. The recent development of relatively inexpensive unmanned aerial vehicles or systems (UAV/UAS) for mapping high resolution snow depth data is helping address some of these scaling issues (e.g. López-Moreno et al., 2015). A recent review of remote sensing applications for monitoring avalanche risk is provided by Eckerstorfer et al. (2016). Current trends in remote sensing are for more synergistic approaches (Tedesco, 2012; Muñoz et al., 2013) that make use of *in situ* data

and multi-sensor information in a data assimilation framework (e.g. Fernandes et al., 2014; Margulies et al., 2015). In the previous SWIPA assessment it was concluded that the ability to assess the current rate of change in Arctic snow cover was hampered by uncertainties in the remotely sensed data and the lack of standardized, validated products (Callaghan et al., 2011c). Some progress can now be reported, through the European Space Agency (ESA) Satellite Snow Product Intercomparison and Evaluation Experiment (SnowPEX) project being carried out in coordination with the WMO Global Cryosphere Watch (GCW) program and the Climate and Cryosphere (CliC) project of the World Climate Research Programme (WCRP). Results from SnowPEX will provide a benchmark for ongoing evaluation of remotely-sensed snow cover datasets. The ESA Cold Regions High Resolution Hydrological Observatory (CoReH2O) mission represented an important opportunity for the development of enhanced satellite SWE products including coverage over Arctic regions. Although CoReH2O was not selected for implementation, it is increasingly clear that there are fundamental challenges to the retrieval of SWE from conventional satellite measurements and novel mission concepts are required. While snow depth estimates from LiDAR (Deems et al., 2013) and SWE retrievals based both on radar volume scattering interactions (Yueh et al., 2009) and interferometry (Deeb et al., 2011; Leinss et al., 2015) show promise, additional study is required to identify potential pathways for new spaceborne mission concepts. The GRACE (Gravity Recovery and Climate Experiment) gravimetry from space mission (Tapley et al., 2004) launched in 2002 offers new opportunities for large-scale monitoring of seasonal and annual variation in the water stored in the seasonal snowpack over the data sparse regions of the Arctic (e.g. Frappart et al., 2006, 2011; Niu et al., 2007).

Snow-cover extent

Snow-cover extent (SCE) information is usually derived from optical satellite systems because of their high resolution but with obvious limitations related to cloud and forest cover (Nolin, 2010). Extensive effort has been focused on these two issues since the previous SWIPA assessment. For example, the SCAMod methodology (Metsämäki, 2013) uses an estimate of 'apparent forest transmissivity' to account for the forest canopy effect in the observed reflectance data. This method is used to provide daily, weekly and monthly fractional snow-cover information at 0.01° resolution through the GlobSnow snow extent products from 1995 based on the European ERS-2/ATSR-2 and EnviSat/AATSR satellites (Metsämäki et al., 2015). MODIS (Hall et al., 2006) snow products are used extensively for Arctic snow cover monitoring and provide daily snow extent and fractional information at varying resolutions from 500 m to 0.05° for the period since 2000. Lindsay et al. (2015) gave a good example of the application of MODIS daily snow cover products for mapping snow-cover onset, snow-off dates and SCD over Alaska, parts of western Canada and the Russian Far East between 2001 and 2013. The latest Collection 6 of MODIS products contains several improvements related to better long-term calibration and improvements to the cloud mask and atmospheric profile algorithms (Crawford, 2015). Improvements in mapping snow-cover fraction from MODIS in transitional periods during accumulation and melt have been demonstrated with the MODSCAG spectral mixing method (Painter et al., 2009; Rittger et al., 2013). The National

Aeronautics and Space Administration (NASA) Visible Infrared Imaging Radiometer Suite (VIIRS) launched in 2011 extends MODIS coverage with comparable performance (Justice et al., 2013; Key et al., 2013) although one issue for Arctic mapping is that VIIRS maps substantially more clouds than MODIS (Key et al., 2013). High resolution Landsat imagery has also proven useful for validating operational snow-cover products (e.g. SnowPEX) and for ecological applications that require snow cover information at spatial scales of less than 50 m (e.g. Maher et al., 2012; Macander et al., 2015).

The NOAA-CDR (Climate Data Record) weekly snow-cover product (Estilow et al., 2015) is the main satellite-derived product used for climate monitoring of Arctic SCE. The method used to generate the weekly snow cover analysis has changed over time as have the sources and frequency of satellite information used in the analysis. There has not been a comprehensive assessment of the homogeneity of the product over the Arctic but results from product inter-comparisons show good consistency in the spring period (Brown et al., 2010), but evidence of an artificial trend to increasing SCE in the snow-onset period likely to be related to improved ability to detect snow cover from increased satellite frequency and resolution over time (Brown and Derksen, 2013). The NOAA-CDR product is not recommended for Arctic snow cover trend analysis during summer months (July and August) when snow is mainly confined to higher elevations (Déry and Brown, 2007). The NOAA-CDR product is derived from daily snow cover analyses produced by NOAA IMS (Interactive Multisensor Snow and Ice Mapping System) since 1998 (Helfrich et al., 2007). The NOAA IMS daily snow extent analysis is an operational multi-sensor product with daily coverage over the northern hemisphere available at 24-km, 4-km and 1-km resolution from 1998, 2004 and 2014, respectively. Production of a 2-km product recently began over the southern hemisphere. Currently available snow cover products over the Arctic show reasonable agreement during months with more-or-less continuous pan-Arctic snow cover but disagreement under conditions of ephemeral, patchy and melting snow (Frei et al., 2012) and over certain regions such as the Canadian High Arctic (Fernandes et al., 2014).

Snow depth and snow water equivalent

There has been relatively little progress in mapping snow depth and SWE over the Arctic with passive microwave satellite data since the GlobSnow product (Takala et al., 2011) was developed. GlobSnow is now considered the current state-of-the-art, albeit with well-documented limitations for SWE >150 mm where retrievals are biased low, and over mountainous terrain where SWE retrievals are masked out due to higher uncertainties induced by sub-grid terrain complexity (Tong et al., 2010). GlobSnow has a more realistic representation of the spatial distribution of SWE over the Arctic than previous standalone passive microwave algorithms (including recent NASA AMSR-E products) as it includes surface observations of snow depth in the SWE retrieval. This corrects the consistent problem in standalone microwave SWE products of large SWE over-estimation over eastern Siberia due to grain size effects, and underestimation over deep boreal snow (Clifford, 2010). Current satellite SWE products are being evaluated in the SnowPEX project. The progress made with GlobSnow is consistent with the assessment of SWE mapping by Tedesco (2012) who concluded that only through the assimilation of

ground observations and model data can satellite-derived snow depth and SWE fields reach the accuracy level required by the current user community (i.e. climatologists, hydrologists, and weather forecasters).

Recent passive microwave research has looked at coupling detailed physical snowpack models into passive microwave emission models to improve SWE estimates over northern regions (Langlois et al., 2012; Rutter et al., 2014). For example, Montpetit et al. (2013) showed that taking account of ice layers in the snowpack significantly improved the simulated brightness temperatures. This knowledge is currently being used to diagnose ice layer formation from passive microwave data in an assessment of grazing conditions of the Peary caribou herd in the Canadian Arctic (Ouellet et al., 2016).

Recent research has shown some potential for Ku-band (King, 2014), C-band (Sun et al., 2015) and X-band (Leinss et al., 2014) radar to estimate snow depth and SWE for shallow dry snow. While the theoretical multi-frequency response of radar backscatter to SWE is well documented (Ulaby and Stiles, 1980), the relationship is indirect because of the influence of snow microstructure. The radar response from two snowpacks with the same SWE but differing snow stratigraphy (for example, predominantly rounded snow grains typical of taiga snow; faceted grains typical of tundra snow) will be strongly influenced by different volume interactions (which is similar to the case for passive microwave radiometry). When the additional complications of surface roughness, within snowpack layer interfaces, and ground surface interactions are considered, there are clear challenges in relating a measurement of radar backscatter to SWE. Recent progress in the development and evaluation of X- and Ku-band radar-based SWE algorithms was motivated in large part by activities related to the CoReH20 mission concept, which completed Phase A under European Space Agency support in 2012 (Rott et al., 2013). While not selected as the ESA Earth Explorer 7 mission, CoReH20 provided the impetus for technical studies on instrument concepts and design, as well as for field and modeling studies on SWE algorithm development and data assimilation. Field campaigns included the acquisition of time series of tower-mounted X- and Ku-band scatterometer measurements in Sodankyla, Finland, over four winter seasons 2009–2013 (Hannula et al., 2016) and airborne synthetic aperture radar (SAR) measurements at the same frequencies over taiga (Finland, 2012 and 2013), alpine (Austria, 2013), and tundra (Canada; Alaska) snow. Collectively, these datasets provide both the temporal and spatial measurements of backscatter necessary for SWE algorithm development and evaluation. The proposed Chinese global Water Cycle Observation Mission (WCOM) will use a dual-band SAR concept similar to CoReH20 for monitoring SWE (Shi et al., 2014).

The recent period has also seen an explosion in the application of UAV/UAS for high resolution mapping of snow depth over relatively small scales (e.g. Jagt et al., 2015; Michele et al., 2015). A pre-snow season survey or digital elevation model is required to estimate the depth of snow with these methods. UAS offer relatively cost-effective high resolution mapping with accuracies <10 cm for snow depths >1 m (Jagt et al., 2015). Work is currently in progress to develop a lightweight compact gamma-ray detector for UAS deployment (Saiet et al., 2014).

The relatively recent GRACE gravimetry from space mission provides monthly information on terrestrial water storage (i.e. the sum of the water stored in aquifers, soil, surface reservoirs, and snow and land ice) from 2002 based on estimates of the time-variations of the Earth's gravity field derived from the GRACE intra-satellites range. Various methods are used to separate SWE from the other water storage terms which requires the use of data and hydrological or land surface models to estimate the non-snow terms of the water storage. A big advantage of GRACE over passive microwave SWE retrieval methods is that the SWE estimates are unaffected by a forest canopy and variable snow grain size, and are not limited in deep snow conditions. The main problem with GRACE is the relatively coarse resolution (~ 330 km for Level-3 land-water solutions) which limits application to larger river basins and continents. These land-water solutions, based on the use of spherical harmonics formalism, are affected by aliasing effects, known as north-south stripes, amplified by the orbital configuration of the GRACE mission, which is also oriented north-south. These effects are partially mitigated by estimating the local variations in water mass on a network of elementary surfaces as proposed in the Mascon (Rowlands et al., 2010) and through regional solution approaches (Ramillien et al., 2012). Removal of the glacial isostatic adjustment signal from GRACE data is required for analysis of trends, and this can be a significant source of uncertainty in some parts of the Arctic (Forman et al., 2012; Wang and Li, 2016). Assimilation of GRACE SWE estimates into land surface models (Su et al., 2010; Forman et al., 2012) resulted in generally improved hydrological simulations, and GRACE-derived solid precipitation estimates over the Arctic (Seo et al., 2010) were found to agree more closely to estimates from the Global Precipitation Climatology Project and ERA-Interim reanalysis than to solid precipitation estimates derived from AMSR-E SWE. Wang and Russell (2016) incorporated GRACE estimates of basin snow water storage into spring runoff forecasts for the Red River Basin demonstrating the utility of GRACE data for hydrological forecasting. The GRACE Follow-on mission (GRACE-FO) scheduled for launch in 2017 will ensure continuity of GRACE data coverage and includes new technology to improve the precision of the measurement system. Current research efforts are focused on downscaling GRACE data to higher spatial and temporal resolutions, and on more accurate segregation of GRACE total water storage into its components.

Melt onset and winter thaw frequency

Knowledge of melt timing and duration, and the frequency of winter thaw events are important in hydrological and ecological applications. For example, winter thaws can contribute to the generation of thick basal ice layers that impede grazing by herbivores and disrupt the sub-nival habitat of small animals (Callaghan et al., 2011c; Reid et al., 2013; Wilson et al., 2013). Winter thaw events and early snowmelt may also damage shrub species and tree roots, affecting plant phenology and reproduction in the Arctic (Bokhorst et al., 2009; Callaghan et al., 2011c). Melt timing and duration also play a role in snow albedo feedbacks to the climate system. Active and passive microwave sensors are very sensitive to liquid water which makes them

ideally suited for mapping melt onset in spring, and winter thaw events (Nolin, 2010). Wang et al. (2011) combined active and passive microwave satellite data to provide an integrated pan-Arctic melt onset dataset for northern high-latitude land surface, ice caps, large lakes, and sea ice over the 2000–2009 decade. Over the terrestrial Arctic, tree fraction and latitude explained more than 60% of the variance in melt onset date, with elevation also an important factor. Mortin et al. (2012) also used Ku-band QuikSCAT daily backscatter data to monitor pan-Arctic seasonal freeze-thaw transitions from 1999 to 2009 and showed that the spatial pattern of the freeze-thaw transition changed substantially from year to year confirming the earlier work of Bartsch (2010) and Bartsch et al. (2010). Wilson et al. (2013) documented substantial interannual variation in the distribution and frequency of thaw-refreeze events in Alaska between 2001 and 2008 from analysis of QuikSCAT data.

These earlier QuikSCAT-based studies were too short for trend analysis. Wang et al. (2013) showed that a satellite passive microwave melt onset retrieval algorithm based on temporal variations in the differences of the brightness temperature between 19 and 37 GHz was as effective as QuikSCAT for melt event detection and provided estimates that were more closely linked to observed snow-off dates than previous studies. Analysis of trends in the integrated pan-Arctic (north of 50°N) melt onset date (MOD) dataset over the 1979–2011 period found significant trends toward earlier MOD of 2 to 3 days per decade were mainly concentrated over the Eurasian land sector of the Arctic, which is consistent with changes in spring SCE observed with visible satellite data. Spring surface air temperature was found to be the dominant factor in explaining interannual variability and trends, with little influence from low-frequency modes of atmospheric circulation.

Semmens and Ramage (2013) used the passive microwave record from 1988 to 2010 to assess snowmelt timing trends for the Yukon River basin, Alaska/Canada and found a lengthening of the melt duration period for the majority of the sub-basins as well as earlier melt onset trends in the higher elevations and northernmost sub-basins (Porcupine, Chandalar, and Koyukuk rivers). Analysis of late winter melt events in the same regions with both active and passive microwave data (Semmens et al., 2013) showed that most early melt events were related to warm air intrusions with only a limited number of events associated with rain-on-snow events. Wang et al. (2016) developed an algorithm for winter melt event detection from passive microwave data and found large temporal and spatial variability in Arctic winter melt events over years and regions, with little evidence of significant trends between 1988 and 2013. Recent work developing a rain-on-snow detection algorithm with the Advanced Microwave Scanning Radiometer for the Earth Observing System (AMSR-E) passive microwave radiometer (Dolant et al., 2016) showed promising results over northern Quebec.

Time series of passive microwave satellite data provide the longest record for melt mapping with data from 1979. This series of data will hopefully be continued to 2025 from the Defense Meteorological Satellite Program (DMSP) Block 5D3 series². Near identical passive microwave instruments are also available from the Chinese meteorological satellite FengYun (FY)-3 series (Yang et al., 2011). The first FY-3 satellite was launched in 2008 with successors planned to potentially provide data through

2025. There are no Ku-band scatterometer data available at present. The C-band Advanced Scatterometer onboard the Meteorological Operational Polar Satellites provides data from 2006 through 2021. The low frequency C-band data are more sensitive to surface soil freeze/thaw than Ku-band but are applicable for snow melt timing detection (Naeimi et al., 2012). The high resolution SAR C-band data (e.g. Radarsat and Sentinel series) make it possible to monitor snowmelt in mountain areas and on glaciers (Rott and Nagler, 1995), but the narrow swath and relatively low temporal resolution make it challenging for large-scale melt mapping. The L-band radiometer on the NASA SMAP (Soil Moisture Active Passive) satellite also has potential for monitoring snowmelt.

3.3.1.3 Reanalyses and reconstructions

The past five to ten years have seen an increase in the availability of gridded snow cover-related information generated by reanalysis systems such as ERA-Interim (Dee et al., 2011) and MERRA (Rienecker et al., 2011; Reichle et al., 2011) or reconstructed from physical snowpack or land surface models driven by reanalysis or observed forcing data (e.g. Liston and Hiemstra, 2011; Brun et al., 2013; Shi et al., 2013). Reanalysis estimates of snow cover may (e.g. ERA-interim) or may not (e.g. MERRA) assimilate *in situ* snow depth observations. These datasets offer the potential for relatively long periods of spatially and temporally complete information. However, great care must be taken in using these datasets for snow cover monitoring as the forcing data may contain discontinuities and/or artificial trends related to changes in observing streams over time (Mudryk et al., 2015). The spatial resolution of gridded SWE datasets also has an impact on SWE climatology and trends. The spatial resolution of reanalyses is typically on the order of 50–100 km which does not adequately resolve the topography of mountainous regions. Higher resolution downscaled reconstructions (Liston and Hiemstra, 2011; Klehmet et al., 2013) were found to give more realistic SWE patterns than the driving reanalyses.

The physical snowpack models used in these reconstructions can also vary greatly in complexity from simple 1-layer schemes (e.g. Balsamo et al., 2009) to distributed snowpack models that include important Arctic processes such as blowing snow sublimation (Liston and Hiemstra, 2011). A recent evaluation of northern hemisphere SWE datasets (Mudryk et al., 2015) found peak seasonal snow water storage over the northern hemisphere to vary by as much as 50% between datasets with a 2–3 factor range in estimated reductions in northern hemisphere SWE over the 1981–2010 period. Differences in snow models were found to be responsible for most of the spatial spread in mean SWE, while meteorological forcing differences were responsible for most of the temporal spread.

3.3.2 Observed trends in snowfall and snow cover

The picture of Arctic snow cover changes presented in the 2011 SWIPA report (Callaghan et al., 2011c) emphasized different responses of snow cover by season, region, and snow cover variable to pan-Arctic warming and increased precipitation. This view still applies but with growing evidence of a strengthening of pan-Arctic trends in earlier snow disappearance in spring linked to polar amplification of

² http://space.skyrocket.de/doc_sdat/dmsp-5d3.htm

warming (Hernández-Henríquez et al., 2015), along with more widespread evidence of trends toward a later start to the snow season for many regions of the Arctic.

3.3.2.1 Solid precipitation

Solid precipitation is the principal input to a snow cover but obtaining reliable estimates of solid precipitation trends over the Arctic is a challenge (Yang et al., 2005; Groisman et al., 2014; Wolff et al., 2015). *In situ* observations are sparse and are subject to many site and gauge issues (e.g. undercatch of solid precipitation, reporting of trace precipitation, station shifts, changes in measurement protocols, automation) while atmospheric reanalyses often contain wet biases linked to inadequate representation of sea ice as well as inhomogeneities from changes in data streams over time (Rapaić et al., 2015; Vihma et al., 2016). The quality of satellite-derived precipitation estimates over the Arctic was considered low by Serreze et al. (2005) but there have been some improvements in processing (Surussavadee and Staelin, 2009) and further improvements are anticipated with data from the Global Precipitation Measurement Mission (Hou et al., 2014; Mateling, 2016) although the spatial coverage (65°S to 65°N) is a major limitation for Arctic applications. The fifth assessment of the Intergovernmental Panel on Climate Change concluded that while there was evidence for increasing precipitation over northern hemisphere high latitudes across multiple data sources, the wide range of magnitudes meant there was low confidence in the average trend (Hartmann et al., 2013). Hinzman et al. (2013) placed high confidence in positive precipitation trends over the Arctic but noted uncertainties in the spatial pattern of the trend. The 2011 SWIPA analysis of pan-Arctic cold season (October–May) precipitation trends from *in situ* data showed a significant increase of 3.6 mm per decade (1.5% per decade) over the 1936–2009 period with significant increases observed over most sectors of the Arctic (Callaghan et al., 2011c). This estimate is comparable to the significant positive trend of 2.1 mm per decade in annual precipitation reported by Rawlins et al. (2010) from the Climatic Research Unit dataset over the 1950–2006 period. A significant 1.5% per decade increase in annual precipitation was obtained from analysis of multidataset trends over Canadian Arctic land areas over the 1950–2010 period (Rapaić et al., 2015). However, most of the increase over the Canadian Arctic occurred over the period 1950–1990 and the period since is characterized by no trend and a marked increase in the spread between data sources. The recent literature indicates widely varying snowfall trends across the Arctic depending on climate regime (Vihma et al., 2016). Negative trends in snowfall are observed in regions with warmer winter climates such as Scandinavia and the Baltic Sea basin (Rasmus et al., 2015; Irannezhad et al., 2016) while increasing snowfall is documented in cold regions such as northern Canada and Siberia (Kononova, 2012; Vincent et al., 2015).

3.3.2.2 Snow-cover extent, snow-cover duration, and snow-on/snow-off date

Snow cover extent (SCE), snow cover duration (SCD), and dates of snow-on and snow-off are routinely monitored from *in situ* and satellite observations. Trends in these variables are more closely linked to air temperature than depth or snow water equivalent (SWE) where trends are driven by non-linear interactions between air temperature and precipitation (Brown

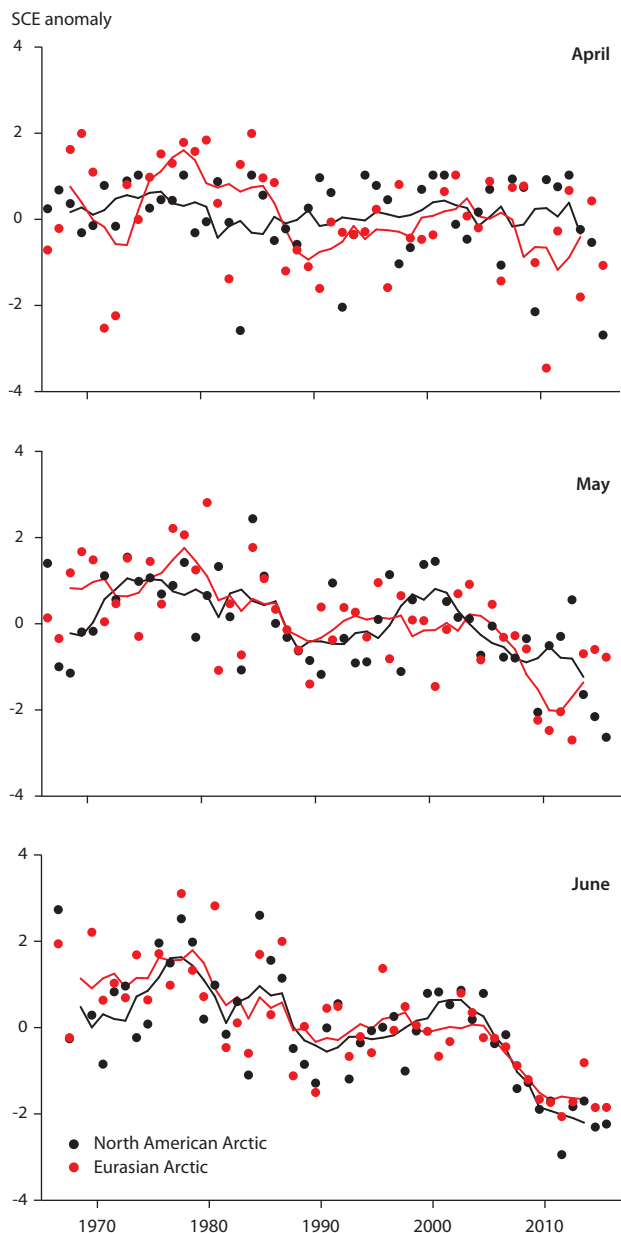


Figure 3.4 Monthly Arctic (land areas $>60^{\circ}\text{N}$) snow cover extent (SCE) standardized (and thus unitless) anomaly time series for 1967–2016 (with respect to the 1981–2010 mean and standard deviation) from the NOAA CDR product (Estilow et al., 2015) for April, May and June. Solid lines depict 5-year running means.

and Mote, 2009). Derksen et al. (2016) estimated the rate of loss of June SCE between 1979 and 2016 from the NOAA CDR data set (Estilow et al., 2015) as -17.8% per decade which is still greater than the loss of September sea-ice extent over the same period (-13.4%). In 2014, a new record low April SCE for the satellite era (1966–) was established for Eurasia (Derksen et al., 2015), while in 2016, new record lows for April and May SCE were reached over the North American sector of the Arctic (Derksen et al., 2016). June 2015 and 2016 had the second and third lowest SCE in North America and Eurasia in the 49-year period of satellite observations (record low in 2012) (Figure 3.4). These rapid reductions are being driven by statistically significant decreases in snow surface albedo and increased air temperatures (Shi et al., 2013), with increased downwelling longwave radiation playing a key role in initiating snow cover anomalies (Wang et al., 2015b). The observed decrease in Arctic spring SCE over the past 30 to

Table 3.1 Summary of trends in Arctic snow cover duration (SCD) for datasets covering at least 30 years.

Region	Period	Data source	Trend in SCD, days/decade			Trend source
			Aug–Jan	Feb–Jul	Annual	
North America						
Arctic (north of 60°N)	1950–2013	Daily snow depth observations from Canada and the USA (56 stations) north of 60°N from the Global Historical Climatology Network (GHCN)	-0.6	-1.5 ^a	-2.2 ^a	This report
High Arctic (north of 66°N)	1955–2013	Daily snow depth observations from Canada and the USA (20 stations) north of 66°N from GHCN	-1.8 ^a	-2.3 ^a	-4.4 ^a	This report
Arctic land area excluding Greenland	1972–2014	Satellite – NOAA CDR Estilow et al. (2015)	-0.4 ^b	-3.9 ^a	-4.3 ^{a,b}	This report
Eastern Canadian Arctic	1950–2011	15 climate stations	-2.5 ^a	-0.7	-3.3 ^a	Brown et al., 2017
Land area north of 60°N, excluding areas of semi-permanent snow	1979–2008	Snow cover reconstruction of Liston and Hiemstra (2011)	-1.0	-0.9	-1.9	This report
Arctic land areas	1979–2011	Passive microwave melt onset date, Wang et al. (2013)	n/a	-1.6	n/a	Wang et al., 2013
Eurasia						
Russian Arctic	1966–2013	<i>In situ</i> daily snow depth observations from Bulygina et al. (2011) updated to 2014	-1.6 ^a	-1.6 ^a	-3.2 ^a	This report
Arctic land area	1972–2014	Satellite – NOAA CDR Estilow et al. (2015)	0.9 ^b	-3.7 ^a	-2.9 ^{a,b}	This report
Land area north of 60°N, excluding areas of semi-permanent snow	1979–2008	Snow cover reconstruction of Liston and Hiemstra (2011)	-0.5	-1.5 ^a	-2.0 ^a	This report
Arctic land areas	1979–2011	Passive microwave melt onset date, Wang et al. (2013)	n/a	-3.3 ^a	n/a	Wang et al., 2013
Pan-Arctic						
Land areas north of 60°N, excluding Greenland	1972–2014	Satellite – NOAA CDR Estilow et al. (2015)	0.4 ^b	-3.8 ^a	-3.4 ^{a,b}	This report
Land areas north of 60°N, excluding areas of semi-permanent snow	1979–2008	Snow cover reconstruction of Liston and Hiemstra (2011)	-0.7	-1.2 ^a	-1.9 ^a	This report

^aStatistically significant trend at 0.05 level; ^btrends in the snow cover onset period contain an artificial increasing trend (Brown and Derksen, 2013).

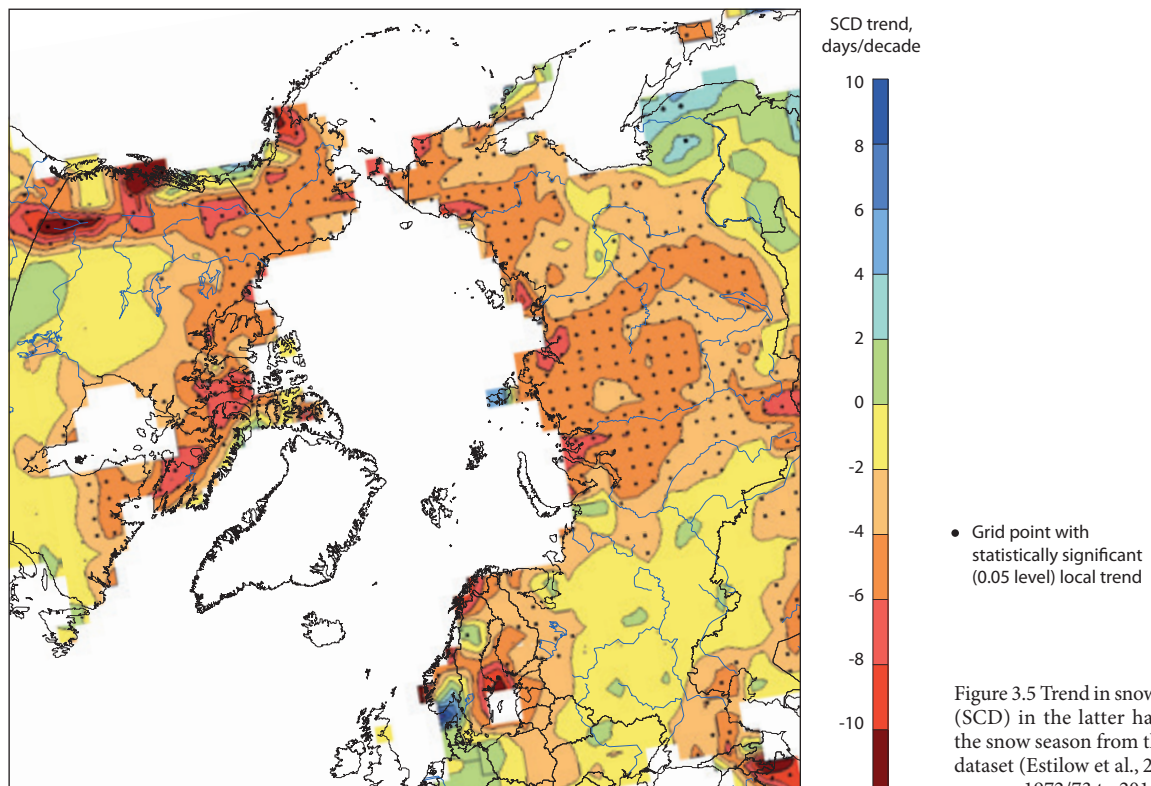


Figure 3.5 Trend in snow cover duration (SCD) in the latter half (Feb–Jul) of the snow season from the NOAA CDR dataset (Estilow et al., 2015) over snow seasons 1972/73 to 2015/16.

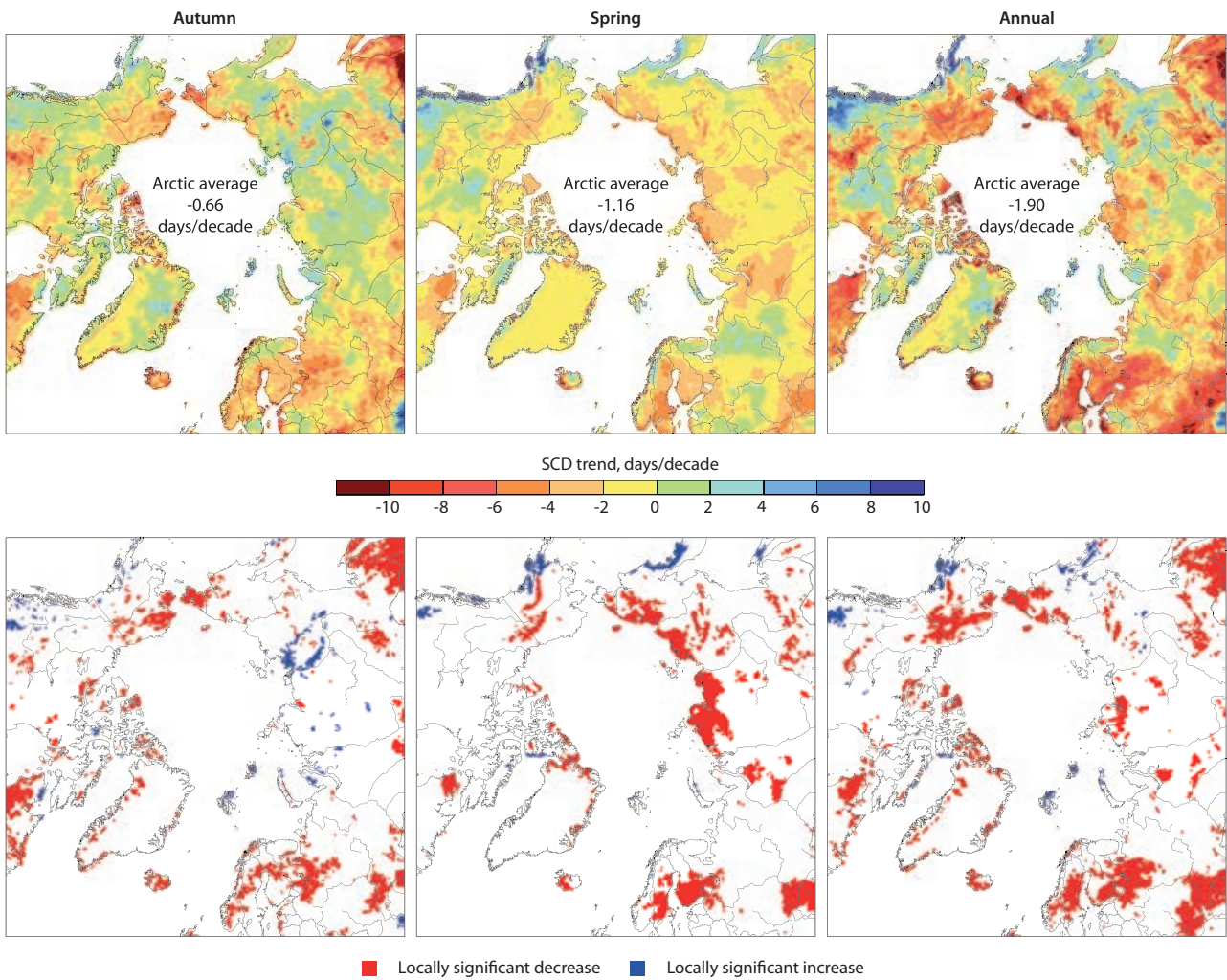


Figure 3.6 The upper panels show trends in snow-cover duration (SCD) in the snow-onset (autumn SCD, Aug–Jan) and melt periods (spring SCD, Feb–Jul) and annual SCD over snow seasons 1979/80 to 2009/10 from the Liston and Hiemstra (2011) snow cover reconstruction. Grid points with statistically significant (0.05 level) local trends for decreasing and increasing SCD are shown in the lower panels.

40 years is only partially captured in the recent CMIP5 climate model historical runs (Derksen and Brown, 2012; Mudryk et al., 2014) and there is evidence that the models underestimate the temperature sensitivity of snow cover (Fletcher et al., 2012; Brutel-Vuilmet et al., 2013) related in part to underestimation of snow albedo feedbacks (Qu and Hall, 2014).

A summary of trends in annual SCD is provided in Table 3.1 for Arctic data sources with at least 30 years of information, along with a breakdown of trends in SCD in the first (Aug–Jan) and second (Feb–Jul) halves of the snow season to provide information on trends in the start and end dates of snow cover. The results provide multi-dataset (*in situ*, satellite, and reanalysis-derived) evidence of significant pan-Arctic reductions in annual SCD of 2–4 days per decade over the past 30 to 40 years, with most of the decreases occurring from earlier disappearance of snow in spring. Significant trends toward later snow cover onset of ~2 days per decade are observed at surface stations in the Russian Arctic, the Canadian eastern Arctic, and the High Arctic region of Canada and Alaska.

The spatial pattern of the SCD trend in the spring half of the snow year from the NOAA-CDR dataset (Figure 3.5) shows clear evidence that the strongest and statistically

significant local trends are located over higher latitudes and higher elevation consistent with polar amplification of warming and enhanced albedo feedbacks (Hernández-Henríquez et al., 2015; Pepin et al., 2015). The corresponding spatial pattern of trends in the snow cover onset period is not shown as it includes an artificial increasing trend related to changes in satellite coverage and resolution over time (Brown and Derksen, 2013). Comparison of SCD trends at the start/end of the snow season between 1979 and 2009 from the snow cover reconstruction of Liston and Hiemstra (2011) (Figure 3.6) shows different spatial patterns with spring decreases more clearly pan-Arctic in nature than SCD trends in the snow cover onset period. Locally significant decreases in spring SCD are mainly located over higher latitudes in agreement with Hernández-Henríquez et al. (2015). SCD trends in the onset period show greater regional variability than spring trends, but locally significant trends typically show decreases consistent with later snow cover onset. Trends to later snow cover onset are reported from analysis of *in situ* observations in Canada (Vincent et al., 2015; Brown et al., 2017), pan-Arctic coastal regions (Rodionov et al., 2013), and northern Eurasia (Kononova, 2012; Popova et al., 2014).

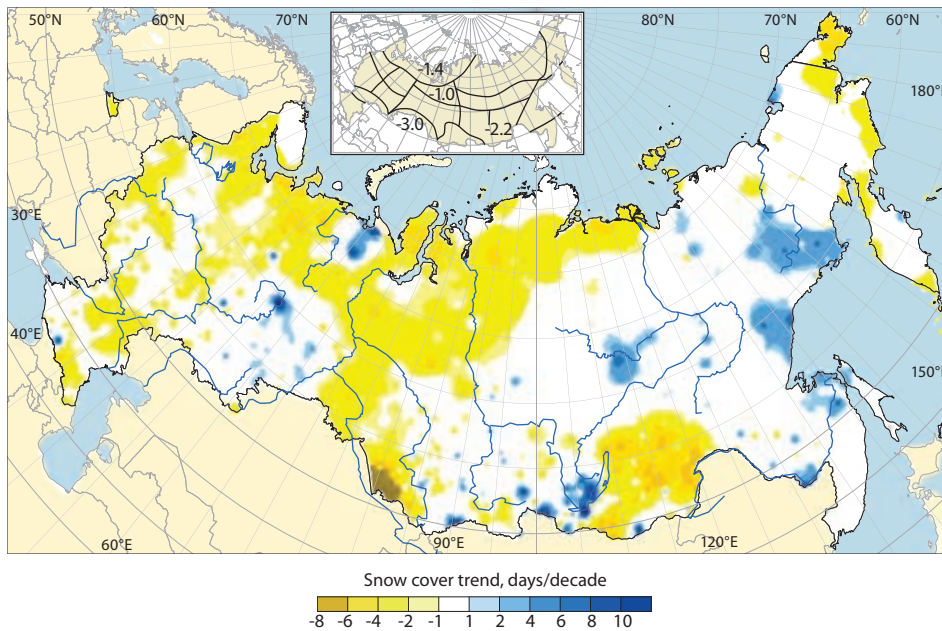


Figure 3.7 Linear trend estimates in time series of the number of days with snow covering more than 50% of the area around a meteorological station for the period 1966–2014. The inset panel shows climate regions where the spatially-averaged trends (% per decade) were statistically significant at the 0.05 level.

The regionally-varying pattern in annual SCD trends over Eurasia from Liston and Hiemstra (2011) (right-hand panels of Figure 3.6) is also observed in updated trends in annual SCD over Russia from *in situ* observations of the number of days with more than 50% of ground covered with snow in the vicinity of the observing station (Figure 3.7). Significant decreases in SCD are observed over regions of European Russia, western Siberia and the Atlantic and Siberian Arctic, while positive SCD trends are infrequent and randomly scattered. Statistically significant estimates of decreasing regional SCD (inset panel Figure 3.7) of -1.0% to -1.4% per decade (~2–3 days per decade) are observed over the Atlantic Arctic and the northern part of the forest and steppe zones of western Siberia. The regionally-averaged SCD series for Russian Arctic stations (north of 60°N) (Figure 3.8) shows evidence of a gradual decline to about 2000 followed by more rapid declines in the post-2000 period in

agreement with results presented by Krenke et al. (2012). SCD in this region decreased by an average 3.2 days per decade (statistically significant at 0.05 level) over the 1966–2014 period (see Table 3.1).

Analysis of changes in melt onset date (MOD) over the northern hemisphere from passive microwave satellite data found MOD occurred 1–2 weeks earlier over the 1979–2012 period with the strongest trends toward earlier MOD over western and central Russia but little change over North America (Mioduszewski et al., 2015). Similar conclusions were obtained from trend analysis of snow-off dates from 636 meteorological stations in the northern hemisphere over the 1980–2006 period by Peng et al. (2013).

An updated analysis of the North American Arctic SCD trends presented in SWIPA 2011 (Callaghan et al., 2011c) was carried out from daily snow depth observations contained in the Global Historical Climatology Network (GHCN) daily archive (Menne et al., 2012). Stations with ≥ 40 years of complete snow cover data in the 1950/51 to 2013/14 snow seasons were used and included 21 Canadian and 35 US stations in the 40–170°W sector. A 1971–2000 reference period was used to compute annual anomaly series at each station for the regional average. The trend in regionally-averaged annual SCD was statistically significant but slightly lower than the value reported in SWIPA 2011 (-2.2 days per decade compared to -2.8 days per decade) with most of the change observed in spring (-1.5 days per decade). The change in the snow onset period (-0.6 days per decade) was not statistically significant. A much stronger negative trend in annual SCD (-4.4 days per decade) was obtained for the 20 stations located above the Arctic Circle over the period 1955/56 to 2013/14 (Figure 3.9).



Figure 3.8 Regionally-averaged variability in annual snow-cover duration (SCD) anomalies (with respect to the 1981–2010 average) over the period 1966–2014 from daily snow depth observations at Russian stations located north of 60°N. Daily snow depths were interpolated to a 200-km grid and the grid values of SCD (days with snow depth >2 cm) used to compute the regional average. The red line is the result of applying a centered 9-term binomial filter. The trend over the period (-3.2 days per decade) is statistically significant at the 0.05 level.

3.3.2.3 Snow depth and snow water equivalent

A summary of regionally-averaged Arctic trends in annual maximum snow depth (SDmax) and SWE for datasets covering a period of at least 30 years is provided in Table 3.2. The trend results show greater regional and temporal variability than for SCD, but with a consensus for declining maximum snow accumulation over the period since 1980 when averaged over the pan-Arctic region.

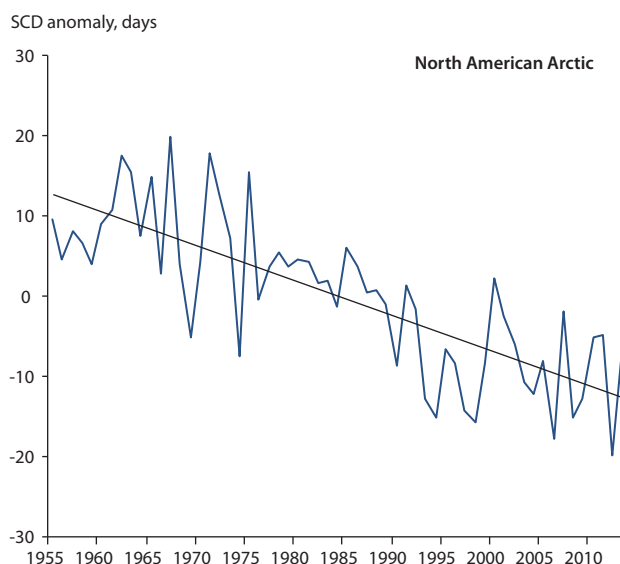


Figure 3.9 Regionally-averaged annual snow-cover duration (SCD) series over the North American Arctic north of 66°N (anomalies with respect to a 1971–2000 reference period) from 20 climate stations in the Global Historical Climate Network archive with ≥ 40 years of daily snow depth data in the 1950/51–2013/14 snow seasons. A 1971–2000 reference period was used to maximize the number of stations in the regional average. The trend over the period (-4.4 days per decade) is statistically significant at the 0.05 level.

Updated trends in SDmax over Russia for the 1966–2014 period (Figure 3.10) show less evidence of significant increases and more evidence of significant decreases compared to the SDmax trends reported by Bulygina et al. (2011) for the 1966–2010 period. Bulygina et al. (2011) found significant increases in SDmax of 3–4% per decade over most of the Russian Arctic west of about 110°E. However, the recent update shows significant increases in only two Russian Arctic regions with trends ranging from 1.4% per decade over the Atlantic Arctic to 2.4% per decade over eastern Siberia (see inset panel in Figure 3.10). These marked changes are attributed to a period of declining SDmax in the post-2000 period (Figure 3.11) driven by a combination of cold dry winters and early spring melt. Osokin and Sosnosky (2014) found that the 2001–2010 decade was characterized by significant reductions in November snow depth over the northeastern European sector, central West Siberia and northeastern Siberia. Warming is also contributing to a declining snowpack by shortening the length of the snow accumulation season and reducing the fraction of precipitation falling as solid precipitation (Gruza and Rankova, 2009; Shmakin, 2010). Corresponding trends in annual maximum snow water equivalent (SWE_{max}) over the 1966–2014 period show some evidence of regionally significant increases at open snow

Table 3.2 Summary of Arctic trends in annual maximum snow depth (SDmax) (cm/decade) and snow water equivalent (SWE) (mm/decade) for datasets covering a period of at least 30 years. SWE trends from gridded datasets were estimated from the annual maximum SWE series computed as the annual maximum water storage north of 60°N divided by the total land area north of 60°N. Greenland was excluded from the trend analysis.

Region	Period	Data source	Trend (units)	Source
North America				
Arctic (north of 60°N)	1950–2013	Daily snow depth observations from Canada and the USA (56 stations) north of 60°N from Global Historical Climatology Network (GHCN)	-0.6 cm/decade	This report
High Arctic (north of 66°N)	1955–2013	Daily snow depth observations from Canada and the USA (20 stations) north of 66°N from GHCN	-0.7 cm/decade	This report
Eurasia				
Russian Arctic	1966/67–2013/14	<i>In situ</i> daily snow depth observations from Bulygina et al. (2011) updated to 2014	0.7 cm/decade	This report
Russian Arctic	1967–2011	Annual SWE _{max} from all snow surveys in Russian Arctic from Bulygina et al. (2011)	-0.2 mm/decade (6.6 ^a mm/decade increase 1967–1993; -4.9 mm/decade decrease 1994–2011)	This report
Pan-Arctic				
Arctic land areas (10-km grid)	1980–2009	Reconstructed daily SWE from snow model driven with downscaled MERRA output (Liston and Hiemstra, 2011)	-0.4 mm/decade	This report
Arctic land areas (75-km grid)	1980–2014	Daily SWE from MERRA Reanalysis (Rienecker et al., 2011)	-3.9 ^a mm/decade	This report
Arctic land areas (75-km grid)	1980–2014	Reconstructed daily SWE from temperature index snowpack model driven with ERA-interim output (Brown and Derksen, 2013)	-4.2 ^a mm/decade	This report
Non-mountainous Arctic land areas (25-km grid)	1980–2014	GlobSnow V2.0 product monthly SWE. Passive microwave satellite algorithm adjusted with available <i>in situ</i> snow depth observations (Takala et al., 2011)	-3.8 ^a mm/decade	This report

^aStatistically significant trend at 0.05 level.

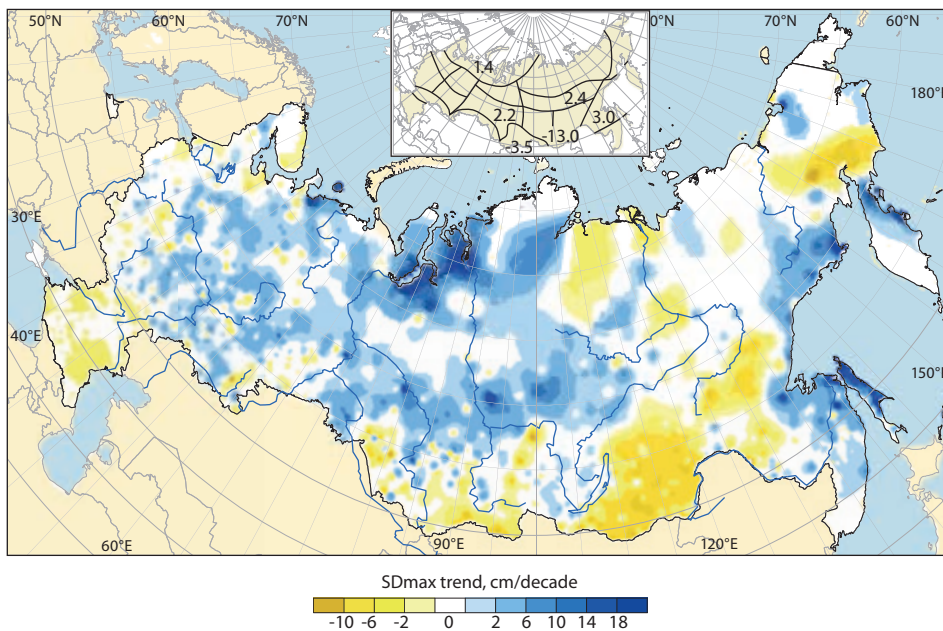


Figure 3.10 Linear trend estimates (1966–2014) in the time series of maximum winter snow depth (SDmax) at meteorological stations. The inset panel shows climate regions where the spatially-averaged trends (%/decade) were statistically significant at the 0.05 level.

survey sites over the northeastern sector of the European Plain (3% per decade) and southwestern Siberia (5% per decade) (Figure 3.12). However, the surveys made in forested terrain show a more patchy response with significant local decreases at many survey sites west of 100°E. The exact reasons for the contrasting response at open and forested sites are unclear but may be partly related to forest growth and increased canopy interception and sublimation of snowfall. Similar contrasting trends in SWEmax between open and forested areas were reported by Maksyutova et al. (2012) over the forest steppe region west of Lake Baikal. The regionally averaged SWEmax series for Russia does not show any evidence of significant trend over the 1967–2011 period (Figure 3.13).

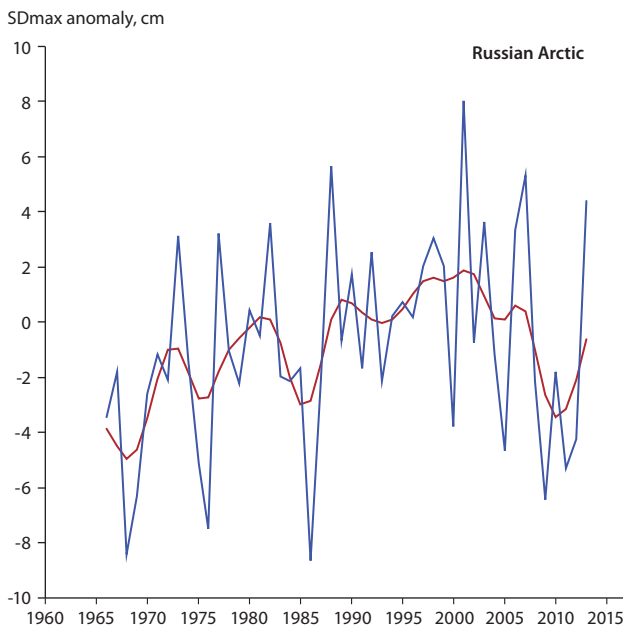


Figure 3.11 Historical variability in regionally-averaged annual maximum snow depth (SDmax) anomalies (with respect to the 1981–2010 average) for Russian stations in the Arctic following the regional averaging method described in Figure 3.8. The red line is the result of applying a centered 9-term binomial filter. The linear trend over the period is not statistically significant.

Some of the largest declines in snowpack have been observed in the relatively ‘warm sector’ of the Arctic (e.g. Alaska, Scandinavia, European Russia, Baltic Sea Basin). In these regions, warming has a strong impact on snow accumulation through reductions in the amount of precipitation falling as snow, particularly in low elevation coastal regions (Rasmus et al., 2015; Irannezhad et al., 2016). In these regions, the sign and magnitude of SWE and SDmax trends can vary significantly with elevation. For example, Skaugen et al. (2012) and Dyrrdal et al. (2013) reported contrasting long-term trends in SDmax and SWE at elevations above and below ~850 meters above sea level (masl) in Norway. SWE trends over southern Norway for the 1931–2009 period for stations located above 850 masl averaged +13 mm per decade in response to precipitation increase of 15–20% over this period (Skaugen et al., 2012). The period 1981–2010 was characterized by predominantly negative SDmax trends over Norway ranging from 5–10% per decade (Dyrrdal et al., 2013). SWE trends in Norway were also found to vary over time in response to the North Atlantic Oscillation (NAO). The 1961–1990 period was characterized by a positive NAO that brought warmer and wetter winters over Norway that contributed to strong elevation gradients in trend sign and magnitude. The relationship between SWE and NAO was less clear in other periods (Skaugen et al., 2012).

Over the North American sector of the Arctic an updated analysis of changes in SDmax at 56 stations in the GHCN dataset over the 1950–2013 period showed less evidence of decreasing snow depth than reported in SWIPA 2011. The trend in SDmax was about one third the value reported in 2011 (-0.6 cm per decade compared to -1.9 cm per decade) and was not statistically significant. However, there was a significant trend toward earlier dates of SDmax of -2.7 days per decade. Vincent et al. (2015) observed significant decreases in SDmax at several stations in the Yukon and Mackenzie Basin over the 1950–2012 period but no significant decreases over the rest of the Canadian Arctic. They reported significant trends toward earlier dates of SDmax at a number of Canadian Arctic stations.

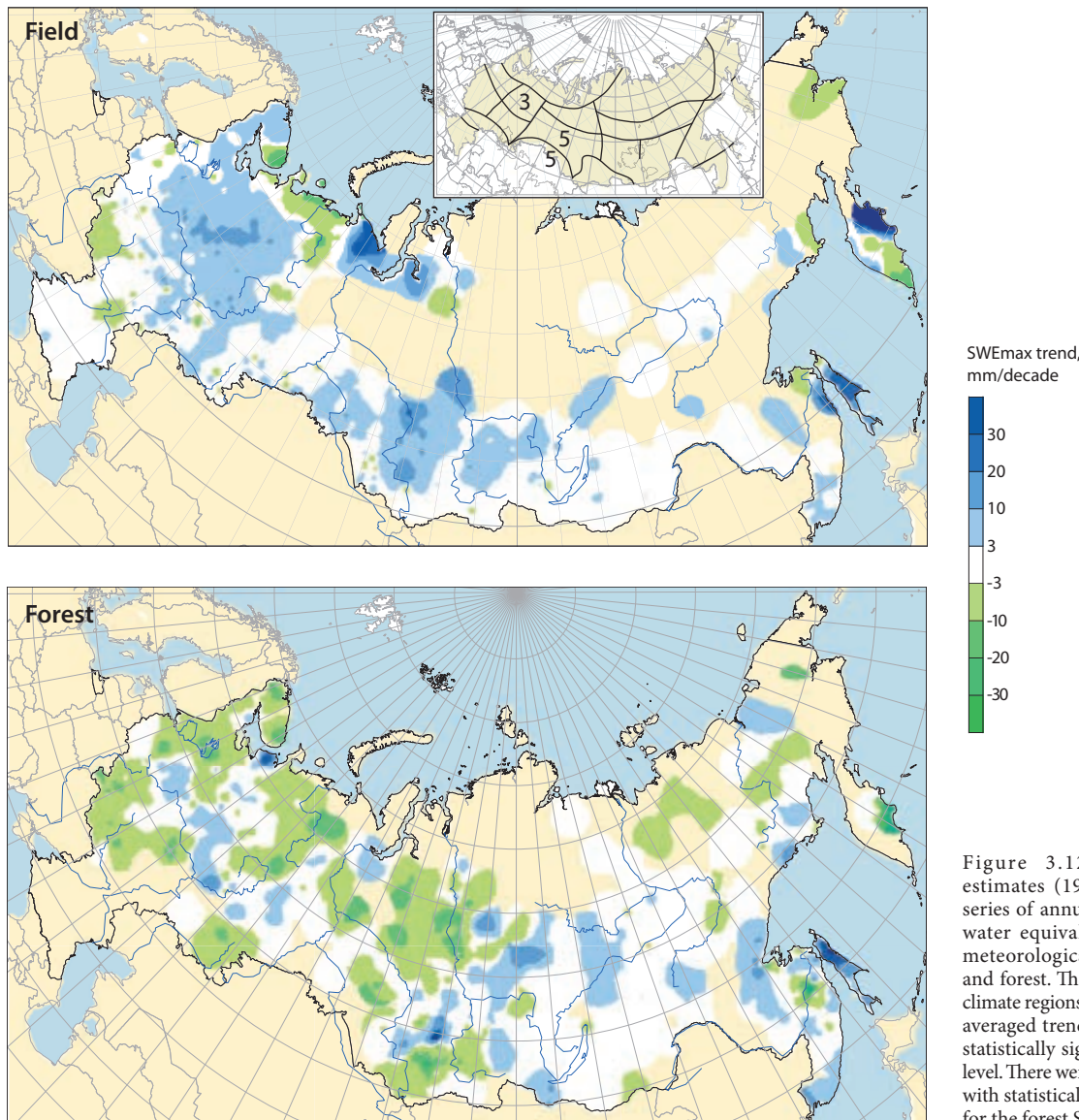


Figure 3.12 Linear trend estimates (1966–2014) in time series of annual maximum snow water equivalent (SWEmax) at meteorological stations in field and forest. The inset panel shows climate regions where the spatially-averaged trends (%/decade) were statistically significant at the 0.05 level. There were no climate regions with statistically significant trends for the forest SWE time series.

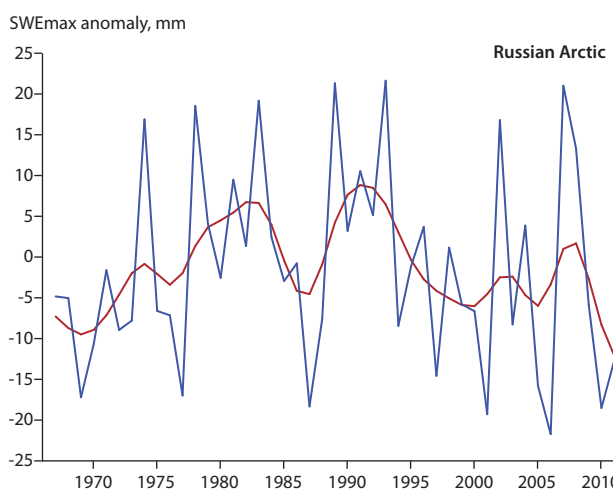


Figure 3.13 Historical variability in regionally-averaged annual maximum snow water equivalent anomalies (SWEmax) (Jan–May period; with respect to the 1981–2010 average) over all snow surveys in the Russian Arctic with at least 40 years of data in the period 1967–2011 following the regional averaging method described in Figure 3.8. The annual SWEmax series is significantly correlated ($r=0.80$) with the annual maximum snow depth series shown in Figure 3.11. The red line is the result of applying a centered 9-term binomial filter. There is no trend over the period of data shown.

Pan-Arctic estimates of trends in snow depth and SWE from recent reconstructions (Liston and Hiemstra, 2011; Park et al., 2012), reanalyses and the new GlobSnow product (Takala et al., 2011) show quite different regional patterns of change around the Arctic (Figures 3.14, 3.15 and 3.16) but with a general decrease when averaged over the Arctic land areas (Table 3.2). Most of the datasets show consistent negative trends in SWEmax over the European Arctic noted previously where snow cover is more sensitive to warming. Bichet et al. (2016) identified an anthropogenic warming signal in the observed SWE decreases over this region. The longer Park et al. (2012) reconstruction (1948–2006) showed mostly positive trends in snow depth up to about 1980 with widespread negative trends established across the pan-Arctic domain after about 1990 in response to rapid warming. A similar trend reversal was observed with Russian Arctic *in situ* SWE observations with significant increases (6.6 mm per decade) in the period 1967–1993, followed by a decline (-4.9 mm per decade) over the period 1994–2011. Observed trends for snow on sea ice are discussed in Chapter 5.

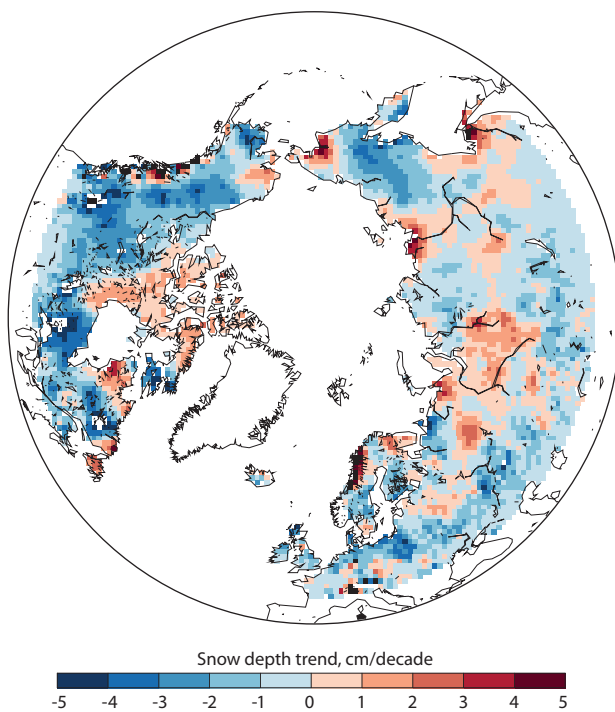


Figure 3.14 Estimated pan-Arctic trend in snow depth (Jan-Mar) over the period 1948–2006 (Park et al., 2012).

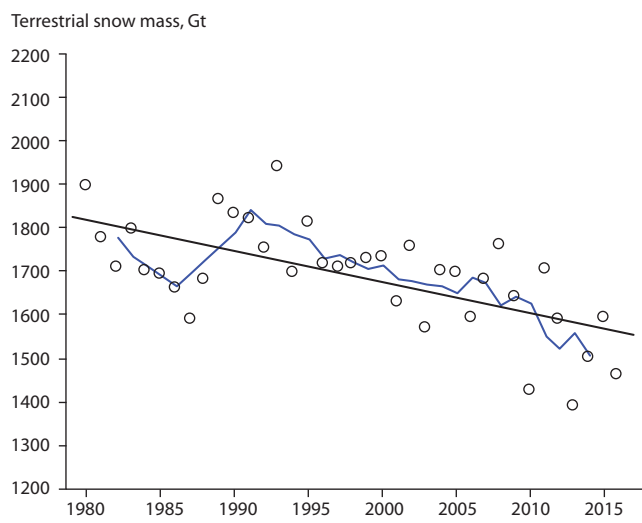


Figure 3.15 Annual variation and trend in maximum values of Arctic land area snow water storage during March from the GlobSnow V2 dataset. March corresponds approximately to the time of annual maximum snow water equivalent (SWEmax) over non-mountainous Arctic land areas. The trend (-4.2% per decade with respect to the 1981–2010 average) is statistically significant.

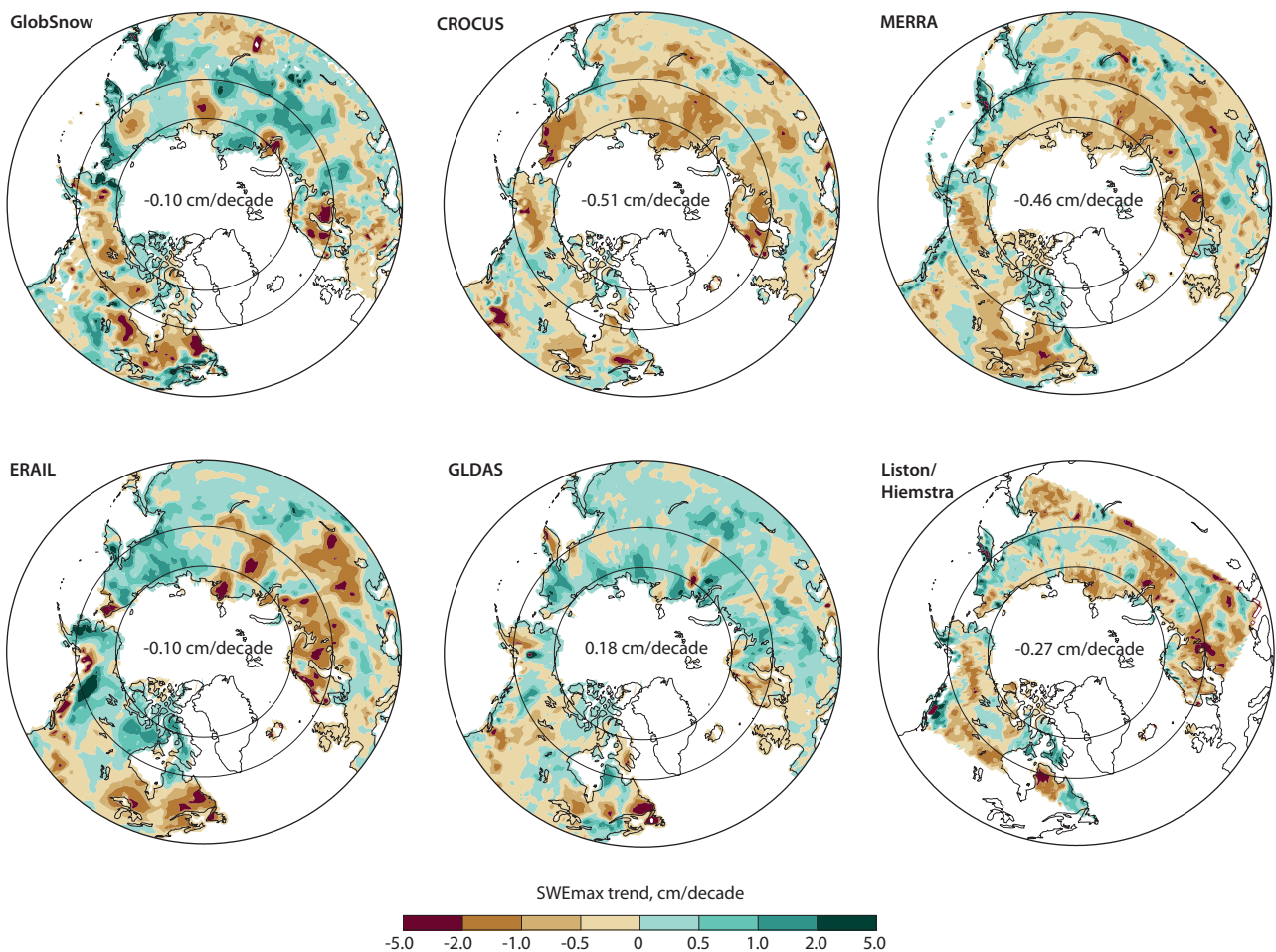


Figure 3.16 Estimated trend in Arctic annual SWEmax over the period 1981–2010 from six datasets (Greenland excluded). The trend in the land area averaged SWEmax series for 60–70°N is shown in each panel. The Liston and Hiemstra trend is computed for the period 1981–2009. Descriptions of the datasets used are provided by Mudryk et al. (2015).

3.3.2.4 Snow properties and winter melt events

Changes in snowpack properties such as albedo, temperature, density, snow grain size distributions, and ice layers are expected from the combined influence of the environmental drivers discussed in Section 3.2. For example, Domine et al. (2015) found that dwarf birch (*Betula glandulosa*) played an important role in modifying the thermal properties of snow by supporting the snowpack and limiting compaction thereby increasing the effective thermal conductivity of the snow layer. However, development of ice layers from winter thaws or rain-on-snow events have the opposite effect on thermal conductivity. Conventional wisdom suggests warming should increase snow density from a decrease in the solid fraction of total precipitation, more rapid metamorphism and potential for more winter thaw events. However, Zhong et al. (2014) showed evidence of significant decreases in snow density from Russian snow surveys over most of the snow season. Repeating the analysis of Zhong and co-workers for Russian snow survey data updated to 2015 confirmed the conclusion of significant decreases in monthly average density over October to February, but with positive trends in May–June snow density. This seasonal response is consistent with concurrent trends to later snow cover onset, increased winter snowfall and earlier spring melt.

Liston and Hiemstra (2011) modelled snow density trends over the period 1979–2009 and found that seasonal snow density increased by 0.29 kg/m³ per decade averaged over the Arctic region (not a significant trend) with a non-significant increase in Arctic-average ROS frequency of 0.03 days per decade. Areas with the largest simulated positive ROS trends were typically located over regions with higher snow accumulation in coastal climates, such as Scandinavia, Baffin Island, Alaska and Kamchatka. Cohen et al. (2015) analyzed ROS events in two reanalyses (MERRA, ERA-interim) and surface observations and concluded that such events are a relatively rare phenomenon over the Arctic with the exception of the same regional hotspots noted by Liston and Hiemstra, with no evidence of robust trends over snow seasons 1979/80 to 2013/14. There was some evidence of ROS variability linked to Arctic Oscillation / North Atlantic Oscillation (AO/NAO) with more ROS events over northeastern Europe in the positive phase of the AO/NAO due to an increased frequency of rainfall. Pedersen et al. (2015) investigated the impact of winter thaw events on snowpack properties in Greenland using the SnowModel physical snowpack model (Liston and Elder, 2006). They found a significant positive trend in the number of winter warming events in parts of western and eastern Greenland for the period 1979–2013. An observational study by Johansson et al. (2011) of 49 years of snow profile stratigraphy data from Abisko, northern Sweden (sub-Arctic region) showed an increase in very hard snow layers between 1961 and 2009, with harder snow in early winter and more moist snow during spring. Toward the end of the observational period the number of occasions with very hard snow layers in the snowpack had more than doubled. In the same period both temperature and precipitation increased, and the air temperature increased particularly at the start and the end of the snow season. Using remote sensing data and ground measurements, Chen et al. (2013) documented a significant increase in the mean ice content of snow over the 1963–2006 period in the regions of northwestern Canada frequented by the Bathurst caribou herd. These results are supported by the recent analysis of satellite passive microwave data

by Langlois et al. (2017) who found a tripling in the occurrence of ice layer formation and ROS events over the Canadian Arctic Archipelago between the periods 1979–1995 and 1996–2011. Care is required in interpreting trend results of melt- and thaw-related phenomena because temporal shifts in snow season timing can generate apparent increasing trends, as noted by Wang et al. (2016).

Changes in winter climate and particularly the frequency and intensity of winter warming events (with or without rain) affect snow properties. There is evidence from satellite data that the duration of melting snow on the ground has increased by 1.3–3.3 days per decade over the period since 1979 (Kim et al., 2015). Melt water percolation into the snowpack accelerates metamorphism affecting density, grain type and grain size. Warming events followed by low temperatures can result in a very dense snowpack and/or ice layers in the snowpack. These ice layers can impede access to forage for caribou and reindeer (*Rangifer tarandus*), and muskox (*Ovibos moschatus*) (Forchhammer and Boertmann, 1993; Hansen et al., 2011, 2014) as well as the small rodents living below the snow (Kausrud et al., 2008). Soil temperatures and thus the permafrost are also affected by ROS-induced changes in snow properties (Westermann et al., 2011). Examples of both ecological and societal consequences were reported from Svalbard during and after the extreme ROS event of February 2012 (Hansen et al., 2014). The event caused a thick ice layer on the ground, increased permafrost temperatures to 5-m depth and triggered slush avalanches with resulting disturbance to infrastructure (a closed airport, restricted traveling in the terrain, closed roads) and wildlife (starvation of reindeer due to the blocked food source). Vikhamar-Schuler et al. (2016) analyzed changes in the frequency and intensity of winter warming events in the Nordic Arctic from long records of daily temperature and precipitation and documented periods with higher frequencies of winter warming events during the 1920s to 1930s and the past 15 years (2000–2014) but found no evidence of significantly increasing trends over the period 1924–2014.

Since few observational time series of snowpack properties are available from the Arctic, the application of physical snowpack modeling is a useful tool for analyzing the response of the snowpack to a changing climate, although the provision of accurate forcing data, particularly precipitation amount and phase, is a challenge (Bokhorst et al., 2016). A number of studies since SWIPA 2011 have applied detailed snowpack models to simulate changes in snowpack conditions and extreme icing events that impede access to grazing or cause vegetation damage (e.g. Vikhamar-Schuler et al., 2013; Bjerke et al., 2014; Rasmus et al., 2014, 2016; Pedersen et al., 2015; Ouellet et al., 2016; Turunen et al., 2016). Vikhamar-Schuler et al. (2013) used the SNOWPACK physical snow model (Bartelt and Lehning, 2002) with meteorological observations from Kautokeino, northern Norway, to relate simulated snowpack properties to historical records of difficult winter grazing conditions for reindeer over the period 1956–2010. Specific years with high reindeer mortality were able to be well reproduced by the model. Rasmus et al. (2014) applied the same snow model with meteorological observations at Muonio, a reindeer district in northern Finland from 1972 to 2010. Winters with icy snow could be distinguished in three out of four reported cases by the SNOWPACK simulations. Similar results were reported by Ouellet et al. (2016) for SNOWPACK simulations over the western Canadian Arctic in a study of factors contributing to the rapid decline of the Peary caribou herd.

3.4 Projected changes in snow cover

3.4.1 Snow-cover change scenarios

There are a number of methods for constructing scenarios (see Mearns et al., 2001 for a discussion of the various methods and their advantages and disadvantages). Physically-based climate models remain a central tool for scenario construction by providing a large ensemble of plausible responses to the increasing concentrations of greenhouse gases in the atmosphere. The 2011 SWIPA report noted a number of shortcomings with the CMIP3 suite of climate models related to their ability to represent Arctic snow processes and feedbacks (Callaghan et al., 2011c). The recent CMIP5 model ensemble (Taylor et al., 2012) includes a larger number of models, higher model resolution, and the inclusion of Earth System Models that include dynamic vegetation and a fully-coupled carbon cycle (Gent, 2012). A comprehensive review of advances in Arctic snow modelling since 2010 is provided by Bokhorst et al. (2016) who concluded that while some progress has been made in model resolution and representation of snow processes, climate models still exhibit a large spread in the strength of snow albedo feedbacks (Qu and Hall, 2014; Thackeray and Fletcher, 2016) that contributes to an underestimate of observed decreases in Arctic spring SCE over the past 30 to 40 years (Derksen and Brown, 2012; Brutel-Vuilmet et al., 2013). The models are also observed to overestimate albedo (Malik et al., 2014; Thackeray et al., 2015) and snow mass during the spring melt season (Shi and Wang, 2015). The treatment of snow in forests (Thackeray et al.,

2014, 2015) and the representation of vegetation distribution and parameters in models (Essery, 2013; Wang et al., 2015a) have been identified as contributing to the observed model spread in snow albedo feedback. Another example comes from a recent Arctic simulation of the HIRHAM5 regional climate model (Zhou et al., 2014) where overestimation of deciduous forest albedo over Siberia contributed to spring temperature biases of approximately -3°C.

The relatively coarse resolution of global climate models (GCMs) is also a contributing factor to spread in snow albedo feedback. Letcher and Minder (2015) showed that realistic representation of snow albedo feedbacks in mountain regions requires model resolutions of ~10 km or better. Crook and Forster (2014) found that CMIP3 climate models underestimated the northern hemisphere surface snow/ice albedo feedback by a factor of 3 to 4 whereas the seasonal cycle feedback was similar in observations and models. This finding suggests the seasonal cycle of albedo is not a good estimate of the strength of a model's snow albedo feedback as initially proposed by Hall and Qu (2006). Some individual models have been shown to have cryospheric radiative feedbacks that agree closely with observational estimates (e.g. CESM1 and CCSM4, Perket et al., 2014). Model differences in snow thermal insulating effects were observed to contribute to large differences in soil temperature (Koven et al., 2013). A series of targeted model intercomparison experiments under the CliC ESM-SnowMIP project (www.climate-cryosphere.org/activities/targeted/esm-snowmip) is planned to help reduce the current model spread by identifying strengths and weaknesses in climate model simulations of global snow cover and providing guidelines for their improvement.

Table 3.3 Climate models used in snow cover change scenarios. Unless indicated, the same model was used for snow cover duration (SCD) and snow water equivalent (SWE) scenarios.

Acronym	Institution	Resolution
BCC-CSM1	BCC (Beijing Climate Center), China Meteorological Administration, China	2.81° × 2.81°
BNU-ESM	College of Global Change and Earth System Science, Beijing Normal University, China	2.81° × 2.81°
CanESM2	CCCma (Canadian Centre for Climate Modelling and Analysis), Canada	2.81° × 2.81°
CCSM4	NCAR (National Center for Atmospheric Research), USA	0.94° × 1.25°
CESM1-BGC	NSF/DOE NCAR (National Center for Atmospheric Research) Boulder, CO, USA	0.94° × 1.25°
CNRM-CM5	CNRM-CERFACS (Centre National de Recherches Météorologiques), France	1.40° × 1.40°
CSIROmk3.6	Commonwealth Scientific and Industrial Research Organisation, Australia	1.88° × 1.88°
GFDL-ESM2M (SWE only)	NOAA Geophysical Fluid Dynamics Laboratory, USA	2.00° × 2.50°
FGOALS-G2 (SCD only)	LASG (Institute of Atmospheric Physics), CESS (Tsinghua University), China	3.00° × 2.81°
FIO-ESM (SCD only)	First Institution of Oceanography, Qingdao, China	2.81° × 2.81°
GISS-E2-R	NASA-GISS, NASA-Goddard Institute for Space Studies, USA	2.00° × 2.50°
HadGEM2-ES (SWE only)	Hadley Centre, UK	1.24° × 1.88°
INMCM4	Institute for Numerical Mathematics, Russian Academy of Sciences, Russia	1.50° × 2.00°
MIROC5	AORI (Atmosphere and Ocean Research Institute), University of Tokyo, Japan	1.40° × 1.40°
MIROC-ESM	Japan Agency for Marine-Earth Science and Technology, Japan	1.88° × 1.88°
MPI-ESM-LR	Max Planck Institute for Meteorology, Germany	1.88° × 1.88°
MRI-CGCM3	Meteorological Research Institute, Tsukuba, Japan	1.13° × 1.13°
NorESM1-M	Norwegian Centre for Climate Services, Norway	1.88° × 2.50°

Dynamical downscaling of snow cover change scenarios with regional climate models (RCMs) provides more detailed spatial information which is important in mountainous regions where the sign of projected snow cover changes can vary with elevation (Kapnick and Delworth, 2013). RCMs are largely constrained by the driving model but do provide potential for added value from more detailed representation of the surface (e.g. land fraction, land cover, topography, ice/water fraction) and surface processes (Koenigk et al., 2015). The resolution of the RCM runs currently available for the Arctic domain of CORDEX (Giorgi et al., 2009) is $\sim 25\text{--}50$ km which may be too coarse for some applications. The Danish RCM HIRHAM5 was run at 0.25° and 0.05° resolution over the Greenland Ice Sheet (Lucas-Picher et al., 2012) to downscale ERA-Interim reanalysis fields for driving ice sheet models. The higher-resolution simulation was considered more realistic but could not be quantified due to a lack of observations.

Statistical downscaling methods can be applied directly to climate model snow cover simulations (e.g. Tryhorn and DeGaetano, 2013) or more typically, to generate bias-corrected time series of driving variables from a reanalysis or climate model that are input to a detailed snowpack (e.g. Brun et al., 2013) or hydrological model (e.g. Deb et al., 2015). McAfee et al. (2014) used statistical downscaling to generate high resolution gridded information on the partitioning of snow and rainfall over mountainous regions of Alaska. High resolution snow cover reconstructions with physical snowpack models (e.g. Liston and Hiemstra 2011; Brun et al. 2013) take account of blowing snow sublimation losses that can be as high as 40% of total snowfall in exposed locations (Reba et al., 2012). Musselman et al. (2015) showed that using physically based windflow models reduces the uncertainty in estimates of blowing snow sublimation losses in complex terrain.

The snow cover change projections developed for the SWIPA update are based on monthly snow cover and SWE output from 16 independent CMIP5 climate models for the historical (1986–2005), RCP4.5 (2006–2099) and RCP8.5 (2006–2099) experiments. Scenarios RCP4.5 and RCP8.5 (van Vuuren et al., 2011) have been adopted as plausible lower and upper bounds for future emission pathways following a recommendation to standardize scenarios across the SWIPA and AAC (Adaptation Actions for a Changing Arctic) assessments. RCP8.5 is similar to the SRES A2 scenario used in SWIPA 2011 to about 2050, but generates stronger warming than the A2 scenario over the latter half of the 21st century. The low emission RCP2.6 scenario was not considered (because it requires extremely aggressive reductions in CO_2 emissions) while RCP6.0 is covered by the spread between RCP4.5 and RCP8.5. The list of models used and their resolution is provided in Table 3.3. Model output was interpolated to a common 200-km polar stereographic grid for computing the multi-model ensemble statistics.

Scenarios of relative change in annual SWEmax and annual SCD over Arctic land areas were generated for three 20-year scenario windows; near-term 2025 (2016–2035), mid-term 2055 (2046–2065) and long-term 2090 (2081–2100), with respect to a 1986–2005 reference period (Figures 3.17 and 3.18). To give some idea of the uncertainty range, the 25th, 50th and 75th percentiles of the 16-model ensemble are plotted following the IPCC (2013) *Atlas of Global and Regional Climate Projections*.

The 50th percentile corresponds to the ensemble median while the 25th and 75th percentiles correspond to the values dividing the distribution of projected changes into the top and bottom 25% (i.e. the highest/lowest four models in the present case). SCD was also separated into the first (Aug–Jan) and second (Feb–Jul) halves of the snow season to analyze changes in snow cover onset and snow-off dates. Regionally-averaged results for projected changes in snow cover were computed over non-glacier grid points because models vary in their treatment of snow in areas where annual accumulation exceeds annual ablation. In light of uncertainties in emission scenarios and the representation of Arctic snow cover in climate models, these projected snow cover changes should be considered rough guidelines as to how the large-scale snow cover climate of the Arctic may evolve in response to two different warming scenarios.

3.4.2 Snow cover and snow water equivalent

Projected changes in SWEmax are shown in Figure 3.17. The RCP8.5 median model results for 2055 are very similar to the 2050 change pattern presented in SWIPA 2011 from the CMIP3 model ensemble showing a region of increasing SWEmax over the cold high latitudes of the Arctic (+15–30%), surrounded by a region of decreasing SWEmax with the largest reductions (>30%) over the European Arctic and western Alaska. This contrasting pattern of projected change in SWEmax is a consequence of non-linear interactions of rising temperature and increasing precipitation on snowfall, the snow accumulation period and winter melt events as noted by Räisänen (2008), and is a robust feature across Figure 3.17. The regions with the largest projected decreases in SWEmax are associated with an increased frequency of low and extremely low snow years (Diffenbaugh et al., 2013).

Annual SCD is projected to decrease by 10–20% over most of the Arctic by 2055 for RCP8.5 (Figure 3.18) but with much larger relative decreases (>30%) over the European Arctic and western Alaska. These results are also very similar to the CMIP3 projected SCD changes presented in SWIPA 2011 (Callaghan et al., 2011c). The magnitude and temporal evolution of the projected SCD changes averaged over the Arctic are strongly dependent on the emission scenario used (Figure 3.19). The RCP4.5 results show evidence of Arctic annual SCD stabilizing at a new equilibrium level about 10% lower than current values by the end of the 21st century while the RCP8.5 results show accelerating losses in snow cover throughout the 21st century. The Arctic-averaged evolution of SWEmax (not shown) exhibits relatively little variation over time and with emission scenario (the shortened accumulation period is offset by increased snowfall). However, the Arctic regionally-averaged monthly SWE results (Figure 3.20) indicate large projected decreases in SWE over the May–October period. The potential for geoengineering to counteract these projected snow cover changes is considered low (Berdahl et al., 2014). Annual maximum accumulations of snow on sea ice are projected to decrease in response to delayed freeze-up (Hezel et al., 2012) and a larger fraction of first-year ice (see Chapter 5).

Some insight into the rate of projected warming for different snow cover variables was obtained by applying the Expected number of Years before Emergence (EYE) method presented by de Elía et al. (2013). This estimates the first year that the climate signal (i.e. the change in snow in response to warming) emerges from the

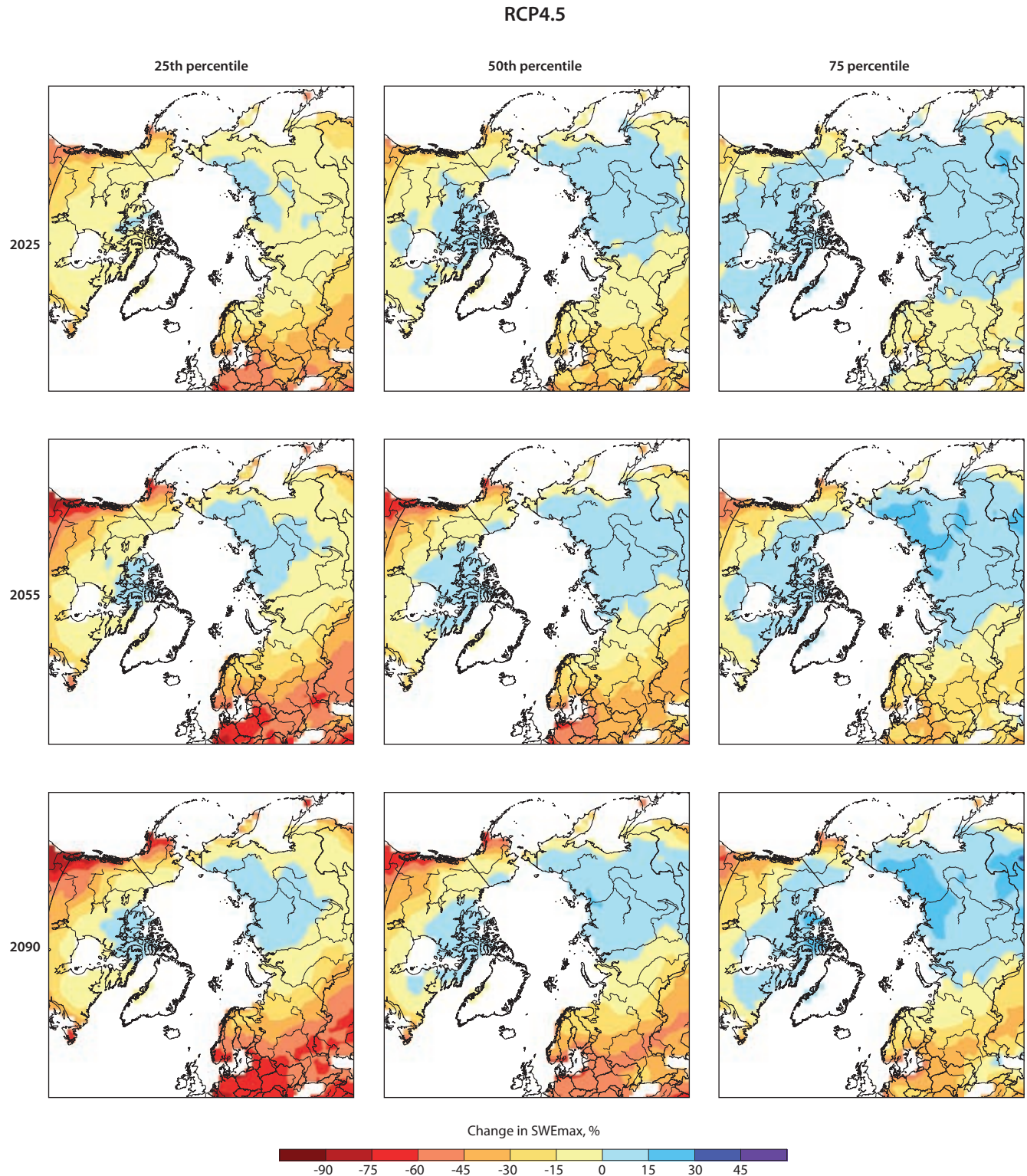


Figure 3.17 Projected relative change (%) in mean annual maximum monthly snow water equivalent (SWE_{max}) for RCP4.5 and RCP8.5 from 16 CMIP5 models with respect to 1986–2005. Results are shown for the 25th, 50th and 75th percentile for three 20-year time slices centered on 2025, 2055 and 2090.

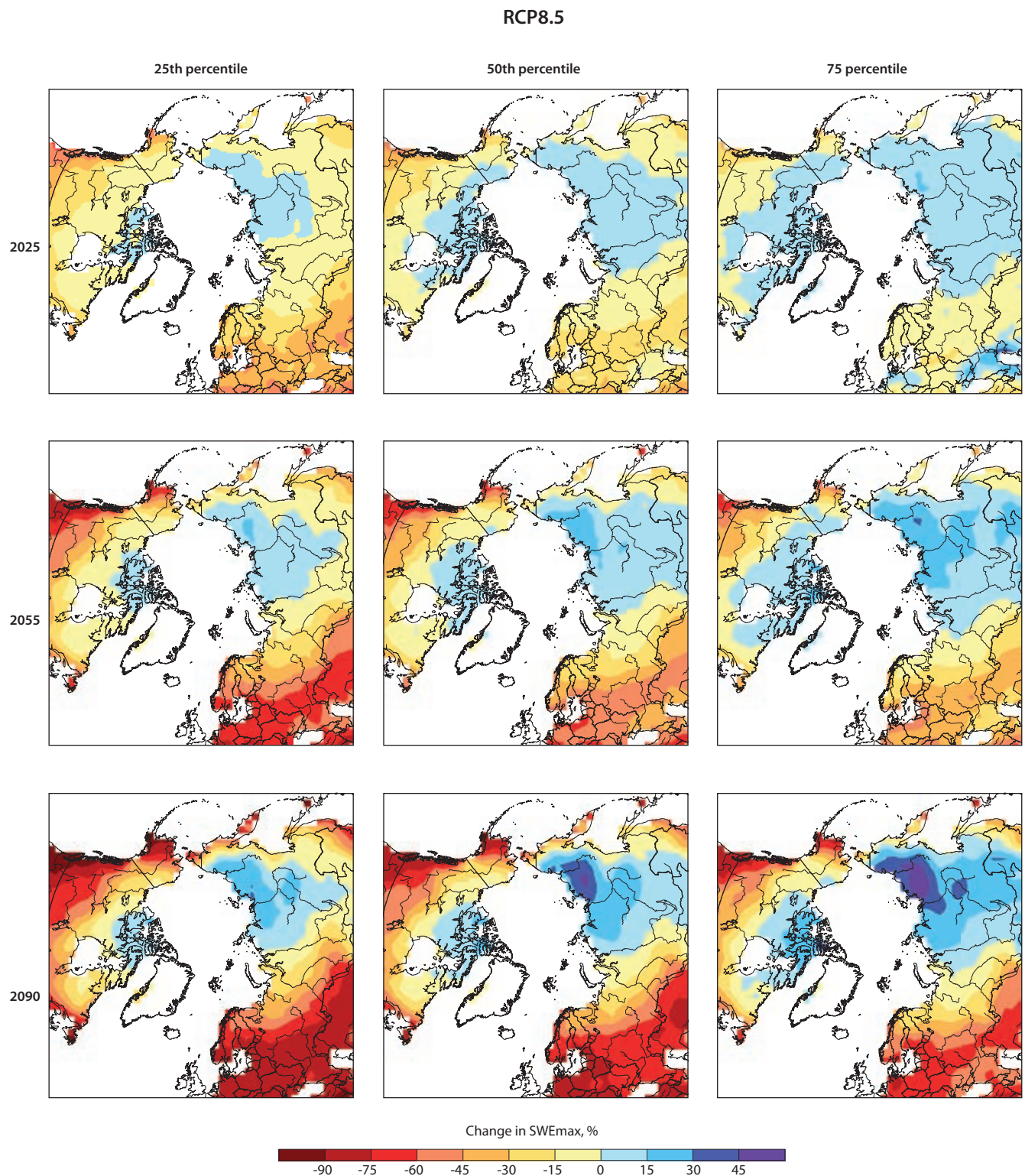


Figure 3.17 (cont.)

RCP4.5

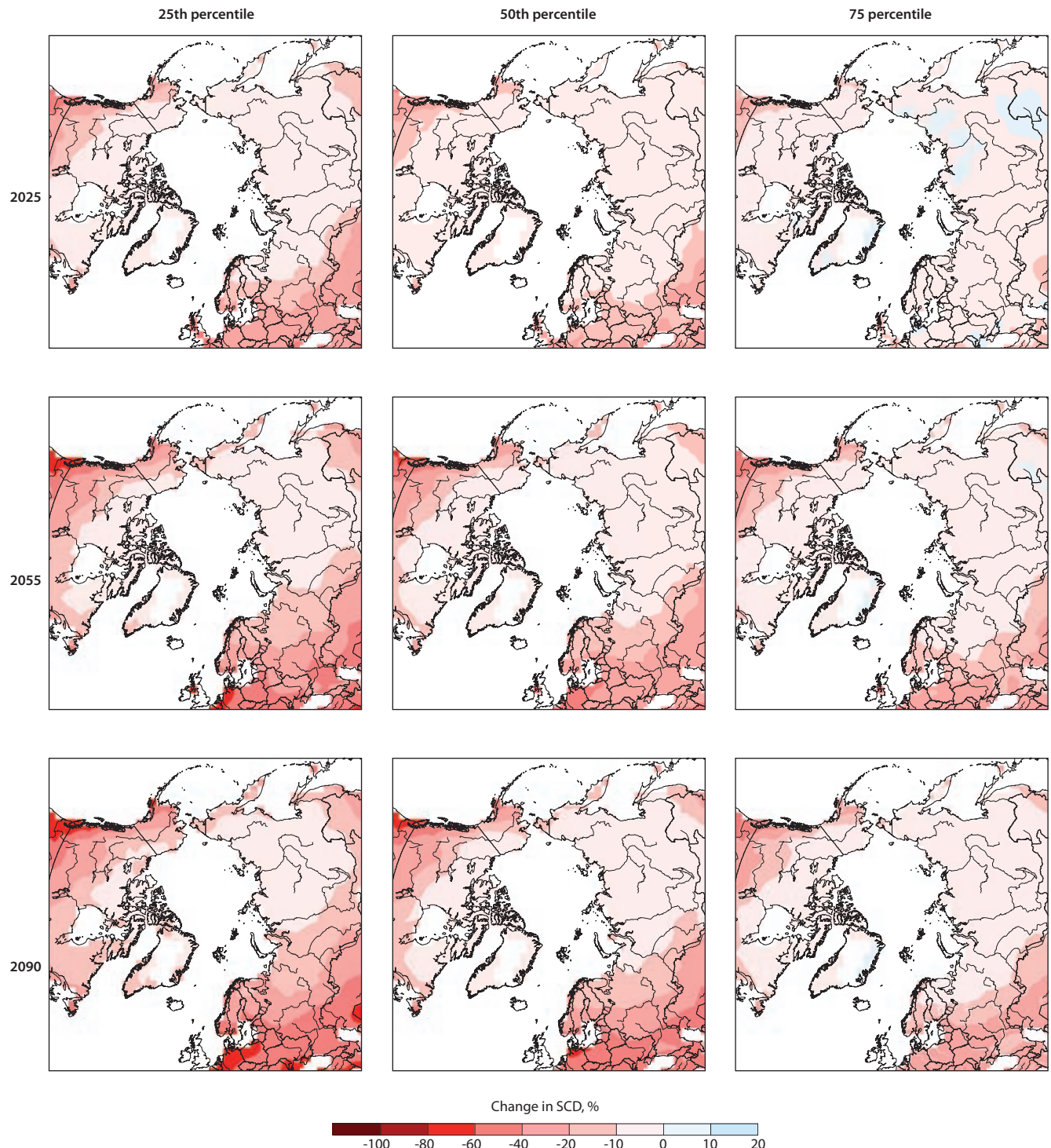


Figure 3.18 Projected relative percentage change in mean annual snow cover duration (SCD) for RCP4.5 and RCP8.5 from 16 CMIP5 models with respect to 1986–2005. Results are shown for the 25th, 50th and 75th percentile for three 20-year time slices centered on 2025, 2055 and 2090.

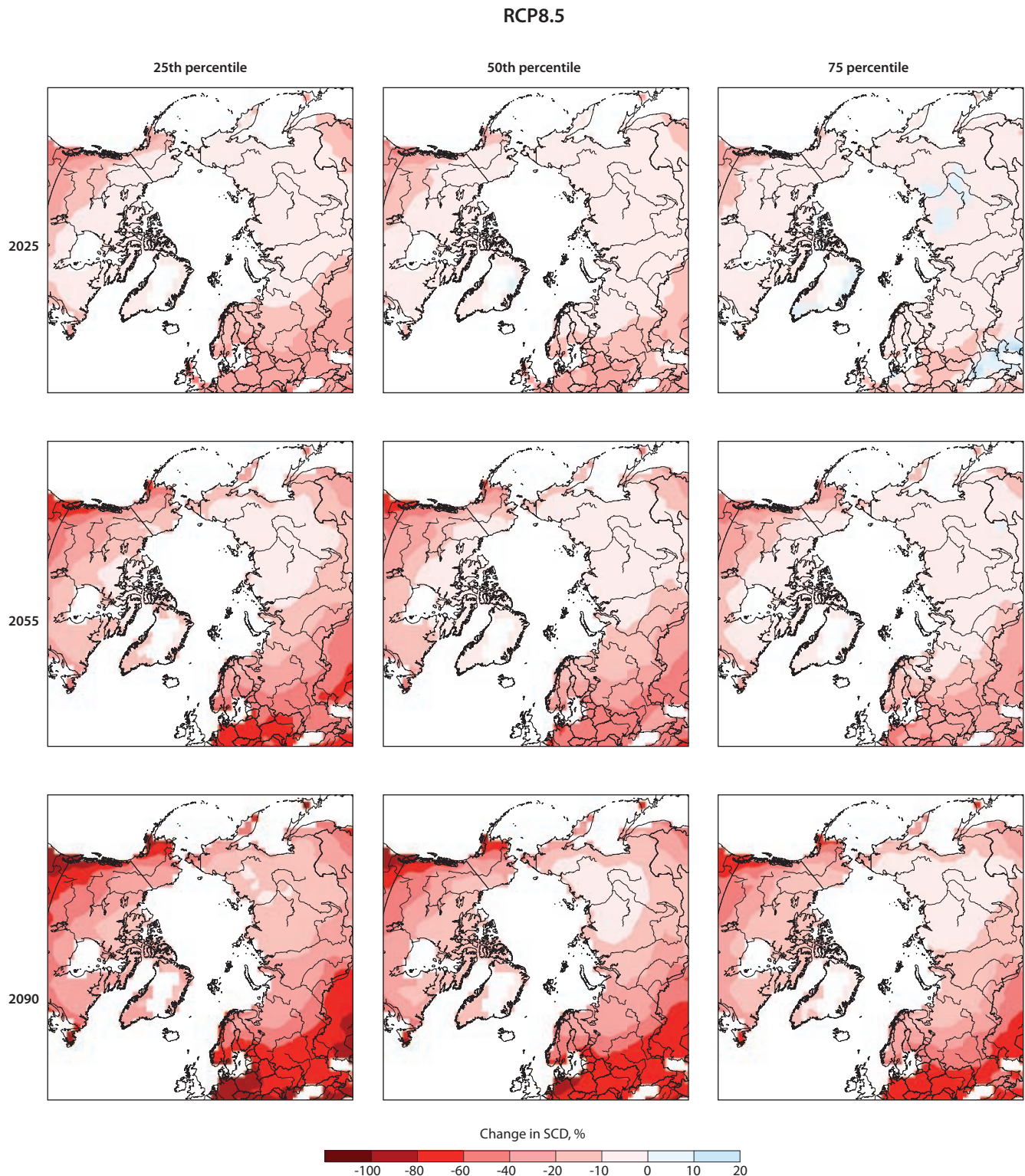


Figure 3.18 (cont.)

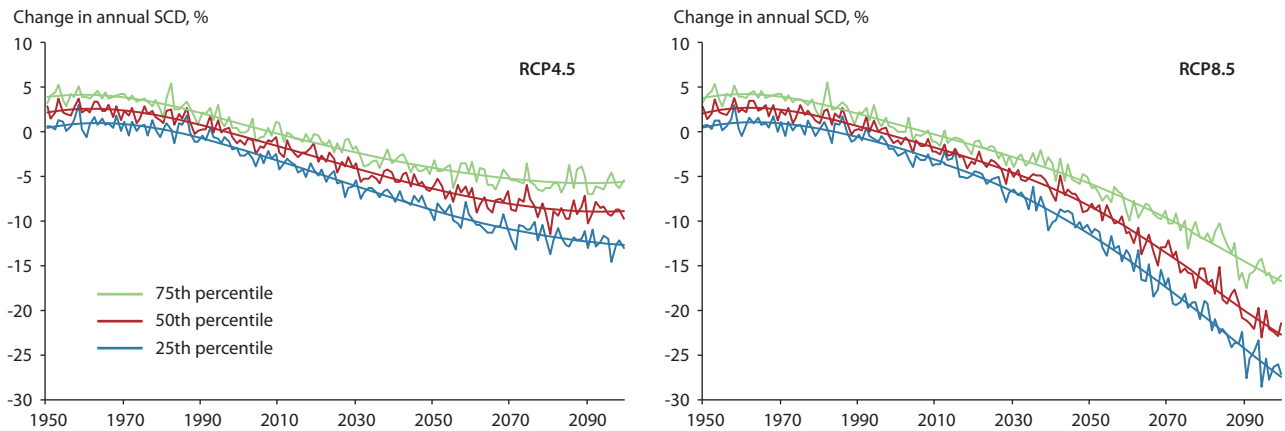


Figure 3.19 Projected relative change in annual snow cover duration (SCD) over Arctic non-glacier land areas under the RCP4.5 and RCP8.5 emission scenarios with respect to the period 1986–2005. The plots show 25th, 50th and 75th percentiles of 16 CMIP5 model runs.

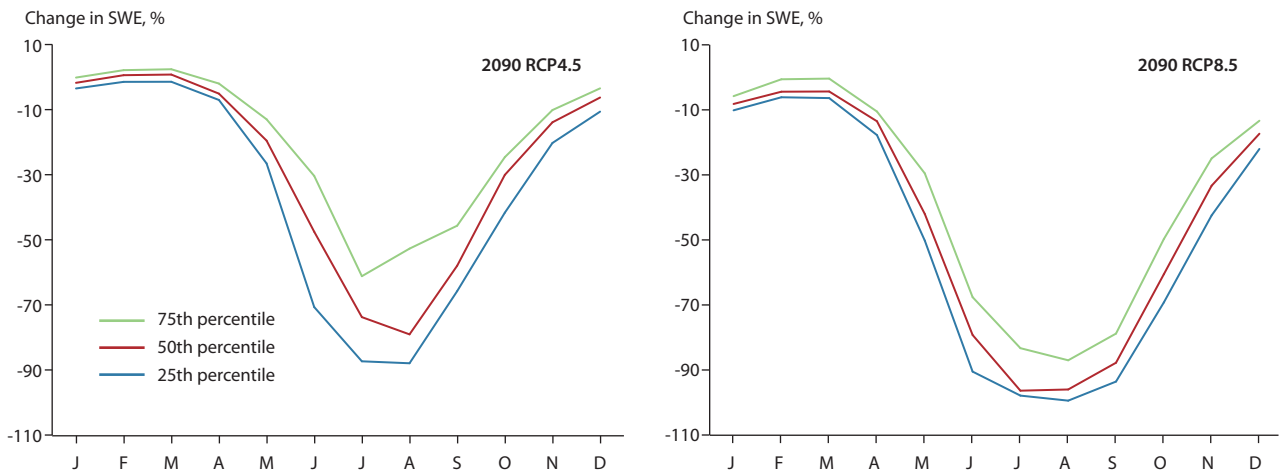


Figure 3.20 Projected relative change in monthly snow water equivalent (SWE) in 2090 over Arctic non-glacier land areas under the RCP4.5 and RCP8.5 emission scenarios with respect to the period 1986–2005. The plots show 25th, 50th and 75th percentiles of 16 CMIP5 model runs.

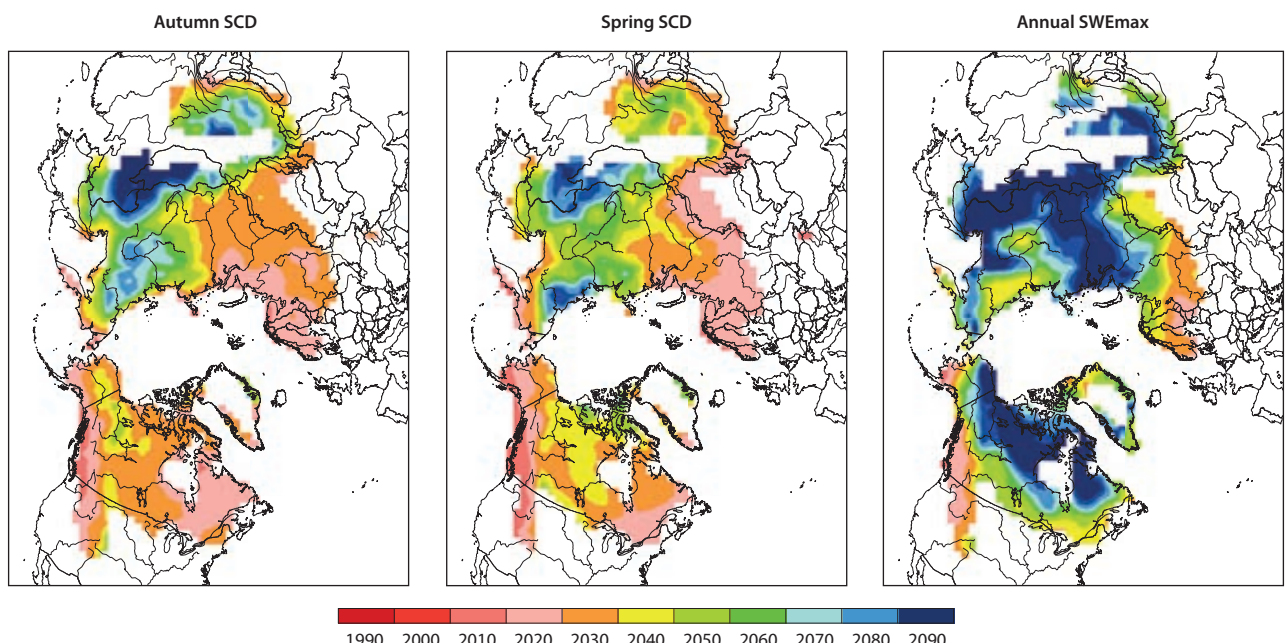


Figure 3.21 Expected year of emergence of climate warming signals in northern hemisphere snow cover in each half of the snow season and for annual maximum snow water equivalent (SWEmax) following de Elía et al. (2013) from an 11-member ensemble of CMIP5 models for emission scenario RCP8.5.

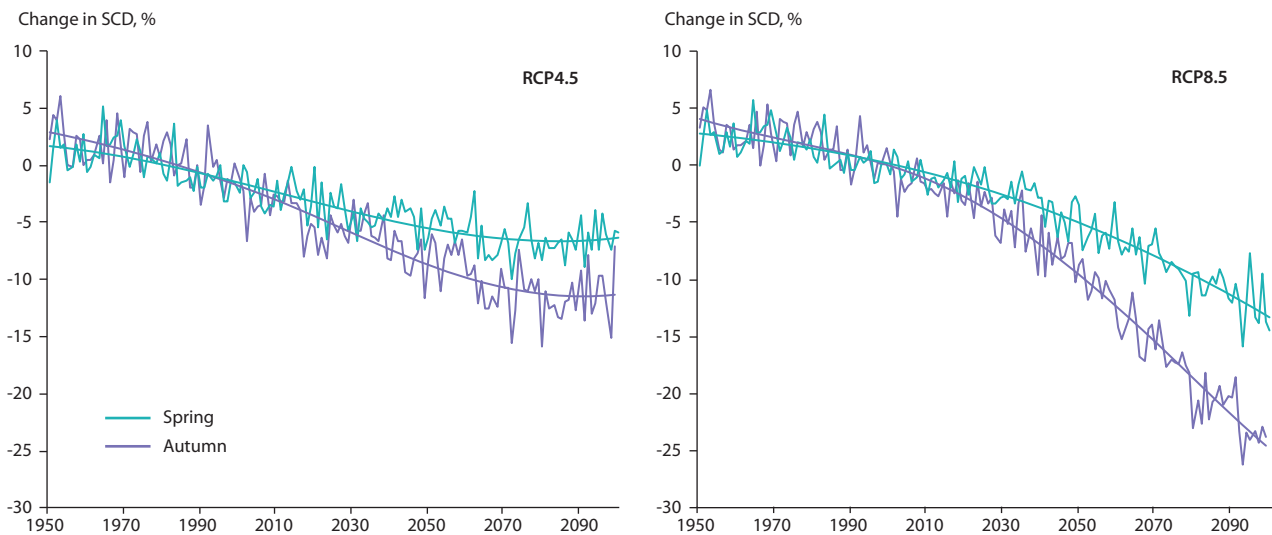


Figure 3.22 50th percentiles of projected relative change in regionally-averaged snow cover duration (SCD) over non-glacier land areas in the Baffin Bay-Davis Strait region in each half of the snow season under the RCP4.5 and RCP8.5 emission scenarios with respect to the period 1986–2005.

‘noise’ that includes the natural variability simulated by the models as well as the between-model spread i.e. where the climate signal is strong and all the models project similar rates of change, the signal will emerge earlier from the noise. This is similar to the ‘time of emergence’ defined by Hawkins and Sutton (2012). The results (Figure 3.21) show that significant change in SCD appears much earlier than in SWE_{max} over most of the Arctic with the exception of northern Siberia where significant increases in SWE_{max} are projected to appear earlier than significant decreases in SCD. The more temperate coastal regions of the Arctic and the European Arctic are projected to have the earliest SCD responses to global warming. This contrasts with most of eastern Siberia where the climate signal is projected to appear much later mainly in response to a large spread in the model projected changes (not shown). The SCD results show evidence of earlier signal emergence in the snow onset period over the Canadian Arctic compared to the spring period in response to enhanced warming from the lengthening of the ice-free season (Steiner et al., 2015). This response is evident in projected SCD results for the Baffin Bay-Davis Strait region (Figure 3.22) and is consistent with observed snow cover trends in the region (Brown et al., 2017).

3.4.3 Snow properties

Changes in snowpack physical properties in response to warming such as albedo, thermal conductivity and ice layers have potentially wide-ranging implications. To date, relatively little work has been carried out to investigate the future response of Arctic snowpack properties to a changing climate. GCMs and RCMs provide large-scale information on changes in snow depth and SWE but the representation of processes influencing snow properties such as metamorphism, water percolation and ice-layer formation varies greatly between models (Bokhorst et al., 2016). Projections of future changes in snow properties (e.g. snow density, snow grain types, liquid water content, ice layers) for local applications such as avalanche risk and winter grazing, requires the use of detailed, multi-layer physical snowpack and land surface process models such as SNOWPACK (Bartelt and Lehning, 2002), SURFEX/CROCUS (Vionnet et al., 2012)

and JULES (Best et al., 2011). Access to winter grazing for reindeer/caribou is a prime example of where higher winter temperatures and more ROS events may contribute to more ice layers in the snow and a denser snowpack from a lower potential for depth hoar formation. Regional projections for the 21st century indicate a significant enhancement of the frequency and intensity of winter warming events over the European Arctic (Vikhamar-Schuler et al., 2016) with a doubling of the current (1985–2014) number of warming events over northern Scandinavia, and a tripling over the Arctic islands.

The SNOWPACK model has been used to investigate the potential impacts of future changes in snowpack properties on reindeer (Vikhamar-Schuler et al., 2013; Turunen et al., 2016). Recent work (Wever et al., 2013, 2015) to include a full solution for the Richards Equation of water flow in SNOWPACK is expected to provide more realistic simulations of melt-freeze crusts and ice lenses. CROCUS has been used to assess projected changes in snow conditions and avalanche activity in the French Alps (Castebrunet et al., 2014) and Canada (Horton et al., 2015). Obtaining sufficient reliable validation data and realistic local-scale model driving data are two ongoing challenges for these types of applied snowpack modelling studies. The sensitivity of the Arctic climate system to changes in snow cover properties is not well-known; this is one of the WCRP-CliC ‘Grand Challenges’ questions for snow cover. Some of the model experiments planned for the ESM-SnowMIP project will help address this question.

3.5 Impacts of a changing Arctic snow cover

Current and projected changes in snow cover generate a cascade of impacts, interactions and feedbacks. These are covered in detail in the review by Bokhorst et al. (2016) and in the regional reports prepared under the AAC-A program. A brief overview of recent work in this vast field is provided in the following sections classified by theme, although it is recognized that the separation is somewhat subjective as there are important linkages and interactions between the identified themes.

3.5.1 Coupled soil-climate-vegetation system

Snow cover is part of a tightly coupled soil-climate-vegetation system with multiple interactions and feedbacks that make it challenging to isolate the impacts of snow cover changes. In this system, snow cover controls winter soil/permafrost temperatures and respiration, provides protection to plants and animals, and controls the timing and amount of liquid water in soil and labile carbon that together determine the magnitude of biogeochemical activity, the exchanges of CO₂ and trace gases, and the export of dissolved nutrients and nitrogen for soil microbes and plants (Brooks et al., 2011; Gouttevin et al., 2012; Reid et al., 2013; Cooper, 2014). Changes in snow cover associated with warming, atmospheric moistening and changing vegetation therefore have the potential to profoundly impact the soil environment and impact long-term patterns of carbon and nitrogen cycling (Leffler et al., 2016) and methane emissions (Zona et al., 2016), but in a complex and non-linear fashion (Rogers et al., 2011).

Unravelling the influence of snow cover in this interlinked system is a challenge. Long-term monitoring of vegetation in Norway over a 30-year period revealed that changing snow cover conditions were contributing to changes in species richness and plant cover (Sandvik and Odland, 2014). However, many of the studies of vegetation response to changing snow conditions reported in the literature are based on local-scale studies with artificially modified snow conditions, usually from installation of snow fences to mimic the effect of increased snowfall (i.e. they are assessing the impact of deeper snow and later melt). According to climate model projections (Figure 3.17), only a few regions of the Arctic are expected to have increased snow accumulations under a warmer climate. These studies typically show substantial warming of the soil and an increase in active layer depth in response to deeper snow (Johansson et al., 2013; Yi et al., 2015), but a range of vegetation responses that vary with species and over small distances (Rumpf et al., 2014; Bjorkman et al., 2015; Semenchuk et al., 2015). In general, tundra plant growth increases under deeper snow in response to increased protection and greater nutrient availability (e.g. Leffler and Welker, 2013; Blok et al., 2015), although in the case of mountain crowberry (*Empetrum hermaphroditum*) in Sweden, the increased plant growth was offset by an outbreak of a host-specific parasitic fungus, *Arwidssonia empetri*, which killed the majority of the shoots of the dominant plant species after six years of increased snow cover (Olofsson et al., 2011). In a more recent study of *E. hermaphroditum* over a wider range of environments, Bienau et al. (2014) found the plant exhibited sufficient elasticity to snow cover conditions that it appeared to have potential to cope with projected changes in snow cover. Semenchuk et al. (2013) found that snow depth influenced flower abundance on Svalbard by altering season length and by protecting flower buds to cold winter air, but most species they studied were insensitive to snow cover changes except for extreme winter warming events that exposed the canopy to cold winter air. Bjorkman et al. (2015) found a complex response of Arctic tundra vegetation flowering phenology to warming and increased snowfall, with increased snowfall observed to offset warming effects. Wheeler et al. (2015, 2016) found evidence that earlier snowmelt could contribute to 'phenological mismatch' by exposing buds to a greater risk of freezing conditions.

The amount of water stored in the winter snowpack also has important implications for vegetation but relationships between SWE, soil moisture and vegetation response are complex and non-linear (Luus et al. 2013). From a 13-year study of vegetation and climate data from High-Arctic northeast Greenland, Westergaard-Nielsen et al. (2017) showed that levels of plant greenness, the timing of peak greenness and the end of the growing season were all significantly correlated to pre-melt snowpack SWE. Water availability had a higher explanatory value than air temperature for growing-season length at the studied site. There are relatively few studies looking at the net impact of greening and shrub expansion on Arctic snow cover and hydrology, and most of the snow-vegetation processes and feedbacks mentioned above are not incorporated in CMIP5 Earth System Models with dynamic vegetation (Pearson et al., 2013). Ménard et al. (2014a,b) modelled the potential impacts of shrub expansion on snowmelt rates and timing and concluded that the net effect involved a complex interaction of sub-grid topography, wind redistribution of snow, and shrub bending and emergence.

3.5.2 Biological systems and geochemical cycling

Snow cover is a dynamic habitat for microorganisms, plants, animals and birds (Larose et al., 2013; Reid et al., 2013; Hodson et al., 2015; Maccario et al., 2015; Rosvold, 2016), and rapidly changing snow conditions may challenge adaptive capacities. Winter thaw and rain-on-snow events can adversely impact grazing animals such as caribou and muskox (Reid et al., 2013) and extreme short-lived winter warming events have potential to damage vegetation (Bokhorst et al., 2011; Semenchuk et al., 2013; Cooper, 2014). Summer snowbeds and permanent snow patches are also highly sensitive to warming. These have been observed to lose their perennial status over the Canadian Arctic Archipelago in recent decades (Woo and Young, 2014) and are likely to become more scattered and tightly linked to local shading in a warmer climate (Kivinen et al., 2012). These play important roles in local ecology and hydrology (Woo and Young, 2014), and are used by ungulates for relief from heat and biting insects (Anderson and Nilssen, 1998; Hagemoen and Reimers, 2002). Hodson et al. (2015) highlighted the importance of understanding algal blooms in snow and their response to warming as they increase surface melting by reducing albedo. Lutz et al. (2016) showed that snow algae are ubiquitous features of Arctic glaciers and estimated the 'bio-albedo feedback' from red snow algal blooms to contribute a 13% reduction in snow albedo over a melt season.

Snow cover sensitivities are complex and may also include timing dependencies. For example, Schmidt et al. (2015) found muskox population dynamics (calf and yearling recruitments) were driven by spring snow cover, while Doiron et al. (2015) observed a trophic mismatch in years with early snow melt between hatch dates of young snow geese (*Chen caerulescens*) and date of peak nitrogen concentration in plants, an index of their nutritive quality for goslings. Gauthier et al. (2013) also found evidence of a trophic mismatch in Bylot Island snow geese in the Canadian Arctic which adjusted their laying date by only 3.8 days on average for a change in snow melt of 10 days over a 24-year period. Fauteux et al. (2015) observed a positive association between snow depth and early summer survival of

lemmings (*Lemmus lemmus*) that they hypothesized is due to the additional protective cover offered by deeper snow against predators. Stien et al. (2012) found that ROS events adversely affected reindeer and sibling voles (*Microtus kuis*) on Svalbard.

Because of its mix of ice, air and impurities, snow cover plays an important role in the storage and cycling of contaminants in the Arctic (Grannas et al., 2013). Solid precipitation is a very effective scavenger of aerosol particles and also absorbs trace gases during its fall to the surface. On the ground, snow metamorphic processes, photochemical reactions and melt events influence the concentration and cycling of contaminants. A detailed review of the current state of knowledge of physical processes and chemical reactivity in surface snow is provided by Bartels-Rausch et al. (2014). Warming temperatures are likely to affect the uptake and cycling of contaminants through changes in solid precipitation, and the partitioning equilibria of contaminants between gas phase and snow and ice (Grannas et al., 2013). However, the ability to model the potential impact of warming on contaminant cycling is limited by a number of major gaps in the current understanding of snow chemistry processes (Domine et al., 2013; Bartels-Rausch et al., 2014).

3.5.3 Hydrological systems

The response of Arctic hydrology to simultaneous changes in air temperature, precipitation (amount, timing and phase), vegetation, active layer thickness, snow cover (accumulation, melt onset timing, melt dynamics) and ice cover (break-up timing and dynamics) are expected to be complex (Shi et al., 2015; Chapter 7). For example, research on the impacts of warming on the hydrology of Trail Valley Creek in the Canadian western Arctic (Shi et al., 2015) revealed unexpected runoff responses related to the interplay between earlier snowmelt onset, temperature fluctuations during the melting period, increasing spring rainfall, and delayed spring rainfall timing in the Arctic headwater basin. Yang et al. (2014, 2015) documented 20% and 60% increases in May flows for the Mackenzie and Yukon Rivers, respectively and decreases in summer flows related to earlier melting of snow. Lesack et al. (2014) found that local spring warming with unexpected snowfall declines, rather than warmer winters, were responsible for earlier ice breakup in the Mackenzie River Delta.

In Norway, Hanssen-Bauer et al. (2015) found that by the end of the 21st century, rain floods are expected to increase and occur more frequently whereas snow melt floods will be smaller and occur less often than under the present climate. These changes are due to the projected changes in seasonal precipitation (amount, intensity and precipitation phase). Over large regions of Eurasia the effects of warming are seen more clearly, with increased winter flows and a shift toward earlier onset of spring runoff and an earlier centroid of annual runoff (Tan et al., 2011). Over the northern part of western Siberia, however, increased evaporation and a deepening active layer are contributing to a reduction in the contribution of meltwater to runoff from 70–80% in the early 1990s to 40–50% expected by the mid-2000s (Zakharova et al., 2011). A shift to more pluvial regimes has potential for drying from lower snowmelt recharge and more evaporation (Wu et al., 2015). However, Conner et al. (2016) suggested that soil moisture response depends on several other factors including landscape characteristics, vegetation, and regional weather patterns.

Climate change is also expected to alter the magnitude, frequency, intensity, duration and persistence of extreme hydroclimate events (Bennett et al., 2015; Yang et al., 2015). For example, Bennett et al. (2015) found contrasting trends in annual maximum (decrease) and minimum (increase) flows for eight Interior Alaskan river basins over the past 50 to 60 years in response to warming. Changes in the frequency of episodic snowmelt events (ESE) occurring prior to the spring snowmelt season can strongly influence runoff in regions such as southwest Greenland where accumulated meltwater from these events accounts for 25–50% of annual precipitation (Pedersen et al., 2015). In this region, ESEs are driven by foehn winds and are an integral component of the snowmelt dynamics. Pedersen et al. (2015) found large interannual variability in ESE frequency over the period 1979–2013 from atmospheric reanalysis data but no evidence of any trends. Late-lying snow banks and snowbeds play important hydrological and ecological roles in High Arctic and elevated areas by supporting wetlands and river flows over summer months (Woo and Young, 2014). Their contribution is especially important in dry polar desert environments and during years with dry summers. Woo and Young (2014) found that summer snow banks over the Canadian Arctic Archipelago have ceased to be perennial features of the landscape over the past decade, with a number of impacts including deepening of seasonal ground thaw in exposed areas, and drying of snow bank-fed tundra ponds and patchy wetlands. Stuefer and Kane (2016) showed there is potential to generate artificial snow drifts with snow fences in critical areas linked to sensitive habitat or water supply. An artificially created snowdrift was able to augment the summer volume of a shallow lake near Prudhoe Bay, Alaska, by over 20% and prevented the lake drying out over the summer.

3.5.4 Human systems

Snow can be a hazard or a benefit for human activities (Callaghan et al., 2011c; Bokhorst et al., 2016). Examples of snow hazards include avalanches, excessive roof snow loads, and blizzards. Removal of snow from critical infrastructure such as key roads and air strips is an important cost item in all northern community operating budgets. The benefits of snow are more difficult to quantify (Sturm et al., 2017). Snow provides easier transport and access to hunting grounds and potential for recreation such as skiing and snowmobiling. Knowledge of local snow cover trends and scenarios of how snow may change in the future are therefore important for decision making and planning. For example, Blair (2015) showed from analysis of satellite data that snow cover days in Hatcher Pass, Alaska, a winter mecca for cross-country skiers, alpine skiers and snowboarders, dropped as much as 47% between 1986 and 2014. Incorporating traditional and local knowledge into decision-making is essential for adapting to a changing climate (Cuerrier et al., 2015). Cuerrier et al. (2015) documented indigenous knowledge of climate change in three communities in Nunavik, Quebec and found a common trend to lower snow cover that impacted travel and traditional activities in various ways. They proposed a novel mix of qualitative and quantitative methods to translate this traditional knowledge into evidence for environmental policy and decision-making.

A review of recent literature related to snow and economy, health and well-being is provided by Bokhorst et al. (2016). Two of the prime snow-related concerns related to projected climate

changes in the Arctic are increased avalanche risk at some locations, and increased risk of flooding from rapid melt events. Eckerstorfer and Christiansen (2012) studied mid-winter extreme weather events (rain on snow) in Svalbard that led to winter slush avalanche activity and damage to infrastructure in the settlement of Longyearbyen. They concluded that the frequency and duration of low-pressure weather systems were the dominant controls of wet snow avalanche activity. Eckerstorfer et al. (2016) provided a review of the applications of remote sensing for avalanche risk monitoring. Another concern is the declining access to country foods (changing snow conditions affect overland transport as well as animal habitat – see Section 3.5.2) which has important implications for the health and disposable income of northern residents (Furgal et al., 2012). Turunen et al. (2016) analyzed the coping capacity and adaptation strategies of reindeer herders to projected changes in snow cover and found that herders were able to combine traditional knowledge skills with technical applications to cope with change. The research also showed that predators, competing land uses and the high prices of supplementary feed and fuel were more important threats than snow cover changes to the herders' coping capacity.

3.5.5 Feedbacks to northern hemisphere atmospheric circulation

While still controversial (Gramling, 2015; Overland, 2016), there is some evidence that snow cover anomalies over Siberia in the early winter period can affect boreal winter condition in the northern hemisphere through dynamical interactions involving the stratosphere and changes in the surface-based AO (Furtado et al., 2015; Orsolini et al., 2016). Chapter 2 provides a detailed discussion of the processes involved in this feedback. The original hypothesis first presented by Cohen and Entekhabi (1999), and further examined by Fletcher et al. (2007, 2009), Smith et al. (2010, 2011), Allen and Zender (2011), and Cohen et al. (2012) was that snow cover anomalies over Eurasia in October acted to reinforce the Siberian high and the negative mode of the AO through a vertically propagating Rossby wave train. A number of studies (Brown and Derksen, 2013; Peings et al., 2013; Popova et al., 2014; Walsh, 2014) have questioned the robustness of this connection showing that it is dataset dependent and primarily the result of internal variability. Cohen et al. (2014) concluded that more knowledge and understanding were needed to advance understanding of the influences of the Arctic snow and ice cover on mid-latitude weather and extreme events. Recent work by Orsolini et al. (2016) suggests that snow depth anomalies rather than SCE are responsible for initiating and maintaining a persistent anomalously negative AO phase. One consistent finding emerging from the modelling studies to date is that current climate models do not appear to adequately capture the observed influence of Siberian snow cover on the northern hemisphere winter atmospheric circulation (Smith et al., 2011; Furtado et al., 2015; Handorf et al., 2015). There is evidence that reductions in northern hemisphere snow and ice are driving changes in atmospheric circulation that favor more frequent extreme summer heat events over northern mid-latitudes (Tang et al., 2014; Petrie et al., 2015). Recent research (Kretschmer et al., 2016) suggests that Arctic sea ice anomalies are a more important driver of mid-latitudinal circulation than snow cover but Furtado et al. (2016) argued that

autumnal sea ice and snow cover anomalies interact differently with the phase and amplitude of the Northern Annular Mode and that both are required to produce skillful forecasts of mid-latitude winter temperature anomalies.

3.6 Conclusions and recommendations

The period since the previous SWIPA assessment (AMAP, 2011) has seen important advances across all the snow sciences and greater understanding of the role and interactions of snow in Arctic soil-climate-vegetation systems. SWIPA 2011 identified a number of major issues and gaps in information and knowledge that impacted on the ability to provide decision-makers with snow-related information that met their needs. In nearly all cases the issues raised are still relevant. However, there has been important progress in some areas that can be highlighted (Table 3.4) and *it is noteworthy that where progress has been made, it is usually because of a focused, coordinated effort to tackle a particular priority item.*

In spite of this progress, there are still fundamental knowledge gaps and scaling issues that need to be addressed in a systematic way to narrow uncertainties in the monitoring and projection of changes in Arctic snow cover. Some of these issues are well articulated in the WCRP-CliC Grand Challenges (www.climate-cryosphere.org/activities/grand-challenges) and “*are linked to fundamental deficiencies in representation of snow physics in models, insufficient in-situ measurement coverage, [...], issues with remote sensing of snow cover (in particular concerning SWE, small-scale snow cover variability, etc.) and overly simplified representation of snow-related processes in ESMs.*” Scaling and the parameterization of sub-grid scale processes remain a high priority particularly for dynamic snow-vegetation interactions in Earth System Models. Reducing the spread in snow albedo feedbacks in climate and Earth System Models and correcting the current damped snow cover temperature sensitivity over northern land areas are key priority areas as these have important consequences for projected rates of snow cover change over the Arctic. Improved understanding of contaminant fate under a changing climate is an ongoing knowledge gap requiring greater interdisciplinary research and collaboration (Grannas et al., 2013).

Workshops and special sessions that encourage greater interaction between the snow process and climate modelling communities will help address these gaps, as will the ESM-SnowMIP activity mentioned in Table 3.4. The European Union has launched an initiative HarmoSnow that aims at building better connections between snow measurements and models, and between snow observers, researchers and forecasters. The action includes initiatives to harmonize practices, standards and retrieval algorithms applied to ground, air- and space-borne snow measurements, and develop a rationale and long-term strategy for snow measurements, their dissemination and archiving (<http://harmosnow.eu/>). These initiatives are closely aligned with the goals of the WMO Global Cryosphere Watch program to provide authoritative information on the cryosphere to decision-makers. Narrowing the uncertainties in observed trends and variability in Arctic SWE is a key priority for climate change detection and for evaluating climate models. Recent work has shown that the use of blended observational datasets provides improved agreement with climate models as well as estimates of the observational uncertainty for evaluating the spread in

Table 3.4 Some examples of progress in meeting gaps in information and knowledge highlighted in the 2011 SIPWA assessment report.

Issue	Progress
There is currently no pan-Arctic historical archive of quality-controlled <i>in situ</i> snow data to support climate monitoring and snow product evaluation in the Arctic	A Copernicus CORE-CLIMAX workshop was held in 2014 to advance the establishment of a global historical snow data archive. A number of recommendations were submitted to the World Meteorological Organization (WMO) to improve snow reporting along with support for a comprehensive land surface archive of <i>in situ</i> data, modelled after the ICOADS dataset. In response to a recommendation at the workshop, the Finnish Meteorological Institute has established a prototype global archive for <i>in situ</i> snow course data ^a with data from Finland, Canada and Russia
A large number of satellite snow cover and SWE datasets exist but there is little guidance for users on the uncertainties	The European Union project CryoLand (2011–2015) has made important progress in the production and implementation of standardized and sustainable snow monitoring services targeted to user needs, which are continuing as a downstream service under the Copernicus framework of the EU (Malnes et al., 2015). The WMO Global Cryosphere Watch (GCW) with financial support from European Space Agency initiated a satellite snow product intercomparison project (SnowPEx) in 2014 to document uncertainties in remotely sensed snow cover products ^b
There is a large spread in snow albedo feedbacks in climate models	The WCRP-CliC ESM–SnowMIP experiment is targeting strengths and weaknesses in the representation of snow in climate models ^c
A large fraction of <i>in situ</i> snow depth network is not reporting in real-time; zero snow depths are not routinely reported	The WMO GWC Snow Watch activity has spearheaded initiatives to improve real-time reporting of snow depth and mandatory reporting of zero depths ^d
Data standardization is an issue for variables such as snowfall where multiple sensor types and configurations are in service	The WMO GCW CryoNet activity ^e is promoting the addition of standardized cryospheric observations to existing facilities; the WMO SPICE solid precipitation intercomparison project is assessing the performance of a wide range of instruments under various climates ^f
Need for improved networking of Arctic community based monitoring programs and greater efforts to record and use traditional knowledge	The Arctic Observing Summit (AOS) of the Sustaining Arctic Observing Networks (SAON) initiative are working to promote these activities. The IASC-SAON Arctic Data Committee is working to develop a broad, globally connected Arctic observing data and information system of systems ^g

^a<http://litdb.fmi.fi/eraclim2.php>; ^b<https://earth.esa.int/web/sppa/activities/qa4eo/snowpex>; ^c<http://www.climate-cryosphere.org/activities/targeted/esm-snowmip>; ^d<http://globalcryospherewatch.org/projects/snowreporting.html>; ^e <http://globalcryospherewatch.org/cryonet/>; ^f<http://www.wmo.int/pages/prog/www/IMOP/intercomparisons/SPICE/SPICE.html>; ^g<http://www.arcticobserving.org/>

simulations (Sospedra-Alfonso et al., 2016). More intensive and comprehensive evaluations of SWE datasets with *in situ* data are needed and the creation of a pan-Arctic quality-controlled historical SWE dataset is an essential step in this process. The remote sensing community also needs to promote more multi-institution, multi-sensor and multi-dataset analyses of Arctic snow cover trends to provide more authoritative guidance to the scientific community following the example of the glaciological community for mass balance trends for the Greenland Ice Sheet (e.g. AMAP, 2009).

Finally, the four imperatives identified by the WCRP-CliC Grand Challenges deserve to be highlighted here as overarching goals for advancing understanding of snow in the Arctic and for responding to user needs. These have been modified to reflect the snow focus of this chapter and the wide range of needs for snow information in application and research:

1. *Datasets*: To have more comprehensive, quality-controlled observational, observationally-based, and proxy datasets of snow variables suitable for a range of Arctic applications and research needs
2. *Processes*: To have a better quantitative understanding of snow processes and snow/climate interactions and better representation of these processes in reanalyses and environmental prediction models
3. *Modelling*: To have increased confidence in snow and climate models and their predictions/projections
4. *Information*: To have improved information regarding observed and projected changes in snow cover, with a specific focus on information relevant for impact assessment and adaptation decision-making.

Acknowledgements

The following people are gratefully acknowledged for providing helpful comments on the draft manuscript: A. Bartsch, T. Callaghan, M. Eckerstorfer, R. Essery, C. Fletcher, F. Frappart, J-C. Gallet, B. Goodison, G. Henderson, M. Johansson, M. Schneebeli and S. Wang, and an anonymous external reviewer. Ross Brown acknowledges the support of Environment and Climate Change Canada to participate in the SWIPA update process.

References

Allen, R.J. and C.S. Zender, 2011. Forcing of the Arctic Oscillation by Eurasian snow cover. *Journal of Climate*, 24:6528–6539.

AMAP, 2009. The Greenland Ice Sheet in a Changing Climate: Snow, Water, Ice and Permafrost in the Arctic (SWIPA). By: Dahl-Jensen, D., J. Bamber, C.E. Bøggild, E. Buch, J.H. Christensen, K. Dethlo, M. Fahnestock, S. Marshall, M. Rosing, K. Steffen, R. Thomas, M. Truffer, M. van den Broeke and C.J. van der Veen. Arctic Monitoring and Assessment Programme (AMAP), Oslo, Norway.

AMAP, 2011. Snow, water, ice and permafrost in the Arctic (SWIPA): Climate change and the cryosphere. Arctic Monitoring and Assessment Programme (AMAP), Oslo, Norway.

AMAP, 2015. Black carbon and ozone as Arctic climate forcers. Arctic Monitoring and Assessment Programme, (AMAP), Oslo, Norway.

Anderson, J.R. and A.C. Nilssen, 1998. Do reindeer aggregate on snow patches to reduce harassment by parasitic flies or to thermoregulate? *Rangifer*, 18:3–17.

Arnaud, L., G. Picard, N. Champollion, F. Domine, J.C. Gallet, E. Lefebvre, M. Fly and J.M. Barnola, 2011. Measurement of vertical profiles of snow specific surface area with a 1 cm resolution using infrared reflectance: instrument description and validation. *Journal of Glaciology*, 57:17–29.

Assini, J. and K.L. Young, 2012. Snow cover and snowmelt of an extensive High Arctic wetland: spatial and temporal seasonal patterns. *Hydrological Sciences Journal*, 57:738–755.

Balsamo, G., P. Viterbo, A. Beljaars, B. Van den Hurk, A.K. Betts and K. Scipal, 2009. A revised hydrology for the ECMWF model: Verification

from field site to terrestrial water storage and impact in the Integrated Forecast System. *Journal of Hydrometeorology*, 10:623-643.

Barnes, E.A. and J.A. Screen, 2015. The impact of Arctic warming on the midlatitude jet-stream: Can it? Has it? Will it? *WIREs: Climate Change* 6:277-286.

Bartels-Rausch, T., H.-W. Jacobi, T.F. Kahan, J.L. Thomas, E.S. Thomson, J.P.D. Abbott, M. Ammann, J.R. Blackford, H. Bluhm, C. Boxe, F. Domine, M.M. Frey, I. Gladich, M.I. Guzman, D. Heger, Th. Huthwelker, P. Klan, W.F. Kuhs, M.H. Kuo, S. Maus, S.G. Moussa, V.F. McNeil, J.T. Newberg, J.B.C. Pettersson, M. Roeselova and J.R. Sodeau, 2014. A review of air-ice chemical and physical interactions (AICI): liquids, quasi-liquids, and solids in snow. *Atmospheric Chemistry and Physics*, 14:1587-1633.

Bartelt, P and M. Lehning, 2002. A physical SNOWPACK model for the Swiss avalanche warning. Part I: numerical model. *Cold Regions Science and Technology*, 35:123-145.

Bartsch, A., 2010. Ten years of sea winds on QuikSCAT for snow applications. *Remote Sensing*, 2:1142-1156.

Bartsch, A., T. Kumpula, B.C. Forbes and F. Stammer, 2010. Detection of snow surface thawing and refreezing in the Eurasian Arctic with QuickSCAT: implications for reindeer herding. *Ecological Applications*, 20:2346-2358.

Belleflamme, A., X. Fettweis and M. Erpicum, 2015. Recent summer Arctic atmospheric circulation anomalies in a historical perspective. *The Cryosphere*, 9:53-64.

Bennett, K.E., A.J. Cannon and L. Hinzman, 2015. Historical trends and extremes in boreal Alaska river basins. *Journal of Hydrology*, 527:590-607.

Berdahl, M., A. Robock, D. Ji, J.C. Moore, A. Jones, B. Kravitz and S. Watanabe, 2014. Arctic cryosphere response in the Geoengineering Model Intercomparison Project G3 and G4 scenarios. *Journal of Geophysical Research: Atmospheres*, 119:1308-1321.

Best, M.J., M. Pryor, D.B. Clark, G.G. Rooney, R.L.H. Essery, C.B. Ménard, J.M. Edwards, M.A. Hendry, A. Porson, N. Gedney, L.M. Mercado, S. Sitch, E. Blyth, O. Boucher, P.M. Cox, C.S.B. Grimmond and R.J. Harding, 2011. The Joint UK Land Environment Simulator (JULES), model description. Part 1: Energy and water fluxes. *Geoscientific Model Development*, 4:677-699.

Bezeau, P., M. Sharp and G. Gascon, 2015. Variability in summer anticyclonic circulation over the Canadian Arctic Archipelago and west Greenland in the late 20th/early 21st centuries and its effect on glacier mass balance. *International Journal of Climatology*, 35:540-557.

Bichet, A., P.J. Kushner and L.R. Mudryk, 2016. Estimating the continental response to global warming using pattern-scaled sea surface temperatures and sea ice. *Journal of Climate*, 29:9125-9139.

Bienau, M.J., D. Hattermann, M. Kröncke, L. Kretz, A. Otte, W.L. Eiserhardt, A. Milbau, B.J. Graae, W. Durka and R.L. Eckstein, 2014. Snow cover consistently affects growth and reproduction of *Empetrum hermaphroditum* across latitudinal and local climatic gradients. *Alpine Botany*, 124:115-129.

Bieniek, P.A., U.S. Bhatt, D.A. Walker, M.K. Raynolds, J.C. Comiso, H.E. Epstein, J.E. Pinzon, C.J. Tucker, R.L. Thoman, H. Tran, N. Mölders, M. Steele, J. Zhang and W. Ermold, 2015. Climate drivers linked to changing seasonality of Alaska coastal tundra vegetation productivity. *Earth Interactions*, 19:1-29.

Bintanja, R. and F.M. Selten, 2014. Future increases in Arctic precipitation linked to local evaporation and sea-ice retreat. *Nature*, 509:479-482.

Bjerke, J.W., S.R. Karlsen, K.A. Hogda, E. Malnes, J.U. Jepsen, S. Lovibond, D. Vikhamer-Schuler and H. Tømmervik, 2014. Record-low primary productivity and high plant damage in the Nordic Arctic Region in 2012 caused by multiple weather events and pest outbreaks. *Environmental Research Letters*, 9:084006 doi:10.1088/1748-9326/9/8/084006.

Bjorkman, A.D., S.C. Elmendorf, A.L. Beamish, M. Vellend and G. Henry, 2015. Contrasting effects of warming and increased snowfall on Arctic tundra plant phenology over the past two decades. *Global Change Biology*, 21:46-51-4661.

Blair, L., 2015. Factoring climate change into recreation investment decisions: evidence from Hatcher's Pass, Alaska. *Symposium of University Research and Creative Expression (SOURCE)*. Paper 94. <http://digitalcommons.cwu.edu/source/2015/posters/94>.

Blok, D., S. Weijers, J.M. Welker, E.J. Cooper, A. Michelsen, J. Löffler and B. Elberling, 2015. Deepened winter snow increases stem growth and alters stem $\delta^{13}\text{C}$ and $\delta^{15}\text{N}$ in evergreen dwarf shrub *Cassiope tetragona* in high-arctic Svalbard tundra. *Environmental Research Letters*, 10:044008 doi:10.1088/1748-9326/10/4/044008.

Boisvert, L.N. and J.C. Stroeve, 2015. The Arctic is becoming warmer and wetter as revealed by the Atmospheric Infrared Sounder. *Journal of Geophysical Research*, 120:4439-4446.

Bokhorst, S., J.W. Bjerke, H. Tømmervik, T.V. Callaghan and G.K. Phoenix, 2009. Winter warming events damage sub-Arctic vegetation: consistent evidence from an experimental manipulation and a natural event. *Journal of Ecology*, 97:1408-1415.

Bokhorst, S., J.W. Bjerke, L.E. Street, T.V. Callaghan and G.K. Phoenix, 2011. Impacts of multiple extreme winter warming events on sub-Arctic heathland: phenology, reproduction, growth, and CO_2 flux responses. *Global Change Biology*, 17:2817-2830.

Bokhorst, S., S.H. Pedersen, L. Brucker, O. Anisimov, J.W. Bjerke, R.D. Brown, D. Ehrlich, R.L. Essery, A. Heilig, S. Ingvander, C. Johansson, M. Johansson, I.S. Jónsdóttir, N. Inga, K. Luojis, G. Macelloni, H. Mariass, D. McLennan, G.N. Rosqvist, A. Sato, H. Savela, M. Schneebeli, A. Sokolov, S.A. Sokratov, S. Terzago, D. Vikhamer-Schuler, S. Williamon, Y. Qiu and T.V. Callaghan, 2016. Changing Arctic snow cover: A review of recent developments and assessment of future needs for observations, modelling, and impacts. *Ambio*, 45:516-537.

Bond, T.C., S.J. Doherty, D.W. Fahey, P.M. Forster, T. Berntsen, B.J. DeAngelo, M.G. Flanner, S. Ghan, B. Kärcher, D. Koch, S. Kinne, Y. Kondo, P.K. Quinn, M.C. Sarofim, M.G. Schultz, M. Schulz, C. Venkataraman, H. Zhang, S. Zhang, N. Bellouin, S.K. Guttikunda, P.K. Hopke, M.Z. Jacobson, J.W. Kaiser, Z. Klimont, U. Lohmann, J.P. Schwarz, D. Shindell, T. Storelvmo, S.G. Warren and C.S. Zender, 2013. Bounding the role of black carbon in the climate system: A scientific assessment. *Journal of Geophysical Research: Atmospheres*, 118:5380-5552.

Brooks, P.D., P. Grogan, P.H. Templer, P. Groffman, M.G. Öquist and J. Schimel, 2011. Carbon and nitrogen cycling in snow-covered environments. *Geography Compass*, 5:682-699.

Brown, R.D. and C. Derksen, 2013. Is Eurasian October snow cover extent increasing? *Environmental Research Letters*, 8:024006.

Brown, R., C. Derksen and L. Wang, 2010. A multi-data set analysis of variability and change in Arctic spring snow cover extent, 1967-2008. *Journal of Geophysical Research*, 115:D16111, doi:10.1029/2010JD013975.

Brown, R.D. and P. Mote, 2009. The response of Northern Hemisphere snow cover to a changing climate. *Journal of Climate*, 22:2124-2145.

Brown, R.D. et al, 2017. Climate variability, trends and projected change for the Eastern Canadian Arctic. In: Bell et al., (eds.) *An Integrated Regional Impact Study for the Canadian Eastern Arctic* (in press).

Brun, E., V. Vionnet, A. Boone, B. Decharme, Y. Peings, R. Valette, F. Karbou and S. Morin, 2013. Simulation of northern Eurasian local snow depth, mass, and density using a detailed snowpack model and meteorological reanalyses. *Journal of Hydrometeorology*, 14:203-219.

Brutel-Vuilmet, C., M. Ménégoz and G. Krinner, 2013. An analysis of present and future seasonal Northern Hemisphere land snow cover simulated by CMIP5 coupled climate models. *The Cryosphere*, 7:67-80.

Bühler, Y., M. Marty, L. Egli, J. Veitinger, T. Jonas, P. Thee, P. and C. Ginzler, 2015. Snow depth mapping in high-alpine catchments using digital photogrammetry. *The Cryosphere*, 9:229-243.

Bulygina, O.N., P. Ya. Groisman, V.N. Razuvayev and N.N. Korshunova, 2011. Changes in snow cover characteristics over Northern Eurasia since 1966. *Environmental Research Letters*, 6:045204.

Burt, M.A. D.A. Randall and M.D. Branson, 2013. Effects of longwave radiation on Arctic sea ice in a warmer climate. *American Geophysical Union, Fall Meeting 2013*, abstract #C31A-0636.

Callaghan, T.V., M. Johansson, R.D. Brown, P.Y. Groisman, N. Labba, V. Radionov, R.G. Barry, O.N. Bulygina, R.L. Essery, D.M. Frolov and V.N. Golubev, 2011a. The changing face of Arctic snow cover: A synthesis of observed and projected changes. *Ambio*, 40:17-31.

Callaghan, T.V., M. Johansson, R.D. Brown, P.Y. Groisman, N. Labba, V. Radionov, R.S. Bradley, S. Blangy, O.N. Bulygina, T.R. Christensen and J.E. Colman, 2011b. Multiple effects of changes in Arctic snow cover. *Ambio*, 40:32-45.

Callaghan, T.V., M. Johansson, R.D. Brown, P.Y. Groisman, N. Labba and V. Radionov, 2011c. Changing snow cover and its impacts. In: *Snow, Water, Ice and Permafrost in the Arctic (SWIPA): Climate Change and the Cryosphere*. Arctic Monitoring and Assessment Programme (AMAP), Oslo, Norway.

Castebrunet, H., N. Eckert, G. Giraud, Y. Durand and S. Morin, 2014. Projected changes of snow conditions and avalanche activity in a warming climate: the French Alps over the 2020-2050 and 2070-2100 periods. *The Cryosphere*, 8:1673-1697.

Chapin III, F., M. Sturm, M. Serreze, J. McFadden, J. Key, A. Lloyd, A. McGuire, T. Rupp, A. Lynch, J. Schimel, J. Beringer, W. Chapman, H. Epstein, E. Euskiachen, L. Hinzman, G. Jia, C. Ping, K. Tape, C. Thompson, D. Walker and J. Welker, 2005. Role of land-surface changes in Arctic summer warming. *Science*, 310:657-660.

Chen, W., D.E. Russell, A. Gunn, B. Croft, W.R. Chen, R. Fernandes, H. Zhao, J. Li, Y. Zhang, K. Koehler, I. Olthof, R.H. Fraser, S.G. Leblanc, G.R. Henry, R.G. White and G.L. Finstad, 2013. Monitoring habitat condition changes during winter and pre-calving migration for Bathurst Caribou in northern Canada. *Biodiversity*, 14:36-44.

Clark, M., A.M. Gurnell, E.J. Milton, M. Seppälä and M. Kyöstiä, 2013. Remotely-sensed vegetation classification as a snow depth indicator for hydrological analysis in sub-arctic Finland. *Fennia-International Journal of Geography*, 163:195-216.

Clifford, D., 2010. Global estimates of snow water equivalent from passive microwave instruments: history, challenges and future developments. *International Journal of Remote Sensing*, 31:3707-3726.

Cohen, J. and D. Entekhabi, 1999. Eurasian snow cover variability and Northern Hemisphere climate predictability. *Geophysical Research Letters*, 26:345-348.

Cohen, J.L., J.C. Furtado, M.A. Barlow, V.A. Alexeev and J.E. Cherry, 2012. Arctic warming, increasing snow cover and widespread boreal winter cooling. *Environmental Research Letters*, 7:014007.

Cohen, J., J.A. Screen, J.C. Furtado, M. Barlow, D. Whittleston, D. Coumou, J. Francis, K. Dethloff, D. Entekhabi, J. Overland and J. Jones, 2014. Recent Arctic amplification and extreme mid-latitude weather. *Nature Geoscience*, 7:627-637.

Cohen, J., H. Ye and J. Jones, 2015. Trends and variability in rain-on-snow events. *Geophysical Research Letters*, 42:7115-7122.

Conner, L.G., R.A. Gill and J. Belnap, 2016. Soil moisture response to experimentally-altered snowmelt timing is mediated by soil, vegetation, and regional climate patterns. *Ecohydrology*, 9:1006-1016.

Cooper, E.J., 2014. Warmer shorter winters disrupt Arctic terrestrial ecosystems. *Annual Review of Ecology, Evolution, and Systematics*, 45:271-295.

Cowtan, K. and R.G. Way, 2014. Coverage bias in the HadCRUT4 temperature series and its impact on recent temperature trends. *Quarterly Journal of the Royal Meteorological Society*, 140:1935-1944.

Crawford, C.J., 2015. MODIS Terra Collection 6 fractional snow cover validation in mountainous terrain during spring snowmelt using Landsat TM and ETM+. *Hydrological Processes*, 29:128-138.

Crook, J.A. and P.M. Forster, 2014. Comparison of surface albedo feedback in climate models and observations. *Geophysical Research Letters*, 41:1717-1723.

Cuerrier, A., N.D. Brunet, J. Gérin-Lajoie, A. Downing and E. Lévesque, 2015. The study of Inuit Knowledge of climate change in Nunavik, Quebec: a mixed methods approach. *Human Ecology*, 43:379-394.

Deb, D., J. Butcher and R. Srinivasan, 2015. Projected hydrologic changes under mid-21st century climatic conditions in a sub-arctic watershed. *Water Resources Management*, 29:1467-1487.

Dee, D.P., S.M. Uppala, A.J. Simmons, P. Berrisford, P. Poli, S. Kobayashi, U. Andrae, M.A. Balmaseda, G. Balsamo, P. Bauer, P. Bechtold, A.C.M. Beljaars, L. van de Berg, J. Bidlot, N. Bormann, C. Delsol, R. Dragani, M. Fuentes, A.J. Geer, L. Haimberger, S.B. Healy, H. Hersbach, E.V. Hólm, L. Isaksen, P. Källberg, M. Köhler, M. Matricardi, A.P. McNally, B.M. Monge-Sanz, J.-J. Morcrette, B.-K. Park, C. Peubey, P. de Rosnay, C. Tavolato, J.-N. Thépaut and F. Vitart, 2011. The ERA-Interim reanalysis: Configuration and performance of the data assimilation system. *Quarterly Journal of the Royal Meteorological Society*, 137:553-597.

Deeb, E., R. Forster and D. Kane, 2011. Monitoring snowpack evolution using interferometric synthetic aperture radar on the North Slope of Alaska, USA. *International Journal of Remote Sensing*, 32:3985-4003.

de Elía, R., S. Biner and A. Frigon, 2013. Interannual variability and expected regional climate change over North America. *Climate Dynamics*, 41:1245-1267.

Deems, J.S., T.H. Painter and D.C. Finnegan, 2013. Lidar measurement of snow depth: a review. *Journal of Glaciology*, 59:467-479.

DerkSEN, C. and R. Brown, 2012. Spring snow cover extent reductions in the 2008-2012 period exceeding climate model projections. *Geophysical Research Letters*, 39:L19504, doi:10.1029/2012GL053387.

DerkSEN, C., M. Sturm, G. Liston, J. Holmgren, H. Huntington, A. Silis, and D. Solie, 2009: Northwest Territories and Nunavut snow characteristics from a sub-Arctic traverse: Implications for passive microwave remote sensing. *Journal of Hydrometeorology*. 10(2): 448-463.

DerkSEN, C., J. Lemmettyinen, P. Toose, A. Silis, J. Pulliainen and M. Sturm, 2014. Physical properties of Arctic versus subarctic snow: Implications for high latitude passive microwave snow water equivalent retrievals. *Journal of Geophysical Research: Atmospheres*, 119:7254-7270.

DerkSEN, C., R. Brown, L. Mudryk and K. Luojus, 2015. Arctic – Terrestrial Snow. State of the Climate in 2014. *Bulletin of the American Meteorological Society: Special supplement*, 96:133-135.

DerkSEN, C., R. Brown, L. Mudryk and K. Luojus, 2016. Terrestrial Snow [in Arctic Report Card]. www.arctic.noaa.gov/reportcard.

de Rosnay, P., G. Balsamo, C. Albergel, J. Muñoz-Sabater and L. Isaksen, 2014. Initialisation of land surface variables for numerical weather prediction. *Surveys in Geophysics*, 35:607-621.

Déry, S.J. and R.D. Brown, 2007. Recent Northern Hemisphere snow cover extent trends and implications for the snow-albedo feedback. *Geophysical Research Letters*, 34:L22504, doi:10.1029/2007GL031474.

Déry, S. and M. Yau, 2002. Large-scale mass balance effects of blowing snow and surface sublimation. *Journal of Geophysical Research: Atmospheres*, 107:4679, doi:10.1029/2001JD001251.

Diffenbaugh, N.S., M. Scherer and M. Ashfaq, 2013. Response of snow-dependent hydrologic extremes to continued global warming. *Nature Climate Change*, 3:379-384.

Doherty, S.J., T.C. Grenfell, S. Forsström, D.L. Hegg, R.E. Brandt and S.G. Warren, 2013. Observed vertical redistribution of black carbon and other insoluble light-absorbing particles in melting snow. *Journal of Geophysical Research: Atmospheres*, 118:5553-5569.

Doiron, M., G. Gauthier and E. Lévesque, 2015. Trophic mismatch and its effects on the growth of young in an Arctic herbivore. *Global Change Biology*, 21:43-64-4376.

Dolant, C., A. Langlois, B. Montpetit, L. Brucker, A. Roy and A. Royer, 2016. Development of a rain-on-snow detection algorithm using passive microwave radiometry. *Hydrological Processes*, 30:3184-3196.

Domine, F., J. Bock, D. Voisin and D.J. Donaldson, 2013. Can we model snow photochemistry? Problems with the current approaches. *The Journal of Physical Chemistry A*, 117:4733-4749.

Domine, F., M. Barrere, D. Sarrazin, S. Morin and L. Arnaud, 2015. Automatic monitoring of the effective thermal conductivity of snow in a low Arctic shrub tundra. *The Cryosphere*, 9:1265-1276.

Donat, M.G., L.V. Alexander, H. Yang, I. Durre, R. Vose, R.J.H. Dunn, K.M. Willett, E. Aguilar, M. Brunet, J. Caesar, B. Hewitson, C. Jack, A.M.G. Klein Tank, A.C. Kruger, J. Marengo, T.C. Peterson, M. Renom, C. Oria Rojas, M. Rusticucci, J. Salinger, A.S. Elrayah, S.S. Sekele, A.K. Srivastava, B. Trewin, C. Villarroel, L.A. Vincent, P. Zhai, X. Zhang and S. Kitching, 2013. Updated analyses of temperature and precipitation extreme indices since the beginning of the twentieth century: the HadEX2 dataset. *Journal of Geophysical Research: Atmospheres*, 118:2098-2118.

Dou, T., C. Xiao, D.T. Shindell, J. Liu, K. Eleftheriadis, J. Ming and D. Qin, 2012. The distribution of snow black carbon observed in the Arctic and compared to the GISS-PUCCINI model. *Atmospheric Chemistry and Physics*, 12:7995-8007.

Dumont, M., E. Brun, G. Picard, M. Michou, Q. Libois, J.-R. Petit, M. Geyer, S. Morin and B. Josse, 2014. Contribution of light-absorbing impurities in snow to Greenland's darkening since 2009. *Nature Geoscience*, 7:509-512.

Dyrrdal, A.V., T. Saloranta, T. Skaugen and H.B. Stranden, 2013. Changes in snow depth in Norway during the period 1961-2010. *Hydrology Research*, 44:169-179.

Ebner, P.P., M. Schneebeli and A. Steinfeld, 2015. Tomography-based observation of sublimation and snow metamorphism under temperature gradient and advective flow. *The Cryosphere Discussions*, 9:4845-4864.

Eckerstorfer, M. and H.H. Christiansen, 2012. Meteorology, topography and snowpack conditions causing two extreme mid-winter slush and wet slab avalanche periods in High Arctic Maritime Svalbard. *Permafrost and Periglacial Processes*, 23:15-25.

Eckerstorfer, M., Y. Bühler, R. Frauenfelder and E. Malnes, 2016. Remote sensing of snow avalanches: Recent advances, potential, and limitations. *Cold Regions Science and Technology*, 121:126-140.

Epstein, H.E., U.S. Bhatt, M.K. Reynolds, D.A. Walker, P.A. Bieniek, C.J. Tucker, J. Pinzon, H. Zeng, G.J. Jia, K.C. Guay and S.J. Goetz, 2014. Tundra greenness. In: Arctic Report Card: Update for 2014. www.arctic.noaa.gov/reportcard

Essery, R., 2013. Large-scale simulations of snow albedo masking by forests. *Geophysical Research Letters*, 40:5521-5525.

Essery, R. and J. Pomeroy, 2004. Vegetation and topographic control of wind-blown snow distributions in distributed and aggregated simulations for an Arctic tundra basin. *Journal of Hydrometeorology*, 5:735-744.

Estilow, T.W., A.H. Young and D.A. Robinson, 2015. A long-term Northern Hemisphere snow cover extent data record for climate studies and monitoring. *Earth System Science Data* 7:137-142.

Fauteux, D., G. Gauthier and D. Berteaux, 2015. Seasonal demography of a cyclic lemming population in the Canadian Arctic. *Journal of Animal Ecology*, 84:1412-1422.

Fensholt, R. and S.R. Proud, 2012. Evaluation of earth observation based global long term vegetation trends – Comparing GIMMS and MODIS global NDVI time series. *Remote Sensing of Environment*, 119:131-147.

Fernandes, R., F. Zhou and H. Song, 2014. Evaluation of multiple datasets for snow cover indicators for Canada. *IEEE International Geoscience and Remote Sensing Symposium, IGARSS 2014*. pp. 239-242.

Fletcher, C.G., P.J. Kushner and J. Cohen, 2007. Stratospheric control of the extratropical circulation response to surface forcing. *Geophysical Research Letters*, 34:L21802, doi:10.1029/2007GL031626.

Fletcher, C.G., S.C. Hardiman, P.J. Kushner and J. Cohen, 2009. The dynamical response to snow cover perturbations in a large ensemble of atmospheric GCM integrations. *Journal of Climate*, 22:1208-1222.

Fletcher, C.G., H. Zhao, P.J. Kushner and R. Fernandes, 2012. Using models and satellite observations to evaluate the strength of snow albedo feedback. *Journal of Geophysical Research: Atmospheres*, 117:D05113, doi:10.1029/2008JD011272.

Forchhammer, M.C. and D. Boertmann, 1993. The muskoxen *Ovibos moschatus* in north and north-east Greenland: population trends and the influence of abiotic parameters on population dynamics. *Ecography*, 16:299-308.

Forman, B.A., R.H. Reichle and M. Rodell, 2012. Assimilation of terrestrial water storage from GRACE in a snow-dominated basin. *Water Resources Research*, 48:W01507, doi:10.1029/2011WR011239.

Forte, E., M. Pipan, R. Francese and A. Godio, 2015. An overview of GPR investigation in the Italian Alps. *First Break*, 33:61-67.

Frappart, F., G. Ramillien, S. Biancamaria, N.M. Mognard and A. Cazenave, 2006. Evolution of high-latitude snow mass derived from the GRACE gravimetry mission (2002–2004). *Geophysical Research Letters*, 33:L02501, doi:10.1029/2005GL024778.

Frappart, F., G. Ramillien and J.S. Famiglietti, 2011. Water balance of the Arctic drainage system using GRACE gravimetry products. *International Journal of Remote Sensing*, 32:431-453.

Frei, A., M. Tedesco, S. Lee, J. Foster, D.K. Hall, R. Kelly and D.A. Robinson, 2012. A review of global satellite-derived snow products. *Advances in Space Research*, 50:1007-1029.

Frost, G.V. and H.E. Epstein, 2014. Tall shrub and tree expansion in Siberian tundra ecotones since the 1960s. *Global Change Biology*, 20:1264-1277.

Furgal, C., L. Chan, M. Tremblay, V. Rajdev, M. Barrett and T. Sheldon, 2012. Impacts of climate change on food security in Nunavik and Nunatsiavut. In: Allard, M. and M. Lemay (eds.), *Nunavik and Nunatsiavut: From Science to Policy*. pp. 156-169. An Integrated Regional Impact Study (IRIS) of Climate Change and Modernization. ArcticNet.

Furtado, J.C., J.L. Cohen, A.H. Butler, E.E. Riddle and A. Kumar, 2015. Eurasian snow cover variability and links to winter climate in the CMIP5 models. *Climate Dynamics*, 1-15, doi:10.1007/s00382-015-2494-4.

Furtado, J.C., J.L. Cohen and E. Tziperman, 2016. The combined influences of autumnal snow and sea ice on Northern Hemisphere winters. *Geophysical Research Letters*, 43:3478-3485.

Fyfe, J.C., G.A. Meehl, M.H. England, M.E. Mann, B.D. Santer, G.M. Flato, E. Hawkins, N.P. Gillett, S.P. Xie, Y. Kosaka and N.C. Swart, 2016. Making sense of the early-2000s warming slowdown. *Nature Climate Change*, 6:224-228.

Gallet, J.-C., F. Domine and M. Dumont, 2014. Measuring the specific surface area of wet snow using 1310 nm reflectance. *The Cryosphere*, 8:1139-1148.

Gauthier, G., J. Béty, M.-C. Cadieux, P. Legagneux, M. Doiron, C. Chevallier, S. Lai, A. Tarroux and D. Berteaux, 2013. Long-term monitoring at multiple trophic levels suggests heterogeneity in responses to climate change in the Canadian Arctic tundra. *Philosophical Transactions of the Royal Society B*, 368:20120482.

Gent, P.R., 2012. Coupled climate and Earth System Models. In: Rasch, P.J. (ed.), *Climate Change Modeling Methodology: Selected Entries from the Encyclopedia of Sustainability Science and Technology*, pp. 5-30. Springer.

Giorgi, F., C. Jones and G.R. Asrar, 2009. Addressing climate information needs at the regional level: the CORDEX framework. *WMO Bulletin*, 58:175-183.

Gouttevin, I., M. Menegoz, F. Dominé, G. Krinner, C. Koven, P. Ciais, C. Tarnocai and J. Boike, 2012. How the insulating properties of snow affect soil carbon distribution in the continental pan-Arctic area. *Journal of Geophysical Research: Biogeosciences*, 117: G02020, doi:10.1029/2011JG001916.

Gramling, C., 2015. The Siberian snow connection. *Science*, 347:821.

Grannas, A.M., C. Bogdal, K.J. Hageman, C. Halsall, T. Harner, H. Hung, R. Kallenborn, P. Klán, J. Klárová, R.W. Macdonald and T. Meyer, 2013. The role of the global cryosphere in the fate of organic contaminants. *Atmospheric Chemistry and Physics*, 13:3271-3305.

Groisman, P.Ya., E.G. Bogdanova, V.A. Alexeev, J.E. Cherry and O.N. Bulygina, 2014. Impact of snowfall measurement deficiencies on quantification of precipitation and its trends over Northern Eurasia. *Ice and Snow*, 2:29-43.

Gruza, G.V. and E.Ya Rankova, 2009. Assessment of the coming climate changes over the Russian Federation Territory. *Russian Meteorology and Hydrology*, 11:15-29.

Hadley, O.L. and T.W. Kirchstetter, 2012. Black-carbon reduction of snow albedo. *Nature Climate Change*, 2:437-440.

Hagemoen, R.I.M. and E. Reimers, 2002. Reindeer summer activity pattern in relation to weather and insect harassment. *Journal of Animal Ecology*, 71:883-892.

Hall, A. and X. Qu, 2006. Using the current seasonal cycle to constrain snow albedo feedback in future climate change. *Geophysical Research Letters*, 30:L03502, doi:10.1029/2005GL025127.

Hall, D.K., G.A. Riggs and V.V. Salomonson, 2006. MODIS snow and sea ice products. In: Qu, J.R., W. Gao, M. Kafatos, R.E. Murphy and V.V. Salomonson (eds.), *Earth Science Satellite Remote Sensing: Science and Instruments*. Vol. 1, pp. 154-181. Springer.

Handorf, D., R. Jaiser, K. Dethloff, A. Rinke and J. Cohen, 2015. Impacts of Arctic sea ice and continental snow cover changes on atmospheric winter teleconnections. *Geophysical Research Letters*, 42:2367-2377.

Hannula, H.-R., J. Lemmettyinen, A. Kontu, C. Derksen and J. Pullainen, 2016. Spatial and temporal variation of bulk snow properties in north boreal and tundra environments based on extensive field measurements. *Geoscientific Instrumentation, Methods and Data Systems*, 5:347-363.

Hansen, B.B., R. Aanes, I.H.J. Kohler and B.E. Saether, 2011. Climate, icing, and wild arctic reindeer: past relationships and future prospects. *Ecology*, 92:1917-1923.

Hansen, B.B., K. Isaksen, R.E. Benestad, J. Kohler, Å.Ø. Pedersen, L.E. Loe, S.J. Coulson, J.O. Larsen and Ø. Varpe, 2014. Warmer and wetter winters: characteristics and implications of an extreme weather event in the High Arctic. *Environmental Research Letters*, 9, 114021.

Hanssen-Bauer, I., E.J. Førland, I. Haddeland, H. Hisdal, S. Mayer, A. Nesje, J.E.Ø. Nilsen, S. Sandven, A.B. Sandø, A. Sorteberg and B. Ådlandsvik, 2015. *Klima i Norge 2100* [Climate in Norway 2100]. Norwegian Centre for Climate Services, Report 2/2015.

Hartmann, D.L., A.M.G. Klein Tank, M. Rusticucci, L.V. Alexander, S. Brönnimann, Y. Charabi, F.J. Dentener, E.J. Dlugokencky, D.R. Easterling, A. Kaplan, B.J. Soden, P.W. Thorne, M. Wild and P.M. Zhai, 2013. Observations: atmosphere and surface. In: Stocker, T.F., D. Qin, G.-K. Plattner, M. Tignor, S.K. Allen, J. Boschung, A. Nauels, Y. Xia, V. Bex and P.M. Midgley (eds.), *Climate Change 2013: The Physical Science Basis. Contribution of Working Group I to the Fifth Assessment Report of the Intergovernmental Panel on Climate Change*. Cambridge University Press.

Havens, S., H-P Marshall, C. Pielmeier and K. Elder, 2013. Automatic grain type classification of snow micro penetrometer signals with random forests. *IEEE Transactions on Geoscience and Remote Sensing*, 51:3328-3335.

Hawkins, E. and R.T. Sutton, 2012. Time of emergence of climate signals. *Geophysical Research Letters*, 39:L01702, doi:10.1029/2011GL050087.

Helfrich, S.R., D. McNamara, B.H. Ramsay, T. Baldwin and T. Kasheta, 2007. Enhancements to, and forthcoming developments in the Interactive Multisensor Snow and Ice Mapping System (IMS). *Hydrological Processes*, 21:1576-1586.

Hernández-Henríquez, M.A., S.J. Déry and C. Derksen, 2015. Polar amplification and elevation-dependence in trends of Northern Hemisphere snow cover extent, 1971–2014. *Environmental Research Letters*, 10:044010.

Hezel, P.J., X. Zhang, C.M. Bitz, B.P. Kelly and F. Massonnet, 2012. Projected decline in spring snow depth on Arctic sea ice caused by progressively

later autumn open ocean freeze-up this century. *Geophysical Research Letters*, 39:L17505, doi:10.1029/2012GL052794.

Hinzman, L.D., C.J. Deal, A.D. McGuire, S.H. Mernild, I.V. Polyakov and J.E. Walsh, 2013. Trajectory of the Arctic as an integrated system. *Ecological Applications*, 23:1837-1868.

Hock, R., 2005. Glacier melt: A review on processes and their modelling. *Progress in Physical Geography*, 29:362-391.

Hodson, A., B. Brock, D. Pearce, J. Laybourn-Parry and M. Tranter, 2015. Cryospheric ecosystems: a synthesis of snowpack and glacial research. *Environmental Research Letters*, 10:110201.

Holbrook, W.S., S.N. Miller and M.A. Provart, 2016. Estimating snow water equivalent over long mountain transects using snowmobile-mounted ground-penetrating radar. *GEOPHYSICS*, 81:WA183-WA193.

Homan, J.W. and D.L. Kane, 2015. Arctic snow distribution patterns at the watershed scale. *Hydrology Research*, 46:507-520.

Horton, S., M. Schirmer and B. Jamieson, 2015. Meteorological, elevation, and slope effects on surface hoar formation. *The Cryosphere*, 9:1523-1533.

Hou, A.Y., R.K. Kakar, S. Neeck, A.A. Azarbarzin, C.D. Kummerow, M. Kojima, R. Oki, K. Nakamura and T. Iguchi, 2014. The global precipitation measurement mission. *Bulletin of the American Meteorological Society*, 95:701-722.

IPCC, 2013. Annex I: Atlas of Global and Regional Climate Projections. In: van Oldenborgh, G.J., M. Collins, J. Arblaster, J.H. Christensen, J. Marotzke, S.B. Power, M. Rummukainen and T. Zhou (eds.), *Climate Change 2013: The Physical Science Basis. Contribution of Working Group I to the Fifth Assessment Report of the Intergovernmental Panel on Climate Change*. Cambridge University Press.

Irannezhad, M., A.-K. Ronkanen and B. Kløve, 2016. Wintertime climate factors controlling snow resource decline in Finland. *International Journal of Climatology*, 36:110-131.

Jagt, B.V., A. Lucieer, L. Wallace, D. Turner and M. Durand, 2015. Snow depth retrieval with UAS using photogrammetric techniques. *Geosciences*, 5:264-285.

Jeong, J.-H., J.-S. Kug, B.-M. Kim, S.-K. Min, H.W. Linderholm, C.-H. Ho, D. Rayner, D. Chen and S.-Y. Jun, 2012. Greening in the circumpolar high-latitude may amplify warming in the growing season. *Climate Dynamics*, 38:1421-1431.

Jin, S., X. Qian and H. Kutoglu, 2016. Snow depth variations estimated from GPS-reflectometry: A case study in Alaska from L2P SNR data. *Remote Sensing*, 8:63, doi:10.3390/rs8010063.

Johansson, C., V.A. Pohjola, C. Jonasson and T.V. Callaghan, 2011. Multi-decadal changes in snow characteristics in sub-Arctic Sweden. *Ambio*, 40:566-574.

Johansson, M., T.V. Callaghan, J. Bosiö, H.J. Åkerman, M. Jackowicz-Korczynski and T.R. Christensen, 2013. Rapid responses of permafrost and vegetation to experimentally increased snow cover in sub-arctic Sweden. *Environmental Research Letters*, 8:035025.

Jones, P.D., D.H. Lister, T.J. Osborn, C. Harpham, M. Salmon and C.P. Morice, 2012. Hemispheric and large-scale land surface air temperature variations: an extensive revision and an update to 2010. *Journal of Geophysical Research*, 117:D05127 doi:10.1029/2011JD017139.

Ju, J. and J.G. Masek, 2016. The vegetation greenness trend in Canada and US Alaska from 1984-2012 Landsat data. *Remote Sensing of Environment*, 176:1-16.

Justice, C.O., M.O. Román, I. Csiszar, E.F. Vermote, R.E. Wolfe, S.J. Hook, M. Friedl, Z. Wang, C.B. Schaaf, T. Miura, M. Tschudi, G. Riggs, D.K. Hall, A.I. Lyaoustin, S. Devadiga, C. Davidson and E.J. Musuoka, 2013. Land and cryosphere products from Suomi NPP VIIRS: Overview and status. *Journal of Geophysical Research: Atmospheres*, 118:9753-9765.

Kaasalainen, S., H. Kaartinen, A. Kukko, K. Anttila and A. Krooks, 2011. Application of mobile laser scanning in snow cover profiling. *The Cryosphere*, 5:135-138.

Kapnick, S.B. and T.L. Delworth, 2013. Controls of global snow under a changed climate. *Journal of Climate*, 26:5537-5562.

Karl, T.R., A. Arguez, B. Huang, J.H. Lawrimore, J.R. McMahon, M.J. Menne, T.C. Peterson, R.S. Vose and H.-M. Zhang, 2015. Possible artifacts of data biases in the recent global surface warming hiatus. *Science Express*, doi:10.1126/science.aaa5632.

Kausrud, K.L., A. Mysterud, H. Steen, J.O. Vik, E. Ostbye, B. Cazelles, E. Framstad, A.M. Eikenes, I. Mysterud, T. Solhøy and C.C. Stenseth, 2008. Linking climate change to lemming cycles. *Nature*, 456:93-97.

Key, J.R., R. Mahoney, Y. Liu, P. Romanov, M. Tschudi, Appel, J. Maslanik, D. Baldwin, X. Wang and P. Meade, 2013. Snow and ice products from Suomi NPP VIIRS. *Journal of Geophysical Research: Atmospheres*, 118:12,816-812,830.

Kim, Y., J.S. Kimball, K. Zhang, K. Didan, I. Velicogna and K.C. McDonald, 2014. Attribution of divergent northern vegetation growth responses to lengthening non-frozen seasons using satellite optical-NIR and microwave remote sensing. *International Journal of Remote Sensing*, 35:3700-3721.

Kim, Y., J.S. Kimball, D.A. Robinson and C. Derksen, 2015. New satellite climate data records indicate strong coupling between recent frozen season changes and snow cover over high northern latitudes. *Environmental Research Letters*, 10:084004.

King, J.M.L., 2014. *Remote Sensing Observations of Tundra Snow with Ku-and X-band Radar*. PhD Thesis. University of Waterloo, Canada.

Kivinen, S., E. Kaarlejärvi, K. Jylhä and J. Räisänen, 2012. Spatiotemporal distribution of threatened high-latitude snowbed and snow patch habitats in warming climate. *Environmental Research Letters*, 7:034024.

Klehmet, K., B. Geyer and B. Rockel, 2013. A regional climate model hindcast for Siberia: analysis of snow water equivalent. *The Cryosphere*, 7:1017-1034.

Koch, F., M. Prasch, L. Schmid, J. Schweizer and M. Mauser, 2014. Measuring snow liquid water content with low-cost GPS receivers. *Sensors*, 14:20975-20999.

Koenigk, T., P. Berg and R. Dösscher, 2015. Arctic climate change in an ensemble of regional CORDEX simulations. *Polar Research*, 34:24603, doi:10.3402/polar.v34.24603.

Kononova, N.K., 2012. The influence of atmospheric circulation on the formation of snow cover on the north eastern Siberia. *Ice and Snow*, 1:38-53. (In Russian, English summary)

Koven, C.D., W.J. Riley and A. Stern, 2013. Analysis of permafrost thermal dynamics and response to climate change in the CMIP5 Earth System Models. *Journal of Climate*, 26:1877-1900.

Krenke, A.N., E.A. Cherenkova and M.M. Chernavskaya, 2012. Stability of snow cover on the territory of Russia in relation to climate change. *Ice and Snow*, 1:29-37.

Kretschmer, M., D. Coumou, J.F. Donges and J. Runge, 2016. Using causal effect networks to analyze different Arctic drivers of mid-latitude winter circulation. *Journal of Climate*, 29:4069-4081.

Langlois, A., A. Royer, C. Derksen, B. Montpetit, F. Dupont and K. Goitia, 2012. Coupling the snow thermodynamic model SNOWPACK with the microwave emission model of layered snowpacks for subarctic and arctic snow water equivalent retrievals. *Water Resources Research*, 48, W12524, doi:10.1029/2012WR012133.

Langlois, A., C.A. Johnson, B. Montpetit, A. Royer, E.A. Blukacz-Richards, E. Neave, C. Dolant, A. Roy, G. Arhonditsis, D.K. Kim, and S. Kaluskar, 2017. Detection of rain-on-snow (ROS) events and ice layer formation using passive microwave radiometry: A context for Peary caribou habitat in the Canadian Arctic. *Remote Sensing of Environment*, 189:84-95.

Larose, C., A. Dommergues and T.M. Vogel, 2013. The dynamic arctic snow pack: an unexplored environment for microbial diversity and activity. *Biology*, 2:317-330.

Leffler, A.J. and J.M. Welker, 2013. Long-term increases in snow pack elevate leaf N and photosynthesis in *Salix arctica*: responses to a snow fence experiment in the High Arctic of NW Greenland. *Environmental Research Letters*, 8:025023.

Leffler, A.J., E.S. Klein, S.F. Oberbauer and J.M. Welker, 2016. Coupled long-term summer warming and deeper snow alters species composition and stimulates gross primary productivity in tussock tundra. *Oecologia*, 181:287-297.

Leinss, S., G. Parrella and I. Hajnsek, 2014. Snow height determination by polarimetric phase differences in X-Band SAR data. *IEEE Journal of Selected Topics in Applied Earth Observations and Remote Sensing*, 7:3794-3810.

Leinss, S., A. Wiesmann, J. Lemmettyinen and I. Hajnsek, 2015. Snow water equivalent of dry snow measured by differential interferometry. *IEEE Journal of Selected Topics in Applied Earth Observations and Remote Sensing*, 8:3773-3790.

Lesack, L.F.W., P. Marsh, F.E. Hicks and D.L. Forbes, 2014. Local spring warming drives earlier river-ice breakup in a large Arctic delta. *Geophysical Research Letters*, 41:1560-1567.

Letcher, T.W. and J.R. Minder, 2015. Characterization of the simulated regional snow albedo feedback using a Regional Climate Model over complex terrain. *Journal of Climate*, 28:7576-7595.

Lindsay, C., J. Zhu, A.E. Miller, P. Kirchner and T.L. Wilson, 2015. Deriving snow cover metrics for Alaska from MODIS. *Remote Sensing*, 7:12961-12985.

Liston, G.E. and K. Elder, 2006. A distributed snow-evolution modeling system (SnowModel). *Journal of Hydrometeorology*, 7:1259-1276.

Liston, G.E. and C.A. Hiemstra, 2011. The changing cryosphere: pan-arctic snow trends (1979–2009). *Journal of Climate*, 24:5691-5712.

López-Moreno, J.I., J. Revuelto, S.R. Fassnacht, C. Azorín-Molina, S.M. Vicente-Serrano, E. Morán-Tejeda and G.A. Sexstone, 2015. Snowpack variability across various spatio-temporal resolutions. *Hydrological Processes*, 29:1213-1224.

Loranty, M.M., L.T. Berner, S.J. Goetz, Y. Jin and J.T. Randerson, 2014. Vegetation controls on northern high latitude snow-albedo feedback: observations and CMIP5 model simulations. *Global Change Biology*, 20:594-606.

Lucas-Picher, P., M. Wulff-Nielsen, J.H. Christensen, G. Aðalgeirsdóttir, R. Mottram, and S.B. Simonsen, 2012. Very high resolution regional climate model simulations over Greenland: Identifying added value. *Journal of Geophysical Research: Atmospheres*, 117:D02108, doi:10.1029/2011JD016267.

Lutz, S., A.M. Anesio, R. Raiswell, A. Edwards, R.J. Newton, F. Gill and L.G. Benning, 2016. The biogeography of red snow microbiomes and their role in melting arctic glaciers. *Nature Communications*, 7: Article no. 11968.

Luus, K.A., J.C. Lin, R.E. Kelly and C.R. Duguay, 2013. Subnivean Arctic and sub-Arctic net ecosystem exchange (NEE) Towards representing snow season processes in models of NEE using cryospheric remote sensing. *Progress in Physical Geography*, 37:484-515.

Ma, Q., K. Wang and M. Wild, 2014. Evaluations of atmospheric downward longwave radiation from 44 coupled general circulation models of CMIP5. *Journal of Geophysical Research: Atmospheres*, 119:4486-4497.

Macander, M.J., C.S. Swingley, K. Joly and M.K. Reynolds, 2015. Landsat-based snow persistence map for northwest Alaska. *Remote Sensing of Environment*, 163:23-31.

Maccario, L., L. Sanguino, T.M. Vogel and C. Larose, 2015. Snow and ice ecosystems: not so extreme. *Research in Microbiology*, 166:782-795.

Maher, A.I., P.M. Treitz and M.A. Ferguson, 2012. Can Landsat data detect variations in snow cover within habitats of arctic ungulates? *Wildlife Biology*, 18:75-87.

Mair, E., G. Leitinger, S. Della Chiesa, G. Niedrist, U. Tappeiner and G. Bertoldi, 2015. A simple method to combine snow height and meteorological observations to estimate winter precipitation at sub-daily resolution. *Hydrological Sciences Journal*, 61:2050-2060.

Maksyutova, E.V., N.V. Kichigina, N.N. Voropai, A.S. Balybina and O.P. Osipova, 2012. Tendencies of hydroclimatic changes on the Baikal natural territory. *Geography and Natural Resources*, 33:304-311.

Malik, M.J., R. Velde, Z. Vekerdy and Z. Su, 2014. Improving modeled snow albedo estimates during the spring melt season. *Journal of Geophysical Research: Atmospheres*, 119:7311-7331.

Malnes, E., A. Buanes, T. Nagler, G. Bippus, D. Gustafsson, C. Schiller, S. Metsämäki, J. Pulliainen, K. Luojus, H.E. Larsen and R. Solberg, 2015. User requirements for the snow and land ice services—CryoLand. *The Cryosphere*, 9:1191-1202.

Margulies, S.A., M. Giroto, G. Cortés and M. Durand, 2015. A particle batch smoother approach to snow water equivalent estimation. *Journal of Hydrometeorology*, 16:1752-1772.

Marsh, P., P. Bartlett, M. MacKay, S. Pohl and T. Lantz, 2010. Snowmelt energetics at a shrub tundra site in the western Canadian Arctic. *Hydrological Processes*, 24:3603-3620.

Mateling, M., 2016. Improving satellite estimates of global snowfall. *Physics Today*, doi.org/10.1063/PT.5.4019.

McAfee, S.A., J. Walsh and T.S. Rupp, 2014. Statistically downscaled projections of snow/rain partitioning for Alaska. *Hydrological Processes*, 28:3930-3946.

McCreight, J.L., E.E. Small and K.M. Larson, 2014. Snow depth, density, and SWE estimates derived from GPS reflection data: Validation in the western US. *Water Resources Research*, 50:6892-6909.

McGrath, D., L. Sass, S. O'Neil, A. Arendt, G. Wolken, A. Gusmeroli, C. Kienholz and C. McNeil, 2015. End-of-winter snow depth variability on glaciers in Alaska. *Journal of Geophysical Research: Earth Surface*, 120:1530-1550.

Mearns, L.O., M. Hulme, T.R. Carter, R. Leemans, M. Lal and P. Whetton, 2001. Climate scenario development. In; *Climate Change 2001. Working Group I: The Scientific Basis*. Third Assessment Report of the Intergovernmental Panel on Climate Change. pp. 739-768. Cambridge University Press.

Ménard, C.B., R. Essery, J. Pomeroy, P. Marsh and D.B. Clark, 2014a. A shrub bending model to calculate the albedo of shrub-tundra. *Hydrological Processes*, 28:341-351.

Ménard, C.B., R. Essery and J. Pomeroy, 2014b. Modelled sensitivity of the snow regime to topography, shrub fraction and shrub height. *Hydrology and Earth System Sciences*, 18:2375-2392.

Ménégoz, M., G. Krinner, Y. Balkanski, A. Cozic, O. Boucher and P. Ciais, 2013. Boreal and temperate snow cover variations induced by black carbon emissions in the middle of the 21st century. *The Cryosphere*, 7:537-554.

Menne, M.J., I. Durre, R.S. Vose, B.E. Gleason and T.G. Houston, 2012. An overview of the Global Historical Climatology Network-Daily Database. *Journal of Atmospheric and Oceanic Technology*, 29:897-910.

Metsämäki, S., 2013. A fractional snow cover mapping method for optical remote sensing data, applicable to continental scale. Doctoral dissertation in Remote Sensing, Aalto University, Finalnd.

Metsämäki, S., J. Pulliainen, M. Salminen, K. Luojus, A. Wiesmann, R. Solberg, K. Böttcher, M. Hiltunen and E. Ripper, 2015. Introduction to GlobSnow Snow Extent products with considerations for accuracy assessment. *Remote Sensing of Environment*, 156:96-108.

Michele, C.D., F. Avanzi, D. Passoni, R. Barzaghi, L. Pinto, P. Dosso, A. Ghezzi, R. Gianatti and G. Della Vedova, 2015. Microscale variability of snow depth using UAS technology. *The Cryosphere Discussions*, 9:1047-1075.

Miller, G.H., S.J. Lehman, K.A. Refsnider, J.R. Southon and Y. Zhong, 2013. Unprecedented recent summer warmth in Arctic Canada. *Geophysical Research Letters*, 40:5745-5751.

Min, S.-K., X. Zhang and F. Zwiers, 2008. Human-induced Arctic moistening. *Science*, 320:518-520.

Min, S.-K., X. Zhang, F.W. Zwiers and G.C. Hegerl, 2011. Human contribution to more-intense precipitation extremes. *Nature*, 470:378-381.

Mioduszewski, J.R., A.K. Rennermalm, D.A. Robinson and L. Wang, 2015. Controls on spatial and temporal variability in Northern Hemisphere terrestrial snow melt timing, 1979-2012. *Journal of Climate*, 28:2136-2153.

Montpetit, B., A. Royer, A. Langlois, P. Cliche, A. Roy, N. Champollion, G. Picard, F. Domine and R. Obbard, 2012. New shortwave infrared albedo measurements for snow specific surface area retrieval. *Journal of Glaciology*, 58:941-952.

Montpetit, B., A. Royer, A. Roy, A. Langlois and C. Derksen, 2013. Snow microwave emission modeling of ice lenses within a snowpack using the Microwave Emission Model for Layered Snowpacks. *IEEE Transactions on Geoscience and Remote Sensing*, 51:4705-4717.

Mortin, J., T.M. Schröder, A. Walloe Hansen, B. Holt and K.C. McDonald, 2012. Mapping of seasonal freeze-thaw transitions across the pan-Arctic land and sea ice domains with satellite radar. *Journal of Geophysical Research: Oceans*, 117:C08004, doi:10.1029/2012JC008001.

Mudryk, L.R., P.J. Kushner and C. Derksen, 2014. Interpreting observed Northern Hemisphere snow trends with large ensembles of climate simulations. *Climate Dynamics*, 43:345-359.

Mudryk, L.R., C. Derksen, P.J. Kushner and R. Brown, 2015. Characterization of Northern Hemisphere snow water equivalent datasets, 1981–2010. *Journal of Climate*, 28:8037-8051.

Muñoz, J., J. Infante, T. Lakhankar, R. Khanbilvardi, P. Romanov, N. Krakauer and A. Powell, 2013. Synergistic use of remote sensing for snow cover and snow water equivalent estimation. *British Journal of Environment and Climate Change*, 3:612-627.

Musselman, K.N., J.W. Pomeroy, R.L. Essery and N. Leroux, 2015. Impact of windflow calculations on simulations of alpine snow accumulation, redistribution and ablation. *Hydrological Processes*, 29:3983-3999.

Myers-Smith, I.H., S.C. Elmendorf, P.S. Beck, M. Wilmking, M. Hallinger, D. Blok, ... and M. Vellend, 2015. Climate sensitivity of shrub growth across the tundra biome. *Nature Climate Change*, 5:887-891.

Naeimi, V., C. Paulik, A. Bartsch, W. Wagner, R. Kidd, S.-E. Park, K. Elger and J. Boike, 2012. ASCAT Surface State Flag (SSF): Extracting information on surface freeze/thaw conditions from backscatter data using an empirical threshold-analysis algorithm. *IEEE Transactions on Geoscience and Remote Sensing*, 50:2566-2582.

Najafi, M.R., F.W. Zwiers and N.P. Gillett, 2016. Attribution of the spring snow cover extent decline in the Northern Hemisphere, Eurasia and North America to anthropogenic influence. *Climatic Change*, 136:571-586.

Namazi, M., K. von Salzen and J.N.S. Cole, 2015. Simulation of black carbon in snow and its climate impact in the Canadian Global Climate Model. *Atmospheric Chemistry and Physics*, 15:10887-10904.

Nitu, R., 2013. Cold as SPICE. *Meteorological Technology International*, August 2013, 148-150.

Niu, G.-Y., K.-W. Seo, Z.-L. Yang, C. Wilson, H. Su, J. Chen and M. Rodell, 2007. Retrieving snow mass from GRACE terrestrial water storage change with a land surface model. *Geophysical Research Letters*, 34:L15704, doi:10.1029/2007GL030413.

Nolin, A., 2010. Recent advances in remote sensing of seasonal snow cover. *Journal of Glaciology*, 56:1141-1150.

Ogden, L.E., 2015. Plants duke it out in a warming Arctic. *BioScience*, 65:220, doi:10.1093/biosci/biu209.

Olofsson, J., L. Ericson, M. Torp, S. Stark and R. Baxter, 2011. Carbon balance of Arctic tundra under increased snow cover mediated by a plant pathogen. *Nature Climate Change*, 1:220-223.

Orsolini, Y.J., R. Senan, F. Vitart, G. Balsamo, A. Weisheimer and F.J. Doblas-Reyes, 2016. Influence of the Eurasian snow on the negative North Atlantic Oscillation in subseasonal forecasts of the cold winter 2009/2010. *Climate Dynamics*, 47:1325-1334.

Osokin, N.I. and A.V. Sosnovsky, 2014. Spatial and temporal variability of depth and density of the snow cover in Russia. *Ice and Snow*, 4:72-80. (In Russian, English summary)

Ouellet, F., A. Langlois, E.A. Blukacz-Richards, C.A. Johnson, A. Royer, E. Neave and N.C. Larter, 2016. Spatialization of the SNOWPACK snow model for the Canadian Arctic to assess Peary caribou winter grazing conditions, *Physical Geography*, doi:10.1080/02723646.2016.1274200.

Overland, J.E., 2016. Is the melting Arctic changing midlatitude weather? *Physics Today*, 69: doi: 10.1063/PT.3.3107.

Overland, J., J. Francis, E. Hanna and M. Wang, 2012. The recent shift in early summer Arctic atmospheric circulation. *Geophysical Research Letters*, 39:L19804, doi:10.1029/2012GL053268.

Painter, T.H., K. Rittger, C. McKenzie, P. Slaughter, R.E. Davis and J. Dozier, 2009. Retrieval of subpixel snow covered area, grain size, and albedo from MODIS. *Remote Sensing of Environment*, 113:868-879.

Park, H., H. Yabuki and T. Ohata, 2012. Analysis of satellite and model datasets for variability and trends in Arctic snow extent and depth, 1948–2006. *Polar Science*, 6:23-37.

Park, H., J.E. Walsh, Y. Kim, T. Nakai and T. Ohata, 2013. The role of declining Arctic sea ice in recent decreasing terrestrial Arctic snow depths. *Polar Science*, 7:174-187.

Park, H., A.B. Sherstiukov, A.N. Fedorov, I.V. Polyakov and J. E. Walsh, 2014. An observation-based assessment of the influences of air temperature and snow depth on soil temperature in Russia. *Environmental Research Letters*, 9:064026.

Park, H., A.N. Fedorov, M.N. Zheleznyak, P.Y. Konstantinov and J.E. Walsh, 2015. Effect of snow cover on pan-Arctic permafrost thermal regimes. *Climate Dynamics*, 44:2873-2895.

Pattison, R.R., J.C. Jorgenson, M.K. Reynolds and J.M. Welker, 2015. Trends in NDVI and tundra community composition in the Arctic of NE Alaska between 1984 and 2009. *Ecosystems*, 18:707-719.

Pearson, R.G., S.J. Phillips, M.M. Loranty, P.S. Beck, T. Damoulas, S.J. Knight and S.J. Goetz, 2013. Shifts in Arctic vegetation and associated feedbacks under climate change. *Nature Climate Change*, 3:673-677.

Pedersen, S.H., G.E. Liston, M.P. Tamstorf, A. Westergaard-Nielsen and N.M. Schmidt, 2015. Quantifying episodic snowmelt events in Arctic ecosystems. *Ecosystems*, 18:839-856.

Peings, Y., E. Brun, V. Mauvais and H. Douville, 2013. How stationary is the relationship between Siberian snow and Arctic Oscillation over the 20th century? *Geophysical Research Letters*, 40:183-188.

Peng, S., S. Piao, P. Ciais, P. Friedlingstein, L. Zhou and T. Wang, 2013. Change in snow phenology and its potential feedback to temperature in the Northern Hemisphere over the last three decades. *Environmental Research Letters*, 8: 014008.

Pepin, N., R.S. Bradley, H.F. Diaz, M. Baraer, E.B. Caceres, N. Forsythe, H. Fowler, G. Greenwood, M.Z. Hashmi, X.D. Liu, J.R. Miller, L. Ning, A. Ohmura, E. Palazzi, I. Rangwala, W. Schöner, I. Severskiy, M. Shahgedanova, M.B. Wang, S.N. Williamson and D.Q. Yang, 2015. Elevation-dependent warming in mountain regions of the world. *Nature Climate Change*, 5:424-430.

Perket, J., M.G. Flanner and J.E. Kay, 2014. Diagnosing shortwave cryosphere radiative effect and its 21st century evolution in CESM. *Journal of Geophysical Research: Atmospheres*, 119:1356-1362.

Petrie, R.E., L.C. Shaffrey and R.T. Sutton, 2015. Atmospheric response in summer linked to recent Arctic sea ice loss. *Quarterly Journal of the Royal Meteorological Society*, 141:2070-2076.

Pithan, F. and T. Mauritsen, 2014. Arctic amplification dominated by temperature feedbacks in contemporary climate models. *Nature Geoscience*, 7:181-184.

Popova, V.V., A.V. Shiryayeva and P.A. Morozova, 2014. Snow cover onset dates in the north of Eurasia: relations and feedback to the macro-scale atmospheric circulation. *Snow and Ice*, 3:39-49. (In Russian, English summary)

Proksch, M., H. Löwe and M. Schneebeli, 2015. Density, specific surface area, and correlation length of snow measured by high-resolution penetrometry. *Journal of Geophysical Research: Earth Surface*, 120:346-362.

Proksch, M., N. Rutter, C. Fierz and M. Schneebeli, 2016. Intercomparison of snow density measurements: bias, precision, and vertical resolution. *The Cryosphere*, 10:371-384.

Qian, Y., T.J. Yasunari, S.J. Doherty, M.G. Flanner, W.K.M. Lau, J. Ming, H. Wang, M. Wang, S.G. Warren and R. Zhang, 2015. Light-absorbing particles in snow and ice: Measurement and modeling of climatic and hydrological impact. *Advances in Atmospheric Sciences*, 32:64-91.

Qu, X. and A. Hall, 2014. On the persistent spread in snow-albedo feedback. *Climate Dynamics*, 42:69-81.

Räisänen, J., 2008. Warmer climate: less or more snow? *Climate Dynamics*, 30:307-319.

Ramillien, G., L. Seoane, F. Frappart, R. Biancale, S. Gratton, X. Vasseur and S. Bourgogne, 2012. Constrained regional recovery of continental water mass time-variations from GRACE-based geopotential anomalies. *Surveys in Geophysics*, 33:887-905.

Rapaic, M., R. Brown, M. Markovic and D. Chaumont, 2015. An evaluation of temperature and precipitation surface-based and reanalysis datasets for the Canadian Arctic, 1950-2010. *Atmosphere-Ocean*, 53:283-303.

Rasmus, S., J. Kumpula and J. Siitari, 2014. Can a snow structure model estimate snow characteristics relevant to reindeer husbandry? *Rangifer*, 34:37-56.

Rasmus, S., J. Boelhouwers, A. Briede, I.A. Brown, M. Falarz, S. Ingvander, J. Jaagus, L. Kitaev, A. Mercer and E. Rimkus, 2015. Recent change – Terrestrial cryosphere. In: *Second Assessment of Climate Change for the Baltic Sea Basin*. pp 117-129. Springer.

Rasmus, S., S. Kivinen, M. Bavay and J. Heiskanen, 2016. Local and regional variability in snow conditions in northern Finland: A reindeer herding perspective. *Ambio*, 45:398-414.

Rasmussen, R., B. Baker, J. Kochendorfer, T. Meyers, S. Landolt, A.P. Fischer, J. Black, J.M. Thériault, P. Kucera, D. Gochis, C. Smith, R. Nitu, M. Hall, K. Ikeda and E. Gutmann, 2012. How well are we measuring snow: the NOAA/FAA/NCAR winter precipitation test bed. *Bulletin of the American Meteorological Society*, 93:811-829.

Rawlins, M.A., M. Steele, M.M. Holland, J.C. Adam, J.E. Cherry, J.A. Francis, P.Ya Groisman, L.D. Hinzman, T.G. Huntington, D.L. Kane, J.S. Kimball, R. Kwok, R.B. Lammers, C.M. Lee, D.P. Lettemaier, K.C. McDonald, E. Podest, J.W. Pundsack, B. Rudels, M.C. Serreze, A. Shiklomanov, Ø. Skagseth, T.J. Troy, C.J. Vörösmarty, M. Wensnahan, E.F. Wood, R. Woodgate, D. Yang, K. Zhang and T. Zhang, 2010. Analysis of the Arctic system for freshwater cycle intensification: observations and expectations. *Journal of Climate*, 23:5715-5737.

Reba, M.L., J. Pomeroy, D. Marks and T.E. Link, 2012. Estimating surface sublimation losses from snowpacks in a mountain catchment using eddy covariance and turbulent transfer calculations. *Hydrological Processes*, 26:3699-3711.

Rees, A., M. English, C. Derksen, P. Toose and A. Silis, 2014. Observations of late winter Canadian tundra snow cover properties. *Hydrological Processes*, 28:3962-3977.

Reichle, R., R. Koster, G. De Lannoy, B. Forman, Q. Liu, S. Mahanam and A. Toure, 2011. Assessment and enhancement of MERRA land surface hydrology estimates. *Journal of Climate*, 24:6322-6338.

Reid, D.G., D. Berteaux and K.L. Laidre, 2013. Mammals. In: Meltofte, H. (ed.), *Arctic Biodiversity Assessment, Status and trends in Arctic biodiversity*. pp. 78-141. *Conservation of Arctic Flora and Fauna (CAFF)*, Akureyri, Iceland.

Revuelto, J., V. Vionnet, J.I. López-Moreno, M. Lafaysse and S. Morin, 2016. Combining snowpack modeling and terrestrial laser scanner observations improves the simulation of small scale snow dynamics. *Journal of Hydrology*, 533:291-307.

Rienecker, M.M., R. Todling, J. Bacmeister, E. Liu, M.G. Bosilovich, S.D. Schubert, L. Takacs, G.-K. Kim, S. Bloom, J. Chen, D. Collins, A. Conaty,

A. da Silva, W. Gu, J. Joiner, R.D. Koster, R. Lucchesi, A. Molod, T. Owens, S. Pawson, P. Pegion, C.R. Redder, R. Reichle, F.R. Robertson, A.G. Ruddick, M. Sienkiewicz and J. Woollen, 2011. MERRA: NASA's Modern-Era Retrospective Analysis for Research and Applications. *Journal of Climate*, 24:3624-3648.

Rittger, K., T.H. Painter and J. Dozier, 2013. Assessment of methods for mapping snow cover from MODIS. *Advances in Water Resources*, 51:367-380.

Rodionov, V.F., E.I. Aleksandrov, N.N. Bryazgin and A.A. Dementiev, 2013. Changes in temperature, precipitation and snow cover in the Arctic Seas region, 1981-2010. *Snow and Ice*, 1:61-68. (In Russian, English summary)

Rogers, M.C., P.F. Sullivan and J.M. Welker, 2011. Evidence of nonlinearity in the response of net ecosystem CO₂ exchange to increasing levels of winter snow depth in the High Arctic of Northwest Greenland. *Arctic, Antarctic, and Alpine Research*, 43:95-106.

Rosvold, J., 2016. Perennial ice and snow-covered land as important ecosystems for birds and mammals. *Journal of Biogeography*, 43:3-12.

Rott, H and T. Nagler, 1995. Monitoring temporal dynamics of snowmelt with ERS-1 SAR. *IEEE International Geoscience and Remote Sensing Symposium*, IGARSS 1995. pp. 1747-1749.

Rott, H., D.W. Cline, C. Duguay, R. Essery, P. Etchevers, I. Hajnsek, M. Kern, G. Macelloni, E. Malnes, J. Pullianen and S.H. Yueh, 2013. COREH20: High-resolution X/Ku-band radar imaging of cold land processes. *IEEE International Geoscience and Remote Sensing Symposium*, IGARSS 2013. pp. 3479-3482.

Rowlands, D.D., S.B. Luthcke, J.J. McCarthy, S.M. Klosko, D.S. Chinn, F.G. Lemoine, J.-P. Boy and T.J. Sabaka, 2010. Global mass flux solutions from GRACE: A comparison of parameter estimation strategies – Mass concentrations versus Stokes coefficients. *Journal of Geophysical Research*, 115:B01403, doi:10.1029/2009JB006546.

Rumpf, S.B., P.R. Semenchuk, S. Dullinger and E.J. Cooper, 2014. Idiosyncratic responses of high arctic plants to changing snow regimes. *PloS one*, 9:e86281.

Rundqvist, S., H. Hedenås, A. Sandström, U. Emanuelsson, H. Eriksson, C. Jonasson and T.V. Callaghan, 2011. Tree and shrub expansion over the past 34 years at the tree-line near Abisko, Sweden. *Ambio*, 40:683-692.

Ruppel, M.M., E. Isaksson, J. Ström, E. Beaudon, J. Svensson, C.A. Pedersen and A. Korhola, 2014. Increase in elemental carbon values between 1970 and 2004 observed in a 300-year ice core from Holtedahlfonna (Svalbard). *Atmospheric Chemistry and Physics*, 14:11447-11460.

Rutter, N., M. Sandells, C. Derksen, P. Toose, A. Royer, B. Montpetit, A. Langlois, J. Lemmettyinen and J. Pulliainen, 2014. Snow stratigraphic heterogeneity within ground-based passive microwave radiometer footprints: Implications for emission modeling. *Journal of Geophysical Research*, 119:550-565.

Saffioti, C., E.M. Fischer and R. Knutti, 2015. Contributions of atmospheric circulation variability and data coverage bias to the warming hiatus. *Geophysical Research Letters*, 42:2385-2391.

Sait, E., D.J. Solie and M. Sturm, 2014. Testing a light-weight compact gamma ray detector for measuring snow water equivalent. In AGU Fall Meeting Abstracts (Vol. 1, p. 0383).

Sandvik, S.M. and A. Odland, 2014. Changes in alpine snowbed-wetland vegetation over three decades in northern Norway. *Nordic Journal of Botany*, 32:377-384.

Sannel, A.B.K., G. Hugelius, P. Jansson and P. Kuhry, 2016. Permafrost warming in a subarctic peatland – which meteorological controls are most important? *Permafrost and Periglacial Processes*, 27:177-188.

Scaff, L., D. Yang, Y. Li and E. Mekis, 2015. Inconsistency in precipitation measurements across the Alaska–Yukon border. *The Cryosphere*, 9:2417-2428.

Schmidt, G.A., D.T. Shindell and K. Tsigaridis, 2014. Reconciling warming trends. *Nature Geoscience*, 7:158-160.

Schmidt, N.M., S.H. Pedersen, J.B. Mosbacher and L.H. Hansen, 2015. Long-term patterns of muskox (*Ovibos moschatus*) demographics in high arctic Greenland. *Journal of Polar Biology*, 38:1667-1675.

Screen, J.A., I. Simmonds, C. Deser and R. Tomas, 2013. The atmospheric response to three decades of observed Arctic sea ice loss. *Journal of Climate*, 26:1230-1248.

Semenchuk, P.R., B. Elberling, C. Amtorp, J. Winkler, S. Rumpf, A. Michelsen and E.J. Cooper, 2015. Deeper snow alters soil nutrient availability and leaf nutrient status in high Arctic tundra. *Biogeochemistry*, 124:81-94.

Semmens, K.A. and J. M. Ramage, 2013. Recent changes in spring snowmelt timing in the Yukon River basin detected by passive microwave satellite data. *The Cryosphere*, 7:905-916.

Semmens, K.A., J. Ramage, A. Bartsch and G.E. Liston, 2013. Early snowmelt events: detection, distribution, and significance in a major sub-arctic watershed. *Environmental Research Letters*, 8:014020.

Seo, K.-W., D. Ryu, B.-M. Kim, D.E. Waliser, B. Tian and J. Eom, 2010. GRACE and AMSR-E-based estimates of winter season solid precipitation accumulation in the Arctic drainage region. *Journal of Geophysical Research*, 115:D20117, doi:10.1029/2009JD013504.

Serreze, M.C., A.P. Barrett and F. Lo, 2005. Northern high-latitude precipitation as depicted by atmospheric reanalyses and satellite retrievals. *Monthly Weather Review*, 133:3407-3430.

Shi, H.X. and C.H. Wang, 2015. Projected 21st century changes in snow water equivalent over Northern Hemisphere landmasses from the CMIP5 model ensemble. *The Cryosphere*, 9:1943-1953.

Shi, X., S.J. Déry, P.Ya. Groisman and D.P. Lettenmaier, 2013. Relationships between recent pan-Arctic snow cover and hydroclimate trends. *Journal of Climate*, 26:2048-2064.

Shi, J., X. Dong, T. Zhao, J. Du, L. Jiang, Y. Du, H. Liu, Z. Wang, D. Ji and C. Xiong, 2014. WCOM: The science scenario and objectives of a global water cycle observation mission. *IEEE International Geoscience and Remote Sensing Symposium*, IGARSS 2014. pp. 3646-3649.

Shi, X., P. Marsh and D. Yang, 2015. Warming spring air temperatures, but delayed spring streamflow in an Arctic headwater basin. *Environmental Research Letters*, 10:064003, doi:10.1088/1748-9326/10/6/064003.

Shmakin, A.B, 2010. Climatic characteristics of snow cover over North Eurasia the last decades. *Ice and Snow*, 1:43-57.

Sicart, J.-E., J.W. Pomeroy, R.L.H. Essery and D. Bewley, 2006. Incoming longwave radiation to melting snow: observations, sensitivity and estimation in northern environments. *Hydrological Processes*, 20:3697-3708.

Skaugen, T., H.B. Strandén and T. Saloranta, 2012. Trends in snow water equivalent in Norway (1931–2009). *Hydrology Research*, 43:489-499.

Skeie, R.B., T. Berntsen, G. Myhre, C.A. Pedersen, J. Ström, S. Gerland and J.A. Ogren, 2011. Black carbon in the atmosphere and snow, from pre-industrial times until present. *Atmospheric Chemistry and Physics*, 11:6809-6836.

Smith, K.L., C.G. Fletcher and P. J. Kushner, 2010. The role of linear interference in the Annular Mode response to extratropical surface forcing. *Journal of Climate*, 23:6036-6050.

Smith, K.L., P.J. Kushner and J. Cohen, 2011. The role of linear interference in Northern Annual Mode variability associated with Eurasian snow cover extent. *Journal of Climate*, 24:6185-6202.

Sospedra-Alfonso, R., W.J. Merryfield and V.V. Kharin, 2016. Representation of snow in the Canadian seasonal to interannual prediction system: Part II. Potential predictability and hindcast skill. *Journal of Hydrometeorology*, 17:2511-2535.

Steiner, N.S., K. Azetsu-Scott, J. Hamilton, K. Hedges, X. Hu, M.Y. Janjua, D. Lavoie, J. Loder, H. Melling, A. Merzouk, W. Perrie, I. Petersen, M. Scarrat, T. Sou and R. Tallmann, 2015. Observed trends and climate projections affecting marine ecosystems in the Canadian Arctic. *Environmental Reviews*, 23:191-239.

Stieglitz, M., S.J. Déry, V.E. Romanovsky and T.E. Osterkamp, 2003. The role of snow cover in the warming of arctic permafrost. *Geophysical Research Letters*, 30:1721, doi:10.1029/2003GL017337.

Stien, A., R.A. Ims, S.D. Albon, E. Fuglei, R.J. Irvine, E. Ropstad, O. Halvorsen, R. Langvatn, L.E. Iøe, V. Veiberg and N.G. Yoccoz, 2012. Congruent responses to weather variability in high arctic herbivores. *Biology Letters*, doi:10.1098/rsbl.2012.0764.

Stuefer, S.L. and D.L. Kane, 2016. Snow retention for increased water supply of shallow Arctic lakes. *Cold Regions Science and Technology*, 123:32-43.

Sturm, M. and S. Stuefer, 2013. Wind-blown flux rates derived from drifts at arctic snow fences. *Journal of Glaciology*, 59:21-34.

Sturm, M., M.A. Goldstein and C. Parr, 2017. Water and life from snow: A trillion dollar science question. *Water Resources Research*, 53, doi:10.1002/2017WR020840.

Su, H., Z.-L. Yang, R.E. Dickinson, C.R. Wilson and G.-Y. Niu, 2010. Multisensor snow data assimilation at the continental scale: The value of Gravity Recovery and Climate Experiment terrestrial water

storage information, *Journal of Geophysical Research*, 115:D10104, doi:10.1029/2009JD013035.

Sun, S., T. Che, J. Wang, H. Li, X. Hao, Z. Wang and J. Wang, 2015. Estimation and analysis of snow water equivalents based on C-Band SAR data and field measurements. *Arctic, Antarctic, and Alpine Research*, 47:313-326.

Surussavadee, C. and D.H. Staelin, 2009. Satellite retrievals of arctic and equatorial rain and snowfall rates using millimeter wavelengths. *IEEE Transactions on Geoscience and Remote Sensing*, 47:3697-3707.

Takala, M., K. Luojus, J. Pulliainen, C. Derksen, J. Lemmetyinen, J.-P. Kärnä, J. Koskinen and B. Bojkov, 2011. Estimating northern hemisphere snow water equivalent for climate research through assimilation of space-borne radiometer data and ground-based measurements. *Remote Sensing of Environment*, 115:3517-3529.

Tan, A., J.C. Adam and D.P. Lettenmaier, 2011. Change in spring snowmelt timing in Eurasian Arctic rivers. *Journal of Geophysical Research: Atmospheres*, 116:D03101, doi:10.1029/2010JD014337.

Tang, Q., X. Zhang and J.A. Francis, 2014. Extreme summer weather in northern mid-latitudes linked to a vanishing cryosphere. *Nature Climate Change*, 4:45-50.

Tapley, B.D., S. Bettadpur, J.C. Ries, P.F. Thompson and M.M. Watkins, 2004. GRACE measurements of mass variability in the Earth system. *Science*, 305:503-505.

Taylor, K.E., R.J. Stouffer and G.A. Meehl, 2012. An Overview of CMIP5 and the experiment design. *Bulletin of the American Meteorological Society*, 93:485-498.

Tedesco, M., 2012. Hemispheric snow water equivalent: The need for a synergistic approach. *Eos*, 93:305-306.

Tedesco, M., S. Doherty, X. Fettweis, P. Alexander, J. Jeyaratnam and J. Stroeve, 2016. The darkening of the Greenland ice sheet: trends, drivers, and projections (1981–2100). *The Cryosphere*, 10:477-496.

Thackeray, C.W. and C.G. Fletcher, 2016. Snow albedo feedback: Current knowledge, importance, outstanding issues and future directions. *Progress in Physical Geography*, 40:392-408.

Thackeray, C.W., C.G. Fletcher and C. Derksen, 2014. The influence of canopy snow parameterizations on snow albedo feedback in boreal forest regions. *Journal of Geophysical Research: Atmospheres*, 119:9810-9821.

Thackeray, C.W., C.G. Fletcher and C. Derksen, 2015. Quantifying the skill of CMIP5 models in simulating seasonal albedo and snow cover evolution. *Journal of Geophysical Research: Atmospheres*, 120:5831-5849.

Tong, J., S.J. Déry, P.L. Jackson and C. Derksen, 2010. Testing snow water equivalent retrieval algorithms for passive microwave remote sensing in an alpine watershed of western Canada. *Canadian Journal of Remote Sensing*, 36:S74-S86.

Tryhorn, L. and A. DeGaetano, 2013. A methodology for statistically downscaling seasonal snow cover characteristics over the Northeastern United States. *International Journal of Climatology*, 33:2728-2743.

Turunen, M.T., S. Rasmus, M. Bavay, K. Ruosteenoja and J. Heiskanen, 2016. Coping with difficult weather and snow conditions: Reindeer herders' views on climate change impacts and coping strategies. *Climate Risk Management*, 11:15-36.

Ulaby, F.T. and W.H. Stiles, 1980. The active and passive microwave response to snow parameters: 2. Water equivalent of dry snow. *Journal of Geophysical Research*, 85(C2):1045-1049.

Urban, M., M. Forkel, J. Eberle, C. Hüttich, C. Schmullius and M. Herold, 2014. Pan-arctic climate and land cover trends derived from multivariate and multi-scale analyses (1981–2012). *Remote Sensing*, 6:2296-2316.

van Vuuren, D.P., J. Edmonds, M. Kainuma, K. Riahi, A. Thomson, K. Hibbard, G.C. Hurtt, T. Kram, V. Krey, J.-F. Lamarque, T. Masui, M. Meinshausen, N. Nakicenovic, S.J. Smith and S.K. Rose, 2011. The representative concentration pathways: an overview. *Climatic Change*, 109:5-31.

Varhola, A., N.C. Coops, M. Weiler and R.D. Moore, 2010. Forest canopy effects on snow accumulation and ablation: An integrative review of empirical results. *Journal of Hydrology*, 392:219-233.

Vihma, T., J. Screen, M. Tjernström, B. Newton, X. Zhang, V. Popova, C. Deser, M. Holland and T. Prowse, 2016. The atmospheric role in the Arctic water cycle: A review on processes, past and future changes, and their impacts. *Journal of Geophysical Research: Biogeosciences*, 121:586-620.

Vikhamar-Schuler, D., I. Hanssen-Bauer, T. Schuler, S.D. Mathiesen and M. Lehning, 2013. Use of a multilayer snow model to assess grazing conditions for reindeer. *Annals of Glaciology*, 54:S214-S226.

Vikhamar-Schuler, D., K. Isaksen, J.E. Haugen, H. Tømmervik, B. Luks, T. Vikhamar-Schuler and J.W. Bjerke, 2016. Changes in winter warming events in the Nordic Arctic Region. *Journal of Climate*, 29:6223-6244.

Vincent, L.A., X. Zhang, R.D. Brown, Y. Feng, E. Mekis, E.J. Milewska, H. Wan and X.L. Wang, 2015. Observed trends in Canada's climate and influence of low-frequency variability modes. *Journal of Climate*, 28:4545-4560.

Vionnet, V., E. Brun, S. Morin, A. Boone, S. Faroux, P. Le Moigne, E. Martin and J.-M. Willemet, 2012. The detailed snowpack scheme Crocus and its implementation in SURFEX v7.2. *Geoscientific Model Development*, 5:773-791.

Walsh, J.E., 2014. Intensified warming of the Arctic: Causes and impacts on middle latitudes. *Global and Planetary Change*, 117:52-63.

Wang, K. and R.E. Dickinson, 2013. Global atmospheric downward longwave radiation at the surface from ground-based observations, satellite retrievals, and reanalyses. *Reviews of Geophysics*, 51:150-185.

Wang, S. and J. Li, 2016. Terrestrial water storage climatology for Canada from GRACE satellite observations in 2002–2014. *Canadian Journal of Remote Sensing*, 42:190-202.

Wang, K. and S. Liang, 2009. Global atmospheric downward longwave radiation over land surface under all-sky conditions from 1973 to 2008. *Journal of Geophysical Research: Atmospheres*, 114:D19101, doi:10.1029/2009JD011800.

Wang, S. and H.A.J. Russell, 2016. Forecasting snowmelt-induced flooding using GRACE satellite data: a case study for the Red River watershed. *Canadian Journal of Remote Sensing*, 42:203-213.

Wang, L., G.J. Wolken, M.J. Sharp, S.E.L. Howell, C. Derksen, R.D. Brown, T. Markus and J. Cole, 2011. Integrated pan-Arctic melt onset detection from satellite active and passive microwave measurements, 2000–2009. *Journal of Geophysical Research: Atmospheres*, 116:D22103, doi:10.1029/2011JD016256.

Wang, L., C. Derksen, R. Brown and T. Markus, 2013. Recent changes in pan-Arctic melt onset from satellite passive microwave measurements. *Geophysical Research Letters*, 40:522-528.

Wang, L., J.N.S. Cole, P. Bartlett, D. Verseghe, V. Arora, C. Derksen, R. Brown and K. von Salzen, 2015a. Investigating the spread of surface albedo in snow covered forests in CMIP5 models. *Journal of Geophysical Research: Atmospheres*, 121:1104-1119.

Wang, T., S. Peng, C. Ottlé and P. Caias, 2015b. Spring snow cover deficit controlled by intraseasonal variability of the surface energy fluxes. *Environmental Research Letters*, 10:024018, doi:10.1088/1748-9326/10/2/024018.

Wang, L., P. Toose, R. Brown and C. Derksen, 2016. Frequency and distribution of winter melt events from passive microwave satellite data in the pan-Arctic, 1988–2013. *The Cryosphere*, 10:2589-2602.

Wegmann, M., Y. Orsolini, M. Vázquez, L. Gimeno, R. Nieto, O. Bulygina, R. Jaiser, D. Handorf, A. Rinke, K. Dethloff, A. Sterin and S. Brönnimann, 2015. Arctic moisture source for Eurasian snow cover variations in autumn. *Environmental Research Letters*, 10:054015, doi:10.1088/1748-9326/10/5/054015.

Westergaard-Nielsen, A., M. Lund, S.H. Pedersen, N.M. Schmidt, S. Klosterman, J. Abermann and B.U. Hansen, 2017. Transitions in high-Arctic vegetation growth patterns and ecosystem productivity tracked with automated cameras from 2000 to 2013. *Ambio*, 46:39-52.

Westermann, S., J. Boike, M. Langer, T.V. Schuler and B. Etzelmüller, 2011. Modeling the impact of wintertime rain events on the thermal regime of permafrost. *The Cryosphere*, 5:945-959.

Wever, N., C. Fierz, C. Mitterer, H. Hirashima and M. Lehning, 2013. Solving Richards Equation for snow improves snowpack meltwater runoff estimations in detailed multi-layer snowpack model. *The Cryosphere*, 8:257-274.

Wever, N., L. Schmid, A. Heilig, O. Eisen, C. Fierz and M. Lehning, 2015. Verification of the multi-layer SNOWPACK model with different water transport schemes. *The Cryosphere Discussions*, 9:2655-2707.

Wheeler, H.C., T.T. Høye, N.M. Schmidt, J.-C. Svenning and M.C. Forchhammer, 2015. Phenological mismatch with abiotic conditions—implications for flowering in Arctic plants. *Ecology*, 96:775-787.

Wheeler, J.A., A.J. Cortés, J. Sedlacek, S. Karrenberg, M. van Kleunen, S. Wipf, G. Hoch, O. Bossdorf and C. Rixen, 2016. The snow and the willows: earlier spring snowmelt reduces performance in the low-lying alpine shrub *Salix herbacea*. *Journal of Ecology*, 104:1041-1050.

Whittington, P., S. Ketcheson, J. Price, M. Richardson and A. Di Febo, 2012. Areal differentiation of snow accumulation and melt between peatland types in the James Bay Lowland. *Hydrological Processes*, 26:2663-2671.

Wilson, R.R., A. Bartsch, K. Joly, J.H. Reynolds, A. Orlando and W.M. Loya, 2013. Frequency, timing, extent, and size of winter thaw-refreeze events in Alaska 2001–2008 detected by remotely sensed microwave backscatter data. *Polar Biology*, 36:419–426.

WMO, 2015. Status of the Global Observing System for Climate, Full Report October 2015. World Meteorological Organization (WMO), Geneva, GCOS-195.

Wolff, M.A., K. Isaksen, A. Petersen-Øverleir, K. Ødemark, T. Reitan and R. Brækkan, 2015. Derivation of a new continuous adjustment function for correcting wind-induced loss of solid precipitation: results of a Norwegian field study. *Hydrology and Earth System Sciences*, 19:951–967.

Woo, M-K. and K.L. Young, 2014. Disappearing semi-permanent snow in the High Arctic and its consequences. *Journal of Glaciology*, 60:192–200.

Wu, W-Y., C-W. Lan, M-H. Lo, J.T. Reager and J.S. Famiglietti, 2015. Increases in the annual range of soil water storage at northern mid-and high-latitudes under global warming. *Geophysical Research Letters*, 42:3903–3910.

Xu, L., R.B. Myneni, R.S. Chapin III, T.V. Callaghan, J.E. Pinzon, C.J. Tucker, Z. Zhu et al., 2013. Temperature and vegetation seasonality diminishment over northern lands. *Nature Climate Change*, 3:581–586.

Yang, D., D. Kane, Z. Zhang, D. Legates and B. Goodison, 2005. Bias-corrections of long-term (1973–2004) daily precipitation data over the northern regions. *Geophysical Research Letters*, 32:L19501. doi: 10.1029/2005GL024057.

Yang, H., L. Lv, H. Xu, J. He and S. Wu, 2011. Evaluation of FY3B-MWRI instrument on-orbit calibration accuracy. *IEEE International Geoscience and Remote Sensing Symposium, IGARSS 2011*. pp. 2252–2254.

Yang, D., P. Marsh and S. Ge, 2014. Heat flux calculations for Mackenzie and Yukon Rivers. *Polar Science*, 8:232–241.

Yang, D., X. Shi and P. Marsh, 2015. Variability and extreme of Mackenzie River daily discharge during 1973–2011. *Quaternary International*, 380–381:159–168.

Yasunari, T.J., R.D. Koster, K-M. Lau and K.-M. Kim, 2015. Impact of snow darkening via dust, black carbon, and organic carbon on boreal spring climate in the Earth system. *Journal of Geophysical Research: Atmospheres*, 120:5485–5503.

Ye, H., E.J. Fetzer, S. Wong, A. Behrangi, D. Yang and B.H. Lambrigton, 2015a. Increasing atmospheric water vapor and higher daily precipitation intensity over northern Eurasia. *Geophysical Research Letters*, 42:9404–9410.

Ye, K., R. Wu and Y. Liu, 2015b. Interdecadal change of Eurasian snow, surface temperature, and atmospheric circulation in the late 1980s. *Journal of Geophysical Research: Atmospheres*, 120:2738–2753.

Yi, Y., J.S. Kimball, M.A. Rawlins, M. Moghaddam and E.S. Eus Kirchen, 2015. The role of snow cover and soil freeze/thaw cycles affecting boreal-arctic soil carbon dynamics. *Biogeosciences Discussions*, 12:11113–11157.

Yueh, S., S. Dinardo, A. Akgiray, R. West, D. Cline and K. Elder, 2009. Airborne Ku-band polarimetric radar remote sensing of terrestrial snow cover. *IEEE Transactions on Geoscience and Remote Sensing*, 47:3347–3364.

Zakharova, E.A., A.V. Kouraev, S. Biancamaria, M.V. Kolmakova, N.M. Mognard, V.A. Zemtsov, S.N. Kirpotin and B. Decharme, 2011. Snow cover and spring flood flow in the Northern Part of Western Siberia (the Poluy, Nadym, Pur, and Taz Rivers). *Journal of Hydrometeorology*, 12:1498–1511.

Zhang, X., J. He, J. Zhang, I. Polyakov, R. Gerdes, J. Inoue and P. Wu, 2013. Enhanced poleward moisture transport and amplified northern high-latitude wetting trend. *Nature Climate Change*, 3:4–51.

Zhong, X., T. Zhang and K. Wang, 2014. Snow density climatology across the former USSR. *The Cryosphere*, 8:785–799.

Zhou, X., H. Matthes, A. Rinke, K. Klehmet, B. Heim, W. Dorn, D. Klaus, K. Dethloff and B. Rockel, 2014. Evaluation of arctic land snow cover characteristics, surface albedo, and temperature during the transition seasons from regional climate model simulations and satellite data. *Advances in Meteorology*, 2014: Article ID 604157.

Zona, D., B. Gioli, R. Commane, J. Lindaas, S.C. Wofsy, C.E. Miller, S.J. Dinardo, S. Dengel, C. Sweeney, A. Karion, R.-Y. Chang, J.M. Henderson, P.C. Murphy, J.P. Goodrich, V. Moreaux, A. Liljedahl, J.D. Watts, J.S. Kimball, D.A. Lipson and W.C. Oechel, 2016. Cold season emissions dominate the Arctic tundra methane budget. *Proceedings of the National Academy of Sciences*, 113:40–45.

4. Changing permafrost and its impacts

LEAD AUTHORS: VLADIMIR ROMANOVSKY, KETIL ISAKSEN, DMITRY DROZDOV, OLEG ANISIMOV, ARNE INSTANES, MARINA LEIBMAN, A. DAVID MCGUIRE, NIKOLAY SHIKLOMANOV, SHARON SMITH, DONALD WALKER

CONTRIBUTING AUTHORS: GUIDO GROSSE, BENJAMIN M. JONES, M. TORRE JORGENSEN, MIKHAIL KANEVSKIY, ALEXANDR KIZYAKOV, ANTONI LEWKOWICZ, GALINA MALKOVA, SERGEY MARCHENKO, DMITRY J. NICOLSKY, DMITRY STERLETSKIY, SEBASTIAN WESTERMANN

Coordinating lead authors shown in bold

Contents

Key Findings	66
4.1 Introduction	66
4.2 Thermal state of permafrost	67
4.2.1 Current conditions	69
4.2.2 Recent changes in permafrost temperature	69
4.2.3 Active-layer thickness	71
4.2.4 Longer-term evidence of change	72
4.2.5 Summary and recommendations	72
4.3 Permafrost modeling and projections of future permafrost states	72
4.3.1 Uncertainties in permafrost response to projected changes in climate	72
4.3.2 Standalone permafrost models	76
4.3.3 Uncertainties in permafrost response to projected changes in climate at sub-regional scales	77
4.3.4 Modeling the effects of vegetation change on permafrost dynamics	79
4.3.5 Modeling sub-sea permafrost dynamics	80
4.3.6 Summary and recommendations	81
4.4 Permafrost-related processes and recent response to climatic changes	81
4.4.1 Thermokarst	81
4.4.2 Thermal erosion	83
4.4.3 Coastal retreat	84
4.4.4 Permafrost-related slope processes	85
4.4.5 Frost heave	86
4.4.6 Summary and recommendations	87
4.5 Effect of infrastructure and climate change on permafrost and permafrost-related hazards	87
4.5.1 Risk assessments and adaptation	87
4.5.2 The RATIC initiative	91
4.5.3 Outlook	94
4.6 Conclusions and knowledge gaps	94
4.6.1 Update of findings on permafrost	94
4.6.2 Knowledge gaps, observational needs and future direction	95
References	95

Key Findings

- New record high mean annual ground temperatures have been observed at many permafrost observatories across the Arctic. The greatest temperature increase since the International Polar Year (2007–2008), more than 0.5°C, occurred in the colder permafrost of the Arctic and High Arctic. In warmer permafrost the temperature increase has been much less or not detectable. At some locations (e.g. in the Alaskan Interior) permafrost temperature has even slightly decreased (typically by 0.1°C).
- Most of the regions where long-term observations of active-layer thickness are available show an increase in active-layer depth over the past five years. During the past 30 years, the average date of freeze-up of the active layer in northern Alaska has become almost two months later. At some locations (such as in the European North of Russia) permafrost degradation has been observed.
- There have been substantial efforts to evaluate large-scale models of permafrost dynamics across the circumpolar north. This has led to a better understanding of the range of uncertainty in projections associated with the models themselves and with the projections of future climate change. Several standalone high resolution permafrost models have been developed to describe potential future changes in permafrost characteristics on regional and local scales. Progress has also been made in modeling the dynamics of sub-sea permafrost.
- There have been no unified trends in thermokarst development associated with global warming observed across the Arctic to date. However, widespread surficial degradation of ice wedges and a significant increase in areas of water-filled polygonal troughs was reported in northern Alaska, the Canadian Arctic Archipelago, and Siberia and linked to climatic change.
- A new phenomenon of deep craters of still unknown origin in permafrost was reported from the western Siberian Arctic. This may indicate a previously overlooked process for a commonly mapped permafrost landform and a potentially rapid pathway for release of long-stored methane in permafrost regions.
- The engineering community has in recent years moved its focus from assessing the consequences of climate change on infrastructure and industrial development to risk assessments and adaptation measures. An unexpected flooding near Prudhoe Bay oilfield in Alaska in 2015 emphasized that many of the future changes in the Arctic will require major funds for repair and adaptation to the changes.

4.1 Introduction

This update of findings on permafrost adds to the benchmark assessments on snow, water, ice and permafrost in the previous SWIPA assessment (AMAP, 2011; Callaghan, et al., 2012). It provides a synthesis of current knowledge across the circumpolar permafrost regions on the thermal state of permafrost (Section 4.2), permafrost modeling and projections of future permafrost states (Section 4.3), permafrost-related processes, coastal erosion, thermokarst and recent changes in thaw lake development (Section 4.4), and cumulative effects of infrastructure and climate change on permafrost and recent advances in understanding permafrost-related geo-hazards (Section 4.5).

Many knowledge sources are drawn on with the focus on new data and results acquired during and after the International Polar Year (IPY, 2007–2009), including the Tenth International Conference on Permafrost (TICOP) in 2012 and the Fourth European Conference on Permafrost (EUCOP 4) in 2014. This update also adds to the results of Working Group I and II to the Fifth Assessment of the Intergovernmental Panel on Climate Change (e.g. Vaughan et al., 2013; Larsen et al., 2014) and the Arctic Resilience Interim Report 2013 (Arctic Council, 2013) by focusing on more recent information and new topics. New knowledge was also gained from ongoing and recent national and international programs and projects such as The Permafrost Carbon Network (www.permafrostcarbon.org), the Study of Environmental Arctic Change (SEARCH, www.arcus.org/search-program), The European Space Agency (ESA) Data User Element (DUE) Permafrost (<http://geo.tuwien.ac.at/permafrost/>), Changing Permafrost in the Arctic and its Global Effects in the 21st Century (PAGE21, www.page21.eu), the NSERC Discovery Frontiers project ADAPT (Arctic Development and Adaptation to Permafrost in Transition), the Next-Generation Ecosystem Experiments (NGEE Arctic, <http://ngee-arctic.ornl.gov/>), and the Global Terrestrial Network for Permafrost (GTN-P, <http://gtnp.arcticportal.org/>).

Section 4.2 provides an update on the current thermal state of permafrost and changes in active-layer thickness (ALT; the top layer of soil that thaws during summer and refreezes in winter) that can be compared to the IPY baseline measurements to assess recent change that has occurred since IPY. The long-term records of permafrost temperature (time series), more than three decades long at some sites, have also been extended and this allows the changes since IPY to be placed within the context of the longer record. Section 4.3 reports the substantial advances regarding incorporation of permafrost in Earth System Models (ESMs) and more comprehensive analysis of the uncertainty of permafrost changes among climate projections and ESMs. It demonstrates the role of benchmark data sets in the selection of realistic ESMs, the reduction of uncertainty and representation of the effects of changing vegetation on permafrost dynamics. Progress in stand-alone permafrost modeling and modeling the dynamics of sub-sea permafrost is also reported. Section 4.4 focusses on the degradation of permafrost – a naturally (or artificially) caused decrease in the thickness and/or areal extent of permafrost – and the related disturbance of the surface and associated processes such as thermokarst, thermal erosion (the erosion of ice-bearing permafrost by the combined thermal and mechanical action of moving water) and slope processes.

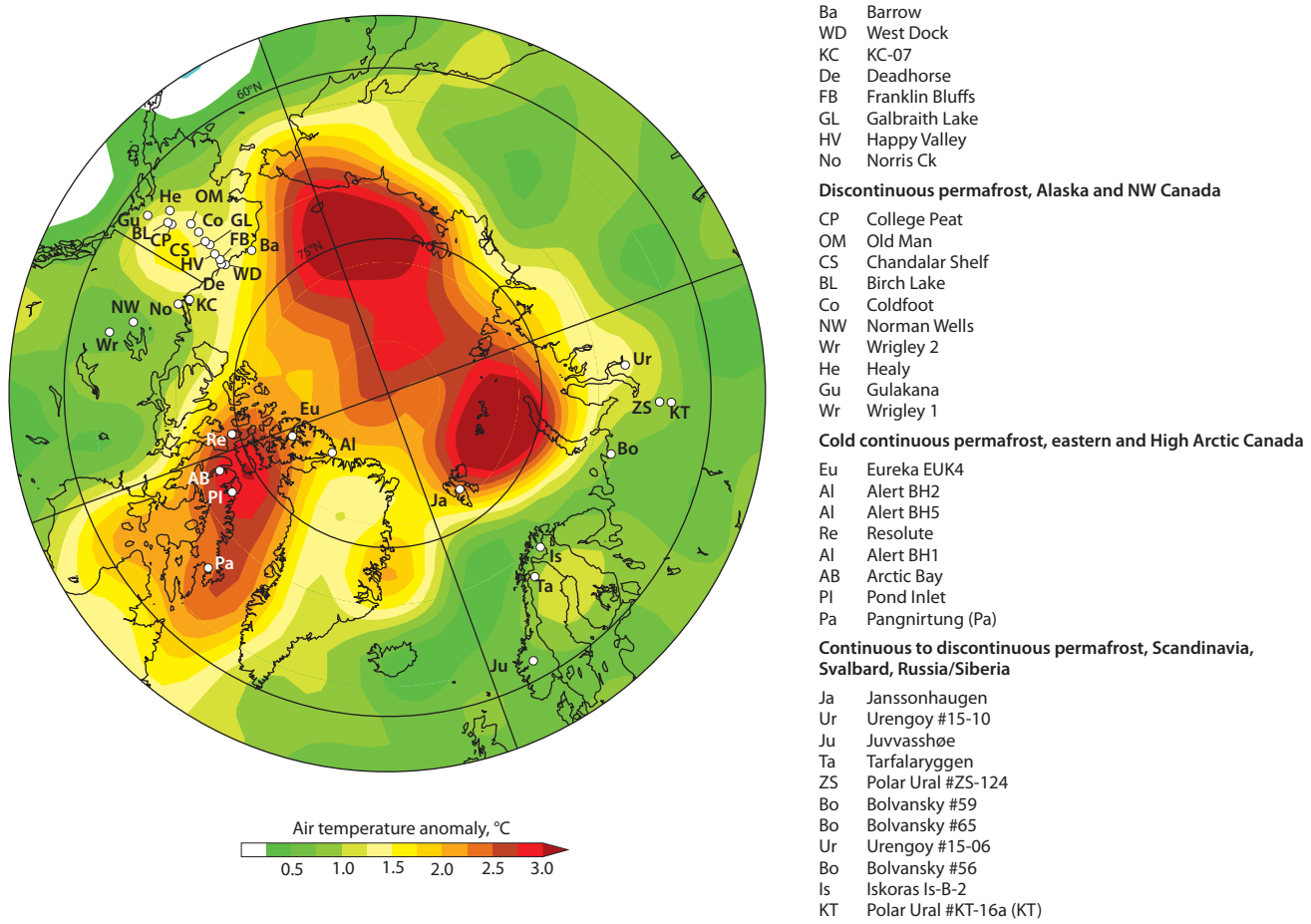


Figure 4.1 Location of the permafrost monitoring sites shown in Figures 4.2 and 4.3 superimposed on average air temperature anomalies for the period 2000–2014 (relative to the 1971–2000 mean) from the NCEP-reanalysis (Kalnay et al., 1996). Following the subdivisions (regions) presented in Figure 4.2, the sites and their abbreviations are listed from coldest to warmest. Climate data provided by the NOAA/ESRL Physical Sciences Division, Boulder Colorado (www.esrl.noaa.gov/psd/).

Studies focusing on recent observations on aggradation of permafrost and related processes are also presented. Section 4.5 focusses on the cumulative effects of infrastructure and climate change on permafrost and advances in understanding of the processes and role of permafrost. New developments in the study of impacts of changing permafrost on infrastructure are also presented.

One of the most dramatic results of thawing permafrost is the potential mobilization of the organic material sequestered to date in perennially frozen deposits (Schuur et al., 2008, 2015). Potential release of carbon dioxide (CO_2) and methane (CH_4) from thawing permafrost may have not only regional but also global impacts on climate (Koven et al., 2015). Owing to the global importance of changes in the carbon cycle resulting from environmental changes in the Arctic, a new chapter on carbon has been included in this report (see Chapter 8). As a consequence, interactions between changes in permafrost and related changes in carbon cycling are addressed in this new chapter and are not considered here.

The SWIPA update on permafrost provides Arctic residents, indigenous peoples, governments, and industry with important information for adapting to global warming. This update was also useful for the regional reports that currently are produced within the project *Adaptation Actions for a Changing Arctic* (AACa).

4.2 Thermal state of permafrost

The most direct indicators of changes in the thermal state of permafrost are permafrost temperature and ALT. Permafrost temperature measured at a depth where there is practically no annual fluctuation in ground temperature is the best indicator of long-term change. This depth varies from a few meters in warm, ice-rich permafrost to 20 m or more in cold permafrost and in bedrock (Romanovsky et al., 2010a; Smith et al., 2010).

During the International Polar Year (IPY) a snapshot of permafrost thermal state for 2007–2009 was developed. This provides a baseline against which future change can be measured. Measurements of ground temperature were made in over 575 boreholes in Canada, Alaska, Russia and Nordic countries representing the range in vegetation, geology and climate found in the permafrost regions of the Arctic and sub-Arctic (Christiansen et al., 2010; Romanovsky et al., 2010a,b; Smith et al., 2010). Measurements continue to be made and data are now available for the 2012–2015 period for many sites (Figure 4.1) which provide an updated picture of the current thermal state of permafrost since IPY. The longer term records (time series), more than three decades long for some sites, have also been extended which allows the changes since IPY to be placed within context of the longer record.

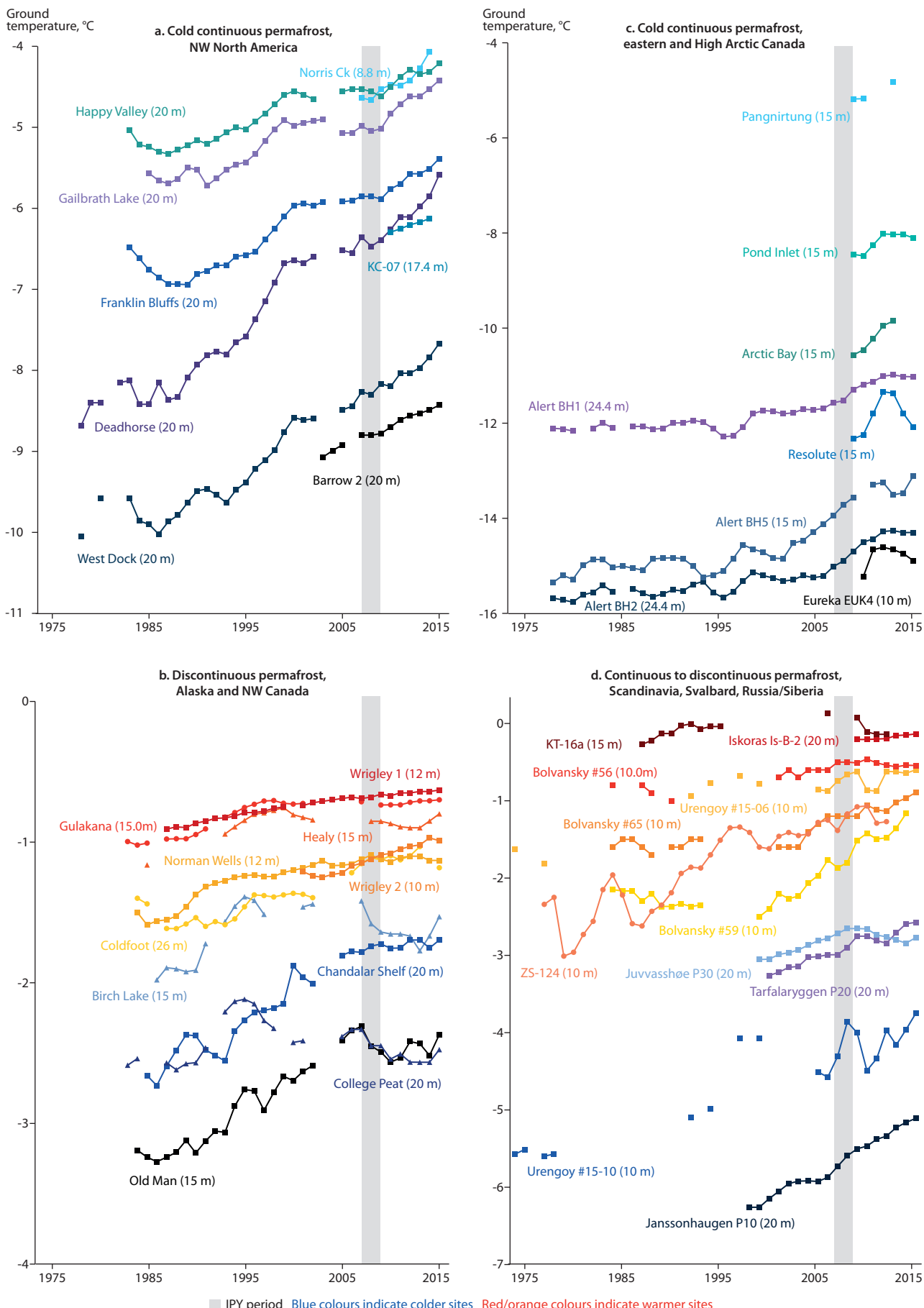


Figure 4.2 Time series of annual mean ground temperature at depths of 9 to 26 m below the surface at selected measurement sites (see Figure 4.1 for locations) that fall roughly into the AACPA priority regions: (a) cold continuous permafrost of northwestern North America (Beaufort-Chukchi region); (b) discontinuous permafrost in Alaska and northwestern Canada; (c) cold continuous permafrost of eastern and High Arctic Canada (Baffin Davis Strait); and (d) continuous to discontinuous permafrost in Scandinavia, Svalbard, Russia/Siberia (Barents region). Temperatures are measured at or near the level of zero annual amplitude. Data series are updated from Christiansen et al. (2010), Romanovsky et al. (2014, 2015) and Ednie and Smith (2015).

4.2.1 Current conditions

Although there is a general decrease in permafrost temperature with increasing latitude, this relationship varies between regions. Warmer permafrost is found in Scandinavia, Svalbard and northwestern Russia compared to other Arctic regions due to the influence of warm ocean currents on climate, while elevation is a modifying factor in the mountains of the Nordic region and western North America (Romanovsky et al., 2010a).

In the discontinuous permafrost zone (as defined by Brown et al., 1997), permafrost temperatures fall within a narrow range and are generally above -2°C . Colder conditions have been found at some sites such as along the Alaska Highway Corridor, southern Yukon, near the Alaska-Canadian border where permafrost can be at temperatures as low as -3°C (Smith and Ednie, 2015) and in the Alaskan Interior (Romanovsky et al., 2014). The range in temperature within the continuous permafrost zone is much larger with the lowest temperatures (-14 to -15°C) measured on northern Ellesmere Island in the Canadian High Arctic (e.g. Smith et al., 2013) and the highest temperatures that may be very close to 0°C in the Russian European Arctic and the Nordic region (Christiansen et al., 2010; Romanovsky et al., 2010b).

4.2.2 Recent changes in permafrost temperature

Based on a selection of sites with both long-term records and good geographic coverage (Figure 4.1) annual mean permafrost temperatures have been increasing at many sites (Figure 4.2). The greatest increase is found in the colder permafrost of the Arctic and High Arctic (Figures 4.2a, 4.2c, and 4.2d) where current permafrost temperatures can be more than 0.5°C higher than during the IPY period (2007–2009). In warmer permafrost such as that in the southern and central Mackenzie Valley, in the Alaskan Interior, or in the discontinuous permafrost zone in Siberia and the Nordic region the temperature difference has been much smaller with increases since IPY generally being less than 0.2°C (Figures 4.2b and 4.2d) and at some sites there has been negligible change in temperature or even slight cooling (Figures 4.2b and 4.3).

The extended time series indicate that the warming documented up to the IPY period (Romanovsky et al., 2010b; Smith et al., 2010) has generally continued in recent years (Figures 4.2 and 4.3). Temperatures measured since IPY in the upper 25 m of the ground at Alert, at the northern edge of Ellesmere Island, Canada, are among the highest recorded since 1978 (Figure 4.2c). Since 2000, permafrost temperatures at Alert have increased at a higher rate than previously. At BH5, temperature at 15 m depth has increased by $\sim 1.3^{\circ}\text{C}$ per decade since 2000, which is about 0.8°C per decade higher than the rate for the entire record (Smith et al., 2015). Even at a depth of 24 m, temperature has increased since 2000 at a rate approaching 1°C per decade. This higher rate of warming since 2000 coincides with a period of higher air temperatures (Figure 4.1) and reduced sea-ice cover (Derkens et al., 2012). The lower rate of temperature increase at 24 m depth and the slight cooling at 15 m depth over the last two years is likely to be a response to a fall in air temperature between 2010 and 2013. A similar pattern is observed in the shorter records from eastern Canadian Arctic sites where permafrost temperatures at 15 m depth increased between 2008 and 2013 (Ednie and Smith, 2015). Temperatures in the warm permafrost of the central Mackenzie River valley in northwestern Canada continue to increase, but at a much lower

rate than in the High Arctic. This increase has slowed further in the last decade (Smith et al., 2015) (Figure 4.2b). At depths of 10–12 m, permafrost temperature at Norman Wells and Wrigley has risen by 0.01 – 0.2°C per decade since 2000 (Figure 4.2b). Permafrost temperatures measured since 2007 at 8.75 m depth in the northern Mackenzie Valley near Inuvik (Norris Ck) have increased by about 0.4°C per decade (Figure 4.2a).

Warming has continued on the North Slope of Alaska (hereafter North Slope) with new record high temperatures at 20 m depth at all permafrost observatories (Figure 4.2a). Recent increases in permafrost temperature are associated with a period of high air temperature (Figure 4.1), including a particularly warm summer in 2013 that contributed to the increase in temperature at 20 m depth (which typically lags changes in surface temperature by about a year).

The increase in permafrost temperature between 2013 and 2015 was substantial on the North Slope ranging from 0.14°C at Happy Valley to 0.39°C at Deadhorse (Figure 4.2a). On the North Slope, temperature at 20 m depth has increased since 2000 by 0.21 – 0.66°C per decade (Figure 4.2a), which is a slightly lower rate than for the period 1986–2000.

In contrast, permafrost temperatures in Interior Alaska (Figure 4.2b) have generally decreased since 2007. Consequently, temperatures in 2014 at some sites in Interior Alaska were lower than those located much further north, for example temperatures at College Peat (64.86°N) are now lower than at Old Man (66.45°N). The cooling trend in Interior Alaska during the early 21st century can be explained by the lack of rise in air temperature and relatively shallow snow cover during this period. However, at two sites, Birch Lake and Healy, this

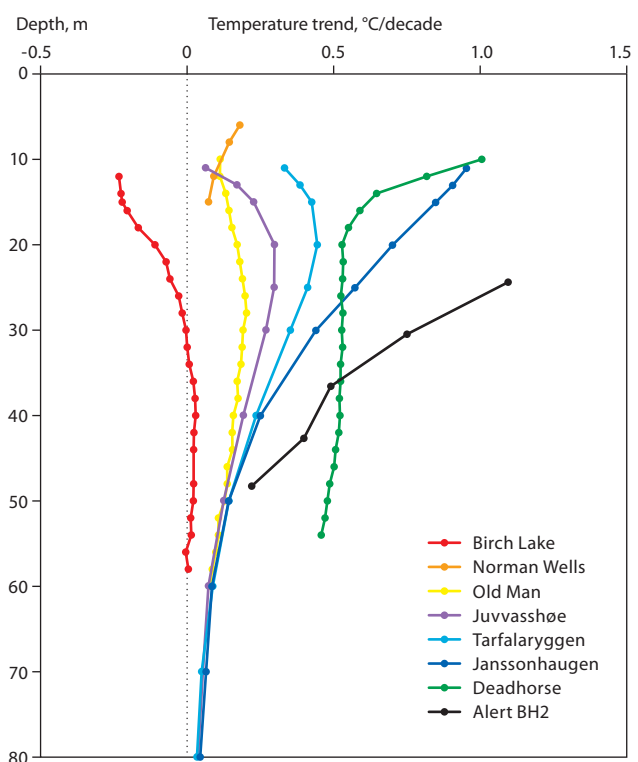


Figure 4.3 Observed linear trends in ground temperature between 2000 and 2014 as a function of depth for the three Nordic key-monitoring sites at Svalbard (Janssonhaugen) and in Scandinavia (Tarfalaryggen and Juvvasshœ), the Canadian sites Alert BH2 and Norman Wells, and the Alaskan sites Deadhorse, Old Man, and Birch Lake. See Figure 4.1 for average air temperature anomalies at these sites for 2000–2014.

cooling trend was interrupted in 2014 by warming of 0.1°C and 0.05°C , respectively (Figure 4.2b). This warming continued in 2015 when the rest of the sites in Interior Alaska showed higher permafrost temperatures than in 2014.

Permafrost temperature has increased by $1\text{--}2^{\circ}\text{C}$ in northern Russia over the last 30 to 35 years (Romanovsky et al., 2010b), similar to that observed in northern Alaska and the Canadian High Arctic. At colder permafrost sites in the Polar Ural Mountains, temperatures at 15 m depth have increased by 0.5°C per decade since the late 1980s (site ZS-124 in Figure 4.2d). Less warming was observed at warm permafrost sites with a slight cooling since 2009 (site KT-16a, Figure 4.2d) (Romanovsky et al., 2014). In the European north of Russia and in the western Siberian Arctic, temperatures at 10 m depth at cold permafrost sites have increased by $\sim 0.4\text{--}0.6^{\circ}\text{C}$ per decade since the late 1980s (Figure 4.2d, Bolvansky #59, Urengoy #15-5 and #15-10) with less warming observed at warm permafrost sites (Figure 4.2d, Bolvansky #56 and Urengoy #15-6). A clear warming trend was also observed during the last seven years at most permafrost monitoring sites in northern East Siberia (e.g. Romanovsky et al., 2013).

Records from the Nordic monitoring sites in Svalbard and Scandinavia (updated from Isaksen et al., 2007) show that ground temperatures at 20 m depth have increased by $0.3\text{--}0.7^{\circ}\text{C}$ per decade since the late 1990s at colder mountain permafrost sites (Figure 4.2d). A significant temperature increase is measurable down to at least 80 m depth (Figure 4.3) reflecting a multi-decadal warming of the permafrost surface. In the Nordic region the largest temperature increases have been at the northernmost sites on Svalbard. The high rate of warming since 1998 on Svalbard coincides with a period of higher air temperatures (Figure 4.1), similar to that observed in the Canadian Arctic. In addition, several extreme and long-lasting warm spells and weather events were superimposed on a significant warming trend (Hansen et al., 2014). Less warming has been observed at warm permafrost sites that are affected by latent heat release at the temperatures close to 0°C when a significant portion of the additional heat flux into the deeper ground generated by rise in atmospheric temperatures is spent on partial melting of the pore ice in the ground. However, at some Nordic and Russian sites ground temperature observations indicate degradation of permafrost over the intervening decade (Isaksen et al., 2011; Drozdzov et al., 2012; Farbrot et al., 2013; Malkova et al., 2014; Melnikov et al., 2015).

This regional contrast in rates of temperature increase (Figure 4.3) is partly due to the difference in changes in climate, particularly air temperature. In the Alaskan and eastern and high Canadian Arctic and the Nordic region, air temperatures since 2000 have been among the highest on record whereas air temperatures in the western North American sub-Arctic have been generally lower since a peak in the 1980s and 1990s. Higher permafrost surface temperatures supply a significant amount of heat to the deeper permafrost. This leads to a substantial increase in permafrost temperatures not only at the surface but also at depth (Figure 4.3). Thus, permafrost temperature at 50 m depth at West Dock and Deadhorse has increased by 1°C during the last 30 years. These data also indicate that the average long-term heat flux into the permafrost at these two sites was on the order of 0.5 W/m^2 in the last 30 years.

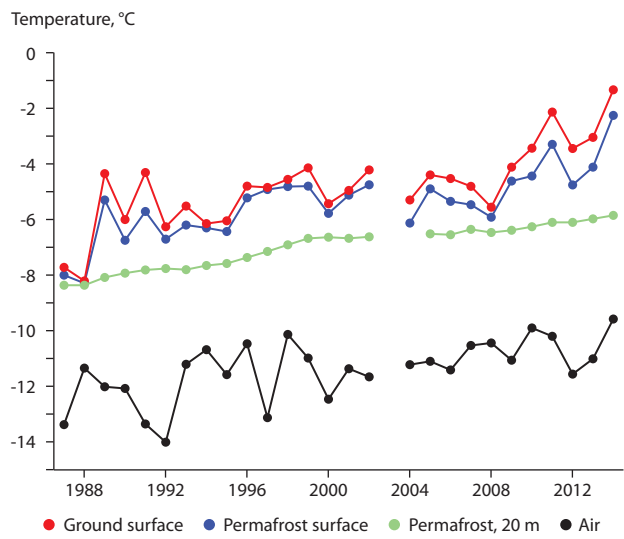


Figure 4.4. Mean annual temperatures of air, ground surface, permafrost surface, and permafrost at 20 m depth recorded at the Deadhorse permafrost observatory in the period 1987–2014 on the North Slope of Alaska.

Figure 4.4 allows better understanding of the causes of the permafrost temperature increase in the North American Arctic. Permafrost temperature follows changes in the mean annual ground surface temperature that, in turn, follows changes in mean annual air temperature. The decadal time scale trend in mean annual near-surface permafrost temperature (1.1°C per decade) is almost identical to the decadal trend in mean annual air temperature (0.9°C per decade) for the entire observational period (Figure 4.4), suggesting that there was no significant trend in snow-cover thickness in the Alaskan Arctic during the last 30 years. Recently (the past five years) however, the rate of increase in near-surface permafrost temperature has exceeded that for air temperature (Figure 4.4). This may be the result of an increase in snow depth during this period. The latest air temperature increase resulted in near-surface ground temperatures on the North Slope of Alaska rising to an unprecedentedly high level. While the mean annual temperatures at the ground and permafrost surfaces at Deadhorse in the mid-1980s were near -8°C (Figure 4.4), in 2014 they were only -1.3°C and -2.2°C , respectively. These temperatures are more typical of Interior Alaska, indicating that permafrost in some areas of the North Slope is losing its thermal stability.

The cold tundra sites also lack a surface buffer layer and are therefore more responsive (Figures 4.2 and 4.3) to changes in air temperature than forested sites of the central Mackenzie Valley (Throop et al., 2012) and Interior Alaska (Shur and Jorgenson, 2007). Where permafrost temperatures are close to 0°C , the high latent heat requirements also result in smaller changes in ground temperature (Figures 4.2 and 4.3) as phase change from ice to liquid water is occurring (Romanovsky et al., 2010a; Throop et al., 2012).

Very warm permafrost can therefore persist even under a rise in atmospheric temperature (e.g. James et al., 2013). In the Canadian High Arctic, increases in air temperature have largely been the result of winter and autumn warming, and windblown tundra sites with little snow cover are therefore more responsive to changes in air temperature (Smith et al., 2012). Similarly, analysis of the seasonality of changes in ground temperature

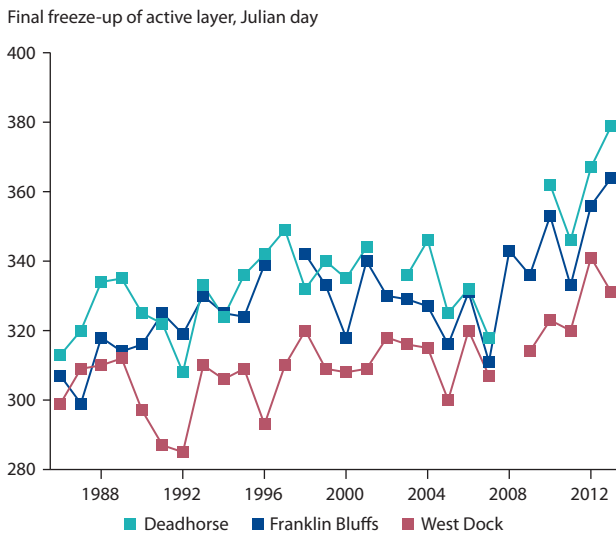


Figure 4.5. Dates of complete freeze-up of the active layer at West Dock, Deadhorse, and Franklin Bluffs on the North Slope of Alaska. See Figure 4.1 for locations.

in the Alaskan Arctic shows that the warming is occurring in both summer and winter with more warming occurring during the cold season. As a result, re-freezing of the active layer takes longer (Figure 4.5). Complete freeze-up of the active layer in northern Alaska in the mid-1980s typically occurred in the first half of October but shifted to mid-December in the first half of the 2010s. In the winter of 2013–2014, an unprecedented late freeze-up (January 15) was observed at the Deadhorse site (Figure 4.5) which is more typical for the Fairbanks area. During the past 30 years, the average date of freeze-up has been almost two months later.

4.2.3 Active-layer thickness

Active-layer thickness responds more to the shorter term variations in climate than does deep ground temperature. Records of ALT therefore exhibit greater interannual variability, primarily in response to variations in summer temperature (e.g. Smith et al., 2009a). Decadal trends in ALT vary by region (Shiklomanov et al., 2012). Nevertheless, most regions for which long-term ALT observations are available show an increase in ALT during the past five years (Figure 4.6) (Romanovsky et al., 2015).

In western North America, ALT has generally increased since IPY (2008). This increase was preceded by a period of thinner active layers which followed the peak ALT in 1998. Generally, recent ALT is less than the 1998 peak value. On the North Slope, ALT has generally increased since 2007 with ALT between 2008 and 2014 being greater than the long-term average (Figure 4.6). The peak ALT value observed in 2013 was the highest since 1998. Active layer data have been obtained from over 40 thaw tubes in the Mackenzie Valley in north-west Canada since the early 1990s (Smith et al., 2009b; Duchesne et al., 2015). Although there is no pronounced trend over the full 1991–2013 period (Figure 4.6), ALT has increased at many sites since 2005 which also appears to coincide with a period of increased summer thawing degree days (Duchesne et al., 2015). This follows a period of thinner active layers that occurred after active layers reached a peak in thickness during the very warm summer of 1998.

In Russia, standardized active layer observations in 2014 were conducted at 36 sites. In western Siberia there is no obvious trend in ALT since IPY (Figure 4.6) although ALT increased between 2010 and 2012 followed by a slight decrease. Locations in the Russian European north have been characterized by almost monotonic deepening of the active

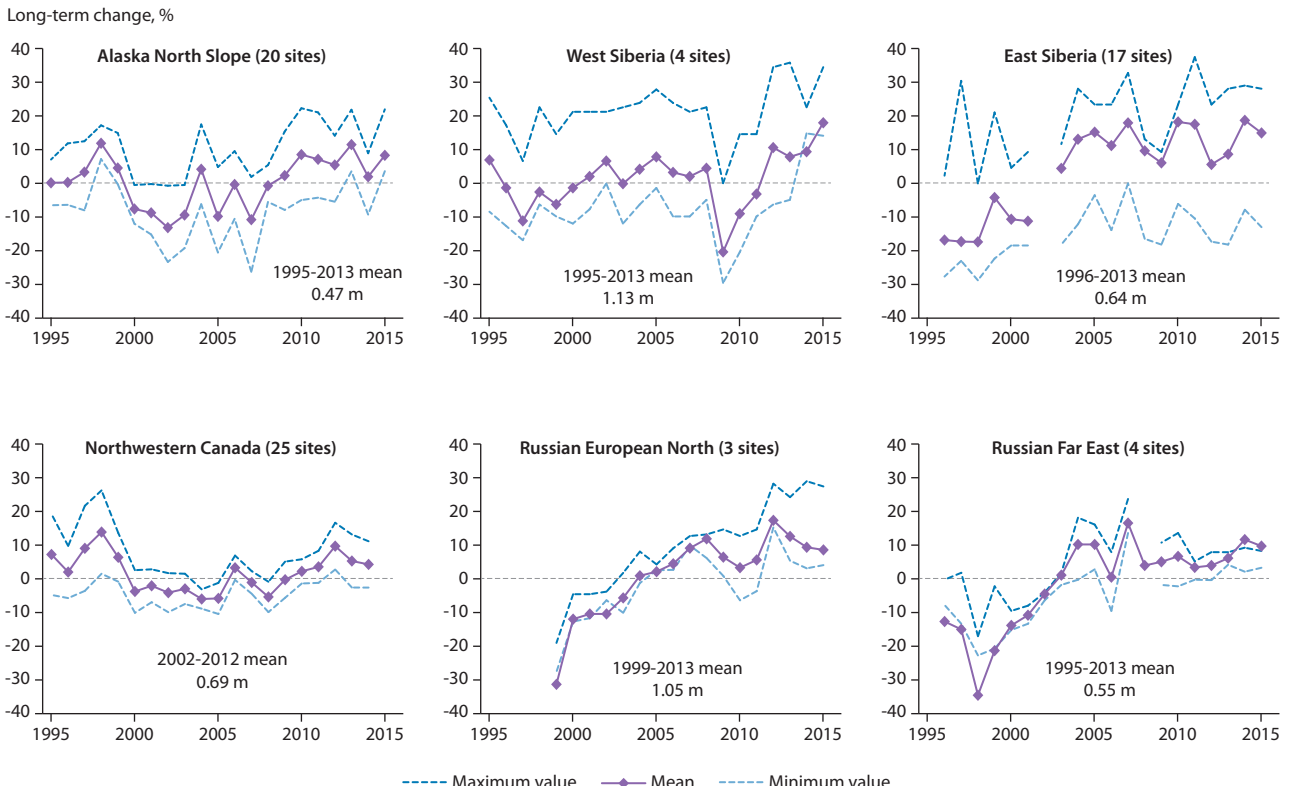


Figure 4.6. Long-term change in active-layer thickness in six Arctic regions as observed during the Circumpolar Active Layer Monitoring project. Data are presented as annual percentage deviations from the mean value for the period of observation. Thaw depth observations from the end of the thawing season were used. Only sites with at least 10 years of continuous thaw depth observations are shown (Romanovsky et al., 2015).

layer over the last 15 years, reaching a maximum in 2012. However, ALT decreased in 2012–2014. In eastern Siberia and the Russian Far East, ALT generally increased between 1996 and 2007 but has since been more stable. An increase in ALT of about 8% was observed between 2013 and 2014 in eastern Siberia, however. In the Russian Far East a slight increase in ALT was observed during 2011–2014 that followed a sharp decrease in 2008–2010 (Figure 4.6).

In the Nordic countries, active layer records (1996–2013) indicate a general increase in ALT since 1999. Maximum ALT was observed in 2011 followed by a period of thinner active layers but ALT was still greater than the long-term average value. Summer 2014 was particularly warm in the Nordic countries and contributed to the thickest active layer measured to date in some places.

4.2.4 Longer-term evidence of change

A recent study by James et al. (2013) which repeated surveys originally conducted in 1964, showed significant degradation of permafrost has occurred since 1964 along the Alaska Highway corridor in the southern Yukon and northern BC Canada. As a result, the southern limit of permafrost appears to have retreated northward by at least 25 km.

The increase in ground surface temperature during the last 30 years triggered long-term permafrost thawing at the Bolvansky site in the European Russian north (Malkova et al., 2014). Although this site is located within the continuous permafrost zone, permafrost temperatures within several landscape types are within 1°C of the freezing point (Figure 4.2d) and thawing has already started at some locations. Surficial geophysics data indicate that a talik (a layer or body of unfrozen ground) 3–8 m thick now exists at these locations (Drozdov et al., 2012; Malkova et al., 2014; Melnikov et al., 2015).

Geophysical surveys performed in Norway in 1999 to delineate the altitudinal limit of mountain permafrost were repeated in 2009–2010 and indicate the degradation of some permafrost over the intervening decade (Isaksen et al., 2011). Since the 1980s, loss of lowland permafrost at mires in northern Sweden has accelerated (Johansson et al., 2011; Callaghan et al., 2013). Increases in ALT and decreases in permafrost thickness have been observed at nine mires, with a complete loss of permafrost at three mires (Åkerman and Johansson, 2008; Callaghan et al., 2013).

4.2.5 Summary and recommendations

A general increase in permafrost temperature that has been observed since the mid-1980s has continued in the period 2011–2015. As in previous years, this increase was not homogeneous in space or time. In colder permafrost within the continuous permafrost zone this increase was particularly strong with warming of 0.4–1°C per decade, similar to the maximum rates observed in the 1990s. Increase in permafrost temperature in the discontinuous permafrost zone was less pronounced and warming was around a few tenths of a degree per decade. At some locations there was even a slight cooling (a few hundredths of a degree) which can be explained by a lack of increase in air temperature and a simultaneous decrease in snow depth. Active layer thickness was increasing at most observation sites, causing thawing of near-surface permafrost and degradation of

ice wedges (see Section 4.4). Present-day permafrost temperature and active layer observing networks provide enough information to determine general trends in permafrost change. However, the spatial distribution of observation sites is very uneven. This causes uneven coverage of different parts of the Arctic and subarctic leaving big gaps in knowledge on changes in permafrost in several large regions, such as the Central Canadian and Central Siberian Arctic and the sub-Arctic. Better coverage is also required for Greenland and the Far North-East of Russia. To make existing and new data on permafrost temperature and active layer thickness readily available to the scientific and engineering communities, climate modelers, educators, stakeholders, and general public, further development of a spectrum of user-friendly databases is required. A good example of development in this direction is the establishment of a database within the WMO/WCRP Global Terrestrial Network for Permafrost project (Biskaborn et al., 2015).

4.3 Permafrost modeling and projections of future permafrost states

The 2011 SWIPA assessment (Callaghan et al., 2012) primarily reported on future projections of soil temperature and top-down thaw of near-surface permafrost in the northern permafrost region and at sub-regional scales of just a few models (e.g. the Geophysical Institute Permafrost Lab, GIPL, model). Uncertainty in the state of future permafrost was primarily quantified by applying one model across a range of climate scenarios. There was little quantitative evaluation of the models in the context of available data or within the context of differences in sensitivity to changes in climate among the models, and there was no attempt at comparing models. Since the SWIPA 2011 assessment, there has been substantial evaluation of large-scale models of permafrost dynamics across the northern permafrost region, and there is now a better understanding of the range of uncertainty in projections associated both with models and future projections of climate change. There has also been progress in evaluating retrospective simulations of models at the sub-regional scale to identify which subset of models should be used for quantifying uncertainty in future projections of permafrost dynamics. Progress has also been made in modeling the effects of vegetation change on permafrost dynamics in response to changing climate. There has also been new progress in modeling the dynamics of sub-sea permafrost beneath the continental shelf of the Arctic Ocean.

4.3.1 Uncertainties in permafrost response to projected changes in climate

McGuire et al. (2016) analyzed uncertainties in the response of permafrost to climate change across the permafrost region of the northern hemisphere since 1960 for 15 permafrost model simulations (Table 4.1) as part of the activities of the Permafrost Carbon Network. Across the permafrost region, the models varied approximately three-fold in their estimates of the area of permafrost (7.6 to 21.1 million km²), defined in these models as the area with an active-layer thickness of less than 3 m. The models all predict a loss in the area of near-surface permafrost (ALT <3 m) between 1960 and 2009, but there are large differences in the magnitude of the predicted

Table 4.1 Comparison of conceptual representation of permafrost dynamics among models compared by McGuire et al. (2016).

Model	Approach to modeling soil thermal dynamics	Depth, m	Moss insulation considered	Organic soil insulation considered	Snow insulation considered	Effect of unfrozen water on phase change considered ^{a,b}
CLM4.5	Multi-layer finite difference heat diffusion	45	No	Yes ^c	Yes (5 layers max)	Yes
CoLM	Multi-layer finite difference heat diffusion	3.4	No	No	Yes (5 layers max)	No
ISBA	Multi-layer Fourier solution	12	No	Yes ^c	Yes (3 layers max)	Yes
JULES	Multi-layer finite difference heat diffusion	3.0	No	No	Yes (3 layers max)	Yes
LPJ-GUESS	Multi-layer finite difference heat diffusion	6-8	No	No	Yes (1 layer)	No
MIROC-ESM	Multi-layer heat conduction	14	No	No	Yes (3 layers max)	No
ORCHa and ORCHb	1D Fourier solution	88	No	No	Yes (1 layer)	Yes
UVic	Multi-layer finite difference heat diffusion	250	No	Yes	Yes (1 layer)	Yes
UW-VIC	Multi-layer finite difference heat diffusion	25	No	Yes	Yes (2 layers max)	Yes
JSBACH	Modified Richtmyr-Morten implicit scheme	10	No	Yes ^c	Yes (5 layers max)	Yes
TEM6	Multi-layer finite difference heat diffusion	36	Yes	No	Yes (1 layer)	No
SiBCASA	Multi-layer finite difference heat diffusion	15	No	Yes	Yes (5 layers max)	Yes
GIPLa	Multi-layer finite difference heat diffusion	200	Yes	Yes	Yes (1 layer)	Yes
GIPLb	Multi-layer finite difference heat diffusion	200	Yes	Yes	Yes (1 layer)	Yes

^aModel implements algorithms for representing the effects of unfrozen water on phase change processes in frozen soil; ^bin all models, soil thermal conductivity is influenced by soil moisture; ^corganic horizon thickness is prescribed and is not prognostic.

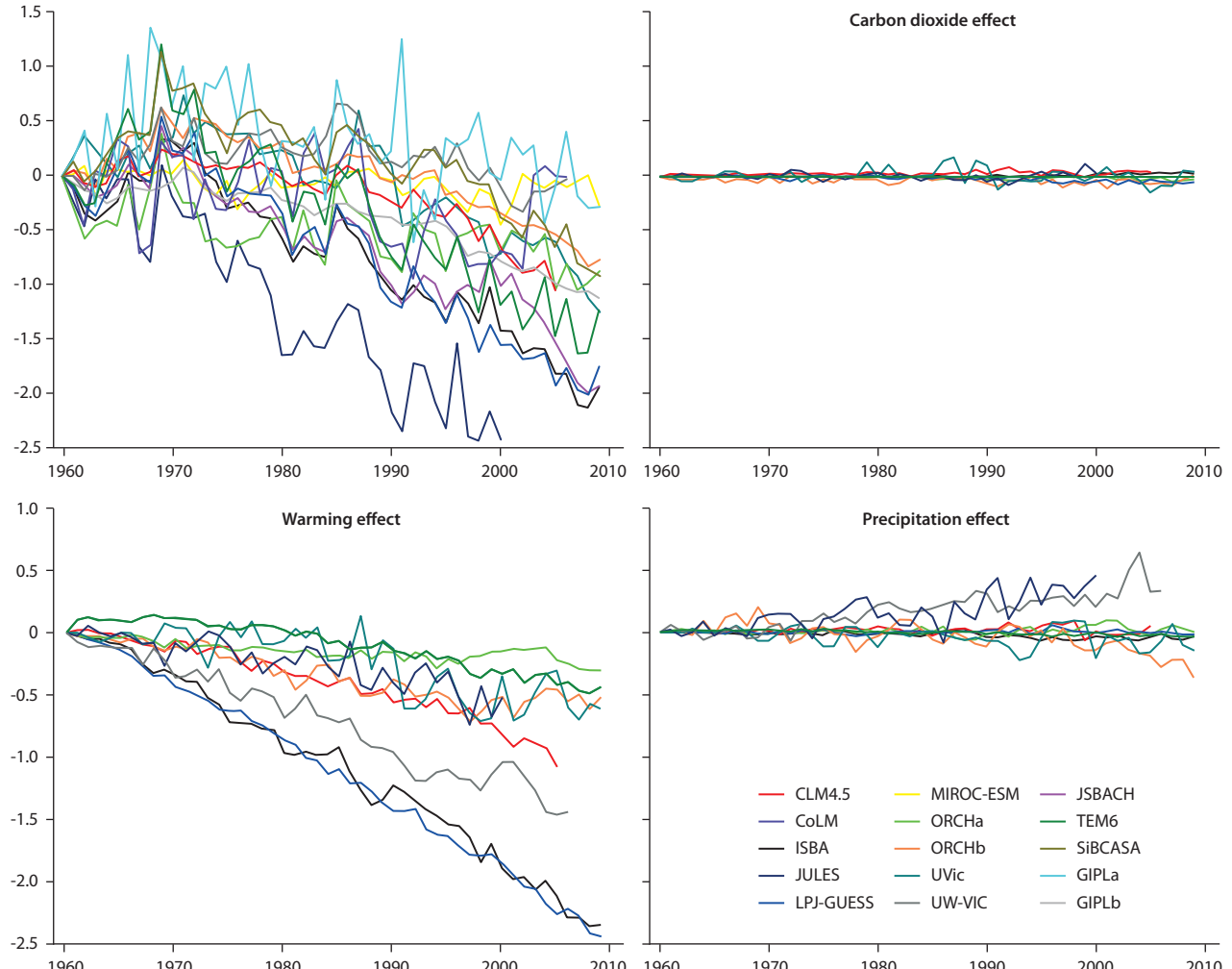
Change in permafrost area, million km²

Figure 4.7 Simulated changes in permafrost area (for ALT <3m) between 1960 and 2009 and the sensitivity of simulated changes in permafrost area to changes in atmospheric carbon dioxide, temperature, and precipitation between 1960 and 2009. See Table 4.1 for model details. (McGuire et al., 2016).

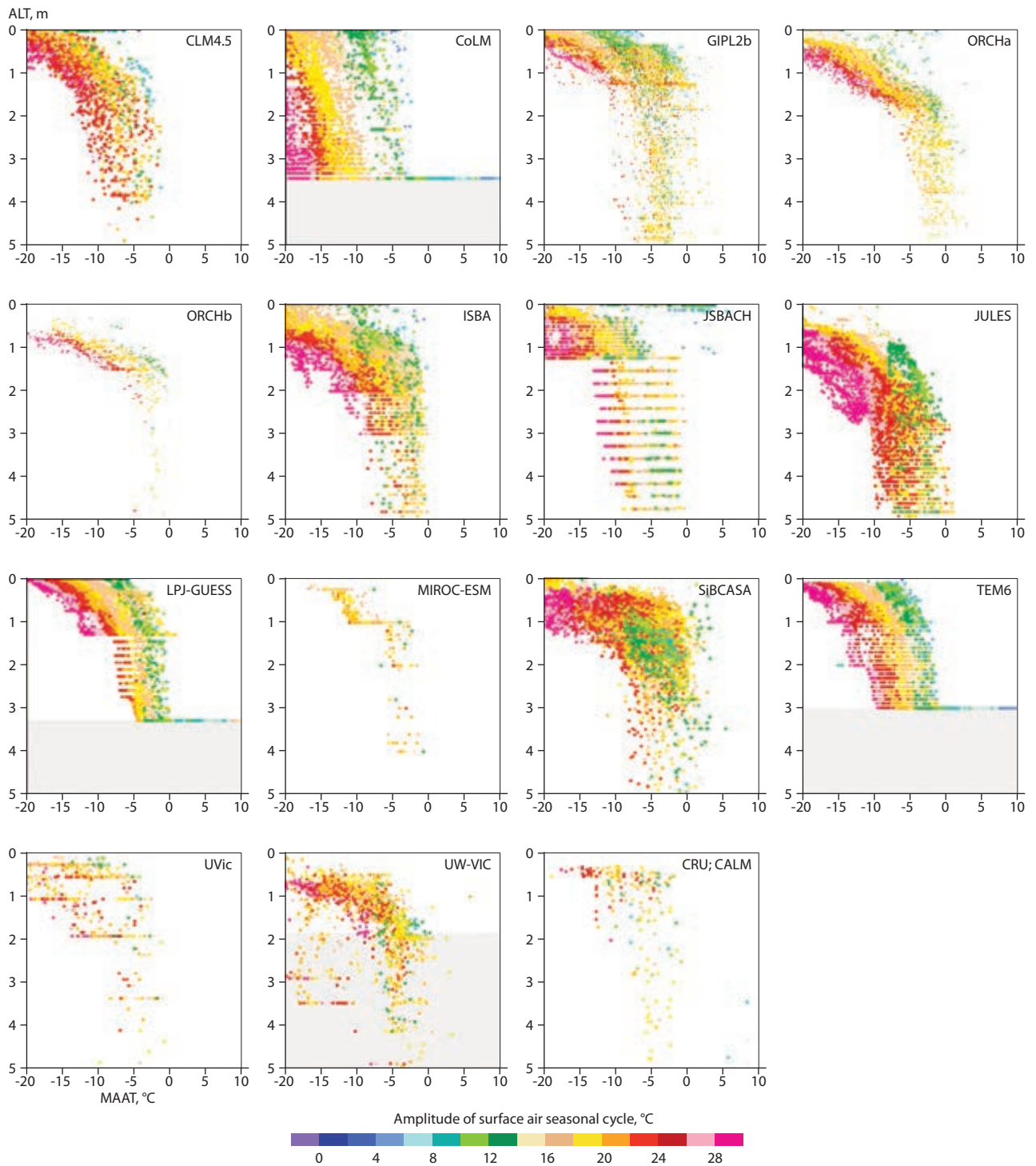


Figure 4.8 Model predictions of initial active-layer thickness (ALT) plotted as functions of mean annual air temperature (MAAT) and the amplitude of the seasonal cycle in surface air temperature, following Koven et al. (2013). Also shown are observations of ALT from the Circumpolar Active Layer Monitoring (CALM) project dataset. See Table 4.1 for model details (McGuire et al., 2016).

rates of loss among models (200 to 58,800 km²/y; Figure 4.7). The analysis also partitioned the loss of permafrost simulated by the models associated with changes in atmospheric CO₂, temperature, and precipitation (Figure 4.7). Among the nine models that ran sensitivity simulations, 84% of the change in permafrost area was explained by model sensitivities to changes in air temperature. In addition to large variations in initial permafrost extent, model predictions of active-layer thickness vary substantially. Figure 4.8 shows initial model predictions of ALT as functions of climate, following

Koven et al. (2013), as compared to observations from the Circumpolar Active Layer Monitoring (CALM) project network. While most models tend to show an overall pattern of climate controls on ALT that is similar to and consistent with observations, key differences can be seen in, for example, the minimum ALT, the maximum mean air temperature at which permafrost occurs, and the slope and shape of the ALT-air temperature relationship. This relationship is clearly shown by observational data for sites ranging from forest and peatlands to tundra (e.g. Smith et al., 2009b). As a whole,

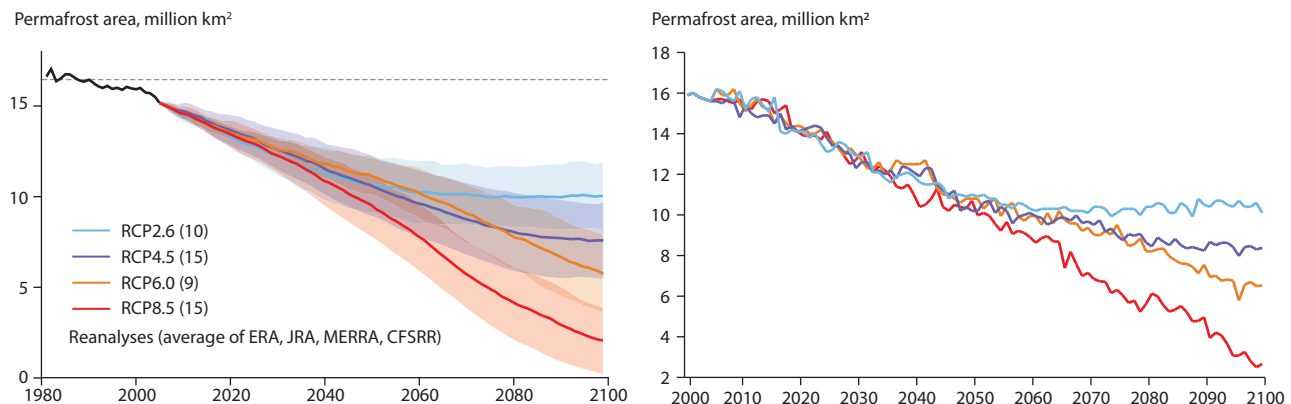


Figure 4.9 Projected northern hemisphere permafrost area from Slater and Lawrence (2013; left) and Arzhanov et al. (2013; right).

the set of models considered by McGuire et al. (2016) shows reduced biases in these comparisons compared to the CMIP5 models (Koven et al., 2013).

Slater and Lawrence (2013) and Koven et al. (2013) analyzed ESM projections of soil temperature from the Coupled Model Intercomparison Project phase 5 (CMIP5) database to assess the models' representation of current-climate soil thermal dynamics. Their analyses indicate that models show a wide range of current area of permafrost (ALT <3 m) (4–25 million km²), active layer statistics (cumulative distributions, correlations with mean annual air temperature, and amplitude of seasonal surface air temperature cycle), and ability to accurately model the coupling between soil and air temperatures at high latitude. Despite large differences between models, all models agree that the projected warming and increases in snow depth will result in near-surface permafrost degradation over large geographic areas.

The sensitivity of the modeled area of permafrost (ALT <3 m) to climate change is 0.8–2.3 million km² per degree centigrade increase in air temperature. The wide range of sensitivity results in a wide range of projected permafrost loss: 15–87% under RCP4.5 and 30–99% under RCP8.5 (Figure 4.9). Slater and Lawrence (2013) estimated that the reduction in near-surface permafrost extent by the end of the century will be about 2.1 million km² under RCP 2.6 and 10 million km² under RCP 8.5. Arzhanov et al. (2013) derived slightly higher estimates of 3 million km² and 10.5 million km², respectively (Figure 4.9). Collectively, the CMIP5 models suggest that for RCP4.5, permafrost will mainly retreat from the present-day discontinuous zone by 2100 (Figure 4.9). Under RCP8.5, sustainable permafrost will probably only occur in the Canadian Arctic Archipelago, the Russian Arctic coast, and the east Siberian uplands (Figure 4.10).

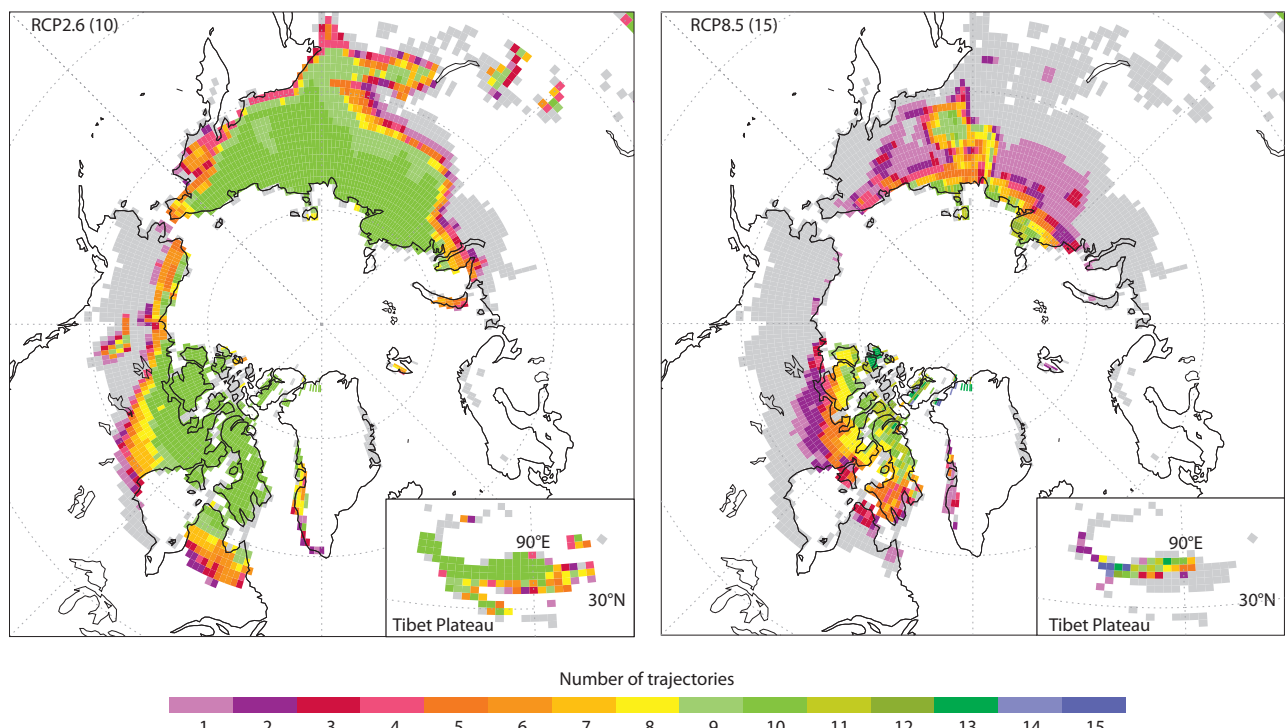


Figure 4.10 Number of climate trajectories with sustainable permafrost in 2099 (Slater and Lawrence, 2013). Numbers in brackets represent the number of different models that were included in the analysis. Present-day continuous and discontinuous permafrost is shown by gray shading.

A key finding is that the models with deeper than average ALT under the current climate were more vulnerable to losing near-surface permafrost for a given amount of warming across the permafrost region. However, it should be noted that some models only consider a limited depth below the ground surface and so overestimate the loss of permafrost when ALT is above 3 m. In areas of the Canadian Arctic and in the Brooks Range in Alaska, for example, where bedrock extends almost to the ground surface, ALT is often more than 3 m.

4.3.2 Standalone permafrost models

Despite a general understanding of how permafrost is changing and may change in the future, it is still unclear how these changes will affect ecosystems and infrastructure on local and regional scales. The major hurdle in addressing this issue lies in limited knowledge of local processes and consequences, owing to insufficient spatial and temporal resolution in models and in projections of changing climate and related changes in other environmental characteristics, including permafrost. A major challenge to the scientific community is to bridge the gaps in spatial scaling to overcome this issue.

To date, numerical standalone permafrost models have proved useful tools for assessing the thermal state of the ground on a range of spatial and temporal scales. To compile 'thermal maps' of the ground, they can be driven by a variety of data sets, from interpolations of in-situ measurements (e.g. Westermann et al., 2013; Zhang et al., 2013) to downscaled climate model output (e.g. Shkol'nik et al., 2010, 2012; Jafarov et al., 2012; Nadyozhina et al., 2013). Recent studies have exemplified the potential of remote sensing data sets, especially of land surface temperature and snow water equivalent, in conjunction with numerical permafrost models (Westermann et al., 2015a). Langer et al. (2013) used a transient permafrost model to infer thaw depth and near-surface ground temperature in a time-resolved way. A large-scale application with a steady-state model was demonstrated by Westermann et al. (2015b) who provided remote-sensing-based maps of ground temperature (Figure 4.11) and permafrost probabilities for the North Atlantic permafrost region. A major

problem is the limited spatial resolution of the remote sensing data so that strategies to represent the considerable subgrid variability of ground temperatures are required (Gisnås et al., 2014; Fiddes et al., 2015). In addition, fine-scale variability in snow depth and surface vegetation cover properties can also lead to spatially different future ground warming and thawing rates as was demonstrated for a site in Greenland by Westermann et al. (2015c). Another caveat for future projections of permafrost evolution is the representation of excess ground ice which can both delay and accelerate permafrost thaw (Lee et al., 2014; Westermann et al., 2016), depending on the hydrological conditions at the site.

Recent assessments demonstrate that permafrost characteristics widely vary, ongoing warming occurs over large areas, and local evidence of permafrost degradation is apparent in parts of Alaska, Russia and Canada (see Sections 4.2, 4.4 and 4.5). As a result, predictive permafrost standalone models of moderate-to-coarse spatial resolution were developed, and substantial permafrost degradation is forecast by the end of the present century. While the projected reductions in permafrost extent ranged from 10% to as much as 40%, these projections are subject to three major caveats (Nicolksy et al., 2007; Lawrence et al., 2008; Saito et al., 2008): (1) they are driven by output from coarse-resolution (~300 km) general circulation models (GCMs) of late-1990s vintage, (2) they do not capture fully the time lags between surface warming and permafrost thaw in areas of thick permafrost, and (3) the climate models suffer from systematic biases (some poorly known) partly caused by an incomplete treatment of snow and subsoil processes. Nevertheless, even small changes in permafrost extent have serious implications for ecosystems, human activities (infrastructure and subsistence lifestyle) and feedbacks within the climate system (especially regarding carbon and water fluxes). To address these problems, new approaches need to be developed to integrate observations, remote sensing data, and GIS technology into retrospective and predictive modeling of permafrost dynamics.

Nicolksy et al. (2017) employed the permafrost module GIPL2 of the Alaska Integrated Ecosystem Model (AIEM) and

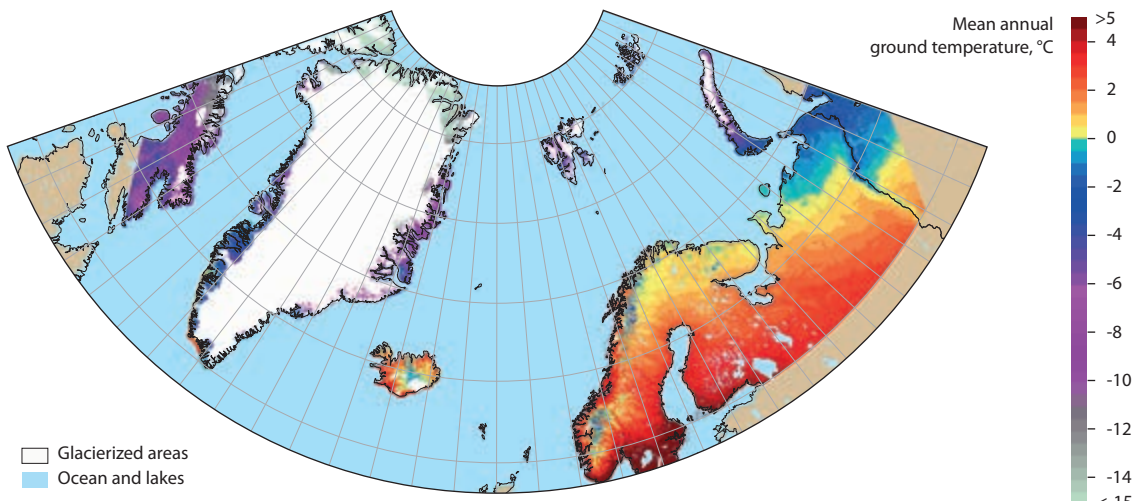


Figure 4.11 Mean annual ground temperature at 1-km spatial resolution simulated by the semi-empirical permafrost model CryoGrid 1 driven by remotely sensed and reanalysis data over the period 2003–2012 (Westermann et al., 2015b).

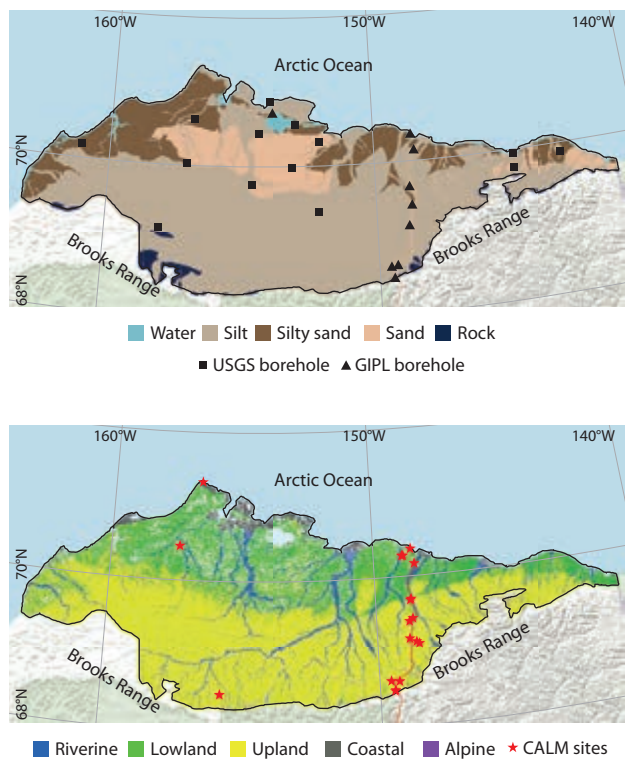


Figure 4.12 Soil texture categories (upper) and ecotype groups (lower) for northern Alaska. 51 different ecotype-soil texture combinations were used to parameterize ground thermal properties for the 770×770 m computational grid cells for use in model applications. The locations of the temperature monitoring sites by the University of Alaska Geophysical Institute and United States Geological Survey are marked in the upper plot and the locations of the Circumpolar Active Layer Monitoring (CALM) sites are marked in the lower plot (Nicolksy et al., 2017).

established several high spatial resolution scenarios of changes in permafrost characteristics in the Alaskan Arctic in response to projected climate change. Properties of surface vegetation, soil type, layering and moisture content are up-scaled using the Landscape/Permafrost database by Jorgenson et al. (2014) and a 30-m resolution unified ecological map by Jorgenson and Heiner (2004). The spatial distribution of the soil texture categories and ecotypes for the Alaska North region is illustrated in Figure 4.12. The soil texture-ecotype pairs provide a decomposition of

the study area into different landscape units with respect to hydrologic, pedologic, and vegetative characteristics of the ground material. The thermal properties for each pair were defined using a temperature data assimilation technique.

Temperature data assimilation techniques allow parameterization of the ground thermal properties for each dominant ecosystem type using the ground temperature records from the shallow boreholes across the Alaska North Slope. Soil temperature dynamics are simulated by solving the 1-D non-linear heat equation with phase change (Nicolksy et al., 2009), while snow temperature and thickness dynamics are simulated by assuming the snow accumulation and compaction processes (Anderson, 1976). To verify the developed model, Nicolksy et al. (2017) compared the modeled and observed ALT, ground temperature and snow depth records from existing permafrost observatories operated by the United States Geological Survey and Geophysical Institute, University of Alaska Fairbanks. The simulated present-day distribution of ALT across the North Slope between the Brooks Range and the Arctic Ocean is shown in Figure 4.13. Potential changes in mean annual ground temperature for the Alaskan Arctic during the 21st century under RCP4.5 and RCP8.5 are reported by Nicolksy et al. (2017).

4.3.3 Uncertainties in permafrost response to projected changes in climate at sub-regional scales

There are two types of uncertainty in permafrost projections: one is associated with the forcing climate, soil, vegetation and other environmental data; and the other is associated with the limitations of permafrost models. The first type of uncertainty for Eurasian permafrost has been assessed in several studies (Anisimov 2011; Anisimov et al., 2011, 2013; Anisimov and Kokorev, 2013; Kokorev and Anisimov, 2013; Zhiltcova and Anisimov 2013; Anisimov and Sherstukov, 2016).

Anisimov and Sherstukov (2016) applied multifactorial regression analysis to climatic data from the full set of roughly 1600 Russian and former Soviet Union weather stations, and evaluated the contribution of air temperature and snow depth to the variation in ground temperature for the period 1972–2012. Neither factor accounted for more than 30% of the permafrost

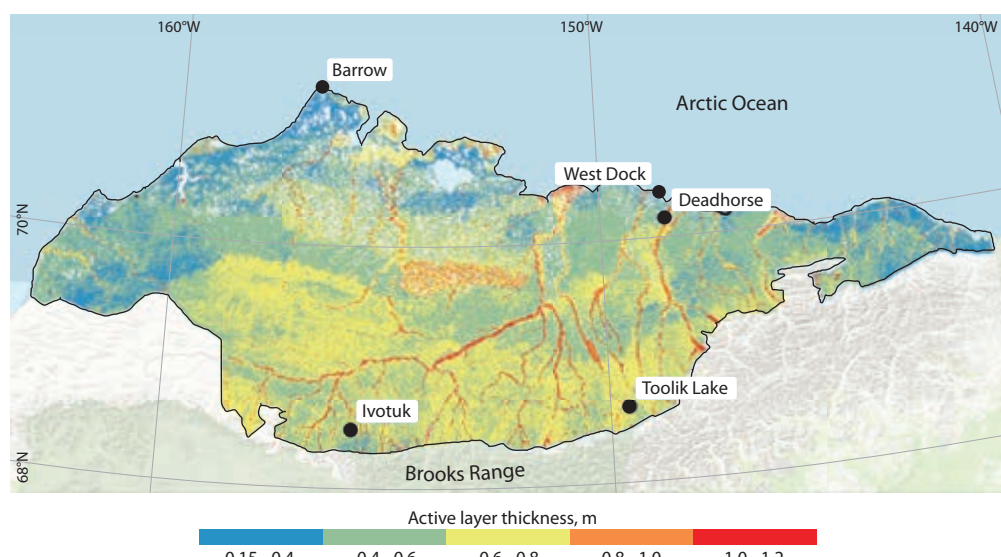


Figure 4.13 A 770×770 m resolution map of the simulated mean active-layer thickness for the Alaska North Slope region for the period 2000–2010 under the RCP4.5 emission scenario. The model was verified using measured ALT at Circumpolar Active Layer Monitoring (CALM) sites (Nicolksy et al., 2017).



Figure 4.14 Percentage of total ground temperature variability attributed to air temperature (upper) and snow depth (lower) (Anisimov and Sherstukov, 2016).

temperature variability (Figure 4.14), with air temperature playing a more important role in the European Arctic region, and snow depth in Siberia.

Anisimov et al. (2013) developed a new climatic regionalization for northern Eurasia and evaluated the skills of ESMs to model the impacts of climate variability and change on the cryosphere. The study area was divided into regions with coherent temperature changes in the period 1972–2012. In the analyses of Anisimov and Kokorev (2013) and Kokorev and Anisimov (2013) regional trends in several climatic

parameters governing permafrost condition were compared with 48 historical runs of CMIP5 ESMs, and the models were ranked according to their skill (Figure 4.15, full data set accessible at <http://permafrost.su/gcm.html>). Results were used to eliminate the outliers and construct an ensemble of models with 'better than average' skill in the Eurasian permafrost region. This procedure of sub-regional and process-specific evaluation of ESMs suggested in these studies markedly lowers the range of uncertainty in predictive permafrost modeling associated with climatic forcing.

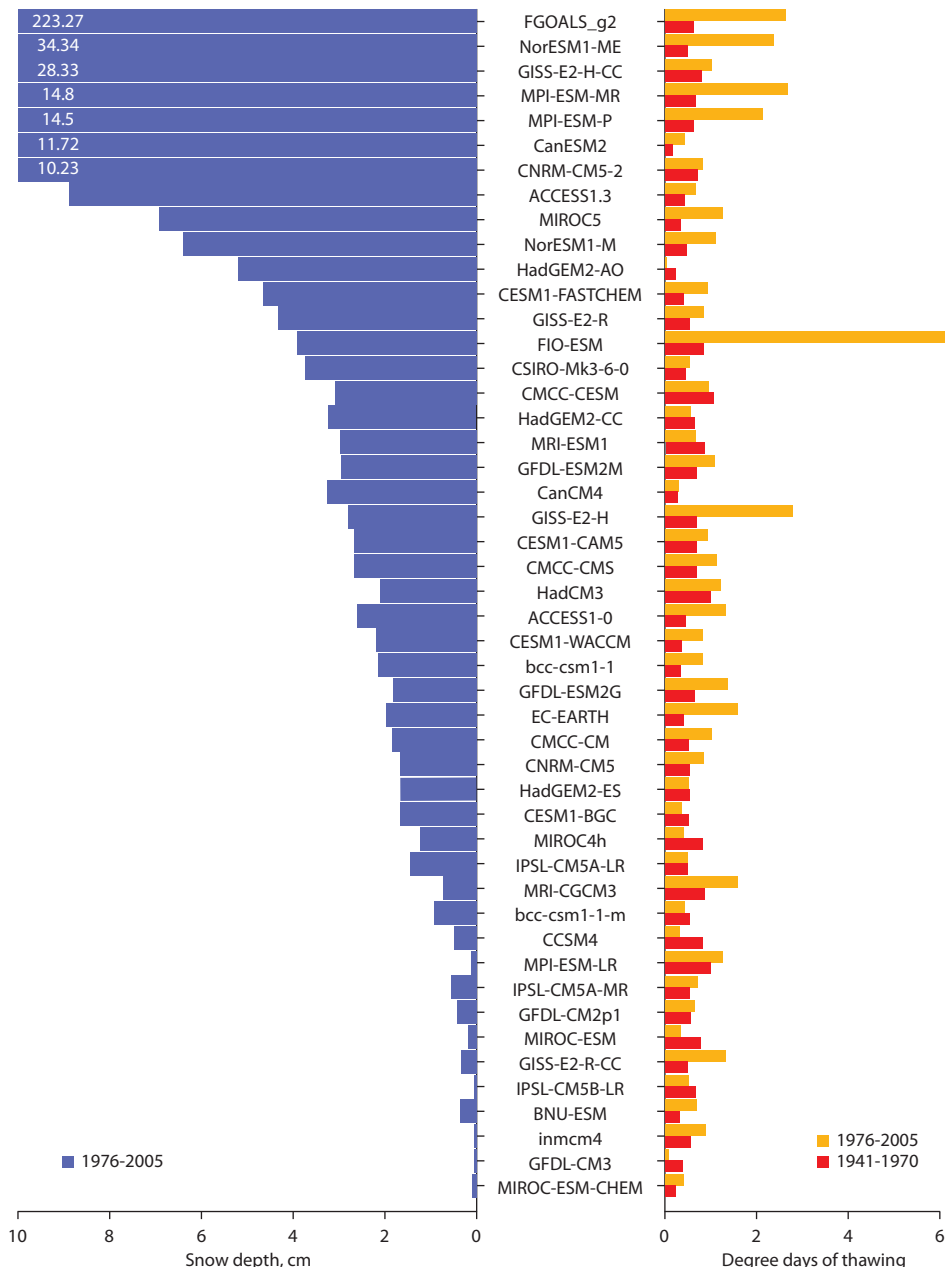


Figure 4.15 Departures of the CMIP5 GCM-based estimates from observations averaged over the Eurasian permafrost region (Anisimov and Kokorev, 2013). The upper bars in the left panel extend beyond the x-axis limits, and the numbers show the actual values of departures for these models.

4.3.4 Modeling the effects of vegetation change on permafrost dynamics

Anisimov and Sherstukov (2016) assessed the uncertainty of permafrost modeling associated with changing vegetation, which acts as a moderator of interactions between the atmospheric and permafrost thermal regime. The role of vegetation is two-fold: (1) non-vascular plants increase thermal insulation and insulate permafrost from warming and (2) enhancement of the leaf area index of shrubs and trees protects permafrost by attenuating the incident solar radiation. Interannual climate-driven variations in plant productivity thus attenuate the direct effect of temperature changes on permafrost. An indirect effect of changing vegetation type (especially growth of shrubs) is also associated with a re-distribution of snow and so these changes may contribute to warming of the ground (Lantz et al., 2010,

2013; Morse et al., 2012; Palmer et al., 2012). However, this effect is not considered in this section.

Field observations over the past 30 years (Elmendorf et al., 2012; Urban et al., 2014) as well as analyses of satellite data (Xu et al., 2013) indicate an increase in plant productivity and 'greening' in many Arctic regions. Shifts in vegetation zones and advancement of shrubs into tundra have been reported in several studies (Hickling et al., 2006; Forbes et al., 2010; Gonzalez et al., 2010), and according to the results from dynamical vegetation models, these changes will continue in the future (Pearson et al., 2013). Vegetation projections are thus needed for predictive permafrost modeling even at relatively short time scales, and at the multi-decadal and century scale vegetation could even act as the key factor governing permafrost response to climatic change.

Climate-induced changes in vegetation, the effect of such changes on permafrost, and dynamically decoupled climate-

Table 4.2 Fraction of the area in northern Eurasia (%) where the vegetation-permafrost system is projected to exceed critical climate thresholds by the 2016–2045 and 2031–2060 time slices. Calculations were made using standalone vegetation and permafrost models forced with CMIP5 climate model output from the RCP8.5 climate experiment. (Anisimov et al., 2011, updated).

Time slice	European North	Western Siberia	Eastern Siberia	Chukotka	Eurasian permafrost average
2016–2045	58	64	55	48	56
2031–2060	71	74	70	57	67

vegetation-permafrost modeling for northern Eurasia have been assessed in several studies (Anisimov et al., 2011, 2015; Zhiltsova and Anisimov, 2013). These studies introduced the concept of region-specific critical climate thresholds, beyond which further climatic forcing leads to irreversible changes in the state of the vegetation-permafrost system. Critical thresholds, or tipping points, are characterized by shifts in the boundaries of biomes, the appearance of new plant species, and abrupt changes in the permafrost thermal regime. Because of the difference in the response rates of permafrost temperature changes and biome boundary shifts, the evolution of the system may be predicted using decoupled standalone climate-driven permafrost and vegetation models. Anisimov et al. (2011) used this approach to calculate the proportion of the permafrost area in four sectors of northern Eurasia that is likely to be affected by critical changes in the first half of the 21st century (Table 4.2).

4.3.5 Modeling sub-sea permafrost dynamics

Since the 2011 SWIPA assessment, there have been major advances in modeling the dynamics of sub-sea permafrost, largely to address the hypothesized thawing of the sediments below the East Siberian Arctic Shelf (ESAS) and potential release of methane from beneath the thawed permafrost. A key difference among the models is whether they account for the effects of salinity. Taylor et al. (2013) used a finite element geothermal model that combines conductive heat transfer with the latent heat of freezing and thawing in porous sediments. This model accounts for the unfrozen pore water through an empirically derived parameterization. Nicolsky et al. (2012)

employed a conventional dynamical model that takes into account the freezing point depression between -0.6°C and -3.1°C in the bottom sediments depending on salinity. In both models salt diffusion from water into bottom sediments is neglected, i.e. salinity remains unchanged. Three other studies by Anisimov et al. (2012a, 2014) and Dmitrenko et al. (2011) used a new type of model (see also Lavrov and Anisimov, 2011 and Anisimov et al., 2012b) which explicitly accounts for salt diffusion from seawater to bottom sediments. Direct effects on the temperature and freezing point depression are thus dynamically calculated.

The major conclusion of Taylor et al. (2013) is that the paleoenvironment of the last 125,000 years is sufficient to develop the depth, seaward extent, and principal features of the sub-sea permafrost body on the Beaufort continental shelf. The computational setup of Nicolsky et al. (2012) accounts for different temperature scenarios in the undisturbed parts of the East Siberian Arctic Shelf and those affected by thermokarst lakes before the inundation of the continental shelf following the last Glacial Maximum (Figure 4.16).

Anisimov et al. (2012a) performed sub-sea permafrost modeling for ESAS over the period from 20,000 years before present, to the present day (2010) and then to year 3000 using a hypothetical climate scenario. Results for the ‘typical’ ESAS conditions are illustrated in Figure 4.17. By 1985, the upper 10 m layer of the bottom sediments has thawed, although the annual-mean near-bottom water temperature remained slightly below zero. Thawing occurred due to salt diffusion in the pore space, which led to the gradual conversion of ice to unfrozen saline water. According to hydrographic data, in the 25 years since

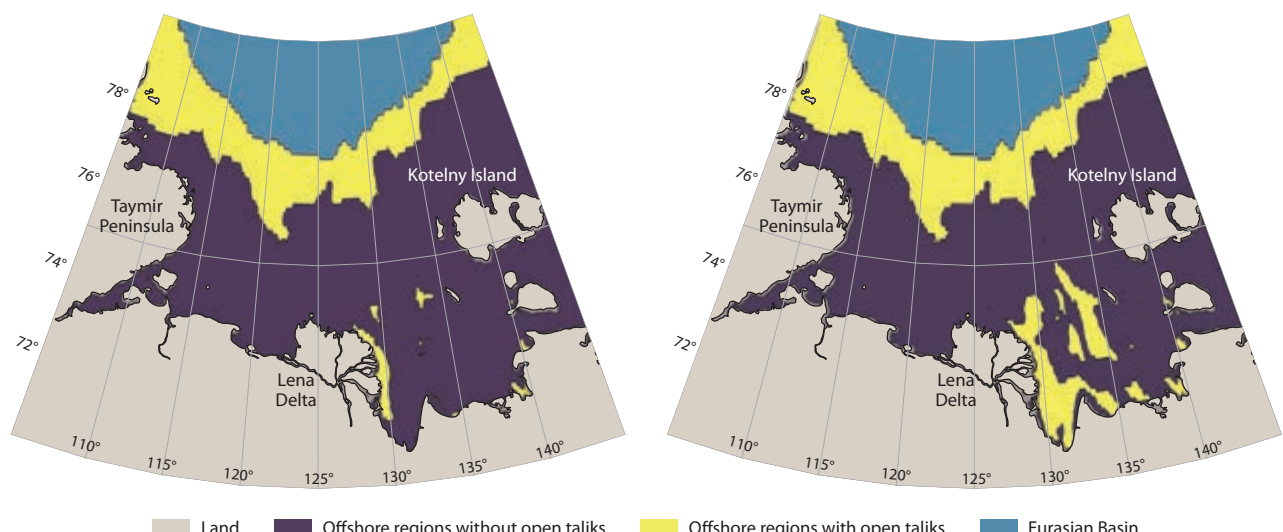


Figure 4.16 Modeled locations of open taliks in the Laptev Sea Shelf in the case of (left) ‘100-year mean’ and (right) ‘1999–2009 mean’ parameterization of benthic temperature (Nicolsky et al., 2012).

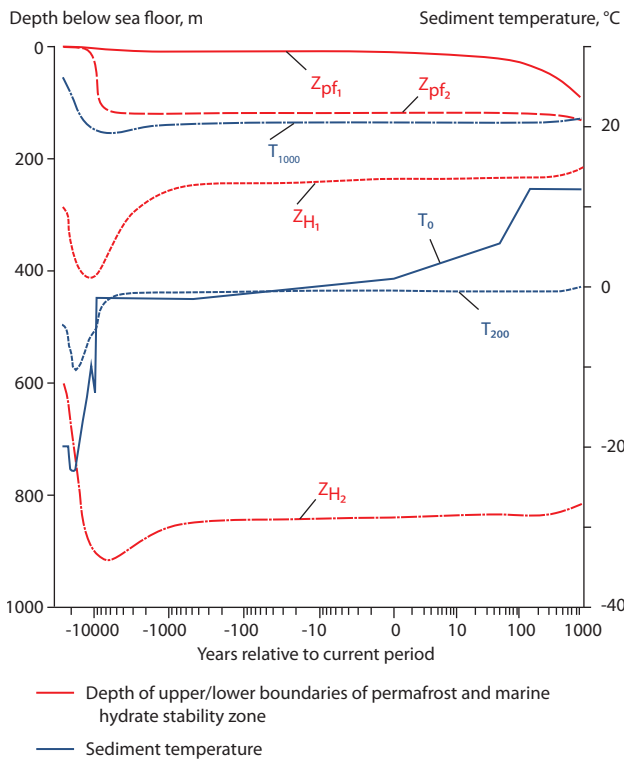


Figure 4.17 Modeled permafrost dynamics over geological time scales (Anisimov et al., 2012a). Blue curves show modeled changes in sediment temperature (vertical axis on right) over time at near-bottom level (T_0), 200 and 1000 m below the sea floor (T_{200} and T_{1000} , respectively). Red curves show depth (vertical axis on left) to upper (Z_{pf1}) and lower (Z_{pf2}) permafrost boundaries, and the upper (Z_{H1}) and lower (Z_{H2}) boundaries of the methane hydrate stability zone. Time (years) is shown on the horizontal axis in a logarithmic scale with respect to the current period (0).

1985 the near-bottom water temperature increased in summer by 2.1°C. This caused further deepening of the upper permafrost boundary by 6–8 m, down to 16–18 m below the sea floor.

4.3.6 Summary and recommendations

There has been substantial progress in analyzing the retrospective simulations of large-scale permafrost models. For models to properly simulate active-layer thickness and soil temperature of near surface permafrost they must adequately simulate snow insulation (including the effect of changing vegetation on snow properties) during winter and the thermal conductivity of near surface organic horizons. A key finding is that it is more important to properly simulate soil temperature at 1-m depth than to simulate the proper initial permafrost area for modeling permafrost degradation in recent decades. This is consistent with the finding of Koven et al. (2013) that models with deeper active-layer thickness under the current climate were more vulnerable to losing near-surface permafrost for a given amount of warming across the permafrost region. These results suggest that uncertainties in future projections can be substantially reduced by benchmarking the retrospective simulations of permafrost models and eliminating from uncertainty analyses those models that do not perform well, as has been demonstrated at the sub-regional scale. Based on recent progress (e.g. Miyazaki et al., 2015; Sueyoshi et al., 2016), the key recommendation here is that benchmark data sets are developed for analyzing the retrospective simulations of permafrost models. It is also important to continue collecting

temperature measurements in various ecosystems in order to capture natural spatial heterogeneity across landscapes. Incorporating thermokarst and thermo-erosion processes (the erosion of ice-bearing permafrost by the combined thermal and mechanical action of moving water) in complex land surface models will be important to fully capture future responses of permafrost dynamics in a warming Arctic and related climatic feedbacks. The additional data could be assimilated in existing permafrost models to further constrain uncertainties in numerical predictions.

4.4 Permafrost-related processes and recent response to climatic changes

Permafrost-related processes directly or indirectly influence northern environments, but the impacts are affected by complex interactions involving positive and negative feedbacks at the surface (Jorgenson et al., 2010), climatic trends and fluctuations (Romanovsky et al., 2010a; Konishchev, 2011), and terrain and ground-ice conditions (French and Shur, 2010; Ukrainsteva et al., 2012; Murton, 2013). Permafrost degradation (reduction in thickness and/or lateral extent) and the related disturbance of the land surface are associated with a diverse set of processes such as thermokarst (thawing of ice-rich permafrost or melting of massive ice followed by subsidence of the ground surface and potential formation of a water body), thermal erosion (downwearing from moving water), thermal abrasion (backwearing from moving water), and thermal denudation associated with hillslope processes (downslope movement of soil or rock, such as frost creep, solifluction and cryogenic landslides including active-layer detachments and retrogressive thaw slumps). At the same time, the aggradation of permafrost and related processes (e.g. frost heave and formation of ice wedges and pingos (a perennial frost mound that comprises a core of massive ice produced primarily by the injection of water and covered by soil and vegetation; van Everdingen, 1998)) are still occurring during the current warming trend in the northern hemisphere. For example, drainage of thermokarst lakes exposes taliks (unfrozen ground beneath the water body) to the negative mean annual ground surface temperatures in the continuous and discontinuous permafrost zone, which results in talik re-freezing accompanied by the accumulation of ground ice. Both permafrost aggradation and degradation associated with thermokarst and other thaw-related features requires further study to determine the pan-Arctic landscape response to climatic trends and fluctuations.

4.4.1 Thermokarst

Thermokarst is the process by which characteristic landforms result from the thawing of *ice-rich permafrost* or the melting of *massive ice* (van Everdingen, 1998). Various types of thermokarst landforms were described by Jorgenson et al. (2008) and Kokelj and Jorgenson (2013). Typical Arctic thermokarst landforms include thermokarst lakes, collapsed pingos, sinkholes, and pits. Accumulation of water in depressions formed by subsidence due to ground ice melt often results in the formation of a small trough pond which may evolve into a lake over time. Depending on the amount of ground ice and depth of thaw beneath the lake, its depth



Figure 4.18 Thermokarst lakes (a), water-filled troughs above degrading ice wedge (b), and overgrowing of draining lake margins (c), Yamal, Russia (photos M.O.Leibman).

can range from 1–3 m to 10–20 m or more (Shur et al., 2012) (Figure 4.18a). Thaw subsidence of more than 20 m is mostly associated with development of thermokarst lakes in the ice-rich yedoma deposits, which contain large volumes of wedge ice (Soloviev, 1962; Romanovskii et al., 2004; Konishchev, 2011; Shur et al., 2012; Grosse et al., 2013; Kokelj and Jorgenson, 2013; Morgenstern et al., 2013; Schirrmeyer et al., 2013; Kanevskiy et al., 2014; Ulrich et al., 2014). In addition to thermokarst processes, lake evolution is driven by the complex interaction of nearshore and slope processes associated with thermal abrasion and thermal denudation (Grosse et al., 2012; Biskaborn et al., 2013).

Thermokarst lake dynamics is an indicator of climate change in the Arctic (Smith et al., 2005; Kravtsova and Tarasenko, 2011). Remote sensing is now widely used to monitor lake area changes in Alaska, where new data on morphometry of thermokarst lakes, shores retreat rates and sedimentation features were also obtained (Hinkel et al., 2007; Arp et al., 2011; Jones et al., 2011, 2012a; Parsekian et al., 2011; Roach et al., 2011; Jones and Arp, 2015; Jorgenson et al., 2012; Necsoiu et al., 2013). In Canada sedimentology and geochemistry of thermokarst ponds were studied in addition to lake dynamics (Bouchard et al., 2011; Carroll et al., 2011; Sannel and Kuhry, 2011; Lantz and Turner, 2015). In the Qinghai-Tibet Plateau of China new data were obtained on hydrological processes near thermokarst lakes and their influence on lake development (Ling et al., 2012; Pan et al., 2014). In Russia the differences and special features of thermokarst lake dynamics were revealed in western Siberia, Yakutia, and northeastern European Russia (Kravtsova and Tarasenko, 2011; Sannel and Kuhry, 2011; Bryksina and Kirpotin, 2012; Iijima, et al. 2012; Sannikov, 2012; Biskaborn et al., 2013; Sjöberg et al., 2013; Trofaier et al., 2013; Manasypov et al., 2014). In Sweden changes in lake extent in peat plateau have been studied (Sannel and Kuhry, 2011).

Increases and decreases in lake area as a response to climate change are of a regional character (Kravtsova and Bystrova, 2009) and are linked to environmental and local climate controls. In general, there is an increase in the number and area of thermokarst lakes in the continuous permafrost zone and a reduction in the number and area of lakes in discontinuous and sporadic permafrost zones (Smith et al., 2005).

The changes observed may differ for large and small lakes. Higher variability is observed for smaller lakes in the tundra zone (Carroll et al., 2011). The formation of new small lakes along with the disappearance of medium and large lakes is noted in western Siberia (Bryksina and Kirpotin, 2012)

(Figure 4.18b) as well as in northeastern Alaska, Seward Peninsula (Jones et al., 2011) and peatlands with sporadic permafrost in northern Sweden (Sannel and Kuhry, 2011). At the same time, lakes are expanding in the allasses (thaw-lake basins) located in the Lena River valley of central Yakutia (Iijima et al., 2012).

Bi-directional resizing of thermokarst lakes is observed in the boreal forests of Alaska (Roach et al., 2011; Jorgenson et al., 2012; Chen et al., 2013). A significant reduction in the areas of lakes in the north and an increase in the areas of lakes in the southern regions were observed in Canada (Carroll et al., 2011), which is the reverse of that observed in western Siberia (Smith et al., 2005). An increase in the total number of water bodies and a decrease in the total area of thermokarst lakes were reported for the southern extent of the continuous permafrost zone in Alaska (Jones et al., 2011). No significant change is observed in the size of thermokarst lakes in the peatlands of continuous and discontinuous permafrost on the coast of Hudson Bay (Canada) or in northeast European Russia (Sannel and Kuhry, 2011).

In addition to interannual dynamics, lakes are subject to seasonal changes in size as well as to catastrophic drainage. For example, lake areas may be reduced by 30% during summer on the lower topographic levels in central Yakutia (Kravtsova and Tarasenko, 2011) and by 42% in the Yukon lowlands (Chen et al., 2013). It is significant that the effect of reducing the water surface area of lakes is observed despite strong thermokarst development (Parsekian et al., 2011; Jorgenson et al., 2012). The formation of floating vegetation mats along thermokarst lake margins indicates the rapid degradation of near-surface permafrost and masks lake expansion (Parsekian et al., 2011; Chen et al., 2013) (Figure 4.18c).

Reduction in a lake area creates numerous climatic feedbacks through changes in lake surface area, evaporation and carbon balance (Carroll et al., 2011). Drainage of thermokarst lakes can lead to permafrost aggradation. In the continuous permafrost zone, freezing of taliks and distinct patterns of soil and vegetation succession begins immediately after drainage (Jones et al., 2012b; Kanevskiy et al., 2014), but may not occur or may be delayed in the discontinuous permafrost zone, where bogs with water are not frozen (Shur and Jorgenson, 2007). Permafrost aggradation here is triggered by accumulation of peat in drained lake basins (Shur and Jorgenson, 2007; Kanevskiy et al., 2014). Permafrost aggradation is accompanied by frost heave and, under certain conditions (mostly in the continuous permafrost zone), by development of ice wedges and pingos.

Expansion of thermokarst lakes may occur through thermal abrasion of lake margins and further subsidence of the lake bottom. The measured rates of shoreline erosion for thermokarst lakes on the Coastal Plain of northern Alaska range from 0–2 m/y in shallow lakes to 1–8 m/y in deeper lakes (Arp et al., 2011). Jones et al. (2011) presented a synthesis of thermokarst lake expansion rates available from studies around the Arctic. The precipitation–evaporation balance rather than air temperature rise may be the primary factor affecting thermokarst processes in some regions (Konishchev, 2011). New subsidence and expansion of existing depressions in the drain-lake basins in central Yakutia are linked to years with higher precipitation, characterized by a thicker and wetter active layer (Iijima et al., 2012).

Widespread surficial degradation of ice wedges has been observed in various permafrost regions of Eurasia and North America during recent decades (Liljedahl et al., 2016). Thermokarst pits and troughs in polygonal terrain are one of the most characteristic thermokarst landforms resulting from thawing of ice-rich permafrost (Kokelj and Jorgenson, 2013). A significant increase in areas of water-filled polygonal troughs was reported in northern Alaska (Jorgenson et al., 2006; Raynolds et al., 2014) and linked to climatic changes. Modern thermal conditions are favorable for the formation of multiple small ponds in early thermokarst stages in the Yakutian Arctic Lowlands, where vast areas of thermokarst depressions exist. Nevertheless, there is low potential for vast thermokarst lake formation because dissected topography provides good drainage conditions and organic matter accumulation in the initial thermokarst depressions provides insulation (Morgenstern et al., 2011; Shur et al., 2012).

Thus, no unified circumpolar trends in thermokarst development associated with global warming have been observed to date. Identified changes in thermokarst lake development are related to both regional and local environmental and climatic factors, including the moisture balance. More studies are required to determine the driving forces for thermokarst lake formation and drainage and subsequent changes in the landscape.

4.4.2 Thermal erosion

Thermal erosion is a dynamic process involving the wearing away of surface deposits by thermal action (the melting of ice) and mechanical action (hydraulic transport) (van Everdingen, 1998). The longest monitoring of gully erosion was conducted on Bylot Island in Canada, where dozens of thermo-erosional gullies ranging from a few meters to 2 km in main axis length

were measured (Godin and Fortier, 2012). The results of spatio-temporal monitoring between 1958 and 2011 using field observations, differential GPS mapping and aerial and satellite imagery analysis indicated that some gullies stabilized while others evolved at rates ranging from 14 ± 3 to 25 ± 4 m/y. One gully mouth was eroded over 82 m in length between 1982 and 2007 by riverbank erosion (Godin and Fortier, 2012). The erosion network in permafrost areas often develops a polygonal pattern because the polygon troughs provide naturally forming flow paths underlain by almost pure ice substrate (Figure 4.19a). Gully formation in polygonal terrain can lead to the development of large gully networks (Fortier et al., 2007; Haltigin et al., 2012) and the drainage of thermokarst lakes (Jones and Arp, 2015). These features are typically 1–5 m deep and may extend for hundreds of meters laterally (Godin and Fortier, 2012).

Thermal erosion rates may increase through positive feedbacks, such as active retrogressive thaw slumps, an unstable permafrost thermal regime following disturbance, streams flowing through gully heads and sinkhole enlargement; while negative feedbacks are associated with surface vegetation regrowth, active-layer drainage and subsequent ground cooling, which can result in gully stabilization (Godin and Fortier, 2012).

River thermal erosion (Figure 4.19b) depends on the spring flood, which combines the mechanical and thermal effects of river flow. River erosion may also occur later in summer if there is a second discharge peak. In the Lena River delta, the retreat of the banks of the river islands indicates high interannual variability that is attributed to variability in the duration and timing of the flood season. Only a few days of contact with floodwaters was required to produce a 22-m bank retreat in 2010 (Costard et al., 2014). The highest long-term rates of erosion of the Collville River bank in the Alaskan Arctic were just over 1 m/y, but in 1962 alone a retreat of about 10 m was reported (Walker and Jorgenson, 2011). River thermal erosion is controlled by water temperature and ice content (Dupeyrat et al., 2011).

River thermal erosion in small river catchments where slopes are proportional in size to the channel geometry is interrelated with other processes. In V-shaped valleys, the influence of cryogenic landsliding on hydrologic processes dominates and dammed lakes may be formed. Thermokarst above ice wedges develops in U-shaped valleys and bead-shaped channels are formed (Figure 4.19c), which contribute to the expansion of thermokarst (Gubarkov and Leibman, 2010; Gubarkov et al., 2014).

Thermo-erosional gullies are long-lasting features in the periglacial landscape. They affect local hydrology, water



Figure 4.19 Polygonal network thermal erosion (a), lateral and river thermal erosion (b), bead-shaped stream (c), Yamal, Russia (photos M.O. Leibman).

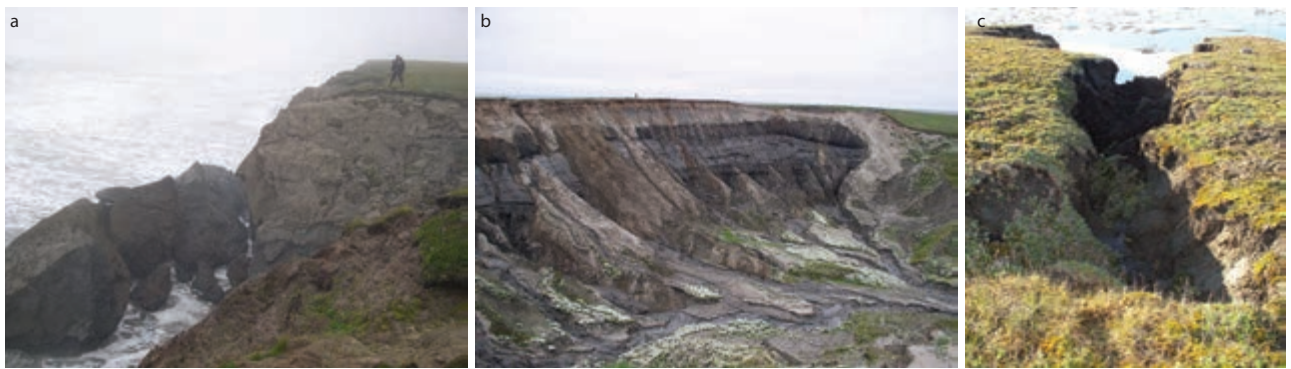


Figure 4.20 Thermal abrasion (a), thermal denudation (b) and thermo-erosional gully (c) at the Kara Sea coast, Yugorsky Peninsula, Russia (photos M.O.Leibman).

availability for vegetation, and thus plant distribution and assemblages. The gullies indicate a likely change in the sedimentary balance of the river system downstream (Godin and Fortier, 2012). Kokelj and Jorgenson (2013) suggested that thermal erosion is accelerating in response to recent atmospheric warming, although site-specific terrain conditions and feedbacks associated with hydrological and ecological processes are contributing to high variability in this process.

4.4.3 Coastal retreat

Coastal erosion includes two main mechanisms: thermal abrasion (this term is mostly used in Russia and is equivalent to coastal and lakeshore thermal erosion) and thermal denudation (Shur et al., 2002; Are, 2012; Günther et al., 2013). In recent years the concept of coastal retreat in the Arctic has developed, with its complex positive and negative feedbacks. The impact of global warming on coastal retreat processes is associated with declining sea-ice cover and increasing seawater temperature (Grigoriev et al., 2006; Vasiliev et al., 2011; Are, 2012).

While the average rate of coastal erosion for the entire Arctic coast is about 0.5 m/y, at many coastal segments the rates are much higher and vary with time (Lantuit et al., 2012, 2013). Long-term monitoring of coastal dynamics in western Yamal near Marre-Sale Polar station during 1979–2010 indicated a long-term average rate of coastal retreat of ~1.7 m/y, with a maximum of 3.3 m/y (Vasiliev et al., 2011).

During 2008–2012, there was an increase in the rate of retreat for the Alaskan coast and coasts of Russia (Lantuit et al., 2013). The north coast of Elson Lagoon on the Beaufort Sea saw an average retreat of 1–4 m/y in the period 2003–2011 (Tweedie et al., 2012). This is lower than the rate observed

in other areas of the Beaufort Sea because the coastal bluff is protected by barrier islands. Jones et al. (2009) found that for a 60-km segment of the Alaskan Beaufort Sea coast, characterized by 2–5 m high bluffs with extremely ice-rich sediments, mean annual erosion reached rates of 6.8 m/y (1955–1979), 8.7 m/y (1979–2002), and 13.6 m/y (2002–2007). Coasts of the Chukchi Sea indicated maximum retreat rates of 2–4 m/y and up to 6 m/y in the period 1930–1950 (Grigoriev et al., 2006).

While thermal abrasion depends on wave action in addition to water temperature (Figure 4.20a), an increase in summer air temperature alone affects the destruction of coasts through thermal denudation (Figure 4.20b), which determines the rate of ice-rich permafrost thaw in the coastal bluffs (Kizyakov et al., 2003, 2013; Are, 2012). In recent years, the western sector of the Russian Arctic has seen an increase in the rate of thermal denudation of coastal bluffs, which has resulted in an increase in the number and size of thermocirques (horseshoe-shaped depressions) associated with the melting of massive ground ice. Monitoring of the Kara Sea coasts showed that the highest rates of coastal retreat occurred during 2007–2010 due to thermal denudation. Thermocirque expansion occurs at an average rate of 13 m/y on Yugorsky Peninsula (Khomutov and Leibman, 2008) and up to 8 m/y at Cape Sopochnaya Karga in Yenisey Bay (Gusev, 2011).

Field monitoring and remote sensing data for the Barents Sea (Kolguev Island) showed a thermocirque growth rate of up to 14.5–15.1 m/y, with an average rate of ~2.6 m/y in 2009–2012. During the same period, there was an increase in the thermal abrasion rate compared to the period 2002–2009, from 0.8 m/y to 2 m/y (Kizyakov et al., 2013). Such high rates are explained by a longer ice-free period in the Barents Sea compared to the Kara and Laptev Seas.



Figure 4.21 Solifluction lobes, northern Yamal, Russia (a) (photo from helicopter, M.O. Leibman), active-layer detachments, central Yamal, Russia (b) (photo from helicopter, M.O. Leibman), retrogressive thaw slump, central Yamal, Russia (c) (photo A.A.Gubarkov).

Lower rates of coastal retreat observed in the Laptev Sea (0.5–5.4 m/y for thermal abrasion and up to 5.9 m/y for thermal denudation) (Pizhankova and Dobrynina, 2010; Pizhankova, 2011) are explained by a large volume of sediment and local topographic features, which restrict the development of waves (Lantuit et al., 2011). Long-term average rates of coastal erosion were estimated at 0.7 m/y for the entire Laptev Sea coast and 1.0 m/y for the East-Siberian Sea (Grigoriev, 2008). Average thermal abrasion and thermal denudation rates of 0.6 m/y and rates of up to 1 m/y were observed for the period 1951–2006 on the coasts of Muostakh Island and Bykovskii Peninsula (Lantuit et al., 2011; Günther et al., 2015). The average rate of thermal denudation in the period 2010–2013 was 3.1 m/y.

A significant role in coastal retreat can also be attributed to gully erosion in the coastal zone related to an increased accumulation of snow providing high moisture supply. One day of snowmelt in 2007 (a year of high snowfall) resulted in a retreat rate an order of magnitude higher than in 2005 and 2006 (Gubarkov et al., 2008) (Figure 4.20c).

4.4.4 Permafrost-related slope processes

Thermal denudation (i.e. slope processes or mass wasting) refers to downslope movements of soil or rock on or near the earth's surface under the influence of gravity. Mass wasting includes slow displacements such as frost creep and solifluction (Figure 4.21a), and more rapid movements such as landslides, earthflows and active-layer failures (Kaplina, 1965; van Everdingen, 1998; French, 2007). This section mainly addresses rapid movements that readily occur as a result of rapid climate change or localized disturbances to the ground thermal regime. Permafrost-related landslides are best understood and subdivided into two main types: retrogressive thaw slumps (earth/mud flows) and translational landslides (active-layer detachments) (Figure 4.21b and c). The first type results from the thawing of massive ground ice within permafrost layers, while the second is triggered by the thawing of ice lenses in the active-layer base (Leibman et al., 2014a).

These thaw-related features are mainly observed in the continuous permafrost zone today, where massive ground ice actively accumulated in the permafrost history and never thawed. Alaska (Balser et al., 2014; Brooker et al., 2014; Pizano et al., 2014), northern Canada (Lewkowicz, 2007; Lantz and Kokelj, 2008; Lacelle et al., 2010; Short et al., 2011; Lantuit et al., 2012; Sloan and Pollard, 2012; Kokelj et al., 2013; Brooker et al., 2014) and central Yamal (Leibman and Kizyakov, 2007; Leibman et al.,

2014a) are the primary regions of landslide occurrence in the Arctic. However, large thaw slumps also occur in regions with ice-rich syngenetic yedoma deposits such as central (Sejourne et al., 2015) and northern Yakutia (Kunitsky et al., 2013). Landslide impacts on the environment and infrastructure are well described (Khomutov, 2012; Yermokhina and Myalo, 2012; Gubarkov et al., 2014; Ukrantseva et al., 2014).

The activation of landslides is controlled by increasing atmospheric precipitation and by changes in summer air temperature. The future occurrence of active-layer detachments will probably shift northward, where conditions for ice formation at the active-layer base are still preserved. The northern limits of the occurrence of retrogressive thaw slumps is probably also shifting northward due to active-layer thickening towards the deep-seated massive ice bodies (Leibman et al., 2014a).

Radiocarbon dating has been used to date ancient landslides (Lantuit et al., 2012; Leibman et al., 2014a) while tree ring dating has been used to date more recent features (Pizano et al., 2014). Previous cycles of activation of retrogressive thaw slumps over a period of 300 to 350 years have been documented on Herschel Island and the Yukon coast (Canada) (Lantuit et al., 2012). Activation of the same features on Yugorsky Peninsula (Russia) was calculated from the rhythms of landslide fan accumulation, in the range of 140 to 770 years, with an average of 455 years (Leibman and Kizyakov, 2007). Taking into account the inaccuracy of the method, it can be assumed that these cycles are of a global nature. Atmospheric warming may cause more frequent activation cycles (Lantuit et al., 2012).

As for active-layer detachments on the central Yamal Peninsula, Russia, the time span separating landslide events as determined by radiocarbon dating ranges from 350 to 500 years (Leibman et al., 2014a). On the Fosheim Peninsula landslide recurrence intervals are much shorter. Within small areas of key-sites at least four different episodes of detachment failure activity have occurred within the last 100 years (Lewkowicz and Harris, 2005). In the northern boreal forest active-layer detachments could be triggered by forest fire. In Mackenzie Valley, fire cycles of 100 to 200 years control landslide activity (Lewkowicz and Harris, 2005).

Slope processes essentially change environmental patterns over vast areas (Abbott et al., 2012; Flinn et al., 2012; Ukrantseva et al., 2012). Redistribution of chemical elements after a landslide event causes changes in the vegetative mosaic in a specific succession (Sloan and Pollard, 2012; Yermokhina and Myalo, 2012). Vegetation is an indicator of the relative age of landslides (Cannone et al., 2010). The azonic high-willow plant community of the Yamal Peninsula, which is characterized



Figure 4.22 Modern frost-heave mounds in central Yamal, Russia (a) (photo M.O. Leibman), old degrading frost heave mound on the Tazovsky Peninsula, Russia (b) (photo O.E. Ponomareva), and a collapsed pingo on the Tazovsky Peninsula, Russia (c) (photo A.I. Kizyakov).

by an abundance of saline deposits is an indicator of ancient landslide activity, and areas of its distribution can be used as a basis for mapping landslides on aerial and satellite images (Ukrainseva et al., 2014).

Permafrost-related slope processes and related environmental patterns are thus highly sensitive to climate change. Knowledge of their distribution and evolution in the landscape is required to assess the potential environmental impacts of these processes.

4.4.5 Frost heave

Frost heave is the upward or outward movement of the ground caused by the formation of ice in the soil by the freezing of both pore water and water migrating to the freezing front, where ice lenses form (van Everdingen, 1998). Perennial frost heave is triggered by permafrost aggradation. Frost heave results in different landforms and causes changes in the landscape. The uplift and drainage associated with frost heave lead to changes in plant assemblages and carbon accumulation in peat deposits due to more intensive aerobic degradation (Routh et al., 2014). In the continuous permafrost zone, frost heave occurs mainly in recently drained lake basins and abandoned fluvial channels. Development of peatlands in the southern limits of the permafrost zone is the main cause of permafrost formation in this region, and so frost heave is an important cryogenic process. Warm summers are favorable for peat accumulation and its action as a thermal insulator. New permafrost may form within peatlands if winters are cold enough (Chizhova et al., 2012; Vasilchuk, 2013) (Figure 4.22a).

Studies in the northern taiga of western Siberia showed that perennial frost heave is ongoing within the peat plateaus and in existing mineral frost-heave mounds, specifically in years with low-snow winters, despite atmospheric warming having been observed there since the 1970s. As a result, all the frost heave mounds and peatlands in the northern taiga of western Siberia have existed in an unstable balance (Figure 4.22b). Active growth of new hillocks and small ridges by frost heave

in the marginal parts of bogs has been reported over this same period (Berdnikov, 2012; Ponomareva et al., 2012).

Frost heave is also involved in pingo formation. Most pingos (82%) are linked to the tundra zone and occupy drained lake basins (Grosse and Jones, 2011; Jones et al., 2012a). The highest number of pingos is found in the western Canadian Arctic. Some pingos collapse through thermokarst, slope failures, sea thermal abrasion (in the coastal zone), erosion or wind action (Mackay and Burn, 2011) (Figure 4.22c). A new permafrost-related process was recently discovered in central Yamal, Russia. A gas-emission crater was reported in summer 2014. This crater was surrounded by a parapet approximately 30 m in diameter at the time of its discovery. Water accumulated at the bottom of the hole. The crater formed in late autumn 2013 (Figure 4.23). The high concentration of methane in the hole measured soon after its discovery indicates the role of methane in its formation. It is highly probable that such landforms will be generated in the future under suitable geological and permafrost conditions. The origin of this crater is still unknown, but some scientists have attributed it to the anomalously warm summer of 2012, specifically the increased ground temperature and amount of unfrozen water in the permafrost, expanding cryopegs (saline water lenses within permafrost) and the formation of a pingo-like mound and its outburst due to high pressure resulting from gas hydrate decomposition within the permafrost (Leibman et al., 2014b). Similar temperature anomalies may increase in number in future decades, presenting risks for human activities in the region (Leibman et al., 2014b; Kizyakov et al., 2015).

More than 10,000 pingos have been mapped on Earth (Grosse and Jones, 2011). However, regional mapping of pingos is typically based on interpretation of imagery showing features in a periglacial landscape context similar to that observed recently on the Yamal Peninsula prior to the formation of the crater. Discovery of the mysterious Siberian landform (Leibman et al., 2014b) may indicate a previously overlooked process for a commonly mapped permafrost landform and a potentially rapid pathway for release of long-stored methane in permafrost regions.

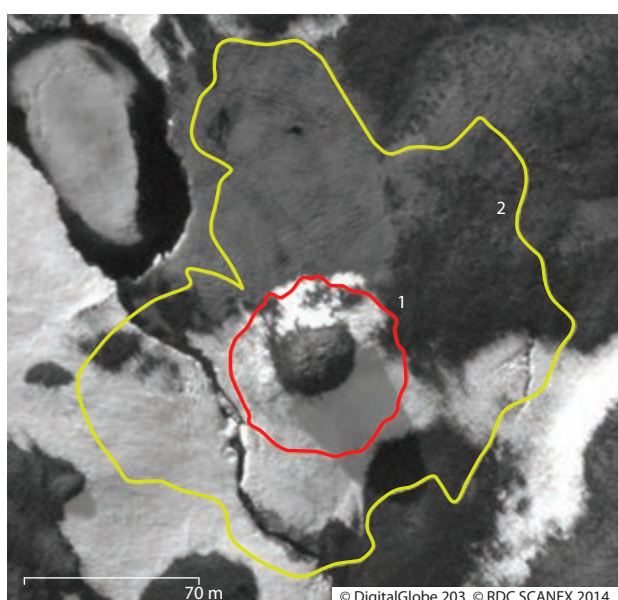
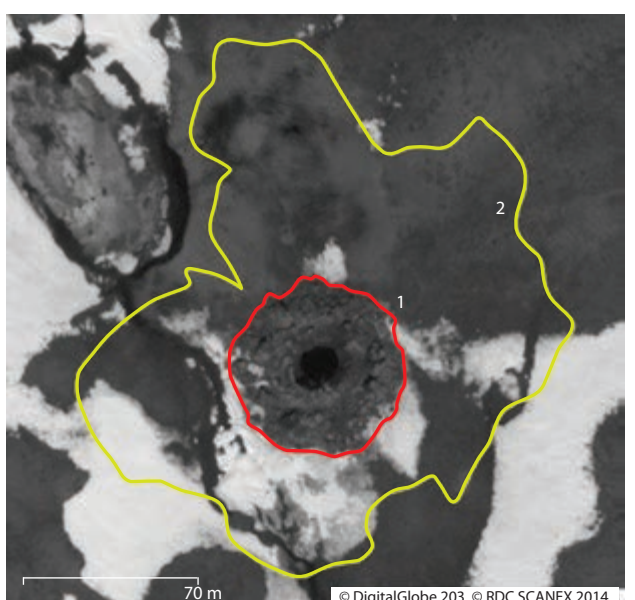


Figure 4.23 High-resolution black and white DigitalGlobe™ satellite imagery (WorldView-1) showing the presence of an 8-m high pingo-like mound on 9 June 2013 (left) and the same location on 15 June 2014 revealing the recently discovered Siberian crater (right). The height of the mound prior to crater formation was estimated using shadow length and sun angle at the time the image was acquired. The red line shows the outline of the surrounding 'parapet'. The yellow line delimits the area where the chunks of soil ejected from the crater were found (Kizyakov et al., 2015).



4.4.6 Summary and recommendations

New field approaches allowing highly precise surface elevation measurements such as differential Global Positioning Systems (DGPS) and terrestrial laser scanners appear promising techniques for capturing surface subsidence or heave associated with ground ice loss and gain, respectively (e.g. Shiklomanov et al., 2013). In addition, modern remote sensing methods such as Interferometric Synthetic Aperture Radar (InSAR), Light Detection and Ranging (LiDAR) and Stereophotogrammetry relying on sub-meter resolution satellite images are now capable of detecting surface subsidence associated with thermokarst or frost heave after lake drainage (Liu et al., 2014a), regional subsidence or heave (Jones et al., 2013; Liu et al., 2014b), and thaw slump formation and coastline migration in permafrost regions (Short et al., 2011; Günther et al., 2013, 2015).

Many of the processes described in this section significantly affect permafrost dynamics. However, general ESMs do not provide the level of detail needed to include such processes. Representation of such processes in new intelligent ways will be important to fully capture future responses of permafrost dynamics in a warming Arctic. Many of the processes observed with field, geophysical, and remote sensing methods are therefore now being implemented in numerical local to regional models and in complex land surface models. For example, the physical and biogeochemical dynamics of thermokarst lake formation and drainage dynamics have been captured in a local-scale 3D model by Kessler et al. (2012). Lee et al. (2014) tested the implementation of excess ground ice content and dynamic changes under a rise in surface air temperature in a land surface scheme. Schneider von Deimling et al. (2014) analyzed the impact of deep permafrost carbon pools and deep thaw by thermokarst on biogeochemical feedbacks from thawing permafrost on climate. To better characterize the response and feedbacks of permafrost to climate change it will be critical to intensify efforts that use a combination of field studies, remote sensing analyses, and modeling approaches to fully describe and quantify periglacial processes and dynamics (Gogineni et al., 2014).

4.5 Effect of infrastructure and climate change on permafrost and permafrost-related hazards

Infrastructure development and climate change are interacting in complex ways to alter permafrost over large areas of the Arctic. Several factors show the need for coordinated interdisciplinary studies to examine infrastructure-related issues, including (1) the large-scale and differing nature of infrastructure and climate change impacts in different parts of the Arctic, (2) the complex, multidisciplinary and cumulative nature of the impacts on social and ecological systems and (3) the need for new methods to assess cumulative effects and promote sustainable methods of infrastructure expansion.

Permafrost thaw and its associated impacts on natural and built environments has been identified as a priority issue across all regions of the Arctic, but the specific issues involved differ by region. Communities, urban environments and infrastructure networks built on ice-rich soils can be significantly affected

by thawing permafrost. At the same time, permafrost thaw due to climate change and the construction and operation of infrastructure can affect natural landscapes and ecosystems in complex ways.

Over the past five years, the understanding of permafrost-related geohazards has focused on risk assessment and adaptation strategies. In addition, the World Climate Research Programme's (WCRP) Climate and the Cryosphere Project (CliC), the International Arctic Science Committee (IASC) and the Arctic Council's Arctic Monitoring and Assessment Programme (AMAP) have supported an internationally authored Arctic Freshwater Synthesis (AFS) report containing a resources component (Prowse et al., 2015). The AFS resources component focuses on the potential impact of future climate change and associated change in water resources in the Arctic, and on how Arctic infrastructure and natural resources are likely to be affected (Instanes et al., 2015). The study emphasizes the uncertainty associated with climate projections in general and with change in the magnitude and frequency of extreme events in particular. These uncertainties make it difficult to accurately assess the impact of current and projected climate change on anthropogenic systems. Other factors, such as human intervention with permafrost soils (for example construction activity and industrial development, and consequent local changes in vegetation and drainage patterns) may overshadow the effect of climate change. The development of rational and efficient infrastructure and transportation systems in the Arctic is costly and sensitive to changes in socio-economic effects often governed by national and international interests and policies. The potential for greater demand for natural resources in the future along with easier access to land areas due to declining sea ice in the Arctic Ocean and previously glaciated land areas becoming ice free, may result in more industrial and development activity in Arctic regions.

The engineering community has in recent years moved its focus from assessing the consequences of climate change on infrastructure and industrial development, to risk assessments and adaptation measures.

4.5.1 Risk assessments and adaptation

For the Arctic region, it is predicted that the general increase in mean hemispheric temperature will lead to increased high-latitude precipitation (ACIA, 2005; IPCC, 2013). Climate change may also alter the amount and type of precipitation, its seasonal distribution, and the timing and rate of snowmelt (Instanes et al., 2015). These changes represent challenges to municipalities and transportation networks in permafrost environments and to current industries and future industrial development.

Risk assessments, taking climate change scenarios into account are becoming more common in the circumpolar Arctic. Current understanding of geohazards such as landslides and avalanches, are updated with input from global climate models and regional climate models (NGI, 2013). However, the large uncertainty associated with these models makes it difficult to make accurate predictions. Projected changes in future incidents related to extreme precipitation events (IPCC, 2012) and consequent slide activity and flooding are especially uncertain. However, national assessments carried out in Canada and Norway seem to support a trend of increased

severity of climatic events (Furgal and Prowse, 2008; NGI, 2013; Warren and Lemmen, 2014). Canada and Norway have made efforts to incorporate risk assessments taking climate change scenarios into account, in new laws, regulations, codes and guidelines. Adaptation techniques vary from site-specific engineering methodology to preserve permafrost under warming scenarios (Lepage and Dore, 2010) using for example artificial cooling techniques such as thermosyphons (Canadian Standards Association, 2014a) and heat pumps (Rongved and Instanes, 2012), to relocation of infrastructure and communities (Tom and Bronen, 2012) and abandonment of industrial sites.

4.5.1.1 Canada

Climate change and its impact on permafrost is a major concern for Canada given that almost half the land mass is underlain by permafrost, and the integrity of many of its northern geosystems, ecosystems and engineered infrastructure is dependent upon the stability of these frozen lands.

In Canada, permafrost engineering research and development is currently focusing on improving climate change assessments and adaptation (e.g. Furgal and Prowse, 2008 and Warren and Lemmen, 2014). An important focus has been on the development of guidelines, standards and best practices related to infrastructure and resource development and climate change in permafrost regions. This includes a technical guideline for adapting infrastructure on permafrost to climate change (Canadian Standards Association, 2010) with a similar document for northern transportation (Transportation Association of Canada, 2010). In addition, new standards were developed for moderating the effect of permafrost degradation on existing building foundations (Canadian Standards Association, 2014b) and for thermosyphon foundations (Canadian Standards Association, 2014a). Emphasis has also been put on the effect of climate change and permafrost degradation on the resource development sector including the need for best practices (e.g. Pearce et al., 2011; IMG-Golder Corporation Environmental Consulting, 2012a,b).

Vulnerability assessments of existing and future infrastructure (e.g. Fortier et al., 2011; Seto et al., 2012; Calmels et al., 2015) which include application of new techniques including inSAR and geophysical surveys (Leblanc et al., 2012, 2015), as well as regional- and community-scale hazard assessments (e.g. Northern Climate Exchange 2013; Blais-Stevens et al., 2015) are informing adaptation planning. Research conducted at large-scale test facilities such as that on the Alaska Highway near Beaver Creek are supporting assessments of techniques to reduce permafrost thaw, such as air convection embankments and snow sheds (Lepage and Dore, 2010; Malenfant-Lepage et al., 2012a,b; Stephani et al., 2014).

Recent large-scale research projects in Canada address the processes and implications of permafrost thaw and degradation. ADAPT (Arctic Development and Adaptation to Permafrost in Transition) (www.cen.ulaval.ca/adapt) was formulated in response to the urgent need to understand how the structure and functioning of these northern systems are linked to permafrost behavior and climate change. In addition, the infrastructure and resources for northern settlements, from drinking water and exploited wildlife to runways, roads and housing, critically depend upon the state of the Arctic permafrost, and ADAPT

is also addressing many of these issues (Vincent et al., 2013). The Integrated Regional Impact Studies (IRIS) of the ArcticNet project summarizes and combines knowledge and models of relevant aspects of the ecosystems of a region affected by change, with the objective of producing a prognosis of the magnitude and socio-economic costs of the impacts of change (Yarnal, 1998). The ArcticNet IRIS approach aims to lay the groundwork for regional models for the Mackenzie Shelf region, the Canadian Arctic Archipelago, the North Water, the terrestrial Eastern Canadian Arctic from Ellesmere Island to James Bay, and for Hudson Bay as a whole. These regional climate change impact assessments will ultimately provide the spatio-temporal resolution necessary to downscale knowledge of the impacts of change to the level of the community.

4.5.1.2 Norway

In Norway, the focus has been on the effect of extreme events and geohazards on the transportation infrastructure and communities in areas subject to natural hazards. The Norwegian Public Roads Administration concluded a six-year research and development program in 2013, addressing the effect of climate change on the transportation network (Norwegian Public Roads Administration, 2013). The program presents recommendations for remedial action related to planning, design, construction and maintenance of roads. Landslides are a major challenge for the Norwegian road network, and around 2000 landslides interfere with roads each year. New guidelines have been developed for rock fall, snow avalanches, slush avalanches and debris flows. A first version of a risk model related to landslides and avalanches has been developed (NGI, 2013).

The impacts of extreme weather events on infrastructure in Norway have been studied through a four-year research project funded by the Norwegian Research Council, also finalized in 2013 (NGI, 2013). This project focused on predicted changes in extreme weather events and impact assessments on infrastructure in Norway. The main features are to better understand the links between climate change and the frequency, intensity and distribution of extreme weather events and to establish a knowledge base of the effect of extreme weather events on transport infrastructure (NGI, 2013). It is believed that the approach and methodology that has been developed related to extreme events and landslides in the two recent research projects in Norway, can be applied to several areas in the Arctic region.

4.5.1.3 Russia

The presence and dynamic nature of ice-rich permafrost constitutes a distinctive engineering environment. Changes in permafrost can lead to loss of soil-bearing strength, increased soil permeability, and increased potential for cryogenic processes such as differential thaw settlement and heave, destructive mass movements, and development of thermokarst terrain. Streletskiy et al. (2012 a,c) provide methodology for geographic assessments of changes in the engineering properties of frozen ground due to observed climatic change. Their analysis is based on Russian methodology utilizing the bearing capacity of a 'standard foundation pile' imbedded in permafrost as a primary variable for engineering assessment of permafrost-affected territory. The bearing capacity of a single post or pile depends on contact with the permafrost

Table 4.3 Decadal changes in the bearing capacity of foundations in Russian permafrost regions due to observed climate change.

Region	Settlement	Bearing capacity of foundations, %				
		1960s	1970s	1980s	1990s	2000s
Western Siberia	Salekhard	100	91–103	72–86	81–82	68–70
	Nadym	100	96–101	77–91	78–100	64–95
	Noviy Urengoy	NA	NA	100	97–116	91–96
	Noviy Port	100	105–114	86–93	87–92	63–76
Central Siberia	Norilsk	100	102–105	88–93	84–92	85–94
	Dudinka	100	103–110	93–94	90–94	74–82
Eastern Siberia	Yakutsk	100	91–98	80–92	59–84	54–80
	Bilibino	NA	100	90–98	97–100	80–91
	Tiksi	100	99–100	96–98	95–97	93–96
	Anadyr	100	101–104	92–100	75–94	52–84
	Chersky	100	100–101	97–98	96	76–84

as well as ground temperature and active-layer thickness. Warming of permafrost and deepening of the active layer can therefore decrease the ability of foundations to support structures to an extent that may not have been anticipated at the time of construction. Historically, engineering standards and designs use climatic 'normals' (long-term mean values) such as the decadal climatic averages recommended under Soviet construction regulations (CNR, 1990). Climatic variability and change are accounted for in engineering procedures through a series of 'safety factors'. While safety coefficients in North America range from 2.5 to 3, in Soviet Russia they rarely exceeded 1.56, making many foundations in Russia especially vulnerable to climate change (Shur and Goering, 2009). The rapid change in climatic conditions can thus affect the stability of structures whose design is based on climatic normals from past decades and relatively low safety coefficients.

Streletskei et al. (2012b) and Shiklomanov and Streletskei (2013) analyzed some of the largest settlements on permafrost representing various regions of the Russian Arctic to determine the relative change in bearing capacity of a standard pile

resulting from climate-induced changes in permafrost. Using the average bearing capacity for the 1960s to 1970 as a reference point and air temperature records from weather stations and information on soil conditions, the average bearing capacity for specific periods between 1960 and 2010 was determined for various regions of Russia (Table 4.3).

The climatic variables (air temperature, precipitation, snow depth) were provided by an ensemble of six CMIP5 GCM models, which most closely reproduce the historical air temperature record for the Russian Arctic (Anisimov and Kokorev, 2013). The hindcast GCM runs were used for climate forcing prior to 2005 with the RCP8.5 (business-as-usual) scenario used for projected future climate. Three periods were used to evaluate climate-induced changes in bearing capacity: decadal differences from 1970 to 2000, 1970 to 2020, and 1970 to 2050. These periods represent conditions faced by infrastructure built during the Soviet construction boom of the 1960s and 1970s. The period 2090 was not used because most infrastructure projects have lifespans of 30 to 100 years (30–50 years for buildings and 75–100 years for bridges and tunnels) (Anisimov et al., 2010). Figure 4.24 shows the change in

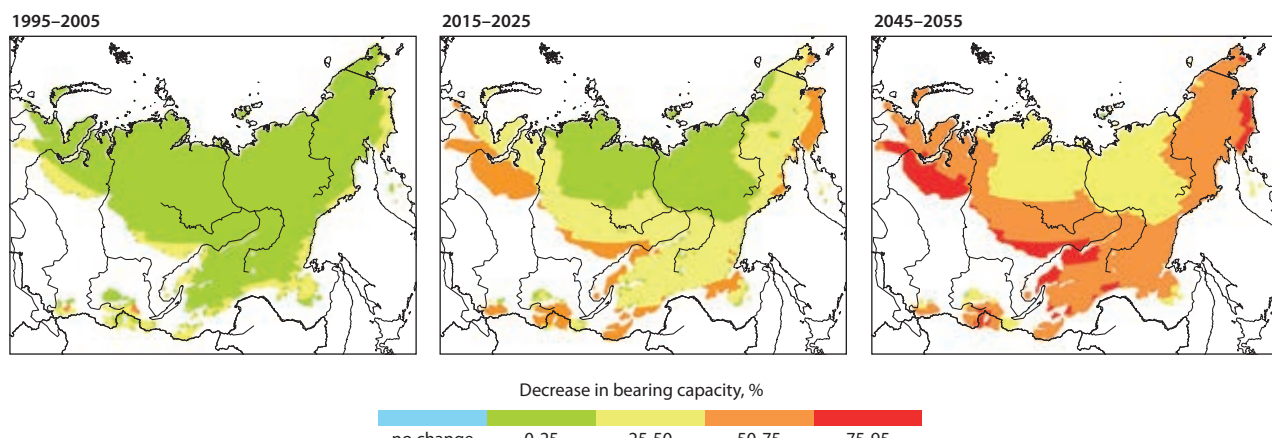


Figure 4.24 Mean changes in bearing capacity of the frozen ground in the Russian permafrost region. Changes are expressed in percentages relative to the 1965–1975 reference period for the periods 1995–2005, 2015–2025 and 2045–2055. Climate forcing is based on an average of results from the six CMIP5 GCM models that most closely reproduce the historical air temperature record for the Russian Arctic (Anisimov and Kokorev, 2013).

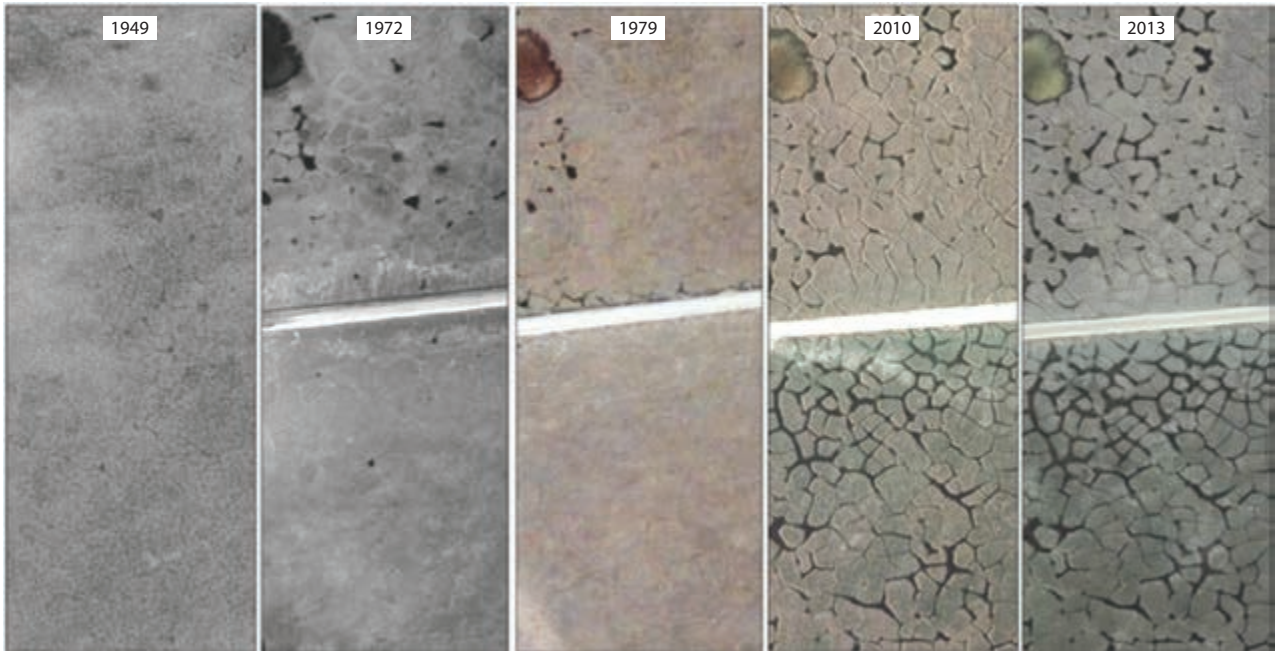


Figure 4.25 Progression of thermokarst from 1949 to 2013 along a section of the Prudhoe Bay Spine Road. The Spine Road was constructed in 1969 so it does not appear on the 1949 image. Thin cloud cover obscures the small lake in the upper left corner of the photo, but most of the thermokarst pits that were present in 1972 are also visible on the 1949 image. In 1972, gravel from road construction occurs on both sides of the road. In 1979, some roadside thermokarst is visible near the road on the north side (above the road in the photo). By 2010, extensive thermokarst is present on both sides of the road, but is most developed south of the road due to periodic flooding from a nearby lake. By 2013, most thermokarst on the south side of the road was connected to Lake Colleen by continuous channels of water in the polygon troughs (Walker et al., 2014).

bearing capacity relative to the 1970 reference period for three periods. The analysis indicates a significant reduction in the ability of the frozen ground to support structures throughout the Russian permafrost regions with the strongest reductions expected at the southern fringes of the permafrost.

4.5.1.4 Social-ecological effects of oil and gas infrastructure

Roads and pipelines associated with oil and gas development have major effects on the adjacent ecosystems and the use of these resources by indigenous peoples. A recent IASC white paper examined two case studies: one from the Prudhoe Bay oilfield in Alaska and one from the Bovanenkovo gas field on the Yamal Peninsula of Russia. These are two of the oldest and largest areas of hydrocarbon development in the Arctic. Differences in the geo-ecological conditions, history of infrastructure expansion, changes in climate patterns, and social-ecological conditions have resulted in different development pathways and consequences for the local landscapes and people (Walker et al., 1987; Walker and Pierce, 2015).

In the Prudhoe Bay oilfield, road networks and infrastructure have caused major changes in the landscapes and ecosystems of this flat thaw-lake region (Walker et al., 1987; Romanovsky et al., 2012; Kanevskiy et al., 2013; Raynolds et al., 2014). Road dust, roadside flooding, changes in snow-melt patterns, and thermokarst are the greatest effects. Thermokarst in the form of ice-wedge degradation (Liljedahl et al., 2016) is occurring along ice-wedges adjacent to roads as well as in areas some distance from roads (Figure 4.25 and Box 4.1). Between 1990 and 2001, coincident with strong atmospheric warming during the 1990s, natural thermokarst resulted in the conversion of low-centered ice-wedge polygons to high-centered polygons, more

active lakeshore erosion and increased landscape and habitat heterogeneity. Earlier snow melt, warmer soils, and extensive new wetlands near roads affect the phenology of vegetation and the use of roadside areas by wildlife. There is a new zone of reduced moss and lichen cover and noticeably high cover of taller, erect dwarf willows (*Salix lanata*) in many roadside areas. The changes in microtopography are of great consequence for roads and infrastructure (see also Section 4.4.1). Large areas adjacent to roads and in open tundra far from infrastructure, which were previously covered by homogeneous networks of wet, low-centered polygons with trough-rim relief of <0.5 m, have been converted to more heterogeneous, high-centered-polygon landscapes with relief of >0.5 m. These more heterogeneous landscapes have deep ponds, extensive channels of water in the polygon troughs, and well-drained polygon centers. The full implications of these ecosystem transitions have not been fully studied, but there are several key questions. (1) What is the effect of landscape fragmentation by roads and pads and the changes in ecosystem properties caused by thermokarst on the diversity and distribution of tundra organisms including plants, invertebrates, small mammals, shorebirds, waterfowl, fish, caribou, and predators? (2) Is it possible to develop models that better link hydrological processes to ice-wedge melting, to better predict pathways of thermokarst and erosion processes in networks of ice-wedge polygons? (3) How do the warmer soils associated with most forms of infrastructure affect a suite of key ecosystem processes, such as plant water uptake, plant productivity, decomposition rates, and trace-gas fluxes? (4) How do heavy dust loads from the roads affect mosses, lichens, biological soil crusts, and the diversity of soil microorganisms that help stabilize and insulate the permafrost?

The permafrost conditions at Prudhoe Bay contrast with those in the Bovanenkovo gas field, where highly erodible sands

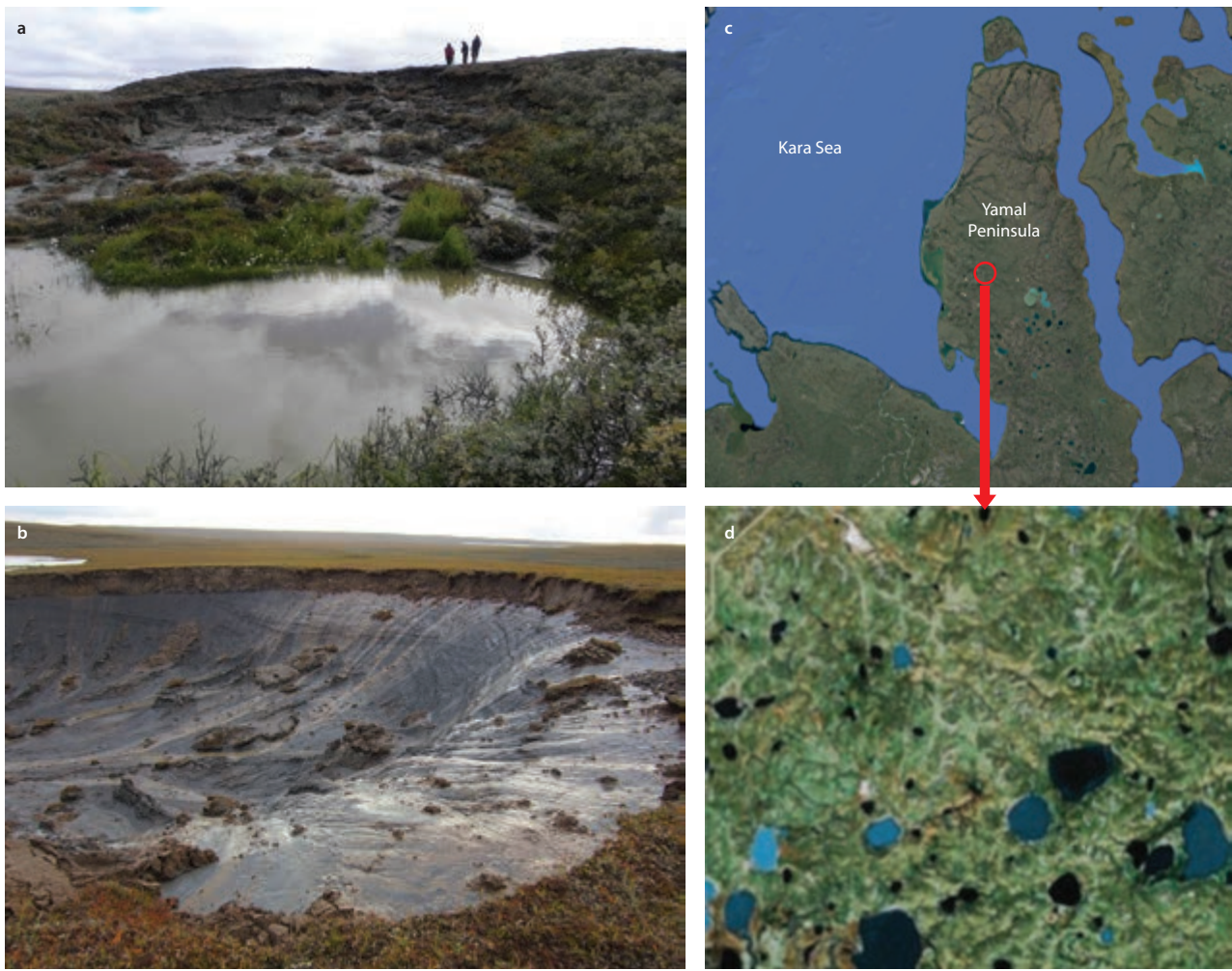


Figure 4.26 Landslides of the central Yamal Peninsula. (a and b) Examples of typical cryogenic landslides and thermocirques of the central Yamal Peninsula. (c) Yamal Peninsula and the location of the key site of landslide research at Vaskiny Dachi (Photos: Marina Leibman and Yuri Dvornikov). (d) Satellite image of highly dissected landscapes caused by cryogenic landslides that are typical of this region. (Images c and d: Google Earth, Digital Globe).

and the presence of massive tabular ground ice near the surface contribute to landslides and thermo-denudation of slopes (Figure 4.26). A large set of cryogenic landslides occurred in the Bovanenkovo region of the central Yamal Peninsula in the late 1980s. Both natural and anthropogenic changes have occurred in this region over the past 40 years. These range from physical obstructions such as roads, railways, and pipelines, to direct and indirect ecological impacts such as changes in vegetation, hydrology and wildlife habitat (Forbes et al., 2009; Khomutov and Leibman, 2010; Kumpula et al., 2011, 2012; Khomutov et al. 2012; Leibman et al., 2015). Expanding networks of petroleum infrastructure on the Yamal Peninsula combined with increasing shrubification, permafrost thaw, rain-on-snow events, and their relationship to the traditional reindeer-herding way of life of the Nenets pose complex questions without immediate answers, including how can development co-exist with reindeer herding in such a manner that traditional herding practices can continue? The sheer scale of the proposed hydrocarbon developments of the next few decades could overwhelm the ability of local communities to adapt to the changing conditions. Future mega-expansion of infrastructure in many areas of the Arctic combined with climate-induced changes in local landscapes and permafrost, present unprecedented challenges

for local communities. Successful adaptations will require the full engagement of local people and governments with industry and governing agencies.

4.5.2 The RATIC initiative

The RATIC (Rapid Arctic Transitions due to Infrastructure and Climate) initiative sponsored by IASC is a forum for developing and sharing new ideas and methods to facilitate the best practices for assessing, responding to, and adaptively managing the cumulative effects of Arctic infrastructure and climate change. These issues were addressed at two recent RATIC workshops (Walker and Peirce, 2015). The report summarizing the workshop results clearly identified permafrost thawing and its associated impacts on natural and built environments as priority issues across all regions of the Arctic, but that specific issues related to permafrost differed in each region studied. In communities and urban environments, changes in the thermal regimes of soils supporting houses, roads, airports, and large buildings have large economic and social consequences. Ecological changes caused by thermokarst and other permafrost-related geomorphic processes are exacerbated by the soil-warming effects of infrastructure and are affecting the structure of landscapes,

Box 4.1 The 2015 aufeis and flooding of the Dalton Highway, Alaska: A perfect storm of infrastructure and climate factors with major economic impacts

The Dalton Highway runs for 668 km between Fairbanks, Alaska, and the Prudhoe Bay oilfield near the Arctic Ocean. The road is the only land link to Alaska's 24 producing North Slope oilfields. The Trans-Alaska Pipeline System (TAPS) (Figure 4.27) is parallel to the road over most of this distance. Starting in mid-March 2015 and continuing through early June 2015, unprecedented aufeis formation and floodwaters up to 75 cm deep inundated the highway between mileposts 390 (km 628) and 414 (km 666) (Figure 4.28). Aufeis is a sheetlike mass of layered ice formed on the ground surface, or on river or lake ice, by freezing of successive flows of water that may seep from the ground, flow from a spring or emerge from below river or lake ice through fractures (van Everdingen, 2005). The source of the flood was the braided Sagavanirktok River (also called the Sag River), which is parallel to the road and where much of the TAPS pipeline is buried in the Sag River floodplain. The northernmost 130 km of the road were closed for extended periods in April and May, forcing Alaska's Governor to declare a disaster emergency twice in spring 2015 (7 April and 22 May).

The event was reported by the state, national and international media (DeMarban, 2015). The magnitude of the event was not, however, conveyed to most readers because of the remoteness of road and no large city or village was directly affected. Most of the direct infrastructure effects occurred to the road and several camps along the Dalton Highway near the Deadhorse Airport (Figures 4.28, 4.29 and 4.30). The Arctic oilfields were strongly affected because they were only accessible by air during the flooding, causing major human and economic

impacts especially to the trucking industry (Nordrum, 2015).

Not noted in any of the media coverage were the major impacts on the permafrost and landscape adjacent to the road. The flood itself caused most impacts but responses to the flood had additional impacts, such as the widening and raising of the roadbed which requires new gravel mines in the river floodplain and adjacent tundra. The immediate cost of road repair was estimated at over USD27 million, with an additional USD40–50 million needed to elevate the road to help prevent a reoccurrence of the flooding in future. Larger long-term impacts could occur if this event is a harbinger of future changes along the Dalton corridor related to a warming Arctic climate, and changes in local hydrology and permafrost.

The causes of the flood are currently not known with certainty, but the event appears to have been a 'perfect storm' of several factors. (1) The autumn season in 2014 was the wettest on record and could have contributed to the large volume of overflow ice (Figure 4.27). (2) Unusual patterns of aufeis and overflow developed in and upstream of the Sag River delta (Figures 4.27 and 4.28). (3) An early initial breakup of the Sagavanirktok River ice in April 2015 initiated the unusual aufeis buildup (or see point 4). (4) Tracks left by a large 3-D seismic geophysical operation in the Sagavanirktok River delta are coincident with and may have had a role in developing the area of most serious and unusual aufeis (Figure 4.28). (5) Thermal infrared imagery of the North Slope in mid-April shows an unusually large amount of overflow water also occurred in the vicinity of Franklin Bluffs, about 35 miles south of Deadhorse. The thawing was apparently in response to a

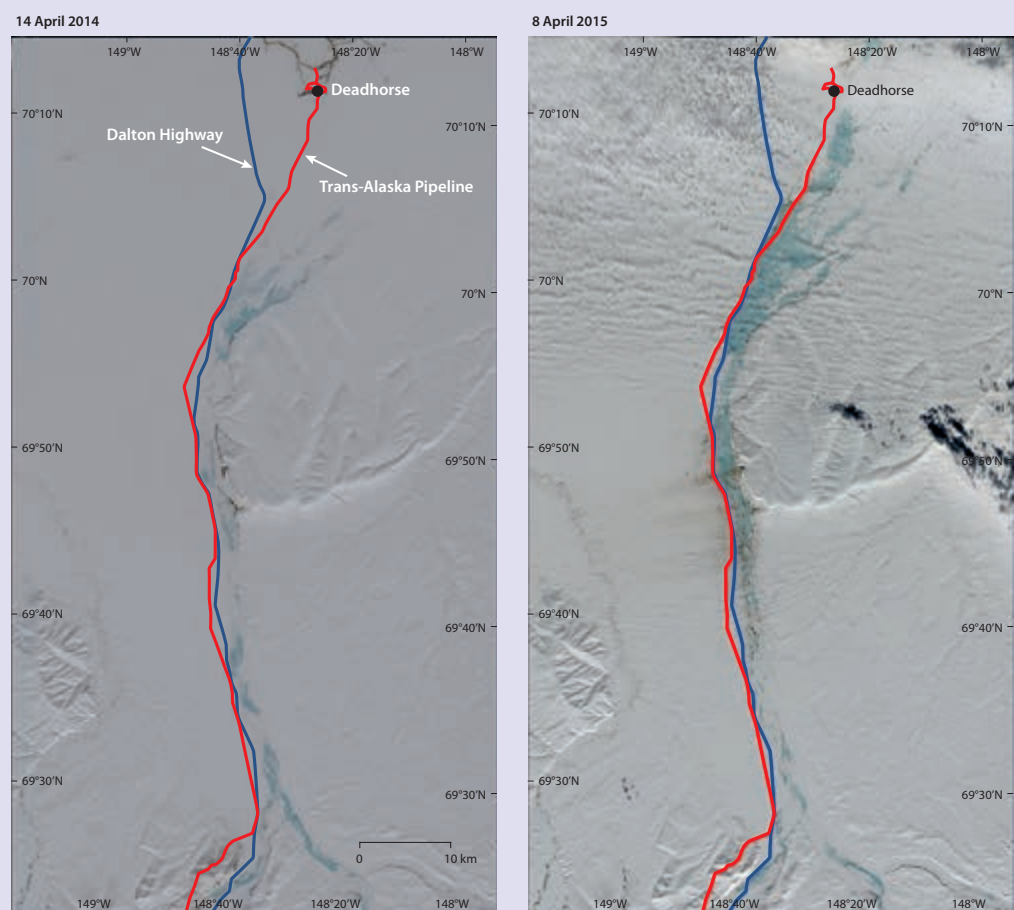


Figure 4.27 Comparison of overflow waters along the coastal plain portion of the Sagavanirktok River in April of a 'normal' year (2014) and during the flood year of 2015. Note the large amount of overflow in the vicinity of Franklin Bluffs in 2015, and in the Sagavanirktok River delta south of Deadhorse adjacent to the Dalton Highway. Images in both years are from Landsat-8. Maps by Lisa Wirth, Geographic Information Network of Alaska, UAF.



Figure 4.28 Area of major washout during the height of the flood on 19 May 2015 (photo: KTUU News).

strong warming wind that was flowing off the bluffs and the area affected stretched from the Sagavanirktok River to the Kuparuk River. (6) A new channel of the river appears to be forming to the west of the existing main channel and contributed to water overflowing over the road toward the west and creating washouts in the road. (7) The nature of sedimentary deposits in the ice-rich permafrost led to very rapid erosion of massive ground ice (Figure 4.30). (8) Inadequate culverts and a road not designed to handle the large amount of auefis and floodwaters. A large area of thermokarst collapse occurred along the Sagavanirktok River south of the Deadhorse Airport (Figure 4.31). As reconstruction proceeds, new gravel mines and gravel placement is destroying much of the historical evidence of the flood event.



Figure 4.29 Deadhorse vicinity at the northern end of the Dalton Highway during peak flood conditions on 19 May 2015. Looking north with the Deadhorse airstrip on the left (photo: KTUU News).



Figure 4.30 Area of thermokarst collapse near Deadhorse Airport as the flood water recedes (upper) and after thermokarst collapse and the start of reconstruction on 11 June 2015 (lower). Courtesy of AKDOT and PF.



Figure 4.31 Large area of massive thermokarst collapse along the Sagavanirktok River, just south of Deadhorse Camp. Looking north (upper). Looking south (lower). Collapse occurred over about 0.5 km along the river and within 20–30 m of the river (photos: D.A. Walker).

hydrological patterns, snow distribution, ecosystems, and land use by northern residents and industry. These cumulative permafrost changes come at a time of intense demographic and socio-economic development in the Arctic. Indirect effects of infrastructure can exceed the direct effects of the planned disturbances, and the evaluation and prediction of the effects of infrastructure and climate must extend beyond the immediate area of the facilities. Environmental impact assessments (EIAs) should therefore include the cumulative impacts of climate change and infrastructure on the adjacent ecosystems. New tools are also needed to monitor infrastructure and landscape changes and to develop sustainable approaches for future development. Of particular relevance to permafrost will be the application of advanced GIS and remote sensing tools for studying change over large areas, including the detection of change in permafrost-related landforms such as landslides, and thermokarst. New scenario modelling approaches integrating landscapes and ecosystems are also required.

4.5.3 Outlook

Several steps are needed to develop scientific research plans aimed at sustainable infrastructure development. The scope of the challenge includes: (1) examining the drivers of Arctic infrastructure in different Arctic cultures, economic systems, political environments, and ecological systems; (2) monitoring and understanding the vulnerabilities, resilience and full cumulative effects of Arctic infrastructure on the diverse group of Arctic social-ecological systems that are currently undergoing change; and (3) planning, managing, and shaping future Arctic infrastructure. Future planning needs to include consideration of the widely divergent political systems, economies, cultures, communities and landscapes present in the Arctic.

The recent RATIC white paper prepared by the IASC Terrestrial, Cryosphere, and Social and Human working groups, made the following recommendation: *Emerging science plans "...need to explicitly address rapidly expanding infrastructure networks. Recent studies indicate that combinations of industrial development and climate change have resulted in major changes to local ecosystems, including the permafrost, hydrology, vegetation, wildlife, and local people. The effects are both positive and negative with respect to biological resources and the local communities and economies. The effects of resource development and fragmentation of large intact ecosystems by extensive networks of roads, railways, and pipelines are apparent and keenly felt by the indigenous people of the Arctic. The effects on broader regions are currently difficult to assess, but require more attention because of the cumulative effects beyond the areas of immediate impact. This topic is internationally important because mineral and hydrocarbon exploration have transnational effects that are broadly occurring across the circumpolar Arctic. The social, economic, regulatory, and political drivers of development vary across the Arctic. The national and international programs supporting research described in the RATIC case studies are examples that need to be built on for the next decade"* (Walker and Peirce, 2015).

4.6 Conclusions and knowledge gaps

4.6.1 Update of findings on permafrost

There is a growing awareness of the consequences of warming and thawing permafrost and its importance for the environment and society. This update on changing permafrost and its impacts provides a synthesis of current knowledge across the circumpolar permafrost regions with the emphasis on progress achieved since the publication of the SWIPA 2011 assessment (AMAP, 2011).

Since the International Polar Year (IPY) in 2007–2008, permafrost temperatures used to document long-term changes show new record high levels at many permafrost observatories across the Arctic. Since IPY the greatest annual mean temperature increases have occurred in the colder permafrost of the Arctic and High Arctic with more than 0.5°C at some sites. In warmer permafrost and in the discontinuous permafrost zone the temperature increase has been much less or not detectable. At some few locations (such as in the Alaskan Interior) annual mean permafrost temperature has even slightly decreased (typically by 0.1°C).

Decadal trends in active-layer thickness (ALT) vary by region. However, an increase in ALT has been observed over the past five years for most of the regions where long-term observations are available, and at several sites the peak ALT year is after IPY. During the past 30 years, the average date of freeze-up of the active layer in northern Alaska has become almost two months later. At some locations (such as in the European North of Russia) permafrost degradation has been observed.

Since SWIPA 2011, there have been many advances in the understanding of possible permafrost responses to the projected global warming. Substantial efforts have been made to evaluate large-scale models of permafrost dynamics across the circumpolar north, and there is now a better understanding of the range of uncertainty in projections associated with both the models themselves and with the projections of future climate change. Interactions between climate-driven thawing of permafrost and vegetation changes are complex but progress has also been made here. In addition, progress has been achieved in standalone permafrost modeling, and advances also include modelling the dynamics of sub-sea permafrost beneath the continental shelf of the Arctic Ocean.

There have been many advances in the understanding of permafrost-related processes, coastal erosion, thermokarst and recent changes in thaw lake development. Widespread surficial degradation of ice wedges has been observed in various permafrost regions of Eurasia and North America during the past two decades. A significant increase in areas of water-filled polygonal troughs was reported in northern Alaska and linked to climatic changes. However, no unified trends in thermokarst development associated with global warming have been observed across the Arctic to date. Changes in thermokarst lake development are related to both regional and local environmental and climatic factors, including the moisture balance. The gas-emission craters recently discovered in north-western Siberia still require scientific explanation, and understanding of the processes leading to their formation is urgently warranted. The importance of this phenomenon to carbon emission from permafrost also needs to be evaluated. Integration of thermokarst and thermo-erosion processes in

complex land surface models will be important to fully capture future responses of permafrost dynamics in a warming Arctic and related climatic feedbacks.

Studies of the cumulative effects of infrastructure and climate change on permafrost geographic assessments of changes in bearing capacity for some of the largest settlements on permafrost in the Russian Arctic indicate significant reduction of this parameter between 1970 and 2050, with the largest decrease in bearing capacity predicted for the southern fringes of the permafrost zone. The Prudhoe Bay oilfield in Alaska and Bovanenkovo gas field on the Yamal Peninsula of Russia have experienced recent changes in permafrost conditions due to a series of warm summers that triggered major increases in thermokarst in the former and thermocirques near the latter. The large-scale damage caused by the 2015 aufeis and flooding event along the Sagavanirktok River in northern Alaska emphasizes that many of the future changes in the Arctic are likely to be surprises that will require major funds for repair and adaptation to the changes.

4.6.2 Knowledge gaps, observational needs and future direction

It is important to continue collecting temperature measurements in various ecosystems in order to capture the natural spatial heterogeneity across the landscapes. This SWIPA update presents ground temperatures from a selection of permafrost monitoring sites with both long-term records and good geographic coverage within the AACIA priority regions: the Beaufort-Chukchi region, Baffin Davis Strait and the Barents area. To support modelling efforts in these regions, for example, more measurements are needed from the High Arctic regions of Russia, Canada and Greenland. The additional data could be assimilated into the existing permafrost models to further constrain uncertainties in the numerical projections.

New field approaches allowing highly precise surface elevation measurements such as differential Global Positioning Systems (DGPS) and terrestrial laser scanners appear promising for capturing surface subsidence or heave associated with ground ice loss and gain, respectively. In addition, modern remote sensing methods such as Interferometric Synthetic Aperture Radar (InSAR), Light Detection and Ranging (LiDAR) and stereophotogrammetry relying on sub-meter resolution satellite images are now capable of detecting surface subsidence associated with thermokarst or frost heave after lake drainage, and thaw slump formation and coastline migration in permafrost regions. Many of the processes significantly affect permafrost dynamics. However, general ESMs do not provide the level of detail to include such processes. Representation of these processes in new intelligent ways will be important to fully capture future responses of permafrost dynamics in a warming Arctic. Incorporating thermokarst and thermo-erosion processes in complex land surface models will be important to fully capture future responses of permafrost dynamics in a warming Arctic and related climatic feedbacks.

Uncertainties in future projections can be reduced by benchmarking the retrospective simulations of permafrost models and eliminating from uncertainty analyses those models that do not perform well with respect to key benchmarks. In addition, future model intercomparisons on permafrost dynamics should

investigate the full uncertainty by conducting simulations for multiple climate-forcing data sets (Peng et al., 2016). Remotely sensed microwave emissivity data related to land surface temperature could also be used to independently evaluate soil surface temperature in models at a large scale or be integrated in ground temperature models (e.g. Westermann et al., 2015b), although they have their own uncertainties (Peng et al., 2016).

Despite the current general understanding of how permafrost is changing and may change in the future, it is still uncertain how these changes will affect ecosystems and infrastructure on local and regional scales. The major hurdle in addressing this problem lies in the limited knowledge of local processes and consequences, due to insufficient spatial and temporal resolution of models and projections of changing climate and resulting changes in other environmental characteristics, including permafrost. To better characterize the response and feedbacks of permafrost to climate change it will be critical to intensify efforts that use a combination of field studies, remote sensing analyses, and modeling approaches to fully describe and quantify the periglacial processes and dynamics (Gogineni et al., 2014). The effects of resource development and fragmentation of large intact ecosystems by extensive networks of roads, railways, and pipelines are apparent and keenly felt by the indigenous people of the Arctic. Effects on broader regions are currently difficult to assess, but require more attention because of the cumulative effects beyond the areas of immediate impact.

References

Abbott, B.W., J.B. Jones Jr., J.R. Larouche and W.B. Bowden, 2012. Hydrologic and gaseous export of carbon and nitrogen from upland thermokarst features on the North Slope of Alaska. *Proceedings of the Tenth International Conference on Permafrost*, 25–29 June, Salekhard, Russia, 4:3–4.

ACIA, 2005. *Impacts of a Warming Arctic: Arctic Climate Impacts Assessment*. Cambridge University Press.

Åkerman, H.J. and M. Johansson, 2008. Thawing permafrost and thicker active layers in sub-arctic Sweden. *Permafrost Periglacial Process*, 19:279–292.

AMAP, 2011. *Snow, Water, Ice and Permafrost in the Arctic (SWIPA): Climate Change and the Cryosphere*. Arctic Monitoring and Assessment Programme (AMAP), Oslo, Norway.

Anderson, E.A., 1976. A point energy and mass balance model of a snow cover. US National Oceanic and Atmospheric Administration (NOAA), Technical Report 19.

Anisimov, O.A., 2011. Permafrost projections. In: Georgiadi A.G. (ed.), *Runoff projections for large Russian rivers. Part 1. Lena river basin*. pp. 75–96. Russian Academy of Science, Moscow. (In Russian)

Anisimov, O.A. and V.A. Kokorev, 2013. Constructing optimal climate ensemble for evaluation of the climate change impacts on the cryosphere. *Ice and Snow*, 1:83–92. (In Russian)

Anisimov, O.A. and A.B. Sherstukov, 2016. Evaluating the effect of environmental factors on permafrost dynamics in Russia. *Earth's Cryosphere*, 2:80–89.

Anisimov, O.A., M.A. Belolutskaya, M.N. Grigoriev, A. Instanes, V.A. Kokorev, N.G. Oberman, S.A. Reneva, Y.G. Strelchenko, D. Strelets'kiy and N.I. Shiklomanov, 2010. Major natural and social-economic consequences of climate change in the permafrost region: predictions based on observations and modeling. Greenpeace.

Anisimov, O.A., E.L. Ziltcova and S.A. Reneva, 2011. Evaluation of thresholds governing the climate change impacts on terrestrial ecosystems in Russia. *Meteorology and Hydrology*, 11:31–41. (In Russian)

Anisimov, O.A., I.I. Borzenkova, S.A. Lavrov and J.G. Strelchenko, 2012a. Dynamics of sub-aquatic permafrost and methane emission at eastern Arctic sea shelf under past and future climatic changes. *Ice and Snow*, 2:97–105. (In Russian)

Anisimov, O.A., Y.A. Anokhin, S.A. Lavrov, G.V. Malkova, A.V. Pavlov, V.E. Romanovsky, D.A. Streletskei, A.L. Kholodov and N.I. Shiklomanov, 2012b. Terrestrial permafrost. In: Semenov, S.M. (ed.), *Methods for Evaluation of the Climate Change Impacts on the Environmental Systems*. pp. 268–328. (In Russian)

Anisimov, O.A., V.A. Kokorev and E.L. Ziltcova, 2013. Temporal and spatial patterns of modern climatic warming: case study of Northern Eurasia. *Climatic Change*, 3:871-883.

Anisimov, O.A., J.G. Zaboikina, V.A. Kokorev and L.N. Yurganov, 2014. Possible reasons of methane emission on the shelf of the seas of the eastern Arctic. *Ice and Snow*, 121:69-81. (In Russian)

Anisimov, O.A., E.L. Ziltcova and V.Y. Razhivin, 2015. Predictive modeling of plant productivity in the Russian arctic using satellite data. *Earth Exploration from Space*, 3:60-70. (In Russian)

Arctic Council, 2013. Arctic Resilience Interim Report 2013. Stockholm Environment Institute and Stockholm Resilience Centre, Stockholm.

Are, F.E., 2012. Coastal Erosion of the Arctic Lowlands. GEO. (In Russian)

Arp, C.D., B.M. Jones, F.E. Urban and G. Grosse, 2011. Hydrogeomorphic processes of thermokarst lakes with grounded-ice and floating-ice regimes on the Arctic coastal plain, Alaska. *Hydrological Processes*, 25:2422-2438.

Arzhanov, M., A. Eliseev and I. Mokhov, 2013. Impact of climate changes over the extratropical land on permafrost dynamics under RCP scenarios in the 21st century as simulated by the IAP RAS climate model. *Russian Meteorology and Hydrology*, 38:456-464. (In Russian)

Balser, A.W., J.B. Jones and R. Gens, 2014. Timing of retrogressive thaw slump initiation in the Noatak Basin, northwest Alaska, USA. *Journal of Geophysical Research: Earth Surface*, 119:1106-1120.

Berdnikov, N.M., 2012. Frost mounds in different landscapes of the Nadym river basin. *Earth's Cryosphere*, XVI:81-86. (In Russian)

Biskaborn, B.K., U. Herzschuh, D.Y. Bolshiyanov, G. Schwamborn and B. Diekmann, 2013. Thermokarst processes and depositional events in a tundra lake, northeastern Siberia. *Permafrost and Periglacial Processes*, 24:160-174.

Biskaborn, B.K., J-P. Lanckman, H. Lantuit, K. Elger, D.A. Streletskei, W.L. Cable and V.E. Romanovsky, 2015. The global terrestrial network for permafrost database: metadata statistics and prospective analysis on future permafrost temperature and active layer depth monitoring site distribution. *Earth System Science Data*, 7:245-259.

Blais-Stevens, A., M. Kremer, P.P. Bonniventure, S.L. Smith, P. Lipovsky and A.G. Lewkowicz, 2015. Active layer detachment slides and retrogressive thaw slumps susceptibility mapping for current and future permafrost distribution, Yukon Alaska Highway Corridor. In: Lollino, G., A. Manconi, J. Clague, W. Shan and M. Chiaro (eds.), *Engineering Geology for Society and Territory*. pp 449-453. Proceedings International Association of Engineering Geology Congress, Torino Italy, Sept 2014. Springer.

Bouchard, F., P. Francus, R. Pienitz and I. Laurion, 2011. Sedimentology and geochemistry of thermokarst ponds in discontinuous permafrost, subarctic Quebec, Canada. *Journal of Geophysical Research*, 116:G00M04, doi:10.1029/2011JG001675.

Brooker, A., R.H. Fraser, I. Olthof, S.V. Kokelj and D. Lacelle, 2014. Mapping the activity and evolution of retrogressive thaw slumps by tasseled cap trend analysis of a landsat satellite image stack. *Permafrost and Periglacial Processes*, 25:243-256.

Brown, J., O.J. Ferrians Jr., J.A. Heginbottom and E.S. Melnikov, 1997. Circum-Arctic map of permafrost and ground-ice conditions. U.S. Department of the Interior, U.S. Geological Survey, Map CP-45.

Bryksina, N.A. and S.N. Kirpotin, 2012. Landscape-space analysis of change of thermokarst lakes areas and number in the permafrost zone of West Siberia. *Tomsk State University Journal of Biology*, 4:185-194. (In Russian)

Callaghan, T.V., M. Johansson, O. Anisimov, H.H. Christiansen, A. Instanes, V. Romanovsky and S. Smith, 2012. Changing permafrost and its impacts. In: *Snow, Water, Ice and Permafrost in the Arctic (SWIPA): Climate Change and the Cryosphere*. Arctic Monitoring and Assessment Programme (AMAP), Oslo, Norway.

Callaghan, T.V., C. Jonasson, T. Thierfelder, Z. Yang, H. Hedenås, M. Johansson, U. Molau, R. Van Bogaert, A. Michelsen, J. Olofsson, D. Gwynn-Jones, S. Bokhorst, G. Phoenix, J.W. Bjerke, H. Tømmervik, T.R. Christensen, E. Hanna, E.K. Koller and V.L. Sloan, 2013. Ecosystem change and stability over multiple decades in the Swedish subarctic: complex processes and multiple drivers. *Philosophical Transactions of the Royal Society B*, 368:20120488, doi:10.1098/rstb.2012.0488.

Calmels, F., L.-P. Roy, C. Laurent, M. Pelletier, L. Kinnear, B. Benkert, B. Horton and J. Pumple, 2015. Vulnerability of the North Alaska highway to permafrost thaw: a field guide and data synthesis. *Northern Climate ExChange, Yukon Research Centre*, Canada.

Canadian Standards Association, 2010. *Technical Guide: Infrastructure in permafrost: a guideline for climate change adaptation*. Canadian Standards Association (CSA), CSA PLUS 4011-2010.

Canadian Standards Association, 2014a. *Thermosyphon foundations for building in permafrost regions*. Canadian Standards Association (CSA), CSA S500-2014.

Canadian Standards Association. 2014b. *Moderating the effects of permafrost degradation on existing building foundations* Canadian Standards Association (CSA), CSA S501-2014.

Cannone, N., A.G. Lewkowicz and M. Guglielmin, 2010. Vegetation colonization of permafrost-related landslides, Ellesmere Island, Canadian High Arctic. *Journal of Geophysical Research*, 115:G04020, doi:10.1029/2010JG001384.

Carroll, M.L., J.R.G. Townshend, C.M. DiMiceli, T. Loboda and R.A. Sohlberg, 2011. Shrinking lakes of the Arctic: spatial relationships and trajectory of change. *Geophysical Research Letters*, 38:L20406, doi:10.1029/2011GL049427.

Chen, M., J.C. Rowland, C.J. Wilson, G.L. Altmann and S.P. Brumby, 2013. The importance of natural variability in lake areas on the detection of permafrost degradation: a case study in the Yukon Flats, Alaska. *Permafrost and Periglacial Processes*, 24:224-240.

Chizhova, Ju.N., A.C. Vasil'chuk, N.A. Budantseva and Yu.K. Vasil'chuk, 2012. Radiocarbon chronology and dynamics of palsas in the Russian European North. *Proceedings of the Tenth International Conference on Permafrost*, 25–29 June, Salekhard, Russia, 2:51-55.

Christiansen, H.H., B. Etzelmüller, K. Isaksen, H. Juliussen, H. Farbrot, O. Humlum, M. Johansson, T. Ingeman-Nielsen, L. Kristensen, J. Hjort, P. Holmlund, A.B.K. Sannel, C. Sigsgaard, H.J. Åkerman, N. Foged, L.H. Blikra, M.A. Pernosky and R. Ødegård, 2010. The thermal state of permafrost in the Nordic area during the International Polar Year. *Permafrost and Periglacial Processes*, 21:156-181.

Costard, F., E. Gautier, A. Fedorov, P. Konstantinov and L. Dupeyrat, 2014. An assessment of the erosion potential of the fluvial thermal process during ice breakups of the Lena River (Siberia). *Permafrost and Periglacial Processes*, 25:162-171.

CNR, 1990. *Stoitelnie Normi i Pravila* [Construction Norms and Regulations]. (Foundations on Permafrost) 2.02.04-88. State Engineering Committee of the USSR. (In Russian).

DeMarban, A., 2015. 'Epic' flooding on Dalton Highway hinders North Slope oil operations. *Alaska Dispatch News*, May 21, 2015.

Derkson, C., S.L. Smith, M. Sharp, L. Brown, S. Howell, L. Copland, D.R. Mueller, Y. Gauthier, C. Fletcher, A. Tivy, M. Bernier, J. Bourgeois, R. Brown, C.R. Burn, C. Duguay, P. Kushner, A. Langlois, A.G. Lewkowicz, A. Royer and A. Walker, 2012. Variability and change in the Canadian cryosphere. *Climatic Change*, 115:59-88.

Dmitrenko, I.A., S.A. Kirillov, B. Tremblay, H. Kassens, O.A. Anisimov, S.A. Lavrov, S.O. Razumov and M.N. Grigoriev, 2011. Recent changes in shelf hydrography in the Siberian Arctic: Potential for subsea permafrost instability. *Journal of Geophysical Research: Oceans*, 116:C10027, doi:10.1029/2011JC007218.

Drozdov, D.S., G.V. Malkova, N.G. Ukrainstseva and Yu.V. Korostelev, 2012. Permafrost monitoring of southern tundra landscapes in the Russian European North and West Siberia. *Proceedings of the Tenth International Conference on Permafrost*, 25–29 June, Salekhard, Russia, 2:65-70.

Duchesne, C., S. Smith, M. Ednie and J. Chartrand, 2015. 20 years of active layer monitoring in the Mackenzie Valley, Northwest Territories. *Geological Survey of Canada, Scientific Presentation SP31*.

Dupeyrat, L., F. Costard, R. Randriamazaoro, E. Gailhardis, E. Gautier and A. Fedorov, 2011. Effects of ice content on the thermal erosion of permafrost: implications for coastal and fluvial erosion. *Permafrost and Periglacial Processes*, 22:179-187.

Ednie, M. and S.L. Smith, 2015. Permafrost temperature data 2008-2014 from community based monitoring sites in Nunavut, *Geological Survey of Canada Open File*, 7784.

Elmendorf, S.C., G.H.R. Henry, R.D. Hollister, R.G. Bjork, N. Boulanger-Lapointe, E.J. Cooper, J.H.C. Cornelissen, T.A. Day, E. Dorrepaal, T.G. Elumeeva, M. Gill, W.A. Gould, J. Harte, D.S. Hik, A. Hofgaard, D.R. Johnson, J.F. Johnstone, I.S. Jonsdottir, J.C. Jorgenson, K. Klanderud, J.A. Klein, S. Koh, G. Kudo, M. Lara, E. Levesque, B. Magnusson, J.L. May, J.A. Mercado-Diaz, A. Michelsen, U. Molau, I.H. Myers-Smith, S.F. Oberbauer, V.G. Onipchenko, C. Rixen, N. Martin Schmidt, G.R. Shaver, M.J. Spasojevic, O.E. orhallsdottir, A. Tolvanen, T. Troxler, C.E. Tweedie, S. Villareal, C.-H. Wahren, X. Walker, P.J. Webber, J.M. Welker

and S. Wipf, 2012. Plot-scale evidence of tundra vegetation change and links to recent summer warming. *Nature Climate Change*, 2:453-457.

Farbrot, H., K. Isaksen, B. Etzelmüller and K. Gisnås, 2013. Ground thermal regime and permafrost distribution under a changing climate in northern Norway. *Permafrost and Periglacial Processes*, 24:20-38.

Fiddes, J., S. Endrizzi and S. Gruber, 2015. Large-area land surface simulations in heterogeneous terrain driven by global data sets: application to mountain permafrost. *The Cryosphere*, 9:411-426.

Flinn, M.B., W.B. Bowden, A.W. Balser, J.B. Jones and M.N. Gooseff, 2012. Soil and water chemistry characteristics of thermo-erosional features in the western Noatak River basin, Alaska, USA. *Proceedings of the Tenth International Conference on Permafrost*, 25–29 June, Salekhard, Russia, 1:101-106.

Forbes, B.C., F. Stammer, T. Kumpula, N. Meschty, A. Pajunen and E. Kaarlejärvi, 2009. High resilience in the Yamal-Nenets social-ecological system, West Siberian Arctic, Russia. *Proceedings of the National Academy of Sciences*, 106:22041-22048.

Forbes, B.C., M.M. Fauria and P. Zetterberg, 2010. Russian Arctic warming and "greening" are closely tracked by tundra shrub willows. *Global Change Biology*, 16:1542-1554.

Fortier, D., M. Allard and Y. Shur, 2007. Observation of rapid drainage system development by thermal erosion of ice wedges on Bylot Island, Canadian Arctic Archipelago. *Permafrost and Periglacial Processes*, 18:229-243.

Fortier, R., A.-M. LeBlanc and W. Yu, 2011. Impacts of permafrost degradation on a road embankment at Umiujaq in Nunavik (Quebec), Canada. *Canadian Geotechnical Journal*, 48:720-740.

French, H.M., 2007. The Periglacial Environment. Third Ed. Wiley and Sons.

French, H. and Y. Shur, 2010. The principles of cryostratigraphy. *Earth-Science Reviews*, 101:190-206.

Furgal, C. and T. Prowse, 2008. Northern Canada. In: Lemmen, D.S., F.J. Warren, J. Lacroix and E. Bush (eds.), *From Impacts to Adaptation: Canada in a Changing Climate 2007*. pp. 57-118. Government of Canada, Ottawa, Ontario.

Gisnås, K., S. Westermann, T.V. Schuler, T. Litherland, K. Isaksen, J. Boike and D. Etzelmüller, 2014. A statistical approach to represent small-scale variability of permafrost temperatures due to snow cover. *The Cryosphere*, 8:2063-2074.

Godin, E. and D. Fortier, 2012. Fine-scale spatio-temporal monitoring of multiple thermo-erosion gully development on Bylot Island, eastern Canadian Archipelago. *Proceedings of the Tenth International Conference on Permafrost*, 25–29 June, Salekhard, Russia, 1:125-130.

Gogineni, P., V.E. Romanovsky, J. Cherry, C. Duguay, S. Goetz, M.T. Jorgenson and M. Moghaddam, 2014. Opportunities to use remote sensing in understanding permafrost and related ecological characteristics. Report of a workshop. National Academies Press.

Gonzalez, P., R.P. Neilson, J.M. Lenihan and R.J. Drapek, 2010. Global patterns in the vulnerability of ecosystems to vegetation shifts due to climate change. *Global Ecology and Biogeography*, 19:755-768.

Grigoriev, M.N., 2008. Kriomorphogenet i litodinamika pribrezhno-shelfovoy zony morey Vostochnoy Sibiri [Cryomorphogenesis and lithodynamics of coastal-shelf zone of the seas of East Siberia]. Avtoreferat dissertatsii na soiskanie uchenoy stepeni doktora geografich-eskikh nauk [Synopsis of the Doctor of Science thesis]. Yakutsk.

Grigoriev, M.N., S.O. Razumov, V.V. Kunitzkiy and V.B. Spektor, 2006. Dynamics of the Russian East Arctic Sea coast: major factors, regularities and tendencies. *Earth's Cryosphere*, X:74-94. (In Russian)

Grosse, G. and B.M. Jones, 2011. Spatial distribution of pingos in northern Asia. *The Cryosphere*, 5:13-33.

Grosse, G., B. Jones and C. Arp, 2012. Thermokarst lakes, drainage, and drained basins. In: Shroder, J.F. (ed.), *Treatise on Geomorphology*. Academic Press.

Grosse, G., J.E. Robinson, R. Bryant, M.D. Taylor, W. Harper, A. DeMasi, E. Kyker-Snowman, A. Veremeeva, L. Schirrmeister and J. Harden, 2013. Distribution of late Pleistocene ice-rich syngenetic permafrost of the Yedoma Suite in East and Central Siberia, Russia. US Geological Survey, Open-File Report 2013-1078.

Gubarkov, A.A. and M.O. Leibman, 2010. Bead-shaped channel forms as evidence of paragenesis of cryogenic and hydrological processes in the small-river valleys of Central Yamal. *Earth's Cryosphere*, XIV:41-49. (In Russian)

Gubarkov, A.A., M.O. Leibman, V.P. Mel'nikov and A.V. Khomutov, 2008. Contribution of lateral thermal erosion and thermal denudation to coastal retreat of the Yugorskii Peninsula. *Doklady Earth Sciences*, 423:1452-1454. (In Russian)

Gubarkov, A., M. Leibman and M. Andreeva, 2014. Cryogenic landslides in paragenetic complexes of slope and channel processes in the central Yamal Peninsula. In: Shan, W. et al. (eds.), *Landslides in Cold Regions in the Context of Climate Change*. pp. 291-308. Springer.

Günther, F., P.P. Overduin, A.V. Sandakov, G. Grosse and M.N. Grigoriev, 2013. Short- and long-term thermo-erosion of ice-rich permafrost coasts in the Laptev Sea region. *Biogeosciences*, 10:4297-4318.

Günther, F., P.P. Overduin, I.A. Yakshina, T. Opel, A.V. Baranskaya and M.N. Grigoriev, 2015. Observing Muostakh disappear: permafrost thaw subsidence and erosion of a ground-ice-rich island in response to arctic summer warming and sea ice reduction. *The Cryosphere*, 9:151-178.

Gusev, E.A., 2011. Observations of geomorphic processes in the North of West Siberia (case study in Sopochnaya Karga). *Successes Contemporary Science*, 9:19-22. (In Russian)

Haltigin, T.W., W.H. Pollard, P. Dutilleul and G.R. Osinski, 2012. Geometric evolution of polygonal terrain networks in the Canadian High Arctic: evidence of increasing regularity over time. *Permafrost and Periglacial Processes*, 23:178-186.

Hansen, B., K. Isaksen, R. Benestad, J. Kohler, Å. Pedersen, L. Loe, S. Coulson, J. Larsen and Ø. Varpe, 2014. Warmer and wetter winters: characteristics and implications of an extreme weather event in the High Arctic. *Environmental Research Letters*, 9:114021, doi:10.1088/1748-9326/9/11/114021.

Hickling, R., D.B. Roy, J.K. Hill, R. Fox and C.D. Thomas, 2006. The distributions of a wide range of taxonomic groups are expanding polewards. *Global Change Biology*, 12:450-455.

Hinkel, K.M., B.M. Jones, W.R. Eisner, C.J. Cuomo, R.A. Beck and R.C. Frohn, 2007. Methods to assess natural and anthropogenic thaw lake drainage on the western Arctic Coastal Plain of northern Alaska. *Journal of Geophysical Research*, 112:F02S16, doi:10.1029/2006JF000584.

Iijima, Y., A.N. Fedorov, T. Ohta, A. Kotani and T.C. Maximov, 2012. Recent hydrological and ecological changes in relation to permafrost degradation under increased precipitation in an eastern Siberian boreal forest. *Proceedings of the Tenth International Conference on Permafrost*, 25–29 June, Salekhard, Russia, 1:161-166.

IMG-Golder Corporation Environmental Consulting, 2012a. Vulnerability assessment of the mining sector to climate change Task 1 Report. Prepared for Nunavut Regional Adaptation Collaborative. www.climatechangenunavut.ca/en/project/nunavut-regional-adaptation-collaborative

IMG-Golder Corporation Environmental Consulting, 2012b. Good environmental practices for northern mining and necessary infrastructure Task 2 Report. Prepared for Nunavut Regional Adaptation Collaborative. www.climatechangenunavut.ca/en/project/nunavut-regional-adaptation-collaborative

Instanes, A., V. Kokorev, R. Janowicz, O. Bruland, K. Sand and T. Prowse, 2015. Changes to freshwater systems affecting Arctic infrastructure and natural resources. The 3rd International Conference on Arctic Research Planning (ICARP-III), 23-30 April, Toyama, Japan. Presentation C07-O15.

IPCC, 2012. Managing the Risks of Extreme Events and Disasters to Advance Climate Change Adaptation. A Special Report of Working Groups I and II of the Intergovernmental Panel on Climate Change. Field, C.B., V. Barros, T.F. Stocker, D. Qin, D.J. Dokken, K.L. Ebi, M.D. Mastrandrea, K.J. Mach, G.-K. Plattner, S.K. Allen, M. Tignor and P.M. Midgley (eds.). Cambridge University Press.

IPCC, 2013. Climate Change 2013: The Physical Science Basis. Contribution of Working Group I to the Fifth Assessment Report of the Intergovernmental Panel on Climate Change. Stocker, T.F., D. Qin, G.-K. Plattner, M. Tignor, S.K. Allen, J. Boschung, A. Nauels, Y. Xia, V. Bex and P.M. Midgley (eds.). Cambridge University Press.

Isaksen, K., J.L. Sollid, P. Holmlund and C. Harris, 2007. Recent warming of mountain permafrost in Svalbard and Scandinavia. *Journal of Geophysical Research*, 112:F02S04, doi:10.1029/2006JF000522.

Isaksen, K., R.S. Ødegård, B. Etzelmüller, C. Hilbich, C. Hauck, H. Farbrot, T. Eiken, H.O. Hygen and T.F. Hipp, 2011. Degrading mountain permafrost in southern Norway - spatial and temporal variability of mean ground temperatures, 1999-2009. *Permafrost Periglacial Processes*, 22:361-377.

Jafarov, E. E., S.S. Marchenko and V.E. Romanovsky, 2012. Numerical modeling of permafrost dynamics in Alaska using a high spatial resolution dataset. *The Cryosphere*, 6:613-624.

James, M., A.G. Lewkowicz, S.L. Smith and C.M. Miceli, 2013. Multi-decadal degradation and persistence of permafrost in the Alaska Highway

corridor, northwest Canada. *Environmental Research Letters*, 8:045013, doi:10.1088/1748-9326/8/4/045013.

Johansson, M., J. Åkerman, F. Keuper, T.R. Christensen, H. Lantuit and T.V. Callaghan, 2011. Past and present permafrost temperatures in the Abisko area: redrilling of boreholes. *Ambio*, 40:558-565.

Jones, B.M. and C.D. Arp, 2015. Observing a catastrophic thermokarst lake drainage in northern Alaska. *Permafrost and Periglacial Processes*, 26:119-128.

Jones, B.M., C.D. Arp, M.T. Jorgenson, K.M. Hinkel, J.A. Schmutz and P.L. Flint, 2009. Increase in the rate and uniformity of coastline erosion in Arctic Alaska. *Geophysical Research Letters*, 36:L03503, doi:10.1029/2008GL036205.

Jones, B.M., G. Grosse, M.C. Arp, K.M. Jones, A. Walter and V.E. Romanovsky, 2011. Modern thermokarst lake dynamics in the continuous permafrost zone, northern Seward Peninsula, Alaska. *Journal of Geophysical Research*, 116:G00M03, doi:10.1029/2011JG001666.

Jones, B.M., G. Grosse, K.M. Hinkel, C.D. Arp, S. Walker, R.A. Beck and J.P. Galloway, 2012a. Assessment of pingo distribution and morphometry using an IfSAR derived DSM, western Arctic Coastal Plain, northern Alaska. *Geomorphology*, 138:1-14.

Jones, M.C., G. Grosse, B.M. Jones and A.K. Walter, 2012b. Peat accumulation in drained thermokarst lake basins in continuous, ice-rich permafrost, northern Seward Peninsula, Alaska. *Journal of Geophysical Research*, 117:G00M07, doi:10.1029/2011JG001766.

Jones, B.M., J.M. Stoker, A.E. Gibbs, G. Grosse, V.E. Romanovsky, T.A. Douglas, N.E.M. Kinsman and B.M. Richmond, 2013. Quantifying landscape change in an arctic coastal lowland using repeat airborne LiDAR. *Environmental Research Letters*, 8:045025.

Jorgenson, M.T. and M. Heiner, 2004. Ecosystems of Northern Alaska. 1:2.5 million-scale map. ABR Inc., Fairbanks, Alaska and The Nature Conservancy, Anchorage, Alaska.

Jorgenson, M.T., Y.L. Shur and E.R. Pullman, 2006. Abrupt increase in permafrost degradation in Arctic Alaska. *Geophysical Research Letters*, 33:L02503, doi:10.1029/2005GL024960.

Jorgenson, T., Y.L. Shur and T.E. Osterkamp, 2008. Thermokarst in Alaska. In: *Proceedings of the Ninth International Conference on Permafrost*, June 29–July 3, University of Alaska Fairbanks, 1:869-876.

Jorgenson, M.T., V. Romanovsky, J. Harden, Y. Shur, J. O'Donnell, E.A.G. Schuur, M. Kanevsky and S. Marchenko, 2010. Resilience and vulnerability of permafrost to climate change. *Canadian Journal of Forest Research*, 40:1219-1236.

Jorgenson, M.T., M. Kanevskiy, Y. Shur, T. Osterkamp, D. Fortier, T. Cater and P. Miller, 2012. Thermokarst lake and shore fen development in boreal Alaska. *Proceedings of the Tenth International Conference on Permafrost*, 25–29 June, Salekhard, Russia, 1:179-184.

Jorgenson, M., M. Kanevskiy, Y. Shur, J. Grunblatt, C. Ping and G. Michaelson, 2014. Permafrost database development, characterization and mapping for northern Alaska. Final report. Prepared for U.S. Fish and Wildlife Service, Arctic Landscape Conservation Cooperative, Anchorage.

Kalnay, E., M. Kanamitsu, R. Kistler, W. Collins, D. Deaven, L. Gandin, M. Iredell, S. Saha, G. White, J. Woollen, Y. Zhu, A. Leetmaa, R. Reynolds, M. Chelliah, W. Ebisuzaki, W. Higgins, J. Janowiak, K.C. Mo, C. Ropelewski, J. Wang, R. Jenne and D. Joseph, 1996. The NCEP/NCAR 40-Year Reanalysis Project. *Bulletin of American Meteorological Society*, 77:437-471.

Kanevskiy, M., Y. Shur, M.T. Jorgenson, C.-L. Ping, G.J. Michaelson, D. Fortier, E. Stephani, M. Dillon and V. Tumskoy, 2013. Ground ice in the upper permafrost of the Beaufort Sea coast of Alaska. *Cold Regions Science and Technology*, 85:56-70.

Kanevskiy, M., M.T. Jorgenson, Y. Shur, J.A. O'Donnell, J.W. Harden, Q. Zhuang and D. Fortier, 2014. Cryostratigraphy and permafrost evolution in lacustrine lowlands of west-central Alaska. *Permafrost and Periglacial Processes*, 25:14-34.

Kaplina, T.N., 1965. *Cryogenic Slope Processes*. Nauka. (In Russian)

Kessler, M.A., L.J. Plug and K.M. Walter Anthony, 2012. Simulating the decadal- to millennial-scale dynamics of morphology and sequestered carbon mobilization of two thermokarst lakes in NW Alaska. *Journal of Geophysical Research: Biogeosciences*, 117:G00M06, doi:10.1029/2011JG001796.

Khomutov, A.V., 2012. Assessment of landslide geohazards in typical tundra of central Yamal. *Proceedings of the Tenth International Conference on Permafrost*, 25–29 June, Salekhard, Russia, 2:157-162.

Khomutov, A.V. and M.O. Leibman, 2008. Landscape controls of thermal denudation rate change on Yugorsky peninsula coast. *Earth's Cryosphere*, XII:24-35. (In Russian)

Khomutov, A.V. and M.O. Leibman, 2010. Landscape pattern and cryogenic landsliding hazard analysis on Yamal peninsula, Russia. In: *Abstracts from the 3rd European Conference on Permafrost*, 254. The University Centre, Svalbard.

Khomutov, A.V., M.O. Leibman and M.V. Andreeva, 2012. Mapping of ground ice in Central Yamal. *Tyumen State University Herald, Earth Sciences*, 7:68-76.

Kizyakov, A.I., D.D. Perednya, Yu.G. Firsov, M.O. Leibman and G.A. Cherkashov, 2003. Character of the coastal destruction and dynamics of the Yugorsky Peninsula coast. *Reports on Polar and Marine Research*, 443:47-49.

Kizyakov, A.I., M.V. Zimin, M.O. Leibman and N.V. Pravikova, 2013. Monitoring of the rate of thermal denudation and thermal abrasion on the western coast of Kolguev Island, using high resolution satellite images. *Earth's Cryosphere*, XVII:36-47. (In Russian)

Kizyakov, A.I., A.V. Sonyushkin, M.O. Leibman, M.V. Zimin and A.V. Khomutov, 2015. Geomorphological conditions of the gas-emission crater and its dynamics in Central Yamal. *Earth's Cryosphere*, XIX:13-22. (In Russian)

Kokelj, S.V. and M.T. Jorgenson, 2013. Advances in thermokarst research. *Permafrost and Periglacial Processes*, 24:108-119.

Kokelj, S.V., D. Lacelle, T.C. Lantz, J. Tunnicliffe, L. Malone, I.D. Clark and K.S. Chin, 2013. Thawing of massive ground ice in mega slumps drives increases in stream sediment and solute flux across a range of watershed scales. *Journal of Geophysical Research: Earth Surface*, 118:681-692.

Kokorev, V.A. and O.A. Anisimov, 2013. Constructing optimal ensemble climatic projection for climate change impact assessment in Russia. In: Izrael, Y. (ed.), *Problems of Ecological Modelling and Ecosystem Monitoring*. pp. 131-153. Planeta. (In Russian)

Konishchev, V.N., 2011. Permafrost response to climate warming. *Earth's Cryosphere*, XV:13-16.

Koven, C.D., W.J. Riley and A. Stern, 2013. Analysis of permafrost thermal dynamics and response to climate change in the CMIP5 Earth System Models. *Journal of Climate*, 26:1877-1900.

Koven, C.D., E.A.G. Schuur, C. Schädel, T. Bohn, E.J. Burke, G. Chen, X. Chen, P. Ciais, G. Grosse, J.W. Harden, D.J. Hayes, G. Hugelius, E.E. Jafarov, G. Krinner, P. Kuhry, D.M. Lawrence, A.H. MacDougall, S.S. Marchenko, A.D. McGuire, S.M. Natali, D.J. Nicolsky, D. Olefeldt, S. Peng, V.E. Romanovsky, K.M. Schaefer, J. Strauss, C. Treat and M. Turetsky, 2015. A simplified, data-constrained approach to estimate the permafrost carbon-climate feedback. *Philosophical Transactions of the Royal Society A*, 373: 20140423.

Kravtsova, V.I. and A.G. Bystrova, 2009. Changes in thermokarst lake size in different regions of Russia for the last 30 years. *Earth's Cryosphere*, XIII:16-26. (In Russian)

Kravtsova, V.I. and T.V. Tarasenko, 2011. The dynamics of thermokarst lakes under climate changes since 1950, Central Yakutia. *Earth's Cryosphere*, XV:31-42. (In Russian)

Kumpula, T., A. Pajunen, E. Kaarlejärvi, B.C. Forbes and F. Stammer, 2011. Land use and land cover change in Arctic Russia: Ecological and social implications of industrial development. *Global Environmental Change*, 21:550-562.

Kumpula, T., B.C. Forbes, F. Stammer and N. Meschtyb, 2012. Dynamics of a coupled system: multi-resolution remote sensing in assessing social-ecological responses during 25 years of gas field development in Arctic Russia. *Remote Sensing*, 4:1046-1068.

Kunitsky, V.V., I.I. Syromyatnikov, L. Schirrmeyer, Yu.B. Skachkov, G. Grosse, S. Wetterich and M.N. Grigoriev, 2013. Ice-rich permafrost and thermal denudation in the Batagay area (Yana Upland, East Siberia). *Kriosfera Zemli*, 17:56-68. (In Russian)

Lacelle, D., B. Björnson and B. Lauriol, 2010. Climatic and geomorphic factors affecting contemporary (1950-2004) activity of retrogressive thaw slumps on the Aklavik Plateau, Richardson Mountains, NWT, Canada. *Permafrost and Periglacial Processes*, 21:1-15.

Langer, M., S. Westermann, M. Heikenfeld, W. Dorn and J. Boike, 2013. Satellite-based modeling of permafrost temperatures in a tundra lowland landscape. *Remote Sensing of Environment*, 135:12-24.

Lantuit, H., D. Atkinson, P.P. Overduin, M. Grigoriev, V. Rachold, G. Grosse and H.-W. Hubberten, 2011. Coastal erosion dynamics on the permafrost-dominated Bykovsky Peninsula, north Siberia, 1951-2006. *Polar Research*, 30:7341, doi:10.3402/polar.v30i0.7341.

Lantuit, H., W.H. Pollard, N. Couture, M. Fritz, L. Schirrmeyer, H. Meyer and H.-W. Hubberten, 2012. Modern and late Holocene retrogressive thaw slump activity on the Yukon coastal plain and Herschel Island, Yukon Territory, Canada. *Permafrost and Periglacial Processes*, 23:39-51.

Lantuit, H., P. Overduin and S. Wetterich, 2013. Recent progress regarding permafrost coasts. *Permafrost and Periglacial Processes*, 24:120-130.

Lantz, T.C. and S.V. Kokelj, 2008. Increasing rates of retrogressive thaw slump activity in the Mackenzie Delta region, N.W.T., Canada. *Geophysical Research Letters*, 35:L06502, doi:10.1029/2007GL032433.

Lantz, T.C. and K.W. Turner, 2015. Changes in lake area in response to thermokarst processes and climate in Old Crow Flats, Yukon. *Journal of Geophysical Research: Biogeosciences*, 120:513-524.

Lantz, T.C., S.E. Gergel and S.V. Kokelj, 2010. Spatial heterogeneity in the shrub tundra ecotone in the Mackenzie Delta region, Northwest Territories: implications for Arctic environmental change. *Ecosystems*, 13:194-204.

Lantz, T.C., P. Marsh and S.V. Kokelj, 2013. Recent shrub proliferation in the Mackenzie Delta uplands and microclimatic implications. *Ecosystems*, 16:47-59.

Larsen, J.N., O.A. Anisimov, A. Constable, A.B. Hollowed, N. Maynard, P. Prestreud, T.D. Prowse and J.M.R. Stone, 2014. Polar regions. In: Barros, V.R., C.B. Field, D.J. Dokken, M.D. Mastrandrea, K.J. Mach, T.E. Bilir, M. Chatterjee, K.L. Ebi, Y.O. Estrada, R.C. Genova, B. Girma, E.S. Kissel, A.N. Levy, S. MacCracken, P.R. Mastrandrea, and L.L. White (eds.), *Climate Change 2014: Impacts, Adaptation, and Vulnerability. Part B: Regional Aspects. Contribution of Working Group II to the Fifth Assessment Report of the Intergovernmental Panel on Climate Change*. Cambridge University Press.

Lavrov, S.A. and O.A. Anisimov, 2011. Modelling of the hydrothermal regime of soils: description of the dynamical model and comparison with observations. In: Izrael, Yu (ed.), *Problems of Ecological Modelling and Ecosystem Monitoring*. pp. 241-255. Hydrometeoizdat. (In Russian)

Lawrence, D.M., A.G. Slater, V.E. Romanovsky and D.J. Nicolsky, 2008. The sensitivity of a model projection of near-surface permafrost degradation to soil column depth and representation of soil organic matter. *Journal of Geophysical Research: Earth Surface*, 113:F02011, doi:10.1029/2007JF000883.

Leblanc, A.-M., N. Short, G. Oldenborger, V. Mathon-Dufour and M. Allard, 2012. Geophysical investigation and InSar mapping of permafrost and ground movement at the Iqaluit airport. In: Doré, G. and B. Morse (eds.), *Cold Regions Engineering 2012, Sustainable Infrastructure Development in a Changing Cold Environment*. pp. 644-665. American Society of Civil Engineers.

LeBlanc, A.-M., G.A. Oldenborger, W.E. Sladen and M. Allard, 2015. Infrastructure and climate warming impacts on ground thermal regime, Iqaluit International Airport, southern Baffin Island, Nunavut. *Summary of Activities 2014*. pp. 119-132. Canada-Nunavut Geoscience Office.

Lee, H., S.C. Swenson, A.G. Slater and D.M. Lawrence, 2014. Effects of excess ground ice on projections of permafrost in a warming climate. *Environmental Research Letters*, 9:124006, doi:10.1088/1748-9326/9/12/124006.

Leibman, M.O. and A.I. Kizyakov, 2007. *Cryogenic Landslides of the Yamal and Yugorsky Peninsulas*. Earth Cryosphere Institute, Moscow-Tyumen. (In Russian)

Leibman, M., A. Khomutov and A. Kizyakov, 2014a. Cryogenic landslides in the West-Siberian Plain of Russia: classification, mechanisms and landforms. In: Shan, W. et al. (eds.), *Landslides in Cold Regions in the Context of Climate Change*. pp. 143-162. Springer.

Leibman, M.O., A.I. Kizyakov, A.V. Plekhanov and I.D. Streletskaia, 2014b. New permafrost feature - deep crater in Central Yamal, West Siberia, Russia, as a response to local climate fluctuations. *Geography, Environment, Sustainability*, 7:68-80.

Leibman, M.O., A.V. Khomutov, A.A. Gubarkov and Y. Dvornikov, 2015. The research station "Vaskiny Dachi" central Yamal, West Siberia, Russia - A review of 25 years of permafrost studies. *Fennia*, 193:3-30.

Lepage, J.M. and G. Dore, 2010. Experimentation of mitigation techniques to reduce the effects of permafrost degradation on transportation infrastructures at Beaver Creek experimental road site (Alaska Highway, Yukon). pp. 526-533. *GEO2010*, 63rd Canadian Geotechnical Conference and 6th Canadian Permafrost Conference, Calgary.

Lewkowicz, A.G., 2007. Dynamics of active-layer detachment failures, Fosheim Peninsula, Ellesmere Island, Nunavut, Canada. *Permafrost and Periglacial Processes*, 18:89-103.

Lewkowicz, A.G. and C. Harris, 2005. Morphology and geotechnique of active-layer detachment failures in discontinuous and continuous permafrost, northern Canada. *Geomorphology*, 69:275-297.

Liljedahl, A.K., J. Boike, R.P. Daanen, A.N. Fedorov, G.V. Frost, G. Grosse, L.D. Hinzman, Y. Iijima, J.C. Jorgenson, N. Matveyeva, M. Necsoiu, M.K. Reynolds, V.E. Romanovsky, J. Schulla, K. Tape, D.A. Walker, C.J. Wilson, H. Yabuki and D. Zona, 2016. Pan-Arctic ice wedge degradation in warming permafrost and its influence on tundra hydrology. *Nature Geoscience*, 9:312-318.

Ling, F., Q. Wu, T. Zhang and F. Niu, 2012. Modelling open-talik formation and permafrost lateral thaw under a thermokarst Lake, Beiluhe basin, Qinghai-Tibet Plateau. *Permafrost and Periglacial Processes*, 23:312-321.

Liu, L., K. Schaefer, A. Gusmeroli, G. Grosse, B.M. Jones, T. Zhang, A.D. Parsekian and H.A. Zebker, 2014a. Seasonal thaw settlement at drained thermokarst lake basins, Arctic Alaska. *The Cryosphere*, 8:815-826.

Liu, L., E.E. Jafarov, K.M. Schaefer, B.M. Jones, H.A. Zebker, C.A. Williams, J. Rogan and T. Zhang, 2014b. InSAR detects increase in surface subsidence caused by an Arctic tundra fire. *Geophysical Research Letters*, 41:3906-3913.

Mackay, J.R. and C.R. Burn, 2011. A century (1910–2008) of change in a collapsing pingo, Parry Peninsula, western Arctic coast, Canada. *Permafrost and Periglacial Processes*, 22:266-272.

Malenfant-Lepage, J., G. Doré and R. Fortier, 2012a. Thermal effectiveness of the mitigation techniques tested at Beaver Creek Experimental road site based on a heat balance analysis (Yukon, Canada). In: Doré, G. and B. Morse (eds.), *Cold Regions Engineering 2012: Sustainable Infrastructure Development in a Changing Cold Environment*. pp. 42-51. American Society of Civil Engineers.

Malenfant-Lepage, J., G. Doré, D. Fortier and P. Murchinson, 2012b. Thermal performance of the permafrost protection techniques at Beaver Creek experimental road site, Yukon Canada. *Proceedings of the Tenth International Conference on Permafrost*, 25–29 June, Salekhard, Russia, 1:261-266.

Malkova, G.D., M.O. Leibman, D.S. Drozdov, A.V. Khomutov, A.A. Guubarkov and A.B. Sherstyukov, 2014. Permafrost. In: *Impact of climate change on terrestrial ecosystems. The Second Assessment Report of ROSHYDROMET on Climate Change and its Consequences within the Territory of Russian Federation*. pp. 410-458, http://downloads.igce.ru/publications/OD_2_2014/v2014/htm/ (in Russian)

Manasypov, R.M., O.S. Pokrovsky, S.N. Kirpotin and L.S. Shirokova, 2014. Thermokarst lake waters across the permafrost zones of western Siberia. *The Cryosphere*, 8:1177-1193.

McGuire, A.D., C. Koven, D.M. Lawrence, J.S. Clein, J. Xia, C. Beer, E. Burke, G. Chen, X. Chen, C. Delire, E. Jafarov, A.H. MacDougall, S. Marchenko, D. Nicolsky, S. Peng, A. Rinke, K. Saito, W. Zhang, R. Alkama, T.J. Bohn, P. Ciais, B. Decharme, A. Ekici, I. Gouttevin, T. Hajima, D.J. Hayes, D. Ji, G. Krinner, D.P. Lettenmaier, P.A. Miller, J.C. Moore, V. Romanovsky, C. Schadel, K. Schaefer, E.A.G. Schuur, B. Smith, T. Suyoshi, and Q. Zhuang, 2016. Variability in the sensitivity among model simulations of permafrost and carbon dynamics in the permafrost region between 1960 and 2009. *Global Biogeochemical Cycles*, 30:1015-1037.

Melnikov, V.P., D.S. Drozdov and V.V. Pendin, 2015. Arctic permafrost: dynamics, risks, problems and solutions. *XXII Int. Science-Practical Conf. New Ideas in Earth Science*. pp. 123-138. 8–10 April, Moscow.

Miyazaki, S., K. Saito, J. Mori, T. Yamazaki, T. Ise, H. Arakida, T. Hajima, Y. Iijima, H. Machiya, T. Suyoshi, H. Yabuki, E.J. Burke, M. Hosaka, K. Ichii, H. Ikawa, A. Ito, A. Kotani, Y. Matsuura, M. Niwano, T. Nitta, R. Oishi, T. Ohta, H. Park, T. Sasai, A. Sato, H. Sato, A. Sugimoto, R. Suzuki, K. Tanaka, S. Yamaguchi and K. Yoshimura, 2015. The GRENE-TEA model intercomparison project (GTMIP): overview and experiment protocol for Stage 1. *Geoscientific Model Development*, 8:2841-2856.

Morgenstern, A., G. Grosse, F. Günther, I. Fedorova and L. Schirrmeister, 2011. Spatial analyses of thermokarst lakes and basins in Yedoma landscapes of the Lena Delta. *The Cryosphere*, 5:849-867.

Morgenstern, A., M. Ulrich, F. Günther, S. Roessler, I.V. Fedorova, N.A. Rudaya, S. Wetterich, J. Boike and L. Schirrmeister, 2013. Evolution of thermokarst in East Siberian ice-rich permafrost: A case study. *Geomorphology*, 201:363-379.

Morse, P., C. Burn and S. Kokelj, 2012. Influence of snow on near-surface ground temperatures in upland and alluvial environments of the outer Mackenzie delta, Northwest Territories. *Canadian Journal of Earth Sciences*, 49:895-913.

Murton, J.B. 2013. Ground ice and cryostratigraphy. In: Shroder, J.F. (ed.), *Treatise on Geomorphology*. Academic Press.

Nadyozhina, E.D., L.R. Olenko and A.A. Pikaleva, 2013. Permafrost evolution in the arctic coastal regions using multi-scale system of climate models. *Proceedings of Main Geophysical Observatory*, 569:62-74. (In Russian)

Necsoiu, M., C.L. Dinwiddie, G.R. Walter, A. Larsen and S.A. Stothoff, 2013. Multi-temporal image analysis of historical aerial photographs and recent satellite imagery reveals evolution of water body surface area

and polygonal terrain morphology in Kobuk Valley National Park, Alaska. *Environmental Research Letters*, 8:025007.

NGI, 2013. Impacts of extreme weather events on infrastructure in Norway (InfraRisk). Norwegian Geotechnical Institute (NGI), NGI-report No. 20091808-01-R.

Nicolsky, D.J., V.E. Romanovsky, V.A. Alexeev and D.M. Lawrence, 2007. Improved modeling of permafrost dynamics in a GCM land-surface scheme. *Geophysical Research Letters*, 34:L08501, doi:10.1029/2007GL029525.

Nicolsky, D.J., V.E. Romanovsky and G.G. Panteleev, 2009. Estimation of soil thermal properties using in-situ temperature measurements in the active layer and permafrost. *Cold Regions Science and Technology*, 55:120-129.

Nicolsky, D.J., V.E. Romanovsky, N.N. Romanovskii, A.L. Kholodov, N.E. Shakhova and I.P. Semiletov, 2012. Modeling sub-sea permafrost in the East Siberian Arctic Shelf: The Laptev Sea region. *Journal of Geophysical Research*, 117:F03028, doi:10.1029/2012JF002358.

Nicolsky, D.J., V.E. Romanovsky, S.K. Panda, S.S. Marchenko, and R. Muskett, 2017. Applicability of the ecosystem type approach to model permafrost dynamics across the Alaska North Slope. *Journal of Geophysical Research*, 122:50-75.

Nordrum, A., 2015. Trucking along the Alaska's 'ice road' to northern oilfields freezes to a halt. *International Business Times*. www.ibtimes.com/trucking-along-alaskas-ice-road-northern-oilfields-freezes-halt-1883163. Accessed 30 August 2015.

Northern Climate Exchange, 2013. Burwash Landing and Destruction Bay Landscape Hazards: Geological Mapping for Climate Change Adaptation Planning. Yukon Research Centre, Yukon College.

Norwegian Public Roads Administration, 2013. Climate and Transport. Report no. 210.

Palmer, M., C. Burn, S. Kokelj and M. Allard, 2012. Factors influencing permafrost temperatures across tree line in the uplands east of the Mackenzie delta. *Canadian Journal of Earth Sciences*, 49:877-894.

Pan, X., Y. You, K. Roth, L. Guo, X. Wang and Q. Yu, 2014. Mapping permafrost features that influence the hydrological processes of a thermokarst lake on the Qinghai-Tibet Plateau, China. *Permafrost and Periglacial Processes*, 25:60-68.

Parsekian, A.D., B.M. Jones, M. Jones, G. Grosse, A.K.M. Walter and L. Slater, 2011. Expansion rate and geometry of floating vegetation mats on the margins of thermokarst lakes, northern Seward Peninsula, Alaska, USA. *Earth Surface Processes and Landforms*, 36:1889-1897.

Pearce, T., J.D. Ford, J. Prino, F. Duerden, J. Pittman, M. Beaumier, L. Berrang-Ford and B. Smit, 2011. Climate change and mining in Canada. *Mitigation and Adaptation Strategies for Global Change*, 16:347-368.

Pearson, R.G., S.J. Phillips, M.M. Loranty, P.S.A. Beck, T. Damoulas, S.J. Knight and S.J. Goetz, 2013. Shifts in Arctic vegetation and associated feedbacks under climate change. *Nature Climate Change*, 3:673-677.

Peng, S., P. Ciais, G. Krinner, T. Wang, I. Gouttevin, A.D. McGuire, D. Lawrence, E. Burke, X. Chen, B. Decharme, C. Koven, A. MacDougall, A. Rinke, K. Saito, W. Zhang, R. Alkama, T.J. Bohn, C. Delire, T. Hajima, D. Ji, D.P. Lettemaier, P.A. Miller, J.C. Moore, B. Smith and T. Suyeshi, 2016. Simulated high-latitude soil thermal dynamics during the past 4 decades. *The Cryosphere*, 10:179-192.

Perednya, D.D., M.O. Leibman, A.I. Kizyakov, B.G. Vanshtein and G.A. Cherkashov, 2003. Coastal dynamics at the western part of Kolguev Island, Barents Sea. *Reports on Polar and Marine Research*, 44:92-94.

Pizano, C., A.F. Barón, E.A.G. Schuur, K.G. Crummer and M.C. Mack, 2014. Effects of thermo-erosional disturbance on surface soil carbon and nitrogen dynamics in upland arctic tundra. *Environmental Research Letters*, 9:075006.

Pizhankova, E.I., 2011. Termodenudation in the coastal zone of the Lyakhovsky islands (interpretation of aerospace images). *Earth's Cryosphere*, XV:61-70. (In Russian)

Pizhankova, E.I. and M.S. Dobrynina, 2010. The dynamics of the Lyakhovsky Islands coastline (results of aerospace image interpretation). *Earth's Cryosphere*, XIV:66-79. (In Russian)

Plug, L.J. and J.J. West, 2009. Thaw lake expansion in a two-dimensional coupled model of heat transfer, thaw subsidence, and mass movement. *Journal of Geophysical Research*, 114:F01002, doi:10.1029/2006JF000740.

Ponomareva, O.E., A.G. Gravis, N.M. Berdnikov and T.A. Blyakharchuk, 2012. Climate change, frost action, and permafrost-related processes in the northern Taiga region of West Siberia. *Proceedings of the Tenth International Conference on Permafrost*, 25-29 June, Salekhard, Russia, 2:343-347.

Prowse, T., A. Bring, E. Carmack and J.M. Karlsson, 2015. Arctic freshwater synthesis: fluxes, storage and effects. The Third International Conference on Arctic Research Planning (ICARP-III), Toyama, Japan, 23-30 April. Presentation C07-O13.

Raynolds, M.K., D.A. Walker, K.J. Ambrosius, J. Brown, K.R. Everett, M. Kanevskiy, G.P. Kofinas, V.E. Romanovsky, Y. Shur and P.J. Webber, 2014. Cumulative geoecological effects of 62 years of infrastructure and climate change in ice-rich permafrost landscapes, Prudhoe Bay Oilfield, Alaska. *Global Change Biology* 20:1211-1224.

Roach, J., B. Griffith, D. Verbyla and J. Jones, 2011. Mechanisms influencing changes in lake area in the Alaskan boreal forest. *Global Change Biology*, 17:2567-2583.

Romanovskii, N.N., H.-W. Hubberten, A.V. Gavrilov, V.E. Tumskoy and A.L. Kholodov, 2004. Permafrost of the east Siberian Arctic shelf and coastal lowlands. *Quaternary Science Reviews*, 23:1359-1369.

Romanovsky, V.E., S.L. Smith and H.H. Christiansen, 2010a. Permafrost thermal state in the polar northern hemisphere during the International Polar Year 2007-2009: a synthesis. *Permafrost and Periglacial Processes*, 21:106-116.

Romanovsky, V.E., D.S. Drozdov, N.G. Oberman, G.V. Malkova, A.L. Kholodov, S.S. Marchenko, N.G. Moskalenko, D.O. Sergeev, N.G. Ukrainstseva, A.A. Abramov, D.A. Gilichinsky and A.A. Vasilev, 2010b. Thermal state of permafrost in Russia. *Permafrost and Periglacial Processes*, 21:136-155.

Romanovsky, V.E., S.L. Smith, H.H. Christiansen et al. 2012. Permafrost. In: *State of the Climate 2011*. Bulletin of the American Meteorological Society, 93:S137-S138.

Romanovsky, V.E., S.L. Smith, H.H. Christiansen, N.I. Shiklomanov, D.S. Drozdov, N.G. Oberman, A.L. Kholodov and S.S. Marchenko, 2013. Permafrost. Arctic Report Card: Update for 2013. NOAA.

Romanovsky, V.E., A.L. Kholodov, S.L. Smith, H.H. Christiansen, N.I. Shiklomanov, D.S. Drozdov, G.V. Malkova, N.G. Oberman and S.S. Marchenko, 2014. Terrestrial permafrost. *Bulletin of the American Meteorological Society*, 95:S139-S141.

Romanovsky, V.E., S.L. Smith, H.H. Christiansen, N.I. Shiklomanov, D.A. Strelets, D.S. Drozdov, G.V. Malkova, N.G. Oberman, A.L. Kholodov and S.S. Marchenko, 2015. Terrestrial permafrost. *Bulletin of the American Meteorological Society*, 96:S139-S141.

Rongved, J.L. and A. Instanes, 2012. Foundation engineering in Svalbard, 1950-2012. *Proceedings of the Tenth International Conference on Permafrost*, 25-29 June, Salekhard, Russia, 1:341-346.

Routh, J., G. Hugelius, P. Kuhry, T. Filley, P. Kaislahti, M. becher and P. Crill, 2014. Multi-proxy study of soil organic matter dynamics in permafrost peat deposits reveal vulnerability to climate change in the European Russian Arctic. *Chemical Geology*, 368:104-117.

Saito, K., 2008. Arctic land hydro-thermal sensitivity under warming: idealized off-line evaluation of physical terrestrial scheme in global climate model. *Journal of Geophysical Research: Atmosphere*, 113:D21106, doi:10.1029/2008JD009880.

Sannel, A.B.K. and P. Kuhry, 2011. Warming-induced destabilization of peat plateau/thermokarst lake complexes. *Journal of Geophysical Research*, 116:G03035, doi:10.1029/2010JG001635.

Sannikov, G.S., 2012. Changes in the areas of thermokarst lakes in the territory of the Bovanenkovo Field (Yamal) over the last 20 years. *Proceedings of the Tenth International Conference on Permafrost*, 25-29 June, Salekhard, Russia, 2:367-370.

Schirrmeister, L., D. Froese, V. Tumskoy, G. Grosse and S. Wetterich, 2013. Yedoma: late Pleistocene ice-rich syngenetic permafrost of Beringia. In: *Encyclopedia of Quaternary Science*. Second Edition, pp. 542-552.

Schneider von Deimling, T., G. Grosse, J. Strauss, J. Boike, L. Schirrmeister, A. Morgenstern, S. Schaphoff and M. Meinshausen, 2014. Observation-based modelling of permafrost carbon fluxes with accounting for deep carbon deposits and thermokarst activity. *Biogeosciences Discussions*, 11:16599-166643.

Schuur, E.A.G., J. Bockheim, J. Canadell, E. Euskrichen, C.B. Field, S.V. Goryachkin, S. Hagemann, P. Kuhry, P. Lafleur, H. Lee, G. Mazhitova, F.E. Nelson, A. Rinke, V.E. Romanovsky, N. Shiklomanov, C. Tarnocai, S. Venevsky, J.G. Vogel and S.A. Zimov, 2008. Vulnerability of permafrost carbon to climate change: implications for the global carbon cycle. *BioScience*, 58:701-714.

Schuur, E.A.G., A.D. McGuire, C. Schädel, G. Grosse, J.W. Harden, D.J. Hayes, G. Hugelius, C.D. Koven, P. Kuhry, D.M. Lawrence, S.M. Natali, D. Olefeldt, V.E. Romanovsky, K. Schaefer, M. Turetsky, C. Treat and J.E. Vonk, 2015. Climate change and the permafrost carbon feedback. *Nature*, 520:171-179.

Séjourné, A., F. Costard, A. Fedorov, J. Gargani, J. Skorve, M. Masse and D. Mege, 2015. Evolution of the banks of thermokarst lakes in Central Yakutia (Central Siberia) due to retrogressive thaw slump activity controlled by insolation. *Geomorphology*, 241:31-40.

Seto, T.C., L.U. Arenson and G. Cousineau, 2012. Vulnerability to climate change assessment for a highway constructed on permafrost. In: *Cold Regions Engineering 2012, Sustainable Infrastructure Development in a Changing Cold Environment*. pp. 515-524. American Society of Civil Engineers.

Shiklomanov, N.I. and D.A. Streletskiy, 2013. Effect of cryosphere changes on Siberian infrastructure. In: Groisman, P.Y. and G. Gutman (eds.), *Environmental Changes in Siberia: Regional Changes and their Global Consequences*. Pp. 155-170. Springer.

Shiklomanov, N.I., D.A. Streletskiy and F.E. Nelson, 2012. Northern Hemisphere component of the global Circumpolar Active Layer Monitoring (CALM) program. Proceedings of the Tenth International Conference on Permafrost, 25-29 June, Salekhard, Russia, 1:377-382.

Shiklomanov, N.I., D.A. Streletskiy, J.D. Little and F.E. Nelson, 2013. Isotropic thaw subsidence in undisturbed permafrost landscapes. *Geophysical Research Letters*, 40:6356-6361.

Shkol'nik, I.M., E.D. Nadyozhina, T.V. Pavlova, E.K. Molkentin and A.A. Semioshina, 2010. Snow cover and permafrost evolution in Siberia as simulated by the MGO regional climate model in the 20th and 21st centuries. *Environmental Research Letters*, 5:015005.

Shkol'nik, I.M., E.D. Nadyozhina, T.V. Pavlova, E.I. Khlebnikova, A.A. Semioshina, E.K. Molkentin and E.N. Stafeeva, 2012. Simulation of the regional features of the seasonal thawing layer in the Siberian permafrost zone. *Earth's Cryosphere*, 16:52-59.

Short, N., B. Brisco, N. Couture, W. Pollard, K. Murnaghna and P. Budkewitsch, 2011. A comparison of TerraSAR-X, RADARSAT-2 and ALOS-PALSAR interferometry for monitoring permafrost environments, case study from Herschel Island, Canada. *Remote Sensing of Environment*, 115:3491-3506.

Shur, Y. and D. Goering, 2009. Climate change and foundations of buildings in permafrost regions. In: Margesin, R. (ed.), *Permafrost Soils. Soil Biology*, 16. pp. 251-260.

Shur, Y.L. and M.T. Jorgenson, 2007. Patterns of permafrost formation and degradation in relation to climate and ecosystems. *Permafrost and Periglacial Processes*, 18:7-19.

Shur, Y., A. Vasiliev, M. Kanevskiy, V. Maksimov, S. Pokrovsky and V. Zaikanov, 2002. Shore erosion in Russian Arctic. *Cold Regions Engineering*. pp. 736-747. doi: 10.1061/(40621(254)63).

Shur, Y., M. Kanevskiy, T. Jorgenson, M. Dillon, E. Stephani, M. Bray and D. Fortier, 2012. Permafrost degradation and thaw settlement under lakes in Yedoma environment. Proceedings of the Tenth International Conference on Permafrost, 25-29 June, Salekhard, Russia, 1:383-388.

Sjöberg, Y., G. Hugelius and P. Kuhry, 2013. Thermokarst lake morphometry and erosion features in two peat plateau areas of northeast European Russia. *Permafrost and Periglacial Processes*, 24:75-81.

Slater, A.G. and D.M. Lawrence, 2013. Diagnosing present and future permafrost from climate models. *Journal of Climate*, 26:5608-5623.

Sloan, H.A. and W.H. Pollard, 2012. Vegetation patterns of retrogressive thaw slumps, Herschel Island, southern Beaufort Sea, Yukon Territory, Canada. Proceedings of the Tenth International Conference on Permafrost, 25-29 June, Salekhard, Russia, 1:389-393.

Solov'ev, P.A., 1962. *Alasniy relief Tsentral'noy Yakutii I ego proiskhozhdenie* [Alas relief of Central Yakutia and its origin]. In: *Mnogoletnemyozlye porody i soputstvuyushchie im yavleniya na territorii Yakutskoy ASSR* [Permafrost and related features in Central Yaku-tia]. pp. 38-54. Academy of Sciences of the USSR Press. (In Russian)

Smith, S.L. and M. Ednie, 2015. Ground thermal data collection along the Alaska Highway easement (KP 1559-1895) Yukon, summer 2014. *Geological Survey of Canada Open File* 7762.

Smith, L.C., Y. Sheng, G.M. MacDonald and L.D. Hinzman, 2005. Disappearing Arctic lakes. *Science*, 308:1429, doi:10.1126/science.1108142.

Smith, S.L., S.A. Wolfe, D.W. Riseborough and F.M. Nixon, 2009a. Active-layer characteristics and summer climatic indices, Mackenzie Valley, Northwest Territories, Canada. *Permafrost and Periglacial Processes*, 20:201-220.

Smith, S.L., D.W. Riseborough, F.M. Nixon, J. Chartrand, C. Duchesne and M. Ednie, 2009b. Data for Geological Survey of Canada active layer monitoring sites in the Mackenzie valley, NWT. *Geological Survey of Canada Open File* 6287.

Smith, S.L., V.E. Romanovsky, A.G. Lewkowicz, C.R. Burn, M. Allard, G.D. Clow, K. Yoshikawa and J. Throop, 2010. Thermal state of permafrost in North America - A contribution to the International Polar Year. *Permafrost and Periglacial Processes*, 21:117-135.

Smith, S.L., J. Throop and A.G. Lewkowicz, 2012. Recent changes in climate and permafrost temperatures at forested and polar desert sites in northern Canada. *Canadian Journal of Earth Sciences*, 49:914-924.

Smith, S.L., D.W. Riseborough, M. Ednie and J. Chartrand, 2013. A map and summary database of permafrost temperatures in Nunavut, Canada. *Geological Survey of Canada Open File* 7393.

Smith, S.L., A.G. Lewkowicz, C. Duchesne and M. Ednie, 2015. Variability and change in permafrost thermal state in northern Canada. *GEOQuébec 2015. Proceedings 68th Canadian Geotechnical Conference and 7th Canadian Conference on Permafrost*.

Stephani, E., D. Fortier, Y. Shur, R. Fortier and G. Doré, 2014. A geosystems approach to permafrost investigations for engineering applications, an example from a road stabilization experiment, Beaver Creek, Yukon, Canada. *Cold Regions Science and Technology*, 100:20-35.

Streletskiy, D.A., N.I. Shiklomanov and V.A. Grebenetz, 2012a. Climate warming-induced changes in bearing capacity of permafrost in the north of West Siberia. *Earth's Cryosphere*, XVI:22-32. (In Russian)

Streletskiy, D.A., N.I. Shiklomanov and E. Hatleberg, 2012b. Infrastructure and a changing climate in the Russian Arctic: A geographic impact assessment. Proceedings of the Tenth International Conference on Permafrost, 25-29 June, Salekhard, Russia, 1:407-414.

Streletskiy, D.A., N.I. Shiklomanov and F.E. Nelson, 2012c. Permafrost, infrastructure, and climate change: A GIS-based landscape approach to geotechnical modelling. *Arctic, Antarctic, and Alpine Research*, 44:368-380.

Sueyoshi, T., K. Saito, S. Miyazaki, J. Mori, T. Ise, H. Arakida, R. Suzuki, A. Sato, Y. Iijima, H. Yabuki, H. Ikawa, T. Ohta, A. Kotani, T. Hajima, H. Sato, T. Yamazaki and A. Sugimoto, 2016. The GRENE-TEA Model Intercomparison Project (GTMIP) stage 1 forcing dataset. *Earth System Science Data*, 8:1-14.

Taylor, A.E., S.R. Dallimore, P.R. Hill, D.R. Issler, S. Blasco and F. Wright, 2013. Numerical model of the geothermal regime on the Beaufort Shelf, arctic Canada since the Last Interglacial. *Journal of Geophysical Research: Earth Surface*, 118:2365-2379.

Throop, J., A.G. Lewkowicz and S.L. Smith, 2012. Climate and ground temperature relations at sites across the continuous and discontinuous permafrost zones, northern Canada. *Canadian Journal of Earth Sciences*, 49:865-876.

Tom, S. and R. Bronen, 2012. Climate change and community-based relocation, Newtok, Alaska. Presentation at the Community Relocation Workshop, Bougainville, Papua New Guinea, September 2012.

Transportation Association of Canada, 2010. *Guidelines for Development and Management of Transportation Infrastructure in Permafrost Regions*. Transportation Association of Canada (TAC), Ottawa.

Trofaiher, A.M., A. Bartsch, W.G. Rees and M.O. Leibman, 2013. Assessment of spring floods and surface water extent over the Yamalo-Nenets Autonomous District. *Environmental Research Letters*, 8:045026.

Tweedie, C.E., A. Aguirre, R. Cody, S. Vargas and J. Brown, 2012. Spatial and temporal dynamics of erosion along the Elson Lagoon coastline near Barrow, Alaska (2002-2011). Proceedings of the Tenth International Conference on Permafrost, 25-29 June, Salekhard, Russia, 1:425-430.

Ukrainseva, N.G., D.S. Drozdov, Y.V. Korostelev and T.A. Korobova, 2012. Terrain indicator approach and results for permafrost studies. Proceedings of the Tenth International Conference on Permafrost, 25-29 June, Salekhard, Russia, 2:463-468.

Ukrainseva, N., M. Leibman, I. Streletskaya and T. Mikhaylova, 2014. Geochemistry of plant-soil-permafrost system on landslide-affected slopes, Yamal, Russia as an indicator of landslide age. In: Shan, W. et al. (eds.), *Landslides in Cold Regions in the Context of Climate Change*. pp. 107-131. Springer.

Ulrich, M., G. Grosse, J. Strauss and L. Schirrmeister, 2014. Quantifying wedge-ice volumes in yedoma and thermokarst basin deposits. *Permafrost and Periglacial Processes*, 25:151-161.

Urban, M., M. Forkel, J. Eberle, C. Huettich, C. Schmullius and M. Herold, 2014. Pan-Arctic climate and land cover trends derived from multivariate and multi-scale analyses (1981-2012). *Remote Sensing*, 6:2296-2316.

van Everdingen, R. (ed.), 1998. *Multi-language glossary of permafrost and related ground-ice terms*. International Permafrost Association.

van Everdingen, R. (ed.), 2005. Multi-language glossary of permafrost related ground-ice terms. 1998 Revised. International Permafrost Association.

Vasil'chuk, Y.K., 2013. Syngenetic ice wedges: cyclical formation, radiocarbon age and stable-isotope records. *Permafrost and Periglacial Processes*, 24:82-93.

Vasiliev, A.A., R.S. Shirokov, G.E. Oblogov and I.D. Streletskaia, 2011. Coastal dynamics of the Western Yamal. *Earth's Cryosphere*, XV:63-65. (In Russian)

Vaughan, D.G., J.C. Comiso, I. Allison, J. Carrasco, G. Kaser, R. Kwok, P. Mote, T. Murray, F. Paul, J. Ren, E. Rignot, O. Solomina, K. Steffen and T. Zhang, 2013. Observations: cryosphere. In: Stocker, T.F., D. Qin, G.-K. Plattner, M. Tignor, S.K. Allen, J. Boschung, A. Nauels, Y. Xia, V. Bex and P.M. Midgley (eds.), *Climate Change 2013: The Physical Science Basis. Contribution of Working Group I to the Fifth Assessment Report of the Intergovernmental Panel on Climate Change*. Cambridge University Press.

Vincent, W.F., M. Lemay, M. Allard and B.B. Wolfe, 2013. Adapting to permafrost change: a science framework. *Eos, Transactions, American Geophysical Union*, 94:373-375.

Walker, H.J. and M.T. Jorgenson, 2011. Tour of the Colville River Delta. In: Jorgenson, M.T. (ed.). *Coastal Region of Northern Alaska. Guidebook to Permafrost and Related Features. Guidebook 10, Part 4*, pp. 85-135. Alaska Division of Geological and Geophysical Surveys.

Walker, D.A. and J. Pierce (eds.), 2015. *Rapid Arctic Transitions due to Infrastructure and Climate (RATIC): A contribution to ICARP III*. Alaska Geobotany Center, University of Alaska Fairbanks.

Walker, D.A., P.J. Webber, E.F. Binnian, K.R. Everett, N.D. Lederer, E.A. Nordstrand and M.D. Walker, 1987. Cumulative impacts of oil fields on northern Alaskan landscapes. *Science*, 238:757-761.

Walker, D.A., M.K. Raynolds, M. Buchhorn and J.L. Peirce (eds.), 2014. *Landscape and permafrost change in the Prudhoe Bay oilfield, Alaska*. Alaska Geobotany Center Report No. AGC 14-01. University of Alaska Fairbanks, Laska.

Warren, F.J. and D.S. Lemmen (eds.), 2014. *Canada in a Changing Climate: Sector Perspectives on Impacts and Adaptation*. Government of Canada, Ottawa.

Westermann, S., T.V. Schuler, K. Gisnås and B. Etzelmüller, 2013. Transient thermal modeling of permafrost conditions in Southern Norway. *The Cryosphere*, 7:719-739.

Westermann, S., C. Duguay, G. Grosse and A. Kääb, 2015a. Remote sensing of permafrost and frozen ground. In: Tedesco, M. (ed.), *Remote Sensing of the Cryosphere*. Wiley Blackwell.

Westermann, S., T. Østby, K. Gisnås, T. Schuler and B. Etzelmüller, 2015b. A ground temperature map of the North Atlantic permafrost region based on remote sensing and reanalysis data. *The Cryosphere*, 9:1303-1319.

Westermann, S., B. Elberling, S. Højlund Pedersen, M. Stendel, B. Hansen and G. Liston, 2015c. Future permafrost conditions along environmental gradients in Zackenberg, Greenland. *The Cryosphere*, 9:719-735.

Westermann, S., M. Langer, J. Boike, M. Heikenfeld, M. Peter, B. Etzelmüller and G. Krinner, 2016. Simulating the thermal regime and thaw processes of ice-rich permafrost ground with the land-surface model CryoGrid 3. *Geoscientific Model Development*, 9:523-546.

Xu, L., R.B. Myneni, F.S. Chapin, T.V. Callaghan, J.E. Pinzon, C.J. Tucker, Z. Zhu, J. Bi, P. Ciais, H. Tommervik, E.S. Euskirchen, B.C. Forbes, S.L. Piao, B.T. Anderson, S. Ganguly, R.R. Nemani, S.J. Goetz, P.S.A. Beck, A.G. Bunn, C. Cao and J.C. Stroeve, 2013. Temperature and vegetation seasonality diminishment over northern lands. *Nature Climate Change*, 3:581-586.

Yarnal, B., 1998. Integrated regional assessment and climate change impacts in river basins. *Climate Research*, 11:65-74.

Yermokhina, K.A. and E.G. Myalo, 2012. Phytoindicators of landslide disturbances in the central Yamal. *Proceedings of the Tenth International Conference on Permafrost*, 25-29 June, Salekhard, Russia, 1:531-536.

Zhang, Y., X. Wang, R. Fraser, I. Olthof, W. Chen, D. McLennan, S. Ponomarenko and W. Wu, 2013. Modelling and mapping climate change impacts on permafrost at high spatial resolution for an Arctic region with complex terrain. *The Cryosphere*, 7:1121-1137.

Zhiltcova, E.L. and O.A. Anisimov, 2013. Empirical-statistical modelling of vegetation zonation under climate change in Russia. In: Izrael, Yu (ed.), *Problems of Ecological Modelling and Ecosystem Monitoring*, pp. 360-374. Planeta. (In Russian)

5. Arctic sea ice

LEAD AUTHORS: DAVID G. BARBER, WALTER N. MEIER, SEBASTIAN GERLAND, C.J. MUNDY, MARIKA HOLLAND, STEFAN KERN, ZHIJUN LI, CHRISTINE MICHEL, DONALD K. PEROVICH, TAKESHI TAMURA

CONTRIBUTING AUTHORS: JØRGEN BERGE, JEFF BOWMAN, JØRGEN S. CHRISTIANSEN, JENS K. EHN, STEVE FERGUSON, MATS A. GRANSKOG, TAKASHI KIKUCHI, HARRI KUOSA, BONNIE LIGHT, NINA LUNDHOLM, IGOR A. MELNIKOV, CHRIS POLASHENSKI, LARS H. SMEDSRUD, GUNNAR SPREEN, MARK TSCHUDI, TIMO VIHMA, MELINDA WEBSTER, LUJUN ZHANG

Coordinating lead authors shown in bold

Contents

Key Findings	104
5.1 Introduction	105
5.2 Changes in sea-ice extent, concentration, and thickness	105
5.2.1 Recent changes in sea-ice extent and concentration	105
5.2.2 Observed changes in sea-ice thickness	107
5.2.3 Projected changes in sea-ice extent, concentration and thickness	109
5.2.4 Comparison between model results and observations	110
5.2.5 Uncertainties and gaps in knowledge	110
5.3 Changes in sea-ice thermodynamics, age and dynamic processes	112
5.3.1 Sea-ice thermodynamic processes	112
5.3.2 Ice age	115
5.3.3 Sea-ice dynamic processes	117
5.3.4 Uncertainties and gaps in knowledge	119
5.4 Biological implications of changing sea ice	119
5.4.1 Impacts on the sea-ice ecosystem	120
5.4.2 Impacts on pelagic ecosystems and food-web transfers	122
5.4.3 Impacts on fish and higher trophic levels	125
5.4.4 Uncertainties and gaps in knowledge	126
References	127

Key Findings

- Arctic sea-ice extent and thickness are continuing to decline, but with high year-to-year variability. The past five years include a record low minimum extent in 2012, followed by the second lowest minimum extent in 2016 and a record low maximum extent in 2016.
- There is increasing evidence for more open water beyond the expected autumn period. The extended periods of open water are dominated by the ice albedo feedback in the Pacific sector, Hudson and Baffin Bay areas, and by ocean heat fluxes in the Atlantic sector of the Arctic.
- New sensors and technologies are providing critical insights into changes in the ice cover. These include continued investigation of thickness and thickness uncertainties from CryoSat-2, new application of SMOS data for thin ice and snow on ice, continued snow and ice observations from Operation IceBridge, and continuing development of ICESat-2 toward a late 2017 launch.
- The CMIP5 model projections for sea ice still lag the rates of decline in both extent and thickness, but are in better agreement with observations than the CMIP3 model runs. There is large variability in model projections and in the short to medium term (up to decadal), natural variability can compensate for anthropogenic greenhouse gas forcing. This suggests that multi-year periods with little or no net ice loss may occur through the rest of the century, although long-term forcing is expected to dominate.
- Ice-related thermodynamic processes are changing. Spring snow cover has thinned in the western Arctic and the greatest thinning is in the Beaufort and Chukchi seas, due to later freeze-up and more first-year ice. There is also a trend towards earlier melt pond formation, particularly north of 80°N. More solar heat is absorbed in the ice-ocean system by first-year ice than multi-year ice – possibly up to 50% more.
- Although the Arctic sea ice is becoming younger, there have been recent regional increases in multi-year ice, suggesting increased interannual variability in recent years. The shift to younger sea ice has several consequences. These include effects on physical sea ice processes, photochemical exchanges with the atmosphere, formation of melt ponds, and the sea-ice energy balance. Mechanical sea ice properties are also being affected, with implications for shipping and ice-associated habitats.
- The Arctic sea-ice circulation has changed and the Beaufort Gyre and Transpolar Drift have strengthened. The speed at which sea ice is moving is increasing almost everywhere in the Arctic Basin because ice strength is decreasing as the ice cover becomes thinner and less compact.
- Evidence for the loss of sea ice biodiversity in the central Arctic Ocean is linked to the decline in thick multi-year ice and its stable environment and to the increasing dominance of seasonal first-year ice. Declining ice cover is causing range contractions for endemic Arctic species and northward extensions for sub-Arctic species. The latter is documented at all trophic levels including primary and secondary producers, fish and marine mammals.
- Thinning ice, decreasing snow cover, and spatial and temporal expansion of open waters provide for increasing primary production (through more favorable light conditions), while stronger stratification due to ice melt and warming are having the opposite effect. The direction and magnitude of change in primary production depends on the outcome of these contrasting effects. There is expected to be a wide range of regional responses.
- Throughout the Arctic, the prolonged open water period due to earlier ice melt and later ice formation is shifting the phenology of the phytoplankton bloom from a unimodal to a bimodal bloom pattern. Changes in sea ice and open water areas are expected to modify the location of areas of high productivity where fish, seabirds and marine mammals congregate, affecting traditional and commercial harvest. The occurrence of toxin-producing algal blooms is an emerging concern throughout the Arctic, especially given the recent extensive observations of algal toxins in marine mammals.

5.1 Introduction

The recent decades have been a time of extraordinary change in the Arctic. Sea ice has experienced unprecedented variability in both the rates and magnitude of change in extent, area, thickness, spatial distribution and most aspects of the temporal and spatial variability of processes controlling snow and frost flower distribution on sea ice. There has been a shift from an environment dominated by multi-year sea ice to one dominated by first-year sea ice (Nghiem et al., 2007; Kwok et al., 2009; Maslanik et al., 2011; Comiso, 2012; Parkinson and Comiso, 2013). Coinciding with this change toward a younger ice cover, and in combination with recent reductions in sea ice extent there is an overall thinning of the Arctic ice pack (Kwok et al., 2009; Kwok and Cunningham, 2015; Lindsay and Schweiger, 2015) with young saline forms providing increased geochemical exchanges across the ocean-ice-atmosphere interface (Nghiem et al., 2012; Barber et al., 2015). Ice motion velocities have been increasing (Rampal et al., 2009; Spreen et al., 2011; Kwok et al., 2013), due primarily to changes in ice thickness and an overall reduction in the mechanical strength of sea ice with slightly increased wind velocities also playing a role. The impacts of these changes in the areal extent, thickness and circulation of sea ice are important throughout all components of the physical, biological, and biogeochemical aspects of the Arctic climate system. This chapter provides an update of current understanding of the processes controlling the forcing of dynamic and thermodynamic processes operating across the ocean-ice-atmosphere interface. This is followed by an examination of the biological implications of these changes in the ice-covered marine environment.

5.2 Changes in sea-ice extent, concentration, and thickness

5.2.1 Recent changes in sea-ice extent and concentration

The decline in Arctic sea-ice extent and concentration has continued, but with substantial year-to-year variability. The most significant change in the sea-ice cover in the Arctic Ocean continues to be the transition from one dominated by old, multi-year ice to one dominated by younger, first-year ice, albeit with significant interannual variability. The loss in extent of older ice types has been documented using various independent methods (e.g. Comiso, 2012; Kwok and Cunningham, 2015; Tschudi et al., 2015; Lindell and Long, 2016). Sea-ice age is addressed in Section 5.3.

5.2.1.1 Changes in space and time

Several authors have reported updated trends for sea-ice extent and area, including Cavalieri and Parkinson (2012) and Meier et al. (2014a), both of which use the NASA Team algorithm for estimates. There are also the related studies of Parkinson (2014a), which examine the hemispheric asymmetry of changes in sea-ice cover. There are several other sea-ice algorithms in addition to those of the NASA Team. Ivanova et al. (2015) compared 11 sea-ice concentration retrieval algorithms over the period from 1979 to 2012. They found that area and

extent computed from sea-ice concentrations using the suite of 11 retrieval algorithms vary by up to 1.5 million km² and 1.0 million km², respectively, but that the linear trends agree reasonably well. Using a 5-algorithm ensemble mean, the trend in annual mean sea-ice area reported by Ivanova et al. (2015) for 1979–2012 was -56,000 km²/y. This indicates an acceleration in sea-ice decline compared to the -49,600 km²/y reported by Cavalieri and Parkinson (2012) for 1979–2010. Using the NASA Team algorithm, Meier et al. (2014a) reported a trend of -52,600 km²/y for the period 1979–2013, which also indicates a slight recent acceleration in the decline.

The NASA Team algorithm product is updated regularly, including a near-real-time version produced by the National Snow and Ice Data Center (NSIDC); both products are archived at NSIDC and areas and extent values are available through the NSIDC Sea Ice Index (Fetterer et al., 2016). The values are provided here because they are widely quoted in the science community, but are not the only source of estimates. Another widely used source of sea ice information is available from the European Meteorological Satellite (EUMETSAT) program Ocean and Sea Ice Satellite Application Facility (OSI-SAF), which uses a combination of two algorithms: the Bristol and Bootstrap algorithms (Eastwood, 2014). The OSI-SAF estimates for updated trends in ice extent through 2015 are also included here (Figure 5.1); the range between the NSIDC Sea Ice Index and the OSI-SAF values suggests an uncertainty range for the extent estimates. The trends from both sources are in good agreement and the uncertainties in the trends are likely to be largely a function of internal variability rather than observational uncertainty, although sensor intercalibration may also be a factor.

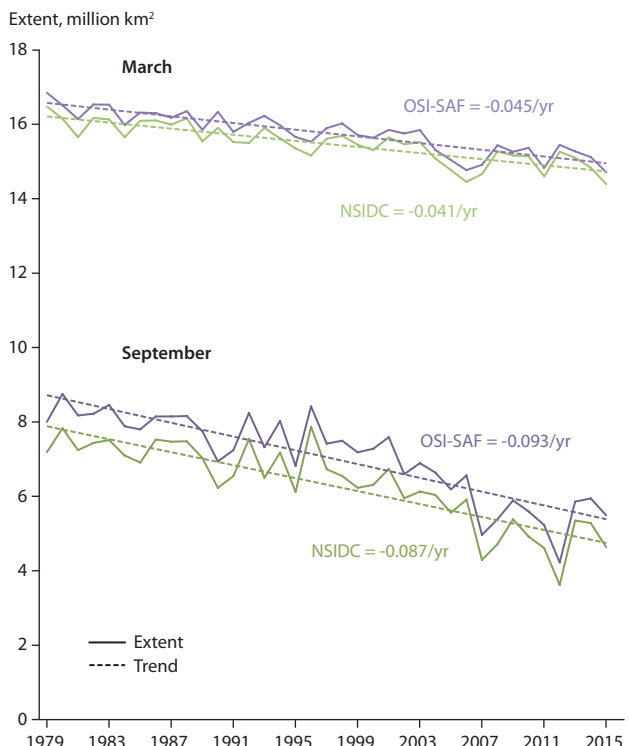


Figure 5.1 March and September Arctic sea-ice extent from the National Snow and Ice Data Center (NSIDC) and the Ocean and Sea Ice Satellite Application Facility (OSI-SAF) and linear trend lines (data source: NSIDC Sea Ice Index and OSI-SAF).

Box 5.1 Sea ice conditions 2016–2017

Arctic sea ice experienced record low conditions throughout 2016, with record low extents in every month from January through June, except for March (which was the second lowest on record). According to NSIDC (<http://nsidc.org/arcticseacenews/>), the maximum extent of 14.52 million km² occurred on 24 March and at the time was the lowest in the passive microwave satellite record. Unfavorable melt conditions during the summer slowed ice loss and led to a 2016 minimum extent on 10 September of 4.14 million km², tied for the second lowest minimum on record. Following the minimum, freeze-up was slow and extents were at or near record lows through the 2016–2017 winter, peaking at 14.42 million km² on 7 March, replacing 2016 as the lowest in the satellite record. Since the maximum, extents remained low into the early summer of 2017 (Figure 5.2).

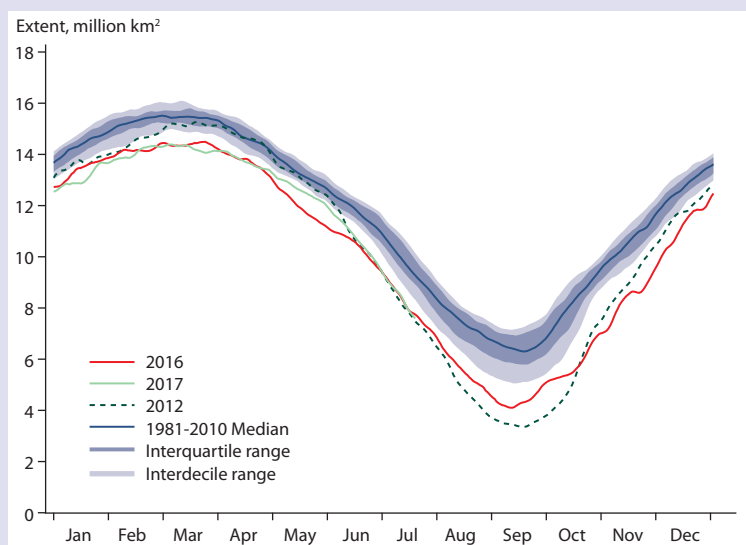


Figure 5.2 Daily Arctic sea-ice extent for 2016–2017 and the record low year of 2012 compared to the 1981–2010 average and two standard deviation range, based on passive microwave data (data source: NSIDC Sea Ice Index).

The mean annual trend values do not capture the temporal or regional variability in the trends, so the trends for March (maximum extent month) and September (minimum extent month) are included here. It is clear that summer trends are much stronger than winter trends (Perovich et al., 2015). In absolute terms (km²/y), the September magnitude is more than double that for March. In addition, the summer trend shows indications of acceleration in recent years with the trend steepening. While summer shows the strongest negative trends, as noted by Cavalieri and Parkinson (2012) and Meier et al. (2014a), all months continue to show statistically significant (>95% confidence level) declines in northern hemisphere extent. Remarkably, while many record low extents have been seen in recent years across all months (including almost every

month in the first half of 2016 – see Box 5.1), the last record high extent in the satellite data occurred in October 1986 (Parkinson and DiGirolamo, 2016).

The downward trend in ice extent has been seen across nearly all ice-covered sectors with almost all regions showing statistically significant declines, with the exception of the Bering Sea during winter (Figure 5.3). The Bering Sea has experienced relatively heavy ice winters in recent years, although 2013–2016 marked a break in the recent trend, with anomalously low ice extents. The Beaufort and Chukchi seas have seen extreme summer ice loss, with trends in September ice extent through 2015 on the order of -20% per decade (Figure 5.3).

Trends have been observed towards an earlier onset of ice surface melt and a longer melt season (i.e. the period between

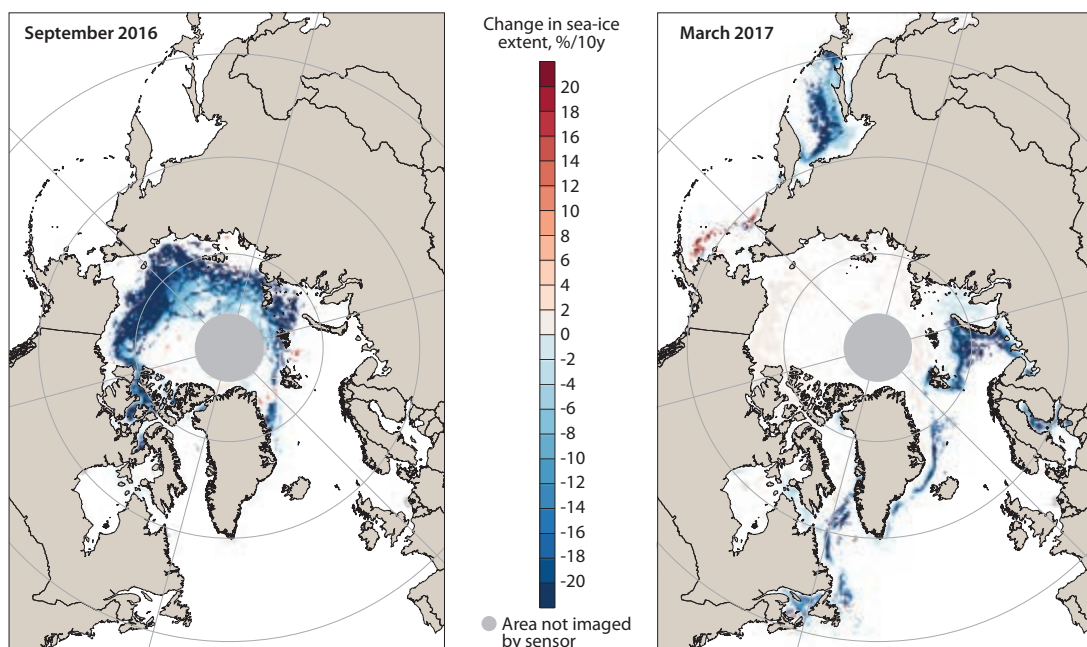


Figure 5.3 Linear trends in sea-ice extent (relative to the 1981–2010 average) for September 2016 and March 2017. Based on the NASA Team algorithm and the NSIDC Sea Ice Index (Fetterer et al., 2016).

the onset of surface melt and surface freezing) (e.g. Bliss and Anderson, 2014; Stroeve et al., 2014a) and are generally in agreement with changes in the length of the open water season (Parkinson, 2014b). Arctic-wide, on average the melt season has lengthened by 5 days per decade; some regions are experiencing even larger increases in melt season length (up to 11 days per decade), particularly in the coastal seas. The increased melt season length is due to later freeze up more than to earlier melt onset; the trend in melt onset is relatively small at 1 to 3 days per decade earlier for most regions. However, earlier melt onset is more important than later freeze-up because it occurs at a time of the year with near 24-hour daylight and thus results in much greater input of solar radiation to the sea ice (Perovich et al., 2011).

Landfast ice grows from the coast, particularly over the shallow shelf regions, and does not drift with the winds and currents. It predominates along the shallow shelf regions of the Siberian coast, but is also found along most coastal regions in the Arctic and throughout the Canadian Arctic Archipelago. Landfast ice distribution and thickness are an important indicator of Arctic climate change because landfast ice is not affected by drift or export. Using sea ice charts for the period 1976–2007, Yu et al. (2014) calculated that the overall Arctic landfast ice area decreased by about 7% per decade over this period. This corresponds to a loss of $\sim 123,000 \text{ km}^2$ per decade, which is about 20–25% of the observed decrease in total ice between 1979 and 2012 (Ivanova et al., 2015).

5.2.1.2 Open water, young ice and frost flowers

The changes in sea ice area and extent are directly related to observations of increasing fractional cover of open water, the formation of young sea ice (ice generally thinner than 30 cm) and the presence of frost flowers on sea ice. These components of the icescape are becoming increasingly important due to their increased coverage both spatially and temporally and to their strong contributions to sensible heat, latent heat and chemical fluxes across the ocean-ice-atmosphere interface. Barber et al. (2015) found statistically significant trends in open-water fraction over the passive microwave record (1979–2010) for each month of the annual cycle. This implies an increasing open-water fraction (and by extension young sea ice) throughout the annual cycle. The trends show a quadratic fit, illustrating strong feedbacks that to a large extent slow the formation of ice in autumn and, to a lesser extent, hasten the decay of sea ice in summer – both causing an increase in open water fraction even in winter. The open-water fraction also plays a significant but as yet poorly defined role in the observed increase in exchange of heat and moisture within the planetary boundary layer (see Section 5.3.3.2). These open-water trends occurred in several regions: the Pacific Sector of the Arctic Ocean including Canada Basin and the Beaufort, Chukchi and East Siberian seas; the Canadian Arctic Archipelago; Baffin Bay and Hudson Bay; and the Barents and Kara seas. The results confirm earlier studies showing that the changes in the Barents and Kara seas are primarily forced by winter ocean heat fluxes (e.g. Polyakov et al., 2010; Dmitrenko et al., 2014), whereas changes observed in the other sectors appear to be summer/autumn related and are primarily atmospherically forced (e.g. Barber et al., 2015; Perovich et al., 2015). The area and extent of young ice cover also increased in various sectors of the Arctic

marginal ice zone over this period. Results are beginning to show the importance of these young ice types to the exchange of heat and mass within the ocean and atmospheric boundary layer, especially the increased role played by highly saline frost flowers on both inorganic and organic chemical fluxes across the ocean-ice-atmosphere interface (e.g. Nghiem et al., 2012). This is further addressed in Section 5.4.

5.2.2 Observed changes in sea-ice thickness

The ESA CryoSat-2 sensor (a radar altimeter) is currently the main source for satellite-based sea ice thickness information, continuing the record from the earlier NASA ICESat laser altimeter. CryoSat-2 and ICESat estimate the elevation of the sea ice above the ocean surface, which is denoted the ‘freeboard’. Freeboard estimates are converted to total thickness using assumptions regarding sea-ice density and properties of the overlying snow cover. The laser altimeter on ICESat actually obtains returns from the top of the snow cover and thus retrieves a snow+ice freeboard; this means that snow must be subtracted from the ICESat measurement before converting freeboard to thickness. However, snow depth/density data are lacking, resulting in potential biases in the estimates (King et al., 2015).

After the first work of Laxon et al. (2013) using CryoSat-2 data to derive sea-ice thickness and volume for the Arctic, Zygmuntowska et al. (2014), Kurtz et al. (2014), Kwok and Cunningham (2015), and Tilling et al. (2015) have contributed to this topic. However, the CryoSat-2 time series is still very short (seven winters) and covers a period with variable summer melt and ice drift conditions (Kwok and Cunningham, 2015). Thus, the trends in ice thickness and volume determined by these authors by extending the CryoSat-2 time series back in time with earlier estimates are quite different. While Laxon et al. (2013) suggested a continued substantial decline in ice volume, Kwok and Cunningham (2015) found no trend could be identified for the short CryoSat-2 time series – especially with the increase in ice volume in winter 2013/14 compared to preceding winters (Figure 5.4). They also found that for the combined ICESat-CryoSat-2 record, the decline in Arctic sea-ice volume had weakened compared to the ICESat time series alone (2003–2008) or in combination with the sea-ice thickness estimates from submarine upward-looking sonar (ULS) data, because the ICESat record is strongly weighted by conditions after the record summer melt in 2007. Tilling et al. (2015) confirmed the results of Kwok and Cunningham (2015) regarding the lack of an ongoing decline in sea ice volume in the CryoSat-2 record.

The L-Band radiometers, such as the ESA SMOS (Soil Moisture and Ocean Salinity) sensor, and on NASA instruments: the SMAP (Soil Moisture Active Passive) and Aquarius (which ceased operations in June 2015) missions allow the retrieval of sea-ice thickness distribution based on a completely different and hence independent method than spaceborne altimetry, although only SMOS has been applied to date (Kaleschke et al., 2012; Huntemann et al., 2014; Tian-Kunze et al., 2014). However, ice thickness retrieval based on SMOS data requires close to 100% SIC (sea ice concentration) and cold conditions and is largely limited to thin sea ice (0.3–0.5 m maximum); the maximum retrievable ice thickness can be higher for low-salinity sea ice such as multi-year ice or sea ice in brackish waters such as the Baltic Sea. Not yet known is the influence of deformation

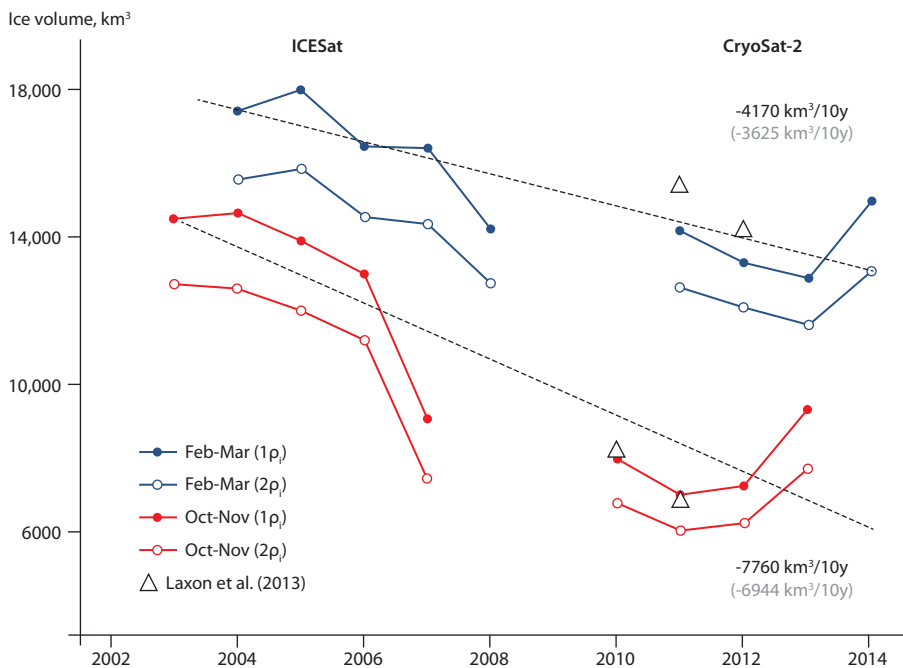


Figure 5.4 ICESat and CryoSat-2 sea-ice volume for late winter (Feb/Mar) and early autumn (Oct/Nov) for two different density values (ρ) (Kwok and Cunningham, 2015).

on the retrieval. Nevertheless, SMOS ice thickness data¹ are valuable for monitoring thickness in thin ice regions such as downstream of polynyas in the Laptev or Kara seas or in the Arctic peripheral seas such as the Barents Sea (Kaleschke et al., 2016). Note that in these regions radar altimetry often fails, either because the sea ice is too thin or because of ocean swell entering the ice cover. There is potential for combining SMOS and altimeter data to obtain hemispheric estimates that span much of the thickness range of sea ice.

Data sets from existing mooring arrays and observatories have continued to deliver extremely useful data, but no definite trends in ice thickness can be reported from North Pole Environmental Observatory (NPEO) Ice Mass Balance (IMB) buoy observations for the nine summers between 2000 and 2013 during which most of the IMBs drifted toward Fram Strait (Perovich et al., 2015), or from the ULS mooring arrays installed through Canadian efforts in the Beaufort Sea, Baffin Bay, Hudson Bay and Canadian Arctic Archipelago (e.g. Barber et al., 2012; Jackson et al., 2015). This contrasts with observations from the Norwegian Polar Institute (NPI) Fram Strait ULS moorings for which a decline in sea-ice thickness has been reported for the period 1990–2011 (Hansen et al., 2013). *In situ* observations in Fram Strait between 2003 and 2012 confirm the decline in ice thickness – at least until winter 2007/08 (Renner et al., 2014). More thin sea ice, and less and thinner multi-year ice is reported for the Beaufort Gyre Exploration Project (BGEPE) mooring array in the Beaufort Sea for the period 2003–2012 (Krishfield et al., 2014).

Airborne observations carried out within the context of Operation IceBridge (Kurtz et al., 2013) and other campaigns (e.g. Armitage and Ridout, 2015; Haas and Howell, 2015) are also covering an increasing number of years. Richter-Menge and Farrell (2013) investigated ice thickness data from Operation IceBridge Arctic airborne surveys in March/April for the period 2009–2013 and reported that ice thickness in the multiyear-ice dominated central Arctic Ocean did not change substantially

over that period, which agrees with findings by Perovich et al. (2015), whereas in the Beaufort and Chukchi seas with their complex mixture of multi-year and first-year ice, mean ice thickness seems to have decreased by ~1 m over that period.

Lindsay and Schweiger (2015) analyzed various sea ice thickness estimates (airborne, spaceborne, mooring-based and submarine-based), extending the unified ice thickness record from 2010 (Lindsay, 2013) with the results of recent years. Their two main findings were that (1) annual mean sea-ice thickness in the region of available submarine data (mostly in the non-shelf regions of the central Arctic) decreased by 65% between 1975 and 2012, and (2) there are substantial differences between mean sea-ice thickness obtained through Operation IceBridge compared to the other data sources used. Together with other results from analyses about the representativeness of the data sets included in their study, this suggests that the inter-comparison and/or combination of ice thickness data across scales has a large potential for biases and misinterpretation of the results. This is not surprising given the newness of the methodology and the disparity in the sources (e.g. radar altimeters vs. laser altimeters). It will take a community-wide effort to reconcile the different ice thickness sources and create a consistent ice thickness time series.

The interplay between thinner, younger sea ice and a longer melt season (see Section 5.3.3) increases the potential for mechanical break-up of sea ice due to wind-induced ocean surface waves and swell, and through this influences both extent and thickness. Mechanical ice break-up used to be most associated with the Antarctic but observations suggest dynamical processes are now becoming an increasing feature across the Arctic. Francis et al. (2011) reported an increase in significant wave height of about 0.5 m per decade in the East Siberian to Beaufort Sea sector of the Arctic Ocean from satellite measurements. Thomson and Rogers (2014) demonstrated that the fetch available with the observed open water area at the end of summer in recent years is becoming long enough to generate swell capable of penetrating deep into the sea-ice cover. This has been observed by Asplin et al. (2012), who showed that on

¹ SMOS sea-ice thickness data are available from <http://icdc.zmaw.de/1/daten/cryosphere/l3c-smos-sit.html>

6 September 2009 swell penetrated as much as 250 km into the Arctic sea-ice cover, leading to a break-up of large (~1 km) multi-year ice floes into smaller floes roughly 100–150 m diameter. This made the remaining sea ice more vulnerable to lateral melt, further break up, increased ice motion and, counter-intuitively, increased the frequency of ice hazards (Barber et al., 2014a) which affected use by indigenous peoples, shipping, and oil and gas infrastructure.

5.2.3 Projected changes in sea-ice extent, concentration and thickness

Under the auspices of the Coupled Model Intercomparison Project 5 (CMIP5; Taylor et al., 2012), several climate modeling centers performed consistent simulations for the 20th and 21st centuries. These were assessed during the Fifth Assessment of the Intergovernmental Panel on Climate Change (IPCC, 2013). For the 20th century, the simulations use specified time-varying external forcings based on the observational record (Lamarque et al., 2010). These can include volcanic emissions, solar input at the top of the atmosphere, aerosols, greenhouse gas concentrations, and ozone changes. For the 21st centuries, the simulations use specified changes in external forcing referred to as representative concentration pathways (RCPs) that are based on a range of different future scenarios (Moss et al., 2010). The RCPs provide information about the uncertainties in projected conditions that are due, for example, to uncertainties in future greenhouse gas emissions. In addition to the CMIP5 simulations, some climate modeling centers have also performed large ensemble experiments with individual climate models (e.g. Kay et al., 2015). These experiments include many realizations (for example, 40 members for the Community Earth System Model large ensemble) of transient simulations over the 20th and 21st centuries. Because these ensemble model runs use the same model subject to the same forcing, differences across the simulations provide information about the role of natural variability on climate trends at different timescales.

The CMIP5 Arctic sea ice simulations have been assessed in various studies (e.g. Massonnet et al., 2012; Stroeve et al., 2012; Wang and Overland, 2012; Liu et al., 2013). The scatter across the models in the late 20th century sea-ice conditions and sea-ice trends remains large. However, as discussed by Stroeve et al. (2012), the CMIP5 climatological ice conditions and trends are more consistent with observations than the earlier CMIP3 models. The transition to ice-free summers also occurs in a similar manner across the models, although the timing differs (Massonnet et al., 2012). Regarding the timing of nearly ice-free summers, Wang and Overland (2012) used a subset of models that perform well in their late 20th century ice extent climatological conditions to estimate that the first ice-free conditions will occur sometime during the 2030s. Using a different method to select a subset of models, Massonnet et al. (2012) projected near ice-free summers between 2041 and 2060 under the RCP8.5 (i.e. high emissions) scenario. Limited analysis has been performed on the regional characteristics of CMIP5 sea ice area projections (e.g. Laliberté et al., 2016). For example, Wang and Overland (2015) found that open water duration in the Beaufort and Chukchi seas increases quickly over the 21st century in a subset of CMIP5 models, which has been observed in the satellite data that dates back to 1979 (Frey et al., 2015).

Projections of future change in sea ice include uncertainty due to model structure, internal variability, and forcing scenarios. These different sources of uncertainty can be estimated from the across-model spread in a multi-model ensemble such as CMIP5 (e.g. Hawkins and Sutton, 2009; Jahn et al., 2016). These analyses suggest that for many variables, including Arctic sea-ice loss (e.g. Lique et al., 2016), internal variability dominates the uncertainty in near-term trends (Swart et al., 2015) and can itself result in a two-decade uncertainty in the timing of ice-free conditions (Jahn et al., 2016). However, there is also growing recognition of the scenario forcing uncertainty on longer timescales (Figure 5.5). An example of uncertainty due to internal variability is ocean heat transport into the Arctic, which demonstrates wide variation under different emission scenarios, as well as under different simulations of the same emission scenario (Koenigk and Brodeau, 2014). This suggests a strong role for natural variability in the influence of ocean heat transport on future sea-ice evolution. And in fact, observational data indicate that up to 50% of ice loss in the Barents Sea from 1998 to 2008 was due to strengthening and warming of the Atlantic Water inflow (Årthun et al., 2012). Shifts in the ice edge north and east due to ocean heat transport during 1979 and 1997 have also been noted (Årthun and Schrum, 2010). Another recent modeling study suggested that low frequency fluctuations in ocean heat transport from the Atlantic and Pacific oceans could account for some of the observed sea-ice decline in the Arctic (Zhang, 2015), and if heat transport slows, there could be a pause in the sea-ice trends.

Model uncertainty is important at all timescales, particularly if there are biases in key model parameters, such as ice thickness (Melia et al., 2015) and albedo. Koenigk et al. (2014) examined ice albedo in the CMIP5 models and found it is strongly related to summer solar insolation of the ice-covered Arctic Ocean region. They found that ice albedo varied widely

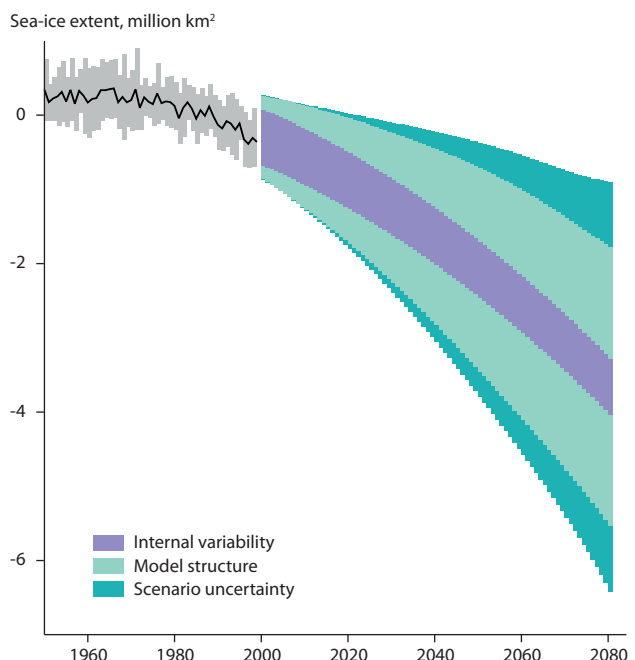


Figure 5.5 Uncertainty range for future sea-ice extent projections due to internal variability, model structure, and scenario uncertainty. Estimated from CMIP3 models based on the method of Hawkins and Sutton (2009) (Lique et al., 2016).

between models, with the main feature being unrealistic spatial variability even though the ensemble mean albedo agreed well with satellite data. Some biases in model albedo are likely to be related to parameterizing minimum ice albedo at a higher level than has been observed.

The role of internal variability for uncertainty in sea-ice projections has been further diagnosed using large ensemble simulations of a single climate model (e.g. Wettstein and Deser, 2014; Swart et al., 2015). These studies confirm the importance of internal variability on multi-decadal timescales. For example, using a particular model ensemble, Wettstein and Deser (2014) found that trends in September ice extent and volume for the period 2020–2059 can exhibit a nearly three-fold difference solely due to internal variability. These studies also indicate that decadal-scale pauses in ice loss are possible even in the 21st century during periods when natural variability counteracts anthropogenic forcing (see also Kay et al., 2011).

Another aspect of variability is the interplay between Arctic internal variability and large-scale externally driven variability. Some studies suggest that external forcing is more important than internal variability in coastal regions (Mikolajewicz et al., 2005; Döscher et al., 2010). Within the central Arctic, both factors are of the same order of magnitude; internal variability is particularly large during times of ice volume increases (Dorn et al., 2012; Döscher et al., 2014).

5.2.4 Comparison between model results and observations

Sea-ice extent (e.g. Massonnet et al., 2012; Stroeve et al., 2012; Wang and Overland, 2012) and sea-ice thickness (e.g. Stroeve et al., 2014b) have been assessed from CMIP5 models via comparisons to historical observations. There is large scatter across the models, with many models having a late 20th century climatology that shows discrepancies with observations. However, the multi-model mean climatology agrees reasonably well with observations (Shu et al., 2015). There are also several individual models that can simulate ice area, its annual cycle, and ice thickness distribution within the Arctic reasonably well. As discussed by Stroeve et al. (2014b), biases in the simulated ice thickness pattern within the Arctic Basin in CMIP5 models are related to atmospheric circulation biases within the models. Model biases in other sea-ice related properties such as the Fram Strait ice area flux (Langehaug et al., 2013), snow cover on sea ice (Hezel et al., 2012; Light et al., 2015a), and the timing of ice melt onset (Jahn et al., 2012) have also been assessed in some CMIP5 models. These properties can affect feedbacks within the climate system and so modify the atmosphere and/or ocean response to changes in sea ice (e.g. Holland and Landrum, 2015). More work is needed to better understand model biases in such properties and their potential influence on the climate system response.

5.2.5 Uncertainties and gaps in knowledge

5.2.5.1 Concentration and extent uncertainty

Estimates of uncertainty from passive microwave sea-ice concentration products is a challenge owing to the large scale, varying surface properties, and limited availability of comparison data; summer is especially challenging due to the effect of melt water on the passive microwave signal (Kern et al.,

2016). Evaluation and validation of sea-ice concentration (SIC) products is an ongoing effort – partly because new algorithms are still being developed and tested (Kongoli et al., 2011; Tikhonov et al., 2015), partly because new satellite sensors are becoming available (e.g. AMSR2; Beitsch et al., 2014), and partly because new independent data sets are emerging which help to better quantify SIC uncertainties. One example is the effort to compute SIC from satellite optical imagery such as MODIS, as is done (see Rösel et al., 2012; Kern et al., 2016) for summer Arctic sea ice. Rösel and Kaleschke (2012b) and Kern et al. (2016) showed that this MODIS-based SIC estimate could help quantify uncertainties in satellite microwave radiometry-based SIC during summer melt. A second example is the possibility, under freezing conditions, to compute the regional- to large-scale thin ice thickness distribution using the ESA SMOS sensor (Kaleschke et al., 2012; Huntemann et al., 2014; Tian-Kunze et al., 2014; Kaleschke et al., 2016); data that can, when carefully referenced as being approximately 100% sea ice, be used to infer biases in SIC over thin ice (Heygster et al., 2014).

More effort has been dedicated during the past five years to assessing the retrieval uncertainty of SIC or at least to providing SIC data sets with an uncertainty estimate – which is an important pre-requisite for assimilating SIC data into numerical models. There are two general approaches. The first is a physical-based approach that applies Gaussian error propagation to the equations used to compute SIC, as proposed by Kern (2004) and Spreen et al. (2008). Input parameters for these uncertainty estimates include the tie point standard deviation and brightness temperature uncertainties. This type of uncertainty estimation is used in the EUMETSAT OSI-SAF SIC data set (Eastwood, 2014) and the ESA-CCI SIC data set (<http://esa-cci.nerc.no>). It should be noted that these uncertainty estimates also include uncertainty caused by the interpolation of the single brightness temperature measurements into a gridded projection (such as the EASE2 or a polar-stereographic grid). The second approach is to use the standard deviation of the SIC within a certain area as a measure for the quality of the SIC estimate (Peng et al., 2013; Meier et al., 2014b). A potential realization of this approach is to compute the standard deviation of the SIC of, for example, a 3×3 grid cell large box centered at the pixel of interest. Peng et al. (2013) even used two different SIC products for this procedure. The advantage of the second approach is that it requires no additional information about uncertainties associated with the input parameters for the SIC retrieval.

Yet another approach was used for the Enhanced NASA Team (also called, NASA Team 2) algorithm, which takes advantage of the iterative nature of the algorithm. Essentially, the uncertainty is estimated from the variability of the concentration as the iteration converges to a minimum cost function (Brucker et al., 2014). The uncertainty is provided completely within the algorithm framework, such that no outside data are required. However, in practice the method can only provide a relative error and must be calibrated and further evaluated before it can provide a quantitative uncertainty estimate.

More difficult is a quantitative estimate of the uncertainty of the sea ice area or sea-ice extent, which goes beyond a simple computation of the variation in these quantities over time. Factors contributing to uncertainty in sea ice area and sea-ice extent are (i) the choice of the threshold ice concentration used,

(ii) whether and which filters are used to flag spurious weather-influence induced SIC over open water, (iii) the accuracy of the SIC itself, and (iv) the reliability of the procedures used to filter land-spillover effects. While the SIC threshold used for 'i' is 15%, the uncertainty at this SIC is usually comparably large. For sea-ice area, 'iii' becomes important and here in particular the dependence of the SIC uncertainty with SIC itself and with season (e.g. underestimation due to surface melt). Contributions from 'ii' and 'iv' are difficult to quantify. Another difficulty is that many of the errors are spatially correlated, complicating the process for deriving regional or hemispheric area and extent uncertainty from grid cell SIC uncertainties. Establishing uncertainties for sea-ice area and extent is a research topic that requires further attention.

Another aspect is the uncertainties in trends. Trend uncertainties are often given as the uncertainty (standard deviation) of the linear fit. However, trend uncertainties are affected by the consistency of the satellite record, meaning that accurate intercalibration between satellites is critical. This issue has not been thoroughly investigated, but Eisenman et al. (2014) found that trend uncertainties may be higher than the quoted standard deviation of the trend. Another issue when examining trends and anomalies is the common assumption that while absolute extent/area values may be biased due to surface melt, snow, and ice conditions, confidence in trends would still be high because these surface effects are consistent over the years (i.e. every summer, surface melt causes an underestimation in concentration and area). But with the surface melt changing (e.g. earlier melt onset) and the discovery that previously unseen or rare conditions of highly degraded (or 'rotten') ice are becoming more common and that these conditions result in a strong underestimation of the ice cover by passive microwave instruments (Barber et al., 2009; Meier et al., 2015) there is concern that these effects may influence the consistency of area trends.

5.2.5.2 Thickness uncertainty

Zygmuntowska et al. (2014) reported that when uncertainties in the input parameters for the freeboard-to-thickness conversion are considered appropriately, the changes in sea ice volume between the ICESat and CryoSat-2 periods are less dramatic than reported in the literature at that time. Uncertainty sources in the freeboard-to-thickness retrieval and the freeboard retrieval itself are manifold. Various publications have shown that both sea ice and snow density play a major role in the uncertainty budget of the sea-ice thickness derived from satellite radar altimetry (e.g. Kern et al., 2015). The different studies mentioned above with regard to sea-ice thickness and volume derived from CryoSat-2 report different uncertainties for their ice thickness estimates based on CryoSat-2 which might lead a user to prefer one estimate over another.

The validation of these data is in its infancy. Many uncertainties still exist in the derivation of the basic parameter, the freeboard (Kwok, 2014b; Ricker et al., 2015). Data used for the validation might also not be free of potential biases and/or are still of unknown uncertainty (e.g. Kurtz et al., 2013; Lindsay and Schweiger, 2015) complicating validation.

Laxon et al. (2013) used additional data to distinguish first-year and multi-year ice and apply different sea ice densities and snow depth values for the freeboard-to-thickness conversion.

Zygmuntowska et al. (2013) suggested an approach that would allow this discrimination by using CryoSat-2 data itself – without the need for additional data and with the potential of improved freeboard retrieval.

At least two recent publications (Ricker et al., 2014; Kurtz et al., 2014) address enhanced solutions for the freeboard retrieval using CryoSat-2 data. The limited range resolution of CryoSat-2, the unknown tracking point of the impinging radar wave in the ice-snow system and the change in radar wave propagation speed in a snow layer of unknown thickness, complicate the freeboard retrieval (Kwok, 2014b). One of the main sources of uncertainty is the snow depth on sea ice (Kwok, 2014b; Ricker et al., 2015). Its retrieval is still a challenge and is addressed in Section 5.3.

ICESat ceased operation in 2009, but is still useful for extending the CryoSat-2 thickness time series. However, stitching together these products is difficult considering the still limited knowledge regarding uncertainties. For example, Bi et al. (2014) analyzed ICESat and found large estimation errors over thick ice. So, there is much work still to do to better understand uncertainties and error sources for altimeter data. The future ICESat-2 satellite will continue the sea ice altimeter record and its new technologies will help refine estimates of thickness, particularly if the radar altimeter on CryoSat-2 continues to operate through and beyond the launch of the laser altimeter on ICESat-2.

5.2.5.3 Gaps in knowledge

The sea ice concentration and extent record from passive microwave instruments provides a nearly complete and consistent record since late 1978. While sensor intercalibration could potentially be improved to enhance confidence in trend estimates (Eisenman et al., 2014) and there is potential for further enhancements, the data provide clear indicators of sea ice change over recent decades. Nevertheless, there is a looming gap due to the potential loss of satellite coverage. Passive microwave sensors have been routinely launched since 1987 and for many years there have been multiple sensors in orbit. However, recent failures have reduced the number currently operating and have significantly increased the risk of a gap in coverage in the next five years. AMSR-E failed in 2011, and the DMSP F-19 SSMIS failed in early 2016 after only two years of operation. In April 2016, the F-17 SSMIS started behaving anomalously and its data quality is reduced. The suite of DMSP SSMI/SSMIS instruments has been the workhorse of passive microwave observations, but all currently operating (as of August 2017) SSMIS instruments (F-15, F-16, F-17, F-18) have been in orbit for between 7 and 18 years, well beyond their design lifetime of three years. The JAXA AMSR2 sensor, operating for five years (as of August 2017) is the only currently operational passive microwave instrument not far beyond its design lifetime (five years). The only remaining sensor potentially ready to be launched in the near future (the DMSP F-20 SSMIS) has been cancelled. While discussions concerning follow-on sensors are ongoing (including an AMSR follow-on, a EUMETSAT instrument on their METOP constellation, and possible new US DMSP radiometers) these are all likely to be a minimum of five years from launch. At that point, the youngest sensor (AMSR-2), if still operating, would be nine years old. This means there is a significant risk of a passive microwave

Box 5.2 Inuit knowledge

Inuit knowledge provides a useful complement to scientific measurements by providing a longer-term context (knowledge has been passed down through many generations) and a qualitative perspective on the nature and impacts of observed changes. In recent years, community-based monitoring networks have been established to complement scientific observations. These provide local-scale information of direct benefit to the community in terms of adaptation to the changing conditions, especially concerning safety issues and emergency preparedness (Pearce et al., 2015). These observations can also inform larger-scale networks, although there are challenges in integrating such information into a wider network (Johnson et al., 2015). Inuit-led teams have also been formed where local (and traditional) knowledge can work alongside science teams to improve integration of these two ways of knowing. Efforts during the International Polar Year increased attention to this approach of integrating local and scientific knowledge (Barber and Barber, 2009).



Jennifer Provencher

Community members and researchers working to track changes in sea ice dynamics near Sanikiluaq, Nunavut.

observation gap in the next five years. If this does occur, direct intercalibration between sensors will not be possible and the consistent, long-term, high quality sea ice concentration and extent record will end.

Sea-ice thickness presents a number of significant gaps in knowledge. First, there is a gap in interpreting the radar and laser returns to yield accurate freeboard measurements. Second, better snow and ice density information is needed to convert the freeboard estimates to total ice thickness. But perhaps the most significant gap is simply the lack of good basin-scale snow depth observations, which are essential for obtaining accurate thickness estimates.

Gaps in western science knowledge can often be supplemented by complementary observations using Inuit knowledge (see Box 5.2). The Inuit have for millennia used the sea ice as a travel corridor, a platform for resource harvesting and a key cultural feature for their way of life. Closer ties are beginning to form where the western science approach is integrated with Inuit knowledge, beginning at the start of the research process and working hand-in hand through to conclusion and reporting.

5.3 Changes in sea-ice thermodynamics, age and dynamic processes

5.3.1 Sea-ice thermodynamic processes

5.3.1.1 Snow cover

Snow plays an integral part in the mass balance of Arctic sea ice cover (Blazey et al., 2013; Webster et al., 2014; Lecomte et al., 2015a). From autumn through spring, snow acts as an insulating barrier between cooler air temperatures and the underlying sea ice. The thermal insulation of the snow cover, which is closely related to its thickness and density, governs the amount of heat loss to the atmosphere and modifies sea

ice growth rates. In some cases, snow contributes to sea ice formation where the snow cover attains sufficient mass to depress and flood sea ice, resulting in snow ice formation, or by refreezing of meltwater or rain, resulting in superimposed ice. These effects are more common in the Antarctic, but with larger amounts of first-year ice they may also be happening more in the Arctic (Wang et al., 2015).

In spring and early summer, the characteristically high albedo of dry snow shields sea ice from solar insolation, reflecting ~85% of incoming solar radiation (Perovich and Polashenski, 2012). Once melt onset begins, snow thickness and roughness influence the location (Petrich et al., 2012), timing (Webster et al., 2015), and formation (Polashenski et al., 2012) of melt ponds, which in turn, control the evolution of the sea ice surface albedo (Perovich and Polashenski, 2012, Landy et al. 2015).

Much of our understanding of snow on sea ice comes from *in situ* data collected at the drifting ice stations of the former Soviet Union during 1937 and 1954–1991. Radionov et al. (1997) and Warren et al. (1999) used these data to produce a snow climatology representative of a multiyear sea ice dominated Arctic. Since then, significant progress has been made towards gathering snow data via multiple field campaigns (e.g. Skourup et al., 2011; Barber et al., 2012; Gardner et al., 2012; Lee et al., 2012; Nghiem et al., 2013), the deployment of ice mass balance buoys (Perovich and Richter-Menge, 2015), annual airborne surveys by NASA's Operation IceBridge (Koenig et al., 2010; Kurtz et al., 2012), and satellite missions: ESA SMOS (Maaß et al., 2013) and AMSR-E (Cavalieri et al., 2014). Although limitations still exist in these data, part of the snow climatology has been extended to the contemporary period, making it possible to conduct a preliminary assessment of snow depth distributions, identify key inter-decadal changes, and make comparisons with model projections.

Information on snow accumulation in the High Arctic is still relatively sparse. On a monthly timescale, snow accumulation rates have changed little from climatology

in the western and central Arctic (Lindsay et al., 2014; Webster et al., 2014). The changes detected in precipitation are sensitive to the period and region analyzed (Vihma et al., 2016). Radionov et al. (2013) reported a winter increase in snowfall over the central Arctic Ocean during the period 1981–2010, but summer snowfall decreased as the proportion of precipitation falling as rain increased (Screen and Simmonds, 2012). The CMIP5 models project a robust increase in precipitation over the Arctic related to warming and increasing available moisture (Collins et al., 2013; Lique et al., 2016; Vihma et al., 2016). September and October remain the maximum snow accumulation period (Radionov et al., 1997; Warren et al., 1999; Webster et al., 2014), largely due to frequent storm events (Sturm et al., 2002) and large moisture fluxes from areas of open water (Boisvert and Stroeve, 2015). As winter progresses, snow accumulation rates decline, but winds continue to redistribute and densify the snow pack, and drifting snow is lost to open leads. The variability in snow depth distribution increases throughout winter (Radionov et al., 1997; Sturm et al., 2002), and by spring the snow distribution has been to a large degree reshaped by winds. Recent studies have shown that melt onset is trending earlier in spring for all Arctic regions (Markus et al., 2009; Stroeve et al., 2014a), largely driven by increased incoming longwave radiation in spring (Maksimovich and Vihma, 2012). Another recent study showed that melt onset coincides with episodic enhanced downwelling longwave radiation, i.e. melt is initiated by storm systems advecting heat and moisture into the Arctic (Kapsch et al., 2016). Earlier melt onset impacts the timing of maximum snow depth and overall seasonal duration.

Warren et al. (1999) observed a decrease in snow depth for all months of a 37-year period (1954–1991) in the Soviet drifting ice station data; the decrease in May, which had the largest negative trend, was attributed to a reduction in accumulation-season snowfall. Extending the analysis to the contemporary period, *in situ* and airborne data have shown that the Arctic snow cover has undergone significant thinning on a decadal timescale (Figure 5.6). Webster et al. (2014) found March and April snow depth in the western Arctic to have thinned by $37 \pm 29\%$ and $56 \pm 33\%$ in the Beaufort and Chukchi seas. Consistent with the model study by Hezel et al. (2012), the decrease in snow depth was attributed to the trend towards later sea ice formation in autumn, which shortens the snow accumulation period. Several observational and modeling studies have shown a strong relationship between thinner snow and the increase in first-year sea ice in the Arctic (Kurtz and Farrell, 2011; Hezel et al., 2012; Blanchard-Wrigglesworth et al., 2015). The impacts of changes in the relative amount of undeformed sea ice and lead openings on drifting snow are not well-observed, but their importance in sea ice mass balance has been clearly demonstrated (Iacozza and Barber, 2010; Leonard and Maksym, 2011; Lecomte et al., 2015b), and highlights the need for continued observational data. Despite the challenges in observing a medium that varies in space and time, collaborative efforts are currently underway between the observational, modeling, and remote sensing communities to identify key snow processes that affect sea ice mass balance, to target data collection needs, and to coordinate future snow analyses.

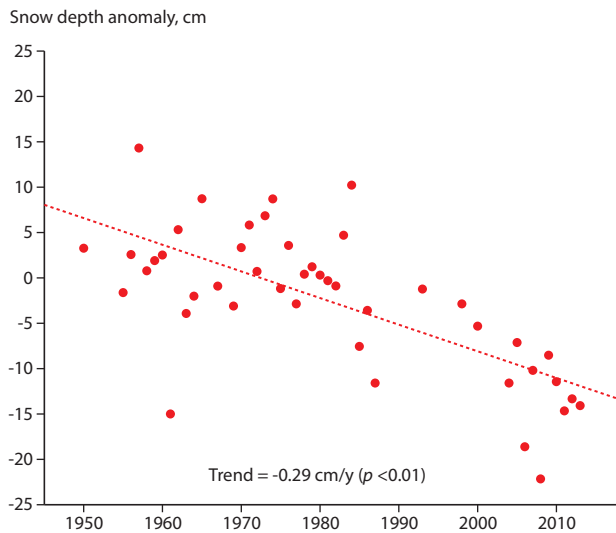


Figure 5.6 Decadal change in snow depth in spring in the Arctic Ocean (Webster et al., 2014). Anomalies were calculated using data from Soviet drifting ice stations (1950–1987), Ice Mass Balance buoys (1993–2013), and the Operation IceBridge snow depth products (2009–2013). The anomaly is the measurement minus the Warren et al. (1999) multi-year average in spring at that location.

5.3.1.2 Melt ponds

Recent years have seen an increased emphasis on understanding the sea ice processes controlling ice decline and climate feedbacks. Among the processes investigated, the formation and evolution of melt ponds on sea ice are particularly important. The implications of the increased presence of melt ponds are important for the ocean-ice-atmosphere energy balance (e.g. Frey et al., 2011; Perovich et al., 2011; Nicolaus et al., 2012; Perovich and Polashenski, 2012; Wang et al., 2014, 2016), ocean and ice biogeochemistry (e.g. Parmentier et al., 2013; Vancoppenolle et al., 2013; Geilfus et al., 2014), and ecosystem function (e.g. Arrigo et al., 2012, 2014; Mundy et al., 2014; Palmer et al., 2014).

Substantial progress has been made in methods for remotely observing melt ponds (Rösel and Kaleschke, 2011; Rösel et al., 2012; Kwok, 2014a; Webster et al., 2015) and understanding the processes that control their formation and seasonal evolution (Petricch et al., 2012; Polashenski et al., 2012; Landy et al., 2014). Early attempts to retrieve their aerial fraction by Yackel and Barber (2000), Markus et al. (2003), and Tschudi et al. (2008) were followed by those of Rösel et al. (2012). A spectral unmixing algorithm and a neural network applied to MODIS L1B reflectances of channels 1, 3 and 4 were used to derive melt pond fraction on Arctic sea ice during summer between 2000 and 2011 (Rösel et al., 2012).

Rösel and Kaleschke (2012a) showed that overall the relative melt pond fraction did not change during the period 2000–2011, but that a trend exists towards earlier melt pond formation particularly in the High Arctic (north of 80°N). In addition, positive melt pond fraction anomalies of between 5% and 10% were found quite early in the melt season north of 75°N in 2007 (Rösel and Kaleschke, 2012a). Studying melt ponds from satellite imagery and *in situ* data, Webster et al. (2015) found evidence that melt ponds formed earlier on multi-year ice

than on first-year ice, and attributed this earlier formation to a thin snow cover.

More work towards deriving melt pond cover fraction is underway using remote sensing frequencies (e.g. Scharien et al., 2014; Zege et al., 2015; Tanaka et al., 2016). Microwave data are particularly sensitive to melt; ongoing attempts at using satellite active microwave data for melt pond fraction retrieval look promising (Scharien et al., 2012) as do attempts using optical data (Mäkynen et al., 2014). Recent work has shown that end-of-winter sea ice roughness from ICESat can predict 85% of the variance in AVHRR-derived surface melt pond albedo (Landy et al., 2015), illustrating the benefits of sensor integration. However, quantitative melt pond observations from satellite remain a challenge due to limitations in spatial resolution and optical transparency due to fog and cloud.

The ability of Earth System Models (ESMs) to capture the impacts of melt ponding on radiative transfer has improved significantly (Pedersen et al., 2009; Flocco et al., 2010; Holland et al., 2012; Hunke et al., 2013), in many cases through the use of resolved-scale process models to bridge the gap between observations and ESM grid-scale parameterizations (Lüthje et al., 2006; Skjelkvåle et al., 2009, 2015). Results from these models have helped to quantify the impact of melt pond processes on sea ice state and potentially to capture the feedback processes through which melt ponds can influence future sea-ice cover in the Arctic (Flocco et al., 2012; Roeckner et al., 2012; Schröder et al., 2014).

5.3.1.3 Ice optics

The transformation of the Arctic sea ice cover from a predominantly perennial ice pack to a predominantly seasonal ice pack (i.e. multi-year ice to first-year ice) is resulting in an ice cover that is younger, thinner, and more likely to form more extensive summer surface melt ponds (Jeffries et al., 2013). These observed changes strongly alter how solar radiation is reflected, absorbed, and transmitted by Arctic sea ice. Perovich et al. (2011) assessed basin-scale increases in heat absorption by the ice cover from 1979 to 2007. The details of how heat is distributed depend on the inherent optical properties of a thinner, more heavily ponded seasonal ice pack. While detailed knowledge of the albedo of different surface conditions is central to this understanding, quantifying light transmission through the ice cover is also critical for determining sea ice mass balance, upper ocean heat, and ecosystem and biogeochemical processes within and beneath the ice.

Long-term monitoring of changes in the inherent optical properties of the ice cover is challenging. However, several studies provide insight on the physical mechanisms of these changes. Albedo and transmittance at a single location were monitored during the drift of the *Tara* over an entire summer (April to September 2007) (Nicolaus et al., 2010). Perovich and Polashenski (2012) documented the seasonal evolution of albedo for a first-year ice cover, finding it to have lower summer values and to decrease faster than multi-year ice. Nicolaus et al. (2012) estimated the surface radiative budget for a large area of the Arctic during August 2011 using an under-ice remotely operated vehicle (ROV). Results show transmittance through first-year ice is almost three-fold higher than through multi-year ice, mainly due to the larger

melt-pond coverage of first-year ice. Energy absorption was 50% higher in first-year ice than multi-year ice. These results are summarized in Figure 5.7. Hudson et al. (2013) documented the aggregate-scale albedo of first-year late summer drift ice, finding it significantly lower than what was documented during the Surface Heat Budget of the Arctic Ocean (SHEBA) experiment (conducted in 1998). They also found ice transmittance to be significantly higher, despite similar pond and open-water fractions. Measurements by Katlein et al. (2015) show that surface features such as melt ponds dominate the spatial distribution of the under-ice light field on scales smaller than 1000 m². Studies of young thin ice (Taskjelle et al., 2016) show transmittance of photosynthetically active radiation of 0.77 to 0.86 for young ice less than 0.15 m thick.

Wang et al. (2014) found that surface conditions and properties played an integral role in the seasonal evolution of albedo and transmittance, and that solar radiation is also a major contributor to ice bottom melt. During the ICESCAPE cruises, Light et al. (2015b) found the enhanced absorption of sunlight by a seasonal ice cover to be caused by ponded and bare ice types. Ponds on first-year ice were found to have thinner floors and bare ice to have diminished freeboard and thinner drained surface scattering layers. Frey et al. (2011) used data from the same experiment to relate the structure of the light field in the upper ocean under the ice to the spatial variation of optical properties in the ice cover.

Optical observations in spring show an increase in visible light transmittance of several orders of magnitude as conditions evolve from snow-covered ice to bare ice to a mix of bare and ponded ice (Nicolaus et al., 2013). As melt progresses, the spatial variability in transmittance increases by as much as an order of magnitude difference between bare and ponded ice (Frey et al., 2011). Furthermore, improved understanding of the decrease in albedo if the ice continues to thin was illustrated by Divine et al. (2015), who found lower aggregate albedo estimates for melting first-year ice than published earlier. This is mainly due to the presence of low albedo melt ponds. Detailed analysis of the angular distribution of the under-ice light field (Katlein et al., 2014) showed that the light field was more forward-directed than would be predicted by the assumption of an isotropic domain, which is useful for interpreting under-ice optical data from ROVs. Ehn et al. (2011) investigated the effects of horizontal spreading of light on the total transmittance by a ponded ice cover and found that, while albedo can be calculated on a fractional-area basis, large-scale estimates of transmittance must account for the distribution of pond sizes. The need to account for the multiple scattering in the bottom layer of sea ice to correctly estimate light availability for primary productivity was demonstrated by Ehn and Mundy (2013).

Significant advances in the treatment of the optical properties of sea ice in General Circulation Models (GCMs) were documented by Holland et al. (2012). Koenigk et al. (2014) and Light et al. (2015a) identified successes and shortcomings of these new schemes. Problems are largely thought to derive from the inability of the models to adequately treat melt ponds, but there are also known problems with the representation of snow and its role in driving the evolution of summer melt.

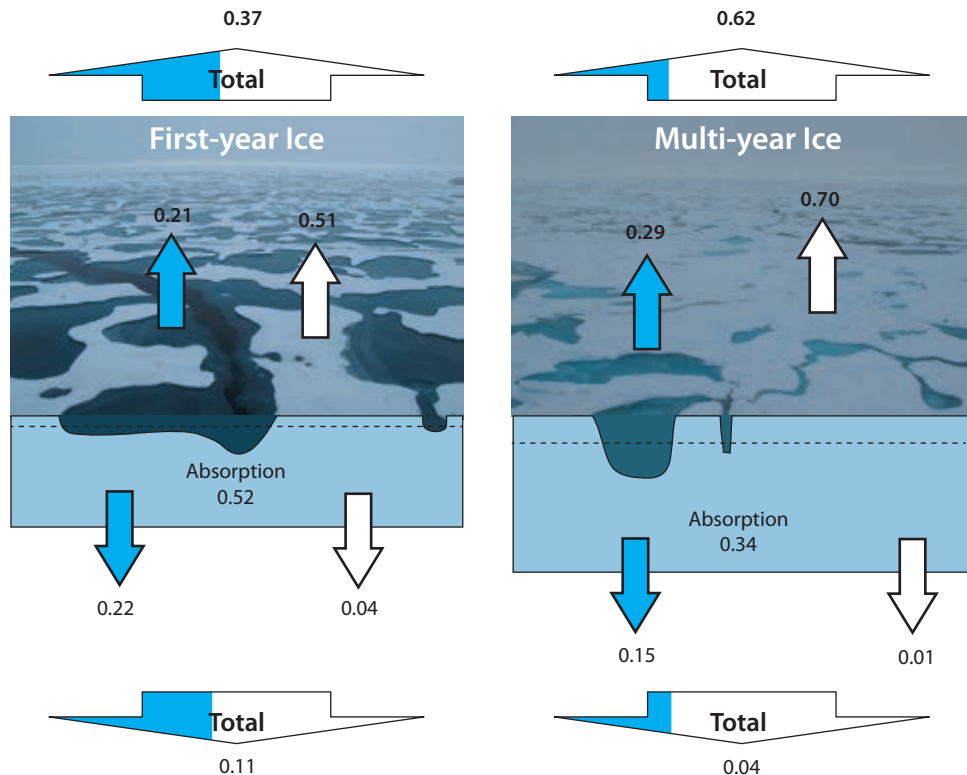


Figure 5.7 Shortwave albedo, transmittance, and absorption of Arctic first-year ice and multi-year ice. The photographs show representative samples of first-year and multi-year ice. The solid line and dashed lines denote the relative freeboard for first-year and multi-year ice. White arrows show results from white ice and blue arrows are for melt ponds. The total arrows show total albedo and transmittance assuming pond fractions of 23% (multi-year ice) and 42% (first-year ice). The shading in the arrows denotes the relative contributions of white ice and melt ponds. Adapted from Nicolaus et al. (2012).

5.3.2 Ice age

5.3.2.1 Transition from a multi-year to a first-year ice system

The age of the sea ice is described by the time span from the initial ice formation to its melt. Because sea ice goes through several stages (WMO, 1970), its age is both a property and a means to describe the state of the ice. Older ice is thicker, less saline and has different roughness and ridge properties (e.g. Lundy et al., 2015), and is thereby more resilient to changes in atmospheric and oceanic forcing compared to younger ice (Perovich et al., 2015). Sea ice in the Arctic has become younger over recent decades. The sea-ice age dataset (Tschudi et al., 2015) confirms the general decline in old ice since the early 1980s (Meier et al., 2014a; Perovich et al., 2015) (Figure 5.8).

These data are derived from Lagrangian tracking of ice parcels, and there is good general agreement between the ice age fields and ice thickness and multi-year ice extent estimates (Maslanik et al., 2011). First-year sea ice is now the dominant ice class. Ice more than three years old represents a minor portion of the Arctic sea-ice cover, and is mainly found only close to the coasts of Greenland and Arctic Canada, and in branches in the Beaufort Sea and Arctic Basin (see Figure 5.8). A new regional study by Howell et al. (2015) on multi-year ice replenishment in the Canadian Arctic Archipelago highlights the large interannual variability in multi-year ice area and its increase after summer 2013.

Another study showing evidence of a younger, thinner and therefore more mobile Arctic sea ice pack is that of Babb et al. (2013). They demonstrated that, for the first time in the observational sea-ice record, multi-year ice was exported southward through the Bering Strait in winter 2011/12. The authors suggested that this was made possible by a predominantly southerly flow and by the lack of ice arch formation in the Bering Strait. The latter being where floes spanning a strait in the form of a arch (seen from above) usually prevents sea ice export to the North Pacific – similar to the Nares Strait bridges (e.g. Kwok et al., 2010) restricting ice export from the Lincoln Sea into northern Baffin Bay. New observational evidence for recent regional changes in the sea ice regimes has been published for Fram Strait (Hansen et al., 2014) and the Chukchi and Beaufort seas (Polashenski et al., 2015).

5.3.2.2 Consequences of the change towards younger Arctic sea ice

The areal reduction of old sea ice has consequences for mean sea-ice thickness, thickness distribution, and surface roughness of Arctic sea ice (Hansen et al., 2014; Renner et al., 2014; Lundy et al., 2015). Reduced ice thickness is related to changes in the forcings, whereas changes in thickness distribution are directly related to the properties of the different ice classes present. Younger sea ice has on average higher salinity than older ice, and this has various consequences, for example how much freshwater is transported with drifting ice and on habitat conditions for organisms living within the ice. The surface albedo and optical properties of

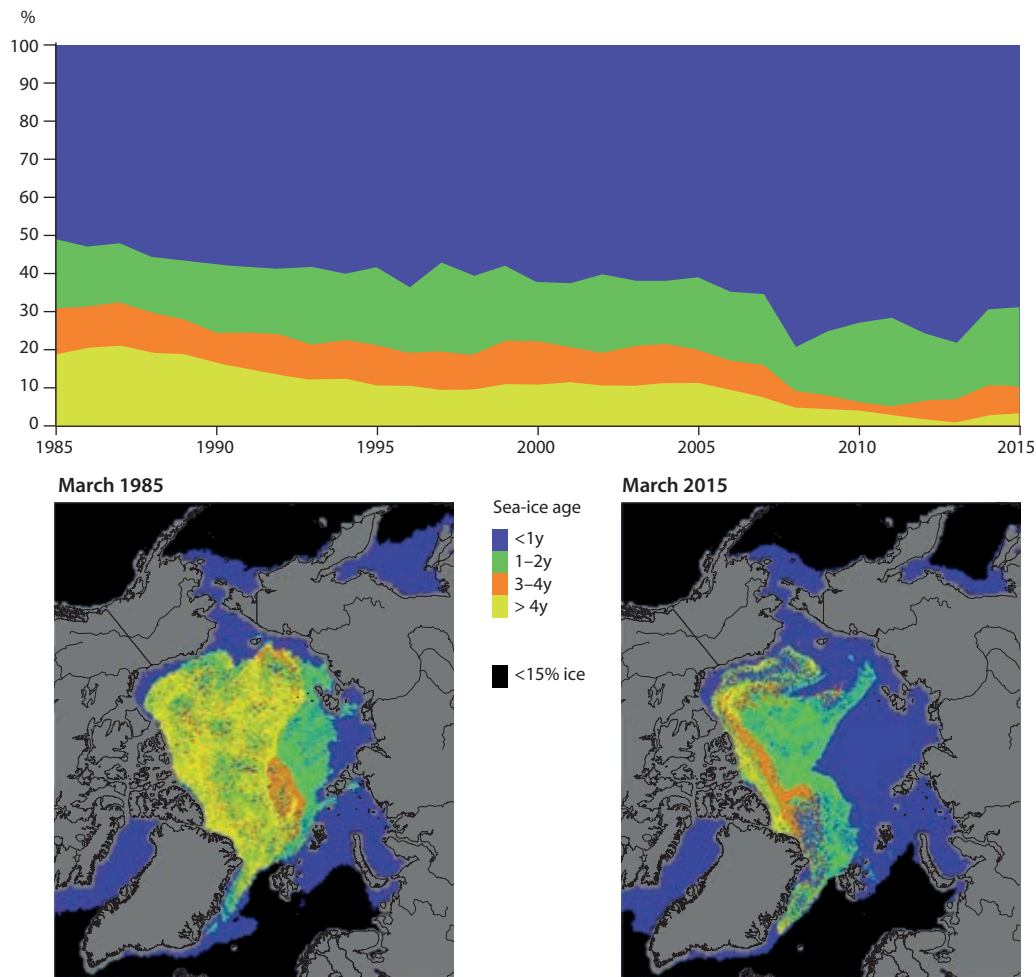


Figure 5.8 A time series of sea-ice age in March from 1985 to the present and maps of sea ice age in March 1985 and March 2015 (Perovich et al., 2015).

young ice and old ice differ (Perovich and Polashenski, 2012; Divine et al., 2015), which affects the seasonal cycle of surface albedo (Figure 5.9) and thus the surface energy balance.

Especially in early and late summer, the albedo of younger sea ice is lower than for older ice. This can enhance melting, creating a positive feedback. Newly published data from the Beaufort and Chukchi seas show that light transmission through ponded first-year sea ice is substantially larger than for ponded multi-year ice (Ehn et al., 2011; Light et al., 2015b).

Younger ice types can have different signatures to multi-year sea ice in remote sensing imagery (e.g. Willmes et al., 2014) due to different surface features and internal structure. Remote sensing signatures can also vary by region and season compounding even relatively simple distinction of multi-year from first-year ice types. Ridges made of younger ice are less consolidated than those made of older ice, but the differences in shape and nature of ridges can be masked by snow in spring. Different types of ridge lead to differences in the mechanical properties of the ice cover. Multi-year ice is getting thinner, and first-year ice can reach similar thicknesses to thin multi-year ice, which can also increase the difficulty of distinguishing between both ice types.

The interplay between thinner, younger sea ice and a longer melt season increases the potential for mechanical break-up

of sea ice from wind-induced ocean surface waves and swell. Francis et al. (2011) observed an increase in significant wave height of about 0.5 m per decade in the East Siberian/Beaufort Sea sector of the Arctic Ocean from satellite measurements. Thomson and Rogers (2014) showed the fetch available with the observed open water area at the end of summer in recent years is becoming long enough to generate a swell capable of penetrating the sea ice cover, thereby affecting both the dynamic and thermodynamic evolution of summer ice (Aspin et al., 2014).

Both a thinning sea ice cover and a projected increase in precipitation, can contribute to increased snow ice formation. Mild spells may trigger superimposed ice formation near the ice surface due to rain or meltwater percolating down through the snow cover and refreezing. Eicken et al. (2004) have already suggested that superimposed ice formation could become a widespread Arctic phenomenon. These upward ice growth mechanisms may be increasingly important for the sea ice mass balance, and for the surface energy balance. Vihma et al. (2014) described the relevance of superimposed ice and snow ice formation in the Arctic and links to other physical processes, while Wang et al. (2015) simulated these upward ice growth mechanisms in a one-dimensional sea ice model along with observations in a Svalbard fjord.

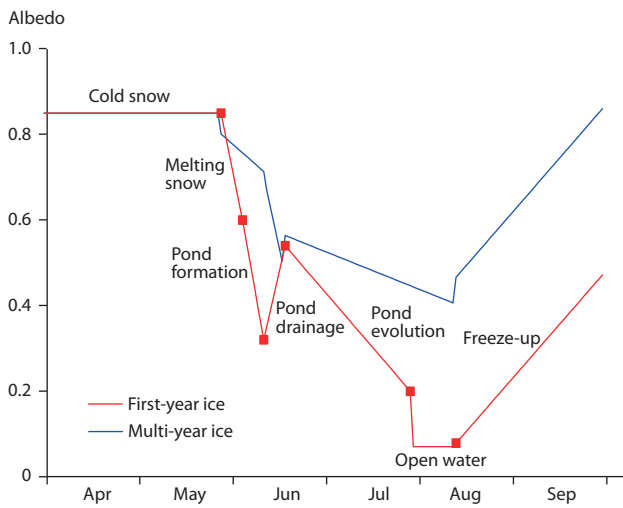


Figure 5.9 Evolution of albedo over first-year ice and multi-year ice (based on Perovich and Polashenski, 2012).

5.3.2.3 Impacts of young saline sea ice

A shift from perennial sea ice to predominantly seasonal ice types will cause changes in the physical properties of the ice cover. These changes are mainly associated with the volume of brine trapped within the ice. In contrast to first-year ice, multi-year ice has undergone a summer melt season and in the process lost most of the brine trapped within. The brine volume, which can be calculated as a function of salinity and temperature, determines the porosity of the ice, which controls many important properties of sea ice, such as its strength, thermal and dielectric properties, mass (chemical and gas) transport, and the development of melt ponds and surface albedo. Salt and heat fluxes are affected by the increased presence of first-year sea ice. First-year ice growth rates are higher than for older ice types, which means more salt is released during autumn and winter ice growth. In summer, the higher melt rates for first-year ice increases freshwater input to the surface ocean, thereby increasing buoyancy flux and stratification. Gas exchange rates through sea ice are also changing: more saline ice means more active exchange processes because gas permeability is higher in more porous sea ice. Recent studies have been conducted to quantify such processes (Loose et al., 2014; Fransson et al., 2015; Sievers et al., 2015; Granskog et al., 2016). Different ages of ice imply changes in freeboard, which trigger more flooding of sea ice (thinner ice may have a negative freeboard with a given snow load, whereas thicker ice would still have a positive freeboard). Flooding affects the salinity and temperature of the sea ice as well as mass exchange (e.g. Nomura et al., 2013) across the ocean-ice-atmosphere interface.

5.3.3 Sea-ice dynamic processes

5.3.3.1 Atmospheric and oceanic forcing of ice motion

Several recent observational studies have addressed the combined effects of atmospheric forcing and changes in the characteristics of the ice pack on ice motion. Previously, Hakkinen et al. (2008) detected a substantial increase in the drift speed of Arctic sea ice between 1950 and 2006, and

attributed this to stronger winds. Recent studies, focusing on the past two or three decades, have revealed an increasing trend in drift speed, but not one dominated by wind forcing. Rampal et al. (2009) observed a positive trend in drift speed and ice deformation using buoy data from 1979 to 2007, but these trends are unlikely to be consequences of stronger atmospheric forcing, suggesting instead that sea ice kinematics play a fundamental role in the albedo feedback loop and sea ice decline. Spreen et al. (2011) found positive trends in the drift speed (10–11% per decade) obtained from satellite observations for the period 1992–2009, which were stronger trends than those for wind speed (1–2% per decade) averaged over the Arctic Basin, and concluded that stronger winds explain part of the increase in drift speed in the central Arctic but not over the entire basin (see Figure 5.10). Thus, drivers other than wind must also be important in this context.

According to Vihma et al. (2012), although variations in the large-scale geostrophic wind dominated interannual variations in drift speed for the period 1989–2009, they did not explain the trend. The variable that best explained the annual mean ice drift speed in the Arctic was the sea-level pressure difference across the Arctic Ocean along the meridians 270°E and 90°E. The large increases in ice drift speed, however, were not explained by the much smaller trends in the wind speed, but were related to a reduced multi-year sea ice cover. For the period 1982–2009, Kwok et al. (2013) found positive trends in drift speed in regions with reduced multi-year ice cover. They saw positive trends in drift speed and negative trends in multi-year sea ice coverage over 90% of the Arctic Ocean. Here also, trends in drift speed were not fully explainable by changes in wind speed. Olason and Notz (2014) concluded that the seasonally varying ice thickness and concentration strongly affect the response of the ice cover to wind forcing. When the ice concentration is low,

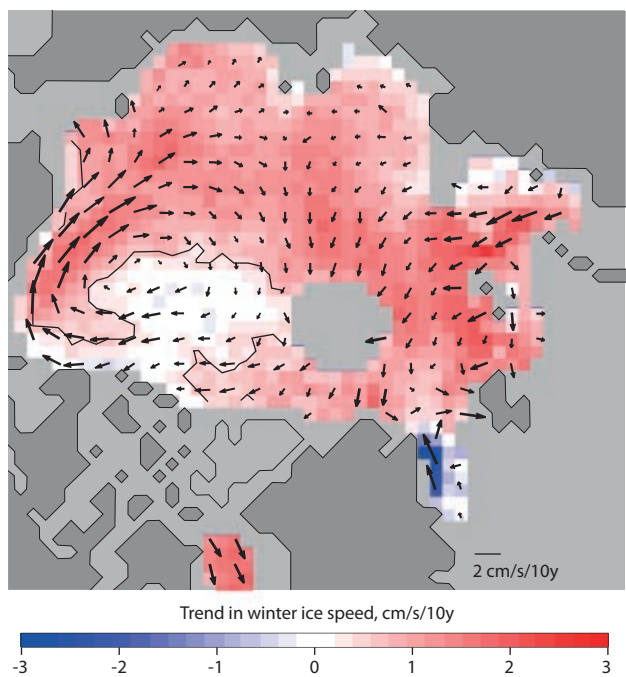


Figure 5.10 Spatial trend in drift speed of Arctic sea ice. Background colors: Linear trend in winter (October to May) sea ice speed for the period 1992–2009. Vectors: changes in sea ice motion for the same period. Data: sea ice drift from SSM/I (Special Sensor Microwave Imager) 85 GHz channels (JPL). Based on Spreen et al. (2011).

the drift speed in the central Arctic is higher, but under high ice concentrations the drift speed depends on ice thickness. At lower ice concentration and thickness, the ice responds more rapidly to synoptic-scale wind forcing as can be observed by an increase in the correlation coefficient between ice drift and geostrophic wind over the past decade (Kwok et al., 2013).

A change in sea ice circulation has also been observed. Kwok et al. (2013) showed the Beaufort Gyre and the Transpolar Drift strengthened between 1982 and 2009. Consistent with that finding, the Arctic Oscillation Index showed a positive trend over that period. The shift in the large-scale atmospheric circulation causes a strengthening of the Beaufort High (Giles et al., 2012; Overland et al., 2012; Ogi and Rigor, 2013), which causes a spin-up of the Beaufort Gyre and thus an accumulation of freshwater in that region (e.g. Giles et al., 2012).

Strengthening of the Transpolar Drift could potentially lead to increased ice export through Fram Strait (e.g. Rigor et al., 2002). The annual export of sea ice through Fram Strait is roughly 10% of the Arctic sea ice area and volume, while export through the other straits is an order of magnitude less (Kwok, 2009). A systematic change in Fram Strait sea ice thickness, or speed and ice concentration, together constituting the ice area export, would alter the composition of the remaining sea ice cover in the Arctic Ocean by tending to preferentially remove ice of particular classes, usually older multi-year ice. According to Ogi and Rigor (2013) the more clockwise, atmospheric circulation in the Arctic has contributed to the recent decrease in sea ice area. Smedsrød et al. (2011) also found an increase in ice area export derived from the across-strait pressure gradient, based on atmospheric reanalysis in combination with satellite data. However, estimates of the sea ice area (Kwok, 2009; Kwok et al., 2013) and volume (Spreen et al., 2009) export based on satellite data do not show a significant change. It is currently unclear whether the ice area flux remains fairly constant (Kwok, 2009; Kwok et al., 2013) or whether there has been a systematic increase (Smedsrød et al., 2011). Even for an increasing area flux it would be unlikely that the sea ice volume flux has increased, because sea ice thickness has strongly decreased in Fram Strait (Hansen et al., 2013), as elsewhere in the Arctic Ocean.

The wind in Fram Strait is not purely geostrophic. On the basis of model experiments and analyses of the atmospheric momentum budget, van Angelen et al. (2011) suggested that thermal wind forcing is important in generating a persistent northerly jet that enhances the southward advection of ice in Fram Strait, while the interannual variations in the ice area flux were better explained by large-scale atmospheric circulation than the thermal wind. The thermal wind originates from the difference between near-surface air temperatures over the ice-covered western Greenland Sea and the ice-free eastern Greenland Sea. According to van Angelen et al. (2011), the forcing has weakened since 1993 due to a stronger warming of the air over the ice-covered regions than over the open ocean.

Shorter-term extremes in the atmospheric forcing can also have profound effects on Arctic sea ice, for example by redistributing sea ice mass. Kwok (2015) reported that the increase in ice thickness after 2013 along the Arctic coasts of Greenland and the Canadian Arctic Archipelago can be mainly attributed to ice convergence in that region. The observed longer tail of the ice thickness distribution with

thicker, more deformed ice in that region during 2013 and 2014 can have longer-lasting effects, at least over the following summer, because deformed, rougher ice exhibits a lower melt pond area fraction and so higher albedo. Also, the reduced ice area in winter following the extreme sea ice minimum in 2007 was mainly attributed to a convergence of sea ice and thereby a redistribution of ice mass towards thicker ice classes rather than a loss of ice mass (Kwok and Cunningham, 2011). Changes in the frequency of such extreme atmospheric events therefore will impact the Arctic sea ice mass balance overall.

Other interesting large-scale features of the Beaufort Sea ice include the seasonal reversals of the sea ice gyre. The reversal from clockwise and anticlockwise was traditionally thought to be restricted to the summer; when the Beaufort High breaks down. Research shows that this reversal now occurs through a much larger part of the annual cycle (Lukovich and Barber, 2005), driven by a change in the climatology of surface pressure patterns over the Beaufort Sea (Aspin et al., 2009) and that such reversals are part of a coherent pattern related to the decreasing thickness and thus increased mobility of sea ice (Lukovich et al., 2015).

Several recent studies therefore draw similar conclusions as to the ongoing metamorphosis of the Arctic sea ice cover. A thinner and mechanically weaker ice pack is more responsive to wind forcing, which explains the increasing trend in drift speed, while the interannual variations are mostly controlled by the large-scale wind field.

Recent studies have evaluated model results for sea ice drift in the Arctic. Rampal et al. (2011) discovered that CMIP3 models fail to capture the accelerated motion of Arctic sea ice. A major reason for this failure is that ice velocity in the models is not strongly affected by ice thickness and concentration. In addition to problems in parameterization of ice dynamics, failures in modelling the ice motion are often related to errors in the large-scale state of the atmosphere. Kwok (2011) found that in the majority of CMIP3 models the mean high-pressure pattern in the southern Beaufort Sea was located too far north, which caused errors in modelled sea ice circulation, thickness, and export. For ice motion at sub-daily scales, challenges remain in observations (Kwok, 2010) and modelling (Vihma et al., 2014). Recent advances have been made in the development of new parameterizations for the form drag generated by ice ridges, floe and melt-pond edges and sastrugi (Andreas, 2011; Lu et al., 2011; Lüpkes et al., 2012a, 2013) and with using improved ice rheologies (Tsamados et al., 2013; Rampal et al., 2016).

The motion of Arctic sea ice is mostly wind-driven, but the ocean plays an important role in some areas such as Fram Strait where it helps drive the sea ice area export, and also transports sea-ice meltwater out of the Arctic Ocean. The East Greenland Current is partly wind-driven, but is also driven by the higher sea level in the Arctic Ocean versus the North Atlantic, related to the large freshwater input to the Arctic Ocean (estuarine circulation) (Macdonald et al., 2015). The mean southward transport is around 6 million m³/s, the speed is reasonably uniform west of the Greenwich Meridian (0–7°W) and there is no evidence of a trend (de Steur et al., 2014). There seems to be an annual cycle south of 79°N with higher flow during winter related to wind-driven forcing of returning Atlantic Water.

5.3.3.2 Effects on the atmospheric and oceanic boundary layers

Sea ice dynamics affect the opening and closing of leads and polynyas, which further affects the thermodynamics and dynamics of the atmospheric boundary layer. Most of the leads in the central Arctic are narrow, but their cumulative effect on boundary-layer temperatures is large when an air mass travels a long distance over a broken sea-ice cover. Tetzlaff et al. (2013) showed that a major part of the variance of 2-m temperature of air masses arriving in Barrow (Alaska) and Alert (Canadian Arctic Archipelago) from the Arctic Ocean is explained by the surface temperature distribution along the air mass trajectory. Some regions are particularly sensitive to sea ice dynamics. In the three winters from 2012 to 2014, the Whalers Bay Polynya north of Svalbard was particularly large, resulting in strong atmospheric convection during cold air outbreaks. Dropsonde measurements from March 2013 showed extreme convective boundary layer heights over the polynya (Tetzlaff et al., 2014). In this area north of Svalbard a feedback mechanism between the younger ice cover and the available ocean heat in the Atlantic layer at about 300 m depth was recently proposed by Ivanov et al. (2015), suggesting stronger coupling between sea ice and the oceanic boundary layer in the future. Studies in Canada have shown that cyclones have a strong impact on heat exchange across the ocean-ice-atmosphere interface into the boundary layer (Raddatz et al., 2014) and that once this ocean heat has entered the boundary layer it can be advected over large distances affecting regional heat and moisture fluxes (Raddatz et al., 2012). The impacts of a more mobile ice cover thus play an important role in both how the atmospheric boundary layer evolves as well as how it scales up to affect regional processes from what are very locally generated points of flux.

In modelling, recent advances have been related to heat and moisture fluxes at lead surface (Lüpkes et al., 2012b; Marcq and Weiss, 2012). In the central Arctic Ocean, leads only cover 1–2% of the ocean during winter, but account for more than 70% of upward heat fluxes, with narrow leads being particularly important (Marcq and Weiss, 2012).

5.3.4 Uncertainties and gaps in knowledge

Information on snow thickness over Arctic sea ice is crucial, since snow strongly affects thermodynamic ice growth, melt pond formation, and radiative transfer. Information on snow thickness on Arctic sea ice is still sparse, although the amount of data has increased recently due to new *in situ*, airborne and satellite surveys (e.g. Laxon et al., 2013; Renner et al., 2014). Autonomous buoys with snow thickness and radiation sensors give quantitative time series data with a higher temporal resolution and also often a smaller footprint than airborne and satellite surveys. However, to collect representative data for a region requires many buoys. Initiatives such as the International Arctic Buoy Programme (IABP) help coordinate deployments of sea ice buoys. Sophisticated buoy setups that combine measurements related to surface energy and mass balance have been developed recently (e.g. Jackson et al., 2013; Wang et al., 2014, 2016; Hoppmann et al., 2015) and will contribute to more dense and accurate autonomously collected sea ice datasets.

Recent Arctic expeditions have made increased use of new technology with mobile sensor platforms. These include AUV

(Autonomous Underwater Vehicle), UAV (Unmanned Aerial Vehicle), ROV (Remotely Operated Vehicle) and instrumented sledges. Some of these systems are still at the development stage, but with new systems becoming standard tools, it will be possible to obtain high quality sea ice data over larger spatial scales in the near future. There are still fewer *in situ* sea ice surveys undertaken in winter months than summer months, but recent (Granskog et al., 2016; Assmy et al., 2017) and planned interdisciplinary expeditions (MOSAiC, www.mosaicobservatory.org) are adding to the existing winter data and providing insights into the changing Arctic sea ice system.

Ice age is now less correlated with ice thickness than it used to be, since the older ice classes have become thinner. Young ice with little snow cover can reach a thickness similar to second-year ice (Notz, 2009), as also found in a recent field experiment in the Arctic Ocean (Granskog et al., 2016). This can be a challenge for deriving ice classes from ice thickness data (Hansen et al., 2014). Distinguishing first- and second-year ice was probably still difficult previously, but in total the range of thicknesses has become narrower, with the thickest ice classes becoming rare. Assessing the age of ice can be supported by information on its physical properties, or by tracking ice movement over time (Tschudi et al., 2015). The Lagrangian tracking of ice parcels used here is subject to errors in the motion tracking; but the general good agreement between the ice age fields and ice thickness and multi-year ice extent estimates (Maslanik et al., 2011) make this pan-Arctic dataset a valuable tool to assess sea ice age on a large spatial scale.

With the observed interannual variability in ice extent, which is expected to increase due to the increasing dominance of first-year sea ice (Gosse et al., 2009), further interannual variability in ice age distribution can be expected in the near future. Years with low summer sea-ice extent will result in increased amounts of first-year ice, relative to other ice classes, in the following year, as occurred after the record minimum-extent years of 2007 and 2012. Years with larger summer ice extent lead to more first-year ice becoming second-year ice for the next season. Swart et al. (2015) showed that internal variability can affect Arctic sea-ice trends, and that there can be pauses in the sea-ice extent trend. As a consequence, ice age and ice type might vary more than in the past within a given region. This would result in varying physical properties (relevant for thermodynamic processes) and varying mechanical properties relevant for ice operations such as shipping and oil and gas development (Galley et al., 2015).

5.4 Biological implications of changing sea ice

Sea ice is a fundamental driver of Arctic marine ecosystem structure and function due to its control of light, heat and momentum across the ocean-ice-atmosphere interface. It controls light transmission (e.g. Nicolaus et al., 2012) and gas exchange (e.g. Rysgaard et al., 2011) between the atmosphere and ocean, regulates physical seawater parameters (e.g. temperature, roughness, salinity), and provides a substrate for the growth of ice algae. Sea ice seasonality is largely responsible for primary productivity patterns across the Arctic (Ardyna et al., 2014; Arrigo and van Dijken, 2015; Leu et al., 2015). The internal sea ice matrix provides a unique polar habitat for a diverse

biological community that includes viruses, archaea, bacteria, algae, heterotrophic protists, and meiofauna (e.g. Thomas and Dieckmann, 2010), and its associated production has trophic links to pelagic and seafloor (benthic) organisms (e.g. Boetius et al., 2013). Sea ice also provides a platform used as a resting and breeding space by marine mammals and birds and a feeding area and refuge to escape predation for larger invertebrates and fishes. The changes observed in sea-ice age, thickness, spatial extent, concentration, and thermodynamic and dynamic processes as well as its snow cover significantly affect the Arctic marine ecosystem. This section reports new knowledge and observed changes in the sea ice-influenced Arctic marine ecosystem with a focus on research published since the previous SWIPA assessment (AMAP, 2011).

5.4.1 Impacts on the sea-ice ecosystem

5.4.1.1 New knowledge on diversity, structure, and function

Sea ice habitats cover a range from moderate to extreme environments. For example, the bottom ice environment is relatively moderate, consistently at or near seawater freezing temperature and salinity. Due to relatively nutrient replete conditions at the end of the polar darkness period, algal diatoms dominate biomass and production during their rapid spring growth, referred to as the spring ice algal bloom (Poulin et al., 2011). A review by Leu et al. (2015) confirmed previous research that showed the spring ice algal bloom (Figure 5.11) is ultimately under bottom-up control, meaning that algal growth is limited by access to critical resources, namely light from above and

nutrients from the underlying ocean. Although the ice algal bloom represents the primary food pulse for the ice-associated food web, most of the biomass produced is funneled into pelagic and benthic food webs (e.g. Boetius et al., 2013; Søreide et al., 2013). In contrast, internal ice communities are exposed to more extreme conditions of very low temperatures, high salinities, low space availability, and a physical separation from nutrients in the underlying water column. While interior ice algal blooms can occur, diatoms and larger metazoans (multicellular organisms) are not as successful in this environment, generally leading to a curtailed microbial food web (Bowman, 2015).

New research and reviews on sea-ice biology have emerged over recent years. The timing of sea ice formation strongly influences pre-spring bloom sea ice bacterial and algal abundance and composition, which is a function of organisms present in the water column during ice formation (Collins et al., 2010; Niemi et al., 2011). Selective pressures on the ice protist community during winter result in the dominance of common sea ice diatom taxa, pre-conditioning the community for its spring bloom (Niemi et al., 2011). In contrast, a sea ice-specific dominated bacterial community develops during spring when bacterial production increases in association with the increase in algal-derived food sources (Bowman, 2015). Recent studies have shown that remineralization of nitrogen, phosphorus and other important elements by sea ice bacteria may be greater than previously thought (Fripiat et al., 2014; Bowman, 2015; Miller et al., 2015). Although many sea ice pennate diatoms are known to be motile along surfaces, *in situ* vertical migration within the ice matrix was only recently shown through a field experiment (Aumack et al., 2014). Furthermore, suspended and sub-ice algal communities were recently brought to the

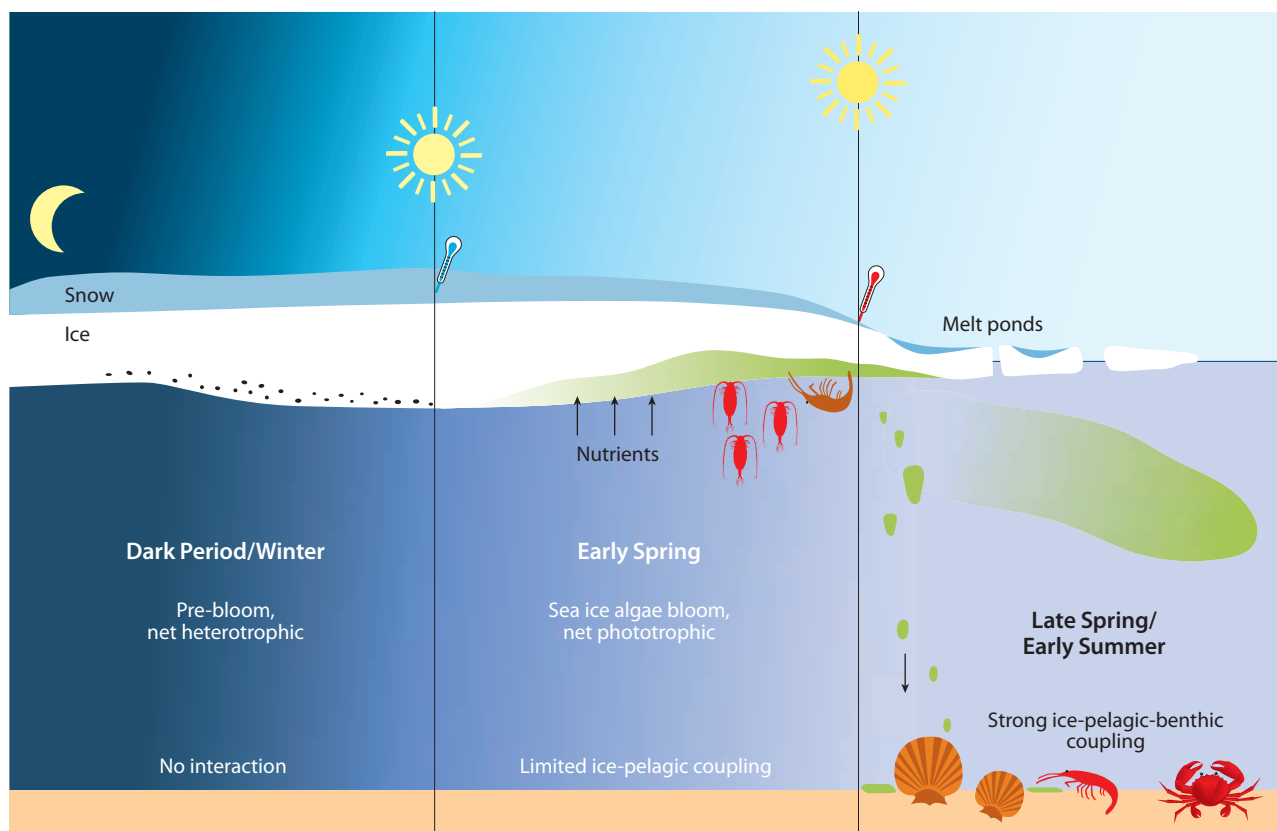


Figure 5.11 Development of a sea-ice algal bloom during the winter-spring-summer transition. The transition from winter to early spring is driven by light limitation and from spring to summer by increasing temperatures and ice melt (based on Leu et al., 2015).

forefront of sea ice ecological research in the Arctic Ocean due to their substantial production during summer, but very little is known about their distribution and timing of production (Assmy et al., 2013; Boetius et al., 2013; Glud et al., 2014).

The use of non-invasive techniques that do not require ice core extraction to follow the dynamics of the ice algal bloom (e.g. Campbell et al., 2015) provides invaluable ecological knowledge confirming the important role of snow cover, melt onset, and particularly early rain events, on bloom termination in late spring, as proposed through previous observations and models (Fortier et al., 2002; Michel et al., 2006). Newly applied imaging tools also provide novel insights into ice algal physiology and ecology (Sackett et al., 2013; Lund-Hansen et al., 2014; Findlay et al., 2015). Advances in the biochemical characterization of substances produced by sea ice diatoms, such as dimethylsulfoniopropionate (Galindo et al., 2014), mycosporine-like amino acids (Elliott et al., 2015; Piiparinens et al., 2015) and dissolved carbohydrates (Underwood et al., 2013; Aslam et al., 2016), are also raising important questions regarding their role in the cycling of carbon in the Arctic Ocean.

5.4.1.2 A shifting multi-year to first-year ice domain

The current balance between multi-year and first-year sea ice in the Arctic Ocean is rapidly shifting towards a predominantly first-year ice regime (Barber et al., 2015), and this is having a fundamental impact on the ice-associated ecosystem. One aspect of this change is an altered light climate. Because light availability constrains the spring ice algal bloom, an increased dominance of thinner and more transparent first-year ice allowing greater light transmission is expected to increase ice algal production (Callaghan et al., 2011; Leu et al., 2015). A contrasting view is that our limited knowledge of multi-year ice ecosystems is biased and lacks an understanding of the role of thick hummocks – a common feature of multi-year ice – that are particularly challenging to sample (Lange et al., 2015). Comparing the ice algal biomass of multi-year and first-year ice, Lange et al. (2015) observed the highest integrated values to be associated with thicker multi-year ice, suggesting that multi-year ice makes a more important contribution to ice algal production in the central Arctic Ocean than previously assumed. Regardless of these contrasting views, regional variations in light availability (e.g. through the influence of snow cover, ridging, melt ponds) and nutrient supply can further influence the magnitude of ice algal production. One of the regions of greatest change is associated with the marginal ice zone, where earlier melt onset and delayed freeze-up are expected to shift the balance between ice algal production and pelagic production (Barber et al., 2015), and thus affect fluxes to the pelagic and benthic food webs (see Box 5.3).

The shift from multi-year to first-year ice also affects the composition of biological communities inhabiting the ice and the ice-water interface. A multi-decadal analysis of dominant groups of algae present in sea ice and invertebrate groups at the ice-water interface reveals changes in species composition (Figure 5.12), attributed to changes in sea-ice cover. The period prior to the early Arctic warming of the 1990s, shows the highest diversity of ice algae (dominated by diatoms) and of under-ice fauna

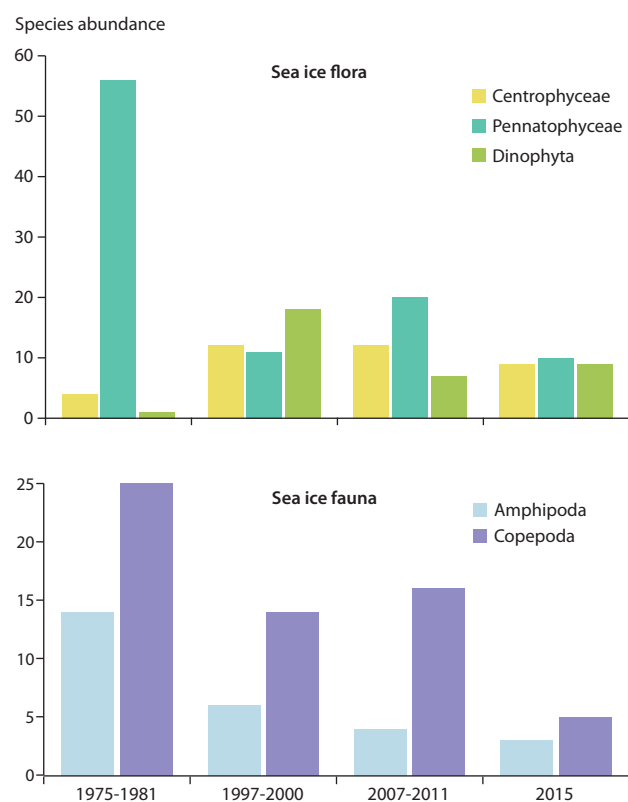


Figure 5.12 Average number of species of sea ice flora and under-ice fauna identified in the Beaufort Gyre (1975–1981 and 1997–2000) and at the North Pole (2007–2011 and 2015). Data for 1975–1981 from Melnikov (1989), 1997–2000 from Melnikov et al. (2002) and 2007–2011 and 2015 from Melnikov et al. (2017).

(dominated by amphipods) (Melnikov, 1989, 1997). The number of species of ice algae and under-ice fauna then decreased and there was a shift in community composition (Melnikov et al., 2002). Recent observations show a shift from pennate to centric diatoms and dinoflagellate species, and a strong reduction in the numbers of copepod and amphipod species (Figure 5.12).

Of the regular inhabitants of the fauna from the undersurface of the ice, only *Apherusa glacialis* has been consistently observed over the past decade (Barber et al., 2015; David et al., 2015). The key species of ice-associated amphipod *Gammarus wilkitzkii* was not observed in any of the many samples collected during summer 2015 near the North Pole, and other ice-associated amphipod species, *Onisimus nanseni*, *O. glacialis*, *Mysis polaris* and *Eusirus holmi* were rarely observed (Melnikov et al., 2017). A decrease in the abundance and biomass of the main ice-associated amphipods is also documented for the Eurasian sector of the Arctic Ocean, with a decrease in abundance of the amphipod *Apherusa glacialis* and a decline, to levels too low for quantitative estimates, in abundance and biomass of *G. wilkitzkii* (Barber et al., 2015).

Changes in the composition of Arctic sea-ice communities can be attributed to the fact that multi-year ice provides a relatively stable habitat that can sustain biodiversity over many years of succession, whereas biodiversity within first-year ice depends on the species present in the water at the time of ice formation and the seasonal succession within the ice matrix (Niemi et al., 2011; Bowman, 2015). Furthermore, Olsen et al. (2017) recently evidenced that the presence of pennate diatoms in first-year sea ice over the Arctic Ocean

Box 5.3 Phenology of Arctic sea ice

Phenology, or the timing of events, is fundamental to the structure and function of Arctic marine ecosystems. The phenology of marine species refers to recurring life-history events, such as the timing of the phytoplankton bloom, the peak in abundance of zooplankton and other species, or the timing of migrations. Increases in temperature have led to important changes in the phenology of marine species in many ocean areas, including advances in the timing of phytoplankton blooms and earlier seasonal cycles (Poloczanska et al., 2013; González and Anadón, 2014). Important changes in phenology are also observed throughout Arctic marine food webs, with changes in the timing and intensity of phytoplankton blooms, earlier zooplankton development, and earlier migrations in beluga (*Delphinapterus leucas*) (Bailleul et al., 2012; Ardyna et al., 2014; Michel et al., 2015).

In the Arctic, the strong seasonality in solar radiation and sea-ice cover constrains the phenology of marine species. The former constitutes a permanent property of the ecosystem that varies with latitude, whereas the latter is subject to rapid ongoing changes (Berge et al., 2015a). These include earlier melt onset and delayed freeze-up resulting in a shorter ice-covered season and, as a corollary, more open water in winter and an extended open-water period (Barber et al., 2015). The changes in sea ice have important consequences for the phenology of the ice algal and phytoplankton production, the timing and activity of grazers, and the phenology of marine mammals and seabirds. Yet, these changes remain constrained within a seasonal context ranging from winter polar night to 24-hour summer daylight.

Recent years have seen increasing research effort to understand the dynamics of Arctic ecosystems during the polar night. Evidence of bacteria-driven nutrient recycling and zooplankton activity reveals complex ecological interactions persisting throughout the dark winter (Berge et al., 2015a; Lønne et al., 2015). Recent evidence of the widespread

occurrence of zooplankton vertical migrations during this period, aptly termed lunar vertical migrations (Last et al., 2016), emphasizes the importance of adaptations to the strong Arctic seasonal cycle in marine species. The ice ecosystem itself remains poorly studied during winter. However, there is now evidence that diverse microbial and protist assemblages, including non-dormant autotrophic cells, persist in low numbers in Arctic sea ice throughout the darkness of winter (Collins et al., 2010; Niemi et al., 2011). For example, Niemi et al. (2011) observed protist diversity in winter sea ice to be comparable to that during the productive spring period, indicating persistence and continuity in the seasonal development of sea ice communities. These results also indicate that the timing of ice formation, when organisms are selectively incorporated into the ice matrix, is a key element in the phenology of ice communities.

The likely impacts of delayed ice formation on the abundance and composition of sea ice communities are unclear. The composition of late winter sea ice communities contrasts markedly with that of surface waters (Druzhkov et al., 2001; Niemi et al., 2011). Overall, the impacts of delayed ice formation on sea ice biogeochemical processes will ultimately result from dual changes affecting the physical-chemical properties of the sea ice and the incorporation of cells into the ice matrix. For example, delayed ice formation and more dynamic conditions in autumn may favor the formation of frost flowers (Figure 5.13). These delicate ephemeral ice crystals can form over large areas of the Arctic Ocean, potentially playing a significant role in biochemical exchanges at the ocean-ice-atmosphere interface (Bowman and Deming, 2010; Douglas et al., 2012; Barber et al., 2014b; Bowman et al., 2014). Changes in the autumn phenology of sea ice, through processes involved in its formation, may thus have large-scale, but largely unknown, impacts on the biogeochemistry of the Arctic Ocean.

basins could be dependent on seeding by adjacent multi-year sea ice. The observed change is likely to be accentuated by the more extensive bottom ice melt of multi-year ice during recent summers.

It is possible that flora and fauna associated with multi-year sea ice will continue to decline and could disappear altogether from the central Arctic Ocean following ice-free Arctic summers. However, there may be mechanisms that could sustain at least some of the species. For example, the amphipod *A. glacialis* is the most numerous of the Arctic ice-associated macrofauna (Arndt and Swadling, 2006; David et al., 2015), and was considered until more recently an obligate ice-associated species, although it has been shown to survive for short periods in the water column (Werner et al., 1999). From a unique set of samples collected during the polar night that documented *A. glacialis* (n=20) at depths between 200 and 2000 m, Berge et al. (2012) proposed a new perspective on the life-history of this species; one involving a pelagic stage during the polar night that would change this species from an obligate to a facultative ice-associated species classification

(Figure 5.14). Deep migrations enable organisms to reach the incoming Atlantic Water, this enables them to avoid export out of the Arctic Ocean and be actively transported back into areas that are more likely to freeze early in winter.

5.4.2 Impacts on pelagic ecosystems and food-web transfers

The changing Arctic sea-ice cover has resulted in effects that reach well beyond the ice ecosystem, and beyond the Arctic Ocean in downstream regions of the North Atlantic. As the ice cover decreases in seasonal and spatial extent, the fraction of open water is increasing significantly. Trends estimated from remote sensing analysis of ocean color indicate a 30% increase in Arctic pelagic primary production between 1998 and 2012 (Arrigo and van Dijken, 2015), which agrees with a 14% per decade estimate for a comparable period (1998–2010; Bélanger et al., 2013). However, these trends vary greatly across regions. The largest increases in primary production are observed in the Barents and Eurasian sectors of the Arctic and in parts of the Canadian

In the sea ice, spring phenology is linked to the timing and speed of snow and ice melt – a function of oceanographic and atmospheric forcing – which is intimately coupled to the release of ice algae into the water column (e.g. Fortier et al., 2002) and their export to the benthos (Boetius et al., 2013; Søreide et al., 2013). Therefore, while earlier ice melt is expected to affect the transfer of ice algae into the marine food web through phenological impacts, the respective influence of atmospheric and oceanic warming on melt processes is also an important aspect to consider in future models.

Under the ice, spring phenology is closely linked to the development of under-ice phytoplankton blooms that require favorable light conditions associated with advanced melt or ice ablation causing the disappearance of the optically dense ice algal layer and snow cover (Mundy et al., 2014). These blooms are expected to be more widespread than previously thought and may be responsible for a large part of the overall

phytoplankton productivity in the Arctic (Arrigo et al., 2012). Because they are not detected by satellite, under-ice blooms are not included in current Arctic primary production estimates based on remote sensing.

At sea ice edges, spring phenology is linked to ice retreat, and so to changes in the location of the marginal ice zone. A recent synthesis of satellite data and modelling indicates that the timing of the phytoplankton bloom is strongly linked to the timing of ice retreat over large parts of the Arctic (Ji et al., 2013). As the marginal ice zone retreats from the shelves towards the central Arctic basins, key questions remain with respect to the cycling and availability of nutrients to sustain production, particularly in relation to the balance between stratification (Li et al., 2009) and wind-driven upwelling in areas off the shelf-break (Carmack and Chapman, 2003) highlighting the important role sea ice plays in momentum exchange.



Figure 5.13 Frost flowers on sea ice showing a refrozen lead with new flowers; (A) an individual flower, (B) a collection of frost flowers and (C) a thermal infra-red image of a single flower (based on Barber et al., 2014b).

Arctic Archipelago, whereas decreases are observed in Baffin Bay, the Beaufort Sea and Fram Strait (Arrigo and Van Dijken, 2015). Nutrient availability, through the balance between water column stratification and mixing continues to be considered a key factor controlling primary production in the changing Arctic (Tremblay et al., 2015). Wind-induced upwelling and mixing are favored under conditions of decreased sea-ice extent (Pickart et al., 2013; Ardyna et al., 2014), as well as at ice edges (Mundy et al., 2009) and can be particularly important during late autumn and winter for preconditioning the water column for enhanced primary production during spring and summer (Tremblay et al., 2011; Falk-Petersen et al., 2015).

Changes in physical and optical properties of the sea ice also affect under-ice production. While blooms have occasionally been reported in the past (e.g. Fortier et al., 2002) recent findings of extensive and highly productive under-ice phytoplankton blooms suggest a much more productive Arctic Ocean than previously assumed (Arrigo et al., 2012, 2014; Mundy et al., 2014; Assmy et al., 2017). The increasing dominance of first-year ice, with its lower albedo compared to multi-year ice, combined

with a decrease in snow cover (see Section 5.3), increases light transmission to the surface ocean and provides an environment where pelagic primary producers can bloom underneath the ice.

The previous SWIPA assessment predicted that the decline in Arctic sea ice would result in an increased frequency and prevalence of autumn phytoplankton blooms (AMAP, 2011). Such a change has now been documented. Ardyna et al. (2014) showed a pan-Arctic increase in the occurrence of autumn blooms (Figure 5.15), with a significant increase over recent decades and near doubling between 1998–2000 and 2007–2012. While sea-ice declines have affected the seasonal dynamics of phytoplankton and the frequency of autumn blooms throughout the Arctic, the strongest increase in the frequency of their occurrence is documented for the Eurasian/Chukchi Sector of the Arctic Ocean (Ardyna et al., 2014).

The regional differences in increased pelagic production and changes in phenology of the spring and autumn blooms largely depend on the balance between the effects of sea-ice decline on surface stratification, mixing and upwelling, and light conditions. Increased surface stratification associated with melt and warming

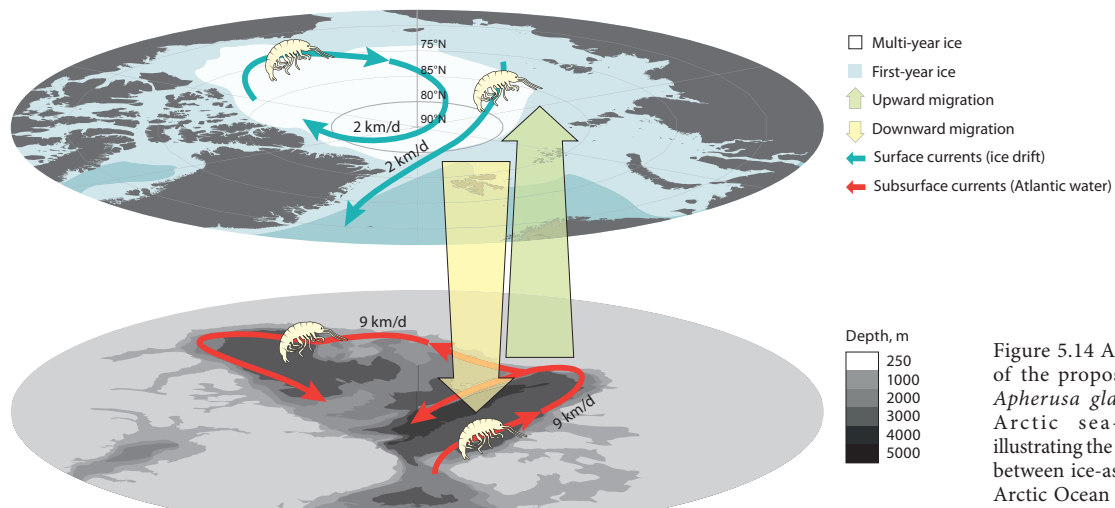


Figure 5.14 A conceptual model of the proposed life history of *Apherusa glacialis*, a common Arctic sea-ice amphipod, illustrating the intimate connection between ice-associated fauna and Arctic Ocean currents (based on Berge et al., 2012).

isolates phytoplankton in the surface sunlit layer from the deeper pool of nutrients, whereas mixing and upwelling bring new nutrients to the surface. Ice melt simultaneously affects all these processes. For example, because wind-induced upwelling and mixing are closely coupled to bathymetric and coastal features, Arctic shelves and deep Arctic basins are expected to respond to sea ice declines differently (Williams and Carmack, 2015). Moreover, the responses of the pelagic ecosystem to sea-ice changes on the inflow and outflow shelves that connect the Arctic to the Pacific and Atlantic oceans can be very different depending on differences in latitude, topography, and ocean dynamics (Michel et al., 2015; Moore and Stabeno, 2015; Wassmann et al., 2015). For the central Arctic Ocean, recent measurements of primary production in thick mats of the chain-forming diatom *Melosira arctica* during the low-ice year 2012 reveal high under-ice production in an area previously considered to show little productivity (Fernández-Méndez et al., 2015). The unexpected finding of these algal masses on the seafloor, to a depth of 4400 m,

also indicates a tight coupling between under-ice production and benthic consumers (Boetius et al., 2013). These recent findings constitute milestones towards a change in understanding of the role of the deep central basins in the productivity and cycling of carbon in the Arctic Ocean.

Recent changes in sea ice type, extent, concentration and timing (formation and melt) are already affecting the distribution and diversity of many Arctic species. A recent switch in dominance from energy-rich diatoms to *Phaeocystis pouchetii* and other small pico- and nanoplankton flagellate species in Fram Strait could indicate a northward extension of these blooms caused by the disappearance of sea ice and an associated northward penetration of warmer Atlantic-influenced water near the surface (Nöthig et al., 2015). Northward range extensions are also now documented for fish, marine mammals, and other species (Moore and Stabeno, 2015; Christiansen et al., 2016; see Section 5.4.3). These northward shifts will undoubtedly influence trophic structures in Arctic

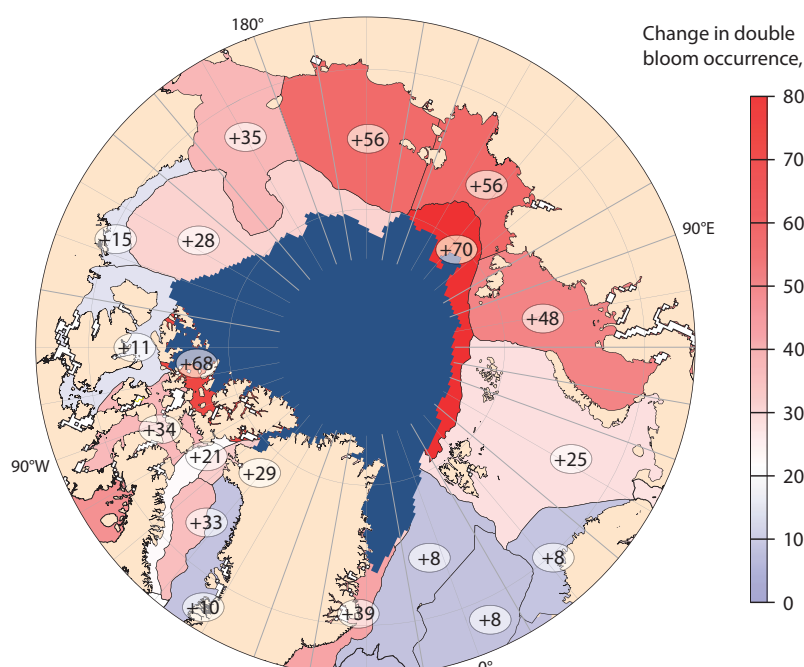


Figure 5.15 Percentage change in pan-Arctic occurrence of autumn blooms between 1998–2001 versus 2007–2012 (adapted from Ardyna et al., 2014).

Box 5.4 Toxic phytoplankton in the Arctic food webs

Blooms of toxin-producing diatoms and dinoflagellates are widely documented in temperate and tropical areas. They can have deleterious effects on ecosystems and human health, and significant economic impacts. Phytoplankton groups known to be harmful in temperate and tropical areas have also been reported in the Arctic. Three major groups of toxin-producing algae are identified based on the type of poisoning they cause in humans: amnesic shellfish poisoning (ASP), diarrhetic shellfish poisoning (DSP) and paralytic shellfish poisoning (PSP). Algal toxins are transported through the food web, from toxin-producing phytoplankton to higher trophic levels (birds, fish, marine mammals, and humans), causing poisoning and even death (e.g. Scholin et al., 2000). ASP is caused by the neurotoxin domoic acid, which can harm wildlife (shellfish, fish, birds, marine mammals) and humans.

Potential domoic acid producers of the diatom genus *Pseudo-nitzschia* are common in Arctic waters and sea ice (Poulin et al., 2011; Percopo et al., 2016), but the frequency and intensity of blooms is not yet known (Lewitus et al., 2012; Matsuno et al., 2014). Strains of two Arctic species, *P. seriata* and *P. obtusa* are known to be toxic (Hansen et al., 2011; Harðardóttir et al., 2015). *P. seriata* is considered a strong toxin producer and toxicity levels in Arctic strains are similar to those found in strains from Canada, Scotland and Denmark, where toxic blooms of *P. seriata* have resulted in toxin levels in blue mussel (*Mytilus edulis*) up to ten times the EU regulatory limit (Bates et al., 2002; Fehling et al., 2005; Lundholm et al., 2005).

Toxin production is regulated by several factors including food-web interactions and photoperiod. Recent findings show that toxin producing *Pseudo-nitzschia* exposed to *Calanus* copepod grazers, increased toxin production and even induced toxicity in a previously non-toxic species (Harðardóttir et al., 2015; Tammilehto et al., 2015). Photoperiod has also been shown to affect toxin production

(Fehling et al., 2005), an important aspect to consider in the Arctic where the productive summer period is characterized by a long photoperiod. ASP toxins from diatoms have been detected in Dungeness crabs (*Cancer magister* Dana) (Horner et al., 1997; Lewitus et al., 2012) which, together with a restricted number of records of dinoflagellate toxins document the presence of algal toxins in the Arctic.

Research on the amount, fate and distribution of algal toxins in Arctic food webs has only very recently begun, and transfer vectors from phytoplankton to higher trophic levels are poorly understood. All three lipid-rich copepod *Calanus* species (*C. finmarchicus*, *C. glacialis* and *C. hyperboreus*) that dominate the Arctic mesozooplankton communities (e.g. Madsen et al., 2001) indiscriminately feed on toxic diatoms and accumulate algal toxins in their tissues (Tammilehto et al., 2012; Harðardóttir et al., 2015).

The risks and impacts of domoic acid accumulation in higher trophic levels via *Calanus* spp. is illustrated by reduced reproductive success in endangered North Atlantic right whale (*Eubalaena glacialis*) attributed to domoic acid exposure via its prey *C. finmarchicus* (Leandro et al., 2010; Doucette et al., 2012). The toxin is otherwise known for having harmful and lethal effects on mammals (e.g. Lewitus et al., 2012). The first report of domoic acid in 13 different species of Alaskan marine mammals has just been published (Lefebvre et al., 2016) and human poisoning by algal toxins is known in Alaska and Arctic Russia (e.g. Vershinin and Orlova, 2008). Under-reporting of the toxin syndromes is considered a major problem in Alaska (RaLonde, 1996; Lewitus et al., 2012) and probably also in other Arctic areas. As pointed out by Levy and Patz (2015), toxic algal blooms are expected to occur more frequently in the future Arctic, in response to changing ocean conditions and the decline in sea ice, potentially resulting in consequential economic and social impacts.

marine food webs (Falk-Petersen et al., 2007). The occurrence of algal toxins is another factor that could strongly influence the Arctic marine ecosystem and which is potentially associated with the decreasing ice cover (see Box 5.4).

5.4.3 Impacts on fish and higher trophic levels

About 220 marine fish species are currently described from the understudied Arctic Ocean and adjacent shelf seas, but only about 25% are considered true Arctic denizens (i.e. species occurring solely or mainly in sub-zero ice-laden waters) (Mecklenburg et al., 2013; Christiansen et al., 2014). This number is likely to change as new sites are explored, taxonomic issues are addressed, and more species of boreal origin spread northward (Fossheim et al., 2015; Mecklenburg and Steinke, 2015; Christiansen et al., 2016). Recent technological advances have also made possible new observations in the Arctic Ocean, including the first large-scale observations of under-ice polar cod (*Boreogadus saida*) in the Eurasian Basin using the icebreaker

towable Surface and Under Ice Trawl (SUIT; David et al., 2016). These findings confirm that this migratory fish is ubiquitous in the ice-covered Arctic Ocean, but that abundance is lower in the central basins than in coastal areas.

The study of Arctic fishes is still exploratory, and forecasts of biological events initiated by sea-ice melt are inevitably conjectures. The present discussion considers three groups of fishes in the marine Arctic: demersal (seafloor), polar cod, and northward range expansions of boreal species. While increased primary production in the Arctic Ocean may benefit higher trophic levels including fishes, the supportive capacity of the ecosystem largely depends on the cycling of this production and its transfer through food webs. Increases in primary production may not increase the supportive capacity for demersal or pelagic fishes if a large part of the production is recycled by a more active microbial food web (e.g. Sherr et al., 2009) or if a shift in species composition impedes efficient pelago-benthos transfer (e.g. Li et al., 2009). Current understanding of the dominant processes on Arctic shelves, and even in the deep basins is one of strong ice-pelagic-benthic coupling (e.g. Boetius et al.,

2013). If increases in production are associated with higher sedimentation of fresh organic material to the seafloor, loss of summer sea ice may improve general living conditions for Arctic demersal fishes in shelf and deep waters. In shallow waters, loss of sea ice and prolonged open water periods may lead to regime shifts where benthic invertebrates are replaced by macroalgae (Clark et al., 2013). Because seaweeds provide essential shelter and nursery habitat for young fish, it may be that such change benefits Arctic intertidal fish fauna. Other factors associated with changes in ice phenology on Arctic shelves, such as changes in water quality (e.g. increased suspended matter due to prevalent mixing during longer open water periods) may have adverse impacts on fish species and kelp production.

The declining ice cover is a more direct threat to polar cod. Although this species is largely confined to sub-zero ice-laden waters in their realized habitat, laboratory studies suggest that polar cod prefer temperatures of 3–6°C and tolerate temperatures up to 14°C (temperatures unlikely to occur in their natural environment) (Christiansen et al., 1997). Considered cold stenotherms in ecological terms but eurytherms in terms of physiological capacity, it is unlikely that this cod species would succumb to higher *in situ* temperatures. However, polar cod rely on sea ice for spawning and it is the main feeding habitat for larval through juvenile stages where they consume ice amphipods and copepods in the sub-ice environment (Craig et al., 1982; Lønne and Gulliksen, 1989; Fortier et al., 1995). In the laboratory, polar cod eggs develop well in ice-free surface layers and hatch after about 75 days at -1°C (Kent et al., 2016). In the natural environment, however, as sea ice is lost, the buoyant eggs and early life stages can be subject to harmful levels of UVB-radiation (Browman et al., 2000), wave action, and avian and other predators (Gradinger and Bluhm, 2004; Christiansen and Reist, 2013). In 2015, the polar cod was reclassified from a species of Least Concern to a species Nearly Threatened on the Norwegian Red List (Henriksen and Hilmo, 2015).

Ocean warming and loss of sea ice also lead to range shifts of fishes from lower latitudes into Arctic waters (Fosheim et al., 2015). There is evidence of range extensions of boreal species such as Atlantic cod (*Gadus morhua*), Atlantic haddock (*Melanogrammus aeglefinus*), Atlantic mackerel (*Scomber scombrus*) and Atlantic herring (*Clupea harengus*). Increasing numbers of Atlantic mackerel near Jan Mayen Island have been documented since 1978 (Wienerroither et al., 2011a) and larvae and adults of this species were observed near Spitsbergen in 2004 and 2013 (Wienerroither et al., 2011b; Berge et al., 2015b). However, Atlantic mackerel is probably a seasonal migrant rather than an established member of the fish fauna near Spitsbergen. Atlantic herring and Atlantic mackerel are visual predators, feeding on zooplankton and fish larvae, and in the case of adult Atlantic mackerel on larger fishes. They are therefore likely to benefit from loss of sea ice and increased visibility in areas with longer periods of open water (Varpe et al., 2015). Overall, the impact on predator-prey relationships of secondary factors from sea ice changes (e.g. water column visibility) are difficult to discern due to confounding effects on both prey and predators. As with other changes associated with sea ice, the effects and interactions are complex, and impacts at physiological, ecological and community levels all contribute to modifications in ecosystem structure.

Arctic marine mammals are of particular concern since they are adapted to living in or in association with sea ice (Laidre et al., 2008, 2015). Loss of sea ice is expected to affect all marine mammal populations, including the ice whales, beluga, narwhal (*Monodon monoceros*) and bowhead (*Balaena mysticetus*); the ice seals, ringed (*Pusa hispida*) and bearded (*Erignathus barbatus*); and the walrus (*Odobenus rosmarus rosmarus*). All three whale species seasonally migrate from temperate regions in winter into High Arctic regions during the ice-free season (Dietz et al., 2008; Ferguson et al., 2010; Bailleul et al., 2012). The ice seals and walrus (and polar bear, *Ursus maritimus*) remain within the ice-covered Arctic area year-round, although seasonal migration occurs to various degrees. All seven of the ice-adapted marine mammals depend on sea ice for survival and reproduction. These species are also important to the Inuit, who harvest them for subsistence food, economic benefits, and cultural wellbeing (e.g. Egeland et al., 2010).

Limited knowledge of the abundance and distribution of whales and pinnipeds in the Arctic makes it difficult to assess their status and trends in relation to the changing sea-ice cover. However, distribution changes related to the opening of previously ice-covered areas have been observed, such as the presence of killer whales (*Orcinus orca*) (Ferguson et al., 2010). Changes in beluga migration patterns have been linked to changes in sea temperature (Bailleul et al., 2012). These observations point to large-scale ice-associated changes impacting the distribution and migration patterns of Arctic marine mammals.

Changes in diet are the best-documented impacts associated with warming for Arctic marine mammals. In particular, loss of access to lipid-rich food chains has resulted in decreased blubber depth and body condition in ringed seals and polar bears (e.g. Kovacs and Lydersen, 2008; Thiemann et al., 2008; Harwood et al., 2012). Similar shifts in the seasonal acquisition and storage of lipids associated with a decreased dietary contribution from large lipid-rich copepods is expected for bowhead whales, but has not yet been observed (e.g. Pomerleau et al., 2012; Falk-Petersen et al., 2015). Shifts in the availability of traditional prey species for beluga and narwhal have been accommodated by varying foraging behavior (Marcoux et al., 2012; Watt et al., 2013). Similarly, walrus are dependent on a benthic-rich food supply associated with first-year ice cover (Grebmeier et al., 2015), but no documented change has yet been shown for this species. Dietary shifts have also been observed in seabirds. For thick-billed murres (*Uria lomvia*), Provencher et al. (2012) observed a dietary shift from polar cod to capelin (*Mallotus villosus*) in the sub-Arctic (Hudson Bay), whereas polar cod remained a significant element of the diet in the High Arctic.

5.4.4 Uncertainties and gaps in knowledge

Knowledge and data gaps continue to limit the certainty of predictions concerning how the ice-associated ecosystem will respond under a changing climate. The relative ease of accessing coastal landfast ice versus the central Arctic ice-pack has resulted in biogeochemical observations being focused in key locations around the periphery of the Arctic Ocean, leaving large data gaps for vast areas of the shelves and central basins. Similarly, logistical considerations, as well as a focus on the biologically productive period, have also skewed the

seasonal observational base towards spring-summer when environmental conditions are more favorable to field studies. The few autumn-winter studies that do exist reveal interesting ecological features of the ice-associated ecosystem, calling for a better characterization of biogeochemical processes during this time of year. Little remains known about the distribution and bloom development of sub- and under-ice primary producers and there are few within-ice primary production estimates. Baseline information on multi-year sea ice communities is also an important knowledge gap. The likelihood of changing ice and ocean conditions enhancing the potential for toxin-producing algal blooms in the Arctic highlights a need for data collection focused specifically on these species and their influence on Arctic food webs, as well as a need to improve the reporting of toxin occurrences across the Arctic. Repeat observations of higher trophic levels are also required, including fishes and marine mammals, in order to constrain their ecological responses and distributional changes in relation to the changing sea-ice cover.

Owing to the interacting effects of light and nutrients as the main factors controlling primary production within and under the sea ice, uncertainties associated with observations and projections of the physical variables by which they are controlled, confound the capacity to predict the future structure and function of the sea-ice ecosystem. Furthermore, these uncertainties increase when predicting the responses at higher trophic levels, due to the added complexity of interactions at the species, population, community and ecosystem level.

The Arctic marine biota has been subject to many glacial-interglacial cycles, including shifts in climate and loss of sea ice during the Quaternary Period, well before the Industrial Revolution (Cronin and Cronin, 2015). However, the rapidity of the current changes in sea ice (thickness, extent, type, timing) and the projections of a continued and rapid sea ice decline, combined with increasing human activities in the previously ice-covered seas, create new Arctic conditions that require the application of a precautionary approach and science-based management of marine resources in the Arctic.

References

AMAP, 2011. Snow, Water, Ice and Permafrost in the Arctic (SWIPA): Climate Change and the Cryosphere. Arctic Monitoring and Assessment Programme (AMAP), Oslo, Norway.

Andreas, E.L., 2011. A relationship between the aerodynamic and physical roughness of winter sea ice. *Quarterly Journal of the Royal Meteorology Society*, 137:1581-1588.

Ardyna, M., M. Babin, M. Gosselin, E. Devred, L. Rainville and J.-É. Tremblay, 2014. Recent Arctic Ocean sea ice loss triggers novel fall phytoplankton blooms. *Geophysical Research Letters*, 41:6207-6212.

Arndt, C.E. and K.M. Swadling, 2006. Crustacea in Arctic and Antarctic sea ice: distribution, diet and life history strategies. *Advances in Marine Biology*, 51:197-315.

Armitage, T.W.K. and A.L. Ridout, 2015. Arctic sea ice freeboard from AltiKa and comparison with CryoSat-2 and Operation IceBridge. *Geophysical Research Letters*, 42:6724-6731.

Arrigo, K.R. and G.L. van Dijken, 2015. Continued increases in Arctic Ocean primary production. *Progress in Oceanography*, 136:60-70.

Arrigo, K.R., D.K. Perovich, R.S. Pickart, Z.W. Brown, G.L. van Dijken, K.E. Lowry, M.M. Mills, M.A. Palmer, W.M. Balch, N.R. Bates, C. Benitez-Nelson, B. Bowler, E. Brownlee, J.K. Ehn, K.E. Frey, R. Garley, S.R. Laney, L. Lubelczyk, J. Mathis, A. Matsuoka, B.G. Mitchell, G.W.K. Moore, E. Ortega-Retuerta, S. Pal, C.M. Polashenski, R.A. Reynolds, B. Schieber, H.M. Sosik, M. Stephens and J.H. Swift, 2012. Massive phytoplankton blooms under Arctic sea ice. *Science*, 336:1408-1408.

Arrigo, K.R., D.K. Perovich, R.S. Pickart, Z.W. Brown, G.L. van Dijken, K.E. Lowry, M.M. Mills, M.A. Palmer, W.M. Balch, N.R. Bates, C.R. Benitez-Nelson, E. Brownlee, K.E. Frey, S.R. Laney, J. Mathis, A. Matsuoka, B.G. Mitchell, G.W.K. Moore, R.A. Reynolds, H.M. Sosik and J.H. Swift, 2014. Phytoplankton blooms beneath the sea ice in the Chukchi Sea. *Deep Sea Research II*, 105:1-16.

Årthun, M. and C. Schrum, 2010. Ocean surface heat flux variability in the Barents Sea. *Journal of Marine Systems*, 83:88-98.

Årthun, M., T. Eldevik, L.H. Smedsrød, Ø. Skagseth and R.B. Ingvaldsen, 2012. Quantifying the influence of Atlantic heat on Barents Sea ice variability and retreat. *Journal of Climate*, 25:4736-4743.

Aslam, S.N., C. Michel, A. Niemi and G.J.C. Underwood, 2016. Patterns and drivers of carbohydrate budgets in ice algal assemblages from first year Arctic sea ice. *Limnology and Oceanography*, 61:919-937.

Asplin, M.G., J.V. Lukovich and D.G. Barber, 2009. Atmospheric forcing of the Beaufort Sea ice gyre: Surface pressure climatology and sea ice motion. *Journal of Geophysical Research*, 114:C00A06, doi:10.1029/2008JC005127.

Asplin, M.G., R. Galley, D.G. Barber and S. Prinsenberg, 2012. Fracture of summer perennial sea ice by ocean swell as a result of Arctic storms. *Journal of Geophysical Research*, C06025, doi:10.1029/2011JC007221.

Asplin, M.G., R. Scharien, B.G.T. Else, D.G. Barber, T. Papakyriakou, S. Howell and S. Prinsenberg, 2014. Implications of fractured arctic perennial ice cover on thermodynamic and dynamic sea ice processes. *Journal of Geophysical Research: Oceans*, 119:2327-2343.

Assmy, P., J.K. Ehn, M. Fernández-Méndez, H. Hop, C. Katlein, A. Sundfjord, K. Bluhm, M. Daase, A. Engel, A. Fransson, M.A. Granskog, S.R. Hudson, S. Kristiansen, M. Nicolaus, I. Peeken, A.H.H. Renner, G. Spreen, A. Tatarak and J. Wiktor, 2013. Floating ice-algal aggregates below melting Arctic sea ice. *PLoS ONE*, 8:e76599.

Assmy, P., M. Fernández-Méndez, P. Duarte, A. Meyer, A. Randelhoff, C.J. Mundy, L.M. Olsen, H.M. Kauko, A. Bailey, M. Chierici, L. Cohen, A.P. Doulgeris, A. Fransson, S. Gerland, H. Hop, S.R. Hudson, N. Hughes, P. Iltkin, G. Johnsen, J.A. King, B. Koch, Z. Koenig, S. Kwasniewski, S.R. Laney, M. Nicolaus, A.K. Pavlov, C.M. Polashenski, C. Provost, A. Rösel, M. Sandbu, G. Spreen, L.H. Smedsrød, A. Sundfjord, T. Taskjelle, A. Tatarak, J. Wiktor, P.M. Wagner, A. Wold, H. Steen and M.A. Granskog, 2017. Leads in Arctic pack ice enable early phytoplankton blooms below snow-covered sea ice. *Scientific Reports*, 7:40850, doi:10.1038/srep40850.

Aumack, C.F., A.R. Juhl and C. Kremlins, 2014. Diatom vertical migration within land-fast Arctic sea ice. *Journal of Marine Systems*, 139:496-504.

Babb, D.G., R.J. Galley, M.G. Asplin, J.V. Lukovich and D.G. Barber, 2013. Multiyear sea ice export through the Bering Strait during winter 2011–2012. *Journal of Geophysical Research: Oceans*, 118:5489-5503.

Bailleul, F., V. Lesage, M. Powers, D.W. Doidge and M.O. Hammill, 2012. Migration phenology of beluga whales in a changing Arctic. *Climate Research*, 53:169-178.

Barber, D.G. and D. Barber, 2009. Two Ways of Knowing: Merging Science and Traditional Knowledge During the Fourth International Polar Year. University of Manitoba Press.

Barber, D.G., R. Galley, M.G. Asplin, R. De Abreu, K.-A. Warner, M. Pućko, M. Gupta, S. Prinsenberg and S. Julien, 2009. Perennial pack ice in the southern Beaufort Sea was not as it appeared in the summer of 2009. *Geophysical Research Letters*, 36:L24501, doi:10.1029/2009GL041434.

Barber, D.G., M.G. Asplin, R. Raddatz, L. Candlish, S. Nickels, S. Meakin, K. Hochheim, J.V. Lukovich, R. Galley and S. Prinsenberg, 2012. Change and variability in sea ice during the 2007–2009 Canadian International Polar Year Program. *Climatic Change*, 115:115-133.

Barber, D.G., G. McCullough, D. Babb, A.S. Komarov, L.M. Candlish, J.V. Lukovich, M. Asplin, S. Prinsenberg, I. Dmitrenko and S. Rysgaard, 2014a. Climate change and ice hazards in the Beaufort Sea. *Elementa*, 2: 000025 doi: 10.12952/journal.elementa.000025.

Barber, D.G., J.K. Ehn, M. Pućko, S. Rysgaard, J.W. Deming, J.S. Bowman, T. Papakyriakou, R.J. Galley and D.H. Søgaard, 2014b. Frost flowers on young Arctic sea ice: the climatic, chemical, and microbial significance of an emerging ice type. *Journal of Geophysical Research*, 119:11,593-11,612.

Barber, D.G., H. Hop, C.J. Mundy, B. Else, I.A. Dmitrenko, J.-E. Tremblay, J.K. Ehn, P. Assmy, M. Daase, L.M. Candlish and S. Rysgaard, 2015. Selected physical, biological and biogeochemical implications of a rapidly changing Arctic marginal ice zone. *Progress in Oceanography*, 139:122-150.

Bates, S.S., C. Léger, J.M. White, N. MacNair, J. Ehrman, M. Levasseur, J.-Y. Couture, R. Gagnon, E. Bonneau, S. Mihaud, G. Sauve', K. Pauley and J.

Chassé, 2002. Domoic acid production by the diatom *Pseudo-nitzschia seriata* causes spring closures of shellfish harvesting for the first time in the Gulf of St. Lawrence, Eastern Canada, In: Book of Abstracts. 10th International Conference on Harmful Algae. Florida.

Beitsch, A., L. Kaleschke and S. Kern, 2014. Investigating high-resolution AMSR2 sea ice concentrations during the February 2013 fracture event in the Beaufort Sea. *Remote Sensing*, 6:3841-3856.

Bélanger, S., M. Babin and J.-É. Tremblay, 2013. Increasing cloudiness in Arctic damps the increase in phytoplankton primary production due to sea ice receding. *Biogeosciences*, 10:4087-4101.

Berge, J., Ø. Varpe, M.A. Moline, A. Wold, P.E. Renaud, M. Daase and S. Falk-Petersen, 2012. Retention of ice-associated amphipods: possible consequences for an ice-free Arctic Ocean. *Biology Letters*, 8:1012-1015.

Berge, J., P.E., Renaud, G. Darnis, F. Cottier, K. Last, T.M. Gabrielsen, G. Johnsen, L. Seuthe, J.M. Weslawski, E. Leu, M. Moline, J. Nahrgang, J.E. Søreide, Ø. Varpe, O.L. Lønne, M. Daase and S. Falk-Petersen, 2015a. In the dark: A review of ecosystem processes during the Arctic polar night. *Progress in Oceanography*, 139:258-271.

Berge, J., K. Heggland, O.J. Lønne, F. Cottier, H. Hop, G.W. Gabrielsen, L. Nøttetstad and O.A. Misund, 2015b. First records of Atlantic mackerel (*Scomber scombrus*) from the Svalbard Archipelago, Norway, with possible explanations for the extension of its distribution. *Arctic*, 68:54-61.

Bi, H., H. Huang, Q. Su, L. Yan, Y. Liu and X. Xu., 2014. An Arctic sea ice thickness variability revealed from satellite altimetric measurements. *Acta Oceanologica Sinica*, 33:134-140.

Blanchard-Wrigglesworth, E., S.L. Farrell, T. Newman and C.M. Bitz, 2015. Snow cover on Arctic sea ice in observations and an Earth System Model. *Geophysical Research Letters*, 42:10,342-10,348.

Blazey, B.A., M.M. Holland and E.C. Hunke, 2013. Arctic Ocean sea ice snow depth evaluation and bias sensitivity in CCSM. *Cryosphere Discussions*, 7:1495-1532.

Bliss, A.C. and M.R. Anderson, 2014. Snowmelt onset over Arctic sea ice from passive microwave satellite data: 1979–2012. *The Cryosphere*, 8:2089-2100.

Boetius, A., S. Albrecht, K. Bakker, C. Bienhold, J. Felsen, M. Fernández-Méndez, S. Hendricks, C. Kattlein, C. Lalande, T. Krumpen, M. Nicolaus, I. Peeken, B. Rabe, A. Rogacheva, E. Rybakova, R. Somavilla, F. Wenzhöfer and RV Polarstern ARK27-3-Shipboard Science Party, 2013. Export of algal biomass from the melting Arctic sea ice. *Science*, 339:1430-1432.

Boisvert, L.N. and J.C. Stroeve, 2015. The Arctic is becoming warmer and wetter as revealed by the Atmospheric Infrared Sounder. *Geophysical Research Letters*, 42:4439-4446.

Bowman, J.S., 2015. The relationship between sea ice bacterial community structure and biogeochemistry: A synthesis of current knowledge and known unknowns. *Elementa*, 3:000072. doi: 10.12952/journal.elementa.000072.

Bowman, J.S. and J.W. Deming, 2010. Elevated bacterial abundance and exopolymers in saline frost flowers and implications for atmospheric chemistry and microbial dispersal. *Geophysical Research Letters*, 37:L13501, doi:10.1029/2010GL043020.

Bowman, J.S., C.T. Berthiaume, E.V. Armbrust and J.W. Deming, 2014. The genetic potential for key biogeochemical processes in Arctic frost flowers and young sea ice revealed by metagenomic analysis. *FEMS Microbiology Ecology*, 89:376-387.

Browman, H.I., C.A. Rodriguez, F. Béland, J.J. Cullen, R.F. Davis, J.H.M. Kouwenberg, P.S. Kuhn, B. McArthur, J.A. Runge, J.-F. St-Pierre and R.D. Vetter, 2000. Impact of ultraviolet radiation on marine crustacean zooplankton and ichthyoplankton: a synthesis of results from the estuary and Gulf of St. Lawrence, Canada. *Marine Ecology Progress Series*, 199:293-311.

Brucker, L., D.J. Cavalieri, T. Markus and A. Ivanov, 2014. NASA Team 2 sea ice concentration algorithm retrieval uncertainty. *IEEE Transactions on Geoscience and Remote Sensing*, 52:7336-7352.

Callaghan, T.V., D. Dahl-Jensen, M. Johansson, R. Kallenborn, J.R. Key, R. Macdonald, T. Prowse, M. Sharp, K. Steffen and W.F. Vincent, 2011. Cross-cutting scientific issues. In: *Snow, Water, Ice and Permafrost in the Arctic (SWIPA): Climate Change and the Cryosphere*. Arctic Monitoring and Assessment Programme (AMAP), Oslo, Norway.

Campbell, K.L., C.J. Mundy, D.G. Barber and M. Gosselin, 2015. Characterizing the ice algae biomass-snow depth relationship over spring melt using transmitted irradiance. *Journal of Marine Systems*, 147:76-84.

Carmack, E. and D.C. Chapman, 2003. Wind-driven shelf/basin exchange on an Arctic shelf: The joint roles of ice cover and shelf-break bathymetry. *Geophysical Research Letters*, 30:1778. doi:10.1029/2003GL017526.

Cavalieri, D.J. and C.L. Parkinson, 2012. Arctic sea ice variability and trends, 1979–2010. *The Cryosphere*, 6:881-889.

Cavalieri, D.J., T. Markus and J.C. Comiso, 2014. AMSR-E/Aqua Daily L3 12.5 km Brightness Temperature, Sea Ice Concentration, and Snow Depth Polar Grids. Version 3. National Snow and Ice Data Center, Boulder, Colorado USA.

Christiansen, J.S. and J.D. Reist, 2013. Fishes. In: *Arctic Biodiversity Assessment. Conservation of Arctic Flora and Fauna (CAFF)*.

Christiansen, J.S., H. Schurmann and L.I. Karamushko, 1997. Thermal behaviour of polar fish: a brief survey and suggestions for research. *Cybium*, 21:353-362.

Christiansen, J.S., C.W. Mecklenburg and O.L. Karamushko, 2014. Arctic marine fishes and their fisheries in light of global change. *Global Change Biology*, 20:352-359.

Christiansen, J.S., E. Bonsdorff, I. Byrkjedal, S.-E. Fevolden, O.V. Karamushko, A. Lynghammer, C.W. Mecklenburg, P.D.R. Møller, J. Nielsen, M.C. Nordström, K. Præbel and R.M. Wienerroither, 2016. Novel biodiversity baselines outpace models of fish distribution in Arctic waters. *The Science of Nature*, 103:8, doi:10.1007/s00114-016-1332-9.

Clark, G.F., J.S. Stark, E.L. Johnston, J.W. Runcie, P.M. Goldsworthy, B. Raymond and M.J. Riddle, 2013. Light-driven tipping points in polar ecosystems. *Global Change Biology*, 19:3749-3761.

Collins, R.E., G. Rocap and J.W. Deming, 2010. Persistence of bacterial and archaeal communities in sea ice through an Arctic winter. *Environmental Microbiology*, 12:1828-1841.

Collins, M., R. Knutti, J. Arblaster, J.-L. Dufresne, T. Fichefet, P. Friedlingstein, X. Gao, W.J. Gutowski, T. Johns, G. Krinner, M. Shongwe, C. Tebaldi, A.J. Weaver and M. Wehner, 2013. Long-term climate change: projections, commitments and irreversibility. In: Stocker, T.F., D. Qin, G.-K. Plattner, M. Tignor, S.K. Allen, J. Boschung, A. Nauels, Y. Xia, V. Bex and P.M. Midgley (eds.), *Climate Change 2013: The Physical Science Basis. Contribution of Working Group I to the Fifth Assessment Report of the Intergovernmental Panel on Climate Change*. Cambridge University Press.

Comiso, J.C., 2012. Large decadal decline of the Arctic multiyear ice cover. *Journal of Climate*, 25:1176-1193.

Craig, P.C., W.B. Griffiths, L. Haldorson and H. McElderry, 1982. Ecological studies of Arctic cod (*Boreogadus saida*) in Beaufort Sea coastal waters, Alaska. *Canadian Journal of Fisheries and Aquatic Sciences*, 39:395-406.

Cronin, T.M. and M.A. Cronin, 2015. Biological response to climate change in the Arctic Ocean: the view from the past. *Arktos*, 1:4, doi:10.1007/s41063-015-0019-3.

David, C., B. Lange, B. Rabe and H. Flores, 2015. Community structure of under-ice fauna in the Eurasian central Arctic Ocean in relation to environmental properties of sea-ice habitats. *Marine Ecology Progress Series*, 522:15-32.

David, C., B. Lange, T. Krumpen, F. Schaafsma, J.A. van Franeker and H. Flores, 2016. Under-ice distribution of polar cod *Boreogadus saida* in the central Arctic Ocean and their association with sea-ice habitat properties. *Polar Biology*, 39:981-994.

de Steur, L., E. Hansen, C. Mauritzen, A. Beszczynska-Möller and E. Fahrbach, 2014. Impact of recirculation on the East Greenland Current in Fram Strait: Results from moored current meter measurements between 1997 and 2009. *Deep Sea Research I*, 92:26-40.

Dietz, R., M.P. Heide-Jørgensen, P. Richard, J. Orr, K. Laidre and H.C. Schmidt, 2008. Movements of narwhals (*Monodon monoceros*) from Admiralty Inlet monitored by satellite telemetry. *Polar Biology*, 31:1295-1306.

Divine, D.V., M.A. Granskog, S.R. Hudson, C.A. Pedersen, T.I. Karlsen, S.A. Divina and S. Gerland, 2015. Regional melt pond fraction and albedo of thin Arctic first-year drift ice in late summer. *The Cryosphere*, 9:255-268.

Dmitrenko, I.A., S.A. Kirillov, N. Serra, N.V. Koldunov, V.V. Ivanov, U. Schauer, I.V. Polyakov, D. Barber, M. Janout, V.S. Lien, M. Makhotin and Y. Aksenov, 2014. Heat loss from the Atlantic water layer in the northern Kara Sea: causes and consequences. *Ocean Science*, 10:719-730.

Dorn, W., K. Dethloff and A. Rinke, 2012. Limitations of a coupled regional climate model in the reproduction of the observed Arctic sea-ice retreat. *The Cryosphere*, 6:985-998.

Dööscher, R., K. Wyser, H.M. Meier, M. Qian and R. Redler, 2010. Quantifying Arctic contributions to climate predictability in a regional coupled ocean-ice-atmosphere model. *Climate Dynamics*, 34:1157-1176.

Dööscher, R., T. Vihma and E. Maksimovich, 2014. Recent advances in understanding the Arctic climate system state and change from a sea ice perspective: a review. *Atmospheric Chemistry and Physics*, 14:13571-13600.

Doucette, G.J., C.M. Mikulski, K.L. King, P.B. Roth, Z. Wang, L.F. Leandro, S.L. DeGrasse, K.D. White, D. De Biase, R.M. Gillett and R.M. Rolland, 2012. Endangered North Atlantic right whales (*Eubalaena glacialis*) experience repeated, concurrent exposure to multiple environmental neurotoxins produced by marine algae. *Environmental Research*, 112:67-76.

Douglas, T.A., F. Domine, M. Barret, C. Anastasio, H.J. Beine, J. Bottenheim, A. Grannas, S. Houdier, S. Netcheva, G. Rowland, R. Staebler and A. Steffen, 2012. Frost flowers growing in the Arctic ocean-atmosphere-sea ice-snow interface: 1. Chemical composition. *Journal of Geophysical Research*, 117:D00R09, doi:10.1029/2011JD016460.

Druzhkov, N.V., E.I. Druzhkova and L.L. Kuznetsov, 2001. The sea-ice algal community of seasonal pack ice in the southwestern Kara Sea in late winter. *Polar Biology*, 24:70-71.

Eastwood, S. (ed.), 2014. Ocean and Sea Ice SAF Sea Ice Product User's Manual. Version 3.11. <http://osisaf.met.no/p/ice/> (accessed 28 December 2015).

Egeland, G.M., A. Pacey, Z. Cao and I. Sobol, 2010. Food insecurity among Inuit preschoolers: Nunavut Inuit child health survey, 2007–2008. *Canadian Medical Association Journal*, 182:243-248.

Ehn, J.K. and C.J. Mundy, 2013. Assessment of light absorption within highly scattering bottom sea ice from under-ice light measurements: Implications for Arctic ice algae primary production. *Limnology and Oceanography*, 58:893-902.

Ehn, J.K., C.J. Mundy, D.G. Barber, H. Hop, A. Rossnagel and J. Stewart, 2011. Impact of horizontal spreading on light propagation in melt pond covered seasonal sea ice in the Canadian Arctic. *Journal of Geophysical Research*, 116:C00G02, doi:10.1029/2010JC006908.

Eicken, H., T.C. Grenfell, D.K. Perovich, J.A. Richter-Menge and K. Frey, 2004. Hydraulic controls of summer Arctic pack ice albedo. *Journal of Geophysical Research*, 109:C08007, doi:10.1029/2003JC001989.

Eisenman, I., W.N. Meier and J.R. Norris, 2014. A spurious jump in the satellite record: has Antarctic sea ice expansion been overestimated? *The Cryosphere*, 8:1289-1296.

Elliott, A., C.J. Mundy, M. Gosselin, M. Poulin, K. Campbell and F. Wang, 2015. Spring production of mycosporine-like amino acids and other UV-absorbing compounds in sea ice-associated algae communities in the Canadian Arctic. *Marine Ecology Progress Series*, 541:91-104.

Falk-Petersen, S., V. Pavlov, S. Timofeev and J.R. Sargent, 2007. Climate variability and possible effects on arctic food chains: The role of *Calanus*. In: Ørbaek, J.B., R. Kallenborn, I. Tombre, E.N. Hegseth, S. Falk-Petersen and A.H. Hoel (eds), *Arctic Alpine Ecosystems and People in a Changing Environment*. pp. 147-166.

Falk-Petersen, S., V. Pavlov, J. Berge, F. Cottier, K.M. Kovacs and C. Lydersen, 2015. At the rainbow's end: high productivity fueled by winter upwelling along an Arctic shelf. *Polar Biology*, 38:5-11.

Fehling, J., K. Davidson and S.S. Bates, 2005. Growth dynamics of non-toxic *Pseudo-nitzschia delicatissima* and toxic *P. seriata* (Bacillariophyceae) under simulated spring and summer photoperiods. *Harmful Algae*, 4:763-769.

Ferguson, S.H., L. Dueck, L.L. Loseto and S.P. Luque, 2010. Bowhead whale *Balaena mysticetus* seasonal selection of sea ice. *Marine Ecology Progress Series*, 411:285-297.

Fernández-Méndez, M., C. Katlein, B. Rabe, M. Nicolaus, I. Peeken, K. Bakker, H. Flores and A. Boetius, 2015. Photosynthetic production in the central Arctic Ocean during the record sea-ice minimum in 2012. *Biogeosciences*, 12:3525-3549.

Fetterer, F., K. Knowles and M. Savoie, 2016, updated daily. Sea Ice Index. Version 2. National Snow and Ice Data Center, Boulder, Colorado USA. <http://dx.doi.org/10.7265/N5736NV7>.

Findlay, C.R., R. Wiens, M. Rak, J. Sedlmair, C.J. Hirschmugl, J. Morrison, C.J. Mundy, M. Kansize and K.M. Gough, 2015. Rapid biodiagnostic ex vivo imaging at 1 μ m pixel resolution with thermal source FTIR FPA. *Analyst*, 140, 2493-2503.

Flocco, D., D.L. Feltham and A.K. Turner, 2010. Incorporation of a physically based melt pond scheme into the sea ice component of a climate model. *Journal of Geophysical Research*, 115:C08012, doi:10.1029/2009JC005568.

Flocco, D., D. Schroeder, D.L. Feltham and E.C. Hunke, 2012. Impact of melt ponds on Arctic sea ice simulations from 1990 to 2007. *Journal of Geophysical Research*, 117:C09032, doi:10.1029/2012JC008195.

Fortier, L., D. Pontona and M. Gilbert, 1995. The match/mismatch hypothesis and the feeding success of fish larvae in ice-covered southeastern Hudson Bay. *Marine Ecology Progress Series*, 120:11-27.

Fortier, M., L. Fortier, C. Michel and L. Legendre, 2002. Climatic and biological forcing of the vertical flux of biogenic particles under seasonal arctic sea ice. *Marine Ecology Progress Series*, 225:1-16.

Fossheim, M., R. Primicerio, E. Johannessen, R.B. Ingvaldsen, M.M. Aschan and A.V. Dolgov, 2015. Recent warming leads to a rapid borealization of fish communities in the Arctic. *Nature Climate Change*, 5:673-677.

Francis, O.P., G.G. Pantaleev and D.E. Atkinson, 2011. Ocean wave conditions in the Chukchi Sea from satellite and in situ observations. *Geophysical Research Letters*, 38:L24610, doi:10.1029/2011GL049839.

Fransson, A., M. Chierici, K. Abrahamson, M. Andersson, A. Gransfors, K. Gärfeldt, A. Torstensson and A. Wulff, 2015. CO₂-system development in young sea ice and CO₂ gas exchange at the ice-air interface mediated by brine and frost flowers in Kongsfjorden, Spitsbergen. *Annals of Glaciology*, 56:245-257.

Frey, K.E., D.K. Perovich and B. Light, 2011. The spatial distribution of solar radiation under a melting Arctic sea ice cover. *Geophysical Research Letters*, 38, L22501, doi:10.1029/2011GL049421.

Frey, K.E., G.W.K. Moore, L.W. Cooper and J.M. Grebmeier, 2015. Divergent patterns of recent sea ice cover across the Bering, Chukchi, and Beaufort seas of the Pacific Arctic region. *Progress in Oceanography*, 136:32-49.

Fripiat, F., J.-L. Tison, L. André, D. Notz and B. Delille, 2014. Biogenic silica recycling in sea ice inferred from Si-isotopes: constraints from Arctic winter first-year sea ice. *Biogeochemistry*, 119:25-33.

Galindo, V., M. Levasseur, C.J. Mundy, M. Gosselin, J.-E. Tremblay, M. Scarratt, Y. Gratton, T. Papakiriakou, M. Poulin and M. Lizotte, 2014. Biological and physical processes influencing sea ice, under-ice algae, and dimethylsulfoniopropionate during spring in the Canadian Arctic Archipelago. *Journal of Geophysical Research*, 119:3746-3766.

Galley, R.J., B.G.T. Else, S.J. Prinsenberg and D.G. Barber, 2013. Sea ice concentration, extent, age, motion and thickness in regions of proposed offshore oil and gas development near the Mackenzie Delta - Canadian Beaufort Sea. *Arctic*, 66:105-116.

Gardner, J., J. Richter-Menge, S. Farrell and J. Brozena, 2012. Coincident multiscale estimates of Arctic sea ice thickness. *Eos, Transactions American Geophysical Union*, 93:57-58.

Geilfus, N.-X., R.J. Galley, O. Crabeck, T. Papakiriakou, J. Landy, J.-L. Tison and S. Rysgaard, 2014. Inorganic carbon dynamics of melt pond-covered first year sea ice in the Canadian Arctic. *Biogeosciences*, 12:2047-2061.

Giles, K.A., S.W. Laxon, A.L. Ridout, D.J. Wingham and S. Bacon, 2012. Western Arctic Ocean freshwater storage increased by wind-driven spin-up of the Beaufort Gyre. *Nature Geoscience*, 5:194-197.

Glud, R.N., S. Rysgaard, G. Turner, D.F. McGinnis and R.J.G. Leakey, 2014. Biological- and physical-induced oxygen dynamics in melting sea ice of the Fram Strait. *Limnology and Oceanography*, 59:1097-1111.

González, T.F. and R. Anadón, 2014. Seasonality of North Atlantic phytoplankton from space: impact of environmental forcing on a changing phenology (1998-2012). *Global Change Biology*, 20:698-712.

Goosse, H., O. Arzel, C.M. Bitz, A. de Montety and M. Vancoppenolle, 2009. Increased variability of the Arctic summer ice extent in a warmer climate. *Geophysical Research Letters*, 36:L23702, doi:10.1029/2009GL040546.

Gradinger, R.R. and B.A. Bluhm, 2004. In-situ observations on the distribution and behavior of amphipods and Arctic cod (*Boreogadus saida*) under the sea ice of the High Arctic Canada Basin. *Polar Biology*, 27:595-603.

Granskog, M.A., P. Assmy, S. Gerland, G. Spreen, H. Steen and L.H. Smedsrød, 2016. Arctic research on thin ice: Consequences of Arctic sea ice loss. *Eos, Transactions American Geophysical Union*, 97:22-26.

Grebmeier, J.M., B.A. Bluhm, L.W. Cooper, S.L. Danielson, K.R. Arrigo, A.L. Blanchard, J.T. Clarke, R.H. Day, K.E. Frey, R.R. Gradinger, M. Kedra, B. Konar, K.J. Kuletz, S.H. Lee, J.R. Lovvord, B.L. Norcross and S.R. Okkonen, 2015. Ecosystem characteristics and processes facilitating persistent macrobenthic biomass hotspots and associated benthivory in the Pacific Arctic. *Progress in Oceanography*, 136:92-114.

Haas, C. and S.E.L. Howell, 2015. Ice thickness in the Northwest Passage. *Geophysical Research Letters*, 42:7673-7680.

Hakkinen, S., A. Proshutinsky and I. Ashik, 2008. Sea ice drift in the Arctic since the 1950s. *Geophysical Research Letters*, 35:L19704, doi:10.1029/2008GL034791.

Hansen, L.R., S. Soylu, Y. Kotaki, Ø. Moestrup and N. Lundholm, 2011. Toxin production and temperature-induced morphological variation of the diatom *Pseudo-nitzschia seriata* from the Arctic. *Harmful Algae*, 10:689-696.

Hansen, E., S. Gerland, M.A. Granskog, O. Pavlova, A.H.H. Renner, J. Haapala, T.B. Løyning and M. Tschudi, 2013. Thinning of Arctic sea ice observed in Fram Strait: 1990-2011. *Journal of Geophysical Research: Oceans*, 118:5202-5221.

Hansen, E., O.-C. Ekeberg, S. Gerland, O. Pavlova, G. Spreen and M. Tschudi, 2014. Variability in categories of Arctic sea ice in Fram Strait. *Journal of Geophysical Research: Oceans*, 119:7175-7189.

Harðardóttir, S., M. Pančić, A. Tammilehto, T.G. Nielsen, B. Krock, E.F. Møller and N. Lundholm, 2015. Dangerous relations in the arctic marine food web – interactions between domoic acid producing *Pseudo-nitzschia* diatoms and *Calanus* copepodites. *Marine Drugs*, 13:3809-3835.

Harwood, L.A., T.G. Smith, H. Melling, J. Alikamik and M.C. Kingsley, 2012. Ringed seals and sea ice in Canada's Western Arctic: Harvest-based monitoring 1992-2011. *Arctic*, 65:377-390.

Hawkins, E. and R. Sutton, 2009. The potential to narrow uncertainty in regional climate predictions. *Bulletin of the American Meteorological Society*, 90:1095-1107.

Henriksen, S. and O. Hilmo (eds), 2015. *Norsk rødliste for arter 2015. Artdatabanken, Norge*.

Heygster, G., M. Huntemann, N. Ivanova, R. Saldo and L.T. Pedersen, 2014. Response of passive microwave sea ice concentration algorithms to thin ice. *Proceedings Geoscience and Remote Sensing Symposium (IGARSS)*, 2014 IEEE International. 13-18 July, Quebec City. pp. 3618-3621.

Hezel, P.J., X. Zhang, C.M. Bitz, B.P. Kelly and F. Massonnet, 2012. Projected decline in spring snow depth on Arctic sea ice caused by progressively later autumn open ocean freeze-up this century. *Geophysical Research Letters*, 39:L17505, doi:10.1029/2012GL052794.

Holland, M.M. and L. Landrum, 2015. Factors affecting projected Arctic surface shortwave heating and albedo change in coupled climate models. *Philosophical Transactions of the Royal Society A*, 373, doi:10.1098/rsta.2014.0162.

Holland, M.M., D.A. Bailey, B.P. Briegleb, B. Light and E. Hunke, 2012. Improved sea ice shortwave radiation physics in CCSM4: the impact of melt ponds and aerosols on arctic sea ice. *Journal of Climate*, 25:1413-1430.

Hoppmann, M., M. Nicolaus, P.A. Hunkeler, P. Heil, L.-K. Behrens, G. König-Langlo and R. Gerdes, 2015. Seasonal evolution of an ice-shelf influenced fast-ice regime, derived from an autonomous thermistor chain. *Journal of Geophysical Research: Oceans*, 120:1703-1724.

Horner, R.A., D.L. Garrison and F.G. Plumley, 1997. Harmful algal blooms and red tide problems on the U.S. west coast. *Limnology and Oceanography*, 42:1076-1088.

Howell, S.E.L., C. Derksen, L. Pizzolato and M. Brady, 2015. Multiyear ice replenishment in the Canadian Arctic Archipelago: 1997–2013. *Journal of Geophysical Research: Oceans*, 120:1623-1637.

Hudson, S.R., M.A. Granskog, A. Sundsfjord, A. Randelhoff, A.H.H. Renner and D.V. Divine, 2013. Energy budget of first-year Arctic sea ice in advanced stages of melt. *Geophysical Research Letters*, 40:2679-2683.

Hunke, E.C., D.A. Hebert and O. Lecomte, 2013. Level-ice melt ponds in the Los Alamos sea ice model. *CICE. Ocean Modelling*, 71:26-42.

Huntemann, M., G. Heygster, L. Kaleschke, T. Krumpen, M. Mäkynen and M. Drusch, 2014. Empirical sea ice thickness retrieval during the freeze up period from SMOS high incident angle observations. *The Cryosphere*, 8:439-451.

Iacozza, J. and D.G. Barber, 2010. An examination of snow redistribution over smooth land-fast sea ice. *Hydrological Processes*, 24:850-865.

IPCC, 2013. *Climate Change 2013: The Physical Science Basis. Contribution of Working Group I to the Fifth Assessment Report of the Intergovernmental Panel on Climate Change*. Stocker, T.F., D. Qin, G.-K. Plattner, M. Tignor, S.K. Allen, J. Boschung, A. Nauels, Y. Xia, V. Bex and P.M. Midgley (eds.). Cambridge University Press.

Ivanov, V., V. Alexeev, N.V. Koldunov, I. Repina, A.B. Sandø, L.H. Smedsrød and A. Smirnov, 2015. Arctic Ocean heat impact on regional ice decay - a suggested positive feedback. *Journal of Physical Oceanography*, 46:1437-1456.

Ivanova, N., L.T. Pedersen, R.T. Tonboe, S. Kern, G. Heygster, T. Lavergne, A. Sørensen, R. Saldo, G. Dybkjær, L. Brucker and M. Shokr, 2015. Inter-comparison and evaluation of sea ice algorithms: towards further identification of challenges and optimal approach using passive microwave observations. *The Cryosphere*, 9:1797-1817.

Jackson, K., J. Wilkinson, T. Maksym, D. Meldrum, J. Beckers, C. Haas and D. Mackenzie, 2013. A novel and low-cost sea ice mass balance buoy. *Journal of Atmospheric and Oceanic Technology*, 30:2676-2688.

Jackson, J.M., H. Melling, J.V. Lukovich, D. Fissel and D.G. Barber, 2015. Formation of winter water on the Canadian Beaufort shelf: new insight from observations during 2009-2011. *Journal of Geophysical Research: Oceans*, 120:4090-4107.

Jahn, A., K. Sterling, M.M. Holland, J.E. Kay, J.A. Maslanik, C.M. Bitz, D.A. Bailey, J. Stroeve, E.C. Hunke, W.H. Lipscomb and D. Pollak, 2012. Late 20th century simulation of Arctic sea ice and ocean properties in CCSM. *Journal of Climate*, 25:1431-1452.

Jahn, A., J.E. Kay, M.M. Holland and D.M. Hall, 2016. How predictable is the timing of a summer ice-free Arctic? *Geophysical Research Letters*, 43:9113-9120.

Jeffries, M.O., J.E. Overland and D.K. Perovich, 2013. The Arctic shifts to a new normal. *Physics Today*, 66:35.

Ji, R., M. Jin and Ø. Varpe, 2013. Sea ice phenology and timing of production pulses in the Arctic Ocean. *Global Change Biology* 19:734-741.

Johnson, N., L. Alessa, C. Behe, F. Danielsen, S. Gearheard, V. Gofman-Wallingfor, A. Kliskey, E.-M. Krummel, A. Lynch, T. Mustonen, P. Pulsifer and M. Svoboda, 2015. The contributions of community-based monitoring and traditional knowledge to Arctic observing networks: Reflections on the state of the field. *Arctic*, 68:28-40.

Kaleschke, L., X. Tian-Kunze, N. Maaß, M. Mäkynen and M. Drusch, 2012. Sea ice thickness retrieval from SMOS brightness temperatures during the Arctic freeze-up period. *Geophysical Research Letters*, 39:L05501, doi:10.1029/2012GL050916.

Kaleschke, L., X. Tian-Kunze, N. Maaß, A. Beitsch, A. Wernecke, M. Miernecki, G. Müller, B.H. Fock, A.M. Gierisch, H.K. Schlünzen, T. Pohlmann, M. Dobrynin, S. Hendricks, J. Asseng, R. Gerdes, P. Jochmann, N. Reimer, J. Holfort, C. Melsheimer, G. Heygster, G. Spreen, S. Gerland, J. King, N. Skou, S.S. Søbjærg, C. Haas, F. Richter and T. Casal, 2016. SMOS sea ice product: operational application and validation in the Barents Sea marginal ice zone. *Remote Sensing of Environment*, 180:264-273.

Kapsch, M.-L., R.G. Graversen, M. Tjernström and R. Bintanja, 2016. The effect of downwelling longwave and shortwave radiation on Arctic summer sea ice. *Journal of Climate*, 29:1143-1159.

Katlein, C., M. Nicolaus and C. Petrich, 2014. The anisotropic scattering coefficient of sea ice. *Journal of Geophysical Research: Oceans*, 119:842-855.

Katlein, C., S. Arndt, M. Nicolaus, D.K. Perovich, M.V. Jakuba, S. Suman, S. Elliott, L.L. Whitcomb, C.J. McFarland, R. Gerdes, A. Boetius and C.R. German, 2015. Influence of ice thickness and surface properties on light transmission through Arctic sea ice. *Journal of Geophysical Research: Oceans*, 120:5932-5944.

Kay, J.E., M.M. Holland and A. Jahn, 2011. Inter-annual to multi-decadal Arctic sea ice extent trends in a warming world. *Geophysical Research Letters*, 38:L15708, doi:10.1029/2011GL048008.

Kay, J.E., C. Deser, A. Phillips, A. Mai, C. Hannay, G. Strand, J.M. Arblaster, S.C. Bates, G. Danabasoglu, J. Edwards, M. Holland, P. Kushner, J.-F. Lamarque, D. Lawrence, K. Lindsay, A. Middleton, E. Munoz, R. Neale, K. Oleson, L. Polvani and M. Vertenstein, 2015. The Community Earth System Model (CESM) Large Ensemble Project: A community Resource for studying climate change in the presence of internal climate variability. *Bulletin of the American Meteorological Society*, doi:10.1175/BAMS-D-13-00255.1.

Kent, D., H.E. Drost, J. Fisher, T. Oyama and A.P. Farrell, 2016. Laboratory rearing of wild Arctic cod *Boreogadus saida* from egg to adulthood. *Journal of Fish Biology*, 88:1241-1248.

Kern, S., 2004. A new method for medium-resolution sea ice analysis using weather-influence corrected Special Sensor Microwave/Imager 85 GHz data. *International Journal of Remote Sensing*, 25:4555-4582.

Kern, S., K. Khorostovsky, H. Skourup, E. Rinne, Z.S. Parsakhoov, V. Djepa, P. Wadhams and S. Sandven, 2015. The impact of snow depth, snow density and ice density on sea ice thickness retrieval from satellite radar altimetry: results from the ESA-CCI Sea Ice ECV Project Round Robin Exercise. *The Cryosphere*, 9:37-52.

Kern, S., A. Roesel, L.T. Pedersen, N. Ivanova, R. Saldo and R.T. Tonboe, 2016. The impact of melt ponds on summertime microwave brightness temperatures and sea-ice concentrations. *The Cryosphere*, 10:2217-2239.

King, J., S. Howell, C. Derksen, N. Rutter, P. Toose, J. Beckers, C. Haas, N. Kurtz and J. Richter-Menge, 2015. Evaluation of Operation IceBridge

quick-look snow depth estimates on sea ice. *Geophysical Research Letters*, 42:9302-9310.

Koenig, L., S. Martin, M. Studinger and J. Sonntag, 2010. Polar airborne observations fill gap in satellite data. *Eos, Transactions American Geophysical Union*, 91:333-334.

Koenigk, T. and L. Brodeau, 2014. Ocean heat transport into the Arctic in the twentieth and twenty-first century in EC-Earth. *Climate Dynamics*, 42:3101-3120.

Koenigk, T., A. Devasthale and K.-G. Karlsson, 2014. Summer Arctic sea ice albedo in CMIP5 models. *Atmospheric Chemistry and Physics*, 14:1987-1998.

Kongoli, C., S.A. Boukabara, B. Yan, F. Weng and R. Ferraro, 2011. A new sea-ice concentration algorithm based on microwave surface emissivities – application to AMSU measurements. *IEEE Transactions on Geoscience and Remote Sensing*, 49:175-189.

Kovacs, K.M. and C. Lydersen, 2008. Climate change impacts on seals and whales in the North Atlantic Arctic and adjacent shelf seas. *Science Progress*, 91:117-150.

Krishfield, R.A., A. Proshutinsky, K. Tateyama, W.J. Williams, E.C. Carmack, F.A. McLaughlin and M.L. Timmermans, 2014. Deterioration of perennial sea ice in the Beaufort Gyre from 2003 to 2012 and its impact on the oceanic freshwater cycle. *Journal of Geophysical Research: Oceans*, 119:1271-1305.

Kuhn, P.S., H.I. Browman, R.F. Davis, J.J. Cullen and B.L. McArthur, 2000. Modeling the effects of ultraviolet radiation on embryos of *Calanus finmarchicus* and Atlantic cod (*Gadus morhua*) in a mixing environment. *Limnology and Oceanography*, 45:1797-1806.

Kurtz, N. and S. Farrell, 2011. Large-scale surveys of snow depth on Arctic sea ice from Operation IceBridge. *Geophysical Research Letters*, 38:L20505, doi:10.1029/2011GL049216.

Kurtz, N., M. Studinger, J. Harbeck, V.D. Onana and S. Farrell, 2012. IceBridge Sea Ice Freeboard, Snow Depth, and Thickness. Version 1. National Snow and Ice Data Center, Boulder, Colorado, USA.

Kurtz, N.T., S.L. Farrell, M. Studinger, N. Galin, J.P. Harbeck, R. Lindsay, V.D. Onana, B. Panzer and J.G. Sonntag, 2013. Sea ice thickness, freeboard, and snow depth products from Operation IceBridge airborne data. *The Cryosphere*, 7:1035-1056.

Kurtz, N., N. Galin and M. Studinger, 2014. An improved CryoSat-2 sea ice freeboard retrieval algorithm through the use of waveform fitting. *The Cryosphere*, 8:1217-1237.

Kwok, R., 2009. Outflow of Arctic Ocean sea ice into the Greenland and Barents Seas: 1979–2007. *Journal of Climate*, 22:2438-2457.

Kwok, R., 2010. Satellite remote sensing of sea ice thickness and kinematics: A review. *Journal of Glaciology*, 56:1129-1140.

Kwok, R., 2011. Observational assessments of Arctic Ocean sea ice motion, export, and thickness in CMIP3 climate simulations. *Journal of Geophysical Research*, 116, C00D05, doi:10.1029/2011JC007004.

Kwok, R., 2014a. Declassified high-resolution visible imagery for Arctic sea ice investigations: An overview. *Remote Sensing of Environment*, 142:44-56.

Kwok, R., 2014b. Simulated effects of a snow layer on retrieval of CryoSat-2 sea ice freeboard. *Geophysical Research Letters*, 41:5014-5020.

Kwok, R., 2015. Sea ice convergence along the Arctic coasts of Greenland and the Canadian Arctic Archipelago: Variability and extremes (1992–2014). *Geophysical Research Letters*, 42:7598-7605.

Kwok, R. and G. Cunningham, 2011. Deformation of the Arctic Ocean ice cover after the 2007 record minimum in summer ice extent. *Cold Regions Science and Technology*, 76-77:17-23.

Kwok, R. and G.F. Cunningham, 2015. Variability of Arctic sea ice thickness and volume from CryoSat-2. *Philosophical Transactions of the Royal Society*, 373(2045), 20140157, doi:10.1098/rsta.2014.0157.

Kwok, R., G.F. Cunningham, M. Wensnahan, I. Rigor, H.J. Zwally and D. Yi, 2009. Thinning and volume loss of the Arctic Ocean sea ice cover: 2003–2008. *Journal of Geophysical Research*, 114:C07005, doi:10.1029/2009JC005312, 2009.

Kwok, R., L. Toudal Pedersen, P. Gudmandsen and S.S. Pang, 2010. Large sea ice outflow into the Nares Strait in 2007. *Geophysical Research Letters*, 37:L03502, doi:10.1029/2009GL041872.

Kwok, R., G. Spreen and S. Pang, 2013. Arctic sea ice circulation and drift speed: Decadal trends and ocean currents. *Journal of Geophysical Research: Oceans*, 118:2408-2425.

Laidre, K.L., I. Stirling, L.F. Lowry, Ø. Wiig, M.P. Heide-Jørgensen and S.H. Ferguson, 2008. Quantifying the sensitivity of Arctic marine mammals to climate-induced habitat change. *Ecological Applications*, 18:S97-S125.

Laidre, K.L., H. Stern, K.M. Kovacs, L. Lowry, S.E. Moore, E.V. Regehr, S.H. Ferguson, Ø. Wiig, P. Boveng, R.P. Angliss, E.W. Born, D. Litovka, L. Quakenbush, C. Lydersen, D. Vongraven and F. Ugarte, 2015. Arctic marine mammal population status, sea ice habitat loss, and conservation recommendations for the 21st century. *Conservation Biology*, 29:724-737.

Laliberté, F., S.E.L. Howell and P.J. Kushner, 2016. Regional variability of a projected sea ice-free Arctic during the summer months. *Geophysical Research Letters*, 43:256-263.

Lamarque, J.-F., T.C. Bond, V. Eyring, C. Granier, A. Heil, Z. Klimont, D. Lee, C. Liouesse, A. Mieville, B. Owen, M.G. Schultz, D. Shindell, S.J. Smith, E. Stehfest, J. Van Aardenne, O.R. Cooper, M. Kainuma, N. Mahowald, J.R. McConnell, V. Naik, K. Riahi and D.P. van Vuuren, 2010. Historical (1850–2000) gridded anthropogenic and biomass burning emissions of reactive gases and aerosols: Methodology and application. *Atmospheric Chemistry and Physics*, 10:7017-7039.

Landy, J., J. Ehn, M. Shields and D. Barber, 2014. Surface and melt pond evolution on landfast first-year sea ice in the Canadian Arctic Archipelago. *Journal of Geophysical Research: Oceans*, 119:3054-3075.

Landy, J.C., J.K. Ehn and D.G. Barber, 2015. Albedo feedback enhanced by smoother Arctic sea ice. *Geophysical Research Letters*, 42:10,714-10,720.

Lange, B., C. Michel, J.F. Beckers, J.A. Casey, H. Flores, I. Hatam, G. Meisterhans, A. Niemi and C. Haas, 2015. Comparing springtime ice-algal chlorophyll *a* and physical properties of multi-year and first-year sea ice from the Lincoln Sea. *PLoS ONE* 10:e0122418.

Langehaug, H.R., F. Geyer, L.H. Smedsrød and Y. Gao, 2013. Arctic sea ice decline and ice export in the CMIP5 historical simulations. *Ocean Modelling*, 71:114-126.

Last, K.S., L. Hobbs, J. Berge, A.S. Brierley and F. Cottier, 2016. Moonlight drives ocean-scale mass vertical migration of zooplankton during the Arctic winter. *Current Biology*, 26:244-251.

Laxon, S.W., K.A. Giles, A.L. Ridout, D.J. Wingham, R. Willatt, R. Ullén, R. Kwok, A. Schweiger, J. Zhang, C. Haas, S. Hendricks, R. Krishfield, N. Kurtz, S. Farrell and M. Davidson, 2013. CryoSat-2 estimates of Arctic sea ice thickness and volume. *Geophysical Research Letters*, 40:732-737.

Leandro, L., R. Rolland, P. Roth, N. Lundholm, Z. Wang and G. Doucette, 2010. Exposure of the North Atlantic right whale *Eubalaena glacialis* to the marine algal biotoxin, domoic acid. *Marine Ecology Progress Series*, 398:287-303.

Lecomte, O., T. Fichefet, F. Massonnet and M. Vancoppenolle, 2015a. Benefits from representing snow properties and related processes in coupled ocean–sea ice models. *Ocean Modelling*, 87:81-85.

Lecomte, O., T. Fichefet, D. Flocco, D. Schroeder and M. Vancoppenolle, 2015b. Interactions between wind-blown snow redistribution and melt ponds in a coupled ocean-sea ice model. *Ocean Modelling*, 87:67-80.

Lee, C.M., S. Cole, M. Doble, L. Freitag, P. Hwang, S. Jayne, M. Jeffries, R. Krishfield, T. Maksym, W. Maslowski, B. Owens, P. Posey, L. Rainville, A. Roberts, B. Shaw, T. Stanton, J. Thomson, M. Timmermans, J. Toole, P. Wadhams, J. Wilkinson and J. Zhang, 2012. Marginal Ice Zone (MIZ) program: science and experiment plan. APL-UW TR 1201. Technical Report, University of Washington, Seattle.

Lefebvre, K.A., L. Quakenbush, E. Frame, K.B. Huntington, G. Sheffield, R. Stimmelmayr, A. Bryan, A. Kendrick, H. Ziel, T. Goldstein, J.A. Snyder, T. Gelatt, F. Gulland, B. Dickerson and V. Gill, 2016. Prevalence of algal toxins in Alaskan marine mammals foraging in a changing arctic and subarctic environment. *Harmful Algae*, 55:13-24.

Leonard, K.C. and T. Maksym, 2011. The importance of wind-blown snow redistribution to snow accumulation on Bellingshausen Sea ice. *Annals of Glaciology*, 52:271-278.

Leu, E., C.J. Mundy, P. Assmy, K. Campbell, T.M. Gabrielsen, M. Gosselin, T. Juul-Pedersen and R. Gradinger, 2015. Arctic spring awakening – steering principles behind the phenology of vernal ice algae blooms. *Progress in Oceanography*, 139:151-170.

Levy, B. and J. Patz, 2015. Climate Change and Public Health. Oxford University Press.

Lewitus, A., R. Horner, D. Caron, E. Garcia-Mendoza, B. Hickey, M. Hunter, D.D. Huppert, R.M. Kuddela, G.W. Lamglois, J.L. Largier, E.J. Lessard, R. RaLonde, J.E.J. Rensel, P.G. Strutton, V.L. Trainer and J.F. Tweddle, 2012. Harmful algal blooms along the North American west coast region: history, trends, causes and impacts. *Harmful Algae*, 19:133-159.

Li, W.K., F.A. McLaughlin, C. Lovejoy and E.C. Carmack, 2009. Smallest algae thrive as the Arctic Ocean freshens. *Science*, 326:539-539.

Light, B., S. Dickinson, D.K. Perovich and M.M. Holland, 2015a. Evolution of summer Arctic sea ice albedo in CCSM4 simulations: Episodic summer snowfall and frozen summers. *Journal of Geophysical Research*, 120:284-303.

Light, B., D.K. Perovich, M.A. Webster, C. Polashenski and R. Dadic, 2015b. Optical properties of melting first-year Arctic sea ice. *Journal of Geophysical Research: Oceans*, 120:7657-7675.

Lindell, D.B. and D.G. Long, 2016. Multiyear Arctic sea ice classification using OSCAT and QuikSCAT. *IEEE Transactions on Geoscience and Remote Sensing*, 54:167-175.

Lindsay, R.W., 2013. Unified Sea Ice Thickness Climate Data Record, 1975-2012. National Snow and Ice Data Center, Boulder, Colorado USA. <http://dx.doi.org/10.7265/N5D50JXV>.

Lindsay, R. and A. Schweiger, 2015. Arctic sea ice thickness loss determined using subsurface, aircraft, and satellite observations. *The Cryosphere*, 9:269-283.

Lindsay, R., M. Wensnahan, A. Schweiger and J. Zhang, 2014. Evaluation of seven different atmospheric reanalysis products in the Arctic. *Journal of Climate*, 27:2588-2606.

Lique, C., M.M. Holland, Y.B. Dibike, D.M. Lawrence and J.A. Screen, 2016. Modeling the arctic freshwater system and its integration in the global system: Lessons learned and future challenges. *Journal of Geophysical Research: Biogeosciences*, 121:540-566.

Liu, J., M. Song, R.M. Horton and Y. Hu, 2013. Reducing spread in climate model projections of a September ice-free Arctic. *Proceedings of the National Academy of Sciences*, 110:12571-12576.

Lønne, O.J. and B. Gulliksen, 1989. Size, age and diet of polar cod *Boreogadus saida* (Lepechin 1773) in ice covered waters. *Polar Biology*, 9:187-191.

Lønne, O.J., S. Falk-Petersen and J. Berge, 2015. Introduction to the special issue on polar night studies conducted onboard RV Helmer Hanssen in the Svalbard area. *Polar Biology*, 38:1-3.

Loose, B., W.R. McGillis, D. Perovich, C.J. Zappa and P. Schlosser, 2014. A parameter model of gas exchange for the seasonal sea ice zone. *Ocean Science*, 10:17-28.

Lu, P., Z. Li, B. Cheng and M. Leppäranta, 2011. A parameterization of the ice-ocean drag coefficient. *Journal of Geophysical Research*, 116:C07019, doi:10.1029/2010JC006878.

Lukovich, J. and D. Barber, 2005. On sea ice concentration anomaly coherence in the Southern Beaufort Sea. *Geophysical Research Letters*, 32:L10705, doi:10.1029/2005GL022737.

Lukovich, J.V., J.K. Hutchings and D.G. Barber, 2015. On sea-ice dynamical regimes in the Arctic Ocean. *Annals of Glaciology*, 56:323-331.

Lund-Hansen, L.C., I. Hawes, B.K. Sorrell and M.H. Nielsen, 2014. Removal of snow cover inhibits spring growth of Arctic ice algae through physiological and behavioral effects. *Polar Biology*, 37:471-481.

Lundholm, N., P. Andersen, K. Jørgensen, B.R. Thorbjørnsen, A. Cembella and B. Krock, 2005. Domoic acid in Danish blue mussels due to a bloom of *Pseudo-nitzschia seriata*. *Harmful Algae News*, 29:8-10.

Lüpkes, C., V. M. Grysanik, J. Hartmann, and E.L. Andreas, 2012a. A parameterization, based on sea ice morphology, of the neutral atmospheric drag coefficients for weather prediction and climate models. *Journal of Geophysical Research*, 117:D13112, doi:10.1029/2012JD017630.

Lüpkes, C., T. Vihma, G. Birnbaum, S. Dierer, T. Garbrecht, V.M. Grysanik, M. Gryschka, J. Hartmann, G. Heinemann, L. Kaleschke, S. Raasch, H. Savijärvi, K.H. Schlünzen and U. Wacker, 2012b. Mesoscale modelling of the Arctic atmospheric boundary layer and its interaction with sea ice. In: Lemke, P. and H.-W. Jacobi (eds.), *Arctic Climate Change: The ACSYS Decade and Beyond*. Atmospheric and Oceanographic Sciences Library, 43:279-324.

Lüpkes, C., V.M. Grysanik, A. Rösel, G. Birnbaum and L. Kaleschke, 2013. Effect of sea ice morphology during Arctic summer on atmospheric drag coefficients used in climate models. *Geophysical Research Letters*, 40:446-451.

Lüthje, M., D.L. Feltham, P.D. Taylor and M.G. Worster, 2006. Modeling the summertime evolution of sea-ice melt ponds. *Journal of Geophysical Research*, 111:C02001, doi:10.1029/2004JC002818.

Maaß, N., L. Kaleschke, X. Tian-Kunze and M. Drusch, 2013. Snow thickness retrieval over thick Arctic sea ice using SMOS satellite data. *The Cryosphere*, 7:1971-1989.

Macdonald, R.W., Z.A. Kuzyk and S.C. Johannessen, 2015. It is not just about the ice: a geochemical perspective on the changing Arctic Ocean. *Journal of Environmental Studies and Sciences*, 5:288-301.

Madsen, S., T. Nielsen and B. Hansen, 2001. Annual population development and production by *Calanus finmarchicus*, *C. glacialis* and *C. hyperboreus* in Disko Bay, western Greenland. *Marine Biology*, 139:75-93.

Maksimovich, E. and T. Vihma, 2012. The effect of surface heat fluxes on interannual variability in the spring onset of snow melt in the central Arctic Ocean. *Journal of Geophysical Research*, 117:C07012, doi:10.1029/2011JC007220.

Mäkynen, M., S. Kern, A. Rösel and L.T. Pedersen, 2014. On the estimation of melt pond fraction on the Arctic sea ice with ENVISAT WSM images. *IEEE Transactions on Geoscience and Remote Sensing*, 52:7366-7379.

Marcq, S. and J. Weiss, 2012. Influence of sea ice lead-width distribution on turbulent heat transfer between the ocean and the atmosphere. *The Cryosphere*, 6:143-156.

Marcoux, M., B.C. McMeans, A.T. Fisk and S.H. Ferguson, 2012. Composition and temporal variation in the diet of beluga whales, derived from stable isotopes. *Marine Ecology Progress Series*, 471:283-291.

Markus, T., D.J. Cavalieri, M.A. Tschudi and A. Ivanoff, 2003. Comparison of aerial video and Landsat 7 data over ponded sea ice. *Remote Sensing of Environment*, 86:458-469.

Markus, T., J.C. Stroeve and J. Miller, 2009. Recent changes in Arctic sea ice melt onset, freezeup, and melt season length. *Journal of Geophysical Research*, 114:C12024, doi:10.1029/2009JC005436.

Maslanik, J., J. Stroeve, C. Fowler and W. Emery, 2011. Distribution and trends in Arctic sea ice age through spring 2011. *Geophysical Research Letters*, 38:L13502, doi:10.1029/2011GL047735.

Massonnet, F., T. Fichefet, H. Goosse, C.M. Bitz, G. Philippon- Berthier, M.M. Holland and P.-Y. Barriat, 2012. Constraining projections of summer Arctic sea ice. *The Cryosphere*, 6:1383- 1394.

Matsuno, K., M. Ichinomiya, A. Yamaguchi, I. Imai and T. Kikuchi, 2014. Horizontal distribution of microprotist community structure in the western Arctic Ocean during late summer and early fall of 2010. *Polar Biology*, 37:1185-1195.

Mecklenburg, C.W. and D. Steinke, 2015. Ichthyofaunal baselines in the Pacific Arctic region and RUSALCA study area. *Oceanography*, 28:158-189.

Mecklenburg, C.W., I. Byrkjedal, J.S. Christiansen, O.V. Karamushko, A. Lynghammar and P.R. Møller, 2013. List of marine fishes of the arctic region annotated with common names and zoogeographic characterizations. *Conservation of Arctic Flora and Fauna (CAFF)*, Akureyri, Iceland.

Meier, W.N., G.K. Hovelsrud, B.E.H. van Oort, J.R. Key, K.M. Kovacs, C. Michel, C. Haas, M.A. Granskog, S. Gerland, D.K. Perovich, A. Makshtas and J.D. Reist, 2014a. Arctic sea ice in transformation: A review of recent observed changes and impacts on biology and human activity. *Reviews of Geophysics*, 52:185-217.

Meier, W.N., G. Peng, D.J. Scott and M.H. Savoie, 2014b. Verification of a new NOAA/NSIDC passive microwave sea-ice concentration climate record. *Polar Research*, 33:21004, doi:/10.3402/polar.v33.21004.

Meier, W.N., F. Fetterer, J. Scott Stewart and S. Helfrich, 2015. How do sea ice concentrations from operational data compare with passive microwave estimates? Implications for improved model evaluations and forecasting. *Annals of Glaciology*, 56:332-340.

Melia, N., K. Haines and E. Hawkins, 2015. Improved Arctic sea ice thickness projections using bias-corrected CMIP5 simulations. *The Cryosphere*, 9:2237-2251.

Melnikov, I.A., 1989. Ecosystem of the Arctic Sea Ice. *Doklady Akademii nauk SSSR*. (In Russian)

Melnikov, I.A., 1997. The Arctic Sea Ice Ecosystem. Gordon and Breach Science Publishers.

Melnikov, I.A., L.G. Kolosova, H.E. Welch and L.S. Zhitina, 2002. Sea ice biological communities and nutrient dynamics in the Canadian Basin of the Arctic Ocean. *Deep Sea Research I*, 49:1623-1649.

Melnikov, I.A., L.S. Zhitina and T.N. Semenova, 2017. Recent condition of the sea ice biodiversity within the North Pole region. *Problemy Arktiki I Antarktiki*, 4(110):104-110.

Michel, C., R.G. Ingram and L. Harris, 2006. Variability of oceanographic and ecological processes in the Canadian Arctic Archipelago. *Progress in Oceanography*, 72:379-401.

Michel, C., J. Hamilton, E. Hansen, D. Barber, M. Reigstad, J. Iacozza, L. Seuthe and A. Niemi, 2015. Arctic Ocean outflow shelves in the changing Arctic: A review and perspectives. *Progress in Oceanography*, 139:66-88.

Mikolajewicz, U., D.V. Sein, D. Jacob, T. Koenigk, R. Podzun and T. Semmler, 2005. Simulating Arctic sea ice variability with a coupled

regional atmosphere-ocean-sea ice model. *Meteorlogische Zeitschrift*, 14:793-800.

Miller, L.A., F. Fripijat, B.G.T. Else, J.S. Bowman, K.A. Brown, R.E. Collins, M. Ewert, A. Fransson and M. Gosselin, 2015. Methods for biogeochemical studies of sea ice: The state of the art, caveats, and recommendations. *Elementa* 3:1-53.

Moore, S.E. and P.J. Stabeno, 2015. Synthesis of Arctic Research (SOAR) in marine ecosystems of the Pacific Arctic. *Progress in Oceanography*, 136:1-11.

Moss, R.H., J.A. Edmonds, K.A. Hibbard, M.R. Manning, S.K. Rose, D.P. van Vuuren, T.R. Carter, S. Emori, M. Kainuma, T. Kram, G.A. Meehl, J.F.B. Mitchell, N. Nakicenovic, K. Riahi, S.J. Smith, R.J. Stouffer, A.M. Thomson, J.P. Weyant and T.J. Wilbanks, 2010. The next generation of scenarios for climate change research and assessment. *Nature*, 463:747-756.

Mundy, C.J., M. Gosselin, J. Ehn, Y. Gratton, A. Rossnagel, D.G. Barber, J. Martin, J.E. Tremblay, M. Palmer, K.R. Arrigo, G. Darnis, L. Fortier, B. Else and T. Papakyriakou, 2009. Contribution of under-ice primary production to an ice-edge upwelling phytoplankton bloom in the Canadian Beaufort Sea. *Geophysical Research Letters*, 36:L17601, doi:10.1029/2009GL038837.

Mundy, C.J., M. Gosselin, Y. Gratton, K. Brown, V. Galindo, K. Campbell, M. Levasseur, D.G. Barber, T. Papakyriakou and S. Bélanger, 2014. Role of environmental factors on phytoplankton bloom initiation under landfast sea ice in Resolute Passage, Canada. *Marine Ecology Progress Series*, 497:39-49.

Nghiem, S.V., I.G. Rigor, D.K. Perovich, P. Clemente-Colon, J.W. Weatherly and G. Neumann, 2007. Rapid reduction of Arctic perennial sea ice. *Geophysical Research Letters*, 34:L19504, doi:10.1029/2007GL031138.

Nghiem, S.V.V., I.G.G. Rigor, A. Richter, J.P.P. Burrows, P.B.B. Shepson, J.W. Bottenheim, D.G. Barber, A. Steffen, J.R. Latonas, F. Wang, G.A. Stern, P. Clemente-Colon, S. Martin, D.K.K. Hall, L. Kaleschke, P.J. Tackett, G. Neumann and M.G. Asplin, 2012. Field and satellite observations of the formation and distribution of Arctic atmospheric bromine above a rejuvenated sea ice cover. *Journal of Geophysical Research*, 117:D00S05, doi:10.1029/2011JD016268.

Nghiem, S.V., P. Clemente-Colon, T. Douglas, C. Moore, D. Obrist, D.K. Perovich, K.A. Pratt, I.G. Rigor, W. Simpson, P.B. Shepson, A. Steffen and J. Woods, 2013. Studying bromine, ozone, and mercury in the Arctic. *Eos, Transactions American Geophysical Union*, 94:289-291.

Nicolaus, M., S. Gerland, S.R. Hudson, S. Hanson, J. Haapala and D.K. Perovich, 2010. Seasonality of spectral albedo and transmittance as observed in the Arctic Transpolar Drift in 2007. *Journal of Geophysical Research*, 115:C11011, doi:10.1029/2009JC006074.

Nicolaus, M., C. Katlein, J. Maslanik and S. Hendricks, 2012. Changes in Arctic sea ice result in increasing light transmittance and absorption. *Geophysical Research Letters*, 39:L24501, doi:10.1029/2012GL053738.

Nicolaus, M., C. Petrich, S.R. Hudson and M.A. Granskog, 2013. Variability of light transmission through Arctic land-fast sea ice during spring. *The Cryosphere*, 7:977-986.

Niemi, A., C. Michel, K. Hille and M. Poulin, 2011. Protist assemblages in winter sea ice: setting the stage for the spring ice algal bloom. *Polar Biology*, 34:1803-1817.

Nomura, D., M.A. Granskog, P. Assmy, D. Simizu and G. Hashida, 2013. Arctic and Antarctic sea ice acts as a sink for atmospheric CO₂ during periods of snowmelt and surface flooding. *Journal of Geophysical Research: Oceans*, 118:6511-6524.

Nöthig, E.-M., A. Bracher, A. Engel, K. Metfies, B. Niehoff, I. Peeken, E. Bauerfeind, A. Cherkasheva, S. Gäßler-Schwarz, K. Hardge, E. Kiliias, A. Kraft, Y.M. Kidane, C. Lalande, J. Piontek, K. Thomisch and M. Wurst, 2015. Summertime plankton ecology in Fram Strait – a compilation of long- and short-term observations. *Polar Research*, 34, 23349, <http://dx.doi.org/10.3402/polar.v34.23349>.

Notz, D., 2009. The future of ice sheets and sea ice: Between reversible retreat and unstoppable loss. *Proceedings of the National Academy of Sciences*, 106:20590-20595.

Ogi, M. and I.G. Rigor, 2013. Trends in Arctic sea ice and the role of atmospheric circulation. *Atmospheric Science Letters*, 14:97-101.

Olason, E. and D. Notz, 2014. Drivers of variability in Arctic sea-ice drift speed. *Journal of Geophysical Research: Oceans*, 119:5755-5775.

Olsen, L.M., S.R. Laney, P. Duarte, H.M. Kauko, M. Fernandez-Mendez, C.J. Mundy, A. Rösel, A. Meyer, P. Itkin, L. Cohen, I. Peeken, A. Tatarek, M. Różańska-Pluta, J. Wiktor, T. Taskjelle, A.K. Pavlov, S.R. Hudson, M.A. Granskog, H. Hop and P. Assmy, 2017. The role of multiyear ice in seeding ice algal blooms in Arctic pack ice. *Journal of Geophysical Research*, doi:10.1002/2016JC012471.

Overland, J.E., J.A. Francis, E. Hanna and M. Wang, 2012. The recent shift in early summer Arctic atmospheric circulation. *Geophysical Research Letters*, 39:L19804, doi:10.1029/2012GL053268.

Palmer, M.A., B.T. Saenz and K.R. Arrigo, 2014. Impacts of sea ice retreat, thinning, and melt-pond proliferation on the summer phytoplankton bloom in the Chukchi Sea, Arctic Ocean. *Deep Sea Research II*, 105:85-104.

Parkinson, C.L., 2014a. Global sea ice coverage from satellite data: Annual cycle and 35-yr trends. *Journal of Climate*, 27:9377-9382.

Parkinson, C.L., 2014b. Spatially mapped reductions in the length of the Arctic sea ice season. *Geophysical Research Letters*, 41:4316-4322.

Parkinson, C.L. and J.C. Comiso, 2013. On the 2012 record low Arctic sea ice cover: Combined impact of preconditioning and an August storm. *Geophysical Research Letters*, 40:1-6.

Parkinson, C.L. and N.E. DiGirolamo, 2016. New visualizations highlight new information on the contrasting Arctic and Antarctic sea-ice trends since the late 1970s. *Remote Sensing of Environment*, 183:198-204.

Parmentier, F.-J.W., T.R. Christensen, L.L. Sørensen, S. Rysgaard, A.D. McGuire, P.A. Miller and D.A. Walker, 2013. The impact of lower sea-ice extent on Arctic greenhouse-gas exchange. *Nature Climate Change*, 3:195-202.

Pearce, T., J. Ford, A. Cunsolo Wilcox and B. Smit, 2015. Inuit Traditional Ecological Knowledge (TEK), subsistence hunting and adaptation to climate change in the Canadian Arctic. *Arctic*, 68:233-245.

Pedersen, C.A., E. Roeckner, M. Lüthje and J.-G. Winther, 2009. A new sea ice albedo scheme including melt ponds for ECHAM5 general circulation model. *Journal of Geophysical Research*, 114:D08101, doi:10.1029/2008JD010440.

Peng, G., W.N. Meier, D.J. Scott and M.H. Savoie, 2013. A long-term and reproducible passive microwave sea ice concentration data record for climate studies and monitoring. *Earth System Science Data*, 5:311-318.

Percopo, I., M.V. Ruggiero, S. Balzano, P. Gourvil, N. Lundholm, R. Siano, A., Tammilehto, D., Vaulot and D. Sarno, 2016. *Pseudo-nitzschia arctica* sp. nov., a new cold-water cryptic *Pseudo-nitzschia* species within the *P. pseudodelicatissima* complex. *Journal of Phycology*, 152:184-199.

Perovich, D.K. and C. Polashenski, 2012. Albedo evolution of seasonal Arctic sea ice. *Geophysical Research Letters*, 39:L08501, doi:10.1029/2012GL051432.

Perovich, D.K. and J.A. Richter-Menge, 2015. Regional variability in sea ice melt in a changing Arctic. *Proceedings of the Royal Society*, 373:20140165, doi:10.1098/rsta.2014.0165.

Perovich, D.K., K.F. Jones, B. Light, H. Eicken, T. Markus, J. Stroeve and R. Lindsay, 2011. Solar partitioning in a changing Arctic sea-ice cover. *Annals of Glaciology*, 52:192-196.

Perovich, D., W. Meier, M. Tschudi, S. Farrel, S. Gerland and S. Hendricks, 2015. Sea Ice. In: Arctic Report Card 2015. www.arctic.noaa.gov/reportcard.

Petrich, C., H. Eicken, C.M. Polashenski, M. Sturm, J.P. Harbeck, D.K. Perovich and D.C. Finnegan, 2012. Snow dunes: A controlling factor of melt pond distribution on Arctic sea ice. *Journal of Geophysical Research*, 117, C09029, doi:10.1029/2012JC008192.

Pickart, R.S., L.M. Schulze, G.W.K. Moore, M.A. Charette, K.R. Arrigo, G. van Dijken and S.L. Danielson, 2013. Long-term trends of upwelling and impacts on primary productivity in the Alaskan Beaufort Sea. *Deep Sea Research I*, 79:106-121.

Piipariinen, J., S. Enberg, J.-M. Rintala, R. Sommaruga, M. Majaneva, R. Autio and A.V. Vähälahti, 2015. The contribution of mycosporine-like amino acids, chromophoric dissolved organic matter and particles to the UV protection of sea-ice organisms in the Baltic Sea. *Photochemical and Photobiological Sciences*, 14:1025-1038.

Polashenski, C., D.K. Perovich and Z. Courville, 2012. The mechanisms of sea ice melt pond formation and evolution. *Journal of Geophysical Research*, 117:C01001, doi:10.1029/2011JC007231.

Polashenski, C., D.K. Perovich, K.E. Frey, L.W. Cooper, C.I. Logvinova, R. Dadic, B. Light, H.P. Kelly, L.D. Trusel and M. Webster, 2015. Physical and morphological properties of sea ice in the Chukchi and Beaufort Seas during the 2010 and 2011 NASA ICESCAPE missions. *Deep Sea Research II*, 118:7-17.

Poloczanska, E.S., C.J. Brown, W.J. Sydeman, W. Kiessling, D.S. Schoeman, P.J. Moore, K. Brander, J.F. Bruno, L.B. Buckley, M.T. Burrows, C.M. Duarte, B.S. Halpern, J. Holding, C.V. Kappel, M.I. O'Connor, J.M. Pandolfi, C. Parmesan, F. Schwing, S.A. Thompson and A.J. Richardson,

2013. Global imprint of climate change on marine life. *Nature Climate Change*, 3:919-925.

Polyakov, I.V., L.A. Timokhov, V.A. Alexeev, S. Bacon, I.A. Dmitrenko, L. Fortier, I.Y. Frolov, J.-C. Gascard, E. Hansen, V.V. Ivanov, S. Laxon, C. Mauritzen, D. Perovich, K. Shimada, H.L. Simmons, V.T. Sokolov, M. Steele and J. Toole, 2010. Arctic Ocean warming contributes to reduced polar ice cap. *Journal of Physical Oceanography*, 40:2743-2756.

Pomerleau, C., V. Lesage, S.H. Ferguson, G. Winkler, S.D. Petersen and J.W. Higdon, 2012. Prey assemblage isotopic variability as a tool for assessing diet and the spatial distribution of bowhead whale *Balaena mysticetus* foraging in the Canadian eastern Arctic. *Marine Ecology Progress Series*, 469:161-174.

Poulin, M., N. Daugbjerg, R. Gradinger, L. Ilyash, T. Ratkova and C. von Quillfeldt, 2011. The pan-Arctic biodiversity of marine pelagic and sea-ice unicellular eukaryotes: a first-attempt assessment. *Marine Biodiversity*, 41:13-28.

Provenccher, J.F., A.J. Gaston, P.D. O'Hara and H.G. Gilchrist, 2012. Seabird diet indicates changing Arctic marine communities in eastern Canada. *Marine Ecology Progress Series*, 454:171-182.

Raddatz, R.L., R.J. Galley and D.G. Barber, 2012. Linking the atmospheric boundary layer to the Amundsen Gulf sea ice cover: a mesoscale to synoptic-scale perspective from winter to summer 2008. *Boundary Layer Meteorology*, 142:123-148.

Raddatz, R.L., R.J. Galley, B.G. Else, T.N. Papakyriakou, M.G. Asplin, L.M. Candlish and D.G. Barber, 2014. Western Arctic cyclones and equilibrium between the atmospheric boundary layer and the sea surface. *Atmosphere-Ocean*, 52:125-141.

Radionov, V.F., N.N. Bryazgin and E.I. Alexandrov, 1997. The snow cover of the Arctic Basin. Technical Report APL-UW-TR 9701. Washington University, Seattle.

Radionov, V.F., E.I. Aleksandrov, N.N. Bryazgin and A.A. Dementiev, 2013. Changes in temperature, precipitation and snow cover in the Arctic seas areas over the period 1981–2010. *Ice and Snow*, No. 1(121):61-68.

RaLonde, R., 1996. Paralytic shellfish poisoning: The Alaska problem. *Alaska's Marine Resources* Vol. 8 No. 2, Alaska Sea Grant Marine Advisory Program, University of Alaska Fairbanks.

Rampal, P., J. Weiss and D. Marsan, 2009. Positive trend in the mean speed and deformation rate of Arctic sea ice. 1979–2007. *Journal of Geophysical Research*, 114:C05013, doi:10.1029/2008JC005066.

Rampal, P., J. Weiss, C. Dubois and J.-M. Campin, 2011. IPCC climate models do not capture Arctic sea ice drift acceleration: Consequences in terms of projected sea ice thinning and decline. *Journal of Geophysical Research*, 116:C00D07, doi:10.1029/2011JC007110.

Rampal, P., S. Bouillon, E. Ólason and M. Morlighem, 2016. neXtSIM: a new Lagrangian sea ice model. *The Cryosphere*, 10:1055-1073.

Renner, A.H., S. Gerland, C. Haas, G. Spreen, J.F. Beckers, E. Hansen, M. Nicolaus and H. Goodwin, 2014. Evidence of Arctic sea ice thinning from direct observations. *Geophysical Research Letters*, 41:5029-5036.

Richter-Menge, J.A. and S.L. Farrell, 2013. Arctic sea ice conditions in spring 2009–2013 prior to melt. *Geophysical Research Letters*, 40:5888-5893.

Ricker, R., S. Hendricks, V. Helm, H. Skourup and M. Davidson, 2014. Sensitivity of CryoSat-2 Arctic sea-ice freeboard and thickness on radar-waveform interpretation. *The Cryosphere*, 8:1607-1622.

Ricker, R., S. Hendricks, D.K. Perovich, V. Helm and R. Gerdes, 2015. Impact of snow accumulation on CryoSat-2 range retrievals over Arctic sea ice: An observational approach with buoy data. *Geophysical Research Letters*, 42:4447-4455.

Rigor, I.G., J.M. Wallace and R.L. Colony, 2002. Response of sea-ice to the Arctic Oscillation. *Journal of Climate*, 15:2648-2663.

Roeckner, E., T. Mauritzen, M. Esch and R. Brokopp, 2012. Impact of melt ponds on Arctic sea ice in past and future climates as simulated by MPI-ESM. *Journal of Advances in Modeling Earth Systems*, 4:M00A02, doi:10.1029/2012MS000157.

Rösel, A. and L. Kaleschke, 2011. Comparison of different retrieval techniques for melt ponds on Arctic sea ice from Landsat and MODIS satellite data. *Annals of Glaciology*, 52:185-191.

Rösel, A. and L. Kaleschke, 2012a. Exceptional melt pond occurrence in the years 2007 and 2011 on the Arctic sea ice revealed from MODIS satellite data. *Journal of Geophysical Research*, 117, C05018, doi:10.1029/2011JC007869.

Rösel, A. and L. Kaleschke, 2012b. Influence of melt ponds on microwave sensors' sea ice concentration retrieval algorithms. In: *Geoscience and Remote Sensing Symposium (IGARSS)*, 2012 IEEE International, 3261-3264.

Rösel, A., L. Kaleschke and G. Birnbaum, 2012. Melt ponds on Arctic sea ice determined from MODIS satellite data using an artificial neural network. *The Cryosphere*, 6:431-446.

Rysgaard, S., J. Bendtsen, B. Delille, G.S. Dieckmann, R.N. Glud, H. Kennedy, J. Mortensen, S. Papadimitriou, D.N. Thomas and J.-L. Tison, 2011. Sea ice contribution to the air-sea CO₂ exchange in the Arctic and Southern Oceans. *Tellus B*, 63:823-830.

Sackett, O., K. Petrou, B. Reedy, A. De Grazia, R. Hill, M. Doblin, J. Beardall, P. Ralph and P. Heraud, 2013. Phenotypic plasticity of Southern Ocean diatoms: Key to success in the sea ice habitat? *PLoS ONE*, 8:e81185.

Scharien, R.K., J.J. Yackel, D.G. Barber, M.G. Asplin, M. Gupta and D. Isleifson, 2012. Geophysical controls on C band polarimetric backscatter from melt pond covered Arctic first-year sea ice: Assessment using high-resolution scatterometry. *Journal of Geophysical Research*, 117:C00G18, doi:10.1029/2011JC007353.

Scharien, R.K., K. Hochheim, J. Landy and D.G. Barber, 2014. Sea ice melt pond fraction estimation from dual-polarization SAR, Part 2. Scaling in situ to Radarsat-2. *The Cryosphere*, 8:2163-2176.

Scholin, C.A., F. Gulland, G.J. Doucette, S. Benson, M. Busman, F.P. Chavez, J. Cordaro, R. DeLong, A. De Vogelaere, J. Harvey, M. Haulena, K. Lefebvre, T. Lipscomb, S. Loscutoff, L.J. Lowenstein, R. Marin III, P.E. Miller, W.A. McLellan, P.D.R. Moeller, C.L. Powell, T. Rowles, P. Silvagni, M. Silver, T. Spraker, V. Trainer and F.M. Van Dolah, 2000. Mortality of sea lions along the central California coast linked to a toxic diatom bloom. *Nature*, 403:80-84.

Schröder, D., D.L. Feltham, D. Flocco and M. Tsamados, 2014. September Arctic sea-ice minimum predicted by spring melt-pond fraction. *Nature Climate Change*, 4:353-357.

Screen, J.A. and I. Simmonds, 2012. Declining summer snowfall in the Arctic: Causes, impacts and feedbacks. *Climate Dynamics*, 38:2243-2256.

Sherr, E.B., B.F. Sherr and A.J. Hartz, 2009. Microzooplankton grazing impact in the Western Arctic Ocean. *Deep Sea Research II*, 56:1264-1273.

Shu, Q., Z. Song and F. Qiao, 2015. Assessment of sea ice simulations in the CMIP5 models. *The Cryosphere*, 9:399-409.

Sievers, J., L.L. Sørensen, T. Papakyriakou, B. Else, M.K. Sejr, D. Haubjerg Søgaard, D. Barber and S. Rysgaard, 2015. Winter observations of CO₂ exchange between sea ice and the atmosphere in a coastal fjord environment. *The Cryosphere*, 9:1701-1713.

Skourup, H., I. Einarsson, L. Sandberg, R. Forsberg, L. Stenseng, S. Hendricks, V. Helm and M. Davidson, 2011. ESA CryoVEx 2011 airborne campaign for CRYOSAT-2 calibration and validation. *Proceedings of the American Geophysical Union Meeting*.

Skiplingstad, E.D., C.A. Paulson and D.K. Perovich, 2009. Simulation of melt pond evolution on level ice. *Journal of Geophysical Research*, 114, C12019, doi:10.1029/2009JC005363.

Skiplingstad, E.D., K.M. Shell, L. Collins and C. Polashenski, 2015. Simulation of the melt season using a resolved sea ice model with snow cover and melt ponds. *Journal of Geophysical Research: Oceans*, 120:5194-5215.

Smedsrød, L.H., A. Sirevaag, K. Kloster, A. Sorteberg and S. Sandven, 2011. Recent wind driven high sea ice area export in the Fram Strait contributes to Arctic sea ice decline. *Cryosphere*, 5:821-829.

Sørensen, J.E., M.L. Carroll, H. Hop, W.G. Ambrose Jr, E.N. Hegseth and S. Falk-Petersen, 2013. Sympagic-pelagic-benthic coupling in Arctic and Atlantic waters around Svalbard revealed by stable isotopic and fatty acid tracers. *Marine Biology Research*, 9:831-850.

Spreen, G., L. Kaleschke and G. Heygster, 2008. Sea ice remote sensing using AMSR-E 89-GHz channels. *Journal of Geophysical Research*, 113:C02S03, doi:10.1029/2005JC003384.

Spreen, G., S. Kern, D. Stammer and E. Hansen, 2009. Fram Strait sea ice volume export estimated between 2003 and 2008 from satellite data. *Geophysical Research Letters*, 36:L19502, doi:10.1029/2009GL039591.

Spreen, G., R. Kwok and D. Menemenlis, 2011. Trends in Arctic sea ice drift and role of wind forcing: 1992–2009. *Geophysical Research Letters*, 38:L19501, doi:10.1029/2011GL048970.

Stroeve, J.C., V. Kattsov, A. Barrett, M. Serreze, T. Pavlova, M. Holland and W.N. Meier, 2012. Trends in Arctic sea ice extent from CMIP5, CMIP3 and observations. *Geophysical Research Letters*, 39:L16502, doi:10.1029/2012GL052676.

Stroeve, J.C., T. Markus, L. Boisvert, J. Miller and A. Barrett, 2014a. Changes in Arctic melt season and implications for sea ice loss. *Geophysical Research Letters*, 41:1216-1225.

Stroeve, J., A. Barrett, M. Serreze and A. Schweiger, 2014b. Using records from submarine, aircraft and satellites to evaluate climate model simulations of Arctic sea ice thickness. *The Cryosphere*, 8:1839-1854.

Sturm, M., J. Holmgren and D.K. Perovich, 2002. Winter snow cover on the sea ice of the Arctic Ocean at the Surface Heat Budget of the Arctic Ocean (SHEBA): Temporal evolution and spatial variability. *Journal of Geophysical Research*, 107:8047, doi:10.1029/2000JC000400.

Swart, N.C., J.C. Fyfe, E. Hawkins, J.E. Kay and A. Jahn, 2015. Influence of internal variability on Arctic sea-ice trends. *Nature Climate Change*, 5:86-89.

Tammilehto, A., T.G. Nielsen, B. Krock, E.F. Møller and N. Lundholm, 2012. *Calanus* spp. – Vectors for the biotoxin, domoic acid, in the Arctic marine ecosystem? *Harmful Algae*, 20:165-174.

Tammilehto, A., T.G. Nielsen, B. Krock, E.F. Møller and N. Lundholm, 2015. Induction of domoic acid production in the toxic diatom *Pseudo-nitzschia seriata* by calanoid copepods. *Aquatic Toxicology*, 159:52-61.

Tanaka, Y., K. Tateyama, T. Kameda and J.K. Hutchings, 2016. Estimation of melt pond fraction over high-concentration Arctic sea ice using AMSR-E passive microwave data. *Journal of Geophysical Research: Oceans*, 121:7056-7072.

Taskjelle, T., S.R. Hudson, M.A. Granskog, M. Nicolaus, R. Lei, S. Gerland, J.J. Stannes and B. Hamre, 2016. Spectral albedo and transmittance of thin young Arctic sea ice. *Journal of Geophysical Research: Oceans*, 121:540-553.

Taylor, K.E., R.J. Stouffer and G.A. Meehl, 2012. An Overview of CMIP5 and the experiment design. *Bulletin of the American Meteorological Society*, 93:485-498.

Tetzlaff, A., L. Kaleschke, C. Lüpkes, F. Ament and T. Vihma, 2013. The impact of heterogeneous surface temperatures on the 2-m air temperature over the Arctic Ocean under clear skies in spring. *The Cryosphere*, 7:153-166.

Tetzlaff, A., C. Lüpkes, G. Birnbaum, J. Hartmann, T. Nygård and T. Vihma, 2014. Brief communication: trends in sea ice extent north of Svalbard and its impact on cold air outbreaks as observed in spring 2013. *The Cryosphere*, 8:1757-1763.

Thiemann, G.W., S.J. Iverson and I. Stirling, 2008. Polar bear diets and arctic marine food webs: insights from fatty acid analysis. *Ecological Monographs*, 78:591-613.

Thomas, D.N. and G.S. Dieckmann, 2010. *Sea Ice*. 2nd Edition. Wiley-Blackwell.

Thomson, J. and W.E. Rogers, 2014. Swell and sea in the emerging Arctic Ocean. *Geophysical Research Letters*, 41:3136-3140.

Tian-Kunze, X., L. Kaleschke, N. Maaß, M. Mäkinen, N. Serra, M. Drusch and T. Krumpen, 2014. SMOS-derived thin sea ice thickness: algorithm baseline, product specifications and initial verification. *The Cryosphere*, 8:997-1018.

Tikhonov, V.V., I.A. Repina, M.D. Raev, E.A. Sharkov, V.V. Ivanov, D.A. Boyarskii, T.A. Alexeeva and N.Y. Komarova, 2015. A physical algorithm to measure sea ice concentration from passive microwave remote sensing data. *Advances in Space Research*, 56:1578-1589.

Tilling, R.L., A. Ridout, A. Shepherd and D.J. Wingham, 2015. Increased Arctic sea ice volume after anomalously low melting in 2013. *Nature Geoscience*, 8:643-646.

Tremblay, J.-É., S. Bélanger, D.G. Barber, M. Asplin, J. Martin, G. Darnis, L. Fortier, Y. Gratton, H. Link, P. Archambault, A. Sallon, C. Michel, W.J. Williams, B. Philippe and M. Gosselin, 2011. Climate forcing multiplies biological productivity in the coastal Arctic Ocean. *Geophysical Research Letters*, 38:L18604, doi:10.1029/2011GL048825.

Tremblay, J.-É., L.G. Anderson, P. Matrai, P. Coupel, S. Bélanger, C. Michel and M. Reigstad, 2015. Global and regional drivers of nutrient supply, primary production and CO₂ drawdown in the changing Arctic Ocean. *Progress in Oceanography*, 139:171-196.

Tsamados, M., D.L. Feltham and A.V. Wilchinsky, 2013. Impact of a new anisotropic rheology on simulations of Arctic sea ice. *Journal of Geophysical Research: Oceans*, 118:91-107.

Tschudi, M.A., J.A. Maslanik and D.K. Perovich, 2008. Derivation of melt pond coverage on Arctic sea ice using MODIS observations. *Remote Sensing of Environment*, 112:2605-2614.

Tschudi, M., C. Fowler and J. Maslanik, 2015. EASE-Grid Sea Ice Age. Version 2. NASA National Snow and Ice Data Center, Boulder, Colorado USA. <http://dx.doi.org/10.5067/IUQJWCYPVX61>.

Underwood, G.J.C., S.N. Aslama, C. Michel, A. Niemi, L. Normanc, K.M. Meiners, J. Laybourn-Parry, H. Paterson and D.N. Thomas, 2013. Broad-scale predictability of carbohydrates and exopolymers in Antarctic and Arctic sea ice. *Proceedings of the National Academy of Sciences*, 110:15734-15739.

van Angelen, J.H., M.R. van den Broeke and R. Kwok, 2011. The Greenland Sea Jet: A mechanism for wind-driven sea ice export through Fram Strait. *Geophysical Research Letters*, 38:L12805, doi:10.1029/2011GL047837.

Vancoppenolle, M., K.M. Meiners, C. Michel, L. Bopp, F. Brabant, G. Carnat, B. Delille, D. Lannuzel, G. Madec, S. Moreau, J.-L. Tison and P. van der Merwe, 2013. Role of sea ice in global biogeochemical cycles: emerging views and challenges. *Quaternary Science Reviews*, 79:207-230.

Varpe, Ø., M. Daase and T. Kristiansen, 2015. A fish-eye view on the new Arctic lightscape. *ICES Journal of Marine Science*, 72:2532-2538.

Vershinin, A. and T.Y. Orlova, 2008. Toxic and harmful algae in the coastal waters of Russia. *Marine Biology*, 48:524-537.

Vihma, T., P. Tisler and P. Uotila, 2012. Atmospheric forcing on the drift of Arctic sea ice in 1989–2009. *Geophysical Research Letters*, 39:L02501, doi:10.1029/2011GL050118.

Vihma, T., R. Pirazzini, I.A. Renfrew, J. Sedlar, M. Tjernström, T. Nygård, I. Fer, C. Lüpkes, D. Notz, J. Weiss, D. Marsan, B. Cheng, G. Birnbaum, S. Gerland, D. Chechin and J.C. Gascard, 2014. Advances in understanding and parameterization of small-scale physical processes in the marine Arctic climate system: a review. *Atmospheric Chemistry and Physics*, 14:9403-9450.

Vihma, T., J. Screen, M. Tjernström, B. Newton, X. Zhang, V. Popova, C. Deser, M. Holland and T. Prowse, 2016. The atmospheric role in the Arctic water cycle: A review on processes, past and future changes, and their impacts. *Journal of Geophysical Research: Biogeosciences*, 121:586-620.

Wang, M. and J.E. Overland, 2012. A sea ice free summer Arctic within 30 years—an update from CMIP5 models. *Geophysical Research Letters*, 39:L18501, doi:10.1029/2012GL052868.

Wang, M. and J.E. Overland, 2015. Projected future duration of the sea-ice-free season in the Alaskan Arctic. *Progress in Oceanography*, 136:50-59.

Wang, C., M. Granskog, S. Gerland, S.R. Hudson, D.K. Perovich, M. Nicolaus, T. Ivan Karlsen, K. Fossan and M. Bratnein, 2014. Autonomous observations of solar energy partitioning in first-year sea ice in the Arctic Basin. *Journal of Geophysical Research: Oceans*, 119:2066-2080.

Wang, C., B. Cheng, K. Wang, S. Gerland and O. Pavlova, 2015. Modelling snow ice and superimposed ice formation on landfast sea ice. *Polar Research*, 34:20828, <http://dx.doi.org/10.3402/polar.v34.20828>.

Wang, C., M.A. Granskog, S.R. Hudson, S. Gerland, A.K. Pavlov, D.K. Perovich and M. Nicolaus, 2016. Atmospheric conditions in the central Arctic Ocean through the melt seasons of 2012 and 2013: Impact on surface conditions and solar energy deposition into the ice-ocean system. *Journal of Geophysical Research: Atmospheres*, 121:1043-1058.

Warren, S., I. Rigor, N. Untersteiner, V.F. Radionov, N.N. Bryazgin, Y.I. Aleksandrov and R. Colony, 1999. Snow depth on Arctic sea ice. *Journal of Climate*, 12:1814-1829.

Wassmann, P., K.N. Kosobokova, D. Slagstad, K.F. Drinkwater, R.R. Hopcroft, S.E. Moore, I. Ellingsen, R.J. Nelson, E. Carmack, E. Popova and J. Berge, 2015. The contiguous domains of Arctic Ocean advection: Trails of life and death. *Progress in Oceanography*, 139:42-65.

Watt, C.A., M.P. Heide-Jørgensen and S.H. Ferguson, 2013. How adaptable are narwhal? A comparison of foraging patterns among the world's three narwhal populations. *Ecosphere*, 4:71, doi:10.1890/ES13-00137.1.

Webster, M.A., I.G. Rigor, S.V. Nghiem, N.T. Kurtz, S.L. Farrell, D.K. Perovich and M. Sturm, 2014. Interdecadal changes in snow depth on Arctic sea ice. *Journal of Geophysical Research: Oceans*, 119:5395-5406.

Webster, M.A., I.G. Rigor, D.K. Perovich, J.A. Richter-Menge, C.M. Polashenski and B. Light, 2015. Seasonal evolution of melt ponds on Arctic sea ice. *Journal of Geophysical Research: Oceans*, 120:5968-5982.

Werner, I., H. Auel, C. Garrity and W. Hagen, 1999. Pelagic occurrence of the sympagic amphipod *Gammarus wilkitzkii* in ice-free waters of the Greenland Sea – dead end or part of life-cycle? *Polar Biology*, 22:56-60.

Wettstein, J.J. and C. Deser, 2014. Internal variability in projections of twenty-first-century Arctic sea ice loss: role of the large-scale atmospheric circulation. *Journal of Climate*, 27:527-550.

Wienerroither, R.M., K.H. Nedreaas, F. Uiblein, J.S. Christiansen, I. Byrkjedal, I. and O. Karamushko, 2011a. The marine fishes of Jan Mayen Island, NE Atlantic – past and present. *Marine Biodiversity*, 41:395-411.

Wienerroither, R., E. Johannessen, A. Dolgov, I. Byrkjedal, O. Bjelland, K.V. Drevetnyak, K.B. Eriksen, A. Hoines, G. Langhelle, H. Langoy, T. Prokhorova, D. Prozorkevich and T. Wennecke, 2011b. *Atlas of the Barents Sea Fishes. IMR/PINRO Joint Report Series 1-2011*.

Williams, W.J. and E.C. Carmack, 2015. The 'interior' shelves of the Arctic Ocean: Physical oceanographic setting, climatology and effects of

sea-ice retreat on cross-shelf exchange. *Progress in Oceanography*, 139:24-41.

Willmes, S., M. Nicolaus and C. Haas, 2014. The microwave emissivity variability of snow covered first-year sea ice from late winter to early summer: a model study. *The Cryosphere*, 8:891-904.

WMO, 1970. Sea-Ice Nomenclature. World Meteorological Organization (WMO), WMO Series, No. 259.

Yackel, J. and D.G. Barber, 2000. Melt ponds on sea ice in the Canadian Arctic Archipelago 2. On the use of RADARSAT-1 synthetic aperture radar for geophysical inversion. *Journal of Geophysical Research: Oceans*, 105:22,061-22,070.

Yu, Y., H. Stern, C. Fowler, F. Fetterer and J. Maslanik, 2014. Interannual variability of Arctic landfast ice between 1976 and 2007. *Journal of Climate*, 27:227-243.

Zege, E.P., A.V. Malinka, I.L. Katsev, A.S. Prikhach, G. Heygster, L.G. Istomina, G. Birnbaum and P. Schwarz, 2015. Algorithm to retrieve the melt pond fraction and the spectral albedo of Arctic summer ice from satellite data. *Remote Sensing of Environment*, 163:153-164.

Zhang, R., 2015. Mechanisms for low-frequency variability of summer Arctic sea ice extent. *Proceedings of the National Academy of Sciences*, 113:4570-4575.

Zygmuntowska, M., K. Khvorostovsky, V. Helm and S. Sandven, 2013. Waveform classification of airborne synthetic aperture radar altimeter over Arctic sea ice. *The Cryosphere*, 7:1315-1324.

Zygmuntowska, M., P. Rampal, N. Ivanova and L.H. Smedsrød, 2014. Uncertainties in Arctic sea ice thickness and volume: new estimates and implications for trends. *The Cryosphere*, 8:705-720.

6. Changes to Arctic land ice

LEAD AUTHORS: **JASON E. BOX, MARTIN SHARP**

CONTRIBUTING AUTHORS: GUÐFINNA ÁDALGEIRSDÓTTIR, MARIA ANANICHEVA, MORTEN L. ANDERSEN, RACHEL CARR, CAROLINE CLASON, WILLIAM T. COLGAN, LUKE COPLAND, ANDREY GLAZOVSKY, ALUN HUBBARD, KRISTIAN K. KJELDSEN, SEBASTIAN MERNILD, GEIR MOHOLDT, TWILA MOON, THOMAS WAGNER, BERT WOUTERS, WESLEY VAN WYCHEN

Coordinating lead authors shown in bold

Contents

Key Findings	138
6.1 Introduction	139
6.2 Arctic glaciers and ice caps	139
6.2.1 Completed inventory	139
6.2.2 Attribution	140
6.2.3 Regional insights	140
6.2.4 Arctic glaciers	145
6.3 Firn changes	147
6.4 Greenland ice sheet	148
6.4.1 Snowfall accumulation	150
6.4.2 Surface melting	150
6.4.3 Surface mass balance	151
6.4.4 Total ice sheet mass balance	151
6.4.5 Floating ice area losses	153
6.4.6 The Northeastern Greenland ice stream	154
6.4.7 Ice sheet surface melt water lakes	154
6.4.8 Internal ice sheet structure	155
6.4.9 Sea level contribution	157
6.5 Projected mass changes	157
6.6 Impacts	158
6.6.1 Nutrient export from glaciated systems	158
6.6.2 Contaminant export from glaciated systems ..	158
6.7 Gaps and observational needs	159
Acknowledgments	160
References	160

Key Findings

- All Arctic regions lost land ice mass between 2003 and 2014, averaging 413 ± 40.6 Gt/y, equivalent to a 1.1 ± 0.1 mm rise in eustatic sea level per year, representing two-thirds of the global land ice contribution to sea level rise. Ice losses were greatest from Greenland (64% of the Arctic total) followed by Arctic Canada (14%) and Alaska (12%). Minor (2-20%) increases in snowfall in the past century were more than offset by increased surface melting and runoff. Rates of mass loss from Arctic land ice have, in most cases, increased compared to those reported in SWIPA 2011. The majority of global glacier mass loss is attributable to anthropogenic climate change.
- New extremes in surface melting of Greenland and Canadian Arctic land ice resulted from warm and moist atmospheric flow over Greenland from North America. The deposition of wildfire black carbon promoted melt through enhanced sunlight absorption. Greenland glaciers surrounding the ice sheet have been losing mass faster (relative to their area) than the ice sheet.
- Floating ice shelves in northern Arctic Canada and Greenland have lost large ice areas since the early 20th century, with some fjords having ice free conditions for the first time in over 3000 years. The Arctic's largest ice shelf (fed by Petermann Glacier, NW Greenland) calved 245 km^2 in August 2010 and 140 km^2 in 2012. The largest Arctic ice shelf now occurs at the terminus of the North East Greenland Ice Stream (NEGIS) that has recently accelerated in response to ocean warming and sea ice decline. The Zachariae glacier of NEGIS is now retreating in some areas into a trough where the ice is grounded 400 m below sea level, suggesting continued marine instability.
- Comprehensive Russian High Arctic survey work reveals substantial ice loss, making this region the fourth largest Arctic contributor to sea level rise after Greenland, Arctic Canada, and Alaska. Siberian glaciers are decreasing in area in response to summer temperature increases and a relatively small snowfall increase.
- Pre-instrumental data from ice cores suggest that melting on Canadian Arctic ice caps is occurring faster now than at any time in the past 4000 years and at rates that were last exceeded during the Holocene Climatic Optimum around 9000 years ago. Dating of plant remains exposed by glacier shrinkage suggests that average summer temperatures in the southern Canadian Arctic are now higher than in the past 44,000 years.
- The increased resolution of Greenland subglacial bed mapping reveals many deeply-incised glacier troughs reaching tens of kilometers further into the ice sheet interior. The existence of many of these subglacial troughs was previously unknown. Side-looking, multi-beam echo sounding observations show Greenland marine frontal ice cliffs are often grounded further below sea level than previously thought, ensuring further marine instability of Greenland glaciers.
- The formation of surface meltwater lakes across the Greenland ice sheet has extended further inland, and the lakes are forming earlier due to increases in summer air temperature.
- Studies of Arctic tidewater glacier behavior show that turbulent aqueous heat transfer from subglacial meltwater discharge is an important melting process that links glacier instability to the atmospheric and oceanic warming.
- The properties of fjord waters contacting major tidewater glaciers have been observed comprehensively only recently, revealing that submarine melting is strongly controlled by the discontinuous presence of warm and saline waters below ~ 300 m depth.
- New studies report changes in near surface snow and firn structure that have important implications for glacier climate response. Atmospheric warming has driven surface meltwater infiltration to higher altitudes, increasing snow and ice column densification and temperature. Extensive and thick ice layers at depth have formed by refreezing of infiltrating meltwater, reducing the capacity of the glacier to absorb meltwater, promoting meltwater runoff increases, especially in successive years of enhanced melting.
- Subglacial lakes have been observed under the Greenland ice sheet for the first time. Their drainage can be rapid and can affect glacier flow. Finer resolution subglacial mapping suggests the existence of many, small subglacial lakes.
- It remains uncertain whether the Greenland ice sheet will undergo more or less dynamic mass loss due to increasing englacial and subglacial water volumes. It is well established that surface melt water-induced basal 'lubrication' decreases as seasonal melt water discharge progresses due to the development of an efficient, lower pressure subglacial drainage network. However, this process of self-regulation seems currently to be limited to within 40 km of the ice sheet margin. Seasonal surface melt-induced flow acceleration has also been shown to occur up to 140 km into the interior.
- The net surface heating effect of clouds has been better quantified, including a powerful heat trapping effect from optically thin liquid clouds and cloud heating that reduces surface refreezing.

6.1 Introduction

This report updates the findings of the previous SWIPA assessment (AMAP, 2011) by presenting new and significant findings from scientific publications since 2009. This information is organized by region, with multi-regional or pan-Arctic findings reported where appropriate. The review draws on more than 330 externally-reviewed journal articles: 172 (55%) of these refer to Greenland, which is more than twice as many as for all other regions (over 60 publications). More than 30 publications (12% of all research papers) are focused at the pan-Arctic or larger scale. The review concludes by identifying current gaps in knowledge.

Satellite and airborne remote sensing are increasingly filling knowledge gaps with new observations, contributing not only to quantifying ice motion and the mass budgets of land ice, but also to illuminating key physical processes. Regional climate modelling studies constrained by *in situ* observational data are increasingly complementing these satellite-based studies.

Effectively completed only in 2014, the global land-ice inventory now enables closure of the Arctic land ice mass budget and the establishment of a baseline for future change assessments.

It is now known not only that the loss rate of Arctic land ice has increased in response to continued climate warming that is linked to anthropogenic forcing, but also that the Arctic is currently the dominant regional source of global sea level rise. In recent years, two-thirds of the Arctic contribution to sea level rise has come from Greenland, and Greenland's peripheral glaciers contribute more runoff per unit area than the coterminous ice sheet. The relative magnitudes of mass changes in small glaciers, ice caps, and the Greenland ice sheet are for the first time largely resolved.

Deeper insight is emerging about the effects on ice dynamics of water movement and storage in the englacial and subglacial environments, and about the role of changes in the oceanic and atmospheric circulations in driving land ice response to climate change. The direct attribution of a definable fraction of land

ice change to anthropogenic activity is a new development. Reduced meltwater retention in firn (multi-year snow on ice sheets and glaciers) in response to the development of massive ice layers that reduce firn permeability suggests that the response of glacier and ice sheet runoff to climate warming is faster than previously assumed. Advances in data availability, synthesis, and knowledge make this SWIPA-update both timely and significant. This report provides new insights into the sources and mechanisms of sea level change, the apparent impacts of changes in the Arctic freshwater budget on North Atlantic ocean circulation, the possible linkage with increased Atlantic storminess, and the impacts of glacier-derived nutrient fluxes on marine fisheries.

6.2 Arctic glaciers and ice caps

In terms of Arctic glaciers and ice caps, numerous major advances have been made since the previous SWIPA assessment (see Sharp et al., 2011a). These advances highlight the disproportionately large contribution to sea level rise from glaciers and ice caps, which together account for 24% of the total land ice area but 40% of the measured sea level rise.

6.2.1 Completed inventory

For the first time, a complete digital inventory exists of all the world's glaciers (Pfeffer et al., 2014), providing a benchmark for glacier change assessment and for evaluating the freshwater and sea level impacts of glacier changes in different regions of the Arctic. The inventory facilitates mass budget closure, leaving bed elevation as the main source of uncertainty for ice volume assessments (Bahr et al., 2015). After the Greenland ice sheet, the region of the Arctic containing most land ice is Arctic Canada, followed by areas peripheral to the Greenland ice sheet and Alaska (Table 6.1).

All Arctic regions lost glacier and ice cap mass between 2003 and 2009 and changes were greatest in Arctic Canada and Alaska (Gardner et al., 2013). Ice loss has continued into 2015

Table 6.1 Glacier population, glacierized area, ice volume and sea level equivalence and the sea level rise contribution of eight Arctic regions.

Region	Number	Area (km ²) ^a	Volume (km ³) ^b	Sea level equivalence (mm) ^c	Mass loss rate (Gt/y) ^d
Arctic Canada North	4540	104,999 ± 3.2%	34,399 ± 4699	85	33 ± 4
Greenland ^e	19306	89,717 ± 5.0%	19,042 ± 2655	53	38 ± 7
Alaska	27108	86,725 ± 5.3%	20,402 ± 1501	51	50 ± 17
Russian Arctic	1069	51,592 ± 2.8%	16,839 ± 2205	42	11 ± 4
Arctic Canada South	7422	40,888 ± 4.9%	9,814 ± 1115	24	27 ± 4
Svalbard and Jan Mayen	1615	33,959 ± 3.5%	9,685 ± 922	24	5 ± 2
Iceland ^f	568	11,060 ± 2.6%	4,441 ± 370	11	10 ± 2
Scandinavia	2668	2,851 ± 9.3%	256 ± 19	0.6	2 ± 0

^aRandolph Glacier Inventory (Pfeffer et al., 2014): Version 5.0 (Arendt et al., 2015); ^bHuss and Farinotti (2012); ^cusing 362 Gt/mm sea level equivalence; ^dreconciled estimates for the period 2003–2009 (Gardner et al., 2013); ^econsiders glaciers with no connection (65,473 km²) and weak connection (24,244 km²) to the ice sheet (Rastner et al., 2012); strongly connected glaciers are not accounted for here (40,354 km²). The no-to-weak ice sheet connectivity has become standard in most publications; ^ffor the period 1995–2010 mass loss of all Icelandic glaciers is 9.5±1.5 Gt/y (Björnsson et al., 2013). For year 2000, Icelandic land ice volume was more precisely determined by radio echo sounding as 3600 km³ and area as 11,100 km² (Björnsson and Pálsson, 2008; Jóhannesson et al., 2013). The Huss and Farinotti (2012) estimate is from relatively uncertain area-volume scaling.

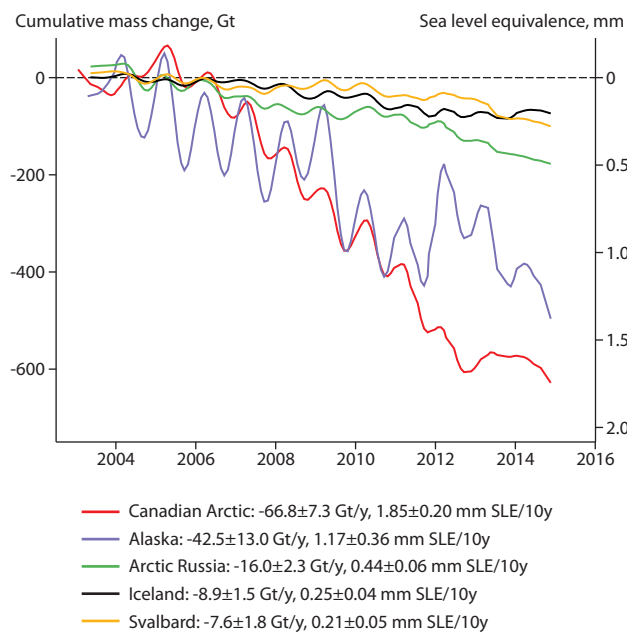


Figure 6.1 Arctic glacier cumulative total mass change and sea level equivalence (SLE) (Wouters et al., 2008; updated by B. Wouters, Utrecht University). Uncertainty ranges represent the standard deviation of least squares fits plus uncertainties in the corrections for glacial isostatic adjustment.

(Figure 6.1). Greenland peripheral glaciers, covering <5% of the island's total ice area are responsible for 14–20% of the whole island mass loss (Bolch et al., 2013). Greenland glacier mass losses are greatest in the southeast and least in the northeast.

Figure 6.1 illustrates how all Arctic regions lost ice mass in the 2003–2015 period. The 2012/2013 increase in mass for the Canadian Arctic was linked to melt suppression by anomalously cool temperatures over the Canadian Arctic islands in summer 2013, when June–August mean air temperatures at 850 hPa were 0.5–2.5°C below the 1981–2010 mean, according to the NCEP–NCAR R1 Reanalysis (Kalnay et al., 1996). The abrupt gain in Alaskan mass around 2011/2012 was due to unusually high snowfall (Beamer et al., 2016).

A global assessment of available mass balance data for glaciers and ice caps shows the monitored Arctic glaciers are more out of balance than the global mean (Mernild et al., 2013a), implying a significant committed loss just to be in equilibrium with the present day climate. While the sample is not comprehensive regionally, it is consistent with the Arctic-wide mass loss evident from satellite gravimetry (Figure 6.1) and includes 18 glaciers from Scandinavia, a region for which gravimetry lacks useful resolution. Accumulation area ratio anomalies suggest that all glaciers in regions north of 25°N were out of equilibrium with climate in the 1979–2009 period (Mernild et al., 2014). In the scenario of a perpetual climate averaging that of 1999–2009, the observed imbalance suggests a committed volume loss of 38±16% and a committed area loss of 32±12%. The 0.71±0.15 mm/y contribution to sea level rise from Arctic glaciers from 1999–2009 was about 40% higher than the 30-year (1979–2009) mean sea level contribution of 0.51±0.16 mm/y. Committed losses (the losses required to bring glacier geometries into equilibrium with the prevailing climate) will increase substantially if the climate continues to warm.

6.2.2 Attribution

Marzeion et al. (2014) used climate modeling to evaluate the relative importance of natural and anthropogenic forcings as drivers of climate change and glacier mass change, and to examine how this varied regionally over time (1851–2010). From 1991 to 2010, they attributed an average of 69±24% of the global glacier mass change to anthropogenic forcing of climate change, a proportion that has increased with time since 1850.

6.2.3 Regional insights

6.2.3.1 Alaska

New studies provide a more comprehensive view of Alaskan ice loss. Airborne laser profiling of 116 glaciers has been used to derive a mean net regional mass balance of -75±11 Gt/y for the period 1994–2013, of which 70% was attributed to land-terminating glaciers, 24% to lake-terminating glaciers, and 6% to ocean-terminating glaciers (Larsen et al., 2015). This is comparable to independent results from spaceborne gravimetry (GRACE) and altimetry (ICESat), which respectively indicate overall regional mass losses of 61±11 Gt/y and 65±12 Gt/y for the period 2003–2009 (Arendt et al., 2013). The interannual variability in glacier mass balance from GRACE is dominated by variability in the summer mass balance which is highly correlated with summer (June, July, August) average temperatures. Accelerated glacier mass losses have been reported for the Wrangell Mountains, increasing from area-averaged values of 0.07±0.19 m water equivalent per year (m w.e./y) (1957–2000) to 0.24±0.16 m w.e./y (2000–2007) (Das et al., 2014). The Wrangell Mountains glaciers are still losing mass but more slowly than for Alaska as a whole. Recently observed mass losses for the bulk of glacierized Alaska south of the Brooks Range correspond to an area-averaged mass change of -0.7 to -0.9 m w.e./y for the period 1994–2013 (Larsen et al., 2015). The mass loss from oceanic ablation (the sum of iceberg calving and submarine melting) has decreased over the past three decades, probably due to the thinning and slowing of many tidewater glaciers (McNabb et al., 2015). However, several fast-flowing tidewater glaciers still lose substantial mass through iceberg calving (Burgess et al., 2013). McNabb et al. (2015) considered Columbia Glacier to have had the highest average rate of frontal ablation over the past three decades, with a mean change of 3.70±0.89 Gt/y.

6.2.3.2 Canadian Arctic

The advent of spaceborne monitoring techniques has enabled a new and spatially comprehensive view of glaciers and ice caps, providing a first complete surface velocity mapping for Canadian Arctic glaciers and a first closure of the total mass balance from satellite gravimetry. For the period 2003–2009, the rate of mass loss from glaciers in Arctic Canada (61±7 Gt/y) was higher than for any other glacier region with the exception of Greenland's coterminous ice sheet (Gardner et al., 2011) and comparable to that from Alaska (Figure 6.1). The short duration satellite measurements (2005–2009) indicate a loss rate five times the 1963–2004 average (Sharp et al., 2011b). The recent high rate of ice loss continued through 2012 (Lenaerts et al., 2013). The recent mass loss from Canadian Arctic glaciers by surface melt and runoff has been 20 times greater than the loss by ice flow discharge (2.6±0.8 Gt in 2012) (van Wychen et al., 2014).

Recent acquisitions of ice thickness data across the Canadian Arctic Archipelago (such as from NASA's Operation IceBridge) now provide the frontal geometry of many of the major outlet glaciers in the Canadian Arctic, and when combined with terminus glacier velocities, enable the calculation of mass loss via ice flux (dynamic discharge) from the Canadian Arctic (van Wychen et al., 2014, 2015, 2016). Overall, dynamic discharge is a small component of mass loss within the Canadian Arctic Archipelago; accounting for ~3.1% of mass loss from the northern Canadian Arctic (when compared to mass balance records in 2012) (van Wychen et al., 2014) and only ~0.1% of mass loss in the southern Canadian Arctic (when compared to mass balance records in 2011) (van Wychen et al., 2015). The lack of major dynamic ice losses further highlights the importance of surface melt and runoff in the Canadian Arctic Archipelago land ice response to climate change.

The increase in Canadian Arctic land ice loss is mainly due to warmer summers in recent years (Gardner et al., 2011) because precipitation rates have remained relatively stable (Gardner et al., 2012), except near polynyas where reduced sea ice cover can enhance snowfall (Mair et al., 2009). 2013 was a positive mass balance year for Canadian Arctic ice. As with western Greenland, summer 2013 experienced anomalously cold northern air flow that suppressed melting (Figure 6.2). In 2012, the opposite atmospheric circulation produced record melting across Greenland and abnormally cold conditions on Svalbard (Figure 6.3). The past decade has had numerous persistent atmospheric circulation patterns. The persistence may be increased due to the reduction in Arctic to mid-latitude temperature differences that drive the Jet Stream (Francis and Vavrus, 2012).

The area of floating ice shelves across northern Ellesmere Island has decreased by more than 90% since the early 20th century, with some fjords having ice-free conditions for the first time in over 3000 years (Sharp et al., 2014). This includes the complete loss of the Markham Ice Shelf in 2008 and the loss of about 61% (29.8 km²) of the Petersen Ice Shelf between 2005 and 2012 (White et al., 2015).

Pre-instrumental data from ice cores suggest that mass loss from Canadian Arctic ice caps is likely to be occurring faster now than at any time in the past 4000 years (Fisher et al., 2012; Zdanowicz et al., 2012). These loss rates were last exceeded in the Holocene Climatic Optimum (a.k.a. Holocene Thermal Maximum) about 9000 years BP, when summer temperatures in this area were 3°C higher than the 20th century average (Kaufman et al., 2004).

Evidence from vegetation remains exposed by glacier retreat on Baffin Island suggests that average summer temperatures during the past 100 years have been higher than in any other century of the past 44,000 years (Miller et al., 2013). The more intense and sustained melt in recent years has resulted from more frequent and sustained summer high atmospheric pressure (Bezeau et al., 2015). This pattern is also recognized as a driver of enhanced Greenland ice melt since 2001 (Rajewicz and Marshall, 2014; McLeod and Mote, 2016). It is not, however, well reproduced by simulations with the CMIP5 Climate models.

6.2.3.3 Svalbard

Recent satellite altimetry provides widespread coverage of Svalbard glaciers, and suggests that they lost 4.3±1.4 Gt/y of ice over the period 2003–2008 (Moholdt et al., 2010). These data

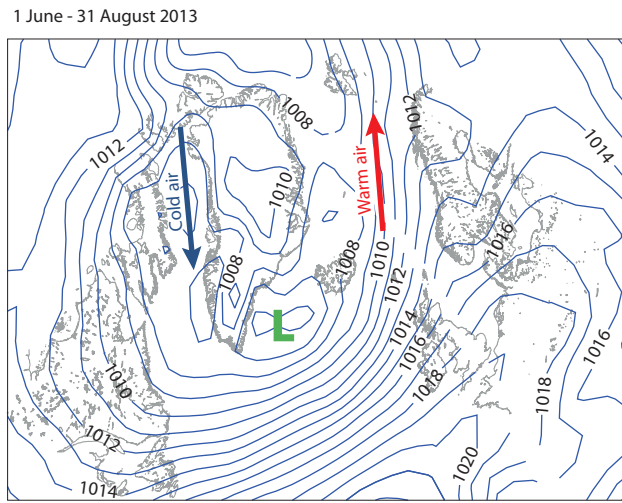


Figure 6.2 Sea level pressure (hPa) 1 June to 31 August 2013. Persistent low atmospheric surface pressure between Arctic Canada and Greenland brought cold air to the region, suppressing melting. The same circulation regime also favored the delivery of relatively warm and moist air to Svalbard, driving its melt rates to twice that of the previous four decades (Jason Box and NCEP/NCAR Reanalysis).

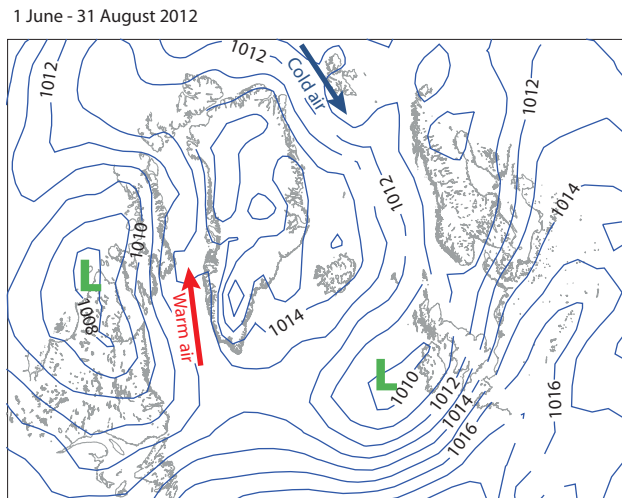


Figure 6.3 Sea level pressure (hPa) 1 June to 31 August 2012. An abnormally persistent atmospheric circulation pattern, brought record melting to western Greenland and the Canadian Arctic at the same time bringing abnormally cold air to Svalbard (Jason Box and NCEP/NCAR Reanalysis).

show a general pattern of high-elevation balance or thickening and low-elevation thinning, combined with a sub-regional pattern of greater rates of thinning in the south and west than in the northeast. Comparisons between the satellite altimetry data and older topographic maps indicate a higher rate of mass loss (~10 Gt/y) for about the past 40 years (Nuth et al., 2010).

The recent relatively low rate of mass loss has been confirmed by GRACE gravimetry (Jacob et al., 2012; Matsuo and Heki, 2013) and by simulations with regional atmosphere-glacier models (Aas et al., 2015; Lang et al., 2015). The models show large interannual variability in climatic mass balance, dominated by variability in summer melting rather than winter accumulation. *In situ* records of climatic surface mass balance for the past 50 years show no acceleration in rates of glacier mass loss, unlike records from most other Arctic regions. The lack of acceleration might be because recent changes in atmospheric circulation favored northwesterly flow in summer over Svalbard

rather than a previously more typical west-southwesterly flow (Lang et al., 2015). However, in 2013, when Greenland and the Canadian Arctic experienced much smaller mass changes, the circulation changed to a south-southwesterly flow over Svalbard causing an anomalously high annual mass loss of 20 Gt (Lang et al., 2015) (Figure 6.2).

The Vestfonna ice cap in eastern Svalbard has a much smaller ice volume than previously thought, suggesting that global ice volume estimates derived using volume-area scaling methods may be problematic (Pettersson et al., 2011). Vestfonna's larger neighbor, the Austfonna ice cap, is currently experiencing one of the largest glacier surges recorded in Svalbard. A smaller flow instability was observed in this glacier in 'Basin 3' in the early 1990s (Dowdeswell et al., 1999), and GPS (global positioning system) observations show a yearly stepwise acceleration in ice-flow speed after melt-induced summer speed-up events from 2008 until autumn 2012 when the fast-flowing region spread to the whole of Basin 3 as a full surge developed (McMillan et al., 2014; Dunse et al., 2015). The iceberg calving flux from Basin 3 exceeded 4 Gt in the following year, and the glacier terminus has advanced more than 5 km into the Barents Sea.

6.2.3.4 Iceland

Owing to its sub-Arctic latitudes and maritime climate, glaciers in Iceland tend to be temperate and to experience relatively high rates of accumulation. As a result they tend to be more sensitive to atmospheric warming than glaciers elsewhere in the Arctic. The region has copious historical information from state documents, written accounts, old maps and photographs. Some recent studies have combined documentary evidence with information from dated end moraines to produce comprehensive reconstructions of glacier fluctuations.

Mass loss rates from Icelandic ice caps were relatively high in the 1930s to 1940s, limited in the 1980s and early 1990s, and increasingly substantial from the mid-1990s onward (Pálsson et al., 2012; Björnsson et al., 2013). Since the Little Ice Age (LIA; ending in the 19th century), Langjökull ice cap has undergone two periods of strongly negative mass balance (1920–1960 and since the mid-1990s) separated by a period of near zero mass balance. Mass balance estimates derived by differencing available elevation maps are -1.6 ± 0.5 m w.e./y for the period 1937–1945 and -1.26 ± 0.15 m w.e./y for the period 1997–2009. The average rate of mass loss from all glaciers in Iceland is estimated at 9.5 ± 1.5 Gt/y for the period 1995–2010, but with large interannual variability (ranging from 2.7 to 25.3 ± 1.5 Gt/y). This is attributable to the combined effects of climate variability and albedo depression by the fallout of ash from volcanic eruptions.

Studies of southeastern Vatnajökull outlet glaciers from the 1600s to present (Hannesdóttir et al., 2014, 2015a) compare recent glacier extent and thickness with historical photographs, maps, and geomorphological data such as moraine dating from the glaciers' maximum extent at the end of 19th century. The size and shape of ten Vatnajökull outlet glaciers at the end of the LIA has been reconstructed. These glaciers advanced in the late 1600s, extended into lowland areas in the 18th century, and reached their LIA maximum around 1880–1890, before retreating in response to climate warming. Since reaching their maximum extent in 1890, the area of the individual outlet glaciers has decreased by 10–30%,

with a total area reduction of 164 km^2 . The volume loss of the outlet glaciers is in the range 15–50%, equivalent to a mass loss of 60 ± 8 Gt ($+0.15 \pm 0.02$ mm mean sea level equivalent). The mean geodetic mass balance for the period 1890–2010 was -0.7 to -0.3 m w.e./y. The most negative mass balance was observed between 2002 and 2010, when the glaciers lost between 0.8 and 2.6 m w.e./y, which are among the highest rates recorded anywhere in the world (Hannesdóttir et al., 2015a). A projected increase in air temperature of $2\text{--}3^\circ\text{C}$ by 2100 is predicted to lead to a total ice volume loss of 50–80% in this area (Hannesdóttir et al., 2015b).

Geodetic data for the entire Drangajökull ice cap show an average mass balance of -0.26 ± 0.04 m w.e./y for the period 1946–2011, corresponding to about 3 km^3 volume loss over the entire period (Magnússon et al., 2015). Over this period, the glacier area decreased from 161 to 144 km^2 . Relatively high mass loss rates were observed for the periods 1946–1960 (0.66 ± 0.17 m w.e./y) and 1994–2011 (0.64 ± 0.10 m w.e./y for 1994–2005 and 0.46 ± 0.15 m w.e./y for 2005–2011). The mass balance of Drangajökull was however close to zero for the period 1960–1985 (-0.07 ± 0.07 m w.e./y for 1960–1975 and 0.07 ± 0.08 m w.e./y for 1975–1985) and significantly positive for the period 1985–1994 (0.26 ± 0.11 m w.e./y). The volume of Drangajökull's three surge-type glaciers is estimated to have been greater during the LIA than at present (Brynjólfsson et al., 2015). The Drangajökull ice cap surge frequency over the past 300 years is about once per century for each glacier. The occurrence of surging does not show a clear relationship with climate fluctuations.

6.2.3.5 Scandinavia

Cumulative mass balance records for northern Scandinavia become more negative from 1948 to about 1970, more positive to about 1995, and then more negative again. The period of increasingly positive cumulative balances is linked to high winter snowfall and a positive phase of the North Atlantic Oscillation (Trachsel and Nesje, 2015), which had a large influence on the maritime glaciers of Norway. Between 2000 and 2010, the average mass loss from glaciers in Norway was estimated at 0.86 ± 0.15 m w.e./y (Engelhardt et al., 2013). Repeat inventories of Norwegian glacier area found an 11% decrease in glacierized area in mainland Norway during the latter half of the 20th century (Winsvold et al., 2014), with a larger (16.5%) decrease in northern Norway. The stable period in the 1970s and 1980s is evident in the mass balance series from Storglaciären in northern Sweden (Box 6.1). The recent trend to more negative cumulative mass balance has continued or accelerated during the period 2001–2009. One third of Storglaciären's cold surface layer was lost during the 12 years from 1989 to 2010 (Gusmeroli et al., 2012). Out of balance conditions suggest that the 18 glaciers monitored in northern Scandinavia would lose $56 \pm 7\%$ of their volume if they came into equilibrium with their 2001–2010 climate (Mernild et al., 2013a).

6.2.3.6 Russian High Arctic

Changes in the mass of land ice in the Russian High Arctic have been comprehensively evaluated for the first time (Moholdt et al., 2012) using a combination of satellite

Box 6.1 Climate change claiming Sweden's highest point

Sweden's highest mountain, Kebnekaise, has two peaks of which the higher is ice-capped. This ice-covered southern peak has been melting at an average rate of 1 m/y for the past 15 years, and its elevation is now within 1 m of that for the rocky northern peak. In what is likely to be an historical

first, a nation's highest point is set to change through climatic warming. The world's longest continuous record of glacier mass balance, which began in the 1945/1946 hydrological year, comes from Storglaciären (Figure 6.4) on the eastern slopes of Kebnekaise.

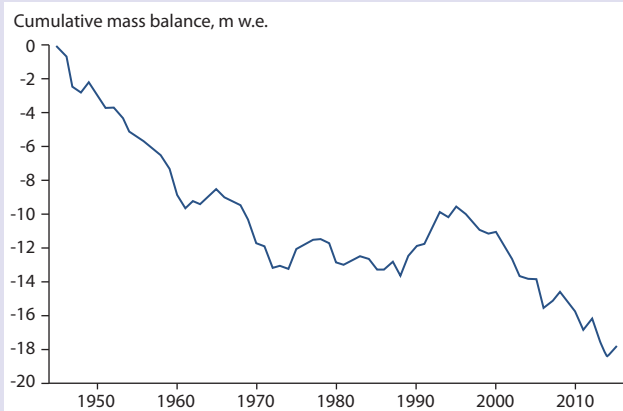


Figure 6.4 Net change in ice mass balance for Storglaciären (see photo), the glacier with the World's longest continuous distributed mass balance record (Peter Jansson, Stockholm University).

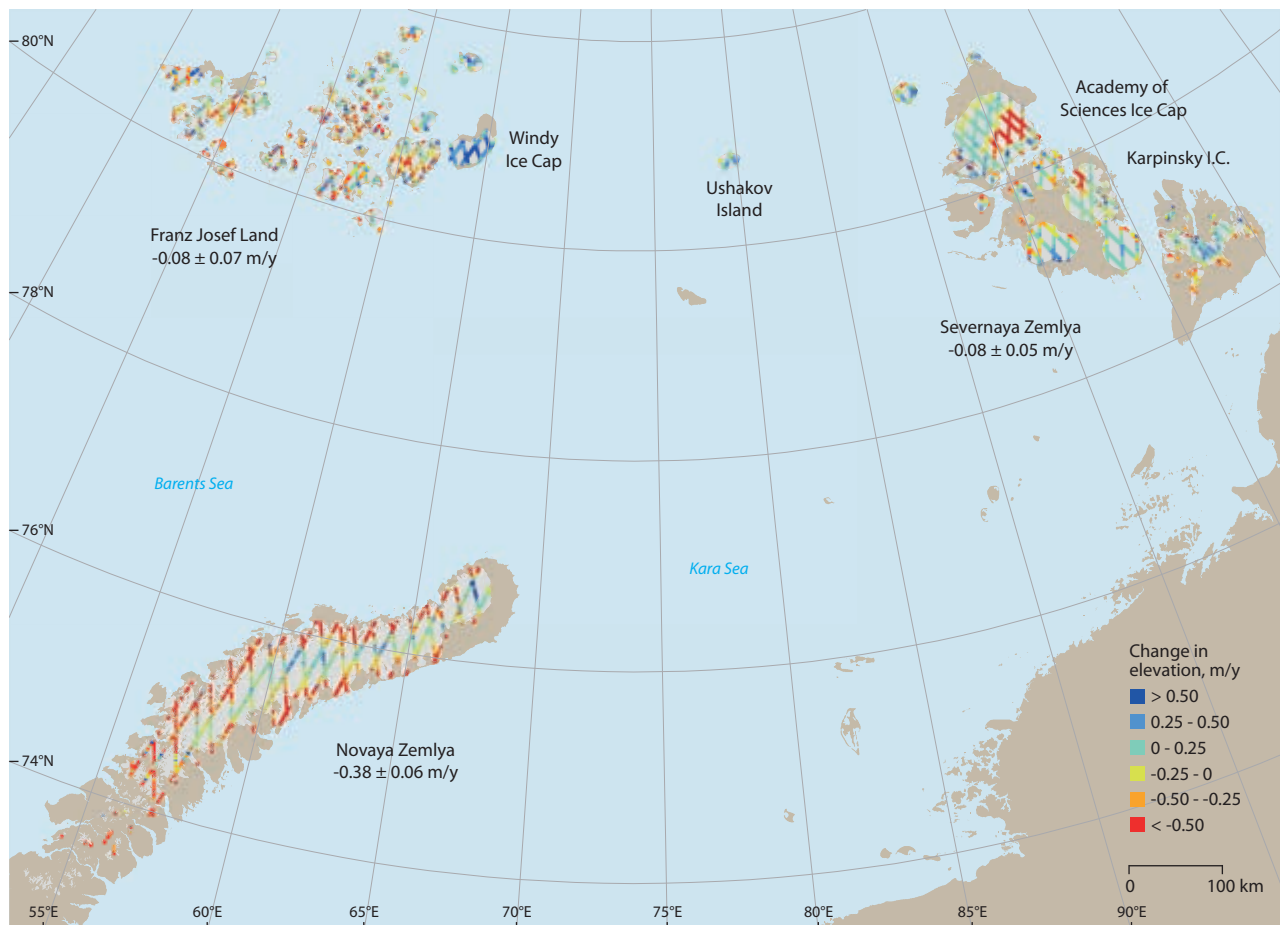


Figure 6.5 ICESat repeat-tracks with average rates of change in elevation for the period October 2003 to October 2009 for glaciers in the Russian High Arctic. Average elevation change rates are given for each of the three named regions (Moholdt et al., 2012).

imagery, altimetry and gravimetry. A mass loss of 9.1 ± 2.0 Gt/y was estimated for the period 2003–2009. This is 7 Gt/y less than that derived by Wouters et al., (2008) from GRACE data alone. The greatest losses are from Novaya Zemlya, where retreat of marine-terminating glaciers has accelerated substantially since 2000 (Carr et al., 2014). Severnaya Zemlya glaciers exhibit highly variable calving rates due to ongoing ice-flow instabilities in the Academy of Sciences Ice Cap (Moholdt et al., 2012) and cyclical collapses of the Matusevich Ice Shelf (Williams and Dowdeswell, 2001). This disintegrated in summer 2012, causing accelerated flow and increased thinning in the tributary glacier basin (Willis et al., 2015).

Reduction in the area of glaciers on Novaya Zemlya between 1952 and 2015 was not less than 812.6 ± 2.7 km². It involved retreat of both marine- and land-terminating glaciers with 507.3 ± 2.4 km² loss from glaciers facing the Barents Sea and 220.8 ± 2.9 km² from glaciers facing the Kara Sea (Lavrentiev, 2016). The rate of glacier area reduction almost doubled over the period 2001–2015, reaching a mean of -20.3 km²/y compared to -10.8 km²/y for 1952–2001.

The current state of the smaller ice shelves on Franz Josef Land (Dowdeswell et al., 1994) is largely unknown, but glaciers in the region appear to be in near balance, with the exception of the Windy Ice Cap, which stands out as a rarity in the present Arctic because it is thickening (Figure 6.5).

6.2.3.7 Siberia

Recent Landsat imagery has been analyzed to make the first complete glacier inventory for continental North Asia. This identifies 5065 glacier units that cover a total area of 2326 ± 186 km² (Earl and Gardner, 2015). Historical USSR glacier inventories indicate a steady glacier shrinkage in all mountain regions over the latter half of the 20th century. Ice loss has increased since the 1980s. Glacier area loss was 22% in the Polar Urals (Khromova et al., 2014).

Between 1968/1969 and 2010, 70% of the glaciers with outlines appearing in a USSR Inventory of Glaciers (1972) have decreased in area (Katalog lednikov SSSR, 1972). The shrinkage is greatest for glaciers in northeastern Siberia (62% area loss; Ananicheva and Karpachevsky, 2015). On average the equilibrium line altitude (ELA) in the Polar Ural mountains rose by 120 m between 1967 and 2010, while ice area decreased by 22%. These changes coincide with a summer warming of 1°C during the latter half of the 20th century (Shahgedanova et al., 2012). ELAs of glaciers in northeastern Siberia and the Koryak Highland have risen by 100–200 m since the 1950s, while ice area has decreased by 20–69% (Ananicheva, 2014). In particular, over the Russian subarctic, glacier area decreased by 15% in Byrranga, 30% in the Suntar-Khayata, Chersky and Meynypilgynsky range (northeast of Koryakia), and 60% in Orulgan (Ananicheva, 2014; Ananicheva and Karpachevsky, 2015). Glacier area in eastern Siberia has decreased by more than one third since 1945 in some areas (Gurney et al., 2008; Galanin et al., 2013).

Relative to a survey during the 1960s (Sedov, 1997a,b) glaciers in the northern Far East of Russia reduced in area by around 30% in the Kolyma Highlands and 60% in the Iskaten Range (Ananicheva and Karpachevsky, 2016) (Figure 6.6).

Aerial photography from August 1950 shows the Kamchatka Peninsula had 448 glaciers with a total area of 905 km². Subsequent satellite observations reveal the separation of glaciers. In the Alney-Chashakondzha region of north-central Kamchatka, glacier area reduced by 11.6 km² (19.2%) over the period 1950–2010. Reduced glacier area is attributed to higher summer air temperatures and lower snowfall (Muravjev and Nosenko, 2013; Muravjev, 2014).

Between 1963 and 2010, the fraction of ice area in the Kodar Mountains of southeastern Siberia that is debris-covered increased by 44%, owing to increased ablation between 1995 and 2010 that coincided with rising summer temperatures (Stokes et al., 2013).



- 1 France Josef Land and Victoria Island
- 2 Ushakov Island
- 3 Severnaya Zemlya
- 4 De Long isles
- 5 Novaya Zemlya
- 6 Caucasus
- 7 Pamir-Alay
- 8 Tien Shan
- 9 Dzhungarsky Alatau
- 10 Khibiny Mountains
- 11 Polar Urals
- 12 Altai Mountains
- 13 Kuznetskii Alatau
- 14 Eastern Sayan
- 15 Kodar Range
- 16 Putorana Plateau (so called passive glaciers)
- 17 Byrranga Mountains
- 18 Orulgan Range
- 19 Wrangel Island
- 20 Chersky Range
- 21 Suntar-Khayata Mountains
- 22 Koryak Highlands and Meynypilgynsky Range
- 23 Kamchatka
- 24 Kolyma Highlands
- 25 Chukchi Highlands (Chukotka)

Figure 6.6 Siberian glacier locations (Maria Ananicheva). Glaciers 7, 8 and 9 not shown.

6.2.3.8 Greenland

The longest surface mass balance record for any Greenland glacier isolated from the ice sheet is from Mittivakkat Gletscher in southeastern Greenland. Between 1986 and 2011, its average thickness decreased by 15%, while its volume decreased by 30%. This is attributed to a combination of warming and reduced snow accumulation (Mernild et al., 2013b). A decline in surface albedo by 0.10 ± 0.05 from 2000–2013 is likely to have contributed to the higher rates of surface melting (Mernild et al., 2011, 2015a).

Comprehensive Greenland glacier surveys from satellite inventories are now available for the first time. Using the new all-Greenland glacier inventory, Bolch et al. (2013) found that all glaciers and ice caps collectively lost 40.9 ± 16.5 Gt/y between October 2003 and March 2008, representing 10% of the estimated contribution of the world's glaciers and ice caps to the rise in global mean sea level.

6.2.4 Arctic glaciers

There had been few detailed studies of Arctic tidewater glacier behavior at the time of the previous SWIPA assessment (see Dahl-Jensen et al., 2011; Sharp et al., 2011a). The situation has now changed dramatically, in terms of observations and the development of theory. Many new satellite and airborne observations of tidewater glacier behavior have been published, and historical photos, maps, and other evidence have been used to reconstruct tidewater glacier terminus fluctuations in Alaska, Svalbard, and Greenland, placing the more finely resolved fluctuations of the satellite era into a longer term context. While regionally diverse, these studies draw consistent conclusions about glacier sensitivity to atmospheric and oceanic warming.

6.2.4.1 Glacier behavior

Alaska

In Alaska, exceptional rates of glacier mass loss have been documented for the marine-terminating Columbia Glacier and the lake-terminating Yakutat Glacier. The discharge of Columbia Glacier increased four-fold between 1948–1981 and 1982–1995, and then doubled from that value in the period 1996–2007 (Rasmussen et al., 2011). Yakutat Glacier is a fast-melting remnant of an LIA glacier, and its recent volume changes suggest that lake-calving dynamics play a significant role in its mass loss despite lower subaqueous melt rates than for saltwater-terminating glaciers (Trüssel et al., 2013).

Canadian Arctic Archipelago

Recent studies have placed an emphasis on determining baseline glacier dynamics at the regional scale across the Canadian Arctic Archipelago (van Wychen et al., 2012, 2014, 2015, 2016) and build upon earlier work (Copland et al., 2003; Short and Gray, 2004, 2005; Burgess et al., 2005; Shepherd et al., 2007). Taken together, these studies give a comprehensive record of tidewater glacier behavior for the Canadian Arctic since 1999 and provide more extensive knowledge of glacier velocities in the Canadian Arctic than was previously available.

Using a ~15-year record of ice motion in the northern part of the Canadian Arctic Archipelago, van Wychen (2015) and

van Wychen et al. (2016) quantified the spatial magnitude of velocity variability and the period over which these processes operate, as well as classifying the behavior of each outlet glacier that displayed variability. In addition to identifying surging as a mechanism that caused variability, new processes have also been identified, such as *pulsing motion* over periods of three to five years confined to specific regions of glaciers defined by basal-topographic features, and *consistent acceleration* where reductions in stresses that resist ice flow in the terminus regions of glaciers facilitate the onset of faster ice motion. Most notably, the consistent acceleration process has been identified as the cause of the recent speed-up of the Trinity–Wykeham Glacier complex of the Prince of Wales Icefield (van Wychen et al., 2016). This glacier has undergone significant thinning, frontal retreat, and acceleration since 2000 and it is speculated that this has been driven by either atmospheric or oceanic warming (or a combination of both) (van Wychen et al., 2016). The speed-up of this glacier basin is reminiscent of recently observed tidewater glacier accelerations in, for example, Helheim Glacier (Greenland) and Columbia Glacier (Alaska), and provides the first example of prolonged and sustained dynamic glacier acceleration in the Canadian Arctic that is not thought to be associated with cyclic (surge or pulse) flow variability (van Wychen et al., 2016).

Several Canadian High Arctic tidewater glaciers have decelerated while a few larger tidewater glaciers increased their discharge over the period 1999–2015 (van Wychen et al., 2014), highlighting the influence of surge-type glaciers for interannual variability in mass change.

Greenland

The mass balance of the Greenland ice sheet's three largest outlet glaciers fluctuated between 2000 and 2010: Helheim Glacier gained mass from 2006 to 2010 (Howat et al., 2011) following a period of sustained terminus retreat (7 km from 2002 to 2006; Jensen et al., 2016). Similarly, mass loss rates from Kangerlussuaq Glacier peaked at seven times the 2000–2010 average in April 2005 and, by summer 2008 had returned to the 2000 rate (Howat et al., 2011). Khan et al. (2014) found that Helheim Glacier thickened by more than 50 m on average from 1981 to 1999. While the strong speed-up observed in southeastern Greenland between 2000 and 2005 has disappeared in recent years, glaciers in northwestern Greenland continue to accelerate (Moon et al., 2012). Jakobshavn Isbræ lost 98 km² of its area from 2002 to 2005, when it retreated by 8 km (Jensen et al., 2016). Its flow accelerated throughout that period (Howat et al., 2011). Jakobshavn Isbræ subsequently exhibited seasonal velocity fluctuations that were 30–50% greater than in earlier summers (Joughin et al., 2014). In northwestern Greenland, glacier retreat rates were rapid but highly variable (McFadden et al., 2011; Carr et al., 2013b).

Compilations of ICESat and IceBridge airborne laser altimetry measurements suggest that dynamic thinning was responsible for half (48%) of the ice mass loss from Greenland between 2003 and 2009, with its contribution peaking in the period 2004–2006 (Csatho et al., 2014). The majority of Greenland outlet glaciers thinned over time interspersed with shorter periods of reduced thinning or even thickening. Examining two periods (1985–1993 and 2005–2010) during which dynamic ice loss dominated total mass loss from the northwest Greenland margin Kjær et al. (2012) found that dynamic thinning may switch on and off.

In a first regional-scale assessment of changes in the velocity and terminus position of Greenland glaciers, Joughin et al. (2010) found widespread outlet glacier acceleration and retreat between 2000 and 2005. Howat et al. (2011) and Moon et al. (2012), and Csatho et al. (2014) found heterogeneous regional patterns of retreat and acceleration. Adjacent outlet glaciers can react differently to a common regional climate forcing (Joughin et al., 2010; Moon et al., 2012; Csatho et al., 2014), highlighting the importance of site-specific controls on tidewater glacier dynamics. Local controlling factors can dominate the climate response of tidewater glaciers. Factors include distance to outer ocean currents, along-fjord width variations, subglacial relief, and the properties and presence of subglacial till (Carr et al., 2013a, 2015; Bougamont et al., 2014).

Andresen et al. (2014) identified retreat episodes for four glaciers terminating in Upernivik Isfjord, in northwestern Greenland. Several glaciers fed a single ice shelf at the time of the first observation (1849), followed by ice shelf disintegration during subsequent periods with higher air temperatures. Glacier retreat phases were roughly synchronous to those observed at Helheim Glacier in southeastern Greenland (Andresen et al., 2012).

Leclercq et al. (2012) reconstructed the terminus positions of 18 land-terminating glaciers in southern and western Greenland since the 19th century, and found an average retreat of 1.2 ± 0.2 km over the 20th century. The retreat rate was largest in the first half of the 20th century, consistent with Bjørk et al. (2012) who found that land-terminating glaciers retreated more rapidly in the 1930s than in the 2000s. This may be because smaller glaciers were already much reduced in size by the 2000s and thus retreated proportionally less in the latter half of the century. In contrast, larger marine-terminating glaciers retreated more rapidly during the recent warming episode (Bjørk et al., 2012) in which the dynamic mass loss response appears to have been triggered by a different forcing. Kjeldsen et al. (2015) produced detailed Greenland maps for three time intervals spanning the end of the LIA, concluding that post-1980s accelerated ice loss and thinning is focused at tidewater glacier outlets.

Andresen et al. (2012) found Helheim Glacier activity to be consistent with oceanic and surface climate fluctuations. For a major tidewater glacier in western Greenland, Lea et al. (2014b) found atmospheric and oceanic data have varied in phase with glacier front position for the past 150 years. For 36 Alaskan glaciers, McNabb and Hock (2014) found that over the 1948–2012 period, the majority of glaciers (66%) retreated, while several underwent rapid, short-term retreats lasting a few years. Retreat occurred following large increases in summer sea surface temperature.

Svalbard

Recent retreat of tidewater glaciers is evident around Svalbard (Nuth et al., 2013), except for surging glaciers (Sund et al., 2014; Dunse et al., 2015). The early 20th century and recent warming periods are well reflected in records of tidewater glacier mass loss rates in Svalbard (Blaszczyk et al., 2013).

6.2.4.2 Tidewater glacier sensitivity

Focus on the importance of submarine melting for mass loss from tidewater glaciers has grown substantially since the previous SWIPA assessment (see Sharp et al., 2011a).

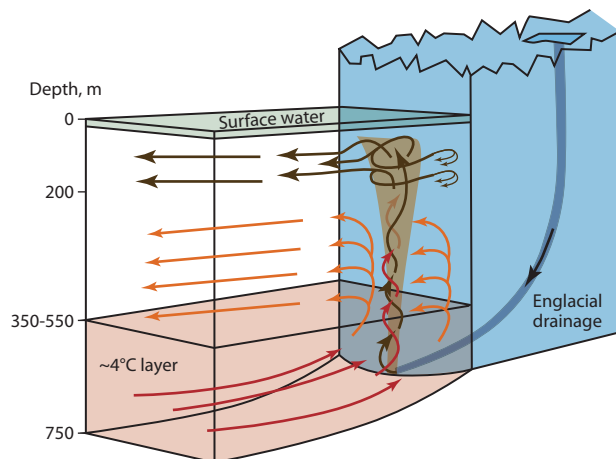


Figure 6.7 Englacial and subglacial meltwater emerges at tidewater glacier fronts, forcing a heat exchange between the ice front and relatively warm ocean waters. In cases where water depth exceeds 350 m, entrainment of water of 4–5°C can enhance melt rates (after Chauché et al., 2014).

The process is recognized not only to be more important than iceberg calving at some glaciers, but also to influence calving rates by introducing instability to tidewater termini by undercutting (Rignot et al., 2010, 2015; Bartholomaus et al., 2013; Motyka et al., 2013; Fried et al., 2015). Buoyant meltwater plumes emerging into the marine environment from the base of the terminal ice cliff can greatly increase rates of terminus melting (Straneo et al., 2011, 2012; Xu et al., 2012) (Figure 6.7).

Side-looking, multi-beam echo sounding observations reveal that Greenland's tidewater glacier termini are grounded further below sea level than previously recognized and that terminal ice cliffs are neither vertical nor smooth, but are often undercut from melting by relatively warm ocean waters below depths of 350 m (Rignot et al., 2015). Side-scan sonar was used to reveal severe undercutting and indirectly infer submarine melt rates of up to 3 m per day at the calving front of an outlet glacier in western Greenland (Fried et al., 2015). This study found that the entire terminus region was undercut and that the resulting notch intersected surface crevasses, thereby promoted enhanced calving-rates. Fried et al. (2015) also speculated that undercut notches constricted outflowing plumes and so amplified submarine melt, which they estimated to account for 85% of total melt losses across the terminus of Kangerlussuup Sermia in central northwestern Greenland.

Direct oceanographic measurements describe the characteristics of fjord waters in contact with major Greenland tidewater glaciers (Straneo et al., 2012; Chauché et al., 2014). A primary factor determining submarine melt rates is the heat input into Greenland's fjords from relatively warm and saline Atlantic Water. This obtains its temperature and salinity from subtropical waters flowing around Greenland that are supplied by the Irminger Current in Denmark Strait and the West Greenland Current from Cape Farvel northward into Baffin Bay and beyond (Straneo et al., 2011) (Figure 6.8). The average summer 2009 energy flux into individual fjords has been estimated at 0.029 TW for Sermilik Fjord, into which the Helheim Glacier discharges (Sutherland and Straneo, 2012). A much

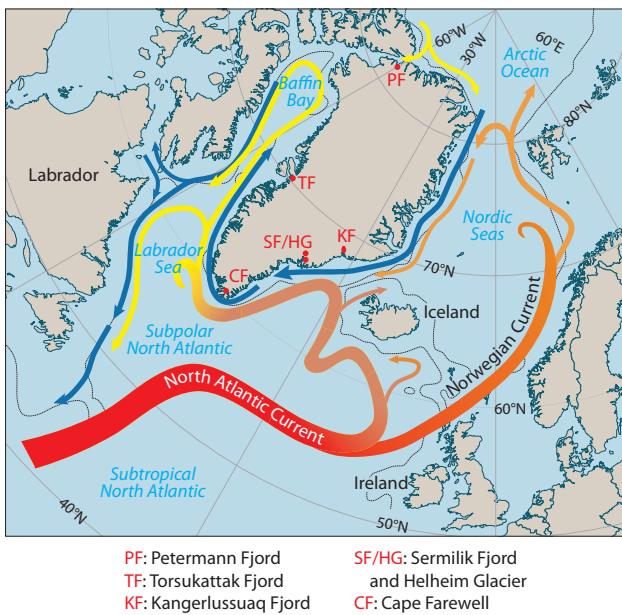


Figure 6.8 Ocean currents delivering heat linked with glacier destabilization (after Straneo and Heimbach, 2013).

higher heat flux (0.26 TW) was estimated for Kangerlussuaq Fjord in southeast Greenland (Bendtsen et al., 2015). Other fluxes include 0.16 TW for Torsukattak Fjord (Rignot and Mouginot, 2012) and 0.31 TW for Petermann Fjord (Johnson et al., 2011). Although these estimates are based on limited CTD measurements (i.e. density/depth profiles) and may overestimate long-term energy fluxes, such high values reveal there is energy available to enhance submarine melting at the calving fronts of many of Greenland's tidewater glaciers provided that the Atlantic Water comes into contact with the glacier fronts. Ocean heat and mass exchanges are driven by shelf circulation, tidal mixing, local winds, and freshwater discharge at glacier fronts (Straneo and Heimbach, 2013). Recent Greenland glacier retreat has coincided with a rapid warming of the sub-polar North Atlantic that began in the mid-1990s and was strongly influenced by persistence in negative phases of the North Atlantic Oscillation (NAO) (Bersch et al., 2007; Yashayaev, 2007; Holland et al., 2008). However, NAO-driven variability cannot account for the recent simultaneous warming of the upper 1000–2000 m of the sub-polar and subtropical North Atlantic that started in the late 1990s and has resulted in a large heat content anomaly over the entire North Atlantic (Straneo and Heimbach, 2013).

6.3 Firn changes

Numerous studies since the previous SWIPA assessment (see Dahl-Jensen et al., 2011; Sharp et al., 2011a) document changes in firn structure and thermodynamics that have important implications for glacier hydrology, ice dynamics and the response of sea level to climate and glacier change. These studies suggest that an increasing proportion of surface melt in firn-covered areas may become runoff as the infilling of firn pore volume with infiltration ice, limits the percolation and storage of liquid water in firn.

Increased melting moves percolation regimes to higher altitudes and increases rates of firn densification (Bezeau et al., 2013). Since the 1980s, the sub-Arctic Penny Ice Cap on Baffin Island has entered a phase of enhanced melt rates owing to rising summer air temperatures across the eastern Arctic. Between 70% and 100% of the annual accumulation at the ice cap summit now occurs in the form of refrozen meltwater (Zdanowicz et al., 2012). Increased surface meltwater infiltration and refreezing caused 10°C of firn warming at 10 m depth on Penny Ice Cap during the period 1990–2011 (Zdanowicz et al., 2012), 5.5°C of firn warming at 10 m depth on the summit of the Devon Ice Cap (Bezeau et al., 2013), and 6°C of firn warming in percolation facies of the Greenland ice sheet over the 1954–2013 period (Polashenski et al., 2014). Surface melt rates such as those recently experienced on ice caps in the Canadian Arctic have not been recorded for more than 3000 years.

The pore volume of the Greenland ice sheet firn provides the capacity to store around 322–1289 Gt of meltwater runoff and may thus buffer the relationship between surface melt and sea level rise in a warming climate (Harper et al., 2012). However this effect will diminish as the pore volume fills, and the sensitivity of sea level to surface melt increase will again increase (Van Angelen et al., 2013).

New Greenland field data indicate the development of extensive and thick ice layers formed by refreezing of percolating meltwater in firn under the warming conditions between the mid-1990s and 2014 (Charalampidis et al., 2015; de La Peña et al., 2015; Machguth et al., 2016; Mikkelsen et al., 2016). Similar observations had previously been reported for the Devon Ice Cap in Arctic Canada (Gascon et al., 2013a,b). Massive ice layers within 5–10 m of the glacier surface reduce the capacity of the firn to absorb meltwater and thus increase the runoff response to warming. The situation is complex, however, as the firn hydrology depends on the local accumulation rate. Under very high accumulation rates, the water can be trapped as a liquid, producing a firn aquifer (Forster et al., 2013). The Greenland firn aquifer persists through winter, occupying 4% of the coterminous ice sheet area with an estimated mass of 140 ± 20 Gt (Koenig et al., 2014). In areas with a low accumulation regime (which are generally colder), however, the meltwater refreezes. It is not known whether, under warming conditions, the aquifer temporarily buffers sea level rise or contributes to it either directly through meltwater drainage, or indirectly through the effects of drainage on ice dynamics.

Melt progressed quickly enough in successive high melt years, most notably 2010 and 2012, that refreezing could promote the development of thick (multi-meter) ice layers in southwestern Greenland. These impermeable layers were sufficient to block meltwater infiltration (Machguth et al., 2016) and to enhance surface runoff. Using meteorological, melt, firn-stratigraphy and proglacial river discharge observations from the extreme 2010 and 2012 summers, Mikkelsen et al. (2016) determined the relationship between surface melting and runoff from the same region of the Greenland ice sheet.

River discharge during the record warm summer of 2012 (6.8 km^3) exceeded that of 2010 (5.3 km^3) by 28%, even though there was only 3% more energy available for melt (Mikkelsen et al., 2016). The difference in discharge response can be explained by diminished firn retention. Runoff was further amplified by a sharp increase in the area contributing to

runoff as the runoff limit rose onto the ice sheet plateau in July 2012. Satellite imagery and photography (Figure 6.9) confirm the existence of a network of supraglacial rivers extending 140 km from the ice margin to an elevation of 1800 m. The extreme melting in 2012 produced flooding that washed out the Watson river bridge in Kangerlussuaq that was built in the 1950s (Figure 6.10).

6.4 Greenland ice sheet

Greenland land ice studies have proliferated since the previous SWIPA assessment (see Dahl-Jensen et al., 2011), producing many headline-grabbing findings about sea level change and impacts on the ocean thermohaline circulation. The number of citations in this assessment to research on Greenland is double that for all other regions. Greenland receives disproportionate attention perhaps because it dominates the contribution of Arctic land ice to sea level change, even though smaller glaciers and ice caps are melting faster (on a unit area basis) than the ice sheet.

The Greenland ice sheet mass balance, like that of other land ice bodies, represents the outcome of competing gains and losses. Gains are almost exclusively from net snow accumulation, although there is evidence of more rime deposition with warming. Losses are from meltwater runoff, iceberg calving, ice-ocean melting and evaporation/sublimation. The following review is organized by mass flux components, beginning with an assessment of the accumulation mass input, followed by the mass loss terms and assessments of net mass change. Subsequent sections document new or enhanced insights into key physical processes of ice-ocean interaction and ice sheet response to climate change. Greenland ice loss is becoming implicated in observed North Atlantic ocean circulation anomalies (Box 6.2).



Figure 6.9 Aerial oblique view on 12 August 2012 of meltwater channeling in the surface snow and firn of the southwestern Greenland ice sheet lower accumulation area at 1800 m elevation, made possible by the development of thick impermeable ice layers in successive previous high melt years.



Figure 6.10 Flooding washing out around the Watson river bridge foundations and over the Kangerlussuaq West Greenland water supply pipeline on 11 July 2012.

Box 6.2 Freshwater fluxes

Freshwater fluxes into the seas south of Greenland, including Canadian sources and snow-on-tundra sources, have accelerated by 50% ($6.3 \pm 0.5 \text{ km}^3/\text{yr}^2$) in less than 20 years (Bamber et al., 2012). For the Greenland ice sheet the rate of mass loss has accelerated. The cumulative freshwater anomaly for the period 1995–2010 is $3200 \pm 358 \text{ km}^3$, about a third of the magnitude of the Great Salinity Anomaly of the 1970s (Dickson et al. 1988; Curry and Mauritzen 2005). Rahmstorf et al. (2015) implicated this flux in a post- year 1900 slow-down of the Atlantic Meridional Overturning Circulation (AMOC) that appears to be unique in at least the past 1000 years. More than two-thirds of the increased freshwater discharged is being driven towards the Labrador Sea in ways that could lead to a weakening of the AMOC (Yang et al., 2016). The freshening seems to be associated with a conspicuous area of cooling sea surface temperatures (SSTs) in the sub-polar North Atlantic (Figure 6.11). An important question is whether the North Atlantic freshening affects Atlantic storminess (Woollings et al., 2012; Lehmann et al., 2014).

Evidence from the release of bottle tracers suggests freshwater recirculation in the North Atlantic could enable an accumulation of increasing amounts of freshwater in the seas north of the Gulf Stream (Ebbesmeyer et al., 2011). Proshutinsky et al. (2015) suggested that additional freshwater fluxes from Greenland land ice melt may be enough to suppress previously established Arctic decadal variability in overturning circulation.

A century-long record of Baffin Bay icebergs is provided by the International Ice Patrol's record of icebergs passing 48°N off Newfoundland (I48N). This dataset exhibits strong interannual variability, with a significant increase in amplitude over recent decades. Bigg et al. (2014) found

this variability is predominantly caused by fluctuations in calving discharge from the Greenland ice sheet. Episodes of high iceberg fluxes are linked with Greenland surface runoff and ocean temperature. They also found the recent increase to be mostly due to calving from west Greenland outlet glaciers.

Thus, Greenland land ice melting and accelerated iceberg discharge have been suggested to influence not only changes in sea level but also changes in North Atlantic thermohaline circulation. Downstream effects of this may be increased storm severity (Jackson et al., 2015) due to an increase in atmospheric baroclinic instability linked to a stronger horizontal temperature gradient between the record 'cold blob' and the (nearly average) warm sub-tropical North Atlantic (Hansen et al., 2016). Duchez et al. (2016) linked the North Atlantic 'cold blob' to the summer of 2015 European heatwave through positioning of the Jet Stream which favors the development of high surface air temperatures over Central Europe.

While measurements indicate increasing average precipitation over Europe (e.g. Denmark, Cappelen, 2015), the increased rainfall is also attributable to an increase in atmospheric moisture content (e.g. Utsumi et al., 2011) which has been attributed to anthropogenic climate change (e.g. Min et al., 2011). The role of atmospheric 'rivers' and a persistent negative NAO is fundamental (Lavers and Villarini, 2013). Meteorological agencies in Ireland and the UK have confirmed that winter (December to February) 2013–2014 set records for precipitation totals and the occurrence of extreme wind speeds (Matthews et al., 2014). Nevertheless, a direct connection between the 'cold blob' and regional weather and climate has yet to be firmly established.

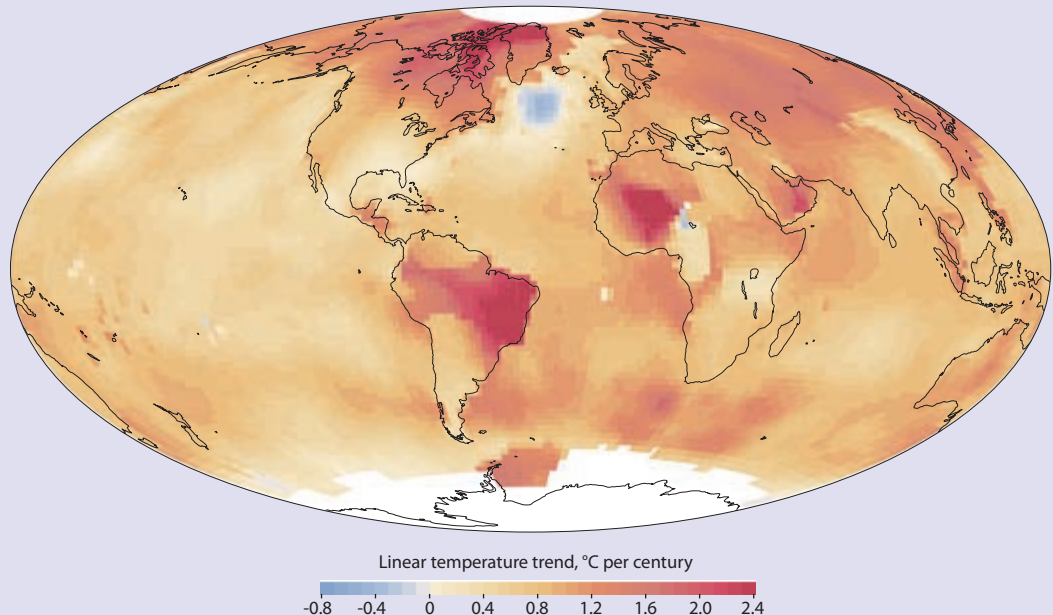


Figure 6.11 Linear trends in annual surface temperature since AD 1901 (after Rahmstorf et al., 2015).

6.4.1 Snowfall accumulation

Ice core and climate model-based accumulation reconstructions indicate substantial inter-decadal variability (Figure 6.12) that correlates with the NAO and with variations in northern hemisphere surface air temperature (Box et al., 2013). The minimum in accumulation in the 1960s, for example, is supported by numerous ice cores and early satellite data, and is largely NAO-driven (Burgess et al., 2010). A 3–20% increase in accumulation rate is evident since the end of the LIA around 1900 (Hanna et al., 2011; Box, 2013; Box et al., 2013; Mernild et al., 2015b). Comparison of Greenland accumulation history with northern hemisphere air temperatures suggests a 6.8% (or 51 Gt) per degree C climate sensitivity (Box et al., 2013). Climate change projections suggest a continuing increase in Greenland precipitation (Fettweis et al., 2013b) possibly promoted by warmer sea surface temperatures that produce stronger evaporation and increased moisture advection from lower latitudes. Rime deposition appears to be a significant mass input (10–20% of accumulation rate) at the highest elevations (Box and Steffen, 2001). For the Summit station, Cullen et al. (2014) found the water vapor flux to be only 2% of the annual accumulation rate, with the main net accumulation of water vapor in winter and net mass loss by sublimation in summer. It is unclear whether net frost deposition increases (Box et al., 2012) or decreases (Cullen et al., 2014) with warming. Box et al. (2012) found higher surface reflectivity in warmer summers.

The differences between reconstructions (Figure 6.12) suggest difficulty in producing an accurate absolute value for the accumulation rate, and trends in the NOAA 20th Century Reanalysis and the ERA-20C appear to be sensitive to data availability, which is limited before 1950.

6.4.2 Surface melting

Persistent anticyclonic circulation over central Greenland in the 2000s has contributed to a strong increase in ice sheet surface melting (Fettweis et al., 2011, 2013a,b; Box et al., 2012; Tedesco et al., 2013a, 2016b; Rajewicz and Marshall, 2014; McLeod and Mote 2016). The annual frequency of extreme high pressure ‘blocking event’ days that deliver warm air onto western Greenland peaked in 2010 and 2012 (McLeod and Mote, 2016), when there was a new record high melt-area extent (Tedesco et al., 2013b). On 11–12 July 2012, 98.6% of the ice sheet underwent surface melt, corresponding to a four-fold increase in the average melt extent at that time of year (Nghiem et al., 2012). The widespread melt in the accumulation area in July 2012 was enhanced by a strong greenhouse effect from low-level liquid clouds (Bennartz et al., 2013) that were promoted by the flow of anomalously warm ‘atmospheric rivers’ (moist air) over Greenland (Neff et al., 2014). Rainfall of 100 mm was observed at 1490 m above sea level on the inland ice of the northwestern ice sheet. During this period, infrared radiation from clouds comprised two-thirds of the surface melt energy for three days (10–12 July 2012; Niwano et al., 2015). For the southern and western ice sheet, Fausto et al. (2016) found advection of sensible and latent heat to be the dominant sources of melt energy during these short-lived melt episodes, and reported the largest observed daily ablation rate of 28 cm ice on 10 July 2012. Together, atmospheric sensible and latent heat delivered

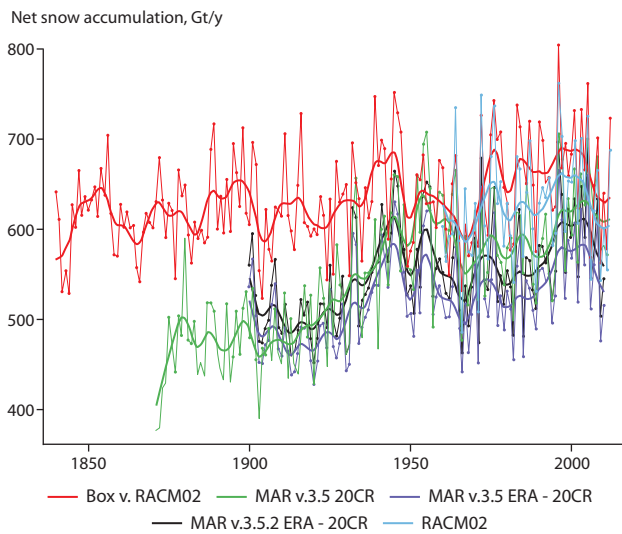


Figure 6.12 Greenland net snow accumulation after Box et al. (2013) based on a statistical reconstruction from 123 ice cores versus the RACMO2.1 model. Also shown is the result from the MAR regional climate model driven by the NOAA 20th Century Reanalysis (Compo et al., 2011) and the ECMWF ERA-20C (Fettweis et al., 2016).

more energy to the lower elevations of the ice sheet than absorbed sunlight during melting episodes linked to the occurrence of atmospheric rivers in July and August 2012 (Fausto et al., 2016). Rainfall events are linked to glacier speedup (Doyle et al., 2015). Furthermore, climate models under-represent the turbulent fluxes of sensible and latent heat by a factor of two, important to address given that the frequency of warmer air masses driven over Greenland is expected to increase with climate change (Collins et al., 2013).

Deposition of black carbon from wildfires also promoted melt through enhanced sunlight absorption (Keegan et al., 2014). Projections suggest that such melt episodes will become increasingly frequent in the coming decades (McGrath et al., 2013). The atmospheric circulation responsible for the extraordinary melt in Greenland in 2012 also caused record melting on Canadian Arctic glaciers and ice caps (e.g. Jeffries et al., 2013). A root cause involves how decreasing Arctic sea ice favors stronger and more frequent occurrences of blocking-high pressure events over Greenland (Liu et al., 2016). Tedesco et al. (2016b) provided evidence of a northward shift in the northern hemisphere jet stream that, together with persistent surface high pressure, promoted extreme melting in northern Greenland.

On average, Greenland clouds enhance meltwater runoff by about a third relative to clear skies because they induce surface heating that limits the refreezing of meltwater (van Tricht et al., 2016).

Climate warming drives many surface darkening processes that increase surface melt of land ice. Increasing snow ablation prolongs the period when darker bare ice is exposed at the surface in summer (Fettweis et al., 2011; Tedesco et al., 2011; Box et al., 2012; van As et al., 2012, 2013). Ice surface microbial communities enhance surface melting due to production of dark UV-shielding pigments (Stibal et al., 2012; Benning et al., 2014; Lutz et al., 2014; Chandler et al., 2015). Snow grain metamorphism (Tedesco et al., 2016a) and changing snow wetness (Charalampidis et al., 2015) also darken snow. An increase in weather conditions conducive

to fire in northern Alaskan, Canadian, and Eurasian regions in the period 1996–2003 (Jolly et al., 2015) reinforces the importance of wildfire-derived black carbon deposition in enhancing Greenland ice melt (Keegan et al., 2014). Projections to 2100 suggest that both air temperatures and fire frequency will increase, such that widespread melt events may become a near-annual occurrence by 2100 (Keegan et al., 2014).

Remotely sensed data, regional climate model simulations, and *in situ* measurements all demonstrate that the ice sheet ablation area albedo decreased at a rate of 0.03–0.06 per decade in the period 2000–2013 (Alexander et al., 2014). Other studies document Greenland darkening (e.g. He et al., 2013; Tedesco et al., 2013a; Dumont et al., 2014), although NASA MODIS Terra sensor degradation contributes to the darkening signal across the northern ice sheet dry snow area (Polashenski et al., 2015). Ground observations from the Greenland Climate Network (Steffen et al., 1996; Box et al., 2012) indicate darkening trends for the southern half of the ice sheet that equal or exceed the satellite-derived trend, showing that some of the darkening is real, but that it may be overestimated by as much as 50% in MODIS data for northern Greenland.

6.4.3 Surface mass balance

Surface climatic mass balance (also known as ‘surface mass balance’, SMB), is the difference between mass gains from net snow accumulation and the sum of mass losses from meltwater runoff, evaporation, and sublimation. Greenland mass loss accelerated between 2003 and 2012 primarily due to increasing surface meltwater runoff ($-6.3 \pm 1.1 \text{ Gt/y}^2$) driven by persistent southerly flow across the western ice sheet (e.g. Rajewicz and Marshall, 2014; McLeod and Mote, 2016) but also as a result of reduced precipitation (Seo et al., 2015). Atmospheric circulation change is closely linked with variance in SMB data (Chen et al., 2015). The recent strong increase in surface melting produced negative surface mass balance along the southwestern ice sheet (van As et al., 2014). The reduced precipitation, like the increased warm air advection and clear sky conditions (Box et al., 2012) between 2003 and 2012 is attributed to NAO-related changes in atmospheric circulation that promoted clear sky conditions over the ice sheet’s upper elevations.

Average summer temperatures on the ice sheet have increased by 1.7°C since 1840, resulting in a 59% increase in surface melt water production (Box, 2013). The concurrent increase in Greenland ice sheet snow accumulation is estimated to be 6.8% per $^\circ\text{C}$ increase in northern hemisphere mean annual air temperature (Box et al., 2013). In terms of SMB, the snowfall increase is more than offset by the increase in surface melting and runoff. The amount of meltwater retained by percolation and refreezing, which delays the response of ice sheet mass balance and sea level to warming (Harper et al., 2012) remains a dominant source of uncertainty in SMB models (Reijmer et al., 2012; Vernon et al., 2013). A higher resolution land/ice/ocean map of the Greenland region (Citterio and Ahlström, 2013) has been published, which better constrains ice sheet area (Kargel et al., 2012). Because surface mass fluxes are largest near the ice/land or ice/ocean boundaries, a comparison of SMB models indicates that common land/sea/ice masks are a prerequisite to reconciling differences among various model-derived estimates (Vernon et al., 2013).

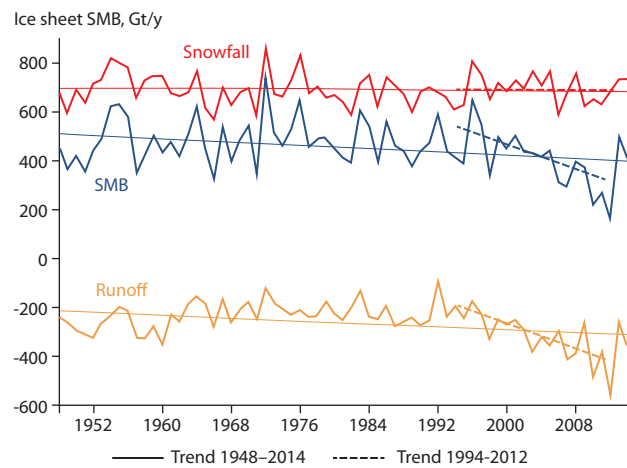


Figure 6.13 Time series of the total Greenland ice sheet surface mass balance (SMB), consisting of the balance between mass inputs from snowfall and mass loss from meltwater runoff, simulated by MARv3.5.2 forced by NCEP–NCARv1 over the period 1948–2014 (Fettweis, University of Liège, Belgium).

Conditions returned to a more positive SMB in 2013 due to reduced melting following a switch to northerly (cold) air flow over western Greenland where most surface melting occurs (Tedesco et al., 2014). Surface melting during summer (June–August) 2013 was near the long-term average for the period 1981–2010. The 2013 and 2015 reduction in surface melting over the southwestern sector of the ice sheet (Tedesco et al., 2015) impacted the total mass budget by ending a six-year period of decreasing SMB (Figure 6.13).

6.4.4 Total ice sheet mass balance

Greenland ice sheet mass balance estimates from multiple independent data sets have for the first time been reconciled (Shepherd et al., 2012), revealing smaller uncertainties than had been reported previously. Ice loss increased from near balance ($51 \pm 65 \text{ Gt/y}$) for the period 1992–2000 to $263 \pm 30 \text{ Gt/y}$ for 2005–2010. An acceleration in ice loss is evident (Rignot et al., 2011). Ice sheet mass loss increased yet further to $375 \pm 30 \text{ Gt/y}$ between 2011 and 2014 (Helm et al., 2014).

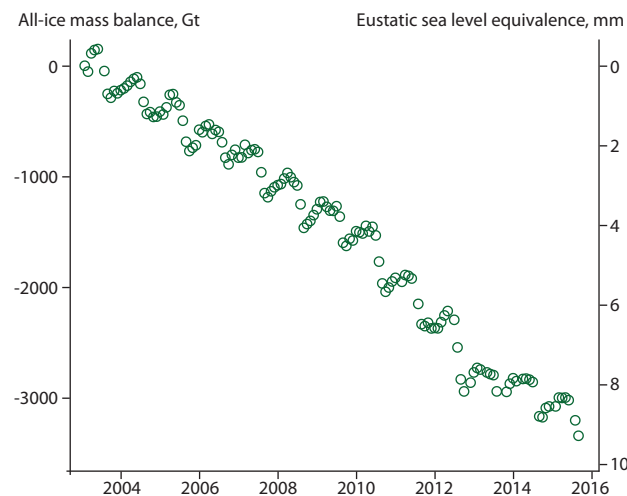


Figure 6.14 Greenland all-ice total ice mass balance from June 2003 to August 2015 according to satellite gravity measurements (after Barletta et al., 2013).

Annual iceberg discharge estimates of Rignot et al. (2011) and Enderlin et al. (2014) provide more complete time-series for constraining the mass budget of the Greenland ice sheet. Dynamical ice flow discharge and SMB were roughly equal contributors to the total mass loss until 2009 after which SMB accounted for about two-thirds of ice loss (Enderlin et al., 2014; Andersen et al., 2015) due to a sharp increase in surface melting. For the period 2007–2011, the total mass balance was -262 ± 21 Gt/y, of which 61% was due to a negative SMB (Andersen et al., 2015).

The period of high mass losses and apparent acceleration of mass loss from Greenland was interrupted in 2013–2014 according to GRACE data (Barletta et al., 2013) (Figure 6.14). In summer 2015, mass loss rates increased again to values similar to those experienced between 2007 and 2012. The pause was linked to increased northerly (cold) atmospheric flow (Tedesco et al., 2013b) (see Figure 6.2).

Regionally, GRACE data demonstrate that Greenland ice loss was concentrated in the southeast and northwest in the 2003–2013 period. The loss is attributed mostly to ice dynamics (Velicogna et al., 2014). The area of negative mass balance spread to the northwest ice sheet margin from the southeast (Khan et al., 2010). Incorporation of higher resolution NASA airborne laser altimetry data from the Land, Vegetation, and Ice Sensor (LVIS) and Airborne Topographic Mapper (ATM) reveals 11% more mass loss from the northwestern sector of the ice sheet than was estimated using ICESat data alone. This shows the importance of incorporating data with high spatial density near the ice sheet margin where the changes are largest (Kjeldsen et al., 2013). Greenland peripheral glaciers, covering 5% of the island's total ice area, are responsible for 14–20% of the mass loss from Greenland as a whole (Bolch et al., 2013) (Figure 6.15).

In the southwest, reductions in SMB explain over half of the acceleration in ice loss (Velicogna et al., 2014). Khan et al. (2014b) found that mass loss from the northeastern Greenland ice stream (NEGIS) catchment increased substantially

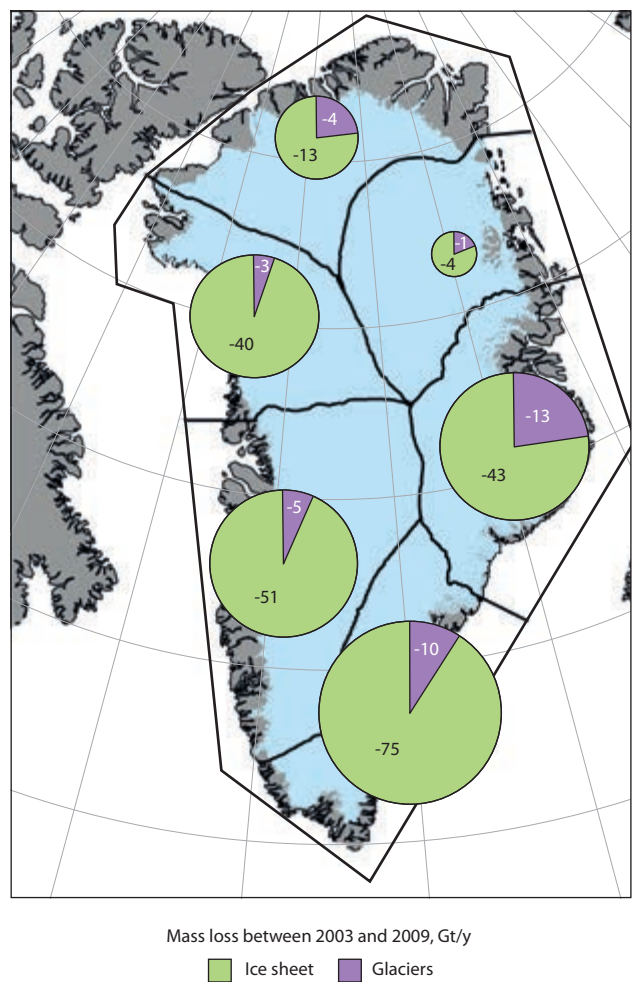


Figure 6.15 Rates of change in the mass of the Greenland Ice Sheet and its surrounding glaciers from 2003 to 2009, based on data from Zwally et al. (2011), Bolch et al. (2013), Gardner et al. (2013), and Colgan et al. (2015b).

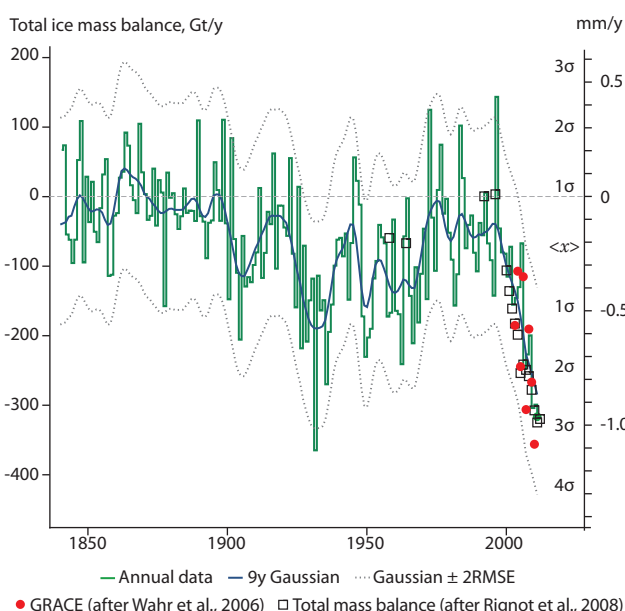


Figure 6.16 Greenland ice sheet total mass balance (after Box and Colgan 2013 and Kjeldsen et al., 2015), derived by modelling ice discharge as a function of runoff and ice discharge (data from Rignot et al., 2008 and Enderlin et al., 2014). The correspondence with GRACE satellite-based Greenland ice mass change estimates is also shown.

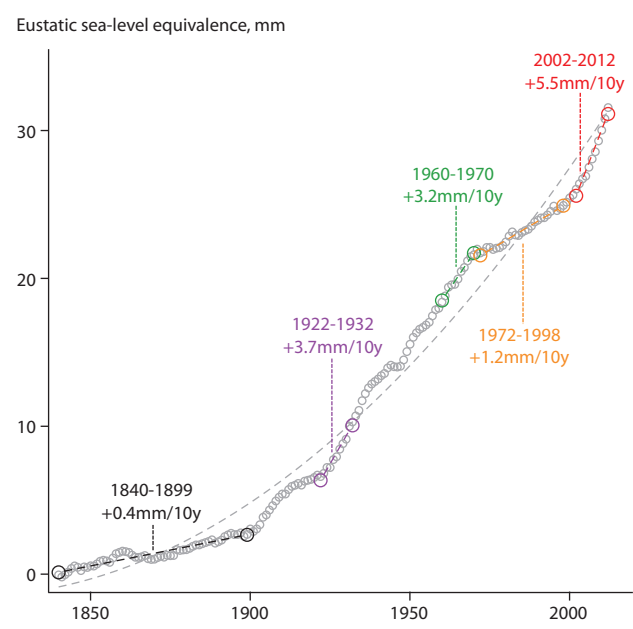


Figure 6.17 Cumulative Greenland ice sheet contribution to global mean sea level for the period 1840–2012; the dashed line indicates acceleration of loss from climate warming (after Box and Colgan, 2013).

after 2006 and attributed this to changes in ice dynamics. Mouginot et al. (2015) also reported a dynamically driven acceleration in mass loss from Zachariae Ice Stream. Between 2003 and 2007, Greenland gained mass in the interior and thinned rapidly at the margins (Zwally et al., 2011) with high interior firn thickening by 1–5 cm/y between 1980 and 2014 (Kuipers Munneke et al., 2015). The total Greenland volume change due to firn and SMB changes between 1980 and 2014 was estimated at $-3295 \pm 1030 \text{ km}^3$, corresponding to an ice-sheet average thinning of $1.96 \pm 0.61 \text{ m}$ (Kuipers Munneke et al., 2015). Since 1995, thinning has intensified and spread across the entire coastal margin. High elevation thickening results from a positive accumulation anomaly relative to the 1961–1990 baseline but also from millennial-scale ice dynamics that favor thickening (Colgan et al., 2015a).

The total mass loss from Greenland reached a record value during June, July, and August 2012 ($-627 \pm 89 \text{ Gt}$) (Tedesco et al., 2013b). This was probably the highest summer mass loss in the period since 1840, which includes the end of the LIA (Box and Colgan, 2013; Kjeldsen et al., 2015) (Figure 6.16).

For the Jakobshavn Isbræ in central western Greenland, Csatho et al. (2008) found balance or advance prior to 1900 and a re-advance as recently as the early 1980s. Since the end of the LIA, the Greenland sea level contribution has exceeded 3.1 cm (Figure 6.17). The estimate suggests a $16 \pm 75 \text{ Gt/y}$ end of LIA (1840–1899) net ice loss increasing to $201 \pm 68 \text{ Gt/y}$ for the period 2002–2012. Short term variations of this type resulting from the 1991–1992 Mt. Pinatubo cooling (e.g. Fettweis et al., 2011) (see Figure 6.13) or the 1965–1970 accumulation low (Burgess et al., 2010) (see Figure 6.17) do not seem to influence the (smoothed) cumulative sea level effect.

While the end of the LIA is apparent from inflections in the reconstructed SMB and total mass balance (Box, 2013; Box and Colgan, 2013), new evidence has emerged of regional variations in its timing. For Kangiata Nunaata Sermia in southwestern Greenland, an LIA maximum extent in 1761 is evident. This was followed by a 5 km retreat by 1808 and a further retreat of 7 km by 1859. This pre-dated the retreat of Jakobshavn Isbræ (Csatho et al., 2008) by at least 43 years (Lea et al., 2014a). Weidick et al. (2012) reported rapid recession of Kangiata Nunaata Sermia in the first half of the 1800s. The first observed retreat of Jakobshavn Isbræ was between 1851 and 1875 (Weidick and Bennike, 2007; Csatho et al., 2008). Andresen et al. (2014) identified some retreat of the Upernivik ice shelf between 1849 and 1886. The contrasting behavior demonstrates the risk of using dated maximum terminus positions from individual tidewater glaciers as indicators of a regional LIA maximum (Lea et al., 2014a). Noting local variability, Kjeldsen et al. (2015) used 1900 as an average date for Greenland-wide LIA termination.

6.4.5 Floating ice area losses

With few exceptions, marine-terminating outlets of the Greenland ice sheet have been retreating. Box and Hansen (2015) surveyed 45 of the widest Greenland glaciers, which between 1999 and 2015 collectively lost an area of 1799 km^2 (Figure 6.18). In August 2010, the longest ice shelf connected to the Greenland ice sheet at Petermann Glacier (also then the Arctic's largest ice shelf) calved 245 km^2 (Falkner et al.,

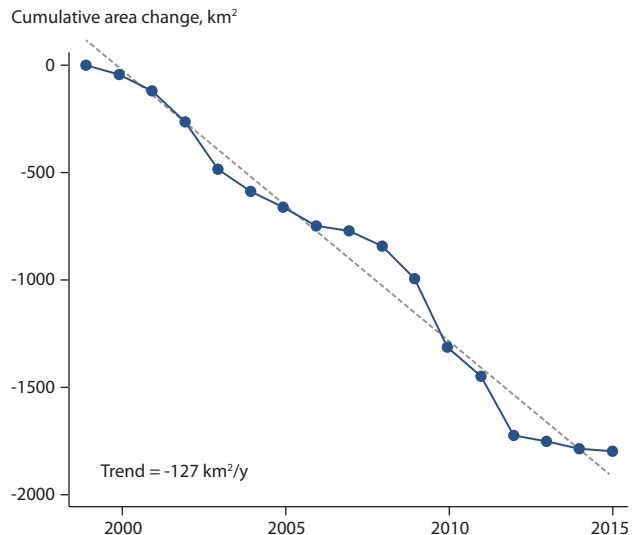


Figure 6.18 Cumulative area change of 45 among the widest Greenland tidewater glaciers (after Jensen et al., 2016 and Box and Hansen, 2015).

2011; Jensen et al., 2016) (Figure 6.19). The Petermann ice shelf disintegration continued with a 140 km^2 calving event in 2012 (Jensen et al., 2016). The largest and most consistent (year-to-year) changes in Greenland glacier area are concentrated in the north of the island (Box and Decker, 2011; Howat and Eddy, 2011). The largest Greenland and Arctic ice shelf is now at the front of the North East Greenland Ice Stream.

Summer air temperature records at all 11 Danish Meteorological Institute stations around Greenland are correlated with glacier front area change: in warm summers, more ice area is lost. At four of the 11 sites, the confidence in that correlation is $>95\%$. At seven of the 11 sites, the confidence is $>80\%$ (Box and Hansen, 2015). The physical mechanism at work is thought to be hydrofracture; namely, that (because water is denser than ice) the weight of water filling an open fracture or void in the ice would be greater than the weight of ice that would fill the same volume. Thus

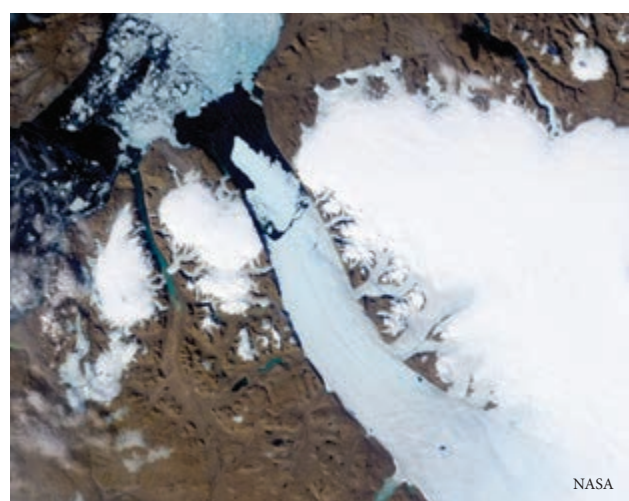


Figure 6.19 The massive (245 km^2) summer 2010 calving event at the floating Petermann Glacier ice shelf in northwestern Greenland (see Figure 6.22 for location).

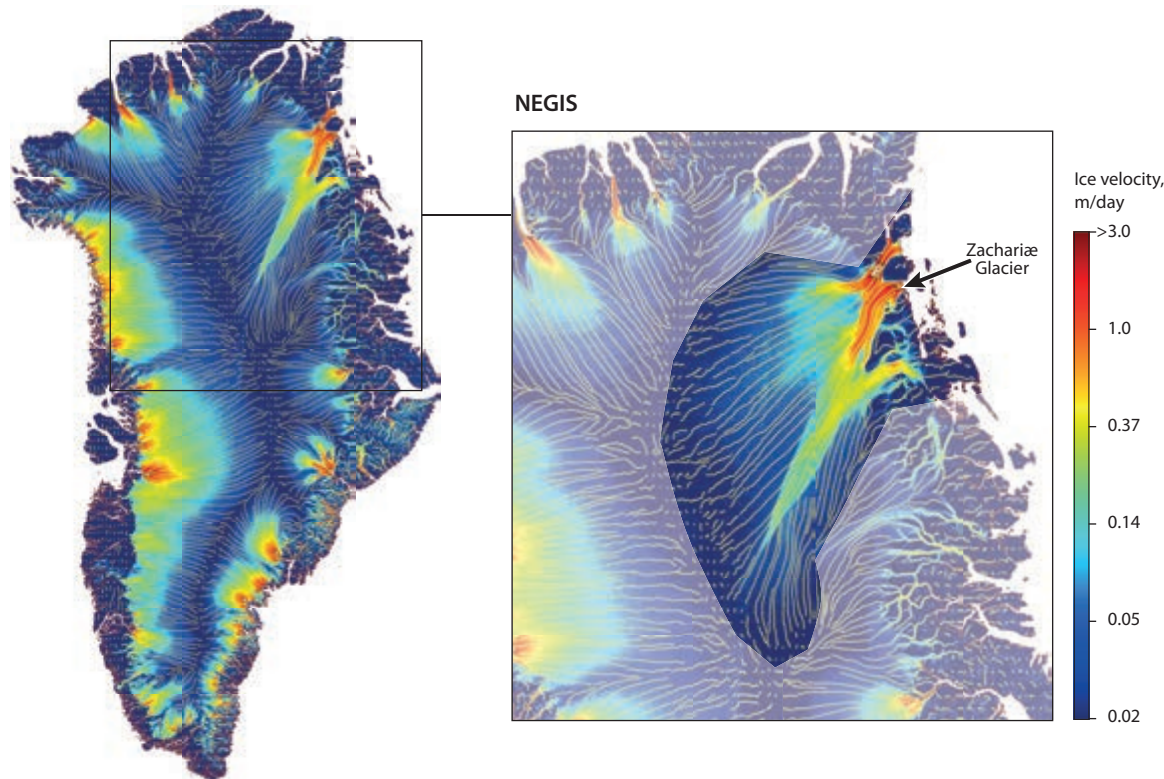


Figure 6.20 Ice velocity map (magnitude, in logarithmic scale) of the Greenland ice sheet derived from SAR data of the EU Copernicus Sentinel-1A satellite, plus an inset showing the Northeastern Greenland ice stream (NEGIS) ice velocity, merging data acquired from 15 October 2014 to 15 October 2016 (data visualization by M. Hermann after Nagler et al., 2015).

a water-filled void creates a stress concentration at the base of the fracture that might cause the fracture to propagate downwards, and possibly reach the base of the glacier, allowing an iceberg to break off if the fracture is extensive enough (e.g. Weertman, 1973; van der Veen, 1998).

6.4.6 The Northeastern Greenland ice stream

The northeastern Greenland ice stream (NEGIS) is the sole Greenlandic ice stream that extends into the deep interior of the ice sheet (Figure 6.20). Fast flow is initiated near the ice divide over a localized area of high geothermal heat flux where the bed comprises water-saturated till (Christianson et al., 2014). The ice stream terminates 1000 km downstream in three large marine-terminating glaciers. At the time of the previous SWIPA assessment (see Dahl-Jensen et al., 2011), studies of NEGIS were limited to a handful of pioneering works (Fahnestock et al., 1993, 2001; Joughin et al., 2000, 2001). NEGIS has now entered a faster flow regime with dynamic thinning in response to ocean warming and sea ice decline (Khan et al., 2014b). Acceleration has extended more than 30 km inland from the NEGIS Zachariæ Glacier grounding line (Mouginot et al., 2015). NEGIS is likely to continue to be drawn down because future retreat will be into areas of the ice sheet bed that lie further below sea level. Because numerical models of ice flux from the ice stream are very sensitive to basal drag (Schlegel et al., 2015), it is hard to precisely predict the future behavior of NEGIS and other Greenland glaciers. The site is to become the focus of a deep ice core drilling program (Vallelonga et al., 2014) that will ensure NEGIS receives more attention.

6.4.7 Ice sheet surface melt water lakes

The distribution of supraglacial lakes on the Greenland ice sheet has extended further inland in response to recent climate warming (Fitzpatrick et al., 2014) and has been predicted to extend to an elevation of 2000 m above sea level under projected warming to 2100 (Leeson et al., 2015). Both studies showed the inland expansion of lakes to be strongly correlated with air temperature increase. During the record melt years of 2010 and 2012, lakes formed and drained earlier, attaining their maximum volume 38 and 20 days earlier than the 11-year average respectively, as well as occupying a greater area and forming at higher elevations (>1800 m) than previously. Despite occupying <2% of the study area, lakes delay runoff by as much as 7–13%. Roughly one third of lakes drain rapidly (<4 days). Clustering of drainage events in space and time suggests a trigger mechanism that is dynamically driven by basal slip (Stevens et al., 2015). The majority of fast lake drainages occur in the southwestern sector of the ice sheet, and fewer are observed in regions with the highest rates of dynamic mass loss (Selmes et al., 2011). The lakes absorb more solar radiation than the ice surface causing a 10–35% increase in ice surface ablation rates relative to surrounding bare ice areas (Tedesco et al., 2012), which is likely to enhance the development of lake basins on the ice surface. Rapid lake drainage occurs in a few hours (Doyle et al., 2013), producing kilometer-long fractures that may trigger further localized lake drainage (Fitzpatrick et al., 2014). Lakes that do not drain can fill and overflow into surface drainage networks that often drain into the ice via fractures, forming so-called moulin. Full lakes can become snow covered and freeze solid over winter. The

freeze-up process may pressurize water in lake bed fractures leading to drainage. Lake water may remain fluid well into the winter while the surface is snow covered.

6.4.8 Internal ice sheet structure

The first comprehensive detailed radar stratigraphy of the Greenland ice sheet was presented by MacGregor et al. (2015). Airborne radar data spanning the 1993–2013 period reveal the ice sheet's regional age structure. Disruption of the otherwise horizontal planar ice structure is evident in several regions where faster flow occurs today or has occurred in the past. Localized basal heating from meltwater infiltration to the bed and consequent changes in ice viscosity (see Box 6.3) are implicated in regional ice-layer deformation patterns (Bell et al., 2014).

Box 6.3 Englacial water and 'thermal collapse'

The additional latent heat entering the ice sheet, associated with the ~50% increase in surface meltwater production over the past two decades (e.g. Box, 2013), is likely to have warmed peripheral areas of the ice sheet, including both land-terminating sectors and marine-terminating outlet glaciers, thereby reducing their viscosity (Phillips et al., 2010, 2013; van der Veen et al., 2011; Lampkin et al., 2013; Lüthi et al., 2015). Looking forward, it is plausible that within four centuries the latent heat associated with refreezing a small fraction of anticipated future surface meltwater production could warm to the pressure melting point the deepest 15% of the ice sheet where the majority of shear deformation occurs. Within five centuries of initiating such a thermal-viscous collapse, modeling by Colgan et al. (2015c) suggests an ice sheet volume decrease of $5\pm2\%$, equivalent to a sea level rise contribution of 330 ± 180 mm. The majority of associated mass wastage would be realized over subsequent millennia. While plausible, no data exist to accurately assess decadal temperature changes within the deepest layers of the ice sheet, and no attempts have been made to assess the likelihood of recent climate change initiating thermal-viscous collapse.



Figure 6.21 Surface meltwater draining into the Greenland ice sheet.

6.4.8.1 Refined Greenland subglacial mapping

The level of detail in subglacial topographic mapping has increased through the compilation of a growing set of ice sounding radar data (Bamber et al., 2013a) and the use of mass-conserving ice flow models to reconstruct bed topographies that are consistent with measured patterns of ice thickness and surface flow velocity (Morlighem et al., 2014) (Figure 6.22). The increased resolution of these bed reconstructions reveals more glacier troughs in which the bed remains below sea level tens of kilometers further inland than was previously thought. Bamber et al. (2013b) documented the existence of a 750-km-long, subglacial canyon beneath the central northern sector of the ice sheet that may have affected subglacial water flow and ice dynamics during past glacial cycles.

6.4.8.2 Subglacial till and sediment

Booth et al. (2012) identified a water-saturated deformable till layer <2 m thick at the bed of the Russell Glacier in western Greenland (~70 km inland of its western margin where the ice is 1.1 km thick) during summer 2010. The deformable layer was stratified and overlay a lodged till unit. Dow et al. (2013) used seismic reflection experiments to reveal extensive saturated sediments underlying Russell Glacier, and Bougamont et al. (2014) used these data to constrain a 3D higher order flow model including a deforming bed, to show that this sector of the ice sheet is dynamically vulnerable to an increase in the intensity and frequency of melt events, such as would be expected under a warmer future climate.

6.4.8.3 Meltwater storage

Both the hydrological budget and the timing of runoff relative to melt onset indicate some water storage in the ablation area of the southwestern ice sheet (Rennermalm et al., 2013; Smith et al., 2015). Eruptions of sediment-laden water were visible at the fjord surface after the cessation of summer runoff at a major western Greenland glacier, and are likely to be indicative of drainage from subglacial meltwater reservoirs (Schild et al., 2016).

6.4.8.4 Subglacial lakes

Thousands of small but distinct subglacial lakes have been predicted to exist under the Greenland ice sheet (Livingstone et al., 2013; Lindbäck et al., 2015), but these features and their drainage have only been observed since the previous SWIPA assessment (see Dahl-Jensen et al., 2011). Airborne radio echo-sounding measurements provide the first clear evidence for the existence of subglacial lakes in Greenland (Palmer et al., 2013). Palmer et al. (2015) reported observations of one lake fed by surface meltwater that enters the ice sheet via a nearby moulin, and drainage of that water from the ice margin via a subglacial tunnel. In an earlier paper, Howat et al. (2015) mapped the footprint of the same subglacial lake as revealed by a 2 km wide, 70 m deep circular depression located 50 km inland of the southwestern margin of the ice sheet. This provides the first direct evidence for concentrated, long-term storage, and sudden release of meltwater at the bed. The abundance of such lakes and their potential importance to the

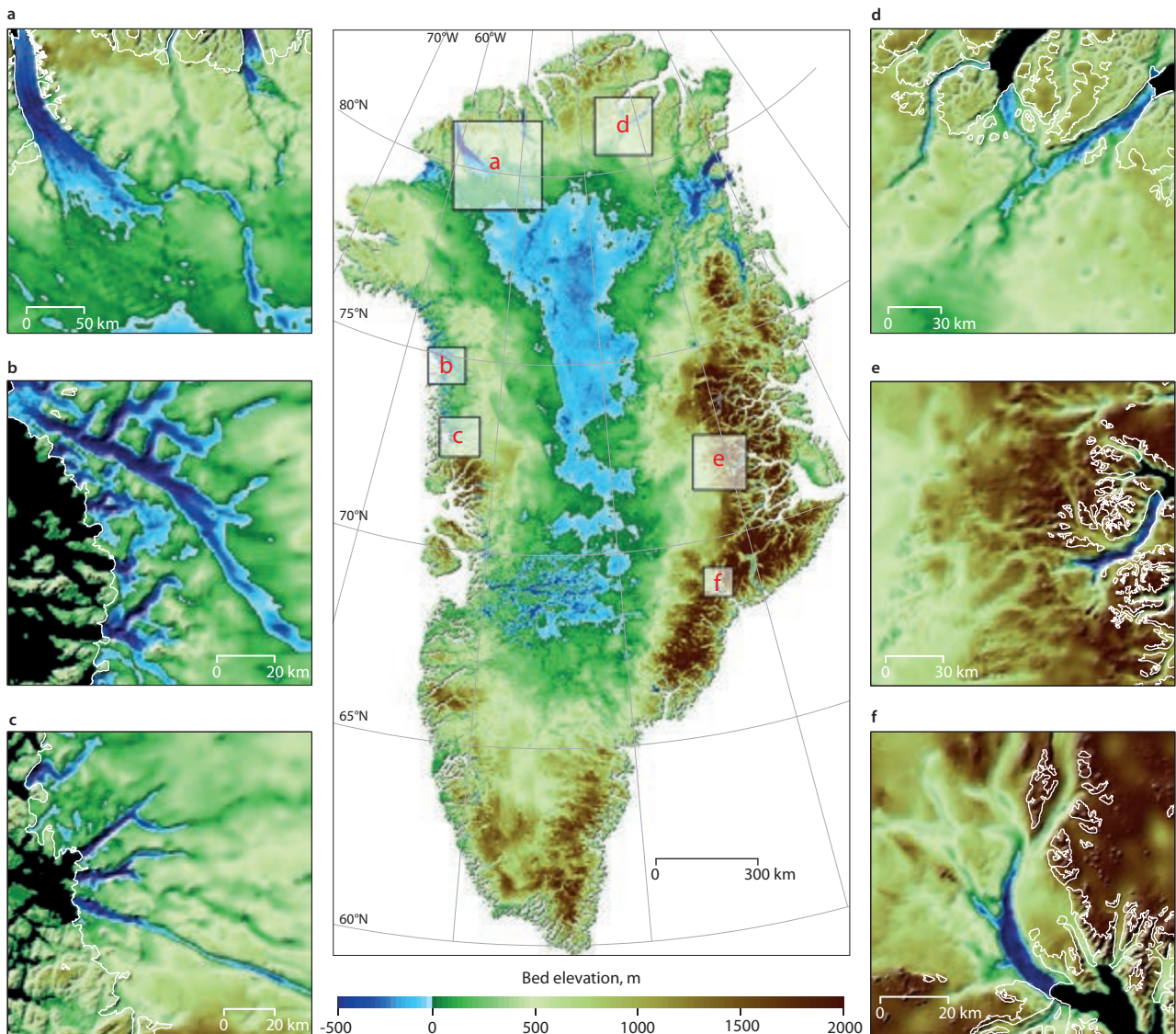


Figure 6.22 Bed elevation of the Greenland ice sheet color-coded up to 2000 m, with submarine areas in blue. Details of the large-scale map for (a) Petermann, Steensby and Ryder Gletscher, (b) Hayes Gletscher, Allison Gletscher and Illulip Sermia, (c) Upernivik Isstrøm and Nunatakassaaq Sermia, (d) Marie Sophie Gletscher, Academy Gletscher and Hagen Bræ, (e) F. Graae, Charcot and Daugaard-Jensen, and (f) Kangerlussuaq Gletscher; glaciers within each of the six categories are listed in clockwise order. The white contour line delineates the limit of land ice. The mass conservation method is employed for the glaciers. Kriging is used to map the interior regions (after Morlighem et al., 2014).

ice sheet's hydrologic system and flow regime remain unknown. Runoff increased over the past decade, with anomalously high melting in 2010 (Van As et al., 2012), which would likely increase subglacial discharge and promote expansion of efficient drainage, potentially triggering drainage of the subglacial reservoir. Both Howat et al. (2015) and Palmer et al. (2015) showed that subglacial drainage of stored water does induce a marked but temporally-limited dynamic response.

Lake drainage events may occur more commonly if surface melting increases in future. Lindbäck et al. (2015) presented a high (150 m) resolution subglacial map covering a 12,000 km² sector of the southwestern ice sheet indicating the probable existence of small subglacial lakes undetectable by surface elevation changes or airborne radar. Their analysis suggests the switching of drainage between competing subglacial catchments driven by seasonal changes in basal hydraulic potential gradients.

6.4.8.5 Subglacial water and ice sheet dynamics

Englacial and subglacial water, its transit, heat transfer to ice, lubricating effect on glacier flow, and subglacial storage have received much attention since the previous SWIPA assessment (see Dahl-Jensen et al., 2011). The work now debates the extent to which lubricating effects are self-regulating as infiltration of surface melt water into englacial and subglacial environments increases.

GPS and surface climate measurements in western Greenland by Bartholomew et al. (2011a,b) confirm an annual cycle in ice flow coupled to surface meltwater production and transport into the subglacial drainage system (Zwally et al., 2002). The observed acceleration decreases as the melt season progresses, indicating the development of an efficient, lower pressure subglacial drainage network (Hofmann, et al., 2011; van de Wal et al., 2015). While this self-regulation is now firmly demonstrated (Sundal et al., 2011; Shannon et al., 2013;

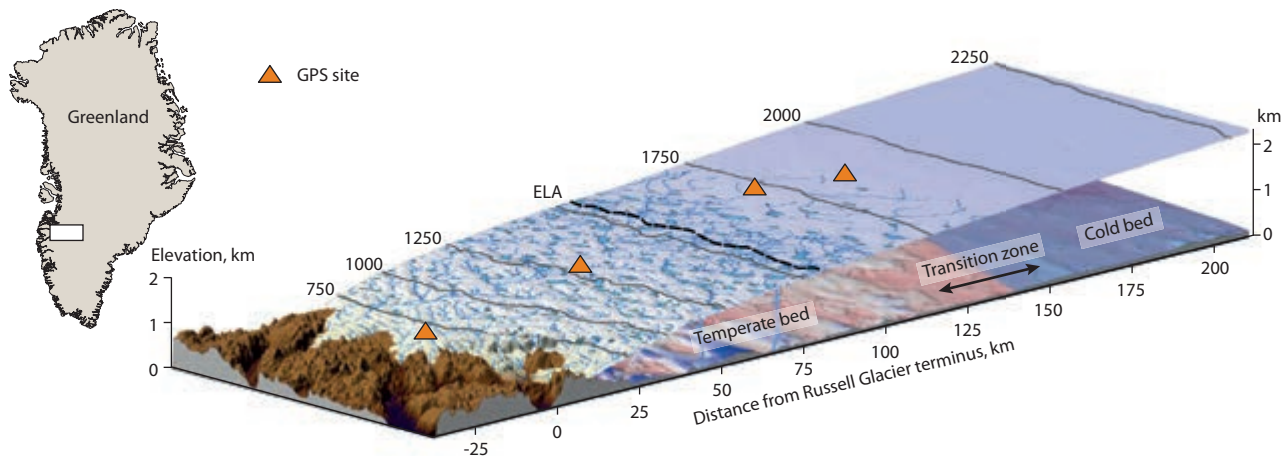


Figure 6.23 Cross-section of the Russell Glacier catchment showing the locations of GPS sites relative to the mean 1990–2011 equilibrium line altitude (ELA) of 1553 m above sea level (after Doyle et al., 2014).

Sole et al., 2013; Tedstone et al., 2015), it has not been observed more than 40 km inland from the ice sheet margin. Subglacial routing plays an important role in shaping the magnitude and extent of seasonal ice sheet acceleration (Palmer et al., 2011) and the basal drainage network is thought to reset annually after the end of each melt season as formerly flooded subglacial tunnels collapse under ice overburden pressure. Yet, the mechanical effect of basal sediment deformation has yet to be unified with the effects of changing basal pressurization from ephemeral meltwater conduits in ice. Bougamont et al. (2014) used modeling to demonstrate a seasonal weakening and strengthening of subglacial sediments, associated with variations in the delivery of surface meltwater to the bed and proposed that ice flow variability linked to changes in subglacial sediment strength is a viable alternative to existing models that link ice flow variability to subglacial drainage system evolution.

Further inland, where thicker ice and lower surface melt rates occur, persistent ice flow acceleration has been observed in winter and summer at and above the equilibrium line altitude, and up to 140 km from the ice margin (Doyle et al., 2014). The underlying cause appears to be upstream migration of a distributed subglacial drainage along with the potential viscous warming and decoupling of a previously frozen bed (Figure 6.23). The area over which such meltwater penetration occurs appears likely to increase under future climate scenarios (Clason et al., 2015). Poinar et al. (2015) countered that even with enhanced surface melt production, meltwater is unlikely to reach the basal environment in the interior of the ice sheet due to low surface strain rates that preclude the formation and propagation of fractures and crevasses. Improved understanding of these processes is therefore imperative to understanding future ice sheet response to a warming climate.

6.4.9 Sea level contribution

Since 1972, the majority (>60%) of observed sea level rise has been due to global glacier and ice sheet contributions, with thermal expansion of ocean water a secondary driver, and increasing human impoundment of water on land in reservoirs roughly canceling the effects of groundwater extraction

(Gregory et al., 2013; Moore et al., 2013). Using a reconciled combination of land ice mass balance estimates from a variety of mostly satellite-based techniques, Shepherd et al. (2012) estimated 0.39 ± 0.14 mm/y of sea level equivalence over the period 1992–2011, increasing to 0.73 ± 0.08 mm/y between 2005 and 2010. Reconciled estimates of local glacier mass loss suggest -259 ± 28 Gt/y between 2003 and 2009, equivalent to $+0.71 \pm 0.08$ mm/y sea level equivalence (Gardner et al., 2013). For the 2004–2010 period, two-thirds of global land ice loss occurred in the Arctic region (Shepherd et al., 2012; Gardner et al., 2013). In its fifth assessment (AR5), the Intergovernmental Panel on Climate Change (IPCC) estimated the Greenland land ice sea level rise contribution on the basis of the average of 18 recent studies for the same period to be 0.34 ± 0.07 mm/y of sea level equivalence (Vaughan et al., 2013). The sea level rise contribution from Greenland has clearly accelerated since 1992: 0.09 (0.02–0.20) mm/y sea level equivalence for the period 1992–2001 to 0.59 (0.43–0.76) mm/y sea level equivalence for the period 2002–2011.

Land ice mass loss leads to solid earth rebound (Bevis et al., 2012) and modifies the global pattern of sea level rise given that ice mass exerts a gravitational influence on its surroundings, including the ocean (Bamber and Riva, 2010). Consequently, the unloading of land masses due to glacier and ice-sheet shrinkage reduces rates of sea level rise locally while increasing effective ‘relative sea level’ further afield. Thus, Arctic land ice change has more influence on sea level in the southern hemisphere and Antarctic land ice change has more impact on sea level in the northern hemisphere (Figure 6.24).

6.5 Projected mass changes

In preparation for the IPCC AR5, increased and coordinated efforts developed regional glacier mass (and sea level contribution) projections that estimate the land ice response to various climate change scenarios. Reporting in this assessment (see Chapter 9) is based on four studies while the previous SWIPA assessment (see Sharp et al., 2011a) was based on one. See Chapter 9 for SWIPA 2017 projections of sea level.

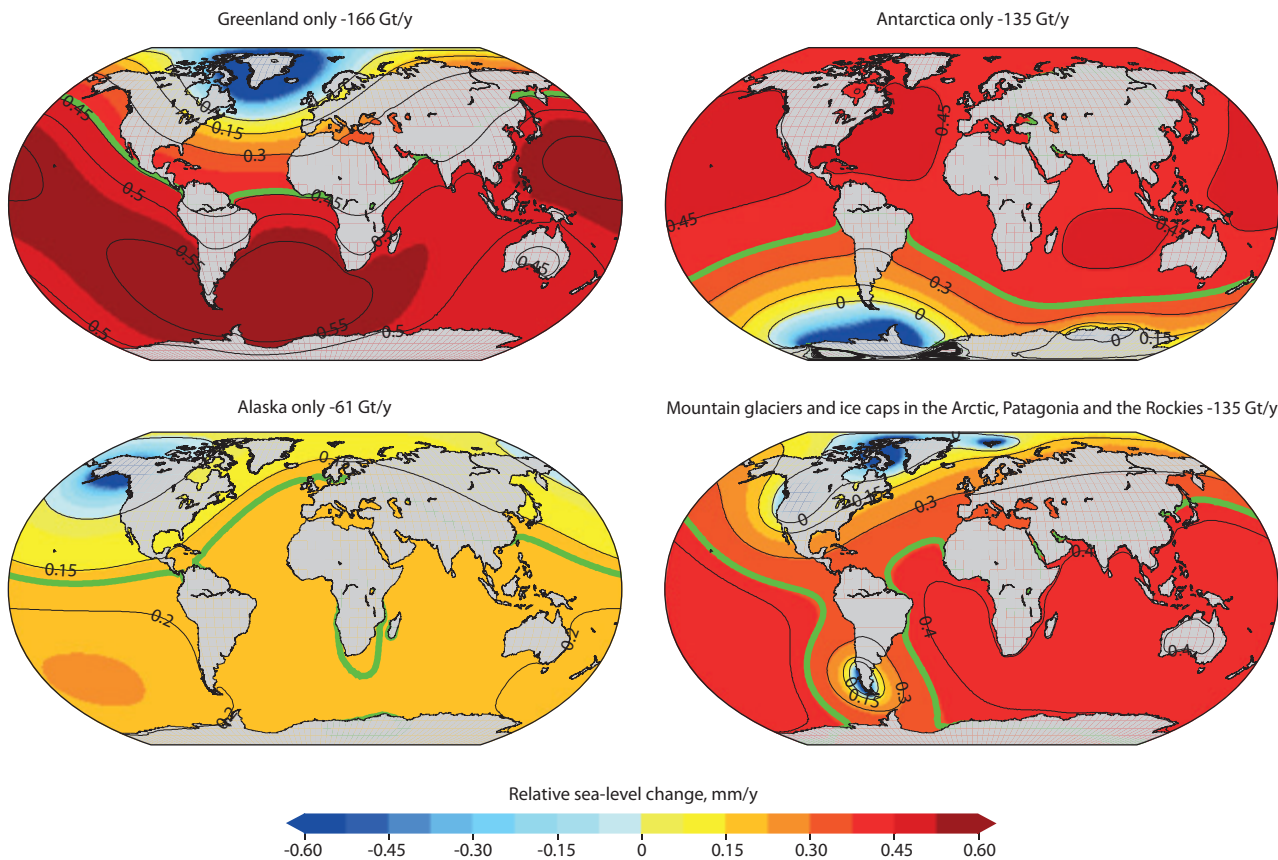


Figure 6.24 Variation in relative sea level (RSL) due to the gravitational and Earth rotational effects of ice mass losses from different sources for the period 2000–2008; Greenland only, Antarctica only, Alaska only, and mountain glaciers and ice caps in the Arctic, Patagonia and the Rockies. The thick green contour indicates the global average eustatic RSL for each source (Bamber and Riva, 2010).

6.6 Impacts

6.6.1 Nutrient export from glaciated systems

The impact of glacial meltwater discharge on nutrient (and contaminant) export into Arctic seas (Figure 6.25) has become a rapidly growing field of study since the previous SWIPA assessment (see Callaghan et al., 2011a,b; Meier et al., 2011; Prowse et al., 2011; Sharp et al., 2011a). Earlier work highlights the importance of catchment geology for water chemistry, especially because glacial catchments have high chemical denudation rates due to high rates of meltwater flushing (Lafrenière and Sharp, 2005). For the Gulf of Alaska, Hood et al. (2009) found that the age of dissolved organic material discharged from glaciers increases with the fraction of the catchment area that is glacierized. Increased freshwater discharge thus alters the age, quantity and reactivity of organic material discharged into the oceans. For one west Greenland catchment, Hawkings et al. (2015) reported increased dissolved nitrogen, phosphorus and silica fluxes during the extreme high melt years of 2010 and 2012. Hawkings et al. (2016) estimated that the Greenland ice sheet contributes about 15% of total bioavailable phosphorus input to the Arctic oceans (~11 Gg/y) and dominates the total phosphorus input (408 Gg/y), which is more than three times that estimated from Arctic rivers (126 Gg/y). The finding of higher nutrient fluxes in high river discharge years leads to the expectation that these fluxes will increase with climate warming.

At present, knowledge of the downstream impacts of variability in nutrient loading is limited. It is known that the coastal waters surrounding the Greenland ice sheet support highly productive ecosystems and are carbon dioxide (CO₂) sinks (Rysgaard et al., 2012). This is also the case for Svalbard, where tidewater glacier fronts are important feeding grounds for marine mammals and seabirds. Glacier meltwater clearly delivers essential nutrients to the polar oceans (Hood et al., 2009; Bhatia et al., 2013; Wadham et al., 2013; Hawkings et al., 2014; Lawson et al., 2014). At the same time, both icebergs and glacial runoff seem to be important vectors for the transport of fine-grained reactive iron into the polar oceans (Raiswell et al., 2008; Raiswell, 2011; Hawkings et al., 2014). However, as pointed out by Hawkings et al. (2015) whether glacier melting provides an important negative climate feedback through its effect on marine primary production and CO₂ drawdown remains unknown.

6.6.2 Contaminant export from glaciated systems

Atmospheric, surface snow, aquatic, and biotic sampling demonstrate the widespread occurrence of organic, inorganic, and particulate pollutants in the Arctic environment (e.g. Butt et al., 2010), including Canadian Arctic ice cores (Zdanowicz et al., 1998, 2000; Zheng et al., 2007; Krachler et al., 2008; Kwok et al., 2013; Zheng, 2015). As glaciers ablate, contaminants are released (e.g. Blais et al., 2001; Bogdal et al., 2010). Mercury is mobilized from Arctic glaciated systems during snowmelt and outburst floods from glacier-dammed lakes (Søndergaard et al., 2015).



Figure 6.25 Aerial view of sediment-rich waters in front of the Humboldt glacier in northwest Greenland, July 2009.

6.7 Gaps and observational needs

Even though an area inventory of land ice is largely completed and surface elevation data exist for most of the Arctic, bed elevation maps are absent for a large fraction (especially for small glaciers), forcing total mass estimates to rely on first-order estimates from area to volume scaling (Bahr et al., 2015). Similarly, many marine-terminating glaciers and fjords lack sufficient bathymetry and bed mapping to constrain their physical dimensions well enough to allow modeling of ice flow and ocean circulation, or even to determine whether or not warm waters may penetrate to the glacier fronts.

Records of land ice extent and volume lack detailed spatial coverage before the era of continuous satellite and airborne remote sensing data, which began around 1992. Over longer, multi-decadal and multi-century timescales, improvements are occurring in the level of detail to which former ice margin positions can be mapped from aerial photos, old maps and information contained in landscapes and landforms. The situation will be further improved as new techniques for dating landscape features related to glacier fluctuations become both available and affordable. However, glaciers present during the Neoglacial cooling (4 ky BP to the end of Little Ice Age c. 1900) are likely to have erased much information about past ice extents from landscapes. During this interval, the minimum configuration of the Greenland ice sheet and major ice caps can only be inferred from relative sea level proxies and ice-core records.

The retention of meltwater in polar firn remains a significant source of uncertainty in estimates of the climatic mass balance

of land ice, particularly owing to its role in delaying the response of the mass balance of accumulation areas to climate warming. Repeat ice cores from single locations have proven to be useful for documenting the history of ice layer development at individual locations, along with repeat borehole temperature profiling, which documents firn warming in response to the release of the latent heat from the freezing of percolating meltwaters. Repeat surveys with ground penetrating radar have proven useful in documenting the three-dimensional evolution of massive ice bodies in firn over time. New methods that may allow such mapping to be extended over whole ice masses using data from airborne radar surveys are emerging. These involve the analysis of the surface scattering component of the radar reflection from glacier surfaces.

Despite receiving a dramatic increase in attention since the previous SWIPA assessment, better understanding of the storage and drainage of subglacial meltwater is needed to rigorously evaluate the role of hydrologically-driven changes in glacier flow in determining how the ice sheet, ice caps and glaciers will respond to a warming climate. Neither the englacial/subglacial drainage pathways followed by meltwaters, nor the timing and extent of subglacial water storage (and how these vary in time and space) are well understood. Nor is it understood how glacier flow and iceberg calving are affected by changes in flow routing and storage of water in glaciers, ice caps and the Greenland ice sheet.

Remote sensing of land ice accumulation rates is becoming possible using ultra-high frequency airborne radio echo sounding in regions where isochronous layering is detectable in radar images, such as through the work of NASA's Operation

IceBridge. Firn cores and density/depth profiles are still needed to calibrate accumulation rates determined by such methods. In any case, the remote sensing of snow mass accumulation rates remains an urgent observational need in many regions of the Arctic.

Available observations show nutrient export from glacial systems increases with increased meltwater discharge. Given the potential impact of these exports on marine primary productivity and CO₂ uptake, more work is clearly needed. There may also be practical implications for the status and distribution of fisheries in the Arctic. Similarly, quantifying and understanding contaminant export in glacial runoff appears to be a high research priority, along with evaluation of the likelihood that glacially-derived contaminants will be incorporated into aquatic food webs. This has already been shown to happen in alpine regions of North America and Europe.

If Arctic land ice loss is affecting ocean thermohaline circulation, and perhaps the intensity or moisture content of storms, it seems clear that extending oceanographic records of change in thermohaline circulation is a high priority.

Ocean warming has been triggering acceleration in the flow of marine-terminating glaciers (Holland et al., 2008), which in turn causes dynamic thinning along major outlet glacier flowlines (Csatho et al., 2014; Mouginot et al., 2015). Thinning is also occurring due to decreasing surface mass balance caused by atmospheric warming. Both thinning mechanisms contribute to Greenland ice sheet thinning both at and above the equilibrium line altitude (Csatho et al., 2014). Thinning moves ice surfaces into lower and therefore warmer parts of the atmosphere, which accelerates the rates of melt and thinning (Rignot et al., 2015). This elevation feedback, operating over decadal to century or more timescales is becoming increasingly important, and will be hard to reverse (Clark et al., 2016) unless there is a compensating feedback involving increased precipitation in a warmer environment where evaporation rates are increased. This is an issue that warrants further investigation using high resolution, state-of-the-art ice sheet models. The work may be facilitated by more studies that use the information contained in ice cores to reconstruct past changes in ice sheet surface elevation and their relationship to changes in ambient air temperature (e.g. Lecavalier et al., 2014).

Acknowledgments

We thank Gerhardt Krinner for constructive and extensive comments in a near-final draft phase.

References

Aas, K.S., T. Dunse, E. Collier, T.V. Schuler, T.K. Berntsen, J. Kohler and B. Luks, 2015. Simulating the climatic mass balance of Svalbard glaciers from 2003 to 2013 with a high-resolution coupled atmosphere-glacier model. *Cryosphere Discussions*, 9:5775-5815.

Alexander, P.M., M. Tedesco, X. Fettweis, R.S.W. van de Wal, C.J.P.P. Smeets and M.R. van den Broeke, 2014. Assessing spatio-temporal variability and trends in modelled and measured Greenland Ice Sheet albedo (2000–2013). *The Cryosphere*, 8:2293-2312.

AMAP, 2011. Snow, Water, Ice and Permafrost in the Arctic (SWIPA): Climate Change and the Cryosphere. Arctic Monitoring and Assessment Programme (AMAP), Oslo, Norway.

Ananicheva, M.D., 2014. Assessment of the area, volume and ELA of glacier systems in Northeast Russia from satellite images in the beginning of the twenty-first century. *Ice and Snow*, 1:35-48.

Ananicheva, M.D. and A. Karpachevsky, 2015. Glaciers of the Orulgan Range, assessment of the current state and possible development for the middle of the 21st century. *Environmental Earth Sciences*, 74:1985-1995.

Ananicheva, M.D. and A.M. Karpachevsky, 2016. The current state of the glaciers of the Chukchi and Kolyma highlands and projection of the glacial systems evolution of the Chukchi Highlands. *Fundamental and Applied Climatology*, 1:64-83.

Andresen, C.S., F. Straneo, M.H. Ribergaard, A.A. Bjørk, T.J. Andersen, A. Kuijpers, N. Nørgaard-Pedersen, K.H. Kjær, F. Schjøth, K. Weckstrøm and A.P. Ahlstrøm, 2012. Rapid response of Helheim Glacier in Greenland to climate variability over the past century. *Nature Geoscience*, 5:37-41.

Andresen, C.S., K.K. Kjeldsen, B. Harden, N. Nørgaard-Pedersen and K.H. Kjær, 2014. Outlet glacier dynamics and bathymetry at Upernivik Isstrøm and Upernivik Isfjord, North-West Greenland. *Geologic Survey of Denmark and Greenland Bulletin*, 31:79-82.

Andersen, M.L., L. Stenseng, H. Skourup, W. Colgan, S.A. Khan, S.S. Kristensen, S.B. Andersen, J.E. Box, A.P. Ahlstrøm, X. Fettweis and R. Forsberg, 2015. Basin-scale partitioning of Greenland ice sheet mass balance components (2007–2011). *Earth and Planetary Science Letters*, 409:89-95.

Arendt, A., S. Luthcke, A. Gardner, S. O’Neil, D. Hill, G. Moholdt and W. Abdalati, 2013. Analysis of a GRACE global mascon solution for Gulf of Alaska glaciers. *Journal of Glaciology*, 59:913-924.

Arendt, A., A. Bliss, T. Bolch, J.G. Cogley, A.S. Gardner, J.-O. Hagen, R. Hock, M. Huss, G. Kaser, C. Kienholz, W.T. Pfeffer, G. Moholdt, F. Paul, V. Radić, L. Andreassen, S. Bajracharya, N.E. Barrand, M. Beedle, E. Berthier, R. Bhamri, I. Brown, E. Burgess, D. Burgess, F. Cawkwell, T. Chinn, L. Copland, B. Davies, H. De Angelis, E. Dolgova, L. Earl, K. Filbert, R. Forester, A.G. Fountain, H. Frey, B. Giffen, N. Glasser, W.Q. Guo, S. Gurney, W. Hagg, D. Hall, U.K. Haritashya, G. Hartmann, C. Helm, S. Herreid, I. Howat, G. Kapustin, T. Khromova, M. König, J. Kohler, D. Kriegel, S. Kutuzov, I. Lavrentiev, R. LeBris, S.Y. Liu, J. Lund, W. Manley, R. Marti, C. Mayer, E.S. Miles, X. Li, B. Menounos, A. Mercer, N. Mölg, P. Mool, G. Nosenko, A. Negrete, T. Nuimura, C. Nuth, R. Pettersson, A. Racoviteanu, R. Ranzi, P. Rastner, F. Rau, B. Raup, J. Rich, H. Rott, A. Sakai, C. Schneider, Y. Seliverstov, M. Sharp, O. Sigurðsson, C. Stokes, R.G. Way, R. Wheate, S. Winsvold, G. Wolken, F. Wyatt, N. Zhelyagina, 2015. Randolph Glacier Inventory – A Dataset of Global Glacier Outlines: Version 5.0. Global Land Ice Measurements from Space, Boulder, Colorado, USA. Digital Media.

Bahr, D.B., W.T. Pfeffer and G. Kaser, 2015. A review of volume-area scaling of glaciers. *Reviews of Geophysics*, 53:95-140.

Bamber, J. and R. Riva, 2010. The sea level fingerprint of recent ice mass fluxes. *The Cryosphere*, 4:621-627.

Bamber, J., M. van den Broeke, J. Ettema, J. Lenaerts and E. Rignot, 2012. Recent large increases in freshwater fluxes from Greenland into the North Atlantic. *Geophysical Research Letters*, 39:L19501, doi:10.1029/2012GL052552.

Bamber, J.L., J.A. Griggs, R.T.W.L. Hurkmans, J. Dowdeswell, S. Gogineni, I. Howat, J. Mouginot, J. Paden, S. Palmer, E. Rignot and D. Steinhage, 2013a. A new bed elevation dataset for Greenland. *The Cryosphere*, 7:499-510.

Bamber, J.L. M.J. Siegert, J.A. Griggs, S.J. Marshall and G. Spada, 2013b. Paleofluvial mega-canyon beneath the central Greenland Ice Sheet. *Science*, 341:997-999.

Barletta, V.R., L.S. Sørensen and R. Forsberg, 2013. Scatter of mass changes estimates at basin scale for Greenland and Antarctica. *The Cryosphere*, 7:1411-1432.

Bartholomaus, T.C., C.F. Larsen and S. O’Neil, 2013. Does calving matter? Evidence for significant submarine melt. *Earth and Planetary Science Letters*, 380:21-30.

Bartholomew, I.D., P. Nienow, A. Sole, D. Mair, T. Cowton, M.A. King and S. Palmer, 2011a. Seasonal variations in Greenland Ice Sheet motion: Inland extent and behaviour at higher elevations. *Earth and Planetary Science Letters*, 307:271-278.

Bartholomew, I., P. Nienow, A. Sole, D. Mair, T. Cowton, S. Palmer and J. Wadham, 2011b. Supraglacial forcing of subglacial drainage in the ablation zone of the Greenland Ice Sheet. *Geophysical Research Letters*, 38, L08502, doi:10.1029/2011GL047063.

Beamer, J.P., D.F. Hill, A. Arendt and G.E. Liston, 2016. High-resolution modeling of coastal freshwater discharge and glacier mass balance in the Gulf of Alaska watershed. *Water Resources Research*, 52:3888-3909.

Bell, R.E., K. Tinto, I. Das, M. Wolovick, W. Chu, T.T. Creyts, N. Frearson, A. Abdi and J.D. Paden, 2014. Deformation, warming and softening of Greenland’s ice by refreezing meltwater. *Nature Geoscience*, 7:497-502.

Bendtsen, J., J. Mortensen, K. Lennert and S. Rysgaard, 2015. Heat sources for glacial ice melt in a West Greenland tidewater outlet glacier fjord: The role of subglacial freshwater discharge. *Geophysical Research Letters*, 42:4089-4095.

Bennartz, R., M.D. Shupe, D.D. Turner, V.P. Walden, K. Steffen, C.J. Cox, M.S. Kulie, N.B. Miller and C. Pettersen, 2013. July 2012 Greenland melt extent enhanced by low-level liquid clouds. *Nature*, 496:83-86.

Benning, L.G., A.M. Anesio, S. Lutz and M. Tranter, 2014. Biological impact on Greenland's albedo. *Nature Geoscience*, 7:691, doi:10.1038/ngeo2260.

Bersch, M., I. Yashayaev and K.P. Koltermann, 2007. Recent changes of the thermohaline circulation in the subpolar North Atlantic. *Ocean Dynamics*, 57:223-235.

Bevis, M., J. Wahr, S.A. Khan, F. Bo Madsen, A. Brown, M. Willis, E. Kendrick, P. Knudsen, J.E. Box, T. van Dam, D.J. Caccamise II, B. Johns, T. Nylen, R. Abbott, S. White, J. Miner, R. Forsberg, H. Zhou, J. Wang, T. Wilson, D. Bromwich and O. Francis, 2012. Bedrock displacements in Greenland manifest ice mass variations, climate cycles and climate change. *Proceedings of the National Academy of Sciences*, 109:11944-11948.

Bezeau, P., M. Sharp, D. Burgess and G. Gascon, 2013. Firn profile changes in response to extreme 21st-century melting at Devon Ice Cap, Nunavut, Canada. *Journal of Glaciology*, 59:981-991.

Bezeau, P., M. Sharp and G. Gascon, 2015. Variability in summer anticyclonic circulation over the Canadian Arctic Archipelago and west Greenland in the late 20th/early 21st centuries and its effect on glacier mass balance. *International Journal of Climatology*, 35:540-557.

Bhatia, M.P., E.B. Kujawinski, S.B. Das, C.F. Breier, P.B. Henderson and M.A. Charette, 2013. Greenland meltwater as a significant and potentially bioavailable source of iron to the ocean. *Nature Geoscience*, 6:274-278.

Bigg, G.R., H.L. Wei, D.J. Wilton, Y. Zhao, S.A. Billings, E. Hanna and V. Kadirkamanathan, 2014. A century of variation in the dependence of Greenland iceberg calving on ice sheet surface mass balance and regional climate change. *Proceedings of the Royal Society A*, 470:doi:10.1098/rspa.2013.0662.

Bjørk, A.A., K.H. Kjær, N.J. Korsgaard, S.A. Khan, K.K. Kjeldsen, C.S. Andresen, J.E. Box, N.K. Larsen and S. Funder, 2012. An aerial view of 80 years of climate-related glacier fluctuations in southeast Greenland. *Nature Geoscience*, 5:427-432.

Björnsson, H. and F. Pálsson, 2008. Icelandic glaciers. *Jökull*, 58:365-386.

Björnsson, H., F. Pálsson, S. Gudmundsson, E. Magnússon, G. Adalgeirsdóttir, T. Jóhannesson, E. Berthier, O. Sigurdsson and T. Thorsteinsson, 2013. Contribution of Icelandic ice caps to sea level rise: trends and variability since the Little Ice Age. *Geophysical Research Letters*, 40:1546-1550.

Blais, J.M., D.W. Schindler, D.C.G. Muir, M. Sharp, D. Donald, M. Lafreniere, E. Braekelveld, W.M.J. Strachan, M. Comba and S. Backus, 2001. Melting glaciers: a major source of persistent organochlorines to subalpine Bow Lake in Banff National Park, Canada. *Ambio*, 30:410-415.

Blaszczyk, M., J.A. Jania and L. Kolondra, 2013. Fluctuations of tidewater glaciers in Hornsund Fjord (Southern Svalbard) since the beginning of the 20th Century. *Polish Polar Research*, 34:327-352.

Bogdal, C., D. Nikolic, M.P. Lüthi, U. Schenker, M. Scheringer and K. Hungerbühler, 2010. Release of legacy pollutants from melting glaciers: model evidence and conceptual understanding. *Environmental Science and Technology*, 44:4063-4069.

Bolch, T., L. Sandberg Sørensen, S.B. Simonsen, N. Mölg, H. Machguth, P. Rastner and F. Paul, 2013. Mass loss of Greenland's glaciers and ice caps 2003–2008 revealed from ICESat laser altimetry data. *Geophysical Research Letters*, 40:875-881.

Booth, A.D., R.A. Clark, B. Kulessa, T. Murray, J. Carter, S. Doyle and A. Hubbard, 2012. Thin-layer effects in glaciological seismic amplitude-versus-angle (AVA) analysis: implications for characterising a subglacial till unit, Russell Glacier, West Greenland. *The Cryosphere*, 6:909-922.

Bougamont, M., P. Christoffersen, A.L. Hubbard, A.A. Fitzpatrick, S.H. Doyle and S.P. Carter, 2014. Sensitive response of the Greenland Ice Sheet to surface melt drainage over a soft bed. *Nature Communications*, 5:5052, doi:10.1038/ncomms6052.

Box, J.E., 2013. Greenland ice sheet mass balance reconstruction. Part II: Surface mass balance (1840-2010). *Journal of Climate*, 26:6974-6989.

Box, J.E. and W. Colgan, 2013. Greenland ice sheet mass balance reconstruction. Part III: Marine ice loss and total mass balance (1840-2010). *Journal of Climate*, 26:6990-7002.

Box, J.E. and D.T. Decker, 2011. Greenland marine-terminating glacier area changes: 2000–2010. *Annals of Glaciology*, 52:91-98.

Box, J.E. and K. Hansen, 2015. Program for the Monitoring of Greenland Ice Sheet (PROMICE). Newsletter 8, December, 2015, http://promice.org/Newsletter_08.pdf

Box, J.E. and K. Steffen, 2001. Sublimation estimates for the Greenland ice sheet using automated weather station observations. *Journal of Geophysical Research*, 106:33965-33982.

Box, J.E., X. Fettweis, J.C. Stroeve, M. Tedesco, D.K. Hall and K. Steffen, 2012. Greenland ice sheet albedo feedback: thermodynamics and atmospheric drivers. *The Cryosphere*, 6:821-839.

Box, J.E., N. Cressie, D.H. Bromwich, J. Jung, M. van den Broeke, J.H. Van Angelen, R.R. Forster, C. Miège, E. Mosley-Thompson, B. Vinther and J.R. McConnell, 2013. Greenland ice sheet mass balance reconstruction. Part I: net snow accumulation (1600-2009). *Journal of Climate*, 26:3919-3934.

Brynjólfsson, S., A. Schomacker, E.R. Guðmundsdóttir and Ó. Ingólfsson, 2015. A 300-year surge history of the Drangajökull ice cap, northwest Iceland, and its maximum during the 'Little Ice Age'. *The Holocene*, 25:1076-1092.

Burgess, D., M. Sharp, D. Mair, J.A. Dowdeswell and T.J. Benham, 2005. Flow dynamics and iceberg calving rates of Devon Ice Cap, Nunavut, Canada. *Journal of Glaciology*, 51:219-230.

Burgess, E.W., R.R. Forster, J.E. Box, E. Mosley-Thompson, D.H. Bromwich, R.C. Bales and L.C. Smith, 2010. A spatially calibrated model of annual accumulation rate on the Greenland Ice Sheet (1958–2007). *Journal of Geophysical Research*, 115:F02004, doi:10.1029/2009JF001293.

Burgess, E.W., R.R. Forster and C.F. Larsen, 2013. Flow velocities of Alaskan Glaciers. *Nature Communications*, 4:2146, doi:10.1038/ncomms3146.

Butt, C.M., U. Berger, R. Bossi and G.T. Tomy, 2010. Levels and trends of poly- and perfluorinated compounds in the Arctic environment. *Science of the Total Environment*, 408:2936-2965.

Callaghan, T.V., M. Johansson, R.D. Brown, P.Y. Groisman, N. Labba and V. Radionov, 2011a. Changing snow cover and its impacts. In: *Snow, Water, Ice and Permafrost in the Arctic (SWIPA): Climate and the Cryosphere. Arctic Monitoring and Assessment Programme (AMAP)*, Oslo, Norway.

Callaghan, T.V., M. Johansson, O. Anisimov, H.E. Christiansen, A. Instanes, V. Romanovsky and S. Smith, 2011b. Changing permafrost and its impacts. In: *Snow, Water, Ice and Permafrost in the Arctic (SWIPA): Climate and the Cryosphere. Arctic Monitoring and Assessment Programme (AMAP)*, Oslo, Norway.

Cappelen, J., 2015. Greenland - DMI Historical Climate Data Collection 1784-2014. Danish Meteorological Institute, Technical Report 15-04.

Carr, J.R., C.R. Stokes and A. Vieli, 2013a. Recent progress in understanding marine-terminating Arctic outlet glacier response to climatic and oceanic forcing: twenty years of rapid change. *Progress in Physical Geography*, 37:435-466.

Carr, J.R., A. Vieli and C.R. Stokes, 2013b. Climatic, oceanic and topographic controls on marine-terminating outlet glacier behavior in north-west Greenland at seasonal to interannual timescales. *Journal of Geophysical Research*, 118:1210-1226.

Carr, J.R., C.R. Stokes and A. Vieli, 2014. Recent retreat of major outlet glaciers on Novaya Zemlya, Russian Arctic, influenced by fjord geometry and sea-ice conditions. *Journal of Glaciology*, 60:155-170.

Carr, J.R., A. Vieli, C.R. Stokes, S.S.R. Jamieson, S. Palmer, P. Christoffersen, J.A. Dowdeswell, F.M. Nick, D.D. Blakemore and D. Young, 2015. Basal topographic controls on rapid retreat of Humboldt Glacier, northern Greenland. *Journal of Glaciology*, 61:137-150.

Chandler, D.M., J.D. Alcock, J.L. Wadham, S.L. Mackie and J. Telling, 2015. Seasonal changes of ice surface characteristics and productivity in the ablation zone of the Greenland Ice Sheet. *The Cryosphere*, 9:487-504.

Charalampidis, C., D. van As, J.E. Box, M.R. van den Broeke, W.T. Colgan, S.H. Doyle, A.L. Hubbard, M. MacFerrin, H. Machguth and C.J.P.P. Smeets, 2015. Changing surface-atmosphere energy exchange and refreezing capacity of the lower accumulation area, West Greenland. *The Cryosphere*, 9:2163-2181.

Chauché, N., A. Hubbard, J.-C. Gascard, J.E. Box, R. Bates, M. Koppes, A. Sole, P. Christoffersen and H. Patton, 2014. Ice-ocean interaction and calving front morphology at two west Greenland tidewater outlet glaciers. *The Cryosphere*, 8:1457-1468.

Chen, L., X. Fettweis, E.M. Knudsen and O.M. Johannessen, 2015. Impact of cyclonic and anticyclonic activity on Greenland ice sheet surface mass balance variation during 1980–2013. *International Journal of Climatology*, 36:3423-3433.

Christianson, K., L.E. Peters, R.B. Alley, S. Anandakrishnan, R.W. Jacobel, K.L. Riverman, A. Muto and B.A. Keisling, 2014. Dilatant till facilitates

ice-stream flow in northeast Greenland. *Earth and Planetary Science Letters*, 401:57-69.

Citterio, M. and A.P. Ahlstrom, 2013. The aerophotogrammetric map of Greenland ice masses. *The Cryosphere*, 7:445-449.

Clark, P.U., J.D. Shakun, S.A. Marcott, A.C. Mix, M. Eby, S. Kulp, A. Levermann, G.A. Milne, P.L. Pfister, B.D. Santer, D.P. Schrag, S. Solomon, T.F. Stocker, B.H. Strauss, A.J. Weaver, R. Winkelmann, D. Archer, E. Bard, A. Goldner, K. Lambeck, R.T. Pierrehumbert and G.-K. Plattner, 2016. Consequences of twenty-first-century policy for multi-millennial climate and sea-level change. *Nature Climate Change*, 6:360-369.

Clason, C.C., D.W.F. Mair, P.W. Nienow, I.D. Bartholomew, A. Sole, S. Palmer and W. Schwanghart, 2015. Modelling the transfer of supraglacial meltwater to the bed of Leverett Glacier, southwest Greenland. *The Cryosphere*, 9:123-138.

Colgan, W., J. Box, M. Andersen, X. Fettweis, B. Csatho, R. Fausto, D. van As and J. Wahr, 2015a. Greenland high elevation mass balance: Inference and implication of reference period (1961-1990) imbalance. *Annals of Glaciology*, 56:105-107.

Colgan, W., W. Abdalati, M. Citterio, B. Csatho, X. Fettweis, S. Luthcke, G. Moholdt, S.B. Simonsen and M. Stober, 2015b. Hybrid glacier Inventory, Gravimetry and Altimetry (HIGA) mass balance product for Greenland and the Canadian Arctic. *Remote Sensing of Environment*, 168:24-39.

Colgan, W., A. Sommers, H. Rajaram, W. Abdalati and J. Frahm, 2015c. Considering thermal-viscous collapse of the Greenland ice sheet. *Earth's Future*, 3:252-267.

Collins, M., R. Knutti, J. Arblaster, J.L. Dufresne, T. Fichefet, P. Friedlingstein, X. Gao, W.J. Gutowski, T. Johns, G. Krinner, M. Shongwe, C. Tebaldi, A.J. Weaver and M. Wehner, 2013. Long-term climate change: projections, commitments and irreversibility. In: Stocker, T.F., D. Qin, G.-K. Plattner, M. Tignor, S.K. Allen, J. Boschung, A. Nauels, Y. Xia, V. Bex and P.M. Midgley (eds.), *Climate Change 2013: The Physical Science Basis. Contribution of Working Group I to the Fifth Assessment Report of the Intergovernmental Panel on Climate Change*. Cambridge University Press.

Compo, G.P., J.S. Whitaker, P.D. Sardeshmukh, N. Matsui, R.J. Allan, X. Yin, B.E. Gleason, R.S. Vose, G. Rutledge, P. Bessemoulin, S. Brönnimann, M. Brunet, R.I. Crouthamel, A.N. Grant, P.Y. Groisman, P.D. Jones, M.C. Kruk, A.C. Kruger, G.J. Marshall, M. Maugeri, H.Y. Mok, Ø. Nordli, T.F. Ross, R.M. Trigo, X.L. Wang, S.D. Woodruff, S.J. Worley, 2011. The twentieth century reanalysis project. *Quarterly Journal of the Royal Meteorological Society*, 137:1-28.

Copland, L., M. Sharp and J.A. Dowdeswell, 2003. The distribution and flow characteristics of surge-type glaciers in the Canadian High Arctic. *Annals of Glaciology*, 36:73-81.

Csatho, B., T. Schenk, C.J. van der Veen and W.B. Krabill, 2008. Intermittent thinning of Jakobshavn Isbræ, West Greenland, since the Little Ice Age. *Journal of Glaciology*, 54:131-144.

Csatho, B., A. Schenk, C. van der Veen, G. Babonis, K. Duncan, S. Rezvanbehbahanic, M. van den Broeke, S. Simonsen, S. Nagarajan and J. van Angelen, 2014. Laser altimetry reveals complex pattern of Greenland Ice Sheet dynamics. *Proceedings of the National Academy of Sciences*, 111:18478-18483.

Cullen, N.J., T. Mölg, J. Conway and K. Steffen, 2014. Assessing the role of sublimation in the dry snow zone of the Greenland ice sheet in a warming world. *Journal of Geophysical Research: Atmosphere*, 119:6563-6577.

Curry, R. and C. Mauritzen, 2005. Dilution of the northern North Atlantic Ocean in recent decades. *Science*, 308:1772-1774.

Dahl-Jensen, D., J. Bamber, C.E. Bøggild, E. Buch, J.H. Christensen, K. Dethloff, M. Fahnestock, S. Marshall, M. Rosing, K. Steffen, R. Thomas, M. Truffer, M. van den Broeke and C. van der Veen, 2011. The Greenland ice sheet in a changing climate. In: *Snow, Water, Ice and Permafrost in the Arctic (SWIPA): Climate and the Cryosphere. Arctic Monitoring and Assessment Programme (AMAP)*, Oslo, Norway.

Das, I., R. Hock, E. Berthier, C.S. Lingle, 2014. 21st-century increase in glacier mass loss in the Wrangell Mountains, Alaska, USA, from airborne laser altimetry and satellite stereo imagery. *Journal of Glaciology*, 60:283-293.

de la Peña, S., I.M. Howat, P.W. Nienow, M.R. van den Broeke, E. Mosley-Thompson, S.F. Price, D. Mair, B. Noël and A.J. Sole, 2015. Changes in the firn structure of the western Greenland Ice Sheet caused by recent warming. *The Cryosphere*, 9:1203-1211.

Dickson, R.R., J. Meincke, S.-A. Malmberg and A.J. Lee, 1988. The "Great Salinity Anomaly" in the northern North Atlantic, 1968-1982. *Progress in Oceanography*, 20:103-151.

Dow, C.F., A. Hubbard, A.D. Booth, S.H. Doyle, A. Gusmeroli and B. Kulessa, 2013. Seismic evidence of a sediment layer underlying Russell Glacier, West Greenland. *Annals of Glaciology*, 54:135-141.

Dowdeswell, J.A., M.R. Gorman, A.F. Glazovsky and Y.Y. Macheret, 1994. Evidence for floating ice shelves in Franz Josef Land, Russian High Arctic. *Arctic and Alpine Research*, 26:86-92.

Dowdeswell, J.A., B. Unwin, A.M. Nuttall and D.J. Wingham, 1999. Velocity structure, flow instability and mass flux on a large Arctic ice cap from satellite radar interferometry. *Earth and Planetary Science Letters*, 167:131-140.

Doyle, S.H., A.L. Hubbard, C.F. Dow, G.A. Jones, A. Fitzpatrick, A. Gusmeroli, B. Kulessa, K. Lindbeck, R. Pettersson and J.E. Box, 2013. Ice tectonic deformation during the rapid in situ drainage of a supraglacial lake on the Greenland Ice Sheet. *The Cryosphere*, 7:129-140.

Doyle, S.H., A. Hubbard, A. Fitzpatrick, D. van As, A. Mikkelsen, R. Pettersson and B.B. Hubbard, 2014. Persistent flow acceleration within the interior of the Greenland ice sheet. *Geophysical Research Letters*, 41:899-905.

Doyle, S.H., A. Hubbard, R.S.W. van de Wal, J.E. Box, D. van As, K. Scharrer, T.W. Meierbachtol, P.C. J. P. Smeets, J.T. Harper, E. Johansson, R.H. Mottram, A.B. Mikkelsen, F. Wilhelms, H. Patton, P. Christoffersen and B. Hubbard, 2015. Amplified melt and flow of the Greenland ice sheet driven by late-summer cyclonic rainfall. *Nature Geoscience*, 8:647-653.

Duchez, A., E. Frajka-Williams, S.A. Josey, D.G. Evans, J.P. Grist, R. Marsh, G.D. McCarthy, B. Sinha, D.I. Berry and J.J.-M. Hirschi, 2016. Drivers of exceptionally cold North Atlantic Ocean temperatures and their link to the 2015 European heat wave. *Environmental Research Letters*, 11:074004, doi:10.1088/1748-9326/11/7/074004.

Dumont, M., E. Brun, G. Picard, M. Michou, Q. Libois, J.-R. Petit, M. Geyer, S. Morin and B. Josse, 2014. Contribution of light-absorbing impurities in snow to Greenland's darkening since 2009. *Nature Geoscience*, 7:509-512.

Dunse, T., T. Schellenberger, J.O. Hagen, A. Kääb, T.V. Schuler and C.H. Reijmer, 2015. Glacier-surge mechanisms promoted by a hydro-thermodynamic feedback to summer melt. *The Cryosphere*, 9:197-215.

Earl, L. and A. Gardner, 2015. A satellite-derived glacier inventory for North Asia. *Annals of Glaciology*, 57:50-60.

Ebbesmeyer, C.C., I.M. Belkin, H.E. Drost, S. Zimmermann and E.C. Carmack, 2011. Wall across the Atlantic: Drift bottles released by students confirm that the Gulf Stream prevents subarctic surface drifters from escaping south. *Oceanography*, 24:172-174.

Enderlin, E., I. Howat, S. Jeong, M. Noh, J. van Angelen and M. van den Broeke, 2014. An improved mass budget for the Greenland ice sheet. *Geophysical Research Letters*, 41:866-872.

Engelhardt, M., T.V. Schuler and L.M. Andreassen, 2013. Glacier mass balance of Norway 1961-2010 calculated by a temperature-index model. *Annals of Glaciology*, 54:32-40.

Fahnestock, M., R. Bindschadler, R. Kwok and K. Jezek, 1993. Greenland ice sheet surface properties and ice dynamics from ERS-1 SAR imagery. *Science*, 262:1530-1534.

Fahnestock, M., W. Abdalati, I. Joughin, J. Brozena and P. Gogineni, 2001. High geothermal heat flow, basal melt, and the origin of rapid ice flow in central Greenland. *Science*, 294:2338-2342.

Falkner, K.K., H. melling, A.M. Münchow, J.E. Box, T. Wohlleben, H.L. Johnson, P. Gudmandson, R. Samelson, L. Copland, K. Steffen, E. Rignot and A.K. Hoggins, 2011. Context for the Recent Massive Petermann Glacier Calving Event. *Eos Transactions American Geophysical Union*, 92:117-118.

Fausto, R.S., D. van As, J.E. Box, W. Colgan, P.L. Langen and R.H. Mottram, 2016. The implication of nonradiative energy fluxes dominating Greenland ice sheet exceptional ablation area surface melt in 2012. *Geophysical Research Letters*, 43:2649-2658.

Fettweis, X., M. Tedesco, M.R. van den Broeke and J. Ettema, 2011. Melting trends over the Greenland ice sheet (1958-2009) from spaceborne microwave data and regional climate models. *The Cryosphere*, 5:359-375.

Fettweis, X., E. Hanna, C. Lang, A. Belleflamme, M. Erpicum and H. Gallée, 2013a. Brief communication Important role of the mid-tropospheric atmospheric circulation in the recent surface melt increase over the Greenland ice sheet. *The Cryosphere*, 7:241-248.

Fettweis, X., B. Franco, M. Tedesco, J. van Angelen, J. Lenaerts, M. van den Broeke and H. Gallée, 2013b. Estimating the Greenland ice sheet surface mass balance contribution to future sea level rise using the regional atmospheric climate model MAR. *The Cryosphere*, 7:469-489.

Fettweis, X., C. Agosta and H. Gallée, 2016. Reconstruction of the Greenland ice sheet surface mass balance over 1900–2015 with the help of the regional climate MARv3.6 model Xavier. *Geophysical Research Abstracts*, Vol. 18, EGU2016-12753. EGU General Assembly.

Fisher, D., J. Zheng, D. Burgess, C. Zdanowicz, C. Kinnard and M. Sharp, 2012. Recent melt rates of Canadian arctic ice caps are the highest in four millennia. *Global and Planetary Change*, 84:3-7.

Fitzpatrick, A.A.W., A.L. Hubbard, J.E. Box, D.J. Quincey, D. van As, A.P.B. Mikkelsen, S.H. Doyle, C.F. Dow, B. Hasholt and G.A. Jones, 2014. A decade (2002–2012) of supraglacial lake volume estimates across Russell Glacier, West Greenland. *The Cryosphere*, 8:107–121.

Forster, R.R., J.E. Box, M.R. van den Broeke, C. Miège, E.W. Burgess, J.H. van Angelen, J.T.M. Lenaerts, L.S. Koenig, J. Paden, C. Lewis, S.P. Gogineni, C. Leuschen and J.R. McConnell, 2014. Extensive liquid meltwater storage in firn within the Greenland ice sheet. *Nature Geoscience*, 7:95–98.

Francis, J.A. and S.J. Vavrus, 2012. Evidence linking Arctic amplification to extreme weather in mid-latitudes. *Geophysical Research Letters*, 39:L06801, doi:10.1029/2012GL051000.

Fried, M., G. Catania, T. Bartholomäus, D. Duncan, M. Davis, L. Stearns, J. Nash, E. Shroyer and D. Sutherland, 2015. Distributed subglacial discharge drives significant submarine melt at a Greenland tidewater glacier. *Geophysical Research Letters*, 42:9328–9336.

Galanin, A.A., V.M. Lytkin, A.N. Fedorov and T. Kadota, 2013. Recession of glaciers in the Suntar-Khayata Mountains and methodological consideration of its assessment. *Ice and Snow*, 53:30–42.

Gardner, A.S., G. Moholdt, B. Wouters, G.J. Wolken, D.D. Burgess, M.J. Sharp, G. Coglet, C. Braun and C. Labine, 2011. Sharply increased mass loss from the glaciers and ice caps in the Canadian Arctic Archipelago. *Nature*, 473:357–360.

Gardner, A., G. Moholdt, A. Arendt and B. Wouters, 2012. Accelerated contributions of Canada's Baffin and Baffin Island glaciers to sea level rise over the past half century. *The Cryosphere*, 6:1103–1125.

Gardner, A., G. Moholdt, J. Cogley, B. Wouters, A. Arendt, J. Wahr, E. Berthier, R. Hock, W. Pfeffer, G. Kaser, S. Ligtenberg, T. Bolch, M. Sharp, J. Hagen, M. van den Broeke and F.A. Paul, 2013. A reconciled estimate of glacier contributions to sea level rise: 2003 to 2009. *Science*, 340:852–858.

Gascon, G., M. Sharp, D. Burgess, P. Bezeau and A.B.G. Bush, 2013a. Changes in accumulation-area firn stratigraphy and meltwater flow during a period of climate warming: Devon Ice Cap, Nunavut, Canada. *Journal of Geophysical Research: Earth Surface*, 118:2380–2391.

Gascon, G., M. Sharp and A.B.G. Bush, 2013b. Changes in melt season characteristics on the Devon Ice Cap, Canada, and their association with the Arctic atmospheric circulation. *Annals of Glaciology*, 54:101–110.

Gregory, J.M., N.J. White, J.A. Church, M.F.P. Bierkens, J.E. Box, M.R. van den Broeke, J.G. Cogley, X. Fettweis, E. Hanna, P. Huybrechts, L.F. Konikow, P.W. Leclercq, B. Marzeion, J. Oerlemans, M.E. Tamisiea, Y. Wada, L.M. Wake and R.S.W. van de Wal, 2012. Twentieth-century global-mean sea-level rise: is the whole greater than the sum of the parts? *Journal of Climate*, 26:4476–4499.

Gurney, S.D., V.V. Popovnin, M. Shahgedanova and C.R. Stokes, 2008. A glacier inventory for the Buordakh Massif, Cherskiy Range, northeast Siberia, and evidence for recent glacier recession. *Arctic Antarctic and Alpine Research*, 40:81–88.

Gusmeroli, A., P. Jansson, R. Pettersson and T. Murray, 2012. Twenty years of cold surface layer thinning at Storglaciären, sub-Arctic Sweden, 1989–2009. *Journal of Glaciology*, 58:3–10.

Hanna, E., P. Huybrechts, J. Cappelen, K. Steffen, R. Bales, E. Burgess, J. McConnell, J. Peder Steffensen, M. van den Broeke, L. Wake, G. Bigg, M. Griffiths and D. Savas, 2011. Greenland Ice Sheet surface mass balance 1870 to 2010 based on Twentieth Century Reanalysis, and links with global climate forcing. *Journal of Geophysical Research*, 116:D24121, doi:10.1029/2011JD016387.

Hannesdóttir, H., H. Björnsson, F. Pálsson, G. Aðalgeirsdóttir and S. Guðmundsson, 2014. Variations of southeast Vatnajökull ice cap (Iceland) 1650–1900 and reconstruction of the glacier surface geometry at the Little Ice Age maximum. *Geografiska Annaler A*, 97:237–264.

Hannesdóttir, H., H. Björnsson, F. Pálsson, G. Aðalgeirsdóttir and S. Guðmundsson, 2015a. Changes in the southeast Vatnajökull ice cap, Iceland, between ~1890 and 2010. *The Cryosphere*, 9:565–585.

Hannesdóttir, H., G. Aðalgeirsdóttir, T. Jóhannesson, Sv. Guðmundsson, P. Crochet, H. Ágústsson, F. Pálsson, E. Magnússon, S.P. Sigurðsson and H. Björnsson, 2015b. Downscaled precipitation applied in modelling of mass balance and the evolution of southeast Vatnajökull, Iceland. *Journal of Glaciology*, 61:799–813.

Hansen, J., M. Sato, P. Hearty, R. Ruedy, M. Kelley, V. Masson-Delmotte, G. Russell, G. Tselioudis, J. Cao, E. Rignot, I. Velicogna, B. Tormey, B. Donovan, E. Kandiano, K. von Schuckmann, P. Kharecha, A.N. Legrande, M. Bauer and K.-W. Lo, 2016. Ice melt, sea level rise and superstorms: evidence from paleoclimate data, climate modeling, and modern observations that 2°C global warming could be dangerous. *Atmospheric Chemistry and Physics*, 16:3761–3812.

Harper, J., N. Humphrey, W. Pfeffer, J. Brown and X. Fettweis, 2012. Greenland ice-sheet contribution to sea-level rise buffered by meltwater storage in firn. *Nature*, 491:240–243.

Hawkins, J.R., J.L. Wadham, M. Tranter, R. Raiswell, L.G. Benning, P.J. Statham, A. Tedstone, P. Nienow, K. Lee and J. Telling, 2014. Ice sheets as a significant source of highly reactive nanoparticulate iron to the oceans. *Nature Communications*, 5:doi:10.1038/ncomms4929.

Hawkins, J.R., J.L. Wadham, M. Tranter, E. Lawson, A. Sole, T. Cowton, A.J. Tedstone, I. Bartholomew, P. Nienow, D. Chandler and J. Telling, 2015. The effect of warming climate on nutrient and solute export from the Greenland Ice Sheet. *Geochemical Perspectives Letters*, 1:94–104.

Hawkins, J., J. Wadham, M. Tranter, J. Telling, E. Bagshaw, A. Beaton, S.-L. Simmons, D. Chandler, A. Tedstone and P. Nienow, 2016. The Greenland Ice Sheet as a hot spot of phosphorus weathering and export in the Arctic. *Global Biogeochemical Cycles*, 30:191–210.

He, T., S. Liang, Y. Yu, D. Wang, F. Gao and Q. Liu, 2013. Greenland surface albedo changes in July 1981–2012 from satellite observations. *Environmental Research Letters*, 8:044043.

Helm, V., A. Humbert and H. Miller, 2014. Elevation and elevation change of Greenland and Antarctica derived from CryoSat-2. *The Cryosphere*, 8:1539–1559.

Hoffman, M.J., G.A. Catania, T.A. Neumann, L.C. Andrews and J.A. Rumrill, 2011. Links between acceleration, melting, and supraglacial lake drainage of the western Greenland ice sheet. *Journal of Geophysical Research*, 116:F04035, doi:10.1029/2010JF001934.

Holland, D.M., R.H. Thomas, B. de Young, M.H. Ribergaard and B. Lyberth, 2008. Acceleration of Jakobshavn Isbræ triggered by warm subsurface ocean waters. *Nature Geoscience*, 1:659–664.

Hood, E., J. Fellman, R.G.M. Spencer, P.J. Hernes, R. Edwards, D. D'Amore and D. Scott, 2009. Glaciers as a source of ancient and labile organic matter to the marine environment. *Nature*, 462:1044–1047.

Howat, I.M. and A. Eddy, 2011. Multidecadal retreat of Greenland's marine-terminating glaciers. *Journal of Glaciology*, 57:389–396.

Howat, I.M., Y. Ahn, I. Joughin, M.R. van den Broeke, J.T.M. Lenaerts and B. Smith, 2011. Mass balance of Greenland's three largest outlet glaciers, 2000–2010. *Geophysical Research Letters*, 38:L12501, doi:10.1029/2011GL047565.

Howat, I.M., C. Porter, M.J. Noh, B.E. Smith and S. Jeong, 2015. Brief communication: sudden drainage of a subglacial lake beneath the Greenland Ice Sheet. *Cryosphere*, 9:103–109.

Huss, M. and D. Farinotti, 2012. Distributed ice thickness and volume of all glaciers around the globe. *Journal of Geophysical Research*, 117:F04010, doi:10.1029/2012JF002523.

Jackson, L.C., R. Kahana, T. Graham, M.A. Ringer, T. Woolings, J.V. Mecking and R.A. Wood, 2015. Global and European climate impacts of a slowdown of the AMOC in a high resolution GCM. *Climate Dynamics*, 45:3299–3316.

Jacob, T., J. Wahr, W.T. Pfeffer and S. Swenson, 2012. Recent contributions of glaciers and ice caps to sea level rise. *Nature*, 482:514–518.

Jeffries, M.O., J. Richter-Menge and J. E. Overland (eds.), 2013. Arctic Report Card 2013. www.arctic.noaa.gov/reportcard.

Jensen, T., J.E. Box and C.S. Hvidberg, 2016. A sensitivity study of annual area change for Greenland ice sheet marine terminating outlet glaciers: 1999–2013. *Journal of Glaciology*, 62:72–81.

Jóhannesson, T., H. Björnsson, E. Magnússon, S. Guðmundsson, F. Pálsson, O. Sigurðsson, Th. Thorsteinsson and E. Berthier, 2013. Ice-volume changes, bias estimation of mass-balance measurements and changes in sub-glacial lakes derived by LiDAR-mapping of the surface of Icelandic glaciers. *Annals of Glaciology*, 54:63–74.

Jolly, M.W., M.A. Cochrane, P.H. Freeborn, Z.A. Holden, T.J. Brown, G.J. Williamson and D.M.J.S. Bowman, 2015. Climate-induced variations in global wildfire danger from 1979 to 2013. *Nature Communications*, 6:7537, doi:10.1038/ncomms8537.

Johnson, H.L., A. Münchow, K.K. Falkner and H. Melling, 2011. Ocean circulation and properties in Petermann Fjord, Greenland. *Journal of Geophysical Research*, 116:C01003, doi:10.1029/2010JC006519.

Joughin, I.R., M.A. Fahnestock and J.L. Bamber, 2000. Ice flow in the northeast Greenland ice stream. *Annals of Glaciology*, 31:141-146.

Joughin, I., M. Fahnestock, D. MacAyeal, J.L. Bamber and P. Gogineni, 2001. Observation and analysis of ice flow in the largest Greenland ice stream. *Journal of Geophysical Research*, 106:34021-34034.

Joughin, I., B. Smith, I. Howat, T. Scambos and T. Moon, 2010. Greenland flow variability from ice-sheet-wide velocity mapping. *Journal of Glaciology*, 56:415-430.

Joughin, I., B.E. Smith, D.E. Shean and D. Floricioiu, 2014. Brief Communication: Further summer speedup of Jakobshavn Isbræ. *The Cryosphere*, 8:209-214.

Kalnay, E., M. Kanamitsu, R. Kistler, W. Collins, D. Deaven, L. Gandin, M. Iredell, S. Saha, G. White, J. Woollen, Y. Zhu, A. Leetmaa, R. Reynolds, M. Chelliah, E. Ebisuzaki, W.E. Higgins, J. Janowiak, K.C. Mo, C. Ropelewski, J. Wang, R. Jenne and D. Joseph, 1996. The NCEP/NCAR 40-Year Reanalysis Project. *Bulletin of the American Meteorological Society*, 77:437-471.

Kargel, J.S., A.P. Ahlström, R.B. Alley, J.L. Bamber, T.J. Benham, J.E. Box, C. Chen, P. Christoffersen, M. Citterio, J.G. Cogley, H. Jiskoot, G.J. Leonard, P. Morin, T. Scambos, T. Sheldon and I. Willis, 2012. Brief Communication: Greenland's shrinking ice cover: "fast times" but not that fast. *The Cryosphere*, 6:533-537.

Katalog lednikov SSSR [The USSR Glacier Inventory], 1972. Part 2. Orulgan range. Hydrometeoizdat, Leningrad. 17(5).

Kaufman, D.S., T.A. Ager, N.J. Anderson, P.M. Anderson, J.T. Andrews, P.J. Bartlein, L.B. Burbaker, L.L. Coats, L.C. Cwynar, M.L. Duval, A.S. Dyke, M.E. Edwards, W.R. Eiser, K. Gajewski, A. Geisodottir, F.S. Hu, A.E. Jennings, M.R. Kaplan, M.W. Kewin, A.V. Lozhkin, G.M. MacDonald, G.H. Miller, C.J. Mock, W.W. Oswald, B.L. Otto-Blisner, D.F. Porinchuk, K. Rühland, J.P. Smol, E.J. Steig and B.B. Wolfe, 2004. Holocene thermal maximum in the western Arctic (0-180° W). *Quaternary Science Reviews*, 23:529-560.

Keegan, K.M., M.R. Albert, J.R. McConnell and I. Baker, 2014. Climate change and forest fires synergistically drive widespread melt events of the Greenland Ice Sheet. *Proceedings of the National Academy of Sciences USA*, 111:7964-7967.

Khan, S., J. Wahr, M. Bevis, I. Velicogna and E. Kendrick, 2010. Spread of ice mass loss into northwest Greenland observed by GRACE and GPS. *Geophysical Research Letters*, 37:L06501, doi:10.1029/2010GL042460.

Khan, S.A., K.K. Kjeldsen, K.H. Kjær, S. Bevan, A. Luckman, A. Aschwanden, A.A. Bjørk, N.J. Korsgaard, J.E. Box, M. van den Broeke, T.M. van Dam and A. Fitzner, 2014a. Glacier dynamics at Helheim and Kangerdlugssuaq glaciers, southeast Greenland, since the Little Ice Age. *The Cryosphere*, 8:1497-1507.

Khan, S.A., K.H. Kjær, M. Bevis, J.L. Bamber, J. Wahr, K.K. Kjeldsen, A.A. Bjørk, N.J. Korsgaard, L.A. Stearns, M.R. van den Broeke, L. Liu, N.K. Larsen and I.S. Muresan, 2014b. Sustained mass loss of the northeast Greenland ice sheet triggered by regional warming. *Nature Climate Change*, 4:292-299.

Khromova, T., G. Nosenko, S. Kutuzov, A. Muraviev and L. Chernova, 2014. Glacier area changes in Northern Eurasia. *Environmental Research Letters*, 9:015003, doi:10.1088/1748-9326/9/1/015003.

Kjær, K.H. S.A. Khan, N.J. Korsgaard, J. Wahr, J.L. Bamber, R. Hurkmans, M. van den Broeke, L.H. Timm, K.K. Kjeldsen, A.A. Bjørk, N.K. Larsen, L.T. Jørgensen, A. Færch-Jensen and E. Willerslev, 2012. Aerial photographs reveal late-20th-century dynamic ice loss in northwestern Greenland. *Science*, 337:569-573.

Kjeldsen, K.K., S.A. Khan, J. Wahr, N.J. Korsgaard, K.H. Kjær, A.A. Bjørk, R. Hurkmans, M.R. van den Broeke, J.L. Bamber and J.H. van Angelen, 2013. Improved ice loss estimate of the northwestern Greenland ice sheet. *Journal of Geophysical Research: Solid Earth*, 118:698-708.

Kjeldsen, K.K., N.J. Korsgaard, A.A. Bjørk, S.A. Khan, J.E. Box, S. Funder, N.K. Larsen, J.L. Bamber, W. Colgan, M. van den Broeke, M.-L. Siggaard-Andersen, C. Nuth, A. Schomacker, C.S. Andresen, E. Willerslev and K.H. Kjær, 2015. Spatial and temporal distribution of mass loss from the Greenland Ice Sheet since AD 1900. *Nature*, 528:396-400.

Koenig, L.S., C. Miege, R.R. Forster and L. Bruckner, 2014. Initial in situ measurements of perennial meltwater storage in the Greenland firn aquifer. *Geophysical Research Letters*, 41:81-85.

Krachler, M., J. Zheng, D. Fisher and W. Shotyk, 2008. Atmospheric Sb in the Arctic during the past 16,000 years: Responses to climate change and human impacts. *Global Biogeochemical Cycles*, 22:GB1015, doi:10.1029/2007GB002998.

Kuipers Munneke, P., S.R.M. Ligtenberg, B.P.Y. Noël, I.M. Howat, J.E. Box, E. Mosley-Thompson, J.R. McConnell, K. Steffen, J.T. Harper, S.B. Das and M.R. van den Broeke, 2015. Elevation change of the Greenland Ice Sheet due to surface mass balance and firn processes, 1960-2014. *The Cryosphere*, 9:2009-2025.

Kwok, K.Y., E. Yamazaki, N. Yamashita, S. Taniyasu, M.B. Murphy, Y. Horii, G. Petrick, R. Kallerborn, K. Kannan, K. Murano and P.K.S. Lam, 2013. Transport of perfluoroalkyl substances (PFAS) from an arctic glacier to downstream locations: Implications for sources. *Science of the Total Environment*, 447:46-55.

Lafrenière, M.J. and M.J. Sharp, 2005. A comparison of solute fluxes and sources from glacial and non-glacial catchments over contrasting melt seasons. *Hydrological Processes*, 19:2991-3012.

Lampkin, D.J., N. Amador, B.R. Parizek, K. Farness and K. Jezek, 2013. Drainage from water-filled crevasses along the margins of Jakobshavn Isbræ: A potential catalyst for catchment expansion. *Journal of Geophysical Research: Earth Surface*, 118:795-813.

Lang, C., X. Fettweis and M. Erpicum, 2015. Stable climate and surface mass balance in Svalbard over 1979-2013 despite the Arctic warming. *The Cryosphere*, 9:83-101.

Larsen, C.F., E. Burgess, A.A. Arendt, S. O'Neil, A.J. Johnson and C. Kienholz, 2015. Surface melt dominates Alaska glacier mass balance. *Geophysical Research Letters*, 42:5902-5908.

Lavers, D.A., and G. Villarini, 2013. The nexus between atmospheric rivers and extreme precipitation across Europe. *Geophysical Research Letters*, 40:3259-3264.

Lavrentiev, I.I., 2016. Change of glaciers of Novaya Zemlya (Russian Arctic) from 1952 to 2015. XVI Glaciological Symposium. Past, Present, and Future of the Earth Cryosphere. 24-29 May 2016, St Petersburg, Russia.

Lawson, E.C., M.P. Bhatia, J.L. Wadham and E.B. Kujawinski, 2014. Continuous summer export of nitrogen-rich organic matter from the Greenland Ice Sheet inferred by ultra-high resolution mass spectrometry. *Environmental Science and Technology*, 48:14248-14257.

Lea, J.M., D.W.F. Mair, F.M. Nick, B.R. Rea, A. Weidick, K.H. Kjær, M. Morlighem, D. van As and J.E. Schofield, 2014a. Terminus-driven retreat of a major southwest Greenland tidewater glacier during the early 19th century: insights from glacier reconstructions and numerical modelling. *Journal of Glaciology*, 60:333-344.

Lea, J.M., D.W.F. Mair, F.M. Nick, B.R. Rea, D. van As, M. Morlighem, P.W. Nienow and A. Weidick, 2014b. Fluctuations of a Greenlandic tidewater glacier driven by changes in atmospheric forcing: observations and modelling of Kangiata Nunaata Sermia, 1859-present. *The Cryosphere*, 8:2031-2045.

Lecavalier, B.S., G.A. Milne, M.J.R. Simpson, L.M. Wake, P. Huybrechts, L. Tarasov, K.K. Kjeldsen, S. Funder, A.J. Long, S. Woodroffe, A.S. Dyke and N.K. Larsen, 2014. A model of Greenland ice sheet deglaciation constrained by observations of relative sea level and ice extent. *Quaternary Science Reviews*, 102:54-84.

Leclercq, P.W., A. Weidick, F. Paul, T. Bolch, M. Citterio and J. Oerlemans, 2012. Brief communication: Historical glacier length changes in West Greenland. *The Cryosphere*, 6:1339-1343.

Leeson, A.A., A. Shepherd, K. Briggs, I. Howat, X. Fettweis, M. Morlighem and E. Rignot, 2015. Supraglacial lakes on the Greenland ice sheet advance inland under warming climate. *Nature Climate Change*, 5:51-55.

Lehmann, J., D. Coumou, K. Frieler, A.V. Eliseev and A. Levermann, 2014. Future changes in extratropical storm tracks and baroclinicity under climate change. *Environmental Research Letters*, 9:084002.

Lenaerts, J., J.H. Angelen, M.R. Broeke, A.S. Gardner, B. Wouters and E. Meijgaard, 2013. Irreversible mass loss of Canadian Arctic Archipelago glaciers. *Geophysical Research Letters*, 40:870-874.

Lindbäck, K., R. Pettersson, A.L. Hubbard, S.H. Doyle, D. van As, A.B. Mikkelsen and A.A. Fitzpatrick, 2015. Subglacial water drainage, storage, and piracy beneath the Greenland ice sheet. *Geophysical Research Letters*, 42:7606-7614.

Liu, J., Z. Chen, J. Francis, M. Song, T. Mote and Y. Hu, 2016. Has Arctic sea-ice loss contributed to increased surface melting of the Greenland ice sheet? *Journal of Climate*, 29:3373-3386.

Livingstone, S.J., C.D. Clark, J. Woodward and J. Kingslake, 2013. Potential subglacial lake locations and meltwater drainage pathways beneath the Antarctic and Greenland ice sheets. *Cryosphere*, 7:1721-1740.

Lüthi, M.P., C. Ryser, L.C. Andrews, G.A. Catania, M. Funk, R.L. Hawley, M.J. Hoffman and T. Neumann, 2015. Heat sources within the Greenland Ice Sheet: dissipation, temperate paleo-firn and cryo-hydrologic warming. *The Cryosphere*, 9:245-253.

Lutz, S., A.M. Anesio, S.E. Jorge Villar and L.G. Benning, 2014. Variations of algal communities cause darkening of a Greenland glacier. *FEMS Microbiology Ecology*, 89:402-414.

MacGregor, J.A., M.A. Fahnestock, G.A. Catania, J.D. Paden, S.P. Gogineni, S.K. Young, S.C. Rybarski, A.N. Mabrey, B.M. Wagman and M. Morlighem, 2015. Radiostratigraphy and age structure of the Greenland Ice Sheet. *Journal of Geophysical Research: Earth Surface*, 120:212-241.

Machguth, H., M. MacFerrin, D. van As, J.E. Box, C. Charalampidis, W. Colgan, R.S. Fausto, H.A.J. Meijer, E. Mosley-Thompson and R.S.W. van de Wal, 2016. Greenland meltwater storage in firn limited by near-surface ice formation. *Nature Climate Change*, 6:390-393.

Magnússon, E., J.M.C. Belart, F. Pálsson, H. Ágústsson and P. Crochet, 2015. Geodetic mass balance record with rigorous uncertainty estimates deduced from aerial photographs and LiDAR data. Case study from Drangajökull ice cap, NW-Iceland. *The Cryosphere Discussions*, 9:4733-4785.

Mair, D., D. Burgess, M. Sharp, J.A. Dowdeswell, T. Benham, S. Marshall and F. Cawkwell, 2009. Mass balance of the Prince of Wales Icefield, Ellesmere Island, Nunavut, Canada. *Journal of Geophysical Research*, 114:F02011, doi:10.1029/2008JF001082.

Marzeion, B., J.G. Cogley, K. Richter and D. Parkes, 2014. Attribution of global glacier mass loss to anthropogenic and natural causes. *Science Express*, 14 August 2014.

Matsuo, K. and K. Heki, 2013. Current ice loss in small glacier systems of the Arctic islands (Iceland, Svalbard, and the Russian High Arctic) from Satellite Gravimetry. *Terrestrial Atmospheric and Oceanic Sciences*, 24:657-670.

Matthews, T., C. Murphy, R.L. Wilby and S. Harrigan, 2014. Stormiest winter on record for Ireland and UK. *Nature Climate Change*, 4:738-740.

McFadden, E.M., I.M. Howat, I. Joughin, B.E. Smith and Y. Ahn, 2011. Changes in the dynamics of marine terminating outlet glaciers in west Greenland (2000–2009). *Journal of Geophysical Research*, 116: F02022, doi:10.1029/2010JF001757.

McGrath, D., W. Colgan, N. Bayou, A. Muto and K. Steffen, 2013. Recent warming at Summit, Greenland: Global context and implications. *Geophysical Research Letters*, 40:2091-2096.

McLeod, J.T. and T.L. Mote, 2016. Linking interannual variability in extreme Greenland blocking episodes to the recent increase in summer melting across the Greenland ice sheet. *International Journal of Climatology*, 36:1484-1499.

McMillan, M., A. Shepherd, N. Gourmelen, A. Dehecq, A. Leeson, A. Ridout, T. Flament, A. Hogg, L. Gilbert, T. Benham, M. van den Broek, J.A. M., Dowdeswell, X. Fettweis, B. Noel and T. Strozzi, 2014. Rapid dynamic activation of a marine-based Arctic ice cap. *Geophysical Research Letters*, 41:8902-8909.

McNabb, R.W. and R. Hock, 2014. Alaska tidewater glacier terminus positions, 1948–2012. *Journal of Geophysical Research: Earth Surface*, 119:153-167.

McNabb, R.W., R. Hock and M. Huss, 2015. Variations in Alaska tidewater glacier frontal ablation, 1985–2013. *J. Geophys. Res. Earth Surf.*, 120:120-136.

Meier, W.N., S. Gerland, M.A. Granskog, J.R. Key, C. Haas, G.K. Hovelsrud, K.M. Kovacs, A. Makshtas, C. Michel, D. Perovich, J.D. Reist and B.E.H. van Oort, 2011. Sea ice. In: *Snow, Water, Ice and Permafrost in the Arctic (SWIPA): Climate and the Cryosphere*. Arctic Monitoring and Assessment Programme (AMAP), Oslo, Norway.

Mernild, S.H., N.T. Knudsen, W.H. Lipscomb, J.C. Yde, J.K. Malmros, B.H. Jakobsen and B. Hasholt, 2011. Increasing mass loss from Greenland's Mittivakkat Gletscher. *The Cryosphere*, 5:341-348.

Mernild, S.H., W.H. Lipscomb, D.B. Bahr, V. Radić and M. Zemp, 2013a. Global glacier retreat: A revised assessment of committed mass losses and sampling uncertainties. *The Cryosphere*, 7:1565-1577.

Mernild, S.H., N.T. Knudsen, M.J. Hoffman, J.C. Yde, W.H. Lipscomb, E. Hanna, J.K. Malmros and R.S. Fausto, 2013b. Volume and velocity changes at Mittivakkat Gletscher, Southeast Greenland, 1994–2012. *Journal of Glaciology*, 59:660-670.

Mernild, S.H., G.E. Liston and C.A. Hiemstra, 2014. Northern hemisphere glaciers and ice caps surface mass balance and contribution to sea-level rise. *Journal of Climate*, 27:6051-6073.

Mernild, S.H., J.K. Malmros, J.C. Yde, R. Wilson, N.T. Knudsen, E. Hanna, R.S. Fausto and D. van As, 2015a, Albedo decline on Greenland's Mittivakkat Gletscher in a warming climate. *International Journal of Climatology*, 35:2294-2307.

Mernild, S.H., E. Hanna, J.R. McConnell, M. Sigl, A.P. Beckerman, J.C. Yde, J. Cappelen and K. Steffen, 2015b. Greenland precipitation trends in a long-term instrumental climate context (1890–2012): Evaluation of coastal and ice core records. *International Journal of Climatology*, 35:303-320.

Mikkelsen, A.B., A. Hubbard, M. MacFerrin, J. Box, S. Doyle, A. Fitzpatrick, B. Hasholt and H. Bailey, 2016. Extraordinary runoff from the Greenland Ice Sheet in 2012 amplified by hypsometry and depleted firn-retention. *The Cryosphere Discussions*, 9:4625-4660.

Miller, G.H., S.J. Lehman, K.A. Refsnider, J.R. Southon and Y. Zhong, 2013. Unprecedented recent summer warmth in Arctic Canada. *Geophysical Research Letters*, 40:5745-5751.

Min, S-K., X. Zhang, F.W. Zwiers and G.C. Hegerl, 2011. Human contribution to more-intense precipitation extremes. *Nature*, 470:378-381.

Moholdt, G., C. Nuth, J.O. Hagen and J. Kohler, 2010. Recent elevation changes of Svalbard glaciers derived from ICESat laser altimetry. *Remote Sensing of Environment*, 114:2756-2767.

Moholdt, G., B. Wouters and A.S. Gardner, 2012. Recent mass changes of glaciers in the Russian High Arctic. *Geophysical Research Letters*, 39:L10502, doi:10.1029/2012GL051466.

Moon, T., I. Joughin, B. Smith and I. Howat, 2012. 21st-Century evolution of Greenland outlet glacier velocities. *Science*, 336:576-578.

Moore, J.C., A. Grinsted, T. Zwinger and S. Jevrejeva, 2013. Semiempirical and process-based global sea level projections. *Reviews of Geophysics*, 51:484-522.

Morlighem, M., E. Rignot, J. Mouginot, H. Seroussi and E. Larour, 2014. Deeply incised submarine glacial valleys beneath the Greenland Ice Sheet. *Nature Geoscience*, 7:418-422.

Motyka, R.J., W.P. Dryer, J. Amundson, M. Truffer and M. Fahnestock, 2013. Rapid submarine melting driven by subglacial discharge, LeConte Glacier, Alaska. *Geophysical Research Letters*, 40:5153-5158.

Mouginot, J., E. Rignot, B. Scheuchl, I. Fenty, A. Khazendar, M. Morlighem, A. Buzzi and J. Paden, 2015. Fast retreat of Zachariae Isstrøm, northeast Greenland. *Science*, 350:1357-1361.

Muravjev, A.Y., 2014. Glacier size changes in Kronotsky Peninsula and Alney-Chashakondzha Massif, Kamchatka Peninsula in the second half of XX century and the beginning of XXI century. *Ice and Snow*, 54:22-28. (In Russian) doi:10.15356/2076-6734-2014-2-22-28.

Muraviev, A.Y. and G.A. Nosenko, 2013. Glaciation change in the northern part of the Middle Range on the Kamchatka Peninsula in the second half of the XX century. *Ice and Snow*, 53:5-11. (In Russian) doi:10.15356/2076-6734-2013-2-5-11.

Nagler, T., H. Rott, M. Hetzenecker, J. Wuite and P. Potin, 2015. The Sentinel-1 mission: new opportunities for ice sheet observations. *Remote Sensing*, 7:9371-9389.

Neff, W.G. F. Compo, M. Ralph and M.D. Shupe, 2014. Continental heat anomalies and the extreme melting of the Greenland ice surface in 2012 and 1889. *Journal of Geophysical Research: Atmospheres*, 119:6520-6536.

Nghiem, S., D. Hall, T. Mote, M. Tedesco, M. Albert, K. Keegan, C. Shuman, N. DiGirolamo and G. Neumann, 2012. The extreme melt across the Greenland ice sheet in 2012. *Geophysical Research Letters*, 39:L20502, doi:10.1029/2012GL053611.

Niwano, M., T. Aoki, S. Matoba, S. Yamaguchi, T. Tanikawa, K. Kuchiki and H. Motoyama, 2015. Numerical simulation of extreme snowmelt observed at the SIGMA-A site, northwest Greenland, during summer 2012. *The Cryosphere*, 9:971-988.

Nuth, C., G. Moholdt, J. Kohler, J.O. Hagen and A. Kääb, 2010. Svalbard glacier elevation changes and contribution to sea level rise. *Journal of Geophysical Research*, 115, F01008, doi:10.1029/2008JF001223.

Nuth, C., J. Kohler, M. König, A. von Deschwanden, J.O. Hagen, A. Kääb, G. Moholdt and R. Pettersson, 2013. Decadal changes from a multi-temporal glacier inventory of Svalbard. *The Cryosphere*, 7:1603-1621.

Palmer, S., A. Shepherd, P. Nienow, I. Joughin, 2011. Seasonal speedup of the Greenland Ice Sheet linked to routing of surface water. *Earth and Planetary Science Letters*, 302:423-428.

Palmer, S.J., J.A. Dowdeswell, P. Christoffersen, D.A. Young, D.D. Blankenship, J.S. Greenbaum, T. Benham, J. Bamber and M.J. Siegert, 2013. Greenland subglacial lakes detected by radar. *Geophysical Research Letters*, 40:6154-6159.

Palmer, S.M., M. McMillan and M. Morlighem, 2015. Subglacial lake drainage detected beneath the Greenland ice sheet. *Nature Communications*, 6:8408, doi:10.1038/ncomms9408.

Pálsson, F., S. Guðmundsson, H. Björnsson, E. Berthier, E. Magnússon, S. Guðmundsson and H.H. Haraldsson, 2012. Mass and volume changes

of Langjökull ice cap, Iceland ~1890 to 2009, deduced from old maps, satellite images and in situ mass balance measurements. *Jökull*, 62:81-96.

Pettersson, R., P. Christoffersen, J.A. Dowdeswell, V.A. Pohjola, A. Hubbard and T. Strozzi, 2011. Ice thickness and basal conditions of Vestfonna ice cap, Eastern Svalbard. *Geografiska Annaler A*, 93:311-322.

Pfeffer W.T., A.A Arendt, A. Bliss, T. Bolch, J.G. Cogley, A.S. Gardner, J.-O. Hagen, R. Hock, G. Kaser, C. Kienholz, E.S. Miles, G. Moholdt, N. Mölg, F. Paul, V. Radić, P. Rastner, B.H. Raup, J. Rich and M.J. Sharp, 2014. The Randolph Glacier Inventory: a globally complete inventory of glaciers. *Journal of Glaciology*, 60:537-552.

Phillips, T., H. Rajaram and K. Steffen, 2010. Cryo-hydrologic warming: A potential mechanism for rapid thermal response of ice sheets. *Geophysical Research Letters*, 37:L20503, doi:10.1029/2010GL044397.

Phillips, T., H. Rajaram, W. Colgan, K. Steffen and W. Abdalati, 2013. Evaluation of cryo-hydrologic warming as an explanation for increased ice velocities in the wet snow zone, Sermeq Avannarleq, West Greenland. *Journal of Geophysical Research: Earth Surface*, 118:1241-1256.

Poinar, K., I. Joughin, S.B. Das, M.D. Behn, J.T.M. Lenaerts and M.R. van den Broeke, 2015. Limits to future expansion of surface-melt-enhanced ice flow into the interior of western Greenland. *Geophysical Research Letters*, 42:1800-1807.

Polashenski, C., Z. Courville, C. Benson, A. Wagner, J. Chen, G. Wong, R. Hawley and D. Hall, 2014. Observations of pronounced Greenland Ice Sheet firm warming and implications for runoff production. *Geophysical Research Letters*, 41:4238-4246.

Polashenski, C., J.E. Dibb, M.G. Flanner, J.Y. Chen, Z.R. Courville, A.M. Lai, J.J. Schauer, M.M. Shafer and M. Bergin, 2015. Neither dust nor black carbon causing apparent albedo decline in Greenland's dry snow zone: implications for MODIS C5 surface reflectance. *Geophysical Research Letters*, 42:9319-9327.

Proshutinsky, A., D. Dukhovskoy, M.-L. Timmermans, R. Krishfield and J.L. Bamber, 2015. Arctic circulation regimes. *Philosophical Transactions of the Royal Society A*, 373:20140160.

Prowse, T., K. Alfredsen, S. Beltaos, B. Bonsal, C. Duguay, A. Korhola, J. McNamara, W.F. Vincent, V. Vuglinsky and G. Weyhenmeyer, 2011. Changing lake and river ice regimes: trends effects and implications. In: *Snow, Water, Ice and Permafrost in the Arctic (SWIPA): Climate and the Cryosphere. Arctic Monitoring and Assessment Programme (AMAP)*, Oslo, Norway.

Rahmstorf, S., J.E. Box, G. Feulner, M.E. Mann, A. Robinson, S. Rutherford and E.J. Schaffernicht, 2015. Exceptional twentieth-century slowdown in Atlantic Ocean overturning circulation. *Nature Climate Change*, 5:475-480.

Raiswell, R., 2011. Iceberg-hosted nanoparticulate Fe in the Southern Ocean: Mineralogy, origin, dissolution kinetics and source of bioavailable Fe. *Deep-Sea Research II*, 58:1364-1375.

Raiswell, R., L.G. Benning, L. Davidson and M. Tranter, 2008. Nanoparticulate bioavailable iron minerals in icebergs and glaciers. *Mineralogical Magazine*, 72:345-348.

Rajewicz, J. and S.J. Marshall, 2014. Variability and trends in anticyclonic circulation over the Greenland ice sheet, 1948–2013. *Geophysical Research Letters*, 41:2842-2850.

Rasmussen, L.A., H. Conway, R.M. Krimmel and R. Hock, 2011. Surface mass balance, thinning and iceberg production, Columbia Glacier, Alaska, 1948–2007. *Journal of Glaciology*, 57:431-440.

Rastner, P., T. Bolch, N. Mölg, H. Machguth, R. Le Bris and F. Paul, 2012. The first complete inventory of the local glaciers and ice caps on Greenland. *The Cryosphere*, 6:1483-1495.

Reijmer, C.H., M.R. van den Broeke, X. Fettweis, J. Ettema and L.B. Stap, 2012. Refreezing on the Greenland ice sheet: a comparison of parameterizations. *The Cryosphere*, 6:743-762.

Rennermalm, A.K., L.C. Smith, V.W. Chu, J.E. Box, R.R. Forster, M.R. Van den Broeke, D. Van As and S.E. Moustafa, 2013. Evidence of meltwater retention within the Greenland ice sheet. *The Cryosphere*, 7:1433-1445.

Rignot, E. and J. Mouginot, 2012. Ice flow in Greenland for the International Polar Year 2008–2009. *Geophysical Research Letters*, 39:L11501, doi:10.1029/2012GL051634.

Rignot, E., J.E. Box, E. Burgess and E. Hanna, 2008. Mass balance of the Greenland ice sheet from 1958 to 2007. *Geophysical Research Letters*, 35, L20502, doi:10.1029/2008GL035417.

Rignot, E., M. Koppes and I. Velicogna, 2010. Rapid submarine melting of the calving faces of West Greenland glaciers. *Nature Geoscience*, 3:187-191.

Rignot, E., I. Velicogna, M.R. van den Broeke, A. Monaghan and J. Lenaerts, 2011. Acceleration of the contribution of the Greenland and Antarctic ice sheets to sea level rise. *Geophysical Research Letters*, 38:L05503, doi:10.1029/2011GL046583.

Rignot, E., I. Fenty, Y. Xu, C. Cai and C. Kemp, 2015. Undercutting of marine-terminating glaciers in West Greenland. *Geophysical Research Letters*, 42:5909-5917.

Rysgaard, S., J. Mortensen, T. Juul-Pedersen, L.L. Sørensen, K. Lennert, D.H. Søgaard, K.E. Arendt, M.E. Bligher, M.K. Sejr and J. Bendtsen, 2012. High air-sea CO₂ uptake rates in nearshore and shelf areas of Southern Greenland: Temporal and spatial variability. *Marine Chemistry*, 128-129:26-33.

Schild, K.M., R.L. Hawley and B.F. Morriss, 2016. Subglacial hydrology at Rink Isbra, West Greenland inferred from sediment plume appearance. *Annals of Glaciology*, 57:118-127.

Schlegel, N.-J., E. Larour, H. Seroussi, M. Morlighem and J.E. Box, 2015. Ice discharge uncertainties in Northeast Greenland from boundary conditions and climate forcing of an ice flow model. *Journal of Geophysical Research: Earth Surface*, 120:29-54.

Sedov, R.V., 1997a. Glaciers of Chukotka. *Data of Glaciological Studies*, 82:213-217. (In Russian)

Sedov, R.V., 1997b. Glaciers Taigonus Peninsula. *Data of Glaciological Studies*, 82:218-221. (In Russian)

Selmes, N., T. Murray and T.D. James, 2011. Fast draining lakes on the Greenland Ice Sheet. *Geophysical Research Letters*, 38:L15501, doi:10.1029/2011GL047872.

Seo, K.-W., D.E. Waliser, C.-K. Lee, B. Tian, T. Scambos, B.-M. Kim, J.H. van Angelen and M.R. van den Broeke, 2015. Accelerated mass loss from Greenland ice sheet: Links to atmospheric circulation in the North Atlantic. *Global and Planetary Change*, 128:61-71.

Shahgedanova, M., G. Nosenko, I. Bushueva and M. Ivanov, 2012. Changes in area and geodetic mass balance of small glaciers, Polar Urals, Russia, 1950–2008. *Journal of Glaciology*, 58:953-964.

Shannon, S., A. Payne, I. Bartholomew, M. van den Broeke, T. Edwards, X. Fettweis, O. Gagliardini, F. Gillet-Chaulete, H. Goelzerg, M. Hoffmann, P. Huybrechts, D. Mair, P. Nienow, M. Perego, S. Price, C. Smeets, A. Sole, R. van de Wal and T. Zwinger, 2013. Enhanced basal lubrication and the contribution of the Greenland ice sheet to future sea-level rise. *Proceedings of the National Academy of Sciences*, 110:14156-14161.

Sharp, M., M. Ananicheva, A. Arendt, J.-O. Hagen, R. Hock, E. Josberger, R.D. Moore, W.T. Pfeffer and G.J. Wolken, 2011a. Mountain glaciers and icecaps. In: *Snow, Water, Ice and Permafrost in the Arctic (SWIPA): Climate and the Cryosphere. Arctic Monitoring and Assessment Programme (AMAP)*, Oslo, Norway.

Sharp, M., D.O. Burgess, J.G. Cogley, M. Ecclestone, C. Labine and G.J. Wolken, 2011b. Extreme melt on Canada's Arctic ice caps in the 21st century. *Geophysical Research Letters*, 38:L11501, doi:10.1029/2011GL047381.

Sharp, M., D.O. Burgess, F. Cawkwell, L. Copland, J.A. Davis, E.K. Dowdeswell, J.A. Dowdeswell, A.S. Gardner, D. Mair, L. Wang, S.N. Williamson, G.J. Wolken and F. Wyatt, 2014. Remote sensing of recent glacier changes in the Canadian Arctic. In: *Global Land Ice Measurements from Space: Satellite Multispectral Imaging of Glaciers*. pp. 205–228.

Shepherd, A., Z. Du, T.J. Benham, J.A. Dowdeswell and E.M. Morris, 2007. Mass balance of Devon Ice Cap, Canadian Arctic. *Annals of Glaciology*, 46:249-254.

Shepherd, A., E.R. Ivins, A. Geruo, V.R. Barletta, M.J. Bentley, S. Bettadpur, K.H. Briggs, D.H. Bromwich, R. Forsberg, N. Galin, M. Horwath, S. Jacobs, I. Joughin, M.A. King, J.T.M. Lenaerts, J. Li, S.R.M. Ligtenberg, A. Luckman, S.B. Luthcke, M. McMillan, R. Meister, G. Milne, J. Mouginot, A. Muir, J.P. Nicolas, J. Paden, A.J. Payne, H. Pritchard, E. Rignot, H. Rott, L.S. Sørensen, T.A. Scambos, B. Scheuchl, E.J.O. Schrama, B. Smith, A.V. Sundal, J.H. van Angelen, W.J. van de Berg, M.R. van den Broeke, D.G. Vaughan, I. Velicogna, J. Wahr, P.L. Whitehouse, D.J. Wingham, D. Yi, D. Young and H.J. Zwally, 2012. A reconciled estimate of ice-sheet mass balance. *Science*, 338:1183-1189.

Short, N.H. and A.L. Gray, 2004. Potential for RADARSAT-2 interferometry: glacier monitoring using speckle tracking. *Canadian Journal of Remote Sensing*, 30:504-509.

Short, N.H. and A.L. Gray, 2005. Glacier dynamics in the Canadian High Arctic from RADARSAT-1 speckle tracking. *Canadian Journal of Remote Sensing*, 31:225-239.

Smith, L.C., V.W. Chu, K. Yang, C.J. Gleason, L.H. Pitcher, A.K. Rennermalm, C.J. Legleiter, A.E. Behar, B.T. Overstreet, S.E. Moustafa, M. Tedesco, R.R. Forster, A.L. LeWinter, D.C. Finnegan, Y. Sheng and J. Balog, 2015. Efficient meltwater drainage through supraglacial streams and rivers on the southwest Greenland Ice Sheet. *Proceedings of the National Academy of Sciences USA*, 112:1001-1006.

Sole, A., P. Nienow, I. Bartholomew, D. Mair, T. Cowton, A. Tedstone and M. King, 2013. Winter motion mediates dynamic response of the Greenland ice sheet to warmer summers. *Geophysical Research Letters*, 40:3940-3944.

Søndergaard, J., M.P. Tamstorf, B. Elberling, M.M. Larsen, M.R. Mylius, M. Lund, J. Abermann and F. Rigét, 2015. Mercury exports from a High-Arctic river basin in Northeast Greenland (74°N) largely controlled by glacial lake outburst floods. *Science of the Total Environment*, 514:83-91.

Steffen, K., J.E. Box and W. Abdalati, 1996. Greenland Climate Network: GC-Net. In: Colbeck, S.C. (ed.), CRREL 96-27 Special Report on Glaciers, Ice Sheets and Volcanoes, pp. 98-103.

Stevens, L.A., M.D. Behn, J.J. McGuire, S.B. Das, I. Joughin, T. Herring, D.E. Shean and M.A. King, 2015. Greenland supraglacial lake drainages triggered by hydrologically induced basal slip. *Nature*, 522:73-76.

Stibal, M., M. Šabacká and J. Žárský, 2012. Biological processes on glacier and ice sheet surfaces. *Nature Geoscience*, 5:771-774.

Stokes, C.R., M. Shahgedanova, I.S. Evans and V.V. Popovniv, 2013. Accelerated loss of alpine glaciers in the Kodar Mountains, south-eastern Siberia. *Global and Planetary Change*, 101:82-96.

Straneo, F. and P. Heimbach, 2013. North Atlantic warming and the retreat of Greenland's outlet glaciers. *Nature*, 504:36-43.

Straneo, F., R. Curry, D.A. Sutherland, G. Hamilton, C. Cenedese, K. Väge and L.A. Stearns, 2011. Impact of fjord dynamics and subglacial discharge on the circulation near Helheim Glacier in Greenland. *Nature Geoscience*, 4:322-327.

Straneo, F., D.A. Sutherland, D. Holland, C. Gladish, G. Hamilton, H. Johnson, E. Rignot, Y. Xu and M. Koppes, 2012. Characteristics of ocean waters reaching Greenland's glaciers. *Annals of Glaciology*, 53:202-210.

Sund, M., T.R. Lauknes and T. Eiken, 2014. Surge dynamics in the Nathorstbreen glacier system, Svalbard. *The Cryosphere*, 8:623-638.

Sundal, A., A. Shepherd, P. Nienow, E. Hanna, S. Palmer and P. Huybrechts, 2011. Melt-induced speed-up of Greenland ice sheet offset by efficient subglacial drainage. *Nature*, 469:521-524.

Sutherland, D.A. and F. Straneo, 2012. Estimating ocean heat transport and submarine melt rate in Sermilik Fjord, Greenland, using lowered ADCP velocity profiles. *Annals of Glaciology*, 53:50-58.

Tedesco, M., X. Fettweis, M.R. Van den Broeke, R.S.W. van de Wal, C.J.P.P. Smeets, W.J. Van de Berg, M.C. Serreze and J.E. Box, 2011. The role of albedo and accumulation in the 2010 melting record in Greenland. *Environmental Research Letters*, 6:014005.

Tedesco, M., M. Lüthje, K. Steffen, N. Steiner, X. Fettweis, I. Willis, N. Bayou and A. Banwell, 2012. Measurement and modeling of ablation of the bottom of supraglacial lakes in western Greenland. *Geophysical Research Letters*, 39:L02502, doi:10.1029/2011GL049882.

Tedesco, M., X. Fettweis, T. Mote, J. Wahr, P. Alexander, J.E. Box and B. Wouters, 2013a. Evidence and analysis of 2012 Greenland records from spaceborne observations, a regional climate model and reanalysis data. *The Cryosphere*, 7:615-630.

Tedesco, M., P. Alexander, J.E. Box, J. Cappelen, T. Mote, K. Steffen, R.S.W. van de Wal, J. Wahr and B. Wouters, 2013b. (Arctic) Greenland ice sheet [in "State of the Climate in 2012"]. *Bulletin of the American Meteorological Society*, 94:S121-123.

Tedesco, M., J.E. Box, J. Cappelen, X. Fettweis, T.S. Jensen, T. Mote, A.K. Rennermalm, L.C. Smith, R.S.W. van de Wal and J. Wahr, 2014. Greenland Ice Sheet [in "State of the Climate in 2013"]. *Bulletin of the American Meteorological Society*, 95:S5-49.

Tedesco, M., J.E. Box, J. Cappelen, R.S. Fausto, X. Fettweis, K. Hansen, T. Mote, C.J.P.P. Smeets, D. van As, R.S.W. van de Wal and J. Wahr, 2015. Greenland. [in Arctic Report Card 2015], Jeffries M. and J. Richter-Menge (eds.).

Tedesco, M., S. Doherty, X. Fettweis, P. Alexander, J. Jeyaratnam and J. Stroeve, 2016a. The darkening of the Greenland ice sheet: trends, drivers, and projections (1981–2100). *The Cryosphere*, 10:477-496.

Tedesco, M., T. Mote, X. Fettweis, E. Hanna, J. Jeyaratnam, J.F. Booth, R. Datta and K. Briggs, 2016b. Arctic cut-off high drives the poleward shift of a new Greenland melting record. *Nature Communications*, 7:11723, doi:10.1038/ncomms11723.

Tedstone, A.J., P.W. Nienow, N. Gourmelen, A. Dehecq, D. Goldberg and E. Hanna, 2015. Decadal slowdown of a land-terminating sector of the Greenland Ice Sheet despite warming. *Nature*, 526:692-695.

Trachsel, M. and A. Nesje, 2015. Modelling annual mass balances of eight Scandinavian glaciers using statistical models. *The Cryosphere*, 9:1401-1414.

Trüssel, B.L., R.J. Motyka, M. Truffer and C.F. Larsen, 2013. Rapid thinning of lake-calving Yakutat Glacier and the collapse of the Yakutat Icefield, southeast Alaska, USA. *Journal of Glaciology*, 59:149-161.

Utsumi, N., S. Seto, S. Kanae, E.E. Maed and T. Oki, 2011. Does higher surface temperature intensify extreme precipitation? *Geophysical Research Letters*, 38:L16708, doi:10.1029/2011GL048426.

Vallelonga, P., K. Christianson, R.B. Alley, S. Anandakrishnan, J.E.M. Christian, D. Dahl-Jensen, V. Gkinis, C. Holme, R.W. Jacobel, N.B. Karlsson, B.A. Keisling, S. Kipfstuhl, H.A. Kjær, M.E.L. Kristensen, A. Muto, L.E. Peters, T. Popp, K.L. Riverman, A.M. Svensson, C. Tibuleac, B.M. Vinther, Y. Weng and M. Winstrup, 2014. Initial results from geophysical surveys and shallow coring of the Northeast Greenland Ice Stream (NEGIS). *The Cryosphere*, 8:1275-1287.

Van Angelen, J.H., J.T.M. Lenaerts, M.R. van den Broeke, X. Fettweis and E. van Meijgaard, 2013. Rapid loss of firn pore space accelerates 21st century Greenland mass loss. *Geophysical Research Letters*, 40:2109-2113.

Van As, D., A.L. Hubbard, B. Hasholt, A.B. Mikkelsen, M.R. van den Broeke and R.S. Fausto, 2012. Large surface meltwater discharge from the Kangerlussuaq sector of the Greenland ice sheet during the record-warm year 2010 explained by detailed energy balance observations. *The Cryosphere*, 6:199-209.

Van As, D., R.S. Fausto, W.T. Colgan, J.E. Box and PROMICE project team, 2013. Darkening of the Greenland ice sheet due to the melt-albedo feedback observed at PROMICE weather stations. *Geological Survey of Denmark and Greenland Bulletin*, 28:69-72.

Van As, D., M.L. Andersen, D. Petersen, X. Fettweis, J.H. Van Angelen, J.T.M. Lenaerts, M.R. Van den Broeke, J.M. Lea JM, C.E. Boggild, A.P. Ahlstrom and K. Steffen, 2014. Increasing meltwater discharge from the Nuuk region of the Greenland ice sheet and implications for mass balance (1960-2012). *Journal of Glaciology*, 60:314-322.

Van de Wal, R.S.W., C.J.P.P. Smeets, W. Boot, M. Stoffelen, R. van Kampen, S.H. Doyle, F. Wilhelms, M.R. van den Broeke, C.H. Reijmer, J. Oerlemans and A. Hubbard, 2015. Self-regulation of ice flow varies across the ablation area in south-west Greenland. *The Cryosphere*, 9:603-611.

Van der Veen, C.J., 1998. Fracture mechanics approach to penetration of surface crevasses on glaciers. *Cold Regions Science and Technology*, 27:31-47.

Van der Veen, C., J. Plummer and L. Stearns, 2011. Controls on the recent speed-up of Jakobshavn Isbræ, West Greenland. *Journal of Glaciology*, 57:770-782.

Van Tricht, K., S. Lhermitte, J.T.M. Lenaerts, I.V. Gorodetskaya, T.S. L'Ecuyer, B. Noël, M.R. van den Broeke, D.D. Turner and N.P.M. van Lipzig, 2016. Clouds enhance Greenland ice sheet meltwater runoff. *Nature Communications*, 7:10266.

Van Wychen, W., 2015. The Dynamics and Dynamic Discharge of the Ice Masses and Tidewater Glaciers of the Canadian High Arctic. Phd. Thesis. University of Ottawa.

Van Wychen, W., L. Copland, L. Gray, D.O. Burgess, B. Danielson and M. Sharp, 2012. Spatial and temporal variation of ice motion and ice flux from Devon Ice Cap, Nunavut, Canada. *Journal of Glaciology*, 58:657-664.

Van Wychen, W., D.O. Burgess, L. Gray, L. Copland, M. Sharp, J.A. Dowdeswell and T.J. Benham, 2014. Glacier velocities and dynamic ice discharge from the Queen Elizabeth Islands, Nunavut, Canada. *Geophysical Research Letters*, 41:484-490.

Van Wychen, W., L. Copland, D.O. Burgess, L. Gray and N. Schaffer, 2015. Glacier velocities and dynamic discharge from the ice masses of Baffin Island and Bylot Island, Nunavut, Canada. *Canadian Journal of Earth Sciences*, 52:980-989.

Van Wychen, W., J. Davis, D.O. Burgess, L. Copland, L. Gray, M. Sharp and C. Mortimer, 2016. Characterizing inter-annual variability of glacier dynamics (1999–2015) and dynamic discharge (2000, 2011–2015) for the ice masses of Ellesmere and Axel Heiberg Islands, Nunavut, Canada. *Journal of Geophysical Research: Earth Surface*, 121:39-63.

Vaughan, D.G., J.C. Comiso, I. Allison, J. Carrasco, G. Kaser, R. Kwok, P. Mote, T. Murray, F. Paul, J. Ren, E. Rignot, O. Solomina, K. Steffen and T. Zhang, 2013. Observations: cryosphere. In: Stocker, T.F., D. Qin, G.-K. Plattner, M. Tignor, S.K. Allen, J. Boschung, A. Nauels, Y. Xia, V. Bex and P.M. Midgley (eds.), *Climate Change 2013: The Physical Science Basis. Contribution of Working Group I to the Fifth Assessment Report of the Intergovernmental Panel on Climate Change*. Cambridge University Press.

Velicogna, I., T.C. Sutterley and M.R. van den Broeke, 2014. Regional acceleration in ice mass loss from Greenland and Antarctica using

GRACE time-variable gravity data. *Journal of Geophysical Research: Space Physics*, 41:8130-8137.

Vernon, C.L., J.L. Bamber, J.E. Box, M.R. van den Broeke, X. Fettweis, E. Hanna and P. Huybrechts, 2013. Surface mass balance model intercomparison for the Greenland ice sheet. *The Cryosphere*, 7:599-614.

Wadham, J., R. De'ath, F.M. Monteiro, M. Tranter, A. Ridgwell, R. Raiswell and S. Tulaczyk, 2013. The potential role of the Antarctic Ice Sheet in global biogeochemical cycles. *Earth and Environmental Science Transactions of the Royal Society of Edinburgh*, 104:55-67.

Weertman, J., 1973. Can a water-filled crevasse reach the bottom surface of a glacier? *International Association of Hydrological Sciences*, 95:139-145.

Weidick, A. and O. Bennike, 2007. Quaternary glaciation history and glaciology of Jakobshavn Isbræ and the Disko Bugt region, West Greenland: a review. *Geological Survey of Denmark and Greenland Bulletin*, 14.

Weidick, A., O. Bennike, M. Citterio and N. Nørgaard-Pedersen, 2012. Neoglacial historical glacier changes around Kangersuneq fjord in southern West Greenland. *Geological Survey of Denmark and Greenland Bulletin*, 27:1-68.

White, A., L. Copland, D. Mueller and W. Van Wychen, 2015. Assessment of historical changes (1959-2012) and the causes of recent break-ups of the Petersen ice shelf, Nunavut, Canada. *Annals of Glaciology*, 56:65-76.

Williams, M. and J.A. Dowdeswell, 2001. Historical fluctuations of the Matusevich Ice Shelf, Severnaya Zemlya, Russian High Arctic. *Arctic Antarctic and Alpine Research*, 33:211-222.

Willis, M.J., A.K. Melkonian and M.E. Pritchard, 2015. Outlet glacier response to the 2012 collapse of the Matusevich Ice Shelf, Severnaya Zemlya, Russian Arctic. *Journal of Geophysical Research: Earth Surface*, 120:2040-2055.

Winsvold, S.H., L.M. Andreassen and C. Kienholz, 2014. Glacier area and length changes in Norway from repeat inventories. *The Cryosphere*, 8:1885-1903.

Woollings, T., J.M. Gregory, J.G. Pinto, M. Reyers and D.J. Brayshaw, 2012. Response of the North Atlantic storm track to climate change shaped by ocean-atmosphere coupling. *Nature Geoscience*, 5:313-317.

Wouters, B., D. Chambers and E.J.O. Schrama, 2008. GRACE observes small-scale mass loss in Greenland. *Geophysical Research Letters*, 35:L20501, doi:10.1029/2008GL034816.

Xu, Y., E. Rignot, D. Menemenlis and M. Koppes, 2012. Numerical experiments on subaqueous melting of Greenland tidewater glaciers in response to ocean warming and enhanced subglacial discharge. *Annals of Glaciology*, 53:229-234.

Yang, Q., T.H. Dixon, P.G. Myers, J. Bonin, D. Chambers and M.R. van den Broeke, 2016. Recent increases in Arctic freshwater flux affects Labrador Sea convection and Atlantic overturning circulation. *Nature Communications*, 7:10525.

Yashayaev, I., 2007. Hydrographic changes in the Labrador Sea, 1960-2005. *Progress in Oceanography*, 73:242-276.

Zdanowicz, C.M., G.A. Zielinski and C.P. Wake, 1998. Characteristics of modern atmospheric dust deposition in snow on the Penny Ice Cap, Baffin Island, Arctic Canada. *Tellus*, 50B:506-520.

Zdanowicz, C.M., G.A. Zielinski and C.P. Wake, 2000. A Holocene record of atmospheric dust deposition on the Penny Ice Cap, Baffin island, Nunavut. *Quaternary Research*, 53:62-69.

Zdanowicz, C., A. Smetny-Sowa, D. Fisher, N. Schaffer, L. Copland, J. Eley and F. Dupont, 2012. Summer melt rates on Penny Ice Cap, Baffin Island: Past and recent trends and implications for regional climate. *Journal of Geophysical Research*, 117, F02006, doi:10.1029/2011JF002248.

Zheng, J., 2015. Archives of total mercury reconstructed with ice and snow from Greenland and the Canadian High Arctic. *Science of the Total Environment*, 509-510:133-144.

Zheng, J., W. Shotyk, M. Krachler and D.A. Fisher, 2007. A 15,800-year record of atmospheric lead deposition on the Devon Island Ice Cap, Nunavut, Canada: Natural and anthropogenic enrichments, isotopic composition, and predominant sources. *Global Biogeochemical Cycles*, 21:GB2027, doi:10.1029/2006GB002897.

Zwally, H.J., W. Abdalati, T. Herring, K. Larson, J. Saba and K. Steffen, 2002. Surface melt-induced acceleration of Greenland ice-sheet flow. *Science*, 297:218-222.

Zwally, H., J. Li, A. Brenner, M. Beckley, H. Cornejo, J. DiMarzio, M. Giovinetto, T. Neumann, J. Robbins, J. Saba, D. Yi and W. Wang, 2011. Greenland ice sheet mass balance: distribution of increased mass loss with climate warming: 2003-07 versus 1992-2002. *Journal of Glaciology*, 57:88-102.

7. Freshwater

LEAD AUTHORS: TERRY D. PROWSE, ARVID BRING, EDDY C. CARMACK, MARIKA M. HOLLAND, ARNE INSTANES, JOHANNA MÅRD, TIMO VIHMA, FREDERICK J. WRONA

Coordinating lead author shown in bold

Contents

Key Findings	170	7.7 Modeling	190
7.1 Introduction	170	7.7.1 Hierarchical modeling approaches	190
7.1.1 The Arctic Freshwater Synthesis	170	7.7.2 Using models to investigate Arctic freshwater variability and change	191
7.1.2 Previous Arctic freshwater programs	170	7.7.3 Knowledge gaps and research direction	192
7.1.3 Defining the geography of an Arctic freshwater domain	171	7.8 Summary	192
7.1.4 Chapter outline	173	7.8.1 Expanded AFD, TCA and role of storm tracks	193
7.2 Atmospheric freshwater	173	7.8.2 New hydro-ecological regimes	193
7.2.1 System function and key processes	173	7.8.3 Enhanced lake moisture flux	195
7.2.2 Observed changes and key drivers	174	7.8.4 Freshwater resources	195
7.2.3 Projected changes and key drivers	174	References	195
7.2.4 Knowledge gaps and future research	174		
7.3 Freshwater in the Arctic marine system	175		
7.3.1 System function and key processes	176		
7.3.2 Observed changes and key drivers	180		
7.3.3 Projected changes and key drivers	182		
7.3.4 Knowledge gaps and future research	183		
7.4 Terrestrial hydrology	183		
7.4.1 System functioning and key processes	184		
7.4.2 Observed changes and key drivers	184		
7.4.3 Projected changes and key drivers	185		
7.4.4 Knowledge gaps and future research	186		
7.5 Terrestrial freshwater ecosystems	186		
7.5.1 Observed and projected ecosystem responses	186		
7.5.2 Knowledge gaps and future research	188		
7.6 Resources	189		
7.6.1 System function and key processes	189		
7.6.2 Projected changes and key drivers	189		
7.6.3 Adaptation	189		
7.6.4 Knowledge gaps and future research	189		

Key Findings

- AMAP has played an active role in the development of an updated, comprehensive, and integrated review of the structure and function of the Arctic freshwater system – the *Arctic Freshwater Synthesis*.
- The Arctic hydrological cycle is accelerating. This highlights the need for more extensive and accurate observations, better process understanding, better models, and more extensive and systematic use of existing models.
- Defining the domain and characteristics of the Arctic freshwater system is critical to its study. The Arctic freshwater domain is broader than previously thought.
- Atmospheric moisture transport to the Arctic freshwater domain has increased, resulting in increased net precipitation and river run-off and a larger liquid freshwater storage in the Arctic. Via increased downward longwave radiation, the increased moisture transport has also contributed to sea ice melt.
- Terrestrial freshwater fluxes are accelerating, especially evapotranspiration and river discharge. Land-surface effects, for example, open-water evaporation from previously ice-covered areas, need better quantifying in climate models.
- Climate-cryospheric-hydrologic changes, coupled with multiple ecological feedbacks, are transforming Arctic landscapes. This is triggering ecosystem shifts and the development of new ecosystems. Projecting the relative geographic extent and magnitudes of such shifts carries great uncertainty. The catchment-scale should be considered an ecological unit of study in future studies. A new nearshore hydro-ecological regime is emerging.
- Employing a hierarchy of modeling approaches provides better insight about the functioning of the Arctic freshwater system. New model validation strategies and enhanced model capabilities are needed to advance modeling of the Arctic freshwater system.
- Efficient water resource management strategies are essential for maintaining freshwater supply and for minimizing the impact of flooding and related hazards associated with changes in freshwater systems. High-latitude terrestrial areas are becoming ‘water rich’, especially in winter, increasing the contrast with more ‘water poor’ regions at lower latitudes and thereby creating potential policy issues regarding future management of such regional water disparities.

7.1 Introduction

7.1.1 The Arctic Freshwater Synthesis

The topic ‘freshwater’ was not treated as a distinct component of the first SWIPA assessment (AMAP, 2011), but rather as an element of various topics and addressed to different levels of detail in several chapters of the report, most of which focused largely on water in its solid, cryospheric state. Since then, however, AMAP has actively supported the production of an *Arctic Freshwater Synthesis* (AFS_{Σ}), in conjunction with the World Climate Research Program’s Climate and Cryosphere Project (WCRP-CliC) and the International Arctic Science Committee. The key rationale for this initiative stems from increasing scientific knowledge and subsequent recognition that changes to the Arctic freshwater system have generated changes in biogeophysical and socio-economic systems of particular importance to northern residents, as well as generating extra-Arctic climatic effects that may have global consequences. To address such concerns, the *Arctic Freshwater Synthesis* focused on assessing the various Arctic freshwater sources, fluxes, storage and effects. Most of these are directly or indirectly controlled by cryospheric components and processes, which are reviewed in other chapters of this assessment.

The key objective of the *Arctic Freshwater Synthesis* – published as a Special Issue of the *Journal of Geophysical Research-Biogeosciences* – was to produce an updated, comprehensive, and integrated review of the structure and function of the entire Arctic freshwater system through an assessment of the most recent literature (Prowse et al., 2015a). As such, it was organized around six key themes: atmosphere (Vihma et al., 2016), oceans (Carmack et al., 2016), terrestrial hydrology (Bring et al., 2016), terrestrial and freshwater ecology (Wrona et al., 2016), resources (Instanes et al., 2016) and modeling (Lique et al., 2016); the review of each co-authored by an international group of over forty scientists from ten countries.

7.1.2 Previous Arctic freshwater programs

Introducing the *Arctic Freshwater Synthesis*, Prowse et al. (2015a) noted that freshwater, in its various physical states, at the northern high latitudes has been the focus of numerous scientific initiatives and related publications that have highlighted its critical role in Arctic ecology, human settlement, hydrology and climate. It is its role in the latter that first focused attention on the importance of the sources, storage and fluxes of freshwater in the Arctic. In fact, it was the effect of freshwater (from atmospheric inputs and continental run-off) on thermohaline circulation, first outlined by Weyl (1968) and then considered in more detail by Rooth (1982) and Aagaard and Carmack (1989), that focused attention on its role in global climate. Examining the sensitivity of the vertical circulation in salinity-stratified northern seas, Aagaard and Carmack (1989) concluded that even small variations in freshwater content could alter or even stop such convection and produce effects analogous to historical halocline catastrophes. Importantly, they extended the overall Arctic hydrologic system to include the freshwater flux generated by the freezing, transporting, and melting of sea ice (see also Chapter 5).

With increasing recognition of the importance of the Arctic freshwater/hydrologic system and how it could be altered by

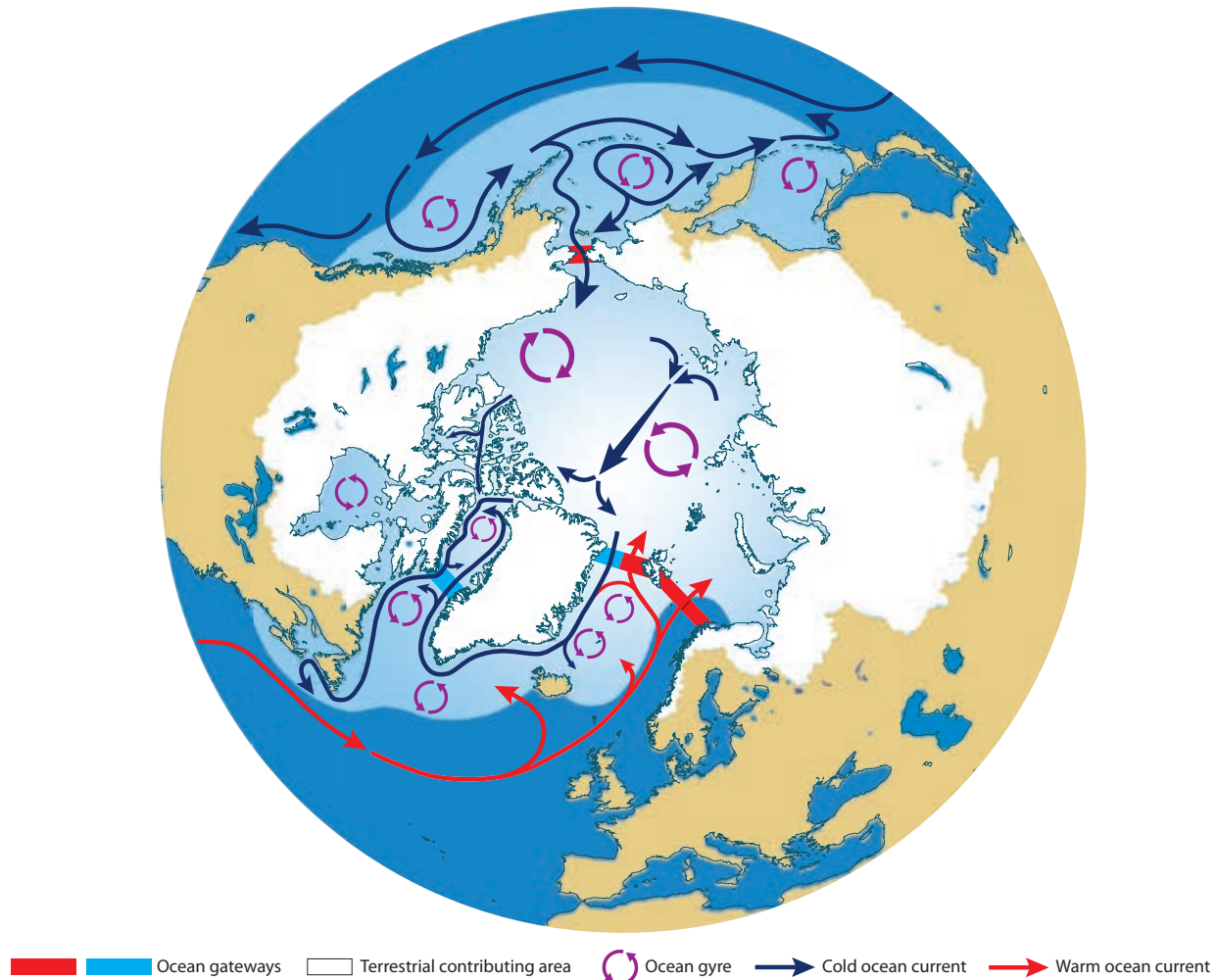


Figure 7.1 Domain of the Arctic Freshwater System (AFD) showing four Arctic Ocean gateways, eleven gyral circulation patterns, major ocean currents, and the All Arctic Regions (AAR) definition of the terrestrial contributing area shown in white (Prowse et al. 2015a).

changes in climate that affect freshwater production, storage and transport, several international scientific assessments, programs and plans began to evolve. These were reviewed by Prowse et al. (2015a), who documented how the foci of such programs gradually expanded from those focused on improving measurement and quantification of major freshwater budget components and fluxes, to those which also considered how changes in these elements affect the broader physical and ecological environment, both terrestrial and marine as well as human activities in the Arctic. The major programs reviewed include the Arctic Climate System Study (ACSYS) developed under the auspices of the World Climate Research Programme; The Freshwater Budget of the Arctic Ocean (FWBAO) generated at a NATO Advanced research workshop; a set of ocean, terrestrial, and socio-economic multi-year science plans produced for the Second International Conference on Arctic Research Planning (ICARP-II, 2005); the U.S. National Science Foundation-Arctic Systems Science, Community-wide Hydrologic Analysis and Monitoring Program (CHAMP) and related Arctic Freshwater Cycle: Land/Upper-Ocean Linkages study, commonly referred to as the Freshwater Integration study (FWI); and the Arctic-Subarctic Ocean Fluxes study (ASOF). One important issue affecting the overall foci of these programs, however, is the lack of a consistent definition of the geographic domain of the Arctic freshwater system (hereafter referred to as the Arctic Freshwater Domain, AFD).

7.1.3 Defining the geography of an Arctic freshwater domain

This section summarizes the findings of Prowse et al. (2015a). In defining the AFD, a number of geographical boundaries can be used based on atmospheric, marine, and terrestrial contexts. The classic Arctic freshwater-marine components include the four main oceanic gateways (Bering Strait, Davis Strait, Fram Strait, Barents Sea Opening) for water flowing into and out of the Arctic Ocean, as well as the extra-Arctic convective gyres located within the adjacent sub-Arctic Atlantic and Pacific oceans. Low-salinity water transported from the Arctic Ocean through the gateways as well as from latitudes south of the sub-Arctic gyres controls the degree of gyral convection. Hence, to obtain a comprehensive understanding of the Arctic freshwater system, requires the analysis of an AFD broader than simply the Arctic Ocean.

From a terrestrial perspective, a marine-based definition of the AFD is critical because it determines the extent of land contributing freshwater, either from river runoff or from glacier melt (Bring et al., 2016; Carmack et al., 2016) – in terms of the latter, contributions from the Greenland Ice Sheet (see Chapter 6) are especially significant because of its proximity to the North Atlantic convective gyres (Figure 7.1). From an atmospheric perspective, defining the geography of the AFD also aids in defining the major source regions and pathways of storm tracks



Figure 7.2 Schematic representation of lower (850 hPa) and upper (250 hPa) troposphere storm tracks (after Hoskins and Hodges, 2002).

(see Figure 7.2) that carry freshwater to the Arctic proper as well as to the major marine and terrestrial 'catchments' that transport the precipitated freshwater to critical regions of the AFD. Figure 7.2 provides a general schematic of such storm tracks. How their alignment, location and structure can be influenced by freshwater fluxes is explored by Carmack et al. (2016), Prowse et al. (2015a), Vihma et al. (2016), and in Section 7.3.

Many freshwater-budget analyses, beginning with that of Agaard and Carmack (1989), indicate that terrestrial rivers make the greatest freshwater contribution to the AFD, with significant variability noted in the size of this input. However, as reported by Prowse et al. (2015a) this is due not to natural variability in the hydro-climatic conditions determining discharge but to different geographical definitions of the terrestrial contributing area (TCA). Historically, there have been four major TCA-definitions: All Arctic Regions (AAR), Arctic Ocean Basin (AOB), Arctic Climate System Study (ACSYS), and Arctic Ocean River Basin (AORB) (Figure 7.3). However, the graphic shows a remarkable linear relationship between total flow and contributing area, indicating comparable runoff yields among the spatially conservative to geographically broader TCA-definitions.

In selecting an appropriate TCA based on knowledge of the 'downstream' marine pathways transporting river runoff, Prowse et al. (2015a) noted that it remains to be determined whether the south-flowing Baffin and Labrador currents

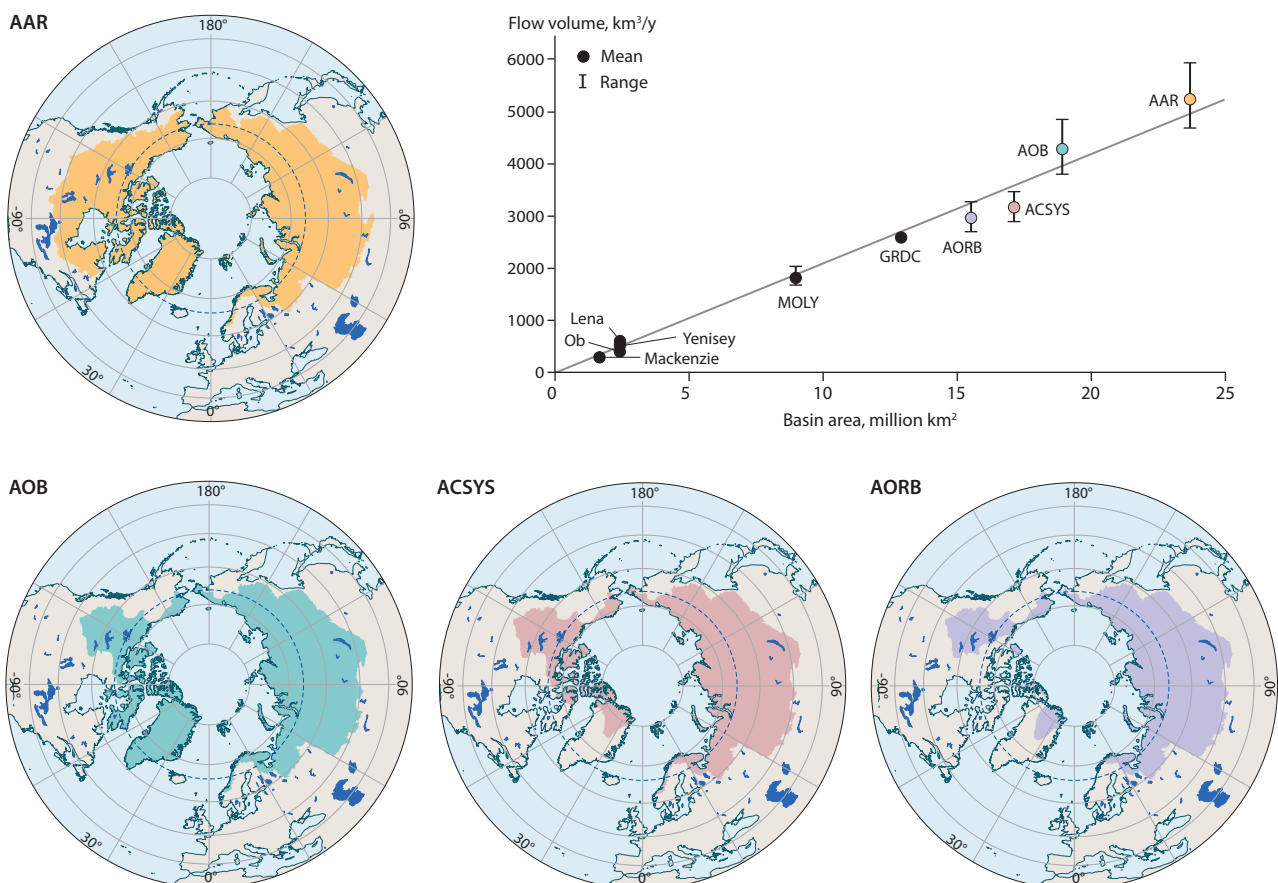


Figure 7.3 Four definitions for the terrestrial contributing area (TCA) part of the Arctic freshwater system: All Arctic Regions (AAR), Arctic Ocean Basin (AOB), Arctic Climate System Study (ACSYS), Arctic Ocean River Basin (AORB), and flow volume versus contributing area for the various TCAs including the Mackenzie, Ob, Lena, and Yenisey Basins (MOLY) and Global Runoff Data Centre (GRDC) (Prowse et al., 2015a).

reflect upon convergence with the Gulf Stream, cross the Atlantic, modify the salinity of subtropical waters en route, and recirculate back into the Arctic via the Fram and Barents Sea branches (Figure 7.1). If this is the case, then runoff from the Canadian Arctic Archipelago, central Canadian Arctic coast, and Hudson Bay would form an important part of the AFD and so be a requisite component to include in the calculation of an Arctic Ocean Freshwater Budget as previously conducted by Lewis et al. (2000).

Although the final marine trajectories and potential diluting effect on the North Atlantic system of freshwater fluxes remains to be fully determined (Carmack et al., 2016; Lique et al., 2016), the TCA considered most appropriate to define the AFD in the *Arctic Freshwater Synthesis*, was the AAR. This definition includes freshwater flowing into Hudson Bay, and discharge from the Yukon and Anadyrsky rivers, which drain into the eastern and western parts of the north Pacific Ocean thereby affecting the salinity of waters passing northward through Bering Strait into the Arctic Ocean. Important physical characteristics of the AAR are that a large majority of its contributing area, precipitation supply and lake storage are found well outside the Arctic Circle (66.6°N). See Section 7.4 and Prowse et al. (2015a) for further details concerning the AAR.

Although the AAR was used to define the AFD in the *Arctic Freshwater Synthesis*, one of the emerging issues (Prowse et al., 2015b; Carmack et al., 2016) was that further extending the AFD is probably warranted – beyond the classical gateways used in most ocean freshwater budgets and beyond the AAR. See Sections 7.3 and 7.8 for further details.

7.1.4 Chapter outline

The following sections provide synopses of the six thematic areas comprising the *Arctic Freshwater Synthesis*: Section 7.2, atmosphere (Vihma et al., 2016); Section 7.3, oceans (Carmack et al., 2016); Section 7.4, terrestrial hydrology (Bring et al., 2016); Section 7.5, terrestrial and freshwater ecosystems (Wrona et al., 2016); Section 7.6, resources (Instanes et al., 2016); and Section 7.7, modeling (Lique et al., 2016). Section 7.8 summarizes key emerging findings based on Prowse et al. (2015b). For more detailed information and a broader listing of references, readers are referred to the seven publications cited here.

7.2 Atmospheric freshwater

The total water content (vapor, liquid, ice) of the Earth's atmosphere is about 13,000 km³, of which 200 km³ occurs over the Arctic. These are very small amounts compared to the storage capacity of the ocean, ice sheets, glaciers, lakes, rivers, and ground, but the atmosphere is an active component of the water cycle. Water vapor in the atmosphere has a residence time of about a week, compared to a decade for freshwater in the Arctic Ocean, and thousands of years for ice sheets and glaciers. Atmospheric moisture, clouds and precipitation simultaneously affect and are affected by the recent rapid climate change in the Arctic. This section presents a summary of key processes as well as past and projected changes in the role of the atmosphere in the Arctic water cycle, and highlights knowledge gaps and future research directions.

7.2.1 System function and key processes

Spatial and temporal distributions of water vapor in the Arctic are closely related to air temperature distributions, with the total water vapor content decreasing poleward and from summer to winter. The occurrence of water vapor and clouds in the Arctic is partly due to local evapotranspiration and condensation and partly due to transport from lower latitudes, which is mostly via transient cyclones. As an annual mean, precipitation exceeds evapotranspiration over almost all land and ocean areas in the Arctic and sub-Arctic.

Water vapor is the source for cloud and fog formation, but also affects evapotranspiration / condensation and radiative transfer, especially of longwave radiation under clear skies. Specific humidity inversions have a high importance for cloud formation and maintenance (Nygård et al., 2014); in the case when cloud layers are decoupled from the Earth surface, the inversions may be the only moisture source for the clouds (Solomon et al., 2014). As water vapor is the strongest greenhouse gas, an increase in its content yields warming at all latitudes. It contributes to the Arctic amplification of climate warming by amplifying the feedbacks due to clouds, surface albedo, and air temperature (Langen et al. 2012).

Arctic cloudiness has a pronounced annual cycle, ranging from 40–70% in winter to 80–95% in summer and autumn (Shupe et al., 2011). Low clouds and fog dominate, predominantly having a warming effect on the surface, especially over the ice-covered Arctic Ocean. In winter, clouds determine the distribution of net thermal radiation (defined positive downward), a distinct bimodal distribution with one peak at about -40 to -50 W/m², with the lowest temperatures and associated with clear conditions, and another near 0 W/m² associated with clouds (Morrison et al., 2011). Due to a high surface albedo and a large solar zenith angle, longwave radiation dominates the cloud radiative effect over sea ice also through a large part of summer, except for, possibly, July and August. Low concentrations of cloud condensation nuclei (CCN) generate clouds with few but large droplets, and hence a relatively low cloud albedo. With exceptionally low concentration, droplets grow large enough to deposit. Since each droplet brings with it the CCN it formed on, this feeds back to an even lower CCN concentration and generates optically thin clouds (Mauritsen et al., 2011). More clouds and water vapor in spring favor early onset of snow melt on sea ice and low sea-ice extent in September. Modeling studies (Kapsch et al., 2016) suggest that a low sea-ice concentration in autumn increases cloudiness and causes thinner ice at lower concentration at the start of winter.

In winter the spatial distributions of precipitation and evaporation are dominated by the difference between large values over the open seas and low values over snow/ice-covered sea and land areas. In summer, however, both precipitation and evaporation over Arctic land areas, except Greenland, exceed the values over sea areas north of 70°N and are comparable to those at lower latitudes. Precipitation and evaporation / evapotranspiration affect the ocean and terrestrial freshwater budgets, the surface albedo and energy budget, and the mass balance of ice sheets, glaciers, and sea ice. Over the Arctic Ocean, net precipitation is strongly positive (by 2000–2200 km³/y) and so freshens the ocean, but an even more important freshening factor is river discharge, which results from a positive net

precipitation over the surrounding continents, especially Eurasia (Bring et al., 2016). Over the Greenland Ice Sheet most precipitation is generated orographically in the coastal regions. Precipitation also affects the mass balance of sea, lake and river ice, but the effects related to surface albedo, thermal insulation by snowpack, and snow-to-ice transformation partly compensate for each other.

7.2.2 Observed changes and key drivers

Past trends in atmospheric water variables in the Arctic include large spatial variations, and are sensitive to the time period and source of data. During recent decades at pan-Arctic scale there seems, however, to be a trend toward wetter conditions; air specific humidity and precipitation have increased (Serreze et al., 2012; Hartmann et al., 2013; Willett et al., 2013). Changes in evapotranspiration are less clear, and trends in clouds vary depending on the region and season (Eastman and Warren, 2013; Nahtigalova, 2013). Models capture the overall wetting trend but have problems reproducing regional detail (see also Lique et al., 2016). The latter may partly result from the larger influence of interannual variability at regional scales and partly (such as in regions of complex orography) from insufficient spatial resolution.

On the basis of climate model experiments addressing the past, the overall wetting is linked to the general warming trend, partly driven by anthropogenic forcing, and amplified in the Arctic due to several feedback effects. The wetter conditions reflect an intensification of the atmospheric water cycle in the Arctic, also seen as an increase in moisture transport from lower latitudes to the Arctic (Zhang et al., 2013). The increased moisture transport has increased downward longwave radiation over most of the year, enhancing sea ice melt (Park et al., 2015). Drivers of interannual variations in the Arctic atmospheric water cycle are related to inherent variability of the polar jet stream, storm tracks, and related synoptic-scale weather. Part of the variability in the jet stream and storm tracks can be characterized by large-scale circulation modes such as the Arctic Oscillation, North Atlantic Oscillation, East Atlantic Pattern, Pacific Decadal Oscillation, and Southern Oscillation, but the relationships vary regionally (Overland et al., 2015).

7.2.3 Projected changes and key drivers

State-of-the-art climate model projections suggest a robust future intensification of the Arctic hydrological cycle during the rest of the 21st century. Mean precipitation and daily precipitation extremes are projected to increase over mid- and high latitudes, largely in response to warming-driven increases in the moisture-holding capacity of the air (i.e. air specific humidity is projected to increase) (Lainé et al., 2014; Lique et al., 2016). The relative increases in precipitation extremes are expected to exceed relative increases in mean values (i.e. precipitation intensity is expected to increase), which may generate challenges in management of water resources (Instanes et al., 2016). The increased atmospheric moisture comes from increased evaporation (itself largely due to the loss of sea-ice cover) and enhanced poleward moisture transport. There is however, significant model divergence in future cloud-cover trends particularly for the months of greatest sea-ice loss.

Model divergence is also large for changes in winter storm tracks (see Figure 7.2 and Section 7.1.3). Evapotranspiration is projected to increase in winter, but in summer to decrease over the oceans and increase over land.

Higher precipitation increases river discharge to the Arctic Ocean (see Bring et al., 2016 and Section 7.4). Over sea ice in summer, the projected increase in rain and decrease in snowfall would lower surface albedo and so further amplify surface melt (Screen and Simmonds, 2012). With reducing sea ice, wind forcing on the Arctic Ocean increases with impacts on ocean currents and freshwater transport out of the Arctic (Carmack et al., 2016; see also Section 7.3).

7.2.4 Knowledge gaps and future research

The main gaps in knowledge about the role of the atmosphere in the Arctic freshwater cycle are due to the sparsity (in space and time) of accurate observations and the complexity of physical processes related to atmospheric moisture, clouds, precipitation, and evaporation. Although understanding of individual processes has increased, challenges remain in the understanding of non-linear interactions of various processes, partly acting at different spatial and temporal scales. This challenge in understanding is reflected in problems with modeling the processes, in particular the sub-grid-scale processes that need to be parameterized in climate and numerical weather prediction models (Vihma et al., 2014). Climate model uncertainties are seen, among others, in the large inter-model scatter in the response of cloud cover to sea-ice loss. Another major factor generating uncertainties in climate model projections for time-scales of the order of years to a few decades is the large natural interannual and decadal variability.

To better quantify the Arctic atmospheric water cycle and its changes, there is a need for more extensive and accurate observations, better process understanding, better models, and more extensive and systematic utilization of existing models. An increase is needed in the amount of radiosonde sounding data from the Arctic. These may be supplemented by vertical profiling of the lower troposphere applying unmanned aerial vehicles (UAVs) and dropsondes (Jonasson et al., 2012; Intrieri et al., 2014). In addition, satellite-, ground- and ship-based remote sensing of cloud properties (such as profiles of water and ice contents) and air humidity have the potential to yield significant further advances in process understanding (Tjernström et al., 2014) and when the time-series become long enough, in climatology of cloud properties (Uttal et al., 2016). More attention is needed on the loss of lake and river ice (Bring et al., 2016; see also Section 7.4) and its effects on local evaporation and the contribution to atmospheric moisture transport to and from the Arctic freshwater system.

Modeling issues that deserve more attention include the representation of unresolved orographic effects on precipitation, storm tracks and atmospheric rivers (narrow bands of enhanced water vapor transport), as well as large-scale effects of sea ice on evaporation and precipitation, and especially on net precipitation which is key to land surface drying/wetting of ecosystems (Wrona et al., 2016) and runoff impacts on ocean salinity. Model results for the recent climate and changes show various discrepancies, but identifying their exact causes is still difficult. Systematic evaluations

of different aspects of the model simulations, such as by Kattsov et al. (2007) may yield more information. Considering future projections of the atmospheric water cycle, there is a need for more model experiments with larger ensembles and a greater range of models. Systematic comparison of the results should allow a better understanding of the sources of uncertainty. There is also a need for updated information on the contributions of anthropogenic and natural forcing to changes in the Arctic freshwater cycle.

7.3 Freshwater in the Arctic marine system

The cycling of freshwater through Earth's atmospheric, terrestrial and oceanic components is a central element in climate and life systems, of which the Arctic Ocean is a major player (Figure 7.4; see also Figure 7.1). Internal to the Arctic there are very few physical, chemical or biological processes that are not influenced or constrained by the local quantities

and geochemical qualities of freshwater (Carmack et al., 2016). Linkages and feedbacks then create strong two-way ties among the Arctic Ocean and atmospheric, terrestrial and extra-Arctic marine components of the system (Bhatt et al., 2014; Bring et al., 2016; Vihma et al., 2016). The sea-ice cover decrease in the Arctic Basin, through its feedback to the atmosphere may also influence the position of the jet stream and storm tracks over the North American and Eurasian continents (Barnes and Screen, 2015). The rate at which such changes within individual systems are occurring is further accelerated by cross-system feedbacks associated with a class of processes termed Arctic amplification (Serreze and Barry, 2011). The rapid cascading of linkages through multiple system components in recent years has led to the possibility of new trajectories within the Arctic system (Carmack et al., 2012; Wassmann and Lenton, 2012). Essential to all the above is evidence of an accelerating hydrological cycle (Zhang et al., 2013); indeed, the acceleration of the Arctic hydrological cycle in the 20th century is without precedence in the Holocene (Wagner et al., 2011).

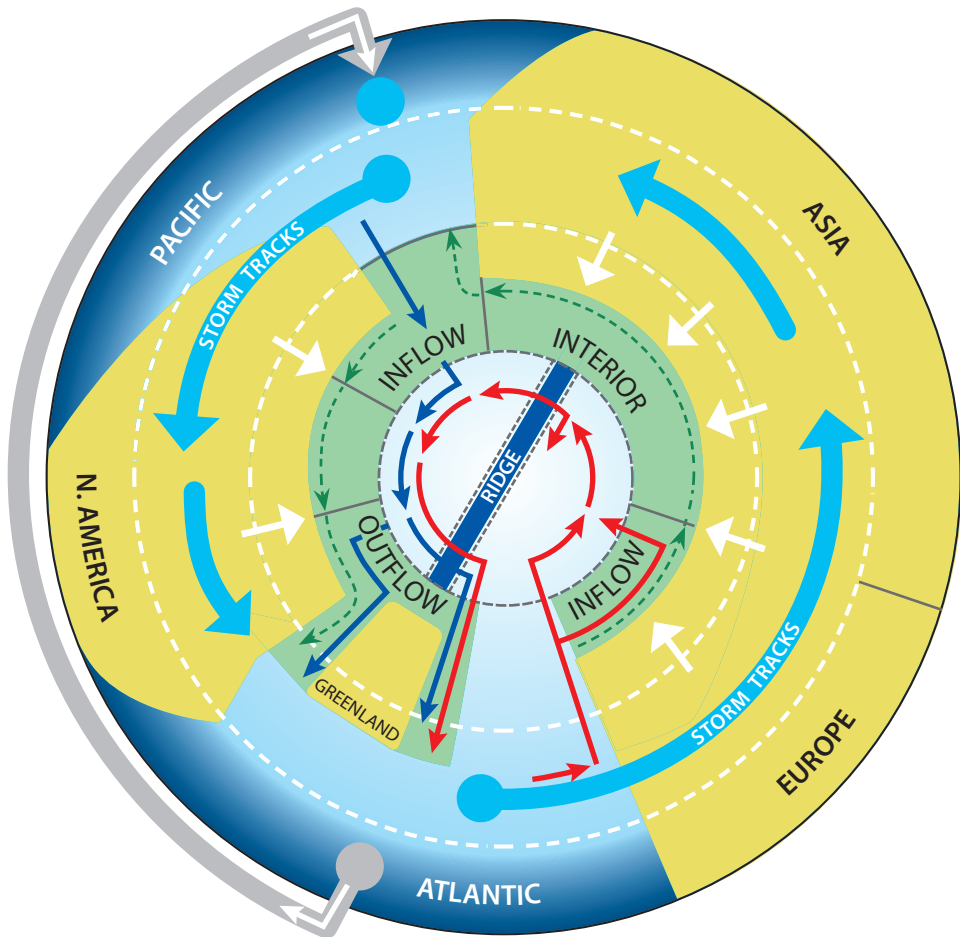


Figure 7.4 Schematic representation of the high-latitude freshwater system as introduced by Prowse et al. (2015a). Moisture is transported from the subtropical and tropical Atlantic Ocean to the Pacific Ocean via the Trade Winds over Central America (thick grey arrow). The sub-Arctic front separates the thermally stratified sub-Arctic oceans (darker blue) from the salt-stratified northern ocean (lighter blue) in both the Atlantic and Pacific Oceans. Moisture is transported from the Pacific and Atlantic Oceans to the Arctic catchment basins by the mid-latitude (Westerlies) storm tracks (thick blue arrows), and subsequently drains into the Arctic Ocean (thick white arrows) where it spreads initially within the Riverine Coastal Domain (dashed green arrows). Warm, salty Atlantic-origin waters (thin red arrows) enter the Arctic Ocean through Fram Strait (the Fram Strait Branch) and the Barents Sea Opening (the Barents Sea Branch) and circulate within the Arctic Basins as subsurface, cyclonic, topographically steered boundary currents along the continental margin and ridge system. Internally modified Atlantic waters exit the Arctic Ocean southward through Fram Strait along eastern Greenland. Cooler and fresher Pacific-origin waters (thin blue arrows) enter the Arctic Ocean through Bering Strait and exit through the Canadian Arctic Archipelago and Fram Strait along eastern Greenland. Within the Arctic Ocean a topological distinction is made between inflow, interior, and outflow shelves (cf. Carmack and Wassmann, 2006; Bluhm et al., 2015).

Table 7.1 Freshwater budgets for the Arctic Ocean from selected published sources. Positive fluxes indicate freshwater sources to the Arctic Ocean. Negative fluxes indicate a freshwater deficit in the outflow from the Arctic Ocean. Uncertainties (on the mean values) are given where available.

	Prior to 1989 (Aagaard and Carmack, 1989) ^a	~1979–2001 (Serreze et al., 2006) ^a	1980–2000 (Haine et al., 2015) ^b	2000–2010 (Haine et al., 2015) ^b
Reservoirs, km ³				
Liquid freshwater	80,000	74,000 ± 7400	93,000	101,000
Sea ice	17,300	10,000	17,800	14,300
Total freshwater	97,300	84,000	110,800	115,300
Fluxes, km ³ /y				
Runoff	3300	3200 ± 110	3900 ± 390	4200 ± 420
P-E ^c	900	2000 ± 200	2000 ± 200	200 ± 220
Bering Strait (total)	1670	2500 ± 300	2540? ± 300	2640 ± 100
Fram Strait liquid ^d	-980	-2700 ± 530	-2700 ± 530	-2800 ± 420
Fram Strait ice	-2790	-2300 ± 340	-2300 ± 340	-1900 ± 280
Davis Strait (total)	-920	-3380 ± 320	-3360 ± 320?	-3220 ± 190
Miscellaneous ^e	-290	-90 ± 90	40 ± 90?	80 ± 90?
Total inflow	6120	7950 ± 400	8800 ± 530?	9400 ± 490
Total outflow	-5520	-8720 ± 700	-8700 ± 700	-8250 ± 550
Residual	890	770 ± 800	100 ± 900?	1200 ± 730

^aAuthors consider the Arctic Ocean to exclude the Canadian Arctic Archipelago and Baffin Bay; ^bAuthors consider the Arctic Ocean to include the Canadian Arctic Archipelago and Baffin Bay; ^cPrecipitation minus Evaporation; ^dincludes the East Greenland Current, the deep outflow, and the West Spitsbergen Current; ^eincludes the Barents Sea Opening, Fury and Hecla Straits, and the freshwater flux from Greenland. They are included separately in the total inflow and outflow fluxes, where possible.

7.3.1 System function and key processes

7.3.1.1 Inexorable poleward transport of freshwater

Freshwater delivery to the Arctic Ocean arises as a consequence of its northward transport as demanded by the climate system to transport heat (in this case as latent heat) from the low to high latitudes. In contrast to the southern hemisphere, the configuration of continents in the northern hemisphere is such that they effectively capture moisture from the atmospheric storm tracks of the Westerlies and redirect in north-flowing drainage basins disproportionate quantities of freshwater into the Mediterranean configuration of the Arctic Ocean (Figure 7.1). Hence, while the Arctic Ocean represents only 1% (in terms of volume) and 3% (in terms of surface area) of the global ocean, it collects over 11% of the global river discharge (Dai and Trenberth, 2002; Carmack et al. 2016). The Trade Winds also transport moisture from the Atlantic Ocean across the Isthmus of Panama to freshen the Pacific Ocean, and some of this freshened water eventually flows into the Arctic Ocean through Bering Strait. The resulting salt stratification or halocline (i.e. a freshened upper ocean and salinity increasing with depth) is the dominant characteristic of high-latitude seas in general and the Arctic Ocean in particular (Carmack, 2007).

The freshwater budget of the Arctic Ocean is governed by the system's key functions and processes: the delivery of fresh and low-salinity waters to the Arctic Ocean by river inflow, net precipitation, distillation during the freeze/thaw cycle and Pacific Ocean inflows; the disposition (e.g. sources, pathways and storage) of freshwater components within various domains of the Arctic Ocean (e.g. basins, shelves,

coastal zone); and the release and net export of freshwater components into the bordering convective domains of the North Atlantic (Carmack et al., 2016).

7.3.1.2 Circulation and water masses

The initial Arctic Ocean freshwater budget presented by Aagaard and Carmack (1989) was recently updated by Haine et al. (2015) (Table 7.1). The distribution of freshwater within the Arctic Ocean is heterogeneous and controlled by circulation and water mass structure. The Arctic Ocean is made integral to the global ocean by the northern hemisphere thermohaline circulation which drives Pacific Water through Bering Strait into Canada Basin, and counter-flowing Atlantic Water through Fram Strait and across the Barents Sea into Nansen Basin. Following Bluhm et al. (2015), it is useful to recognize four vertically-stacked circulation layers (Figure 7.5): (1) the wind-driven surface layer circulation that is characterized by the cyclonic Trans-Polar Drift from Siberia to Fram Strait and the anticyclonic Beaufort Gyre in southern Canada Basin; (2) the underlying circulation of waters that comprise the halocline complex, composed largely of Pacific Water and Atlantic Water that are modified during their passage over the Bering/Chukchi and Barents/Siberian shelves, respectively; (3) the topographically-trapped Arctic Circumpolar Boundary Current that carries Atlantic Water cyclonically around the boundaries of the entire suite of basins; and (4) the very slow exchange of Arctic Ocean Deep Waters. Within the basin domain two water mass assemblies are observed, the difference between them being the absence or presence of Pacific Water sandwiched between Arctic Surface Waters above and the Atlantic Water complex below; the boundary between these domains forms the Atlantic/Pacific halocline front (McLaughlin et al., 1996;

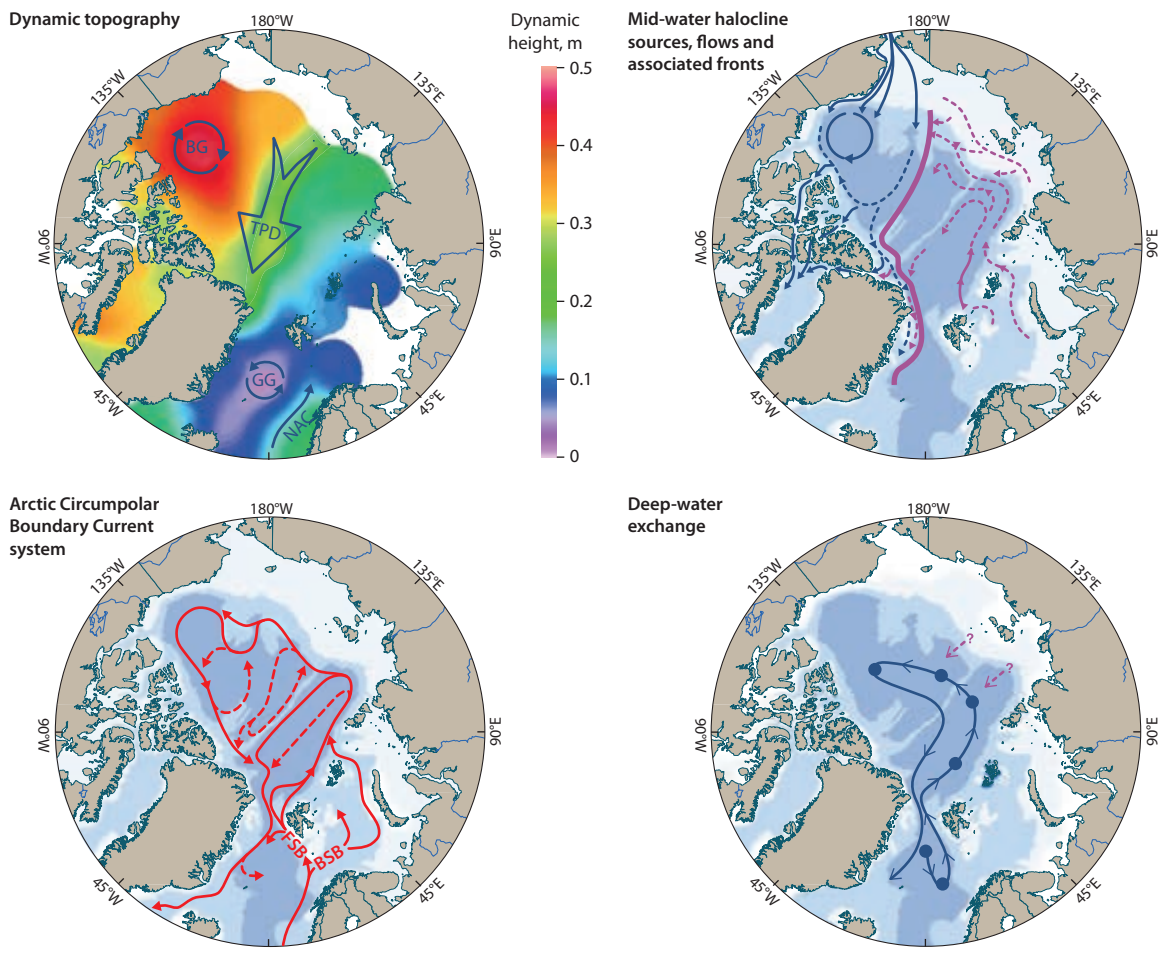


Figure 7.5 Schematic representations of Arctic Ocean circulation: Surface circulation of the Arctic Ocean as shown by dynamic topography (20/400 db); mid-water halocline sources, flows and associated fronts (blue shows Pacific-origin waters, maroon shows Atlantic-origin waters, thick maroon line depicts the front between them) (after McLaughlin et al., 1996); the Arctic Circumpolar Boundary Current system derived from Atlantic water inflows (after Rudels et al., 1999; Aksenov et al., 2011); and deep-water exchange (Aagaard et al., 1985). BG is the Beaufort Gyre, BSB is the Barents Sea Branch, FSB is the Fram Strait Branch, GG is the Greenland Gyre, NAC is the Norwegian-Atlantic Current, TPD is the Transpolar Drift. (Bluhm et al., 2015).

Carmack et al., 2015), which is roughly aligned with the Trans-Polar Drift although its position changes with time (Steele and Boyd, 1998; Alkire et al., 2007).

7.3.1.3 Role in regulating physical processes

One key consequence of salt stratification is that sea ice can only form over deep oceans where a permanent halocline limits deep thermally-driven convection (Bulgakov, 1962). Salt stratification thus plays an indirect but key role in determining the planetary albedo and ice/albedo feedback effects (Aagaard and Carmack, 1994). Salt stratification also constrains the upward diffusive flux of heat from the underlying and warmer inflows from the Atlantic and Pacific Oceans, thus also allowing persistence of ice cover (Polyakov et al., 2013b; Carmack et al., 2015). It also forces the density-driven estuarine circulation of the Arctic Ocean. But the distribution of freshwater within the Arctic Ocean is not uniform, and salinities range from about 35 where Atlantic Water enters the basin to near zero adjacent to river mouths and along the coast (Carmack et al., 2016). This huge range in salinity, the main parameter that determines density stratification in high-latitude oceans, affects almost every aspect of circulation and mixing within the Arctic Ocean.

7.3.1.4 Role in regulating biogeochemical processes

The freshwater cycle in the Arctic Ocean influences most biological and geochemical processes. Very importantly, each source of freshwater has a different biogeochemical role. Freshwater derived from terrestrial sources transports dissolved and particulate materials and plays a major role in setting rates of geochemical transformations in coastal regions (Dittmar and Kattner, 2003). Along with their freshwater anomaly and effects on stratification, Pacific-origin waters advect heat, nutrients (Codispoti et al., 2013) and zooplankton (Nelson et al., 2009), and are preconditioned for low calcium carbonate saturation state (Ω), making these waters vulnerable to ocean acidification (Yamamoto-Kawai et al., 2013). Mixing with freshwater from river inflow and ice melt decreases Ω and accelerates ocean acidification, but the local degree of acidification depends on the chemical properties of the specific freshwater source (Yamamoto-Kawai et al., 2009). Surface freshening suppresses the supply of nutrients from depth, decreases primary production, promotes formation of a subsurface chlorophyll maximum layer, and changes plankton size structure in the euphotic zone (Li et al., 2009; Tremblay and Gagnon, 2009;

McLaughlin and Carmack, 2010). On shelves, salt stratification restricts deep and bottom water from contact with the atmosphere and results in a decrease in oxygen content and an accumulation of carbon dioxide (CO_2), and can have negative impacts on benthic communities (Bates et al., 2013). Formation of sea ice and associated brine release redistributes freshwater and materials from the surface to depth by convection. Drifting sea ice transports freshwater and sediments from shelves to deep basins (e.g. Nürnberg et al., 1994). The formation and outflow of brine-enriched shelf water also transports terrestrial and remineralized material to intermediate and deep layers (Guéguen et al., 2007; Nakayama et al., 2011). Arctic outflows into the Labrador Sea and sub-Arctic North Atlantic have clear biological consequences (Drinkwater and Harding, 2001; Greene and Pershing, 2007).

7.3.1.5 Role in terrestrial and atmospheric processes

The net poleward atmospheric moisture flux is largely compensated by the net oceanic export of freshened seawater and sea ice back to lower latitudes. These freshwater exports also carry large amounts of carbon (MacGilchrist et al., 2014) and nutrients (Torres-Valdés et al., 2013). When freshwater exports reach the sub-Arctic Nordic Seas, they influence surface salinity (Dickson et al., 1988; Haak et al., 2003) and the rate of dense water formation, with potential feedbacks on Arctic climate (Dukhovskoy et al., 2004) and implications for the strength of the Atlantic meridional overturning circulation (AMOC) (Rahmstorf et al., 2015). Through its associated transport of heat, the AMOC plays a key role in regulating global climate (Vellinga and Wood, 2002) and weather in western Europe through a

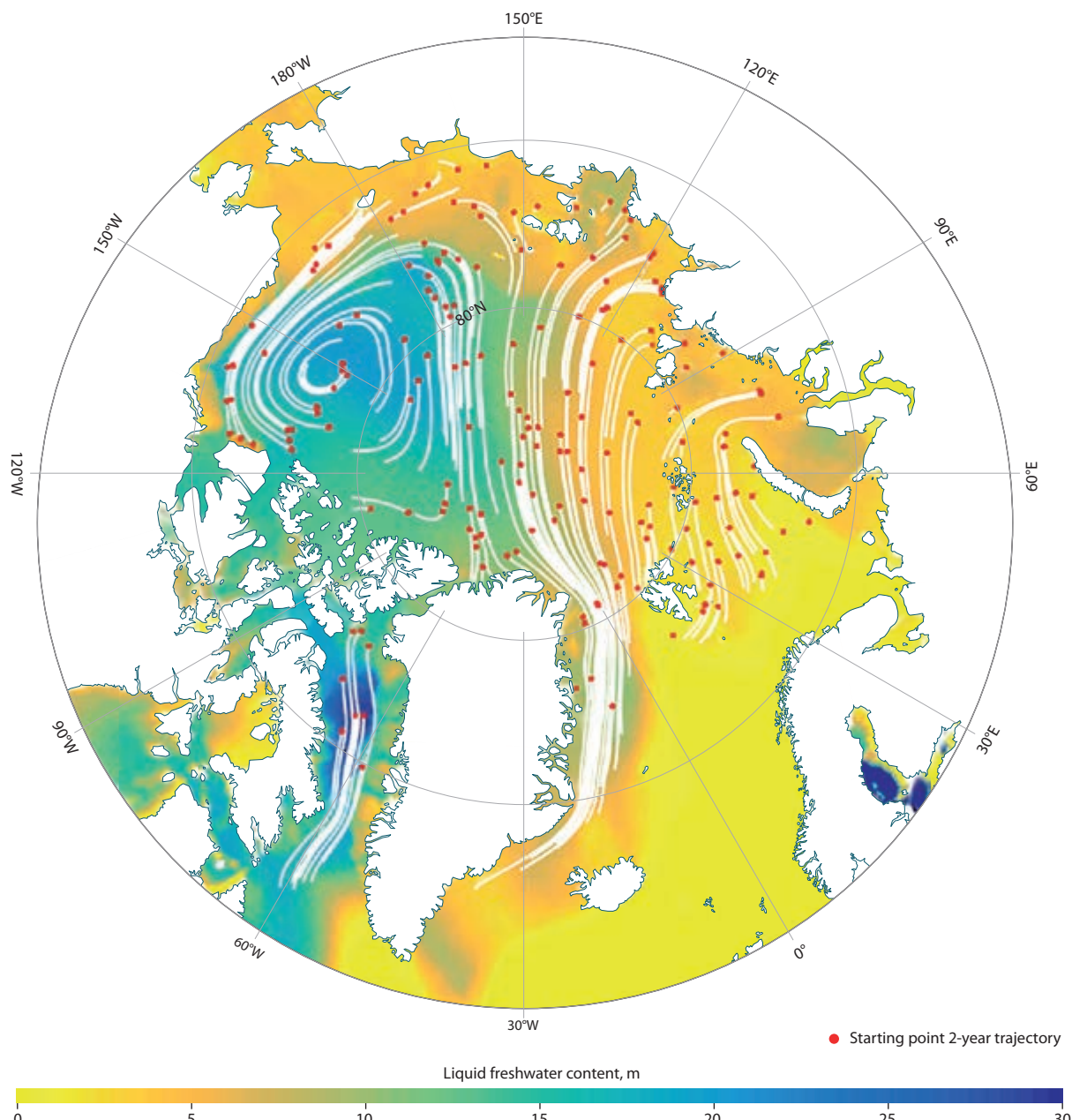


Figure 7.6 Liquid freshwater content (i.e., thickness of freshwater anomaly relative to a reference salinity of 34.8) from the PHC (Polar Science Center Hydrographic Climatology) 3.0 climatology (Steele et al., 2001) and trajectories of sea ice computed using 2000–2010 satellite ice velocities from the Polar Pathfinder Sea Ice Motion data (Fowler et al., 2013). The small red dots indicate the starting points of the trajectories, which last two years.

strong modulation of the storm track (Woollings et al., 2012). The decrease in sea-ice cover in the Arctic Basin, a phase change from solid to liquid freshwater, may also influence the position of the jet stream and storm tracks over the North American and Eurasian continents (Francis and Vavrus, 2012; Screen et al., 2013; Barnes and Screen, 2015; Francis and Skific, 2015).

7.3.1.6 Freshwater storage and export

Relative to a reference salinity of 34.8, about 101,000 km³ of freshwater are stored in the Arctic Ocean (this is an estimate of the 2000–2010 annual average volume by Haine et al., 2015; Table 7.1). The largest freshwater reservoir exists in the Amerasian Basin, specifically in the Beaufort Gyre where about 23,500 km³ freshwater are stored and the accumulated freshwater anomaly diluting the upper ocean above the 34.8 isohaline surface is about 20 m thick. In the Eurasian Basin, typical liquid freshwater thicknesses are 5–10 m. This pattern of liquid freshwater storage reflects the dominant surface circulation (Figure 7.6): Eurasian Basin surface water flows toward the Trans-Polar Drift and so leaves via Fram Strait. In contrast, Amerasian Basin surface water circulates clockwise in the Beaufort Gyre leaking into the Trans-Polar Drift or into the Canadian Arctic Archipelago.

Freshwater in the solid phase as sea ice is another important reservoir in the Arctic (see Krishfield et al., 2014). About 14,300 km³ of freshwater are stored in sea ice (2000–2010 average from Haine et al., 2015). The largest sea ice volumes are north of the Canadian Arctic Archipelago and Greenland and across the pole, where the ice is still relatively thick (Kwok et al., 2009). The seasonal freeze-thaw cycle acts to exchange freshwater between the liquid and solid phases. Its amplitude is about 13,400 km³ (averaged over the decade of the 2000s; Haine et al., 2015), close to the annual average freshwater volume stored in sea ice. Sea-ice formation in winter occurs throughout the Arctic Ocean but the prevailing currents tend to export ice frozen over the Eurasian shelves toward the central Arctic and the Trans-Polar Drift (Figure 7.5). Under current climate conditions only about 35% of the sea ice present at the end of winter, when the ice volume peaks survives the summer to become multiyear ice. Of the remaining 65%, most melts within the Arctic although some is exported south.

Storage of freshwater varies seasonally in the upper mixed layer with freshwater removal (and storage in sea ice) taking place during autumn and winter and freshwater addition during the summer melt period. The seasonal cycle of river input (and net precipitation) further modifies the liquid freshwater content of the surface layer. Superimposed on this predominantly solar-forced variability are dynamical processes that redistribute freshwater laterally as well as vertically within the water column. Beginning around May–June each year, the ocean surface layer warms due to absorption of solar radiation through open water and areas of thin ice. The resulting structure is a relatively fresh, thin (a few meters to about 20 m) surface layer. Beginning in September, penetrative convection occurs as a result of sea-ice growth and brine rejection; the summer-generated mixed layer becomes saltier and deepens through April. In a closed one-dimensional system, the net change in freshwater content integrated over the surface layer would equal that estimated from the net change in sea-ice volume (provided winter convective deepening of the surface layer does not exceed the depth of the surface layer at the start of the melt season).

Arctic freshwater is released to lower latitudes via two marine export pathways. First, and largest is the pathway east of Greenland through Fram Strait. Oceanographic moorings, ocean models, and satellite observations are used to estimate the flux of liquid and solid freshwater through this gateway. The 2000–2010 average estimates are 2800±420 km³/y as liquid and 1900±280 km³/y as ice (Haine et al., 2015). The second pathway is through the Canadian Arctic Archipelago and Davis Strait, which currently carries about 2900±190 km³/y as liquid freshwater and 320±32 km³/y as ice (Curry et al., 2011, 2015). From the total average volume in liquid and ice (115,300 km³, see above), a bulk freshwater residence time of about 14 years can be inferred (recognizing that in reality a broad range of residence times exist depending on the specific reservoir). Although 88% of Arctic freshwater is in liquid form, only about 73% leaves in that phase; as such, export as ice is disproportionately important.

Sources, storage reservoirs and sinks for freshwater in the Arctic Ocean, and the changes observed between 1980–2000 and 2000–2010 are summarized in Figure 7.7.

7.3.1.7 Geochemical tracers and source waters

Each source of freshwater has a unique geochemical composition and will thus influence different regions of the Arctic Ocean in different ways. In a changing climate, each individual freshwater source is likely to change disproportionately relative to one another in both volume and phenology. Distillation and export associated with the seasonal sea-ice cycle will certainly change in ways that are poorly understood, as will the flux and distribution of freshwater from net precipitation across the basin. Pacific Water, for example, can be distinguished from Atlantic Water using nutrient characteristics: dissolved inorganic nitrate and phosphate ratios, and silicate concentration (e.g. Ekwurzel et al., 2001; Jones et al., 2003). The oxygen isotope ratio of water ($\delta^{18}\text{O}$) and alkalinity have been used to differentiate meteoric water (river runoff plus precipitation) from sea-ice meltwater (e.g. Macdonald et al., 1999; Yamamoto-Kawai et al., 2005). Alkalinity and barium concentrations reflect the source of meteoric water as they are present in high concentrations in North American rivers and low in Eurasian runoff, and are absent in precipitation (e.g. Guay and Falkner, 1997; Yamamoto-Kawai et al., 2005). A recently developed satellite observation of colored dissolved organic matter enabled a real-time, synoptic monitoring of river runoff spreading in open-water areas (Fichot et al., 2013).

The spatial distribution of each freshwater source has been determined from observations of these geochemical tracers. Pacific Water spreads within the Amerasian Basin and flows out through Fram Strait and the Canadian Arctic Archipelago, and is traceable as far south as the Grand Banks near 42°N (Jones et al., 2003). A high concentration of sea-ice meltwater is found in summer surface waters of the inflow shelves (Barents and Chukchi shelves), whereas the central Arctic is the region of net ice formation (Yamamoto-Kawai et al., 2005). The Beaufort Gyre accumulates not only freshwater from Pacific Water, runoff, and precipitation but also salt (brine) rejected during sea-ice formation on shelves surrounding the Canada Basin (Yamamoto-Kawai et al., 2005). Runoff from Eurasian rivers flows toward the Trans-Polar Drift and Fram Strait, but a significant proportion also enters the Amerasian Basin (Carmack et al., 2008; Morison et al., 2012). Eurasian runoff

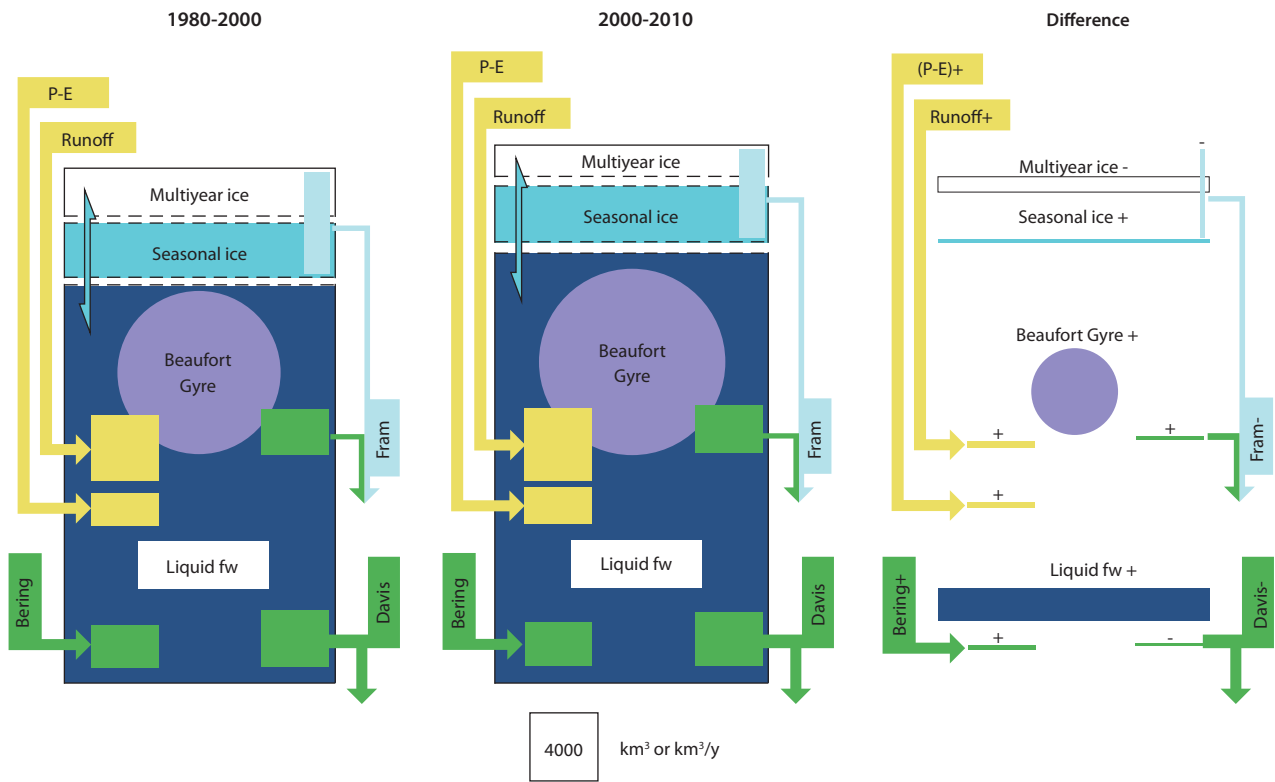


Figure 7.7 Schematic illustration of the freshwater budget for the Arctic Ocean for the period (nominally) 1980–2000, the decade of the 2000s, and the difference between them. In each diagram, the principal freshwater sources are precipitation minus evaporation (P-E), runoff, and flow through Bering Strait. The principal sinks are outflow through Davis and Fram Straits. The freshwater reservoirs are split between liquid freshwater (with the Beaufort Gyre shown in the circle) and sea ice (seasonal and multiyear). The area of each shape is proportional to the corresponding freshwater flux or reservoir volume (see the white box for scale). (Haine et al., 2015).

is, in fact, the major source of meteoric water found in Canada Basin and the Beaufort Gyre (Carmack et al., 2008; Guay et al., 2009). Runoff from the Mackenzie River flows northwestward into Canada Basin or eastward toward the Canadian Arctic Archipelago. The routing of river runoff varies with local winds as well as with atmospheric circulation patterns (e.g. Guay et al., 2001; Anderson et al., 2004; Morison et al., 2012; Fichot et al., 2013).

7.3.2 Observed changes and key drivers

7.3.2.1 Storage

The Arctic freshwater reservoirs are changing on interannual and multi-decadal time-scales. There has been an especially rapid increase in liquid freshwater storage since 2000 over the basins and a rapid decline in summer sea ice (see Table 7.1). In contrast, over the 20th century the central Arctic Ocean became increasingly saltier (Polyakov et al., 2008); this salinification led to a substantial decrease (1478 ± 17 km 3) in freshwater content between 1976 and 1999. Polyakov et al. (2008) argued that ice production and sustained draining of freshwater from the Arctic Ocean in response to winds were the key contributors to the salinification of the upper Arctic Ocean during the 20th century. However, the freshwater content anomalies extant in the 2000s and 2010s stand out: the freshening is dramatic with no analogy in almost a century-long history of oceanographic observations (Polyakov et al., 2013b). The expansion of the liquid freshwater reservoir amounts to about 8000 km 3 for the 2000s compared to

the 1980–2000 average (Giles et al., 2012). The increase is seen mainly in the western Arctic Ocean and in the Beaufort Gyre specifically, which has increased its volume over the past two decades by about 5000 km 3 . Relatedly, upper ocean salinity in Canada Basin was 1–3 practical salinity units fresher in 2008 than prior to 1990 (Morison et al., 2012). Rabe et al. (2014) found an annual increase in liquid freshwater of 600 ± 300 km 3 /y between 1992 and 2012. Satellite measurements of sea level concur. Giles et al. (2012) estimated that the inflated Beaufort Gyre contributed to 8000 ± 2000 km 3 more western Arctic freshwater in 2010 than in 1995. The total liquid freshwater store is increasing but not in all parts of the Arctic Ocean. Morison et al. (2012) used hydrography, geochemistry, satellite altimetry, and satellite bottom pressure data to show that the freshwater content of the Amerasian Basin increased while in the Eurasian Basin it decreased. Upper ocean salinity was 1–2 practical salinity units higher in the Makarov Basin in 2008 compared to before 1990, for instance. At least some of the increased freshwater observed in the Beaufort Gyre has been redistributed from the Eurasian Basin.

The Arctic sea-ice reservoir is losing volume especially in summer. It declined at an average annual rate of $-3.8 \pm 0.3\%$ per decade between November 1979 and December 2012 (Vaughan et al., 2013). Sea-ice thickness is also in decline. Kwok and Rothrock (2009) reported submarine and satellite data that show the average end-of-melt season ice thickness was 3.02 m in 1958–1976 but just 1.43 m in 2003–2007. Because both ice extent and ice thickness are declining, sea-ice volume is also declining. The Pan-Arctic Ice Ocean Modeling and Assimilation

System (PIOMAS) (Zhang and Rothrock, 2003) estimates of the freshwater stored in seasonal ice are nearly constant at 13,000 km³ over the period 1980 to 2010. However, the volume of freshwater in multiyear ice declined from 10,900 km³ for 1980–2000 to 7400 km³ for the 2000s. Over this period, the annual average volume of freshwater in sea ice declined from 17,800 to 14,300 km³ (Table 7.1) (Schweiger et al., 2011; Haine et al., 2015). Collectively, the loss of ice and increased flux convergence accounts for the greater volume of liquid freshwater observed in the 2000s (Haine et al., 2015).

7.3.2.2 Freshwater trajectories and pathways

The processes that store and export freshwater from the Arctic are connected to the surface circulation and hence to winds. Figure 7.6 shows the 2000–2010 average sea-ice drift trajectories which reflect ocean surface flows and in turn the sea-level pressure. Average sea-level pressure is relatively high over Canada Basin (the Beaufort High) and low over the Eurasian Basin, Barents Sea, and Nordic Seas (Serreze and Barrett, 2011). The associated sea-level slope acquires geostrophic balance with a clockwise surface flow parallel to the wind, namely, the Beaufort Gyre and Trans-Polar Drift. Analysis of freshwater-content anomalies suggests that sustained phases of freshening in the central Arctic Ocean are associated with salinification in the Barents and western Greenland seas (with much stronger anomalies in the Greenland Sea) and vice versa (Polyakov et al., 2008). These estimates strongly suggest that at decadal and longer time-scales, the magnitudes of ice and freshwater exchange through straits connecting the Arctic Ocean to the sub-Arctic basins are of primary importance for stratification within the sub-Arctic basins. Long-term variations in freshwater storage and export were examined by Proshutinsky et al. (2015), who noted that between 1948 and 1996 the mean annual environmental parameters in the Arctic experienced well-defined decadal variability with two basic circulation regimes, cyclonic and anticyclonic, alternating at 5- to 7-year intervals (Proshutinsky and Johnson, 1997; Proshutinsky et al., 2002). Since 1997, however, the Arctic system has been under the influence of the anticyclonic circulation regime, with an attendant increase in freshwater storage. Proshutinsky et al. (2015) employed box model results to explain this and to demonstrate the importance of treating the Arctic Ocean and North Atlantic sub-Arctic region as a coupled ocean/ice/atmosphere system and to suggest that additional freshwater arising from Greenland ice melt is altering system behavior.

7.3.2.3 Ice volume and transport

Ice draft from naval submarine sonar during the ‘old’ Arctic regime (1960–1982) was mapped by Bourke and Garrett (1987), revealing an average 3–8 m for the central Arctic pack ice of the time and an average 1–3 m for the peripheral areas of first-year ice. This average draft has declined greatly over the past quarter century. Kwok and Rothrock (2009) gave a recent perspective that combines the analysis of pre-2000 sonar data from submarines (Rothrock et al., 1999) with post-2000 data from satellite altimetry (Kwok et al., 2009). They found a decrease of 40% or more in all subregions between 1958–1976 and 1993–1997; Tucker et al. (2001) using data from an often surveyed path northward along 150°W showed the change actually occurred within a few years

of 1990. The subsequent change to the mid-2000s was less, about 6.5%. Meanwhile, the expanse of decades-old ice has shrunk by 45%. Rigor and Wallace (2004) argued that the impetus for multiyear ice loss was a change in wind-driven ice circulation – caused by an interval of high Arctic Oscillation conditions – that forced old ice out to the Atlantic. The substitutions of open water for almost half of the pre-existing multiyear ice in summer and of much thinner first-year ice for the same multiyear ice in winter can explain much of the drop in average ice thickness. Moreover, loss of summer ice has exposed a larger area of water to insolation in summer, creating a warmer sea surface and accelerated melting of ice – the positive albedo feedback effect (Perovich et al., 2011).

7.3.2.4 Duration and thickness of ice cover near the coast

There are very few systematic long-term thickness observations for seasonal Arctic sea ice. The longest data series, built by Canadian and Russian weather services since the mid-1900s, document the annual growth and decay cycle of fast-ice close to shore. End-of-winter data from both Siberia and Canada reveal only weak trends in thickness (a few centimeters per decade), with a decrease at some sites and an increase at others (Brown and Coté, 1992; Polyakov et al., 2003). Observations in the Canadian Arctic reveal that variation in snow depth strongly influences variation in ice thickness (Brown and Coté, 1992; Dumas et al., 2005; Melling, 2012). Polyakov et al. (2013a) prepared a 15-station composite of Siberian observations that began in the 1930s; this shows a decrease of 13 cm between 1960 and 2009 (2.2 cm per decade), which was, however, preceded by a 20-cm increase between 1934 and 1960; snow depth was not measured. Data, such as they exist, suggest that the impact of climate change on coastal fast-ice thickness has been much less than its impact on pack ice in the central Arctic.

7.3.2.5 Sea level along the Arctic coastlines

Proshutinsky et al. (2004) provided estimates of sea level trends from the 1950s to the 1990s. For the period 1954–1989, sea level was rising at about 0.185 cm/y. Using atmospheric observations and reanalysis products and modeling, they inferred that about a third of this rise was due to steric effects. Another third may be explained by falling sea-level pressure (the so-called reverse barometer effect). The remainder may be explained by effects of winds and change in Arctic Ocean mass. Danielson et al. (2014) showed a recent increase in polar easterlies to be associated with a decline in sea-surface height along the Siberian Arctic coast (2006–2011 relative to 2000–2005) and proposed that fluctuations in sea-surface height at this location contributed in part to variations in the Pacific–Arctic pressure head and the Bering Strait fluxes. Analysis of more recent observations suggests a drastic change in sea-level variability along the Siberian Arctic coast (Ashik et al., 2015). Starting from around 1985 there was a rapid increase in sea level; this may be characterized by a linear trend of 0.244 ± 0.097 cm/y. The maximum trend (0.441 cm/y) was observed in the southwestern part of the Kara Sea. Ashik et al. (2015) argued that this substantial acceleration in sea-level rise may be explained by an increased frequency and intensity of Arctic cyclones which depress sea level offshore while raising sea level at the coast.

7.3.2.6 Nutrient supply and primary producers

Two factors limit productivity in the Arctic Ocean: light (photosynthetically active radiation) and nutrients (primarily nitrate). For the latter, the Arctic can be considered an advective ocean (Carmack and Wassmann, 2006; Grebmeier et al., 2015; Wassmann et al., 2015) through which nutrients are transported and transformed between the Pacific and Atlantic Oceans (Yamamoto-Kawai et al., 2006). However, it is important to distinguish between new and recycled primary production, with the former limited by the supply of nitrate to the euphotic zone during the vegetative growing season (see Codispoti et al., 2013). In turn, this supply has three seasonal modes of delivery: replenishment by haline convection during the winter non-vegetative season; vertical mixing at the base of the mixed layer in summer; and enhanced mixing by winds and convection in autumn when sufficient light is still available to support an autumn bloom. As shown by Codispoti et al. (2013), nutrient replenishment in winter is very small owing to robust freshwater stratification. The importance of vertical mixing at the base of the surface mixed layer in summer is confirmed by the ubiquitous presence of the subsurface chlorophyll maximum (Martin et al., 2013; Bluhm et al., 2015; Tremblay et al., 2015). The increasing importance of the autumn bloom following sea-ice retreat was discussed by Ardyna et al. (2014). At present, there are insufficient data to provide a quantitative Arctic-wide assessment of temporal trends in nutrient supply. There is evidence, however, that freshwater capping is suppressing the supply of nutrients in Canada Basin, as shown by the recent deepening of the chlorophyll maximum (McLaughlin and Carmack, 2010) and by the increased fraction of smaller phytoplankton in the upper ocean (Li et al., 2009), whereas ice retreat beyond the shelf break may be increasing nutrient supply on shelves due to enhanced upwelling (Tremblay et al., 2015; Williams and Carmack, 2015).

7.3.2.7 Ocean acidification

Changes in environmental parameters over the past two decades (increased river discharge, warming, loss of sea ice, and increased primary productivity) are affecting the rate of acidification in the Arctic Ocean. Time series observations reveal significant decreases in pH and Ω in the Nordic Seas between 1985 and 2008 (Olafsson et al., 2009), and in the Canada Basin between 1997 and 2008 (Yamamoto-Kawai et al., 2009; Miller et al., 2014). In the former region, ocean acidification was enhanced by a surface ocean $p\text{CO}_2$ increase slightly exceeding the atmospheric CO_2 trend, probably due to decadal-scale climate variability (Thomas et al., 2008; McKinley et al., 2011). In the latter region, the increase in atmospheric CO_2 could account only for half the decrease in Ω , with the rest due to the extensive loss of sea ice in the 2000s (Yamamoto-Kawai et al., 2011). Melting of sea ice has also enhanced the uptake of CO_2 by the surface water and meltwater that are diluted in alkalinity and calcium ion concentration. These combined effects resulted in a large decrease in Ω and undersaturation of surface water with respect to aragonite-type calcium carbonate in the Canada Basin. Aragonite undersaturation has also been observed in the low-salinity surface waters in coastal regions of the Bering Sea (Mathis et al., 2011), East Siberian Sea (Anderson et al., 2011), Canadian Arctic Archipelago (Chierici and Fransson, 2009; Azetsu-Scott et al., 2010; Chierici et al., 2011; Yamamoto-Kawai et al., 2013), and Hudson Bay (Azetsu-Scott et al., 2014).

These observations indicate that freshwater input significantly exacerbated ocean acidification in surface waters. In contrast, warming and increased primary productivity in surface waters serve to increase surface Ω (e.g. Chierici et al., 2011).

Freshwater inputs also affect ocean acidification by stratifying the surface layer. A stronger and shallower halocline results in a higher temperature and lower biological productivity in surface waters and prevents the transport of anthropogenic CO_2 into deeper layers (Cai et al., 2010). In shelf seas, stratification also results in low pH and low Ω bottom waters by accumulating remineralized CO_2 at the seabed. Aragonite-undersaturated shelf bottom waters have been observed in the Bering Sea (Mathis et al., 2011), Chukchi Sea (Bates et al., 2009), East Siberian Sea (Anderson et al., 2011), Canadian Arctic Archipelago (Yamamoto-Kawai et al., 2013), and Hudson Bay as well as in the intermediate layer of the Canada Basin where shelf-derived water occurs (Jutterström and Anderson, 2005). Calcite-undersaturated bottom waters are now observed in the East Siberian Sea and Hudson Bay (Anderson et al., 2011; Azetsu-Scott et al., 2014). Although Arctic waters were originally characterized by low Ω , largely due to high freshwater inputs, calculations have shown that the observed undersaturation is a recent phenomenon. In fact, Yamamoto-Kawai et al. (2013) showed that most of the Arctic Ocean would be oversaturated if there were no uptake of anthropogenic CO_2 . An increase in freshwater supply to the Arctic Ocean will act to further exacerbate ocean acidification and expand the area of calcium carbonate undersaturation.

7.3.3 Projected changes and key drivers

Currently, the Arctic Ocean is freshening (Haine et al., 2015), warming (Polyakov et al., 2012), losing sea ice (Stroeve et al., 2012), and its ice cover is changing properties and moving faster (Kwok et al., 2013). Internal to the Arctic Ocean, the distribution and spreading pathways of stored freshwater are shifting on a variety of time-scales (Mauritzen, 2012). External to the Arctic Ocean, the exchanges of heat, salt and biogeochemical properties with the bordering subarctic oceans are undergoing substantial change (Carmack and McLaughlin, 2011). As the physical attributes of the overall Arctic freshwater system undergo change, so too do its geochemical components (McLaughlin and Carmack, 2010) and biological components (Petrenko et al., 2013). Modeling studies project major changes in the Arctic Ocean freshwater system with substantial intra-Arctic and extra-Arctic effects (Lique et al., 2016).

Coupled climate models provide information about potential future change in the Arctic freshwater system (Lique et al., 2016; Section 7.7) but model results are inherently uncertain and different coupled models are often in mutual contradiction. Nevertheless, some projections are robust across current climate models that derive from two well-accepted predictions: (1) that the global hydrological cycle will intensify in a warmer climate and (2) that Arctic warming will exceed the global average. Future conditions under warming scenarios are likely to include increased runoff, increased inputs from glacier melt and permafrost thaw, and changes in the phenology of discharge (Bring et al., 2016; Section 7.4). Freshwater supply into oceanic regions to the south of the conventional Arctic Ocean gateways may recirculate back into the Arctic Ocean or influence the convective gyres in the subarctic North Atlantic to influence the strength of the Atlantic meridional overturning cell. Better

understanding of the Arctic freshwater system thus requires an expanded geographical domain. A larger-scale perspective for the marine freshwater system should also help improve understanding of ocean-atmosphere coupling at boundaries between salt-stratified ocean and temperature stratified ocean, which in turn appear to constrain storm tracks.

An intensifying hydrological cycle magnifies the atmospheric convergence of water vapor in the Arctic (Zhang et al., 2013) and so increases precipitation and runoff. One CMIP5 model, for example, projects a 40% increase in precipitation north of 70°N over the 21st century (Vavrus et al., 2012; Vihma et al., 2016; Section 7.2). Most of this is likely to be due to an intensifying Arctic hydrological cycle (i.e. greater evaporation linked to sea-ice retreat) rather than to water vapor flux from lower latitudes (Bintanja and Selten, 2014). Haine et al. (2015) concluded that the total P-E freshwater source to the ocean would be about 30% higher by 2100, with total runoff about 14% higher. The Bering Strait freshwater flux is also projected to increase but by an unknown amount.

The total volume of freshwater stored in the Arctic will probably increase due to these larger inflows. Based on results from a selection of CMIP models, Haine et al. (2015) speculated that an extra 50,000 km³ could be stored by the end of the century, a growth of 50% (but did note significant differences between models). This increase will occur in the liquid reservoir as the sea ice volume will continue to decline. Most of the liquid reservoir increase will presumably occur in the Canada Basin. It is unclear whether the Beaufort Gyre has reached, or is approaching maximum capacity.

For the outflow fluxes, Fram Strait will probably transition to more liquid export – perhaps doubling by 2100 – and less ice export, which may shrink to become just a minor term in the budget (Vavrus et al., 2012). The flux through Davis Strait is uncertain; one model projects that it will increase to 2070 as the outflow freshens and then decrease as its volume flux drops (Vavrus et al., 2012). Haine et al. (2015) projected that the total Arctic freshwater outflow will increase this century but maybe by less than the freshwater sources increase. On this basis the Arctic Ocean would be freshening in 2100, perhaps even at a faster rate than during the 2000s.

7.3.4 Knowledge gaps and future research

Improved quantification of the freshwater budget in the marine system is needed by managers and policy-makers (Prowse et al., 2015b). A three-step approach is proposed for future research:

1. *Improved hydrographic mapping of system components.* Change cannot be quantified without robust monitoring data, and it is not possible to monitor what has not been adequately mapped. Fundamental knowledge of Arctic Ocean hydrography is currently rudimentary, spatially and temporally.
2. *Increased monitoring of system components.* Detection of change requires sustained monitoring. Time-series data for the Arctic Ocean are extremely sparse. This makes it almost impossible to distinguish variability and trends at different time-scales. Remote sensing and ground-based measurements are both required, since neither can provide a complete picture without the other.
3. *Focused studies of fundamental concepts and processes.* Improved understanding and parameterization is required for processes that control freshwater delivery, transport, storage and discharge back to lower latitudes; the role that atmospheric and terrestrial system components play in terms of two-way interactions and system feedbacks; and the joint effects of sea-ice decline and an intensified hydrological cycle on northern hemisphere weather and global climate (Carmack et al., 2016; Prowse et al., 2015b).

7.4 Terrestrial hydrology

An All Arctic Regions (AAR) delineation was selected as the terrestrial contributing area (TCA) for the *Arctic Freshwater Synthesis* based largely on the nature of the downstream marine pathways that transport the flow of rivers from this terrestrial region (see Section 7.1). As previously stated, an important geographical characteristic of the AAR is that a majority (about 77%) of its total contributing area lies outside the classical definition of the Arctic (i.e. south of the Arctic Circle at 66.6°N; see Figures 7.3 and 7.8). Moreover, if just the

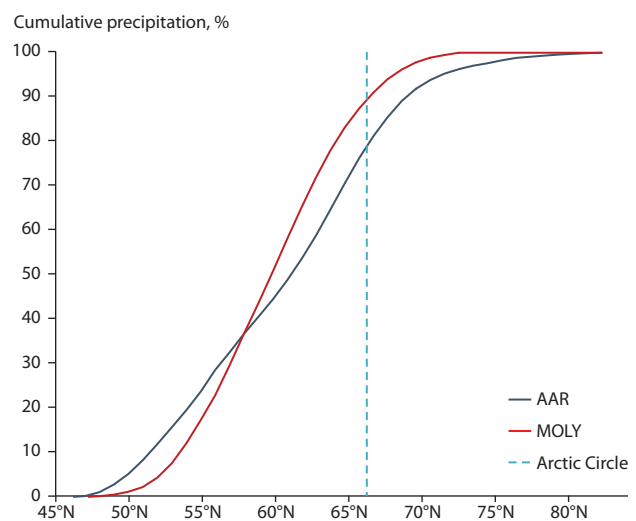
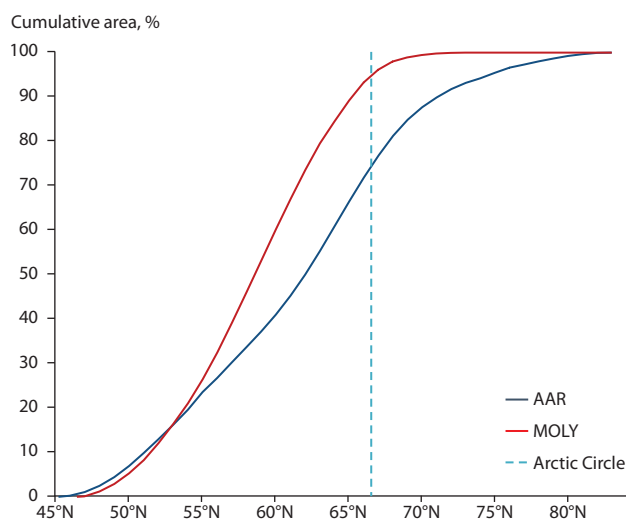


Figure 7.8 Cumulative area by latitude (left) and cumulative precipitation by latitude (right) for the All Arctic Regions (AAR) contributing area and the four major river basins (MOLY; Mackenzie, Ob, Lena, Yenisey) (Prowse et al., 2015a).

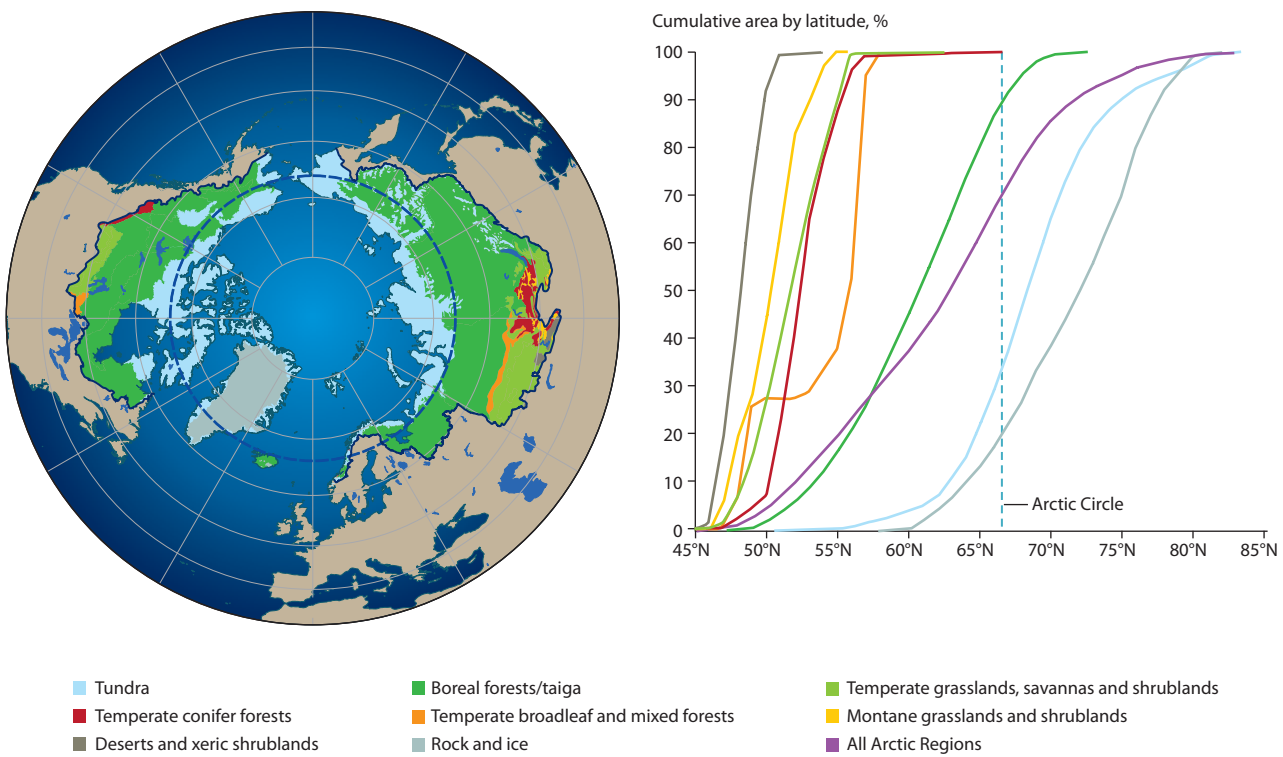


Figure 7.9 Major ecoregions within the All Arctic Regions (AAR) contributing area and cumulative area by latitude for each ecoregion (Prowse et al., 2015a).

contributing area of the four major rivers that empty directly into the Arctic Ocean (Mackenzie, Ob, Lena, Yenisey; herein referred to as MOLY) is included, the percentage area south of the Arctic Circle is about 95%. A large percentage of the total basin precipitation that supplies the various Arctic-flowing rivers is also delivered at latitudes south of the Arctic Circle: 80% in the case of the AAR and 90% for MOLY (Figure 7.8), and across a diverse range of ecoregions and hydro-physiographic regions (Figures 7.9 and 7.10) with different water-balance, runoff and storage characteristics as controlled by variations in precipitation-evapotranspiration regimes, cryospheric components, elevation effects and lake area. For the latter, a majority of lake storage within the AAR also occurs at more southerly latitudes, with about 85% of total area below the Arctic Circle, due primarily to the area of relatively large lakes (Prowse et al., 2015a). Many smaller lakes and ponds are found above the Arctic Circle, however, an important issue in Arctic aquatic ecology (Wrona et al., 2016 and Section 7.5).

7.4.1 System functioning and key processes

The cryospheric components, including their ongoing spatial and temporal changes (see also Chapters 3, 4 and 6) play a large role in determining hydrologic responses across the diverse range of hydro-climatic regions within the AAR (Bring et al., 2016). They also play a key role in producing changes in terrestrial vegetation and the related hydrologic response, particularly evapotranspiration and runoff (Wrona et al., 2016; see Section 7.5; see also Chapter 10).

Terrestrial freshwater fluxes through river basins are central to many of the environmental changes currently underway in the Arctic. Water added as precipitation over Arctic river basins (see Prowse et al., 2015a; Lique et al., 2016; Vihma et al., 2016 for overviews and quantitative estimates)

mostly returns to the atmosphere as evapotranspiration. The magnitude of the evapotranspiration flux then largely determines the proportion of the water that forms river discharge and eventually reaches the Arctic Ocean. The river discharge in turn transports freshwater, heat, sediment, carbon and nutrients across vast distances, while runoff regimes and river ice conditions control winter transportation, infrastructure and resource extraction, carbon release from permafrost, and ecosystem dynamics. Lake and river ice peak at a volume of about 1600 km³ in winter, which is roughly equal to the volume of the northern hemisphere land snow pack, and covers an area similar to that of the Greenland Ice Sheet (Brooks et al., 2013). Although most direct effects of freshwater ice are local or regional (e.g. changes in radiation and convective fluxes) (Rouse et al., 2005), the impact on evapotranspiration, precipitation, and their feedbacks on hydrology may act at much larger scales, even influencing the water balance of large Arctic basins (Rouse et al., 2008).

7.4.2 Observed changes and key drivers

Although uncertain, observations and models suggest terrestrial freshwater fluxes have intensified over the past few decades (Haine et al., 2015). Here, the key focus is on evapotranspiration, runoff, and changes in lake and river ice. Evapotranspiration is the major component of water flux out of the pan-Arctic drainage basin. The annual evapotranspiration flux, which ranges from averages of 141±8 mm/y in the tundra to 426±16 mm/y in grasslands (based on long-term satellite estimates; Bring et al., 2016) is generally less than precipitation, except over a few southern inland areas. Over time, landscape variations such as changes in lake area may have considerable effects on evapotranspiration and runoff (Karlsson et al., 2015). Measurements of evapotranspiration rates are difficult

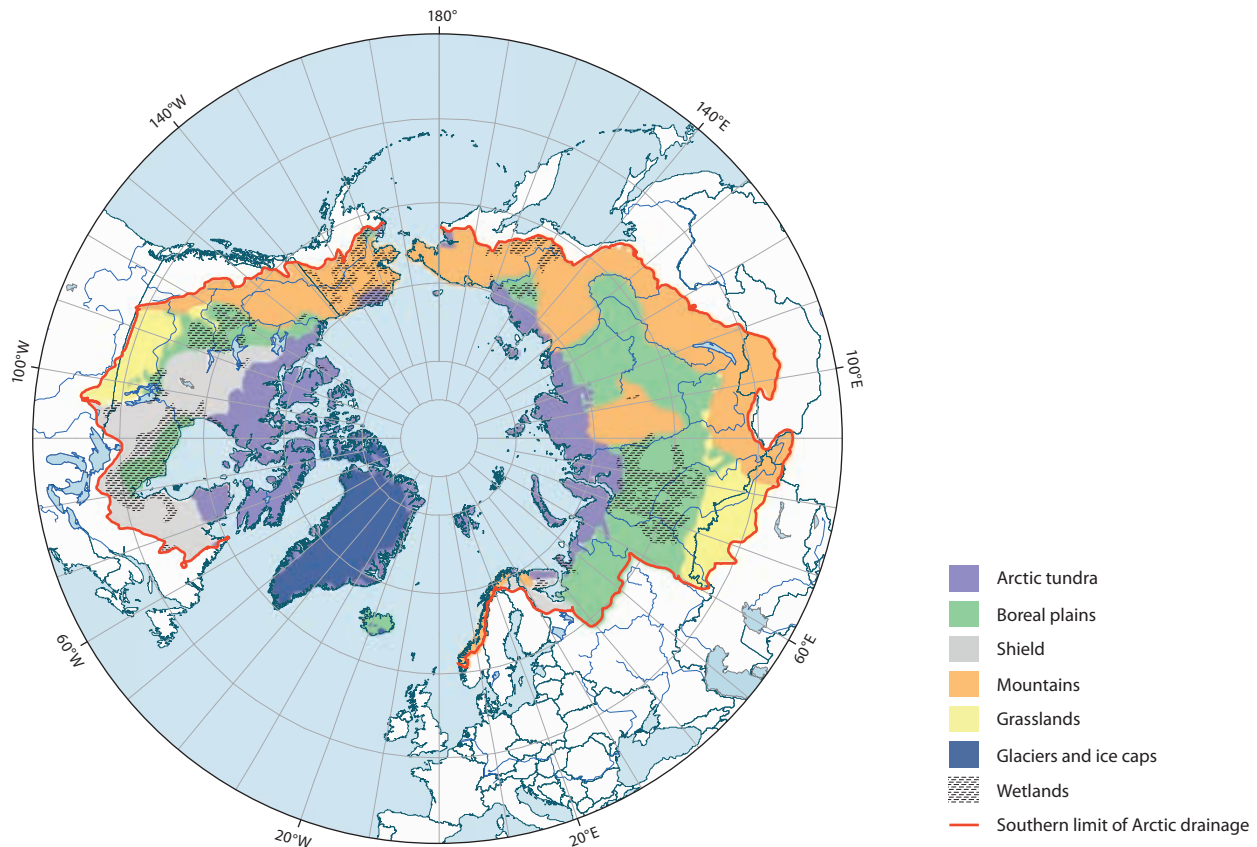


Figure 7.10 Major hydro-physiographic regions within the All Arctic Regions (AAR) contributing area (Bring et al., 2016).

to undertake over large areas, but model analyses of historical data suggest that evapotranspiration has accelerated over the pan-Arctic basin as a whole, with mean trends of $+0.17 \text{ mm/y}^2$ ($p<0.1$) for the period 1950–1999 (Rawlins et al., 2010) increasing to $+0.38 \text{ mm/y}^2$ ($p<0.05$) for the period 1983–2005 (Zhang et al., 2009). Liu et al. (2014) reported a similar rate of increase at $+0.13 \text{ mm/y}^2$ ($p<0.05$) for northern Eurasia during 1948–2009, with some decreases reported in the boreal forests of southern and central Canada. A longer growing season, increased water availability, and higher temperatures may all have contributed to increasing evapotranspiration.

Discharge is the other major terrestrial freshwater flux. River flows have generally increased for the pan-Arctic (Holmes et al., 2013; Haine et al., 2015), rising from $3900 \pm 390 \text{ km}^3/\text{y}$ for the period 1980–2000 to $4200 \pm 420 \text{ km}^3/\text{y}$ for the period 2000–2010 (Haine et al., 2015). There is evidence for a central role of increased atmospheric moisture transport as a driver of the flow increases (Troy et al., 2012; Zhang et al., 2013; see discussion on atmospheric changes in Section 7.2, and Vihma et al., 2016). Factors such as fires, permafrost decay, and landscape changes also affect flow but to a lesser degree (Zhang et al., 2013; Karlsson et al., 2014). An exact quantification of such effects remains elusive.

Ice-cover duration on lakes has declined, with breakup dates changing more rapidly than freeze-up (Prowse, 2011; Benson et al., 2012). Although the change is greatest over the longest term (the period 1855–2004 shows more change than the period 1905–2004), the rate of change has increased over recent decades with freeze-up later by 1.6 days per decade in the past 30 years, breakup earlier by 1.9 days per decade, and ice

duration shorter by 4.3 days per decade (Benson et al., 2012). River ice has changed in similar ways, but with more variation in freeze-up trends (Beltaos and Prowse, 2009). Although ice cover tends to be more sensitive to changes in air temperature at lower latitudes than at higher latitudes (Livingstone et al., 2010), the decline in ice cover appears to have been faster in very high-latitude lakes (Latifovic and Pouliot, 2007), which lost 1.75 days of ice cover per year over the period 1970–2004 – more than 4.5 times the rate in southern Canada. It is unclear whether this reflects the more recent and greater high-latitude warming, or potential differences in methodology.

7.4.3 Projected changes and key drivers

Arctic evapotranspiration is generally expected to increase during the 21st century (Lainé et al., 2014), with changes in daily evapotranspiration in the order of 0.05 mm/day in winter and 0.25 mm/day in summer over a 100-year period for the terrestrial pan-Arctic (1980–2000 vs 2080–2100), based on the RCP4.5 greenhouse gas emissions scenario (Lainé et al., 2014), but the redistribution of vegetation will also alter other local climate feedbacks, with complex changes (Pearson et al., 2013). Other estimates, based on earlier models, indicate trends of between 0.24 and 0.92 mm/y^2 , with a mean of 0.65 mm/y^2 for the period 1950–2049 (Rawlins et al., 2010). In general, results suggest an acceleration in evapotranspiration increase over the latter half of the 21st century. In contrast to the historical importance of atmospheric moisture transport in increased river flows, simulations project that open-water evaporation from previously ice-covered areas will play an increasingly

important role in freshwater supply to the Arctic basins (Bintanja and Selten, 2014; see also Section 7.2 and Vihma et al., 2016).

Increased evapotranspiration is unlikely to fully compensate for increases in precipitation, and so water flows are also projected to increase. Simulations with global hydrological models, using input from climate models show increases in the order of 25–50% over most of the pan-Arctic region (van Vliet et al., 2013). Although decreases are projected for some regions, model consistency is generally higher for increases.

Another potential change in evaporation regimes concerns the loss of freshwater ice cover. While lake-ice cover is projected to decrease in thickness (10–50 cm) and duration (15–50 days) over the period 2040–2079 compared to 1960–1999 (Dibike et al., 2011), the same is not projected for river ice. Given that the total area of freshwater ice in the northern hemisphere is $1.7 \times 10^6 \text{ km}^2$, roughly equal to that of the Greenland Ice Sheet (Brooks et al., 2013) there is large potential for increased open-water evaporation from the vast lakes and ponds that populate the TCA. The implications of this are addressed in Section 7.8.

As south-to-north air temperature gradients decrease along northward-flowing rivers, the magnitude of spring floods is likely to decline owing to less severe ice jamming (Prowse et al., 2010). However, more water may be released from melting snow as spring snow-water-equivalent is projected to increase at high latitudes (Adam et al., 2009). The net result of these two factors on flooding remains to be quantified but will vary by river basin. Changes in river-ice floods are important to rivers of the TCA, because such events are the main agent of sediment transport and morphological change (Turcotte et al., 2011).

7.4.4 Knowledge gaps and future research

Accurately representing precipitation in the high latitudes, by better remote sensing technology and more skillful models from a terrestrial hydrology perspective is an important research direction that would enhance the ability to understand and model Arctic freshwater dynamics (see also Lique et al., 2016). Studies that examine changes in land surface variables and fluxes (e.g. Dirmeyer et al., 2013) but which focus on the terrestrial Arctic may improve understanding of land–atmosphere interactions with respect to soil moisture and evapotranspiration. There is a strong need for more accurate representation of land surface effects concerning vegetation, lakes, and human interventions, in climate models (Bring et al., 2015). Moreover, given that ice-covered freshwater bodies comprise a significant proportion of the TCA and are projected to be increasingly less ice covered, the local and wider-scale atmospheric and hydrologic effects of this new moisture source need to be included in climate modeling of the Arctic freshwater system (Prowse et al., 2015b; Lique et al., 2016; Vihma et al., 2016).

Overall, knowledge of water and waterborne material flows is limited, largely reflecting the scope of surface-water and water-chemistry monitoring (McClelland et al., 2015). Potential improvements have been suggested by Azcárate et al. (2013) and McClelland et al. (2015). Use of remote-sensing technology, where some recent studies have shown promising results (e.g. Gleason and Smith, 2014) should be investigated further as a complement to increasing ground-based observations.

7.5 Terrestrial freshwater ecosystems

Alterations in precipitation, the annual evapotranspiration flux, landscape-level changes in lake and drainage area and runoff regimes, and associated changes in the spatial and temporal distribution and properties of snow, ice and permafrost collectively have been identified as key hydrological and cryospheric drivers of ecosystem change (Bring et al., 2016; Vihma et al., 2016; Wrona et al., 2016). In turn, these environmental drivers affect landscape geomorphological processes resulting in changes in the distribution and types of ecosystems/habitats, biological productivity, biogeochemical processes and exports, and species gains/losses, including phenological mismatches leading to trophic alterations. Given the complex inter-relationships among the drivers, significant uncertainty remains in forecasting the local and regional impacts of an intensified Arctic water cycle and related cryospheric change on Arctic terrestrial and freshwater ecosystems within the various ecoregions (Figure 7.9).

There is a broad range of geographical and ecological conditions in the Arctic, with river, lake, pond, and wetland complexes providing key geographical linkages across landscapes and environmental gradients. A range of terrestrial vegetation zones occur in the Arctic as well as a continuous gradient of environmental severity, from the boreal ecozone at the southern boundary to the open tundra and polar deserts of the far north, with freshwater ecosystems prevalent along this entire gradient (Vincent and Laybourn-Parry, 2008). From south to north, the vertical and horizontal dimensions in structural complexity of the vegetation also decrease (Walker et al., 2005; Callaghan et al., 2011; Ims et al., 2013). The Arctic tundra biome is also strongly influenced by coastal maritime climatic and hydrological regimes (AMAP, 2011; Ims et al., 2013). While temperature is a driver of ecological processes in tundra ecosystems, it is hydrological interactions that mediate the climate responses of these systems.

A large variety of freshwater ecosystem types occur in the Arctic (Huryn et al., 2005; White et al., 2007; Vincent and Laybourn-Parry, 2008; Moss et al., 2009; Wrona et al., 2013), ranging from ephemeral shallow ponds to large lakes, small intermittent streams to more permanently flowing large rivers, and intricate wetland complexes composed of fens, bogs, and marshes (Vincent and Laybourn-Parry, 2008). Hydrological processes and associated freshwater ecosystems in the Arctic are controlled by local and regional catchment characteristics, such as geology and landscape geomorphology, the associated terrestrial vegetation cover, and the presence or absence of permafrost (White et al., 2007). Freshwater ecosystems often form a highly interconnected network at the landscape scale, thus serving as important integrators of hydrological, atmospheric, and terrestrial processes (Williamson et al., 2008, 2009; Schindler, 2009).

7.5.1 Observed and projected ecosystem responses

7.5.1.1 Changing landscapes

Changes in permafrost thaw, snow distribution, runoff regimes and drainage systems collectively contribute to transformations of the landscape, resulting in gains and losses of ecosystems (e.g. reduction in the areal extent of high-

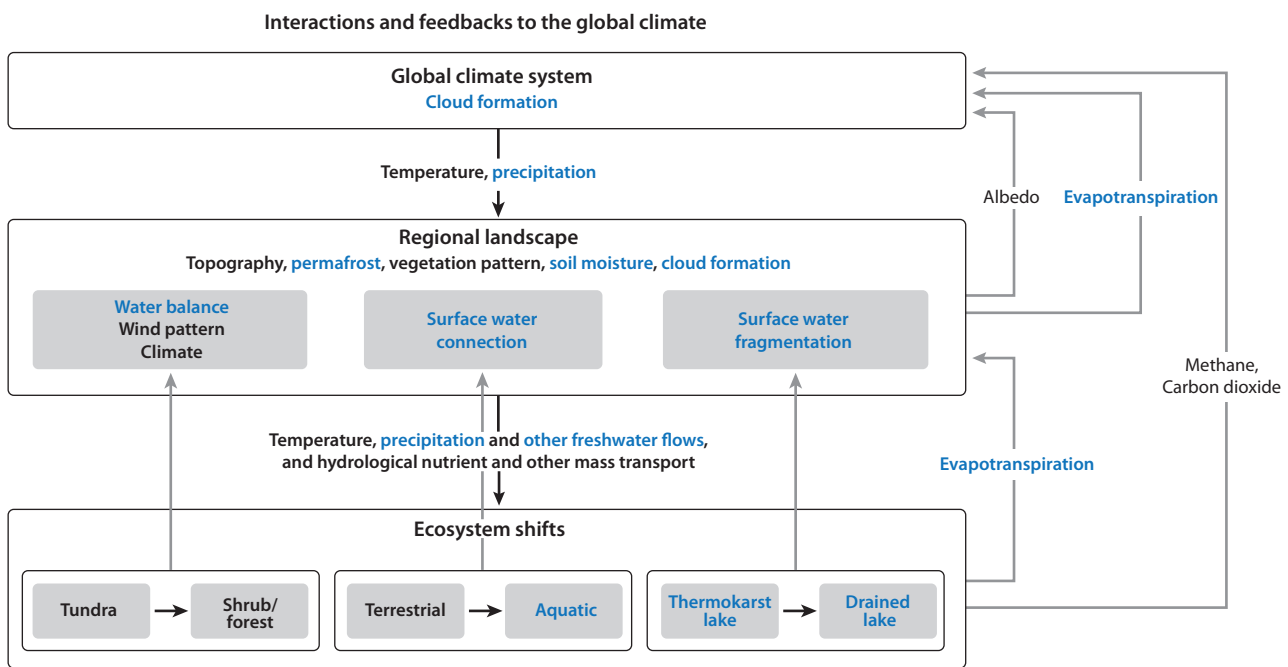


Figure 7.11 Interactions and feedbacks from three general types of ecosystem shift in Arctic terrestrial and freshwater environments: tundra to shrub/forest, terrestrial to aquatic, and thermokarst lakes to drained lakes (Wrona et al., 2016 – adapted from Karlsson et al., 2011).

latitude wetlands/ponds), changing river-lake connectivity, and altering ecosystem structure and function (Avis et al., 2011; Ims et al., 2013; Wrona et al., 2013, 2016; Karlsson et al., 2014; Andresen and Lougheed, 2015). The combination of climate-cryospheric-hydrologic change, coupled with multiple ecological feedback processes, may in turn, cause unexpected reorganizations of ecological structure and function and trigger ecosystem shifts (Figure 7.11) or the development of novel ecosystems. Several such shifts have been observed in the Arctic, including vegetation shifts and conversions between terrestrial and aquatic ecosystems (e.g. thermokarst lakes and wetlands developing in ice-rich terrestrial environments, and draining of lakes and wetlands causing conversion from aquatic to terrestrial ecosystems) (Wrona et al., 2016). There is great uncertainty in the projections of the relative geographic extent and magnitudes of such shifts.

7.5.1.2 Productivity

‘Terrestrial greening’ is the most conspicuous productivity-related change observed in the Arctic (e.g. Macias-Fauria et al., 2012; Gamon et al., 2013; Xu et al., 2013; Guay et al., 2014; see also Chapter 9), exemplified by ‘shrubification’ in the tundra biome (e.g. Myers-Smith et al., 2011; Elmendorf et al., 2012; Tape et al., 2012). Shrub encroachment and other vegetation productivity change could cause shifts in trophic dynamics, community composition and biogeochemical cycling on land and associated aquatic ecosystems (DeMarco et al., 2014; Stewart et al., 2014). Removal of shrub canopies can encourage permafrost thaw and the transition of ecosystems from terrestrial to aquatic, undergoing anaerobic rather than aerobic decomposition, and leading to greater methane release (Nauta et al., 2015). Productivity change has also been linked to warming, altered moisture and disturbance regimes related to permafrost thaw, fire and changing herbivore pressure

(e.g. Lantz et al., 2010; Frost et al., 2013; Kerby and Post, 2013). Enhanced nutrient fluxes from land to water, from a deepening of the active layer and increased thermokarst activity, have been associated with increasing ion and nutrient concentrations in receiving waters, in some cases leading to enhanced autotrophic productivity (e.g. Thompson et al., 2012; Kokelj et al., 2013, 2015; Thienpont et al., 2013). While decreasing ice-cover thickness, duration and optical quality have been documented in freshwater ecosystems (e.g. Wrona et al., 2013, 2016; Surdu et al., 2014), the geographic extent and rate of possible aquatic greening are still uncertain.

7.5.1.3 Biogeochemical processes and exports

The proportion of snow and rainfall, snow depth and distribution, seasonal ice cover, and permafrost dynamics have direct and indirect effects on ecosystem biophysical and biochemical processes (Bring et al., 2016; Wrona et al., 2016). Together with other environmental drivers such as shifts in plant community structure and productivity relationships and fire, these changes will influence the rates and magnitudes of nutrient cycling and export, the release and transport of bound or deposited contaminants, and biophysical properties such as successional patterns in terrestrial and freshwater ecosystems (Wookey et al., 2009; Holmes et al., 2013; Ims et al., 2013; Wrona et al., 2016). Increased terrestrial productivity in boreal forest, and sub-Arctic and Arctic tundra regions (Epstein et al., 2012; Guay et al., 2014; Urban et al., 2014) may have significant consequences for biogeochemical export to catchment lakes and rivers and eventually the ocean (Carmack et al., 2016; Section 7.3). Based on current knowledge, it is only possible to speculate about these potential (or actual) effects, partly because interacting eco-hydro-geomorphic factors do not enable simple causalities to be established.

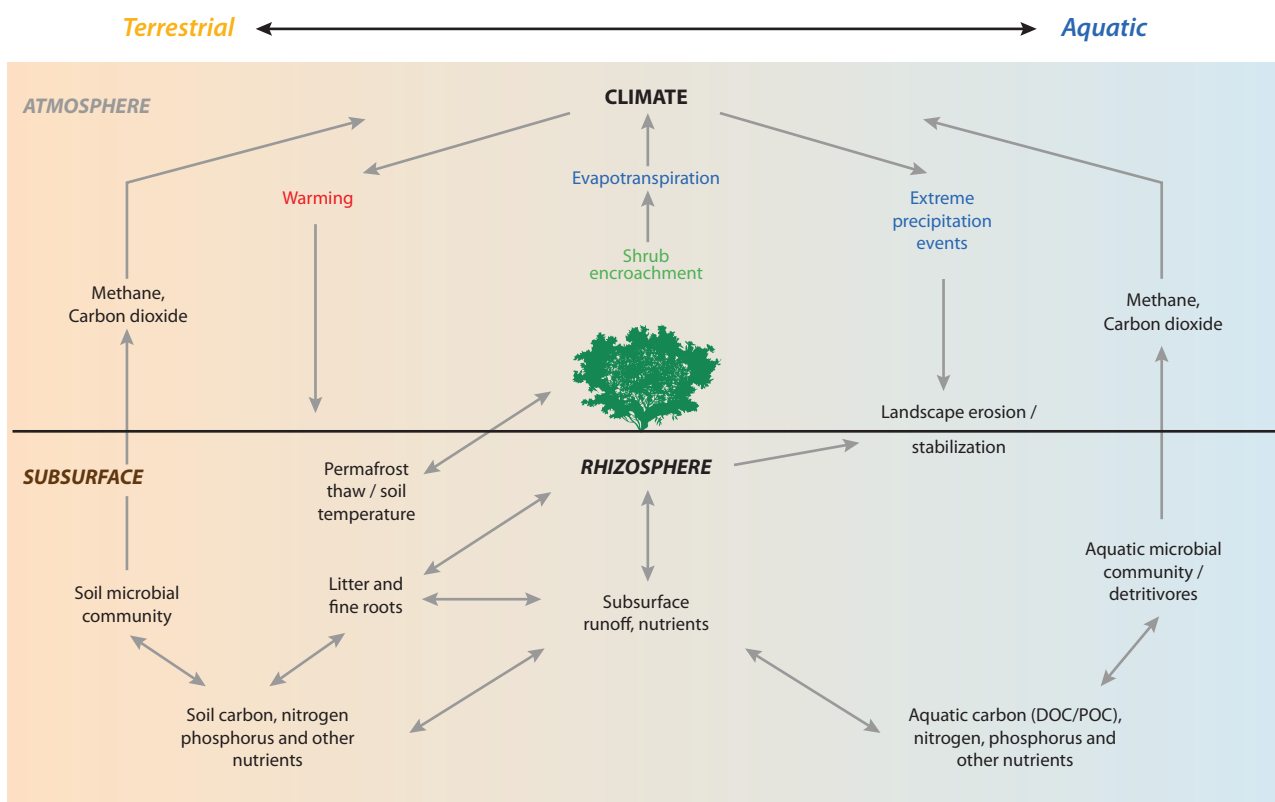


Figure 7.12 Linkages and possible effects of vegetation change on Arctic terrestrial and aquatic biogeochemical and ecological processes (Wrona et al., 2016 – adapted from Myers-Smith et al., 2011).

7.5.1.4 Species and trophic alterations

A changing Arctic freshwater system and cryosphere have significant cascading effects on species range expansion or contraction, food web complexity and trophic coupling (Christiansen et al., 2013; Ims et al., 2013; Wrona et al., 2013). This is largely associated with the potential loss of species from northern ecological communities but also to the arrival of new species from the south, either through gradual range expansions or long-distance dispersal of invasive species. Changes in snow and ice-cover duration and extent, frequency and intensity of rain-on-snow events, and earlier river and lake-ice break-up can result in seasonal and phenological mismatches in terrestrial and aquatic food webs, where trophic interactions between consumers and resources become weakened or broken (Post and Forchhammer, 2008; Miller-Rushing et al., 2010; Woodward et al., 2010; Prowse et al., 2011; Ims et al., 2013; Wrona et al., 2013). In freshwater ecosystems, higher water temperature and longer open-water periods are expected to shift seasonal phenology, and to cause decreases in cold stenotherms (algae, benthic macroinvertebrates, fish) and range alteration for cold-intolerant taxa.

Figure 7.12 shows linkages between aquatic and terrestrial ecosystems and changes in vegetation, while Figure 7.11 shows interactions and feedbacks for three types of ecosystem shift in the Arctic. In terms of linkages and vegetation shifts, increases in shrub species could lead to enhanced litter and fine root inputs and nitrogen-fixation in terrestrial soils, thereby altering nutrient cycling and leading to greater runoff into aquatic systems. Furthermore, proliferation of shrubs may influence evapotranspiration rates and the stability of stream banks, and pond and lake shores. In contrast, removal of shrub canopies can

lead to permafrost thaw and the transition of ecosystems from terrestrial to aquatic. Collectively, these ecological feedbacks of vegetation change can influence inputs of nutrients and fluxes of gaseous, particulate organic carbon and dissolved organic carbon, potentially leading to enhanced productivity across both terrestrial and aquatic Arctic ecosystems. As shown in Figure 7.11, climate change drives changes in regional temperature and precipitation, and these exogenous changes interact with regional topography and landscape patterns of permafrost and plant communities, and are mediated and propagated by hydrology (blue text indicating hydrologic variables) in pushing Arctic ecosystems toward directional ecosystem shifts (black arrows). Ecosystem shifts occur at the local landscape scale, but the consequences can feed back to regional and global scales (gray arrows), through reshaping of hydrology (changes in evapotranspiration, water balance, and surface water connection/fragmentation) and by altering albedo and carbon (as carbon dioxide and methane) energy fluxes. If these changes accumulate across large geographic areas, they can also affect global climate.

7.5.2 Knowledge gaps and future research

There is a need for an improved process-based understanding of inter-ecosystem interactions addressing key uncertainties, plus improved predictive models of ecosystem responses to alterations in hydrologic, cryospheric and atmospheric drivers. Consideration should be given to the catchment-scale as an ecological unit of study (e.g. Skeffington et al., 2010), thereby more explicitly considering the physical, chemical and ecological processes and fluxes across a full freshwater continuum in a geographic region and spatial range of hydro-ecological units

(e.g. stream-pond-lake-river-nearshore marine environments). Key knowledge gaps that need to be addressed through enhanced interdisciplinary research and monitoring include: (1) forecasting the rates and relative importance of greening and browning in terrestrial and freshwater systems, including an improved process-based understanding of inter-ecosystem interactions that involve terrestrial landscape-freshwater-nearshore marine coupling; (2) predicting how an altered and intensified hydrological cycle affects terrestrial and freshwater productivity and influences biogeochemical processes such as net emissions of greenhouse gases and geochemical export to the ocean; (3) identifying specific Arctic regions that may be particularly vulnerable to ecosystem shifts in the future (e.g. shrubification, species gains and losses, enhanced landscape disturbance/alterations such as thermokarst development and slumping) and determining whether tipping points exist that lead to irreversible ecosystem state changes; (4) projecting how altered hydrological and climatic seasonality will influence the structure and function of Arctic ecosystems and determining whether phenological mismatches will result in restructuring of Arctic food webs and corresponding cascades to ecological processes; and (5) improving process-based understanding and prediction of hydrological and cryospheric change at relevant spatial and temporal scales to assess corresponding changes in geochemical, biological and ecosystem-level attributes and properties.

7.6 Resources

Annual precipitation in the mid- and high-latitude areas has increased over the past century (Vihma et al., 2016) and models project that Arctic-mean precipitation will continue to increase in the future (Lique et al., 2016; Vihma et al., 2016). This implies that freshwater availability may also increase. Climate change may alter the amount and type of precipitation, its seasonal distribution, and the timing and rate of snowmelt (Bring et al., 2016; Vihma et al., 2016). Current knowledge of system function and key physical processes affecting northern water resources, industry and other sectorial infrastructure was summarized by Instanes et al. (2016) and this summary provides the basis of this section.

7.6.1 System function and key processes

Water resource management in the Arctic provides opportunities for socio-economic growth and industrial development. Efficient water resource management strategies are essential for maintaining water security and for minimizing the impact of flooding and related hazards associated with changes in freshwater systems.

7.6.2 Projected changes and key drivers

A projected increase in precipitation and thus total freshwater system volume in the Arctic, coupled with more frequent droughts at lower latitudes will increase the importance of the Arctic as a source of water supply for southern population centers. Hence, requests for the export of freshwater to more southerly latitudes is likely to grow, particularly by the end of the century, and become an increasing concern for policymakers.

Deeper active layers and higher permafrost temperatures under a warming climate could increase the risk of freshwater contamination associated with municipal and industrial waste

disposal. Municipal water resources could also become more vulnerable to extreme flood and drought events.

Transportation networks are also threatened by climate warming. Decreasing river and lake ice thickness (see Section 7.4) is affecting the viability of ice roads through shorter operational seasons (Hori et al., 2016; Mullan et al., 2016). A trend towards reduced transportation efficiency of temporary winter roads is increasing demand for all-weather roads and river transport. All-weather roads and railroads in the Arctic could be affected by accelerated rates of erosion, slumps and landslides due to permafrost thaw.

Higher winter and mean annual flows are projected to increase potential for hydropower generation. Arctic residents could even develop small-scale hydro-electric units in some areas. Projected changes in the timing and magnitude of snowmelt runoff and river-ice conditions could cause reservoir related and downstream flood hazards.

Declining sea ice and retreating glaciers will result in a longer operational season. Easier access to land areas through the opening up of the Arctic Ocean and previously glaciated land areas becoming ice free, coupled with increased demand for natural resources and raw materials, are projected to result in increased industrial activity by the end of the century.

7.6.3 Adaptation

Risk assessments taking climate change scenarios into account are becoming more common in the circumpolar Arctic (Instanes, 2012). Canada and Norway have already made efforts to incorporate climate change scenarios and risk assessments within new laws, regulations, codes, and guidelines. Climate change adaptation is challenging, especially given the large uncertainty associated with climate model results (Lique et al., 2016). In particular, uncertainty related to the amount and type of precipitation, its seasonal distribution, and frequency of extreme events makes it difficult to accurately estimate the impact of current and projected climate change on anthropogenic systems. Other factors may overshadow the effect of climate change such as construction activity and industrial developments that degrade permafrost soils, and so cause changes in local vegetation and drainage patterns.

There are also many sources of uncertainty in the projections of hydrological impacts; in the climate modeling, which is used to transfer a projected climate change signal to meteorological station sites; in the seasonality of the runoff; and in the hydrological modeling. The choice of regional climate scenarios is a crucial factor in any impact study. Future work should pay more attention to this issue to ensure that the ensemble of regional climate scenarios used is as unbiased as possible and covers a reasonable spread of future developments. Climate change adaption and an ability to exploit the potential benefits associated with climate change require multidisciplinary and cross-sectional research.

7.6.4 Knowledge gaps and future research

The major knowledge gap concerning water resources is a lack of historical site-specific observations and data (Bates et al., 2008). Knowledge of past, present and future variability in climate and hydrological response is essential for planning future water-resource management and planning for domestic/

industrial water use. Most hydrological models are built and calibrated for current and historical physical and ecological conditions of the land surface. Given that future climate in the Arctic is likely to be characterized by higher temperatures and higher precipitation, and so changes in land surface properties, vegetation cover and evapotranspiration (Bring et al., 2016; Lique et al., 2016; Wrona et al., 2016 and Sections 7.4, 7.7, and 7.5, respectively), advances in the current suite of hydrological models are required to fully assess the hydrological impacts of a changing climate on different water-resource sectors. Specifically, there is currently insufficient information on how climate change and variability affect water consumption, water quality, irrigation and groundwater supplies. Such information is essential for effective multi-use management of Arctic water resources under changing climatic conditions. Moreover, achieving an effective balance between the effects of a changing climate on water-resource supply and use, means water-resource management requires information from the application of a wide range of regional climate scenarios that also employ a plausible range of type and scale of future water-resource developments. Acquiring such information is key to designing effective adaptation measures for managing Arctic freshwater resources.

7.7 Modeling

There have been large-scale changes in the Arctic freshwater system (e.g. White et al., 2007; Prowse et al., 2015a). Investigating the mechanisms responsible for these changes is challenging based on observations alone. This is particularly true in the Arctic where measurements are generally sparse in space and time. Modeling systems can act as a ‘virtual laboratory’ and through appropriate experimental design can provide a powerful means to investigate the mechanisms of variability and change. Models also have a predictive capability, making it possible to investigate potential response to continued greenhouse gas emissions.

7.7.1 Hierarchical modeling approaches

Many different types of model have been used to investigate processes and interactions in the Earth’s system (Figure 7.13). These range from conceptual models that describe linkages across system components, such as discussed by Francis et al. (2009), to complex global Earth System models that solve extensive sets of equations on some of the world’s fastest supercomputers (e.g. Collins et al., 2011; Hurrell et al., 2013). These different modeling types are important tools in the

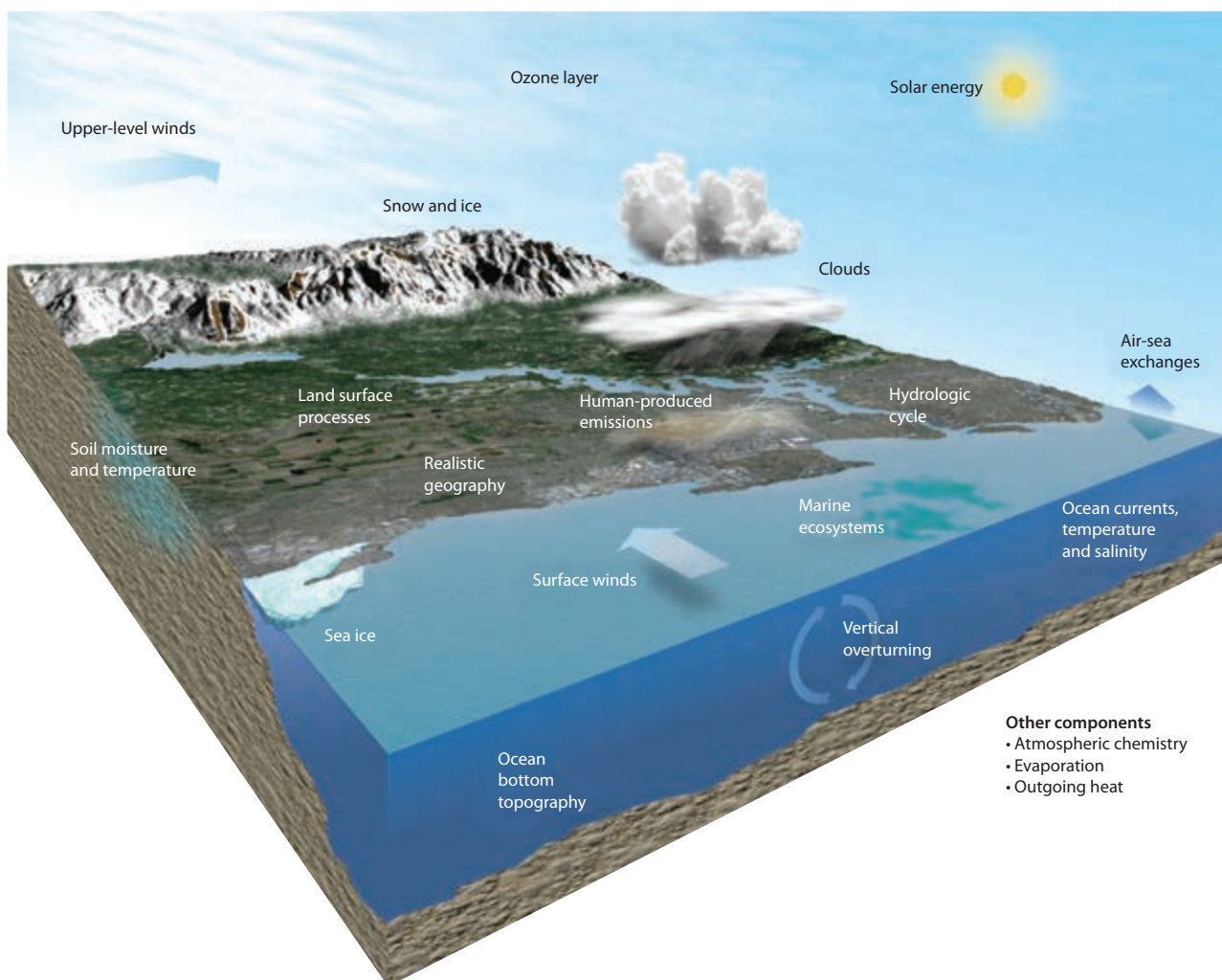


Figure 7.13 Schematic representation of Earth system model processes. Within a hierarchy of models, process models may focus on a single element of this schematic (such as permafrost), component models isolate a particulate component (such as the ocean or atmosphere) subject to prescribed boundary conditions, and fully coupled models include interactions across components. Copyright UCAR. Illustration courtesy of Warren Washington, NCAR (as shown in Lique et al., 2016).

attempt to better understand the Arctic freshwater system. The application of a hierarchy of modeling approaches is particularly useful as it can provide insights on many aspects of the system. For example, process models, which isolate a specific element of the system and allow the study of factors that determine the functioning of that element. Large-scale component models, such as atmosphere-only or ocean-only systems provide a means to explore variability and changes within these systems. Fully-coupled climate or earth system models enable studies on the role of feedbacks and coupled interactions on system functioning.

While models are powerful tools for studying the Arctic freshwater system, their limitations must be considered. Models can omit processes of relevance to a specific problem. This could include the lack of coupled interactions for a single-component model or the exclusion of a component of the system, such as ice sheets and glaciers (as has traditionally been the case in most Earth System Models). Models also exhibit biases in their mean climate conditions, which can affect simulations of variability and feedbacks. Finally, many large-scale models use relatively coarse resolution (around 100 km) and do not resolve finer-scale processes such as ocean eddies. The effects of unresolved processes can be parameterized, but these parameterizations themselves have deficiencies and uncertainties that must also be considered.

7.7.2 Using models to investigate Arctic freshwater variability and change

Studies using a hierarchy of models, with different levels of complexity and component interactions have provided considerable insight into processes affecting the Arctic freshwater system. The Arctic freshwater budget (see Figure 7.14) is determined by factors that affect the land, atmosphere, ocean, and sea ice. Investigating the processes within these components, using process models for example is a useful way to better understand the functioning of the system. This includes process models for various elements of the Arctic freshwater system. For example, models of permafrost dynamics (Lawrence et al., 2008; Frampton et al., 2013), high-latitude lakes (Dibike et al., 2011), and change in terrestrial snow cover (Liston and Elder, 2006) have been used to study the sensitivity and functioning of these various elements. Such models have provided insights on the factors influencing individual elements of the Arctic freshwater system.

Component and coupled models of the Arctic and/or global system enable the study of factors affecting the hydrological cycle in systems subject to additional climate system interactions. For example, the Arctic Ocean Model Intercomparison Project (AOMIP; Proshutinsky et al., 2001) employed ice-ocean coupled models to investigate mechanisms driving variability in Arctic Ocean freshwater budgets in the late 20th century (Jahn et al., 2012). Several studies have used model simulations for the historical period to attribute some fraction of observed Arctic change to anthropogenic factors. This includes attribution studies on changes in northern hemisphere snow-cover extent (Rupp et al., 2013), Arctic river discharge (Wu et al., 2005), and Arctic sea-ice cover (Min et al., 2008).

Coupled climate models provide a means to investigate projected future change subject to an assumed emissions scenario. While models differ considerably in the simulated

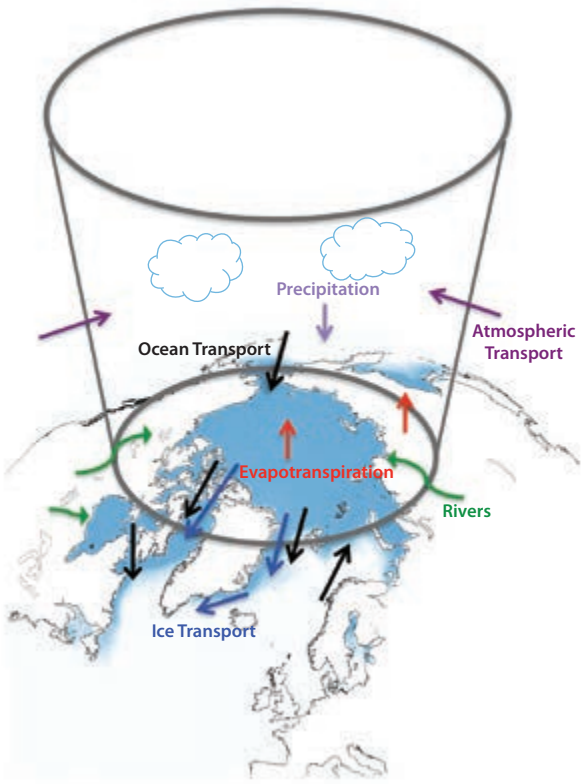


Figure 7.14 Schematic illustration of the Arctic freshwater budget. In addition to water fluxes (represented by arrows), water is also stored in the form of low-salinity ocean water, sea ice, glaciers, groundwater, and permafrost. The blue region indicates the average March sea-ice extent for the period 1980–1989 from satellite passive microwave data (Lique et al., 2016).

magnitude of future change, they do show consistency in the general sign of change. In particular, coupled models project an acceleration of the Arctic freshwater cycle in that there is an increase in the flux of water passing through the hydrological elements (e.g. Holland et al., 2007; Rawlins et al., 2010; Haine et al., 2015; Lique et al., 2016). This includes enhanced Arctic precipitation due to increased poleward moisture transport and local evaporation (e.g. Held and Soden, 2006; Bintanja and Selten, 2014; Vihma et al., 2016). The phase of precipitation also changes under Arctic warming, with a generally shorter snowfall season and implications for the terrestrial snow pack (Räisänen, 2008; Bring et al., 2016). With enhanced precipitation, increasing river discharge to the Arctic Ocean results as the Arctic warms (Mokhov et al., 2003; Holland et al., 2007). This acts with increased Arctic basin net sea-ice melt to freshen the Arctic Ocean. As a result, enhanced ocean freshwater is transported to the northern North Atlantic, which can have downstream implications and lead to a reduction in deep water formation and weakening of the Meridional Overturning Circulation (Jahn and Holland, 2013).

While there are many consistencies in the sign of projected future change simulated by models, the magnitude of that change can differ considerably and is quite uncertain (e.g. Holland et al., 2007). There are several sources for that uncertainty, including components associated with internal variability, model structure, and scenario or forcing uncertainty (e.g. Hawkins and Sutton, 2009; Hodson et al., 2013; Lique et al.,

2016). Uncertainty associated with the models themselves (model structure) is important for all timescales, whereas uncertainty associated with internal variability dominates in the near term (decadal scales) and scenario forcing uncertainty is important on longer timescales.

Improvements in models can help narrow uncertainty associated with model structure. The use of initialized decadal predictions (e.g. Meehl et al., 2009) may provide better predictive skill on interannual to decadal timescales.

7.7.3 Knowledge gaps and research direction

The Arctic freshwater system is controlled by processes within and across multiple Earth System components. Variability and change in Arctic freshwater budgets can in turn affect ocean circulation, biogeochemical cycles, and sea-level rise with far-reaching implications. Models are useful tools to understand both the functioning of the Arctic freshwater system and the larger implications of its variability and change. However, in applying models to these topics the limitations of modeling systems, including the influence of model biases and missing processes need to be carefully considered.

New strategies to facilitate comparisons between models and observations, such as use of satellite simulators (Cesana et al., 2012) and tracer-enabled ocean simulations (Newton et al., 2008; Jahn et al., 2010) are providing fresh insights about the causes for model biases and should be continued and expanded. Process-oriented observations have been beneficial for improved model parameterizations (Tjernström et al., 2005) and the need remains for observations to inform model developments. Conversely,

model simulations can be used to determine the added value of new observations and can help to inform observing system design (Lindsay and Zhang, 2006).

To better represent the Arctic freshwater system, new model capabilities are also needed. Models currently exclude some processes and interactions that are important for the functioning of the Arctic freshwater system. For example, many climate or Earth system models currently exclude explicit treatments of land ice, although there is progress in this area (Ridley et al., 2005; Lipscomb et al., 2013). Large-scale models also generally include only simple representations of lake processes and exclude many aspects important for high latitude river networks, such as their capacity to freeze and transport heat, carbon, nutrients and sediment. To better understand changing Arctic freshwater systems and their larger implications, model developments are needed to better incorporate these and other missing processes.

7.8 Summary

An integrated assessment of the major findings from the six thematic foci of the *Arctic Freshwater Synthesis* (see Section 7.1) indicates several key emerging scientific issues and related research needs (Prowse et al., 2015b). These include changes in the geography of the AFD, TCA and related storm tracks; the emergence of new hydro-ecological regimes with both terrestrial and marine components; the development of enhanced moisture fluxes from lake regimes; and changes in the relative importance of different freshwater resources.

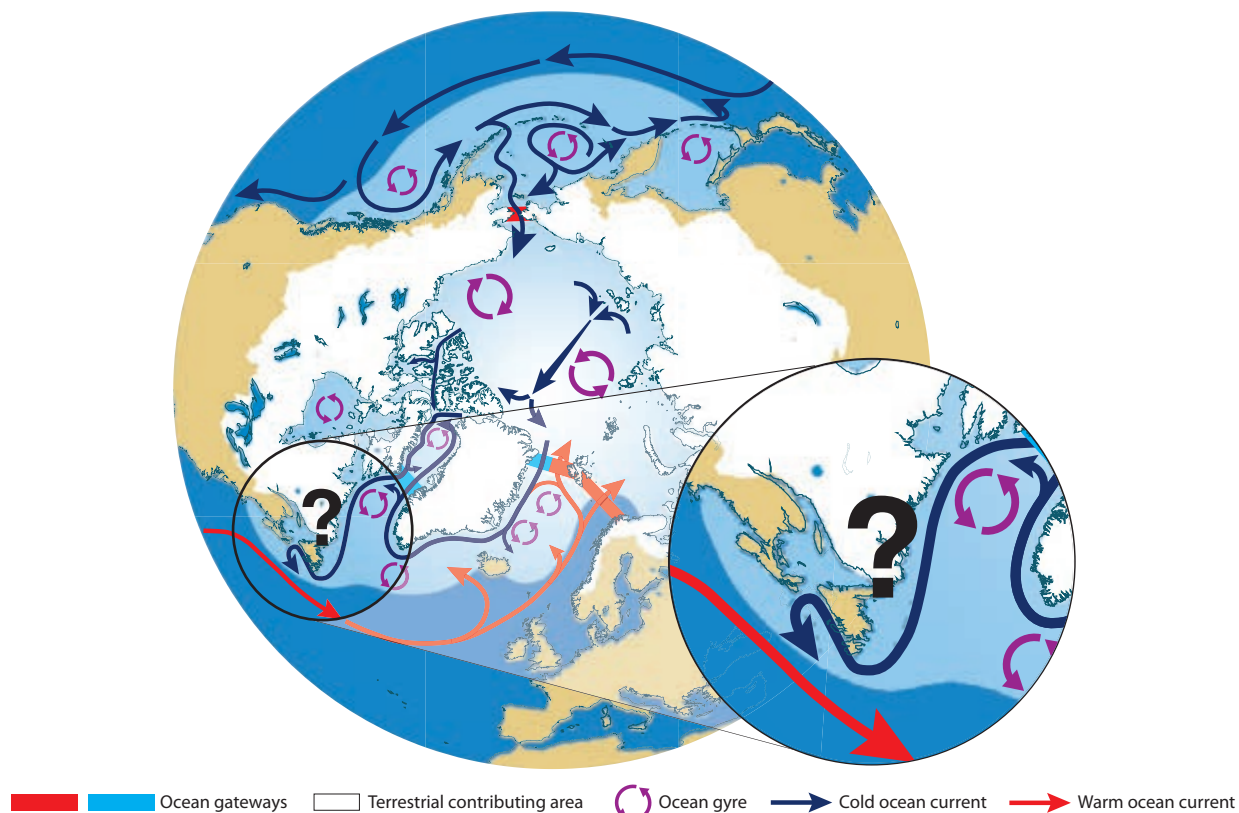


Figure 7.15 Expanded domain of the Arctic freshwater system showing four Arctic Ocean gateways, eleven gyral circulation patterns, major ocean currents including the newly identified pathway originating from the Laurentian Great Lakes/St. Lawrence River system – the final trajectory of which remains to be determined (identified by question mark), and the related expanded terrestrial-contributing area (shown in white) (Prowse et al., 2015b).

7.8.1 Expanded AFD, TCA and role of storm tracks

Although several geographical boundaries could have been used to define the overall domain of the Arctic freshwater system for the *Arctic Freshwater Synthesis*, an ocean-based definition was chosen, which also defined the related TCA. An important southern marine delimiter for the selected AFD was the location of the sub-Arctic seas, which contain the convective gyres that are influenced by the input of low-salinity water exported from the Arctic Ocean. As explored in the *Arctic Freshwater Synthesis* (Carmack et al., 2016), such gyral activity could also be influenced by additional freshwater sources originating from latitudes south of the gyres. One source area with emerging evidence is the St. Lawrence River system, and the subsequent marine trajectory of its freshwater flux to the North Atlantic Ocean (Figure 7.15). While additional research is required to confirm the nature, magnitude and effect of this additional freshwater flux, verification of such would also mean an enlarged TCA (see red area in Figure 7.16), and an increase in the total contributing terrestrial river flow (as indicated by 'AFD' on the area-discharge plot in Figure 7.16). Moreover, extending the logic for an expansion of the TCA means that other freshwater sources originating from additional extra-Arctic river basins should also be evaluated for potential inclusion. In the case of the Bering Strait gateway, this could mean the addition of rivers draining into the northern Pacific Ocean from the east coast of Russia and west coast of North America.

An additional consideration in defining a broader TCA for the Arctic freshwater system is how such new contributing areas, both marine and terrestrial, align with the freshwater-delivering storm tracks. As reviewed by Prowse et al. (2015a), storm track location and structure are controlled by various factors including orography, land-sea contrasts, and ocean temperature gradients, such as found along ocean fronts. Marine fronts exist where there is a strong contrast in sea-surface temperature, particularly at depth. The strong influence of freshwater in determining the boundary between temperature-stratified subtropical seas and salt-stratified high-latitude seas (Carmack et al., 2016), indicates the need for a greater emphasis on evaluating the importance of freshwater-controlled marine boundaries in affecting ocean-atmosphere coupling and thus the direction and intensity of the related storm tracks that deliver freshwater to the Arctic freshwater system.

7.8.2 New hydro-ecological regimes

As reviewed by Bring et al. (2016) and Wrona et al. (2016), the aquatic and terrestrial landscape of the Arctic freshwater system has experienced various changes in successional patterns and geographic extent of biomes (i.e. transition of tundra to shrubland/forest) and ecosystem types (i.e. terrestrial to thermokarst lakes/wetlands and the reverse). To a large degree, these are climatically driven and hydrologically mediated, particularly by the effects of permafrost thaw and related modifications to flow pathways. Given the importance of such

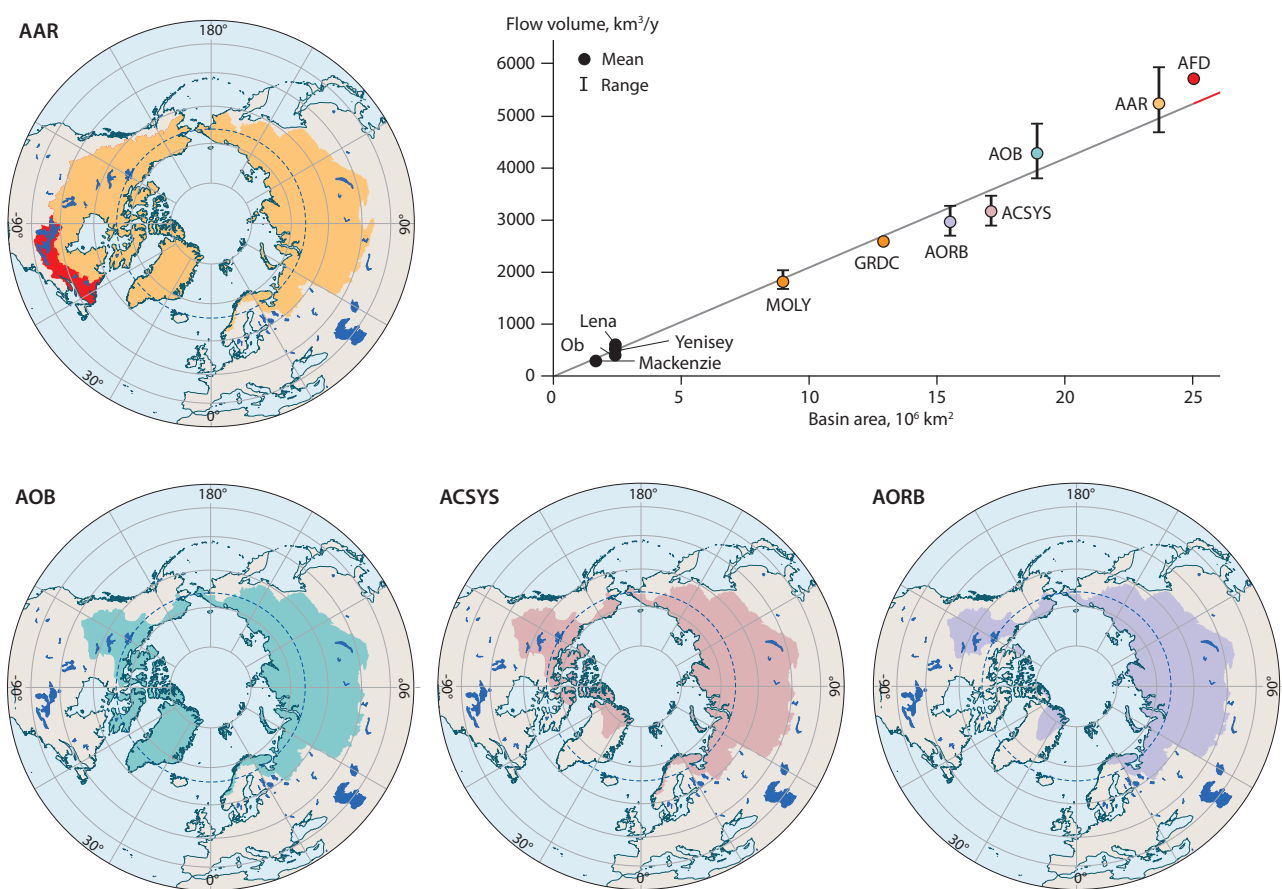


Figure 7.16 Based on Figure 7.3, the newly defined Arctic Freshwater Domain (AFD) is shown with the Laurentian Great Lakes / St Lawrence River system noted in Figure 7.15 (here outlined in red) added to the All Arctic Regions (AAR) definition shown in yellow (after Prowse and Flegg, 2000a); plus an update of the flow volume by contributing area relationship (after Prowse and Flegg, 2000b), which includes in the upper right, the largest area and flow volume TCA - the newly defined AFD (Prowse et al., 2015b).

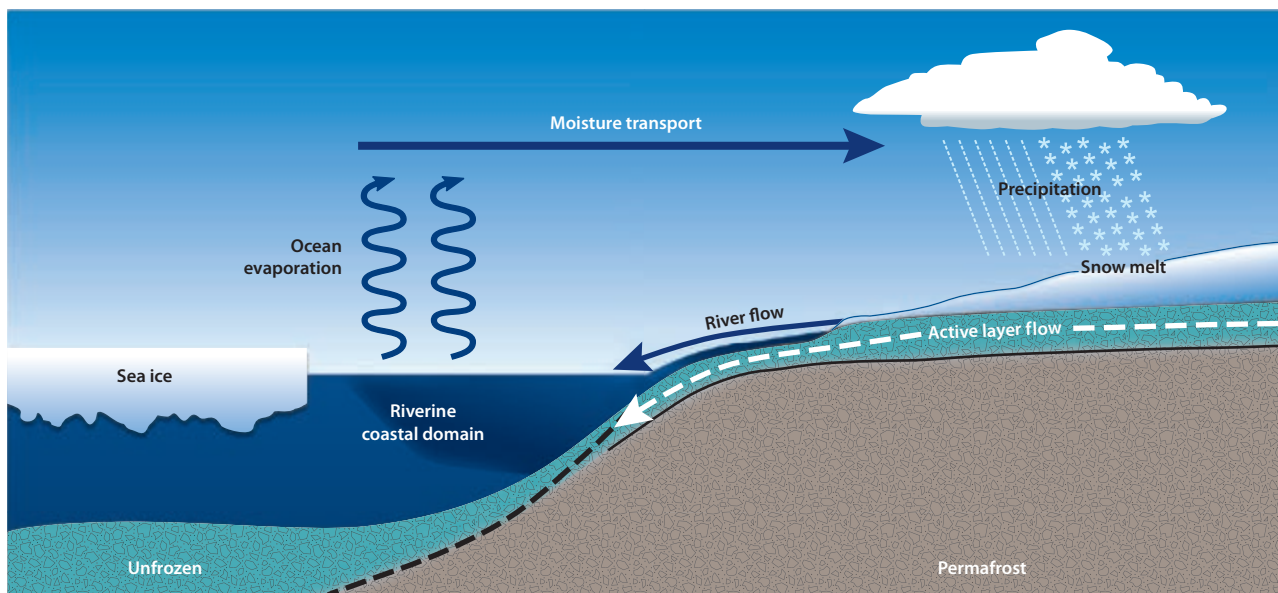


Figure 7.17 Schematic representation of the nearshore hydro-ecological regime, which includes illustrations of ocean-to-land moisture transport, precipitation on land, thawing permafrost with a deepening active layer, surface and groundwater flows and geochemical flux, transport to the riverine coastal domain, and subsequent trajectory to the broader ocean environment (after Prowse et al., 2015b).

changes in affecting key climate-related fluxes (e.g. carbon, methane, energy, and water; Wrona et al., 2016), there is an emerging need to be able to fully quantify the spatial extent of ecosystem transformations. Given the large spatial discord between hydrological and ecological monitoring that currently exists within the TCA and thus a related lack of integrated hydrologic-ecosystem field studies, new field-based scientific programs are required that can provide the requisite data to achieve higher-resolution modeling of freshwater systems (Lique et al., 2016; Section 7.7). To this end, Wrona et al. (2016; see also Section 7.5.2) recommended the adoption of a full freshwater continuum for study – one that considers fluxes and processes across a full spatial range of hydro-ecological units, that is, using a catchment-based approach that considers both landscape and hydrological gradients, which exist between ponds and streams, to lakes and rivers, and ultimately to coastal marine environments.

The emergence of a new nearshore hydro-ecological regime was identified during the *Arctic Freshwater Synthesis* (Figure 7.17) characterized by changes in nearshore hydrogeochemical fluxes on the landscape but with significant ecological implications for the coastal, and possibly broader, marine environment. The creation of this new regime was noted to be primarily driven by changes in two cryospheric components: sea ice and permafrost. Specifically, the retreat of sea ice from coastal margins has created a new moisture supply to the atmosphere and resultant increases in precipitation to the nearshore terrestrial landscape (Bring et al., 2016; Vihma et al., 2016). While the magnitude of resulting runoff from surface and groundwater flow systems remains to be quantified, such flow should be geochemically enriched because of the related thawing of permafrost and deepening of the active layer. Moreover, given that the total length of northern hemisphere coastline affected by permafrost is about 408,000 km, or 34% of the world's coastline (Lantuit et al., 2012), this effect could have a significant impact on marine productivity, especially given that the Arctic Ocean is roughly 53% continental shelf (Krause-Jensen and Duarte, 2014). Future research to assess the

magnitude and spatial extent of changing geochemical fluxes associated with permafrost thaw also needs to consider the role of the riverine coastal domain (Figure 7.4), which is driven by continental runoff (Carmack et al., 2016) and could transport 'enriched' discharge well beyond the mouths of streams forming this new nearshore hydrologic regime. To fully evaluate the changing sources, quantity, quality, seasonality, and fate/effect of freshwater in this newly developing nearshore regime, new field studies are needed. However, such studies will involve a considerable logistical challenge since the deep-draft vessels commonly used in marine research will not be suitable for this shallow, nearshore marine environment.

As outlined by Carmack et al. (2016; Section 7.3), new nearshore fluxes are likely to alter ocean primary production, pH, and the carbon cycle, and in the nearshore environment promote the emergence of new marine ecosystems. Overall, it remains to be seen whether new primary production will increase or decrease (Nishino et al., 2011). In the deep basins of the Arctic Ocean, which are notably oligotrophic new production is mainly nutrient-limited (Bluhm et al., 2015). However, earlier melt and retreat of sea ice well into the deep basins will enhance wind- and ice-forced shelf-break upwelling (Carmack and Chapman, 2003) thereby increasing nutrient fluxes and solar radiation and thus, new production. In contrast, it is coastal domains that are likely to experience the greatest change depending on the combined effects of at least five distinct but interacting mechanisms: (1) enhanced river discharge and freshwater stratification, which limit vertical nutrient supply; (2) increased light limitation from enhanced turbidity resulting from increased permafrost erosion along coasts and within coastal rivers, and via increased wind-driven sediment resuspension; (3) consequences of terrestrial and marine permafrost thaw in altering riverine and coastal geochemistry; (4) improved conditions for northward expansion of vegetated coastal ecosystems (Krause-Jensen and Duarte, 2014); and (5) biodiversity changes related to poleward migrations of boreal species. The cascading effects of such changes on higher trophic levels, including fish, marine mammals, and subsistence hunting are not yet clear.

7.8.3 Enhanced lake moisture flux

Owing to the vast area of ice-covered lakes within the Arctic (Prowse et al., 2015a) it has been suggested that decreases in lake-ice cover and duration (Bring et al., 2016; Section 7.4) have the potential to generate a new major supply of freshwater to the atmosphere through enhanced water-column heating and thus evaporation (Vihma et al., 2016; Section 7.2). The magnitude, fate, and effects (intra-lake and downwind) of such a new freshwater moisture source remain to be assessed. However, intra-lake effects are likely to be significant given the potential for an enhanced flux to the atmosphere to change lake water budgets/levels and, as a consequence to alter the physical, chemical, and biological conditions controlling carbon and methane fluxes (Wrona et al., 2016; Section 7.5).

7.8.4 Freshwater resources

Although the final effects on freshwater supply and distribution of the various processes outlined above (such as increased evapotranspiration from changes in vegetation regimes, increased evaporation from an ice-diminished ocean and ponds/lakes/rivers, and modified intensity and direction of storm tracks) need to be fully determined, the higher-latitude terrestrial areas of the AFD are generally becoming more ‘water rich’ (i.e. water availability meets or exceeds the needs of human development and ecosystem services) (Bring et al., 2016; Lique et al., 2016). This is particularly the case during winter when precipitation increases exceed those for evaporation (Vihma et al., 2016). Such a situation could translate into an economic benefit via the additional hydropower generation capacity created, especially when augmented by other freshwater sources, for example enhanced glacier melt (see also Chapter 6), as is already occurring in Greenland (Instanes et al., 2016). Although large-scale hydropower facilities are located only in currently strategic watersheds, increases in the flow of northern rivers might lead to a geographical expansion of facilities, especially if energy demands at high latitudes also increase. The opportunity for small-scale hydropower generation to supply energy to northern communities and resource sectors could also emerge with increases in the flow of even small rivers and streams. However, better knowledge of the risks of extreme events in these rivers is essential for securing the safe and efficient operation of all such facilities (Instanes et al., 2016); information that can only be obtained through enhanced multiscale models of the complete freshwater system (Lique et al., 2016; Section 7.7).

An additional policy issue that could develop as the high latitudes become ‘water rich’ is the possibility of using some of this excess freshwater to supply more southerly latitudes (Prowse et al., 2015b), especially if they become increasingly affected by prolonged drought conditions and so effectively ‘water poor’ (i.e. water availability does not meet the needs of human development and ecosystem services). Improved ability to model future regional differences in water availability, especially between northern and southern latitudes is essential to guide the emergence of policy-related discussion on this issue, and achieving a more comprehensive understanding of the full Arctic freshwater system is central to this.

References

Aagaard, K. and E.C. Carmack, 1989. The role of fresh water in ocean circulation and climate. *Journal of Geophysical Research*, 94:14,485-14,498.

Aagaard K. and E.C. Carmack, 1994. The Arctic Ocean and climate: a perspective. In: Johannessen, O.M., R.D. Muench, and J.E. Overland (eds.), *The Polar Oceans and their Role in Shaping the Global Environment*. pp 5-20. American Geophysical Union.

Aagaard, K., J.H. Swift and E.C. Carmack, 1985. Thermohaline circulation in the Arctic Mediterranean Seas. *Journal of Geophysical Research*, 90:4833-4846.

Adam, J.C., A.F. Hamlet and D.P. Lettenmaier, 2009. Implications of global climate change for snowmelt hydrology in the twenty-first century. *Hydrological Processes*, 23:962-972.

Aksenov, Y., V.V. Ivanov, A.J.G. Nurser, S. Bacon, I.V. Polyakov, A.C. Coward, A.C. Naveira-Garabato and A. Beszczynska-Moeller, 2011. The Arctic circumpolar boundary current. *Journal of Geophysical Research*, 116:C09017, doi:10.1029/2010JC006637.

Alkire, M.B., K.K. Falkner, I. Rigor, M. Steele and J. Morison, 2007. The return of Pacific waters to the upper layers of the central Arctic Ocean. *Deep Sea Research I*, 54:1509-1529.

AMAP, 2011. *Snow, Water, Ice and Permafrost in the Arctic (SWIPA): Climate Change and the Cryosphere*. Arctic Monitoring and Assessment Programme (AMAP), Oslo, Norway.

Anderson, L.G., S. Jutterström, S. Kaltin, E.P. Jones and G. Björk, 2004. Variability in river runoff distribution in the Eurasian Basin of the Arctic Ocean. *Journal of Geophysical Research*, 109:C01016, doi:10.1029/2003JC001773.

Anderson, L.G., G. Björk, S. Jutterström, I. Pipko, N. Shakhova, I. Semiletov and I. Wählström, 2011. East Siberian Sea, an Arctic region of very high biogeochemical activity. *Biogeosciences*, 8:1745-1754.

Andresen, C.G. and V.L. Lougheed, 2015. Disappearing Arctic tundra ponds: Fine-scale analysis of surface hydrology in drained thaw lake basins over a 65 year period (1948-2013). *Journal of Geophysical Research: Biogeosciences*, 120:466-479.

Ardyna, M., M. Babin, M. Gosselin, E. Devred, L. Rainville and J.-É. Tremblay, 2014. Recent Arctic Ocean sea ice loss triggers novel fall phytoplankton blooms. *Geophysical Research Letters*, 41:6207-6212.

Ashik, I.M., V.V. Ivanov, H. Kassens, M.S. Makhotin, I.V. Polyakov, L.A. Timokhov, I.E. Frolov and J. Holemann, 2015. Major results of oceanographic studies of the Arctic Ocean during the last decade: Problems of the Arctic and Antarctic. *Problems of the Arctic and Antarctic*, 1:42-56. [in Russian]

Avis, C.A., A.J. Weaver and K.J. Meissner, 2011. Reduction in areal extent of high-latitude wetlands in response to permafrost thaw. *Nature Geoscience*, 4:444-448.

Azcárate, J., B. Balfors, A. Bring and G. Destouni, 2013. Strategic environmental assessment and monitoring: Arctic key gaps and bridging pathways. *Environmental Research Letters*, 8:044033, doi:10.1088/1748-9326/8/4/044033.

Azetsu-Scott, K., A. Clarke, K. Falkner, J. Hamilton, E.P. Jones, C. Lee, B. Petrie, S. Prinsenberg, M. Starr and P. Yeats, 2010. Calcium carbonate saturation states in the waters of the Canadian Arctic Archipelago and the Labrador Sea. *Journal of Geophysical Research*, 115:C11021, doi:10.1029/2009JC005917.

Azetsu-Scott, K., M. Starr, Z.P. Mei and M. Granskog, 2014. Low calcium carbonate saturation state in an Arctic inland sea having large and varying fluvial inputs: The Hudson Bay system. *Journal of Geophysical Research: Oceans*, 119:6210-6220.

Barnes, E.A. and J.A. Screen, 2015. The impact of Arctic warming on the midlatitude jet-stream: Can it? Has it? Will it? *WIREs Climate Change*, 6:277-286.

Bates, B., Z.W. Kundzewicz, S. Wu and J. Palutikof (eds.), 2008. *Climate Change and Water*. Technical Paper of the Intergovernmental Panel on Climate Change (IPCC).

Bates, N.R., J.T. Mathis and L. Cooper, 2009. Ocean acidification and biologically induced seasonality of carbonate mineral saturation states in the western Arctic Ocean. *Journal of Geophysical Research*, 114:C11007, doi:10.1029/2008JC004862.

Bates, N.R., M.I. Orchowska, R. Garley and J.T. Mathis, 2013. Summertime calcium carbonate undersaturation in shelf waters of the western Arctic Ocean: How biological processes exacerbate the impact of ocean acidification. *Biogeosciences*, 10:5281-5309.

Beltaos, S. and T. Prowse, 2009. River-ice hydrology in a shrinking cryosphere. *Hydrological Processes*, 23:122-144.

Benson, B.J., J.J. Magnuson, O.P. Jensen, V.M. Card, G. Hodgkins, J. Korhonen, D.M. Livingstone, K.M. Stewart, G.A. Weyhenmeyer and N.G. Granin, 2012. Extreme events, trends, and variability in Northern Hemisphere lake-ice phenology (1855–2005). *Clim. Change*, 112:299–323.

Bhatt, U.S., D.A. Walker, J.E. Walsh, E.C. Carmack, K.E. Frey, W.N. Meier, S.E. Moore, F.-Y.W. Parmentier, E. Post, V.E. Romanovsky and W.R. Simpson, 2014. Implications of Arctic sea ice decline for the earth system. *Annual Review of Environment and Resources*, 39:57-89.

Bintanja, R. and F.M. Selten, 2014. Future increases in Arctic precipitation linked to local evaporation and sea-ice retreat. *Nature*, 509:479-482.

Bluhm, B.A., K.N. Kosobokova and E.C. Carmack, 2015. A tale of two basins: An integrated physics and biology perspective of the deep Arctic Ocean. *Progress in Oceanography*, 139:89-121.

Bourke, R.H. and R.P. Garrett, 1987. Sea ice thickness distribution in the Arctic Ocean. *Cold Regions Science and Technology*, 13:259-280.

Bring, A., S.M. Asokan, F. Jaramillo, J. Jarsjö, L. Levi, J. Pietron, C. Prieto, P. Rogberg and G. Destouni, 2015. Implications of freshwater flux data from the CMIP5 multi-model output across a set of Northern Hemisphere drainage basins. *Earth's Future*, 3:206-217.

Bring, A., I. Fedorova, Y. Dibike, L. Hinzman, J.M. Karlsson, S.H. Mernild, T. Prowse, O. Semenova, S. Stuefer and M.-K. Woo, 2016. Arctic terrestrial hydrology: A synthesis of processes, regional effects and research challenges. [Special Issue] *Journal of Geophysical Research: Biogeosciences*, 121:621-649.

Brooks, R.N., T.D. Prowse and I.J. O'Connell, 2013. Quantifying Northern Hemisphere freshwater ice. *Geophysical Research Letters*, 40:1128-1131.

Brown, R.D. and P. Coté, 1992. Inter-annual variability of land-fast ice thickness in the Canadian High Arctic, 1950–89. *Arctic*, 45:273-284.

Bulgakov, N.P., 1962. Determination of functional graphs of the time at which water reaches the freezing point and the depth of density mixing. *Problems of the North*, 4:141-148.

Cai, W.J., L. Chen, B. Chen, Z. Gao, S.H. Lee, J. Chen, D. Pierrot, K. Sullivan, Y. Wang, X. Hu, W.-J. Huang, Y. Zhang, S. Xu, A. Murata, J.M. Grebmeier, E.P. Jones and H. Zhang, 2010. Decrease in the CO₂ uptake capacity in an ice-free Arctic Ocean basin. *Science*, 329:556-559.

Callaghan, T.V., M. Johansson, R.D. Brown, P.Ya. Groisman, N. Labba, V. Radionov, R.S. Bradley, S. Blangy, O.N. Bulygina, T.R. Christensen, J.E. Colman, R.L.H. Essery, B.C. Forbes, M.C. Forchhammer, V.N. Golubev, R.E. Honrath, G.P. Juday, A.V. Meshcherskaya, G.K. Phoenix, J. Pomeroy, A. Rautio, D.A. Robinson, N.M. Schmidt, M.C. Serreze, V.P. Shevchenko, A.I. Shiklomanov, A.B. Shmakin, P. Sköld, M. Sturm, M. Woo and E.F. Wood, 2011. Multiple effects of changes in Arctic snow cover. *Ambio*, 40:32-45.

Carmack, E.C., 2007. The alpha/beta ocean distinction: A perspective on freshwater fluxes, convection, nutrients and productivity in high-latitude seas. *Deep Sea Research II*, 54:2578-2598.

Carmack, E. and D.C. Chapman, 2003. Wind-driven shelf/basin exchange on an Arctic shelf: The joint roles of ice cover extent and shelfbreak bathymetry. *Geophysical Research Letters*, 30:1778, doi:10.1029/2003GL017526.

Carmack, E. and F. McLaughlin, 2011. Towards recognition of physical and geochemical change in Subarctic and Arctic Seas. *Progress in Oceanography*, 90:90-104.

Carmack, E.C. and P. Wassmann, 2006. Food-webs and physical biological coupling on pan-arctic shelves: Perspectives, unifying concepts and future research. *Progress in Oceanography*, 71:446-477.

Carmack, E.C., F.A. McLaughlin, M. Yamamoto-Kawai, M. Itoh, K. Shimada, R. Krishfield and A. Proshutinsky, 2008. Freshwater storage in the Northern Ocean and the special role of the Beaufort Gyre. In: Dickson, R.R., J. Meincke and P. Phinnes (eds.), *Arctic–Subarctic Ocean Fluxes, Defining the Role of the Northern Seas in Climate*. pp. 145-169. Springer.

Carmack, E.C., G. Whiteman, T. Homer-Dixon and F.A. McLaughlin, 2012. Detecting and coping with potentially disruptive shocks and flips in complex-adaptive Arctic marine systems: A resilience approach to place and people. *Ambio*, 41:56-65.

Carmack, E., I. Polyakov, L. Padman, I. Fer, E. Hunke, J. Hutchings, J. Jackson, D. Kelley, R. Kwok, C. Layton, D. Perovich, O. Persson, B. Ruddick, M.-L. Timmermans, J. Toole, T. Ross, S. Vavrus and P. Winsor, 2015. Towards quantifying the increasing role of oceanic heat flux in sea ice loss in the new Arctic. *Bulletin of the American Meteorological Society*, 96:2079-2105.

Carmack, E., M. Yamamoto-Kawai, S. Bacon, B. Bluhm, T. Haine, C. Lique, H. Melling, I. Polyakov, F. Straneo, M.-L. Timmermans and W. Williams, 2016. Freshwater and its role in the Arctic Marine System: sources, disposition, storage, export, and physical and biogeochemical consequences in the Arctic and global oceans. [Special Issue] *Journal of Geophysical Research: Biogeosciences*, 121:675-717.

Cesana, G., J.E. Kay, H. Chepfer, J.M. English and G. Boer, 2012. Ubiquitous low-level liquid-containing Arctic clouds: New observations and climate model constraints from CALIPSO-GOCCP. *Geophysical Research Letters*, 39:L20804, doi:10.1029/2012GL053385.

Chierici, M. and A. Fransson, 2009. Calcium carbonate saturation in the surface water of the Arctic Ocean: Undersaturation in freshwater influenced shelves. *Biogeosciences*, 6:2421-2431.

Chierici, M., A. Fransson, B. Lansard, L.A. Miller, A. Mucci, E. Shadwick, H. Thomas, J.-E. Tremblay and T.N. Papakyriakou, 2011. Impact of biogeochemical processes and environmental factors on the calcium carbonate saturation state in the Circumpolar Flaw Lead in the Amundsen Gulf, Arctic Ocean. *Journal of Geophysical Research*, 116:C00G09, doi:10.1029/2011JC007184.

Christiansen J.S., J.D. Reist, R. Brown, V. Brykov, G. Christensen, K. Christoffersen, P. Cott, P. Crane, J. Dempson, M. Docker, K. Dunmall, A. Finstad, V. Gallucci, J. Hammar, L. Harris, J. Heino, E. Ivanov, O. Karamushko, A. Kirillov, A. Kucheryavy, H. Lehtonen, A. Lynghammar, C. Mecklenburg, P. Möller, T. Mustonen, A. Oleinik, M. Power, Y. Reshetnikov, V. Romanov, O. Sandlund, C. Sawatzky, M. Svenning, H. Swanson and F.J. Wrona, 2013. Arctic fishes. In: *Arctic Biodiversity Assessment*. pp. 192-245. Conservation of Arctic Flora and Fauna (CAFF), Arctic Council Working Group.

Codispoti, A., V. Kelly, A. Thessen, P. Matrai, S. Suttles, V. Hill and B. Light, 2013. Synthesis of primary production in the Arctic Ocean: III. Nitrate and phosphate based estimates of net community production. *Progress in Oceanography*, 110:126-150.

Collins, B., N. Bellouin, M. Doutriaux-Boucher, N. Gedney, P. Halloran, T. Hinton, J. Hughes, C.D. Jones, M. Joshi, S. Liddicoat, G. Martin, F. O'Connor, J. Rae, C. Senior, S. Sitch, I. Totterdell, A. Wiltshire and S. Woodward, 2011. Development and evaluation of an Earth-system model-HadGEM2. *Geoscientific Model Development*, 4:1051-1075.

Curry, B., C.M. Lee and B. Petrie, 2011. Volume, freshwater, and heat fluxes through Davis Strait, 2004–05. *Journal of Physical Oceanography*, 41:429-436.

Curry, B., C.M. Lee, B. Petrie, R.E. Moritz and R. Kwok, 2015. Multiyear volume, liquid freshwater, and sea ice transports through Davis Strait, 2004–10. *Journal of Physical Oceanography*, 44:1244-1266.

Dai, A. and K.E. Trenberth, 2002. Estimates of freshwater discharge from continents: Latitudinal and seasonal variations. *Journal of Hydrometeorology*, 3:660-687.

Danielson, S.L., T.W. Weingartner, K. Hedstrom, K. Aagaard, R. Woodgate, E. Curchitser and P. Stabeno, 2014. Coupled wind-forced controls of the Bering–Chukchi shelf circulation and the Bering Strait throughflow: Ekman transport, continental shelf waves, and variations of the Pacific–Arctic sea surface height gradient. *Progress in Oceanography*, 125:40-61.

DeMarco, J., M.C. Mack and M.S. Bret-Harte, 2014. Effects of arctic shrub expansion on biophysical vs. biogeochemical drivers of litter decomposition. *Ecology*, 95:1861-1875.

Dibike, Y., T. Prowse, T. Saloranta and R. Ahmed, 2011. Response of Northern Hemisphere lake-ice cover and lake-water thermal structure patterns to a changing climate. *Hydrological Processes*, 25:2942-2953.

Dickson, R.R., J. Meincke, S.A. Malmberg and A.J. Lee, 1988. The great salinity anomaly in the North Atlantic. *Nature*, 256:479-482.

Dirmeyer, P.A., Y. Jin, B. Singh and X. Yan, 2013. Trends in land–atmosphere interactions from CMIP5 simulations. *Journal of Hydrometeorology*, 14:829-849.

Dittmar, T. and G. Kattner, 2003. The biogeochemistry of the river and shelf ecosystem of the Arctic Ocean: A review. *Marine Chemistry*, 83:103-120.

Drinkwater, K.F. and G.C. Harding, 2001. Effects of the Hudson Strait outflow on the biology of the Labrador shelf. *Canadian Journal of Fisheries and Aquatic Sciences*, 58:171-184.

Dukhovskoy, D., M. Johnson and A. Proshutinsky, 2004. Arctic decadal variability: An auto-oscillatory system of heat and fresh water exchange. *Geophysical Research Letters*, 31:L03302, doi:10.1029/2003GL019023.

Dumas, J., E. Carmack and H. Melling, 2005. Climate change impacts on the Beaufort shelf landfast ice. *Cold Regions Science and Technology*, 42:41-51.

Eastman, R. and S.G. Warren, 2013. A 39-Yr survey of cloud changes from land stations worldwide 1971–2009: Long-term trends, relation to aerosols, and expansion of the tropical belt. *Journal of Climate*, 26:1286–1303.

Ekwarzel, B., P. Schlosser, R.A. Mortlock and R.G. Fairbanks, 2001. River runoff, sea ice meltwater, and Pacific water distribution and mean residence times in the Arctic Ocean. *Journal of Geophysical Research*, 106:9075–9092.

Elmendorf, S.C., G.H.R. Henry, R.D. Hollister, R.G. Björk, N. Boulanger-Lapointe, E.J. Cooper, J.H.C. Cornelissen, T.A. Day, E. Dorrepaal, T.G. Elumeeva, M. Gill, W.A. Gould, J. Harte, D.S. Hik, A. Hofgaard, D.R. Johnson, J.F. Johnstone, I.S. Jónsdóttir, J.C. Jorgenson, K. Klanderud, J.A. Klein, S. Koh, G. Kudo, M. Lara, E. Lévesque, B. Magnússon, J.L. May, J.A. Mercado-Díaz, A. Michelsen, U. Molau, I.H. Myers-Smith, S.F. Oberbauer, V.G. Onipchenko, C. Rixen, N.M. Schmidt, G.R. Shaver, M.J. Spasojevic, P.E. Þórhallsdóttir, A. Tolvanen, T. Troxler, C.E. Tweedie, S. Villareal, C.-H. Wahren, X. Walker, P.J. Webber, J.M. Welker and S. Wipf, 2012. Plot-scale evidence of tundra vegetation change and links to recent summer warming. *Nature Climate Change*, 2:453–457.

Epstein, H.E., M.K. Raynolds, D.A. Walker, U.S. Bhatt, C.J. Tucker and J.E. Pinzon, 2012. Dynamics of aboveground phytomass of the circumpolar Arctic tundra during the past three decades. *Environmental Research Letters*, 7:015506, doi.org/10.1088/1748-9326/7/1/015506.

Fichot, G.G., K. Kaise, S.B. Hooker, R.M.W. Amon, M. Babin, S. Bélanger, S.A. Walker and R. Benner, 2013. Pan-Arctic distributions of continental runoff in the Arctic Ocean. *Scientific Reports*, 3:1053, doi:10.1038/3501053.

Fowler, C., W. Emery and M. Tschudi, 2013. Polar pathfinder daily 25 km EASE-grid sea ice motion vectors. Version 2. National Snow and Ice Data Center, Boulder, Colorado.

Frampton, A., S.L. Painter and G. Destouni, 2013. Permafrost degradation and subsurface-flow changes caused by surface warming trends. *Hydrogeology Journal*, 21:271–280.

Francis, J. and N. Skific, 2015. Evidence linking rapid Arctic warming to mid-latitude weather patterns. *Philosophical Transactions of the Royal Society A*, 373, doi:10.1098/rsta.2014.0170.

Francis, J.A. and S.J. Vavrus, 2012. Evidence linking Arctic amplification to extreme weather in mid-latitudes. *Geophysical Research Letters*, 39:L06801, doi:10.1029/2012GL051000.

Francis, J.A., D.M. White, J.J. Cassano, W.J. Gutowski Jr., L.D. Hinzman, M.M. Holland, M.A. Steele and C.J. Vörösmarty, 2009. An arctic hydrologic system in transition: Feedbacks and impacts on terrestrial, marine, and human life. *Journal of Geophysical Research*, 114:G04019, doi:10.1029/2008JG000902.

Frost, G.V., H.E. Epstein, D.A. Walker, G. Matyshak and K. Ermokhina, 2013. Patterned-ground facilitates shrub expansion in Low Arctic tundra. *Environmental Research Letters*, 8:015035.

Gamon, J.A., K.F. Huemmrich, R.S. Stone and C.E. Tweedie, 2013. Spatial and temporal variation in primary productivity (NDVI) of coastal Alaskan tundra: Decreased vegetation growth following earlier snowmelt. *Remote Sensing of Environment*, 129:144–153.

Giles, K.A.S., W.A. Laxon, L. Ridout, D.J. Wingham and S. Bacon, 2012. Western Arctic Ocean freshwater storage increased by wind-driven spin-up of the Beaufort Gyre. *Nature Geoscience*, 5:194–197.

Gleason, C.J. and L.C. Smith, 2014. Toward global mapping of river discharge using satellite images and at-many-stations hydraulic geometry. *Proceedings of the National Academy of Sciences*, 111:4788–4791.

Grebmeier, J.M., B.A. Bluhm, L.W. Cooper, S.L. Danielson, K.R. Arrigo, A.L. Blanchard, J.T. Clarke, R.H. Day, K.E. Frey, R.R. Gradinger, M. Kędra, B. Konar, K.J. Kuletz, S.H. Lee, J.R. Lovvold, B.L. Norcross and S.R. Okkonen, 2015. Ecosystem characteristics and processes facilitating persistent macrobenthic biomass hotspots and associated benthivory in the Pacific Arctic. *Progress in Oceanography*, 136:92–114.

Greene, C.H. and P.J. Pershing, 2007. Climate drives sea change. *Science*, 315:1084–1085.

Guay, C.K. and K.K. Falkner, 1997. Barium as a tracer of Arctic halocline and river waters. *Deep Sea Research II*, 44:1543–1569.

Guay, C.K., K.K. Falkner, R.D. Muench, M. Mensch, M. Frank and R. Bayer, 2001. Wind-driven transport pathways for Eurasian Arctic river discharge. *Journal of Geophysical Research*, 106:11,469–11,480.

Guay, C.K., F.A. McLaughlin and M. Yamamoto-Kawai, 2009. Differentiating fluvial components of upper Canada Basin waters on the basis of measurements of dissolved barium combined with other physical and chemical tracers. *Journal of Geophysical Research*, 114:C00A09, doi:10.1029/2008JC005099.

Guay, K.C., P.S.A. Beck, L.T. Berner, S.J. Goetz, A. Baccini and W. Buermann, 2014. Vegetation productivity patterns at high northern latitudes: a multi-sensor satellite data assessment. *Global Change Biology*, 20:3147–3158.

Guéguen, C., L. Guo, M. Yamamoto-Kawai and N. Tanaka, 2007. Colored dissolved organic matter dynamics across the shelf-basin interface in the western Arctic Ocean. *Journal of Geophysical Research*, 112:C05038, doi:10.1029/2006JC003584.

Haak, H., J. Jungclaus, U. Mikolajewicz and M. Latif, 2003. Formation and propagation of great salinity anomalies. *Geophysical Research Letters*, 30:1473–1476.

Haine, T.W.N., B. Curry, R. Gerdes, E. Hansen, M. Karcher, C. Lee, B. Rudels, G. Spreen, L. de Steur, K.D. Stewart and R. Woodgate, 2015. Arctic freshwater export: Status, mechanisms, and prospects. *Global Planetary Change*, 125:13–35.

Hartmann, D.L., A.M.G. Klein Tank, M. Rusticucci, L.V. Alexander, S. Brönnimann, Y. Charabi, F.J. Dentener, E.J. Dlugokencky, D.R. Easterling, A. Kaplan, B.J. Soden, P.W. Thorne, M. Wild and P.M. Zhai, 2013. Observations: atmosphere and surface. In: Stocker, T.F., D. Qin, G.-K. Plattner, M. Tignor, S.K. Allen, J. Boschung, A. Nauels, Y. Xia, V. Bex and P.M. Midgley (eds.), *Climate Change 2013: The Physical Science Basis. Contribution of Working Group I to the Fifth Assessment Report of the Intergovernmental Panel on Climate Change*. Cambridge University Press.

Hawkins, E. and R. Sutton, 2009. The potential to narrow uncertainty in regional climate predictions. *Bulletin of the American Meteorological Society*, 90:1095–1107.

Held, I.M. and B.J. Soden, 2006. Robust responses of the hydrological cycle to global warming. *Journal of Climate*, 19:5686–5699.

Hodson, D.L., S.P. Keeley, A. West, J. Ridley, E. Hawkins and H.T. Hewitt, 2013. Identifying uncertainties in Arctic climate change projections. *Climate Dynamics*, 40:2849–2865.

Holland, M.M., J. Finniss, A.P. Barrett and M.C. Serreze, 2007. Projected changes in Arctic Ocean freshwater budgets. *Journal of Geophysical Research*, 112:G04S55, doi:10.1029/2006JC000354.

Holmes, R.M., M.T. Coe, G.J. Fiske, T. Gurtovaya, J.W. McClelland, A.I. Shiklomanov, R.G. Spencer, S.E. Tank and A.V. Zhulidov, 2013. Climate change impacts on the hydrology and biogeochemistry of Arctic rivers. In: Goldman, C.R., M. Kumagai and R.D. Robarts (eds.), *Climatic Change and Global Warming of Inland Waters: Impacts and Mitigation for Ecosystems and Societies*. pp. 3–26. John Wiley & Sons.

Hori, Y., W.A. Gough, K. Butler and L.J.S. Tsuji, 2016. Trends in the seasonal length and opening dates of a winter road in the western James Bay region, Ontario, Canada. *Theoretical and Applied Climatology*, doi: 10.1007/s00704-016-1855-1.

Hoskins, B.J. and K.I. Hodges, 2002. New perspectives on the Northern Hemisphere winter storm tracks. *Journal of the Atmospheric Sciences*, 59:1041–1061.

Hurrell, J.W., M.M. Holland, P.R. Gent, S. Ghan, J.E. Kay, P.J. Kushner, J.-F. Lamarque, W.G. Large, D. Lawrence, K. Lindsay, W.H. Lipscomb, M.C. Long, N. Mahowald, D.R. Marsh, R.B. Neale, P. Rasch, S. Vavrus, M. Vertenstein, D. Bader, W.D. Collins, J.J. Hack, J. Kiehl and S. Marshall, 2013. The Community Earth System model: A framework for collaborative research. *Bulletin of the American Meteorological Society*, 94:1339–1360.

Huryn, A.D., K.A. Slavik, R.L. Lowe, S.M. Parker, D.S. Anderson and B.J. Peterson, 2005. Landscape heterogeneity and the biodiversity of Arctic stream communities: A habitat template analysis. *Canadian Journal of Fisheries and Aquatic Sciences*, 62:1905–1919.

ICARP-II, 2005. Arctic Research: A Global Responsibility. An Overview of the Second International Conference on Arctic Research Planning. 10–12 November 2005, Copenhagen, Denmark.

Ims, R.A., D. Ehrlich, B.C. Forbes, B. Huntley, D.A. Walker, P.A. Wookey, D. Berteaux, U.S. Bhatt, K.A. Bräthen, M.E. Edwards, H.E. Epstein, M.C. Forchhammer, E. Fuglei, G. Gauthier, S. Gilbert, M. Leung, I.E. Menyushina, N. Ovsyanikov, E. Post, M.K. Raynolds, D.G. Reid, N.M. Schmidt, A. Stien, O.I. Sumina and R. van der Wal, 2013. Terrestrial ecosystems. In: Arctic Biodiversity Assessment, pp. 385–440. Conservation of Arctic Flora and Fauna (CAFF), Arctic Council Working Group.

Instanes, A., 2012. Permafrost engineering design utilising climate change information. In: *Proceedings of the 10th International Conference on Permafrost (TICOP)*, 25–29 June 2012, vol. I, pp. 167–172, Salekhard, Russia.

Instanes, A., V. Kokorev, R. Janowicz, O. Bruland, K. Sand and T. Prowse, 2016. Changes to freshwater systems affecting Arctic infrastructure

and natural resources. [Special Issue] *Journal of Geophysical Research: Biogeosciences*, 121, 567-585.

Intrieri, J.M., G. de Boer, M.D. Shupe, J.R. Spackman, J. Wang, P.J. Neiman, G.A. Wick, T.F. Hock and R.E. Hood, 2014. Global Hawk dropsonde observations of the Arctic atmosphere obtained during the Winter Storms and Pacific Atmospheric Rivers (WISPAR) field campaign. *Atmospheric Measurement Techniques*, 7:3917-3926.

Jahn, A. and M.M. Holland, 2013. Implications of Arctic sea ice changes for North Atlantic deep convection and the meridional overturning circulation in CCSM4-CMIP5 simulations. *Geophysical Research Letters*, 40:1206-1211.

Jahn, A., L.B. Tremblay, R. Newton, M.M. Holland, L.A. Mysak and I.G. Dmitrenko, 2010. A tracer study of the Arctic Ocean's liquid freshwater export variability. *Journal of Geophysical Research*, 115:C07015, doi:10.1029/2009JC005873.

Jahn, A., Y. Aksenov, B.A. de Cuevas, L. de Steur, S. Häkkinen, E. Hansen, C. Herbaut, M.-N. Houssais, M. Karcher, F. Kauker, C. Lique, A. Nguyen, P. Pemberton, D. Worthen and J. Zhang, 2012. Arctic Ocean freshwater: How robust are model simulations? *Journal of Geophysical Research*, 117:C00D16, doi:10.1029/2012JC007907.

Jonassen, M.O., H. Ólafsson, H. Ágústsson, Ó. Rögnvaldsson and J. Reuder, 2012. Improving high-resolution numerical weather simulations by assimilating data from an unmanned aerial system. *Monthly Weather Review*, 140:3734-3756.

Jones, E.P., J.H. Swift, L.G. Anderson, M. Lipizer, G. Civitarese, K.K. Falkner, G. Kattner and F. McLaughlin, 2003. Tracing Pacific water in the North Atlantic ocean. *Journal of Geophysical Research*, 108:3116, doi:10.1029/2001JC001141.

Jutterström, S. and L.G. Anderson, 2005. The saturation of calcite and aragonite in the Arctic Ocean. *Marine Chemistry*, 94:101-110.

Kapsch, M., R. Graversen, M. Tjernström and R. Bintanja, 2016. The effect of downwelling longwave radiation on Arctic summer sea ice. *Journal of Climate*, 29:1143-1159.

Karlsson, J.M., A. Bring, G.D. Peterson, L.J. Gordon and G. Destouni, 2011. Opportunities and limitations to detect climate-related regime shifts in inland Arctic ecosystems through eco-hydrological monitoring. *Environmental Research Letters*, 6:014015.

Karlsson, J.M., S.W. Lyon and G. Destouni, 2014. Temporal behavior of lake size-distribution in a thawing permafrost landscape in northwestern Siberia. *Remote Sensing*, 6:621-636.

Karlsson, J.M., F. Jaramillo and G. Destouni, 2015. Hydro-climatic and lake change patterns in Arctic permafrost and non-permafrost areas. *Journal of Hydrology*, 529:134-145.

Kattsov, V.M., J.E. Walsh, W.L. Chapman, V.A. Govorkova, T.V. Pavlova and X. Zhang, 2007. Simulation and projection of Arctic freshwater budget components by the IPCC AR4 Global Climate Models. *Journal of Hydrometeorology*, 8:571-589.

Kerby, J.T. and E. Post, 2013. Advancing plant phenology and reduced herbivore production in a terrestrial system associated with sea ice decline. *Nature Communications* 4:2514, doi:10.1038/ncomms3514.

Kokelj, S.V., D. Lacelle, T.C. Lantz, J. Tunnicliffe, L. Malone, I.D. Clark and K.S. Chin, 2013. Thawing of massive ground ice in mega slumps drives increases in stream sediment and solute flux across a range of watershed scales. *Journal of Geophysical Research: Earth Surface*, 118:681-692.

Kokelj, S.V., J. Tunnicliffe, D. Lacelle, T.C. Lantz, K.S. Chin and R. Fraser, 2015. Increased precipitation drives mega slump development and destabilization of ice-rich permafrost terrain, northwestern Canada. *Global and Planetary Change*, 129:56-68.

Krause-Jensen, D. and C.M. Duarte, 2014. Expansion of vegetated coastal ecosystems in the future Arctic. *Frontiers in Marine Science*, 1:doi:10.3389/fmars.2014.00077.

Krishfield, R.A., A. Proshutinsky, K. Tateyama, W.J. Williams, E.C. Carmack, F.A. McLaughlin and M.-L. Timmermans, 2014. Deterioration of perennial sea ice in the Beaufort Gyre from 2003 to 2012 and its impact on the oceanic freshwater cycle. *Journal of Geophysical Research: Oceans*, 119:1271-1305.

Kwok, R. and D.A. Rothrock, 2009. Decline in Arctic sea ice thickness from submarine and ICESat records: 1958-2008. *Geophysical Research Letters*, 36:L15501, doi:10.1029/2009GL039035.

Kwok, R., G.F. Cunningham, M. Wensnahan, I. Rigor, H.J. Zwally and D. Yi, 2009. Thinning and volume loss of Arctic sea ice: 2003-2008. *Journal of Geophysical Research*, 114:C07005, doi:10.1029/2009JC005312.

Kwok, R., G. Spreen and S. Pang, 2013. Arctic sea ice circulation and drift speed: Decadal trends and ocean currents. *Journal of Geophysical Research: Oceans*, 118:2408-2425.

Lainé, A., H. Nakamura, K. Nishii and T. Miyasaka, 2014. A diagnostic study of future evaporation changes projected in CMIP5 climate models. *Climate Dynamics*, 42:2745-2761.

Langen, P.L., R.G. Graversen and T. Mauritsen, 2012. Separation of contributions from radiative feedbacks to polar amplification on an aquaplanet. *Journal of Climate*, 25:3010-3024.

Lantuit, H., P.P. Overduin, N. Couture, S. Wetterich, F. Aré and D. Atkinson, 2012. The Arctic coastal dynamics database: A new classification scheme and statistics on Arctic permafrost coastlines. *Estuaries and Coasts*, 35:383-400.

Lantz, T.C., S.E. Gergel and G.H.R. Henry, 2010. Response of green alder (*Alnus viridis* subsp. *fruticosa*) patch dynamics and plant community composition to fire and regional temperature in north-western Canada. *Journal of Biogeography*, 37:1597-1610.

Latifovic, R. and D. Pouliot, 2007. Analysis of climate change impacts on lake ice phenology in Canada using the historical satellite data record. *Remote Sensing of Environment*, 106:492-507.

Lawrence, D.M., A.G. Slater, V.E. Romanovsky and D.J. Nicolsky, 2008. The sensitivity of a model projection of near-surface permafrost degradation to soil column depth and inclusion of soil organic matter. *Journal of Geophysical Research*, 113:F02011, doi:10.1029/2007JF000883.

Lewis, E.L., E.P. Jones, P. Lemke, T.D. Prowse and P. Wadhams (eds.), 2000. *The Freshwater Budget of the Arctic Ocean*. Proceedings of the NATO Advanced Research Workshop on the Freshwater Budget of the Arctic Ocean. Kluwer Academic.

Li, W.K.W., F.A. McLaughlin, C. Lovejoy and E.C. Carmack, 2009. Smallest algae thrive as the Arctic Ocean freshens. *Science*, 326:539, doi:10.1126/science.1179798.

Lindsay, R.W. and J. Zhang, 2006. Arctic Ocean ice thickness: Modes of variability and the best locations from which to monitor them. *Journal of Physical Oceanography*, 36:496-506.

Lipscomb, W.H., J.G. Fyke, M. Vizcaíno, W.J. Sacks, J. Wolfe, M. Vertenstein, A. Craig, E. Kluzek and D.M. Lawrence, 2013. Implementation and initial evaluation of the Glimmer Community ice sheet model in the community Earth System Model. *Journal of Climate*, 26:7352-7371.

Lique, C., N.N. Holland, Y.B. Dibike, D.M. Lawrence and J. Screen, 2016. Modeling the Arctic Freshwater System and its integration in the global system: Lessons learned and future challenges. [Special Issue] *Journal of Geophysical Research: Biogeosciences*, 121:540-566.

Liston, G.E. and K. Elder, 2006. A distributed snow-evolution modeling system (SnowModel). *Journal of Hydrometeorology*, 7:1259-1276.

Liu, Y., Q. Zhuang, Z. Pan, D. Miralles, N. Tchekakova, D. Kicklighter, J. Chen, A. Sirin, Y. He, G. Zhou and J. Melillo, 2014. Response of evapotranspiration and water availability to the changing climate in Northern Eurasia. *Climatic Change*, 126:413-427.

Livingstone, D.M., R. Adrian, T. Blenckner, G. George and G.A. Weyhenmeyer, 2010. Lake ice phenology. In: George, D.G. (ed.), *The Impact of Climate Change on European Lakes*. pp. 51-61. Springer.

Macdonald, R.W., E.C. Carmack, F.A. McLaughlin, K.K. Falkner and J.H. Swift, 1999. Connections among ice, runoff and atmospheric forcing in the Beaufort Gyre. *Geophysical Research Letters*, 26:2223-2226.

MacGilchrist, G.A., A.C. Naveira Garabato, T. Tsubouchi, S. Bacon, S. Torres-Valdés and K. Azetsu-Scott, 2014. The Arctic Ocean carbon sink. *Deep Sea Research I*, 86:39-55.

Macias-Fauria, M., B.C. Forbes, P. Zetterberg and T. Kumpula, 2012. Eurasian Arctic greening reveals teleconnections and the potential for structurally novel ecosystems. *Nature Climate Change*, 2:613-618.

Martin, J., D. Dumont and J.E. Tremblay, 2013. Contribution of subsurface chlorophyll maxima to primary production in the coastal Beaufort Sea (Canadian Arctic): A model assessment. *Journal of Geophysical Research: Oceans*, 118:5873-5886.

Mathis, J.T., J.N. Cross and N.R. Bates, 2011. Coupling primary production and terrestrial runoff to ocean acidification and carbonate mineral suppression in the eastern Bering Sea. *Journal of Geophysical Research*, 116:C02030, doi:10.1029/2010JC006453.

Mauritsen, T., J. Sedlar, M. Tjernström, C. Leck, M. Martin, M. Shupe, S. Sjögren, B. Sierau, P.O.G. Persson, I.M. Brooks and E. Swietlicki, 2011. An Arctic CCN-limited cloud-aerosol regime. *Atmospheric Chemistry and Physics*, 11:165-173.

Mauritzen, C., 2012. Arctic freshwater. *Nature-Geosciences*, 5:162-164.

McClelland, J.W., S.E. Tank, R.G.M. Spencer and A.I. Shiklomanov, 2015. Coordination and sustainability of river observing activities in the Arctic. *Arctic*, 68:59-68.

McKinley, G.A., A.R. Fay, T. Takahashi and N. Metzl, 2011. Convergence of atmospheric and North Atlantic carbon dioxide trends on multidecadal timescales. *Nature Geoscience*, 4:606-610.

McLaughlin, F.A. and E.C. Carmack, 2010. Nutricline deepening in the Canada Basin, 2003–2009. *Geophysical Research Letters*, 37:L24602, doi:10.1029/2010GL045459.

McLaughlin, F.A., E.C. Carmack, R.W. Macdonald and J.K.B. Bishop, 1996. Physical and geochemical properties across the Atlantic/Pacific water mass front in the southern Canadian Basin. *Journal of Geophysical Research*, 101:1183-1197.

Meehl, G.A., L. Goddard, J. Murphy, R. J. Stouffer, G. Boer, G. Danabasoglu, K. Dixon, M. A. Giorgetta, A. M. Greene, E. Hawkins, G. Hegerl, D. Karoly, N. Keenlyside, M. Kimoto, B. Kirtman, A. Navarra, R. Pulwarty, D. Smith, D. Stammer and T. Stockdale, 2009. Decadal prediction: Can it be skillful? *Bulletin of the American Meteorological Society*, 90:1467-1485.

Melling, H., 2012. Sea-ice observation: Advances and challenges. In: Lemke, P. and H.-W. Jacobi (eds.), *Arctic Climate Change*. pp. 27-115. Springer.

Miller, L.A., R.W. Macdonald, F. McLaughlin, A. Mucci, M. Yamamoto-Kawai, K.E. Giesbrecht and W.J. Williams, 2014. Changes in the marine carbonate system of the western Arctic: Patterns in a rescued data set. *Polar Research*, 33:20577, doi:10.3402/polar.v33.20577.

Miller-Rushing, A.J., T.T. Hoyer, D.W. Inouye and E. Post, 2010. The effects of phenological mismatches on demography. *Philosophical Transactions of the Royal Society B*, 365:3177-3186.

Min, S.-K., X.B. Zhang, F.W. Zwiers and T. Agnew, 2008. Human influence on Arctic sea ice detectable from early 1990s onwards. *Geophysical Research Letters*, 35:L21701, doi: 10.1029/2008GL035725.

Mokhov, I.I., V.A. Semenov and V.C. Khon, 2003. Estimates of possible regional hydrologic regime changes in the 21st century based on global climate models. *Atmospheric and Oceanic Physics*, 39:130-144.

Morison, J., R. Kwok, C. Peralta-Ferriz, M. Alkire, I. Rigor, R. Andersen and M. Steele, 2012. Changing Arctic Ocean freshwater pathways. *Nature*, 481:66-70.

Morrison, H., P. Zuidema, A.S. Ackerman, A. Avramov, G. De Boer, J. Fan, A.M. Fridlind, T. Hashino, J.Y. Harrington, Y. Luo, M. Ovchinnikov and B. Shipway, 2011. Intercomparison of cloud model simulations of Arctic mixed-phase boundary layer clouds observed during SHEBA/FIRE-ACE. *Journal of Advances in Modeling Earth Systems*, 3:M06003, doi:10.1029/2011MS000066.

Moss, B., D. Hering, A.J. Green, A. Aidoud, E. Becares, M. Beklioglu, H. Bennion, L. Carvalho, S. Declerck, M. Dobson, E. van Donk, H. Feuchtmayr, N. Friberg, G. Grenouillet, A. Hobæk, K. Irvine, R. Johnson, M. Meerhoff, S. Ormerod, E. Papastergiadou, R. Ptacnik, P. Verdonck, B. Clement, T. Davidson, B. Dudley, E. Jeppesen, M. Kernan, L. Sandin, G. Simpson, G.A. Weyhenmeyer, D. Box, S. Brucet, H. Hillebrand, I. Jones, M. Manca, J. Olafsson, E. Penning, X. Quintana, M. Seferlis, C. Triga and A.M. Verschoor, 2009. Climate change and the future of freshwater biodiversity in Europe: A primer for policy makers. *Freshwater Reviews*, 2:103-130.

Mullan, D., G. Swindles, T. Patterson, J. Galloway, A. Macumber, H. Falck, L. Crossley, J. Chen and M. Pisaric, 2016. Climate change and the long-term viability of the world's busiest heavy haul ice road. *Theoretical and Applied Climatology*, doi:10.1007/s00704-016-1830-x.

Myers-Smith, I.H., B.C. Forbes, M. Wilmking, M. Hallinger, T. Lantz, D. Blok, K.D. Tape, M. Macias-Fauria, U. Sassi-Klaassen, E. Lévesque, S. Boudreau, P. Ropars, L. Hermanutz, A.J. Trant, L.S. Collier, S. Weijers, J. Rozema, S.A. Rayback, N.M. Schmidt, G. Schaeppman-Strub, S. Wipf, C. Rixen, C.B. Ménard, S. Venn, S. Goetz, L. Andreu-Hayles, S. Elmendorf, V. Ravolainen, J. Welker, P. Grogan, H.E. Epstein and D.S. Hik, 2011. Shrub expansion in tundra ecosystems: dynamics, impacts and research priorities. *Environmental Research Letters*, 6, 045509.

Nahtigalova, D.P., 2013. Long-term conditions of cloudage over the territory of the Siberian region and its modern changes. *Modern Problems of Science and Education*, 4:science-education.ru/110-a9820.

Nakayama, Y., S. Fujita, K. Kuma and K. Shimada, 2011. Iron and humic-type fluorescent dissolved organic matter in the Chukchi Sea and Canada Basin of the western Arctic Ocean. *Journal of Geophysical Research*, 116:C07031, doi:10.1029/2010JC006779.

Nauta, A.L., M.M.P.D. Heijmans, D. Blok, J. Limpens, B. Elberling, A. Gallagher, B. Li, R.E. Petrov, T.C. Maximov, J. van Huissteden and F. Berendse, 2015. Permafrost collapse after shrub removal shifts tundra ecosystem to a methane source. *Nature Climate Change*, 5:67-70.

Nelson, R.J., E.C. Carmack, F.A. McLaughlin and G. Cooper, 2009. Tracking penetration of Pacific zooplankton into the western Arctic Ocean with molecular population genetics. *Marine-Ecology Progress Series*, 381:129-138.

Newton, R., P. Schlosser, D.G. Martinson and W. Maslowski, 2008. Freshwater distribution in the Arctic Ocean: Simulation with a high-resolution model and model-data comparison. *Journal of Geophysical Research*, 113:doi:10.1029/2007JC004111.

Nishino, S., T. Kikuchi, M. Yamamoto-Kawai, Y. Kawaguchi, T. Hirawake and M. Itoh, 2011. Enhancement/reduction of biological pump depends on ocean circulation in the sea-ice reduction regions of the Arctic Ocean. *Journal of Oceanography*, 67:305-314.

Nürnberg, D., I. Wollenburg, D. Dethleff, H. Eicken, H. Kassens, T. Letzig, E. Reimann and J. Thiede, 1994. Sediments in Arctic sea ice: Implications for entrainment, transport and release. *Marine Geology*, 119:185-214.

Nygård, T., T. Valkonen and T. Vihma, 2014. Characteristics of Arctic low-tropospheric humidity inversions based on radio soundings. *Atmospheric Chemistry and Physics*, 14:1959-1971.

Olafsson, J., S.R. Olafsdottir, A. Benoit-Cattin, M. Danielsen, T.S. Arnarson and T. Takahashi, 2009. Rate of Iceland Sea acidification from time series measurements. *Biogeosciences*, 6:2661-2668.

Overland, J., J. Francis, R. Hall, E. Hanna, S.-J. Kim and T. Vihma, 2015. The melting Arctic and mid-latitude weather patterns: Are they connected? *Journal of Climate*, 28:7917-7932.

Park, H.-S., S. Lee, S.-W. Son, S.B. Feldstein and Y. Kosaka, 2015. The impact of poleward moisture and sensible heat flux on Arctic winter sea ice variability. *Journal of Climate*, 28:5030-5040.

Pearson, R.G., S.J. Phillips, M.M. Loranty, P.S.A. Beck, T. Damoulas, S.J. Knight and S.J. Goetz, 2013. Shifts in Arctic vegetation and associated feedbacks under climate change. *Nature Climate Change*, 3:673-677.

Perovich, D.K., J.A. Richter-Menge, K.F. Jones, B. Light, B.C. Elder, C. Polashenski, D. LaRoche, T. Markus and R. Lindsay, 2011. Arctic sea-ice melt in 2008 and the role of solar heating. *Annals of Glaciology*, 52:355-359.

Petrenko, D., D. Pozdnyakov, J. Johannessen, F. Counillon and V. Sychov, 2013. Satellite-derived multi-year trend in primary production in the Arctic Ocean. *International Journal of Remote Sensing*, 34:3903-3937.

Polyakov, I.V., G.V. Alekseev, R.V. Bekryaev, U.S. Bhatt, R. Colony, M.A. Johnson, V.P. Karklin, D. Walsh and A.V. Yulin, 2003. Long-term ice variability in Arctic marginal seas. *Journal of Climate*, 16:2078-2085.

Polyakov, I.V., V.A. Alexeev, G.I. Belchansky, I. Dmitrenko, V.V. Ivanov, S. Kirillov, A. Koralev, M. Steele, L. Timokhov and I. Yashayev, 2008. Arctic Ocean freshwater changes over the past 100 years and their causes. *Journal of Climate*, 21:364-384.

Polyakov, I.V., A.V. Pnyushkov and T.A. Timokhov, 2012. Warming of the intermediate Atlantic Water of the Arctic Ocean in the 2000s. *Journal of Climate*, 25:8362-8370.

Polyakov, I.V., U.S. Bhatt, J.E. Walsh, E.P. Abrahamsen, A.V. Pnyushkov and P.F. Wassmann, 2013a. Recent oceanic changes in the Arctic in the context of long-term observations. *Ecological Applications*, 23:1745-1764.

Polyakov, I.V., A.V. Pnyushkov, R. Remer, L. Padman, E.C. Carmack and J.M. Jackson, 2013b. Winter convection transports Atlantic water heat to the surface layer in the eastern Arctic Ocean. *Journal of Physical Oceanography*, 43:2142-2155.

Post, E. and M.C. Forchhammer, 2008. Climate change reduces reproductive success of an Arctic herbivore through trophic mismatch. *Philosophical Transactions of the Royal Society B*, 363:2369-2375.

Proshutinsky, A.Y. and M.A. Johnson, 1997. Two circulation regimes of the wind driven Arctic Ocean. *Journal of Geophysical Research*, 102:12,493-12,514.

Proshutinsky, A., M. Steele, J. Zhang, G. Holloway, N. Steiner, S. Häkkinen, D. Holland, R. Gerdes, C. Koerber, M. Karcher, M. Johnson, W. Maslowski, W. Walczowski, W. Hibler and J. Wang, 2001. Multinational effort studies differences among Arctic Ocean models. *Eos Transactions American Geophysical Union*, 82:643-644.

Proshutinsky, A., R.H. Bourke and F.A. McLaughlin, 2002. The role of the Beaufort Gyre in Arctic climate variability: Seasonal to decadal climate scales. *Geophysical Research Letters*, 29:2100, doi:10.1029/2002GL015847.

Proshutinsky, A., I.M. Ashik, E.N. Dvorkin, S. Häkkinen, R.A. Krishfield and W.R. Peltier, 2004. Secular sea level change in the Russian sector of the Arctic Ocean. *Journal of Geophysical Research*, 109:C03042, doi:10.1029/2003JC002007.

Proshutinsky, A., D. Dukhovskoy, M.-L. Timmermans, R. Krishfield and J. Bamber, 2015. Arctic circulation regimes. *Philosophical Transactions of the Royal Society A*, 373:20140160, doi:10.1098/rsta.2014.0160.

Prowse, T.D., 2011. Lake and river ice in Canada. In: French, H. and O. Slaymaker (eds.), *Changing Cold Environments*. pp. 163–181. John Wiley and Sons.

Prowse, T.D. and P.O. Flegg, 2000a. Arctic river flow: A review of contributing areas. In: Lewis, E.L., E.P. Jones, P. Lemke, T.D. Prowse, and P. Wadhams (eds.), *The Freshwater Budget of the Arctic Ocean*. pp 269–280. NATO Science Series. Kluwer Academic.

Prowse, T.D. and P.O. Flegg, 2000b. The magnitude of river flow to the Arctic Ocean: dependence on contributing area. *Hydrological Processes*, 14:3185–3188.

Prowse, T., R. Shrestha, B. Bonsal and Y. Dibike, 2010. Changing spring air-temperature gradients along large northern rivers: Implications for severity of river-ice floods. *Geophysical Research Letters*, 37:L19706, doi:10.1029/2010GL044878.

Prowse, T.D., K. Alfredsen, S. Beltaos, B. Bonsal, C. Duguay, A. Korhola, J. McNamara, W. Vincent, V. Vuglinsky and G. Weyhenmeyer, 2011. Changing lake and river ice regimes: trends, effects, and implications. In: *Snow, Water, Ice Permafrost in the Arctic (SWIPA)*. Arctic Monitoring and Assessment Program (AMAP), Oslo, Norway.

Prowse, T., A. Bring, J.M. Karlsson and E. Carmack, 2015a. Arctic freshwater synthesis: Introduction. [Special Issue] *Journal of Geophysical Research: Biogeosciences*, 120: 2121–2131.

Prowse, T., A. Bring, J.M. Karlsson, E. Carmack, M. Holland, A. Instanes, T. Vihma and F.J. Wrona, 2015b. Arctic freshwater synthesis: Summary of key emerging issues. [Special Issue] *Journal of Geophysical Research: Biogeosciences*, 120:1887–1893.

Rabe, B., M. Karcher, F. Kauker, U. Schauer, J.M. Toole, R.A. Krishfield, S. Pisarev, T. Kikuchi and J. Su, 2014. Arctic Ocean basin liquid freshwater storage trend 1992–2012. *Geophysical Research Letters*, 41:961–968.

Rahmstorf, S., J.E. Box, G. Feulner, M.E. Mann, A. Robinson, S. Rutherford and E.J. Chaffernicht, 2015. Exceptional twentieth-century slowdown in Atlantic Ocean overturning circulation. *Nature Climate Change*, 5:475–480.

Räisänen, J., 2008. Warmer climate: less or more snow? *Climate Dynamics*, 30:307–319.

Rawlins, M., M. Steele, M.M. Holland, J.C. Adam, J.E. Cherry, J.A. Francis, P.Y. Groisman, L.D. Hinzman, T.G. Huntington, D.L. Kane, J.S. Kimball, R. Kwok, R.B. Lammers, C.M. Lee, D.P. Lettenmaier, K.C. McDonald, E. Podest, J.W. Pundsack, B. Rudels, M.C. Serreze, A. Shiklomanov, Ø. Skagseth, T.J. Troy, C.J. Vörösmarty, M. Wensnahan, E.F. Wood, R. Woodgate, D. Yang, K. Zhang and T. Zhang, 2010. Analysis of the Arctic system for freshwater cycle intensification: observations and expectations. *Journal of Climate*, 23:5715–5737.

Ridley, J.K., P. Huybrechts, J.M. Gregory and J.A. Lowe, 2005. Elimination of the Greenland Ice Sheet in a High CO₂ Climate. *Journal of Climate*, 18:3409–3427.

Rigor, I.G. and J.M. Wallace, 2004. Variations in the age of Arctic sea-ice and summer sea-ice extent. *Geophysical Research Letters*, 31:L09401, doi:10.1029/2004GL019492.

Rothrock, D.A., Y. Yu and G.A. Maykut, 1999. Thinning of the Arctic sea-ice cover. *Geophysical Research Letters*, 26:3469–3472.

Rooth, C., 1982. Hydrology and ocean circulation. *Progress in Oceanography*, 11:131–149.

Rouse, W.R., C.J. Oswald, J. Binyamin, C. Spence, W.M. Schertzer, P.D. Blanken, N. Bussières and C.R. Duguay, 2005. The role of northern lakes in a regional energy balance. *Journal of Hydrometeorology*, 6:291–305.

Rouse, W.R., P.D. Blanken, C.R. Duguay, C.J. Oswald and W.M. Schertzer, 2008. Climate-lake interactions. In: *Cold Region Atmospheric and Hydrologic Studies*. The Mackenzie GEWEX Experience. pp. 139–160. Springer.

Rudels, B., H.J. Friedrich and D. Quadfasel, 1999. The Arctic circumpolar boundary current. *Deep-Sea Research II*, 46:1023–1062.

Rupp, D.E., P.W. Mote, N.L. Bindoff, P.A. Stott and D.A. Robinson, 2013. Detection and attribution of observed changes in northern hemisphere spring snow cover. *Journal of Climate*, 26:6904–6914.

Schindler, D.W., 2009. Lakes as sentinels and integrators for the effects of climate change on watersheds, airsheds, and landscapes. *Limnology and Oceanography*, 54:2349–2358.

Schweiger, A., R. Lindsay, J. Zhang, M. Steele, H. Stern and R. Kwok, 2011. Uncertainty in modeled Arctic sea ice volume. *Journal of Geophysical Research*, 116:C00D06, doi:10.1029/2011JC007084.

Screen, J.A. and I. Simmonds, 2012. Declining summer snowfall in the Arctic: causes, impacts and feedbacks. *Climate Dynamics*, 38:2243–2256.

Screen, J.A., I. Simmonds, C. Deser and R. Tomas, 2013. The atmospheric response to three decades of observed Arctic sea ice loss. *J. Clim.*, 26:1230–1248.

Serreze, M.C. and A.P. Barrett, 2011. Characteristics of the Beaufort Sea High. *Journal of Climate*, 24:159–182.

Serreze, M.C. and R.G. Barry, 2011. Processes and impacts of Arctic amplification: A research synthesis. *Global Planetary Change*, 77:85–96.

Serreze, M.C., A.P. Barrett, A.G. Slater, R.A. Woodgate, K. Aagaard, R.B. Lammers, M. Steele, R. Moritz, M. Meredith and C.M. Lee, 2006. The large-scale freshwater cycle of the Arctic. *Journal of Geophysical Research*, 111:C11010, doi:10.1029/2005JC003424.

Serreze, M.C., A.P. Barrett and J. Stroeve, 2012. Recent changes in tropospheric water vapor over the Arctic as assessed from radiosondes and atmospheric reanalyses. *Journal of Geophysical Research*, 117:D10104, doi:10.1029/2011JD017421.

Shupe, M.D., V.P. Walden, E. Eloranta, T. Uttal, J.R. Campbell, S.M. Starkweather and M. Shiobara, 2011. Clouds at Arctic atmospheric observatories. Part I: Occurrence and macrophysical properties. *Journal of Applied Meteorology and Climatology*, 50:626–644.

Skeffington, R.A., A.J. Wade, P.G. Whitehead, D. Butterfield, Ø. Kaste, H.E. Andersen, K. Rankinen and G. Grenouillet, 2010. Modelling catchment scale responses to climate change. In: Kernan, M., R.W. Battarbee and B. Moss (eds.), *Climate Change Impacts on Freshwater Ecosystems*. pp. 236–261. Blackwell.

Solomon, A., M.D. Shupe, P.O.G. Persson, H. Morrison, T. Yamaguchi, P.M. Caldwell and G. de Boer, 2014. The sensitivity of springtime Arctic mixed-phase stratocumulus clouds to surface layer and cloud-top inversion layer moisture sources. *Journal of the Atmospheric Sciences*, 71:574–595.

Steele, M. and T. Boyd, 1998. Retreat of the cold halocline layer in the Arctic Ocean. *Journal of Geophysical Research*, 103:10,419–10,435.

Steele, M., R. Morley and W. Ermold, 2001. A global ocean hydrography with a high quality Arctic Ocean. *Journal of Climate*, 14:2079–2087.

Stewart, K.J., P. Grogan, D.S. Coxson and S.D. Siciliano, 2014. Topography as a key factor driving atmospheric nitrogen exchanges in arctic terrestrial ecosystems. *Soil Biology and Biochemistry*, 70:96–112.

Stroeve, J.C., M.C. Serreze, M.M. Holland, J.E. Kay, J. Masklinik and A.P. Barrett, 2012. The Arctic's rapidly shrinking sea ice cover: a research synthesis. *Climate Change*, 110:1005–1027.

Surdu, C.M., C.R. Duguay, L.C. Brown and D. Fernández Prieto, 2014. Response of ice cover on shallow lakes of the North Slope of Alaska to contemporary climate conditions (1950–2011): Radar remote-sensing and numerical modeling data analysis. *Cryosphere*, 8:167–180.

Tape, K.D., M. Hallinger, J.M. Welker and R.W. Ruess, 2012. Landscape heterogeneity of shrub expansion in Arctic Alaska. *Ecosystems*, 15:711–724.

Thienpont, J.R., K.M. Rühland, M.F.J. Pisaric, S.V. Kokelj, L.E. Kimpe, J.M. Blais and J.P. Smol, 2013. Biological responses to permafrost thaw slumping in Canadian Arctic lakes. *Freshwater Biology*, 58:337–353.

Thomas, H., A.E.F. Prowe, I.D. Lima, S.C. Doney, R. Wanninkhof, R.J. Greatbatch, U. Schuster and A. Corbière, 2008. Changes in the North Atlantic Oscillation influence CO₂ uptake in the North Atlantic over the past 2 decades. *Global Biogeochemical Cycles*, 22:GB4027, doi:10.1029/2007GB003167.

Thompson, M.S., F.J. Wrona, F.J. and T.D. Prowse, 2012. Shifts in plankton, nutrient and light relationships in small tundra lakes caused by localized permafrost thaw. *Arctic*, 65:367–376.

Tjernström, M., M. Žagar, G. Svensson, J.J. Cassano, S. Pfeifer, A. Rinke, K. Wyser, K. Dethloff, C. Jones, T. Semmler and M. Shaw, 2005. Modelling the Arctic boundary layer: An evaluation of size ARCMIP regional-scale models using data from the SHEBA Project. *Boundary-Layer Meteorology*, 117:337–381.

Tjernström, M., C. Leck, C.E. Birch, J.W. Bottenheim, B.J. Brooks, I.M. Brooks, L. Bäcklin, R.Y.-W. Chang, G. de Leeuw, L. Di Liberto, S. de la Rosa, E. Granath, M. Graus, A. Hänsel, J. Heintzenberg, A. Held, A. Hind, P. Johnston, J. Knulst, M. Martin, P.A. Matrai, T. Mauritsen, M. Müller, S.J. Norris, M.V. Orellana, D.A. Orsiini, J. Paatero, P.O.G. Persson, Q. Gao, C. Rauschenberg, Z. Ristovski, J. Sedlar, M.D. Shupe, B. Sierau, A. Sirevaag, S. Sjogren, O. Stetzer, E. Swietlicki, M. Szczodrak, P. Vaattovaara, N. Wahlberg, M. Westberg and C.R. Wheeler, 2014. The Arctic Summer Cloud Ocean Study (ASCOS): Overview and experimental design. *Atmospheric Chemistry and Physics*, 14:2823–2869.

Torres-Valdés, S., T. Tsubouchi, S. Bacon, A.C. Naveira-Garabato, R. Sanders, F.A. McLaughlin, B. Petrie, G. Kattner, K. Azetsu-Scott and T.E. Whitledge, 2013. Export of nutrients from the Arctic Ocean. *Journal of Geophysical Research: Oceans*, 118:1625-1644.

Tremblay, J.E. and J. Gagnon, 2009. The effects of irradiance and nutrient supply on the productivity of Arctic waters: A perspective on climate change. In: Nihoul, C.J. and A. G. Kostianoy (eds.), *Influence of Climate Change on the Changing Arctic and Subarctic Conditions*. pp. 73-92. Springer.

Tremblay, J.É., L.G. Anderson, P. Matrai, P. Coupel, S. Bélanger, C. Michel and M. Reigstad, 2015. Global and regional drivers of nutrient supply, primary production and CO₂ drawdown in the changing Arctic Ocean. *Progress in Oceanography*, 139:171-196.

Troy, T.J., J. Sheffield and E.F. Wood, 2012. The role of winter precipitation and temperature on northern Eurasian streamflow trends. *Journal of Geophysical Research: Atmospheres*, 117:D05131, doi:10.1029/2011JD016208.

Tucker, W.B., J.W. Weatherly, D.T. Eppler and D.L. Bentley, 2001. Evidence for rapid thinning of sea ice in the western Arctic Ocean at the end of the 1980s. *Geophysical Research Letters*, 28:2851-2854.

Turcotte, B., B. Morse, N.E. Bergeron and A.G. Roy, 2011. Sediment transport in ice-affected rivers. *Journal of Hydrology*, 409:561-577.

Urban, M., M. Forke, J. Eberle, C. Huttich, C. Schmullius and M. Herold, 2014. Pan-Arctic climate and land cover trends derived from multi-variate and multi-scale analyses (1981-2012). *Remote Sensing*, 6:2296-2316.

Uttal, T., S. Starkweather, J. Drummond, T. Vihma, C.J. Cox, E. Drugokencky, J. Ogren, B. McArthur, L. Schmeisser, V. Walden, T. Laurila, L. Darby, A. P. Makshtas, J. Intrieri, J. Burkhart, T. Haiden, B. Goodison, M. Maturilli, M. Shupe, G. de Boer, R. Stone, A. Saha, A. Grachev, L. Bruhwiler, O. Persson, G. Lesins, S. Crepinsek, C. Long, S. Sharma, A. Massling, D.D. Turner, D. Stanitski, E. Asmi, M. Aurela, H. Skov, K. Eleftheriades, A. Virkkula, A. Platt, E. Forland, J. Verlinde, I. Yoshihiroo, I.E. Nielsen, M. Bergin, L. Candalish, N. Zimov, S. Zimov, N. O'Neil, P. Fogal, R. Kivi, E. Konopleva, V. Kustov, B. Vasel, Y. Viisanen and V. Ivakhov, 2016. International Arctic Systems for Observing the Atmosphere (IASOA): An International Polar Year Legacy Consortium. *Bulletin of the American Meteorological Society*, doi: <http://dx.doi.org/10.1175/BAMS-D-14-00145.1>

Van Vliet, M.T.H., W.H.P. Franssen, J.R. Yearsley, F. Ludwig, I. Haddeland, D.P. Lettenmaier and P. Kabat, 2013. Global river discharge and water temperature under climate change. *Global Environmental Change*, 23:450-464.

Vaughan, D.G., J.C. Comiso, I. Allison, J. Carrasco, G. Kaser, R. Kwok, P. Mote, T. Murray, F. Paul, J. Ren, E. Rignot, O. Solomina, K. Steffen and T. Zhang, 2013. Observations: cryosphere. In: Stocker, T.F., D. Qin, G.-K. Plattner, M. Tignor, S.K. Allen, J. Boschung, A. Nauels, Y. Xia, V. Bex and P.M. Midgley (eds.), *Climate Change 2013: The Physical Science Basis. Contribution of Working Group I to the Fifth Assessment Report of the Intergovernmental Panel on Climate Change*. Cambridge University Press.

Vavrus, S.J., M.M. Holland, A. Jahn, D. Bailey and B.A. Blazey, 2012. Twenty-first-century Arctic climate change in CCSM4. *Journal of Climate*, 25:2696-2710.

Vellinga, M. and R.A. Wood, 2002. Global climatic impacts of a collapse of the Atlantic thermohaline circulation. *Climatic Change*, 54:251-267.

Vihma, T., R. Pirazzini, I. Fer, I.A. Renfrew, J. Sedlar, M. Tjernström, C. Lüpkes, T. Nygård, D. Notz, J. Weiss, D. Marsan, B. Cheng, G. Birnbaum, S. Gerland, D. Chechin and J.C. Gascard, 2014. Advances in understanding and parameterization of small-scale physical processes in the marine Arctic climate system: a review. *Atmospheric Chemistry and Physics*, 14:9403-9450.

Vihma, T., J. Screen, M. Tjernström, B. Newton, X. Zhang, V. Popova, C. Deser, M. Holland and T. Prowse, 2016. The atmospheric role in the Arctic water cycle: processes, past and future changes, and their impacts. [Special Issue] *Journal of Geophysical Research: Biogeosciences*, 121:586-620.

Vincent, W.F. and J. Laybourn-Parry (eds.), 2008. *Polar Lakes and Rivers: Limnology of Arctic and Antarctic Aquatic Ecosystems*. Oxford University Press.

Wagner, A., G. Lohmann and M. Prange, 2011. Arctic river discharge trends since 7 ka BP. *Global Planetary Change*, 79:48-60.

Walker, D.A., M.K. Reynolds, F.J.A. Daniels, E. Einarsson, A. Elvebakk, W.A. Gould, A.E. Katenin, S.S. Kholod, C.J. Markon, E.S. Melnikov, N.G. Moskalenko, S.S. Talbot, B.A. Yurtev and The other members of the CAVM Team, 2005. The circumpolar Arctic vegetation map. *Journal of Vegetation Science*, 16:267-282.

Wassmann, P. and T. Lenton, 2012. Arctic tipping points in the Earth System perspective. *Ambio*, 41:1-9.

Wassmann, P., K.N. Kosobokova, D. Slagstad, K.F. Drinkwater, R.R. Hopcroft, S.E. Moore, I. Ellingsen, R.J. Nelson, E. Carmack, E. Popova and J. Berge, 2015. The contiguous domains of Arctic Ocean advection: trails of life and death. *Progress in Oceanography*, 139:42-65.

Weyl, P.K., 1968. The role of the oceans in climatic change: A theory of the ice ages. *Meteorological Monographs*, 8:37-62.

White, D., L. Hinzman, L. Alessa, J. Cassano, M. Chambers, K. Falkner, J. Francis, W.J. Gutkowsky, M. Holland, R.M. Holmes, H. Huntington, D. Kane, A. Kliskey, C. Lee, J. McClelland, B. Peterson, T.S. Rupp, F. Straneo, M. Steele, R. Woodgate, D. Yang, K. Yoshikawa and T. Zhang, 2007. The arctic freshwater system: Changes and impacts. *Journal of Geophysical Research: Biogeosciences*, 112:G04S54, doi:10.1029/2006JG000353.

Willett, K.M., C.N. Williams Jr, R.J. Dunn, P.W. Thorne, S. Bell, M.D. Podesta, P.D. Jones and D.E. Parker, 2013. HadISDH: an updateable land surface specific humidity product for climate monitoring. *Climate of the Past*, 9:657-677.

Williams, W.J. and E.C. Carmack, 2015. The 'interior' shelves of the Arctic Ocean: Physical oceanographic setting, climatology and effects of sea-ice retreat on cross-shelf exchange. *Progress in Oceanography*, 139:24-41.

Williamson, C.E., W. Dodds, T.K. Kratz and M.A. Palmer, 2008. Lakes and streams as sentinels of environmental change in terrestrial and atmospheric processes. *Frontiers in Ecology and the Environment*, 6:247-254.

Williamson, C.E., J.E. Saros, W.F. Vincent and J.P. Smol, 2009. Lakes and reservoirs as sentinels, integrators, and regulators of climate change. *Limnology and Oceanography*, 54:2273-2282.

Woollings, T., J.M. Gregory, J.G. Pinto, M. Reyers and D.J. Brayshaw, 2012. Response of the North Atlantic storm track to climate change shaped by ocean-atmosphere coupling. *Nature Geoscience*, 5:313-317.

Woodward, G., D.M. Perkins and L.E. Brown, 2010. Climate change and freshwater ecosystems: impacts across multiple levels of organization. *Philosophical Transactions of the Royal Society B*, 365:2093-2106.

Wookey, P.A., R. Aerts, R.D. Bardgett, F. Baptist, K.A. Bräthen, J.H.C. Cornelissen, L. Gough, I.P. Hartley, D.W. Hopkins, S. Lavorel and G.R. Shaver, 2009. Ecosystem feedbacks and cascade processes: understanding their role in the responses of Arctic and alpine ecosystems to environmental change. *Global Change Biology*, 15:1153-1172.

Wrona, F., J.D. Reist, P. Amundsen, P. Chambers, K. Christoffersen, J. Culp, P. di Cenzo, L. Forsström, J. Hammar, R. Heikkinen, J. Heino, K. Kahlainen, H. Lehtonen, J. Lento, L. Lesack, M. Luoto, D. Marcogliese, P. Marsh, P. Moquin, T. Mustonen, M. Power, T. Prowse, M. Rautio, H. Swanson, M. Thompson, H. Toivonen, V. Vasiliev, R. Virkkala and S. Zavalko, 2013. Freshwater ecosystems. In: *Arctic Biodiversity Assessment*. pp. 390-433. *Conservation of Arctic Flora and Fauna (CAFF)*, Arctic Council Working Group.

Wrona, F.J., M. Johansson, J.M. Culp, A. Jenkins, J.M. Karlsson, I.H. Myers-Smith, T.D. Prowse, W.F. Vincent and P.A. Wookey, 2016. Transitions in Arctic Ecosystems: Ecological Implications of a changing freshwater system. [Special Issue] *Journal of Geophysical Research: Biogeosciences*, 121:650-674.

Wu, P., R. Wood and P. Stott, 2005. Human influence on increasing Arctic river discharges. *Geophysical Research Letters*, 32:L02703, doi:10.1029/2004GL021570.

Xu, L., R.B. Myreni, F.S. Chapin, T.V. Callaghan, J.E. Pinzon, C.J. Tucker, Z. Zhu, J. Bi, P. Ciais, H. Tommervik, E.S. Euskirchen, B.C. Forbes, S.L. Piao, B.T. Anderson, S. Ganguly, R.R. Nemani, S.J. Goetz, P.S.A. Beck, A.G. Bunn, C. Cao and J.C. Stroeve, 2013. Temperature and vegetation seasonality diminishment over northern lands. *Nature Climate Change*, 3:581-586.

Yamamoto-Kawai, M., N. Tanaka and S. Pivovarov, 2005. Freshwater and brine behaviors in the Arctic Ocean deduced from historical data of δ¹⁸O and alkalinity (1929–2002 AD). *Journal of Geophysical Research*, 110:C10003, doi:10.1029/2004JC002793.

Yamamoto-Kawai, M., E.C. Carmack and F.A. McLaughlin, 2006. Nitrogen balance and Arctic throughflow. *Nature*, 443, 43.

Yamamoto-Kawai, M., F.A. McLaughlin, E.C. Carmack, S. Nishino, K. Shimada and N. Kurita, 2009. Surface freshening of the Canada Basin, 2003–2007: River runoff versus sea ice meltwater. *Journal of Geophysical Research*, 114:C00A05, doi:10.1029/2008JC005000.

Yamamoto-Kawai, M., F.A. McLaughlin and E.C. Carmack, 2011. Effects of ocean acidification, warming and melting of sea ice on aragonite

saturation of the Canada Basin surface water. *Geophysical Research Letters*, 38:L03601, doi:10.1029/2010GL045501.

Yamamoto-Kawai, M., F. McLaughlin and E. Carmack, 2013. Ocean acidification in the three oceans surrounding northern North America. *Journal of Geophysical Research: Oceans*, 118:6274-6284.

Zhang, J. and D.A. Rothrock, 2003. Modeling global sea ice with a thickness and enthalpy distribution model in generalized curvilinear coordinates. *Monthly Weather Review*, 131:845-861.

Zhang, K., J.S. Kimball, Q. Mu, L.A. Jones, S.J. Goetz and S.W. Running, 2009. Satellite based analysis of northern ET trends and associated changes in the regional water balance from 1983 to 2005. *Journal of Hydrology*, 379:92-110.

Zhang, X., J. He, J. Zhang, I. Polyakov, R. Gerdes, J. Inoue and P. Wu, 2013. Enhanced poleward moisture transport and amplified northern high-latitude wetting trend. *Nature Climate Change*, 3:47-51.

8. Arctic carbon cycling

LEAD AUTHORS: **TORBEN R. CHRISTENSEN, SØREN RYSGAARD, JØRGEN BENDTSEN, BRENT ELSE, RONNIE N. GLUD, KO VAN HUISSTEDEN, FRANS-JAN W. PARMENTIER, TORSTEN SACHS, JORIEN E. VONK**

Coordinating lead authors shown in bold

Contents

Key Findings	204
8.1 Introduction	204
8.2 Marine carbon cycling	204
8.2.1 Defining the borders of the marine Arctic	204
8.2.2 Carbon exchange across the air-sea interface	205
8.2.3 Carbon transport in the marine Arctic	206
8.2.4 Sea ice and the carbon cycle	207
8.3 Arctic terrestrial carbon cycling	207
8.3.1 Magnitude of the soil carbon reservoir	207
8.3.2 Vulnerability of the soil carbon reservoir	209
8.3.3 Carbon exchange across the soil-air interface	210
8.4 Integration and projections	211
8.4.1 Projections for change and its possible radiative impact	212
8.4.2 Modeling the integrated Arctic terrestrial and marine system	213
8.5 Conclusions and recommendations	214
References	214

Key Findings

- The marine Arctic is considered a net carbon sink, with large regional differences in uptake rates. More regional modelling and observational studies are required to reduce the uncertainty among current estimates. Robust projections for how the Arctic Ocean carbon sink may evolve in the future are currently lacking.
- Direct connections have been documented between sea-ice dynamics and carbon cycling in marine ecosystems and on land. Projections suggest further sea-ice decline may accelerate changes in carbon cycling dynamics at sea and on land. Although river-transported organic and inorganic carbon plays a major role in the marine Arctic carbon cycle this is not well studied. Changes in terrestrial ecosystems may also affect sea-ice decline – at least in the long term.
- Permafrost underlies ~75% of the area draining into the Arctic Ocean but its hydrology is poorly understood, especially under global warming. Arctic tundra is a net sink for atmospheric carbon dioxide (CO_2) in the growing season and the sink strength has more than doubled since 2000 in Eurasia. In contrast, the few winter data available show tundra ecosystems are a net source of atmospheric CO_2 in winter. Small features below the resolution of current lake and wetland databases may be important controls on carbon transfer from permafrost soils to the atmosphere.
- Earth System Models (ESMs) are not yet able to reliably simulate the full dynamics of the Arctic carbon cycle. This is mainly because such models still address terrestrial and marine systems separately and because they vary widely in their representation of permafrost. Further development of ESMs should include a focus on improving the connections between ocean and land, especially in the representation of lateral fluxes.

8.1 Introduction

Many recent changes in the Arctic cryosphere have been dramatic and have exceeded even the most extreme projections of future change. Some of these changes in the cryosphere are expected to affect local climate and through distant connections, regional and even global climate. However, climate feedbacks associated with the changing cryosphere are complex, vary over space and time, and are generally poorly understood. These feedback mechanisms include both biogeophysical and biogeochemical aspects. This chapter reviews recent information on ecosystem-atmosphere interactions within the Arctic, especially in relation to marine and terrestrial carbon cycling.

Although the previous SWIPA report did not include a specific chapter on Arctic carbon cycling, this topic was still addressed. The difference is that the results formed part of several different chapters, whereas this update on Arctic carbon cycling is presented as a single chapter and so provides a more comprehensive and all-encompassing view of current understanding (see Box 8.1 for an overview of Arctic carbon fluxes).

From the perspective of an astronaut looking down on Earth from high above the North Pole it is immediately obvious that to understand the Arctic carbon cycle, ocean and land cannot be considered separately. Huge rivers discharge into the Arctic Ocean, carrying vast amounts of sediment that can be seen from space as enormous swirls in the coastal zone. In addition, roughly 80% of lowland tundra occurs within 100 km of the coast (Walker et al., 2005) – emphasizing the maritime nature of this ecosystem's climate. This coastal climate has changed over recent decades due to the rapidly diminishing sea ice (Screen et al., 2012; Barber et al., 2015), causing feedbacks that affect both marine and terrestrial greenhouse-gas exchange (Parmentier et al., 2013) and ultimately permafrost thaw (Schuur et al., 2015). But despite this obvious interlinkage, ocean and land are too often considered as separate systems. To truly grasp the impact of climate change on the Arctic as a whole an integrated approach is essential.

8.2 Marine carbon cycling

8.2.1 Defining the borders of the marine Arctic

The marine Arctic is broadly defined as the ocean area receiving runoff and calved glacial ice from areas with an Arctic climate. The present assessment uses the more specific AMAP definition of the marine Arctic (ACIA, 2005), namely the Arctic Ocean with adjacent continental shelf areas, the Nordic Seas (i.e. the Norwegian, Greenland and Iceland Seas), the waters surrounding Greenland south of the Denmark Strait (i.e. in the northern North Atlantic), Baffin Bay, the Canadian Arctic archipelago, the connection to Hudson Bay, and the northern part of the Labrador Sea. Thus, the marine Arctic comprises deep ocean areas in the Arctic Ocean, Nordic Seas, Baffin Bay and northern North Atlantic as well as shallow coastal and shelf areas in contact with large drainage areas where freshwater or ice, via rivers or glaciers, enter the ocean. The marine Arctic carbon cycle thus affects a much larger area than the central Arctic Ocean itself.

Box 8.1 Arctic carbon fluxes

On land, plants take up carbon while microorganisms in the soil produce methane (CH_4) and respire carbon dioxide (CO_2). In the ocean, CH_4 is released from thawing subsea permafrost, while CO_2 is absorbed due to an undersaturation of CO_2 in the water compared with the atmosphere. CO_2 is then photosynthesized into organic carbon or converted into calcium carbonate (CaCO_3) by the biological and solubility pumps, maintaining low $p\text{CO}_2$ levels. Near the ice edge, cooling

induces sinking of the surface water, and with it CO_2 . Above the ice, the air-ice exchange depends on the carbonate chemistry and temperature of the ice. CO_2 can also be discharged into brine channels in the ice, where transport is downwards due to the density difference. In polynyas and leads, CO_2 can be taken up from the atmosphere, but CH_4 can also be produced in surface waters. Transport into the deeper and interior waters of the Arctic Ocean ensures storage of carbon.

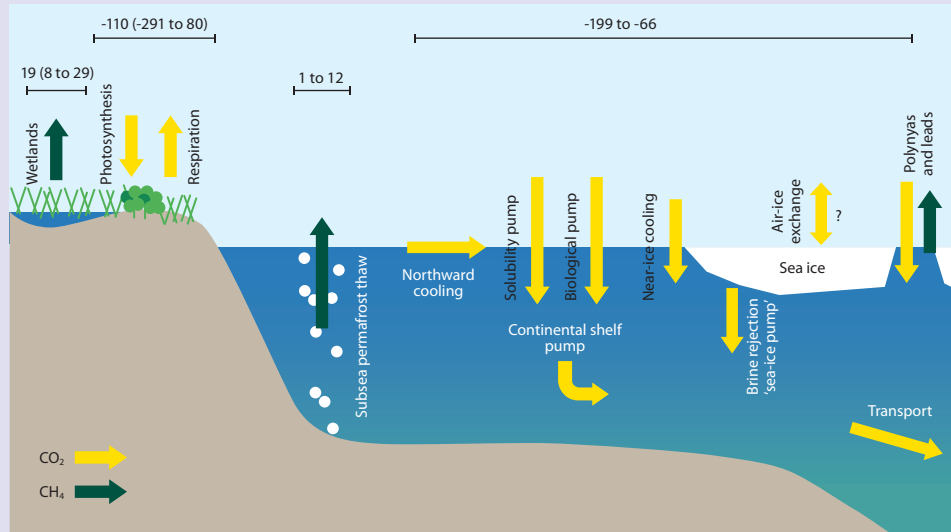


Figure 8.1 Simplified representation of those Arctic carbon fluxes that may be influenced by sea-ice retreat (Parmentier et al., 2013). Current best estimates of sink/source strengths are shown in TgC/y , where available. The uncertainty ranges of the terrestrial fluxes are shown in brackets. The arrows do not indicate the strength of each flux.

8.2.2 Carbon exchange across the air-sea interface

The amount of atmospheric carbon dioxide (CO_2) absorbed by the Arctic Ocean may be significantly affected by changes in sea-ice cover, the structure and functioning of marine ecosystems, and the hydrological cycle. The controls on this 'carbon sink' can be broadly categorized into two classes: the biogeochemical processes that determine the partial pressure of CO_2 in seawater (i.e. $p\text{CO}_{2\text{sw}}$) and the physical processes that determine the rate of gas exchange across the air-sea interface (i.e. the gas transfer velocity, k). Solubility and the diffusivity of CO_2 in seawater (characterized by the Schmidt number) also control the carbon sink, although to a much lesser degree than k or $p\text{CO}_{2\text{sw}}$ (Wanninkhof, 1992). Changes in both $p\text{CO}_{2\text{sw}}$ and k are expected under a warming climate, making the Arctic Ocean carbon sink vulnerable to climate change. Arguably the most important biogeochemical process for CO_2 uptake is primary production.

Satellite data show the decline in Arctic sea ice has been accompanied by a significant increase in primary productivity (Arrigo and van Dijken, 2011). However, recent discoveries of significant under-ice phytoplankton blooms, which are poorly represented by traditional remote sensing data suggest current estimates of Arctic productivity could be underestimated (Arrigo et al., 2012). Several recent studies have also reported the widespread occurrence of ice-algal aggregates below melting summer ice in the central Arctic

Ocean and Fram Strait (Assmy et al., 2013; Boetius et al., 2013; Fernández-Méndez et al., 2014; Glud et al., 2014). Although their productivity is considerably less than the pelagic primary production they do represent an important food source for the sympagic community and – after sinking – for the benthic food web and carbon export to the seabed. It is not clear whether the many recent reports on ice-algae aggregates reflect an actual increase in their numbers potentially related to increased melt pond coverage (Lee et al., 2012; Palmer et al., 2014) or whether they have just been overlooked in past studies (Boetius et al., 2013; Glud et al., 2014).

There are even fewer studies of benthic primary production, even in the Arctic which includes 25% of the global coastal area. Here, the nutrient requirements of benthic primary producers in the form of micro- and macroalgae are largely met by regenerated nutrients from the sediment. In areas with sufficient light, benthic primary producers can make a substantial contribution to the overall production (Glud et al., 2002, 2009; Krause-Jensen et al., 2007; Woelfel et al., 2010; Attard et al., 2014). Using remote sensing data for the period 1998–2003, Gattuso et al. (2006) found that although up to 25% of the Arctic coastal seabed received only about 1% of the incoming irradiance during summer, this could be enough to sustain benthic primary production. By combining the light distribution data reported by Gattuso et al. (2006) with data from studies on the relation between light and benthic primary production in different Arctic settings it is clear that benthic primary production in the Arctic is significant – representing

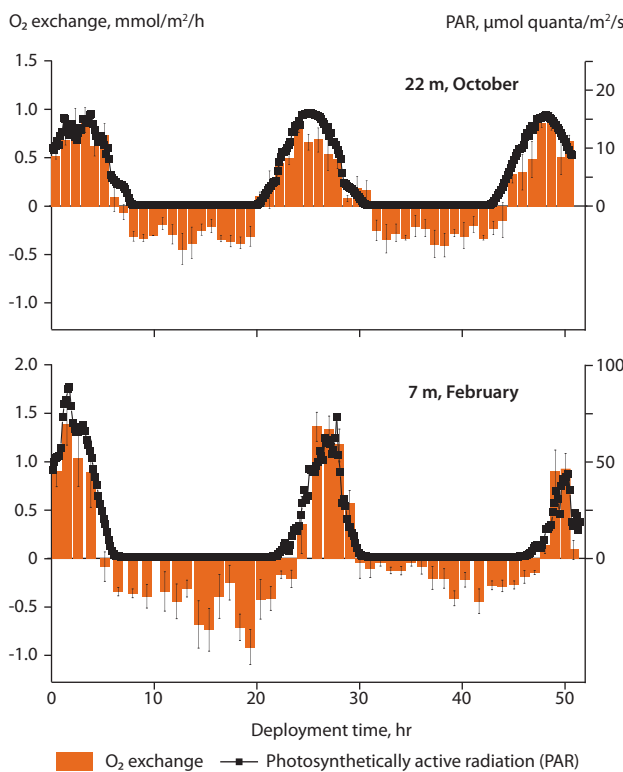


Figure 8.2 Net oxygen (O_2) production by benthic diatoms in Nuuk fjord (Greenland) in daytime at 22 m water depth in October and 7 m water depth in February. The light level required to induce net O_2 production was between 2 and 4 $\mu\text{mol quanta}/\text{m}^2/\text{s}$ (Attard et al., 2014).

between 10% and 40% (Glud et al., 2009; Attard et al., 2014, 2016) of the estimated annual pelagic production (Subba-Rao and Platt, 1984; Pabi et al., 2008). Figures 8.2 and 8.3 show that benthic algal communities in the Arctic are well adapted to low light levels.

More open water and higher primary production should drive a lower $p\text{CO}_{2\text{sw}}$ and increased CO_2 uptake. However, there is some uncertainty about this because ice loss has so far occurred primarily over nutrient-rich shelf seas, and observations in the deep basins indicate low CO_2 uptake capacities owing to stratification and nutrient limitation (Cai et al., 2010; Else et al., 2013). Nutrient limitation may become more widespread in the future as freshening from higher river runoff and ice melt (Morison et al., 2012) suppresses vertical mixing (Nummelin et al., 2015) and reduces light availability through increased turbidity. This could lead to lower levels of primary production. Other factors limiting production-driven CO_2 drawdown include warmer surface waters (Steele et al., 2008), higher river fluxes of organic and inorganic carbon (Tank et al., 2012a), and coastal erosion (Vonk et al., 2012). This indicates the need for a greater focus on the potential impacts of reduced sea-ice cover and enhanced river run-off on net productivity in the coastal Arctic.

A continued decline in Arctic sea ice is also expected to drive an increase in gas exchange across the ocean–atmosphere interface. Particularly because longer open water seasons will increase the amount of time seawater is in direct contact with the air, thus increasing mean annual k . Similarly, increased fetch lengths are causing increased wave generation (Aspin et al., 2014), which may in turn increase gas transfer. Gas transfer may also increase in ice-affected areas as the extent of the marginal

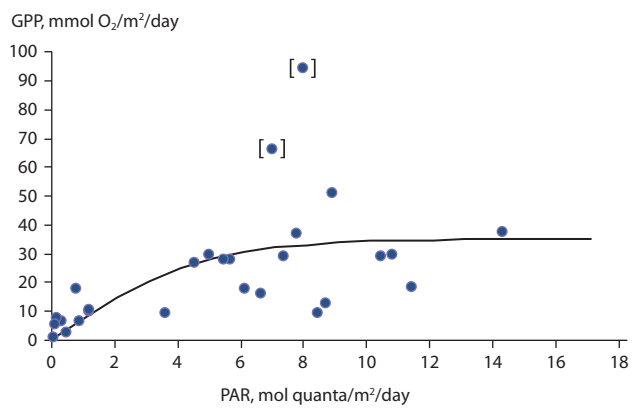


Figure 8.3 Gross benthic primary production (GPP) as derived from benthic oxygen (O_2) exchange as a function of integrated daily light availability (photosynthetically active radiation; PAR) at a range of Arctic and subarctic settings, outliers in square brackets (Attard et al., 2016).

ice zone changes (Strong and Rigor, 2013), and increasing ice drift (Spreen et al., 2011) results in more lead and polynya activity. Recent observations (Else et al., 2011) and modeling studies (Loose et al., 2014) show k is higher in these regions, making them potentially important for gas exchange in the Arctic. But it should also be noted that not all studies show enhanced gas transfer in such environments (Rutgers van der Loeff et al., 2014; Butterworth and Miller, 2016). Gases can also move through first-year sea ice (Loose et al., 2010), potentially extending the seasons and locations involved in air-sea gas exchange. Current estimates suggest this exchange may be insignificant compared to direct air-sea exchange (Loose et al., 2010; Crabeck et al., 2014), but observations for the more dynamic spring break-up and autumn freeze-up periods are currently lacking.

In general, the marine Arctic is considered to be a net carbon sink and several studies agree on an overall uptake of about 0.1–0.2 PgC/y. However, this overall agreement includes estimates with large regional differences in uptake rates; for example, 0.2 PgC/y in the Nordic Seas (Jeansson et al., 2011), and 0.12 PgC/y for the Arctic Ocean north of 76°N and 0.21 PgC/y for the north subpolar North Atlantic (49–76°N) (Schuster et al., 2013). Arrigo et al. (2010) used satellite data to derive an estimated uptake of 0.12 PgC/y for an area covering most of the marine Arctic and MacGilchrist et al. (2014) estimated a total air-sea exchange of 0.17 PgC/y for this same area. Model studies for the Arctic Ocean suggest an uptake of 0.06 PgC/y for the entire Arctic region (Manizza et al., 2013). Further regional modelling and observational studies of the marine Arctic are required to reduce the uncertainty among current estimates.

8.2.3 Carbon transport in the marine Arctic

The observational database for marine carbon compounds such as dissolved inorganic carbon (DIC), pH, surface $p\text{CO}_2$ and alkalinity, has increased significantly over the past decade. The international effort of collating quality checked data in the open CARINA (CARbon dioxide IN the Atlantic Ocean) data base (Key et al., 2010; Tanhua et al., 2010), including data from the marine Arctic (Olsen, 2009; Jutterström et al., 2010) has resulted in several studies of the marine Arctic carbon cycle. Jeansson et al. (2011) used carbon data for the Nordic Seas together with previous estimates of volume transports to the

area and found that the largest carbon transport to the marine Arctic takes place across the Greenland-Scotland Ridge – estimating the corresponding fluxes of DIC as an outflow of ~ 3.4 PgC/y and an inflow (including the area between Scotland and Norway) of ~ 4.2 PgC/y. They also found ~ 1.8 PgC/y was transported through the Barents Sea towards the Arctic Ocean and ~ 0.8 PgC/y was transported across Fram Strait into the Greenland Sea. Kivimäe et al. (2010) found a higher net DIC transport through the Barents Sea (~ 2.7 PgC/y). MacGilchrist et al. (2014) found a net DIC transport from the Nordic Seas to the Arctic Ocean of ~ 1.5 PgC/y, which is $\sim 50\%$ larger than the estimate of Jeansson et al. (2011). A large carbon transport also takes place through the Canadian Arctic Archipelago and into Baffin Bay. MacGilchrist et al. (2014) estimated a total transport, based on observations from Shadwick et al. (2011) of ~ 2.6 PgC/y into Baffin Bay and a slightly larger southward carbon flux through Davis Strait. DIC transport from the Pacific Ocean through Bering Strait has been estimated at ~ 0.6 PgC/y based on observed DIC concentrations and volume fluxes (Cai et al., 2014).

Analysis of the transient change in DIC in subsurface water masses in the Arctic Ocean shows no significant trend for water masses below 2000 m whereas water masses above 1400 m show a significant increase of 0.4 to 0.9 $\mu\text{mol C/kg/y}$ and because no corresponding change in nutrient concentrations has been observed, this increase in DIC has been explained by an increased uptake of anthropogenic carbon (Ericson et al., 2014). The accumulated inventory of anthropogenic DIC in the Nordic Seas and the Arctic Ocean has been estimated to account for about 2% of the total anthropogenic DIC load (Olsen et al., 2010; Tanhua et al., 2010) although the corresponding water volume constitutes only about 1% of the global ocean.

River-transported organic and inorganic carbon plays a major role in the marine Arctic carbon cycle (McGuire et al., 2009; MacDonald et al., 2010). A total river transport of 0.06 PgDIC/y has been estimated for the Arctic region (Tank et al., 2012a) and is comparable to the air-sea net exchange of CO₂. Riverborne organic carbon influences carbon cycling in Arctic shelf regions (Alling et al., 2010) and a study in the Laptev and East Siberian Shelf Seas showed that remineralization of organic carbon explains the net-outgassing in these areas (Anderson et al., 2009). Runoff from glacier systems may also make a significant contribution to the Arctic carbon budget (Lawson et al., 2014) but these systems are less studied (Meire et al., 2015). These issues are further discussed in Section 8.3.

8.2.4 Sea ice and the carbon cycle

The role of ice-covered oceans in the CO₂ balance has been largely ignored because sea ice is assumed to impede gaseous exchange with the atmosphere (Tison et al., 2002). However, sea ice is permeable when warm enough (e.g. Golden et al., 1998) and can support gas exchange (e.g. Delille et al., 2007; Nomura et al., 2010; Miller et al., 2011; Geilfus et al., 2013; Sørensen et al., 2014; Sieverts et al., 2015). In addition, recent studies have shown that physical and chemical processes in the sea ice itself may act as an important control on $p\text{CO}_2$ at the sea surface (Rysgaard et al., 2009, 2012, 2013; Jones et al., 2010; Fransson et al., 2013; Parmentier et al., 2013; Delille et al., 2014). During ice growth, precipitation of the carbonate

crystal ikaite increases the CO₂ concentration in brine. If most of this CO₂ is rejected via brine drainage and mixed into the ocean interior while the ikaite crystals remain trapped in the sea ice matrix, then the release of the alkalinity to the surface ocean by the dissolution of ikaite lowers $p\text{CO}_2$ and so enhances the air-sea CO₂ flux. Budget calculations of the potential size of this sea-ice pump during summer ice melt show a net uptake of 14–31 TgC/y in the Arctic and 19–52 TgC/y in the Antarctic (Rysgaard et al., 2011; Delille et al., 2014). This process could be an important element of the ocean CO₂ sink, not only today but also during the Last Glacial Maximum (Bouttes et al., 2010). As well as influencing the CO₂ flux, ikaite production in sea ice also generates divergent paths of pH evolution from seawater pH to that of exterior and interior ice, frost flowers and brine (Hare et al., 2013). A typically high pH of exterior layers in bulk sea ice cores indicates the presence of a large pH gradient from internal ice layers to the snow-ice-water surface and at the ice-water interface, which may be significant for biochemical and geophysical processes in ocean surface waters.

Recent studies indicate significant sources of CH₄ in the Arctic Ocean (e.g. Damm et al., 2010; Shakhova et al., 2010; Kort et al., 2012; Vancoppenolle et al., 2013), although atmospheric measurements suggest previous bottom-up estimates have overestimated the importance of the Arctic Ocean as a CH₄ source (Berchet et al., 2016). It has been suggested that sea ice in the Arctic Ocean regulates CH₄ levels through two mechanisms: by shielding CH₄ emission from the ocean and through CH₄ consumption (He et al., 2013). Other studies suggest river runoff may be an important source of CH₄ for sea ice in coastal areas, and that sea ice can be both a sink for CO₂ and a source for CH₄ (Crabeck et al., 2014).

Robust projections for how the Arctic Ocean carbon sink may evolve in the future are currently lacking. Attempts to quantify past changes using biogeochemical models have suggested an increasing sink of 0.9 TgC/y (Schuster et al., 2013) to 1.4 TgC/y (Manizza et al., 2013). These estimates are in line with those of Jutterström et al. (2010) who estimated 1.3 TgC/y based simply on increased exposure of the surface ocean to the atmosphere. Whether this rate of increase can be sustained long-term remains unclear.

8.3 Arctic terrestrial carbon cycling

8.3.1 Magnitude of the soil carbon reservoir

Low temperatures, wet conditions and permafrost (soil or peat with below-zero temperature for at least two consecutive years) are favorable for the accumulation and preservation of organic matter in soils because decomposition rates are low. In the northern hemisphere, permafrost soils occur on about 25% of the land area (23 million km²), either as a continuous cover (continuous permafrost, >90% of the area) or as patchy (discontinuous, 50–90% of the area) and sporadic permafrost (10–50% of the area) (Brown et al., 2014). Estimates of the amount of global organic carbon in Arctic soils have recently been revised upward, amounting to about 50% of the world's global soil carbon (Tarnocai et al., 2009; Hugelius et al., 2014). Decomposition of this carbon in a rapidly warming Arctic, and the resulting emissions of CO₂ or CH₄, is a potentially

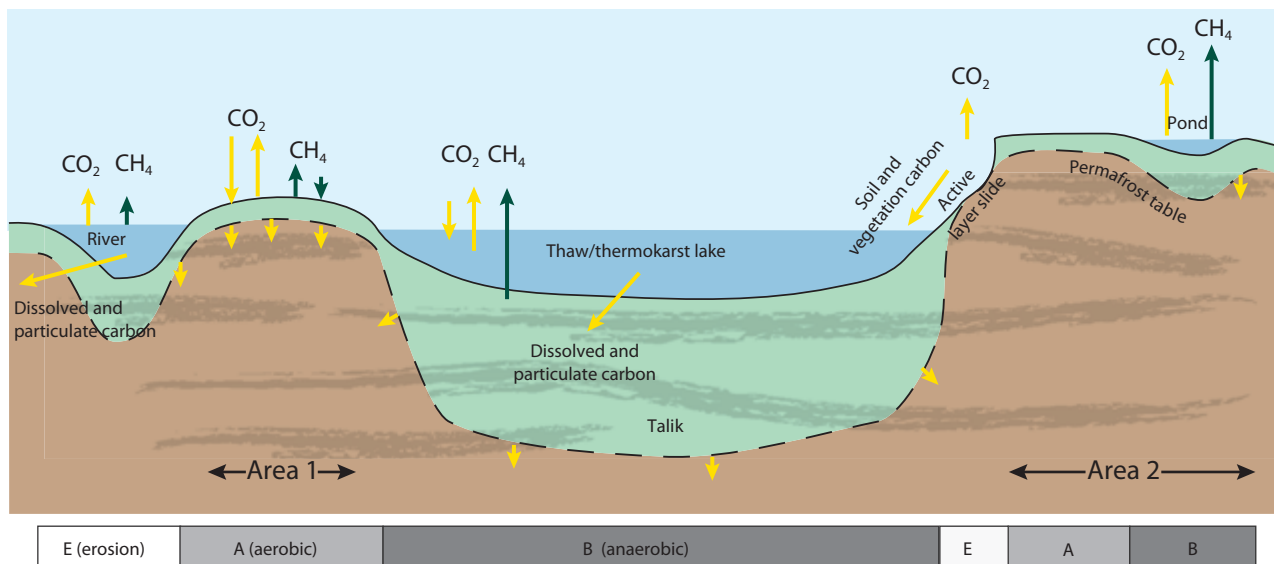


Figure 8.4 Mechanisms by which carbon may be lost from Arctic soils in permafrost areas (excluding fire). Area 1 has a spatially homogenous increase in active layer thickness and Area 2 has spatially heterogeneous permafrost thaw driven by differences in soil ice content (after van Huissteden and Dolman, 2013).

important feedback to climate warming. However, the extent to which this carbon is available for decomposition is dependent on its conservation in frozen ground and vulnerability to permafrost degradation, burial depth, and how easily the organic material is decomposed (McGuire et al., 2010; Van Huissteden and Dolman, 2013). Cryoturbation (vertical movement of soil resulting from freeze-thaw processes) mixes carbon to deeper levels, potentially removing it from the layers of rapid decomposition (Kaiser et al., 2007; Koven et al., 2009). Conversely, permafrost thaw may result in a range of soil erosion processes and in lake/pond formation through soil subsidence, meaning soil carbon can be exposed to anaerobic (resulting in CH_4 and CO_2 emission) and aerobic (resulting in CO_2 emission) decomposition, and to transport as dissolved organic carbon (DOC) and particulate organic carbon (POC) through streams/rivers to lakes and the sea (Van Huissteden and

Dolman, 2013; Vonk and Gustafsson, 2013; Figure 8.4). These lateral processes have largely been neglected in Arctic carbon cycling studies but have attracted more attention recently (Vonk and Gustafsson, 2013; Cory et al., 2014).

Older inventories of Arctic soil carbon included only the top 100 cm of soil; however, because permafrost thaw may affect soil organic matter (SOM) at greater depths, Tarnocai et al. (2009) also included soil layers up to 300 cm depth in their inventory. They also accounted for variability in soils and organic deposits across the Arctic by distinguishing between peatland areas, alluvial deposits, and yedoma. The highest organic carbon contents occurred in peat soils and peaty cryoturbated mineral soils ($32.2\text{--}69.6\text{ kg/m}^2$). Although yedoma soils have a low carbon content, the vast extent of these deposits means they represent a large carbon pool (Zimov et al., 2006; Schirrmeister et al., 2010, 2011).

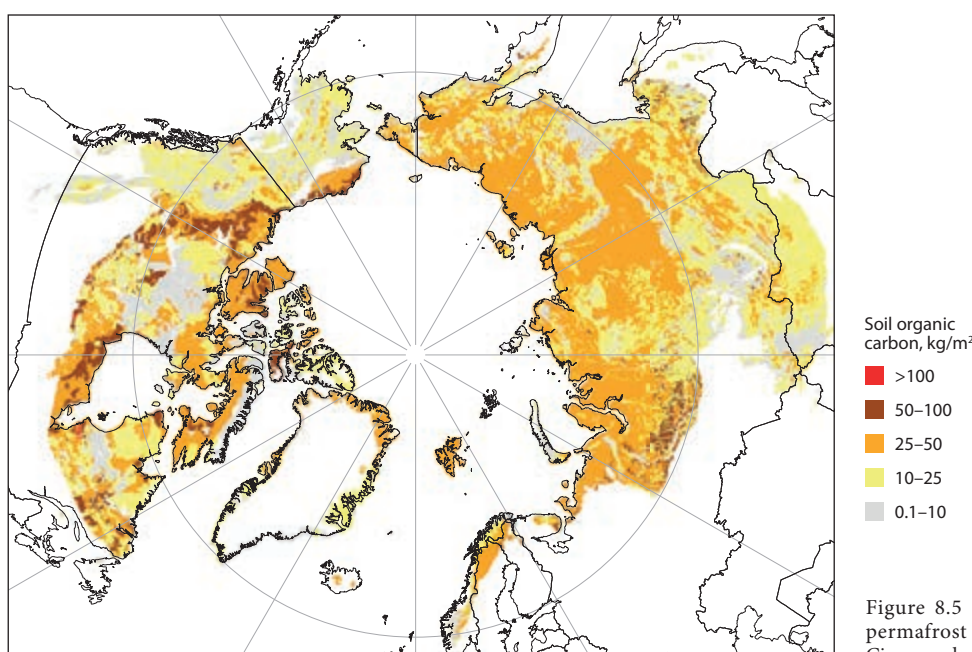


Figure 8.5 Carbon distribution of northern permafrost soils derived from the Northern Circumpolar Soil Database (Hugelius et al., 2013).

Table 8.1 Recent estimates of Arctic soil carbon stocks.

Soil carbon stock, PgC				Source
0–100 cm	0–300 cm	>300 cm	Total	
496	1024	407	1672	Tarnocai et al. (2009)
		241 ^a		
nd	750	400	1400–1850	Schuur et al. (2008)
		250 ^a		McGuire et al. (2009)
472±27	1035±150	181±54	1307±170	Hugelius et al. (2014)
		91±52 ^a		

nd: Not determined. ^adelta/alluvial sediments.

The most recent estimates for Arctic soil carbon stocks converge on the range 1400–1850 PgC for all northern permafrost soils (750–1024 PgC for peatlands, 241–250 PgC for alluvial deposits, 400–407 PgC for yedoma). However, the uncertainties associated with these estimates are large, especially for the amount of carbon at deeper levels and the thickness of these carbon deposits. The Northern Circumpolar Soil Database is being developed to help reduce these uncertainties (Hugelius et al., 2013). Hugelius et al. (2014) arrived at lower estimates in particular for yedoma (181±54 PgC) and alluvial deposits (91±52 PgC) (Table 8.1 and Figure 8.5); the yedoma estimate being in line with the sediment analysis data of Strauss et al. (2013).

The lability (decomposability) of SOM strongly determines the rate at which carbon stored in soil reservoirs can be transferred to the atmosphere after thaw and shows considerable variability. Schädel et al. (2014) analyzed the lability of SOM using aerobic incubation experiments on organic and mineral soil cores collected from Alaska and northern Siberia. The fraction of SOM that is decomposed in less than a year (the ‘fast pool’ fraction) was less than 5% in all soils. However, the ‘slow pool’ fraction (defined here by decomposition taking 5 to 15 years) varied between organic and mineral soils, with organic soils showing the fastest decomposition rates and greatest variability. The carbon/nitrogen ratio is a good proxy for slow pool size. Treat et al. (2015) analyzed a large database of anaerobic incubation studies. This showed differences in the anaerobic CO₂:CH₄ production ratio (lowest for tundra sites) and overall anaerobic CO₂ and CH₄ production (greatest for organic soils and inundated soils, and least for deeper horizons). Methane production was more than four times higher in soil from graminoid (grass) and shrub-dominated sites than in soils from forested sites, suggesting that the vegetation community can have a significant influence on CH₄ fluxes, as found in field observations (e.g. Strömgren et al., 2003; Turetsky et al., 2007). In the absence of any other changes, a shift in graminoid species composition may therefore affect the CO₂:CH₄ production ratio (Strömgren et al., 2003). Pedersen et al. (2011) examined a range of drained thermokarst lake basins of various age in northern Alaska and found evidence of substantial decomposable carbon deposits in even the oldest lake beds (5500 years) and deepest soil horizons.

8.3.2 Vulnerability of the soil carbon reservoir

The vulnerability of the Arctic soil carbon pool to climate change depends on its position with respect to the surface. Deeper (below 1 m) permafrost carbon is less vulnerable to short-term changes in temperature. A distinction can be made between gradual changes (‘press disturbances’ such as changes in active layer thickness, soil wetness, and microbial process rates) and rapid changes (‘pulse disturbances’ such as wildfires and thermal disturbance of permafrost – thermokarst) (Grosse et al., 2011). The latter depend on the distribution of ice in the subsoil and on geomorphological processes resulting from soil subsidence and erosion (Figure 8.4). Carbon that is lost from soils is either emitted as CO₂ and CH₄ to the atmosphere or is transported as DOC and POC in rivers. About two-thirds of this riverborne carbon is outgassed to the atmosphere during transport, but a large proportion may be sequestered again in lake, river, and marine sediments (Van Huissteden et al., 2013).

In an ‘expert opinion’ survey conducted in 2012, experts were asked to provide quantitative estimates of permafrost change in response to four scenarios of warming (Schuur et al., 2013). For the intermediate warming scenario (RCP4.5), experts hypothesized that carbon release from permafrost zone soils over the 2010–2040 period could total 11–25 PgC in CO₂ equivalents using a 100-year CH₄ global warming potential (GWP). These values increased by 50% for a 20-year CH₄ GWP, with between 25% and 50% of expected climate forcing coming from CH₄ even though CH₄ accounted for only ~2% of the expected carbon release. However, the numbers from this first survey do not represent a net flux into the atmosphere because changes in biomass, fires and DOC/POC fluxes were not accounted for. A second expert opinion survey was thus conducted to quantify potential change in these components of the carbon cycle (Abbott et al., 2016). Expert opinion of biomass change within the boreal zone varied strongly under the RCP4.5 scenario, from -6 to 12 PgC by 2040 (1st and 3rd quartiles reported), while tundra biomass was generally considered to increase over this period from ~0.5 to 1.7 PgC. However, the latter range is the same as that estimated for carbon loss from boreal forest fires. Tundra fires and DOC/POC fluxes were considered small, with increases of less than ~0.5 PgC by 2040. The survey results indicate that permafrost carbon release may be larger than gains in biomass, but large uncertainties exist up until 2040. On longer timescales – up to 2100 and 2300 – expert opinion tended to agree that carbon losses from permafrost soils would exceed gains in biomass.

Changes in temperature and precipitation both affect permafrost soils. Ijima et al. (2010) reported higher soil temperatures and soil wetness after four years of high rainfall and snowfall in the central Lena basin in Siberia. These changes resulted locally in taiga forest die-back (Ijima et al., 2014) and lower boreal forest carbon sequestration. In contrast, water-limited plant communities in High Arctic settings may benefit from increased soil moisture (Elberling et al., 2008). Climate manipulation experiments show increased active layer thickness enhances decomposition of older soil carbon (Natali et al., 2014). For example, Dorrepaal et al. (2009) reported that more

than 69% of the increase in soil respiration was attributed to soil organic matter near the base of the active layer in a warming experiment in a subarctic peatland.

While expansion of existing lakes may increase in a warmer and wetter climate, this is ultimately limited by fluvial and subsurface drainage of lakes (Jones et al., 2011; Van Huissteden et al., 2011). There is little reliable information on lake expansion, and even less on how this may affect lake CH₄ emission, since this requires extensive multi-year high resolution remote sensing studies and must take into account any non-climatic lake level changes (Plug et al., 2008; Jones et al., 2011). In southern discontinuous permafrost areas, lake area tends to decrease by regrowth (filling in of lakes to become wetlands) and subsurface drainage (Roach et al., 2011). Observation data from the Seward Peninsula (Alaska) indicate a net decrease in lake area resulting from the drainage of large lakes, while the number of smaller lakes and ponds is growing rapidly (Jones et al., 2011). In other areas, there are also indications of rapidly increasing numbers of small lakes and ponds (Jorgenson et al., 2006). In western Siberia, a relationship was established between lake size and lake water CO₂ and CH₄ concentration, with the smaller lakes showing the highest gas concentrations (Shirakova et al., 2013). This pattern indicates that small features below the resolution of current lake and wetland databases may be important controls on carbon transfer from permafrost soils to the atmosphere.

8.3.3 Carbon exchange across the soil-air interface

Most of the direct observational studies of the exchange of CO₂ between tundra and the atmosphere have been conducted during the summer growing season. These studies generally indicate that Arctic tundra has been a sink for atmospheric CO₂ during summer in all subregions of the Arctic, with no substantial change in sink strength before or after 2000 (McGuire et al., 2012). But this is not the case for Eurasia, for which sink strength has more than doubled since 2000. However, the difference between the mean exchange rates for before and after 2000 is not significant owing to the substantial overlap between the ranges reported (-50 to -1 gC/m² and -141 to -4 gC/m², respectively). Nevertheless, existing observations suggest there are differences among different tundra types in net summer CO₂ exchange. There is little overlap in reported net CO₂ uptake in wet tundra (-59 to -27 gC/m²) and dry tundra (-11 to 21 gC/m²).

Very few studies have estimated CO₂ exchange in winter. However, those data that do exist suggest tundra ecosystems are a net source of CO₂ to the atmosphere in winter. The few studies available appear to show no difference in source strength among subregions or tundra types (Pirk et al., 2016).

An episodic release of stored gases may be triggered by physical pressure build-up in permafrost soil when the active layer starts freezing from the top downwards toward the permanently frozen soil in autumn (Mastepanov et al., 2008,

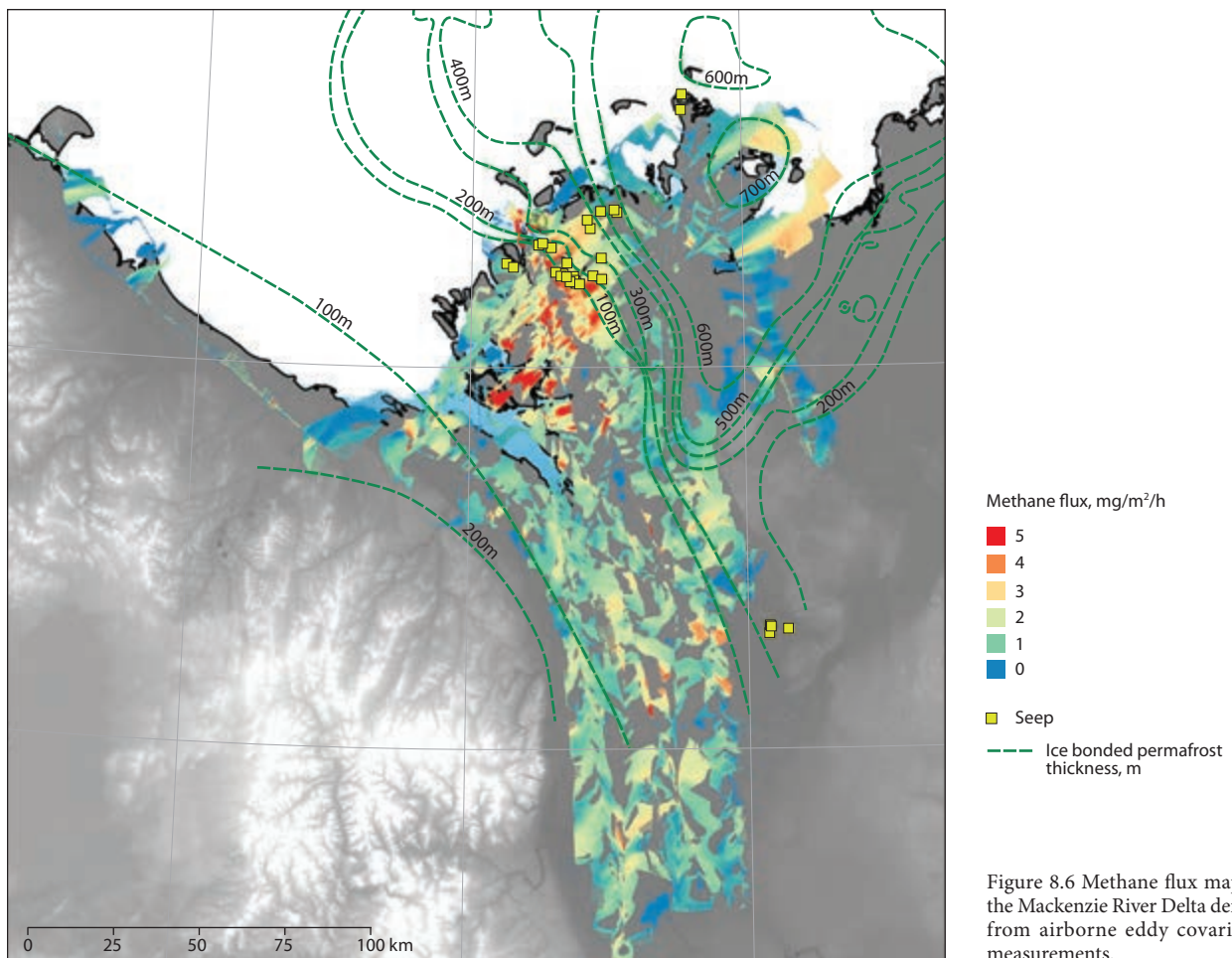


Figure 8.6 Methane flux map for the Mackenzie River Delta derived from airborne eddy covariance measurements.

2013). Zona et al. (2016) estimated that cold season (September to May) emission of CH_4 during freeze-up of the active layer may exceed summer emissions in Alaska. There may also be sudden CH_4 emissions during the growing season related to atmospheric pressure change (Klapstein et al., 2014). In a related ecosystem, Wik et al. (2014) found CH_4 transport to the atmosphere in gas bubbles from subarctic lakes shows a highly predictable relationship with energy input. However, ebullition (bubble emission) and storage/transport issues as well as microbial community shifts may complicate seasonal emission patterns as they do not follow simple relationships with variations in temperature and plant productivity.

A growing number of observation-based studies are attempting to estimate annual CO_2 exchange between tundra and the atmosphere. In general, the range in variability among estimates is scattered around neutral annual CO_2 exchange in all subregions. In North America, the data indicate that tundra ecosystems could have been net sources of CO_2 to the atmosphere before 2000, but broadly neutral or weak sinks since 2000 (McGuire et al., 2012). The estimates of annual exchange differ among tundra types with wet tundra and treeline tending to act as a CO_2 sink and dry tundra tending to act as a CO_2 source.

There is still large variability in Arctic tundra CH_4 emission estimates, mainly because spatio-temporal variability is not adequately captured by the current sparse measurement networks. Observational studies reviewed by McGuire et al. (2012) indicate that through the 1990s and 2000s, tundra emitted $14.7 \text{ TgCH}_4/\text{y}$ (0–29.3 TgCH_4/y uncertainty range). This largely supports the review of bottom-up and top-down CH_4 emission estimates by Kirschke et al. (2013), who suggested a Eurasian boreal wetland source of $14 \text{ TgCH}_4/\text{y}$ (range: 9–23 TgCH_4/y) and $9 \text{ TgCH}_4/\text{y}$ (range: 4–13 TgCH_4/y) for top-down and bottom-up estimates, respectively, and a top-down estimated soil sink of $3 \text{ TgCH}_4/\text{y}$ (range: 1–5 TgCH_4/y). For North American wetlands, the top-down estimates are lower than the bottom-up estimates with $9 \text{ TgCH}_4/\text{y}$ (range: 6–17 TgCH_4/y) and $16 \text{ TgCH}_4/\text{y}$ (range: 9–28 TgCH_4/y), respectively, as well as a top-down estimated soil sink of $2 \text{ TgCH}_4/\text{y}$ (range: 1–2 TgCH_4/y).

Observations that typically feed into bottom-up estimates were compiled by Olefeldt et al. (2013), who derived a median CH_4 flux of $34 \text{ mgCH}_4/\text{m}^2/\text{d}$ (range: 3–80 $\text{mgCH}_4/\text{m}^2/\text{d}$) for tundra regions, based on eddy covariance (EC) and gradient tower measurements. Most recently, Petrescu et al. (2015) reported a flux of $19.6 \text{ mgCH}_4/\text{m}^2/\text{d}$ averaged from seasonally operated EC sites in the circumpolar Arctic and boreal region, while Watts et al. (2014) estimated emissions of $<65.8 \text{ mgCH}_4/\text{m}^2/\text{d}$ at circumpolar EC sites based on a satellite data driven biophysical modeling approach. These fluxes are dynamic and also subject to change following permafrost thaw (e.g. Christensen et al., 2003).

Recent developments include increased use of airborne measurements, which have the advantage of avoiding biases induced by logistical constraints on ground-based study site selection or by hotspot-focused studies that ignore potentially vast areas of CH_4 uptake ($-3.2 \pm 1.4 \text{ mgCH}_4/\text{m}^2/\text{d}$ in dry tundra and $-1.2 \pm 0.6 \text{ mgCH}_4/\text{m}^2/\text{d}$ in wet tundra) as reported for north-eastern Greenland by Jørgensen et al. (2015). Airborne measurements (Figure 8.6) also inherently include previously often neglected freshwater systems, which are estimated to contribute as much as $13 \text{ TgCH}_4/\text{y}$ north of 54°N (Bastviken et al., 2011).

Chang et al. (2014) used aircraft concentration data and inverse modeling to derive regional fluxes averaged across Alaska integrated to $2.1 \pm 0.5 \text{ TgCH}_4$ for the period May to September 2012. This value includes all biogenic, anthropogenic, and geological sources (e.g. seeps), which Walter Anthony et al. (2012) estimated to contribute $1.5\text{--}2 \text{ TgCH}_4/\text{y}$ alone, based on extrapolating ground-based measurements.

Chang et al. (2014) estimated a North Slope contribution of $7 \pm 2 \text{ mgCH}_4/\text{m}^2/\text{d}$ (0.2 TgCH_4 total for May–September). Using airborne eddy covariance, Kohnert et al. (2017) derived July median surface fluxes in the Mackenzie Delta of $26 \pm 8 \text{ mgCH}_4/\text{m}^2/\text{d}$ at a spatial resolution of 100 m. In northern Scandinavia, O’Shea et al. (2014) reported an aircraft derived regional CH_4 flux estimate of $29 \pm 12 \text{ mgCH}_4/\text{m}^2/\text{d}$ for a single day in July 2012.

8.4 Integration and projections

The hydrological cycle is an important connecting factor between the Arctic Ocean and the surrounding land. Freshwater systems integrate terrestrial processes, serve as reactive transport pathways, and provide locations for short- or long-term burial along the path from land to ocean (Cole et al., 2007; Battin et al., 2009; Vonk and Gustafsson, 2013). The freshwater carries sediments, nutrients, and organic matter, and has a relatively large influence on the adjacent ocean: despite holding only 1% of the global ocean volume, the Arctic Ocean receives approximately 10% of all river discharge. Combined, the eight largest Arctic rivers export an estimated $\sim 249 \text{ Tg}$ of sediment and $\sim 40 \text{ Tg}$ organic carbon to the Arctic Ocean each year (Holmes et al., 2002, 2012; McGuire et al., 2009). In addition, coastal erosion (Figure 8.7) is estimated to deliver 430 Tg sediment (Rachold et al., 2004) and $5\text{--}14 \text{ Tg}$ organic carbon per year (Rachold et al., 2004; Streletskaya et al., 2009; Vonk et al., 2012; Günther et al., 2013). Once these carbon flows arrive in the ocean they may be (further) degraded, released to the atmosphere (Anderson et al., 2009), or buried for long-term storage in sediments. All these processes may be influenced by climate change, altering the interaction between ocean and land.

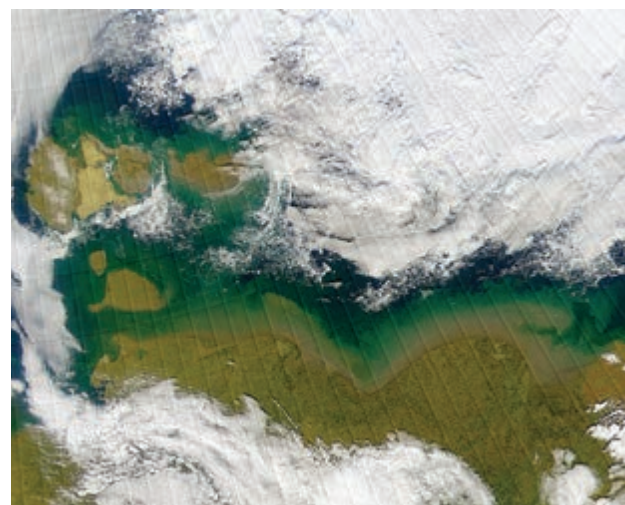


Figure 8.7 Satellite image showing very turbid waters along the East Siberian Coast where coastal erosion delivers large quantities of sediment to the shelf sea. Image acquired from the Sea-Viewing Wide Field-of-View Sensor (SeaWiFS) on-board GeoEye’s OrbView-2 satellite on 24 August 2000.

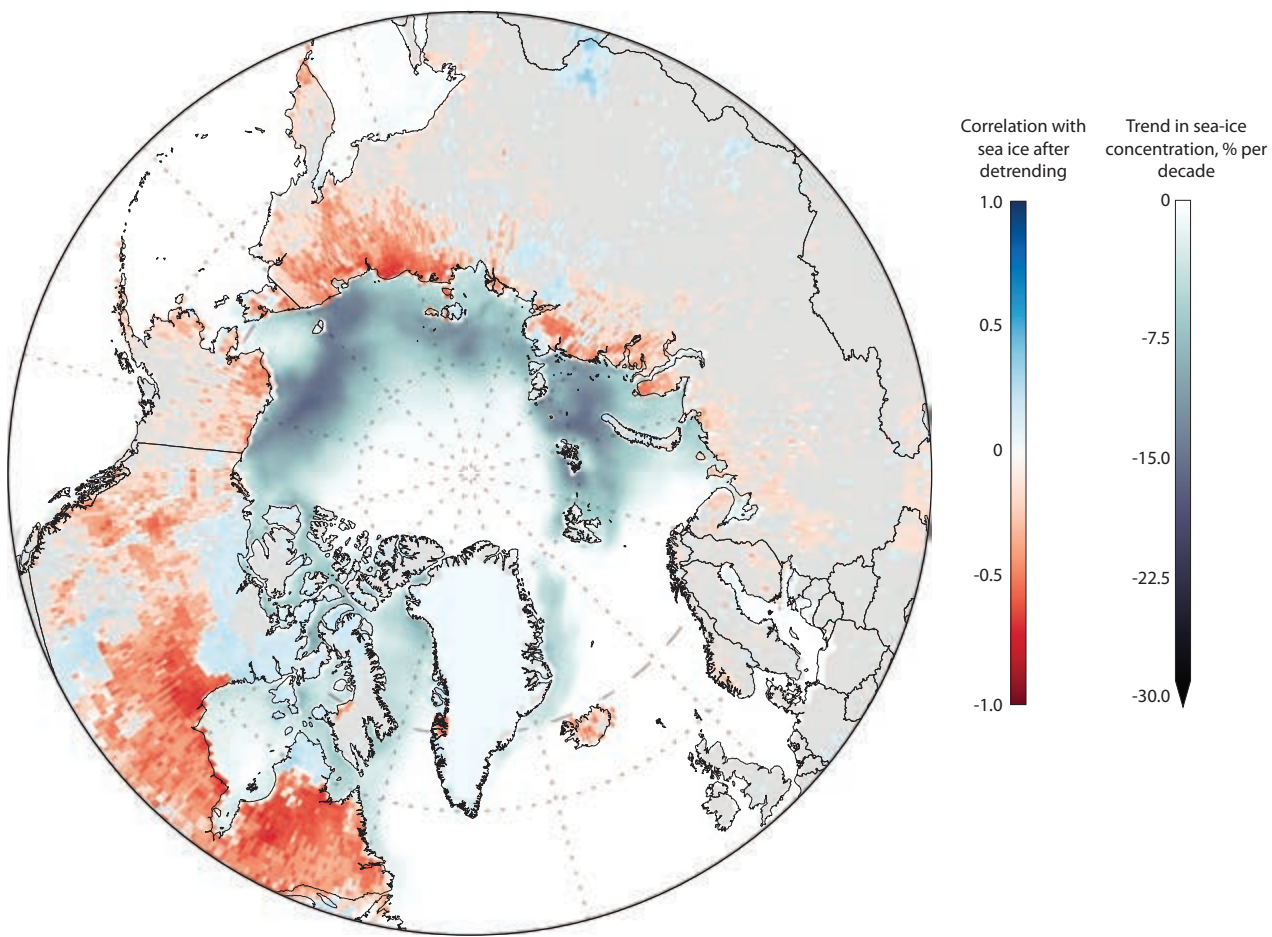


Figure 8.8 Correlation between terrestrial methane (CH_4) emissions and sea ice for May–October over the period 1981–2010. The color of each grid cell indicates the strength of the correlation between modeled CH_4 emissions and sea-ice concentration within a radius of 2000 km from the grid cell. The linear trend in sea-ice concentration is shown to indicate areas of high retreat (Parmentier et al., 2015).

In addition to the carbon flow from land to ocean, the ocean can itself affect carbon flow on land especially through the marked decline in sea ice over recent decades. The decline in sea ice has exposed more open ocean water and because this has a lower albedo, the result is increased absorption of solar radiation by the ocean (Pistone et al., 2014). This leads to higher air temperatures (Screen et al., 2012) and may increase precipitation on land (Bintanja and Selten, 2014) – both of which strongly influence the terrestrial carbon cycle. Some studies have also linked sea-ice decline to enhanced circumpolar vegetation growth and CH_4 emissions (Bhatt et al., 2014; Parmentier et al., 2015; Figure 8.8). Long time series over decades are required to separate such connections from internal climate variations (Bhatt et al., 2013).

8.4.1 Projections for change and its possible radiative impact

A better understanding of permafrost dynamics is essential to resolve the interplay between land and ocean of relevance to future changes in the Arctic carbon cycle. Although permafrost underlies about three-quarters of the area draining into the Arctic Ocean the hydrology of this complex environment, especially under global warming is poorly understood. The interplay between permafrost and the hydrological cycle will significantly affect the lateral flows of carbon within the Arctic,

and ultimately the flux to the atmosphere. For example, a deepening of the active layer and melting of ice wedge polygons may increase the drainage of water, and thus increase runoff (Liljedahl et al., 2016). Alternatively, soil subsidence due to permafrost thaw may create new depressions in the landscape, increasing wetness (Nauta et al., 2015). Trends continuing from present-day warming can be informative about future change. Throughout the permafrost zone, lakes are expanding in some areas and diminishing in others (Smith et al., 2005; Walter et al., 2006; Jones et al., 2011). These differences are probably related to varying stages of permafrost degradation, the drainage capacity of the landscape, and associated changes in hydrology. Overall, however, permafrost thaw increases hydrological connectivity within landscapes, which leads to increased groundwater input and winter base flow (Walvoord and Striegl, 2007; Bense et al., 2009; Liljedahl et al., 2016). Research has shown that Arctic rivers have discharged more water into the ocean, both in Eurasia (Peterson et al., 2002) and North America (Déry et al., 2009).

Changes in the Arctic hydrological cycle are likely to affect the transport of organic matter and sediments from land to ocean. The presence or absence of water, snow and ice play an important role in determining the rate of carbon release from thawing permafrost. However, it is unclear whether climate change is more likely to increase or decrease the net organic carbon export from the Arctic Ocean watershed. This is partly

due to the lack of long time series (Holmes et al., 2012), but also to the region- and landscape-specific responses of organic carbon export to permafrost thaw (Tank et al., 2012b). For example, the Yukon River showed a 40% decrease in discharge-normalized DOC export from 1978 to 2003 – probably due to increasing hydrological flow path lengths that allow for a higher degree of organic carbon processing in soils prior to aquatic release (Striegl et al., 2005). On the other hand, DOC concentrations are significantly higher in permafrost-free watersheds than permafrost-dominated watersheds in western Siberian peatlands (Frey et al., 2007) and in small watersheds in interior Alaska (MacLean et al., 1999), suggesting that DOC export will increase when permafrost thaws. The degradation potential of organic carbon released from thawing permafrost is also important: carbon released during river base flow in winter is more labile than summer carbon fluxes (Wickland et al., 2012) and old-permafrost carbon is more labile than surface-soil carbon (Vonk et al., 2013; Abbott et al., 2014). The fluxes of both types of labile carbon are likely to increase under a warming climate, potentially leading to increased conversion of organic carbon in the aquatic environment to greenhouse gases. On the other hand, thermokarst lakes formed through permafrost thaw can evolve from being net emitters of greenhouse gases to sites of long-term carbon sequestration, converting these lake basins to net carbon sinks (Walter Anthony et al., 2014).

The increased growth in terrestrial plants that has been associated with sea-ice decline (Bhatt et al., 2010) suggests an increase in CO₂ uptake by tundra. But because respiration releases CO₂ and because this process is also temperature dependent, it could compensate (partly or even completely) for the enhanced plant growth. For example, a 20-year warming study in Alaska showed that while plant productivity and soil litter input increased, this was offset by greater soil respiration (Sistla et al., 2013). As a result, although the amount of carbon stored in above-ground biomass rose, the net carbon balance in the soil was near zero.

A connection between warming from sea-ice decline and changes in terrestrial greenhouse gas exchange appears likely, although the magnitude of this impact is unclear (Parmentier et al., 2013) due to various complicating factors. A change in the vegetation structure of tundra, for example, can have a large impact on the underlying permafrost. Locally, shrubs shield the ground from solar radiation, effectively cooling the ground (Blok et al., 2010). An expansion of shrubs could therefore counteract permafrost thaw. However, the reverse is also true: the removal of shrubs leads to permafrost collapse, wetter conditions and an increase in CH₄ emissions (Nauta et al., 2015). The way in which Arctic shrubs respond to sea-ice decline and associated warming is thus of high importance to the stability of permafrost soils. Another important control on the stability of permafrost soils is snow depth. A thick snow pack in winter insulates the ground from the lowest temperatures, effectively raising annual ground temperature. A simple snow manipulation experiment in subarctic Sweden showed that a doubling of snow depth led to permafrost degradation and vegetation change in just a few years (Johansson et al., 2013). Because sea-ice decline is expected to result in higher air temperatures, as well as higher precipitation (Bintanja and Selten, 2014), it is important to assess how these climatic changes lead to a change in vegetation structure, snow distribution and ultimately permafrost stability.

Moreover, the highest temperature increases related to sea-ice decline occur in autumn, when photosynthesis has ceased but soil respiration and CH₄ emissions are still occurring. Sea-ice decline may therefore lead to a greater release of greenhouse gases at that time of year. Although model simulations indicate that sea-ice decline forced an increase in CH₄ emissions (Parmentier et al., 2015), empirical verification of this in the field is not possible due to a lack of observations. More directly, the declining sea ice results in greater coastal erosion due to the combined effect of warmer air and water temperatures, and increasing storm, wave and tidal activity (Jones et al., 2009; Günther et al., 2015). This shows the effects of sea-ice decline on the Arctic carbon cycle can be direct, indirect and can act on many different processes.

8.4.2 Modeling the integrated Arctic terrestrial and marine system

Despite the many connections outlined here as well as their potential for change, Earth System Models (ESMs) tend to address terrestrial and marine systems separately (Anav et al., 2013) – even though it has long been known that riverine carbon input can have a significant impact on the marine system (Aumont et al., 2001). This input may be especially significant for the Arctic Ocean with its relatively large riverine inflow. However, accurate simulation of small-scale coastal processes is often complicated by the low resolution (i.e. large grid cell size) of these models. ESMs also tend to vary widely in their representation of permafrost (Koven et al., 2013) and this indicates they still need considerable improvement before being able to simulate the full dynamics of the Arctic carbon cycle reliably, including land-ocean transport.

Although studies using ESMs do tend to acknowledge the warming impact of sea-ice decline on the terrestrial environment, they often omit the additional step of examining the consequences for the terrestrial carbon cycle (Lawrence et al., 2008; Screen et al., 2012) – despite the many connections and potential for change as outlined in this chapter. Moreover, simulating sea-ice decline at the same high rate as has been observed remains difficult, despite recent model improvement (Wang and Overland, 2012). Nevertheless, ESMs may be useful tools to test the response of terrestrial ecosystems to different future sea ice scenarios.

Regional models may be more effective at representing interactions between ocean and land. For example, coupling DOC export from a terrestrial biosphere model to an ocean model, enables these two parts of the carbon cycle to interact. Indeed, a modeling effort focused on the Arctic Basin showed that changes in DOC become significant at the decadal scale (McGuire et al., 2010). However, lateral transport of river POC, as well as lateral release of DOC and POC from increasingly frequent pulse disturbances (Schuur et al., 2015) are currently not included in any ESMs or regional models. In their absence, current terrestrial biosphere models can be useful tools to identify the distant links to sea-ice decline. A comparison of three biogeochemical models showed CH₄ emissions and sea-ice decline to co-vary across large parts of the Arctic (see Figure 8.8). As a result, 2005–2010 emissions were 1.7 TgCH₄/y higher than in the 1980s (Parmentier et al., 2015). In this case, the warming effect of sea-ice decline was not modeled directly,

but implied through the reanalysis products used as input to the models. Such analyses can be valuable to identify whether these links exist, and by what magnitude amplified warming induced by sea-ice decline has increased CH₄ emissions or altered CO₂ exchange. Changes in terrestrial ecosystems may also affect sea-ice decline – at least in the long term. A recent study showed that under a doubling of atmospheric CO₂ concentrations, the expansion of vegetation predicted in the Arctic leads to a lower albedo, in turn leading to additional atmospheric warming, and ultimately more sea-ice decline (Jeong et al., 2014).

These regional modeling studies show that sea ice, the atmosphere and the adjacent land area are strongly connected and should not be considered in isolation. Development of ESMs should therefore include a focus on improving the connections between ocean and land, primarily in the representation of lateral fluxes. To achieve this, representation of permafrost environments must be improved such that the changes in hydrology following permafrost thaw and their effect on organic carbon export can be accurately predicted. Carbon flows from land to sea should not remain a fixed boundary condition but should be considered dynamically in light of the dramatic changes expected in the Arctic environment under continued warming.

8.5 Conclusions and recommendations

Direct connections have been documented between sea-ice dynamics and carbon cycling related processes in marine ecosystems and on land. Projections suggest further sea-ice decline may accelerate changes in carbon cycling dynamics at sea and on land. Greater emphasis is needed on studies that connect sea ice decline and the carbon cycle, and the prognostic modelling of these connections.

Recent studies show non-growing season processes strongly influence Arctic carbon cycling. In fact, wintertime CH₄ emissions may even exceed summer emissions. Further support is needed for the development of infrastructure to facilitate field research and monitoring during winter, and so improve the modeling of wintertime impacts.

Sea ice formation and melt processes have been shown to affect CO₂ transport into the ocean as well as pH conditions in surface waters. Many of these processes have only recently been documented. Support is needed for experimental work on these issues under controlled conditions and in the field.

Increased discharge and a shift from surface-water to groundwater-dominated systems within the Arctic are having major impacts on the hydrological cycle. These changes in the hydrological cycle are influencing organic matter and sediment transport, with large regional differences. Support is needed for the field monitoring necessary to continue building long time series, with increasing emphasis given to regional variation.

Physical soil pressure related processes have an impact on gas releases from permafrost soils and can affect the seasonal dynamics and scale of CH₄ emissions from terrestrial environments. These findings may help explain hitherto unexplained atmospheric dynamics of CH₄. Support is needed for experimental work on these issues under controlled conditions and in the field.

References

Abbott, B.W., J.R. Larouche, J.B. Jones, W.B. Bowden and A.W. Balser, 2014. Elevated dissolved organic carbon biodegradability from thawing and collapsing permafrost, *Journal of Geophysical Research: Biogeosciences*, 119:2049-2063.

Abbott, B.W., J.B. Jones, E.A.G. Schuur, F.S. Chapin III, W.B. Bowden, et al., 2016. Biomass offsets little or none of permafrost carbon release from soils, streams, and wildfire: an expert assessment. *Environmental Research Letters*, 11:034014, doi:10.1088/1748-9326/11/3/034014.

ACIA, 2005. *Arctic Climate Impact Assessment*. Cambridge University Press.

Alling, V., L. Sanchez-Garcia, D. Porcelli, S. Pugach, J.E. Vonk, B. van Dongen, C.-M. Mörth, L.G. Anderson, A. Sokolov, P. Andersson, C. Humborg, I. Semiletov and Ö. Gustafsson, 2010. Nonconservative behavior of dissolved organic carbon across the Laptev and East Siberian seas. *Global Biogeochemical Cycles*, 24:GB4033, doi:10.1029/2010GB003834.

Anav, A., P. Friedlingstein, M. Kidston, L. Bopp, P. Ciais, P. Cox, C. Jones, M. Jung, R. Myneni and Z. Zhu, 2013. Evaluating the land and ocean components of the global carbon cycle in the CMIP5 Earth System Models. *Journal of Climate*, 26:6801-6843.

Anderson, L.G., S. Jutterström, S. Hjalmarsson, I. Wählström and I.P. Semiletov, 2009. Out-gassing of CO₂ from Siberian Shelf seas by terrestrial organic matter decomposition. *Geophysical Research Letters*, 36:L20601, doi:10.1029/2009GL040046.

Arrigo, K.R. and G.L. van Dijken, 2011. Secular trends in Arctic Ocean net primary production. *Journal of Geophysical Research*, 116:C09011, doi:10.1029/2011JC007151.

Arrigo, K.R., S. Pabi, G.L. van Dijken and W. Maslowski, 2010. Air-sea flux of CO₂ in the Arctic Ocean, 1998–2003. *Journal of Geophysical Research*, 115:G04024, doi:10.1029/2009JG001224.

Arrigo, K.R., D.K. Perovich, R.S. Pickart, G.L. van Dijken, K.E. Lowry, M.M. Mills, M.A. Palmer, W.M. Balch, F. Bahr, N.R. Bates, C. Benitez-Nelson, B. Bowler, E. Brownlee, J.K. Ehn, K.E. Frey, R. Garley, S.R. Laney, L. Lubelczyk, J. Mathis, A. Matsuoka, B.G. Mitchell, G.W. Moore, E. Ortega-Retuerta, S. Pal, C.M. Polashenski, R.A. Reynolds, B. Schieber, H.M. Sosik, M. Stephens and J.H. Swift, 2012. Massive phytoplankton blooms under Arctic sea ice. *Science*, 15:336(6087):1408, doi:10.1126/science.

Asplin, M.G., R. Scharien, B. Else, S. Howell, D.G. Barber, T. Papakyriakou and S. Prinsenberg, 2014. Implications of fractured Arctic perennial ice cover on thermodynamic and dynamic sea ice processes. *Journal of Geophysical Research: Oceans*, 119:2327-2343.

Assmy, P., J.K. Ehn, M. Fernández-Méndez, H. Hop, C. Katlein, A. Sundfjord, K. Bluhm, M. Daase, A. Engel, A. Fransson, M.A. Granskog, S.R. Hudson, S. Kristiansen, M. Nicolaus, I. Peeken, A.H.H. Renner, G. Spreen, A. Tatarék and J. Wiktor, 2013. Floating ice-algal aggregates below melting Arctic sea ice. *PLoS ONE* 8, (10):e76599.

Attard, K.M., R.N. Glud, D.F. McGinnis and S. Rysgaard, 2014. Seasonal rates of benthic primary production in a Greenlandic fjord measured by aquatic eddy-correlation. *Limnology and Oceanography*, 59:1555-1569.

Attard, K.M., K. Hancke, M.K. Sejr and R.N. Glud, 2016. Benthic primary production and mineralization in a high Arctic fjord: in situ assessments by aquatic eddy covariance. *Marine Ecology Progress Series*, 554:35-50.

Aumont, O., J.C. Orr, P. Monfray, W. Ludwig, P. Amiotte Suchet and J.L. Probst, 2001. Riverine-driven interhemispheric transport of carbon. *Global Biogeochemical Cycles*, 15:393-405.

Barber, D.G., H. Hop, C.J. Mundy, B. Else, I. Dmitrenko, J.-E. Tremblay, J.K. Ehn, P. Assmy, M. Daase, L. Candlish and S. Rysgaard, 2015. Selected physical, biological and biogeochemical implications of a rapidly changing Arctic Marginal Ice Zone. *Progress in Oceanography*, 139:122-150.

Bastviken, D., L.J. Tranvik, J.A. Downing, P.M. Crill and A. Enrich-Prast, 2011. Freshwater methane emissions offset the continental carbon sink. *Science*, 331:50.

Battin, T.J., S. Luyssaert, L.A. Kaplan, A.K. Aufdenkampe, A. Richter and L.J. Tranvik, 2009. The boundless carbon cycle. *Nature Geoscience*, 2:598-600.

Bense, V.F., G. Ferguson and H. Kooi, 2009. Evolution of shallow groundwater flow systems in areas of degrading permafrost. *Geophysical Research Letters*, 36:L22401, doi:10.1029/2009GL039225.

Berchet, A., P. Bousquet, I. Pison, R. Locatelli, F. Chevallier, J.-D. Paris, E.J. Dlugokencky, T. Laurila, J. Hatakka, Y. Viisanen, D.E.J. Worthy, E. Nisbet, R. Fisher, J. France, D. Lowry, V. Ivakhov and O. Hermansen, 2016. Atmospheric constraints on the methane emissions from the East Siberian Shelf. *Atmospheric Chemistry and Physics*, 16:4147-4157.

Bhatt, U.S., D.A. Walker, M.K. Reynolds, J.C. Comiso, H.E. Epstein, G. Jia, R. Gens, J.E. Pinzon, C.J. Tucker, C.E. Tweedie and P.J. Webber, 2010. Circumpolar Arctic tundra vegetation change is linked to sea ice decline. *Earth Interactions*, 14: doi:10.1175/2010EI315.1.

Bhatt, U., D. Walker, M. Reynolds, P. Bieniek, H. Epstein, J. Comiso, J. Pinzon, C. Tucker and I. Polyakov, 2013. Recent declines in warming and vegetation greening trends over pan-Arctic tundra. *Remote Sensing*, 5:4229-4254.

Bhatt, U.S., D.A. Walker, J.E. Walsh, E.C. Carmack, K.E. Frey, W.N. Meier, S.E. Moore, F.-J.W. Parmentier, W. Post, V.E. Romanovsky and W.R. Simpson, 2014. Implications of Arctic sea ice decline for the Earth system. *Annual Review of Environment and Resources*, 39:57-89.

Bintanja, R. and F.M. Selten, 2014. Future increases in Arctic precipitation linked to local evaporation and sea-ice retreat. *Nature*, 509:479-482.

Blok, D., M.P.D. Heijmans, G. Schaeppman-Strub, A.V. Kononov, T.C. Maximov and F. Berendse, 2010. Shrub expansion may reduce summer permafrost thaw in Siberian tundra. *Global Change Biology*, 16:1296-1305.

Boetius, A., S. Albrecht, K. Bakker, C. Bienhold, J. Felsen, M. Fernández-Méndez, S. Hendricks, C. Kattlein, C. Lalande, T. Krumpen, M. Nicolaus, I. Peeken, B. Rabe, A. Rogacheva, E. Rybakova, R. Somavilla, F. Wenzhöfer and RV Polarstern ARK27-3-Shipboard Science Party, 2013. Export of algal biomass from melting Arctic sea-ice. *Science*, 339:1430-1432.

Bouttes, N., D. Paillard and D.M. Roche, 2010. Impact of brine-induced stratification on the glacial carbon cycle. *Climate of the Past*, 6:575-589.

Brown, J., O. Ferrians, J.A. Heginbottom and E. Melnikov, 2014. Circum-Arctic Map of Permafrost and Ground-Ice Conditions. National Snow and Ice Data Center, Boulder, Colorado, USA.

Butterworth, B.J. and S.D. Miller, 2016. Air-sea exchange of carbon dioxide in the Southern Ocean and Antarctic marginal ice zone. *Geophysical Research Letters*, 43:7223-7230.

Cai, W., L. Chen, B. Chen, Z. Gao, S.H. Lee, J. Chen, D. Pierrot, K. Sullivan, Y. Wang, X. Hu, W.-J. Huang, Y. Zhang, S. Xu, A. Murata, J.M. Grebmeier, E.P. Jones and H. Zhang, 2010. Decrease in the CO₂ uptake capacity in an ice-free Arctic Ocean basin. *Science*, 329:556-559.

Cai, W.-J., N.R. Bates, L. Guo, L.G. Anderson, J.T. Mathis, R. Wanninkhof, D.A. Hansell, L. Chen and I.P. Semiletov, 2014. Carbon fluxes across boundaries in the Pacific sector of the Arctic Ocean in a changing environment. In: The Pacific Arctic region: Ecosystem Status and Trends in a Rapidly Changing Environment. pp. 199-222. Springer.

Chang, R.Y.-W., C.E. Miller, S.J. Dinardo, A. Karion, C. Sweeney, B.C. Daube, J.M. Henderson, M.E. Mountain, J. Eluszkiewicz, J.B. Miller, L.M.P. Bruhwiler and S.C. Wofsy, 2014. Methane emissions from Alaska in 2012 from CARVE airborne observations. *Proceedings of the National Academy of Sciences of the United States of America*, 111:16694-16699.

Christensen, T.R., A. Joabsson, L. Ström, N. Panikov, M. Mastepanov, M. Öquist, B.H. Svensson, H. Nykänen, P. Martikainen and H. Oskarsson, 2003. Factors controlling large scale variations in methane emissions from wetlands. *Geophysical Research Letters*, 30:1414, doi: 10.1029/2002GL016848.

Cole, J.J., Prairie, Y.T., Caraco, N.F., McDowell, W.H., Tranvik, L.J., Striegl, R.G., Duarte, C.M., Kortelainen, P., Downing, J.A., Middelburg and J.J. Melack, 2007. Plumbing the global carbon cycle: integrating inland waters into the terrestrial carbon budget. *Ecosystems*, 10:172-185.

Cory, R.M., C.P. Ward, B.C. Crump and G.W. Kling, 2014. Sunlight controls water column processing of carbon in arctic fresh waters. *Science*, 345:925-928.

Crabeck, O., B. Delille, S. Rysgaard, D.N. Thomas, N.-X. Geilfus, B. Else and J.-L. Tison, 2014. First "in situ" determination of gas transport coefficients (DO₂, DN₂, DAr) from bulk gas concentration measurements (O₂, N₂, Ar) in natural sea ice. *Journal of Geophysical Research: Oceans*, 119:6655-6668.

Damm, E., E. Helmke, S. Thoms, U. Schauer, E. Nothig, K. Bakker and R.P. Kiene, 2010. Methane production in aerobic oligotrophic surface water in the central Arctic Ocean. *Biogeosciences*, 7:1099-1108.

Delille, B., B. Jourdain, A.V. Borges, J.-L. Tison and D. Delille, 2007. Biogas (CO₂, O₂, dimethylsulfide) dynamics in spring Antarctic fast ice. *Limnology and Oceanography*, 52:1367-1379.

Delille, B., M. Vancoppenolle, N.-X. Geilfus, B. Tilbrook, D. Lannuzel, V. Schoemann, S. Becquevert, G. Carnat, D. Delille, C. Lancelot, L. Chou, G.S. Dieckmann and J.-L. Tison, 2014. Southern Ocean CO₂ sink: The contribution of the sea ice. *Journal of Geophysical Research: Oceans*, 119:6340-6355.

Déry, S.J., M.A. Hernández Henríquez, J.E. Burford and E.F. Wood, 2009. Observational evidence of an intensifying hydrological cycle in northern Canada. *Geophysical Research Letters*, 36:L13402, doi:10.1029/2009GL038852.

Dorrepal, E., S. Toet, R.S.P. Van Logtestijn, E. Swart, M.J. Van de Weg, T.V. Callaghan and R. Aerts, 2009. Carbon respiration from subsurface peat accelerated by climate warming in the subarctic. *Nature*, 460:616-620.

Elberling, B., C. Nordström, L. Grøndahl, H. Søgaard, T. Friberg, T.R. Christensen, L. Ström, F. Marchand and I. Nijs, 2008. High-Arctic soil CO₂ and CH₄ production controlled by temperature, water, freezing and snow. In: Meltofte, H., T.R. Christensen, M.C. Forchhammer and M. Rasch (eds.), *High-Arctic Ecosystem Dynamics in a Changing Climate*, pp. 441-472. Academic Press.

Else, B.G.T., T.N. Papakyriakou, R.J. Galley, W.M. Drennan, L.A. Miller and H. Thomas, 2011. Wintertime CO₂ fluxes in an Arctic polynya using eddy covariance: Evidence for enhanced air-sea gas transfer during ice formation. *Journal of Geophysical Research*, 116:C00G03, doi:10.1029/2010JC006760.

Else, B.G.T., R.J. Galley, B. Lansard, D.G. Barber, K. Brown, L.A. Miller, A. Mucci, T.N. Papakyriakou, J.É. Tremblay and S. Rysgaard, 2013. Further observations of a decreasing atmospheric CO₂ uptake capacity in the Canada Basin (Arctic Ocean) due to sea ice loss. *Geophysical Research Letters*, 40:1132-1137.

Ericson, Y., A. Ulfso, S. van Heuven, G. Kattner and L.G. Anderson, 2014. Increasing carbon inventory of the intermediate layers of the Arctic Ocean. *Journal of Geophysical Research: Oceans*, 119:2312-2326.

Fernández-Méndez, M., F. Wenzhöfer, I. Peeken, H.L. Sørensen, R.N. Glud and A. Boetius, 2014. Composition, buoyancy regulation and fate of ice algal aggregates in the Central Arctic Ocean. *PLoS ONE*, 9(9): e107452.

Fransson, A., M. Chierici, L.A. Miller, G. Carnat, E. Shadwick, H. Thomas, S. Pineault and T.N. Papakyriakou, 2013. Impact of sea-ice processes on the carbonate system and ocean acidification at the ice-water interface of the Amundsen Gulf, Arctic Ocean. *Journal of Geophysical Research: Oceans*, 118:7001-7023.

Frey, K.E., D.I. Siegel and L.C. Smith, 2007. Geochemistry of west Siberian streams and their potential response to permafrost degradation. *Water Resources Research*, 43:W03406, doi:10.1029/2006WR004902.

Gattuso, J.P., B. Gentili, C.M. Duarte, J.A. Kleypas, J.J. Middelburg and D. Antoinne, 2006. Light availability in the coastal ocean: Impact on the distribution of benthic photosynthetic organisms and their contribution to primary production. *Biogeosciences*, 3:489-513.

Geilfus, N.-X., G. Carnat, G.S. Dieckmann, N. Halden, G. Nehrke, T. Papakyriakou, J.-L. Tison and B. Delille, 2013. First estimates of the contribution of CaCO₃ precipitation to the release of CO₂ to the atmosphere during young sea ice growth. *Journal of Geophysical Research: Oceans*, 118:244-255.

Glud, R.N., M. Kühl, F. Wenzhöfer and S. Rysgaard, 2002. Benthic diatoms of a high Arctic fjord (Young Sound, NE Greenland): Importance for ecosystem primary production. *Marine-Ecology Progress Series*, 238:15-29.

Glud, R.N., J. Wöbel, U. Karsten, M. Kühl and S. Rysgaard, 2009. Benthic microalgal production in the Arctic: applied methods and status of the current database. *Botanica Marina*, 52:559-571.

Glud, R.N., S. Rysgaard, G. Turner, D.F. McGinnis and R.J.G. Leaky, 2014. Biological and physical induced oxygen dynamics in melting sea ice of the Fram Strait. *Limnology and Oceanography*, 59:1097-1111.

Golden, K.M., S.F. Ackley and V.I. Lytle, 1998. The percolation phase transition in sea ice. *Science*, 282:2238-2241.

Grosje, G., J. Harden, M. Turetsky, A.D. McGuire, P. Camill, C. Tarnocai, S. Frolking, E.A.G. Schuur, T. Jorgenson, S. Marchenko, V. Romanovsky, K.P. Wickland, N. French, M. Waldrop, L. Bourgeau Chavez and R.G. Striegl, 2011. Vulnerability of high latitude soil organic carbon in North America to disturbance. *Journal of Geophysical Research*, 116:G00K06, doi:10.1029/2010JG001507.

Günther, F., P.P. Overduin, A.V. Sandakov, G. Grosje and M.N. Grigoriev, 2013. Short- and long-term thermo-erosion of ice-rich permafrost coasts in the Laptev Sea region. *Biogeosciences*, 10:4297-4318.

Günther, F., P.P. Overduin, I.A. Yakshina, T. Opel, A.V. Baranskaya and M.N. Grigoriev, 2015. Observing Muostakh disappear: permafrost thaw subsidence and erosion of a ground-ice-rich island in response to arctic summer warming and sea ice reduction. *The Cryosphere*, 9:151-178.

Hare, A., F. Wang, R. Galley, N.-X. Geilfus, D. Barber and S. Rysgaard, 2013. pH evolution in sea ice grown at an outdoor experimental facility. *Marine Chemistry*, 154:46-64.

He, X., L. Sun, Z. Xie, W. Huang, N. Long and G. Xing, 2013. Sea ice in the Arctic Ocean: Role of shielding and consumption of methane. *Atmospheric Environment*, 67:8-13.

Holmes, R.M., J.W. McClelland, B.J. Peterson, I.A. Shiklomanov, A.I. Shiklomanov, A.V. Zhulidov, V.V. Gordeev and N.N. Bobrovitskaya, 2002. A circumpolar perspective on fluvial sediment flux to the Arctic ocean. *Global Biogeochemical Cycles*, 16:45-1-45-14.

Holmes, R.M., M.T. Coe, G.J. Fiske, T. Gurtovaya, J.W. McClelland, A.I. Shiklomanov, R.G.M. Spencer, S.E. Tank and A.V. Zhulidov, 2012. *Climate Change Impacts on the Hydrology and Biogeochemistry of Arctic Rivers*. Wiley & Sons.

Hugelius, G., C. Tarnocai, G. Broll, J.G. Canadell, P. Kuhry and D.K. Swanson, 2013. The northern circumpolar soil carbon database: spatially distributed datasets of soil coverage and soil carbon storage in the northern permafrost regions. *Earth System Science Data*, 5:3-13.

Hugelius, G., J. Strauss, S. Zubrzycki, J.W. Harden, E.A.G. Schuur, C.L. Ping, L. Schirrmeyer, G. Grosse, G.J. Michaelson, C.D. Koven, J.A. O'Donnell, B. Elberling, U. Mishra, P. Camill, Z. Yu, J. Palmtag and P. Kuhry, 2014. Estimated stocks of circumpolar permafrost carbon with quantified uncertainty ranges and identified data gaps. *Biogeosciences*, 11:6573-6593.

Ijima, Y., A.N. Fedorov, H. Park, K. Suzuki, H. Yabuki, T.C. Maximov and T. Ohata, 2010. Abrupt increases in soil temperatures following increased precipitation in a permafrost region, Central Lena River Basin, Russia. *Permafrost and Periglacial Processes*, 21:30-41.

Ijima, Y., T. Ohta, A. Kotani, A.N. Fedorov, Y. Kodama and T.C. Maximov, 2014. Sap flow changes in relation to permafrost degradation under increasing precipitation in an eastern Siberian larch forest. *Ecohydrology*, 7:177-187.

Jeansson, E., A. Olsen, T. Eldevik, I. Skjelvan, A.M. Omar, S.K. Lauvset, J.E.Ø. Nilsen, R.G.J. Bellerby, T. Johannessen and E. Falck, 2011. The Nordic Seas carbon budget: Sources, sinks, and uncertainties. *Global Biogeochemical Cycles*, 25:GB4010, doi:10.1029/2010GB003961.

Jeong, J.-H., J.-S. Kug, H.W. Linderholm, D. Chen, B.-M. Kim and S.-Y. Jun, 2014. Intensified Arctic warming under greenhouse warming by vegetation-atmosphere-sea ice interaction. *Environmental Research Letters*, 9:094007, doi:10.1088/1748-9326/9/9/094007.

Johansson, M., T.V. Callaghan, J. Bosiö, H.J. Åkerman, M. Jackowicz-Korczyński and T.R. Christensen, 2013. Rapid responses of permafrost and vegetation to experimentally increased snow cover in sub-arctic Sweden. *Environmental Research Letters*, 8:035025, doi:10.1088/1748-9326/8/3/035025.

Jones, B.M., C.D. Arp, M.T. Jorgenson, K.M. Hinkel, J.A. Schmutz and P.L. Flint, 2009. Increase in the rate and uniformity of coastline erosion in Arctic Alaska. *Geophysical Research Letters*, 36:L03503, doi:10.1029/2008GL036205.

Jones, E.M., D.C.E. Bakker, H.J. Venables, M.J. Whitehouse, R.E. Korb and J. Watson, 2010. Rapid changes in surface water carbonate chemistry during Antarctic sea ice melt. *Tellus*, 62B:621-635.

Jones, B.M., G. Grosse, C.D. Arp, M.C. Jones, K.M. Walter Anthony and V.E. Romanovsky, 2011. Modern thermokarst lake dynamics in the continuous permafrost zone, northern Seward Peninsula, Alaska. *Journal of Geophysical Research*, 116:G00M03, doi:10.1029/2011JG001666.

Jorgenson, M.T., Y.L. Shur and E.R. Pullman, 2006. Abrupt increase in permafrost degradation in arctic Alaska. *Geophysical Research Letters*, 33:L02503, doi:10.1029/2005GL024960.

Juncher Jørgensen, C., K.M. Lund Johannsen, A. Westergaard-Nielsen and B. Elberling, 2015. Net regional methane sink in High Arctic soils of northeast Greenland. *Nature Geoscience*, 8:20-23.

Jutterström, S., L.G. Anderson, N.R. Bates, R. Bellerby, T. Johannessen, E.P. Jones, R.M. Key, X. Lin, A. Olsen and A.M. Omar, 2010. Arctic Ocean data in CARINA. *Earth System Science Data*, 2:71-78.

Kaiser, C., H. Meyer, C. Biasi, O. Rusalimova, P. Barsukov and A. Richter, 2007. Conservation of soil organic matter through cryoturbation in arctic soils in Siberia. *Journal of Geophysical Research*, 112:G02017, doi:10.1029/2006JG000258.

Karlsson, J. and G. Svensson, 2013. Consequences of poor representation of Arctic sea-ice albedo and cloud-radiation interactions in the CMIP5 model ensemble. *Geophysical Research Letters*, 40:4374-4379.

Key, R.M., T. Tanhua, A. Olsen, M. Hoppema, S. Jutterström, C. Schirnick, S. Van Heuven, A. Kozyr, X. Lin, A. Velo, D.W.R. Wallace and L. Mintrop, 2010. The CARINA data synthesis project: Introduction and overview. *Earth System Science Data*, 2:105-121.

Kirschke, S., P. Bousquet, P. Ciais, M. Saunois, J.G. Canadell, E.J. Dlugokencky, et al., 2013. Three decades of global methane sources and sinks. *Nature Geoscience*, 6:813-823.

Kivimäe, C., R.J. Bellerby, A. Fransson, M. Reigstad and T. Johannessen, 2010. A carbon budget for the Barents Sea. *Deep-Sea Research*, 57:1532-1542.

Klapstein, S.J., M.R. Turetsky, A.D. McGuire, J.W. Harden, C.I. Czimczik, X. Xu, J.P. Chanton and J.M. Waddington, 2014. Controls on methane released through ebullition in peatlands affected by permafrost degradation. *Journal of Geophysical Research: Biogeosciences*, 119:418-431.

Kohnert, K., A. Serafimovich, S. Metzger, J. Hartmann and T. Sachs, 2017. Strong geologic methane emissions from discontinuous terrestrial permafrost in the Mackenzie Delta, Canada. *Scientific Reports*, 7:5828, doi:10.1038/s41598-017-05783-2.

Kort, E.A., S.C. Wofsy, B.C. Daube, M. Diao, J.W. Elkins, R.S. Gao, E.J. Hintsa, D.F. Hurst, R. Jimenez, F.L. Moore, J.R. Spackman and M.A. Zondlo, 2012. Atmospheric observations of Arctic Ocean methane emissions up to 82° north. *Nature Geoscience*, 5:318-321.

Koven, C., P. Friedlingstein, P. Ciais, D. Kholostyanov, G. Krinner and C. Tarnocai, 2009. On the formation of high-latitude soil carbon stocks: Effects of cryoturbation and insulation by organic matter in a land surface model. *Geophysical Research Letters*, 36:L21501, doi:10.1029/2009GL040150.

Koven, C.D., W.J. Riley and A. Stern, 2013. Analysis of permafrost thermal dynamics and response to climate change in the CMIP5 Earth System Models. *Journal of Climate*, 26:1877-1900.

Krause-Jensen, D., M. Kuhl, P.B. Christensen and J. Borum, 2007. Carbon cycling in Arctic marine ecosystems: Case study Young Sound. *Meddelser om Grönland*, Bioscience, 58:159-175.

Lawrence, D.M., A.G. Slater, R.A. Tomas, M.M. Holland and C. Deser, 2008. Accelerated Arctic land warming and permafrost degradation during rapid sea ice loss. *Geophysical Research Letters*, 35:L11506, doi:10.1029/2008GL033985.

Lawson, E.C., J.L. Wadham, M. Tranter, M. Stibal, G.P. Lis, C.E.H. Butler, J. Laybourn-Parry, P. Nienow, D. Chandler and P. Dewsbury, 2014. Greenland Ice Sheet exports labile organic carbon to the Arctic oceans. *Biogeosciences*, 11:4015-4028.

Lee, S.H., D. Stockwell, H.-M. Joo, Y.B. Son, C.-K. Kang and T.E. Whittlett, 2012. Phytoplankton production from melting ponds on Arctic sea ice. *Journal of Geophysical Research*, 117:C04030, doi:10.1029/2011JC007717.

Liljedahl, A.K., J. Boike, R.P. Daanen, A.N. Fedorov, G.V. Frost, G. Grosse, L.D. Hinzman, Y. Iijima, J.C. Jorgenson, N. Matveyeva and M. Necsoiu, 2016. Pan-Arctic ice-wedge degradation in warming permafrost and its influence on tundra hydrology. *Nature Geoscience*, 9:312-318.

Loose, B., P. Schlosser, D. Perovich, D. Ringelberg, D. Ho, T. Takahashi, J. Richter-Menge, C. Reynolds, W. McGillis and J.-L. Tison, 2010. Gas diffusion through columnar laboratory sea ice: Implications for mixed layer ventilation of CO₂ in the seasonal sea ice zone. *Tellus B*, 63:23-39.

Loose, B., W.R. McGillis, D. Perovich, C.J. Zappa and P. Schlosser, 2014. A parameter model of gas exchange for the seasonal sea ice zone. *Ocean Science*, 10:17-28.

MacDonald, R.W., L.G. Anderson, J. Christensen, L.A. Miller, I.P. Semiletov and R. Stein, 2010. The Arctic Ocean. In: Liu, K.-K., L. Atkinson, R. Quinones and L. Talaue-McManus (eds.), *Carbon and Nutrient Fluxes in Continental Margins: A Global Synthesis*. pp. 289-303. Springer.

MacGilchrist, G.A., A.C.N. Garabato, T. Tsubouchi, S. Bacon, S. Torres-Valdés and K. Azetsu-Scott, 2014. The Arctic Ocean carbon sink. *Deep-Sea Research I*, 86:39-55.

MacLean, R., M.W. Oswood, J.G. Irons III and W.H. McDowell, 1999. The effect of permafrost on stream biogeochemistry: A case study of two streams in the Alaskan (U.S.A.) taiga. *Biogeochemistry*, 47:239-267.

Manizza, M., M.J. Follows, S. Dutkiewicz, D. Menemenlis, C.N. Hill and R.M. Key, 2013. Changes in the Arctic Ocean CO₂ sink (1996-2007): A regional model analysis. *Global Biogeochemical Cycles*, 27:1108-1118.

Mastepanov, M., C. Sigsgaard, E.J. Dlugokencky, S. Houweling, L. Strom, M.P. Tamstorf and T.R. Christensen, 2008. Large tundra methane burst during onset of freezing. *Nature*, 456:628-631.

Mastepanov, M., C. Sigsgaard, T. Tagesson, L. Ström, M. Tamstorf, M. Lund and T.R. Christensen, 2013. Revisiting factors controlling methane emissions from high-Arctic tundra. *Biogeosciences*, 10:5139-5158.

McGuire, D., L.G. Anderson, T.R. Christensen, S. Dallimore, L. Guo, D.J. Hayes, M. Heimann, T.D. Lorenson, R.W. Macdonald and N. Roulet, 2009. Sensitivity of the carbon cycle in the Arctic to climate change. *Ecological Monographs*, 79:523-555.

McGuire, A.D., D.J. Hayes, D.W. Kicklighter, M. Manizza, Q. Zhuang, M. Chen, M.J. Follows, K.R. Gurney, J.W. McClelland, J.M. Melillo, B.J. Peterson and R.G. Prinn, 2010. An analysis of the carbon balance of the Arctic Basin from 1997 to 2006. *Tellus B*, 62:455-474.

McGuire, A.D., T.R. Christensen, D. Hayes, A. Heroult, E. Euskirchen, Y. Yi, J.S. Kimball, C. Koven, P. Lafleur, P.A. Miller, W. Oechel, P. Peylin and M.

Williams, 2012. An assessment of the carbon balance of Arctic tundra: comparisons among observations, process models, and atmospheric inversions. *Biogeosciences*, 9:3185–3204.

Meire, L., S. Søgaard, J. Mortensen, F.J.R. Meysman, K. Soetaert, K. Arendt, T. Juul-Pedersen, M.E. Blicher and S. Rysgaard, 2015. Glacial meltwater and primary production as drivers for strong CO₂ uptake in fjord and coastal waters adjacent to the Greenland Ice Sheet. *Biogeosciences*, 12:2347–2363.

Miller, L.A., T.N. Papakyriakou, R.E. Collins, J.W. Deming, J.K. Ehn, R.W. Macdonald, A. Mucci, O. Owens, M. Raudsepp and N. Sutherland, 2011. Carbon dynamics in sea ice: A winter flux time series. *Journal of Geophysical Research*, 116:C02028, doi:10.1029/2009JC006058.

Morison, J., R. Kowk, C. Peralta-Ferriz, M. Alkire, I. Rigor, R. Anderson and M. Steele, 2012. Changing Arctic Ocean freshwater pathways. *Nature*, 481:66–70.

Natali, S., E.A.G. Schuur, E.E. Webb, C.E. Hicks Pries and K.G. Crummer, 2014. Permafrost degradation stimulates carbon loss from experimentally warmed tundra. *Ecology*, 95:602–608.

Nauta, A.L., M.M.P.D. Heijmans, D. Blok, J. Limpens, B. Elberling, A. Gallagher, B. Li, R.E. Petrov, T.C. Maximov, J. van Huissteden and F. Berendse, 2015. Permafrost collapse after shrub removal shifts tundra ecosystem to a methane source. *Nature Climate Change*, 5:67–70.

Nomura, D., H. Eicken, R. Gradinger and K. Shirasawa, 2010. Rapid physically driven inversion of the air-sea ice CO₂ flux in the seasonal landfast ice off Barrow, Alaska after onset surface melt. *Continental Shelf Research*, 30:1998–2004.

Nummelin, A., C. Li and L.H. Smedsrød, 2015. Response of Arctic Ocean stratification to changing river runoff in a column model. *Journal of Geophysical Research: Oceans*, 126:2655–2675.

Olefeldt, D., M.R. Turetsky, P.M. Crill and A.D. McGuire, 2013. Environmental and physical controls on northern terrestrial methane emissions across permafrost zones. *Global Change Biology*, 19:589–603.

Olsen, A., 2009. Nordic Seas total dissolved inorganic carbon data in CARINA. *Earth System Science Data*, 1:35–43.

Olsen, A., A.M. Omar, E. Jeansson, L.G. Anderson and R.G.J. Bellerby, 2010. Nordic seas transit time distributions and anthropogenic CO₂. *Journal of Geophysical Research*, 115:C05005, doi:10.1029/2009JC005488.

O'Shea, S.J., G. Allen, M.W. Gallagher, K. Bower, S.M. Illingworth, J.B.A. Muller, B.T. Jones, C.J. Percival, S.J.-B. Bauguitte, M. Cain, N. Warwick, A. Quiquet, U. Skiba, J. Drewer, K. Dinsmore, E.G. Nisbet, D. Lowry, R.E. Fisher, J.L. France, M. Aurela, A. Lohila, G. Hayman, C. George, D.B. Clark, A.J. Manning, A.D. Friend and J. Pyle, 2014. Methane and carbon dioxide fluxes and their regional scalability for the European Arctic wetlands during the MAMM project in summer 2012. *Atmospheric Chemistry and Physics*, 14:13159–13174.

Pabi, S., G.L. van Dijken and K.R. Arrigo, 2008. Primary production in the Arctic Ocean 1998–2006. *Journal of Geophysical Research*, 113:C08005.

Palmer, M.A., B.T. Saenz and K.R. Arrigo, 2014. Impacts of sea ice retreat, thinning and melt-pond proliferation on the summer phytoplankton bloom in the Chukchi Sea, Arctic Ocean. *Deep Sea Research II*, 105:85–104.

Parmentier F.J.W., T.R. Christensen, L.L. Sørensen, S. Rysgaard, A.D. McGuire, P.A. Miller and D.A. Walker, 2013. The impact of a lower sea-ice extent on Arctic greenhouse-gas exchange. *Nature Climate Change*, 3:195–202.

Parmentier, F.J.W., W. Zhang, Y. Mi, X. Zhu, J. Huissteden, D.J. Hayes, Q. Zhuang, T.R. Christensen and A. David McGuire, 2015. Rising methane emissions from northern wetlands associated with sea ice decline. *Geophysical Research Letters*, 42:7214–7222.

Pedersen, J.A., M.A. Simpson, J.G. Bockheim and K. Kumar, 2011. Characterization of soil organic carbon in drained thaw-lake basins of Arctic Alaska using NMR and FTIR photoacoustic spectroscopy. *Organic Geochemistry*, 42:947–954.

Peterson, B.J., R.M. Holmes, J.W. McClelland, C.J. Vörösmarty, R.B. Lammers, A.I. Shiklomanov, I.A. Shiklomanov and S. Rahmstorf, 2002. Increasing river discharge to the Arctic Ocean. *Science*, 298:2171–2173.

Petrescu, A.M.R., A. Lohila, J.-P. Tuovinen, D.D. Baldocchi, A.R. Desai, et al., 2015. The uncertain climate footprint of wetlands under human pressure. *Proceedings of the National Academy of Sciences*, 112:4594–4599.

Pirk, N., M.P. Tamstorf, M. Lund, M. Mastepanov, S.H. Pedersen, M.R. Mylius, F.-J.W. Parmentier, H.H. Christiansen and T.R. Christensen, 2016. Snowpack fluxes of methane and carbon dioxide from high Arctic tundra. *Journal of Geophysical Research: Biogeosciences*, 121:2886–2900.

Pistone, K., I. Eisenman and V. Ramanathan, 2014. Observational determination of albedo decrease caused by vanishing Arctic sea ice. *Proceedings of the National Academy of Sciences*, 111:9322–3326.

Plug, L.J., C. Walls and B.M. Scott, 2008. Tundra lake changes from 1978 to 2001 on the Tuktoyaktuk Peninsula, western Canadian Arctic. *Geophysical Research Letters*, 35:L03502, doi:10.1029/2007GL032303.

Rachold, V., H. Eicken, V.V. Gordeev, M.N. Grigoriev, H.W. Hubberten, A.P. Lisitzin, V.P. Shevchenko and L. Schirrmeyer, 2004. Modern terrigenous organic carbon input to the Arctic Ocean. In: *The Organic Carbon Cycle in the Arctic Ocean*, pp. 33–55. Springer.

Roach, J., B. Griffith, D. Verbyla and J. Jones, 2011. Mechanisms influencing changes in lake area in Alaskan boreal forest. *Global Change Biology*, 17:2567–2583.

Rutgers van der Loeff, M.M., N. Cassar, M. Nicolaus, B. Rabe and I. Stimac, 2014. The influence of sea ice cover on air-sea gas exchange estimated with radon-222 profiles. *Journal of Geophysical Research: Oceans*, 119:2735–2751.

Rysgaard, S., J. Bendtsen, L.T. Pedersen, H. Ramløv and R.N. Glud, 2009. Increased CO₂ uptake due to sea ice growth and decay in the Nordic Seas. *Journal of Geophysical Research*, 114:C09011, doi:10.1029/2008JC005088.

Rysgaard, S., J. Bendtsen, B. Delille, G. Dieckmann, R.N. Glud, H. Kennedy, J. Mortensen, S. Papadimitriou, D. Thomas and J.-L. Tison, 2011. Sea ice contribution to air-sea CO₂ exchange in the Arctic and Southern Oceans. *Tellus*, 63B:823–830.

Rysgaard, S., R.N. Glud, K. Lennert, M. Cooper, N. Halden, R. Leaky, F.C. Hawthorne and D. Barber, 2012. Ikaite crystals in melting sea ice leads to low pCO₂ levels and high pH in Arctic surface waters. *The Cryosphere*, 6:1–8.

Rysgaard, S., D. Søgaard, M. Cooper, M. Pucko, K. Lennert, T.N. Papakyriakou, F. Wang, N.X. Geilfus, R.N. Glud, J. Ehn, D. McGinnies, K. Attard, J. Siverts, J.W. Deming and D. Barber, 2013. Ikaite crystal distribution in Arctic winter sea ice and its implications for CO₂ system dynamics. *The Cryosphere*, 7:1–12.

Schädel, C., E.A.G. Schuur, R. Bracho, B. Elberling, C. Knoblauch, H. Lee, Y. Luo, G.R. Shaver and M. Turetsky, 2014. Circumpolar assessment of permafrost C quality and its vulnerability over time using long-term incubation data. *Global Change Biology*, 20:641–652.

Schirrmeyer, L., V. Kunitsky, G. Grosse, S. Wetterich, H. Meyer, G. Schwamborn, O. Babiy, A. Derevyagin and C. Siegert, 2010. Sedimentary characteristics and origin of the Late Pleistocene Ice Complex on northeast Siberian Arctic coastal lowlands and islands. A review. *Quaternary International*, 241:3–25.

Schirrmeyer, L., G. Grosse, S. Wetterich, P.P. Overduin, J. Strauss, E.A.G. Schuur and H.W. Hubberten, 2011. Fossil organic matter characteristics in permafrost deposits of the northeast Siberian Arctic. *Journal of Geophysical Research*, 116:G00M02, doi:10.1029/2011JG001647.

Schuster, U., G.A. McKinley, N. Bates, F. Chevallier, S.C. Doney, A.R. Fay, M. González-Dávila, N. Gruber, S. Jones, J. Krijnen, P. Landschützer, N. Lefèvre, M. Manizza, J. Mathis, N. Metzl, A. Olsen, A.F. Rios, C. Rödenbeck, J.M. Santana-Casiano, T. Takahashi, R. Wanninkhof and A.J. Watson, 2013. An assessment of the Atlantic and Arctic sea-air CO₂ fluxes, 1990–2009. *Biogeosciences*, 10:607–627.

Schuur, E.A.G., J. Bockheim, J.G. Canadell, E. Euskirchen, C.B. Field, S.V. Goryachkin, S. Hagemann, P. Kuhry, P.M. Lafleur, H. Lee, G. Mazhitova, F.E. Nelson, A. Rinke, V.E. Romanovsky, N. Shiklomanov, C. Tarnocai, S. Venevsky, J.G. Vogel and S.A. Zimov, 2008. Vulnerability of permafrost carbon to climate change: Implications for the global carbon cycle. *BioScience*, 58:701–714.

Schuur, E.A.G., B.W. Abbott, W.B. Bowden, V. Brovkin, P. Camill, et al., 2013. Expert assessment of vulnerability of permafrost carbon to climate change. *Climatic Change*, 119:359–374.

Schuur, E.A.G., A.D. McGuire, C. Schädel, G. Grosse, J.W. Harden, D.J. Hayes, G. Hugelius, C.D. Koven, P. Kuhry, D.M. Lawrence, S.M. Natali, D. Olefeldt, V.E. Romanovsky, K. Schaefer, M.R. Turetsky, C.C. Treat and J.E. Vonk, 2015. Climate change and the permafrost carbon feedback. *Nature*, 520:171–179.

Screen, J.A., C. Deser and I. Simmonds, 2012. Local and remote controls on observed Arctic warming. *Geophysical Research Letters*, 39:L10709, doi:10.1029/2012GL051598.

Shadwick, E.H., A.H. Thomas, Y. Gratton, D. Leong, S.A. Moore, T. Papakyriakou and A.E.F. Prowe, 2011. Export of Pacific carbon through the Arctic Archipelago to the North Atlantic. *Continental Shelf Research*, 31:806–816.

Shakhova, N., I. Semiletov, A. Salyuk, V. Yusupov, D. Kosmach and Ö. Gustafsson, 2010. Extensive methane venting to the atmosphere from sediments of the East Siberian Arctic Shelf. *Science*, 327:1246.

Shirakova, L.S., O.S. Pokrovsky, S.N. Kirpotin, C. Desmukh, B.G. Pokrovsky, S. Audry and J. Viers, 2013. Biogeochemistry of organic carbon, CO₂, CH₄ and trace elements in thermokarst water bodies in discontinuous permafrost zones of Western Siberia. *Biogeochemistry*, 113:573-593.

Sieverts, J., T. Papakyriakou, S. Larsen, M.M. Jammet, S. Rysgaard, M.K. Sejr and L.L. Sørensen, 2015. Estimating local atmosphere-surface fluxes using eddy covariance and numerical ogive optimization. *Atmospheric Chemistry and Physics*, 15:2081-2013.

Sistla, S.A., J.C. Moore, R.T. Simpson, L. Gough, G.R. Shaver and J.P. Schimel, 2013. Long-term warming restructures Arctic tundra without changing net soil carbon storage. *Nature*, 497:615-618.

Smith, L.C., Y. Sheng, G.M. MacDonald and L.D. Hinzman, 2005. Disappearing Arctic lakes. *Science*, 308:1429-1429.

Sørensen, L.L., B. Jensen, R.N. Glud, D.F. McGinnia, M. Sejr, J. Sieverts, D.H. Søgaard and S. Rysgaard, 2014. Parameterization of atmosphere-surface exchange of CO₂ over sea ice. *The Cryosphere*, 8:853-866.

Spreen, G., R. Kwok and D. Menemenlis, 2011. Trends in Arctic sea ice drift and role of wind forcing: 1992–2009. *Geophysical Research Letters*, 38:L19501, doi:10.1029/2011GL048970.

Steele, M., W. Ermold and J. Zhang, 2008. Arctic Ocean surface warming trends over the past 100 years. *Geophysical Research Letters*, 35:L02614, doi:10.1029/2007GL031651.

Strauss, J., L. Schirrmeister, G. Grosse, S. Wetterich, M. Ulrich, U. Herzschuh and H.W. Hubberten, 2013. The deep permafrost carbon pool of the Yedoma region in Siberia and Alaska. *Geophysical Research Letters*, 40:6165-6170.

Streltskaya, I.D., A.A. Vasiliev and B.G. Vanstein, 2009. Erosion of sediment and organic carbon from the Kara Sea coast. *Arctic Antarctic and Alpine Research*, 41:79-87.

Striegl, R.G., G.R. Aiken, M.M. Dornblaser, P.A. Raymond and K.P. Wickland, 2005. A decrease in discharge-normalized DOC export by the Yukon River during summer through autumn. *Geophysical Research Letters*, 32:L21413, doi:10.1029/2005GL024413, 2005.

Stroeve, J.C., V. Kattsov, A. Barrett, M. Serreze, T. Pavlova, M. Holland and W.N. Meier, 2012. Trends in Arctic sea ice extent from CMIP5, CMIP3 and observations. *Geophysical Research Letters*, 39:L16502, doi:10.1029/2012GL052676.

Ström, L., A. Ekberg and T.R. Christensen, 2003. Species-specific effects of vascular plants on carbon turnover and methane emissions from a tundra wetland. *Global Change Biology*, 9:1185-1192.

Strong, C. and I.G. Rigor, 2013. Arctic marginal ice zone trending wider in summer and narrower in winter. *Geophysical Research Letters*, 40:4864-4868.

Subba-Rao, D.V. and T. Platt, 1984. Primary production of Arctic waters. *Polar Biology*, 3:191-201.

Tanhua, T., S. van Heuven, R.M. Key, A. Velo, A. Olsen and C. Schirnick, 2010. Quality control procedures and methods of the CARINA database. *Earth System Science Data*, 2:35-49.

Tank, S.E., P.A. Raymond, R.G. Striegl, J.W. McClelland, R.M. Holmes, G.J. Fiske and B.J. Peterson, 2012a. A land-to-ocean perspective on the magnitude, source and implication of DIC flux from major Arctic rivers to the Arctic Ocean. *Global Biogeochemical Cycles*, 26:GB4018, doi:10.1029/2011GB004192.

Tank, S.E., K.E. Frey, R.G. Striegl, P.A. Raymond, R.M. Holmes, J.W. McClelland and B.J. Peterson, 2012b. Landscape-level controls on dissolved carbon flux from diverse catchments of the circumboreal. *Global Biogeochemical Cycles*, 26:GB0E02, doi:10.1029/2012GB004299.

Tarnocai, C., J.G. Canadell, E.A.G. Schuur, P. Kuhry, G. Mazzitova and S. Zimov, 2009. Soil organic carbon pools in the northern circumpolar permafrost region. *Global Biogeochemical Cycles*, 23:GB2023, doi:10.1029/2008GB003327.

Tison, J.-L., C. Haas, M.M. Gowing, S. Sleewaegen and A. Bernard, 2002. Tank study of physio-chemical controls on gas content and composition during growth of young sea ice. *Journal of Glaciology*, 48:177-191.

Treat, C., S.M. Natali, J. Ernakovich, C.M. Iversen, M. Lupascu, A.D. McGuire, R.J. Norby, T. Roy Chowdhury, A. Richter, H. Santruckova, C. Schädel, E.A.G. Schuur, V.L. Sloan, M.R. Turetsky and M. Waldrop, 2015. A pan-Arctic synthesis of potential CH₄ and CO₂ production under saturated conditions. *Global Change Biology*, doi:10.1111/gcb.12875.

Turetsky, M.R., R.K. Wieder, D.H. Vitt, R.J. Evans and K.D. Scott, 2007. The disappearance of relict permafrost in boreal North America: Effects on peatland carbon storage and fluxes. *Global Change Biology*, 13:1922-1934.

Van Huissteden, J. and A.J. Dolman, 2013. Soil carbon in the Arctic and the permafrost carbon feedback. *Current Opinions in Environmental Sustainability*, 4:545-551.

Van Huissteden, J., C. Berrittella, F.J.W. Parmentier, Y. Mi, T.C. Maximov and A.J. Dolman, 2011. Methane emissions from permafrost thaw lakes limited by lake drainage. *Nature Climate Change*, 1:119-123.

Van Huissteden, J., J. Vandenberghe, P.L. Gibbard and J. Lewin, 2013. Periglacial fluvial sediments and forms. *Encyclopedia of Quaternary Science*, 3:440-499.

Vancoppenolle, M., K.M. Meiners, C. Michel, L. Bopp, F. Brabant, G. Carnat, B. Delille, D. Lannuzel, G. Madec, S. Moreau, J.-L. Tison and P. van der Merwe, 2013. Role of sea ice in global biogeochemical cycles: emerging views and challenges. *Quaternary Science Reviews* 79:207-230.

Vonk, J.E. and Ö. Gustafsson, 2013. Permafrost-carbon complexities. *Nature Geoscience*, 6:675-676.

Vonk, J.E., L. Sánchez-García, B.E. van Dongen, V. Alling, D. Kosmach, A. Charkin, I.P. Semiletov, O.V. Dudarev, N. Shakhova, P. Roos, T.I. Eglington, A. Andersson and Ö. Gustafsson, 2012. Activation of old carbon by erosion of coastal and subsea permafrost in Arctic Siberia. *Nature*, 489:137-140.

Vonk, J.E., P.J. Mann, S. Davydov, A. Davydova, R.G.M. Spencer, J. Schade, W.V. Sobczak, N. Zimov, S. Zimov, E. Bulygina, T.I. Eglington and R.M. Holmes, 2013. High biolability of ancient permafrost carbon upon thaw. *Geophysical Research Letters*, 40:2689-2693.

Walker, D.A., M.K. Reynolds, F.J.A. Daniels, E. Einarsson, A. Elvebakk, W.A. Gould, A.E. Katenin, S.S. Kholod, C.J. Markon, E.S. Melnikov, N.G. Moskalenko, S.S. Talbot and B.A. Yurtsev, 2005. The circumpolar Arctic vegetation map. *Journal of Vegetation Science*, 16:267-282.

Walter, K.M., S.A. Zimov, J.P. Chanton, D. Verbyla and F.S. Chapin III, 2006. Methane bubbling from Siberian thaw lakes as a positive feedback to climate warming. *Nature*, 443:71-75.

Walter Anthony, K.M., P. Anthony, G. Grosse and J. Chanton, 2012. Geologic methane seeps along boundaries of Arctic permafrost thaw and melting glaciers. *Nature Geoscience*, 5:419-426.

Walter Anthony, K.M., S.A. Zimov, G. Grosse, M.C. Jones, P.M. Anthony, F.S. Chapin, J.C. Finlay, M.C. Mack, S. Davydov, P. Frenzel and S. Frolking, 2014. A shift of thermokarst lakes from carbon sources to sinks during the Holocene epoch. *Nature*, 511:452-456.

Walvoord, M.A. and R.G. Striegl, 2007. Increased groundwater to stream discharge from permafrost thawing in the Yukon River basin: Potential impacts on lateral export of carbon and nitrogen. *Geophysical Research Letters*, 34:L12402, doi:10.1029/2007GL030216.

Wang, M. and J.E. Overland, 2012. A sea ice free summer Arctic within 30 years: An update from CMIP5 models. *Geophysical Research Letters*, 39:L18501, doi:10.1029/2012GL052868.

Wanninkhof, R., 1992. Relationship between wind speed and gas exchange over the ocean. *Journal of Geophysical Research: Oceans*, 97:7373-7382.

Watts, J.D., J.S. Kimball, F.J.W. Parmentier, T. Sachs, J. Rinne, D. Zona, W. Oechel, T. Tagesson, M. Jackowicz-Korczyński and M. Aurela, 2014. A satellite data driven biophysical modeling approach for estimating northern peatland and tundra CO₂ and CH₄ fluxes. *Biogeosciences*, 11:1961-1980.

Wickland, K.P., G.R. Aiken, K. Butler, M.M. Dornblaser, R.G.M. Spencer and R.G. Striegl, 2012. Biodegradability of dissolved organic carbon in the Yukon River and its tributaries: Seasonality and importance of inorganic nitrogen. *Global Biogeochemical Cycles*, 26:GB0E03, doi:10.1029/2012GB004342.

Wik, M., B.F. Thornton, D. Bastviken, S. MacIntyre, R.K. Varner and P.M. Crill, 2014. Energy input is primary controller of methane bubbling in subarctic lakes. *Geophysical Research Letters*, 41:555-560.

Woelfel, J., R. Schumann, F. Peine, A. Flohr, A. Kruss, J. Tegowski, P. Blondel, C. Wiencke and U. Karsten, 2010. Microphytobenthos of Arctic Kongsfjorden (Svalbard, Norway): Biomass and potential primary production along the shore line. *Polar Biology*, 33:1239-1253.

Zimov, S.A., S.P. Davydov, G.M. Zimova, A.I. Davydova, E.A.G. Schuur, K. Dutta and F.S. Chapin III, 2006. Permafrost carbon: Stock and decomposability of a globally significant carbon pool. *Geophysical Research Letters*, 33:L20502, doi:10.1029/2006GL027484.

Zona, D., B. Gioli, R. Commane, J. Lindaas, S.C. Wofsy, C.E. Miller, S.J. Dinardo, S. Dengel, C. Sweeney, A. Karion and R.Y.W. Chang, 2016. Cold season emissions dominate the Arctic tundra methane budget. *Proceedings of the National Academy of Sciences*, 113:40-45.

9. Sea level rise contribution from Arctic land ice: 1850-2100

LEAD AUTHORS: JASON E. BOX, WILLIAM T. COLGAN

Contents

Key Findings	220
9.1 Introduction	220
9.2 Sea level rise	221
9.2.1 How important is Arctic land ice to present sea level rise?	221
9.2.2 Non-ice sea level forcings	222
9.2.3 The future	223
9.3 Data and methodology	223
9.4 Results and discussion	224
9.4.1 Past sea level reconstruction	224
9.4.2 Arctic land ice and the Paris Agreement	225
9.4.3 Uncertainties and potential for low-biased projections	225
9.5 Conclusions	227
Acknowledgments	228
References	228

Key Findings

- Arctic land ice is estimated to have been responsible for 0.10 m (or 48%) of global sea level rise over the period 1850–2010. For 2004–2010, for which precise estimates are available, 72% of the land ice contribution to sea level rise came from the Arctic. During this period, Arctic land ice was responsible for 35% of all global sea level rise.
- Including all sources (net land ice loss, ocean thermal expansion, changes in land water storage), global sea-level rise this century (2006–2100) is projected to range from at least 0.52 m (RCP4.5) to at least 0.74 m (RCP8.5). These projections are likely to represent minimum bounds because some processes, for example, thinning-based amplification of land ice response or irreversible loss of some sectors of the West Antarctic ice sheet, already appear to be underway.

9.1 Introduction

This chapter evaluates the potential impact of the 2015 Paris Agreement on the sea-level rise contribution from Arctic land ice. When reassessing sea level rise, SWIPA 2017 finds that the Intergovernmental Panel on Climate Change (IPCC) Fifth Assessment Report (AR5) values (Church et al., 2013b) are likely to be underestimated owing to a variety of unaccounted for processes, including warming-based amplification of land ice response to climate warming.

Contemporary regional and global sea level changes are influenced by a wide variety of factors, including thermal expansion of seawater, contributions from land ice mass change, human impoundment of water in reservoirs, human extraction of groundwater that runs off to the sea, changing atmospheric and oceanic circulation patterns, changes to Earth's gravity field and changes in planetary rotation speed (e.g. Bamber and Riva, 2010; Mitrovica et al., 2011; Kopp et al., 2015; Thompson et al., 2016). Multiple studies have now inferred rates of sea-level change, due to land ice and other components, over various periods of the past (e.g. Ray and Douglas, 2011; Church et al., 2013a; Gregory et al., 2012), as well as from the past into the future (e.g. Rahmstorf, 2007; Grinsted et al., 2009), or focused on projecting future sea level contributions (e.g. Slagmolen et al., 2012; Giesen and Oreleemanns, 2013; Hirabayashi et al., 2013; Radic et al., 2014). In addition to temporal differences, studies also vary in spatial coverage, data and methodology, and reported uncertainty.

Land ice mass changes influence sea level through net mass transfers, more specifically mass gains from snow, rainfall, condensation and frost, and mass losses from meltwater runoff, solid ice discharge and water vapor loss. The transfer of land ice into the oceans weakens the gravitational field in the immediate vicinity of shrinking land ice, causing a redistribution of ocean mass from near-field regions of decreasing gravity to far-field regions where gravitational changes are minimal (Rietbroeka et al., 2016). Land ice mass loss also causes upward glacial isostatic rebound (Bevis et al., 2012; Lecavalier et al., 2013). Glacial isostatic rebound is believed to slightly increase ocean basin volume, resulting in a subtle global sea-level fall. This ocean basin volume increase is due to ultra-viscous mantle slowly flowing from regions of oceanic crust to continental crust (Tamisiea, 2011). Local sea-level decrease can also arise when the rate of glacial isostatic adjustment, or upwards crustal rebound, exceeds absolute sea level rise (SLR). The absolute SLR is the net result of solid-earth and oceanic factors contributing to sea level change (Cazenave and Llovel, 2010) (Figure 9.1). At any coastal location, the net change in sea level due to cryospheric processes is the site-specific sum of all mechanisms (Alison et al., 2015). See also Kopp et al. (2015) for a detailed review of factors influencing geographic variability in sea level.

The gravitational effects stemming from Arctic land ice loss are such that the resulting SLR is felt most in Southeast Asia and least in the immediate vicinity of Greenland and Baffin Bay (Figure 9.2). During the period 2002–2014, the combined effects of changes in the Earth's gravitational field and ocean thermal expansion produced SLR three to five times the global mean rate in equatorial regions, which have large coastal populations, such as in the Philippines and Indonesia (Rietbroeka et al., 2016).

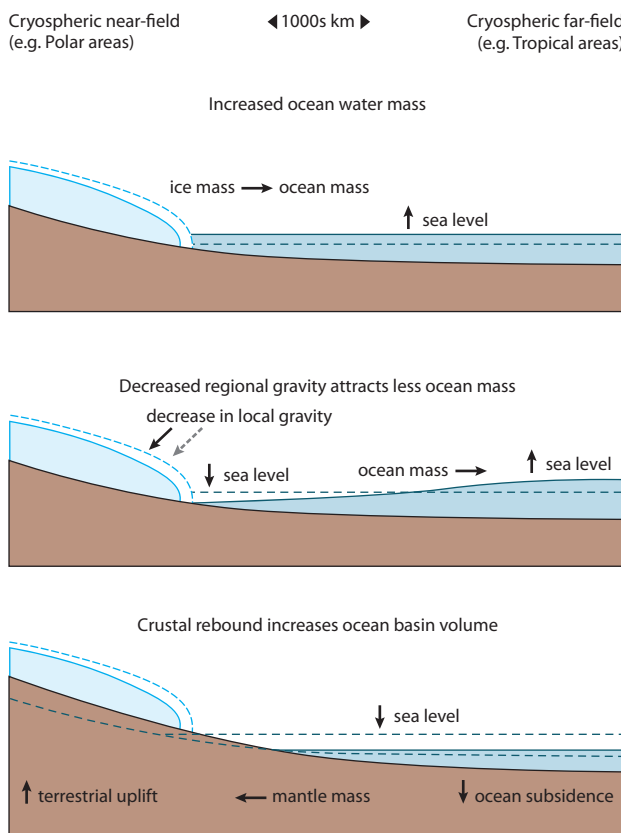


Figure 9.1 Schematic overview of cryospheric processes that influence absolute and relative sea level.

Recent studies add detail to sea level projections. Kopp et al. (2014) projected future local and global sea level changes, exploring how the different SLR components (i.e. ocean dynamics, Arctic and Antarctic ice melt) contribute to the uncertainty in sea level projections. They found that the Antarctic ice sheet contributes a growing share of variance in global and local sea level projections and that it is likely

to become the dominant source of SLR in late 21st century projections, although at some sites oceanographic processes contribute the largest share throughout the century. Jevrejeva et al. (2016) employed a globally distributed probabilistic sea level calculation, resolving each component of the sea level budget. In 2100, under an RCP8.5 scenario, they suggested a global mean SLR of 0.86 m relative to 2006, with a 5% chance of global mean SLR exceeding 1.78 m. For the analogous climate scenario, the IPCC AR5 suggested that SLR by 2100 would be in the 0.53–0.97 m range (Church et al., 2013a). The geographic distribution of this SLR will be non-uniform, owing to gravitational, dynamic and solid-earth effects. SLR, however, is likely to exceed the global median SLR along 80% of coastlines (Jevrejeva et al., 2016).

Here, this study assesses the global sea level budget to achieve closure during a 250-year period spanning the past and future (1850–2100). It highlights the role of Arctic land ice to anticipated mid- to late 21st century SLR and by comparing the SLR contributions from Arctic land ice, including the Greenland ice sheet, under RCP4.5 and RCP8.5 at the mid-century years 2030 and 2080, also evaluates the potential impact of the 2015 Paris Agreement.

9.2 Sea level rise

9.2.1 How important is Arctic land ice to present sea level rise?

During the 2004–2010 period, for which a global land ice inventory is sufficiently complete and multiple independent methods are reconcilable (Shepherd et al., 2012; Gardner et al., 2013), Arctic land ice loss was responsible for 72% of the cryospheric contribution to SLR (Table 9.1). The coterminous Greenland ice sheet was the single largest Arctic land ice source of SLR, contributing 41% of the global land ice sea level forcing. Arctic Canada and Alaska were the next largest Arctic sources: together contributing about 40% of the Greenland ice sheet

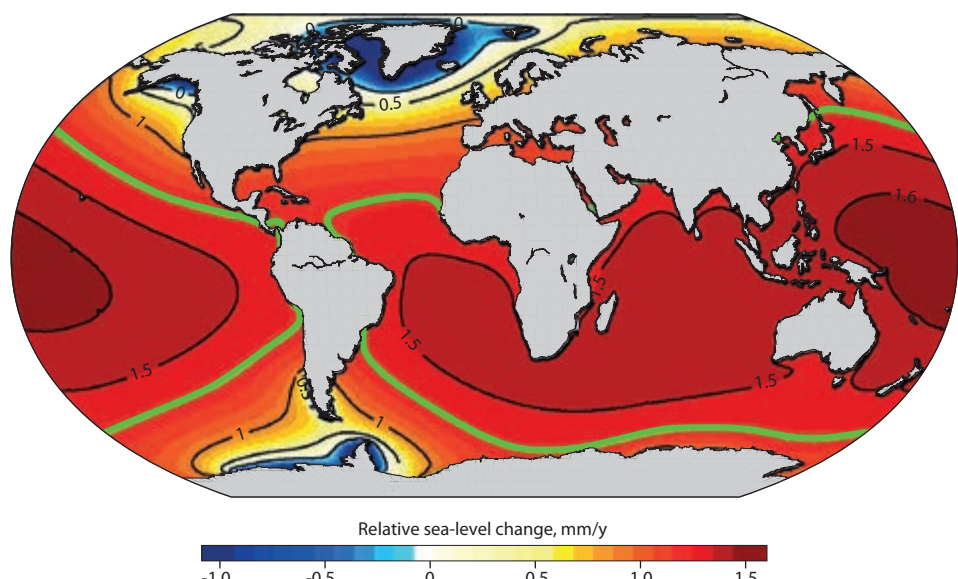


Figure 9.2 Relative sea level variations due to the gravitational and Earth rotational effects of ice mass losses from different sources for the period 2000–2008 (Bamber and Riva, 2010). The thick green contour indicates the sum of the fingerprints from different sources.

Table 9.1 Global land ice contribution to sea-level rise during the 2004 to 2010 period. Randolph Glacier Inventory regional identification shown in parentheses where applicable (Pfeffer et al., 2014).

Region	Mass balance, Gt/y	Uncertainty, Gt/y	Global fraction	Start year	End year	Method(s)	Source
Greenland ice sheet	-225	26	40.8%	2005	2010	altimetry, gravimetry, input-output	Shepherd et al. (2012), Gardner et al. (2013)
Canadian Arctic (3,4)	-60	8	10.9%	2003	2009	altimetry	Gardner et al. (2013)
Alaska (1)	-50	17	9.1%	2003	2009	altimetry	Gardner et al. (2013)
Greenland glaciers (5)	-38	7	6.9%	2003	2008	altimetry	Gardner et al. (2013)
Iceland (6)	-10	2	1.8%	2004	2011	altimetry	Matsuo and Heki (2013), Gardner et al. (2013), uncertainties from latter
Russian Arctic (9)	-7	4	1.3%	2004	2012	altimetry	Matsuo and Heki (2013), uncertainties from latter
Svalbard (7)	-4	2	0.7%	2004	2012	altimetry	Matsuo and Heki (2013), uncertainties from latter
Scandinavia (8)	-2	0	0.4%	2003	2009	altimetry	Gardner et al. (2013)
Arctic ice	-396	66	71.7%				
West Antarctic ice sheet	-102	18	18.5%	2005	2010	altimetry, gravimetry, input-output	Shepherd et al. (2012)
Antarctic peninsula	-36	10	6.5%	2005	2010	altimetry, gravimetry	Shepherd et al. (2012)
East Antarctic ice sheet	58	31	-10.5%	2005	2010	altimetry, gravimetry, input-output	Shepherd et al. (2012)
Non-Arctic or Antarctic glaciers (10–18)	-76	25	13.8%	2003	2009	altimetry	Gardner et al. (2013)
Non-Arctic ice	-156	84	28.3%	2004	2010	average	Gardner et al. (2013)
Global, Gt/y	-552	150					
Global, mm/y	-1.5	0.4					

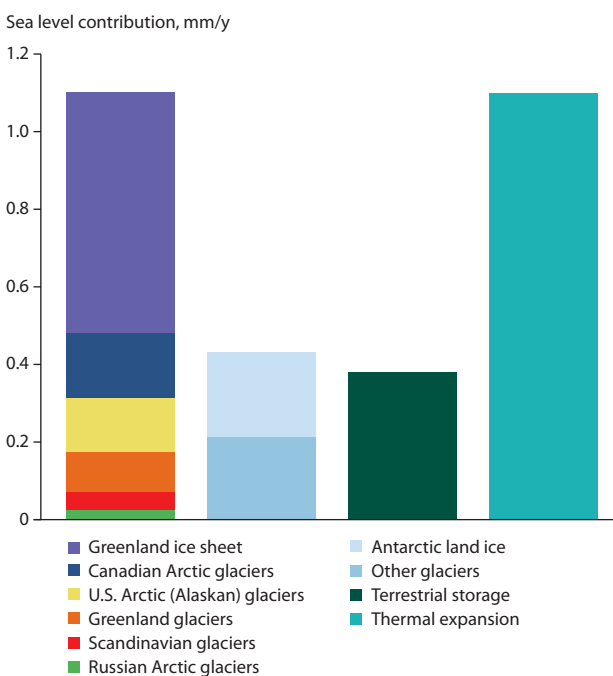


Figure 9.3 Comparison of Arctic sea level rates 2004–2010 with other global sea level components. ‘Scandinavian glaciers’ includes both Iceland and Svalbard. ‘Other glaciers’ includes, for example, Patagonian, Himalayan, African, and Indonesian land ice sources.

contribution. The magnitude of the different rates is shown in Figure 9.3. The global budget shows that roughly a third of global SLR is attributable to Arctic land ice melt of which more than half is from Greenland, roughly a third is from thermal expansion, and the remainder is from other sources (Antarctica, other glaciers and terrestrial storage).

9.2.2 Non-ice sea level forcings

Ocean thermal expansion, due to decreasing seawater density with increasing water temperature, is the second largest sea level forcing after land ice mass change (e.g. Gregory et al., 2012). Because, ocean observations before about 1960 are too sparse for robust observationally-constrained estimates of the global ocean thermal expansion, numerical models are relied upon to estimate both pre-1960 and future rates of thermal expansion of seawater. While continued climate warming will increase ocean thermal expansion, it is unlikely that thermal expansion will outpace land ice contributions to SLR in the next century owing to the expected acceleration of land ice loss (e.g. DeConto and Pollard, 2016; Jevrejeva et al., 2016).

Human activities introduce changes in land water storage, such as groundwater extraction from natural aquifers and water impoundment in artificial reservoirs. During the period 1900–1970, global impoundment slightly exceeded global extraction,

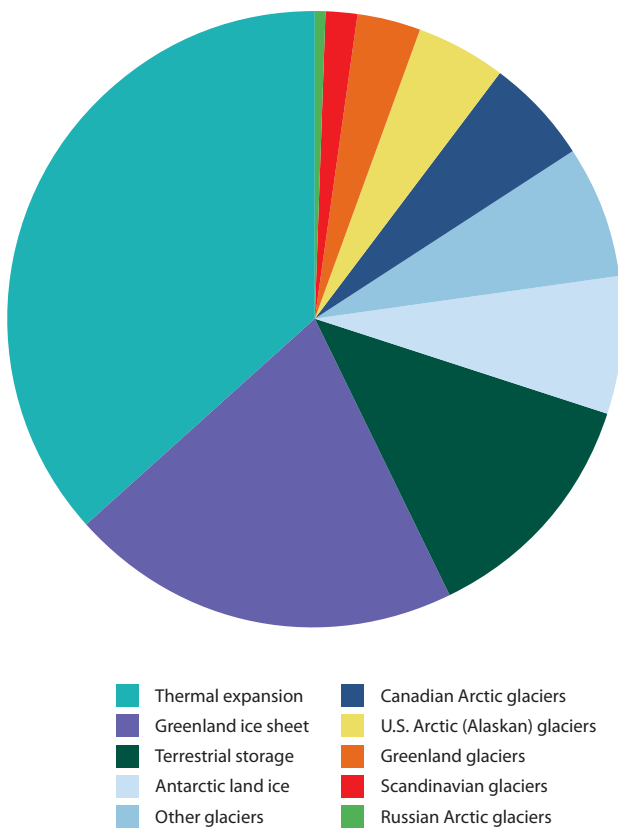


Figure 9.4 Global sea-level rise sources with Arctic land ice contributions highlighted relative to Antarctic land ice, thermal expansion and terrestrial water storage during the 2004–2010 period. ‘Scandinavian glaciers’ includes both Iceland and Svalbard. ‘Other glaciers’ includes, for example, Patagonian, Himalayan, African, and Indonesian land ice sources. The sources are sorted from largest to smallest.

while for 1970–2010 the pattern was reversed (Church et al., 2013a). Today, land water storage is a source of SLR.

The relative proportion of land ice and other contributions to SLR are illustrated in Figure 9.4.

9.2.3 The future

This chapter examines the RCP4.5 and RCP8.5 climate scenarios used in the IPCC AR5 to compare possible anthropogenic impacts on future SLR (van Vuuren et al., 2011; Church et al., 2013a; Myhre et al., 2013). RCP8.5 represents ‘business-as-usual’, which yields a 1350 ppmv atmospheric CO₂-equivalent concentration and a projected 4.9°C global average warming associated with a 8.5 W/m² enhanced greenhouse effect by 2100. In contrast, the RCP4.5 scenario reflects a future with significant greenhouse gas emission reductions, similar to a slightly less aggressive carbon emission implementation of the 2015 Paris Agreement, with a projected 2.4°C global average warming, a 650 ppmv CO₂-equivalent concentration and a 4.5 W/m² enhanced greenhouse effect by 2100 relative to a pre-industrial baseline (Figure 9.5).

9.3 Data and methodology

This new study assesses the 1850–2100 SLR contribution of land ice within nineteen glacierized regions of the world. The SLR contributions of land ice are discretized into ‘Arctic’ (Randolph Glacier Inventory (RGI) regions 1, 3–9 plus Greenland Ice

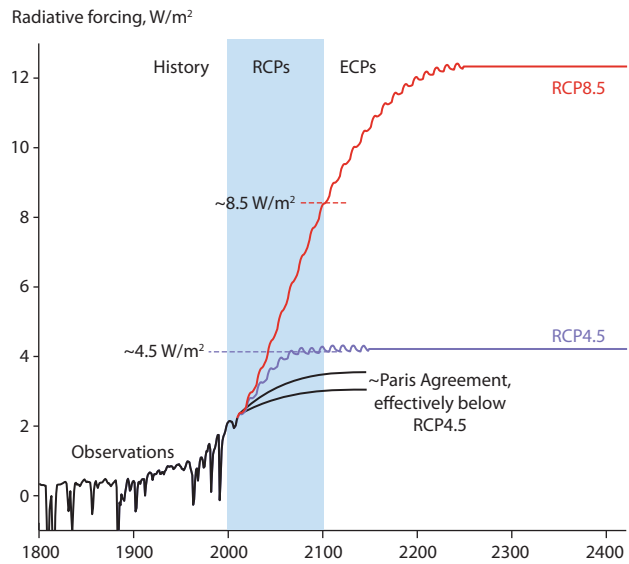


Figure 9.5 Representative Concentration Pathway (RCP) scenarios RCP4.5 and RCP8.5 including Extended Concentration Pathways (ECPs) after Meinshausen et al. (2011). The graphic indicates an approximate trajectory for the Paris Agreement. RCP8.5 is conceptualized as relatively slow adoption of low-carbon energy systems and weak international cooperation in reducing carbon emissions. RCP4.5, by contrast, is conceptualized as rapid development and implementation of low-carbon technology under strong international cooperation.

Sheet), ‘Antarctic’ (RGI region 19 plus Antarctic ice sheet) and ‘Other’ (RGI region 2, 10–18; Pfeffer et al., 2014). There are no new glacier and ice sheet simulations presented here.

Similar to Kopp et al. (2014), this study uses the AR5 model ensemble average glacier mass balance model output from Marzeion et al. (2012), which simulates the surface mass balance of a global inventory of glaciers and ice caps under RCP4.5 and RCP8.5 using 15 global circulation models (GCMs). This study adopts published uncertainties, derived from the standard deviation of ensemble spread, for these regional surface mass balance time-series.

For the Antarctic ice sheet, the present study uses the RCP4.5 and RCP8.5 2006–2100 SLR contributions estimated by IPCC AR5 and applies published relative uncertainties of $\pm 100\%$. This thereby assumes no sea level change associated with the Antarctic ice sheet during the period 1850–2005 (Church et al., 2013a). For the Greenland ice sheet, this study employs the 1850–2005 total mass balance time-series of Kjeldsen et al. (2015), and an associated relative uncertainty of $\pm 39\%$ after Box (2013) and Box and Colgan (2013). For the 2006–2100 period, it is assumed that the Greenland ice sheet contribution to SLR is six times that simulated for Greenland local glaciers after Marzeion et al. (2012).

The scaling factor (6.0 ± 0.3) is derived from observations indicating that local glacier mass loss was one sixth of ice sheet mass loss observed by satellite during the 2004–2010 period (Colgan et al., 2015) and is consistent with Gardner et al. (2013) and Shepherd et al. (2012). The scaled Greenland ice sheet mass loss under RCP8.5 (0.11 m sea level equivalence, hereafter SLE from 2006–2100) is also consistent with the ice sheet mass loss from IPCC AR5 under RCP8.5 (0.12 m SLE). The scaling factor and uncertainty are taken to be the same for the different RCPs. The present study assumes a relative uncertainty of 50% in this scaling term.

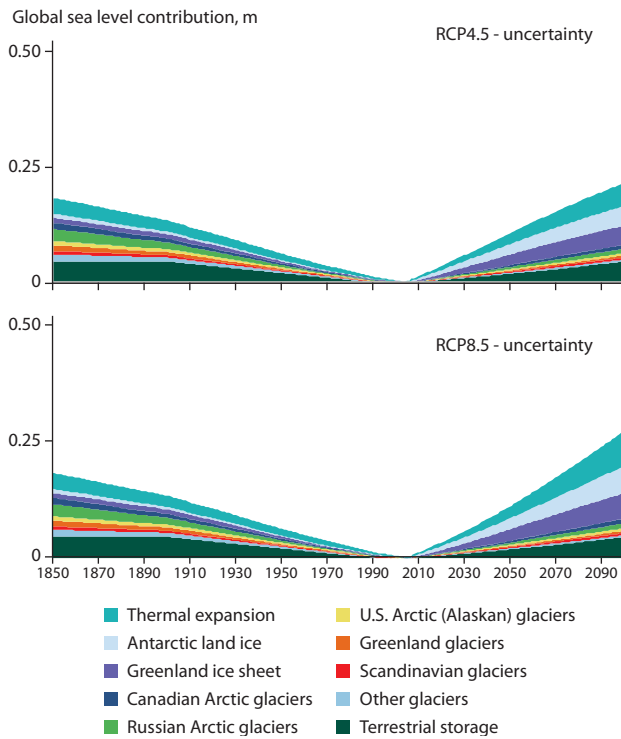


Figure 9.6 An uncertainty budget that sums sea level uncertainties described in Section 9.3.

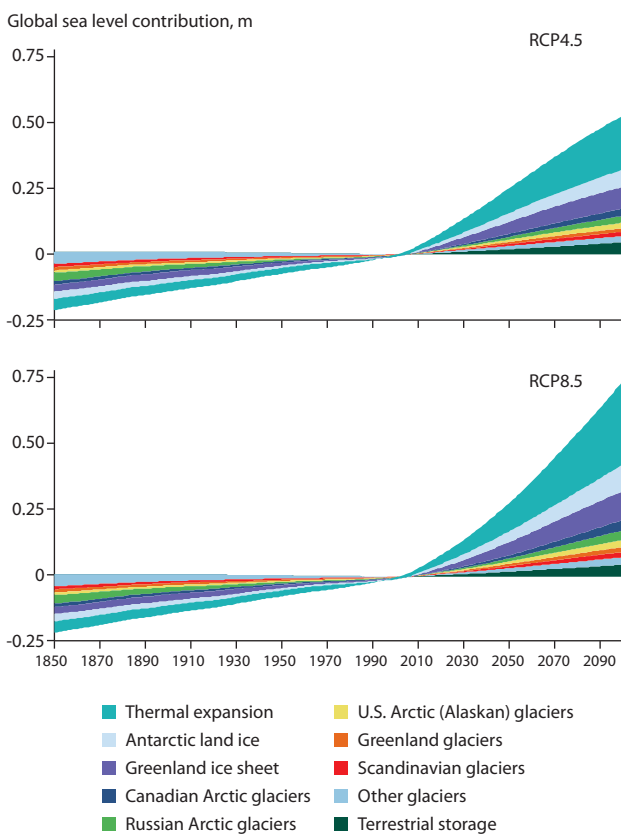


Figure 9.7 Historical (1850–2005) and projected (2006–2100) terms influencing global mean sea level under the RCP4.5 and the RCP8.5 scenarios. Sea-level rise expressed relative to 2006. Arctic land ice contributions highlighted relative to Antarctic land ice, thermal expansion and terrestrial water storage contributions to the global budget. ‘Scandinavian glaciers’ includes both Iceland and Svalbard. ‘Other glaciers’ includes, for example, Patagonian, Himalayan, African, and Indonesian land ice sources.

For thermal expansion, this study employs the RCP4.5 and RCP8.5 2006–2100 estimated SLR from IPCC AR5, to which published relative uncertainties of ± 24 and 22% , respectively, are applied. A thermal expansion contribution of 0.8 ± 0.3 mm per year during the 1971–2005 period adopted, and an analogous rate of 0.2 mm per year is assumed for the preceding 1850–1970 period (Church et al., 2013a). This assumed rate of thermal expansion, which is under 20% of the rate observed during the 1993–2010 period, yields a cumulative SLR of 2.4 cm during the 1850–1970 period. This pre-observational period thermal expansion rate is plausible in the context of the expectation of increasing ocean temperatures in response to documented atmospheric warming since about 1850.

For land water storage, this study adopts RCP4.5 and RCP8.5 values for the 2006–2100 period from IPCC AR5, with a climate-independent relative uncertainty of $\pm 100\%$ in both scenarios. This study prescribes a net sea level drawdown of 0.1 mm per year during the 1901–1990 period, and no sea level change associated with terrestrial water storage during the 1850–1900 and 1991–2005 periods (Church et al., 2013a).

Because the uncertainty budget zeros out in 2000 (see Figure 9.6), making it impossible to provide an uncertainty value near that time, an uncertainty value for 2000 was developed by integrating uncertainty backwards in time from 2000 to 1850, reaching a very conservative year 2000 value of ± 0.18 m.

9.4 Results and discussion

9.4.1 Past sea level reconstruction

Summing historical land ice mass changes, ocean thermal expansion and terrestrial storage yields a total SLR of 0.19 ± 0.18 m for the period 1850–2000, which is consistent with the best estimate of 0.21 m for 1880–2010 from tide-gauge records reported in IPCC AR5 (Church et al., 2013a). According to the present study, Arctic land ice was responsible for 48% (or 0.10 m) of the 1850–2000 SLR (Figure 9.7).

Summing future projections yields a total SLR of 0.52 ± 0.21 m under RCP4.5 and 0.74 ± 0.28 m under RCP8.5 during 2006–2100, with Arctic land ice responsible for 0.19 ± 0.07 m (or 37%) and 0.25 ± 0.09 m (or 34%), respectively. Under both the RCP4.5 and RCP8.5 scenarios, the Greenland ice sheet is the largest land-ice contributor to SLR during 2000–2100. Using 1850 as the base year to denote the onset of significantly enhanced greenhouse gas concentrations, rather than the arbitrary base year of 2006, then the year 2100 SLR projected in this study is 0.83 ± 0.21 and 0.98 ± 0.28 m under RCP4.5 and RCP8.5, respectively. Over the entire 1850–2100 period, Arctic land ice will contribute between 0.29 ± 0.15 and 0.35 ± 0.17 m to SLR under RCP4.5 and RCP8.5, respectively. The substantial Antarctic contribution uncertainty is discussed later.

RCP8.5 produces 43% (or 0.23 m) more SLR by 2100 than RCP4.5 (Figure 9.8). Including all sources (net land ice loss, ocean thermal expansion, changes in land water storage), global sea-level rise this century (2006–2100) is projected to range from at least 0.52 m (RCP4.5) to at least 0.74 m (RCP8.5). These projections are likely to represent minimum bounds because some processes, for example, thinning-based amplification of land ice response or irreversible loss of some sectors of the West Antarctic ice sheet, already appear to be underway.

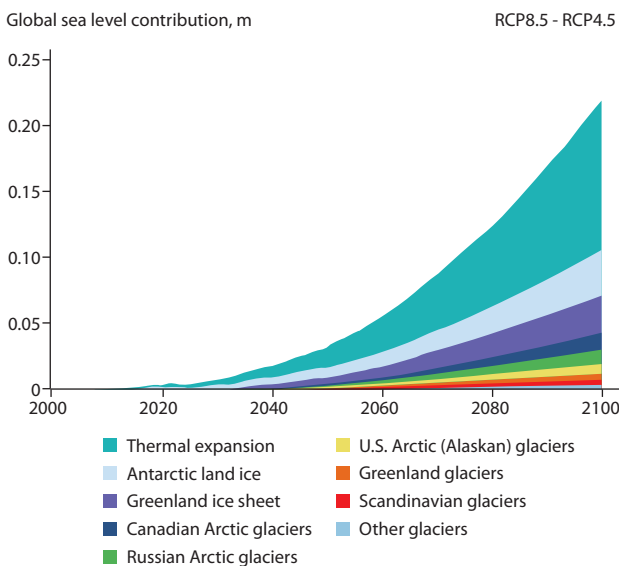


Figure 9.8 Sea level component summed difference: RCP8.5 minus RCP4.5. ‘Scandinavian glaciers’ includes both Iceland and Svalbard. ‘Other glaciers’ includes, for example, Patagonian, Himalayan, African, and Indonesian land ice sources.

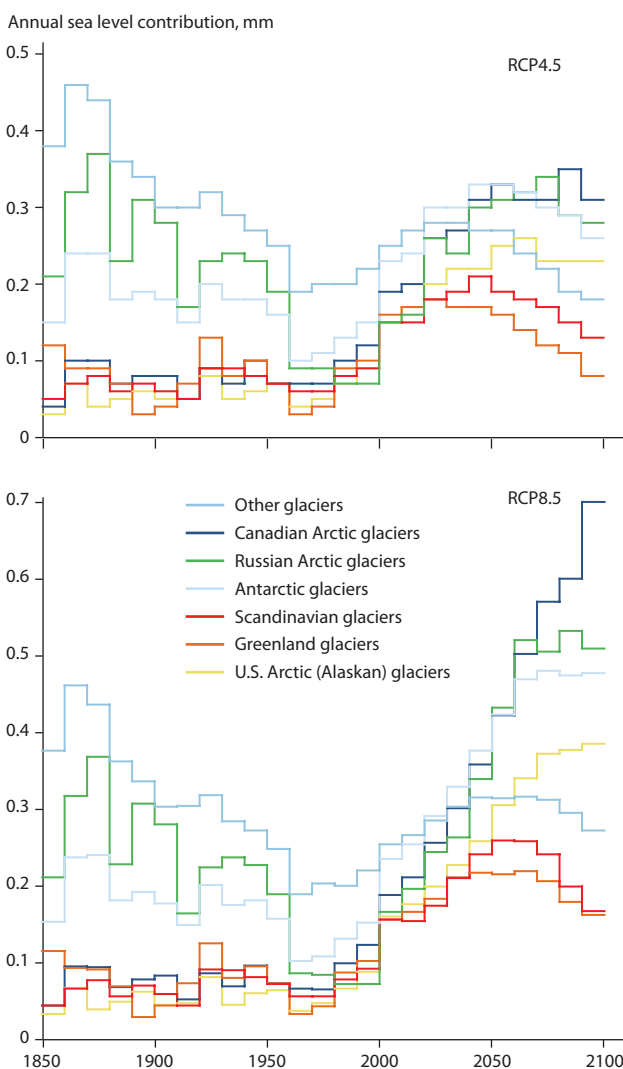


Figure 9.9 Annual sea level contribution, averaged per decade between 1850–2100, from the Arctic land ice and other regions simulated by Marzeion et al. (2012) under RCP4.5 and RCP8.5.

The choice of RCP4.5 or RCP8.5 climate scenario appears to have a strong influence on whether the Arctic land ice contribution to SLR peaks prior to 2100. Under RCP8.5, only Greenland peripheral glacier and Scandinavian glacier mass loss is projected to peak prior to 2100, with all other Arctic land ice contributions to SLR increasing beyond 2100 (Figure 9.9). Under the RCP8.5 scenario, the Arctic glacier contribution to SLR would only begin to decrease post-2100 once increases in specific runoff are eventually offset by decreases in glacier area (e.g. Flowers et al., 2005). Under RCP4.5, by contrast, the sea level contributions of all Arctic land ice regions, except for the Greenland ice sheet and the Canadian Arctic, exhibit a clear peak prior to 2100.

The year 2006–2100 SLR projected in this study (0.52 ± 0.21 to 0.74 ± 0.28 m) differs from the 0.90 to 1.60 m presented in SWIPA 2011 (Callaghan et al., 2011) for several reasons. First, the SWIPA 2011 SLR projection for 2100 may be considered an expert elicitation (i.e. ‘educated guess’), which was informed, but not based, on models. In contrast, this study uses physically-based projections of individual components of the global water budget. Second, SWIPA 2011 did not examine specific climate scenarios, but implicitly based projections on the A1B-type business-as-usual scenario that pre-dated the RCP scenarios (IPCC, 2000). As a result, the 0.70 m range in global mean sea level assessed by SWIPA 2011 reflects uncertainty within a single scenario, whereas the 0.22 m range presented here reflects the spread between two scenarios. Substantial uncertainty is associated with the projections within each scenario (see Figure 9.6). Finally, SWIPA 2011 used 1990, rather than 2006, as the base year for sea-level projections. Approximately 0.04 m of SLR occurred during the period 1990–2006. A substantial number of sea level projections, including those developed during IPCC AR5, use 2006 as the base year.

9.4.2 Arctic land ice and the Paris Agreement

By 2030, the Arctic land ice contribution to SLR is only 5% less under RCP4.5 than under RCP8.5 (Figure 9.10). Thus, the Arctic land-ice contribution to SLR may now be considered effectively ‘locked-in’ until about 2035 as a consequence of historically integrated greenhouse gas emissions. By 2080, however, the Arctic land ice contribution to global sea level is 27% higher under RCP8.5 than under RCP4.5. By 2080, the total sea level contribution, including thermal expansion, is 30% higher under RCP8.5 than RCP4.5. This proportion grows with time, reaching a difference of 43% by 2100. The difference between SLR under RCP4.5 and RCP8.5 for the next 85 years (2015–2100) is greater than the entire SLR contribution from all Arctic land ice over the past 165 years (1850–2015). The potential increase in ocean thermal expansion and accelerated land ice loss highlights a strong impetus for immediate and effective implementation of the 2015 Paris Agreement.

9.4.3 Uncertainties and potential for low-biased projections

The assumptions adopted here, suggest that the Arctic land ice fraction (0.35) to global SLR will remain relatively constant through 2100. Yet, as IPCC AR5 cautioned, “*the collapse of marine-based sectors of the Antarctic ice sheet, if initiated, could cause global mean sea level to rise substantially during the 21st century*” (IPCC, 2014). Indeed, Rignot et al. (2014) has since reinforced this

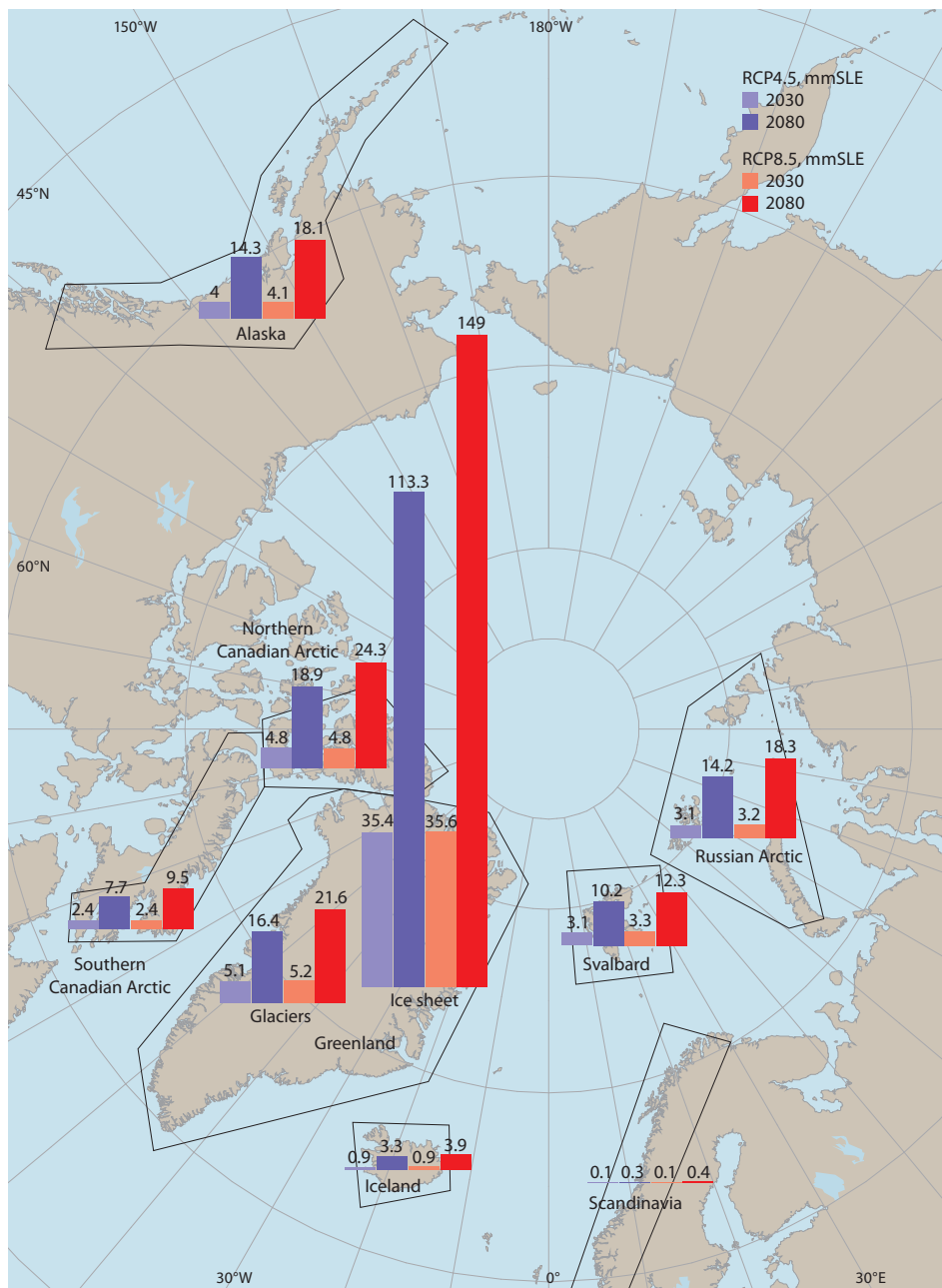


Figure 9.10 Projected land ice loss (expressed in millimeters sea level equivalence; SLE) from different Arctic regions in 2030 and 2080 under the RCP4.5 and RCP8.5 scenarios, based on the 2006–2100 sea level budget described in Section 9.4. The relatively small mainland Eurasian glaciers do not appear here owing to incomplete assessment.

concern, indicating that some marine-based collapse is already underway. A related NASA press release headlined *West Antarctic Glacier Loss Appears Unstoppable*. Rignot et al. (2014) noted that although the Amundsen Sea region is not the whole West Antarctic ice sheet, it does contain enough land ice to raise global sea level by 1.2 m and its collapse is now likely to be irreversible on a policy-relevant time-scale. Using a model that includes Antarctic ice shelf hydrofracturing, DeConto and Pollard (2016) found that Antarctica has the potential to contribute more than 1 m to SLR by 2100. However, it is fair to be critical of the notion that Antarctic de-glaciation will soon outpace Arctic deglaciation, and especially that of smaller Arctic glaciers and ice caps. First, the DeConto and Pollard (2016) treatment of meltwater retention in snow probably overestimates the speed of meltwater delivery into crevasses to promote hydrofracturing. Second, understanding the behavior of the smaller but faster-

responding Arctic glaciers is crucial for accurate and robust SLR projections in the years before 2100.

Meanwhile, marine-based sectors of the Greenland ice sheet now appear to be undergoing similar irreversible collapse, with a committed 0.5 m SLR contribution now anticipated from the Zachariae Isstrøm sector (Rignot et al., 2015).

Thus, while the 21st century sea-level estimates discussed here may be useful interim planning targets, they are likely to represent an underestimate of a larger committed SLR from global land ice. More context is given by the finding that global mean sea level has been 6 to 9 m higher as recently as the previous interglacial period (115–130 k years ago), when atmospheric CO₂ concentrations were below 280 ppmv (e.g. Dutton et al., 2015).

The 2005–2010 East Antarctic ice sheet surface mass gain of 80 Gt/y (Shepherd et al., 2012) is expected to persist

into the future, owing to climate warming adding moisture to the atmosphere and increasing potential snowfall rates. Recent observations and modelling studies, however, have suggested the potential for rapid and substantial retreat of large sectors of the East Antarctic ice sheet post-2100 (Mengel and Levermann, 2014).

Marzeion et al. (2012) concluded that until 2100, ensemble uncertainty (i.e. the envelope of results from the use of different global climate models) within each scenario dominates the uncertainty for the future glacier mass loss, despite several of the different models incorporating some of the same physics packages.

Not explicitly accounted for in the Marzeion et al. (2012) data used here to represent land ice outside the Greenland and Antarctic ice sheets is hypsometry, the non-linear increase in land ice surface area with increasing elevation. In a warming scenario, hypsometry causes melt to expand sharply over the increasingly gradual surface slopes of the ice sheet and ice cap upper elevations (e.g. McGrath et al., 2013). While meltwater retention will work against the sea level response (Pfeffer et al., 1991; Harper et al., 2012), in cases of successive high melt years, the retention capacity may become limited by the development of impermeable layers that leave porous firn below stranded from the meltwater retention process (Machguth et al., 2016).

Increases in ice cap and ice sheet melt area, if sustained over long periods, promote dynamic thinning that reinforces hypsometric melt area amplification (Carlson et al., 2009). Dynamic thinning causes surface slumping into lower parts of the atmosphere. Lowered areas gain more atmospheric heat from sensible, condensational, and thermal infrared energy that produce more surface melting and dynamic thinning. The magnitude of thinning reinforcing melting should be addressed using approaches after, for example, Bahr et al. (2015).

Climate warming provides the conditions for enhanced growth of snow and bare ice algae, which darken the surface, causing enhanced melt (Lutz et al., 2014, 2016) not captured by the temperature dependence used by Marzeion et al. (2012). Also not captured, the deposition of wildfire black carbon promotes melt through enhanced sunlight absorption, forcing snow grain metamorphosis that further darkens snow (Tedesco et al. 2015). Wildfire events are linked with enhanced Greenland land ice melting (Keegan et al., 2014). Climate projections suggest wildfires will become more frequent (Young et al., 2016).

Thermal-viscous ice sheet collapse is a process not included in modeling, whereby enhanced surface meltwater production results in enhanced warming throughout the ice column. The warmer ice deforms more readily and what follows is enhanced ice thinning (Phillips et al., 2010; Colgan et al., 2015).

Finally, although this study has focused on assessing the potential sea level contribution of Arctic land ice to 21st century SLR, thermal expansion of seawater may play an increasingly important role in global SLR. Under the RCP8.5 scenario, the IPCC projected a year 2100 thermal expansion SLR of 0.32 m, and a global land ice (including both the Arctic and Antarctic) contribution of 0.38 m (Church et al., 2013a). More recent simulations, however, which examined spatial patterns of dynamic changes in sea level using an ensemble of GCMs, suggest 16% greater global SLR in 2100 under

RCP8.5 than stated in the IPCC AR5 (Jevrejeva et al., 2016). A substantial proportion of the 0.12 m increase in projected SLR is associated with improved scientific understanding of thermal expansion.

9.5 Conclusions

The present sea level budget suggests that global mean sea level will rise at equivalent rates under RCP4.5 and RCP8.5 until about year 2030, with both scenarios responsible for similar committed land ice loss and sea level rise until that time. Thus, the effectiveness of the Paris Agreement implementation becomes very important for sea level rise only after mid-century.

Between 2030 and 2080 there is a growing divergence between the RCP4.5 and RCP8.5 land ice contributions to SLR, which results from the degree to which amplifying glacier-climate feedback processes like hypsometric amplification operate. It seems likely that the future land ice mass balance simulations after Marzeion et al. (2012) may underestimate land ice loss by not simulating emerging feedbacks, such as surface darkening via biological growth or wildfire increase.

Atmospheric warming is poised to drive a list of additional land ice melt amplifiers, in addition to hypsometric amplification. For example, surface darkening from increased surface water concentration; more exposure of relatively dark bare glacier ice at the expense of brighter snow cover, leading to more sunlight absorption; more rainfall at the expense of snow accumulation; more downward thermal infrared radiation from a more humid and warmer atmosphere; more condensation heating of the surface; and more sensible heating of the surface. Many of these glacier processes respond to climate on seasonal time-scales.

On multi-year time-scales, sustained warming promotes ice dynamic thinning that reinforces the amplified melt area from hypsometry. In areas of accelerated flow, dynamic thinning causes surface slumping into lower and therefore warmer parts of the atmosphere. While some self-regulation from increased sub-glacial water flow efficiency is evident, flow acceleration propagates inland, ensuring flow speed sensitivity to warming well into the future.

It is fair to be critical of the notion that Antarctic deglaciation will soon outpace Arctic deglaciation, and especially that of smaller Arctic glaciers and ice caps. First, the DeConto and Pollard (2016) treatment of meltwater retention in snow probably overestimates the speed of meltwater delivery into crevasses to promote hydrofracturing. Second, understanding the behavior of the smaller but faster-responding Arctic glaciers is crucial for accurate and robust SLR projections in the years before 2100. The pre-2100 years are of first concern to the users of today's sea level projections – planners, risk managers, policymakers, re-insurers, etc. This is not to say that SLR after 2100 is not of concern, but that knowledge is of less use if what will happen before 2100 is not first understood.

Land ice responds over a spectrum of time scales with the longer term processes gaining in importance mid-century, about the time the success of the Paris Agreement could be felt. Failure to adopt the Paris Agreement would result in direct sea level impacts for hundreds of millions of people, especially near end of century and beyond.

Acknowledgments

Digital copies of the annual time-series of SLR terms during the 1850-2100 period presented in Figure 9.7, under both RCP4.5 and RCP8.5 scenarios, are available by contacting info@amap.no. The data set includes both regionally discretized land ice terms, as well as thermal expansion and terrestrial storage terms. W.T. Pfeffer and R.E. Kopp are thanked for constructive review comments on this chapter.

References

Alison, I., W. Colgan, M. King and F. Paul. 2015. Ice sheets, glaciers, and sea level. In: Haeberli, W. and C. Whiteman (eds.), *Snow and Ice-Related Hazards, Risks, and Disasters*. pp. 714-747. Elsevier.

Bahr, D.B., W.T. Pfeffer and G. Kaser, 2015. A review of volume-area scaling of glaciers. *Reviews of Geophysics*, 53:95-140.

Bamber, J. and R. Riva, 2010. The sea level fingerprint of recent ice mass fluxes. *The Cryosphere*, 4:621-627.

Bevis, M., J. Wahr, S.A. Khan, F.Bo Madsen, A. Brown, M. Willis, E. Kendrick, P. Knudsen, J.E. Box, T. van Dam, D.J. Caccamise II, B. Johns, T. Nylen, R. Abbott, S. White, J. Miner, R. Forsberg, H. Zhou, J. Wang, T. Wilson, D. Bromwich and O. Francis, 2012. Bedrock displacements in Greenland manifest ice mass variations, climate cycles and climate change. *Proceedings of the National Academy of Sciences*, 109:11944-11948.

Box, J.E., 2013. Greenland ice sheet mass balance reconstruction. Part II: Surface mass balance (1840–2010). *Journal of Climate*, 26:6974-6989.

Box, J.E. and W. Colgan, 2013. Greenland ice sheet mass balance reconstruction. Part III: Marine ice loss and total mass balance (1840–2010). *Journal of Climate*, 26:6990-7002.

Callaghan, T.V., D. Dahl-Jense, M. Johansson, R. Kellenborn, R.R. Key, R. Macdonald, T. Prowse, M. Sharp, K. Steffen and W.F. Vincent, 2011. Cross-cutting scientific issues. In: *Snow, Water, Ice and Permafrost in the Arctic (SWIPA): Climate Change and the Cryosphere*. Arctic Monitoring and Assessment Programme (AMAP), Oslo, Norway.

Carlson, A., F. Anslow, E. Obbink, A. LeGrande, D. Ullman and J. Licciardi, 2009. Surface-melt driven Laurentide Ice Sheet retreat during the early Holocene. *Geophysical Research Letters*, 36:L24502, doi:10.1029/2009GL040948.

Cazenave, A. and W. Llovel, 2010. Contemporary sea level rise. *Annual Review of Marine Science*, 2:145-173.

Church, J.A. D. Monselesan, J.M. Gregory and B. Marzeion, 2013a. Evaluating the ability of process based models to project sea-level change. *Environmental Research Letters*, 8:014051, doi:10.1088/1748-9326/8/1/014051.

Church, J.A., P.U. Clark, A. Cazenave, J.M. Gregory, S. Jevrejeva, A. Levermann, M.A. Merrifield, G.A. Milne, R.S. Nerem, P.D. Nunn, A.J. Payne, W.T. Pfeffer, D. Stammer and A.S. Unnikrishnan, 2013b. Sea level change. In: *Climate Change 2013: The Physical Science Basis. Contribution of Working Group I to the Fifth Assessment Report of the Intergovernmental Panel on Climate Change*. Cambridge University Press.

Colgan, W., A. Sommers, H. Rajaram, W. Abdalati and J. Fahrm, 2015. Considering thermal-viscous collapse of the Greenland ice sheet. *Earth's Future*, 3:252-267.

DeConto, R.M. and D. Pollard, 2016. Contribution of Antarctica to past and future sea-level rise. *Nature*, 531:591-597.

Dutton, A., A.E. Carlson, A.J. Long, G.A. Milne, P.U. Clark, R. DeConto, B.P. Horton, S. Rahmstorf and M.E. Raymo, 2015. Sea-level rise due to polar ice-sheet mass loss during past warm periods. *Science*, 349: doi:10.1126/science.aaa4019.

Flowers, G., S. Marshall, H. Björnsson and G. Clarke, 2005. Sensitivity of Vatnajökull ice cap hydrology and dynamics to climate warming over the next 2 centuries. *Journal of Geophysical Research*, 110:F02011, doi:10.1029/2004F000200.

Gardner, A., G. Moholdt, J. Cogley, B. Wouters, A. Arendt, J. Wahr, E. Berthier, R. Hock, W. Pfeffer, G. Kaser, S. Ligtenberg, T. Bolch, M. Sharp, J. Hagen, M. van den Broeke and F.A. Paul, 2013. A reconciled estimate of glacier contributions to sea level rise: 2003 to 2009. *Science*, 340:852-858.

Giesen, R.H. and J. Oerlemans, 2013. Climate-model induced differences in the 21st century global and regional glacier contributions to sea-level rise. *Climate Dynamics*, 41:3283-3300.

Gregory, J.M., N.J. White, J.A. Church, M.F.P. Bierkens, J.E. Box, M.R. van den Broeke, J.G. Cogley, X. Fettweis, E. Hanna, P. Huybrechts, L.F. Konikow, P.W. Leclercq, B. Marzeion, J. Oerlemans, M.E. Tamisiea, Y. Wada, L.M. Wake and R.S.W. van de Wal, 2012. Twentieth-century global-mean sea-level rise: is the whole greater than the sum of the parts? *Journal of Climate*, 26:4476-4499.

Grinsted, A., J.C. Moore and S. Jevrejeva, 2009. Reconstructing sea level from paleo and projected temperatures 200 to 2100 AD. *Climate Dynamics*, 34:461-472.

Harper, J., N. Humphrey, W.T. Pfeffer, J. Brown and X. Fettweis, 2012. Greenland ice-sheet contribution to sea-level rise buffered by meltwater storage in firn. *Nature*, 491:240-243.

Hirabayashi, Y., Y. Zang, S. Watanabe, S. Koirala and S. Kanae, 2013. Projection of glacier mass changes under a high-emission climate scenario using the global glacier model HYOGA2. *Hydrological Research Letters*, 7:6-11.

IPCC, 2000. Special Report on Emission Scenarios. Nakicenovic, N. and R. Swart (eds.), Intergovernmental Panel on Climate Change (IPCC). Cambridge University Press.

IPCC, 2014. Summary for policymakers. In: *Synthesis Report. Contribution of Working Groups I, II and III to the Fifth Assessment Report of the Intergovernmental Panel on Climate Change*. Intergovernmental Panel on Climate Change (IPCC). Cambridge University Press.

Jevrejeva, S., L.P. Jackson, R.E.M. Riva, A. Grinsted and J.C. Moore, 2016. Coastal sea level rise with warming above 2°C. *Proceedings of the National Academy of Sciences*, 113:13342-13347.

Keegan, K.M., M.R. Albert, J.R. McConnell and I. Baker, 2014. Climate change and forest fires synergistically drive widespread melt events of the Greenland Ice Sheet. *Proceedings of the National Academy of Sciences USA*, 111:7964-7967.

Kjeldsen, K.K., N.J. Korsgaard, A.A. Bjørk, S.A. Khan, J.E. Box, S. Funder, N.K. Larsen, J.L. Bamber, W. Colgan, M. van den Broeke, M.-L. Sigaard-Andersen, C. Nuth, A. Schomacker, C.S. Andresen, E. Willerslev and K.H. Kjær, 2015. Spatial and temporal distribution of mass loss from the Greenland Ice Sheet since AD 1900. *Nature*, 528:396-400.

Kopp, R.E., R.M. Horton, C.M. Little, J.X. Mitrovica, M. Oppenheimer, D.J. Rasmussen, B.H. Strauss and C. Tebaldi, 2014. Probabilistic 21st and 22nd century sea-level projections at a global network of tide-gauge sites. *Earth's Future*, 2:383-406.

Kopp, R.E., C.C. Hay, C.M. Little and J.X. Mitrovica, 2015. Geographic variability of sea-level change. *Current Climate Change Reports*, 1:192-204.

Lecavalier, B.S., G.A. Milne, B.M. Vinther, D.A. Fisher, A.S. Dyke and M.J.R. Simpson, 2013. Revised estimates of Greenland ice sheet thinning histories based on ice-core records. *Quaternary Science Reviews*, 63:73-82.

Lutz, S., A.M. Anesio, S.E. Jorge Villar and L.G. Benning, 2014. Variations of algal communities cause darkening of a Greenland glacier. *FEMS Microbiology Ecology*, 89:402-414.

Lutz, S., A.M. Anesio, R. Raiswell, A. Edwards, R.J. Newton, F. Gill and L.G. Benning, 2016. The biogeography of red snow microbiomes and their role in melting arctic glaciers. *Nature Communications*, 7:11968, doi:10.1038/ncomms11968.

Machguth, H., H.H. Thomsen, A. Weidick, A.P. Ahlstrøm, J. Abermann, M.L. Andersen, S.B. Andersen et al., 2016. Greenland surface mass-balance observations from the ice-sheet ablation area and local glaciers. *Journal of Glaciology*, 62:861-887.

Marzeion, B., A.H. Jarosch and M. Hofer, 2012. Past and future sea-level change from the surface mass balance of glaciers. *The Cryosphere*, 6:1295-1322.

Matsuo, K. and K. Heki, 2013. Current ice loss in small glacier systems of the Arctic Island (Iceland, Svalbard, and the Russian High Arctic) from satellite gravimetry. *Terrestrial Atmospheric and Oceanic Sciences*, 24:657-670.

McGrath, D., W. Colgan, N. Bayou, A. Muto and K. Steffen, 2013. Recent warming at Summit, Greenland: global context and implications. *Geophysical Research Letters*, 40:2091-2096.

Meinshausen, M., S.J. Smith, K.V. Calvin, J.S. Daniel, M.L.T. Kainuma, J.-F. Lamarque, K. Matsumoto, S.A. Montzka, S.C.B. Raper, K. Riahi, A.M. Thomson, G.J.M. Velders and D.P. van Vuuren, 2011. The RCP greenhouse gas concentrations and their extensions from 1765 to 2300. *Climatic Change*, 109:213-241.

Mengel, M. and A. Levermann, 2014. Ice plug prevents irreversible discharge from East Antarctica. *Nature Climate Change*, 4:451-455.

Mitrovica, J.X., N. Gomez, E. Morrow, C. Hay, K. Latychev and M.E. Tamisiea, 2011. On the robustness of predictions of sea level fingerprints. *Geophysical Journal International*, 187:729-742.

Myhre, G., D. Shindell, F.-M. Bréon, W. Collins, J. Fuglestvedt, J. Huang, D. Koch, J.-F. Lamarque, D. Lee, B. Mendoza, T. Nakajima, A. Robock, G. Stephens, T. Takemura and H. Zhang, 2013. Anthropogenic and Natural Radiative Forcing. In: Climate Change 2013: The Physical Science Basis. Contribution of Working Group I to the Fifth Assessment Report of the Intergovernmental Panel on Climate Change [Stocker, T.F., D. Qin, G.-K. Plattner, M. Tignor, S.K. Allen, J. Boschung, A. Nauels, Y. Xia, V. Bex and P.M. Midgley (eds.)]. Cambridge University Press.

Pfeffer, W., M. Meier and T. Illangasekare, 1991. Retention of Greenland runoff by refreezing: Implication for projected future sea level change. *Journal of Geophysical Research*, 96:22,117-22,124.

Pfeffer, W.T., A.A. Arendt, A. Bliss, T. Bolch, J.G. Cogley, A.S. Gardner, J.-O. Hagen, R. Hock, G. Kaser, C. Kienholz, E.S. Miles, G. Moholdt, N. Mölg, F. Paul, V. Radić, P. Rastner, B.H. Raup, J. Rich and M.J. Sharp, 2014. The Randolph Glacier Inventory: a globally complete inventory of glaciers. *Journal of Glaciology*, 60:537-552.

Phillips, T., H. Rajaram and K. Steffen, 2010. Cryo-hydrologic warming: A potential mechanism for rapid thermal response of ice sheets. *Geophysical Research Letters*, 37:L20503. doi:10.1029/2010GL044397

Radic, V., A. Bliss, A. Beedlow, R. Hock, E. Miles and J. Cogley, 2014. Regional and global projections of twenty-first century glacier mass changes in response to climate scenarios from global climate models. *Climate Dynamics*, 42:37-58.

Rahmstorf, S., 2007. Response to comments on "A semi-empirical approach to projecting future sea-level rise". *Science*, 317:5846, doi:10.1126/science.1141283.

Ray, R.D. and B.C. Douglas, 2011. Experiments in reconstructing twentieth-century sea levels. *Progress in Oceanography*, 91:496-515.

Rietbroek, R., S. Brunnabend, J. Kusche, J. Schröterb and C. Dahlec, 2016. Revisiting the contemporary sea-level budget on global and regional scales. *Proceedings of the National Academy of Sciences*, 113:1504-1509.

Rignot, E., J. Mouginot, M. Morlighem, H. Seroussi and B. Scheuchl, 2014. Widespread, rapid grounding line retreat of Pine Island, Thwaites, Smith, and Kohler glaciers, West Antarctica, from 1992 to 2011. *Geophysical Research Letters*, 41:3502-3509.

Rignot, E., I. Fenty, Y. Xu, C. Cai and C. Kemp, 2015. Undercutting of marine-terminating glaciers in West Greenland. *Geophysical Research Letters*, 42:5909-5917.

Shepherd, A., E. Ivins, A. Geruo, V. Barletta, M. Bentley, S. Bettadpur, K. Briggs, D. Bromwich, R. Forsberg, N. Galin, M. Horwath, S. Jacobs, I. Joughin, M. King, J. Lenaerts, J. Li, S. Ligtenberg, A. Luckman, S. Luthcke, M. McMillan, R. Meister, G. Milne, J. Mouginot, A. Muir, J. Nicolas, J. Paden, A. Payne, H. Pritchard, E. Rignot, H. Rott, L. Sørensen, T. Scambos, B. Scheuchl, E. Schrama, B. Smith, A. Sundal, J. van Angelen, W. van de Berg, M. van den Broeke, D. Vaughan, I. Velicogna, J. Wahr, P. Whitehouse, D. Wingham, D. Yi, D. Young and H. Zwally, 2012. A reconciled estimate of ice-sheet mass balance. *Science*, 338:1183-1190.

Slangen, A.B.A., C.A. Katsman, R.S.W. Van de Wal, L.L.A. Vermeersen and R.E.M. Riva, 2012. Towards regional projections of twenty-first century sea-level change based on IPCC SRES scenarios. *Climate Dynamics*, 38:1191-1209.

Tamisiea, M., 2011. Ongoing glacial isostatic contributions to observations of sea level change. *Geophysical Journal International*, 186:1035-1044.

Tedesco, M., S. Doherty, W. Warren, M. Tranter, J. Stroeve, X. Fettweis and P. Alexander, 2015. What darkens the Greenland ice sheet? *Eos*, 96: doi:10.1029/2015EO035773.

Thompson, P.R., B.D. Hamlington, F.W. Landerer and S. Adhikari, 2016. Are long tide gauge records in the wrong place to measure global mean sea level rise? *Geophysical Research Letters*, 43: 10,403-10,411.

van Vuuren, J. Edmonds, M. Kainuma, K. Riahi, A. Thomson, K. Hibbard, G.C. Hurtt, T. Kram, V. Krey, J.-F. Lamarque, T. Masui, M. Meinshausen, N. Nakicenovic, S.J. Smith and S.K. Rose, 2011. The Representative Concentration Pathways: An Overview. *Climatic Change*, 109:5-31.

Young, A.M., P.E. Higuera, P.A. Duffy and F.S. Hu, 2016. Climatic thresholds shape northern high-latitude fire regimes and imply vulnerability to future climate change. *Ecography*, 39:001-012.

10. Cross-cutting scientific issues

LEAD AUTHORS: **JOHANNA MÅRD, JASON E. BOX, ROSS BROWN, MICHELLE MACK, SEBASTIAN H. MERNILD, DONALD WALKER, JOHN WALSH**

CONTRIBUTING AUTHORS: **UMA S. BHATT, HOWARD E. EPSTEIN, ISLA H. MYERS-SMITH, MARTHA K. RAYNOLDS, E.A.G. SCHUUR**

Coordinating lead authors shown in bold

Contents

Key Findings	232
10.1 Introduction	232
10.2 Thresholds and irreversibilities	232
10.2.1 Context	232
10.2.2 Abrupt historical changes	233
10.2.3 Potential future Arctic climate shifts	234
10.2.4 Knowledge gaps and recommendations ..	235
10.3 Arctic tundra vegetation: greening and browning	235
10.3.1 Context	235
10.3.2 Circumpolar level	235
10.3.3 Regional level	239
10.3.4 Landscape level	240
10.3.5 Plot level	241
10.3.6 Knowledge gaps and recommendations ..	241
10.4 Physical disturbance in Arctic terrestrial ecosystems	242
10.4.1 Context	242
10.4.2 Wildfire	242
10.4.3 Abrupt permafrost thaw	243
10.4.4 Mercury cycling and toxicity	245
10.4.5 Knowledge gaps and recommendations ..	246
10.5 Precipitation effects	247
10.5.1 Context	247
10.5.2 Precipitation interaction with climate change processes	247
10.5.3 Rain-on-snow events	248
10.5.4 Ground moisture content	249
10.5.5 Future projections	250
10.5.6 Knowledge gaps and recommendations ..	250
References	250

Key Findings

- Arctic warming projected for 2100 will exceed irreversible thresholds for sea ice, the Greenland ice sheet and possibly the boreal forest.
- Midsummer tundra biomass, as indicated by a greenness index (MaxNDVI), has been increasing, while total seasonal productivity, as indicated by the time-integrated greenness index (TI-NDVI), has recently declined in many areas. These trends from 1982–2015 are likely to be due to a variety of multi-scale hydrological factors, such as late frosts, late snowmelt, increased clouds, and increased surface water due to thermokarst. Field-level studies are needed at a variety of scales to verify and attribute the vegetation productivity trends.
- More frequent physical disturbance events such as wildfire and abrupt permafrost thaw could accelerate biome shifts, including increasing tree density in taiga, expansion of tall shrubs and trees into tundra, and conversion between terrestrial and aquatic ecosystems.
- Increasing disturbance, such as abrupt permafrost thaw is likely to continue to influence the cycling and toxicity of mercury in the Arctic system.
- The pattern of change in Arctic precipitation is complex, with increases in some areas and decreases in others but with an overall increase. Future projections suggest a continued widespread increase in precipitation, especially over the Arctic Ocean.
- Climate-driven increases in the fraction of precipitation falling as rain will accelerate the loss of snow, influencing wildlife and hydrological conditions.

10.1 Introduction

Recent warming in the Arctic has driven significant changes in the cryosphere and the freshwater system. The consequences of Arctic change are complicated by shifting hydrological connections, and ecological dynamics that interact within the Arctic and with the global climate system. Gradual climate change, together with multiple feedbacks, increases the possibility that thresholds are being crossed, and may result in, for example, loss of summer sea ice (see Chapter 5), accelerating Greenland ice sheet loss (see Chapter 6) and ecosystem shifts (this chapter). Previous chapters of this report present a summary of the changes observed since SWIPA 2011 in different components of the Arctic system (snow, freshwater, land ice, sea ice, permafrost), as well as their emerging effects on carbon cycling. This chapter presents an assessment of cross-cutting scientific issues that involve one or more of these components. These include assessments of thresholds and irreversibilities within the Arctic system (Section 10.2), greening and browning of Arctic tundra vegetation (Section 10.3), physical disturbance in Arctic terrestrial ecosystems (Section 10.4) and precipitation effects (Section 10.5).

The topics selected for the current report were identified as being particularly important, and some differ from those covered by SWIPA 2011. Revisited themes include impacts of the changing cryosphere on Arctic ecosystems, and contaminant pathways (with focus on mercury).

Key findings identified here update some of those identified in the cross-cutting chapter of SWIPA 2011 (Callaghan et al., 2011a) and include: changes in hydrologic properties are continuing to affect tundra by introducing spatial complexity into the recently observed trend of greening (i.e. with browning trends in some areas); physical disturbance events (such as wildfire and abrupt permafrost thaw) are continuing to become more frequent and could accelerate biome shifts, and are continuing to affect the cycling and toxicity of mercury; precipitation is still increasing, with the fraction falling as rain increasing due to warming; and Arctic warming projected for 2100 is still likely to exceed thresholds estimated for climate shifts involving sea ice, the Greenland ice sheet and possibly the boreal forest.

10.2 Thresholds and irreversibilities

10.2.1 Context

The rapidity of the ongoing changes discussed in other chapters of this report raises the possibility that thresholds are being approached or crossed. The fact that each year of the past decade has been warmer in the Arctic than the warmest year (1998) of the 20th century suggests that the Arctic climate system may have entered a new regime during the early 2000s. Reid et al. (2016) presented evidence of a global regime shift in the 1980s from sea ice, snow cover and Arctic temperature data. Advances in complex systems theory provide a framework for assessing stability thresholds and irreversibilities in the Arctic system. In this respect, the Arctic's role as a sentinel of global change provides opportunities to bring new perspectives to the global relevance of ongoing environmental change in the Arctic.

Reviews of thresholds and irreversibilities have been recently provided for broader Arctic climate changes (Lenton, 2012) and for Arctic marine ecosystems (Duarte et al., 2012). These studies build on previous research on seasonal sea ice loss and its potential to contribute to a regime shift in Arctic climate (Lindsay and Zhang, 2005; Livina and Lenton, 2013).

There is emerging acceptance in the field of geosciences that there are situations in which a small change in forcing (e.g. global temperature) causes a qualitative change in the future state of the climate system or a subsystem thereof (Lenton, 2012). The resulting change can be abrupt and can be irreversible, although it need not be. The forcing can be external (solar, volcanic, anthropogenic) or can arise from internal climate variability (El Niño Southern Oscillation, Arctic Oscillation). The attribution of abrupt changes and regime shifts in this region is complicated by the large internal variability of the Arctic climate.

10.2.2 Abrupt historical changes

Abrupt climate changes include those during the Eemian interglacial (~125 k BP) when the Arctic Ocean was seasonally ice-free, the treeline underwent a major northward advance, and the Greenland ice sheet shrank enough to raise sea level

by several meters. The Dansgaard-Oeschger events of the past glacial period were characterized by abrupt $\sim 5^{\circ}\text{C}$ temperature shifts occurring over periods of a few years to a few decades at most (e.g. Alley et al., 1993). The rapid cooling of the Younger Dryas (c. 12.9 to 11.7 k BP) persisted for about 1000 years before ending with an abrupt warming of $\sim 7^{\circ}\text{C}$ over just a few years in the North Atlantic.

While paleo changes occurred with external forcing different from the present, more recent changes have occurred with external forcing similar to that of today. In cases of abrupt climate change, positive feedbacks within the climate system became key. Recent (post-1900) Arctic temperatures indicate an abrupt warming ($\sim 1^{\circ}\text{C}$ in the past 100 years) reversing the slow 2000-year cooling ($\sim -0.025^{\circ}\text{C}$ per 100 years) in response to orbitally-driven changes in solar irradiance (Kaufman et al., 2009). Sea ice decline during the past three decades has been attributed to a combination of atmospheric warming, variations in atmospheric circulation and oceanic heat transport into the Arctic, and the albedo-temperature feedback that has accelerated the reduction in sea ice (Kattsov et al., 2011; Stroeve et al., 2012; Overland et al., 2014). A freshwater release from the Beaufort Gyre is likely to have contributed

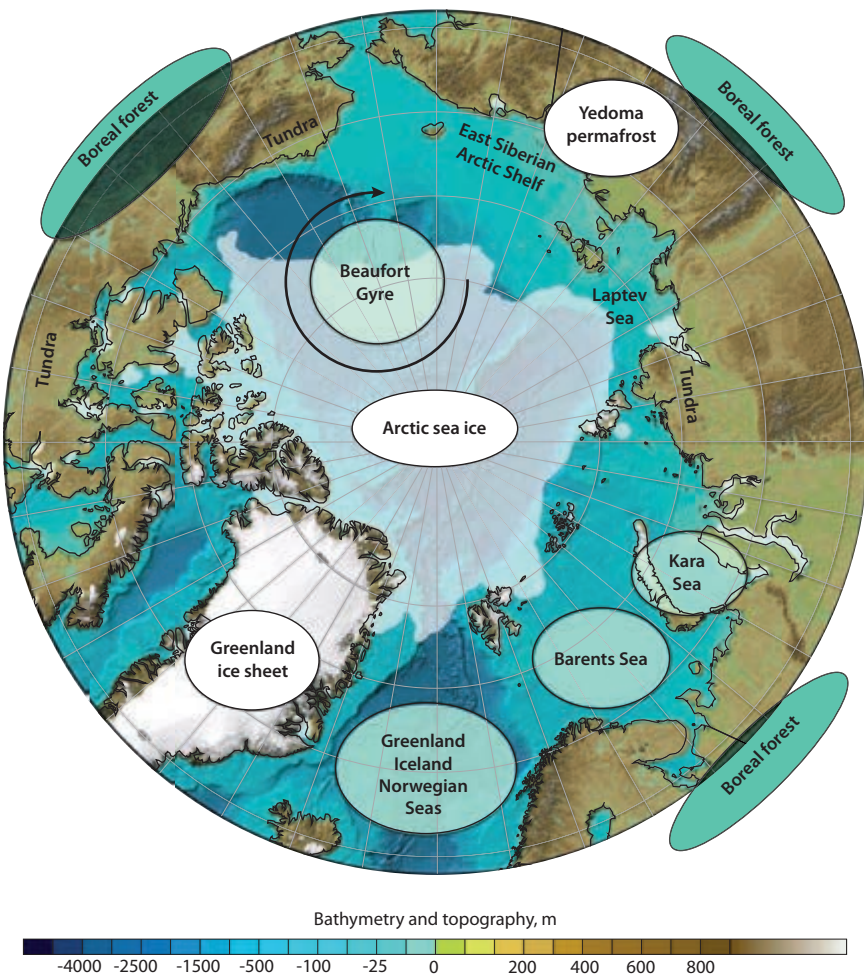


Figure 10.1 Arctic climate system elements involved in abrupt changes and thus representing potential sources of abrupt climate change associated with threshold exceedances (Lenton, 2012). Boreal forest regions have an increased risk of wildfire.

to North Atlantic salinity anomalies during the late 1960s, early 1970s, and late 1990s (Aagaard and Carmack, 1989; Belkin, 2004). The Greenland ice sheet's accelerating loss of mass is linked to increased surface melting (e.g. Box and Colgan, 2013) and the destabilizing effect of warm ocean waters on marine terminating glaciers (e.g. Rignot et al., 2010, 2015; Straneo et al., 2011, 2012). Warmer Atlantic waters are affecting the Arctic Ocean's shelf seas, where submerged permafrost contains large stores of methane, a potential source of abrupt climate change (Shakhova et al., 2015). On land, river discharge has increased (Peterson et al., 2002; McClelland et al., 2006; Shiklomanov and Lammers, 2009; Overeem and Syvitski, 2010; Rawlins et al., 2010), and the lengthening of the snow-free season (Derksen et al., 2015) has led to increased shrub growth at the forest margins as well as to increased wildfire activity in the boreal forest. The fire-climate relationship exhibits thresholds, with a sharp increase in fire probability with increasing summer temperature (Young et al., 2016) and a 1996–2003 increase in 'fire weather' conditions (Jolly et al., 2015). Water temperatures in Arctic streams and rivers are also rising, with implications ranging from a greater contribution to sea ice melt to new risks for temperature-sensitive riverine fish species (Prowse et al., 2011; Wrona et al., 2016). The foci of these ongoing abrupt changes, as well as the potential threshold exceedances and regime shifts discussed in the following section, are highlighted in Figure 10.1.

10.2.3 Potential future Arctic climate shifts

Following the framework of Lenton (2012), Figure 10.2 places the potential Arctic climate regime shifts within a framework of projected global warming to 2100, although the findings of this review are due for a significant update given the substantial increase in new knowledge. The projected warming ranges from about 1.5 to 6°C, depending on the model and the assumed greenhouse gas/aerosol forcing scenario (RCP2.6 to RCP8.5).

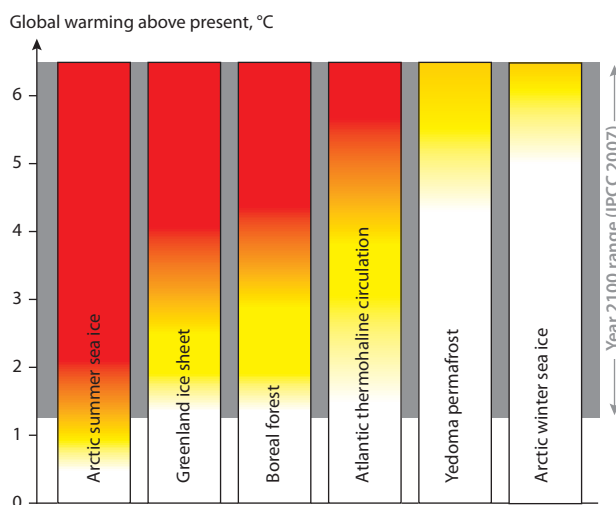


Figure 10.2 Proximity of different threshold exceedances that may alter the state of the Arctic system (Lenton, 2012). Colors represent the likelihood of a regime shift as a function of the increase in global temperature above the 1980–1999 mean. The transition from white to yellow indicates that the likelihood becomes non-zero, while the transition from yellow to red indicates that a regime shift is as likely as not. Dark red indicates that a regime shift is more likely than not.

10.2.3.1 Arctic sea ice

The key feedback for sea-ice loss is the albedo-temperature feedback (Riihelä et al., 2013), although cloud, moisture and atmosphere-ocean circulation feedbacks are also likely to be important (Pithan and Mauritsen, 2014). While sea-ice area and volume have declined during summer by about 40% and 60%, respectively, as compared to mid-20th century values (Kwok and Rothrock, 2009), the loss of summer sea ice is not necessarily irreversible if cooling were to ensue (Eisenman and Wettlaufer, 2009). Moreover, any shift to a regime in which the Arctic Ocean is ice-free all year round appears to require a warming of ~13°C (Winton, 2006), which is highly unlikely during the present century (Figure 10.2, far right).

10.2.3.2 Greenland ice sheet instability

A key feedback in the climate response of the Greenland ice sheet is the elevation-surface temperature feedback. New research lowers the threshold air temperature increase that is potentially capable of triggering irreversible wastage of the Greenland ice sheet from the 2–5°C range (Gregory and Huybrechts, 2006; Kriegler et al., 2009; Huybrechts et al., 2011) to as low as 1.6°C above pre-industrial conditions (with a 95% confidence interval of 0.8–3.2°C; Robinson et al., 2012). Even before the surface mass balance becomes negative, there is a distinct possibility of shrinkage of the ice sheet with multiple paths to different stable states for ice sheet volume. One such transition, possibly already underway, could ultimately lead to a 15% loss of the ice sheet over several centuries and could contribute about 50 cm to global sea-level rise by 2100 (Pfeffer et al., 2008; Colgan et al., 2015).

10.2.3.3 Boreal forest

When summers become too warm for tree species such as spruce, aspen and birch, boreal forests become increasingly vulnerable to drought-driven productivity decline, pests and disease, with more frequent wildfires and decreased reproduction rates. Estimates of thresholds for the warming that would result in boreal forest dieback are in the range 3–4°C of global warming (Lenton, 2012). If such thresholds are crossed, open woodlands or grasslands would replace large areas of the present boreal forest. The reduction in forest canopy area would lead to a reinforcing feedback as the surface would be subject to greater summer warming and drying, which would further increase wildfire frequency (Shuman et al., 2015; Tchebakova et al., 2016).

10.2.3.4 Atlantic thermohaline circulation

While a collapse or stagnation of the North Atlantic thermohaline circulation would have profound consequences for the climate of northern Europe and even globally, a total shutdown over the next century is unlikely (Collins et al., 2013). Nevertheless, global climate models do project a gradual weakening of the North Atlantic thermohaline circulation over the next century, and the Atlantic meridional overturning circulation has weakened over the past few decades in a way that appears unprecedented in at least 1000 years (Rahmstorf et al., 2015). However, the time series of direct ocean measurements supporting this weakening

may be too short to be conclusive given that the Atlantic meridional overturning circulation is known to exhibit low-frequency variations with typical timescales of 50 to 100 years.

10.2.3.5 Permafrost carbon release

While permafrost warming has been detected in many areas (see Chapter 4), thawing will primarily affect the near-surface permafrost layer with significant effects on local ecosystems and the global carbon cycle. The downward progression of thaw is a slow process, so much of the deep permafrost (i.e. tens to hundreds of meters deep) will remain frozen for at least the next century under almost any climate scenario. Moreover, even the upper layers of warming permafrost will reach the freezing point at different times in different areas. While Figure 10.2 depicts permafrost to be stable relative to the other system components, this is likely to be true only for deep permafrost. Surface permafrost is highly likely to transition to a new state by 2100 under the current path of warming. It is the surface permafrost (0–3m soil depth) that contains a large quantity of organic carbon that is vulnerable to thaw and release to the atmosphere. As one example, the Yedoma region of northeastern Siberia, containing large amounts of carbon in the form of frozen loess and subject to thaw by heat generated internally through biogeochemical decomposition of carbon-containing material (Khvorostyanov et al., 2008), could release large amounts of carbon dioxide (CO_2) and methane (CH_4). Methane release from thermokarst expansion zones of Arctic lakes is projected to increase in the 21st century (Walter Anthony et al., 2016; see also Section 10.4.3). Large reservoirs of permafrost-held CH_4 are also present in the subsea permafrost of the Siberian shelf seas. Again, however, catastrophic releases (large quantities in less than a decade) over the next century are considered unlikely although other opinions exist (Shakhova et al., 2015). There is the potential for 130 to 160 billion tonnes of carbon to be released to the atmosphere by 2100 as the greenhouse gases CO_2 and CH_4 under the current warming trajectory, which would accelerate climate change (Schuur et al. 2015).

10.2.3.6 Others

The five system components highlighted in this review are arguably among the most likely to contribute to regime shifts in the Arctic system. However, there are also other possibilities, including range expansion of shrub and forest biomes into today's tundra regions, Arctic stratospheric ozone loss, changes in location of oceanic deep convection associated with changes in the subpolar gyre, changes in primary production in the Arctic (see Section 5.4.2), and other marine ecosystem changes (Duarte et al., 2012). Finally, there remains the possibility of a surprise threshold or source of regime shift, especially given the poorly understood processes and linkages in the Arctic climate system. Unanticipated external influences such as catastrophic volcanic eruptions and meteor impacts fall within this category of potential surprises (Stenchikov et al., 2002; Robock and Oppenheimer, 2003).

10.2.4 Knowledge gaps and recommendations

The amount of warming needed to effect a regime shift in the Arctic system remains uncertain. For example, Arctic terrestrial system regime shifts, especially in the boreal forest, are poorly known and in need of quantification. Observation-

driven modeling represents a way forward for addressing this knowledge gap. The irreversibility of regime shifts for sea ice is also not well understood. Given the importance of sea ice for the future rate of Arctic warming, the irreversibility of large and rapid sea ice changes (including those of the past decade) must be a priority for research. Evaluating Greenland's regime shifts must also be a priority, especially in the context of the Greenland ice sheet mass balance and its impacts on global sea level and ocean thermohaline circulation. Further, the strength of the Atlantic thermohaline circulation, which may undergo a regime shift associated with Arctic change, represents a major observational need with direct observational records too short to separate inter-decadal internal variability from a clear climate change signal. Systematic monitoring of oceanic heat transport into the Arctic, together with an improved understanding of the fate of this heat, are keys to the explanation of sea ice retreat and associated Arctic Ocean regime shifts.

10.3 Arctic tundra vegetation: greening and browning

10.3.1 Context

Arctic greening has been observed across tundra ecosystems over the past 30 years, with a shift towards browning in some areas since the early 2000s. This section examines observed changes in vegetation productivity over the past 34 years (1982–2015) and relates these to climate variables and their effects on greening at different spatial scales.

Circumpolar studies of the spatial and temporal variations in Arctic vegetation derived from satellite data and field observations are increasingly pointing to causal factors of change that are linked to snow, freshwater availability, ice distribution, and permafrost (Raynolds and Walker, 2008, 2009; Elmendorf et al., 2012; Bhatt et al., 2013; Piao et al., 2014; Forkel et al., 2015; Myers-Smith et al., 2015). Because these causal factors are interrelated in complex ways involving geography and geology, a hierarchical approach is useful for examining some of the cross-linkages between Arctic system elements (snow, water, ice, permafrost) and greening patterns at circumpolar, regional, landscape and plot scales (Figure 10.3). A current challenge is to interpret and link the information derived from observations at different scales.

10.3.2 Circumpolar level

Decadal-scale positive trends in Arctic productivity were first noted at the circumpolar level (Myneni et al., 1997; Jia et al., 2003; Goetz et al., 2005; Bunn and Goetz, 2006; Bhatt et al., 2010). The main Arctic-system factors affecting circumpolar tundra greening patterns involve atmospheric and oceanic circulation, sea-ice distribution, and river input of relatively warm freshwater into the Arctic Ocean (Figure 10.3). These factors affect atmospheric moisture and land-surface temperatures at the circumpolar scale, which in turn influence circumpolar snow, cloudiness, summer temperatures, and spatial and temporal greening patterns.

The normalized difference vegetation index (NDVI) derived from GIMMS (Global Inventory Modeling and Mapping Studies) data (Tucker, 1979) is the most commonly used

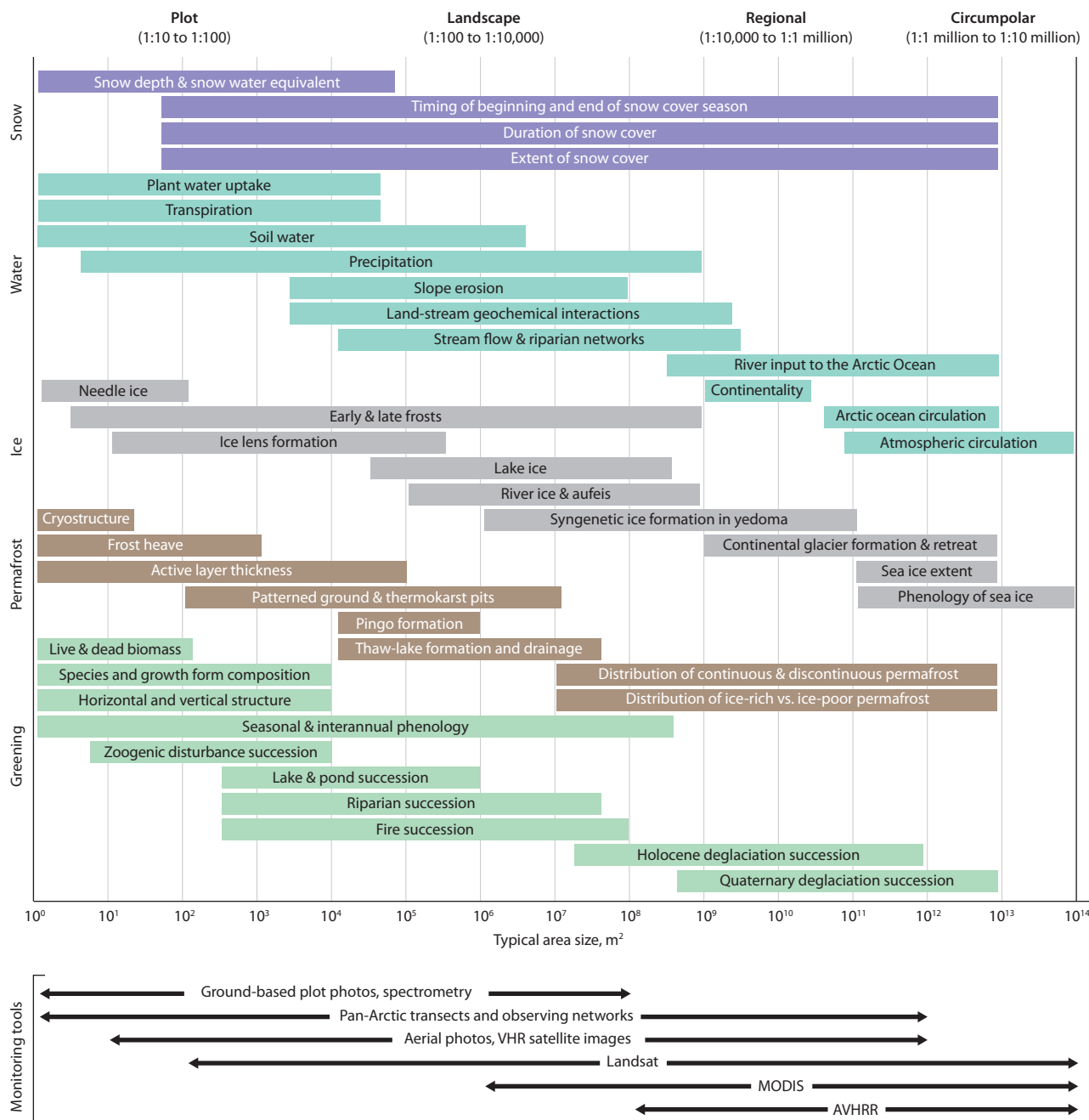


Figure 10.3 A hierarchical framework for examining vegetation greening in relation to snow, water, ice and permafrost. Reading downwards within a hierarchical level gives an impression of the main snow, water, ice, and permafrost factors affecting tundra greening patterns at each scale. The horizontal arrows below the graphic show scales for some of the common monitoring tools used to observe patterns at each scale.

index of vegetation biomass and productivity (see Box 10.1). A spatial comparison of change in AVHRR-derived annual maximum NDVI (MaxNDVI) between 1982 and 2015 provides a long-term view of the general trend in annual maximum aboveground green biomass (Figure 10.6). The graphic also shows spatial differences in the change in the annual sum of bi-weekly maximum NDVI values that exceed a minimum threshold value. Time-integrated NDVI (TI-NDVI) is generally considered a robust proxy for annual net primary productivity (Goward et al., 1985; Justice et al., 1985).

MaxNDVI increased in most areas of the Arctic tundra between 1982 and 2015 (green areas in Figure 10.6 and positive trend lines in Figure 10.7), with exceptions in the delta regions of the Yukon and Kuskokwim rivers of Alaska, the northern

High Arctic of Canada, northwestern Siberia, and parts of Chukotka, which show negative MaxNDVI trends (brown areas in Figure 10.6). The positive trends for the entire Arctic (+12%), Eurasian Arctic (+7%), and North American Arctic (+17%) (Figure 10.7) probably indicate a general increase in biomass over most of the Arctic except in the areas of declining MaxNDVI (Epstein et al., 2017).

TI-NDVI shows more variable trends, with positive changes in most of the Arctic, but also large areas of negative trends in the delta regions of the Yukon and Kuskokwim rivers of Alaska, the Seward Peninsula, northern High Arctic of Canada, northwestern Siberia, northern Yamal and Gydan peninsulas, western and northern Taymir Peninsula, and northern Chukotka (Figure 10.6). TI-NDVI has declined since 2001 over much of the

Box 10.1 Normalized difference vegetation index

The normalized difference vegetation index (NDVI) is the most common satellite-derived index used to monitor global-scale vegetation patterns. NDVI contrasts the reflectance in the visible portion of the spectrum, where plant chlorophyll absorbs maximally, with the near infra-red portion, where leaf and canopy structure cause strong reflectance (Figure 10.4). This response increases with vegetation amount and differs strongly compared to the reflectance of bare soil or water.

The difference between reflectance in the satellite channels that measure these parts of the spectrum (AVHRR Channels 1 (visible) and 2 (near infrared)) is then divided by the sum, to normalize the index for variations in incident radiation due to sun angle and other illumination factors.

AVHRR Channel 2 – AVHRR Channel 1

AVHRR Channel 2 + AVHRR Channel 1

The result is a robust index of vegetation that is interpreted as the photosynthetic capacity of the vegetation (Tucker and Sellers, 1986) or its 'greenness' and is correlated with ground measurements of biomass, leaf-area index, intercepted photosynthetically active radiation, carbon dioxide flux and other measures of tundra photosynthetic activity (Stow et al., 1993). Maximum annual NDVI (MaxNDVI) is more closely related to biomass, while time-integrated NDVI across the growing season (TI-NDVI) is a better measure of seasonal productivity (Goward et al., 1985). NDVI saturates at high

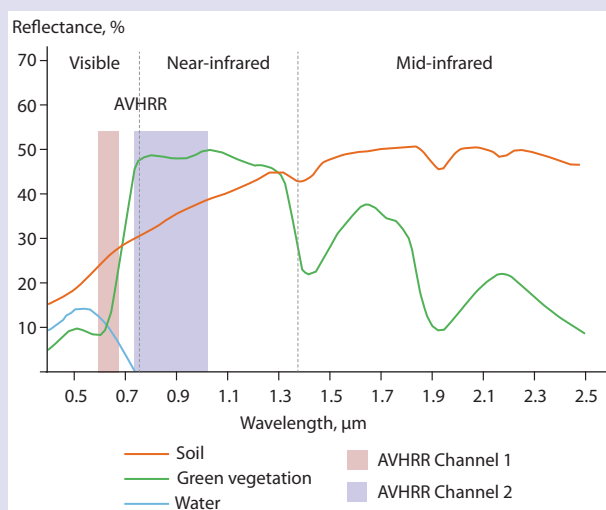


Figure 10.4 Typical top-of-atmosphere reflectance of soil, vegetation and water. The spectrum is divided to show the wavelengths used to calculate NDVI. The colored bars show the band-widths measured by the Advanced Very High Resolution Radiometer (AVHRR) on NOAA satellites.

levels of vegetation cover, so is especially effective for non-forested and sparsely vegetated areas such as the Arctic. A circumpolar map of aboveground phytomass was created using the correlation between zonal aboveground biomass and NDVI along two transects in North America and Eurasia (Figure 10.5) (Raynolds et al., 2012).

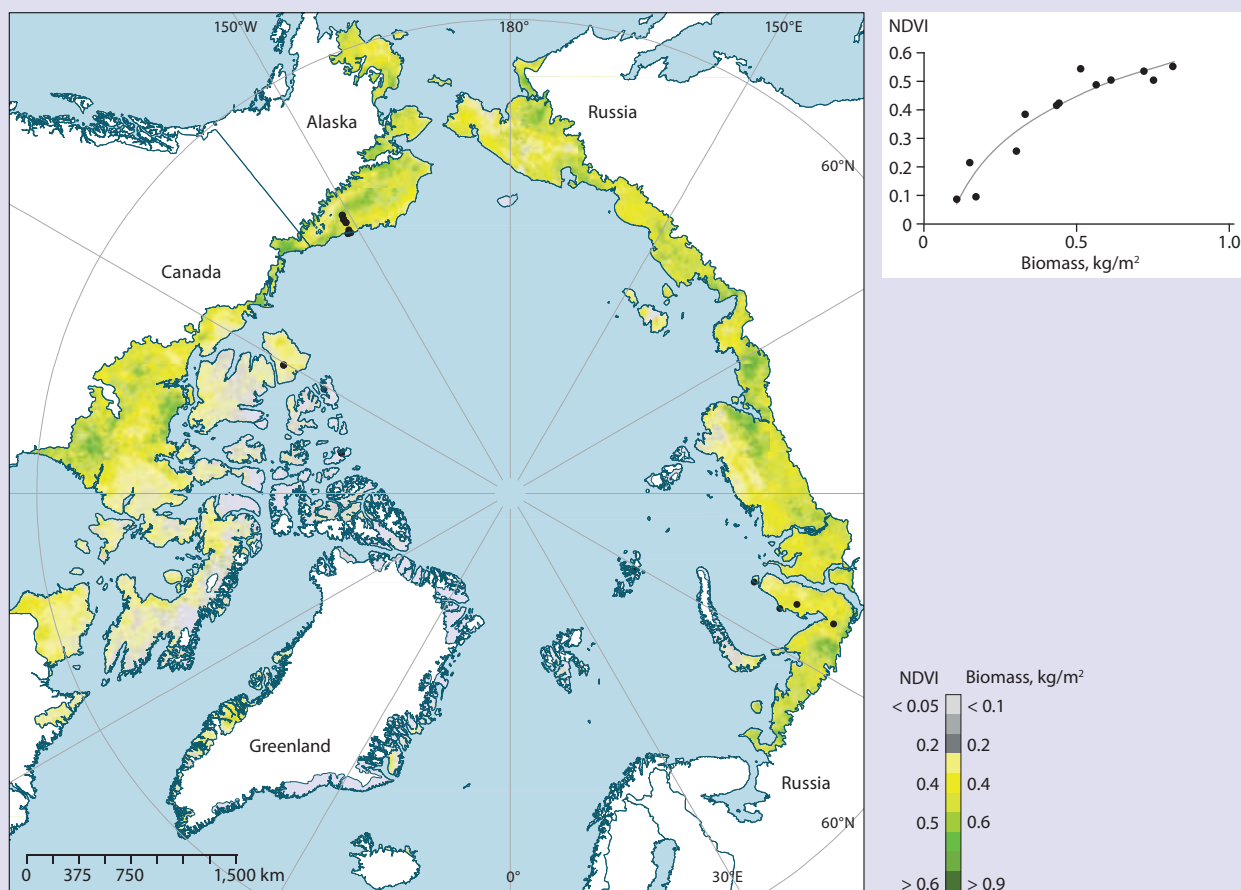


Figure 10.5 NDVI from the Global Inventory Modelling and Mapping Studies (GIMMS3g, Pinzon and Tucker 2014) and related above-ground plant biomass in the Arctic in 2010. The relationship between plant biomass and NDVI, shown in the graph in the upper right, was developed from field sampling of zonal sites in North America and Eurasia (Raynolds et al., 2012).

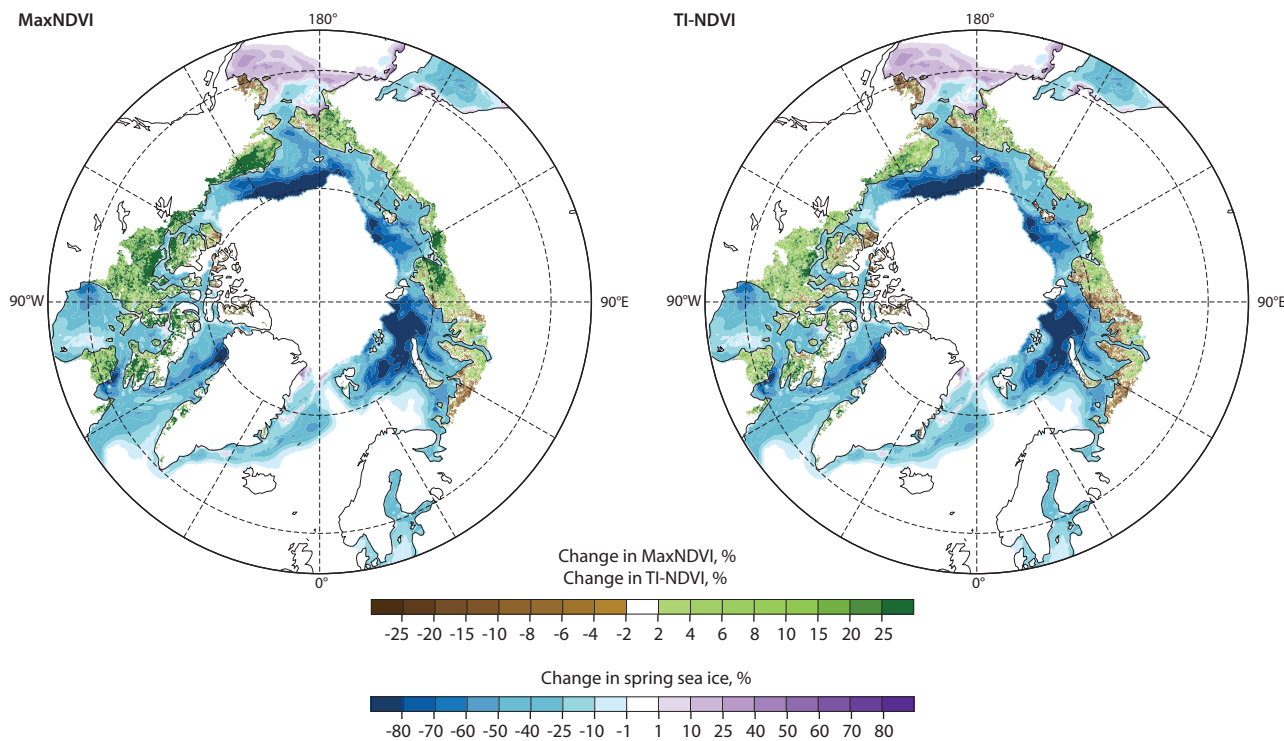


Figure 10.6 Change in annual maximum NDVI (MaxNDVI; left) and time-integrated NDVI (TI-NDVI; right) between 1982 and 2015 (Bhatt et al., 2010, updated to 2015). Both graphics also show change in spring sea-ice concentration. Change in NDVI is determined from the Global Inventory Modeling and Mapping Studies datasets (Pinzon and Tucker, 2014) and change in sea ice from Special Sensor Microwave Imager sea-ice concentrations (Comiso and Nishio, 2008).

Eurasian Arctic while the trend in the North American Arctic has been fairly flat (Figure 10.7) (Bhatt et al., 2017; Epstein et al., 2017). MaxNDVI increased from 1982 to 2002 in the Eurasian Arctic and until 2010 in the North American Arctic. MaxNDVI then declined by 8.4% between 2011 and 2015, and TI-NDVI by 8.7% (12% for the Eurasian Arctic) (Figure 10.7). The negative trends may indicate declining annual productivity, but this needs to be confirmed with field data. Long-term monitoring of High Arctic stations shows generally positive increases in plant cover and biomass (Hudson and Henry, 2009).

A recent global analysis of NDVI and the fraction of absorbed photosynthetically active radiation at the global

scale found seasonal freshwater availability and land-cover/land-use changes have major effects on trends in peak greenness in all regions of the globe (Forkel et al., 2015). In tundra regions, warming trends are amplified by feedbacks associated with the reduction in the extent of highly reflective sea ice (Serreze and Francis, 2006) and greater absorption of heat by the ocean (Steele et al., 2008). The warming trends also extend to land areas (Lawrence et al., 2008), where there is an increased risk of permafrost degradation (Shur and Jorgenson, 2007; Jorgenson et al., 2010; see also Chapter 4) and increased quantities of freshwater on low-lying landscapes (Liljedahl et al., 2016; Raynolds and Walker, 2016b; see also

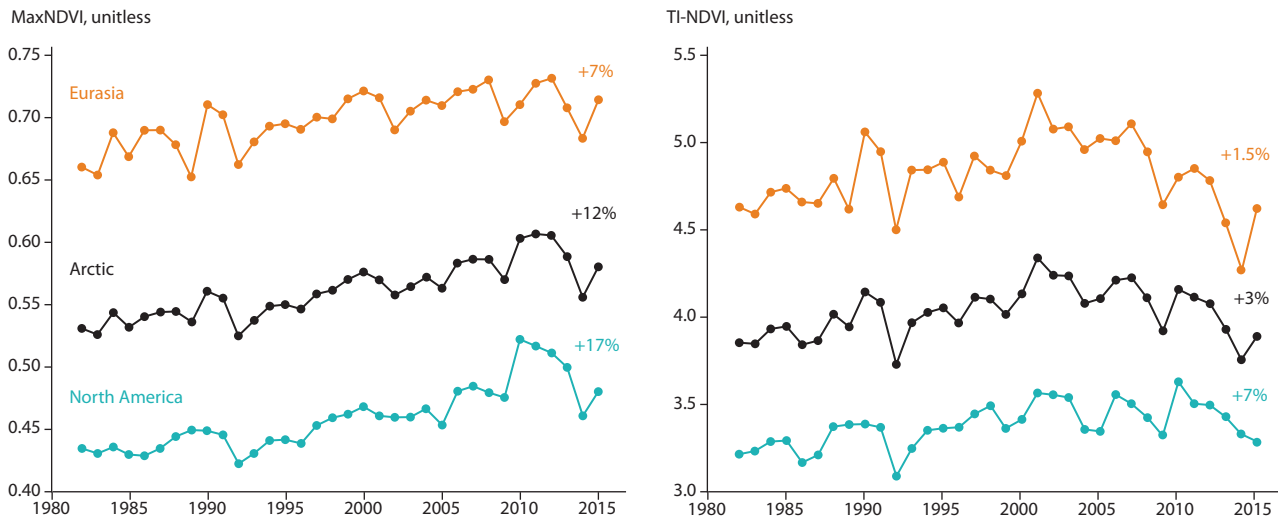


Figure 10.7 Change over time in annual maximum NDVI (MaxNDVI; left) and time-integrated NDVI (TI-NDVI; right) for the North American Arctic, Eurasian Arctic and Arctic as a whole (1982–2015) (Bhatt et al., 2010, updated to 2015).

Chapter 7). These changes are not limited to warm permafrost areas in the Low Arctic. Widespread and rapid thermokarst with extensive ponded freshwater occurred during the last decade within 1 km at all three of Vladimir Romanovsky's High Arctic long-term permafrost monitoring sites on Ellef Ringnes, Prince Patrick, and Banks Island, Canada (Farquharson et al., 2016). A warming summer climate caused warmer ground temperature, increased active layer depth, ice wedge melt, subsequent ground subsidence, and ponding. Between 2005 and 2013, active layer depth increased at Isachsen, Mould Bay and Green Cabin by up to 20, 30, and 40 cm respectively. Permafrost thaw and the resulting changes in soil moisture and nutrient dynamics are likely to be related to greening of tundra vegetation particularly in areas of subsidence where water accumulates but does not pond. Increased water availability is thought to increase greening

through increase in productivity of all plant growth forms, and especially increased shrub cover in the Low Arctic tundra (Elmendorf et al., 2012; Myers-Smith et al., 2015).

10.3.3 Regional level

Earlier analyses indicated that regions with large sea-ice declines generally showed increased terrestrial warming and positive NDVI (Bhatt et al., 2010). However, the situation has become more complicated since about 2002; the latest trends are shown in Figure 10.8. For example, the Baffin Bay region showed the expected trends (based on earlier observations) with strong sea-ice retreat, a strong increase in the summer warmth index (SWI, i.e. sum of mean monthly temperatures exceeding 0°C) on land, and a strong increase in MaxNDVI. The Beaufort Sea region also exhibited a strong and highly variable negative trend in spring

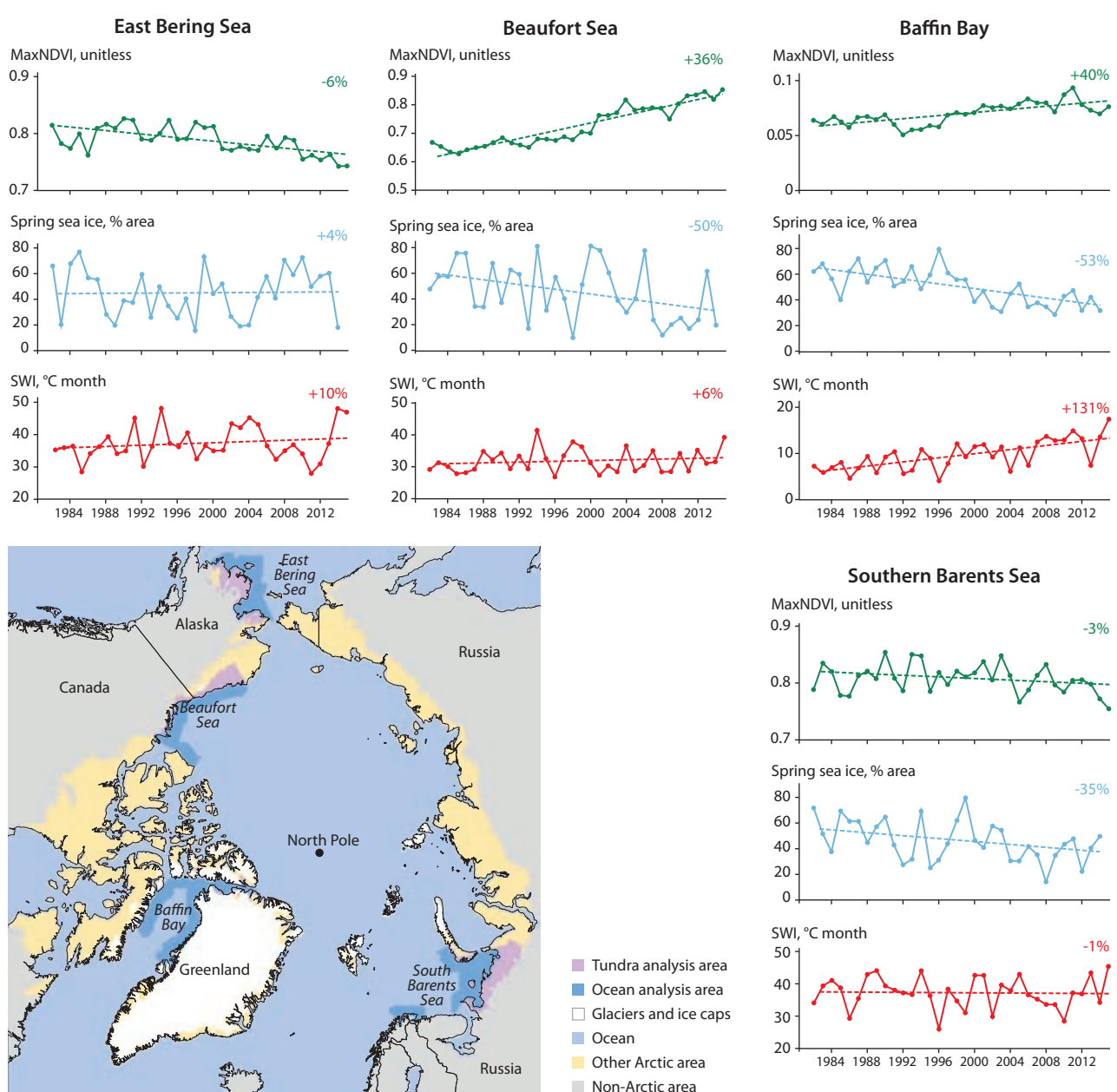


Figure 10.8 Trends in spring sea-ice extent within 100 km of the coast, Summer Warmth Index (SWI), and MaxNDVI for the period 1982–2015, for four areas exhibiting large and contrasting changes in sea-ice extent: East Bering Sea, Beaufort Sea, Baffin Bay and southern Barents Sea (Bhatt et al., 2010 updated to 2015). Sectoral divisions in the Arctic Ocean are according to the Russian Arctic Atlas (Treshnikov, 1985) and the adjacent land areas according to the phytogeographic subdivisions (Yurtsev, 1994).

ice-extent, but a non-significant SWI trend, and a strong increase in MaxNDVI. In contrast, the East Bering Sea is one of the few areas showing a positive sea-ice trend. This was accompanied by a slight increase in SWI, and a negative MaxNDVI trend. In the southern Barents Sea, a negative sea-ice trend was accompanied by a negative SWI trend and slightly negative trend in the MaxNDVI (Bhatt et al., 2010, updated to 2015).

The reversal of earlier positive trends in NDVI in some parts of the Arctic is thought to be due, in part, to reduced mid-summer coastal sea ice, and to increased amounts of open water and increased ocean-heat content, which influence atmospheric moisture levels over the Arctic Ocean and nearshore environments, and in turn affect fog, cloud cover, mid-summer air temperatures, and the length of the snow-free season (Bhatt et al., 2013). The interplay between these factors varies regionally. A detailed analysis in Alaska examined the sea-ice, land-surface temperature, NDVI, snow (1982–2013), and ocean-heat (1988–2013) trends in the Beaufort, East Chukchi, and East Bering regions (Bieniek et al., 2015). Sea ice declined throughout summer and autumn in the Beaufort and East Chukchi Seas, and increased through winter and spring in the Bering Sea. Ocean heat in summer showed warming trends in the Beaufort and East Chukchi seas, and cooling trends in the East Bering Sea. On land, surface temperatures warmed from late summer to autumn but cooled during midsummer in all three regions (Bieniek et al., 2015). The summer cooling was attributed to increased summer cloudiness in all three areas. NDVI showed increases over most of the summer (except late May) in the Beaufort and East Chukchi seas, and a decline in the East Bering Sea. The early summer declines were thought to be due to increased winter and spring snow in all three areas. The longer open-water season could be causing increased atmospheric moisture and cloud cover, which could in turn lead to large-scale climate change. Further investigations with field data and models would be useful for trend confirmation.

Detailed examination of variations in regional NDVI patterns due to geographic and terrain factors could help clarify causes for the circumpolar patterns. For example, latitudinal variations in NDVI (Raynolds et al., 2008) are constrained by historical differences in glacial geology because of relatively low productivity on younger glacial surfaces (Walker et al., 1995; Raynolds and Walker, 2009). Elevation gradients and different types of bedrock affect vegetation in the Arctic mountains (Cooper, 1986; Sieg and Daniëls, 2005). Studies in mountainous regions outside the Arctic have shown strong correspondence between elevation and NDVI patterns (Walker et al., 1993; Asner et al., 2014). Permafrost-related characteristics accounted for about 11% of the regional variation in NDVI; high-ice-content permafrost with shallow overburden is strongly correlated with lower NDVI (Raynolds and Walker, 2008). Thick moss layers and erect shrubs have the greatest effect on soil-temperature regimes, and vegetation types with both of these components occur in areas with medium to high permafrost ice-content, and in areas with discontinuous permafrost.

Snow-related factors include phenology patterns that are affected by snow extent and the timing of snow cover along latitudinal and elevational temperature gradients (Oberbauer et al., 2013; Bjorkman et al., 2015). Pan-Arctic studies of snowmelt patterns (Liston and Hiemstra, 2011; Derksen et al., 2015) have generally not supported the hypothesis that later snow melt is contributing to the recent

early-summer declines in NDVI as noted by Bhatt et al. (2013). Other hydrologically-related regional-scale factors that could reasonably cause negative NDVI patterns include early or late frost events (Wheeler et al., 2014), rain-on-snow events (Bartsch et al., 2010), the regional effect on temperatures of near-coastal oceanic currents, continentality gradients such as those in long Greenland fjords, and large north-flowing rivers discharging relatively warm freshwater into the Arctic Ocean. These other factors have not been systematically linked to the observed global and regional variations in greening, but such studies are needed.

The main Arctic-system factors affecting regional patterns of tundra greening are summarized in Figure 10.3 and include the timing of the snow-cover season; the duration and extent of snow cover; freshwater inputs to the Arctic Ocean from rivers; regional continentality; the distribution of continuous and discontinuous permafrost, and ice-rich vs. ice-poor permafrost; the amount of syngenic ice in regional Yedoma deposits; and landscape and vegetation succession related to continental-scale glaciations.

10.3.4 Landscape level

Greenness patterns at the landscape level are mostly related to mesoscale differences in water, snow, and vegetation distribution associated with slopes and small watersheds. Predictable relationships between soil moisture, snow, active layer, plant community structure, composition and productivity, NDVI, and trace-gas flux have been described along toposequences (Billings, 1973; Giblin et al., 1991; Shaver et al., 1996; Walker and Walker, 1996; Birkeland, 1999; Jorgenson, 2000; Euskirchen et al., 2012; Ropars et al., 2015).

Slope-stream interfaces are another focus of research (Stieglitz et al., 2003) where, for example, small drainage channels (water tracks) on hill slopes are sites of enhanced productivity (Tape et al., 2012; Swanson, 2015). Figure 10.9 illustrates the striking differences in productivity associated with water tracks, as implied by the strong differences in reflectance in the near infrared part of the spectrum in the false-color infrared images of a watershed in the northern foothills of Arctic Alaska (Tape et al., 2012).

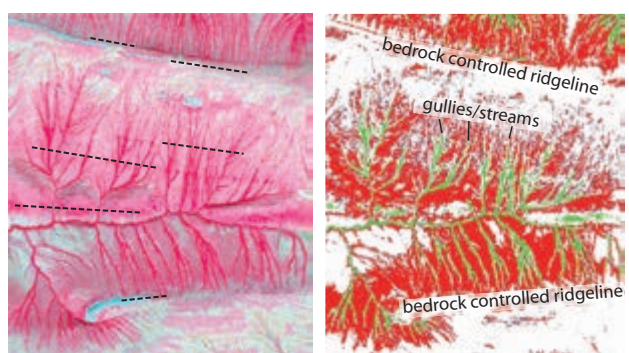


Figure 10.9 False color-infrared satellite image near the Chandler River in Alaska showing tall shrubs (dark red) distributed along streams and sedimentary rock outcrops (left) and a supervised classification of the image, showing expanding alder patches (green) in the centers of the water tracks, stable alder patches on hill slopes (red), and short- or non-shrub tundra elsewhere (white) (right). Each image is 5.5-km wide, with a center point at 68.917°N, 151.765°E; north is up (Tape et al., 2012).

Greenness patterns at the landscape level also include responses to disturbance (see Section 10.4), including thermokarst (Jorgenson et al., 2006; Raynolds et al., 2014a; Jones et al., 2015), landslides (Lantz et al., 2009; Ukrainstseva et al., 2014), fire (Mack et al., 2011; Bret-Harte et al., 2013), herbivory (Johnson et al., 2011; Väistönen et al., 2014), small-scale patterned ground features (e.g. frost boils; Frost et al., 2013), and human activities (Kumpula et al., 2012; Raynolds et al., 2014b). Such disturbances typically enhance snow cover, water, soil temperatures, and nutrient regimes, resulting in increased productivity.

In summary, Arctic-system factors related to tundra greening that are important at the landscape level (Figure 10.3) include those related to snow (timing of the snow-cover season and extent of snow cover); water (local precipitation, landscape-scale variations in soil-water availability, slope erosion, land-stream geochemical interactions, and streamflow in riparian networks), ice (early and late frost, effects of lake ice, river ice and aufeis, and ice wedges), permafrost (landscapes with small-scale patterned ground and thermokarst pits, pingos, and thaw-lake formation and drainage), and disturbances (natural and human).

10.3.5 Plot level

Most observations of water, nutrient availability, and plant growth are conducted at the plot level (e.g. Chapin et al., 1988; Kjelland and Chapin, 1992), but plot-based studies examining vegetation transformation due to actual climate change (as opposed to experimental warming, fertilization, watering, and snow-fence experiments) are rare. Most studies of the effects of climate change at the plot scale have examined warming in control plots of experimental manipulations, such as those of the International Tundra Experiment (ITEX; Elmendorf et al., 2012, 2015), or the effects of climate on radial growth of shrub species including willow, alder, *Cassiope*, and other tall and dwarf species (Myers-Smith et al., 2015). A synthesis of plant phenological responses to temperature variation within the ITEX control plots did not show any systematic advance in phenology related to warming; instead, temperature variability during the years sampled and an absence of warming at some sites resulted in mixed responses (Oberbauer et al., 2013). Plants of different communities and growth forms differed in their phenological responses. These results point to complex changes in plant communities and ecosystem function at high latitudes and elevations as the climate warms.

Only a few studies have attempted to examine changes to the full suite of habitat types and associated plant communities within large landscapes (Daniëls et al., 2010; Callaghan et al., 2011b; Villarreal et al., 2012). Even fewer have examined variations in the spectral properties of the diversity of plant communities across large landscapes (Shippert et al., 1995; Laidler et al., 2008; Boelman et al., 2011; Atkinson and Treitz, 2013; Buchhorn et al., 2013; Bratsch et al., 2016). These studies reveal site-specific factors that are often more important than regional temperature for controlling productivity, population structure and populations of Arctic plants (Elmendorf et al., 2012, 2015; Oberbauer et al., 2013). Changes in snow cover, water availability, and freeze-thaw events are likely to influence tundra vegetation, particularly shrubs (Preece and Phoenix, 2014; Wheeler et al., 2014), but also graminoid species (Gould and Mercado-Díaz, 2014), and mosses (Jägerbrand et al., 2012), especially in maritime areas of extensive paludification

(Crawford et al., 2003). The timing of snowmelt strongly affects the phenology of plants (Walker et al., 2001; Høye et al., 2007; Bjorkman et al., 2015; Wheeler et al., 2015). Plot-level studies at the High Arctic research site, Zackenberg, in Greenland revealed that during a period of strong regional warming, when the date of snowmelt became earlier by over two weeks (Høye et al., 2007; Wheeler et al., 2015), there was a strong negative trend in NDVI in all six vegetation types studied, indicating that factors other than warming were driving the negative trends in greenness (Ellebjerg et al., 2008). The study concluded that earlier snowmelt limits summer moisture availability and plant productivity unless compensated for by summer precipitation.

In summary, a large suite of Arctic system factors affect the greenness of vegetation at the plot level (Figure 10.3), including microscale and landscape variations in the depth, water equivalent, timing and duration of snow cover; soil water availability; plant-water uptake and transpiration; needle-ice disturbance; early and late frosts, and frost heave; active-layer thickness; development of small-scale patterned-ground features; and thermokarst of ice wedges. These, in turn, affect a wide range of plant factors that influence vegetation greenness as seen from space, including the amount of live and dead biomass, the species and growth-form composition of the plant canopy, horizontal and vertical structure of the plant canopy, seasonal and interannual variation in phenology, and succession following small-scale disturbances such as those related to small animals and larger grazing herbivores, or larger-scale succession following fire, thaw-lake drainage, or river-channel changes.

10.3.6 Knowledge gaps and recommendations

The large number of water-related variables affecting plant-related factors, makes field studies to determine actual hydrological causes of greenness change at plot to regional scales a desirable focus of future research. Coordinated ecological, hydrological and cryospheric monitoring efforts are needed to improve understanding of Arctic tundra greening and its interactions with changes in climate. Analyzing the spatio-temporal patterns in Arctic greening in conjunction with Arctic-system hydrological elements (e.g. snow, water, ice, permafrost) will be important for identifying the key variables, characteristics, and types of related changes that trigger vegetation responses. A coordinated monitoring approach of this type will also be useful for linking ground-based and satellite-derived observations across spatial and temporal scales.

A coordinated approach for collecting plot-based information and for linking ground-based observations to satellite-derived observations in a hierarchy of spatial scales would be facilitated by standardized interdisciplinary monitoring methods. Coordinated methods can be used to examine the variations in a set of site factors, including Arctic-system elements, vegetation, and spectral properties from a full suite of vegetation-habitat types and mapping units in a hierarchy of spatial scales across a broad range of terrestrial locations within the Arctic Observing Network (Lee et al., 2015; Walker et al., 2016). Increased application of time series of very-high-resolution satellite imagery and inexpensive means to obtain airborne images, such as drones and balloons, would help efforts to extrapolate the results of ground-based studies to broader regions and the circumpolar Arctic.

10.4 Physical disturbance in Arctic terrestrial ecosystems

10.4.1 Context

Disturbance is integral to most ecosystems on Earth, and their dynamics are largely shaped by patterns and processes of post-disturbance recovery (White and Jentsch, 2001). As climate changes, however, the nature of disturbance in many ecosystems is also changing, increasing uncertainty about how ecosystem and regional dynamics will play out in the future. In the Arctic, where average surface air temperatures are increasing at around twice the global average (Bindoff et al., 2013), physical disturbances are intensifying. Recent observations suggest that climate-sensitive disturbance events, such as wildfire and abrupt permafrost thaw, are increasing in frequency, intensity, and magnitude across many Arctic regions, driven by gradual climate warming (Jorgenson et al., 2013), extreme weather events (Balser et al., 2014), and interactions between disturbances, such as those between abrupt thaw and wildfire (Hu et al., 2015; Jones et al., 2015) or human activities (Jorgenson et al., 2006). In the case of coastal ecosystems, increased wave action due to loss of shore-fast ice is an additional driver of increased erosion rates and, in the case of permafrost coastlines, abrupt thaw (Lantuit et al., 2012). Because these disturbances affect permafrost (Schuur et al., 2008; Grosse et al., 2011), hydrology (Osterkamp et al., 2009; Vonk et al., 2015), and vegetation composition (Lantz et al., 2009; Pizano et al., 2014), increased rates have the potential to catalyze rapid and persistent changes in the structure and function of Arctic ecosystems. Understanding the mechanisms that determine when and where climate-sensitive disturbances fundamentally alter ecosystem dynamics is critical for predicting the future state of the Arctic system, its ability to support the health and wellbeing of local stakeholders, and its changing impacts on global climate.

10.4.2 Wildfire

One of the most rapid pathways by which climate warming can alter the structure and function of Arctic ecosystems – and their impact on the Earth system – is through intensification of wildfires (Figure 10.10; Kasischke et al., 1995; Harden et al., 2000; Chapin et al., 2008; Hu et al., 2010, 2015; Mack et al., 2011; Turetsky et al., 2011; Kelly et al., 2016). The majority of organic carbon sequestered in Arctic tundra and taiga ecosystems resides in a thick soil organic layer that can be hundreds to thousands of years old; this is a carbon legacy of past fire cycles (Harden et al., 2000). Combustion of the soil organic layer dominates carbon emissions during fire (Kasischke et al., 1995;

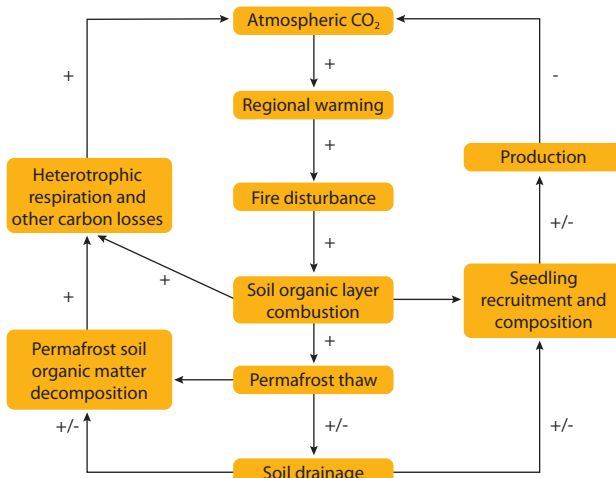


Figure 10.10 Hypothesized indirect radiative forcing of climate change through the effects of increased fire disturbance on the structure and function of Arctic ecosystems.

Boby et al., 2010; Mack et al., 2011), and more intense fires result in deeper burning (Turetsky et al., 2011). Because rates of soil carbon accumulation vary across the landscape (Hobbie et al., 2000), deeper burning may not always combust legacy carbon (Mack et al., 2011). But deeper burning that does combust legacy carbon could rapidly shift ecosystems across a carbon cycling threshold: from net accumulation of carbon from the atmosphere over multiple fire cycles to net loss.

Disturbances that impact the organic soil layer can persistently alter both physical and biological controls over carbon cycling, including permafrost stability, hydrology, and vegetation (Figure 10.10). Reduction or loss of the soil organic layer decreases ground insulation (Shur and Jorgenson, 2007; Jorgenson et al., 2013; Jiang et al., 2015), warming permafrost soils and exposing organic matter that has been frozen for hundreds to thousands of years to microbial decomposition, mineralization, and atmospheric release of greenhouse gases (Schuur et al., 2008). Degradation of permafrost can also increase or decrease soil drainage, leading to changes in soil moisture regimes that impact both decomposition and production (Schuur et al., 2009; Jorgenson et al., 2013). These changes may also lead to abrupt thaw and thermal erosion events (see Section 10.4.3) that drive further change in ecosystem processes. Loss of the soil organic layer also exposes mineral soil seedbeds (Johnson, 1992; Johnstone et al., 2009) leading to recruitment of deciduous tree and shrub species that do not establish on organic soil (Johnstone and Chapin, 2006). This has been shown to shift post-fire vegetation to alternate successional trajectories (Figure 10.11; Johnstone et al., 2010).

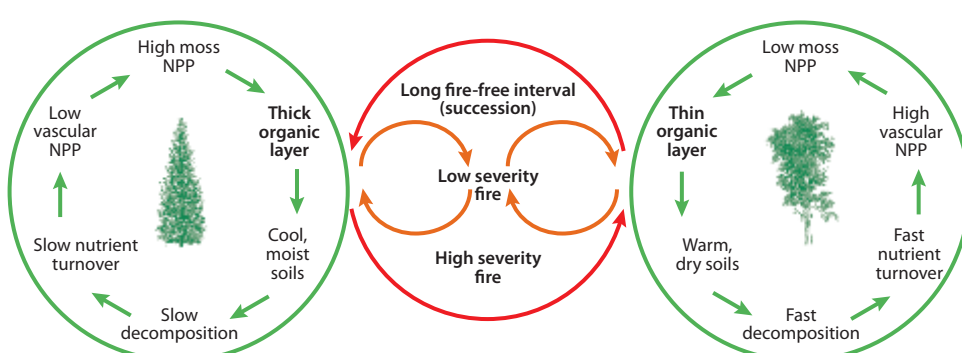


Figure 10.11 Soil organic layer dynamics across fire and successional cycles in taiga forest in interior Alaska. Adapted from Johnstone et al. (2010). NPP: net primary productivity.

Indeed, model projections suggest that Alaskan taiga may soon cross a threshold, where recent increases in fire activity have made deciduous stands as abundant as spruce stands on the landscape (Mann et al., 2012). In the Arctic larch forests of northeastern Siberia, increased fire severity may lead to increased tree density in forested areas and forest expansion into tundra (Alexander et al., 2012). Finally, burned graminoid tundra has been observed to increase in greenness after fire (Hu et al., 2015). This has been linked to increased dominance of tall deciduous shrubs (Racine et al., 1987). Plant-soil-microbial feedbacks within new vegetation types (Figure 10.11) determine long-term trajectories of nutrient dynamics (Melvin et al., 2015), which constrain ecosystem carbon storage (Johnstone et al., 2010; Alexander and Mack, 2016) and resultant climate feedbacks via carbon and energy (Randerson et al., 2006; Rocha et al., 2012).

Although increased fire activity is expected to transfer surface and permafrost soil carbon to the atmosphere, fire effects on plant community composition and post-fire successional trajectories may actually increase plant productivity. In the thick organic layer domain where spruce and moss dominate plant communities after low severity fires (left circle of Figure 10.11), the accumulation of soil organic layers in mesic-to-moist sites is associated with feedbacks among cool, moist soils, low rates of decomposition and nutrient cycling, and high net primary productivity of poorly decomposable moss. Alternatively, in the shallow organic layer domain, shallow organic layers in mesic-to-dry sites are associated with feedbacks among warm dry soils, high rates of decomposition, and high vascular plant productivity that smothers mosses with deciduous leaf fall. In permafrost terrain, thick organic layers maintain ecosystem-protected permafrost (Shur and Jorgenson, 2007). Severe fires can drive a shift to the thin organic layer domain, where permafrost is degraded or lost. A key knowledge gap is identifying when and where increased fire activity drives a net loss versus a net gain in ecosystem carbon pools, and thus a net positive or net negative feedback to climate warming.

Wildfire has played a variable role in the historic disturbance regime of taiga and tundra regions of western North America and northeastern Eurasia. Forecasts for future climate-fire interactions point towards increasing fire activity throughout the taiga regions of northern North America and northeastern Eurasia and expansion of novel fire regimes into tundra regions previously protected by a cool moist climate (Hu et al., 2015). In Alaska, it is expected that the rate of tundra burning will double during this century. For the taiga forests of interior Alaska, Kelly et al. (2013) used paleoecological reconstructions of fire history to show that fire frequency and severity are now higher than at any time in the past 10,000 years (Figure 10.12), but few other studies have placed current fire characteristics into the context of the historic regime. More studies are needed that explore pan-Arctic directional change in fire regimes.

10.4.3 Abrupt permafrost thaw

Abrupt permafrost thaw occurs when ground ice melts in thawing permafrost soils (Shur and Jorgenson, 2007; Grosse et al., 2011). At the scale of the ecosystem or hill slope, the physical impacts of these events are relatively well understood (Jorgenson, 2013). Because ice in fine-grained sediments often exceeds the pore space, melting can cause the surface to settle or liquefy. The amount of settlement and liquefaction is related to the amount and type of ice in the soil, and in concert with soil

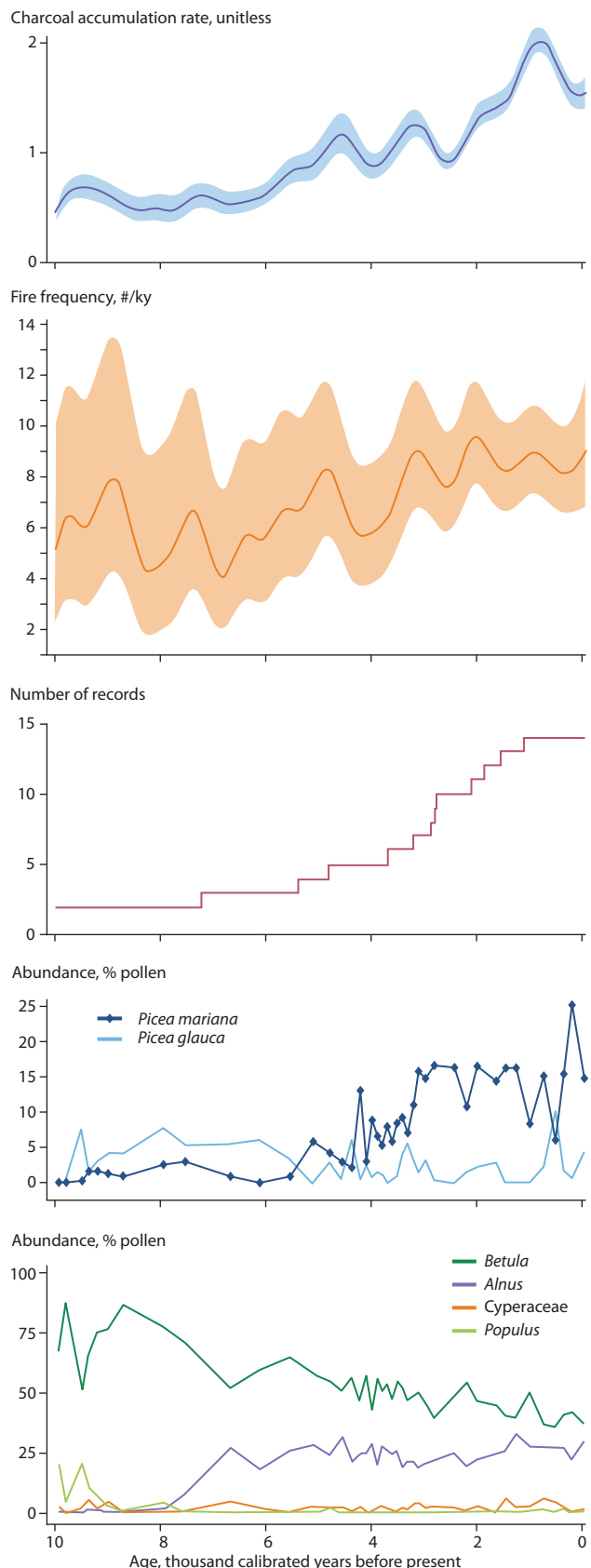


Figure 10.12 Proxy records of ecosystem change, highlighting millennial patterns of the past 10,000 years. Plots indicate: millennial composite records of charcoal accumulation rate and fire frequency from sediment charcoal analysis (with 90% confidence intervals); number of records contributing to composite charcoal records; pollen abundance of key conifer species black and white spruce (*Picea mariana* and *P. glauca*) and other major taxa at Screaming Lynx Lake, Alaska. Diamond symbols on the *P. mariana* curve indicate sampling resolution for all pollen data. Figure from Kelly et al. (2013).

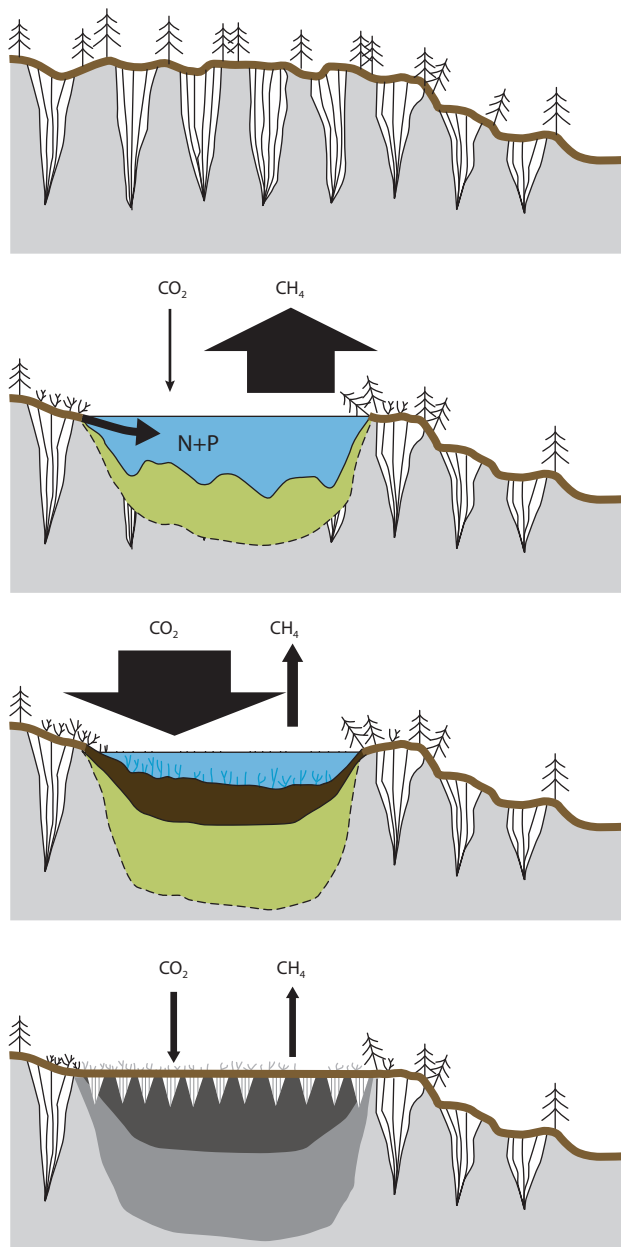


Figure 10.13 Thermokarst lake disturbance and recovery cycle in northeastern Siberian yedoma soils. Soil profile from northeastern Siberia, termed yedoma, with massive Pleistocene-aged ice wedges (upper). Thermokarst-lake expansion (thaw bulb shown in yellow; thaw boundary shown as a dotted line) accompanied by Pleistocene-aged methane (CH_4) emissions and release of nitrogen and phosphorus ($\text{N}+\text{P}$) from yedoma into lakes, stimulating aquatic productivity and carbon dioxide (CO_2) uptake, which offset Pleistocene-aged CO_2 emissions from yedoma decay (upper middle). Partially drained lake with atmospheric CO_2 uptake by plants forming thick Holocene-aged organic carbon deposits (brown) exceeding CH_4 emissions from contemporary organic matter decay (lower middle). Refreezing of remaining Pleistocene and Holocene carbon in sediments following complete lake drainage (new ice wedges are shown as triangles), with peatland-type CH_4 emissions and CO_2 uptake (lower). The thicknesses of CH_4 and CO_2 arrows are scaled by relative magnitude on a carbon-mass basis. From Walter Anthony et al. (2014).

type, topographic relief, and other environmental factors, determines the characteristics of the resultant disturbance event (Shur and Jorgenson, 2007). On relatively flat landscapes, settlement can range from low intensity disturbance, such as irregular surface subsidence that alters microtopography and soil drainage (Lee et al., 2011), to high intensity subsidence that turns terrestrial ecosystems into thermokarst lakes (Figure 10.13;

Walter Anthony et al., 2014). In both cases, changing hydrology can feed back positively to accelerate permafrost thaw. Deepening flow paths channel water towards thawing areas, and flowing or pooling water causes more localized thawing, often at rates substantially higher than would be predicted from changes in air temperature alone (Osterkamp et al., 2009; Jorgenson et al., 2010).

On hill slopes, soil liquefaction can result in abrupt landslides or gully formation: thermo-erosional mass wasting events that move large volumes of soil and sediment downslope. These events kill vegetation, mix and bury organic matter-rich surface soils into sediments, expose long-buried mineral soil and unweathered sediments, and transfer terrestrial material to lakes, streams and rivers. Loss of terrestrial material results in the formation of new flow paths and concavities in the landscape that can similarly channel water and accelerate local permafrost thaw, leading to repeating cycles of erosion (Kokelj et al., 2009).

Abrupt thaw events that damage and kill dominant plant species initiate successional processes, and in some cases permanently shift vegetation composition, plant biomass, and productivity (Jorgenson et al., 2006; Schuur et al., 2007; Baltzer et al., 2014). These disturbances offer an opportunity for plant community reorganization that may, under current trajectories of warming, accelerate biome shifts such as range expansion of tall shrubs and trees into tundra or the conversion of terrestrial to aquatic ecosystems (Karlsson et al., 2011). Although similar patterns have been identified in studies from many regions of the Arctic, little is known about the spatial extent or persistence of disturbance-driven biome shifts. In low intensity abrupt thaw events, vegetation composition is altered when changing flow paths shift soil moisture regimes. Shrubs and trees have been observed to increase in upland tundra ecosystems when thaw increases soil drainage (Schuur et al., 2007; Frost and Epstein, 2014), while in lowlands, thaw and subsidence inundates the rooting zone, killing trees and shrubs and favoring wetland sedges and mosses (Baltzer et al., 2014). At the extreme end of subsidence, thermokarst lake formation leads to a complete turnover in the plant community and replacement of low-productivity terrestrial species with high-productivity aquatic mosses that maintain the ecosystem as a carbon sink relative to the atmosphere (Figure 10.13; Walter Anthony et al., 2014).

Thermo-erosional events that kill vegetation and expose mineral soil open up unique opportunities for community change as new individuals recruit from seed, spores, or vegetative propagules on a novel seedbed. Tall deciduous shrub species such as willow and alder (Frost et al., 2013) and tree species such as aspen and birch (Johnstone et al., 2010) have tiny, wind-dispersed seeds that preferentially recruit on mineral soil seedbeds, leading to rapid and persistent increases in both biomass and productivity of these species, at least during the early decades after disturbance. (Pizano et al., 2014). Increasing rates of disturbance could create more seed sources, accelerating regional rates of expansion. Once established, functional traits of shrub and deciduous tree species bring into play plant-soil-microbial feedbacks that reinforce high rates of productivity over longer timescales via effects on nutrient cycling (DeMarco et al., 2011, 2014).

In addition to impacts on carbon inputs to ecosystems, abrupt thaw events also alter decomposition and carbon loss pathways by exposing previously frozen carbon to microbial processes and by altering the environment where decomposition occurs.

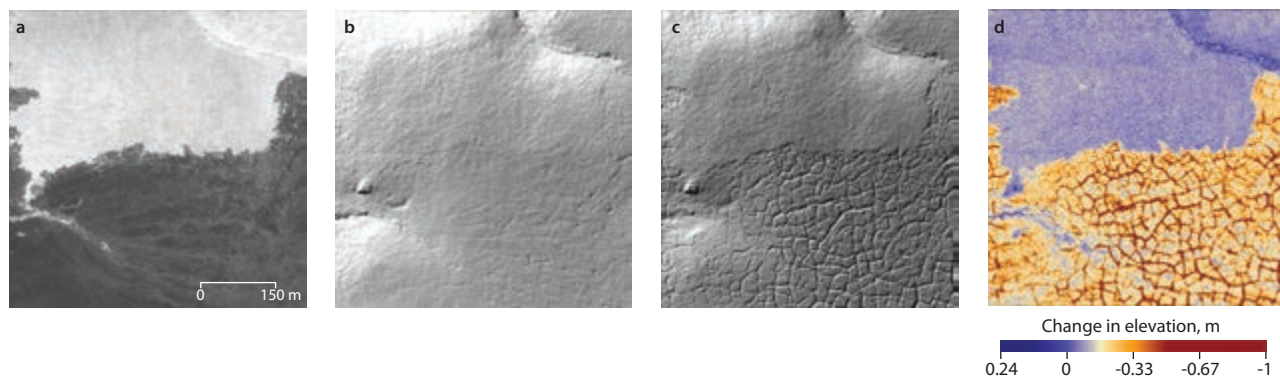


Figure 10.14 Detection of permafrost thaw subsidence and thermokarst initiation in burned tundra using multi-temporal Light Detection and Ranging (LiDAR) remote sensing (Jones et al., 2015). (a) Quickbird image from 5 July 2008, the year following fire, showing part of the northern extent of the burn area and the distinction between burned (dark) and unburned (light) tundra. Shaded contour images of the (b) 2009 and (c) 2014 1-m resolution LiDAR digital terrain models showing ice wedge degradation in the burn area. (d) The change in terrain created by subtracting the 2009 DTM from the 2014 DTM.

Because of the large size and potential lability of the permafrost soil carbon pool (Schuur and Abbott, 2011), there is substantial interest in understanding how abrupt thaw might accelerate its decomposition or alter the ratio of the greenhouse gasses carbon dioxide (CO_2) and methane (CH_4) released to the atmosphere (Schuur et al., 2015). In the few studies of carbon balance following surface subsidence in tundra ecosystems, increases in plant productivity outweighed enhanced decomposition relatively soon after disturbance (Schuur et al., 2009; Natali et al., 2012). Over longer periods, however, losses of old, deep permafrost carbon outweighed enhanced plant uptake, causing the ecosystem to become a carbon source relative to the atmosphere (Dorrepaal et al., 2009; Schuur et al., 2009).

In thermo-erosional features, where vegetation is killed and sediments are moved downslope, the fate of plant and soil carbon pools involved in the disturbance event is a key unknown for understanding impacts on ecosystem carbon balance. Studies of carbon fate tend to focus on one or a few fates; no studies or syntheses have examined the mass balance of carbon pools impacted by this type of disturbance. Soil organic carbon, previously stabilized in permafrost, may be exposed to thaw and/or moved to aerobic surface environments where decomposition and loss to the atmosphere is stimulated by higher temperature (Schuur et al., 2008; Grosse et al., 2011) and photo-oxidation (Cory et al., 2014). Alternatively, plant and soil carbon may be churned into deeper sediments and stabilized by freezing, low oxygen, or mineral sorption (Koven et al., 2009), or exported to aquatic ecosystems (Kokelj and Burn, 2005; Ping et al., 2011; Kokelj et al., 2013). Inputs to lakes may be stabilized in anaerobic sediments (Walter Anthony et al., 2007), while in streams or rivers, rapid aerobic processing may result in rapid return to the atmosphere (Kokelj et al., 2013). Studies are needed that examine the balance between stabilization and loss of carbon pools impacted by thermo-erosional disturbances.

Both surface subsidence and thermo-erosion affect hydrologic processes critical for determining soil oxygen availability and the balance between CO_2 and CH_4 release from decomposing carbon. Some of the highest CH_4 emissions in the permafrost region have been observed in lakes and wetlands formed through abrupt thaw. At the same time, accumulation of new carbon under anaerobic conditions in peat (Bockheim et al., 2004) and in lake sediments can be greater than carbon loss from thawing permafrost (Walter

Anthony et al., 2014). Understanding where abrupt thaw shifts ratios of CO_2 to CH_4 , as well as its impacts on net ecosystem carbon balance, is key for predicting feedbacks between increasing disturbance and climate.

Concurrent with permafrost warming throughout much of the northern hemisphere, observations of abrupt thaw have increased, yet relatively few studies have placed these observations in an historic context that would enable detection of a regime shift. Ice-rich permafrost that has undergone abrupt thaw events is described as thermokarst terrain, typified by irregular surface topography, thermokarst lakes and thermo-erosional gullies and landslide scars (Jorgenson, 2013). Retrospective studies of thermokarst terrain indicate northward expansion over the past century in Canada, China, Mongolia, Alaska, and northeastern Russia (Jorgenson, 2013). Regional studies in Alaska and Canada have documented expansion of lake and wetland area (Beilman et al., 2001; Baltzer et al., 2014), while others, some but not all discontinuous permafrost regions, have established patterns of decreasing lake cover associated with rapid drainage and drying (Lantz and Turner, 2015). Local studies point towards regional climate drivers, such as decadal warming (Jorgenson et al., 2006), extreme weather events (e.g. record warm precipitation) (Balser et al., 2014), and interactions with other physical disturbance agents (e.g. wildfire) (Jones et al., 2015), as drivers of increased frequency of and area affected by abrupt thaw events. New approaches are linking sediment records to thermokarst terrain formation over centennial to millennial timescales (Chipman et al., 2015). Optical and radar remote sensing as well as repeat airborne LiDAR measurements are enabling detection of abrupt thaw at larger spatial scales than before (Figure 10.14; Balser et al., 2014; Jones et al., 2015; Li et al., 2015). These observations are critical for developing the diagnostic models that can detect regime shifts, as well as the prognostic models that will forecast surface disturbance events in future climate and link them to the function of the Arctic system.

10.4.4 Mercury cycling and toxicity

Climate change is influencing the cycling of mercury (Hg) within the Arctic system (Stern et al., 2012). Stronger climate-sensitive disturbances, such as wildfire and abrupt permafrost thaw, could further exacerbate these changes, altering Hg transport, mass balance, and speciation. The latter is of particular concern due to increasing bioaccumulation in aquatic food webs, toxicity

of wild/local foods, and health risks to humans (Gordon et al., 2016). Inorganic forms of Hg are readily eliminated by animals, but in anaerobic environments such as peat soils, sediments, or lake water columns, bacteria can methylate elemental or oxidized Hg (Hu et al., 2013), resulting in the formation of methylmercury (MeHg). This is a potent neurotoxin that is of increasing concern in Arctic and sub-Arctic areas where indigenous peoples rely on subsistence hunting and fishing for their nutritional, social and cultural wellbeing (AMAP, 2011). Although recent decreases in human Hg levels have been observed in communities where there have been efforts to increase understanding of Hg risks, the Hg levels of individuals in many communities still exceed guideline values set by the US Environmental Protection Agency, Health Canada, and the World Health Organization (AMAP, 2011).

Long-range atmospheric transport of Hg from anthropogenic sources at lower latitudes has led to enhanced Hg deposition and accumulation in the vegetation, soils and sediments of northern ecosystems (Fitzgerald et al., 1998). Peatlands and permafrost soils retain the record of industrial deposition, primarily from coal burning, as well as long-term natural rates of deposition (Rydberg et al., 2010). Boreal peatlands and permafrost soils may contain some of the largest northern stocks of Hg, up to ten times greater than stocks in forested upland soils (Turetsky et al., 2006).

Because Hg is linked to the organic carbon cycle by affinities in transport and controls over methylation processes, disturbances that affect carbon cycling will also affect Hg cycling. For example, climate-driven increases in wildfire intensity and areal extent that accelerate carbon release to the atmosphere should thus also influence the rate of Hg release. Mercury stocks once protected in cold, wet soils will become increasingly vulnerable to combustion as boreal forests, peatlands and tundra experience increasing fire disturbance. Burning of peat may be a particularly important yet unconstrained component of Hg release, and is also a key unknown in the mass balance of Hg in Arctic and boreal ecosystems. Turetsky et al. (2006) found that including peat soil combustion in circumboreal estimates of fire-driven Hg emissions resulted in a 15-fold increase in emissions over studies that did not include peat soils. In their Canadian study region alone, Hg emissions during drought years approached industrial emissions of Hg in North America, suggesting that large fire years could lead to a net regional loss of Hg. It follows that disturbances that alter drainage and water table depth, making peat more vulnerable to deep combustion, must also increase Hg emissions. Clearly, regional studies that focus on carbon emission from fire could be synthesized with soil Hg data to improve estimates of fire-driven Hg emissions. Emitted Hg is dominated by elemental Hg, which has a one-year residence time in the atmosphere (Friedli et al., 2003), so it is unclear whether wildfire emissions will result in regional or even circumpolar re-deposition: tracking the fate of this fire-emitted Hg is a key research need.

Abrupt permafrost thaw that increases hydrologic connectivity between terrestrial and aquatic ecosystems is likely to increase Hg transport to aquatic ecosystems and the formation of MeHg (Gordon et al., 2016). Thaw that leads to landscape drying, by contrast, could stabilize Hg stocks in aerobic soils and sediments. Subsidence that alters flow pathways may increase the volume of organic soil that is

hydraulically connected to aquatic ecosystems, increasing the lateral transport of organic matter-bound Hg as newly thawed permafrost soil is exposed (Rydberg et al., 2010). Mass wasting events transport particulate organic matter downslope and into aquatic ecosystems, where Hg can be stabilized through burial in sediments or could again be subject to methylation as it is moved through the water column or downstream. Thawing and subsiding permafrost peatlands are observed to be hotspots for Hg mobilization (Rydberg et al., 2010) and MeHg export (Gordon et al., 2016), but few studies have examined the fate of Hg in mass wasting events, such as active layer detachment slides or riverine coastal erosion.

In summary, Hg cycling and toxicity are likely to be highly sensitive to how climate change and disturbance impact drainage – whether landscapes become drier or wetter and more hydrologically connected. Mercury may be stabilized in soils that become drier after permafrost thaw, yet this Hg may also be vulnerable to combustion and emission to the atmosphere in a warmer, drier climate. In soils that become wetter, Hg is more likely to become mobile in the toxic form of MeHg.

10.4.5 Knowledge gaps and recommendations

Although regional records of recent (~50 year) wildfire activity exist for some areas of the Arctic (i.e. Alaska and Canada), recent fire activity in Arctic Russia remains a key knowledge gap. Syntheses of pan-Arctic observations of wildfire characteristics – frequency, intensity, severity, size – are needed for assessment of the current Arctic fire regime, comparison with historic regimes, and for prognostic modeling of future regimes. Current regional synthesis efforts in North America, such as that undertaken by the US NASA Arctic Boreal Vulnerability Experiment, should be coordinated with regional syntheses of Russian and European regions.

Substantially less is known about abrupt thaw disturbance events at regional scales than wildfire events; observations of surface subsidence, mass wasting, and post-disturbance recovery are crucial for understanding the current and future trajectory of ecosystems as permafrost soils warm. Moreover, wildfire could greatly accelerate rates of permafrost degradation and vegetation change, thus research on post-fire ecosystems that integrates changes in plant productivity with changes in deep permafrost soil carbon decomposition should be a high priority.

For understanding the ecological mechanisms through which abrupt thaw affects the ecosystem carbon balance and carbon cycling feedbacks to climate, critical knowledge gaps remain in terms of understanding the ratio of CO₂ to CH₄ emitted, the partitioning of respiration between winter and summer, decomposition of old permafrost carbon, and the fate of carbon pools displaced laterally by the disturbance event. Future research is needed that combines measurements of net ecosystem exchange with the additional components of net ecosystem carbon balance, and that incorporates the direct impacts of the disturbance on lateral carbon fluxes as well as changes over the post-disturbance recovery period.

Finally, better predictions of when and where ecosystems become wetter or drier after disturbance and how flow paths change would help constrain predictions of climate impacts on biogeochemical cycles, such as carbon and Hg. Research is needed that improves regional understanding of ecosystem vulnerability to changes in drainage.

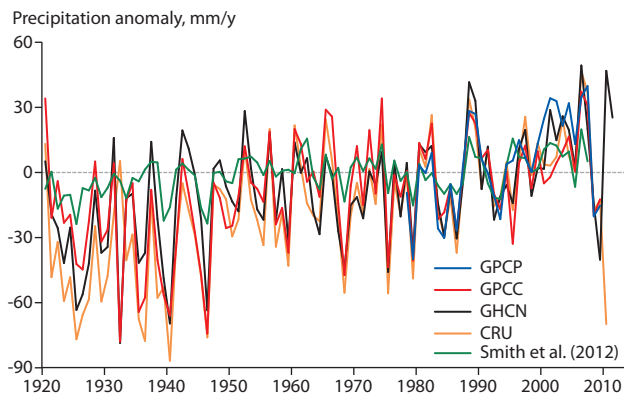


Figure 10.15 Annual precipitation anomalies averaged over land areas for Arctic latitudes from five global precipitation data sets relative to a 1981–2000 climatology (after Hartmann et al., 2013). GPCP (Global Precipitation Climatology Project), GPCC (Global Precipitation Climatology Centre), GHCN (Global Historical Climatology Network) and CRU (Climatic Research Unit).

10.5 Precipitation effects

10.5.1 Context

Precipitation, whether liquid or solid, affects numerous physical processes including: surface albedo change, glacier surface ablation, snowpack heat transfer, snowpack ice layer formation, surface energy exchanges, snow metamorphism, melt timing and duration, permafrost stability, nutrient cycling, vegetation growth patterns, vegetation community composition, animal grazing, animal habitats and fire frequency. Present and future changes in Arctic precipitation thus have the potential to influence (if not dominate) radiative, thermal and biological feedbacks. However, even though Arctic precipitation is increasing overall, spatial patterns of change are complex and the sign and relative importance of feedback processes to the climate and hydrological systems of the Arctic remain unclear.

The IPCC AR5 found increasing precipitation over northern hemisphere high latitudes across multiple data sources (Figure 10.15) concurrent with increasing northern hemisphere air temperature (Walsh et al., 2008) and increasing absolute humidity (Hartmann et al., 2013). The concurrent variability

suggests an increase in precipitation of around 2% per decade over the Arctic from the observed warming (Chapter 3), a positive feedback between warming and precipitation, and a reduction in the fraction of precipitation falling as solid precipitation (Chapter 3). Future climate warming is therefore expected to further increase Arctic precipitation (Flato et al., 2013). An increase in Arctic precipitation is one of the most robust signals in the global climate models under all forcing scenarios and is consistent with long-term observational precipitation records from sub-Arctic locations (e.g. Denmark, see Cappelen, 2015).

There is evidence from Greenland ice cores of a 15% increase in Greenland ice sheet snow accumulation over the period 1900–1999 (Box et al., 2013; Mernild et al., 2015). Monitoring at near-coastal Greenland meteorological stations suggests an increase in winter precipitation between 1900 and 2012 (Mernild et al., 2015). Yet, deducing trends from precipitation records is not straightforward. This is arguably due to inhomogeneities caused by automation in Canadian and United States networks in recent decades; Russian precipitation data may lack bias-adjustments; strong wind effects on the gauge catch along the Arctic coasts, where most of the Arctic meteorological stations are situated; and network paucity everywhere in the Arctic, except Fennoscandia. As a result, some researchers consider the empirical evidence of precipitation increase in the Arctic to be inconclusive despite most observations indicating precipitation increase. One of the factors that may act against the ‘theoretical’ expectations of current and future increase in terrestrial precipitation at high latitudes is a weakening of cyclonic activity, because this would reduce water vapor transport inside the continents (Groisman et al., 2014).

10.5.2 Precipitation interaction with climate change processes

Arctic precipitation change contributes to rainfall-induced-darkening of Greenland snow (Charalampidis et al., 2015; Mernild et al., 2015) and other albedo feedbacks on land ice in which low snow cover anomalies amplify bare ice sheet surface melting (Tedesco et al., 2011; Box et al., 2012). For the terrestrial and marine environment, absorbed sunlight is

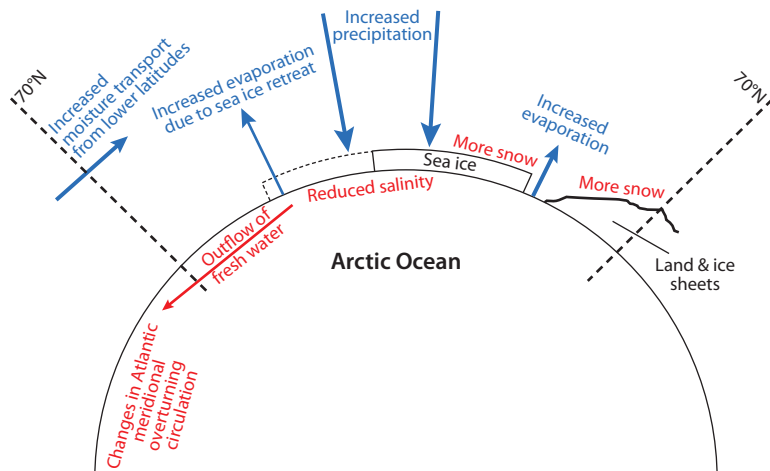


Figure 10.16 Sea-land moisture exchange within the Arctic and between the Arctic and lower latitudes (Bintanja and Selten, 2014). Blue arrows denote future changes in Arctic moisture exchanges, with arrow size loosely depicting the magnitude of change. The red text and red arrows represent the associated climatic consequences.

a driver of decline in snow cover and sea ice (Flanner et al., 2011; Shi et al., 2013). Heavy rainfall events promote land ice acceleration (Doyle et al., 2015) and snowpack and permafrost heating (Westermann et al., 2011).

This assessment (see Chapter 4) documents further that in Alaska, permafrost warming of the past five years has been linked with reduced insulation from declining snow cover. The evolution of thermokarst lakes appears more the result of precipitation and evaporation changes than temperature change. Permafrost abrasion, denudation, and gully formation are influenced by summer and winter precipitation. Landslide activation is partly controlled by increasing precipitation.

Retreating winter sea ice promotes stronger local ocean surface evaporation (especially in winter), and this is projected to amplify future Arctic precipitation increase more than the enhanced moisture inflow from lower latitudes (Bintanja and Selten, 2014) (Figure 10.16).

10.5.3 Rain-on-snow events

Rain-on-snow events impact humans, vegetation, hydrology, and wildlife by altering snowmelt, runoff, soil temperature, and sea ice (Cohen et al., 2015) (see also Chapter 3). Liston and Hiemstra (2011) found possible increases in snow density and rain-on-snow events in the period 1979–2009. Yet, trends in rain-on-snow events are small and of opposite sign, probably due to the competing consequences of higher temperatures causing more frequent rainfall relative to snowfall but also less snow cover.

While shrubification in some parts of the Arctic (Tape et al., 2006; Myers-Smith et al., 2011) modifies snow layer heat conduction by limiting compaction and thereby decreasing the effective thermal conductivity (Domine et al., 2015), ice layers from winter thaws or rain-on-snow events often have the opposite effect of increasing thermal conductivity. It is unclear whether rain-on-snow events are increasing and to what extent

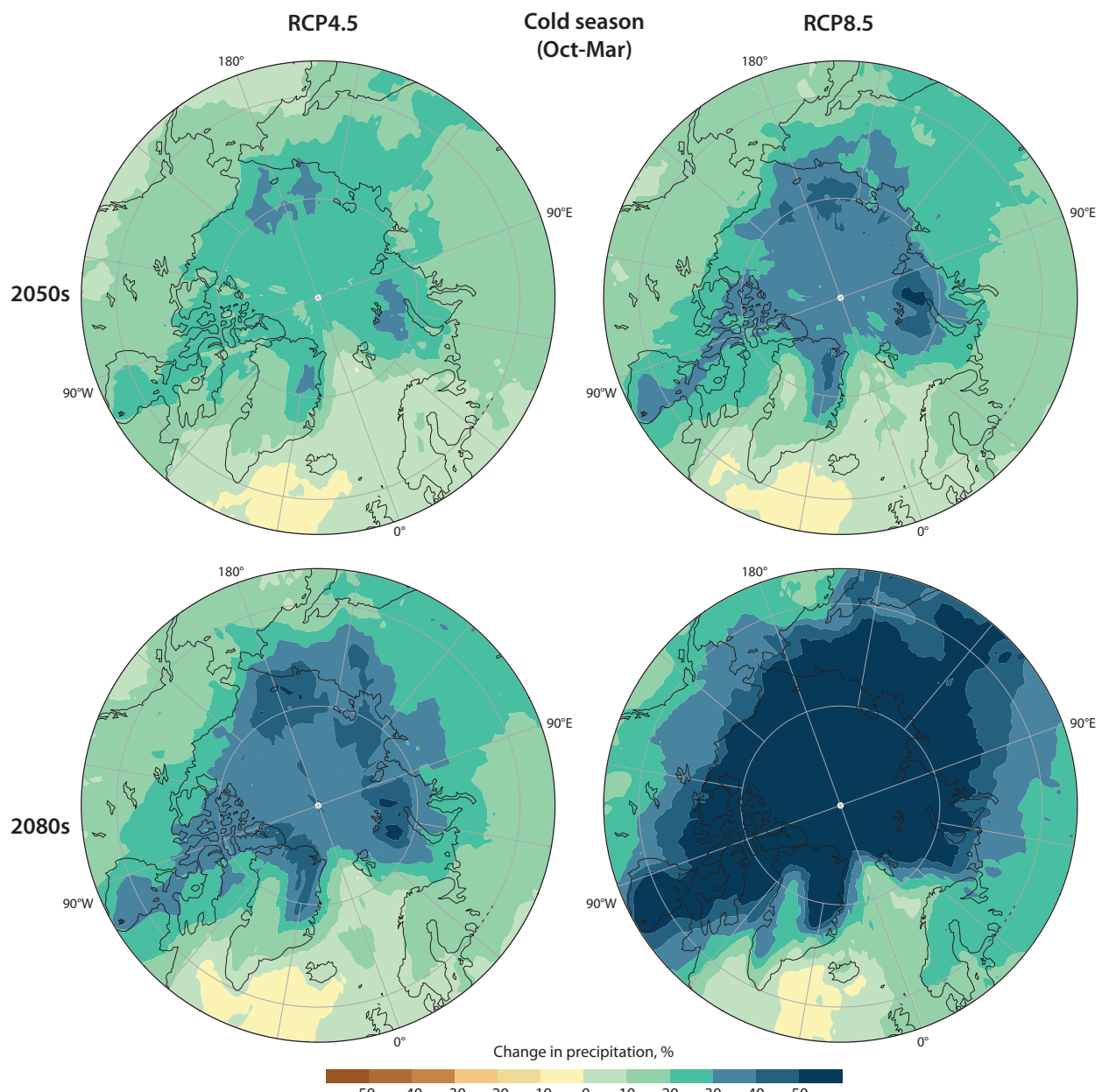


Figure 10.17 Projected changes in precipitation (50th percentile), relative to 1986–2005, for October–March under the RCP4.5 scenario (left panels) and the RCP8.5 scenario (right panels). Upper panels are for the 2050s and lower panels are for the 2080s (G. Flato, Environment Canada).

they will affect the thermal insulating effect of the snow cover. Rain-on-snow events occur over relatively small spatial scales and have high interannual variability (Wilson et al., 2013). Snowpack heating from rainfall can be important especially during heavy rain events (Westermann et al., 2011) but is not expected to be a major effect in a warmer climate because of shorter snow cover duration. On sea ice, for example, rain-on-snow events are known to change the physical properties of the snow and in turn the microwave properties of the snow with consequences for sea ice concentration retrieval (see Chapter 5).

Rain-on-snow events have the potential to indirectly drive the population dynamics of overwintering vertebrates (Hansen et al., 2013). Both ecological and societal consequences were reported from Svalbard during and after an extreme rain-on-snow event in February 2012 (Hansen et al., 2014) which resulted in a thick ground ice layer that prevented caribou from grazing, increased permafrost temperatures

to 5 m depth, and triggered slush avalanches with resulting disturbance to infrastructure (including closed roads and restricted off road travel). Hansen et al. (2014) concluded that the frequency of Arctic rain-on-snow events is likely to increase with climate change.

10.5.4 Ground moisture content

It is unclear whether declining Arctic snow cover will increase or decrease ground moisture content. Climate warming is advancing the onset of spring snowmelt and decreasing snow cover duration (Derkzen and Brown, 2012) and this may lengthen the summer dry state and ultimately cause drier soil conditions and a changing runoff regime, where the Arctic hydrologic system is changing in response to a seasonal shift in solid and liquid precipitation (see Chapter 3). An increasing rain to snowfall ratio creates potential for drying through lower

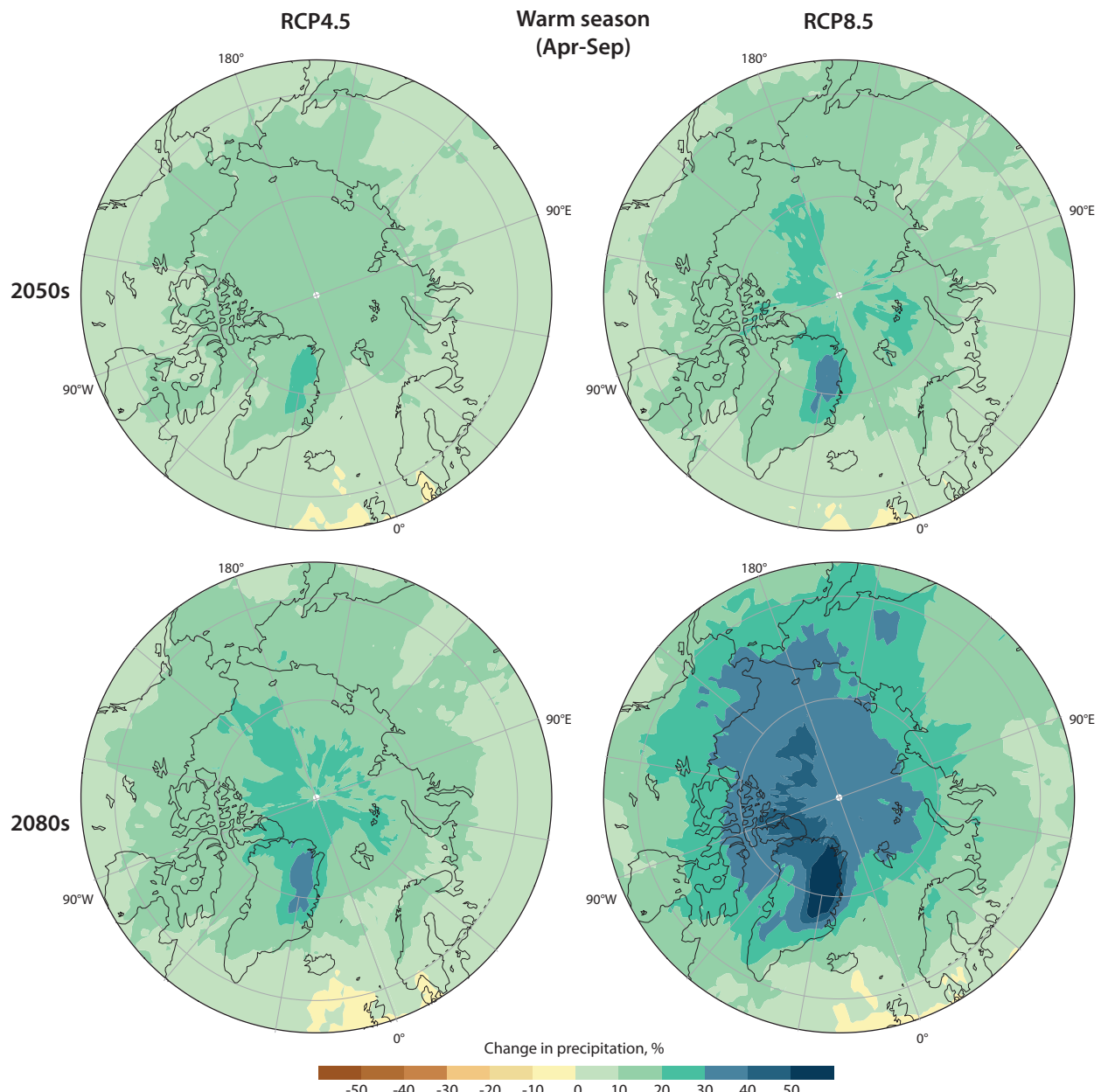


Figure 10.18 Projected changes in precipitation (50th percentile), relative to 1986–2005, for April–September under the RCP4.5 scenario (left panels) and the RCP8.5 scenario (right panels). Upper panels are for the 2050s and lower panels are for the 2080s (G. Flato, Environment Canada).

snowmelt recharge and more evaporation (Wu et al., 2015). However, Conner et al. (2016) found that the soil moisture response depends on many other factors including landscape characteristics, vegetation, and regional weather patterns.

For inland areas of the Greenland ice sheet, years with low surface meltwater runoff are synchronous with years of relatively high previous winter snow accumulation, as more surface melt water can be retained in a thicker drier and cold polar snowpack (Hanna et al., 2008; Mernild et al., 2009). However, in maritime regions such as southeastern Greenland, high runoff can result from abnormally wet conditions (Mernild et al., 2014).

10.5.5 Future projections

In climate projections, Arctic precipitation shows a greater percentage increase than in all other regions except the tropical Pacific Ocean. As shown in Figures 10.17 and 10.18, the percentage increases are greatest in the cold season and for the RCP8.5 scenario. Spatially, the increases are greatest over the Arctic Ocean, where they exceed 50% over some areas in the cold season under RCP8.5. The increase in precipitation in the Arctic is one of the most robust signals in the global climate models under all forcing scenarios. While the precipitation increases are larger in a percentage sense than elsewhere because the Arctic precipitation totals are relatively small, the actual amounts of the increase are smaller than in many other regions globally. Moreover, it should be emphasized that increases in precipitation do not necessarily imply increases in ground wetness. Increasing evapotranspiration generally results in decreasing runoff. The model-projected changes in soil moisture in the Arctic are generally small, ranging from decreases in some areas to increases in others (Collins et al., 2013). While highly uncertain owing to their dependence on the model-simulated precipitation, evapotranspiration and runoff, these changes in ground wetness have potentially important impacts on vegetation, fire regime and land use.

Maximum 5-day precipitation amounts within a year are projected to increase by 20–30% over most Arctic land areas by 2081–2100 under the RCP8.5 scenario (Collins et al., 2013). An increase in snow accumulation over the cold season increases the risk of strong runoff pulses and flooding on rivers such as the Yenisey and Lena in Siberia. Also consistent with the projected increase in precipitation in the Arctic is a projected reduction of 5–10 days in the yearly maximum number of consecutive dry days (Collins et al., 2013).

10.5.6 Knowledge gaps and recommendations

Observational data indicate an overall rise in Arctic temperature and precipitation (and change in the fraction of precipitation falling as snow or rain) that not only strengthens the hydrological system but drives amplifying feedback processes such as enhanced land ice melting. While a widespread pattern of snow cover decline is evident, it is unclear whether this change will increase or decrease ground moisture content. Shrubification of the Arctic modifies snow layer heat conduction with opposite effects on the thermal conductivity from compaction and ice layer development. Permafrost and snowpack base heating are evident from winter rainfall episodes. Cold season heavy rainfall events have negative societal and wildlife impacts. Yet, it is unclear if there are trends in rain-on-snow events.

The complexity of Arctic precipitation change, both geographically and temporally highlights the need for a denser and higher accuracy network of precipitation records by improving precipitation/snowfall observation technology. It should help to develop remote sensing of precipitation and to continue to assess reanalysis precipitation estimates and compare these with surface and remotely sensed precipitation.

References

Aagaard, K. and E.C. Carmack, 1989. The role of sea ice and other fresh water in the Arctic circulation. *Journal of Geophysical Research*, 94:14485-14498.

Alexander, H.D. and M.C. Mack, 2016. A canopy shift in interior Alaskan boreal forests: consequences for above-and belowground carbon and nitrogen pools during post-fire succession. *Ecosystems*, 19:98-114.

Alexander, H.D., M.C. Mack, S. Goetz, M.M. Loranty, P.S.A. Beck, K. Earl, S. Zimov, S. Davydov and C.C. Thompson, 2012. Carbon accumulation patterns during post-fire succession in Cajander larch (*Larix cajanderi*) forests of Siberia. *Ecosystems*, 15:1065-1082.

Alley, R.B., D.A. Meese, C.A. Shuman, A.J. Gow, K.C. Taylor, P.M. Grootes, J.W.C. White, M. Ram, E.D. Waddington, P.A. Mayewski and G.A. Zielinski, 1993. Abrupt increase in Greenland snow accumulation at the end of the Younger Dryas event. *Nature*, 362:527-529.

AMAP, 2011. AMAP Assessment 2011: Mercury in the Arctic. Arctic Monitoring and Assessment Programme (AMAP), Oslo, Norway.

Asner, G.P., C.B. Anderson, R.E. Martin, D.E. Knapp, R. Tupayachi, F. Sinca and Y. Malhi, 2014. Landscape-scale changes in forest structure and functional traits along an Andes-to-Amazon elevation gradient. *Biogeosciences*, 11:843-856.

Atkinson, D. and P. Treitz, 2013. Modeling biophysical variables across an arctic latitudinal gradient using high spatial resolution remote sensing data. *Arctic, Antarctic and Alpine Research*, 45:161-178.

Balser, A.W., J.B. Jones and R. Gens, 2014. Timing of retrogressive thaw slump initiation in the Noatak Basin, northwest Alaska, USA. *Journal of Geophysical Research: Earth Surface*, 119:1106-1120.

Baltzer, J.L., T. Veness, L.E. Chasmer, A.E. Sniderhan and W.L. Quinton, 2014. Forests on thawing permafrost: fragmentation, edge effects, and net forest loss. *Global Change Biology*, 20:824-834.

Bartsch, A., T. Kumpula, B.C. Forbes and F. Stammiller, 2010. Detection of snow surface thawing and refreezing in the Eurasian Arctic with QuickSCAT: implications for reindeer herding. *Ecological Applications*, 20:2346-2358.

Beilman, D.W., D.H. Vitt and L.A. Halsey, 2001. Localized permafrost peatlands in western Canada: definition, distributions, and degradation. *Arctic, Antarctic, and Alpine Research*, 33:70-77.

Belkin, I.M., 2004. Propagation of the “Great Salinity Anomaly” of the 1990s around the northern North Atlantic. *Geophysical Research Letters*, 31:L08306, doi:10.1029/2003GL019334.

Bhatt, U.S., D.A. Walker, M.K. Raynolds, J.C. Comiso, H.E. Epstein, G. Jia, R. Gens, J.E. Pinzon, C.J. Tucker, C.E. Tweedie and P.J. Webber, 2010. Circumpolar Arctic tundra vegetation change is linked to sea ice decline. *Earth Interactions*, 14:1-20.

Bhatt, U.S., D.A. Walker, M.K. Raynolds, P.A. Bieniek, H.E. Epstein, J.C. Comiso, J.E. Pinzon, C.J. Tucker and I.V. Polyakov, 2013. Recent declines in warming and vegetation greening trends over pan-Arctic tundra. *Remote Sensing*, 5:4229-4254.

Bhatt, U.S., D.A. Walker, M.K. Raynolds, P.A. Bieniek, H.E. Epstein, J.C. Comiso, J.E. Pinzon, C.J. Tucker, M.A. Steele, W. Ermold and J. Zhang, 2017. Changing seasonality of Panarctic tundra vegetation in relationship to climatic variables. *Environmental Research Letters*, special biomass issue, 12:055003 <https://doi.org/10.1088/1748-9326/aa6b0b>.

Bieniek, P., U. Bhatt, D. Walker, M.K. Raynolds, J. Comiso, H. Epstein, J. Pinzon, C. Tucker, R. Thoman, H. Tran, N. Mölders, M. Steele, J. Zhang and W. Ermold, 2015. Climate drivers linked to changing seasonality of Alaska coastal tundra vegetation productivity. *Earth Interactions*, 19:151016095240009.

Billings, W.D., 1973. Arctic and alpine vegetations: similarities, differences, and susceptibility to disturbances. *Bioscience*, 23:697-704.

Bindoff, N.L., P.A. Stott, K.M. AchutaRao, M.R. Allen, N. Gillett, D. Gutzler, K. Hansingo, G. Hegerl, Y. Hu, S. Jain, I.I. Mokhov, J. Overland, J. Perlitz, J. Pitman, J. T. Randall, J. Schellnhuber, J. Smith, J. Tschirhart, J. T. F. Wallen, J. Wiltshire, J. Zhou and J. Zhou, 2013. Changes in the Arctic. *Climate Change 2013: The Physical Science Basis. Contribution of Working Group I to the Fifth Assessment Report of the Intergovernmental Panel on Climate Change*, Cambridge University Press, Cambridge, United Kingdom and New York, NY, USA, pp. 95-128.

R. Sebbari and X. Zhang, 2013. Detection and attribution of climate change: from global to regional. In: Climate Change 2013: The Physical Science Basis. Contribution of Working Group I to the Fifth Assessment Report of the Intergovernmental Panel on Climate Change. pp. 867-952. Cambridge University Press.

Bintanja, R. and F.M. Selten, 2014. Future increases in Arctic precipitation linked to local evaporation and sea-ice retreat. *Nature*, 509:479-482.

Birkeland, P.W., 1999. Soils and Geomorphology. Third edition. Oxford University Press.

Bjorkman, A.D., S.C. Elmendorf, A.L. Beamish, M. Vellend and G.H.R. Henry, 2015. Contrasting effects of warming and increased snowfall on Arctic tundra plant phenology over the past two decades. *Global Change Biology*, 21:4651-4661.

Boby, L.A., E.A.G. Schuur, M.C. Mack, D. Verbyla and J.F. Johnstone, 2010. Quantifying fire severity, carbon, and nitrogen emissions in Alaska's boreal forest. *Ecological Applications*, 20:1633-1647.

Bockheim, J.G., K.M. Hinkel, W.R. Eisner and X.Y. Dai, 2004. Carbon pools and accumulation rates in an age-series of soils in drained thaw-lake basins, Arctic Alaska. *Soil Science Society of America Journal*, 68:697-704.

Boelman, N.T., L. Gough, J.R. McLaren and H. Greaves, 2011. Does NDVI reflect variation in the structural attributes associated with increasing shrub dominance in arctic tundra. *Environmental Research Letters*, 6:035501, doi:10.1088/1748-9326/6/3/035501.

Box, J.E. and W. Colgan, 2013. Greenland ice sheet mass balance reconstruction. Part III: Marine ice loss and total mass balance (1840-2010). *Journal of Climate*, 26:6990-7002.

Box, J.E., X. Fettweis, J.C. Stroeve, M. Tedesco, D.K. Hall and K. Steffen, 2012. Greenland ice sheet albedo feedback: thermodynamics and atmospheric drivers. *The Cryosphere*, 6:821-839.

Box, J.E., N. Cressie, D.H. Bromwich, J. Jung, M. van den Broeke, J.H. van Angelen, R.R. Forster, C. Miège, E. Mosley-Thompson, B. Vinther and J.R. McConnell, 2013. Greenland ice sheet mass balance reconstruction. Part I: net snow accumulation (1600-2009). *Journal of Climate*, 26:3919-3934.

Bratsch, S.N., H.E. Epstein, M. Buchhorn and D.A. Walker, 2016. Differentiating among four Arctic tundra plant communities at Ivvotuk, Alaska using field spectroscopy. *Remote Sensing*, 8:51, doi:10.3390/rs8010051.

Bret-Harte, M.S., M.C. Mack, G.R. Shaver, D.C. Huebner, M. Johnston, C.A. Mojica, C. Pizano and J.A. Reiskind, 2013. The response of Arctic vegetation and soils following an unusually severe tundra fire. *Philosophical Transactions of the Royal Society B*, 368:20120490, doi:10.1098/rstb.2012.0490.

Buchhorn, M., D.A. Walker, B. Heim, M.K. Raynolds, H.E. Epstein and M. Schwieder, 2013. Ground-based hyperspectral characterization of Alaska tundra vegetation along environmental gradients. *Remotes Sensing*, 5:3971-4005.

Bunn, A.G. and S.J. Goetz, 2006. Trends in satellite-observed circumpolar photosynthetic activity from 1982 to 2003: The influence of seasonality, cover type, and vegetation density. *Earth Interactions*, 10:1-19.

Callaghan, T.V., D. Dahl-Jensen, M. Johansson, R. Kallenborn, R.R. Key, R. Macdonald, T. Prowse, M. Sharp, K. Steffen and W.F. Vincent, 2011a. Cross-cutting scientific issues. In: Snow, Water, Ice and Permafrost in the Arctic (SWIPA): Climate Change and the Cryosphere. Arctic Monitoring and Assessment Programme (AMAP), Oslo, Norway.

Callaghan, T.V., C.E. Tweedie, J. Åkerman, C. Andrews, J. Bergstedt, M.G. Butler, T.R. Christensen, D. Cooley, U. Dahlberg, R.K. Danby, F.J.A. Daniëls, J.G. de Molenaar, J. Dick, C. Ebbe Mortensen, D. Ebert-May, U. Emanuelsson, H. Eriksson, H. Hedenås, G.H.R. Henry, D.S. Hik, J.E. Hobbie, E.J. Jantze, C. Jaspers, C. Johansson, M. Johansson, D.R. Johnson, J.F. Johnstone, C. Jonasson, C. Kennedy, A.J. Kenney, F. Keuper, S. Koh, C.J. Krebs, H. Lantuit, M.J. Lara, D. Lin, V.L. Lougheed, J. Madsen, N. Matveyeva, D.C. McEwen, I.H. Myers-Smith, Y.K. Narozhniy, H. Olsson, V.A. Pohjola, L.W. Price, F. Rigét, S. Rundqvist, A. Sandström, M. Tamstorf, R. Van Bogaert, S. Villarreal, P.J. Webber and V.A. Zemtsov, 2011b. Multi-decadal changes in tundra environments and ecosystems: Synthesis of the International Polar Year – Back to the Future Project (IPY-BTF). *Ambio*, 40:705-716.

Cappelen, J., 2015. Greenland - DMI Historical Climate Data Collection 1784-2014. Danish Meteorological Institute, Technical Report No. 15-02.

Chapin III, F.S., N. Fetcher, K. Kielland, K.R. Everett and A.E. Linkins, 1988. Productivity and nutrient cycling of Alaskan tundra: enhancement by flowing soil water. *Ecology*, 69:693-702.

Chapin, F.S., S.F. Trainor, O. Huntington, A.L. Lovecraft, E. Zavaleta, D.C. Natcher, A.D. McGuire, J.L. Nelson, L. Ray, M. Calef, N. Fresco, H. Huntington, T.S. Rupp, L. Dewilde and R.L. Naylor, 2008. Increasing wildfire in Alaska's boreal forest: Pathways to potential solutions of a wicked problem. *Bioscience*, 58:531-540.

Charalampidis, C., D. van As, J.E. Box, M.R. van den Broeke, W.T. Colgan, S.H. Doyle, A.L. Hubbard, M. MacFerrin, H. Machguth and C.J.P.P. Smeets, 2015. Changing surface-atmosphere energy exchange and refreezing capacity of the lower accumulation area, West Greenland. *The Cryosphere*, 9:2163-2181.

Chipman, M.L., C. Reents, J.A. Greenberg and F. Hu, 2015. Impact of climate and fires on abrupt permafrost thaw in Alaskan tundra. In: American Geophysical Union, Fall Meeting, 14-18 December 2015. San Francisco.

Cohen, J., H. Ye and J. Jones, 2015. Trends and variability in rain-on-snow events. *Geophysical Research Letters*, 42:7115-7122.

Colgan, W., A. Sommers, H. Rajaram, W. Abdalati and J. Fahrm, 2015. Considering thermal-viscous collapse of the Greenland ice sheet. *Earth's Future*, 3:252-267.

Collins, M., R. Knutti, J. Arblaster, J.-L. Dufresne, T. Fichefet, P. Friedlingstein, X. Gao, W.J. Gutowski, T. Johns, G. Krinner, M. Shongwe, C. Tebaldi, A.J. Weaver and M. Wehner, 2013. Long-term climate change: projections, commitments and irreversibility. In: Climate Change 2013: The Physical Science Basis. Contribution of Working Group I to the Fifth Assessment Report of the Intergovernmental Panel on Climate Change. pp. 1029-1136. Cambridge University Press.

Comiso, J.C. and F. Nishio, 2008. Trends in the sea ice cover using enhanced and compatible AMSR-E, SSM/I, and SMMR data. *Journal of Geophysical Research*, 113:C02S07, doi:10.1029/2007JC004257.

Conner, L.G., R.A. Gill and J. Belnap, 2016. Soil moisture response to experimentally-altered snowmelt timing is mediated by soil, vegetation, and regional climate patterns. *Ecohydrology*, 9:1006-1016.

Cooper, D.J., 1986. Arctic-alpine tundra vegetation of the Arrigetch Creek Valley, Brooks Range, Alaska. *Phytocoenologia*, 14:467-555.

Cory, R.M., C.P. Ward, B.C. Crump and G.W. King, 2014. Sunlight controls water column processing of carbon in arctic fresh waters. *Science*, 345:925-928.

Crawford, R.M.M., C.E. Jeffree and W.G. Rees, 2003. Paludification and forest retreat in northern oceanic environments. *Annals of Botany*, 91:213-226.

Daniëls, F.J.A., J.G. de Molenaar, M. Chytrý and L. Tichý, 2010. Vegetation change in Southeast Greenland? Tasiilaq revisited after 40 years. *Applied Vegetation Science*, 14:230-241.

DeMarco, J., M.C. Mack and M.S. Bret-Harte, 2011. The effects of snow, soil microenvironment, and soil organic matter quality on N availability in three Alaskan Arctic plant communities. *Ecosystems*, 14:804-817.

DeMarco, J., M.C. Mack and M.S. Bret-Harte, 2014. Effects of arctic shrub expansion on biophysical vs. biogeochemical drivers of litter decomposition. *Ecology*, 95:1861-1875.

Derkens, C. and R. Brown, 2012. Spring snow cover extent reductions in the 2008–2012 period exceeding climate model projections. *Geophysical Research Letters*, 39:L19504, doi:10.1029/2012GL053387.

Derkens, C., R. Brown, L. Mudryk and K. Luojus, 2015. Terrestrial snow cover. Arctic Report Card: Update for 2015. NOAA.

Domine, F., M. Barrere, D. Sarrazin, S. Morin and L. Arnaud, 2015. Automatic monitoring of the effective thermal conductivity of snow in a low-Arctic shrub tundra. *The Cryosphere*, 9:1265-1276.

Dorrepaal, E., S. Toet, R.S.P. van Logtestijn, E. Swart, M.J. van de Weg, T.V. Callaghan and R. Aerts, 2009. Carbon respiration from subsurface peat accelerated by climate warming in the subarctic. *Nature*, 460:616-619.

Doyle, S.H., A. Hubbard, R.S.W. van de Wal, J.E. Box, D. van As, K. Scharrer, T.W. Meierbach, P.C.J.P. Smeets, J.T. Harper, E. Johansson, R.H. Mottram, A.B. Mikkelsen, F. Wilhelms, H. Patton, P. Christoffersen and B. Hubbard, 2015. Amplified melt and flow of the Greenland ice sheet driven by late-summer cyclonic rainfall. *Nature Geoscience*, 8:647-653.

Duarte, C.M., S. Agusti, P. Wassmann, J.M. Arrieta, M. Alcaraz, A. Coello, N. Marba, I.E. Hendriks, J. Holding, I. Garcia-Zarandona, E. Kritzberg and D. Vaque, 2012. Tipping elements in the Arctic marine ecosystem. *Ambio*, 41:44-55.

Eisenman, I. and J. Wettlaufer, 2009. Nonlinear threshold behavior during the loss of Arctic sea ice. *Proceedings of the National Academy of Sciences*, 106:28-32.

Ellebjerg, S.M., M.P. Tamstorf, L. Illeris, A. Michelsen and B.U. Hansen, 2008. Inter-annual variability and controls of plant phenology and productivity at Zackenberg. In: Advances in Ecological Research:

High Arctic Ecosystem Dynamics in a Changing Climate. pp. 250-273. Amsterdam.

Elmendorf, S.C., G.H.R. Henry, R.D. Hollister, R.G. Björk, N. Boulanger-Lapointe, E.J. Cooper, J.H.C. Cornelissen, T.A. Day, E. Dorrepaal, T.G. Elmeeva, M. Gill, W.A. Gould, J. Harte, D.S. Hik, A. Hofgaard, D.R. Johnson, J.F. Johnstone, I.S. Jónsdóttir, J.C. Jorgenson, K. Klanderud, J.A. Klein, S. Koh, G. Kudo, M. Lara, E. Lévesque, B. Magnusson, J.L. May, J.A. M.-D. Az, A. Michelsen, U. Molau, I.H. Myers-Smith, S.F. Oberbauer, V.G. Onipchenko, C. Rixen, N.M. Schmidt, G.R. Shaver, M.J. Spasojevic, P.E. Þórhallsdóttir, A. Tolvanen, T. Troxler, C.E. Tweedie, S. Villareal, C.-H. Wahren, X. Walker, P.J. Webber, J.M. Welker and S. Wipf, 2012. Plot-scale evidence of tundra vegetation change and links to recent summer warming. *Nature Climate Change*, 2:453-457.

Elmendorf, S.C., G.H.R. Henry, R.D. Hollister, A.M. Fosaa, W.A. Gould, L. Hermanutz, A. Hofgaard, I.I. Jónsdóttir, J.C. Jorgenson, E. Lévesque, B. Magnusson, U. Molau, I.H. Myers-Smith, S.F. Oberbauer, C. Rixen, C.E. Tweedie and M. Walker. 2015. Experiment, monitoring, and gradient methods used to infer climate change effects on plant communities yield consistent patterns. *Proceedings of the National Academy of Sciences of the United States of America*, 112:448-452.

Epstein, H.E., U.S. Bhatt, M.K. Reynolds, D.A. Walker, B.C. Forbes, M. Macias-Fauria, M. Loranty, G. Phoenix and J. Bjerke, 2017. Tundra greenness. In: *State of the Climate in 2016*. Bulletin of the American Meteorological Society, 98:S145-S147.

Euskirchen, E.S., M.S. Bret-Harte, G.J. Scott, C. Edgar and G.R. Shaver, 2012. Seasonal patterns of carbon dioxide and water fluxes in three representative tundra ecosystems in northern Alaska. *Ecosphere*, 3:1-19.

Farquharson, L.M., V.E. Romanovsky, W.L. Cable and D.A. Walker, 2016. Widespread and rapid thermokarst development in a region of very cold permafrost in the Canadian High Arctic. Abstract GC33G06, AGU Fall Meeting, San Francisco, CA, 12-16 December.

Fitzgerald, W.F., D.R. Engstrom, R.P. Mason and E.A. Nater, 1998. The case for atmospheric mercury contamination in remote areas. *Environmental Science and Technology*, 32:1-7.

Flanner, M.G., K.M. Shell, M. Barlage, D.K. Perovich and M.A. Tschudi, 2011. Radiative forcing and albedo feedback from the Northern Hemisphere cryosphere between 1979 and 2008. *Nature Geoscience*, 4:151-155.

Flato, G., J. Marotzke, B. Abiodun, P. Braconnot, S.C. Chou, W. Collins, P. Cox, F. Driouech, S. Emori, V. Eyring, C. Forest, P. Gleckler, E. Guilyardi, C. Jakob, V. Kattsov, C. Reason and M. Rummukainen, 2013. Evaluation of climate models. In: Stocker, T.F., D. Qin, G.-K. Plattner, M. Tignor, S.K. Allen, J. Boschung, A. Nauels, Y. Xia, V. Bex and P.M. Midgley (eds.), *Climate Change 2013: The Physical Science Basis. Contribution of Working Group I to the Fifth Assessment Report of the Intergovernmental Panel on Climate Change*. Cambridge University Press.

Forkel, M., M. Migliavacca, K. Thonicke, M. Reichstein, S. Schaphoff, U. Weber and N. Carvalhais, 2015. Codominant water control on global interannual variability and trends in land surface phenology and greenness. *Global Change Biology*, 21:3414-3435.

Friedli, H., L. Radke, J. Lu, C. Banic, W. Leaitch and J. MacPherson, 2003. Mercury emissions from burning of biomass from temperate North American forests: laboratory and airborne measurements. *Atmospheric Environment*, 37:253-267.

Frost, G.V. and H.E. Epstein, 2014. Tall shrub and tree expansion in Siberian tundra ecotones since the 1960s. *Global Change Biology*, 20:1264-1277.

Frost, G.V., H.E. Epstein, D.A. Walker, G. Matyshak and K. Ermokhina, 2013. Patterned-ground facilitates shrub expansion in Low Arctic tundra. *Environmental Research Letters*, 8:15035-15043.

Giblin, A.E., K.J. Nadelhoffer, G.R. Shaver, J.A. Laundre and A.J. McKerrow, 1991. Biogeochemical diversity along a riverside toposequence in arctic Alaska. *Ecological Monographs*, 61:415-435.

Goetz, S.J., A.G. Bunn, G.J. Fiske and R.A. Houghton, 2005. Satellite-observed photosynthetic trends across boreal North America associated with climate and fire disturbance. *Proceedings of the National Academy of Sciences*, 102:13521-13525.

Gordon, J., W. Quinton, B. Branfireun and D. Olefeldt, 2016. Mercury and methylmercury biogeochemistry in a thawing permafrost wetland complex, Northwest Territories, Canada. *Hydrological Processes*, 30:3627-3638.

Gould, W.A. and J.A. Mercado-Díaz, 2014. Decadal-scale changes of vegetation from long-term plots in Alaskan tundra. In: Hobbie, J.E. and G.W. Kling (eds.), *Alaska's Changing Arctic: Ecological Consequences for Tundra, Streams, and Lakes*. pp. 130-131.

Goward, S.N., C.T. Tucker and D.G. Dye, 1985. North American vegetation patterns observed with the NOAA-7 advanced very high resolution radiometer. *Vegetatio*, 64:3-14.

Gregory, J.M. and P. Huybrechts, 2006. Ice-sheet contributions to future sea level change. *Philosophical Transactions of the Royal Society A*, 364:1709-1731.

Groisman, P.Y., E.G. Bogdanova, V.A. Alexeev, J.E. Cherry and O.N. Bulygina, 2014. Impact of snowfall measurement deficiencies on quantification of precipitation and its trends over Northern Eurasia. *Ice and Snow, 2:29-43*.

Grosse, G., J. Harden, M. Turetsky, A.D. McGuire, P. Camill, C. Tarnocvai, S. Froliking, E.A.G. Schuur, T. Jorgenson, S. Marchenko, V. Romanovsky, K.P. Wickland, N. French, M. Waldrop, L. Bourgeau-Chavez and R.G. Striegl, 2011. Vulnerability of high-latitude soil organic carbon in North America to disturbance. *Journal of Geophysical Research*, 166:G00K06, doi:10.1029/2010JG001507.

Hanna, E., P. Huybrechts, K. Steffen, J. Cappelen, R. Huff, C. Shuman, T. Irvine-Fynn, S. Wise and M. Griffiths, 2008. Increased runoff from melt from the Greenland Ice Sheet: A response to global warming. *Journal of Climate*, 21:331-341.

Hansen, B.U., V. Grøtan, R. Aanes, B.-E. Sæther, A. Stien, E. Fuglei, R.A. Ims, N.G. Yoccoz and Å.Ø. Pedersen, 2013. Climate events synchronize the dynamics of a resident vertebrate community in the High Arctic. *Science*, 339:313-315.

Hansen, B.B., K. Isaksen, R.E. Benestad, J. Kohler, A.Ø. Pedersen, L.E. Loe, S.J. Coulson, J.O. Larsen and Ø. Varpe, 2014. Warmer and wetter winters: characteristics and implications of an extreme weather event in the High Arctic. *Environmental Research Letters*, 9:114021.

Harden, J., S. Trumbore, B. Stocks, A. Hirsch, S. Gower, K. O'Neill and E. Kasischke, 2000. The role of fire in the boreal carbon budget. *Global Change Biology*, 6(Suppl):174-184.

Hartmann, D.L., A.M.G. Klein Tank, M. Rusticucci, L.V. Alexander, S. Brönnimann, Y. Charabi, F.J. Dentener, E.J. Dlugokencky, D.R. Easterling, A. Kaplan, B.J. Soden, P.W. Thorne, M. Wild and P.M. Zhai, 2013. Observations: atmosphere and surface. In: Stocker, T.F., D. Qin, G.-K. Plattner, M. Tignor, S.K. Allen, J. Boschung, A. Nauels, Y. Xia, V. Bex and P.M. Midgley (eds.), *Climate Change 2013: The Physical Science Basis. Contribution of Working Group I to the Fifth Assessment Report of the Intergovernmental Panel on Climate Change*. Cambridge University Press.

Hobbie, S.E., J.P. Schimel, S.E. Trumbore and J.R. Randerson, 2000. Controls over carbon storage and turnover in high-latitude soils. *Global Change Biology*, 6:196-210.

Høye, T.T., E. Post, H. Meltofte, N.M. Schmidt and M.C. Forchhammer, 2007. Rapid advancement of spring in the High Arctic. *Current Biology*, 17:R449-R451.

Hu, F.S., P.E. Higuera, J.E. Walsh, W.L. Chapman, P.A. Duffy, L.B. Brubaker and M.L. Chipman, 2010. Tundra burning in Alaska: Linkages to climatic change and sea ice retreat. *Journal of Geophysical Research*, 115:G04002, doi:10.1029/2009JG001270.

Hu, H., H. Lin, W. Zheng, S.J. Tomanicek, A. Johs, X. Feng, D.A. Elias, L. Liang and B. Gu, 2013. Oxidation and methylation of dissolved elemental mercury by anaerobic bacteria. *Nature Geoscience*, 6:751-754.

Hu, F.S., P.E. Higuera, P. Duffy, M.L. Chipman, A.V. Rocha, A.M. Young, R. Kelly and M.C. Dietze, 2015. Arctic tundra fires: natural variability and responses to climate change. *Frontiers in Ecology and the Environment*, 13:369-377.

Hudson, J.M.G. and G.H.R. Henry, 2009. Increased plant biomass in a High Arctic heath community from 1981 to 2008. *Ecology*, 90:2657-2663.

Huybrechts, P., H. Goelzer, I. Janssens, E. Driesschaert, T. Fichefet, H. Goosse and M.F. Loutre, 2011. Response of the Greenland and Antarctic ice sheets to multi-millennial greenhouse warming in the earth system model of intermediate complexity LOVECLIM. *Surveys in Geophysics*, 32:397-416.

Jägerbrand, A.K., G. Kudo, J.M. Alatalo and U. Molau, 2012. Effects of neighboring vascular plants on the abundance of bryophytes in different vegetation types. *Polar Science*, 6:200-208.

Jia, G.J., H.E. Epstein and D.A. Walker, 2003. Greening of arctic Alaska, 1981-2001. *Geophysical Research Letters*, 30:2067, doi:10.1029/2003GL018268.

Jiang, Y., A.V. Rocha, J.A. O'Donnell, J.A. Drysdale, E.B. Rastetter, G.R. Shaver and Q. Zhuang, 2015. Contrasting soil thermal responses to fire in Alaskan tundra and boreal forest. *Journal of Geophysical Research: Earth Surface*, 120:363-378.

Johnson, E.A., 1992. *Fire and Vegetation Dynamics. Studies from the North American Boreal Forest*. Cambridge University Press.

Johnson, D.R., M.J. Lara, G.R. Shaver, G.O. Batzli, J.D. Shaw and C.E. Tweedie, 2011. Exclusion of brown lemmings reduces vascular plant

cover and biomass in Arctic coastal tundra: resampling of a 50+ year herbivore exclusion experiment near Barrow, Alaska. *Environmental Research Letters*, 6:045507.

Johnstone, J.F. and F.S. Chapin III, 2006. Effects of burn severity on patterns of post-fire tree recruitment in boreal forests. *Ecosystems*, 9:14-31.

Johnstone, J.F., L. Boby, E. Tissier, M.C. Mack, D.L. Verbyla and X. Walker, 2009. Post-fire seed rain of black spruce, a semi-serotinous conifer, in forests of interior Alaska. *Canadian Journal of Forest Research*, 39:1575-1588.

Johnstone, J.F., F.S. Chapin, T.N. Hollingsworth, M.C. Mack, V. Romanovsky and M. Turetsky, 2010. Fire, climate change, and forest resilience in interior Alaska. *Canadian Journal of Forest Research*, 40:1302-1312.

Jolly, M.W., M.A. Cochrane, P.H. Freeborn, Z.A. Holden, T.J. Brown, G.J. Williamson and D.M.J.S. Bowman, 2015. Climate-induced variations in global wildfire danger from 1979 to 2013. *Nature Communications*, 6:7537, doi:10.1038/ncomms8537.

Jones, B.M., G. Grosse, C.D. Arp, E. Miller, L. Liu, D.J. Hayes and C.F. Larsen, 2015. Recent Arctic tundra fire initiates widespread thermokarst development. *Scientific Reports*, 5:15865.

Jorgenson, M.T., 2000. Hierarchical organization of ecosystems at multiple spatial scales on the Yukon-Kuskokwim Delta, Alaska, U.S.A. *Arctic, Antarctic, and Alpine Research*, 32:221-239.

Jorgenson, M.T., 2013. Thermokarst terrains. In: Shroder, J. (ed.), *Glacial and Periglacial Geomorphology*. pp. 313-324. Academic Press.

Jorgenson, M.T., Y.L. Shur and E.R. Pullman, 2006. Abrupt increase in permafrost degradation in Arctic Alaska. *Geophysical Research Letters*, 25:L02503, doi:10.1029/2005GL024960.

Jorgenson, M.T., V. Romanovsky, J. Harden, Y. Shur, J. O'Donnell, E.A.G. Shuur, M. Kanevskiy and S. Marchenko, 2010. Resilience and vulnerability of permafrost to climate change. *Canadian Journal of Forest Research*, 40:1219-1236.

Jorgenson, M.T., J. Harden, M. Kanevskiy, J. O'Donnell, K. Wicklund, S. Ewing, K. Manies, Q. Zhuang, Y. Shur, R. Striegl and K. Koch, 2013. Reorganization of vegetation, hydrology and soil carbon after permafrost degradation across heterogeneous boreal landscapes. *Environmental Research Letters*, 8:035017.

Justice, C.O., J.R.G. Townshend, B.N. Holben and C.J. Tucker, 1985. Analysis of the phenology of global vegetation using meteorological satellite data. *International Journal of Remote Sensing*, 6:1271-1318.

Karlsson, J., A. Bring, G.D. Peterson, L.J. Gordon and G. Destouni, 2011. Opportunities and limitations to detect climate-related regime shifts in inland Arctic ecosystems through eco-hydrological monitoring. *Environmental Research Letters*, 6:014015.

Kasischke, E.S., N.L. Christensen and B.J. Stocks, 1995. Fire, global warming, and the carbon balance of boreal forests. *Ecological Applications*, 5:437-451.

Kattsov, V., V. Ryabinin, J. Overland, M. Serreze, M. Visbeck, J. Walsh, W. Meier and X. Zhang, 2011. Arctic sea ice change: a grand challenge of climate science. *Journal of Glaciology*, 56:1115-1121.

Kaufman, D.S., D.P. Schneider, N.P. McKay, C.M. Ammann, R.S. Bradley, K.R. Briffa, G.H. Miller, B.L. Otto-Bliesner, J.T. Overpeck, B.M. Vinther and Arctic Lakes 2K Project Members, 2009. Recent warming reverses long-term Arctic cooling. *Science*, 325:1236-1239.

Kelly, R., M.L. Chipman, P.E. Higuera, I. Stefanova, L.B. Brubaker and F.S. Hu, 2013. Recent burning of boreal forests exceeds fire regime limits of the past 10,000 years. *Proceedings of the National Academy of Sciences*, 110:13055-13060.

Kelly, R., H. Genet, A.D. McGuire and F.S. Hu, 2016. Palaeodata-informed modelling of large carbon losses from recent burning of boreal forests. *Nature Climate Change*, 6:79-82.

Khvorostyanov, D.V., G. Krinner, P. Cais, M. Heimann and S.A. Zimov, 2008. Vulnerability of permafrost carbon to global warming. Part 1: Model description and the role of heat generated by organic matter decomposition. *Tellus B*, 60:250-264.

Kielland, K. and F.S.I. Chapin, 1992. Nutrient absorption and accumulation in arctic plants. In: Chapin, F.S.I., R.L. Jefferies, J.F. Reynolds, G.S. Shaver and J. Svoboda (eds.), *Arctic Ecosystems in a Changing Climate: An Ecophysiological Perspective*. pp. 321-335. Academic Press.

Kokelj, S.V. and C.R. Burn, 2005. Geochemistry of the active layer and near-surface permafrost, Mackenzie delta region, Northwest Territories, Canada. *Canadian Journal of Earth Sciences*, 42:37-48.

Kokelj, S.V., T.C. Lantz, J. Kanigan, S.L. Smith and R. Coutts, 2009. Origin and polycyclic behaviour of tundra thaw slumps, Mackenzie Delta region, Northwest Territories, Canada. *Permafrost and Periglacial Processes*, 20:173-184.

Kokelj, S.V., D. Lacelle, T.C. Lantz, J. Tunnicliffe, L. Malone, I.D. Clark and K.S. Chin, 2013. Thawing of massive ground ice in mega slumps drives increases in stream sediment and solute flux across a range of watershed scales. *Journal of Geophysical Research: Earth Surface*, 118:681-692.

Koven, C., P. Friedlingstein, P. Cais, D. Khvorostyanov, G. Krinner and C. Tarnocai, 2009. On the formation of high-latitude soil carbon stocks: effects of cryoturbation and insulation by organic matter in a land surface model. *Geophysical Research Letters*, 36: L21501, doi:10.1029/2009GL040150.

Kriegler, E., J.W. Hall, H. Held, R. Dawson and H.J. Schellnhuber, 2009. Imprecise probability assessment of tipping points in the climate system. *Proceedings of the National Academy of Sciences*, 106:5041-5046.

Kumpula, T., B.C. Forbes, F. Stammer and N. Meschtyb, 2012. Remote sensing and GIS analysis of anthropogenic and natural land use and land cover changes in tundra environments in Bovanenkovo gas field on Yamal Peninsula, Russia. Third Yamal Land-Cover Land-Use Change Workshop Arctic Centre, Rovaniemi, Finland, 19-21 May 2012.

Kwok, R. and D.A. Rothrock, 2009. Decline in Arctic sea ice thickness from submarine and ICESat records: 1958-2008. *Geophysical Research Letters*, 36:L15501, doi:10.1029/2009GL039035.

Laidler, G.J., P.M. Treitz and D.M. Atkinson, 2008. Remote sensing of arctic vegetation: relations between the NDVI, spatial resolution and vegetation cover on Boothia Peninsula, Nunavut. *Arctic*, 61:1-13.

Lantuit, H., P.P. Overduin, N. Couture, S. Wetterich, F. Aré, D. Atkinson, J. Brown, G. Cherkashov, D. Drozdov, D.L. Forbes, A. Graves-Gaylord, M. Grigoriev, H.-W. Hubberten, J. Jordan, T. Jorgenson, R. Strand Ødegård, S. Ogorodov, W.H. Pollard, V. Rachold, S. Sedenko, S. Solomon, F. Steenhuisen, I. Streletskaya and A. Vasiliev, 2012. The Arctic coastal dynamics database: a new classification scheme and statistics on Arctic permafrost coastlines. *Estuaries and Coasts*, 35:383-400.

Lantz, T.C. and K.W. Turner, 2015. Changes in lake area in response to thermokarst processes and climate in Old Crow Flats, Yukon. *Journal of Geophysical Research: Biogeosciences*, 120:513-524.

Lantz, T.C., S.V. Kokelj, S.E. Gergel and G.H.R. Henry, 2009. Relative impacts of disturbance and temperature: persistent changes in microenvironment and vegetation in retrogressive thaw slumps. *Global Change Biology*, 15:1664-1675.

Lawrence, D.M., A.G. Slater, R.A. Tomas, M.M. Holland and C. Deser, 2008. Accelerated Arctic land warming and permafrost degradation during rapid sea ice loss. *Geophysical Research Letters*, 35:L11506, doi:10.1029/2008GL033985.

Lee, H., E.A.G. Schuur, J.G. Vogel, M. Lavoie, D. Bhadra and C. Staudhammer, 2011. A spatially explicit analysis to extrapolate carbon fluxes in upland tundra where permafrost is thawing. *Global Change Biology*, 17:1379-1393.

Lee, O., H. Eicken, G. Kling and C. Lee, 2015. A framework for prioritization, design and coordination of Arctic long-term observing networks: A perspective from the U.S. SEARCH Program. *Arctic*, 68:76-88.

Lenton, T.M., 2012. Arctic climate tipping points. *Ambio*, 41:10-22.

Li, Z., R. Zhao, L. Wen, G. Feng, Z. Zhang and Q. Wang, 2015. InSAR analysis of surface deformation over permafrost to estimate active layer thickness based on one-dimensional heat transfer model of soils. *Scientific Reports*, 5:15542, doi:10.1038/srep15542.

Liljedahl, A.K., J. Boike, R.P. Daanen, A.N. Fedorov, G.V. Frost, G. Grosse, L.D. Hinzman, Y. Lijma, J.C. Jorgenson, N. Matveyeva, M. Necsoiu, M.K. Reynolds, V.E. Romanovskiy, J. Schulla, K.D. tape, D.A. Walker, C.J. Wilson, H. Yabuki and D. Zona, 2016. Pan-Arctic ice-wedge degradation in warming permafrost and its influence on tundra hydrology. *Nature Geoscience*, 9:312-318.

Lindsay, R.W. and J. Zhang, 2005. The thinning of Arctic sea ice, 1988-2003: Have we passed a tipping point? *Journal of Climate*, 18:4879-4894.

Liston, G.E. and C.A. Hiemstra, 2011. The changing cryosphere: Pan-Arctic snow trends (1979-2009). *Journal of Climate*, 24:5691-5712.

Livina, V.N. and T.M. Lenton, 2013. A recent tipping point in the Arctic sea ice cover: abrupt and persistent increase in the seasonal cycle since 2007. *The Cryosphere*, 7:275-286.

Mack, M.C., M.S. Bret-Harte, T.N. Hollingsworth, R.R. Jandt, E.A.G. Schuur, G.R. Shaver and D.L. Verbyla, 2011. Carbon loss from an unprecedented Arctic tundra wildfire. *Nature*, 475:489-492.

Mann, D.H., T.S. Rupp, M.A. Olson and P.A. Duffy, 2012. Is Alaska's boreal forest now crossing a major ecological threshold? *Arctic Antarctic and Alpine Research*, 44:319-331.

McClelland, J.W., S.J. Dery, J. Peterson, R.M. Holmes and E.F. Woods, 2006. A pan-arctic evaluation of changes in river discharge during the latter half of the 20th century. *Geophysical Research Letters*, 33:L06715, doi:10.1029/2006GL025753.

Melvin, A.M., M.C. Mack, J.F. Johnstone, A.D. McGuire, H. Genet and E.A.G. Schuur, 2015. Differences in ecosystem carbon distribution and nutrient cycling linked to forest tree species composition in a mid-successional boreal forest. *Ecosystems*, 18:1472-1488.

Mernild, S.H., G.E. Liston, C.A. Hiemstra, K. Steffen, E. Hanna and J.H. Christensen, 2009. Greenland ice sheet surface mass-balance modeling and freshwater flux for 2007, and in a 1995–2007 perspective. *Hydrological Processes*, 23:2470-2484.

Mernild, S.H., Liston, G.E. and C.A. Hiemstra, 2014. Northern Hemisphere glaciers and ice caps surface mass balance and contribution to sea-level rise. *Journal of Climate*, 27:6051-6073.

Mernild, S.H., E. Hanna, J.R. McConnell, M. Sigl, A.P. Beckerman, J.C. Yde, J. Cappelen and K. Steffen, 2015. Greenland precipitation trends in a long-term instrumental climate context (1890–2012): Evaluation of coastal and ice core records. *International Journal of Climatology*, 35:303–320.

Myers-Smith, I.H., B.C. Forbes, M. Wilmking, M. Hallinger, T. Lantz, D. Blok, K.D. Tape, M. Macias-Fauria, U. Sass-Klaassen, E. Lévesque, S. Boudreau, P. Ropars, L. Hermanutz, A. Trant, L.S. Collier, S. Weijers, J. Rozema, S.A. Rayback, N.M. Schmidt, G. Schaepman-Strub, S. Wipf, C. Rixen, C.B. Ménard, S. Venn, S. Goetz, L. Andreu-Hayles, S. Elmendorf, V. Ravolainen, J. Welker, P. Grogan, H.E. Epstein and D.S. Hik, 2011. Shrub expansion in tundra ecosystems: dynamics, impacts, and research priorities. *Environmental Research Letters*, 6:045509.

Myers-Smith, I.H., S.C. Elmendorf, P.S.A. Beck, M. Wilmking, M. Hallinge, D. Blok, K.D. Tape, S.A. Rayback, M. Macias-Fauria, B.C. Forbes, J.D.M. Speed, N. Boulanger-Lapointe, C. Rixen, E. Lévesque, N.M. Schmidt, C. Baittinger, A.J. Trant, L. Hermanutz, L.S. Collier, M.A. Dawes, T.C. Lantz, S. Weijers, R.H. Jørgensen, A. Buchwal, A. Buras, A.T. Naito, V. Ravolainen, G. Schaepman-Strub, J.A. Wheeler, S. Wipf, K.C. Guay, D.S. Hik and M. Vellend, 2015. Climate sensitivity of shrub growth across the tundra biome. *Nature Climate Change*, 5:887-891.

Myneni, R.B., C.D. Keeling, C.J. Tucker, G. Asrar and R.R. Nemani, 1997. Increased plant growth in the northern high latitudes from 1981 to 1991. *Nature*, 386:698-702.

Natali, S.M., E.A.G. Schuur and R.L. Rubin, 2012. Increased plant productivity in Alaskan tundra as a result of experimental warming of soil and permafrost. *Journal of Ecology*, 100:488-498.

Oberbauer, S.F., S.C. Elmendorf, T.G. Troxler, R.D. Hollister, A.V. Rocha, M.S. Bret-Harte, M.A. Dawes, A.M. Fosaa, G.H.R. Henry, T.T. Hoye, F.C. Jarrad, I.S. Jonsdottir, K. Klanderud, J.A. Klein, U. Molau, C. Rixen, N.M. Schmidt, G.R. Shaver, R.T. Slider, O. Totland, C.H. Wahren and J.M. Welker, 2013. Phenological response of tundra plants to background climate variation tested using the International Tundra Experiment. *Philosophical Transactions of the Royal Society B*, 368:20120481.

Osterkamp, T.E., M.T. Jorgenson, E.A.G. Schuur, Y.L. Shur, M.Z. Kanevskiy, J.G. Vogel and V.E. Turnskoy, 2009. Physical and ecological changes associated with warming permafrost and thermokarst in Interior Alaska. *Permafrost and Periglacial Processes*, 20:235-256.

Overeem, I. and J.P.M. Syvitski, 2010. Shifting discharge peaks in Arctic rivers, 1977–2007. *Geografiska Annaler A*, 92:285-296.

Overland, J.E., M. Wang, J.E. Walsh and J.C. Stroeve, 2014. Future Arctic climate changes: Adaptation and mitigation timescales. *Earth's Future*, 2:68-74.

Peterson, B.J., R.M. Holmes, J.W. McClelland, C.J. Vorusmarty, R.B. Lammers, A.I. Shiklomanov, I.A. Shiklomanov and S. Rahmstorf, 2002. Increasing river discharge to the Arctic Ocean. *Science*, 298:2171-2173.

Pfeffer, W.T., J.T. Harper and S. O'Neil, 2008. Kinematic constraints on glacier contributions to 21st-century sea level rise. *Science*, 321:1340-1343.

Piao, S., H. Nan, C. Huntingford, P. Ciais, P. Friedlingstein, S. Sitch, S. Peng, A. Ahlström, J.G. Canadell, N. Cong, S. Lewis, P.E. Levy, L. Liu, M.R. Lomas, J. Mao, R.B. Myneni, P. Peylin, B. Poulter, X. Shi, G. Yin, N. Viovy, T. Wang, X. Wang, S. Zaeble, N. Zeng, Z. Zeng and A. Chen, 2014. Evidence for a weakening relationship between interannual temperature variability and northern vegetation activity. *Nature Communications*, 5:5018, doi:10.1038/ncomms6018.

Ping, C.-L., G.L. Michaelson, L. Guo, T. Jorgenson, M. Kanesskiy, Y. Shur, F. Dou and J. Liang, 2011. Soil carbon and material fluxes across the eroding Alaska Beaufort Sea coastline. *Journal of Geophysical Research: Biogeosciences*, 116: G02004, doi:10.1029/2010JG001588.

Pinzon, J. and C. Tucker, 2014. A non-stationary 1981–2012 AVHRR NDVI3g time series. *Remote Sensing*, 6:6929-6960.

Pithan, F. and T. Mauritsen, 2014. Arctic amplification dominated by temperature feedbacks in contemporary climate models. *Nature Geoscience*, 7:181-184.

Pizano, M.C., A.F. Barón, E.A.G. Schuur, K.G. Crummer and M.C. Mack, 2014. Effects of thermo-erosional disturbance on surface soil carbon and nitrogen dynamics in upland arctic tundra. *Environmental Research Letters*, 9:075006, doi:10.1088/1748-9326/9/7/075006.

Preece, C. and G.K. Phoenix, 2014. Impact of early and late winter icing events on sub-arctic dwarf shrubs. *Plant Biology*, 16:125-132.

Prowse, T., K. Alfredsen, S. Beltaos, B. Bonsal, C. Duguay, A. Korhola, J. McNamara, W.F. Vincent, V. Vuglinsky and G. Weyhennmeyer, 2011. Changing lake and river ice regimes: trends effects and implications. In: *Snow, Water, Ice and Permafrost in the Arctic (SWIPA): Climate and the Cryosphere*. Arctic Monitoring and Assessment Programme (AMAP), Oslo, Norway.

Racine, C.H., L.A. Johnson and L.A. Viereck, 1987. Patterns of vegetation recovery after tundra fires in northwestern Alaska, USA. *Arctic and Alpine Research*, 19:461-469.

Rahmstorf, S., J. Box, G. Feulner, M. Mann, A. Robinson, S. Rutherford and E. Schaffernicht, 2015. Exceptional twentieth-century slowdown in Atlantic Ocean overturning circulation. *Nature Climate Change*, 5:475-480.

Randerson, J.T., H. Liu, M.G. Flanner, S.D. Chambers, Y. Jin, P.G. Hess, G. Pfister, M.C. Mack, K.K. Treseder, L.R. Welp, F.S. Chapin, J.W. Harden, M.L. Goulden, E. Lyons, J.C. Neff, E.A.G. Schuur and C.S. Zender, 2006. The impact of boreal forest fire on climate warming. *Science*, 314:1130-1132.

Rawlins, M.A., M. Steele, M.M. Holland, J.C. Adam, J.E. Cherry, J.A. Francis, P.Ya Groisman, L.D. Hinzman, T.G. Huntington, D.L. Kane, J.S. Kimball, R. Kwok, R.B. Lammers, C.M. Lee, D.P. Lettenmaier, K.C. McDonald, E. Podest, J.W. Pundsack, B. Rudels, M.C. Serreze, A. Shiklomanov, Ø. Skagseth, T.J. Troy, C.J. Vörösmarty, M. Wensnahan, E.F. Wood, R. Woodgate, D. Yang, K. Zhang and T. Zhang, 2010. Analysis of the arctic system freshwater cycle intensification: observations and expectations. *Journal of Climate*, 23:5715-5737.

Raynolds, M.K. and D.A. Walker, 2008. Relationship of permafrost characteristics, NDVI, and arctic vegetation types. pp. 1469-1474. Ninth International Conference on Permafrost, Fairbanks, Alaska.

Raynolds, M.K. and D.A. Walker, 2009. Effects of deglaciation on circumpolar distribution of arctic vegetation. *Canadian Journal of Remote Sensing*, 35:118-129.

Raynolds, M.K. and D.A. Walker, 2016. Increased wetness confounds Landsat-derived NDVI trends in the central Alaska North Slope region, 1985–2011. *Environmental Research Letters*, 11:085004.

Raynolds, M.K., J.C. Comiso, D.A. Walker and D. Verbyla, 2008. Relationship between satellite-derived land surface temperatures, arctic vegetation types, and NDVI. *Remote Sensing of Environment*, 112:1884-1894.

Raynolds, M.K., D.A. Walker, H.E. Epstein, J.E. Pinzon and C.J. Tucker, 2012. A new estimate of tundra-biome phytomass from trans-Arctic field data and AVHRR NDVI. *Remote Sensing Letters*, 3:403-411.

Raynolds, M.K., D.A. Walker, K.J. Ambrosius, J. Brown, K.R. Everett, M. Kanevskiy, G.P. Kofinas, V.E. Romanovsky, Y. Shur and P.J. Webber, 2014a. Cumulative geoecological effects of 62 years of infrastructure and climate change in ice-rich permafrost landscapes, Prudhoe Bay Oilfield, Alaska. *Global Change Biology*, 20:1211-1224.

Raynolds, M.K., D.A. Walker, M. Buchhorn and L. Wirth, 2014b. Vegetation changes related to 45 years of heavy road traffic along the Spine Road at Prudhoe Bay, Alaska. In: *Arctic Change 2014*, pp. 138-139.

Reid, P.C., R.E. Hari, G. Beaugrand, D.M. Livingstone, C. Marty, D. Straile, J. Barichivich, E. Goberville, R. Adrian, Y. Aono, R. Brown, J. Foster, P. Groisman, P. Hélaouët, H.-H. Hsu, R. Kirby, J. Knight, A. Kraberg, J. Li, T.-T. Lo, R.B. Myneni, R.P. North, J.A. Pounds, T. Sparks, R. Stübi, Y. Tian, K.H. Wiltshire, D. Xiao and Z. Zhu, 2016. Global impacts of the 1980s regime shift. *Global Change Biology*, 22:682-703.

Rignot, E., M. Koppes and I. Velicogna, 2010. Rapid submarine melting of the calving faces of West Greenland glaciers. *Nature Geoscience*, 3:187-191.

Rignot, E., I. Fenty, Y. Xu, C. Cai and C. Kemp, 2015. Undercutting of marine-terminating glaciers in West Greenland. *Geophysical Research Letters*, 42:5909-5917.

Riihelä, A., T. Manninen and V. Laine, 2013. Observed changes in the albedo of the Arctic sea-ice zone for the period 1982 to 2009. *Nature Climate Change*, 3:895-898.

Robinson, A., R. Calov and A. Ganopolski, 2012. Multistability and critical thresholds of the Greenland ice sheet. *Nature Climate Change*, 2:429-432.

Robock, A. and C. Oppenheimer (eds.), 2003. *Volcanism and the Earth's Atmosphere*. Geophysical Monograph 139, American Geophysical Union.

Rocha, A.V., M.M. Loranty, P.E. Higuera, M.C. Mack, F.S. Hu, B.M. Jones, A.L. Breen, E.B. Rastetter, S.J. Goetz and G.R. Shaver, 2012. The footprint of Alaskan tundra fires during the past half-century: implications for surface properties and radiative forcing. *Environmental Research Letters*, 7:044039.

Ropars, P., E. Lévesque and S. Boudreau, 2015. How do climate and topography influence the greening of the forest-tundra ecotone in northern Québec? A dendrochronological analysis of *Betula glandulosa*. *Journal of Ecology*, 103:679-690.

Rydberg, J., J. Klaminder, P. Rosén and R. Bindler, 2010. Climate driven release of carbon and mercury from permafrost mires increases mercury loading to sub-arctic lakes. *Science of the Total Environment*, 408:4778-4783.

Schuur, E.A.G. and B. Abbott, 2011. Climate change: High risk of permafrost thaw. *Nature*, 480:32-33.

Schuur, E.A.G., K.G. Crummer, J.G. Vogel and M.C. Mack, 2007. Plant species composition and productivity following permafrost thaw and thermokarst in Alaskan tundra. *Ecosystems*, 10:280-292.

Schuur, E.A.G., J. Bockheim, J.G. Canadell, E. Euskirchen, C.B. Field, S.V. Goryachkin, S. Hagemann, P. Kuhry, P.M. Lafleur, H. Lee, G. Mazhitova, F.E. Nelson, A. Rinke, V.E. Romanovsky, N. Shiklomanov, C. Tarnocai, S. Venevsky, J.G. Vogel and S.A. Zimov, 2008. Vulnerability of permafrost carbon to climate change: Implications for the global carbon cycle. *Bioscience*, 58:701-714.

Schuur, E.A.G., J.G. Vogel, K.G. Crummer, H. Lee, J.O. Sickman and T.E. Osterkamp, 2009. The effect of permafrost thaw on old carbon release and net carbon exchange from tundra. *Nature*, 459:556-559.

Schuur, E.A.G., A.D. McGuire, C. Schädel, G. Grosse, J.W. Harden, D.J. Hayes, G. Hugelius, C.D. Koven, P. Kuhry, D.M. Lawrence, S.M. Natali, D. Olefeldt, V.E. Romanovsky, K. Schaefer, M.R. Turetsky, C.C. Treat and J.E. Vonk, 2015. Climate change and the permafrost carbon feedback. *Nature*, 520:171-179.

Serreze, M. and J. Francis, 2006. The Arctic amplification debate. *Climate Change*, 76:241-264.

Shakhova, N. I. Semiletov, V. Sergienko, L. Lobkovsky, V. Yusupov, A. Salyuk, A. Salomatin, D. Chernykh, D. Kosmach, G. Panteleev, D. Nicolsky, V. Samarkin, S. Joye, A. Charkin, O. Dudarev, A. Meluzov and O. Gustafsson, 2015. The East Siberian Arctic Shelf: towards further assessment of permafrost-related methane fluxes and role of sea ice. *Philosophical Transactions of the Royal Society A*, 373:20140451, doi:10.1098/rsta.2014.0451.

Shaver, G.R., J.A. Laundre, A.E. Giblin and K.J. Nadelhoffer, 1996. Changes in live plant biomass, primary production, and species composition along a riverside toposequence in arctic Alaska, USA. *Arctic and Alpine Research*, 28:363-379.

Shi, X., S.J. Déry, P.Ya. Groisman and D.P. Lettenmaier, 2013. Relationships between recent pan-Arctic snow cover and hydroclimate trends. *Journal of Climate*, 26:2048-2064.

Shiklomanov, A.I. and R.B. Lammers, 2009. Record Russian river discharge in 2007 and the limits of analysis. *Environmental Research Letters*, 4 (4):045015.

Shippert, M.M., D.A. Walker, N.A. Auerbach and B.E. Lewis, 1995. Biomass and leaf-area index maps derived from SPOT images for Toolik Lake and Innnavait Creek areas, Alaska. *Polar Record*, 31:147-154.

Shuman, J.K., N.M. Tchekakova, E.I. Parfenova, A.J. Soja, H.H. Shugart, D. Ershov and K. Holcomb, 2015. Forest forecasting with vegetation models across Russia. *Canadian Journal of Forest Research*, 45:175-184.

Shur, Y.L. and M.T. Jorgenson, 2007. Patterns of permafrost formation and degradation in relation to climate and ecosystems. *Permafrost and Periglacial Processes*, 18:7-19.

Sieg, B. and F.J.A. Daniëls, 2005. Altitudinal zonation of vegetation in continental West Greenland with special reference to snowbeds. *Phytocoenologia*, 35:887-908.

Smith, T.M., P.A. Arkin, L. Ren and S.S.P. Shen, 2012. Improved reconstruction of global precipitation since 1900. *Journal of Atmospheric and Oceanic Technology*, 29:1505-1517.

Steele, M., W. Ermold and J. Zhang, 2008. Arctic Ocean surface warming trends over the past 100 years. *Geophysical Research Letters*, 35: L02614, doi:10.1029/2007GL031651.

Stenchikov, G., A. Robock, V. Ramaswamy, M.D. Schwarzkopf, K. Hamilton and S. Ramachandran, 2002. Arctic Oscillation response to the 1991 Mount Pinatubo eruption: Effects of volcanic aerosols and ozone depletion. *Journal of Geophysical Research: Atmospheres*, 107:ACL 28-1-ACL 28-16.

Stern, G.A., R.W. Macdonald, P.M. Outridge, S. Wilson, J. Chetelat, A. Cole, H. Hintelmann, L.L. Loseto, A. Steffen and F. Wang, 2012. How does climate change influence Arctic mercury? *Science of the Total Environment*, 414:22-42.

Stieglitz, M., J. Shaman, J. McNamara, V. Engel, J. Shanley and G.W. Kling, 2003. An approach to understanding hydrologic connectivity on the hillslope and the implications for nutrient transport. *Global Biogeochemical Cycles*, 17:1105, doi:10.1029/2003GB002041.

Straneo, F., R. Curry, D.A. Sutherland, G. Hamilton, C. Cenedese, K. Väge and L.A. Stearns, 2011. Impact of fjord dynamics and subglacial discharge on the circulation near Helheim Glacier in Greenland. *Nature Geoscience*, 4:322-327.

Straneo, F., D.A. Sutherland, D. Holland, C. Gladish, G. Hamilton, H. Johnson, E. Rignot, Y. Xu and M. Koppes, 2012. Characteristics of ocean waters reaching Greenland's glaciers. *Annals of Glaciology*, 53:202-210.

Stroeve, J.C., M.C. Serreze, M.M. Holland, J.E. Kay, J. Masklinik and A.P. Barrett, 2012. The Arctic's rapidly shrinking sea ice cover: a research synthesis. *Climate Change*, 110:1005-1027.

Stow, D.A., A.S. Hope and T.H. George, 1993. Reflectance characteristics of arctic tundra vegetation from airborne radiometry. *International Journal of Remote Sensing*, 14:1239-1244.

Swanson, D.K., 2015. Environmental limits of tall shrubs in Alaska's Arctic national parks. *PLoS One*, 10:e0138387.

Tape, K., M. Sturm and C. Racine, 2006. The evidence for shrub expansion in Northern Alaska and the Pan-Arctic. *Global Change Biology*, 12:686-702.

Tape, K.D., M. Hallinger, J.M. Welker and R.W. Ruess, 2012. Landscape heterogeneity of shrub expansion in Arctic Alaska. *Ecosystems*, 15:711-724.

Tchekakova, N.M., E.I. Parfenova and A.I. Soja, 2016. Significant Siberian vegetation change is compelled by the changing climate. In: Mueller, L., E. Smolentseva, A. Syso and G. Licheid (eds.), *Novel Methods for Monitoring and Management of Land and Water Resources of Siberia*. Springer.

Tedesco, M., X. Fettweis, M.R. van den Broeke, R.S.W. van de Wal, C.J.P.P. Smeets, W.J. van de Berg, M.C. Serreze and J.E. Box, 2011. The role of albedo and accumulation in the 2010 melting record in Greenland. *Environmental Research Letters*, 6:014005, doi: 10.1088/1748-9326/6/1/014005.

Treshnikov, A.F., 1985. *Atlas of the Arctic*. Arctic and Antarctic Scientific Research Institute (AANII), Moscow. (In Russian)

Tucker, C.J., 1979. Red and photographic infrared linear combinations for monitoring vegetation. *Remote Sensing of Environment*, 8:127-150.

Tucker, C.J. and P.J. Sellers, 1986. Satellite remote sensing of primary production. *International Journal of Remote Sensing*, 7:1395-1416.

Turetsky, M.R., J.W. Harden, H.R. Friedli, M. Flannigan, N. Payne, J. Crock and L. Radke, 2006. Wildfires threaten mercury stocks in northern soils. *Geophysical Research Letters*, 33:L16403, doi:10.1029/2005GL025595.

Turetsky, M.R., E.S. Kane, J.W. Harden, R.D. Ottmar, K.L. Manies, E. Hoy and E.S. Kasischke, 2011. Recent acceleration of biomass burning and carbon losses in Alaskan forests and peatlands. *Nature Geoscience*, 4:27-31.

Ukraintseva, N., M. Leibman, I. Streletskaya and T. Mikhaylova, 2014. Geochemistry of plant-soil-permafrost system on landslide-affected slopes, Yamal, Russia as an indicator of landslide age. In: Shan, W., Y. Guo, F. Wang, H. Marui and A. Strom (eds.), *Landslides in Cold Regions in the Context of Climate Change*. pp. 107-131. Springer.

Väistönen, M., H. Ylännö, E. Kaarlejärvi, S. Sjögersten, J. Olofsson, N. Crout and S. Stark, 2014. Consequences of warming on tundra carbon balance determined by reindeer grazing history. *Nature Climate Change*, 4:384-388.

Villarreal, S., R.D. Hollister, D.R. Johnson, M.J. Lara, P.J. Webber and C.E. Tweedie, 2012. Tundra vegetation change near Barrow, Alaska (1972-2010). *Environmental Research Letters*, 7:015508.

Vonk, J.E., S.E. Tank, W.B. Bowden, I. Laurion, W.F. Vincent, P. Alekseychik, M. Amyot, M.F. Bilett, J. Canário, R.M. Cory, B.N. Deshpande, M. Helbig, M. Jammes, J. Karlsson, J. Larouche, G. MacMillan, M. Rautio, K.M. Walter Anthony and K.P. Wicklund, 2015. Reviews and syntheses: Effects of permafrost thaw on Arctic aquatic ecosystems. *Biogeosciences*, 12:7129-7167.

Walker, D.A. and M.D. Walker, 1996. Terrain and vegetation of the Imnavait Creek Watershed. In: Reynolds, J.F. and J.D. Tenhunen (eds.), *Landscape Function: Implications for Ecosystem Disturbance, a Case Study in Arctic Tundra*. pp. 73-108. Springer.

Walker, D.A., J.C. Halfpenny, M.D. Walker and C. Wessman, 1993. Long-term studies of snow-vegetation interactions. *Bioscience*, 43:287-301.

Walker, D.A., N.A. Auerbach and M.M. Shippert, 1995. NDVI, biomass, and landscape evolution of glaciated terrain in northern Alaska. *Polar Record*, 31:169-178.

Walker, D.A., W.D. Billings and J.G. de Molenaar, 2001. Snow-vegetation interactions in tundra environments. In: Jones, H.G., R.W. Hoham, J.W. Pomeroy and D.A. Walker (eds.), *Snow Ecology*. pp. 266-324. Cambridge University Press.

Walker, D.A., A.L. Breen, L.A. Druckenmiller, L.W. Wirth, W. Fisher, M.K. Raynolds, J. Šíbík, M.D. Walker, S. Hennekens, K. Boggs, T. Boucher, M. Buchhorn, H. Bültmann, D.J. Cooper, F.J.A. Daniëls, S.J. Davidson, J.J. Ebersole, S.C. Elmendorf, H.E. Epstein, W.A. Gould, R.D. Hollister, C.M. Iversen, M.T. Jorgenson, A. Kade, M.T. Lee, W.H. MacKenzie, R.K. Peet, J.L. Peirce, U. Schickhoff, V.L. Sloan, S.S. Talbot, C.E. Tweedie, S. Villarreal, P.J. Webber and D. Zona, 2016. The Alaska Arctic Vegetation Archive (AVA-AK). *Phytocoenologia*, 46:221-229.

Walsh, J.E., W.L. Chapman, V. Romanovsky, J.H. Christensen and M. Stendel, 2008. Global climate model performance over Alaska and Greenland. *Journal of Climate*, 21:6156-6174.

Walter Anthony, K.M., M.E. Edwards, G. Grosse, S.A. Zimov and F.S. Chapin III, 2007. Thermokarst lakes as a source of atmospheric CH₄ during the last deglaciation. *Science*, 318:633-636.

Walter Anthony, K.M., S.A. Zimon, G. Grosse, M.C. Jones, P.M. Anthony, F.S. Chapin III, J.C. Finlay, M.C. Mack, S. Davydov, P. Frenzel and S. Froliking, 2014. A shift of thermokarst lakes from carbon sources to sinks during the Holocene epoch. *Nature*, 511:452-456.

Walter Anthony, K., R. Daanen, P. Anthony, T.S. von Deimling, C.-L. Ping, J.P. Chanton and G. Grosse, 2016. Methane emissions proportional to permafrost carbon thawed in Arctic lakes since the 1950s. *Nature Geosciences*, 9:679-682.

Westermann, S., J. Boike, M. Langer, T.V. Schuler and B. Etzelmüller, 2011. Modeling the impact of wintertime rain events on the thermal regime of permafrost. *The Cryosphere*, 5:945-959.

Wheeler, J.A., G. Hoch, A.J. Cortés, J. Sedlacek, S. Wipf and C. Rixen, 2014. Increased spring freezing vulnerability for alpine shrubs under early snowmelt. *Oecologia*, 175:219-229.

Wheeler, H.C., T.T. Hoye, N.M. Schmidt, J.-C. Svenning and M.C. Forchammer, 2015. Phenological mismatch with abiotic conditions-implications for flowering in Arctic plants. *Ecology*, 96:775-787.

White and A. Jentsch, 2001. The search for generality in studies of disturbance and ecosystem dynamics. *Progress in Botany*, 62:399-450.

Wilson, R.R., A. Bartsch, K. Joly, J.H. Reynolds, A. Orlando and W.M. Loya, 2013. Frequency, timing, extent, and size of winter thaw-refreeze events in Alaska 2001–2008 detected by remotely sensed microwave backscatter data. *Polar Biology*, 36:419-426.

Winton, M., 2006. Does the Arctic sea ice have a tipping point? *Geophysical Research Letters*, 33:L23504, doi:10.1029/2006GL028017.

Wrona, F.J., M. Johansson, J.M. Culp, A. Jenkins, J.M. Karlsson, I.H. Myers-Smith, T.D. Prowse, W.F. Vincent and P.A. Wookey, 2016. Transitions in Arctic ecosystems: ecological implications of a changing freshwater system [Special issue]. *Journal of Geophysical Research: Biogeosciences*, 121:650-674.

Wu, W.-Y., C.-W. Lan, M.-H. Lo, J.T. Reager and J.S. Famiglietti, 2015. Increases in the annual range of soil water storage at northern middle and high latitudes under global warming. *Geophysical Research Letters*, 42:3903-3910.

Young, A.M., P.E. Higuera, P.A. Duffy and F.S. Hu, 2016. Climatic thresholds shape northern high-latitude fire regimes and imply vulnerability to future climate change. *Ecography*, 39:001-012.

Yurtsev, B.A., 1994. The floristic division of the Arctic. *Journal of Vegetation Science*, 5:765-776.

11. SWIPA 2017 Synthesis: summary and implications of findings

LEAD AUTHORS: JAMES OVERLAND, JOHN WALSH, VLADIMIR KATTSOV, DAVID BARBER, JASON E. BOX, ROSS BROWN, JOHANNA MÅRD, MORTEN S. OLSEN, VLADIMIR ROMANOVSKY

Coordinating lead authors shown in bold

Contents

SWIPA 2017: Summary and implications of findings	258
11.1 Introduction and scope	259
11.2 Ongoing change in the cryosphere	259
11.2.1 Climate trends	260
11.2.2 Snow on land	260
11.2.3 Permafrost	260
11.2.4 Sea ice	260
11.2.5 Land ice	261
11.2.6 Freshwater	261
11.2.7 Carbon cycling	261
11.2.8 Terrestrial ecosystems	261
11.3 Projected change in the cryosphere	261
11.4 Linkage between cryospheric change and lower latitudes	262
11.4.1 Patterns of atmospheric circulation	262
11.4.2 Greenhouse gas release	262
11.4.3 Sea-level rise	263
11.4.4 Freshwater outflow	263
11.5 Consequences of cryospheric-driven change	264
11.5.1 Changes in marine and terrestrial access	264
11.5.2 Land use	264
11.5.3 Industrialization and development	264
11.5.4 Hazards	265
11.5.5 Ecosystem and biodiversity losses	265
11.5.6 Shift in lifestyles, culture and socio-economics	265
11.6 Research priorities from the SWIPA 2017 assessment	265
11.7 Conclusion	266
References	268

SWIPA 2017: Summary and implications of findings

Summary of observations and projections

- The period since SWIPA 2011 has seen a continuation of cryospheric trends consistent with rapid warming of the Arctic. These trends are very likely to continue past mid-century, with more frequent and stronger extremes and the passing of no-return thresholds ('irreversibilities').
- Observed and projected changes in Arctic temperature are more than double those at mid-latitudes.
- Sea ice is undergoing a regime shift from multi-year ice to predominantly first-year ice. Summer sea ice is very likely to be essentially gone within the next few decades.
- Loss of land-based ice – from mountain glaciers and ice caps – is expected to accelerate because committed loss will increase with warming, with implications for global sea-level rise.
- Ongoing reductions in Arctic snow cover and warming permafrost are both manifestations of change in the Arctic terrestrial coupled soil-vegetation-climate system, with impacts on energy, freshwater and carbon cycling. Specific humidity and precipitation have generally increased.
- There are emerging impacts of Arctic change on mid-latitude weather/climate and global sea-level rise.

Summary of implications

- The Arctic climate will continue to change over the coming decades with major consequences for ecosystems and society. Adaptation efforts need to begin now, because foreseeable Arctic temperature changes are large (4–5°C for autumn/winter by 2040–2050). In addition to climate change, adaptation planning should take into account economic and societal drivers.
- Substantial and immediate mitigation in greenhouse gas emissions (at least at the level of RCP4.5) should reduce the risk of further future change for most cryospheric components after mid-century, and reduce the likelihood of potential irreversible melt of the Greenland ice sheet and glaciers and the associated impact on sea-level rise.
- Cumulative global impacts related to Arctic change are expected to be large; adaptation costs and economic opportunities are estimated in the tens of trillions of US dollars.
- Prudent adaptation and risk management require better quantitative predictions. This means:
 - determining which feedbacks involving the Arctic cryosphere are most consequential for rapid Arctic warming
 - having a better understanding of interactions between different parts of the Arctic system. In particular, reducing uncertainties in snow-vegetation interactions, reducing uncertainties in snow and ice albedo feedbacks, and developing more detailed representation of vegetation, lakes and rivers
 - enhancing Arctic observing systems and the interpretation of *in situ* observations, satellite data, and model results; as well as improving coordination between monitoring efforts, process studies, and modeling.
- Determining the impacts of Arctic climate change outside of the Arctic region requires improved understanding of atmospheric and ocean connectivities.

11.1 Introduction and scope

The key finding of SWIPA 2017 is continued change in all components of the Arctic cryosphere since the first SWIPA assessment – SWIPA 2011 (AMAP, 2011). Six additional years of data and new understanding from an increasing body of peer-reviewed scientific literature add certainty relative to the findings of SWIPA 2011 on near future (decadal) trends across multiple processes. SWIPA 2017 provides evidence that interacting Arctic changes will continue and are likely to accelerate in some components of the cryosphere given the continued increase in greenhouse gas (GHG) emissions. In combination with natural variability in weather and climate, this GHG-forced change will result in more extreme events. Driven mainly by warming, cryospheric changes involve a decrease in terrestrial spring snow, warming permafrost and increased active layer depth, continued mass loss from glaciers and ice sheets, and a shift from mostly thick multi-year sea ice to thinner first-year sea ice. Cryospheric changes are having, and will continue to have for the foreseeable future, profound impacts on physical, biological, and geochemical systems and on human activities in the Arctic (Figure 11.1). Impacts are beginning to extend beyond the Arctic, with changes in the Arctic cryosphere contributing to global sea-level rise and influencing mid-latitude weather.

Multiple lines of evidence showing a continuing shift in the climate state of the Arctic are presented in Chapter 2, and discussed in relation to projections of Arctic-wide changes in temperature for the coming decades driven by scenarios of increased GHG concentrations. The remaining chapters detail recent data and relevant new scientific literature for the major components of the cryosphere. There are four main issues: the nature and magnitude of the changes, their timing relative to the seasonal/annual cycle, the spatial and temporal scales on which they occur, and their local and large-scale consequences

for physical and biological systems. This chapter provides a summary of cryospheric changes documented in the preceding chapters, shows their projections, and provides a synthesis of their combined impact on the Arctic environment and its inhabitants. It addresses potential global impacts where this is possible. A new emphasis relative to SWIPA 2011 is that, while climate models project that temperatures, spring snow cover, and sea-ice extent and thickness will continue to follow the same broad trends over the next three decades, other elements of the cryosphere such as mass loss from glaciers and ice sheets are projected to accelerate in the latter half of the century. Societal and infrastructure impacts such as those related to permafrost thawing are expected to substantially increase before mid-century and will require major adaptation efforts.

11.2 Ongoing change in the cryosphere

The Arctic as a system (Figure 11.1) is undergoing transformations that cut across all components of the cryosphere (Figure 11.2). A warming trajectory toward a summer that is essentially sea ice-free and a spring that is snow-free on land ensures profound disruption of the Arctic biogeophysical state involving major changes in ground hydrology, vegetation, marine production (including fisheries in the coastal seas), more wildfires and permafrost thaw, and conversion between terrestrial and aquatic ecosystems. Permafrost thaw accelerates the decomposition of plant material and carbon release to the atmosphere. Changes in snow distribution, lake drainage, thermo-erosional features and fire will influence the cycling and toxicity of contaminants. Arctic precipitation is increasing overall, yet some areas are drying and tundra is browning. SWIPA 2017 highlights the complexity of interactions within the Arctic system and emphasizes the importance of such a perspective to provide accurate projections of different cryospheric elements.

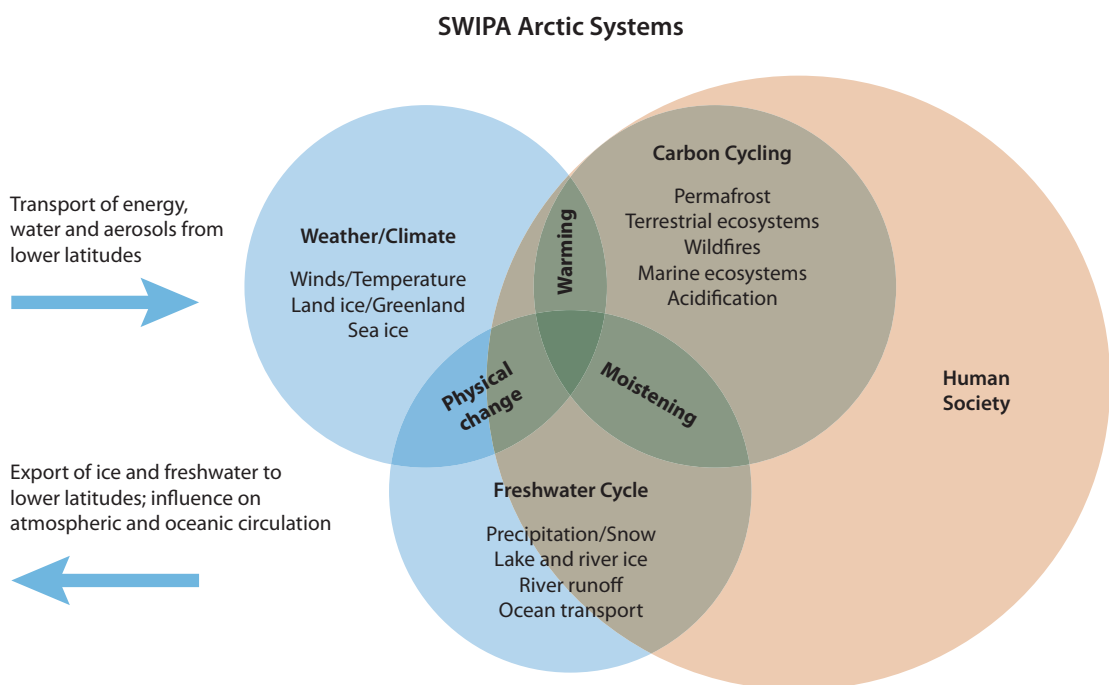


Figure 11.1 Conceptualized view of the interactions between the three main system elements of the Arctic cryosphere (climate, carbon, freshwater) set within the human dimension, and their emerging links with the mid-latitudes.

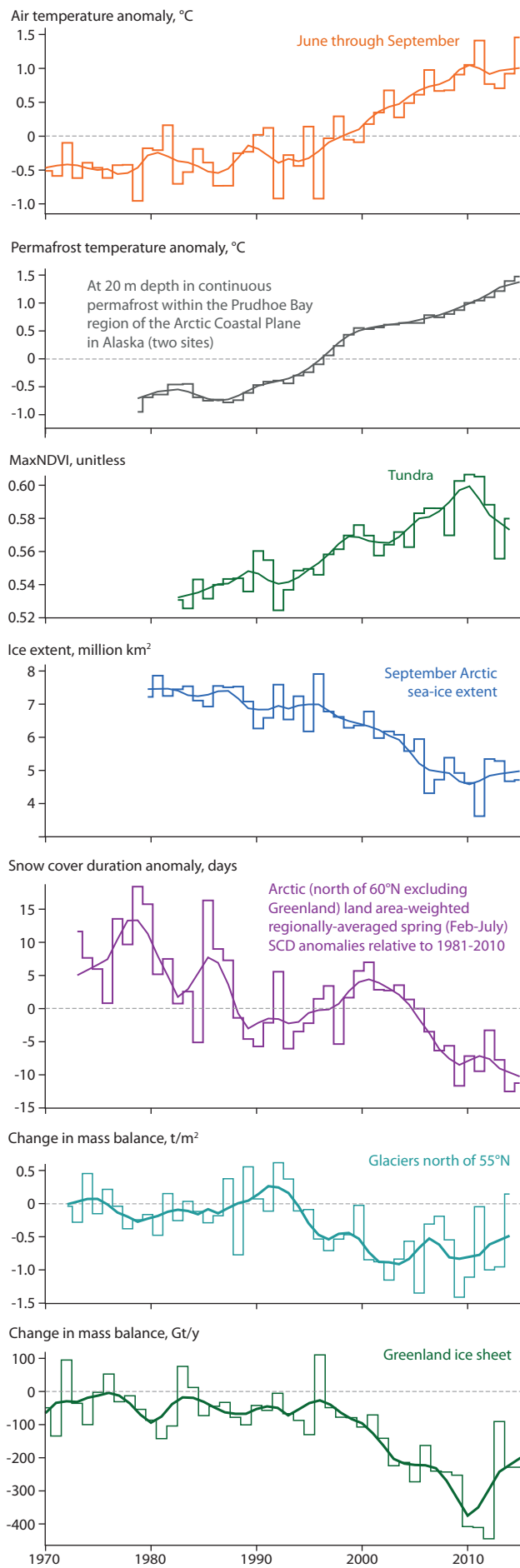


Figure 11.2 Relative change in multiple Arctic cryospheric indicators since 1970.

11.2.1 Climate trends

In response to continued GHG forcing and multiple polar amplification processes the Arctic has continued to warm at over twice the rate of the global average (Figure 2.2) since SWIPA 2011. The warming is most marked in autumn and winter. Advection of moisture into the Arctic and a reduction in fine particulate material carried into the Arctic from mid-latitudes have also contributed to the rise in temperature. Natural atmospheric variability also impacts the Arctic; during 1939–1970 it counteracted the GHG contribution; during 2008–2012 it contributed to the rapid loss observed in Greenland glacier area; and in autumn and winter 2016 it contributed to record regional temperatures of more than 6°C above average (Figure 2.3). Other striking new findings are the confirmation of loss of sea ice volume and the transition across most of the Arctic from multi-year sea ice to first-year sea ice (Figure 2.5), with nearly Arctic-wide low ice concentrations in summer 2012 and 2016. Increased long-term greening is now apparent across many Arctic and subarctic land areas, although some areas have recently shown increased variability and browning (Figures 2.7 and 10.6).

11.2.2 Snow on land

There is widespread multi-dataset evidence of continued reductions in Arctic snow cover since SWIPA 2011. Arctic spring (May, June) snow cover on land has now decreased by more than two standard deviations over the period of satellite observations beginning in the late 1960s (Figure 3.4). Trends in annual maximum snow accumulation are more uncertain but suggest a trend to pan-Arctic land area decreases in the amount of water stored in seasonal snow cover over the past ~20 years. There is evidence of increased ice layer development in snowpack from several regions in response to winter thaw and rain-on-snow events.

11.2.3 Permafrost

Since 2007/2008, new record high mean annual ground temperatures in the upper 10–20 m have been observed at many permafrost observatories with the greatest temperature increases (>0.5°C) occurring in the colder permafrost of the northern Arctic (Figure 4.2). In warmer permafrost, temperature increases are lower or not detectable. In northern Alaska, the active layer freeze-up date in the early 2010s (mid-December) was almost two months later than in the mid-1980s (first half of October).

11.2.4 Sea ice

The recent decade continues the unprecedented change in Arctic sea ice, in both the rates and magnitude of change in extent, area, thickness, spatial distribution, and most aspects of temporal and spatial variability. The Arctic has transformed from an environment dominated by thick multi-year sea ice to one dominated by thinner first-year sea ice (Figures 5.1 and 5.8). Sea-ice extent and thickness continue their downward trend. The past six years have seen high variability; with record low extent in summer 2012 and 2016 and substantially greater extent and thickness in 2013 and 2014. The Pacific sector of the Arctic Ocean, Hudson Bay and Baffin Bay show increased open water from August through December; the autumn open-water extension period is dominated by the ice albedo feedback and heat capture in the upper ocean. The Atlantic sector shows

increased open water in winter; the open-water period is dominated by horizontal ocean heat fluxes. Understanding the evolution of snow on sea ice remains a scientific challenge. There is evidence for a loss of biodiversity in sea-ice habitats in the central Arctic Ocean, linked to the decline in thick multi-year sea ice. The increasing presence of very young ice types results in high salinity ice covers (e.g. frost flowers) that are reactive in chemical exchanges with the atmosphere and ocean.

11.2.5 Land ice

All Arctic regions lost land ice mass between 2003 and 2014, representing a large regional contribution to global sea-level rise. Rates of mass loss from land ice have, in most cases, increased in comparison with rates reported in SWIPA 2011 (Table 6.1, Figures 6.1 and 6.14). Ice mass losses were greatest from the Greenland ice sheet and peripheral ice caps (64% of the Arctic total), followed by Arctic Canada (14%) and Alaska (12%). Of the global glacier mass loss between 1991 and 2010, 70% has been attributed to anthropogenic causes. Shifts in summer atmospheric circulation patterns between years strongly influence the relative rates of glacier melt in different regions (Figures 6.2 and 6.3). Surface melting over the entire Greenland ice sheet in 2012 represented a new extreme. Glacier, ice cap, and ice sheet mass balance estimates from multiple independent data sets have, for the first time, been reconciled, indicating widespread acceleration of ice loss across the Arctic, with the exception of Svalbard.

11.2.6 Freshwater

Liquid freshwater storage has increased since 2000 within the Arctic marine basins (Figure 7.6). Specific humidity and precipitation have generally increased in the Arctic, in part related to the advection of moist air from mid-latitudes, which has also contributed to an increase in Arctic surface temperature through increased downwelling of long-wave radiation, and from a longer open water season. Runoff into the Arctic Basin increased by 8% between 1980–2000 and 2000–2010 (Table 7.1).

11.2.7 Carbon cycling

Recent changes in biogeophysical energy exchange and transport within the Arctic, and between this complex region and the atmosphere exceeded even extreme projections. There is now clear evidence for both the marine and terrestrial Arctic environments that winter is not, as has previously been assumed, a dormant time for ecosystem processes. This includes carbon exchange through sea ice in the winter via recently discovered calcium carbonate-related processes. Terrestrial carbon exchange is complicated by the role of thawing permafrost, increased hydrological processes, and coupling between the land and ocean.

11.2.8 Terrestrial ecosystems

Arctic greening (overall color changes as seen from satellite; Chapter 10) has been observed across tundra ecosystems over the past 30 years. However, recent hydrological and cryospheric changes are influencing greening/browning patterns. Increasing frequency of wildfires and abrupt thaw events can accelerate biome shifts, such as increased tree density in taiga, spread of tall shrubs and trees into tundra, or conversion between terrestrial and aquatic ecosystems.

11.3 Projected change in the cryosphere

General circulation model (GCM) projections based on scenarios of anthropogenic GHG concentrations (IPCC, 2013) suggest the Arctic will continue to warm over the coming decades at a rate at least double that for other regions of the world (Figure 2.15), with related changes throughout the cryosphere driven in part by feedbacks among cryospheric and other climate system components. The Arctic of the foreseeable future (decades) is projected to be very different to that of today.

Natural variability can result in occasional short-term cooling trends set within the context of longer-term warming, or can combine with the long-term warming trend to produce regional and temporal extremes. For example, January through April and October/December 2016 showed extreme Arctic-wide temperatures; January 2016 was 5°C above the 1981–2010 average, and 2°C above the previous record (Figure 2.3).

Given the current and projected increase in global GHG levels over the next two decades, it is likely that average autumn and winter temperatures in the Arctic will increase by 4–5°C by 2040–2050 relative to a 1981–2005 baseline (Figure 2.13). Differences arising from the choice of GHG scenario only start to emerge after this period. An essentially ice free Arctic Ocean in summer is likely within the next few decades. These changes are now 'locked' into the Arctic climate system due to the cumulative effect of past GHG emissions and the GHG increase projected for the next few decades. Glacier mass shows the potential for accelerated loss in the latter half of the century. For temperatures and Arctic systems to stabilize in the latter half of the century would require substantial global climate mitigation efforts.

Some Arctic warming projections for 2100 exceed thresholds for internal tipping points, including rapid loss of the Greenland ice sheet and autumn/spring sea ice, and changes in boreal forest extent.

Future projections suggest Arctic precipitation will increase, especially over the Arctic Ocean. The fraction falling as rain rather than snow will increase with warming.

Similar to SWIPA 2011, projected changes in Arctic snow cover have a snow-cover duration decrease of 10–20% over most of the Arctic by mid-century but with larger decreases (>30%) over the European sector and western Alaska, and during late spring. The largest and most rapid reductions in snow cover are projected in the warmer coastal regions of the Arctic, such as Alaska and Scandinavia. Northern Siberia and the Canadian Arctic Archipelago are projected to have increased snow accumulation in a warmer climate (Figures 3.17 and 3.18). Climate model projections based on the RCP4.5 scenario show that efforts to reduce carbon dioxide emissions can contribute to a stabilization of Arctic snow cover loss by the end of the 21st century. Climate models still exhibit a large spread in the strength of snow albedo feedbacks during the snowmelt period that hindcast studies show contributed to an underestimate of the observed decreases in terrestrial spring snow-cover extent over the past 30 to 40 years. This suggests that the models may also underestimate the rate of future change projected for Arctic snow cover. Current and projected changes in snow cover generate a cascade of interactions and feedbacks that affect Arctic climate, the sublayer (ground or ice) thermal regime, hydrology, vegetation, marine primary production, biogeochemical activity, exchanges of carbon dioxide and trace gases, and ecosystem services.

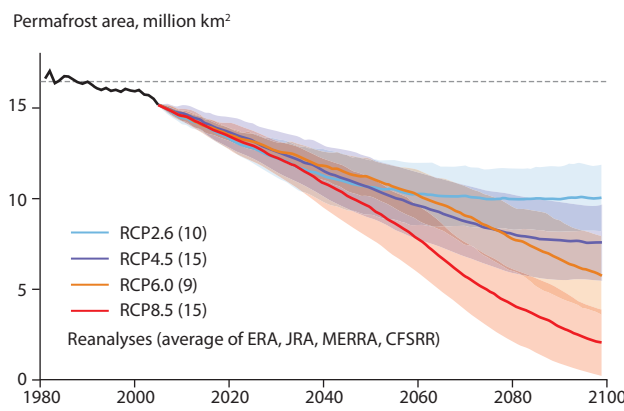


Figure 11.3 Projected change in permafrost area under different greenhouse gas scenarios; the number of models contributing to each RCP estimate is given in brackets, the shaded area is one standard deviation across the models, and the dashed black line represents the present-day total permafrost area (Slater and Lawrence, 2013).

Since SWIPA 2011, there have been substantial efforts to evaluate large-scale models of permafrost dynamics across the circumpolar north. Projections show a decrease in northern hemisphere permafrost area from roughly 15 million km² at present to 12 million km² by 2040 followed by a rapid decrease to 5 million km² by 2080 under the RCP8.5 scenario, and stabilization at around 8 million km² under RCP4.5 (Figure 11.3). Thus societal/engineering impacts associated with permafrost warming could increase substantially by mid-century.

Projected warming will involve a shift from snow-dominated to rain-dominated hydrologic regimes in some terrestrial areas, which will generally become more 'water rich', where water availability meets or exceeds the needs of human development and ecosystem services. Inadequate knowledge of the spatial and temporal distribution of freshwater is a key uncertainty. Freshwater represents a complex of interacting systems and thus projections for any one subsystem are challenging, for example due to increased influences from changes in vegetation, increased evaporation from an ice-diminished ocean and ponds/lakes/rivers, and modified intensity, direction and heat and moisture content of storm tracks. Delivery of freshwater to the marine system is also poorly understood. Climate change and human regulation of water systems both affect how freshwater is delivered to the ocean and the commensurate impacts.

Projected land ice changes in SWIPA 2017 are based on four studies, while the corresponding projections in SWIPA 2011 were based on one. Glaciers in some parts of north-eastern Siberia and the Kamchatka Peninsula are projected to disappear by 2060, with other glaciers undergoing substantial reductions. Projected mass loss from glaciers and icecaps is greater in the latter half of the century under both the RCP4.5 and RCP8.5 scenarios (Figure 11.4).

There is large variability between different model projections for sea-ice extent and thickness. Models show essentially ice-free summers by the mid-21st century; this is later than data extrapolation and process studies suggest. While models suggest summer open water duration will increase by several months over the next three decades, winters will remain ice covered. Results from model projections also agree with recent observations for an increasing frequency and spatial extent of young ice forms in winter, thereby affecting thermal and chemical coupling with the atmosphere.

In summary, climate models suggest that while temperatures, spring snow cover, and sea-ice extent and thickness are likely to continue to exhibit the same major trends over the next three decades, other elements of the cryosphere such as mass loss from glaciers, in turn driving sea-level rise, may accelerate (Figure 11.4). Infrastructure impacts such as those from permafrost thaw are also foreseen to increase until mid-century and will rise substantially in the latter half of the century under continued increases in atmospheric GHG concentrations.

11.4 Linkage between cryospheric change and lower latitudes

The Arctic is linked with the global climate system through north-south heat and moisture exchanges in the atmosphere and ocean, and through carbon cycling. There is growing evidence that the Arctic cryosphere has potential to impact society at lower latitudes through sea-level rise and an influence on atmospheric circulation.

11.4.1 Patterns of atmospheric circulation

Shifts in Arctic sea ice and snow cover and increased heating are warming the lower atmosphere in the Arctic. Rising air temperatures decrease air density and the north-south horizontal pressure gradients, and thus shift wind patterns. Whether these changes affect weather at lower latitudes of the northern hemisphere is a difficult question because Arctic forcing is but one impact on mid-latitude weather along with natural variability and equatorial forcing. It has also been a relatively short period (~15 years) since Arctic forcing was strong enough to have an impact at lower latitudes, so it is difficult to separate potential Arctic forcing from random processes. The key issue is not whether the warming Arctic will influence mid-latitude weather patterns over the coming decades, but rather what is the nature and magnitude of this influence relative to non-Arctic factors, and is it limited to specific regions, seasons, or types of weather event? Hemispheric data over multiple decade-long time series do not as yet show appreciable Arctic-forced impacts on mid-latitude climate. Warming in all seasons will continue for the Arctic and subarctic into the future (Figures 2.13 and 2.14). However, there is evidence for regional causal connections, such as Barents-Kara sea ice loss, a stronger Siberian High, and cold air outbreaks into eastern Asia. Recent (December 2016) cold air penetrating into the southeastern United States was related to a shift in the large-scale atmospheric wind patterns and was reinforced by higher temperatures north of Alaska and west of Greenland. Arctic/mid-latitude weather linkages are a major research challenge because Arctic forcing will continue to strengthen, with potential for improving mid-latitude extended range weather forecasts for large populations.

11.4.2 Greenhouse gas release

Over the recent geological past, the GHG balance in the Arctic has been toward the storage of carbon. However, recent changes suggest the storage capacity may be declining or even reversing. Permafrost degradation in some areas exacerbates carbon loss and may potentially release stores of trapped GHGs over decadal to centennial time scales.

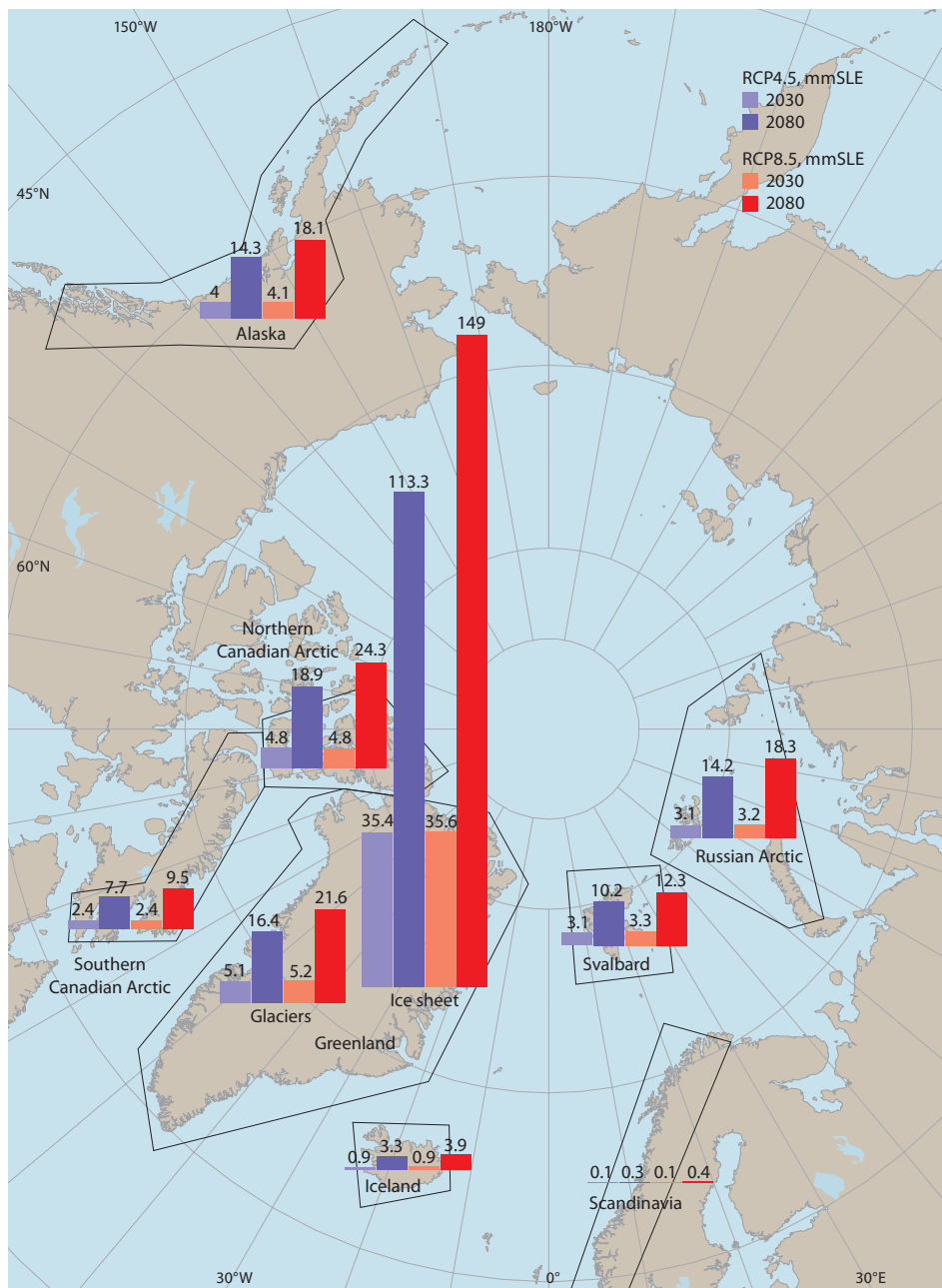


Figure 11.4 Projected land ice loss (expressed in millimeters sea level equivalence; mmSLE) from different Arctic regions in 2030 and 2080 under the RCP4.5 and RCP8.5 scenarios, based on the 2006–2100 sea level budget described in Section 9.4. The relatively small mainland Eurasian glaciers do not appear here owing to incomplete assessment.

11.4.3 Sea-level rise

Climate change affects sea level primarily through thermal expansion of seawater in the global oceans due to warming, and mass losses from glaciers and Antarctic and Greenland ice masses. NASA estimates that global sea level rose by 8.6 cm over the period 1993–2016. More than half the change in global sea level results from land ice change, and two-thirds of global land ice loss occurs in the Arctic region. Glaciers and ice sheets represent a large reservoir for future contributions to sea-level rise (Table 9.1). Uncertainty about the future volume change of Greenland's ice is a major concern. New information (Section 6.4.4) suggests a disturbing recent (2002–2012) increase in the Greenland ice sheet loss contribution to global mean sea level relative to the previous century. For

the future, significant effects of sea-level rise will become increasingly evident beyond mid-century (Figure 11.4). A key issue is that the current and near future rise in temperature commits the system to future long-term ice loss. Sea-level rise increases coastal flooding, beach erosion, infrastructure damage, environmental impacts on ecosystems, and saltwater intrusion into groundwater. Such effects are exacerbated when combined with storm tides, such as happened in the New York area in 2012 during hurricane Sandy.

11.4.4 Freshwater outflow

Recent estimates (Chapter 7) suggest increased storage of freshwater has occurred in Canada Basin and that export of freshwater stores from the Eurasian Basin has increased. Large-scale export of freshwater from the Arctic over

geological time has been linked with large-scale cooling of the northern hemisphere. Factors driving such export are poorly understood, although regional air/sea interaction is implicated. Thus, if Arctic freshwater storage were to be replaced by freshwater export, there could be unexpected consequences for northern hemisphere climate, based on interaction between the freshwater outflow and the Atlantic Ocean circulation and heat content, ultimately interacting with atmospheric circulation.

11.5 Consequences of cryospheric-driven change

The SWIPA 2017 update has been conducted under a different assessment landscape than SWIPA 2011, as it is concurrent with the AMAP *Adaptation Actions for a Changing Arctic* (AACa) activity. With a focus on three Arctic subregions (the Barents Sea area; the Bering, Chukchi, and Beaufort seas region; and Baffin Bay and Davis Strait region) the AACa is an integrated assessment of the impacts of Arctic change and is intended to inform adaptation actions. The AACa assessment examines the impacts of climate drivers, other environmental stressors, and socio-economic drivers of Arctic change. SWIPA 2017 is the peer-reviewed scientific assessment documenting current and future cryospheric changes that support the magnitude and locations of adaptation actions for AACa. Given the imminent publication of the full AACa assessment reports, the SWIPA 2017 update has been limited to an assessment of the consequences of physical changes in cryospheric system components – snow, water, ice, permafrost and carbon cycling – especially during the period since SWIPA 2011, as a contribution to the AACa process.

The consequences of Arctic change include economic costs, and estimating the cryosphere's contribution to the costs of ongoing and future climate change is an emerging research area. Such studies, using econometric strategies for converting incremental warming to equivalent GHG amounts and their estimated damage potential, place the cumulative costs of Arctic warming at USD 7–100 trillion (i.e. million million), or EUR 6–80 trillion by 2100 under a warming scenario corresponding to the current trajectory of future GHG emissions (Euskirchen et al., 2013). While these estimates are *cumulative* over the period 2010–2100, the corresponding annual average cost is USD 77 billion to USD 1 trillion. These estimates take into account the warming effect of the reduction in surface albedo resulting from diminished sea ice and terrestrial snow cover, and increased methane emissions from thawed permafrost. The costs are associated with sea-level rise as well as with impacts on water availability, agriculture and other industries. The large range reflects economic uncertainties as well as uncertainty in future climate change in the Arctic. Nevertheless, the range represents a substantial economic impact and equates to 0.4–5.6% of the U.S. Gross Domestic Product in 2015. More recently, Hope and Schaefer (2015) used an integrated assessment model to estimate the economic impacts of only permafrost thaw through the associated releases of carbon dioxide and methane. The mean of the cumulative cost estimates by 2200 was USD 43 trillion under a mid-range global warming scenario.

11.5.1 Changes in marine and terrestrial access

Changes in sea ice, snow cover and land ice have consequences for access in the marine and terrestrial domains. The open water season has already increased by one to three months in the last two decades over much of the Arctic Ocean (Chapter 5), and ship traffic has shown a marked increase. The transit of a large cruise ship through the Northwest Passage in 2016 highlights the new regime of increased marine access. However, season length for overland transportation via ice roads, which are vital for wintertime resupply of industries and remote communities in Alaska and Canada, has decreased.

11.5.2 Land use

Changes in human land use are closely tied to permafrost and erosion. Changes in permafrost are well documented (Chapter 4). In communities and urban environments, changes in the thermal regime of soils that support houses, roads, airports, and buildings have large economic and societal consequences. New findings since SWIPA 2011 show increasing thermokarst activity in permafrost areas (Liljedahl et al., 2016; Reynolds et al., 2014).

Rain-on-snow events during the Arctic winter affect road transportation, electrical power systems, and access to forage foods by wildlife. Recent studies point to ongoing and projected increases in freezing rain in a warming climate, with impacts on wildlife and human activities.

11.5.3 Industrialization and development

Resource extraction, commercial fishing and tourism are three key industries in the Arctic. All are affected by climate change, although non-climate drivers are also important to the trajectories of these activities.

Arctic nations derive major economic benefit from the extractive resources industries. Mining is a significant industry in Russia, Canada, Alaska, and northern Scandinavia. The extent to which climate change will influence industry planning will likely be for the issue of access, but will also depend on market forces and government incentives.

Commercial fishing is a major activity in the Arctic and its periphery, and some fishing grounds could shift northward. Direct linkage between fisheries and future climate change is difficult to establish because fish stocks are also strongly affected by fishing pressure and related management decisions. Compounding uncertainty in the climate-fisheries connection is ocean acidification, which is a fisheries-related risk associated with increased GHG emissions.

A longer warm season in the Arctic has implications for Arctic tourism, especially if the shoulder seasons of spring and autumn create additional opportunities for outdoor activities. Skiing and other winter recreation may face challenges. In view of the rapid rate of summer sea-ice retreat, cruise ship tourism is already increasing. As access to coastal communities increases, cruise ship tourism will be affected as much or more by local infrastructure and permit requirements than by ice conditions, highlighting the interplay between climate and non-climate drivers.

Significant hydroelectric generation already exists in northern watersheds that empty into Arctic or subarctic marine waters (such as in Canada and Russia). The potential for new hydropower sources is being exploited, for example in Greenland.

11.5.4 Hazards

Climate change (specifically the projected changes in seasonal precipitation amount, intensity and type) is expected to alter the magnitude, frequency, intensity, duration and persistence of extreme weather/hydrological events. Over large parts of Eurasia the effects of warming are manifesting as increased winter river flow and a shift toward an earlier start to spring runoff and an earlier peak in annual runoff.

Snow can be a hazard for human activities. Examples include avalanches, excessive roof snow loads and blizzards. Removal of snow from critical infrastructure such as key roads and airstrips is an important cost in all northern community budgets. Although snow season length is projected to decrease under a warming climate, the future trend in heavy snow events is unclear.

Despite the ongoing decrease in multi-year sea-ice extent, sea ice hazards may be increasing in some parts of the Arctic. There is evidence that wind speeds increase ice velocity in marginal ice zones, making it difficult to model ice hazards affecting offshore industries. Sea-based subsistence activities are increasingly subject to the hazards associated with a thinner, more mobile and less stable ice cover (Eicken and Mahoney, 2015).

Various studies project an increase in summer wildfires. Even with an increase in precipitation, the summer surface water balance may become increasingly negative as evapotranspiration increases owing to higher temperatures and a longer summer season. The projected increase in wildfires represents a continuation of the trend in recent decades for more frequent severe fire years in Alaska, Canada and Russia.

11.5.5 Ecosystem and biodiversity losses

Terrestrial ecosystem findings beyond SWIPA 2011 suggest additional variability in greening and browning at the land surface and the frequency of wildfire and abrupt thaw events has increased. These landform changes are accelerating biome shifts; for example, increasing tree density in taiga, range expansion of tall shrubs and trees into tundra, and conversion between terrestrial and aquatic ecosystems. Abrupt thaw also accelerates decomposition and release of permafrost carbon to the atmosphere.

Changes in climate, especially in sea ice and its associated snow cover, have consequences for Arctic marine ecosystems and biodiversity. Increased ice algal production is expected with thinner and more transparent first-year ice in the Arctic. As shown in Chapters 2 and 5, the prolonged open water period due to earlier ice melt and later ice formation is shifting the phenology of the phytoplankton bloom from a unimodal to a bimodal bloom pattern. This shift was not documented in the Arctic Climate Impact Assessment (ACIA, 2005) or SWIPA 2011 (AMAP, 20011). The occurrence of toxin-producing algal blooms is an emerging concern and is supported by recent extensive

observations of algal toxins in marine mammals, and the call for monitoring of these toxins in Arctic marine food webs.

The decline in Arctic sea ice is dictating range contractions for endemic Arctic species and poleward extensions for subarctic species. The latter is documented at all trophic levels: primary and secondary producers, fishes and marine mammals. While more extensive and longer open water periods may favor increased primary production, stronger stratification due to sea ice melt and warming have opposing effects on primary production. Whales are favored over ice-obligate species such as walrus and polar bears.

11.5.6 Shift in lifestyles, culture and socio-economics

Food security lies at the intersection of culture, socio-economics, and lifestyle for many Arctic communities. Climate-related threats occur at many levels, including physical, ecological, technological, cultural, economic, and societal (AMAP 2017a,b,c). Availability of subsistence food species may shift due to more difficult/hazardous travel to traditional hunting areas, altered wildlife habitats and distributions, local extinction of food plants, and spoilage of meat in food cellars built into thawing permafrost.

Climate change has already affected the range and abundance of important marine and terrestrial food sources such as salmon, herring, char, cod, walrus, seals, whales, caribou, moose and some species of seabird, with the spread of new southern species into northern areas having both ecological and food security implications. Adequate safe water supplies for many communities depend on natural surface features (ponds, streams, lakes), which are vulnerable to thermokarst disturbance and drainage, as well as bacterial contamination.

Solid precipitation is a very effective scavenger of aerosol particles and also absorbs trace gases during its fall to the surface. On land and ice, snow metamorphic processes, photochemical reactions and melt events influence the concentrations and cycling of many contaminants. Warming is expected to further impact the uptake and cycling of contaminants through changes in snow, and the partitioning equilibria of contaminants between the gas phase and snow and ice.

11.6 Research priorities from the SWIPA 2017 assessment

Previous chapters, and Sections 11.2 and 11.3, outline the prospect of a ice-free Arctic Ocean in summer and autumn, thawing permafrost, glacier and ice sheet contributions to sea-level rise, and shifts in Arctic/mid-latitude climate connections and in the freshwater and carbon system. Societal impacts from Arctic climate change will be large relative to the rest of the globe (Section 11.4 and 11.5). The cryosphere also contains important records of past climate providing benchmarks for interpreting current and future climate change.

The World Climate Research Programme (WCRP) has developed Grand Challenges, including one for the cryosphere, focused on improvements to climate models (Kattsov et al., 2012; Flato et al., 2016) in preparation for the next model intercomparison (CMIP6) for next (sixth) assessment of the

Intergovernmental Panel on Climate Change. The SWIPA 2017 findings corroborate and endorse their overarching perspective:

How will melting ice respond to, and feedback on, the climate response to increasing greenhouse gases, and what will the impacts be?

The WCRP Grand Challenge proposed three foci: sea ice and snow modeling, ice sheet modeling, and permafrost carbon release.

- Assembling the most reliable observational data on sea ice and snow, and using these data to evaluate and improve climate model simulations of the remarkable changes that have already been observed and to enhance confidence in future projections.
- Assembling glacier and ice sheet models for use in projecting melt rates and corresponding sea-level rise. Shrinking glaciers will also have profound and direct impacts on millions of people whose water resources depend on the summertime storage provided by mountain glaciers.
- Quantifying the amount of carbon available in permafrost areas, evaluating the potential for release of this carbon, and improving our capability to simulate the response of permafrost thaw, and its connection to the global carbon cycle.

In contrast to SWIPA 2011, SWIPA 2017 shifts the discussion from mostly known individual cryospheric processes to the uncertain future interaction of these processes, with consequences at an Arctic-wide and global scale (Figure 11.1). Acting on the SWIPA 2017 assessment requires addressing two critical goals:

- Improve quantitative predictions for the timing of future Arctic changes. This includes further understanding of the cryospheric feedbacks consequential for amplification of Arctic temperatures forced by GHGs.
- Improve confidence in quantitative predictions of interactions between the Arctic and global systems, on monthly to multi-decadal time scales.

While the framework for comparative assessment of cryospheric feedbacks has improved since SWIPA 2011, evaluations to date are model-based and have not included potentially important terrestrial and marine feedbacks. Further evaluation is a prerequisite for quantitative predictions of future change.

Several knowledge gaps and research needs have been identified:

- Overarching knowledge gap:* Despite qualitative progress, the overarching knowledge gap is poor quantification of the timing, magnitude, and risk of future Arctic change, especially for those changes that involve multiple Arctic feedbacks.
- Changing climate system:* Determine the amount of global warming that would trigger an unstable abrupt shift in the Arctic system (sea ice, Greenland ice sheet, permafrost, boreal forest). Better document and project changes in storms, precipitation/evaporation, Arctic vegetation, moisture fluxes, and the influence of freshwater-marine coupling on the Arctic and through teleconnections to the North Atlantic.

- Declining sea ice:* Improve timing estimates for future loss of regional sea ice and increase understanding of the change from multi-year sea ice to first-year sea ice. Determine the impacts of sea ice loss on Arctic and mid-latitude weather, climate variability and predictability. Data gaps impede projections of the ice-associated ecosystem response to a changing climate.
- Thawing permafrost:* Investigate how changes in permafrost affect coastal erosion, ecosystems, and infrastructure on local and regional scales. A major unknown is quantifying the strength of the positive feedback between thawing permafrost and warming climate in terms of natural carbon emissions.
- Melting ice sheets/glaciers:* Quantitative rates are needed for the processes (ice dynamics, subglacial meltwater, ocean interaction) that accelerate melting. Also needed is a more complete quantitative evaluation of the contribution of the Greenland ice sheet and Arctic glaciers to future sea-level rise relative to non-Arctic contributions.
- Shifts in terrestrial ecosystems:* Improve understanding of snow-land type-hydrologic changes coupled with ecological feedbacks that together transform Arctic landscapes. Scaling challenges arise because many landscape changes occur at small scales but their aggregate changes have regional and global impacts. Develop syntheses of pan-Arctic observations of wildfire characteristics (frequency, intensity, severity, size).
- Observations:* All aspects of Arctic research can benefit from better monitoring and satellite interpretations, and improved coordination between monitoring efforts, process studies, and modeling.
- Modeling:* How to use climate model results in future climate and risk assessments is a significant scientific issue in itself. Improvements include the need for better approaches to multi-model evaluations, determining confidence levels in model projections for different variables, development of strategies for using model ensembles to assess probabilities and uncertainties, and using downscaling techniques to add resolution and uncertainty estimates.
- Costs:* There is a need for better quantification of the impacts of Arctic change in terms of economic and societal costs. Current cost estimates have uncertainties spanning a full order of magnitude and are greater than the uncertainties in the climate projections on which they are based.

11.7 Conclusion

SWIPA 2017 confirms, with increased confidence, the Arctic cryospheric trends reported in SWIPA 2011, consistent with amplified warming of the Arctic due to anthropogenic climate forcing. This warming is driving change throughout the cryosphere, and these changes are expected to continue in the foreseeable (decades) future. The Arctic is showing clear evidence of evolving to a new state before mid-century. Change in the Arctic is expected to accelerate in the latter half of the century for some components such as glaciers, ice sheets and permafrost. Based on extensive new peer-reviewed literature, the preceding chapters collectively provide new insights into the scope and

nature of cryospheric change. The summary of observations and projections, and summary of implications presented at the beginning of the chapter are repeated in Box 11.1.

Changes in the Arctic cryosphere have consequences for ecosystems, infrastructure, and human wellbeing in and beyond the Arctic. These changes combine with non-climate environmental stressors (contaminants, land use) and socio-economic drivers (global economy, management decisions) to amplify impacts. Among the most visible impacts of cryospheric change are the effects of a reduced sea-ice cover on coastal erosion, river flooding and water supply in coastal communities, access to the Arctic, and marine ecosystems (including marine mammals). Increased algal production and loss of sea-ice biodiversity in the central Arctic Ocean are among the key impacts of the shift from a multi-year to predominantly first-year sea ice. The warming climate and reductions in terrestrial snow cover and freshwater ice are having negative impacts on overland transportation needed for community resupply, industrial transport and winter subsistence hunting, whereas loss of sea ice is increasing opportunities for shipping and resource development. The loss of snow cover feeds back to spring temperatures, impacts vegetation in the boreal forest and tundra biomes, and favors a longer warm season and

associated drying. Snow cover on sea ice is poorly understood. Together with increased pest infestations, the warmer and drier conditions have contributed to an increase in severe wildfire years in North America and Eurasia. Thawing permafrost damages infrastructure and has the potential to require billions of dollars (euros) in additional maintenance and building replacement costs. The major high-latitude industries (resource extraction, subarctic fisheries, tourism, transportation) may experience increased opportunities from cryospheric changes under a warming climate, but global demand and commodity prices remain the primary driver for resource exploitation. Food security in Arctic communities is affected by changes in the availability of subsistence foods and interplay with the growing cash economy in Arctic communities.

SWIPA 2011 pointed to a highly variable and uncertain present and future for the Arctic; climate projections were becoming less trustworthy predictors of future risk. The report pointed to difficulties in extrapolating from past trends, and with assuming smooth transitions, slow rates of change, and low frequencies of extreme events. Six more years of data and new analyses in SWIPA 2017 add increased certainty to near future trends across multiple processes. This assessment presents evidence that changes will continue for the foreseeable future

Box 11.1 SWIPA 2017: Summary and implications of findings

Summary of observations and projections

- The period since SWIPA 2011 has seen a continuation of cryospheric trends consistent with rapid warming of the Arctic. These trends are very likely to continue past mid-century, with more frequent and stronger extremes and the passing of no-return thresholds ('irreversibilities').
- Observed and projected changes in Arctic temperature are more than double those at mid-latitudes.
- Sea ice is undergoing a regime shift from multi-year ice to predominantly first-year ice. Summer sea ice is very likely to be essentially gone within the next few decades.
- Loss of land-based ice – from mountain glaciers and ice caps – is expected to accelerate because committed loss will increase with warming, with implications for global sea-level rise.
- Ongoing reductions in Arctic snow cover and warming permafrost are both manifestations of change in the Arctic terrestrial coupled soil-vegetation-climate system, with impacts on energy, freshwater and carbon cycling. Specific humidity and precipitation have generally increased.
- There are emerging impacts of Arctic change on mid-latitude weather/climate and global sea-level rise.

Summary of implications

- The Arctic climate will continue to change over the coming decades with major consequences for ecosystems and society. Adaptation efforts need to begin now, because foreseeable Arctic temperature changes are large (4–5°C for autumn/winter by 2040–2050). In addition to climate

change, adaptation planning should take into account economic and societal drivers.

- Substantial and immediate mitigation in greenhouse gas emissions (at least at the level of RCP4.5) should reduce the risk of further future change for most cryospheric components after mid-century, and reduce the likelihood of potential irreversible melt of the Greenland ice sheet and glaciers and the associated impact on sea-level rise.
- Cumulative global impacts related to Arctic change are expected to be large; adaptation costs and economic opportunities are estimated in the tens of trillions of dollars.
- Prudent adaptation and risk management require better quantitative predictions. This means:
 - determining which feedbacks involving the Arctic cryosphere are most consequential for rapid Arctic warming
 - having a better understanding of interactions between different parts of the Arctic system. In particular, reducing uncertainties in snow-vegetation interactions, reducing uncertainties in snow and ice albedo feedbacks, and developing more detailed representation of vegetation, lakes and rivers
 - enhancing Arctic observing systems and the interpretation of *in situ* observations, satellite data, and model results; as well as improving coordination between monitoring efforts, process studies, and modeling.
- Determining the impacts of Arctic climate change outside of the Arctic region requires improved understanding of atmospheric and ocean connectivities.

(decades) and beyond, given the committed climate forcing from past, present and future GHG emissions. The key finding of SWIPA 2017 is that Arctic changes will be large and early relative to the rest of the globe, and will require major adaptation. This adaptation to GHG-induced changes in the Arctic cryosphere remains a challenge for Arctic and global communities. Halting changes beyond those foreseen by mid-century could be possible through the full implementation of a major mitigation strategy. Providing increased certainty to present and future cryospheric changes and their associated impacts, the key findings of SWIPA 2017 motivate the need for improvement in quantitative prediction of underlying processes, their interactions, and the timing of future Arctic temperature increases, cryospheric shifts, and ecosystem and societal impacts.

References

ACIA, 2005. Arctic Climate Impact Assessment. Cambridge University Press.

AMAP, 2011. Snow, Water, Ice and Permafrost in the Arctic (SWIPA): Climate Change and the Cryosphere. Arctic Monitoring and Assessment Programme (AMAP), Oslo, Norway.

AMAP, 2017a. Adaptation Actions for a Changing Arctic: Perspectives from the Barents Area. Arctic Monitoring and Assessment Programme (AMAP), Oslo, Norway.

AMAP, 2017b. Adaptation Actions for a Changing Arctic: Perspectives from the Bering-Chukchi-Beaufort region. Arctic Monitoring and Assessment Programme (AMAP), Oslo, Norway.

AMAP, 2017c. Adaptation Actions for a Changing Arctic: Perspectives from the Baffin Bay/Davis Strait region. Arctic Monitoring and Assessment Programme (AMAP), Oslo, Norway.

Eicken, H. and A.R. Mahoney, 2015. Sea ice: Hazards, risks and implications for disasters. In: Ellis, J., J. Douglas and J.F. Shroder (eds.), *Coastal and Marine Hazards, Risks and Disasters*. pp. 381-401. Elsevier.

Euskirchen, E.S., E.S. Goodstein and H.P. Huntington, 2013. An estimated cost of lost climate regulation services caused by thawing of the Arctic cryosphere. *Ecological Applications*, 23:1869-1880.

Flato, G., V. Kattsov and J. Baeseman, 2016. Melting Ice – Global Consequences. Initial implementation plan for the WCRP Grand Challenge on the Cryosphere in a Changing Climate. www.wcrp-climate.org/melting-ice-global-consequences-documents.

Hope, C. and K. Schaefer, 2015. Economic impacts of carbon dioxide and methane released from thawing permafrost. *Nature Climate Change*, 6:56-59.

IPCC, 2013. Climate Change 2013: The Physical Science Basis. Contribution of Working Group I to the Fifth Assessment Report of the Intergovernmental Panel on Climate Change. Stocker, T.F., D. Qin, G.-K. Plattner, M. Tignor, S.K. Allen, J. Boschung, A. Nauels, Y. Xia, V. Bex and P.M. Midgley (eds.). Cambridge University Press.

Kattsov, V., G. Flato, S. Bony, S. Gille, B. Kirtman, V. Ryabinin, A. Scaife and K. Trenberth, 2012. Cryosphere in a changing climate: A grand challenge of climate science. WCRP White paper. www.wcrp-climate.org/images/documents/grand_challenges/GC_cryo.pdf

Liljedahl, A.K., J. Boike, R.P. Daanen, A.N. Fedorov, G.V. Frost, G. Grosse, L. Hinzman, Y. Iijima, J.C. Jorgenson, N. Matveyeva, M. Necsoiu, M.K. Raynolds, V.E. Romanovsky, J. Schulla, K. Tape, D.A. Walker, C.J. Wilson, H. Yabuki and D. Zona, 2016. Pan-Arctic ice wedge degradation in warming permafrost and its influence on tundra hydrology. *Nature Geoscience*, 9:312-318.

Raynolds, M.K., D.A. Walker, K.J. Ambrosius, J. Brown, K.R. Everett, M. Kanavskiy, G.P. Kofinas, V.E. Romanovsky, Y. Shur and P.J. Webber, 2014. Cumulative geoecological effects of 62 years of infrastructure and climate change in ice-rich permafrost landscapes, Prudhoe Bay Oilfield, Alaska. *Global Change Biology*, 20:1211-1224.

Slater, A.G. and D.M. Lawrence, 2013. Diagnosing present and future permafrost from climate models. *Journal of Climate*, 26:5608-5623.

Acronyms and abbreviations

Ω	Saturation state	OSI-SAF	Ocean and Sea Ice Satellite Application Facility
AACA	Adaptation Actions for a Changing Arctic	$p\text{CO}_2$	Partial pressure of carbon dioxide
AAR	All Arctic Regions (a TCA definition)	POC	Particulate organic carbon
ACIA	Arctic Climate Impact Assessment	RATIC	Rapid Arctic Transitions due to Infrastructure and Climate
AFD	Arctic Freshwater Domain	RCM	Regional climate model
ALT	Active-layer thickness	RCP	Representative Concentration Pathway (IPCC)
AMAP	Arctic Monitoring and Assessment Programme	ROS	Rain-on-snow event
AMOC	Atlantic Meridional Overturning Circulation	SCD	Snow-cover duration
AO	Arctic Oscillation	SCE	Snow-cover extent
AR5	Fifth Assessment Report (IPCC)	SDmax	Maximum snow depth
AVHRR	Advanced Very High Resolution Radiometer	SIC	Sea-ice concentration
BC	Black carbon	SLE	Sea level equivalence
BP	Before present	SLR	Sea-level rise
CALM	Circumpolar Active Layer Monitoring	SMB	Surface mass balance
CH_4	Methane	SOM	Soil organic matter
CMIP5	Coupled Model Intercomparison Project phase 5	SRES	Special Report on Emission Scenarios (IPCC)
CO_2	Carbon dioxide	SWE	Snow water equivalent
DOC	Dissolved organic carbon	SWEmax	Maximum SWE
DLR	Downward longwave radiation	TAPS	Trans-Alaska Pipeline System
ELA	Equilibrium line altitude	TCA	Terrestrial contributing area
ESM	Earth system model	TI-NDVI	Time-integrated NDVI
GCM	Global climate model / General circulation model	UAV/UAS	Unmanned aerial vehicle or system
GHG	Greenhouse gas	UNFCCC	United Nations Framework Convention on Climate Change
GWP	Global warming potential	USD	United States dollar
Hg	Mercury	WCRP-CliC	World Climate Research Program's Climate and Cryosphere Project
IASC	International Arctic Science Committee	w.e.	Water equivalent
IPCC	Intergovernmental Panel on Climate Change	WMO	World Meteorological Organization
IPY	International Polar Year		
IRIS	Integrated Regional Impact Studies		
LIA	Little Ice Age		
LAP	Light absorbing particle		
MaxNDVI	Maximum NDVI		
MeHg	Methylmercury		
MOD	Melt onset date		
NAO	North Atlantic Oscillation		
NASA	National Aeronautics and Space Administration (US)		
NDVI	Normalized Difference Vegetation Index		
NEGIS	North East Greenland Ice Stream		
NOAA	National Oceanic and Atmospheric Administration (US)		
NSIDC	National Snow and Ice Data Center (US)		

Arctic Monitoring and Assessment Programme

The Arctic Monitoring and Assessment Programme (AMAP) was established in June 1991 by the eight Arctic countries (Canada, Denmark, Finland, Iceland, Norway, Russia, Sweden and the United States) to implement parts of the Arctic Environmental Protection Strategy (AEPS). AMAP is now one of six working groups of the Arctic Council, members of which include the eight Arctic countries, the six Arctic Council Permanent Participants (indigenous peoples' organizations), together with observing countries and organizations.

AMAP's objective is to provide 'reliable and sufficient information on the status of, and threats to, the Arctic environment, and to provide scientific advice on actions to be taken in order to support Arctic governments in their efforts to take remedial and preventive actions to reduce adverse effects of contaminants and climate change'.

AMAP produces, at regular intervals, assessment reports that address a range of Arctic pollution and climate change issues, including effects on health of Arctic human populations. These are presented to Arctic Council Ministers in 'State of the Arctic Environment' reports that form a basis for necessary steps to be taken to protect the Arctic and its inhabitants.

This report has been subject to a formal and comprehensive peer review process. The results and any views expressed in this series are the responsibility of those scientists and experts engaged in the preparation of the reports.

The AMAP Secretariat is located in Oslo, Norway. For further information regarding AMAP or ordering of reports, please contact the AMAP Secretariat (Gaustadalléen 21, N-0349 Oslo, Norway) or visit the AMAP website at www.apam.no.



ARCTIC COUNCIL

AMAP
Arctic Monitoring and
Assessment Programme

AMAP Secretariat

Gaustadalléen 21
N-0349 Oslo, Norway

T +47 21 08 04 80

F +47 21 08 04 85

www.amap.no

ISBN 978-82-7971-101-8

